VOLUME 28 / NUMBER 13
JULY 8, 1990
ACC. NOS. N90-20044 TO N90-20919

STAR

AN ABSTRACT JOURNAL

Scientific and Technical Aerospace Reports

PRODUCED BY THE
SCIENTIFIC AND TECHNICAL
INFORMATION
DIVISION

NASA

NATIONAL AERONAUTICS AND SPACE ADMINISTRATION

WHAT YOU CAN DO FOR *STAR*

All users of this abstract service are urged to forward reports to be considered for announcement in *STAR*. This will aid NASA in its efforts to provide the fullest possible coverage of all scientific and technical publications that might support aeronautics and space research and development. If you have prepared relevant reports (other than those that you will transmit to NASA, DOD, or DOE through the usual contract- or grant-reporting channels), please send them for consideration to the NASA Scientific and Technical Information Facility, P.O. Box 8757, BWI Airport, MD 21240.

Reprints of journal articles, book chapters, and conference papers are also welcome. These will be considered for announcement in *STAR*'s companion journal, *International Aerospace Abstracts*.

You may specify a particular source to be included in a report announcement if you wish; otherwise the report will be placed on public sale at the National Technical Information Service. Copyrighted publications will be announced but not distributed or sold.

PURCHASE OF *STAR*

The semimonthly issues are available to registered users on annual subscription from the NASA Scientific and Technical Information Facility, ATTN: Registration Services, P.O. Box 8757, BWI Airport, MD 21240. *STAR* is publicly available on annual subscription from the Superintendent of Documents, U.S. Government Printing Office, Washington, DC 20402.

PUBLISHED BY:

UNITED STATES GOVERNMENT
NATIONAL AERONAUTICS AND SPACE ADMINISTRATION
SCIENTIFIC AND TECHNICAL INFORMATION DIVISION
Scientific and Technical Aerospace Reports, Volume 28, is prepared by the NASA Scientific and Technical Information Facility operated for the National Aeronautics and Space Administration by RMS Associates.

The Administrator of the National Aeronautics and Space Administration has determined that the publication of this periodical is necessary in the transaction of the public business required by law of this agency. Use of funds for printing this periodical has been approved by the Director of the Office of Management and Budget through March 22, 1991.

US ISSN 0036-8741

Scientific and Technical Aerospace Reports (STAR) is issued twice a month and contains abstracts and indexes of meeting papers, conference proceedings, and unlimited distribution reports that have been added to the NASA Scientific and Technical Information Database during the preceding period. These citations may also be accessed online via NASA/RECON or via AIAA's Aerospace Database (File 108) through Dialog Information Services, Inc.

STAR subject coverage includes all aerospace-related areas that will help NASA achieve its mission. Material is gathered from all over the world and includes significant input from many countries under exchange and access agreements.

Consult the indexes at the back of this volume to help zero in on what you are looking for. These include:

Subject Index
Personal Author Index
Corporate Source Index
Contract Number Index
Report/Accession Number Index

STAR's companion abstract journal *International Aerospace Abstracts* should be used if you are looking for references to periodicals, books, and published meeting papers or conference proceedings.

Questions and comments should be addressed to:

NASA Scientific and Technical Information Facility
User Services
P.O. Box 8757
BWI Airport, MD 21240
301-621-0150

VOLUME 28 NUMBER 13 / JULY 8, 1990

TABLE OF CONTENTS

AERONAUTICS

Includes aeronautics (general); aerodynamics; air transportation and safety; aircraft communications and navigation; aircraft design, testing and performance; aircraft instrumentation; aircraft propulsion and power; aircraft stability and control; and research and support facilities (air).

For related information see also *Astronautics.*

01 AERONAUTICS (GENERAL) **N.A.**

02 AERODYNAMICS **1749**

Includes aerodynamics of bodies, combinations, wings, rotors, and control surfaces; and internal flow in ducts and turbomachinery.

For related information see also *34 Fluid Mechanics and Heat Transfer.*

03 AIR TRANSPORTATION AND SAFETY **1751**

Includes passenger and cargo air transport operations; and aircraft accidents.

For related information see also *16 Space Transportation* and *85 Urban Technology and Transportation.*

04 AIRCRAFT COMMUNICATIONS AND NAVIGATION **N.A.**

Includes digital and voice communication with aircraft; air navigation systems (satellite and ground based); and air traffic control.

For related information see also *17 Space Communications, Spacecraft Communications, Command and Tracking* and *32 Communications and Radar.*

05 AIRCRAFT DESIGN, TESTING AND PERFORMANCE **1754**

Includes aircraft simulation technology.

For related information see also *18 Spacecraft Design, Testing and Performance* and *39 Structural Mechanics.* For land transportation vehicles see *85 Urban Technology and Transportation.*

06 AIRCRAFT INSTRUMENTATION **1756**

Includes cockpit and cabin display devices; and flight instruments.

For related information see also *19 Spacecraft Instrumentation* and *35 Instrumentation and Photography.*

07 AIRCRAFT PROPULSION AND POWER **1756**

Includes prime propulsion systems and systems components, e.g., gas turbine engines and compressors; and onboard auxiliary power plants for aircraft.

For related information see also *20 Spacecraft Propulsion and Power, 28 Propellants and Fuels,* and *44 Energy Production and Conversion.*

08 AIRCRAFT STABILITY AND CONTROL **1758**

Includes aircraft handling qualities; piloting; flight controls; and autopilots.

For related information see also *05 Aircraft Design, Testing and Performance.*

09 RESEARCH AND SUPPORT FACILITIES (AIR) **1758**

Includes airports, hangars and runways; aircraft repair and overhaul facilities; wind tunnels; shock tubes; and aircraft engine test stands.

For related information see also *14 Ground Support Systems and Facilities (Space).*

ASTRONAUTICS

Includes astronautics (general); astrodynamics; ground support systems and facilities (space); launch vehicles and space vehicles; space transportation; space communications, spacecraft communications, command and tracking; spacecraft design, testing and performance; spacecraft instrumentation; and spacecraft propulsion and power.

For related information see also *Aeronautics.*

12 ASTRONAUTICS (GENERAL) **1759**

For extraterrestrial exploration see *91 Lunar and Planetary Exploration.*

13 ASTRODYNAMICS **1760**

Includes powered and free-flight trajectories; and orbital and launching dynamics.

14 GROUND SUPPORT SYSTEMS AND FACILITIES (SPACE) **1760**

Includes launch complexes, research and production facilities; ground support equipment, e.g., mobile transporters; and simulators.

For related information see also *09 Research and Support Facilities (Air).*

15 LAUNCH VEHICLES AND SPACE VEHICLES **1761**

Includes boosters; operating problems of launch/space vehicle systems; and reusable vehicles.

For related information see also *20 Spacecraft Propulsion and Power.*

16 SPACE TRANSPORTATION **N.A.**

Includes passenger and cargo space transportation, e.g., shuttle operations; and space rescue techniques.

For related information see also *03 Air Transportation and Safety* and *18 Spacecraft Design, Testing and Performance.* For space suits see *54 Man/System Technology and Life Support.*

17 SPACE COMMUNICATIONS, SPACECRAFT COMMUNICATIONS, COMMAND AND TRACKING **1761**

Includes telemetry; space communications networks; astronavigation and guidance; and radio blackout.

For related information see also *04 Aircraft Communications and Navigation* and *32 Communications and Radar.*

18 SPACECRAFT DESIGN, TESTING AND PERFORMANCE 1762

Includes satellites; space platforms; space stations; spacecraft systems and components such as thermal and environmental controls; and attitude controls.

For life support systems see *54 Man/System Technology and Life Support.* For related information see also *05 Aircraft Design, Testing and Performance, 39 Structural Mechanics,* and *16 Space Transportation.*

19 SPACECRAFT INSTRUMENTATION N.A.

For related information see also *06 Aircraft Instrumentation* and *35 Instrumentation and Photography.*

20 SPACECRAFT PROPULSION AND POWER 1765

Includes main propulsion systems and components, e.g. rocket engines; and spacecraft auxiliary power sources.

For related information see also *07 Aircraft Propulsion and Power, 28 Propellants and Fuels, 44 Energy Production and Conversion,* and *15 Launch Vehicles and Space Vehicles.*

CHEMISTRY AND MATERIALS

Includes chemistry and materials (general); composite materials; inorganic and physical chemistry; metallic materials; nonmetallic materials; propellants and fuels; and materials processing.

23 CHEMISTRY AND MATERIALS (GENERAL) 1765

24 COMPOSITE MATERIALS 1766

Includes physical, chemical, and mechanical properties of laminates and other composite materials.

For ceramic materials see *27 Nonmetallic Materials.*

25 INORGANIC AND PHYSICAL CHEMISTRY 1769

Includes chemical analysis, e.g., chromatography; combustion theory; electrochemistry; and photochemistry.

For related information see also *77 Thermodynamics and Statistical Physics.*

26 METALLIC MATERIALS 1774

Includes physical, chemical, and mechanical properties of metals, e.g., corrosion; and metallurgy.

27 NONMETALLIC MATERIALS 1779

Includes physical, chemical, and mechanical properties of plastics, elastomers, lubricants, polymers, textiles, adhesives, and ceramic materials.

For composite materials see *24 Composite Materials.*

28 PROPELLANTS AND FUELS 1783

Includes rocket propellants, igniters and oxidizers; their storage and handling procedures; and aircraft fuels.

For related information see also *07 Aircraft Propulsion and Power, 20 Spacecraft Propulsion and Power,* and *44 Energy Production and Conversion.*

29 MATERIALS PROCESSING 1783

Includes space-based development of products and processes for commercial application.

For biological materials see *55 Space Biology.*

ENGINEERING

Includes engineering (general); communications and radar; electronics and electrical engineering; fluid mechanics and heat transfer; instrumentation and photography; lasers and masers; mechanical engineering; quality assurance and reliability; and structural mechanics.

For related information see also *Physics.*

31 ENGINEERING (GENERAL) 1787

Includes vacuum technology; control engineering; display engineering; cryogenics; and fire prevention.

32 COMMUNICATIONS AND RADAR 1788

Includes radar; land and global communications; communications theory; and optical communications.

For related information see also *04 Aircraft Communications and Navigation* and *17 Space Communications, Spacecraft Communications, Command and Tracking.* For search and rescue see *03 Air Transportation and Safety,* and *16 Space Transportation.*

33 ELECTRONICS AND ELECTRICAL ENGINEERING 1791

Includes test equipment and maintainability; components, e.g., tunnel diodes and transistors; microminiaturization; and integrated circuitry.

For related information see also *60 Computer Operations and Hardware* and *76 Solid-State Physics.*

34 FLUID MECHANICS AND HEAT TRANSFER 1798

Includes boundary layers; hydrodynamics; fluidics; mass transfer and ablation cooling.

For related information see also *02 Aerodynamics* and *77 Thermodynamics and Statistical Physics.*

35 INSTRUMENTATION AND PHOTOGRAPHY 1803

Includes remote sensors; measuring instruments and gauges; detectors; cameras and photographic supplies; and holography.

For aerial photography see *43 Earth Resources and Remote Sensing.* For related information see also *06 Aircraft Instrumentation* and *19 Spacecraft Instrumentation.*

36 LASERS AND MASERS 1805

Includes parametric amplifiers.

For related information see also *76 Solid-State Physics.*

37 MECHANICAL ENGINEERING 1809

Includes auxiliary systems (nonpower); machine elements and processes; and mechanical equipment.

38 QUALITY ASSURANCE AND RELIABILITY 1813

Includes product sampling procedures and techniques; and quality control.

39 STRUCTURAL MECHANICS 1814

Includes structural element design and weight analysis; fatigue; and thermal stress.

For applications see *05 Aircraft Design, Testing and Performance* and *18 Spacecraft Design, Testing and Performance.*

GEOSCIENCES

Includes geosciences (general); earth resources and remote sensing; energy production and conversion; environment pollution; geophysics; meteorology and climatology; and oceanography.

For related information see also *Space Sciences.*

42 GEOSCIENCES (GENERAL) **N.A.**

43 EARTH RESOURCES AND REMOTE SENSING **1819**

Includes remote sensing of earth resources by aircraft and spacecraft; photogrammetry; and aerial photography.

For instrumentation see *35 Instrumentation and Photography.*

44 ENERGY PRODUCTION AND CONVERSION **1821**

Includes specific energy conversion systems, e.g., fuel cells; global sources of energy; geophysical conversion; and windpower.

For related information see also *07 Aircraft Propulsion and Power, 20 Spacecraft Propulsion and Power,* and *28 Propellants and Fuels.*

45 ENVIRONMENT POLLUTION **1829**

Includes atmospheric, noise, thermal, and water pollution.

46 GEOPHYSICS **1831**

Includes aeronomy; upper and lower atmosphere studies; ionospheric and magnetospheric physics; and geomagnetism.

For space radiation see *93 Space Radiation.*

47 METEOROLOGY AND CLIMATOLOGY **1843**

Includes weather forecasting and modification.

48 OCEANOGRAPHY **1848**

Includes biological, dynamic, and physical oceanography; and marine resources.

For related information see also *43 Earth Resources and Remote Sensing.*

LIFE SCIENCES

Includes life sciences (general); aerospace medicine; behavioral sciences; man/system technology and life support; and space biology.

51 LIFE SCIENCES (GENERAL) **1848**

52 AEROSPACE MEDICINE **1850**

Includes physiological factors; biological effects of radiation; and effects of weightlessness on man and animals.

53 BEHAVIORAL SCIENCES **1854**

Includes psychological factors; individual and group behavior; crew training and evaluation; and psychiatric research.

54 MAN/SYSTEM TECHNOLOGY AND LIFE SUPPORT **1855**

Includes human engineering; biotechnology; and space suits and protective clothing.

For related information see also *16 Space Transportation.*

55 SPACE BIOLOGY **N.A.**

Includes exobiology; planetary biology; and extraterrestrial life.

MATHEMATICAL AND COMPUTER SCIENCES

Includes mathematical and computer sciences (general); computer operations and hardware; computer programming and software; computer systems; cybernetics; numerical analysis; statistics and probability; systems analysis; and theoretical mathematics.

59 MATHEMATICAL AND COMPUTER SCIENCES (GENERAL) **1856**

60 COMPUTER OPERATIONS AND HARDWARE **1856**

Includes hardware for computer graphics, firmware, and data processing.

For components see *33 Electronics and Electrical Engineering.*

61 COMPUTER PROGRAMMING AND SOFTWARE **1864**

Includes computer programs, routines, algorithms, and specific applications, e.g., CAD/CAM.

62 COMPUTER SYSTEMS **1871**

Includes computer networks and special application computer systems.

63 CYBERNETICS **1873**

Includes feedback and control theory, artificial intelligence, robotics and expert systems.

For related information see also *54 Man/System Technology and Life Support.*

64 NUMERICAL ANALYSIS **1875**

Includes iteration, difference equations, and numerical approximation.

65 STATISTICS AND PROBABILITY **1879**

Includes data sampling and smoothing; Monte Carlo method; and stochastic processes.

66 SYSTEMS ANALYSIS **1879**

Includes mathematical modeling; network analysis; and operations research.

67 THEORETICAL MATHEMATICS **1880**

Includes topology and number theory.

PHYSICS

Includes physics (general); acoustics; atomic and molecular physics; nuclear and high-energy physics; optics; plasma physics; solid-state physics; and thermodynamics and statistical physics.

For related information see also *Engineering.*

70 PHYSICS (GENERAL) **1880**

For precision time and time interval (PTTI) see *35 Instrumentation and Photography;* for geophysics, astrophysics or solar physics see *46 Geophysics, 90 Astrophysics,* or *92 Solar Physics.*

71 ACOUSTICS 1881
Includes sound generation, transmission, and attenuation.
For noise pollution see *45 Environment Pollution.*

72 ATOMIC AND MOLECULAR PHYSICS 1883
Includes atomic structure, electron properties, and molecular spectra.

73 NUCLEAR AND HIGH-ENERGY PHYSICS 1886
Includes elementary and nuclear particles; and reactor theory.
For space radiation see *93 Space Radiation.*

74 OPTICS 1887
Includes light phenomena and optical devices.
For lasers see *36 Lasers and Masers.*

75 PLASMA PHYSICS 1889
Includes magnetohydrodynamics and plasma fusion.
For ionospheric plasmas see *46 Geophysics.* For space plasmas see *90 Astrophysics.*

76 SOLID-STATE PHYSICS 1892
Includes superconductivity.
For related information see also *33 Electronics and Electrical Engineering* and *36 Lasers and Masers.*

77 THERMODYNAMICS AND STATISTICAL PHYSICS 1899
Includes quantum mechanics; theoretical physics; and Bose and Fermi statistics.
For related information see also *25 Inorganic and Physical Chemistry* and *34 Fluid Mechanics and Heat Transfer.*

SOCIAL SCIENCES

Includes social sciences (general); administration and management; documentation and information science; economics and cost analysis; law, political science, and space policy; and urban technology and transportation.

80 SOCIAL SCIENCES (GENERAL) 1899
Includes educational matters.

81 ADMINISTRATION AND MANAGEMENT 1899
Includes management planning and research.

82 DOCUMENTATION AND INFORMATION SCIENCE 1900
Includes information management; information storage and retrieval technology; technical writing; graphic arts; and micrography.
For computer documentation see *61 Computer Programming and Software.*

83 ECONOMICS AND COST ANALYSIS N.A.
Includes cost effectiveness studies.

84 LAW, POLITICAL SCIENCE AND SPACE POLICY N.A.
Includes NASA appropriation hearings; aviation law; space law and policy; international law; international cooperation; and patent policy.

85 URBAN TECHNOLOGY AND TRANSPORTATION N.A.
Includes applications of space technology to urban problems; technology transfer; technology assessment; and surface and mass transportation.
For related information see *03 Air Transportation and Safety, 16 Space Transportation,* and *44 Energy Production and Conversion.*

SPACE SCIENCES

Includes space sciences (general); astronomy; astrophysics; lunar and planetary exploration; solar physics; and space radiation.
For related information see also *Geosciences.*

88 SPACE SCIENCES (GENERAL) N.A.

89 ASTRONOMY 1901
Includes radio, gamma-ray, and infrared astronomy; and astrometry.

90 ASTROPHYSICS 1902
Includes cosmology; celestial mechanics; space plasmas; and interstellar and interplanetary gases and dust.
For related information see also *75 Plasma Physics.*

91 LUNAR AND PLANETARY EXPLORATION N.A.
Includes planetology; and manned and unmanned flights.
For spacecraft design or space stations see *18 Spacecraft Design, Testing and Performance.*

92 SOLAR PHYSICS N.A.
Includes solar activity, solar flares, solar radiation and sunspots.
For related information see *93 Space Radiation.*

93 SPACE RADIATION 1903
Includes cosmic radiation; and inner and outer earth's radiation belts.
For biological effects of radiation see *52 Aerospace Medicine.* For theory see *73 Nuclear and High-Energy Physics.*

GENERAL

Includes aeronautical, astronautical, and space science related histories, biographies, and pertinent reports too broad for categorization; histories or broad overviews of NASA programs.

99 GENERAL 1903

Note: N.A. means that no abstracts were assigned to this category for this issue.

SUBJECT INDEX I-1
PERSONAL AUTHOR INDEX I-61
CORPORATE SOURCE INDEX I-69
CONTRACT NUMBER INDEX I-81
REPORT/ACCESSION NUMBER INDEX .. I-85
APPENDIX—ABOUT STAR A-1

TYPICAL CITATION AND ABSTRACT

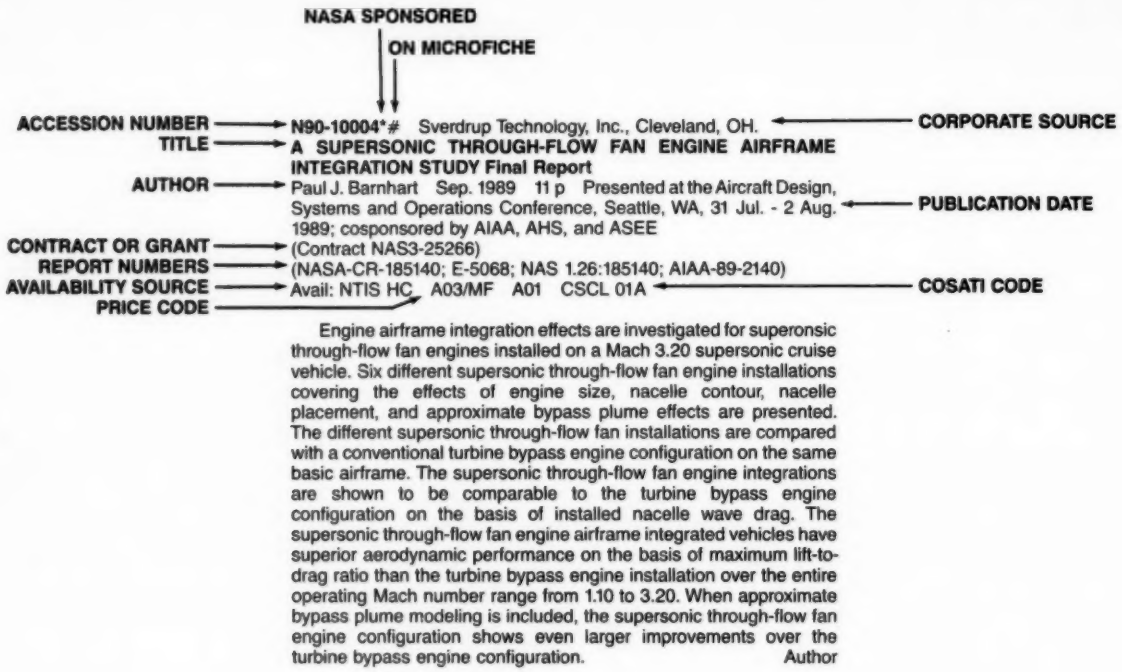
NASA SPONSORED
ON MICROFICHE
ACCESSION NUMBER
N90-10004*# Sverdrup Technology, Inc., Cleveland, OH.
CORPORATE SOURCE
TITLE
A SUPERSONIC THROUGH-FLOW FAN ENGINE AIRFRAME INTEGRATION STUDY Final Report
AUTHOR
Paul J. Barnhart Sep. 1989 11 p Presented at the Aircraft Design, Systems and Operations Conference, Seattle, WA, 31 Jul. - 2 Aug. 1989; cosponsored by AIAA, AHS, and ASEE
PUBLICATION DATE
CONTRACT OR GRANT
(Contract NAS3-25266)
REPORT NUMBERS
(NASA-CR-185140; E-5068; NAS 1.26:185140; AIAA-89-2140)
AVAILABILITY SOURCE
Avail: NTIS HC A03/MF A01 CSCL 01A
COSATI CODE
PRICE CODE
Engine airframe integration effects are investigated for superonsic through-flow fan engines installed on a Mach 3.20 supersonic cruise vehicle. Six different supersonic through-flow fan engine installations covering the effects of engine size, nacelle contour, nacelle placement, and approximate bypass plume effects are presented. The different supersonic through-flow fan installations are compared with a conventional turbine bypass engine configuration on the same basic airframe. The supersonic through-flow fan engine integrations are shown to be comparable to the turbine bypass engine configuration on the basis of installed nacelle wave drag. The supersonic through-flow fan engine airframe integrated vehicles have superior aerodynamic performance on the basis of maximum lift-to-drag ratio than the turbine bypass engine installation over the entire operating Mach number range from 1.10 to 3.20. When approximate bypass plume modeling is included, the supersonic through-flow fan engine configuration shows even larger improvements over the turbine bypass engine configuration. Author

VOLUME 28 NUMBER 13 / JULY 8, 1990

Scientific and Technical Aerospace Reports

A Semimonthly Publication of the National Aeronautics and Space Administration

01 AERONAUTICS (GENERAL)

No abstracts in this category.

02 AERODYNAMICS

Includes aerodynamics of bodies, combinations, wings, rotors, and control surfaces; and internal flow in ducts and turbomachinery.

For related information see also *34 Fluid Mechanics and Heat Transfer.*

N90-20044 Stanford Univ., CA.
COMPUTATION OF HYPERSONIC LOW DENSITY FLOWS WITH THERMOCHEMICAL NONEQUILIBRIUM Ph.D. Thesis
Tahir Goekcen 1989 128 p
Avail: Univ. Microfilms Order No. DA8925870

Recent interest in hypersonic transitional flows, transitional referring to the flow regime between continuum, and free-molecular flows, is motivated by the current and projected flight activities at high altitudes and at high speeds. A new thermochemical nonequilibrium formulation appropriate to hypersonic transitional flows of air was developed. The present nonequilibrium gas model for air consists of five chemical species: diatomic species; molecular nitrogen N2, molecular oxygen O2, nitric oxide NO, and atomic species; atomic nitrogen N and atomic oxygen O. The local thermodynamic state of the gas is described by three temperatures corresponding to three internal energy modes, i.e., translational temperature T, vibrational temperature T (sub v), and rotational temperature T (sub r). The thermal and chemical nonequilibrium processes are vibrational and rotational relaxation for the diatomic species and chemical reactions among the five chemical species. Slip and catalytic wall boundary conditions are included in the formulation. The governing partial differential equations with the proper boundary conditions are solved numerically using an implicit time marching finite volume technique. The computed results are compared with the existing Monte Carlo simulations in terms of surface quantities such as drag and heat transfer and in terms of nonequilibrium flow structure. Dissert. Abstr.

N90-20045 Florida Univ., Gainesville.
APPLICATION OF A THREE-DIMENSIONAL NAVIER-STOKES MODEL FOR A SUBSONIC JET IN A CROSSFLOW Ph.D. Thesis
Karlin Renee Roth 1988 157 p
Avail: Univ. Microfilms Order No. DA8924020

The aerodynamic/propulsive interaction between a subsonic jet exhausting perpendicularly through a flat plate into a crossflow is investigated numerically. An approximately factored, partially flux split, implicit solver for the 3-D thin layer Navier-Stokes equations is used for the computations. This algorithm is applied to flows with a range of jet to crossflow velocity ratios between 4 and 8. Both qualitative and quantitative agreement between the computed results and the existing experimental database are demonstrated. Qualitatively, all of the pertinent flow features, including the jet trajectory, the contrarotating vortex pair and the wake region near the flat plate, are captured numerically. Flow visualization of the computed results on a graphics workstation is instructive for understanding the complex interaction between the jet and the crossflowing fluid in the region near the jet exit. The computed jet centerlines deviate less than one jet diameter from the empirically predicted and experimentally located centerlines for all cases tested, including an inviscid computation. The computed velocity field is analyzed so that a direct comparison can be made with the experimentally determined properties of the contrarotating vortex pair. Good agreement between the vortex properties calculated for the simulation and the experiment is demonstrated for the most refined computations. Dissert. Abstr.

N90-20046*# National Aeronautics and Space Administration. Langley Research Center, Hampton, VA.
EXPERIMENTAL AND THEORETICAL AERODYNAMIC CHARACTERISTICS OF A HIGH-LIFT SEMISPAN WING MODEL
Zachary T. Applin and Garl L. Gentry, Jr. Washington May 1990 111 p
(NASA-TP-2990; L-16441; NAS 1.60:2990) Avail: NTIS HC A06/MF A01 CSCL 01A

Experimental and theoretical aerodynamic characteristics were compared for a high-lift, semispan wing configuration that incorporated a slightly modified version of the NASA Advanced Laminar Flow Control airfoil section. The experimental investigation was conducted in the Langley 14- by 22-Foot Subsonic Tunnel at chord Reynolds numbers of 2.36 and 3.33 million. A two-dimensional airfoil code and a three-dimensional panel code were used to obtain aerodynamic predictions. Two-dimensional data were corrected for three-dimensional effects. Comparisons between predicted and measured values were made for the cruise configuration and for various high-lift configurations. Both codes predicted lift and pitching moment coefficients that agreed well with experiment for the cruise configuration. These parameters were overpredicted for all high-lift configurations. Drag coefficient was underpredicted for all cases. Corrected two-dimensional pressure distributions typically agreed well with experiment, while the panel code overpredicted the leading-edge suction peak on the wing. One important feature missing from both of these codes was a capability for separated flow analysis. The major cause of disparity between the measured data and predictions presented herein was attributed to separated flow conditions. Author

N90-20047*# National Aeronautics and Space Administration. Langley Research Center, Hampton, VA.
USING TRANSONIC SMALL DISTURBANCE THEORY FOR PREDICTING THE AEROELASTIC STABILITY OF A FLEXIBLE WIND-TUNNEL MODEL
Walter A. Silva (Lockheed Engineering and Sciences Co., Hampton, VA.) and Robert M. Bennett Mar. 1990 13 p Presented at the AIAA 31st Structures, Structural Dynamics, and Materials Conference, Long Beach, CA, 2-4 Apr. 1990
(NASA-TM-102617; NAS 1.15:102617) Avail: NTIS HC A03/MF A01 CSCL 01A

The CAP-TSD (Computational Aeroelasticity Program - Transonic Small Disturbance) code, developed at the NASA - Langley Research Center, is applied to the Active Flexible Wing (AFW) wind tunnel model for prediction of the model's transonic

aeroelastic behavior. Static aeroelastic solutions using CAP-TSD are computed. Dynamic (flutter) analyses are then performed as perturbations about the static aeroelastic deformations of the AFW. The accuracy of the static aeroelastic procedure is investigated by comparing analytical results to those from previous AFW wind tunnel experiments. Dynamic results are presented in the form of root loci at different Mach numbers for a heavy gas and air. The resultant flutter boundaries for both gases are also presented. The effects of viscous damping and angle-of-attack, on the flutter boundary in air, are presented as well. Author

N90-20048# Boston Univ., MA.
UNSTEADY FREE-WAKE VISCOUS AERODYNAMIC ANALYSIS OF HELICOPTER ROTORS Final Report, 9 Feb. 1987 - 8 Oct. 1989
Luigi Morino, Slobodan Sipcic, and Mark Downey Nov. 1989 24 p
(Contract DAAL03-87-K-0022; ARO Proj. P-24025-EG)
(AD-A217166; ARO-24025.12-EG) Avail: NTIS HC A03/MF A01 CSCL 01/1

This report contains the results for research on unsteady free-wake viscous aerodynamic analysis of helicopter rotors. The effort may be divided into three general areas. The first deals with further developments of the zeroth-order potential-flow analysis; the second with the first-order analysis; and the third with the Poincare decomposition for the analysis of viscous flows. GRA

N90-20049*# Institute for Computer Applications in Science and Engineering, Hampton, VA.
VISCOUS SHOCK PROFILES AND PRIMITIVE FORMULATIONS Final Report
S. Karni (Cranfield Inst. of Tech., Bedford, England) Mar. 1990 25 p Submitted for publication
(Contract NAS1-18605)
(NASA-CR-182029; NAS 1.26:182029; ICASE-90-28) Avail: NTIS HC A03/MF A01 CSCL 01A

Weak solutions of hyperbolic systems in primitive (non-conservation) form for which a consistent conservation form exists are considered. It is shown that primitive formulations, shock relations are not uniquely defined by the states to either side of the shock but also depend on the viscous path connecting the two. Scheme-dependent high order correction terms are derived that enforce consistent viscous shock profiles. The resulting primitive algorithm is conservative to the order of approximation. One dimensional Euler calculations of flows containing strong shocks clearly show that conservation errors in primitive flow calculations are of comparable quality. Author

N90-20050*# Institute for Computer Applications in Science and Engineering, Hampton, VA.
SPECTRAL SIMULATION OF UNSTEADY COMPRESSIBLE FLOW PAST A CIRCULAR CYLINDER Final Report
Wai-Sun Don and David Gottlieb (Brown Univ., Providence, RI.) Apr. 1990 25 p Submitted for publication
(Contracts NAS1-18107; NAS1-18605; NAG1-703; AF-AFOSR-0303-85; NSF DMS-88-10150)
(NASA-CR-182030; NAS 1.26:182030; ICASE-90-29) Avail: NTIS HC A03/MF A01 CSCL 01A

An unsteady compressible viscous wake flow past a circular cylinder was successfully simulated using spectral methods. A new approach in using the Chebyshev collocation method for periodic problems is introduced. It was further proved that the eigenvalues associated with the differentiation matrix are purely imaginary, reflecting the periodicity of the problem. It was been shown that the solution of a model problem has exponential growth in time if improper boundary conditions are used. A characteristic boundary condition, which is based on the characteristics of the Euler equations of gas dynamics, was derived for the spectral code. The primary vortex shedding frequency computed agrees well with the results in the literature for Mach = 0.4, Re = 80. No secondary frequency is observed in the power spectrum analysis of the pressure data. Author

N90-20051*# National Aeronautics and Space Administration. Lewis Research Center, Cleveland, OH.
NUMERICAL SIMULATIONS OF SUPERSONIC FLOW THROUGH OSCILLATING CASCADE SECTIONS
Dennis L. Huff and T. S. R. Reddy (Toledo Univ., OH.) 1990 10 p Presented at the 15th Southeastern Conference on Theoretical and Applied Mechanics, Atlanta, GA, 22-23 Mar. 1990; sponsored by Georgia Inst. of Technology
(NASA-TM-103100; E-5421; NAS 1.15:103100) Avail: NTIS HC A02/MF A01 CSCL 01A

A finite difference code was developed for modeling inviscid, unsteady supersonic flow by solution of the compressible Euler equations. The code uses a deforming grid technique to capture the motion of the airfoils and can model oscillating cascades with any arbitrary interblade phase angle. A flat plate cascade is analyzed, and results are compared with results from a small perturbation theory. The results show very good agreement for both the unsteady pressure distributions and the integrated force predictions. The reason for using the numerical Euler code over a small perturbation theory is the ability to model real airfoils that have thickness and camber. Sample predictions are presented for a cascade of loaded airfoils and show appreciable differences in the unsteady surface pressure distributions when compared with the flat plate results. Author

N90-20052*# Stanford Univ., CA. Dept. of Aeronautics and Astronautics.
TRANSPIRATION COOLING IN HYPERSONIC FLIGHT
Domingo Tavella and Leonard Roberts Jun. 1989 31 p
(Contract NCC2-543)
(NASA-CR-186435; NAS 1.26:186435; SU-JIAA-TR-92) Avail: NTIS HC A03/MF A01 CSCL 01A

A preliminary numerical study of transpiration cooling applied to a hypersonic configuration is presented. Air transpiration is applied to the NASA all-body configuration flying at an altitude of 30500 m with a Mach number of 10.3. It was found that the amount of heat disposal by convection is determined primarily by the local geometry of the aircraft for moderate rates of transpiration. This property implies that different areas of the aircraft where transpiration occurs interact weakly with each other. A methodology for quick assessments of the transpiration requirements for a given flight configuration is presented. Author

N90-20053# Computational Mechanics Co., Austin, TX.
ANALYSIS OF FLOW-, THERMAL-, AND STRUCTURAL-INTERACTION OF HYPERSONIC STRUCTURES SUBJECTED TO SEVERE AERODYNAMIC HEATING Annual Technical Report No. 2, 1 Nov. 1988 - 1 Nov. 1989
30 Nov. 1989 109 p
(Contract F49620-88-CK-0001; AF Proj. 2302)
(AD-A217882; TR-89-15; AFOSR-90-0050TR) Avail: NTIS HC A06/MF A01 CSCL 01/1

Over the past two years a unique collection of algorithms have been developed for the analysis of hypersonic structures subjected to severe aerodynamic heating. These algorithms employ adaptive computational methods to resolve many of the complex structural and flow features such as nonelastic, large, time dependent structural deformations, shock interaction boundary layers and shock interactions. Local error estimates were used to evaluate the quality of the computed solutions and subsequently optimize the structure of the grids to deliver a specified level of accuracy with a minimum of computational effort. In addition, implicit/explicit solution algorithms for the fluid modeling were employed which exploit the speed and simplicity of explicit methods and the stability of implicit methods. Zoning techniques for automatically selecting the implicit and explicit zones were studied with optimization of the computational effort as the central goal. The modeling of the structural problems incorporated a version of the Bodner-Partom constitutive model for time dependent viscoplastic materials. This model was extended to include a damage parameter which was treated as an additional internal state variable. A number of validation cases were run to test the

various components of the package and prepare for the experimental verification which was planned for year three. GRA

03 AIR TRANSPORTATION AND SAFETY

Includes passenger and cargo air transport operations; and aircraft accidents.

For related information see also *16 Space Transportation* and *85 Urban Technology and Transportation.*

N90-20054# Advisory Group for Aerospace Research and Development, Neuilly-Sur-Seine (France). Aerospace Medical Panel.

IMPLICATIONS OF ADVANCED TECHNOLOGIES FOR AIR AND SPACECRAFT ESCAPE

Feb. 1990 108 p In ENGLISH and FRENCH Symposium held in Munich, Fed. Republic of Germany, 24-28 Apr. 1989 (AGARD-CP-472; ISBN-92-835-0539-5) Copyright Avail: NTIS HC A06/MF A01; Non-NATO Nationals requests available only from AGARD/Scientific Publications Executive

With reduction of escape fatalities or injuries and improvement of out-of-the envelope ejection safety as primary goals, this Symposium addressed the latest technological advances in all areas which affect overall escape system performance and capabilities. Escapes from hypersonic vehicles and spacecraft were also considered. For individual titles, see N90-20055 through N90-20066.

N90-20055# Aerospace Medical Research Labs., Wright-Patterson AFB, OH. Human Systems Div.

DEVELOPMENT OF ACCELERATION EXPOSURE LIMITS FOR ADVANCED ESCAPE SYSTEMS **c54**

James W. Brinkley, Lawrence J. Specker, and Stephen E. Mosher (DynCorp., Wright-Patterson AFB, OH.) *In* AGARD, Implications of Advanced Technologies for Air and Spacecraft Escape Feb. 1990 14 p (For primary document see N90-20054 13-03)

Copyright Avail: NTIS HC A06/MF A01; Non-NATO Nationals requests available only from AGARD/Scientific Publications Executive

Transient and angular accelerations significantly affect aircrew safety during emergency escape from aerospace vehicles. However, due to the scarcity of laboratory data on the response of the human body to transient, multiaxial acceleration, criteria for design and evaluation of escape systems were restricted to relatively simplistic limits of acceleration magnitude and rate of acceleration onset for acceleration vectors acting in three orthogonal axes, with the exception of the foot-to-head direction (+Z axis). Mathematical models were only used to assess the probability of injury for acceleration acting in the +Z axis. Limits were not specified for angular acceleration. The United States Air Force is currently engaged in an advanced development program to demonstrate the feasibility of three-dimensional thrust-vector control to provide ejection seat attitude control and trajectory steering. This program has served to stimulate the development of more comprehensive design and evaluation criteria to assure that the thrust-vector control system functions without causing an unacceptable risk of injury to the escape system occupant. A method was developed to limit acceleration exposure on the basis of the computed responses of three orthogonal dynamic models. The method was initially developed using existing data from tests with human subjects and experience with operational escape systems. More extensive research is now ongoing to evaluate and improve the method. Impact experiments with volunteers were accomplished to more precisely define the properties of the dynamic response models. Escape system test data were analyzed, including measurements of linear acceleration and angular velocity. The acceleration exposure limit method is described, the results of recent impact tests accomplished with volunteers provided, and revised dynamic response model coefficients derived from the results of these tests. Recent applications of the acceleration exposure method include evaluation of the performance of the ACES II ejection seat, development of the CREST advanced escape system technologies demonstrator, and study of crew escape systems for hypersonic flight vehicles. Author

N90-20056# Laboratoire de Medecine Aerospatiale, Bretigny-sur-Orge (France).

PARACHUTE OPENING SHOCKS DURING HIGH SPEED EJECTIONS: NORMALIZATION [CHOCS A L'OUVERTURE LORS DES EJECTIONS A GRANDE VITESSE? QUELLES NORMES?] **c05**

A. Leger, P. Dolou, P. Sandor, and P. Beaudouin (Service Technique des Programmes Aeronautiques, Paris, France) *In* AGARD, Implications of Advanced Technologies for Air and Spacecraft Escape Feb. 1990 7 p In FRENCH (For primary document see N90-20054 13-03)

Copyright Avail: NTIS HC A06/MF A01; Non-NATO Nationals requests available only from AGARD/Scientific Publications Executive

Conditions which evolve during combat flight leads to the consideration of the probability of pilot ejection at low altitude high speed flight. Problems associated with wind blast and the stability of the ejection seat could lead to the risk of injury connected to parachute opening. A study demonstrating the compatibility of the MK 10 seat ejection with different combat aircraft was carried out by testing on a dynamic rail. The results show a significant increase in recorded G(z) acceleration during the opening of the main parachute. A biomechanical analysis of the shocks shows the role played by different phases during the opening. These data are given so that the normalization problem and useful criteria can be considered. Author

N90-20057# Institute of Aviation Medicine, Farnborough (England).

DEVELOPMENT OF AN EJECTION SEAT SPECIFICATION FOR A NEW FIGHTER AIRCRAFT

D. J. Anton *In* AGARD, Implications of Advanced Technologies for Air and Spacecraft Escape Feb. 1990 7 p (For primary document see N90-20054 13-03)

Copyright Avail: NTIS HC A06/MF A01; Non-NATO Nationals requests available only from AGARD/Scientific Publications Executive

The development of a new aircraft brings with it the opportunity to incorporate improvements, and new features, in the design of the escape system that experience with previous systems has shown to be necessary. Just such an opportunity occurred with the announcement of the development of the European Fighter Aircraft. The United Kingdom input to the specification of the ejection seat for this aircraft was derived from accident experience and from analysis of ejection test data from previous marks of ejection seat. The aim is to discuss the problem of impairment of consciousness on ejection, the rationale for improvements in ejection seat stability, and measures taken to improve ejection seat headbox impact attenuation. Author

N90-20058# Royal Aerospace Establishment, Farnborough (England).

ESCAPE SYSTEMS RESEARCH AT RAE

D. J. Gilson *In* AGARD, Implications of Advanced Technologies for Air and Spacecraft Escape Feb. 1990 15 p (For primary document see N90-20054 13-03)

Copyright Avail: NTIS HC A06/MF A01; Non-NATO Nationals requests available only from AGARD/Scientific Publications Executive

A range of recent topics in the escape systems research program at the Establishment is described. Prominent among these is the computer simulation of ejection seat dynamics which enables prediction of the behavior of escape systems in different conditions, and complements the experimental methods of investigation. Other topics described include passive methods of seat stabilization using plates to supplement a bridle-mounted drogue, use of a reefed drogue to improve deceleration characteristics, consideration of some methods of deceleration, and use of inflatable restraint devices. Electronic sequencer developments are described, leading

to provision of a high capacity, high reliability sequencer for trials use. A Biodynamic modeling and dummy development are considered. Author

N90-20059# Martin-Baker Aircraft Co. Ltd., Denham (England).
FIGHTER ESCAPE SYSTEM: THE NEXT STEP FORWARD
B. A. Miller *In* AGARD, Implications of Advanced Technologies for Air and Spacecraft Escape Feb. 1990 6 p (For primary document see N90-20054 13-03)
Copyright Avail: NTIS HC A06/MF A01; Non-NATO Nationals requests available only from AGARD/Scientific Publications Executive

Ejection seats have become increasingly complex, heavier and bulkier in recent years. This growth in response to the increasing demands for greater performance, under more severe conditions. It is also due to the relocation onto the seat of equipment which was previously aircraft mounted such as anti-g valve, oxygen regulator, NBC equipment, and OBOGS auxiliary oxygen equipment. In the Tornado, the Mk10A ejection seat even gained outlets for the cabin conditioning system, becoming the world's first air conditioned ejection seat. This trend has persisted for some 15 years, but now new design derivers are becoming dominant with an increasing and urgent need for lightweight and low cost. The Martin-Baker developments of the past 15 years are briefly reviewed and the new trends which are shaping future Fighter Escape Systems discussed. Author

N90-20060# Douglas Aircraft Co., Inc., Long Beach, CA.
POTENTIAL ROLE OF AVIONICS IN ESCAPE SYSTEMS
James J. Schoen *In* AGARD, Implications of Advanced Technologies for Air and Spacecraft Escape Feb. 1990 4 p (For primary document see N90-20054 13-03)
Copyright Avail: NTIS HC A06/MF A01; Non-NATO Nationals requests available only from AGARD/Scientific Publications Executive

The role of avionics in escape systems for high-performance aircraft is rapidly expanding. In the most advanced systems currently in service, an electronic controller, in conjunction with mechanical sensors, selects the recovery sequence and controls event timing. More advanced avionics systems under development feature improved microprocessors and solid-state sensors. These slightly improve performance by modifying system timing based on airspeed and altitude conditions. They also introduce desirable black-box features such as built-in-test and fault isolation. Avionics has the potential to contribute far more to escape systems based on the current development of controllable propulsion systems. Typically these systems would consist of multiple rocket engines under the command of a microprocessor/controller. The controllable propulsion system would control attitude and would also control the acceleration forces on the crew member. The avionics system would therefore include attitude and acceleration sensors. In smarter systems,the propulsion system could be used to control the escape trajectory for ground avoidance or to reduce forces on the crew member in an escape under benign conditions. Thus, the avionics system may include ground direction and proximity sensors. Real-time control of an escape system vehicle under the dynamic conditions associated with high airspeed or rapid maneuvering requires a comprehensive avionics system with high-frequency response. However, the technology is available, and this type of system could be a basic feature of any next-generation escape system. Author

N90-20061# German Air Force, Fuerstenfeldbruk (Germany, F.R.). Inst. of Aerospace Medicine.
EJECTION SEAT TRAINING OF JET PILOTS AND WEAPON SYSTEM OFFICERS AT THE GERMAN AIR FORCE SCHOOL OF AVIATION MEDICINE
R. O. Amendt *In* AGARD, Implications of Advanced Technologies for Air and Spacecraft Escape Feb. 1990 2 p (For primary document see N90-20054 13-03)
Copyright Avail: NTIS HC A06/MF A01; Non-NATO Nationals requests available only from AGARD/Scientific Publications Executive

Ejection seat systems have been in use since World War II in most jet aircraft in Air Forces all over the world and nowadays have reached a high technical performance standard. There is no doubt that any escape system can only be as efficient as its operator and user and how he knows and correctly applies it within the system performance limits. For these reasons academic and practical training of pilots and weapon system officers in two-seater aircraft has become mandatory. The objectives of this training are as follows: inform the pilot about the physical stress on his body during ejection from aircraft in order to safe his life and avoid injuries; drill safe operating procedures of the respective escape system so they become routine and instinctive, emphasizing what can happen if the system is not used correctly or in good time; and eliminate the psychological threshold to actually get out of the protecting cockpit in case of emergency simply by having already practiced this situation in a simulator. The primary objective with this new device was to simulate ejection from the aircraft as realistic as possible under training conditions on the ground. The new training device and some first experiences with it are described. Author

N90-20062# Aerospace Medical Research Labs., Wright-Patterson AFB, OH. Biodynamics and Bioengineering Div.
THE USAF ADVANCED DYNAMIC ANTHROPOMORPHIC MANIKIN (ADAM) **c54**
Roy R. Rasmussen and Ints Kaleps *In* AGARD, Implications of Advanced Technologies for Air and Spacecraft Escape Feb. 1990 7 p (For primary document see N90-20054 13-03)
Copyright Avail: NTIS HC A06/MF A01; Non-NATO Nationals requests available only from AGARD/Scientific Publications Executive

Ejection from aircraft at high speeds poses severe injury hazards to the crewmember. As performance characteristics of aircraft are further improved, the protection capabilities of ejection systems must also be improved to assure the safety of the crewmember. The demonstration of these ejection system improvements requires extensive testing with manikins to effectively evaluate the performance of the ejection seat and assess the injury potential to the crewmember. The United States Air Force (USAF) has embarked on a new effort to design and develop an Advanced Dynamic Anthropomorphic Manikin (ADAM) with improved human-like fidelity and data collection capability over currently available escape system testing manikins. This effort has resulted in the development and fabrication of two prototype (one small and one large) instrumented, anthropomorphic manikins for testing and evaluation and the production of ten manikins to be used in ejection and other protection system testing. Discussed will be the design objectives and resulting features of ADAM and a summary of testing results for exposure to extreme temperature and humidity environments; Gz low level vibration; and Gx, Gy and Gz whole body impacts. Author

N90-20063# Aerospace Medical Research Labs., Wright-Patterson AFB, OH. Human Systems Div.
WINDBLAST PROTECTION FOR ADVANCED EJECTION SEATS
Lawrence J. Specker and James W. Brinkley *In* AGARD, Implications of Advanced Technologies for Air and Spacecraft Escape Feb. 1990 11 p (For primary document see N90-20054 13-03)
Copyright Avail: NTIS HC A06/MF A01; Non-NATO Nationals requests available only from AGARD/Scientific Publications Executive

The United States Air Force is currently engaged in an advanced development program to demonstrate the feasibility of extending the capability of open ejection seats to 700 KEAS. The probability of injury at this airspeed is estimated to be 100 percent, based on the current injury statistics. Past approaches to windblast protection have involved the use of harnesses and limb tethers which have proved to be unacceptable to pilots. Therefore, advanced unencumbering techniques are required to provide the needed protection. The USAF has developed and tested a windblast protection concept that utilizes high-strength, deployable

fabric panels. The panels capture and slow the aerodynamic flow impinging on the ejection seat occupant's extremities and torso and reduce the probability of windblast induced flail injury. Wind tunnel tests were conducted in low- and high-speed wind tunnels using one-half scale models of a fiftieth percentile crewman and ejection seat as well as full-scale manikins and modified ACES 2 ejection seats equipped with the flow-stagnation panels. The tests were accomplished to determine the degree of protection for the crewmember, the influence of the flow-stagnation panels on ejection seat aerodynamics, and the effects of design changes to the panel shape and material. The wind tunnel tests have demonstrated the protective potential of the flow-stagnation concept, but classical aerodynamic and windblast tests have indicated the configuration of the panels is critical to the protection of the crewmember's head. Configuration of the panels is also critical for the reduction of the total loads acting on the crewmember and seat combination. Without passive aerodynamic reduction of the forces and moments, a larger catapult and stabilization system thrust must be used to maintain stabilized flight through the ejection sequence. An overview of the flow-stagnation windblast protection system tests, the implications of its use and required future tests are discussed. Author

N90-20064# Douglas Aircraft Co., Inc., Long Beach, CA.
CONTROLLABLE PROPULSION FOR ESCAPE SYSTEMS CONTROL
A. Blair McDonald *In* AGARD, Implications of Advanced Technologies for Air and Spacecraft Escape Feb. 1990 6 p (For primary document see N90-20054 13-03)
Copyright Avail: NTIS HC A06/MF A01; Non-NATO Nationals requests available only from AGARD/Scientific Publications Executive

Current escape systems for military aircraft use solid-grain rockets for propulsion. These provide a fixed level of thrust for a fixed period of time. Since the escape system has no function over a wide range of conditions, this approach is a compromise. Significant improvements in escape capability could be achieved by introducing a propulsion system in which the thrust-time profile could be varied to suit the circumstances of each emergency. The technology now exists to introduce a fully controllable propulsion system. Such a system would not only provide a variable thrust-time profile but would also permit the propulsion system to provide stabilization, to control the forces applied to the crew member, and to control the escape trajectory. These capabilities would allow improved system operation throughout an expanded escape envelope. The technology for a fully controllable propulsion system was already demonstrated in a development program. Author

N90-20065# Avions Marcel Dassault-Breguet Aviation, Saint-Cloud (France).
REQUIREMENTS FOR PROTECTIVE PRESSURE SUITS FOR THE HERMES SPACECREW [EXIGENCES DU SCAPHANDRE DE PROTECTION DE L'EQUIPAGE D'HERMES]
L. Simionesco and C. Fagot *In* AGARD, Implications of Advanced Technologies for Air and Spacecraft Escape Feb. 1990 10 p In FRENCH (For primary document see N90-20054 13-03)
Copyright Avail: NTIS HC A06/MF A01; Non-NATO Nationals requests available only from AGARD/Scientific Publications Executive

In its present configuration, the Hermes space plane is equipped with a pressurized ejection capsule designed to assure crew protection during the critical phases of both launching and atmospheric reentry. The capability of operating in large areas (up to M = 7, Z = 60 km) is required of the launcher. The capsule provides the 3 man space crew the physical protection necessary during ejection in either landing or splashdown. The fear of accidental loss of pressure in the Hermes cabin requires the crew to be equipped with individual protective pressure suits. From analyses of missions and results, the functions of the pressure suits are described, and the physical limits and operating constraints are proven. The pressure suit systems can be integrated with the space plane. Of concern is the resolution of the insertion interface procedures used in mission rescue scenarios and emergencies. Author

N90-20066# Martin-Baker Aircraft Co. Ltd., Denham (England).
SPACECRAFT ESCAPE **c18**
B. A. Miller *In* AGARD, Implications of Advanced Technologies for Air and Spacecraft Escape Feb. 1990 7 p (For primary document see N90-20054 13-03)
Copyright Avail: NTIS HC A06/MF A01; Non-NATO Nationals requests available only from AGARD/Scientific Publications Executive

The currently preferred option from among the designs so far studied are described. Alternatives for seat design will still be studied to identify systems which offer the best possible approach with minimum design risk. Martin-Baker will continue to study the overall design and also initiate more detailed studies of the main elements, such as drogue stabilization, temperature extremes protection, and rocket motor thrust vectoring. The study of program management and the testing and qualification of such a system will also be initiated. It is already apparent that the test program would, at some point, require testing of the seat under actual conditions, if the required level of confidence is to be achieved. The Hermes Management Team are meeting the crew safety challenge by initiating and funding wide ranging feasibility studies. They are placing equal emphasis on the Crew Escape Module concept and this study is also most promising. Hermes has the enormous advantage of hindsight which, we all know is perfect, and this valuable experience is being put to good use. This is believed to be pioneering work, whether by CEM or encapsulated ejection seats can provide an effective and efficient means of safe crew escape. Such a valuable prize will however not be obtained without continuing to commit the necessary resources and dedication. Author

N90-20067# Ministerie van Verkeer en Waterstaat, 's-Gravenhage (Netherlands).
[ACTIVITIES REPORT IN CIVIL AVIATION] Annual Report, 1987 [RIJKSLUCHTVAARTDIENST: JAARVERSLAG 1987]
1987 55 p In DUTCH
(ETN-90-95471) Avail: NTIS HC A04/MF A01

The activities in the fields of airworthiness, airports, air traffic policy, and flight safety are reported. The activities of the civil aviation school, the national aeronautics and astronautics museum Aviodome, and the national aeronautics and astronautics laboratory are presented. The economic significance of the Dutch aviation sector is discussed. The type specification of the Fokker 100 is outlined. ESA

N90-20068*# National Aeronautics and Space Administration. Langley Research Center, Hampton, VA.
A REVIEW OF THE ANALYTICAL SIMULATION OF AIRCRAFT CRASH DYNAMICS
Edwin L. Fasanella, Huey D. Carden, Richard L. Boitnott (Army Aviation Systems Command, Hampton, VA.), and Robert J. Hayduk Jan. 1990 25 p
(NASA-TM-102595; NAS 1.15:102595) Avail: NTIS HC A03/MF A01 CSCL 01C

A large number of full scale tests of general aviation aircraft, helicopters, and one unique air-to-ground controlled impact of a transport aircraft were performed. Additionally, research was also conducted on seat dynamic performance, load-limiting seats, load limiting subfloor designs, and emergency-locator-transmitters (ELTs). Computer programs were developed to provide designers with methods for predicting accelerations, velocities, and displacements of collapsing structure and for estimating the human response to crash loads. The results of full scale aircraft and component tests were used to verify and guide the development of analytical simulation tools and to demonstrate impact load attenuating concepts. Analytical simulation of metal and composite aircraft crash dynamics are addressed. Finite element models are examined to determine their degree of corroboration by

experimental data and to reveal deficiencies requiring further development. Author

N90-20069# Dayton Univ., OH. Research Inst.
FULL-SCALE BIRDSTRIKE TESTING OF IN-SERVICE AGED F-111 ADBIRT WINDSHIELD TRANSPARENCIES Interim Report, May 1985 - Nov. 1987
Daniel R. Bowman, Gregory J. Stenger, and Blaine S. West Aug. 1989 297 p
(Contract F33615-84-C-3404; AF Proj. 1926)
(AD-A218035; UDR-TR-88-39; WRDC-TR-89-3075) Avail: NTIS HC A13/MF A02 CSCL 01/2

A test program consisting of 22 full scale birdstrike tests of F-111 ADBIRT windshield transparencies was conducted. Test hardware was developed to simulate flight structure, and four pound artificial birds were used to impact the transparencies at the most critical location, the upper inboard corner. Testing was completed on windshield panels ranging from unaged baseline windshields to windshields which had been in service for more than five years. The structural integrity of F-111 ADBIRT windshield transparencies was found to be significantly reduced by in-service aging. GRA

04 AIRCRAFT COMMUNICATIONS AND NAVIGATION

Includes digital and voice communication with aircraft; air navigation systems (satellite and ground based); and air traffic control.

For related information see also *17 Space Communications, Spacecraft Communications, Command and Tracking* and *Communications and Radar.*

No abstracts in this category.

05 AIRCRAFT DESIGN, TESTING AND PERFORMANCE

Includes aircraft simulation technology.

For related information see also *18 Spacecraft Design, Testing and Performance* and *39 Structural Mechanics.* For land transportation vehicles see *85 Urban Technology and Transportation.*

N90-20070 Maryland Univ., College Park.
AEROELASTIC CHARACTERISTICS OF AIRCRAFT WITH CIRCULATION CONTROL WINGS Ph.D. Thesis
David Joseph Haas 1989 159 p
Avail: Univ. Microfilms Order No. DA8924160

The aeroelastic characteristics of high aspect ratio circulation control (CC) wings cantilevered at the root and attached to a free flying aircraft are investigated. Several analytical models are developed with varying degree of complexity. First, a cantilevered CC wing is examined. Static divergence and a circulation control reversal phenomenon are investigated through the use of lift and control effectiveness ratios. The flutter instability is analyzed using an elastic beam model in conjunction with a modified strip analysis method based on classical unsteady airfoil theory. Then, aeroelastic stability of a free flying aircraft with rigid body pitch and plunge motions is examined using the finite element method. For this, unsteady aerodynamic loads are calculated using a time domain, unsteady aerodynamic model based on the indicial response method. Steady experimental circulation control airfoil data are used to determine the airfoil lift curve slope and aerodynamic center location as a function of angle of attack, blowing level, and Mach number. The effects of several design parameters on aeroelastic stability are examined including; wing sweep angle, elastic axis location, wing torsion and bending stiffness, fuselage inertia, blowing level, and span-wise blowing distribution. Loss of control effectiveness was found to be critical on the aft-swept wing. A low speed flutter instability, unique to wings employing circulation control blowing, was identified. Dissert. Abstr.

N90-20071*# National Aeronautics and Space Administration. Langley Research Center, Hampton, VA.
THE APPLICATION OF ACTIVE CONTROLS TECHNOLOGY TO A GENERIC HYPERSONIC AIRCRAFT CONFIGURATION
M. G. Gilbert, J. Heeg, A. S. Pototzky, C. V. Spain, D. L. Soistmann (Lockheed Engineering and Sciences Co., Hampton, VA.), and H. J. Dunn Jan. 1990 16 p Presented at the 7th National Aero-Space Plane Technology Symposium, Cleveland, OH, Oct. 1989
(NASA-TM-101689; NAS 1.15:101689) Avail: NTIS HC A03/MF A01 CSCL 01C

Analytical methods are described for the prediction of aerothermoelastic stability of hypersonic aircraft including active control systems. Thermal loads due to aerodynamic heating were applied to the finite element model of the aircraft structure and the thermal effects on flutter were determined. An iterative static aeroelastic trim analysis procedure was developed including thermal effects. And active control technology was assessed for flutter suppression, ride quality improvement, and gust load alleviation to overcome any potential adverse aeroelastic stability or response problems due to aerodynamic heating. A generic hypersonic aircraft configuration was selected which incorporates wing flaps, ailerons, and all moveable fins to be used for active control purposes. The active control system would use onboard sensors in a feedback loop through the aircraft flight control computers to move the surfaces for improved structural dynamic response as the aircraft encounters atmospheric turbulence. Author

N90-20072# Federal Aviation Administration, Atlantic City, NJ. Technical Center.
FLOOR PULL TEST OF A TRANSPORT AIRFRAME SECTION
Dick Johnson and Anthony Wilson Dec. 1989 71 p
(DOT/FAA/CT-TN88/14) Avail: NTIS HC A04/MF A01

An 8-foot length of a transport airplane airframe and cabin floor structure, located at the Federal Aviation Administration Technical Center, was statically pull tested to failure. Two tests were conducted and consisted of vertically loading the floor structure in an upward direction at both the four and two intersecting seat track/floor beam locations, respectively. This test procedure was used to simulate the magnitude and direction of external loads that could be applied to the floor track by an aft seat leg fitting during a longitudinal impact occurrence. Floor load, deflection, and strain data were obtained for each of the two loading conditions. The first test, which involved the uniform loading of a center position floor beam and related floor track structure at four track locations (body station 540), resulted in the failure of track and floor beam under a maximum beam failure load of 21,859 pounds. The second test condition, involving a subsequent loading of the same beam but at only two track locations (with the remaining half of beam restrained), resulted in track failure at a maximum load of 14,169 pounds. These failure loads were within 20 percent of those identified under a prior analytical analysis of the fuselage/floor structure. Dissert. Abstr.

N90-20073# Air Force Inst. of Tech., Wright-Patterson AFB, OH. School of Engineering.
F-15B HIGH ANGLE-OF-ATTACK PHENOMENA AND SPIN PREDICTION USING BIFURCATION ANALYSIS M.S. Thesis
Daniel D. Baumann Dec. 1989 143 p
(AD-A217366; AFIT/GAE/ENY/89D-01) Avail: NTIS HC A07/MF A01 CSCL 01/1

Modern fighter aircraft are being designed to be operated at higher and higher angles-of-attack. The resulting increase in maneuverability is offset however by an increase in susceptibility to departure from controlled flight. An investigation of the F-15B fighter aircraft was undertaken to predict high angle-of-attack phenomena such as flat spins. Aerodynamic forces and moments as a function of control surface deflections were modeled over a

wide angle-of-attack range (-20 deg less than or equal to alpha less than or equal to +90 deg) and were then used to formulate a non-linear eight state (alpha, beta, p, q, r, Theta, Psi, V) aircraft model. Equilibrium and periodic solutions to the resulting equations of motion were then computed using a bifurcation analysis package. A number of bifurcation points, limit points and Hopf bifurcation points were detected indicating changes in flight stability. Several stable equilibrium solution branches at angles-of-attack greater than 70 degrees were observed which correspond to flat spin behavior. Theoretically predicted flat spin conditions correlated well with empirical flight test data. In addition stable equilibrium and periodic surveyed resulting in a global map of stability as a function of control surface deflection for the F-15B. GRA

N90-20074# Oklahoma Univ., Norman.
HYPERSONIC WAVERIDER CONFIGURATIONS FOR TRANS-ATMOSPHERIC VEHICLES M.S. Thesis
William P. Martin 1989 197 p Sponsored by AFIT, Wright-Patterson AFB, OH
(AD-A217925; AFIT/CI/CIA-89-105) Avail: NTIS HC A09/MF A02 CSCL 01/3

The development of a catalogue of waverider shapes generated from axisymmetric conical flow is described. A simple but reliable method of calculating the viscous drag is presented and over one-hundred configurations are shown with various aerodynamic and pertinent geometric design factors. All of the configurations presented are based on Mach number of 10 and Reynolds number (based on the length of the waverider) of 10 to the 6th power. However, the analysis presented adapts itself to any Mach or Reynolds number. The lift-to-drag ratios presented range from 4.32 to 5.06 while the average skin friction coefficient ranged from 0.00176 to 0.00205. The volume to area ratio V2/3/S(p) ranged from 0.224 to 0.153. GRA

N90-20075# Texas A&M Univ., College Station.
A VIDEO-BASED EXPERIMENTAL INVESTIGATION OF WING ROCK Ph.D. Thesis
Steven Lynn Morris 1989 261 p
(Contract F49620-87-C-0069)
(AD-A218244; AD-E501191; AFIT/CI/CIA-89-148) Avail: NTIS HC A12/MF A02 CSCL 01/1

This research developed a definitive theory on the cause of wing rock. The study was based on dynamic measurements in both a water tunnel and a wind tunnel on a sharp edged delta wing with an 80 deg. leading edge sweep angle. Experimental data were compared with analytical results from a mathematical model and a fourth order Runge-Kutta integration. In the water tunnel tests, conducted at alpha = 35 deg. and Reynolds numbers from 30000/ft to 75000/ft, the movement of the leading edge vortices and the model motion were simultaneously tracked and analyzed using a video-based motion analysis system, ExpertVision. ExpertVision accuracy was validated using stationary and forced oscillation tests on 70 and 80 deg. delta wings. Vortex trajectory, core velocity, and burst point results from stationary tests were in good agreement with published data. Forced oscillation tests proved that ExpertVision could simultaneously track and analyze the movement of leading edge vortices and model motion. Wing rock is caused by the dynamic behavior of the leading edge vortices. The alternate lift-off and reattachment of the vortices generate an asymmetry in vortex lift and cause changes in rolling moment that initiate and sustain roll oscillations. Wing rock dynamics were significantly different water tunnel and wind tunnel experiments. Apparent mass terms must be included in the equations of motion when converting water tunnel acceleration data to rolling moment coefficients. GRA

N90-20076# Army Aviation Engineering Flight Activity, Edwards AFB, CA.
AIRWORTHINESS AND FLIGHT CHARACTERISTICS EVALUATION OF THE MCDONNELL DOUGLAS HELICOPTER CORPORATION (MDHC) 530FF HELICOPTER Final Report, Aug. 1987 - Sep. 1988
James L. Webre, William Y. Abbott, Michael White, William Stormer, and Warren Gould May 1989 299 p Sponsored by Army Aviation Systems Command, Saint Louis, MO
(AD-A218253; USAAEFA-86-15) Avail: NTIS HC A13/MF A02 CSCL 01/3

An Airworthiness and Flight Characteristics Evaluation of the McDonnell Douglas 530FF helicopter (also known as the AH-6G or MH-6H) was performed. The test consumed 94 productive flight test hours in 152 total hours. Many configurations were flown at gross weights up to 3950 pounds. Three deficiencies related to the handling qualities, and one related to the inability to observe a sideslip/tail rotor flapping limit were identified. Twelve shortcomings were also identified. GRA

N90-20077# Naval Postgraduate School, Monterey, CA.
AERODYNAMIC ANALYSIS OF A US NAVY AND MARINE CORPS UNMANNED AIR VEHICLE M.S. Thesis
Daniel F. Lyons Jun. 1989 204 p
(AD-A218282) Avail: NTIS HC A10/MF A02 CSCL 01/3

An aerodynamic analysis was performed on a U.S. Navy and Marine Corps Unmanned Air Vehicle (UAV) called PIONEER. A low-order panel method called PMARC (Panel Method Ames Research Center) was used to obtain various aerodynamic parameters and to evaluate the longitudinal and directional stability and control of the vehicle. In addition, a drag analysis of the vehicle was performed using techniques described in Fluid Dynamic Drag by Hoerner. Drag reduction methods were also investigated. The neutral point of the large tail PIONEER was calculated to be at 74 percent of the mean aerodynamic chord (MAC). The small tail neutral point was calculated to be at the 51 percent MAC position. Cross wind limitations were obtained for PIONEER. The maximum sideslip angles due to cross wind were determined to be 8.5 and 18. For an approach speed of 65 knots, cross wind limits were calculated to be ten knots and 22 knots for the single rubber and dual rudder cases, respectively. Drag polars were plotted for PIONEER. It was determined that drag on the vehicle could be reduced by 29 percent using simple and cost effective modifications to the vehicle. Follow-on analysis of PIONEER through the Naval Postgraduate School UAV Flight Test Research Program and through full-scale wind tunnel testing at the National Full-Scale Aerodynamics Complex were also discussed. GRA

N90-20078* National Aeronautics and Space Administration. Langley Research Center, Hampton, VA.
COMPRESSION PYLON Patent
James C. Patterson, Jr., inventor (to NASA) 19 Sep. 1989 10 p Filed 23 Jun. 1988
(NASA-Case-LAR-13777-1; US-Patent-4,867,394;
US-Patent-Appl-SN-210480; US-Patent-Class-244-54;
US-Patent-Class-244-55; US-Patent-Class-244-130) Avail: US Patent and Trademark Office CSCL 01C

A compression pylon for an aircraft with a wing-mounted engine, that does not cause supersonic airflow to occur within the fuselage-wing-pylon-nacelle channel is presented. The chord length of the pylon is greater than the local chord length of the wing to which it is attached. The maximum thickness of the pylon occurs at a point corresponding to the local trailing edge of the wing. As a result, the airflow through the channel never reaches supersonic velocities.

Official Gazette of the U.S. Patent and Trademark Office

N90-20079* National Aeronautics and Space Administration. Langley Research Center, Hampton, VA.
PASSIVE VENTING TECHNIQUE FOR SHALLOW CAVITIES Patent
Robert L. Stallings, Jr., inventor (to NASA) and Floyd J. Wilcox, Jr., inventor (to NASA) 30 Sep. 1988 5 p Filed 30 Sep. 1988
(NASA-Case-LAR-14031-1; US-Patent-4,863,118;
US-Patent-Appl-SN-252081; US-Patent-Class-244-130;
US-Patent-Class-244-137.4) Avail: US Patent and Trademark Office CSCL 01C

A device is introduced for reducing drag and store separation difficulties caused by shallow cavities on aircraft in supersonic flight consisting of a group of hollow pipes the same length as

the cavity. The pipes are attached to the cavity floor so as to allow air to flow through the pipes. This device allows air to flow through the pipes opposite to the direction of flow outside the pipes. This results in reduced drag and improved store separation characteristics.

Official Gazette of the U.S. Patent and Trademark Office

N90-20056# Laboratoire de Medecine Aerospatiale, Bretigny-sur-Orge (France).
PARACHUTE OPENING SHOCKS DURING HIGH SPEED EJECTIONS: NORMALIZATION [CHOCS A L'OUVERTURE LORS DES EJECTIONS A GRANDE VITESSE? QUELLES NORMES?]
A. Leger, P. Dolou, P. Sandor, and P. Beaudouin (Service Technique des Programmes Aeronautiques, Paris, France) *In* AGARD, Implications of Advanced Technologies for Air and Spacecraft Escape Feb. 1990 7 p In FRENCH (For primary document see N90-20054 13-03)
Copyright Avail: NTIS HC A06/MF A01; Non-NATO Nationals requests available only from AGARD/Scientific Publications Executive

06 AIRCRAFT INSTRUMENTATION

Includes cockpit and cabin display devices; and flight instruments.

For related information see also *19 Spacecraft Instrumentation* and *35 Instrumentation and Photography.*

N90-20080*# Eagle Engineering, Inc., Hampton, VA.
THE NASA DIGITAL VGH PROGRAM: EXPLORATION OF METHODS AND FINAL RESULTS. VOLUME 2: L 1011 DATA 1978-1979: 1619 HOURS
Norman L. Crabill Dec. 1989 175 p
(Contracts NASw-4430; DTFA03-890-A-00019)
(NASA-CR-181909-Vol-2; NAS 1.26:181909-Vol-2; DOT/FAA-CT-89/36-2) Avail: NTIS HC A08/MF A01 CSCL 01D

Data obtained from the digital flight data recorder system of a L 1011 aircraft in 914 flights and 1619 hours of airline revenue operations are presented. Data on conditions with flap deployment and autopilot use are given. In addition, acceleration statistics are presented from 23 hours on nonrevenue flights. Author

N90-20081*# Eagle Engineering, Inc., Hampton, VA.
THE NASA DIGITAL VGH PROGRAM. EXPLORATION OF METHODS AND FINAL RESULTS. VOLUME 1: DEVELOPMENT OF METHODS
Norman L. Crabill Dec. 1989 131 p
(Contract NASw-4430)
(NASA-CR-181909-Vol-1; NAS 1.26:181909-Vol-1; DOT/FAA-CT-89/36-1) Avail: NTIS HC A07/MF A01 CSCL 01D

Two hundred hours of Lockheed L 1011 digital flight data recorder data taken in 1973 were used to develop methods and procedures for obtaining statistical data useful for updating airliner airworthiness design criteria. Five thousand hours of additional data taken in 1978 to 1982 are reported in volumes 2, 3, 4 and 5. Author

N90-20082*# Eagle Engineering, Inc., Hampton, VA.
THE NASA DIGITAL VGH PROGRAM. EXPLORATION OF METHODS AND FINAL RESULTS. VOLUME 3: B 727 DATA 1978-1980: 1765 HOURS
Norman L. Crabill Dec. 1989 175 p
(Contract NASw-4430)
(NASA-CR-181909-Vol-3; NAS 1.26:181909-Vol-3; DOT/FAA-CT-89/36-3) Avail: NTIS HC A08/MF A01 CSCL 01D

B 727 digital flight data recorder data taken in 1978 through 1980 were analyzed to provide many statistical data useful for updating airliner airworthiness design criteria. Author

N90-20083*# Eagle Engineering, Inc., Hampton, VA.
THE NASA DIGITAL VGH PROGRAM: EXPLORATION OF METHODS AND FINAL RESULTS. VOLUME 4: B 747 DATA 1978-1980, 1689 HOURS
Norman L. Crabill Dec. 1989 174 p
(Contract NASw-4430)
(NASA-CR-181909-Vol-4; NAS 1.26:181909-Vol-4; DOT/FAA-CT-89/36-4) Avail: NTIS HC A08/MF A01 CSCL 01D

B 747 digital flight data taken in 1978 through 1980 were analyzed to provide many statistical data useful for updating airliner airworthiness design criteria. Author

N90-20084*# Eagle Engineering, Inc., Hampton, VA.
THE NASA DIGITAL VGH PROGRAM: EXPLORATION OF METHODS AND FINAL RESULTS. VOLUME 5: DC 10 DATA 1981-1982, 129 HOURS
Norman L. Crabill Dec. 1989 139 p
(Contract NASw-4430)
(NASA-CR-181909-Vol-5; NAS 1.26:181909-Vol-5; DOT/FAA-CT-89/36-5) Avail: NTIS HC A07/MF A01 CSCL 01D

DC 10 digital flight data recorder data taken in 1981 through 1982 were analyzed to provide statistical data useful for updating airliner airworthiness design criteria. Author

07 AIRCRAFT PROPULSION AND POWER

Includes prime propulsion systems and systems components, e.g., gas turbine engines and compressors; and onboard auxilliary power plants for aircraft.

For related information see also *20 Spacecraft Propulsion and Power, 28 Propellants and Fuels,* and *44 Energy Production and Conversion.*

N90-20085*# National Aeronautics and Space Administration. Lewis Research Center, Cleveland, OH.
AEROSPACE INDUCTION MOTOR ACTUATORS DRIVEN FHOM A 20-kHz POWER LINK
Irving G. Hansen Jan. 1990 5 p Presented at the 4th International Conference on Power Electronics and Variable Speed Drives, London, England, 17-19 Jul. 1990; sponsored by Institution of Electrical Engineers
(NASA-TM-102482; E-5272; NAS 1.15:102482) Avail: NTIS HC A01/MF A01 CSCL 21E

Aerospace electromechanical actuators utilizing induction motors are under development in sizes up to 40 kW. While these actuators have immediate application to the Advanced Launch System (ALS) program, several potential applications are currently under study including the Advanced Aircraft Program. Several recent advances developed for the Space Station Freedom have allowed induction motors to be selected as a first choice for such applications. Among these technologies are bi-directional electronics and high frequency power distribution techniques. Each of these technologies are discussed with emphasis on their impact upon induction motor operation. Author

N90-20086*# National Aeronautics and Space Administration. Hugh L. Dryden Flight Research Facility, Edwards, CA.
THE IMPLEMENTATION AND OPERATION OF A VARIABLE-RESPONSE ELECTRONIC THROTTLE CONTROL SYSTEM FOR A TF-104G AIRCRAFT
Bradford Neal and Upal Sengupta Dec. 1989 18 p
(NASA-TM-101696; H-1542; NAS 1.15:101696) Avail: NTIS HC A03/MF A01 CSCL 21E

During some flight programs, researchers have encountered problems in the throttle response characteristics of high-performance aircraft. To study and to help solve these problems, the National Aeronautics and Space Administration Ames Research Center's Dryden Flight Research Facility (Ames-Dryden) conducted a study using a TF-104G airplane modified with a

variable-response electronic throttle control system. Ames-Dryden investigated the effects of different variables on engine response and handling qualities. The system provided transport delay, lead and lag filters, second-order lags, command rate and position limits, and variable gain between the pilot's throttle command and the engine fuel controller. These variables could be tested individually or in combination. Ten research flights were flown to gather data on engine response and to obtain pilot ratings of the various system configurations. The results should provide design criteria for engine-response characteristics. The variable-response throttle components and how they were installed in the TF-104G aircraft are described. How the variable-response throttle was used in flight and some of the results of using this system are discussed. Author

N90-20087*# National Aeronautics and Space Administration. Ames Research Center, Moffett Field, CA.

STATIC AEROELASTIC ANALYSIS OF A THREE-DIMENSIONAL GENERIC WING

John A. Green, In Lee, and Hirokazu Miura Feb. 1990 29 p (NASA-TM-102231; A-89239; NAS 1.15:102231) Avail: NTIS HC A03/MF A01 CSCL 21E

A continuation of research on the static aeroelastic analysis of a generic wing configuration is presented. Results of the study of the asymmetric oblique wing model developed by Rockwell International, in conjunction with the NASA Oblique Wing Research Aircraft Program, are reported. The capability to perform static aeroelastic analyses of an oblique wing at arbitrary skew positions is demonstrated by applying the MSC/NASTRAN static analysis scheme modified by the aerodynamic influence coefficient matrix created by the NASA Ames aerodynamic panel codes. The oblique wing is studied at two skew angles, and in particular, the capability to calculate 3-D thickness effects on the aerodynamic properties of the wing is investigated. The ability to model asymmetric wings in both subsonic and supersonic Mach numbers is shown. The aerodynamic influence coefficient matrix computed by the external programs is inserted in MSC/NASTRAN static aeroelasticity analysis run stream to compute the aeroelastic deformation and internal forces. Various aerodynamic coefficients of the oblique wing were computed for two Mach numbers, 0.7 and 1.4, and the angle of attach -5 through 15 deg. Author

N90-20088*# Allied-Signal Aerospace Co., Torrance, CA. AiResearch Los Angeles Div.

DEVELOPMENT AND FABRICATION OF STRUCTURAL COMPONENTS FOR A SCRAMJET ENGINE Final Report, Mar. 1980 - May 1989

O. A. Buchmann Mar. 1990 234 p
(Contract NAS1-16097)
(NASA-CR-181945; Rept-89-62543; NAS 1.26:181945) Avail: NTIS HC A11/MF A02 CSCL 21E

A program broadly directed toward design and development of long-life (100 hours and 1,000 cycles with a goal of 1,000 hours and 10,000 cycles) hydrogen-cooled structures for application to scramjets is presented. Previous phases of the program resulted in an overall engine design and analytical and experimental characterization of selected candidate materials and concepts. The latter efforts indicated that the basic life goals for the program can be reached with available means. The main objective of this effort was an integrated, experimental evaluation of the results of the previous program phases. The fuel injection strut was selected for this purpose, including fabrication development and fabrication of a full-scale strut. Testing of the completed strut was to be performed in a NASA-Langley wind tunnel. In addition, conceptual designs were formulated for a heat transfer test unit and a flat panel structural test unit. Tooling and fabrication procedures required to fabricate the strut were developed, and fabrication and delivery to NASA of all strut components, including major subassemblies, were completed. Author

N90-20089# Oxford Univ. (England). Dept. of Engineering Science.

HEAT TRANSFER NEAR THE ENTRANCE TO A FILM COOLING HOLE IN A GAS TURBINE BLADE M.S. Thesis

Aaron R. Byerley 1989 240 p Sponsored by AFIT (AD-A217396; AFIT/CI/CIA-89-107) Avail: NTIS HC A11/MF A02 CSCL 20/13

Film cooling is a method used to prevent jet engine turbine blade failure due to overheating. It consists of bleeding relatively cool air from the engine's compressor stage and discharging it through small holes in the turbine blade surface. This air provides a protective, insulating film which keeps the blade surface temperature well below the destructively high temperature levels of the combustor gases. This thesis presents for the first time, detailed pictures of the convective heat transfer distribution on the wall of an internal turbine blade passage near the entrance to a film cooling hole. The physical situation was modelled at 100X geometric scale as flow extraction into a single circular hole from a two-dimensional, fully developed, turbulent channel flow. High resolution heat transfer measurements were made using a transient technique with liquid crystals as surface temperature indicators. During the experiments, the two-dimensional channel Reynolds number was held constant while the flow extraction rate was varied for each of four hole inclination angles. The main region of heat transfer enhancement was found to be downstream with local heat transfer levels up to 6.5 times the levels associated with turbulent channel flow. Additional experimental, analytical, and computational flow field studies showed that the enhancement was caused mainly by the removal of the upstream boundary layer and the formation of a new laminar boundary layer at the down-stream hole edge. GRA

N90-20090*# National Aeronautics and Space Administration. Lewis Research Center, Cleveland, OH.

COMPARISON OF 3-D VISCOUS FLOW COMPUTATIONS OF MACH 5 INLET WITH EXPERIMENTAL DATA

D. R. Reddy (Sverdrup Technology, Inc., Cleveland, OH.), T. J. Benson, and L. J. Weir Jan. 1990 15 p Presented at the 28th Aerospace Sciences Meeting, Reno, NV, 8-11 Jan. 1990; sponsored by AIAA Previously announced in IAA as A90-26970 (NASA-TM-102518; E-5322; NAS 1.15:102518) Avail: NTIS HC A03/MF A01 CSCL 21E

A time marching 3-D full Navier-Stokes code, called PARC3D, is validated for an experimental Mach 5 inlet configuration using the data obtained in the 10 x 10 ft supersonic wind tunnel at the NASA Lewis Research Center. For the first time, a solution is obtained for this configuration with the actual geometry, the tunnel conditions, and all the bleed zones modeled in the computation. Pitot pressure profiles and static pressures at various locations in the inlet are compared with the corresponding experimental data. The effect of bleed zones, located in different places on the inlet walls, in eliminating the low energy vortical flow generated from the 3-D shock-boundary layer interaction is simulated very well even though some approximations are used in applying the bleed boundary conditions and in the turbulence model. A further detailed study of the effect of individual bleed ports is needed to understand fully the actual mechanism of efficiently eliminating the vortical flow from the inlet. A better turbulence model would help to improve the accuracy even further in predicting the corner flow boundary layer profiles. Author

N90-20091# General Motors Corp., Indianapolis, IN. Gas Turbine Div.

IN-LINE WEAR MONITOR Final Report, Jul. 1988 - Apr. 1989

Keith A. Pieper and Ivor J. Taylor (Princeton Gamma Tech, Inc., NJ.) Nov. 1989 51 p
(Contract F33615-85-C-2537)
(AD-A217799; ALLISON-EDR-14074; WRDC-TR-89-2118) Avail: NTIS HC A04/MF A01 CSCL 21/5

This report describes construction and test results of an in-line monitor for critical ferrous and nonferrous metal debris in turbine engine lubrication systems. The in-line wear monitor (ILWM) uses the x ray fluorescence principle for detecting metal debris on a

continuous basis while the engine is running. The sensor portion of the system is engine mounted and contains a radioactive x ray source, a flow cell to direct the oil across an x ray permeable window, a proportional counter x ray detector and its associated preamplifier and amplifier electronics. The data acquisition electronics is mounted on the airframe and contains a microprocessor based system for inputting pulses from the sensor, classifying and counting them according to energy bands, and analyzing the data and outputting metal concentration values to the engine monitoring system. The sensor portion of the system is designed to fit on a TF41 turbine engine in place of a tube between the oil tank and the oil pump. A TF41 engine monitoring system has been modified to accept the new signals from the ILWM on spare inputs so that none of the existing functions were disturbed. The ILWM has been flow tested at various flow rates, concentration levels, oil temperatures, and aerations. The wear monitor detected iron, copper, and both iron and copper together. GRA

08 AIRCRAFT STABILITY AND CONTROL

Includes aircraft handling qualities; piloting; flight controls; and autopilots.

For related information see also *05 Aircraft Design, Testing and Performance.*

N90-20092# Range Commanders Council, White Sands Missile Range, NM. Range Safety Group.
FLIGHT TERMINATION SYSTEM BATTERY GUIDELINES
Oct. 1989 20 p
(AD-A217310; RCC/RSG-318-89) Avail: NTIS HC A03/MF A01 CSCL 10/3

This document is intended to be used as a guide for range users requiring a flight termination battery. It will provide the user with guidelines for incorporating technical and safety criteria necessary to describe a power source (battery) which will be compatible with the mission critical needs of a flight termination system (FTS). All batteries used to provide the electrical power for an FTS shall have a proven performance reliability of .999 at the 95 percent confidence level. Performance reliability shall be established through statistically based testing. The battery specification, as a minimum, shall include all of the applicable operational, mechanical, electrical, and environmental characteristics of the FTS. As a final product, any battery to be used with an FTS shall be from those units for which lot-acceptance data is in compliance with the specification and the data evaluation requirements of this document. A quality assurance program, such as MIL-Q-9858, must be invoked in the purchase document and placed in operation concurrent with the qualification program so as to allow its assessment prior to beginning production. GRA

N90-20093*# National Aeronautics and Space Administration. Langley Research Center, Hampton, VA.
DIGITAL-FLUTTER-SUPPRESSION-SYSTEM INVESTIGATIONS FOR THE ACTIVE FLEXIBLE WING WIND-TUNNEL MODEL
Boyd Perry, III, Vivek Mukhopadhyay, Sherwood T. Hoadley, Stanley R. Cole, Carey S. Buttrill, and Jacob A. Houck Mar. 1990 13 p Presented at the AIAA 31st Structures, Structural Dynamics, and Materials Conference, Long Beach, CA, 2-4 Apr. 1990
(NASA-TM-102618; NAS 1.15:102618) Avail: NTIS HC A03/MF A01 CSCL 01C

Active flutter suppression control laws were designed, implemented, and tested on an aeroelastically-scaled wind tunnel model in the NASA Langley Transonic Dynamics Tunnel. One of the control laws was successful in stabilizing the model while the dynamic pressure was increased to 24 percent greater than the measured open-loop flutter boundary. Other accomplishments included the design, implementation, and successful operation of a one-of-a-kind digital controller, the design and use of two simulation methods to support the project, and the development and successful use of a methodology for on-line controller performance evaluation. Author

N90-20094# Wright Research Development Center, Wright-Patterson AFB, OH. Flight Dynamics Lab.
LABORATORY IMPLEMENTATION OF THE CONTINUOUSLY RECONFIGURING MULTI-MICROPROCESSOR FLIGHT CONTROL SYSTEM (CRMMFCS) Final Report, Apr. 1980 - Jun. 1984
Bill Rollison, Dan Thompson, Ray Bortner, Stan Pruett, and Mark Mears Oct. 1989 98 p
(AD-A217730; WRDC-TR-89-3114) Avail: NTIS HC A05/MF A01 CSCL 01/4

The initial CRMMFSC report highlighted the theoretical concepts and established the boundaries for realizing an autonomously distributed control system. The hardware and software methods used in the laboratory model to achieve the goals as set down in the concept phase are discussed. The discussion highlights the hardware construction, revealing the operations and the reasoning behind the choices made. The section on software reviews the techniques used to glue the hardware together to become a system. The completed laboratory model and its testing under a number of conditions are discussed. GRA

N90-20095# Human Engineering Labs., Aberdeen Proving Ground, MD.
INTERACTION OF SWITCH ACTUATION ON TRACKING WITH A FOUR-AXIS FLIGHT CONTROL (CROSS-COUPLING) Final Report
William B. DeBellis Dec. 1989 49 p
(DA Proj. 1L1-62716-AH-70)
(AD-A217981; HEL-TM-17-89) Avail: NTIS HC A03/MF A01 CSCL 01/4

This is the third in a series of investigations to generate a data base for multiaxis side arm flight controls. The purpose of this research is to determine the interaction between switch actuation and tracking performance while tracking in four axes. The research is required to specify the number and locations of switches that can be placed on the flight control. The long range goal is to provide design recommendations and input to military specifications and standards. Tracking errors increase when switches associated with this control grip and controller mechanism are operated. GRA

09 RESEARCH AND SUPPORT FACILITIES (AIR)

Includes airports, hangars and runways; aircraft repair and overhaul facilities; wind tunnels; shock tubes; and aircraft engine test stands.

For related information see also *14 Ground Support Systems and Facilities (Space).*

N90-20096* National Aeronautics and Space Administration. Langley Research Center, Hampton, VA.
AIRPLANE TAKEOFF AND LANDING PERFORMANCE MONITORING SYSTEM Patent
David B. Middleton, inventor (to NASA), Raghavachari Srivatsan, inventor (to NASA), and Lee H. Person, inventor (to NASA) 27 Jun. 1989 25 p Filed 6 Aug. 1987 Prepared in cooperation with Kansas Univ., Lawrence
(NASA-Case-LAR-13734-1-CU; US-Patent-4,843,554; US-Patent-Appl-SN-082766; US-Patent-Class-364-427; US-Patent-Class-73-178-T) Avail: US Patent and Trademark Office CSCL 14B

The invention is a real-time takeoff and landing performance monitoring system which provides the pilot with graphic and metric information to assist in decisions related to achieving rotation speed (V sub R) within the safe zone of the runway or stopping the aircraft on the runway after landing or take off abort. The system processes information in two segments: a pretakeoff segment and a real-time segment. One-time inputs of ambient conditions and

airplane configuration information are used in the pretakeoff segment to generate scheduled performance data. The real-time segment uses the scheduled performance data, runway length data and transducer measured parameters to monitor the performance of the airplane throughout the takeoff roll. An important feature of this segment is that it updates the estimated runway rolling friction coefficient. Airplane performance predictions also reflect changes in headwind occurring as the takeoff roll progresses. The system displays the position of the airplane on the runway, indicating runway used and runway available, summarizes the critical information into a situation advisory flag, flags engine failures and off-nominal acceleration performance, and indicates where on the runway particular events such as decision speed (V sub 1), rotation speed (V sub R) and expected stop points will occur based on actual or predicted performance. The display also indicates airspeed, wind vector, engine pressure ratios, second segment climb speed, and balanced field length (BFL). The system detects performance deficiencies by comparing the airplane's present performance with a predicted nominal performance based upon the given conditions.

Official Gazette of the U.S. Patent and Trademark Office

N90-20097# Army Cold Regions Research and Engineering Lab., Hanover, NH.

AIRFIELDS ON ANTARCTIC GLACIER ICE

Malcolm Mellor and Charles Swithinbank Dec. 1989 106 p
(Grant NSF DPP-87-001)
(AD-A217638; CRREL-89-21) Avail: NTIS HC A06/MF A01 CSCL 01/5

The physical characteristics of blue ice ablation areas in Antarctica are described and some representative ablation rates are given. The possibilities for using blue-ice areas as airfields are outlined and exploratory surveys are mentioned. Site details are given for icefields at Mount Howe, Mill Glacier, Patriot Hills, Rosser Ridge, Mount Lechner, S1 near Casey station, and on the Ross Ice Shelf near McMurdo station. The surface roughness of blue ice is discussed, microrelief surveys are presented for Mount Howe and Patriot Hills, and spectral analyses are used to develop relations between bump height and wavelength. U.S. military specifications for the roughness limits of various types of runways are summarized and graphical comparisons are made with the roughness analyses for Mount Howe and Patriot Hills. Special machines for smoothing ice runways are discussed and design specifications are developed. Some notes on ground facilities and ground transport are included. Appendices give discussions of weather patterns in the Transantarctic Mountains and methodology for making spectral analyses of surface roughness. It is concluded that glacier-ice airfields for conventional transport aircraft can be developed at low cost in Antarctica. Recommendations for further work are offered. GRA

N90-20098# Aeronautical Research Labs., Melbourne (Australia).

A DATA ACQUISITION PARALLEL BUS FOR WIND TUNNELS AT ARL (AERONAUTICAL RESEARCH LABORATORY)

J. F. Harvey Aug. 1989 34 p
(AD-A218052; ARL-FLIGHT-MECH-TM-412; DODA-AR-005-629)
Avail: NTIS HC A03/MF A01 CSCL 05/2

The data acquisition system used by the Subsonic Wind Tunnel at Aeronautical Research Laboratory, Melbourne, was designed in 1972. Tunnel productivity was further improved during 1982 with the installation of a dedicated computer (PDP11/44) which eliminated the time sharing access with the site's central computer. The dedicated computer also provides real-time processing of data and supports graphical displays for interactive operation with wind tunnel tests. In recent years this dedication minicomputer has become unreliable and the high cost of maintenance has led to its replacement with a micro VAX which is intended to be connected to similiar data gathering equipment to that used in the Subsonic Wind Tunnel. A data bus was developed to provide bi-directional communication between the dedicated master mini computer and the numerous microprocessor slave modules which form the new system. GRA

N90-20099# Air Force Inst. of Tech., Wright-Patterson AFB, OH.

DESIGN OF A HIGH ANGLE OF ATTACK ROBOTIC STING MOUNT FOR TESTS IN A LOW SPEED WIND TUNNEL M.S. Thesis

Tommy Jack Kubler 1989 152 p
(AD-A218105; AFIT/CI/CIA-89-104) Avail: NTIS HC A08/MF A01 CSCL 14/2

A sting mounting system designed for high angle of attack (AOA) testing has been developed for the 7x10 foot low-speed wind tunnel (LSWT). The mechanism was able to position the model from -15 deg to +90 deg of pitch with accuracy to within 0.2 deg, while keeping the model near the center of the test section. Compatible with the current turntable apparatus, the high angle of attack robotic sting (HARS) retained the turntable's full range of yaw movement of + or - 90 deg. All model positioning was done without shutting the tunnel down to manually alter the sting or mounting apparatus. Pitch adjustment progressed at about 4 deg per second, with final position tuning taking nearly 15 seconds. The mechanism consisted of two square steel telescoping tube struts that were joined at the ends in the test section by a cross link that held the existing LSWT small Langley sting. Wind tunnel blockage and flow irregularities near the model were minimized by mounting drive hardware under the tunnel floor. An IBM/AT compatible microcomputer equipped with an analog-to-digital conversion board provided position control, drive motor signaling, and input signal filtering. GRA

N90-20100# Air Force Inst. of Tech., Wright-Patterson AFB, OH.

RUNAWAY RUBBER REMOVAL M.S. Thesis

Dean W. Simpson 1989 112 p
(AD-A218349; AFIT/CI/CIA-89-186) Avail: NTIS HC A06/MF A01 CSCL 01/5

When the wheels of landing aircraft impact a runway pavement, they deposit rubber on the pavement surface. As deposited rubber accumulates, the available friction between aircraft tires and the runway surface is reduced. This results in hazardous aircraft operating conditions. Factors affecting the need, method, and timing of rubber removal are addressed. GRA

12 ASTRONAUTICS (GENERAL)

For extraterrestrial exploration see *91 Lunar and Planetary Exploration.*

N90-20101# Utah State Univ., Logan. Center for Atmospheric and Space Sciences.

USU CENTER OF EXCELLENCE IN THEORY AND ANALYSIS OF THE GEO-PLASMA ENVIRONMENT Final Technical Report

Robert W. Schunk 30 Nov. 1989 49 p
(Contract F49620-86-C-0109)
(AD-A217736; AFOSR-90-0106TR) Avail: NTIS HC A03/MF A01 CSCL 20/14

A team of eleven Ph.D. scientists and several graduate students was assembled at USU to work in close collaboration with scientists at the Air Force Geophysics Lab on a number of problems that are relevant to Air Force systems, including OTH radars, communications, and orbiting space structures. The overall goal of the research was to obtain a better understanding of the basic chemical and physical processes operating in the geoplasma environment, including the ionosphere, thermosphere, and magnetosphere. Some of the specific tasks included the following: (1) Studies of ionospheric structure and irregularities; (2) Study the feasibility of developing better operational ionospheric models for the Air Force; (3) Conduct model/data comparisons in order to validate the ionospheric models; (4) Study plasma convection characteristics in the high latitude ionosphere; (5) Study magnetosphere-ionosphere coupling problems; (6) Construct a thermospheric general circulation model; (7) Develop a 3D, time dependent model of the outer plasmasphere; (8) Develop a 3D, time dependent MHD model of the earth's magnetosphere; (9)

Conduct satellite drag studies; and (10) Study certain spacecraft-environment interaction problems, including those related to high voltage power sources, spacecraft outgassing, and spacecraft charging at LEO altitudes. GRA

N90-20457*# National Aeronautics and Space Administration. Lewis Research Center, Cleveland, OH.
HUMAN EXPLORATION MISSION STUDIES
Robert L. Cataldo *In its* Space Electrochemical Research and Technology (SERT), 1989 Dec. 1989 p 9-15 (For primary document see N90-20454 13-44)
Avail: NTIS HC A16/MF A02 CSCL 22A

13 ASTRODYNAMICS

Includes powered and free-flight trajectories; and orbital and launching dynamics.

N90-20102 Illinois Univ., Urbana-Champaign.
OPTIMAL, IMPULSIVE, TIME-FIXED ORBITAL RENDEZVOUS AND INTERCEPTION WITH PATH CONSTRAINTS Ph.D. Thesis
Der-Ren Taur 1989 241 p
Avail: Univ. Microfilms Order No. DA8924957

Minimum-fuel, impulsive, time-fixed extremal solutions are obtained for the problem of orbital rendezvous and interception with path constraints. The coplanar case and a restricted class of path constraints are analyzed. A theory based on the extended problem of Bolza in the calculus of variations was established to determine optimal impulsive trajectories with state variable inequality constraints. According to this newly developed theory, all the necessary conditions including the optimal corner conditions were obtained for both constrained and unconstrained arcs. The constrained extremal solutions, including the optimal number of impulses, their times and positions were studied under a conjecture proposed for the minimization process on the constrained arc. The fundamental problems such as the existence of boundary arcs or boundary points, absorbing boundaries or non-absorbing boundaries, and the continuity of the Hamiltonian function with a scleronomic constraint in infinite control problems were studied and answered. A bifurcation phenomenon and the non-uniqueness of the extremal solutions having the same cost were found during the research. The extended principles of dynamical reversibility and reflectability of the impulsive solution were developed to obtain the conjugate solutions belonging to the same cost function. In addition, the local-optimal time-fixed solutions obtained can be used to perform time versus fuel trade-offs for missions which have time constraints. Dissert. Abstr.

N90-20103# Air Force Wright Research and Development Center, Wright-Patterson AFB, OH.
ETO (EARTH-TO-ORBIT): A TRAJECTORY PROGRAM FOR AEROSPACE VEHICLES Final Report, Jan. 1987 - Jul. 1988
John L. Leingang, Wayne A. Donaldson, Kenneth A. Watson, and Louis R. Carreiro Jun. 1989 90 p
(AD-A218157; WRDC-TR-89-2023) Avail: NTIS HC A05/MF A01 CSCL 01/3

This is a formulation report and user guide for a two degree-of-freedom flight trajectory computer program. The program, called ETO, runs on IBM/compatible XT/AT microcomputers. It is designed for very short run times, i.e., less than 1 to 3 minutes. Horizontal or low angle takeoff single-stage or two-stage vehicles can be studies. Ascent to earth orbit or constant speed cruise can be studied. Any combination of airbreathing or rocket propulsion may be used. Working from tabular data for propulsion performance, aerodynamics, and vehicle weight and fuel, the governing equations of motion are integrated forward in time to track velocity, altitude, range, flight path angle, and weight. GRA

N90-20104# Draper (Charles Stark) Lab., Inc., Cambridge, MA.
TRAJECTORY OPTIMIZATION IN THE PRESENCE OF CONSTRAINTS M.S. Thesis - Massachusetts Inst. of Tech.
Timothy E. McQuade Jun. 1989 123 p Sponsored by AFIT, Wright-Patterson AFB, OH
(AD-A218271; AFIT/CI/CIA-89-096) Avail: NTIS HC A06/MF A01 CSCL 01/1

In many aerospace problems, it is necessary to determine vehicle trajectories that satisfy constraints. Typically two types of constraints are of interest. First, it may be desirable to satisfy a set of boundary conditions. Second, it may be necessary to limit the motion of the vehicle so that physical limits and hardware limits are not exceeded. In addition to these requirements, it may be necessary to optimize some measure of vehicle performance. In this thesis, the square root sweep method is used to solve a discrete-time linear quadratic optimal control problem. The optimal control problem arises from a Mayer form continuous-time nonlinear optimization problem. A method for solving the optimal control problem is derived. Called the square root sweep algorithm, the solution consists of a set of backward recursions for a set of square root parameters. The square root sweep algorithm is shown to be capable of treating Mayer form optimization problems. Heuristics for obtaining solutions are discussed. The square root sweep algorithm is used to solve several example optimization problems. GRA

14 GROUND SUPPORT SYSTEMS AND FACILITIES (SPACE)

Includes launch complexes, research and production facilities; ground support equipment, e.g., mobile transporters; and simulators.

For related information see also *09 Research and Support Facilities (Air).*

N90-20105# Army Armament Research and Development Command, Dover, NJ. Artillery Armaments Div.
ARDEC (ARMAMENT RESEARCH, DEVELOPMENT AND ENGINEERING CENTER) ELECTRIC GUN IN-HOUSE TEST PROGRAM Annual Report, Oct. 1987 - Sep. 1988
Curtis Dunham, Thomas Coradeschi, Duk In Chang, Kenneth VanCamp, Gregory Colombo, Michael Wie, Ing Woo Chin, and William Juhasz Jan. 1990 53 p
(AD-A217337; ARFSD-TR-89021) Avail: NTIS HC A04/MF A01 CSCL 19/6

This report summarizes the experimental testing conducted on three railguns. It discusses improvements to the 30-megajoule homopolar generator and 250-kilojoule capacitor bank as well as instrumentation techniques and analysis capabilities. It also describes the planned high energy lab. The 50-mm square bore railgun demonstrated dramatic improvements in barrel wear with solid armatures of proper design. Tests on the short prototype of the 20-mm round bore railgun indicated that the composite structure will withstand the forces involved in the upcoming 5 km/sec tests using plasma armatures. The 50-mm round bore railgun short prototype tests pointed out the difficulties of designing solid round bore armatures and the importance of matching barrel stiffness and armature compliance. GRA

N90-20106# Sandia National Labs., Albuquerque, NM. Electromagnetic Launcher Div.
A 10-STAGE RECONNECTION DEMONSTRATION LAUNCHER
Eugene C. Cnare, Melvin M. Widner, and Billy W. Duggin 1989 3 p Presented at the 5th IEEE Symposium on Electromagnetic Launch Technology, Destin, FL, 1-5 Apr. 1990
(Contract DE-AC04-76DP-00789)
(DE90-007653; SAND-89-2111C; CONF-9004136-4) Avail: NTIS HC A01/MF A01

A small-scale, 10-stage cylindrical reconnection launcher has been designed, fabricated, and tested. Ten-gram projectiles are accelerated from rest to 317 m/s through the 0.44 m launcher assembly with a projectile kinetic energy to capacitor stored energy efficiency of 9 percent. Comparison of test results and computer code predictions will be presented. Results of these studies have substantiated launcher scaling at small size and have provided a useful test bed for launcher components and diagnostics. DOE

N90-20107# Sandia National Labs., Albuquerque, NM. Electromagnetic Launcher Div.
DIAGNOSTICS AND FIRING CONTROL FOR THE CYLINDRICAL RECONNECTION LAUNCHER
Billy W. Duggin 1989 4 p Presented at the 5th IEEE Symposium on Electromagnetic Launch Technology, Destin, FL, 1-5 Apr. 1990
(Contract DE-AC04-76DP-00789)
(DE90-007677; SAND-89-2113C; CONF-9004136-5) Avail: NTIS HC A01/MF A01

A real-time firing control system has been developed which controls the operation of multi-stage electromagnetic reconnection launchers. This controller, facility diagnostics, and data acquisition capabilities are described. DOE

N90-20108# Sandia National Labs., Albuquerque, NM.
DESIGN AND PERFORMANCE OF A MULTI-STAGE CYLINDRICAL RECONNECTION LAUNCHER
Ronald J. Kaye, Edwin L. Brawley (Rockwell International Corp., Albuquerque, NM.), Billy W. Duggin, Eugene C. Cnare, Dean C. Rovang, and Melvin M. Widner 1989 14 p Presented at the 5th IEEE Symposium on Electromagnetic Launch Technology, Destin, FL, 1-5 Apr. 1990
(Contract DE-AC04-76DP-00789)
(DE90-007820; SAND-89-2112C; CONF-9004136-6) Avail: NTIS HC A03/MF A01

A multi-stage, cylindrical, reconnection launcher is being tested to demonstrate electrically-contactless, induction-launch technology for solenoidal coil geometry. A 6-stage launcher system is being developed to accelerate a 5 kg mass from rest to 300 m/s with a stored energy of (ge)200 kJ per coil stage. This launcher will provide data for model verification and the engineering basis for proceeding with larger multistage systems. The design of the multi-stage, discrete-coil launcher is described. Integration of coils, projectile, power systems, and real-time fire control are discussed. Results of multi-stage firings are presented. DOE

N90-20109# Illinois Univ., Urbana. Dept. of Electrical and Computer Engineering.
APPLICATION OF RAILGUN PRINCIPLE TO HIGH-VELOCITY HYDROGEN PELLET INJECTION FOR MAGNETIC FUSION REACTOR REFUELING
Kyekyoon Kim Dec. 1989 9 p
(Contract DE-FG02-84ER-52111)
(DE90-008281; DOE/ER-52111/T6; FCPRL-8903) Avail: NTIS HC A02/MF A01

The research effort on using railgun accelerators to injection hydrogen fuel pellets in magnetically confined plasmas is briefly discussed. DOE

15 LAUNCH VEHICLES AND SPACE VEHICLES

Includes boosters; operating problems of launch/space vehicle systems; and reusable vehicles.

For related information see also *20 Spacecraft Propulsion and Power.*

N90-20110*# National Aeronautics and Space Administration. Lewis Research Center, Cleveland, OH.
ADVANCED LAUNCH VEHICLE PROPULSION AT THE NASA LEWIS RESEARCH CENTER
Bryan A. Palaszewski 1990 6 p Presented at the High Energy Density Materials Contractors' Conference, Long Beach, CA, 26-28 Feb. 1990; sponsored by AFOSR
(NASA-TM-103096; E-5417; NAS 1.15:103096) Avail: NTIS HC A02/MF A01 CSCL 22B

Several programs are investigating the benefits of advanced propellant and propulsion systems for future launch vehicles and upper stages. The two major research areas are the Metallized Propellants Program and the Advanced Concepts Program. Both of these programs have theoretical and experimental studies underway to determine the system-level performance effects of these propellants on future NASA vehicles. Author

16 SPACE TRANSPORTATION

Includes passenger and cargo space transportation, e.g., shuttle operations; and space rescue techniques.

For related information see also *03 Air Transportation and Safety* and *18 Spacecraft Design, Testing and Performance.* For space suits see *54 Man/System Technology and Life Support.*

No abstracts in this category.

17 SPACE COMM., SPACECRAFT COMM., COMMAND & TRACKING

Includes telemetry; space communications networks; astronavigation and guidance; and radio blackout.

For related information see also *04 Aircraft Communications and Navigation* and *32 Communications and Radar.*

N90-20111# Midwest Research Inst., Golden, CO. Wind Research Branch.
PC-BASED PCM TELEMETRY DATA REDUCTION SYSTEM SOFTWARE
D. A. Simms Feb. 1990 11 p Presented at the 36th ISA International Instrumentation Symposium, Denver, CO, 6-10 May 1990
(Contract DE-AC02-83CH-10093)
(DE90-000317; SERI/TP-257-3663; CONF-900599-3) Avail: NTIS HC A03/MF A01

The Solar Energy Research Institute's (SERI) Wind Research Program is using pulse code modulation (PCM) telemetry systems to study horizontal-axis wind turbines. SERI has developed a low-cost PC-based PCM data-acquisition system to facilitate quick PCM data analysis in the field. The SERI PC-PCM system consists of AT-compatible hardware boards for decoding and combining PCM data streams and DOS software for control and management of data acquisition. Up to four boards can be installed in a single PC, providing the capability to combine data from four PCM streams direct to disk or memory. This paper describes the SERI Quick-Look Data Management Program, which is a comprehensive software package used to organize, acquire, process, and display information from PCM data streams. The software was designed for use in conjunction with SERI's PC-PCM hardware described in a related paper. Features of the Quick-Look program are highlighted, including those which make it useful in an experiment test environment to quickly examine and verify incoming data. Also discussed are problems and techniques associated with PC-based PCM data acquisition, processing, and real-time display. DOE

N90-20112*# Harris Corp., Palm Bay, FL. Government Aerospace Systems Div.
PROXIMITY OPERATIONS CONCEPT DESIGN STUDY, TASK 6 Final Report
A. N. Williams Apr. 1990 294 p
(Contract NAS1-18225)
(NASA-CR-181971; JA-1264-6; NAS 1.26:181971) Avail: NTIS HC A13/MF A02 CSCL 17B

The feasibility of using optical technology to perform the mission of the proximity operations communications subsystem on Space Station Freedom was determined. Proximity operations mission requirements are determined and the relationship to the overall operational environment of the space station is defined. From this information, the design requirements of the communication subsystem are derived. Based on these requirements, a preliminary

design is developed and the feasibility of implementation determined. To support the Orbital Maneuvering Vehicle and National Space Transportation System, the optical system development is straightforward. The requirements on extra-vehicular activity are such as to allow large fields of uncertainty, thus exacerbating the acquisition problem; however, an approach is given that could mitigate this problem. In general, it is found that such a system could indeed perform the proximity operations mission requirement, with some development required to support extra-vehicular activity. Author

18 SPACECRAFT DESIGN, TESTING AND PERFORMANCE

Includes satellites; space platforms; space stations; spacecraft systems and components such as thermal and environmental controls; and attitude controls.

For life support systems see *54 Man/System Technology and Life Support.* For related information see also *05 Aircraft Design, Testing and Performance, 39 Structural Mechanics,* and *16 Space Transportation.*

N90-20113*# TRW, Inc., Huntsville, AL. System Development Div.

SPACE STATION SIMULATION COMPUTER SYSTEM (SCS) STUDY FOR NASA/MSFC. VOLUME 1: OVERVIEW AND SUMMARY Final Technical Report, Aug. 1988 - Oct. 1989

31 Oct. 1989 61 p Prepared in cooperation with Essex Corp., Huntsville, AL and Grumann Data Systems Corp., Woodbury, NY (Contract NAS8-37745)

(NASA-CR-183840; NAS 1.26:183840; TRW-SCS-89-T7-Vol-1)

Avail: NTIS HC A04/MF A01 CSCL 22B

NASA's Space Station Freedom Program (SSFP) planning efforts have identified a need for a payload training simulator system to serve as both a training facility and as a demonstrator to validate operational concepts. The envisioned Marshall Space Flight Center (MSFC) Payload Training Complex (PTC) required to meet this need will train the space station payload scientists, station scientists, and ground controllers to operate the wide variety of experiments that will be onboard the Space Station Freedom. The Simulation Computer System (SCS) is the computer hardware, software, and workstations that will support the Payload Training Complex at MSFC. The purpose of this SCS study is to investigate issues related to the SCS, alternative requirements, simulator approaches, and state-of-the-art technologies to develop candidate concepts and designs. This study was performed August 1988 to October 1989. Thus, the results are based on the SSFP August 1989 baseline, i.e., pre-Langley configuration/budget review (C/BR) baseline. Some terms, e.g., combined trainer, are being redefined. An overview of the study activities and a summary of study results are given here. Author

N90-20114*# TRW, Inc., Huntsville, AL. System Development Div.

SPACE STATION SIMULATION COMPUTER SYSTEM (SCS) STUDY FOR NASA/MSFC. VOLUME 2: CONCEPT DOCUMENT Final Technical Report

31 Oct. 1989 151 p Prepared in cooperation with Essex Corp., Huntsville, AL and Grumann Data Systems Corp., Woodbury, NY (Contract NAS8-37745)

(NASA-CR-183841; NAS 1.26:183841; MSFC-SPEC-1764-Vol-2)

Avail: NTIS HC A08/MF A01 CSCL 22B

The Simulation Computer System (SCS) concept document describes and establishes requirements for the functional performance of the SCS system, including interface, logistic, and qualification requirements. The SCS is the computational communications and display segment of the Marshall Space Flight Center (MSFC) Payload Training Complex (PTC). The PTC is the MSFC facility that will train onboard and ground operations personnel to operate the payloads and experiments on board the international Space Station Freedom. The requirements to be satisfied by the system implementation are identified here. The SCS concept document defines the requirements to be satisfied through the implementation of the system capability. The information provides the operational basis for defining the requirements to be allocated to the system components and enables the system organization to assess whether or not the completed system complies with the requirements of the system. Author

N90-20115*# TRW, Inc., Huntsville, AL. System Development Div.

SPACE STATION SIMULATION COMPUTER SYSTEM (SCS) STUDY FOR NASA/MSFC. VOLUME 3: REFINED CONCEPTUAL DESIGN REPORT Final Technical Report

31 Oct. 1989 110 p Prepared in cooperation with Essex Corp., Huntsville, AL and Grumann Data Systems Corp., Woodbury, NY (Contract NAS8-37745)

(NASA-CR-183842; NAS 1.26:183842; TRW-SCS-89-T5-Vol-3)

Avail: NTIS HC A06/MF A01 CSCL 22B

The results of the refined conceptual design phase (task 5) of the Simulation Computer System (SCS) study are reported. The SCS is the computational portion of the Payload Training Complex (PTC) providing simulation based training on payload operations of the Space Station Freedom (SSF). In task 4 of the SCS study, the range of architectures suitable for the SCS was explored. Identified system architectures, along with their relative advantages and disadvantages for SCS, were presented in the Conceptual Design Report. Six integrated designs-combining the most promising features from the architectural formulations-were additionally identified in the report. The six integrated designs were evaluated further to distinguish the more viable designs to be refined as conceptual designs. The three designs that were selected represent distinct approaches to achieving a capable and cost effective SCS configuration for the PTC. Here, the results of task 4 (input to this task) are briefly reviewed. Then, prior to describing individual conceptual designs, the PTC facility configuration and the SSF systems architecture that must be supported by the SCS are reviewed. Next, basic features of SCS implementation that have been incorporated into all selected SCS designs are considered. The details of the individual SCS designs are then presented before making a final comparison of the three designs. Author

N90-20116*# TRW, Inc., Huntsville, AL. System Development Div.

SPACE STATION SIMULATION COMPUTER SYSTEM (SCS) STUDY FOR NASA/MSFC. VOLUME 4: CONCEPTUAL DESIGN REPORT Final Technical Report

31 Oct. 1989 63 p Prepared in cooperation with Essex Corp., Huntsville, AL and Grumann Data Systems Corp., Woodbury, NY (Contract NAS8-37745)

(NASA-CR-183843; NAS 1.26:183843; TRW-SCS-89-T4-Vol-4)

Avail: NTIS HC A04/MF A01 CSCL 22B

The Simulation Computer System (SCS) is the computer hardware, software, and workstations that will support the Payload Training Complex (PTC) at Marshall Space Flight Center (MSFC). The PTC will train the space station payload scientists, station scientists, and ground controllers to operate the wide variety of experiments that will be onboard the Space Station Freedom. In the first step of this task, a methodology was developed to ensure that all relevant design dimensions were addressed, and that all feasible designs could be considered. The development effort yielded the following method for generating and comparing designs in task 4: (1) Extract SCS system requirements (functions) from the system specification; (2) Develop design evaluation criteria; (3) Identify system architectural dimensions relevant to SCS system designs; (4) Develop conceptual designs based on the system requirements and architectural dimensions identified in step 1 and step 3 above; (5) Evaluate the designs with respect to the design evaluation criteria developed in step 2 above. The results of the method detailed in the above 5 steps are discussed. The results of the task 4 work provide the set of designs which two or three candidate designs are to be selected by MSFC as input to task 5-refine SCS conceptual designs. The designs selected for

refinement will be developed to a lower level of detail, and further analyses will be done to begin to determine the size and speed of the components required to implement these designs. Author

N90-20117*# TRW, Inc., Huntsville, AL. System Development Div.
SPACE STATION SIMULATION COMPUTER SYSTEM (SCS) STUDY FOR NASA/MSFC. VOLUME 5: STUDY ANALYSIS REPORT Final Technical Report
31 Oct. 1989 96 p Prepared in cooperation with Essex Corp., Huntsville, AL and Grumann Data Systems Corp., Woodbury, NY
(Contract NAS8-37745)
(NASA-CR-183844; NAS 1.26:183844; TRW-SCS-89-T2-Vol-5)
Avail: NTIS HC A05/MF A01 CSCL 22B

The Simulation Computer System (SCS) is the computer hardware, software, and workstations that will support the Payload Training Complex (PTC) at the Marshall Space Flight Center (MSFC). The PTC will train the space station payload scientists, station scientists, and ground controllers to operate the wide variety of experiments that will be on-board the Freedom Space Station. The further analysis performed on the SCS study as part of task 2-Perform Studies and Parametric Analysis-of the SCS study contract is summarized. These analyses were performed to resolve open issues remaining after the completion of task 1, and the publishing of the SCS study issues report. The results of these studies provide inputs into SCS task 3-Develop and present SCS requirements, and SCS task 4-develop SCS conceptual designs. The purpose of these studies is to resolve the issues into usable requirements given the best available information at the time of the study. A list of all the SCS study issues is given. Author

N90-20118*# TRW, Inc., Huntsville, AL. System Development Div.
SPACE STATION SIMULATION COMPUTER SYSTEM (SCS) STUDY FOR NASA/MSFC. VOLUME 6: STUDY ISSUES REPORT Final Technical Report
31 Oct. 1989 85 p Prepared in cooperation with Essex Corp., Huntsville, AL and Grumann Data Systems Corp., Woodbury, NY
(Contract NAS8-37745)
(NASA-CR-183845; NAS 1.26:183845; TRW-SCS-89-T1-Vol-6)
Avail: NTIS HC A05/MF A01 CSCL 22B

The Simulation Computer System (SCS) is the computer hardware, software, and workstations that will support the Payload Training Complex (PTC) at the Marshall Space Flight Center (MSFC). The PTC will train the space station payload specialists and mission specialists to operate the wide variety of experiments that will be on-board the Freedom Space Station. This simulation Computer System (SCS) study issues report summarizes the analysis and study done as task 1-identify and analyze the CSC study issues- of the SCS study contract.This work was performed over the first three months of the SCS study which began in August of 1988. First issues were identified from all sources. These included the NASA SOW, the TRW proposal, and working groups which focused the experience of NASA and the contractor team performing the study-TRW, Essex, and Grumman. The final list is organized into training related issues, and SCS associated development issues. To begin the analysis of the issues, a list of all the functions for which the SCS could be used was created, i.e., when the computer is turned on, what will it be doing. Analysis was continued by creating an operational functions matrix of SCS users vs. SCS functions to insure all the functions considered were valid, and to aid in identification of users as the analysis progressed. The functions will form the basis for the requirements, which are currently being developed under task 3 of the SCS study. Author

N90-20119 Virginia Polytechnic Inst. and State Univ., Blacksburg.
DISCRETE-TIME CONTROL OF A SPACECRAFT WITH RETARGETABLE FLEXIBLE ANTENNAS Ph.D. Thesis
Martin Ernest Bartea France 1989 132 p
Avail: Univ. Microfilms Order No. DA8922350

The discrete-time control of a spacecraft consisting of a rigid-platform with retargetable flexible antennas is considered. The mission consists of independent minimum-time manuevers of each antenna to coincide with predetermined lines of sight, while the platform is stabilized in an inertial space and elastic vibration of the antennas is suppressed. A discrete-time approach permits consideration of the time-varying nature of the system in designing the control law. Both global and decentralized controls are proposed for a noise-free system with full-state feedback. Initially, a time-varying linear quadratic regulator (LQR) is implemented, followed by two types of decentralized controllers. First, a collocated control law is devised in which actuator forces are based on the position and velocity at the actuator locations. Next, a new method called Substructure Decentralized Control (SDC) is proposed, where each flexible substructure is controlled based on state measurements associated with the substructure modes of the separately modeled appendages. In both global and decentralized cases, a linear control law is first implemented coupled with an open-loop disturbance-accommodating control based on the known inertial disturbances caused by the maneuver. Elastic motion is next controlled using non-linear (on-off) antenna controllers for each decentralized case. For SDC, the controls translate into quantized actual controls. Lastly, nonlinear (on-off) control laws are also used to control the rigid-body motion for each case. The problem of controlling the time-varying system in the presence of noisy actuators and sensors is also examined.
Dissert. Abstr.

N90-20120*# Arinc Research Corp., Annapolis, MD.
SPACE STATION FREEDOM ELECTRIC POWER SYSTEM AVAILABILITY STUDY Final Report
Scott R. Turnquist Feb. 1990 139 p Prepared for Analex Corp., Cleveland, OH
(Contract NAS3-24564)
(NASA-CR-185181; NAS 1.26:185181; ARINC-4247-01-01-5032)
Avail: NTIS HC A07/MF A01 CSCL 22B

The results are detailed of follow-on availability analyses performed on the Space Station Freedom electric power system (EPS). The scope includes analyses of several EPS design variations, these are: the 4-photovoltaic (PV) module baseline EPS design, a 6-PV module EPS design, and a 3-solar dynamic module EPS design which included a 10 kW PV module. The analyses performed included: determining the discrete power levels that the EPS will operate at upon various component failures and the availability of each of these operating states; ranking EPS components by the relative contribution each component type gives to the power availability of the EPS; determining the availability impacts of including structural and long-life EPS components in the availability models used in the analyses; determining optimum sparing strategies, for storing space EPS components on-orbit, to maintain high average-power-capability with low lift-mass requirements; and analyses to determine the sensitivity of EPS-availability to uncertainties in the component reliability and maintainability data used. Author

N90-20121*# National Aeronautics and Space Administration. Langley Research Center, Hampton, VA.
COMPONENT COUNT AND PRELIMINARY ASSEMBLY CONSIDERATIONS FOR LARGE SPACE TRUSS STRUCTURES
W. Scott Kenner, Marvin D. Rhodes, and W. B. Fichter Feb. 1990 25 p
(NASA-TM-102604; NAS 1.15:102604) Avail: NTIS HC A03/MF A01 CSCL 22B

Expressions for the number of truss components per truss division are presented along with expressions for the area and dimensions of mosaic hexagonal panel arrangements. The expressions were developed by substituting the number of truss components in specific truss divisions into associated polynomial equations and solving for the coefficients of the polynomials. To assist in automated or astronaut truss/panel assembly operations, a concept for assembling a tetrahedral truss with hexagonal panels is presented. The assembly concept minimizes the exchange of truss assembly devices and panel attachment devices, assuming

that the number of exchanges is a driving assembly concern.
Author

N90-20122*# National Aeronautics and Space Administration. Langley Research Center, Hampton, VA.
USE OF RANDOM MARTIAN ATMOSPHERE TO EVALUATE POTENTIAL ENTRY GUIDANCE SCHEMES
Barbara S. Tomlinson and William T. Suit Jan. 1990 29 p
(NASA-TM-102606; NAS 1.15:102606) Avail: NTIS HC A03/MF A01 CSCL 22B

A random Martian atmosphere was developed and was used with three guidance schemes to determine the effect of random density variations on the guidance. This random atmosphere was shown to be useful for testing the robustness of guidance schemes for vehicles encountering random disturbances during aerobraking for capture into planetary orbit. Levels of disturbance that could be tolerated and areas where performance could be improved were established. The need for Monte Carlo studies to define the excursion boundaries of capture orbit parameters was indicated.
Author

N90-20123# Michigan Univ., Ann Arbor. Dept. of Electrical Engineering and Computer Science.
AIMING CONTROL: THEORY AND APPLICATIONS TO DYNAMIC CONTROL OF SPACE STRUCTURES Annual Report, 1 Aug. 1988 - 31 Jul. 1989
Semyon M. Meerkov 15 Jul. 1989 90 p
(Contract F49620-87-C-0079; AF Proj. 2304)
(AD-A217877; AFOSR-90-0035TR) Avail: NTIS HC A05/MF A01 CSCL 22/1

The goal of the project as a whole is the investigation of fundamental bounds on the maximal achievable precision of aiming of dynamical systems with random perturbations and application of these bounds to control of space structures. To this end, during the second year of the project the following results were obtained: it has been shown that linear systems with small additive noise can be pointed with any desired accuracy by output feedback if and only if the system is invertable and minimum phase in an approximate sense; when the measurements noise is present, the maximal achievable precision of aiming is bounded, even if the conditions mentioned above are satisfied; thus, the measurement noise has a more severe effect on the pointability of dynamical system than the input noise. In addition, the problem of residence probability control has been investigated and its relation to the problem of residence time control was analyzed. GRA

N90-20124# Naval Postgraduate School, Monterey, CA.
A SATELLITE SIMULATION PROGRAM
Rex H. Shudde Sep. 1989 58 p
(AD-A218079) Avail: NTIS HC A04/MF A01 CSCL 22/3

This report presents a satellite simulation written for the IBM PC and clones in Microsoft QuickBASIC 4.5. The program can either generate an ephemeris of satellite ground-track position and location with respect to a fixed ground station, or determine the position and time the satellite is above the horizon of a specified ground station. Provision is made for the program to handle multiple satellites and multiple ground stations. Input is either by way of the computer keyboard or by separate files for satellites and ground stations. Output is written both on the screen and to an ASCII output file which can be accessed by a data based management program. GRA

N90-20125# Air Force Inst. of Tech., Wright-Patterson AFB, OH.
DISCRETE-TIME CONTROL OF A SPACECRAFT WITH RETARGETABLE FLEXIBLE ANTENNAS Ph.D. Thesis
Martin E. France 25 May 1989 134 p
(AD-A218345; AFIT/CI/CIA-89-070) Avail: NTIS HC A07/MF A01 CSCL 22/2

The discrete time control of a spacecraft consisting of a rigid platform with retargetable flexible antennas is considered. The mission consists of independent minimum time maneuvers of each antenna to coincide with predetermined lines of sight, while the platform is stabilized in an inertial space and elastic vibration of the antennas is suppressed. The system is governed by a set of linearized time varying equations of motion. A discrete time approach permits consideration of the time varying nature of the system in designing the control law. Both global and decentralized controls are proposed for a noise free system with full state feedback. Initially, a time varying linear quadratic regulator (LQR) is implemented, followed by two types of decentralized controllers. GRA

N90-20126* National Aeronautics and Space Administration. Lyndon B. Johnson Space Center, Houston, TX.
DOCKING MECHANISM FOR SPACECRAFT Patent
Gregory A. Lange, inventor (to NASA), John P. McManamen, inventor (to NASA), and John A. Schliesing, inventor (to NASA) 30 Dec. 1988 24 p Filed 30 Dec. 1988
(NASA-Case-MSC-21386-1; US-Patent-4,858,857;
US-Patent-Appl-SN-292123; US-Patent-Class-244-161;
US-Patent-Class-244-159; US-Patent-Class-405-188;
US-Patent-Class-166-343) Avail: US Patent and Trademark Office CSCL 22B

A system is presented for docking a space vehicle to a space station where a connecting tunnel for in-flight transfer of personnel is required. Cooperable coupling mechanisms include docking rings on the space vehicle and space station. The space station is provided with a tunnel structure, a retraction mechanism, and a docking ring. The vehicle coupling mechanism is designed to capture the station coupling mechanism, arrest relative spacecraft motions while limiting loads to acceptable levels, and then realign the spacecraft for final docking and tunnel interconnection. The docking ring of the space vehicle coupling mechanism is supported by linear attentuator actuator devices, each of which is controlled by a control system which receives loading information signals and attenuator stroke information signals from each device and supplies output signals for controlling its linear actuation to attenuate impact loading or to realign the spacecraft for final docking and tunnel interconnection. The retraction mechanism is used to draw the spacecraft together after initial contact and coupling. Tunnel trunnions, cooperative with the latches on the space vehicle constitute the primary structural tie between the spacecraft in final docked configuration.
Official Gazette of the U.S. Patent and Trademark Office

N90-20066# Martin-Baker Aircraft Co. Ltd., Denham (England).
SPACECRAFT ESCAPE
B. A. Miller *In* AGARD, Implications of Advanced Technologies for Air and Spacecraft Escape Feb. 1990 7 p (For primary document see N90-20054 13-03)
Copyright Avail: NTIS HC A06/MF A01; Non-NATO Nationals requests available only from AGARD/Scientific Publications Executive

19 SPACECRAFT INSTRUMENTATION

For related information see also *06 Aircraft Instrumentation* and *35 Instrumentation and Photography.*

No abstracts in this category.

20 SPACECRAFT PROPULSION AND POWER

Includes main propulsion systems and components, e.g., rocket engines; and spacecraft auxilliary power sources.

For related information see also *07 Aircraft Propulsion and Power, 28 Propellants and Fuels, 44 Energy Production and Conversion,* and *15 Launch Vehicles and Space Vehicles.*

N90-20127*# Thiokol Corp., Brigham City, UT. Space Operations.

THIOKOL/WASATCH INSTALLATION EVALUATION OF THE REDESIGNED FIELD JOINT PROTECTION SYSTEM (CONCEPTS 1 AND 3) Final Report

M. Cook 13 Dec. 1989 45 p

(Contract NAS8-30490)

(NASA-CR-183860; NAS 1.26:183860; TWR-50138) Avail: NTIS HC A03/MF A01 CSCL 21H

The procedures, performance, and results obtained from the Thiokol Corporation/Wasatch Redesigned Field Joint Protection System (FJPS) Installation Evaluation are documented. The purpose of the evaluation was to demonstrate and develop the procedures required to install two different concepts (referred to as Concepts 1 and 3) of the redesigned FJPS. The processing capability of each configuration was then evaluated and compared. The FJPS is installed on redesigned solid rocket motors (RSRM) to protect the field joints from rain intrusion and to maintain the joint temperature sensor measurement between 85 and 122 F while the boosters are on the launch pad. The FJPS is being redesigned to reduce installation timelines at KSC and to simplify or eliminate installation processing problems related to the present design of an EPDM moisture seal/extruded cork combination. Several installation techniques were evaluated, and a preferred method of application was developed for each concept. The installations were performed with the test article in the vertical (flight) position. Comparative timelines between the two concepts were also developed. An additional evaluation of the Concept 3 configuration was performed with the test article in the horizontal position, to simulate an overhead installation on a technical evaluation motor (TEM). Author

N90-20128# Instituto de Pesquisas Espaciais, Sao Jose dos Campos (Brazil).

EXPERIMENTAL PROPOSITION ABOARD THE SECOND DATA COLLECTING SATELLITE-SCD 2 OF THE MECB [PROPOSTA DE EXPERIMENTO A BORDO DO SEGUNDO SATELITE DE COLETA DE DADOS-SCD2 DA MECB]

Gilberto MarregaSandonato, Antonio MontesFilho, Gerson Otto Ludwig, Jose Leonardo Ferreira, and Julio GuimaraesFerreira Nov. 1989 44 p In PORTUGUESE; ENGLISH summary

(INPE-4980-RPE/606) Avail: NTIS HC A03/MF A01

A proposition presented to MECB for the realization of tests of an ion thruster aboard the data collecting satellite SCD-2 is described. The study is aimed at making compatible the operational characteristics of the ion thruster to the specifications of SCD-2 satellite Author

23 CHEMISTRY AND MATERIALS (GENERAL)

N90-20129# Northwestern Univ., Evanston, IL. Dept. of Physics and Astronomy.

STUDIES OF THE STRUCTURE AND PROPERTIES OF ORGANIC MONOLAYERS, MULTILAYERS AND SUPERLATTICES

P. Dutta and J. B. Ketterson 1990 29 p

(Contract DE-FG02-84ER-45125)

(DE90-008330; DOE/ER-45125/T2) Avail: NTIS HC A03/MF A01

Organic monolayers and multilayers are both scientifically fascinating and technologically promising; they are, however, both complex systems and relatively inaccessible to experimental probes. The x ray diffraction studies are described which have given substantial new information about the structures and phase transitions in monolayers on the surface of water; use of these monolayers as a unique probe of the dynamics of wetting and spreading; and studies of monolayer mechanical properties using a simple but effective technique available to anyone using the Wilhelmy method to measure surface tension. DOE

N90-20130*# National Aeronautics and Space Administration. Lewis Research Center, Cleveland, OH.

EXPERIMENTALLY DETERMINED WEAR BEHAVIOR OF AN Al2O3-SiC COMPOSITE FROM 25 TO 1200 C

Christopher DellaCorte, Serene C. Farmer, and Patricia O. Book (Cleveland State Univ., OH.) 1990 22 p Presented at the Tribology of Composite Materials, 1-3 May 1990, Oak Ridge, TN; sponsored by ASM International

(NASA-TM-102549; E-5361; NAS 1.15:102549) Avail: NTIS HC A03/MF A01 CSCL 07A

The sliding wear behavior of a self-mated alumina-silicon carbide whisker toughened composite was studied using optical, scanning electron (SEM) and transmission electron (TEM) microscopy. Because of its excellent strength and toughness properties this composite material is under consideration for use in heat engine applications for sliding contacts which operate at elevated temperatures. The composite's wear behavior and especially its wear mechanisms are not well understood. Pin-on-disk specimens were slid in air at 2.7 m/s sliding velocity, under a 26.5-N load, at temperatures 25 to 1200 C. Pin wear increased with increasing temperature. Based upon the microscopic analyses, the wear mechanism seems to be loosening of the reinforcing whiskers due to frictional and bulk heating. This leads to whisker pullout and increased wear. Author

N90-20131# Department of Energy, Washington, DC. Materials Sciences Div.

MATERIALS SCIENCE PROGRAMS, FISCAL YEAR 1989

Mar. 1990 181 p

(DE90-008169; DOE/ER-0447P) Avail: NTIS HC A09/MF A01

The Division of Materials Sciences is located within the Department of Energy in the Office of Basic Energy Sciences. The Office of Basic Energy Sciences reports to the Director of the Office of Energy Research. The Director of this office is appointed by the President with Senate consent. The Director advises the Secretary on the physical research program; monitors the Department's R and D programs; advises the Secretary on management of the laboratories under the jurisdiction of the Department, excluding those that constitute part of the nuclear weapon complex; and advises the Secretary on basic and applied research activities of the Department. The research covers a spectrum of scientific and engineering areas of interest to the Department of Energy and is conducted generally by personnel trained in the disciplines of Solid State Physics, Metallurgy, Ceramics, Chemistry, Polymers and Materials Science. The Materials Sciences Division supports basic research on materials properties and phenomena important to all energy systems. The aim is to provide the necessary base of materials knowledge required to advance the nation's energy programs. This report contains a listing of research underway in FY 1989 together with a convenient index to the Division's programs. DOE

N90-20132# Vanderbilt Univ., Nashville, TN. Dept. of Chemistry.

QUANTUM-THEORETICAL METHODS AND STUDIES RELATING TO PROPERTIES OF MATERIALS Final Report, 1 Jun. 1986 - 30 Jun. 1989

Cari S. Ewig 19 Dec. 1989 49 p

(Grant AF-AFOSR-0146-86; AF Proj. 2303)

(AD-A217843; AFOSR-90-0126TR) Avail: NTIS HC A03/MF A01 CSCL 20/10

This research concerned the development of new ab initio

nonempirical quantum-theoretical methods and computational techniques for studying molecular properties related to those of advanced materials. Extensive computations were performed to demonstrate the quality of the theoretically predicted results. These techniques were employed to study in detail several specific molecular species, focussing on those with unusual and potentially useful energies, structures, spectra, and related properties. GRA

N90-20133* National Aeronautics and Space Administration. Ames Research Center, Moffett Field, CA.
THE 1-(DIORGANOOXYPHOSPHONYL)-METHYL)-2,4- AND -2,6-DIAMIDO BENZENES Patent
John A. Mikroyannidis, inventor (to NASA) and Demetrius A. Kourtides, inventor (to NASA) (National Academy of Sciences - National Research Council, Washington, DC.) 5 Sep. 1989 7 p Filed 28 May 1987 Division of US-Patent-4,689,421, US-Patent-Appl-SN-641152, filed 16 Aug. 1984; Continuation-in-part of US-Patent-Appl-SN-522629, filed 12 Aug. 1983, abandoned; Continuation-in-part of US-Patent-Appl-SN-493864, filed 12 May
(NASA-Case-ARC-11425-4; US-Patent-4,864,050; US-Patent-Appl-SN-054985; US-Patent-Appl-SN-641152; US-Patent-Appl-SN-522629; US-Patent-Appl-SN-493864; US-Patent-Class-558-190) Avail: US Patent and Trademark Office CSCL 07A

1-((Diorgano oxyphosphonyl) methyl)-2,4- and -2,6-dinitro and diamino benzenes are prepared by nitrating an (organophosphonyl) methyl benzene to produce the dinitro compounds which are then reduced to the diamino compounds. The organo grounds (alkyl, haloalkyl, aryl) on the phosphorus may be removed to give the free acids (HO)2P(double bond O)single bond. The diamino compounds may be polymerized with dianhydrides or diacyl halides to produce fire and flame resistant polymers which are useful in the manufacture of aircraft structures.
Official Gazette of the U.S. Patent and Trademark Office

24 COMPOSITE MATERIALS

Includes physical, chemical, and mechanical properties of laminates and other composite materials.
For ceramic materials see *27 Nonmetallic Materials.*

N90-20134# United Kingdom Atomic Energy Authority, Harwell (England). Materials Physics and Metallurgy Div.
INFILTRATION MECHANICS IN CONVENTIONAL AND HYBRIDISED FIBRE REINFORCED METAL MATRIX COMPOSITES
R. M. K. Young Nov. 1988 26 p
(AERE-R-13330) Avail: NTIS HC A03/MF A01

An analysis is presented for the prediction of the pressures required to effect the infiltration of both conventional and hybridized aligned fiber bundles, taking into account the exact meniscus configuration and the effect of entrapped gas. This allows the prediction of the existence, and size, of defects formed under particular infiltration conditions. The strength of the cohesive forces acting between the fibers during infiltration is also calculated.
Author

N90-20135*# Virginia Polytechnic Inst. and State Univ., Blacksburg. Dept. of Engineering Science and Mechanics.
INNOVATIVE DESIGN OF COMPOSITE STRUCTURES: THE USE OF CURVILINEAR FIBER FORMAT TO IMPROVE BUCKLING RESISTANCE OF COMPOSITE PLATES WITH CENTRAL CIRCULAR HOLES Report, 16 Feb. - 15 Aug. 1989
M. W. Hyer and H. H. Lee Mar. 1990 28 p
(Grant NAG1-901)
(NASA-CR-186454; NAS 1.26:186454; VPI-E-90-05) Avail: NTIS HC A03/MF A01 CSCL 11D

The gains in buckling performance are explored that can be achieved by deviating from the conventional straightline fiber format and considering the situation whereby the fiber orientation in a layer, or a group of layers, can vary from point to point. The particular situation studied is a simply supported square plate with a centrally located hole loaded in compression. By using both a sensitivity analysis and a gradient-search technique, fiber orientation in a number of regions of the plate are selected so as to increase the buckling load relative to baseline straightline designs. The sensitivity analysis is used to determine which regions of the plate have the most influence on buckling load, and the gradient search is used to find the design that is believed to represent the absolute maximum buckling load for the conditions prescribed. Convergence studies and sensitivity of the final design are discussed. By examining the stress resultant contours, it is shown how the curvilinear fibers move the load away from the unsupported hole region of the plate to the supported edges, thus increasing the buckling capacity. The tensile capacity of the improved buckling design is investigated, and it is shown that both tensile capacity and buckling capacity can be improved with the curvilinear fiber concept.
Author

N90-20136*# Virginia Polytechnic Inst. and State Univ., Blacksburg. Dept. of Engineering Science and Mechanics.
INNOVATIVE DESIGN OF COMPOSITE STRUCTURES: THE USE OF CURVILINEAR FIBER FORMAT IN COMPOSITE STRUCTURE DESIGN Report, 16 Aug. 1988 - 15 Feb. 1989
M. W. Hyer and R. F. Charette (Naval Ship Research and Development Center, Bethesda, MD.) Mar. 1990 18 p
(Grant NAG1-901)
(NASA-CR-186453; NAS 1.26:186453; VPI-E-90-04) Avail: NTIS HC A03/MF A01 CSCL 11D

The gains in structural efficiency are investigated that can be achieved by aligning the fibers in some or all of the layers in a laminate with the principal stress directions in those layers. The name curvilinear fiber format is given to this idea. The problem studied is a plate with a central circular hole subjected to a uniaxial tensile load. An iteration scheme is used to find the fiber directions at each point in the laminate. Two failure criteria are used to evaluate the tensile load capacity of the plates with a curvilinear format, and for comparison, counterpart plates with a conventional straightline fiber format. The curvilinear designs for improved tensile capacity are then checked for buckling resistance. It is concluded that gains in efficiency can be realized with the curvilinear format.
Author

N90-20137*# National Aeronautics and Space Administration. Langley Research Center, Hampton, VA.
A STUDY OF PHYSICAL PROPERTIES OF ODPA-p-PDA POLYIMIDE FILMS
Jag J. Singh, Abe Eftekhari (Analytical Services and Materials, Inc., Hampton, VA.), and Terry L. St.Clair Mar. 1990 17 p
(NASA-TM-102625; NAS 1.15:102625) Avail: NTIS HC A03/MF A01 CSCL 11D

Physical properties were investigated of ODPA-p-PDA polyimide films, including their lower molecular weight versions with phthalimide endcaps. Free volume, determined by low energy positron annihilation in the test films, was the major parameter of interest since all other physical properties are ostensibly related to it. It affects the dielectric constant as well as the saturation moisture pickup of the test films. An empirical relation was developed between the free volume and molecular weight of the test films, comparable to the Mark-Houwink relation between the polymer solution viscosity and the molecular weight. Development of such a relation constitutes a unique achievement since it enables researchers to estimate the molecular weight of an intractable polymer in solid state for the first time.
Author

N90-20138*# National Aeronautics and Space Administration. Lewis Research Center, Cleveland, OH.
COMPOSITE LAMINATE TAILORING WITH PROBABILISTIC CONSTRAINTS AND LOADS
P. B. Thanedar and C. C. Chamis 1990 18 p Presented at the Energy Technology Conference and Exhibition, New Orleans, LA, 14-18 Jan. 1990; sponsored by ASME
(NASA-TM-102515; E-5182; NAS 1.15:102515) Avail: NTIS HC A03/MF A01 CSCL 11D

A reliability-based structural synthesis procedure was developed

to tailor laminates to meet reliability-based (ply) strength requirements and achieve desirable laminate responses. The main thrust is to demonstrate how to integrate the optimization technique in the composite laminate tailoring process to meet reliability design requirements. The question of reliability arises in fiber composite analysis and design because of the inherent scatter that is observed in the constituent (fiber and matrix) material properties during experimentation. Symmetric and asymmetric composite laminates subject to mechanical loadings are considered as application examples. These application examples illustrate the effectiveness and ease with which reliability considerations can be integrated in the design optimization model for composite laminate tailoring. Author

N90-20139*# National Aeronautics and Space Administration. Lewis Research Center, Cleveland, OH.
EVALUATION OF THERMAL AND MECHANICAL LOADING EFFECTS ON THE STRUCTURAL BEHAVIOR OF A SiC/TITANIUM COMPOSITE
Joseph E. Grady and Bradley A. Lerch Apr. 1990 15 p Presented at the 31st Structures, Structural Dynamics and Materials Conference, Long Beach, CA, 2-4 Apr. 1990; sponsored in part by AIAA, ASME, ASCE, AHS, and ASC
(NASA-TM-102536; E-5349; NAS 1.15:102536) Avail: NTIS HC A03/MF A01 CSCL 11D

Composite specimens of titanium-15-3 matrix reinforced with continuous SCS-6 silicon carbide fibers were tested under a variety of thermal and mechanical loadings. A combined experimental/finite element approach was used to estimate the effective in-situ modulus of the matrix material and to evaluate changes in modulus due to the applied loads. Several fiber orientations were tested. Results indicate that the effect of the thermal loads on composite stiffness varies with fiber orientation. Applications of this method to test specimens damaged by uniaxial tension, thermal cycling, and isothermal fatigue loadings are used to illustrate that by monitoring overall structural behavior, changes in stiffness caused by thermomechanical loading can be detected. Author

N90-20140# Rensselaer Polytechnic Inst., Troy, NY.
COMPENDIUM OF ABSTRACTS AND VIEWGRAPHS. Report, for 1 Dec. 1988 - 30 Nov. 1989
R. J. Diefendorf 30 Nov. 1989 549 p Presented at the 2nd International Workshop on Composite Materials and Structures for Rotorcraft, Troy, NY, 14-15 Sep. 1989
(Contract DAAL03-89-G-0003)
(AD-A217189; ARO-26588.1-EG-CF) Avail: NTIS HC A23/MF A03 CSCL 11/4

A workshop was conducted, dealing with the fundamentals of composite constituent materials and laminates as they influence applications to advanced rotorcraft developments. Included in the purview of the workshop were the theory, numerical analysis, fabrication, testing, and inspection of thermoset and thermoplastic resin matrix and metal matrix composites as they may have advantage for rotors, fixed airframe, drive system, controls, and engine cold section components. GRA

N90-20141# Naval Ship Research and Development Center, Bethesda, MD. Ship Materials Engineering Dept.
THROUGH-THICKNESS STRAIN RESPONSE OF THICK COMPOSITES IN COMPRESSION Report, Aug. 1987 - Aug. 1989
Eugene T. Camponeschi, Jr. 5 Sep. 1989 40 p
(AD-A217233; DTRC/SME-89-67) Avail: NTIS HC A03/MF A01 CSCL 11/4

With the continued success of composite materials in high performance structures, new applications for Navy primary structures are being identified. Many of these applications require designs with composite materials having section thicknesses greater than those that have been used and studied to date. Along with this interest in thick composite structures comes the need for full three-dimensional stress analysis. The limits and accuracy of existing three-dimensional data bases will dictate the limit and accuracy of corresponding analyses. This report summarizes an investigation of the through-thickness strain response of thick composite materials subjected to compressive loading. One-half inch thick (96 ply) carbon and S2 glass reinforced composites were studied. A thick-section compression test method was developed for the purpose of this investigation. Using this test method the longitudinal and through-thickness strain to failure, longitudinal modulus, inplane and through-thickness Poisson's ratio, and ultimate strength of these materials was determined. The through-thickness data from the 96 ply 0 coupons show the materials to be transversely isotropic. The through-thickness data from 96 ply 0/0/90 laminates show good correlation with a theoretical solution that provides the nine elastic constants for thick orthotropic plates. GRA

N90-20142# Naval Ship Research and Development Center, Bethesda, MD. Ship Materials Engineering Dept.
COMPRESSION TESTING OF THICK-SECTION COMPOSITE MATERIALS Report, Sep. 1987 - Sep. 1989
E. T. Camponeschi, Jr. 1 Oct. 1989 42 p
(AD-A217234; DTRC/SME-89-73) Avail: NTIS HC A03/MF A01 CSCL 11/4

Interest in the compressive response of fiber-reinforced composite materials has resulted in numerous research programs addressing the theoretical and experimental response of composites subjected to compressive loading. These research programs have dealt exclusively with the response of composite materials 6.4 mm (0.25 inches) in thickness and less. As composite materials become more attractive for use in large Navy structures, the need to understand the mechanical response of composites greater than 6.4 mm (0.25 inches) in thickness becomes a necessity. In this program a compression test fixture that allows the testing of composites up to one inch thickness and greater was designed and refined. This fixture was used to evaluate the effects of constituents, fiber orientation, and thickness on the compressive response of composite materials. In addition the fixture was used to determine if the failure mechanisms observed for thick composites are similar to those that have been observed and reported for composite materials less than 6.4 mm (0.25 in.) thick. The strength, stiffness, and failure characteristics of 48 ply, 96 ply and 192 ply carbon/epoxy and S2 glass/epoxy are discussed. Unidirectional and (O/O/90) style laminates have been investigated. The thickness of the 96 and 192 ply coupons allows the direct measurement of NU13 for the constituents and orientations listed above and this data is also reported. GRA

N90-20143# Michigan Univ., Ann Arbor. Dept. of Chemical Engineering.
SUMMARY REPORT OF THE SUMMER CONFERENCE OF THE DARPA-MATERIALS RESEARCH COUNCIL Report, 1 May 1987 - 30 Apr. 1990
M. J. Sinnott 4 Aug. 1989 356 p Conference held in La Jolla, CA, 10 Jul. - 4 Aug. 1989
(Contract N00014-87-G-0217; DARPA Order 6029)
(AD-A217380) Avail: NTIS HC A16/MF A02 CSCL 05/2

The proceedings are presented for the conference. Some of the contents are: Fundamentals of Manufacturing Advanced Materials; DARPA Initiative to Establish a U.S. Base for Multi-Chip Module Substates; U.S. Competitiveness in Ceramics; Mathematical Modeling; Designing with Advanced Composites; The Fracture Energy of Metal/Ceramic Interfaces; Twin Induced Toughening in Gamma TiAL; The Critical Reinforcement Size for the Avoidance of Matrix Cracking; Advanced Composites with Improved Compressive Properties; Coatings for Fiber Reinforced Intermetallics; Interatomic Potentials; Refractory Compounds; Limitations of Processing Future VLSI Circuits; Advanced Packaging for Digital Silicon and GaAs; Sensors in Semiconductor Device Processing; Advanced Acoustic Sensors; Energetic Materials; Biomimetric Design; Neural Networks and Cellular Automata; Electrochemical Power Sources; Magnetic and Magnetoopitcal Recording; Photonic Manufacturing; Biotechnology; Jet Engines; Relative Reaction Rates of Methane Versus Acetylene in the

Formation of C-13 Diamonds Films; Spectral Emissivities of Liquid Transition Metals as Functions of Temperature and wavelengths; and Advanced Systems for Adsorption of Toxic Gases. GRA

N90-20144# Auburn Univ., AL. Dept. of Mechanical Engineering.
OPTIMIZATION OF FRACTURE RESISTANCE IN COMPOSITES Final Report, 30 Sep. 1986 - 14 Mar. 1990
Bor Z. Jang, Jeff Suhling, Bruce Valaire, and Ralph H. Zee 21 Dec. 1989 25 p
(Contract DAAL03-86-G-0211)
(AD-A217431; ARO-24804.26-MS) Avail: NTIS HC A03/MF A01 CSCL 11/4

An interdisciplinary approach was taken to investigate structure property relationships in fibrous composites subjected to various stress states and environmental conditions. The ultimate goal was to reinforce the ability to optimize the fracture resistance in composites. The concept of controlled interlaminar bonding (CIB) was proposed and evaluated as a possible approach of improving the impact energy-absorbing capability or the damage tolerance in composites. Thickness-direction fibers, as introduced by stitching or braiding, can improve the interlaminar shear strength and interlaminar fracture toughness, thereby reducing or suppressing delamination in advanced composites. Failure mechanisms in the composites subjected to impact loading were investigated. The most critical material parameters that dictate the impact penetration resistance of composites were identified. Failure mechanisms of hybrid composites were studied as a ballistic impact study was developed. The effect of residual thermal stresses on the impact response of composites was measured. New techniques for determining residuals stresses and internal damages in composites were discussed. A new energy-based fracture criterion for composites was proposed. Equations for determining the strain energy densities in composites under various loading modes were derived. A new way of determining the stress intensity factor in composite was developed, and applications of the J-integral approach to composites fracture problems are discussed. GRA

N90-20145# Institute for Defense Analyses, Alexandria, VA.
SUMMARY OF THE DoD METAL MATRIX COMPOSITES (MMC) STEERING COMMITTEE MEETING, HOSTED BY THE INSTITUTE FOR DEFENSE ANALYSIS Final Report
Michael A. Rigdon and Donald Groves Nov. 1989 204 p Meeting held in Alexandria, VA, 5-6 Oct. 1989
(Contract MDA903-84-C-0031)
(AD-A217611; AD-E501190; IDA-D-696; IDA/HQ-89-34987)
Avail: NTIS HC A10/MF A02 CSCL 11/4

Metal Matrix Composites (MMC) exhibit a number of properties that make these materials attractive candidates for use in advanced Department of Defense and Strategic Defense Initiative systems. Because of this potential it has been the practice of the various government agencies involved in metal matrix composites research and development to convene meetings periodically in order to discuss the nature and progress of the MMC work being carried on. The proceedings are presented of such a meeting in which two current aspects, the agency programs and funding and systems transitions/applications, were addressed. GRA

N90-20146# Systran Corp., Dayton, OH.
OPTIMIZATION OF LAMINATED COMPOSITE PLATES Final Report, Sep. 1988 - Aug. 1989
Antonio Miravete Sep. 1989 190 p
(Contract F33615-88-C-5402)
(AD-A217621; WRDC-TR-89-4107) Avail: NTIS HC A09/MF A01 CSCL 11/4

Optimal laminate configurations for laminated rectangular plates under transverse and buckling loads are investigated. Laminate thickness and fiber orientation are treated as design variables, the thickness laminate being variable along the plate. A fully stressed iterative procedure and a quadratic failure criterion were applied in order to get the minimum weight plate using strength as a design criterion. A finite element method accounting for in-plane and interlaminar stresses was used. Results for thin and thick plates, different boundary conditions and some types of loading are shown. GRA

N90-20147# California Univ., Berkeley. Lawrence Berkeley Lab. Materials and Chemical Sciences Div.
SYNTHESIS OF ALUMINA-COATED SiC WHISKERS FOR PRODUCTION OF SiC WHISKER-REINFORCED ALUMINA COMPOSITE MATERIALS M.S. Thesis
David Kapolnek Dec. 1989 59 p Prepared in cooperation with California Univ., Berkeley
(Contract DE-AC03-76SF-00098)
(DE90-007778; LBL-28263) Avail: NTIS HC A04/MF A01

Thick coatings of hydrated basic aluminum sulfate, an alumina precursor, were precipitated on the surfaces of SiC whiskers from an aqueous solution. These coatings were then thermally decomposed to obtain alumina coatings on the SiC whiskers. Both high aspect ratio as-received SiC whiskers and reduced aspect ratio whiskers were used as core particles in the coating process. SiC content in the composite powders was controlled by either varying the amount of SiC whiskers that were added to the original coating solution, or by using multiple coating steps in the original SiC core particles. Coated whiskers were characterized before and after calcination using scanning electron microscopy and x ray diffraction. Samples of these composite powders were hot-pressed at 1600 C and 35 MPA pressure to obtain dense SiC whiskers-reinforced alumina composite materials. Polished surfaces of these composites were observed using optical microscopy and SEM to qualitatively analyze whisker distribution in the matrix and residual porosity in the material. In all composites using reduced aspect ratio whiskers, whisker distribution was uniform throughout the material, and residual porosity was very low. Fracture surfaces of some materials were observed in SEM, showing that a limited amount of whisker pull-out had occurred. DOE

N90-20148# California Univ., Berkeley. Lawrence Berkeley Lab. Materials and Chemical Sciences Div.
SYMPOSIUM ON HIGH TEMPERATURE AND MATERIALS CHEMISTRY
Gerd M. Rosenblatt Oct. 1989 252 p Symposium held in Berkeley, CA, 24-25 Oct. 1989
(Contract DE-AC03-76SF-00098)
(DE90-008047; LBL-27905; CONF-8910302-1) Avail: NTIS HC A12/MF A02

This volume contains the written proceedings of the Symposium on High Temperature and Materials Chemistry held in Berkeley, California on October 24 to 25, 1989. The Symposium was sponsored by the Materials and Chemical Sciences Division of Lawrence Berkeley Laboratory and by the College of Chemistry of the University of California at Berkeley to discuss directions, trends, and accomplishments in the field of high temperature and materials chemistry. Its purpose was to provide a snapshot of high temperature and materials chemistry and, in so doing, to define status and directions. DOE

N90-20149# Oak Ridge National Lab., TN.
CHARACTERIZATION OF CERAMIC MATRIX COMPOSITES FABRICATED BY CHEMICAL VAPOR INFILTRATION
D. P. Stinton, D. M. Hembree, Jr., K. L. More, B. W. Sheldon, and T. M. Besmann 1989 8 p Presented at the Materials Research Society Fall Meeting, Boston, MA, 27 Nov. - 2 Dec. 1989
(Contract DE-AC05-84OR-21400)
(DE90-008409; CONF-891119-107) Avail: NTIS HC A02/MF A01

A process for the preparation of fiber-reinforced SiC composites by chemical vapor deposition has been developed at Oak Ridge National Laboratory. Composites are prepared by infiltrating fibrous preforms with reactant gases that decompose at elevated temperatures to deposit silicon carbide between and around the fibers. Because the infiltration process utilizes both temperature and pressure gradients, SiC is deposited under conditions that vary considerably from the hot face to the cool face of the

composite. Matrix characterization of composite samples by transmission electron microscopy and Raman spectroscopy are described. DOE

N90-20150# Brookhaven National Lab., Upton, NY. Materials Science Div.
EXTENDED X RAY ABSORPTION FINE STRUCTURE ANALYSIS APPLIED TO COMPOSITE MATERIALS
Benji Maruyama, Enrique V. Barrera, Richard K. Everett (Naval Research Lab., Washington, DC.), and Steve M. Heald 1990 10 p Presented at the International Conference on Composite Interfaces, Cleveland, OH, 21-24 May 1990
(Contracts DE-AC02-76CH-00016; DE-AC05-80ER-10742)
(DE90-008575; BNL-43876; CONF-9005133-1) Avail: NTIS HC A02/MF A01

Extended X ray Absorption Fine Structure (EXAFS) is a spectroscopic technique which allows the determination of the atomic structure of materials. EXAFS can be used to determine nearest neighbor identity, coordination number, interatomic distance and degree of disorder, and therefore is particularly useful for investigation of the atomistic structure of composite interfaces. Using EXAFS and related techniques, the structure of an interface can be investigated in a non-destructive manner. After a brief description of the EXAFS technique, its utility will be demonstrated through a study of vanadium barriers at aluminum-graphite interfaces. It is found that the vanadium reacts strongly, forming vanadium oxide and carbide, while little unreacted metallic vanadium remains. DOE

N90-20151*# National Aeronautics and Space Administration. Lewis Research Center, Cleveland, OH.
FUNDAMENTAL ASPECTS OF AND FAILURE MODES IN HIGH-TEMPERATURE COMPOSITES
Christos C. Chamis and Carol A. Ginty 1990 16 p Presented at the 35th International SAMPE Symposium and Exhibition, Anaheim, CA, 2-5 Apr. 1990
(NASA-TM-102558; E-5378; NAS 1.15:102558) Avail: NTIS HC A03/MF A01 CSCL 11D

Fundamental aspects of and attendant failure mechanisms for high temperature composites are summarized. These include: (1) in-situ matrix behavior; (2) load transfer; (3) limits on matrix ductility to survive a given number of cyclic loadings; (4) fundamental parameters which govern thermal stresses; (5) vibration stresses; and (6) impact resistance. The resulting guidelines are presented in terms of simple equations which are suitable for the preliminary assessment of the merits of a particular high temperature composite in a specific application. Author

N90-20152# Army Lab. Command, Watertown, MA. Material Technology Lab.
OXYGEN CONCENTRATIONS ON SURFACES OF CARBON FIBERS Final Report
Sin-Shong Lin Nov. 1989 18 p
(AD-A217724; MTL-TR-89-99) Avail: NTIS HC A03/MF A01 CSCL 11/2

Performance of carbon fiber reinforced composites depends significantly on the interface between the fiber surfaces and the resin matrix. Good adhesion is a precondition for the intended transfer of stresses in the fiber polymer composites. For carbon fibers, the oxidized surface treatment is a widely accepted method used to achieve good adhesion. Five pitch/polyacrylonitrile-based carbon fibers were surface treated with various chemical agents such as nitric acid, peroxide, oxygen, and acid/hydrogen. The oxidized surfaces were characterized by scanning electron microscopy (SEM), x ray photoelectron spectroscopy (XPS), and Auger spectroscopy for surface morphology, carbon-oxygen functional groups, and oxygen distributions. In particular, scanning Auger microanalysis was extensively employed for the detailed determinations of oxygen distributions on the fiber surfaces. These results indicate that the formation of oxides on the fiber surfaces vary widely from region-to-region, segment-to-segment, and strand-to-strand. The available amounts of surface oxides are dependent on the fiber structure, as well as the precursors. GRA

N90-20153# MSNW, Inc., San Marcos, CA.
DETERMINATION OF FUNDAMENTAL THERMODYNAMIC PROPERTIES OF CONSTITUENT MATERIALS AND PERFORMANCE SCREENING OF CANDIDATE SYSTEMS Final Report, Oct. 1987 - Dec. 1988
John T. Porter and G. H. Reynolds May 1989 82 p
(Contract F33615-88-C-5401; AF Proj. 2420)
(AD-A218089; WRDC-TR-89-4035) Avail: NTIS HC A05/MF A01 CSCL 11/4

The Phase 1 results of a program directed at a validation of thermochemical modeling, combined with selection supplemental experimental techniques, as a basis for screening materials for application in ultra-high temperature composites are presented. The experimental techniques employed were laser probe spectroscopy and high temperature mass spectroscopy. Representative candidate constituents, drawn from oxides, carbides, borides, and intermetallics, were assessed under neutral and oxidizing conditions. The modeling approach can, in most cases, define probable limits for material stability. The experimental approaches provide a useful supplement to available data. Improved sensitivity in the laser spectroscopic measurement would be useful and the mass spectrometric technique would benefit from extended pressure sampling capability and reduced cell/heater interactions. GRA

25 INORGANIC AND PHYSICAL CHEMISTRY

Includes chemical analysis, e.g., chromatography; combustion theory; electrochemistry; and photochemistry.

For related information see also *77 Thermodynamics and Statistical Physics.*.

N90-20154* National Aeronautics and Space Administration. Langley Research Center, Hampton, VA.
ISOTOPE EXCHANGE IN OXIDE-CONTAINING CATALYST Patent
Kenneth G. Brown, inventor (to NASA), Billy T. Upchurch, inventor (to NASA) (Chemicon Corp., Virginia Beach, VA.), Robert V. Hess, inventor (to NASA), Irvin M. Miller, inventor (to NASA), David R. Schryer, inventor (to NASA), Barry D. Sidney, inventor (to NASA), George M. Wood, inventor (to NASA), and Ronald F. Hoyt, inventor (to NASA) 13 Jun. 1989 5 p Filed 15 Jan. 1988
(NASA-Case-LAR-13542-2-SB; US-Patent-4,839,330; US-Patent-Appl-SN-145719; US-Patent-Class-502-53; US-Patent-Class-204-157.51; US-Patent-Class-372-59; US-Patent-Class-502-38; US-Patent-Class-502-339; US-Patent-Class-502-352) Avail: US Patent and Trademark Office CSCL 07D

A method of exchanging rare-isotope oxygen for common-isotope oxygen in the top several layers of an oxide-containing catalyst is disclosed. A sample of an oxide-containing catalyst is exposed to a flowing stream of reducing gas in an inert carrier gas at a temperature suitable for the removal of the reactive common-isotope oxygen atoms from the surface layer or layers of the catalyst without damaging the catalyst structure. The reduction temperature must be higher than any at which the catalyst will subsequently operate. Sufficient reducing gas is used to allow removal of all the reactive common-isotope oxygen atoms in the top several layers of the catalyst. The catalyst is then reoxidized with the desired rare-isotope oxygen in sufficient quantity to replace all of the common-isotope oxygen that was removed.

Official Gazette of the U.S. Patent and Trademark Office

N90-20155# Max-Planck-Inst. fuer Stroemungsforschung, Goettingen (Germany, F.R.).
EXPERIMENTAL INVESTIGATION OF THE THERMOCAPILLARY MIGRATION OF WATER DROPLETS IN BUTYLBENZOATE Thesis [EXPERIMENTELLE UNTERSUCHUNG DER THERMOKAPILLAREN BEWEGUNG VON WASSERTROPFEN IN BUTYLBENZOAT]
M. Haehnel Jun. 1988 65 p In GERMAN
(MPIS-14/1988; ISSN-0436-1199; ETN-90-95330) Avail: NTIS HC A04/MF A01; Max-Planck Institut fuer Stroemungsforschung, Bunsenstrasse 10, D-3400 Goettingen, Fed. Republic of Germany, 28 DM

The migration of single water droplets in the vertical temperature field of the matrix fluid butylbenzoate was investigated using an arrangement for the perturbation-free droplet production, removal by section, and a suitable measuring cell. The dependence of the reciprocal droplet diameter on the deviation of the droplets was calculated. The deviation from the linear relation increases for stronger temperatures. The vertical position of droplets of several diameters confirms the thermocapillary convection found by Delitzsch et al. ESA

N90-20156# Air Force Academy, CO.
CONDENSED PHASE KINETIC DEUTERIUM ISOTOPE EFFECTS IN HIGH ENERGY PHENOMENA: MECHANISTIC INVESTIGATIONS AND RELATIONSHIPS Technical Report, Jan. 1975 - Dec. 1989
Scott A. Shackelford Dec. 1989 52 p Presented at the NATO Advanced Study Inst. on Chemistry and Physics of the Molecular Processes in Energetic Materials, Attaville Milicia, Italy, 3-15 Sep. 1989
(AF Proj. 2303)
(AD-A217161; FJSRL-TR-89-0010) Avail: NTIS HC A04/MF A01 CSCL 07/4

The rate-controlling mechanistic step of an energetic material's condensed phase thermochemical decomposition process is determined directly using the kinetic deuterium isotope effect (KDIE) approach. The KDIE is used with isothermal DSC and isothermal TGA analyses of TNT, HNBB, TATB, RDX, HMX, and their deuterium labeled analogs. The decomposition processes' rate-controlling step possibly can change as the energetic material physical state varies. The condensed phase KDIE approach that determines the rate-controlling mechanistic step in a slow thermochemical decomposition process, can be extended into the progressively more drastic high energy regimes encountered with the rapid pyrolytic decomposition/deflagration process, plus the higher temperature/pressure combustion, thermal explosion, and detonation events. The KDIE determined mechanistic relationships between the slow thermochemical decomposition process and more hostile high energy events are individually described for HMX, RDX, TATB, and TNT. GRA

N90-20157# Case Western Reserve Univ., Cleveland, OH.
ELECTROCHEMICAL PHASE DIAGRAMS FOR AQUEOUS REDOX SYSTEMS Final Report, 1 Aug. 1986 - 31 Jul. 1989
John C. Angus, Michael J. Zappia, and Rebecca C. Yung 22 Dec. 1989 29 p
(Contract DAAL03-86-K-0062)
(AD-A217168; ARO-23359.1-MS) Avail: NTIS HC A03/MF A01 CSCL 07/4

A completely new phase diagram, the electron number diagram, has been developed for aqueous redox systems. The electron number diagram is a transformed potential-pH diagram in which potential is replaced by its thermodynamic conjugate, the number of electrons. The relationship between electron number diagrams and potential-pH diagrams, which provide complementary information, is explained in thermodynamic and geometric terms. Electron number diagrams show similarities to metallurgical T-x diagrams. Because electron number is a conserved quantity, material balances can be performed on electron number diagrams, and process trajectories can be followed. The mass and electron balance equations are derived, and electron number diagrams are used to illustrate a variety of process trajectories. The diagrams are of particular value in describing the complex phase chemistry involved in aqueous corrosion, hydrometallurgical ore processing, nuclear waste disposal, geochemical processes and some fuel sulfur removal processes. A detailed thermodynamic analysis of complex aqueous redox systems was the basis for algorithms for construction of generalized chemical potential diagrams, potential-pH diagrams and electron number diagrams. Computer programs were used to construct diagrams for a variety of systems, including the following which include two active redox elements: the aqueous U-C, Cd-Te and Ga-As systems. GRA

N90-20158# Connecticut Univ., Storrs. Liquid Crystalline Polymer Research Center.
RIGID ROD MOLECULES AS LIQUID CRYSTAL THERMOSETS Interim Technical Report No. 36
Andrea E. Hoyt, Brian Benicewicz, and Samuel J. Huang 29 Jan. 1990 18 p Submitted for publication
(Contract N00014-86-K-0772)
(AD-A217573; TR-36) Avail: NTIS HC A03/MF A01 CSCL 07/6

Rigid rod molecules endcapped with conventional crosslinking groups such as maleimide and nadimide were prepared and studied by differential scanning calorimetry and hot stage polarized light microscopy. Nematic liquid crystalline phases were identified in several of the new monomers. Thermally induced polymerization occurred in the nematic phase region and resulted in retention of the nematic texture in the final crosslinked solid. In many cases, isotropization was not observed at normal heating rates due to crosslinking and solidification in the nematic phase. GRA

N90-20159# Colorado State Univ., Fort Collins. Dept. of Mechanical Engineering.
STRUCTURE OF MODEL GAS FLAMES IN NITRAMINES Final Technical Report, 1 Oct. 1988 - 30 Nov. 1989
Melvyn C. Branch Dec. 1989 14 p
(Grant AF-AFOSR-0331-88; AF Proj. 2308)
(AD-A217578; AFOSR-90-0116TR) Avail: NTIS HC A03/MF A01 CSCL 21/9

The current status of studies undertaken of model gas phase flames associated with the combustion of nitramine based solid rocket propellants is summarized. These studies consist of measurements of the structure of stable and unstable species concentration profiles and temperature in laminar, premixed, flat flames of fuel nitrogen oxide mixtures at low pressure. The experimental measurements are then compared to calculations of the concentration profiles using a one dimensional flame code which models the transport processes and chemistry of the flame. The transport processes include species diffusion and thermal conduction through the flame and the chemistry is modeled by a detailed chemical kinetic reaction mechanism. The flames which were studied thus far are supplied with Methane, CH2O or CO as fuel and NO2, N2O or O2 as oxidizer. The overall characteristics of the flames are presented in the paper and the preliminary conclusions of the flame modeling are discussed. GRA

N90-20160# Princeton Univ., NJ. Dept. of Chemistry.
MECHANISMS OF REACTIVE ETCHING Final Technical Report, 1 May 1985 - 30 Jun. 1989
Steven L. Bernasek Dec. 1989 14 p
(Grant AF-AFOSR-0209G-85; AF Proj. 2303)
(AD-A217679; AFOSR-90-0122TR) Avail: NTIS HC A03/MF A01 CSCL 07/4

Several aspects of the surface chemistry of electronic materials are addressed. COF2 was shown to be an effective thermal and photochemical etchant of Si and SiO2. A general purpose molecular beam scattering apparatus was constructed to investigate the mechanism of COF2 etching of Si. H2 and CH4 scattering from the FE (111) surface was studied in order to characterize the operation of this system. Dynamics of van der Waals bound clusters interacting with solid surfaces were investigated. Deposition of metallic layers from organometallic precursors was also studied. GRA

N90-20161# Sandia National Labs., Albuquerque, NM. Inorganic Materials Chemistry Div.
HYDROUS METAL OXIDE-SUPPORTED CATALYSTS. PART 1: PREPARATION CHEMISTRY AND PHYSICAL AND CHEMICAL PROPERTIES
R. G. Dosch, H. P. Stephens, F. V. Stohl, B. C. Bunker, and C. H. Peden Feb. 1990 89 p
(Contract DE-AC04-76DP-00789)
(DE90-007607; SAND-89-2399) Avail: NTIS HC A05/MF A01

This report describes the development of the following new catalytic materials based on hydrous metal oxide (HMO) ion exchange materials: Na-Ti, Nb, Zr, and mixtures of hydrated silica with hydrous Ti-oxide. HMO's provide a versatile system for the preparation of heterogeneous catalysts. The preparation chemistry allows synthesis of catalysts that can be tailored to particular processes with respect to both chemical and physical properties. Bulk catalysts with surface areas over 300 sq m/g and pore volumes up to 0.4 cc/g as well as thin films of the HMO materials can be prepared on supports having a wide range of catalytically important physical properties. This report, the first of two parts, presents research performed to date regarding the preparation chemistry, and physical and chemical properties of HMO materials which may be used to develop heterogeneous catalysts for direct coal liquefaction processes. During the course of this work, new ideas for research areas relative to direct coal liquefaction were briefly explored. Two of them that merit further work, catalyst-anchored hydrogen donors and alkoxide-derived crystalline titanate compounds, are briefly described. DOE

N90-20162# Sandia National Labs., Albuquerque, NM. Solar Thermal Collector Technology Div.
DEVELOPMENTS IN SOLAR PHOTOCATALYSIS FOR DESTRUCTION OF ORGANICS IN WATER
James E. Pacheco, Cliff Carwile, Kimberly A. Magrini, and Mark Mehos (Midwest Research Inst., Golden, CO.) 1989 10 p Presented at the 16th Annual Waste Management Symposium: Working Towards A Cleaner Environment, Tucson, AZ, 25 Feb. - 1 Mar. 1990
(Contract DE-AC04-76DP-00789)
(DE90-007685; SAND-89-2236C; CONF-900210-23) Avail: NTIS HC A02/MF A01

A process is being developed that has the potential to destroy a wide range of organic contaminants in water using solar energy and a titanium dioxide photocatalyst, TiO2. Contaminated water flows through a reactor on which sunlight is focused to activate the catalyst forming hydroxyl radicals and super oxide ions. These reactive species readily attack and decompose organics in solution producing only water, CO2 and halo acids. Tests were conducted at three levels: at a benchtop scale (liter), with a small outdoor trough (100 liters) and with a large outdoor parabolic trough (2000 liters). The experimental variables examined include ultraviolet light intensity, catalyst loading, the effect of adding hydrogen peroxide, and the performance of catalyst supports. The intensity of ultraviolet irradiation significantly affected decomposition rates of a chlorinated solvent, trichloroethylene (TCE) yielding faster reaction rates at higher intensities. The amount of catalyst in suspension affected the destruction rate of trichloroethylene; the rate increased as the amount of catalyst was increased from 0.01 to 0.1 wt percent. Hydrogen peroxide used in conjunction with TiO2 significantly enhanced the photocatalytic decomposition rate of a model compound, salicylic acid, by as much as 8 times over the rate with TiO2 alone. Supported TiO2 on silica glass beads performed less effectively compared to suspended TiO2 for TCE decomposition with simulated sunlight as did TiO2 on alumina ceramic frits for decomposing salicylic acid in natural sunlight. TiO2 on fiberglass mesh performed about as well as the ceramic frits. DOE

N90-20163# Florida Univ., Gainesville. Dept. of Chemistry.
THE GLOW DISCHARGE AS AN ATOMIZATION AND IONIZATION SOURCE Technical Progress Report
1990 5 p
(Contract DE-FG05-89ER-14018)
(DE90-007693; DOE/ER-14018/1) Avail: NTIS HC A01/MF A01

This is to summarize the research progress in this project at the University of Florida over the past 13 months. In keeping with the directions of the Federal Demonstration Project, the report will be brief, presenting an overview of the major findings. The study of the glow discharge, primarily as an ionization source for elemental analysis was continued. Glow discharge interest continues to grow in the analytical chemistry community as evidenced by the number of special symposia at major conferences, by the new researchers entering the field, and by the introduction of new instrumentation. There is little doubt that glow discharge mass spectrometry, for example, is now a major technique in the elemental analysis of solids. DOE

N90-20164# California Univ., Berkeley. Lawrence Berkeley Lab. Center for Advanced Materials.
INFRARED ABSORPTION STUDY OF ZINC-DOPED SILICON
E. Merk, J. Heyman, and E. E. Haller Nov. 1989 7 p Presented at the Materials Research Society Fall Meeting, Boston, MA, 27 Nov. - 2 Dec. 1989
(Contract DE-AC03-76SF-00098)
(DE90-007779; LBL-28206; CONF-891119-102) Avail: NTIS HC A02/MF A01

We report high resolution infrared absorption spectra associated with the deep zinc acceptor in silicon. The optical transitions between ground and bound excited p-like states of the neutral helium-like double acceptor Zn(exp 0) center have been observed for the first time. The absorption cross section for the hole transition is found to be very small, of the order of 10(exp -17) sq cm. Energy spacings of the P(exp 3/2) Rydberg series are very similar to the spacings of the group-III acceptors, suggesting that, in spite of the large ground state binding energy, effective mass approximation still applies to the bound excited states. This represents one more case where the strong central cell potential does not significantly disturb the neutral helium-like bound excited states. Similar observations have been made for the less deep neutral double acceptor Be, and for the chalcogens donors S, Se and Te. The optical ionization energy of Zn(exp 0/-) has been determined to be 2575 cm(exp -1) (319 MeV). Two additional sets of absorption lines related to zinc have been observed at 2130 cm(exp 11) and 2758 cm(exp -1). Their origin will be discussed. DOE

N90-20165# California Univ., Berkeley. Lawrence Berkeley Lab.
ENHANCEMENT OF MASS TRANSFER TO A ROTATING CYLINDER ELECTRODE BY INERT PARTICLES SUSPENDED IN THE ELECTROLYTE
L. H. Kim, R. H. Muller, and C. W. Tobias Jun. 1989 34 p
(Contract DE-AC03-76SF-00098)
(DE90-008054; LBL-27473) Avail: NTIS HC A03/MF A01

Mass-transfer rates were investigated to a rotating cylindrical electrode in the presence of suspended particles either more or less dense than the electrolyte. In the case of low-density particles, the limiting-current density for the reduction of ferricyanide increases rapidly with volume fraction of solids up to about 10%, then gradually declines to values near those for the particle-free electrolyte. The transport process is interpreted by a three-zone model in which mass-transfer rate is controlled by different modes of particle behavior in the centrifugal force field. For high-density particles, limiting currents increase monotonically with increasing particle concentration, and the enhancement caused by suspended particles decreases with increasing rotation speed. DOE

N90-20166# Sandia National Labs., Albuquerque, NM.
MOISTURE CONTROL IN SEALED ELECTRONIC PACKAGES
M. R. Keenan Feb. 1990 68 p
(Contract DE-AC04-76DP-00789)
(DE90-008136; SAND-89-2106) Avail: NTIS HC A04/MF A01

A number of issues associated with controlling the internal moisture content of sealed packages are examined. The basic

strategy for maintaining a dry internal environment is to incorporate desiccant into the package and it is shown that molecular sieves are well suited to this task. Expressions are developed that predict the moisture content of the package in terms of package design and the external storage environment. Both moisture sealed into the package during assembly and water that leaks or permeates into the package over its lifetime are accounted for. In this development, the temperature dependences of all quantities of interest are explicitly treated and the actual Langmuir-like adsorption isotherm exhibited by molecular sieves is employed. These equations allow the quantity of desiccant required to meet design objectives to be computed. They also permit one to evaluate the sensitivity of the internal environment to design parameters and storage conditions, and a number of these are discussed. A computer program that has been written to perform these calculations is also described. DOE

N90-20167# Oak Ridge National Lab., TN.
CORROSION PROPERTIES OF Fe3Al IN H2S-H2-H2O MIXTURES
J. H. DeVan 1989 2 p Presented at the Meeting of the Electrochemical Society, Montreal, Quebec, 6-11 May 1990
(Contract DE-AC05-84OR-21400)
(DE90-004936; CONF-900562-2) Avail: NTIS HC A01/MF A01

Compatibility with mixed gases containing sulfur, oxygen, and chlorine is a critical requirement for high-temperature alloys used in coal conversion applications. The studies had two primary objectives: to evaluate the effects of low concentrators (1 to 2 percent) of elemental additions, such as Nb, Y, and Zr, on the sulfidation resistance of Fe3Al, and to establish the cause of the detrimental effect of Cr on the sulfidation resistance of these alloys at concentrations above 2 percent. All experiments were conducted in flowing H2S-H2-H2O mixtures with relatively low oxygen activities and high sulfur activities. Alloys were exposed at 700 and 800 C in isothermal tests and between 25 and 800 C in thermal transient tests. The resultant weight changes during microbalance exposures of 120 to 300 h were analyzed to establish reaction kinetics for scale growth and exfoliation. The scales and underlying alloy were also analyzed to relate oxidation and sulfidation processes to alloy content. DOE

N90-20168# Los Alamos National Lab., NM.
THE CALCULATION OF HYDROGEN-BONDING PROPERTIES
James P. Ritchie, Edward M. Kober, and Ian C. Faloona 1989 7 p Presented at the US Army CRDEC Scientific Conference on Chemical Defense Research, Aberdeen Proving Ground, MD, 14-17 Nov. 1989
(Contract W-7405-eng-36)
(DE90-007534; LA-UR-90-485; CONF-8911171-1) Avail: NTIS HC A02/MF A01

Hydrogen-bonding characteristics of molecules are extremely important in determining their boiling points, densities and water-solubilities, and these properties are important in understanding the adsorption of gases on charcoal. We show that empirical scales that measure hydrogen-bonding interactions can be correlated with the electrostatic properties of the molecules which agrees with previous worker's assessment that the hydrogen-bonding interaction is electrostatic in nature. Correlations both with single molecule properties as well as with the interaction energy between two molecules are found. This establishes a method for calculating these important properties which were previously available only through experiment or empirical scales. DOE

N90-20169# California Univ., Davis. Dept. of Electrical and Computer Engineering.
DEEP LEVEL TRANSIENT SPECTROSCOPY IN RESISTIVE LAYERS
Charles E. Hunt and Kim Ng Jun. 1989 4 p
(Contract W-7405-eng-48)
(DE90-008349; UCRL-21268) Avail: NTIS HC A01/MF A01

The application of the Deep Level Transient Spectroscopy (DLTS) technique to resistive semiconductor thin films, such as Silicon-On-Insulator (SOI) and thin layer of GaAs formed on semi-insulating material is investigated. Schottky diodes made of these materials were used. The effect of the series resistance inherent in these types of thin-film test structures on the interpretation of data obtained from the measurement apparatus is discussed. It is observed that inverted DLTS signals occur in these structures because of the high series resistance. It is shown that ignoring this effect can lead to erroneous values of the activation energy and the density of traps. DOE

N90-20170# Little (Arthur D.), Inc., Cambridge, MA.
TECHNO-ECONOMIC ASSESSMENT OF A CARBOTHERMIC ALUMINA REDUCTION PROCESS
C. L. Kusik, Andrew Syska, John Mullins, and V. Vejins 1989 26 p Presented at the 118th AIME Annual Meeting, Las Vegas, NV, 26 Feb. 1989
(Contracts DE-AC07-76ID-01570; DE-FG07-83ID-12467)
(DE90-007018; EGG-M-88425; CONF-890201-2) Avail: NTIS HC A03/MF A01

Arthur D. Little, Inc., undertook an assessment of a process for the carbothermic reduction of alumina based on prior work and a flowsheet developed by a technical committee for the U.S. Department of Energy. This paper summarizes the techno-economic assessment which identified potentially viable sub-process steps and their economic viability based on past research findings. Economic comparisons show the carbothermic process has the potential for lower capital and operating costs than the conventional Hall cell. Potential energy savings would be substantial through the use of carbothermic reduction of alumina, in the order of 230 trillion Btu's annually. However, several of the selected subprocesses have not been reduced to practice, and an opportunity exists to further improve the process economics through research and development. DOE

N90-20171# Lawrence Livermore National Lab., CA.
EXPERIMENTAL VALIDATION OF EXTENDED IMAGE RECONSTRUCTION USING BISPECTRAL SPECKLE INTERFEROMETRY
Taylor W. Lawrence, J. Patrick Fitch, Dennis M. Goodman, Norbert A. Massie, and Robert J. Sherwood Jan. 1990 17 p Presented at the SPIE Astronomical Telescopes and Instrumentation for the 21st Century Symposium, Tucson, AZ, 11-17 Feb. 1990
(Contract W-7405-eng-48)
(DE90-008545; UCRL-101575; CONF-900285-2) Avail: NTIS HC A03/MF A01

Results will be presented from a horizontal path imaging experiment in which a 0.5 meter telescope is used to focus on a target located at a range of 1.2 km. The targets included various extended objects from a simple binary letters to extended representations of satellites with grey scale and size variations. Imaging at a center wavelength of 0.7 microns, an atmospheric degradation factor of D/r(sub o) = 17, on average was found. A slow read-rate bare CCD detector was used to effectively deal with additive noise in the speckle measurements. The image reconstruction algorithms are based on the use of the complex bispectrum and diffraction-limited imaging was demonstrated down to light levels approaching a few photons per speckle resolution area. Careful attention was paid to the effects of additive noise on the reconstruction process and it was shown that they can be adequately overcome. DOE

N90-20172# Pacific Northwest Lab., Richland, WA.
VIBRATIONAL SPECTROSCOPY OF BORON NITRIDE AT HIGH TEMPERATURES AND PRESSURES
Gregory J. Exarhos and Nancy J. Hess (Washington Univ., Seattle.) Dec. 1989 6 p Presented at the Materials Research Society Fall Meeting, Boston, MA, 27 Nov. - 2 Dec. 1989
(Contract DE-AC06-76RL-01830)
(DE90-008633; PNL-SA-17226; CONF-891119-113) Avail: NTIS HC A02/MF A01

Raman scattering measurements are used to distinguish between amorphous and crystalline phases in sputter deposited boron nitride coatings and bulk materials. Changes in vibrational

line frequency and linewidth can be attributed to differences in particle size or inherent strain which can be quantified from pressure-dependent measurements of the bulk material. The response of the Raman-allowed E(sub 2g) modes (hexagonal phase) to temperature is described by a forced damped harmonic oscillator model from which the intra- and interplanar lattice thermal expansion can be estimated. DOE

N90-20173# Lehigh Univ., Bethlehem, PA.
ANALYTICAL ELECTRON MICROSCOPY OF CATALYST PREPARATIONS Progress Report, 15 Jul. 1989 - 14 Jul. 1990
Charles E. Lyman 1990 6 p
(Contract DE-FG02-86ER-45269)
(DE90-008699; DOE/ER-45269/T1) Avail: NTIS HC A02/MF A01

This program seeks to analyze supported metal catalysts by analytical electron microscopy (AEM) at an analytical sensitivity is pursued with the electron probe microanalyzer (EPMA) at about 10 micron resolution, while high spatial resolution is pursued with the field-emission STEM used as an AEM. The catalyst preparations examined are two important classes of pollution control catalysts. Rhodium supported on Al2O3 is a candidate catalyst for reduction of NO(x) in flue stack gases of stationary power sources. Rh and Pt together on Al2O3 is a candidate catalyst for both the reduction of NO(x) and the oxidation of CO and hydrocarbons in automobile exhaust. The overriding theme of this program is to use analytical electron microscopy techniques to understand elemental distributions in experimental catalysts so that catalysts with optimal microstructures can be prepared. This requires very sophisticated electron beam instrumentation to perform the analyses, an understanding of the electron beam interactions with the catalyst in the guise of electron beam damage, and a catalytic testing program to assess the success of individual experimental preparations. All of these are components of the present program. DOE

N90-20174# Utah Univ., Salt Lake City. Dept. of Chemistry.
DURIP FTIR STUDIES OF SOLID STATE REACTION DYNAMICS Final Report, 15 Nov. 1988 - 14 Nov. 1989
Charles A. Wight 24 Jan. 1990 35 p
(Grant AF-AFOSR-0108-89; AF Proj. 3842)
(AD-A217713; AFOSR-90-0004TR) Avail: NTIS HC A03/MF A01 CSCL 07/5

The origin of metastability in high symmetry molecules was studied by photoionization and photodissociation techniques. One- and two-photon ionization processes were studied in the triatomic hydrogen molecule and photodissociation of H3. Photoionization of diatomic helium, triatomic nitrogen, and D3O were observed, and a background study of metastable HD, H2, and He2 was performed. A new source for formation of H3 and H5 was developed. GRA

N90-20175# State Univ. of New York, Buffalo. Dept. of Chemistry.
CHEMICAL AND ELECTROCHEMICAL STUDIES IN IONIC LIQUIDS Final Report, 1 Dec. 1986 - 30 Nov. 1989
Robert A. Osteryoung 12 Jan. 1990 39 p
(Grant AF-AFOSR-0088-87; AF Proj. 2303)
(AD-A217742; AFOSR-90-0084TR) Avail: NTIS HC A03/MF A01 CSCL 07/2

Chemical and electrochemical studies were carried out in ambient temperature chloroaluminate molten salts composed of aluminum chloride and 1-ethyl-3-methylimidazolium chloride. Simultaneous electrochemical in electrochemistry on polypyrrole (EPR) work was performed on polypyrrole and polyfluorene in the molten salts. The chemistry and electrochemistry of a number of solutes, benzoquinone, several molybdenum dimers, and ferro/ferricyanide, were examined. Oxygen 17 NMR spectroscopy was employed to assess the behavior of oxide in the molten salts. Gutmann donor-acceptor numbers were obtained making use of electrochemical and NMR, Phosphorus 31, measurements. GRA

N90-20176# California Univ., Davis. Dept. of Mechanical Engineering.
AERODYNAMIC AND KINETIC PROCESSES IN FLAMES Final Report, 1 Mar. 1985 - 28 Feb. 1989
Chung K. Law 15 Sep. 1989 74 p
(Grant AF-AFOSR-0147-85; AF Proj. 2308)
(AD-A217796; AFOSR-90-0087TR) Avail: NTIS HC A04/MF A01 CSCL 21/2

An extensive experimental, numerical and analytical study of the dynamics and chemical kinetics of flames was conducted. Specific phenomena investigated included an asymptotic simulation of hydrocarbon oxidation kinetics, an analysis of nonadiabatic flame propagation in dissociation equilibrium, a 3-step modeling of diffusion flames, detailed experimental and numerical determination of the laminar flame speeds of methane/air mixtures, experimental and analytical quantification of the propagation, extinction and interaction of laminar flames, experimental quantification of the structure and propagation of turbulent premixed flames in stagnation flow, and the influence of dilution, inert addition, preferential diffusion, and aerodynamic straining on soot formation in diffusion flames. A total of fourteen journal publications resulted from the present program. GRA

N90-20177# Texas A&M Univ., College Station.
LIGAND-CENTERED ELECTRON-TRANSFER REDOX PROCESSES FOR MANGANESE, IRON, AND COBALT COMPLEXES IN RELATION TO SELECTED CATALYTIC SYSTEMS Ph.D. Thesis
Silvia Ann Richert 1989 146 p Sponsored in part by AFIT, Wright-Patterson AFB, OH, and NSF
(AD-A217957; AFIT/CI/CIA-89-025) Avail: NTIS HC A07/MF A01 CSCL 07/3

The oxidation potentials for a series of Manganese L3, Iron L3 and Cobalt L3 complexes (L = acetylacetonate, 8-quinolinolate, picolinate, 2,2'-bipyridine, and 1,10-phenanthroline) were determined by cyclic voltammetry. The oxidations of these complexes occur at substantially less positive potentials than those for their zinc analogues and care clearly ligand-centered. The removal of an electron from the valence shell of the ligand is facilitated by the formation of a metal (d-electron)-ligand (p-electron) covalent bond. Other hydrocarbon substrates are transformed to ketones via the oxygenation of a methylenic carbon. Acetylenes and arylolefins are dioxygenated to alpha-dicarbonyls and aldehydes. A micron-dioxygen binuclear iron picolinate intermediate appears to be the active form of the catalyst. GRA

N90-20178# Air Force Inst. of Tech., Wright-Patterson AFB, OH.
THE EXTINCTION AND STRUCTURE OF COUNTERFLOW PREMIXED FLAMES M.S. Thesis
Jesse Keith Crump 1989 61 p
(AD-A218106; AFIT/CI/CIA-89-026) Avail: NTIS HC A04/MF A01 CSCL 21/2

A theoretical and experimental investigation of the extinction of a counterflow premixed flame was performed using methane as the fuel. The extinction limits were measured for a premixed flame stabilized between a premixed, fuel lean stream of methane, air and nitrogen and a stream of hot combustion product. The composition of the reactant mixture as a function of the strain rate was measured at extinction over a wide range of conditions. The results are interpreted using previously developed theories to derive overall chemical kinetic rate parameters. Temperature and composition profiles were obtained for several premixed flames near extinction. GRA

N90-20179# Minnesota Univ., Minneapolis.
INFRARED AND X RAY PHOTOELECTRON SPECTROSCOPY STUDIES OF THE POLYIMIDE/METAL INTERFACE M.S. Thesis
William Creed Stewart Apr. 1989 109 p Sponsored by AFIT, Wright-Patterson AFB, OH
(AD-A218249; AFIT/CI/CIA-89-023) Avail: NTIS HC A06/MF A01 CSCL 07/6

This thesis considers the chemical interactions which occur at the interface of a polymer and a metal. Polyimides were chosen for this study because of their application in microelectronic devices, flexible interconnects, solar cells, and printed circuit boards. In these applications, a polyimide typically forms an interface with chromium, aluminum, copper, or gold. Numerous results have been published on the processes which occur when metals are deposited on cured polyimide. Less attention has been given to the equally important sequence of polyimide curing on a metal. The interfaces studied for this thesis were those formed by imidization of polyamic acid on gold, chromium, and copper. Infrared spectroscopy (IR) and x-ray photoelectron spectroscopy (XPS) were used to study these interfaces. Polyimide films as thin as 34 A were prepared on metallized silicon wafers for these analyses. The IR and XPS results indicated the gold interacted very little with the polyimide, while copper produced significant changes in the IR and XPS spectra. At elevated cure temperatures chromium also reacted with the polyimide. In the structures with chromium and copper, the thermal stability of the polyimide at the interface was reduced from that of bulk polyimide. The data showed that the metals interact with the polymer structure at the point where ring closure occurs to form the polyimide from polyamic acid. GRA

N90-20180* National Aeronautics and Space Administration. Langley Research Center, Hampton, VA.

PROCESS FOR MAKING A NOBLE METAL ON TIN OXIDE CATALYST Patent

Billy T. Upchurch, inventor (to NASA), Patricia A. Davis, inventor (to NASA), and Irvin M. Miller, inventor (to NASA) (Science and Technology Corp., Hampton, VA.) 8 Aug. 1989 10 p Filed 31 Aug. 1987

(NASA-Case-LAR-13741-1-SB; US-Patent-4,855,274; US-Patent-Appl-SN-090874; US-Patent-Class-502-339; US-Patent-Class-502-325; US-Patent-Class-502-344) Avail: US Patent and Trademark Office CSCL 07D

A quantity of reagent grade tin metal or compound, chloride-free, and high-surface-area silica spheres are placed in deionized water, followed by deaerating the mixture by boiling and adding an oxidizing agent, such as nitric acid. The nitric acid oxidizes the tin to metastannic acid which coats the spheres because the acid is absorbed on the substrate. The metastannic acid becomes tin oxide upon drying and calcining. The tin-oxide coated silica spheres are then placed in water and boiled. A chloride-free precious metal compound in aqueous solution is then added to the mixture containing the spheres, and the precious metal compound is reduced to a precious metal by use of a suitable reducing agent such as formic acid. Very beneficial results were obtained using the precious metal compound tetraammine platinum(II) hydroxide. Official Gazette of the U.S. Patent and Trademark Office

26 METALLIC MATERIALS

Includes physical, chemical, and mechanical properties of metals, e.g., corrosion; and metallurgy.

N90-20181*# National Aeronautics and Space Administration. Lewis Research Center, Cleveland, OH.

MECHANICAL PROPERTIES OF PURE NICKEL ALLOYS AFTER LONG TERM EXPOSURES TO LIOH AND VACUUM AT 775 K

J. Daniel Whittenberger and E. J. Vesely, Jr. (IIT Research Inst., Chicago, IL.) Jan. 1990 23 p

(NASA-TM-102403; E-5142; NAS 1.15:102403) Avail: NTIS HC A03/MF A01 CSCL 11F

The solid to liquid phase transformation of LiOH at 744.3 K is considered to be an ideal candidate thermal energy storage (TES) mechanism for a Rankine heat engine based solar dynamic system operating at approximately 682 K. While pure nickel is thought to be a suitable containment material for LiOH, long term containment is of concern because molten hydroxides are usually corrosive. Two commercially pure nickel alloys, Ni-200 and Ni-201, were exposed to molten LiOH, its vapor, and vacuum at 775 K for periods ranging from 50 to 5000 h, and simple mechanical property measurements (77 to 900 K tensile and 750 K creep rupture) of exposed alloys were undertaken. The mechanical property test procedures are described and tabular lists of the test data are presented. Author

N90-20182# United Kingdom Atomic Energy Authority, Harwell (England). Materials Physics and Metallurgy Div.

EFFECT OF HEAT TREATMENT ON THE FRACTURE TOUGHNESS TRANSITION PROPERTIES OF AN A508 CLASS 3 STEEL

G. P. Gibson, M. Capel, and S. G. Druce Sep. 1989 75 p

(AERE-R-13548) Avail: NTIS HC A04/MF A01

Quenched and tempered low alloy steels such as ASTM (American Society for Testing and Materials) A508 class 3 were used in the manufacture of the reactor pressure vessel, pressurizer, and steam generators of pressurized water reactors. These steels undergo a transition in fracture toughness properties with temperature, due to a change in fracture mode from microvoid coalescence to cleavage fracture with decreasing temperature. The effect of heat treatment on the fracture toughness transition properties of an A508 class 3 forging was studied. Fractographic examination of broken specimens revealed that cleavage fracture is initiated by the cracking of brittle second phase particles, primarily iron based carbides, but in a few cases titanium carbides or manganese sulphide inclusions. The critical state in the cleavage fracture process is particle size dependent. In the case of the carbides, all smaller than 1.2 micrometers, the critical stage is the propagation of a particle sized microcrack into the ferritic matrix. For the manganese sulphide inclusions which nucleated fracture, all larger than 1.5 micrometers, the critical stage was the cracking of the particle. Decreasing the rate of cooling from the austenitization temperature from 40 to 6 C/min resulted in an increase in the transition temperature of 30 C. An increase in the degree of tempering from 610 C for five hours to 675 C for 20 hours raised the transition temperature by 70 C. The range of tempering studied was chosen to sample the plausible extremes of commercial practice and exceeded those allowed by the ASTM standard. The effect of cooling rate on the transition temperature is primarily due to the effect on the ferritic grain size, while the effect of tempering is to increase the carbide size. The effect of carbide and grain size on the transition temperature is apparently due to their effect on the number of particles which crack and act as potential cleavage nucleation sites. Author

N90-20183# United Kingdom Atomic Energy Authority, Harwell (England). Materials Physics and Metallurgy Div.

HYDROGEN, THERMAL AGEING AND THE ROLE OF CARBIDES IN FATIGUE OF A HIGH STRENGTH STEEL

C. A. Hippsley and C. E. Lane Jul. 1989 18 p

(AERE-R-13599) Avail: NTIS HC A03/MF A01

The influences of thermal aging and environment on Paris-Erdogan regime fatigue crack growth rates and mechanisms in a high strength NiCr steel (300 M) were investigated. Crack growth rates were measured in inert (vacuum) and aggressive (hydrogen) environments, for quenched-and-tempered material before and after thermal aging at 500 C. Aging induced an acceleration of crack growth in vacuum at low delta K levels, but a retardation at high delta K levels. The crack path was transgranular throughout, and followed carbide/matrix interfaces. These effects were associated with the embrittlement of carbide/matrix interfaces by phosphorus segregation, which facilitated transgranular crack growth at low delta K, but produced crack tip shielding from voids surrounding the crack at high delta K. Hydrogenacted synergistically with phosphorus to embrittle carbide/matrix interfaces, but also localized slip deformation at crack tips, reducing void formation in surrounding material, and associated shielding. Consequently, aging enhanced crack growth rates in hydrogen for all delta K levels examined. The role of carbide/matrix interface embrittlement constitutes a third mechanism of hydrogen and temper embrittlement interaction in fatigue crack growth, additional to those of carbide precipitation and grain boundary embrittlement previously reported. Author

N90-20184# United Kingdom Atomic Energy Authority, Harwell (England). Fracture Studies Group.
THE EFFECT OF THE SiC/Al INTERFACE ON MATRIX MICROSTRUCTURE IN 2xxx-SiCp METAL MATRIX
M. Strangwood Aug. 1989 21 p
(AERE-R-13591) Avail: NTIS HC A03/MF A01

The microstructures of an Al-Mg-Si alloy with three levels of SiC(p) reinforcement (0, 14 and 20 volume percent) in both an under- and over-aged condition were determined by transmission electron microscopy (TEM). In addition, fine scale chemical analysis was performed using a FED-STEM in the SiC/Al interfacial region of the alloy reinforced with 15 volume percent SiC(p). The presence of the reinforcement caused an acceleration of the aging process through increased dislocation densities arising from thermal expansivity mismatch between matrix and reinforcement. In addition, a modification in the matrix grain structure was noted with refinement in areas of high reinforcement density, but grain growth in regions with a lower SiC(p) content due to strain concentration. The SiC/Al interface acted as a sink for vacancies resulting in both equilibrium and non-equilibrium segregation of Mg and Cu to that site in the underaged condition. In the overaged condition, desegregation had taken place to leave only equilibrium segregation at the interface. Author

N90-20185# United Kingdom Atomic Energy Authority, Harwell (England). Materials Physics and Metallurgy Div.
WETTING OF METALLIC CARBIDES BY NON-REACTIVE LIQUID METALS
A. M. Stoneham and P. W. Tasker Sep. 1989 19 p
(AERE-M-3759) Avail: NTIS HC A03/MF A01

The systematics of the wetting of metallic carbides by liquid copper are analyzed. Subject to a simple assumption relating the plasmon energy of a carbide to the parent metal, the results can be understood in terms of dispersion forces, unlike the wetting of ionic oxides. The wetting angle correlates with the enthalpy of carbide formation since both can be linked to the carbide electron density. The carbide enthalpy of formation correlates with the incorporation energy of carbon in the carbide-forming substrate metal, which depends on electron density; the wetting angle depends on the electron density via the plasmon energy in the frequency-dependent dielectric function. The analysis explains systematic data by Ramqvist. Author

N90-20186# United Kingdom Atomic Energy Authority, Harwell (England). Materials Physics and Metallurgy Div.
CONSTITUTIVE DATA ACQUISITION AND MODELLING IN ALUMINIUM 2014 ALLOY
R. M. K. Young and M. J. Holmes Sep. 1989 27 p
(AERE-R-13651) Avail: NTIS HC A03/MF A01

The deformation behavior of the aluminum 2014 alloy system was examined using compression and torsion test techniques over the temperature range 623 K to 773 K and over the strain rate range 0.23 to 8/s. IM (ingot metallurgy) material was examined in naturally aged and normalized tempers, and the consolidated billet as well as extruded material were examined for the PM (powder metallurgy) route study. Flow stress results were fitted to the generalized hot working equation using an iterative regression method to generate the constitutive constants. Significant differences are found in the constitutive behavior of the different materials. Author

N90-20187# United Kingdom Atomic Energy Authority, Harwell (England). Materials Physics and Metallurgy Div.
SHAPING THE INSONIFYING PULSE TO OPTIMISE B-SCANS OBTAINED IN AUSTENITE
E. E. Aldridge and B. M. Hawker May 1989 34 p
(AERE-R-13518) Avail: NTIS HC A03/MF A01

The dependence of inspection capability for coarse-grained equiaxed cast austenitic steel on the total transfer function of the ultrasonic system is examined and work done to adapt an inspection system to given it a pre-defined idealized transfer function is described. Two approaches are used to examine the variation of signal-to-noise level with the transfer function. Firstly a computer model of an electrical pulse passing along a multiple-element delay line with randomized impedance levels simulates the transmission of ultrasound through a coarse-grained anisotropic material, and the short circuited end represents a specular reflector. The signal/reverberation noise level of the reflected wave is examined as a function of the equivalent mean grain size and of the input waveform. Secondly the quality of signals from a side-drilled hole at depth 60 mm is studied experimentally using a digital waveform synthesizer to generate various drive waveforms, including gated sinusoidal waveforms as used in previous work. From these results the transfer function of the rest of the system is derived and a new drive waveform is computed in an effort to achieve an idealized pulse shape at the receiver. The improvement is judged by subjective assessment of the unprocessed B-scan images and is quantified by measuring the signal to peak noise ratio for a side-drilled hole at depth 60 mm after the data were processed using synthetic aperture focusing. Author

N90-20188# United Kingdom Atomic Energy Authority, Harwell (England). Materials Physics and Metallurgy Div.
AGEING EFFECTS IN WELDED CAST CF3 STAINLESS STEEL
M. Strangwood and S. G. Druce Aug. 1989 40 p
(AERE-R-13559) Avail: NTIS HC A03/MF A01

Welded duplex stainless steel castings are used widely in the PWR (pressurized water reactor) primary coolant circuit at operational temperatures close to 300 C and design lifetimes of several hundred thousand hours. Under these conditions, microstructural changes are known to occur which affect the tensile and fracture properties. Results from aging studies over a range of temperatures from 300 C to 425 C for durations up to 10,000 h are presented. Hardness, impact fracture, and microstructural data are presented for weldmetal, heat affected zone (HAZ), and parent casting microstructures. Particular emphasis is given to HAZ properties and the determination of the fracture mechanism in aged materials. Comparison is made of the activation energy associated with aging induced changes in hardness and impact fracture properties for parent casting and HAZ microstructures. The weldmetal is highly resistant to the effects of aging, preventing any determination of activation energy. Author

N90-20189# United Kingdom Atomic Energy Authority, Harwell (England). Materials Development Div.
SPALLATION OF OXIDE SCALES FROM 20 PERCENT Cr/25 PERCENT Ni/Nb STAINLESS STEEL
M. J. Bennett, D. J. Buttle, P. D. Colledge, J. B. Price, C. B. Scruby, and K. A. Stacey May 1989 21 p
(AERE-R-13464) Avail: NTIS HC A03/MF A01

Acoustic emission (AE) monitoring was used both during the formation of scale on the 20Cr/25Ni/Nb stabilized stainless steel during isothermal exposures to carbon dioxide at 1123 to 1273 K and on subsequent furnace cooling to ambient temperature. Developments are reported whereby the AE technique may be used in conjunction with a controlled atmosphere microbalance to provide simultaneously two parameters describing the phenomenon occurring. Results obtained on cooling concerning the initiation and kinetics of spallation are discussed in terms of a strain energy model. Author

N90-20190# United Kingdom Atomic Energy Authority, Harwell (England). Materials Development Div.
STOCHASTIC APPROACH TO THE INITIATION OF PITTING CORROSION
P. H. Balkwill, C. Westcott, and D. E. Williams Dec. 1988 21 p
(AERE-R-13348) Avail: NTIS HC A03/MF A01

The parameters of a general stochastic model which was previously developed to describe the initiation phase of pitting corrosion were determined for a variety of austenitic stainless steels in dilute chloride solution. Alloys may be ranked from a knowledge of the frequency of occurrence of propagating pits Lambda (s(exp -1)/sq cm) This parameter gives the probability per unit area and time that a propagating pit will form. While reliable determinations of Lambda require a large number of experiments, it is shown that reasonable estimates of lambda can be made from a

knowledge of the frequency of nucleation of unstable pits lambda (s(exp -1)/sq cm) which can be obtained conveniently from relatively few specimens. The reduction in passive current density as the oxide film thickness increases is demonstrated. It is shown lambda varies strongly with passive film thickness and passive current density. These effects illustrate how the observed nucleation frequency for pits can depend on experimental conditions such as the pretreatment of the specimen, which may include exposure to air or solution after polishing and the potential ramp rate used in a potentiodynamic experiment. The identification of events arising at particular microstructural features is possible using an analysis of the shape distribution of current transients due to unstable pitting. Author

N90-20191# United Kingdom Atomic Energy Authority, Harwell (England). Materials Physics and Metallurgy Div.

FATIGUE CRACK GROWTH IN MARTENSITIC 2 1/4Cr-1Mo STEEL AT ELEVATED TEMPERATURES

C. A. Hippsley, P. Bowen, and J. F. Knott (Cambridge Univ., England) Jun. 1989 54 p

(AERE-R-13524) Avail: NTIS HC A04/MF A01

Mechanisms of sub-critical high temperature intergranular crack growth were studied during fatigue loading in air and in vacuum for coarse-grained martensitic 2 1/4Cr-1Mo steel. The crack increment per cycle, da/dN, is increased greatly under high mean stress conditions as the cyclic frequency is reduced. In addition, fatigue crack growth rates as a function of frequency can be predicted accurately from base-line fatigue data (obtained at low mean stress) and static crack growth resistance curves. The cyclic and static components of crack growth appear to be essentially independent. The importance of the average value of stress intensity over the fatigue cycle, K(mean), was identified. More generally, these cyclic-static crack growth mechanisms may have some potential use for modeling fatigue-creep interactions. Author

N90-20192# United Kingdom Atomic Energy Authority, Harwell (England). Materials Development Div.

TELLURIUM EMBRITTLEMENT OF TYPE 316 STEEL

J. A. Hemsworth, M. G. Nicholas, and R. M. Crispin Mar. 1989 34 p

(AERE-R-13440) Avail: NTIS HC A03/MF A01

The effects of molten tellurium and tellurium/caesium mixtures on the mechanical properties of Type 316 steel tensile test pieces were assessed at temperatures between 460 and 800 C using slow and fast strain rates. Tellurium embrittled the steel at temperatures above 600 C and this was associated with extensive chemical interaction and grain boundary penetration. At 600 C, the addition of even 2 percent of caesium caused tellurium to embrittle the steel severely. Similarities to zinc embrittlement exist that suggest tellurium also degrades by a two step process, with cracks being initiated due to the chemical interaction but propagating because of surface energy reductions. Author

N90-20193# United Kingdom Atomic Energy Authority, Harwell (England). Fracture Studies Group.

THE AGEING EFFECT OF THE MATRIX-REINFORCEMENT INTERFACE ON THE AGEING RESPONSE OF AN ALUMINIUM 6061 ALLOY REINFORCED WITH 20VOL PERCENT SiC PARTICULATES

M. Strangwood, N. J. Taylor (Salford Univ., England), and C. A. Hippsley Jan. 1989 43 p

(AERE-R-13361) Avail: NTIS HC A03/MF A01

The effect of the SiC/Al interface upon precipitation processes during aging of a 20 wt percent SiC(sub P)/6061 metal matrix composite was studied using SEM, (S) TEM, and AES. The results were compared with an unreinforced 6061 alloy subjected to the same heat treatments. The microstructural effects were related to tensile properties and matrix hardness. The reinforcement caused accelerated aging due to higher dislocation densities and Mg2Si formation at the SiC/Al interface. The latter precipitation occurred as a result of Mg and Si segregation and depleted the matrix in solute, leading to lower levels of MgAl precipitation compared with the unreinforced 6061. This was reflected by lower matrix hardnesses in the reinforced alloy. Ductility in the unreinforced alloy fell with increasing hardness, but, while uniformly lower, was largely insensitive to matrix hardness in the reinforced alloy. This was attributed to domination of the fracture process by large SiC particles. Author

N90-20194*# National Aeronautics and Space Administration. Marshall Space Flight Center, Huntsville, AL.

SECONDARY ARM COARSENING AND MICROSEGREGATION IN SUPERALLOY PWA-1480 SINGLE CRYSTALS: EFFECT OF LOW GRAVITY

M. Vijayakumar, S. N. Tewari (Cleveland State Univ., OH.), J. E. Lee, and P. A. Curreri Jan. 1990 12 p Proposed for presentation at the CSME Mechanical Engineering Forum 1990, Toronto, Ontario, 3-9 Jun. 1990; sponsored by Canadian Society for Mechanical Engineering

(Grant NAG8-091)

(NASA-TM-102445; E-5220; NAS 1.15:102445) Avail: NTIS HC A03/MF A01 CSCL 11F

Single crystal specimens of nickel base superalloy PWA-1480 were directionally solidified on ground and during low gravity (20 sec) and high gravity (90 sec) parabolic maneuver of KC-135 aircraft. Thermal profiles were measured during solidification by two in-situ thermocouples positioned along the sample length. The samples were quenched during either high or low gravity cycles so as to freeze the structures of the mushy zone developing under different gravity levels. Microsegregation was measured by examining the solutal profiles on several transverse cross-sections across primary dendrites along their length in the quenched mushy zone. Effect of gravity level on secondary arm coarsening kinetics and microsegregation have been investigated. The results indicate that there is no appreciable difference in the microsegregation and coarsening kinetics behavior in the specimens grown under high or low gravity. This suggests that short duration changes in gravity/levels (0.02 to 1.7 g) do not influence convection in the interdendritic region. Examination of the role of natural convection, in the melt near the primary dendrite tips, on secondary arm spacings requires low gravity periods longer than presently available on KC-135. Secondary arm coarsening kinetics show a reasonable fit with the predictions from a simple analytical model proposed by Kirkwood for a binary alloy. Author

N90-20195# Stuttgart Univ. (Germany, F.R.). Fakultaet Physik.

RESEARCH OF THE INTERACTION BETWEEN HYDROGEN AND DEUTERIUM WITH ATOMIC EIGEN DEFECTS AND DISLOCATIONS IN NICKEL AND IRON Ph.D. Thesis [UNTERSUCHUNG DER WECHSELWIRKUNG VON WASSERSTOFF UND DEUTERIUM MIT ATOMAREN EIGENFEHLSTELLEN UND VERSETZUNGEN IN NICKEL UND EISEN]

Michael Hirscher 1987 151 p In GERMAN

(ETN-90-95380) Avail: NTIS HC A08/MF A01

The object is to examine hydrogen influence on the free migration of eigen defects and their role in hydrogen diffusion by magnetic resonance measurements made by the LC oscillator method. Hydrogen shows in metal a very great diffusion capacity and a high solubility. Diffusivity and solubility of hydrogen in nickel are similar to that of hydrogen in austenitic steels. In alpha-iron hydrogen has a very high mobility. Nickel radiation at 77 k brings about several processes with the following defects: they can regenerate by recombination with their eigen location other an empty place; they can create interstitial atom clusters; they can be captured by contamination and at this temperature then become immobile. During a radiation at 77 k alpha-iron defects are immobile too and fixed in the state produced by this radiation. ESA

N90-20196# Army Lab. Command, Watertown, MA. Material Technology Lab.

EVALUATION OF 2090-T8E48 ALUMINUM-LITHIUM PLATES Final Report

Ernest S. Chin, Marietta R. Cappucci, Robert M. Huie, and Robert E. Pasternak Nov. 1989 22 p

(DA Proj. 1L1-62105-AH-84)
(AD-A217262; MTL-TR-89-97) Avail: NTIS HC A03/MF A01 CSCL 11/6

A 1.5-inch-thick 2090-T8E48 aluminum-lithium (Al-Li) alloy plate was evaluated in conjunction with the Navy Cooperative Test Program. Mechanical characterization included testing of tensile specimens in the longitudinal, transverse, and short direction, and testing of compact tension/slow bend specimens covering the L-T, T-L, L-S, S-L, S-T, and T-S directions. In addition, ballistic tolerance against caliber .30 armor piercing projectile and 20-mm fragment simulated projectile was determined. Corrosion and stress corrosion studies were made in accordance with ASTM standards. Microstructural characterization was performed through optical metallography and transmission electron microscopy. Consolidation and discussion of all the results in comparison with previously evaluated 0.5-inch-thick X2090-T8 is presented. GRA

N90-20197# Lawrence Livermore National Lab., CA. Dept. of Material Sciences and Mineral Engineering.
DESIGN AND PROCESSING OF STRONG-TOUGH MICROCOMPOSITE STEELS
Gareth Thomas Dec. 1989 19 p Presented at the Poland Steel Conference, Krynica, Poland, 23-26 Apr. 1990
(Contract DE-AC03-76SF-00098)
(DE90-007764; LBL-28294; CONF-9004139-1) Avail: NTIS HC A03/MF A01

Microcomposite HSLA steels based on Fe/Cr/Mn/C were designed as a result of sophisticated electron microscopy and microanalytic studies so as to consist of fine packet lath dislocated martensite and interlath austenite films in order to obtain steels with superior combinations of strength, fracture toughness, and formability. Such properties can be obtained directly by on-line controlled rolling and cooling directly in a hot mill, so that post tempering can be eliminated. For long products and plates of low to medium carbon compositions, the processing requires accelerated water cooling. Niobium is effective in increasing hardenability, in grain refinement, and without adversely modifying the microcomposite morphology of the steels. DOE

N90-20198# California Univ., Davis. Div. of Materials Science and Engineering.
AN INVESTIGATION OF THE MECHANISMS OF SOLID STATE POWDER REACTION IN THE COMBUSTION SYNTHESIS AND SINTERING OF HIGH TEMPERATURE MATERIALS
Zuhair A. Munir Aug. 1989 15 p
(Contract DE-FG03-86ER-45249)
(DE90-007880; DOE/ER-45249/T1) Avail: NTIS HC A03/MF A01

The progress made over the period of May 27, 1986 to August 15, 1989, on a DOE-supported research aimed at providing a fundamental understanding of combustion-synthesis related reactions is discussed. Accomplishments made over the stated period are given below under two categories: Completed Work and Work in Progress. Because reprints and preprints of Completed Work are attached to this report, only a brief description of each of the items is given below. For items listed under Work in Progress, a brief summary of the most important results is provided. DOE

N90-20199# General Electric Co., Schenectady, NY. Atomic Power Lab.
THE STRESS CORROSION PERFORMANCE OF DIFFUSION BONDED NICKEL BASE ALLOYS
1989 24 p
(Contract DE-AC12-76SN-00052)
(DE90-008130; KAPL-4713) Avail: NTIS HC A03/MF A01

Excellent mechanical strength can be achieved in diffusion bonded nickel-base alloys when approximately 0.01 mm of nickel is plated on the surfaces before bonding. However, rapid stress corrosion cracking takes place in the bond line region when such materials are tested in high purity water at 360 C. The failures are caused by the low concentration of chromium in the nickel-rich bond line region. Long-time high temperature anneals to diffuse chromium into the bond line dramatically improve the stress corrosion resistance. Measurements of the local chromium in the bond line and separate tests of Ni-Cr binary alloys show that chromium contents approaching that of the bulk alloy are necessary to eliminate the cracking susceptibility. DOE

N90-20200*# National Aeronautics and Space Administration. Marshall Space Flight Center, Huntsville, AL.
ROLLING CONTACT FATIGUE OF SURFACE MODIFIED 440C USING A 'Ge-POLYMET' TYPE DISC ROD TEST RIG
Robert L. Thom Mar. 1989 23 p
(NASA-TM-100390; NAS 1.15:100390) Avail: NTIS HC A03/MF A01 CSCL 11F

Through hardened 440 C martensitic stainless steel test specimens were surface modified and tested for changes in rolling contact fatigue using a disc on rod test rig. The surface modifications consisted of nitrogen, boron, titanium, chromium, tantalum, carbon, or molybdenum ion implantation at various ion fluences and energies. Tests were also performed on specimens reactively sputtered with titanium nitride. Author

N90-20201# Argonne National Lab., IL. Materials Science Div.
PHYSICAL SPUTTERING OF METALLIC SYSTEMS BY CHARGED-PARTICLE IMPACT
Nghi Q. Lam Dec. 1989 123 p Presented at the 8th Pfefferkorn Conference on Fundamental Beam Interactions with Solids for Microscopy, Microanalysis and Microlithograph, Park City, UT, 7-12 May 1989
(Contract W-31-109-eng-38)
(DE90-007803; CONF-8905179-3) Avail: NTIS HC A07/MF A01

A brief overview is provided of the current understanding of physical sputtering by charged particle impact, with the emphasis on sputtering of metals and alloys under bombardment with particles that produce knock-on collisions. Fundamental aspects of ion-solid interactions, and recent developments in the study of sputtering of elemental targets and preferential sputtering in multicomponent materials are reviewed. A few specific topics of sputter emission are concentrated on, including the various properties of the sputtered flux and depth of origin, and on connections between sputtering and other radiation induced and enhanced phenomena that modify the near surface composition of the target. The synergistic effects of these diverse processes in changing the composition of the integrated sputtered atom flux is described in simple physical terms, using selected examples of recent important progress. DOE

N90-20202# Sandia National Labs., Albuquerque, NM.
EVALUATION OF MATERIAL HOMOGENEITY AS A FUNCTION OF THICKNESS OF LOW-ALLOY FERRITIC STEEL Final Report
T. L. Anderson and M. A. Lambert (Texas A&M Univ., College Station.) Nov. 1989 35 p
(Contract DE-AC04-76DP-00789)
(DE90-008069; SAND-89-7096) Avail: NTIS HC A03/MF A01

A series of Charpy and nil-ductility transition temperature (NDTT) tests were performed on 8 in. and 12 in. thick forgings of A508-4A, A508-4B, and A350-LF3 steels. Three different positions in thickness were tested in the 12 in. forgings, while two locations in the forging were analyzed. Chemical analysis and metallographic examination were also performed on each material and in each thickness location. The material toughness tended to be lower in the thicker forgings and in the center of a given forging. Low relative toughness coincided with well tempered microstructures, where equiaxed ferrite grains had begun to form. These grains are coarser than the packet structure that existed at earlier stages of tempering. Low quench rates (associated with thick sections and central regions of a given thickness) apparently accelerated the structural changes during tempering, which led to microstructures with low toughness. The NDTT results were suspect because most arrests occurred in the heat affected zones (HAZs) of the welds rather than in the parent metal. The measured NDTT values were lower than expected, based on published empirical correlations with Charpy energy. This was particularly true for the

A508-4A steel. This provided further evidence that the drop weight tests were actually measuring the arrest properties of the HAZ in most cases. DOE

N90-20203# Lawrence Livermore National Lab., CA. Chemistry and Materials Science.
ELECTRONIC STRUCTURE, ALLOY PHASE STABILITY, AND PHASE DIAGRAMS
A. Gonis, M. Sluiter, P. E. A. Turchi, G. M. Stocks, and D. M. Nicholson (Oak Ridge National Lab., TN.) 16 Feb. 1990 35 p Presented at the 119th TMS (The Minerals, Metals and Metallurgical Society) Annual Meeting and Exhibit, Anaheim, CA, 18-22 Feb. 1990
(Contract W-7405-eng-48)
(DE90-008306; UCRL-102971; CONF-900206-4) Avail: NTIS HC A03/MF A01

The relevance of electronic structure calculations to the determination of alloy phase stability and alloy phase diagrams was reviewed. The Connolly-Williams method, the generalized perturbation method, the embedded cluster method, and the method of concentration waves are presented and their main features are discussed and compared. The results of calculations of effective cluster interactions in substitutionally disordered alloys and of phase diagrams for specific alloy systems, e.g., PdRh, PdV and AlLi, are shown and work currently in progress is briefly described. DOE

N90-20204# Lawrence Livermore National Lab., CA.
REACTIVE SPUTTERING OF MOLYBDENUM
A. F. Jankowski and L. R. Schrawyer Jan. 1990 27 p Presented at the 8th International Triennial Conference on Thin Films and the 17th International Conference on Metallurgical Coatings, San Diego, CA, 1-6 Apr. 1990
(Contract W-7405-eng-48)
(DE90-008307; UCRL-102017; CONF-900419-2) Avail: NTIS HC A03/MF A01

The composition and crystalline structure of molybdenum-oxide thin films is controlled through the process of reaction dc magnetron sputtering. A systematic variation in target power density results in a continuous transition in the appearance of molybdenum-oxide from a translucent glass to a metallic-like film. New molybdenum-oxide crystal structures and compositions are found using XRD, SAD, AES depth profiling and STEM. DOE

N90-20205# Lawrence Livermore National Lab., CA.
A UNIFIED INTEGRATED MODEL FOR SPUTTER COATING UNIFORMITY
R. S. Upadhye and E. J. Hsieh Aug. 1989 10 p Presented at the 36th American Vacuum Society National Vacuum Symposium, Boston, MA, 23-27 Oct. 1989
(Contract W-7405-eng-48)
(DE90-008322; UCRL-98747; CONF-891093-26) Avail: NTIS HC A02/MF A01

The coating flux received by substrates in a sputter coating process consists of two components: the diffusive flux, contributed by fully thermalized atoms, and the directed flux, contributed by atoms which have retained a major part of their original velocity (i.e., both speed and direction). Near the source, the directed flux prevails, whereas far away from the source, the diffusive flux dominates. The sputtered source atoms undergo collisions with the inert gas atoms and become thermalized. The fraction of thermalized atoms increases with distance from the source, and so does the diffusive component of the net flux. The two different process mechanisms have often been modeled separately. Such models work only in the extremes, and are not useful in situations where both mechanisms contribute significantly. We have developed an integrated model of the process which assigns weights to the two mechanisms; the weighting factors are then related to the process and equipment parameters. DOE

N90-20206# California Univ., Berkeley. Lawrence Berkeley Lab. Center for Advanced Materials.
THE METALLURGICAL MECHANISMS OF SOLDER FATIGUE
J. W. Morris, Jr., D. Tribula, T. S. E. Summers, and D. Grivas Dec. 1989 7 p Presented at NEPCON '90: National Electronic Packaging and Production Conference, Anaheim, CA, 26 Feb. - 1 Mar. 1990 Prepared in cooperation with California Univ., Berkeley
(Contract DE-AC03-76SF-00098)
(DE90-008390; LBL-28405; CONF-900271-2) Avail: NTIS HC A02/MF A01

Thermal fatigue of solder joints is an important source of failure in electronic devices. Failures arise from the strain, most often in shear, imposed on the solder joint by the uneven thermal expansions of the joint constraining surfaces. Increased solder joint reliability and improved fatigue resistant solders require an understanding of the metallurgical mechanisms operative during the fatigue cycle. The work that is reviewed here concentrates on the mechanisms of thermal fatigue and, in particular, their association with the solder microstructure. While the fatigue life of Pb-Sn solder joints is strongly dependent on operating conditions, the metallurgical mechanisms of failure are surprisingly constant for joints where the deformation occurs predominantly in shear at elevated temperatures and the solder exhibits the classic lamellar eutectic microstructure. Under these conditions, the shear strain in the joint is inhomogeneous and initiates a local recrystallization and softening of the solder microstructure. Fatigue cracks initiate in this softer microstructure to cause ultimate failure. The results outlined here identify and elucidate the role of the solder microstructure during thermal fatigue and suggest specific paths toward the design of superior solder alloys. DOE

N90-20207# Oak Ridge National Lab., TN. Metals and Ceramics Div.
AN INTRODUCTION TO NICKEL ALUMINIDE ALLOY
J. R. Weir, Jr. 1990 49 p Presented at the 1990 International Manufacturing Conference, Atlanta, GA, 26 Mar. 1990
(Contract DE-AC05-84OR-21400)
(DE90-008565; CONF-9003111-1) Avail: NTIS HC A03/MF A01

The properties of the alloys were measured on an entirely new and different alloy system. The alloys are based on the intermetallic compound Ni3Al with the substitution of alloying elements for the nickel or aluminum atoms, or both, to produce alloys of differing properties. Intermetallic compounds are brittle (including Ni3Al). However, it was found that by changing the composition from Ni75Al25 to Ni76Al24 and adding approximately 200 ppm (by weight) boron the material becomes ductile and, therefore, a potentially useful structural material. This report consists of viewgraphs for the seminar presentation an introduction to nickel aluminide alloy. DOE

N90-20208# Pratt and Whitney Aircraft, West Palm Beach, FL.
IMPROVED TOUGHNESS ALLOYS BASED ON TITANIUM ALUMINIDES Final Report, Aug. 1985 - Mar. 1989
Martin J. Blackburn and Michael P. Smith 26 Oct. 1989 222 p
(Contract F33615-85-C-5030)
(AD-A218149; PW-FR-20760; WRDC-TR-89-4095) Avail: NTIS HC A10/MF A01 CSCL 21/5

Alloy development programs over the past decade have identified alloys, based on the compound Titanium aluminide (alpha-two) with tensile and creep properties that indicate applications at temperatures as high as 760 C (1400 F) should be possible. However, rather low values of toughness and impact resistance at temperatures less than 260 C (500 F) lead to concerns over component durability during assembly and service. The objective of this program was to improve the toughness of Ti3Al based alloys. In Phase I, solid solution modifications (Task 1), development of a tough second phase (Task 2), and formation of rare earth oxide dispersions by rapid solidification (Task 3) were investigated. Task 4 evaluated a combination of those alloys and processing techniques from the first three tasks. In Phase II, three alloy systems were selected for scale-up and extensive mechanical property testing. GRA

27 NONMETALLIC MATERIALS

Includes physical, chemical, and mechanical properties of plastics, elastomers, lubricants, polymers, textiles, adhesives, and ceramic materials.

For composite materials see *24 Composite Materials.*

N90-20209# United Kingdom Atomic Energy Authority, Harwell (England). Materials Development Div.

THE EFFECTS OF RADIATION ON THE MECHANICAL PROPERTIES OF POLYMERS USED AS ELECTRICAL CABLE INSULATION AND JACKETING MATERIALS

D. I. Johnson Jan. 1989 25 p

(AERE-R-13286) Avail: NTIS HC A03/MF A01

Available information on the effects of radiation on polymers which are being considered for use, or are used, in nuclear power plants are summarized. Data are presented in such a way as to indicate whether dose-rate effects are likely to occur. Information was obtained from a variety of sources and is supplemented in some cases by data generated in current Harwell work carried out for a General Nuclear Safety Research program. Author

N90-20210# Brookhaven National Lab., Upton, NY. Dept. of Applied Science.

SOL-GEL DERIVED POLYTITANOSILOXANE COATINGS

Toshifumi Sugama Sep. 1989 21 p Presented at the Corrosion '90, Las Vegas, NV, 23-27 Apr. 1990

(Contracts DE-AC02-76CH-00016; MIPR-ARO-102-89)

(DE90-004186; BNL-43358; CONF-900403-4) Avail: NTIS HC A03/MF A01

Amorphous polytitanosiloxane (PTS) was formed by hydrolysis polycondensation and hydrolysis polycondensation pyrolysis reaction of precursor sol solutions consisting of monomeric organosilanes, Ti(OC2H5)4, methanol, water and hydrochloric acid, over the temperature range 100 to 500 C. These reaction processes which are responsible for the assemblage of PTS networks were found to depend mainly on the species of organosilane used. The PTS was applied as a coating on aluminum substrates, and the factors which play an important role in providing corrosion protection were investigated. Three major findings are as follows: (1) the addition of HCl, which was used as hydrolysis accelerator for the organosilanes and Ti(OC2H5)4, acts to produce a clear sol solution, thereby aiding in the formation of smooth and uniform coating layers; (2) the organosilane to Ti(OC2H5)4 ratios are critical for the fabrication of PTS films; and (3) moderate densifications of the Si-O-Ti bond in PTS networks are needed to produce a good film. DOE

N90-20211# Massachusetts Inst. of Tech., Cambridge. Dept. of Chemical Engineering.

CO2 DIFFUSION AND SOLUBILITY IN A POLYSTYRENE/POLYBUTADIENE BLOCK COPOLYMER WITH HIGHLY ORIENTED LAMELLAR MORPHOLOGY

D. H. Rein, J. J. Csernica, R. F. Baddour, and R. E. Cohen 8 Dec. 1989 34 p

(Contract N00014-87-K-0517)

(AD-A217165; TR-9) Avail: NTIS HC A03/MF A01 CSCL 07/6

Solubility and diffusion coefficients for CO2 in polystyrene polybutadiene (SB) block copolymer films were measured in a pressure decay sorption apparatus at 1 atm over a temperature range of 20 to 90 C. The morphology of the block copolymer specimens consisted of alternating S and B lamellae of approximately 100 angstrom thickness with excellent long range orientation perpendicular to the surface of the 0.02 to 0.05 cm thick films. Diffusion behavior in the copolymer was simulated using homopolybutadiene and homopolystyrene data along with a finite difference model based on the well-ordered morphology. Comparisons of model predictions with the measured values of the effective diffusion coefficient for CO2 in the copolymer revealed that the diffusion coefficient of CO2 in the polybutadiene region of the copolymer was lower than in homopolybutadiene by a factor of 1.9 at 20 C. This difference disappeared at the glass transition temperature of the polystyrene in SB. This temperature-dependent reduction of CO2 diffusion in the polybutadiene regions of the block copolymer results from restrictions on chain motions of the polybutadiene blocks arising from their connection to polystyrene blocks. GRA

N90-20212# Research Triangle Inst., Research Triangle Park, NC.

RESEARCH AND DEVELOPMENT ON ENHANCED DEGRADABLE PLASTICS Report, for 16 Dec. 1987 - 31 Dec. 1988

Anthony L. Andrady and Todd M. Olson (Naval Ship Research and Development Center, Bethesda, MD.) 1 Jan. 1989 84 p

(Contract N61533-88-C-0002)

(AD-A217180; DTRC/SME-CR-08-89) Avail: NTIS HC A05/MF A01 CSCL 11/9

Three major activities carried out during the report period are those relating to: (1) development of definitions, standards and test protocols for enhanced biodegradable plastics, (2) the testing of selected starch-based plastic films for biodegradation under marine conditions, and (3) assessment of two approaches to improved biodegradability in plastic films. Commercial starch-containing plastic films degrade slower at sea than that claimed for soil exposure. Moderate rates of degradation of greater than 9 to 12 months require high levels of starch, thus making it difficult to design a film thick enough for heavy-duty bags, yet retaining moderate biodegradability. Coextrusion of films with the starch (or other degradable material) in the middle layer coated on either side with unfilled plastic material may have improved surface and other properties. These too, however, degrade at rates comparable or slower than the commercial materials. Blends of two plastics, polyethylene and polycaprolactone (PCL) (where the latter is biodegradable in soil), performed well under marine exposure. Films of blends with up to 10 percent of PCL had acceptable physical strength and moderate biodegradability. GRA

N90-20213# Harvard Univ., Cambridge, MA. Dept. of Physics.

X RAY SPECULAR REFLECTION STUDIES OF SILICON COATED BY ORGANIC MONOLAYERS (ALKYLSILOXANES) Interim Technical Report

I. M. Tidswell, B. M. Ocko, P. S. Pershan, S. R. Wasserman, G. M. Whitesides, and J. D. Axe (Brookhaven National Lab., Upton, NY.) Nov. 1989 79 p Submitted for publication

(Contract N00014-86-K-0756)

(AD-A217418; TR-21) Avail: NTIS HC A05/MF A01 CSCL 11/3

X ray specular reflectivity is used to characterize the structure of silicon/silicon-oxide surfaces coated with chemisorbed hydrocarbon monolayer films (alkylsiloxanes). Using synchrotron radiation the reflectivity could be followed over 9 orders of magnitude, from grazing incidence to an incident angle allowing a spatial resolution of features along the surface normal. Analysis was performed by fitting the data to reflectivities calculated from models of the surface electron density and by calculation of Patterson functions directly from the data. These procedures allow identification of an approx. 17A thick SiO2 layer, a layer of head group region where the alkyl siloxane adsorbs to the SiO2, and the hydrocarbon layer. The data also requires that the various interface have different widths. The fact that the same local hydrocarbon density is observed for both fully formed and partially formed monolayers with alkane chains of varying length excludes a model in which the partially formed monolayer is made up of separated islands of well formed monolayers. Measurements before and after chemical reaction of a monolayer in which the alkyl chain is terminated by an olefinic group demonstrates the ability to use x ray reflectivity to characterize chemical changes. Effects of radiation damage on these types of measurements are described. GRA

N90-20214# Aerodyne Research, Inc., Billerica, MA.

FLUORINATED DIAMOND THIN FILMS FOR TRIBOLOGICAL APPLICATIONS Final Report, Apr. - Oct. 1989

Andrew Freedman and Charter Stinespring 4 Jan. 1990 22 p

(Contract N00014-89-C-0140)
(AD-A217452; ARI-RR-750) Avail: NTIS HC A03/MF A01 CSCL 11/8

Diamond (100) substrates were fluorinated with both atomic and molecular fluorine under ultrahigh vacuum conditions using molecular beams. X ray photoelectron spectra of the resulting samples indicate that atomic fluorine, F, reacts with an initial accommodation coefficient of 0.25 (+ or - 0.1) at 298 K; a saturation coverage of about three quarters of a monolayer is obtained. The carbon fluoride adlayer is thermally stable to 700 K, but slowly desorbs at temperatures above this. In contrast, molecular fluorine, F2, reacts quite slowly; a saturation coverage of less than one fifth of a monolayer after several hundred monolayers exposure to F2 at temperatures from 300 to 700 K is achieved. In addition, diamond substrates saturated with fluorine atoms showed no loss of fluorine after exposure to beams of H2 and O2 at temperatures between 300 and 700 K. GRA

N90-20215# Connecticut Univ., Storrs. Liquid Crystalline Polymer Research Center.
COPOLYMER-LIKE STRUCTURES OF NEMATIC NITROIMINE DIMERS Interim Technical Report No. 35
L. V. Azaroff, Jack M. Gromek, Agya R. Saini, and Anselm C. Griffin 29 Jan. 1990 19 p Submitted for publication
(Contract N00014-86-K-0772)
(AD-A217574) Avail: NTIS HC A03/MF A01 CSCL 07/6

A series of nitroimine, Siamese-twin dimers joined by an aliphatic chain with n = 2 to 10 were examined by DSC, microscopy, and x ray diffraction. All dimers except the one having n = 3 undergo transitions to a nematic mesophase without exhibiting distinct relationships. The N-I transitions, in contrast, exhibit a very pronounced alternation with even numbered spacers having much higher clearing temperatures. Magnetically aligned monodomains of the nematic mesophase were examined by x ray diffraction. In addition to the broad equatorial arcs (yielding interchain separations 1.5 to 5.7A), up to eight aperiodically spaced meridional reflections were recorded. By positing two possible coupling modes in which either one or both phenyl rings in neighboring dimers overlap, a linear array of coupled nitroimine dimers having two repeating distances along its length is produced. Using such a copolymer-like model, the spacings of the aperiodic meridional reflections and their relative intensities could be reproduced for a random sequence of the two repeat distances and an equal (50:50) probability of single or double overlapped phenyl rings. GRA

N90-20216# Pennsylvania State Univ., University Park. Dept. of Chemistry.
SYNTHESIS OF NEW POLYPHOSPHAZENE ELASTOMERS
Harry R. Allcock, Gayann S. McDonnell, and James L. Desorcie 1 Feb. 1990 31 p
(Contract N00014-84-K-0447)
(AD-A217585; TR-52) Avail: NTIS HC A03/MF A01 CSCL 07/6

A new class of phosphazene elastomer was synthesized. The cyclic phosphazenes, N3P3F5(CMe3), N3P3F5Ph, non-gem-N3P3C14Me2, non-gem-N3P3C14E12, (NPC1Me)3, and (NPC1Me)4 were polymerized to macromolecules of formula (NPF2)2NPFR(n), NPC12(NPC1R)2(n), and (NPC1R)(n). Species (NPC1Me)3 and (NPC1Et)3 were copolymerized with (NPC12)3 to yield polymers of type NPC12)x(NPC1R)yn. The halogen atoms in the high polymers were replaced by trifluoroethoxy groups to yield hydrolytically-stable derivatives. The influence of the alkyl or aryl groups on the properties of the polymers is described. The new polymers are elastomers, with glass transition temperatures in the -40 to -60 C range. GRA

N90-20217# North Carolina State Univ., Raleigh. Dept. of Nuclear Engineering.
MAGNETIC VAPOR SHIELD MECHANISM FOR PROTECTION OF MATERIAL SURFACES EXPOSED TO HIGH HEAT LOAD Final Report
J. G. Gilligan 11 Dec. 1989 36 p
(Contract DAAL03-86-K-0029)
(AD-A217667; ARO-22678.3-MS) Avail: NTIS HC A03/MF A01 CSCL 20/3

This project was successful in predicting decreased erosion of surfaces exposed to high heat fluxes under railgun or electromagnetic launcher conditions. The significant reduction has come as a result of the proper modeling of the vapor shielding (VS) effect. Favorable comparison with experimental results supports the conclusion. A further decrease in surface erosion should come as a result of an applied magnetic field which should reduce turbulence in the VS boundary layer. Preliminary experimental measurements support this claim, but further theoretical work must be done which would include 2-D, and turbulent effects. GRA

N90-20218# Brookhaven National Lab., Upton, NY.
THE ROLE OF POLARITY ON THE STABILITY OF GRAPHITIC COMPOUNDS
Renata M. Wentzcovitch, Alessandra Continenza, and A. J. Freeman (Northwestern Univ., Evanston, IL.) 1989 4 p Presented at the Materials Research Society Meeting on Diamond, Boron Nitride, Silicon Carbide, and Related Wide Bandgap Semiconductors, Boston, MA, 27 Nov. - 2 Dec. 1989 Sponsored in part by National Center for Supercomputing Applications, Illinois Univ., Urbana-Champaign
(Contract DE-AC02-76CH-00016; NSF DMR-88-21571)
(DE90-006528; BNL-43772; CONF-8911168-1) Avail: NTIS HC A01/MF A01

There is an old puzzle associated with the series of compounds formed by first row elements, C, BN, and BeO: similar to the other members of the family of octet semiconductors, these compounds exist in dense phases like diamond and zincblende, or hexagonal diamond (lonsdaleite) and wurtzite; however, whereas C and BN also exist in low density graphitic phases, BeO does not. Until now it has not been understood if the absence of BeO in this latter series is caused by simple technical difficulties in preparing the compound or by an intrinsic structural instability of the graphitic phase with respect to the dense wurtzite phase. There is some interest in layered BeO because of its expected exotic intercalation chemistry, as well as some possible unusual properties in this highly polar 2-D oxide. In this report, the stability of graphitic BeO is discussed based on all-electron full-potential linearized augmented plane wave method. DOE

N90-20219# Cornell Univ., Ithaca, NY. Dept. of Materials Science and Engineering.
INTERFACE SCIENCE IN DEFORMATION PROCESSING OF CERAMICS Progress Report, 1 May 1989 - 29 Feb. 1990
Rishi Raj 15 Dec. 1989 11 p
(Contract DE-FG02-87ER-45303)
(DE90-008424; DOE/ER-45303/2) Avail: NTIS HC A03/MF A01

The two major themes of the current work are: the study of the mechanical properties of interfaces in ceramic materials in terms of their structure and chemistry, and the development of techniques for studying the growth of multilayer thin films of ceramics by vapor phase techniques. The thin film approach is useful because interfacial reactions under controlled oxygen activities can be studied in one-dimensional multilayers that contain flat interfaces. State-of-the-art techniques such as high resolution electron microscopy and Rutherford Backscattering can be used to obtain definitive results for the chemistry and structure of interfaces, and these results can then be applied to understand the mechanical properties of complex ceramic materials at high temperatures. DOE

N90-20220# Midwest Research Inst., Golden, CO. Chemical Conversion Research Branch.
ASSESSMENT OF BIOBASED MATERIALS
Helena L. Chum, ed. Dec. 1989 175 p
(Contract DE-AC02-83CH-10093)
(DE90-000300; SERI/TR-234-3610) Avail: NTIS HC A08/MF A01

Biobased materials are polymers derived from renewable resources by chemical or combined chemical and mechanical methods, or produced directly in biological processes. Combinations of renewable and conventional fossil-fuel-derived plastics are also biobased materials. This assessment reviews materials from renewable resources and their properties including major biopolymers produced by plants and selected animal sources. Examples discussed are wood, its polymeric components such as cellulose and lignin, related polymers such as chitin, other carbohydrate polymers such as starch, which when combined with plastics can impart environmental degradability to the resulting material. The conventional role of inexpensive wood flour as a filler is reviewed as well as the future research necessary to bring these materials into a higher value use as a reinforcing material for composites. Automotive, building, and packaging materials applications are considered. Bioproduction of materials is reviewed for selected polymers such as cellulose, other plant cell wall polymers, and proteins, with emphasis on silk and wool. These materials can be produced with specific properties such as biodegradability (e.g., polyhydroxybutyrate and valerate copolymers, polylactide polymers) or specific mechanical properties. DOE

N90-20221# Sandia National Labs., Albuquerque, NM.
THE VISCOELASTICITY OF CURING THERMOSETS
Douglas Adolf and James E. Martin 1990 8 p Presented at the ANTEC 1990: Society of Plastics Engineers Meeting, Dallas, TX, 7-11 May 1990
(Contract DE-AC04-76DP-00789)
(DE90-006535; SAND-90-0077C; CONF-9005107-1) Avail: NTIS HC A02/MF A01

As a crosslinking polymer cures, dramatic changes in molecular architecture occur. These structural changes in turn affect the viscoelastic behavior of the material. At a critical extent of reaction (the gel point), the polymer undergoes a transition from a viscous liquid to an elastic solid. The evolution of structure and viscoelasticity were monitored in an epoxy encapsulant used at Sandia, the diglycidyl ether of Bisphenol A cured with diethanolamine (DEA). The structure evolves according to percolation theory, and the viscoelasticity evolves according to out dynamic scaling theory for branched polymers. DOE

N90-20222# Massachusetts Inst. of Tech., Cambridge. Dept. of Materials Science and Engineering.
RADIATION DISORDER AND APERIODICITY IN IRRADIATED CERAMICS Progress Report, 22 Jun. - 31 Dec. 1989
Linn W. Hobbs, Merton C. Flemings, and David J. Harrigan 1989 3 p
(Contract DE-FG02-89ER-45396)
(DE90-008253; DOE/ER-45396/1) Avail: NTIS HC A01/MF A01

Two lines of research have been pursued in the six months since the program funding began on 22 June 1989. These are: to provide computer graphic representation of the physical models of tetrahedral network glass structure that Dr. Carol Marians had developed during a previous DOE-funded program, to assign coordinates to the tetrahedron vertices, and to minimize the energies of these configurations in order to provide a relaxed set of coordinates which could be compared to diffraction data; and to initiate ion implantation into pyrophosphates in order to investigate radiation-induced disorder of partial network structures. DOE

N90-20223# Brown Univ., Providence, RI. Div. of Engineering.
TENSILE FRACTURE TOUGHNESS OF CERAMIC MATERIALS: EFFECTS OF DYNAMIC LOADING AND ELEVATED TEMPERATURES
S. Suresh, T. Nakamura (State Univ. of New York, Stony Brook.), K. Yang, and J. Duffy 1990 39 p
(Contract DE-FG02-84ER-45167)
(DE90-008329; DOE/ER-45167/T1) Avail: NTIS HC A03/MF A01

Experimental methods are presented for the determination of fracture initiation toughness of ceramics and ceramic composites in pure tension under quasi-static and dynamic loading conditions over a range of temperature spanning 20 C to 1300 C. Circumferentially notched and cyclic fatigue pre-cracked rods of a variety of ceramic materials were subjected to quasi-state tensile fracture in an electro-servohydraulic test machine and to dynamic tensile fracture using a modified tensile Kolsky (split-Hopkinson) bar. Dynamic finite element analyses of the circumferentially notched cylindrical rod have been conducted to develop the optimum specimen dimensions and tests procedures for ambient and elevated temperature dynamic fracture initiation toughness measurement. Experiments conducted on Al2O3, Si3N4 and SiC, and an Al2O3 - 25 volume percent SiC whisker composite at room temperature indicate that the dynamic to quasi-state fracture initiation toughness ratio K(sub Id)/K(sub Ic) is in the range of 1.1 to 1.4. Scanning electron microscopy observations show that failure above 1100 C usually evolves by the nucleation, growth and coalescence of cavities. The mechanisms of elevated temperature quasi-state and dynamic fracture in polycrystalline Al2O3 are examined and possible causes for the apparently higher dynamic fracture initiation resistance are discussed. The significance and limitations of the proposed experimental techniques are highlighted. DOE

N90-20224# Oak Ridge National Lab., TN. Metals and Ceramics Div.
MECHANICAL BEHAVIOR OF WHISKER REINFORCED CERAMICS
Paul F. Becher and H. T. Lin (Oak Ridge Associated Universities, Inc., TN.) 1990 12 p Presented at the International Forum on Fine Ceramics '90, Nagoya, Japan, 12-16 Mar. 1990
(Contract DE-AC05-84OR-21400)
(DE90-008758; CONF-900393-2) Avail: NTIS HC A03/MF A01

The interest in ceramics and ceramic composites has prompted research concerned with mechanisms to toughen them and to improve their elevated temperature mechanical performance. The beneficial effects of ceramic whiskers on fracture toughness are derived from the high strength of the reinforcing phases and from crack deflection at interfaces. As described earlier, bridging of a crack by these reinforcing phases increases the fracture toughness by the formation of a bridging zone behind the crack tip wherein the bridging ligaments impose a closure stress on the crack. Similar toughening effects due to crack bridging are observed in silicon nitride ceramics containing elongated grains and in ceramics containing plate-like grains or reinforcing phases. The question that remained is whether or not such reinforced ceramics would exhibit attractive mechanical properties at elevated temperatures. This paper will review results that indicate that whisker reinforcement, and similar reinforcing approaches, improves the mechanical performance of ceramics at elevated temperatures. DOE

N90-20225# Pacific Northwest Lab., Richland, WA.
CERAMIC OXIDE THIN FILM FORMATION UTILIZING BIOLOGICAL PROCESSES
B. J. Tarasevich and P. C. Rieke Jan. 1990 9 p Presented at the Materials Research Society Fall Meeting, Boston, MA, 27 Nov. - 2 Dec. 1989
(Contract DE-AC06-76RL-01830)
(DE90-008599; PNL-SA-17271; CONF-891119-112) Avail: NTIS HC A02/MF A01

Mineralization processes used by bioorganisms were adapted for the nucleation and growth of ceramic oxide thin films onto surfaces from aqueous solutions. These strategies include the use of surfaces derivatized with specific functional groups that control the nucleation and growth and properties of materials deposited. Initial experiments have involved the precipitation of iron oxide materials onto functionalized polystyrene surfaces. Deposition resulted in the formation of thin films composed of densely packed, nanometer-sized crystallites and evidence for the formation of oriented crystallites was found. This process may have advantages over conventional thin film processing methods due to the ability to systematically control surface properties to systematically control properties of materials deposited. DOE

N90-20226# Duke Univ., Durham, NC. Dept. of Mechanical Engineering and Materials Science.
POSITRON ANNIHILATION SPECTROSCOPY: A NONDESTRUCTIVE, SUBMICROSCOPIC CHARACTERIZATION TECHNIQUE FOR STRUCTURAL POLYMERS Final Report, 1 Sep. 1986 - 31 Aug. 1989
Phillip L. Jones 16 Nov. 1989 3 p
(Contract DAAL03-86-G-0046)
(AD-A217748; ARO-23791.2-MS-F) Avail: NTIS HC A01/MF A01 CSCL 07/6

Positron annihilation lifetime spectroscopy (PALS) was used to characterize as extruded and aged LEXAN polycarbonate. The long lived component of the PALS analysis is attributed to orthoPositronium (oPs) pick off annihilations. The oPs pickoff component lifetime and intensity decrease as the result of the aging heat treatment, and this decrease is associated with a decrease in the free volume site size and concentration in glassy polycarbonate due to aging. Isothermal relaxation experiments performed over the range 12 to 30 C performed on as-extruded and aged polycarbonate indicate that the relaxation kinetics are significantly different, and are consistent with a decrease in molecular mobility as the result of aging. An activation energy for structural relaxation of 8.2 kcal/mole for aged polycarbonate versus 3.0 kcal/mole for unaged polycarbonate was determined. The relaxation kinetics observed using PALS is related to the structural state and molecular mobility of the polymer. GRA

N90-20227# National Inst. of Standards and Technology, Gaithersburg, MD. Ceramics Div.
STRENGTH AND MICROSTRUCTURE OF CERAMICS Final Technical Report, 1987 - 1989
Brian R. Lawn, C. J. Alpert, S. J. Bennison, H. M. Chan, S.-J. Cho, R. F. Cook, C. J. Fairbanks, M. P. Harmer, B. J. Hockey, and D. B. Marshall et al Nov. 1989 243 p
(Contracts AFOSR-ISSA-87-0034; AFOSR-ISSA-88-0005; AF Proj. 2306; NIST Proj. 4202464)
(AD-A217752; AFOSR-90-0013TR) Avail: NTIS HC A11/MF A02 CSCL 11/2

Results of a study program on the toughness properties of monophase ceramics are summarized. In situ observations of crack propagation in alumina and other monophase ceramics show crack interface bridging to be the principal source of increasing toughness with crack size, i.e., R-curve behavior. Fracture mechanics models describing this behavior, in the particular context of strength, are developed. Results of strengths tests confirming the essential predictions of the theory are presented. Results of wear and fatigue tests are also described. The model has strong implications concerning the controlled processing of ceramics for optimum toughness and strength properties. GRA

N90-20228# Oklahoma State Univ., Stillwater.
POLYMER LIQUID CRYSTALS WITH SIDE CHAIN DISCOGENS Final Report, 1 Apr. 1987 - 30 Sep. 1989
Warren T. Ford 5 Feb. 1990 9 p Sponsored by ONR, Arlington, VA
(AD-A218013) Avail: NTIS HC A02/MF A01 CSCL 07/6

With the long term goal of creating new polymers that have novel optical and electronic properties and can be fabricated as thin films, three classes of liquid crystalline materials were investigated. Discotic aza-macrocycles that may form complexes with metal ions with high selectivity, discotic phthalocyanines that may have strong nonlinear optical properties and are semiconductors, and polarized stilbenes that have strong second and third order nonlinear optical responses were the classes. GRA

N90-20229# Texas Univ., Arlington. Center for Advanced Polymer Research.
ELECTRONIC AND IONIC TRANSPORT IN PROCESSABLE CONDUCTING POLYMERS Quarterly Technical Report, No. 18, 1 Oct. - 31 Dec. 1989
Martin Pomerantz, John R. Reynolds, Krishnan Rajeshwar, and Dennis S. Marynick 10 Jan. 1990 7 p
(Contract N00014-90-J-1320)
(AD-A218093) Avail: NTIS HC A02/MF A01 CSCL 07/4

Stability studies of the electrical conductivity of poly(pyrrole tosylate) (PPTOS); poly(pyrrole dodecylbenzenesulfonate) (PPDBS) and polypyrrole/poly(styrene sulfonate) (PP/PSS) films and their laminated composites with epoxy/glass have been carried out at 160 F and 95 percent relative humidity. GPC molecular weight studies of poly(3-alkylthiophenes) has shown that the use of a multiangle laser light scattering (MALLS) detector, which provides absolute molecular weights, gives much higher values (2 to 5 times) than using polystyrene standards and an RI or UV-VIS detector. Thus, polystyrene is a poor molecular weight standard for these rigid rod poly(3-alkylthiophenes). Ion binding studies have been extended to polypyrrole/poly(styrene sulfonate) using Ru(bpy)3(2+) (bpy=2,2'-bipyridyl) and Ru(NH3)6(3+) as redox probes. Copolymers of pyrrole and 3-(1-pyrrolyl) propanesulfonate were also studied this way. Partition coefficients were determined with a combination of UV-VIS spectrophotometric and voltammetric data. GRA

N90-20230# Pennsylvania State Univ., University Park. Dept. of Chemistry.
RING EXPANSION AND EQUILIBRATION IN ORGANOPHOSPHAZENES, AND THE RELATIONSHIP TO POLYMERIZATION
Harry R. Allcock, Gayann S. McDonnell, and James L. Desorcie 15 Feb. 1990 39 p Submitted for publication
(Contract N00014-84-K-0477)
(AD-A218234; AD-E501191; TR-54) Avail: NTIS HC A03/MF A01 CSCL 07/6

A series of cyclic trimeric phosphazenes that bear both halogen and organic side groups have been found to undergo ring expansion-equilibration reactions at elevated temperatures. Compounds non-gem N3P3F5CMe3, N3P3F5Ph, N3P3F4 (CMe-3)2,N3P3F4Ph2, hexamers, and in some cases, heptamers, octamers, and nonamers when heated. The cyclic tetramers (NPC1Me)4 and (NPC1Et)4 also equilibrate to a range of cyclic species that range from trimer to hexamer. Several of these equilibrations also lead to the formation of high polymers. The results are discussed in terms of possible mechanisms for ring-ring equilibration and polymerization. GRA

N90-20231# Boeing Aerospace Co., Seattle, WA.
PROCESSING, FABRICATION, CHARACTERIZATION AND DEVICE DEMONSTRATION OF HIGH TEMPERATURE SUPERCONDUCTING CERAMICS Final Report, 30 Sep. 1988 - 30 Nov. 1989
Thomas S. Luhman and Ilhan Aksay Jan. 1990 185 p
(Contract F49620-88-C-0143)
(AD-A218330; AFOSR-90-0236TR) Avail: NTIS HC A09/MF A01 CSCL 20/3

Success with organometallics, citrates, and sintered powder compacts has resulted in two approaches for further development of strain tolerant conductors. They are, thin fibers and tapes, and bulk monoliths. A thorough understanding of the phase relationships in high temperature superconductors, including those phase relationships exhibited by the oxygen sublattice has been developed. This has allowed approaches for addressing the weak-link problem. Processes are being developed to reduce the grain size of fibers, tapes and monoliths. This approach offers the potential to deliver strong, fine-grained material and, with the correct alteration of grain boundaries, the elimination of poor electrical conduction across the weak-links. Other facets of this approach include attempts to texture the fine grains, produce adequate porosity to ensure good oxygenation, and the possible incorporation of silver for matrix strengthening. Work was pursued for producing candidate material for devices based on controlling high temperature peritectic reactions, for example seeding of fibers and tapes with yttrium oxide. The goal of this program is to develop material processes for new high temperature superconducting ceramics and to demonstrate these processes in a high current device. GRA

N90-20232# Johns Hopkins Univ., Baltimore, MD.
ULTRASTRUCTURE PROCESSING OF ORDERED POLYMERS Final Report, 1 Aug. 1987 - 31 May 1989
Ronald K. Eby 18 Jan. 1990 156 p
(Grant AF-AFOSR-0320-87; AF Proj. 2303)
(AD-A218331; AFOSR-90-0240TR) Avail: NTIS HC A08/MF A01 CSCL 07/6

In order to explore the nonlinear elasticity of high performance PBZT fibers, a method using laser-generated ultrasound was developed to measure the Young's modulus of the fibers as a function of temperature and static tensile stress. X ray diffraction was also used to measure both the crystal modulus and aspects of the ultra-structure such as crystal size, unit cell structure and orientation. It is shown that improved crystal orientation with increased tensile stress is one of the most important mechanisms of the nonlinear elasticity. GRA

N90-20233# General Atomic Co., San Diego, CA.
HIGH-TEMPERATURE CERAMIC SUPERCONDUCTORS Report, 1 Oct. - 31 Dec. 1989
K. S. Mazdiyasni, A. Chen, K. C. Chen, D. M. Duggan, E. I. Glatter, F. C. Montgomery, S. S. Pak, M. B. Maple, L. Paulius, and P. K. Tasai (California Univ., San Diego.) 10 Jan. 1990 46 p
(Contract N00014-88-C-0714)
(AD-A218347) Avail: NTIS HC A03/MF A01 CSCL 09/1

The principal objectives of this program are to demonstrate fabrication of high temperature ceramic superconductors that can operate at or above 90 Kelvin with appropriate current density, (Jc), in forms useful for application in resonant cavities, magnets, motors, sensors, computers, and other devices; and to fabricate and demonstrate selected components made of these materials, including microwave cavities and magnetic shields. GRA

28 PROPELLANTS AND FUELS

Includes rocket propellants, igniters, and oxidizers; their storage and handling procedures; and aircraft fuels.

For related information see also *07 Aircraft Propulsion and Power, 20 Spacecraft Propulsion and Power,* and *44 Energy Production and Conversion.*

N90-20234# Sandia National Labs., Albuquerque, NM.
PYROTECHNIC DEVICE TECHNOLOGY
P. D. Wilcox 1989 18 p Presented at the 14th International Pyrotechnics Seminar, Jersey, England, 18-22 Sep. 1989
(Contract DE-AC04-76DP-00789)
(DE90-007683; SAND-90-0259C; CONF-8909113-7) Avail: NTIS HC A03/MF A01

The current technology of pyrotechnic devices is surveyed and trends are examined for the future. Pyrotechnic can have several meanings. Pyrotechnic devices here are devices in which porous materials undergo reduction-oxidation reactions and produce useful products. The pyrotechnic materials are generally fuel-oxidizer systems without binders, in contrast to primary or secondary explosives or propellants. The word pyrotechnic is often used to include explosive, squib, propellant, or other ordnance type devices, especially in the European community. The major need for pyrotechnic devices was always military and defense; however, as technology advances, the civilian uses of pyrotechnics will continue to grow. If every automobile had a pyrotechnic device to trigger its air or crash bag, that application alone would mean millions of devices per year. Applications in safety, fire fighting, law enforcement, and other commercial applications are likely to increase due to the increased capability of pyrotechnic devices and the integration of such devices in system designs. DOE

N90-20235# Scientific Computing Associates, Inc., New Haven, CT.
MODIFICATION AND IMPROVEMENT OF SOFTWARE FOR MODELING MULTIDIMENSIONAL REACTING FUEL FLOWS Final Report, 1 Nov. 1986 - 31 Jan. 1989
David E. Keyes, Dennis J. Philbin, and Mitchell D. Smooke Jul. 1989 97 p
(Contract F33615-86-C-2694)
(AD-A217789; SCA-142; WRDC-TR-89-2056) Avail: NTIS HC A05/MF A01 CSCL 21/2

The flame type of most practical combustion devices is the diffusion flame. These flames are important in the interaction of heat and mass transfer with chemical reactions in ramjets, jet turbines and commercial burners. Three-dimensional models that couple the effects of fluid flow with detailed chemical reaction are as yet computationally infeasible. We focus our attention on axisymmetric laminar and turbulent diffusion flames in which a cylindrical fuel stream is surrounded by a coflowing oxidizer jet. In this configuration we can study the interaction of fluid flow with chemical reactions while obtaining a computationally feasible problem. The work centers on the development and application of accurate and efficient computational methods for the solution of the two-dimensional nonlinear boundary value problems describing the reacting systems. In particular, our goals involve the generalization of our one-dimensional fluid-chemistry model to two dimensions. We also focus on the use of two-dimensional flame sheet models as starting estimates for the nonlinear equation solver. Both confined and free methane-air flames have been studied. The results of the research are applicable to problems in: (1) turbulent reacting flows, (2) engine efficiency, (3) commercial power generation units, and (4) pollutant formation. GRA

29 MATERIALS PROCESSING

Includes space-based development of products and processes for commercial applications.

For biological materials see *55 Space Biology.*

N90-20236* National Aeronautics and Space Administration. John F. Kennedy Space Center, Cocoa Beach, FL.
VORTEX MOTION PHASE SEPARATOR FOR ZERO GRAVITY LIQUID TRANSFER Patent
Frank S. Howard, inventor (to NASA) and Wilson M. Fraser, Jr., inventor (to NASA) 18 Jul. 1989 8 p Filed 16 Aug. 1988
(NASA-Case-KSC-11387-1; US-Patent-4,848,987;
US-Patent-Appl-SN-232734; US-Patent-Class-55-160;
US-Patent-Class-55-182; US-Patent-Class-55-205;
US-Patent-Class-141-45) Avail: US Patent and Trademark Office CSCL 22A

A vortex motion phase separator is disclosed for transferring a liquid in a zero gravity environment while at the same time separating the liquid from vapors found within either the sender or the receiving tanks. The separator comprises a rigid sender tank having a circular cross-section and rigid receiver tank having a circular cross-section. A plurality of ducts connects the sender tank and the receiver tank. Disposed within the ducts connecting the receiver tank and the sender tank is a pump and a plurality of valves. The pump is powered by an electric motor and is adapted to draw either the liquid or a mixture of the liquid and the vapor from the sender tank. Initially, the mixture drawn from the sender tank is directed through a portion of the ductwork and back into the sender tank at a tangent to the inside surface of the sender tank, thereby creating a swirling vortex of the mixture within the sender tank. As the pumping action increases, the speed of the swirling action within the sender tank increases creating an increase in the centrifugal force operating on the mixture. The effect of the centrifugal force is to cause the heavier liquid to migrate to the inside surface of the sender tank and to separate from the vapor. When this separation reaches a predetermined degree, control means is activated to direct the liquid conveyed by the pump directly into the receiver tank. At the same time, the vapor within the receiver tank is directed from the receiver tank back into the sender tank. This flow continues until substantially all of the liquid is transferred from the sender tank to the receiver tank.

Official Gazette of the U.S. Patent and Trademark Office

N90-20237*# Case Western Reserve Univ., Cleveland, OH. Dept. of Material Science and Engineering.
INSTANTANEOUSLY GENERATED FOAM AND ITS APPLICABILITY TO REDUCED GRAVITY Final Report
Ali Ilhan, Dong-Sang Kim, and Pavel Hrma Feb. 1990 58 p (Grant NAG3-740)
(NASA-CR-185208; E-5282; NAS 1.26:185208) Avail: NTIS HC A04/MF A01 CSCL 22A

The objective of this study is two-fold: (1) understanding the generation and collapse of foam in molten glass, and (2) determining the role of gravity in transient foam dynamics. Both theoretical considerations and experiments show that gravity affects evolution of transient foams. Provided that Marangoni forces are absent, the lack of bubble motion under microgravity will prevent formation of surface foam and, as a result, only bulk foam will be generated. Also, the absence of gravity drainage will affect the foam collapse rate and mode when a surface foam has been produced prior to its exposure to microgravity. The progress follows three steps: (1) selection of appropriate materials and development of experimental techniques; (2) experimental study of transient foams on earth and developing a theoretical model; and (3) experimental study of transient foams under microgravity during free fall in a drop tower. The main results are presented of the first phase of the research which involves most of the ground based work needed to accomplish the first two steps. The suggestions for the final stage is also included. Earth bound experiments have shown that it is possible to produce transient foams suitable for drop tower experiments and to record their behavior by a video or still camera in a simple experimental set-up. Transient cellular foams were produced and studied in soda lime glass with sulfate at 1400 to 1500 C. The study of foams in model systems under convenient ambient temperature conditions helped to gather a significant amount of information in a short time. The relationship between foam behavior and structure was analyzed and the relationship between foam structure and the system properties is currently under development. Author

N90-20238# Deutsche Forschungsanstalt fuer Luft- und Raumfahrt, Cologne (Germany, F.R.). Inst. fuer Raumsimulation.
CENTER OF GRAVITY: METALLIC SOLIDIFICATION [SCHWERPUNKT: METALLISCHE ERSTARRUNG]
G. Otto, ed. Jun. 1989 220 p In ENGLISH and GERMAN Presented at 3rd Summer School Session on Microgravity, Cologne, Fed. Republic of Germany, 19-22 Jun. 1989
(DFVLR-IB-333-89/3; ETN-90-95850) Avail: NTIS HC A10/MF A02

An introduction to the principles of the germ formation and growth and the interaction of a solidification front with scattered particles is presented. The main topics were: German microgravity program and flight opportunities; user center and assistance; principles of the metallic solidification; supercooling and germ formation; dynamics of the solidification front; dispersion reinforced materials; systems with a miscibility gap in the liquid state; molding solidification; microgravity conditions of a space vehicle; fusion furnaces for Spacelab; electromagnetic fusion process and position research; diffusion and germ formation in glasses. For individual titles, see N90-20239 through N90-20250.

N90-20239# Deutsche Forschungsanstalt fuer Luft- und Raumfahrt, Cologne (Germany, F.R.). Haupabteilung Projekte und Mikrogravitation.
GERMAN MICROGRAVITY PROGRAM AND FLIGHT OPPORTUNITIES [DEUTSCHES MIKROGRAVITATIONSPROGRAMM UND FLUGGELEGENHEITEN]
H. Binnenbruck *In its* Center of Gravity: Metallic Solidification Jun. 1989 p 1-18 In GERMAN (For primary document see N90-20238 13-29)
Avail: NTIS HC A10/MF A02

A research on weightlessness was carried out covering three themes: the scientific program, the flight program and the program assistance measures. The scientific program is particularly centered on the boundary surface and transfer phenomena (form and stability of capillary surfaces, thermodynamics), the metals and binder materials (fusion, supercooling), the crystals, and the physical chemical and technical questions. The problems of biology, biotechnology and medicine are also examined. Some information about the Columbus shuttle module is given in example. ESA

N90-20240# Deutsche Forschungsanstalt fuer Luft- und Raumfahrt, Cologne (Germany, F.R.). Inst. fuer Raumsimulation.
USER CENTER AND ASSITANCE [NUTZERZENTRUM UND NUTZERUNTERSTUETZUNG]
K. Wittmann *In its* Center of Gravity: Metallic Solidification Jun. 1989 p 19-32 In GERMAN (For primary document see N90-20238 13-29)
Avail: NTIS HC A10/MF A02

The user center of Cologne (Germany, F.R.) is dedicated to weightlessness experiments in medical, biological, and chemical areas. It is based on the research results that were gathered during the first Spacelab flight. The aims of this center are to facilitate the access to the space experiments, to reduce the costs by efficient utilization of the expensive space experiment time and by the use of concentrated experience. The center works principally for the D2-Spacelab mission and for Eureca, an uninhabited experiment platform of ESA. The structure studies were sufficiently advanced for the preparation phase for these flights to begin by 1987. The future achievement for the space station was flexibly planned, so that the center can be adaptated to the immediate need. ESA

N90-20241# Deutsche Forschungsanstalt fuer Luft- und Raumfahrt, Cologne (Germany, F.R.). Inst. fuer Raumsimulation.
PRINCIPLES OF METALLIC SOLIDIFICATION [GRUNDLAGEN DER METALLISCHEN ERSTARRUNG]
B. Feuerbacher *In its* Center of Gravity: Metallic Solidification Jun. 1989 p 33-41 In GERMAN (For primary document see N90-20238 13-29)
Avail: NTIS HC A10/MF A02

In a dynamic equilibrium between fusion and solidification, a continuous supercooling is necessary with a limited solidification velocity. The latent heat must be evacuated to stabilize the solidification front and avoid a dendritic growth of the crystal. On the solidification front, a local negative temperature gradient appears. Liquidus and solidus concentrations are different with a constant temperature, which causes segregation. The special case of the supercooling, which appears only in alloy systems, must be considered: before the solidification front, the temperature drops locally under the liquidus temperature, despite the increasing temperature gradient, which determines the crystal structure in the fusion phase. ESA

N90-20242# Deutsche Forschungsanstalt fuer Luft- und Raumfahrt, Cologne (Germany, F.R.). Inst. fuer Raumsimulation.
SUPERCOOLING AND GERM FORMATION [UNTERKUEHLUNG UND KEIMBILDUNG]
D. M. Herlach *In its* Center of Gravity: Metallic Solidification Jun. 1989 p 43-75 In GERMAN (For primary document see N90-20238 13-29)
Avail: NTIS HC A10/MF A02

If a fusion phase is cooled down at an equilibrium temperature, the thermodynamic conditions can predict a spontaneous crystallization of the fusion phase, but experimental observation of the supercooling phenomenon shows that it is possible to see no solidification. To understand this the atomic and microscopic phenomena must be taken into account, with the macroscopic thermodynamics. A fluid with free, arbitrarily moving atoms is considered. The atoms are statistically gathered in agglomerates all the time, whose near organization corresponds to the solid phase. Such an agglomerate implies a boundary surface between liquid and solid phase with a boundary surface energy which is an energy barrier against the crystallization. The supercooling is characterized by an activation threshold for the crystallization of the fusion phase, the classical germ formation theory. Using the nucleation theory, the activation energy for heterogeneous germ

formation is always lower than for homogeneous germ formation. ESA

N90-20243# Aachener Centrum fuer Erstarrung unter Schwerelosigkeit e.V. (Germany, F.R.).
DYNAMICS OF THE SOLIDIFICATION FRONT [DYNAMIK DER ERSTARRUNGSFRONT]
S. Rex *In* DLR, Center of Gravity: Metallic Solidification Jun. 1989 p 77-89 In GERMAN (For primary document see N90-20238 13-29)
Avail: NTIS HC A10/MF A02

The heat and mass transfer at the solidification front is studied and the anisotropy and the grain junctions are determined. A quasi isothermal solidification and a solidification in a temperature gradient field must be distinguished. In alloys the conditions are difficult, because the local equilibrium temperature between solidus and liquidus line can vary. During the solidification of a binary alloy, a surplus of one component appears in the fusion phase, because of the lower solubility in the crystal. A concentration drop is developed, whose profile is determined by the crystallization velocity and the diffusive or convective transfer in the fusion volume. The difficulties of the quantitative tests of solidification models are caused by the inaccuracy of the thermophysical magnitudes of fusion for the alloys, whose measurements are altered by the free convection. ESA

N90-20244# Krupp (Fried.) G.m.b.H., Essen (Germany, F.R.).
DISPERSION REINFORCED MATERIALS [DISPERSIONSVERSTAERKTE WERKSTOFFE]
Juergen Poetschke *In* DLR, Center of Gravity: Metallic Solidification Jun. 1989 p 91-93 In GERMAN (For primary document see N90-20238 13-29)
Avail: NTIS HC A10/MF A02

Research was carried for the manufacture of a material in which the particles or filaments are equally distributed. For economical reasons, it is interesting to produce these binders by solidification or casting. A theoretical approach to the behavior at advancing solid-liquid interfaces of foreign particles present in the melt as a separate phase was taken. The temperature field and the influence of a contaminant in the melt were taken into account. The equations chosen were solved numerically. The numerical data can be described with satisfactory accuracy by a function, so that the results can be communicated in the form of a self-contained expression. The use of this equation is found to be in good agreement with recent measurements of latex particles in water: the model gives the critical solidification velocity at which the latex particles of a specific size are only just pushed along by the ice front. An assessment of other measured values given in the literature is not possible since the material values and experimental parameters are not completely known. ESA

N90-20245# Max-Planck-Inst. fuer Metallforschung, Stuttgart (Germany, F.R.). Inst. fuer Werkstoffwissenschaften.
SYSTEMS WITH A MISCIBILITY GAP IN THE LIQUID STATE
B. Predel, L. Ratke, and H. Fredriksson (Royal Inst. of Tech., Stockholm, Sweden) *In* DLR, Center of Gravity: Metallic Solidification Jun. 1989 p 108-140 (For primary document see N90-20238 13-29)
Avail: NTIS HC A10/MF A02

Immiscible alloys have gained a renewed scientific and technological interest, because they allow production of fine, homogeneous dispersion alloys, that is possible in the absence of gravity driven convection and sedimentation. An overview of metallic immiscible alloys is presented. The Ga-Hg system is suitable for the experiments because of its low critical temperature. The asymmetry of the miscibility gap is especially marked in the Bi-Ga and Bi-Zn systems. Even with combinations of elements which are very similar with regard to their atomic size, as well as to their general chemical properties, positive enthalpy values can be observed when they are mixed in the liquid state so that a miscibility gap ensues. This is the case for some rare Earth metal combinations. The principle processes governing the two phase microstructure in immiscible alloys are: nucleation of the minority phase, growth of the nuclei, various types of matter transports, coalescence of nuclei and droplets. The gravity influences separation processes and the morphology of the microstructure. ESA

N90-20246# INTOSPACE G.m.b.H., Hanover (Germany, F.R.).
MOLDING SOLIDIFICATION [FORMGEBENDE ERSTARRUNG]
H. J. Sprenger *In* DLR, Center of Gravity: Metallic Solidification Jun. 1989 p 141-152 In GERMAN Sponsored by BMFT and DLR (For primary document see N90-20238 13-29)
Avail: NTIS HC A10/MF A02

By means of protective coating technology, the remelting of alloys and binders can be achieved if the deformation forces are well compensated. Such forces can be created by boundary and surface tensions, residual acceleration, cavities or gaseous bubbles in the melt, moving in the melt, external influences and volume increase. The experimental observations showed that nearly all deformation forces are surmountable by an appropriate choice of the test parameters. Only the volume increase, which appears in nearly all interesting technical alloys, by phase transistions solid-liquid, is difficult in microgravity laboratories. The tests with special alloys establish that few deformations appear with experiments made with very thin protective coatings. It can be concluded that the forces which are exerted on the protective coating by the volume variation in the melting have the greatest influence in the deformations, even under microgravity. ESA

N90-20247# Deutsche Forschungsanstalt fuer Luft- und Raumfahrt, Cologne (Germany, F.R.). Inst. fuer Raumsimulation.
MICROGRAVITY CONDITIONS OF A SPACE VEHICLE [MIKROGRAVITATIONSBEDINGUNGEN EINES RAUMFAHRZEUGS]
R. Jilg and H. Hamacher *In its* Center of Gravity: Metallic Solidification Jun. 1989 p 159-175 In GERMAN (For primary document see N90-20238 13-29)
Avail: NTIS HC A10/MF A02

A gravity field can be locally compensated by an acceleration field. A free drifting space vehicle is in a state of free fall. Its trajectory is generally elliptic in the inhomogeneous gravity field of the Earth. The observations show that the weightlessness can be simulated. Near the Earth surface, where the gravity field is nearly homogeneous, the fall curve becomes a parabola. The terrestrial field does not vary with time and location; the field in the space vehicle is dynamic and has a broad frequency spectrum; so that for many problems, a similarity between the tests in space and terrestrial laboratory is not possible; the establishment of the microgravity field is essential. For some physical processes, analytic results are obtained which indicate the maximal accelerations to be dependent on the frequency. ESA

N90-20248# Deutsche Forschungsanstalt fuer Luft- und Raumfahrt, Cologne (Germany, F.R.).
FUSION FURNACES FOR SPACELAB [SCHMELZOEFEN FUER SPACELAB]
F. Claasen *In its* Center of Gravity: Metallic Solidification Jun. 1989 p 185-192 In GERMAN (For primary document see N90-20238 13-29)
Avail: NTIS HC A10/MF A02

The performances, dimensions and characteristics of some fusion furnaces used in spacelab are given. Data on the power, the maximum temperature and the gradients are presented. The information is presented in the form of datasheets. ESA

N90-20249# Deutsche Forschungsanstalt fuer Luft- und Raumfahrt, Cologne (Germany, F.R.). Inst. fuer Raumsimulation.
ELECTROMAGNETIC FUSION PROCESS AND POSITION RESEARCH [ELEKTROMAGNETISCHE SCHMELZVERFAHREN UND POSITIONIERUNG]
I. Egry *In its* Center of Gravity: Metallic Solidification Jun. 1989 p 193-203 In GERMAN (For primary document see N90-20238 13-29)
Avail: NTIS HC A10/MF A02

Inductive heating is an efficient method to heat and melt

electrical conductive materials. Electromagnetic alternative fields produce Joule heating and thereby heat them. Moving by means of electromagnetic fields is applied to a cooled metal melt. All levitation devices use a high frequency generator, which produces the electromagnetic field. It is made of an oscillating circuit and an amplifier. The inductivity of the coil establishes the frequency of the field and its geometry determines the location dependence of the field. Conic open coils are used, which produce approximately a quadrupole field. Since, for heating, a dipole field is optimal, a two coil system is used which is more expensive but separates levitation and heating. ESA

N90-20250# Technische Univ., Clausthal-Zellerfeld (Germany, F.R.). Inst. fuer Nichtmetallische Werkstoffe.
DIFFUSION AND GERM FORMATION IN GLASSES [DIFFUSION UND KEIMBILDUNG IN GLAESERN]
G. Frischat *In* DLR, Center of Gravity: Metallic Solidification Jun. 1989 p 205-206 Sponsored by BMFT and DLR (For primary document see N90-20238 13-29)
Avail: NTIS HC A10/MF A02

An experiment was developed by which the behavior of a helium bubble in a soda-lime-silica glass melt at about 1100 C can be observed photographically under weightless conditions for 93 minutes. The experience ran successfully aboard the Space Shuttle Challenger during its mission in February 1987. Different compositions of the glass forming systems Li2O-SiO2 and Na2O-B2O3-SiO2 were melted and solidified both under microgravity and normal gravity conditions. The flight samples turned out to be more homogeneous than the terrestrial reference samples. This can be explained by the fact that heterogeneous nuclei from the contact zone container wall-melt are transported into the bulk of the melt by no convection under normal gravity, causing partial crystallization there. Also the morphologies of the crystalline phase were different between both sets of experiments. The addition of Pt as a nucleating agent lead to a more fine-grained microstructure for the microgravity samples. ESA

N90-20251*# National Aeronautics and Space Administration. Marshall Space Flight Center, Huntsville, AL.
THE NASA, MARSHALL SPACE FLIGHT CENTER DROP TUBE USER'S MANUAL
Thomas J. Rathz (Alabama Univ., Huntsville.) and Michael B. Robinson Mar. 1990 52 p
(NASA-TM-100392; NAS 1.15:100392) Avail: NTIS HC A04/MF A01 CSCL 22A

A comprehensive description of the structural and instrumentation hardware and the experimental capabilities of the 105-meter Marshall Space Flight Center Drop Tube Facility is given. This document is to serve as a guide to the investigator who wishes to perform materials processing experiments in the Drop Tube. Particular attention is given to the Tube's hardware to which an investigator must interface to perform experiments. This hardware consists of the permanent structural hardware (with such items as vacuum flanges), and the experimental hardware (with the furnaces and the sample insertion devices). Two furnaces, an electron-beam and an electromagnetic levitator, are currently used to melt metallic samples in a process environment that can range from 10(exp -6) Torr to 1 atmosphere. Details of these furnaces, the processing environment gases/vacuum, the electrical power, and data acquisition capabilities are specified to allow an investigator to design his/her experiment to maximize successful results and to reduce experimental setup time on the Tube. Various devices used to catch samples while inflicting minimum damage and to enhance turnaround time between experiments are described. Enough information is provided to allow an investigator who wishes to build his/her own furnace or sample catch devices to easily interface it to the Tube. The experimental instrumentation and data acquisition systems used to perform pre-drop and in-flight measurements of the melting and solidification process are also detailed. Typical experimental results are presented as an indicator of the type of data that is provided by the Drop Tube Facility. A summary bibliography of past Drop Tube experiments is provided, and an appendix explaining the noncontact temperature determination of free-falling drops is provided. This document is to be revised occasionally as improvements to the Facility are made and as the summary bibliography grows. Author

N90-20252*# National Aeronautics and Space Administration, Washington, DC.
MICROGRAVITY SCIENCE AND APPLICATION PROGRAM TASKS, 1989 REVISION
May 1990 219 p
(NASA-TM-4191; NAS 1.15:4191) Avail: NTIS HC A10/MF A02 CSCL 22A

The active research tasks, as of the fiscal year 1989, of the Microgravity Science and Applications Program, NASA Office of Space Science and Applications, involving several NASA Centers and other organizations are compiled. The purpose is to provide an overview of the program scope for managers and scientists in industry, university, and government communities. The scientists in industry, university, and government communities. An introductory description of the program, the strategy and overall goal, identification of the organizational structures and people involved, and a description of each task are included. Also provided is a list of recent publications. The tasks are grouped into several major categories: electronic materials, solidification of metals, alloys, and composites; fluids, interfaces, and transport; biotechnology; glasses and ceramics; combustion science; physical and chemistry experiments (PACE); and experimental technology, facilities, and instrumentation. Author

N90-20253*# National Aeronautics and Space Administration. Lewis Research Center, Cleveland, OH.
DESIGN AND TEST OF A COMPACT OPTICS SYSTEM FOR THE POOL BOILING EXPERIMENT
Jerri S. Ling and James R. Laubenthal Mar. 1990 17 p
(NASA-TM-102530; E-5339; NAS 1.15:102530) Avail: NTIS HC A03/MF A01 CSCL 22A

The experiment described seeks to improve the understanding of the fundamental mechanisms that constitute nucleate pool boiling. The vehicle for accomplishing this is an investigation, including tests to be conducted in microgravity and coupled with appropriate analyses, of the heat transfer and vapor bubble dynamics associated with nucleation, bubble growth/collapse and subsequent motion, considering the interrelations between buoyancy, momentum and surface tension which will govern the motion of the vapor and surrounding liquid, as a function of the heating rate at the heat transfer surface and the temperature level and distribution in the bulk liquid. The experiment is designed to be contained within the confines of a Get-Away-Special Canister (GAS Can) installed in the bay of the space shuttle. When the shuttle reaches orbit, the experiment will be turned on and testing will proceed automatically. In the proposed Pool Boiling Experiment a pool of liquid, initially at a precisely defined pressure and temperature, will be subjected to a step imposed heat flux from a semitransparent thin-film heater forming part of one wall of the container such that boiling is initiated and maintained for a defined period of time at a constant pressure level. Transient measurements of the heater surface and fluid temperatures near the surface will be made, noting especially the conditions at the onset of boiling, along with motion photography of the boiling process in two simultaneous views, from beneath the heating surface and from the side. The conduct of the experiment and the data acquisition will be completely automated and self-contained. For the initial flight, a total of nine tests are proposed, with three levels of heat flux and three levels of subcooling. The design process used in the development and check-out of the compact photographic/optics system for the Pool Boiling Experiment is documented.
Author

31 ENGINEERING (GENERAL)

Includes vacuum technology; control engineering; display engineering; cryogenics; and fire prevention.

N90-20254* National Aeronautics and Space Administration. Lyndon B. Johnson Space Center, Houston, TX.
SYSTEM FOR VENTING GAS FROM A LIQUID STORAGE TANK Patent
Regina E. Dugan, inventor (to NASA) 11 Jul. 1989 8 p Filed 30 Sep. 1988
(NASA-Case-MSC-21253-1; US-Patent-4,846,854; US-Patent-Appl-SN-251439; US-Patent-Class-55-46; US-Patent-Class-55-159; US-Patent-Class-137-154; US-Patent-Class-141-93; US-Patent-Class-239-543) Avail: US Patent and Trademark Office CSCL 13B

Gas is vented from a non-cryogenic liquid storage tank while discharging pressurized liquid from a tube into the tank through a plurality of inclined jets, circumferentially spaced about an end of a vent tube positioned within the tube. Each jet is directed toward a central axis of the vent tube, such that the end of the vent tube receives gas from the vessel passing between individual jetstreams, which in combination form a conical shaped barrier to liquid droplets which would otherwise also pass to the vent tube and out the tank. Gas is thus vented through the central tube while pressurized liquid flows in an axially opposite direction in the annulus between the inner vent tube and the outer liquid tube. The system of the present invention is prarticularly well suited for venting gas from a tank being replenished with liquid at a zero or near zero gravity environment. A screen-type liquid acquisition device employing surface tension is provided for withdrawing substantially liquid from the tank. The withdrawn liquid may be resupplied to the liquid tube under pressure supplied by a circulating pump, thereby releasing substantially only gas from the storage tank to reduce the pressure in the tank.
Official Gazette of the U.S. Patent and Trademark Office

N90-20255# Drexel Univ., Philadelphia, PA. Dept. of Materials Engineering.
SPRAY DEPOSITION: A FUNDAMENTAL STUDY OF DROPLET IMPINGEMENT, SPREADING AND CONSOLIDATION Final Report
D. Apelian, A. Lawley, and P. Mathur Dec. 1989 99 p
(Contract N00014-84-K-0472)
(AD-A217202; TR-14) Avail: NTIS HC A05/MF A01 CSCL 13/8

This report summarizes the objectives, approach and salient results of a program on spray casting. Spray casting via the Osprey (TM) process is emerging as a promising technology to produce near-net-shaped components of advanced materials. The process involves the sequential stages of gas atomization and droplet consolidation on a substrate to produce a disk, billet, tube and/or strip. The major advantage of spray casting is the ability to produce uniform, fine grained materials at deposition rates in the range 0.25 to 2.5 kg/s in a single operation from the melt. Composite materials can be manufactured by injecting second phase particles into the spray of droplets, or by in situ reactions between the droplets and the gas during flight. The objectives were to develop a scientific understanding of the physical and thermal phenomena that are active during spray casting and which govern the shape and microstructural integrity of the preforms and to evaluate the Osprey process for processing bulk high strength low alloy steels.
GRA

N90-20256# Michigan Univ., Ann Arbor. Coll. of Engineering.
FLEXIBLE AUTOMATIC DISCRETE PARTS ASSEMBLY Final Report, 1 Sep. 1987 - 31 Aug. 1988
D. E. Atkins and R. A. Volz Sep. 1989 110 p
(Contract F33615-85-C-5105; AF Proj. 2306)
(AD-A217401; RSD-TR-14-88; WRDC-TR-89-8037) Avail: NTIS HC A06/MF A01 CSCL 13/8

There is great emphasis today on the development of fully integrated manufacturing, including both the automation of individual manufacturing operations and the integration of all phases of manufacturing, from design through planning through production. The associated problems, however, are extremely complex and will require a large research effort over an extended period of time. This project is focused on an important category of flexible automation problems, in itself quite large, for which there are yet very few operational systems, flexible automated assembly. Assembly is the most highly labor intensive manufacturing process in the production of durable goods. There is thus great potential for direct cost saving through the development of flexible automated systems for assembly, as well as the indirect benefits mentioned above. The long term goal is to develop technologies that can be applied to many different aspects of assembly automation and that can be evolved to successively higher levels of abstraction, i.e., that will eventually allow high level commands, such as assembly product X, to be given. Three aspects of the problem are addressed: vision, planning/programming, and system integration. The first year's effort on this project toward these goals is described.
GRA

N90-20257# Lawrence Livermore National Lab., CA.
HIGH-EXPLOSIVES APPLICATIONS FACILITY (HEAF)
J. L. Morse, comp. and R. C. Weingart, comp. Mar. 1989 300 p
(Contract W-7405-eng-48)
(DE90-008122; UCID-21864) Avail: NTIS HC A13/MF A01

This Safety Analysis Report (SAR) reviews the safety and environmental aspects of the High Explosives Applications Facility (HEAF). Topics covered include the site selected for the HEAF, safety design criteria, operations planned within the facility, and the safety and environmental analyses performed on this project to date. Provided in the Summary section is a review of hazards and the analyses, conclusions, and operating limits developed in this SAR. Appendices provide supporting documents relating to this SAR. This SAR is required by the LLNL Health and Safety Manual and DOE Order 5481.1B(2) to document the safety analysis efforts. The SAR was assembled by the Hazards Control Department, B-Division, and HEAF project personnel. This document was reviewed by B Division, the Chemistry Department, the Hazards Control Department, the Laboratory Associate Director for Administration and Operations, and the Associate Directors ultimately responsible for HEAF operations.
DOE

N90-20258# Argonne National Lab., IL.
EVALUATION OF INDUSTRIAL MAGNETIC HEAT PUMP/REFRIGERATOR CONCEPTS THAT UTILIZE SUPERCONDUCTING MAGNETS
J. A. Waynert, A. J. DeGregoria, R. W. Foster, and J. A. Barclay Jun. 1989 66 p Prepared in cooperation with Astronautics Technology Center, Madison, WI
(Contract W-31-109-eng-38)
(DE90-008093; ANL-89/23) Avail: NTIS HC A04/MF A01

A preliminary assessment is provided of some magnetic heat pump (MHP)/refrigeration concepts for cryogen liquefaction and other industrial applications. Applications of interest range from the liquefaction of gases (20 to 100 K) to cold storage refrigeration for food preservation (250 to 320 K) to heat pumps utilizing industrial waste heat (350 to 400 K). Initial market penetration of magnetic refrigeration devices is anticipated for low temperature industrial applications such as the cryogen liquefaction field, and the major focus of the study is on hydrogen liquefaction (20 K) utilizing a liquid nitrogen heat sink (77 K). A brief market analysis indicated that there is a need for small (approx. 1 ton/day liquid hydrogen) hydrogen liquefiers with dispersed usage at appropriate sites in the country to reduce distribution costs. This provides an ideal market niche for magnetic liquefiers since conventional gas cycle liquefiers cannot be economically scaled to small sizes. A number of design options for hydrogen liquefiers are analyzed, including thermodynamic cycles; magnetic materials; heat exchangers; process of magnetization/demagnetization; magnet configurations; source/sink connections; and regenerative, recuperative, and active magnetic regenerative concepts.
DOE

N90-20259# Sandia National Labs., Albuquerque, NM. Thermal Test and Analysis Div.
THE THERMAL RESPONSE OF GENERIC OBJECTS IN JP-4 POOL FIRES
J. T. Nakos, W. Gill, and N. R. Keltner 1990 33 p Presented at the 1990 JANNAF Propulsion Systems Hazards Meeting, Laurel, MD, 3-5 Apr. 1990
(Contract DE-AC04-76DP-00789)
(DE90-008503; SAND-89-0412C; CONF-9004147-1) Avail: NTIS HC A03/MF A01

The measured thermal response of generic objects in engulfing pool fires is presented. The objects include cylinders and flat plates of various sizes and materials. A simple radiation/convection model of the heat transfer from the fire to the object is developed and discussed in light of the experimental data. DOE

N90-20260# Lawrence Livermore National Lab., CA.
A GUIDE TO PERFORMING AND DOCUMENTING SAFETY ANALYSES
Edward J. Hallinan Feb. 1989 89 p
(Contract W-7405-eng-48)
(DE90-008687; LLNL-M-243-Vol-1) Avail: NTIS HC A05/MF A01

Safety analysis has been one of the most volatile technical fields in recent times. In fact, some have questioned whether it qualifies as a technical field. Controversies have arisen because: safety analysis results are prophesies and not exact predictions; most of the results are qualitative rather than quantitative; exact quantitative criteria for comparison are scarce. Terms such as unlikely for event frequency and major for consequences are frequently used. These terms are hard to define and assess; data for predictions is also scarce, may not exactly apply, and is subject to large uncertainties; most accidents can involve human errors, and human response cannot be accurately estimated; safety analysis is a relatively new field with ever-changing rules and requirements; relatively few personnel were trained in safety analysis techniques and have operations experience, both in the organizations that perform the safety analyses and those that regulate how safety analyses are to be done; safety analysis budgets are usually controlled by line organizations that must also design, build, and operate the facility. Line organizations usually perceive such safety analysis costs as nonproductive and thus provide only minimum funding; in general, radiological impacts are overemphasized, and nonradiological impacts are superficially treated. This leads to inconsistencies in analyzing and designing against hazards; and safety analyses are not performed, reviewed, or documented consistently throughout the U.S. Department of Energy (DOE) complex. DOE

N90-20261# Lawrence Livermore National Lab., CA.
A GUIDE TO PERFORMING AND DOCUMENTING SAFETY ANALYSES
Edward J. Hallinan Mar. 1989 60 p
(Contract W-7405-eng-48)
(DE90-008688; LLNL-M-243-Vol-2) Avail: NTIS HC A04/MF A01

The detailed example included demonstrates how the guidelines in Volume 1 can help safety analysts and managers achieve their goals by illustrating the process and the result. The example was chosen from a familiar operation to highlight the process and sample report without getting lost in explaining technical details or creating a forum for disagreements over fine points rather than concentrating on approach and presentation. (The example would really fall into the category of routinely accepted and not need a safety analysis as defined by DOE Order 5480.1B and 5481.1B. However, for the purposes of this document, it is assumed that a safety analysis is needed for the example). Although this volume reviews basic concepts from Volume 1 that will be needed for the example, consult the main text for more detailed information. DOE

N90-20262# Air Force Inst. of Tech., Wright-Patterson AFB, OH.
AN EXPERT SYSTEM FOR THE DESIGN OF HEATING, VENTILATING, AND AIR-CONDITIONING SYSTEMS M.S. Thesis - Purdue Univ.
Pedro Jose Camejo Dec. 1989 154 p
(AD-A218287; AFIT/CI/CIA-89-178) Avail: NTIS HC A08/MF A01 CSCL 12/9

Expert systems are computer programs that seek to mimic human reason. An expert system shell, a software program commonly used for developing expert systems in a relatively short time, was used to develop a prototypical expert system for the design of heating, ventilating, and air-conditioning (HVAC) systems in buildings. Because HVAC design involves several related knowledge domains, developing an expert system for HVAC design requires the integration of several smaller expert systems known as knowledge bases. A menu program and several auxiliary programs for gathering data, completing calculations, printing project reports, and passing data between the knowledge bases are needed and have been developed to join the separate knowledge bases into one simple-to-use program unit. GRA

32 COMMUNICATIONS AND RADAR

Includes radar; land and global communications; communications theory; and optical communications.

For related information see also *04 Aircraft Communications and Navigation* and *17 Space Communications, Spacecraft Communications, Command and Tracking.* For search and rescue see *03 Air Transportation and Safety,* and *16 Space Transportation.*

N90-20263*# Notre Dame Univ., IN. Dept. of Electrical and Computer Engineering.
ERROR CONTROL TECHNIQUES FOR SATELLITE AND SPACE COMMUNICATIONS Semiannual Status Report
Daniel J. Costello, Jr. Feb. 1990 83 p
(Grant NAG5-557)
(NASA-CR-186221; NAS 1.26:186221) Avail: NTIS HC A05/MF A01 CSCL 17B

An expurgated upper bound on the event error probability of trellis coded modulation is presented. This bound is used to derive a lower bound on the minimum achievable free Euclidean distance d sub (free) of trellis codes. It is shown that the dominant parameters for both bounds, the expurgated error exponent and the asymptotic d sub (free) growth rate, respectively, can be obtained from the cutoff-rate R sub O of the transmission channel by a simple geometric construction, making R sub O the central parameter for finding good trellis codes. Several constellations are optimized with respect to the bounds. Author

N90-20264*# National Aeronautics and Space Administration. Lewis Research Center, Cleveland, OH.
NUMERICAL ARC SEGMENTATION ALGORITHM FOR A RADIO CONFERENCE-NASARC (VERSION 4.0) TECHNICAL MANUAL
Wayne A. Whyte, Jr., Ann O. Heyward, Denise S. Ponchak, Rodney L. Spence, and John E. Zuzek 6 Oct. 1988 156 p
(NASA-TM-101453; E-4736; NAS 1.15:101453) Avail: NTIS HC A08/MF A01 CSCL 17B

The information contained in the NASARC (Version 4.0) Technical Manual and NASARC (Version 4.0) User's Manual relates to the Numerical Arc Segmentation Algorithm for a Radio Conference (NASARC) software development through November 1, 1988. The Technical Manual describes the NASARC concept and the algorithms used to implement the concept. The User's Manual provides information on computer system considerations, installation instructions, description of input files, and program operation instructions. Significant revisions were incorporated in the Version 4.0 software over prior versions. These revisions have further enhanced the modeling capabilities of the NASARC procedure and provide improved arrangements of predetermined

arcs within the geostationary orbits. Array dimensions within the software were structured to fit within the currently available 12 megabyte memory capacity of the International Frequency Registration Board (IFRB) computer facility. A piecewise approach to predetermined arc generation in NASARC (Version 4.0) allows worldwide planning problem scenarios to be accommodated within computer run time and memory constraints with enhanced likelihood and ease of solution. Author

N90-20265# Illinois Univ., Urbana-Champaign. Coordinated Science Lab.
TOMOGRAPHIC PROCESSING OF SYNTHETIC APERTURE RADAR SIGNALS FOR ENHANCED RESOLUTION Ph.D. Thesis - 1990
Jerald Lee Bauck Nov. 1989 219 p
(Contract DAAL03-86-K-0111)
(AD-A217178; UILU-ENG-89-2236; ARO-24370.41-MA) Avail: NTIS HC A10/MF A02 CSCL 17/9

Spotlight-mode synthetic aperture radar imaging is studied from the viewpoint of tomographic signal processing which allows the relaxation of the nearly-universal assumption that plane waves pass over the ground patch. This allows high-quality image reconstruction in the face of arbitrary amounts of wavefront curvature such as would be present when the angle subtended by the ground patch, as seen by the radar, is not small. One such application is wide-area surveillance. A methodology is used which has the benefits of a wideband transmitted signal (impulse) and a sensible simulation. Image reconstruction algorithms are developed for monostatic and bistatic systems. Simulation results using these algorithms compare favorably with baseline simulations which use a more conventional algorithm operating on data which do not embody the effects of wavefront curvature. Comments on system design and computational implementation are made as necessary. A new set of problems which appear to benefit from the tomographic viewpoint is posed. This work may also find applications in some forms of reflection tomography. GRA

N90-20266# Army Inst. for Research in Management Information and Computer Sciences, Atlanta, GA.
TECHNOLOGY ASSESSMENT OF VIDEO TELECONFERENCING
Feb. 1989 13 p
(AD-A217318; ASQBG-A-89-010) Avail: NTIS HC A03/MF A01 CSCL 25/3

There are three major types of video teleconferencing (VTC) available today, they are: Ad hoc VTC, Slow-scan VTC, and Full-motion VTC. Ad hoc VTC refers to the transmission of a full-motion TV image from one site to many. This form of VTC has been mainly used for product announcements by companies and is usually done over a network of public VTC rooms on a one time basis. This approach is expensive, but effective in reaching a targeted group of people at one time. Slow-scan VTC transmits a picture over a low speed line (telephone lines), in a few seconds a retransmission occurs for only the parts of the picture that have changed. This low cost method is good for a few applications where very little motion is involved. Full-motion VTC most nearly recreates the face to face meeting. Depending on transmission rates, this method can approach the quality of a TV transmission. The major cost factors in this approach are transmission speed and the equipment to code and decode the signals. AT and T was awarded the contract for the Defense Commercial Telecommunications Network (DCTN) in March of 1984 for the period January 1986 to January 1996. DCTN is a leased communications service that provides voice, data, and video service for DOD and GSA. The major advance that DCTN provides over standard voice and data service is VTC. DCTN is the standard vehicle for VTC within the DOD. The use of any other network requires a waiver from the Defense Communications Agency. GRA

N90-20267# Columbia Univ., New York, NY. Radiation Lab.
RESEARCH INVESTIGATION DIRECTED TOWARD EXTENDING THE USEFUL RANGE OF THE ELECTROMAGNETIC SPECTRUM Annual Progress Report No. 39, 1 Oct. 1988 - 30 Sep. 1989
George W. Flynn and Richard M. Osgood, Jr. 31 Dec. 1989 97 p Sponsored in part by IBM Corp.
(Contracts DAAL03-88-C-0009; DAAL03-89-K-0028; F49620-86-C-0067; DE-FG02-88ER-13937; N00014-86-K-0694; N00014-88-K-0299; SRC-88-SJ-055; NSF CHE-88-16581; NSF PHY-88-20540)
(AD-A217460) Avail: NTIS HC A05/MF A01 CSCL 20/14

JSEP research has yielded two new laser microprobes for use in electronics fabrication. The development of such probes is increasingly important because of the need for precision in situ monitoring in advanced electronics fabrication. In the first, photoelectric emission induced by a focused UV laser beam was used for the first time to make a scanning photoemission microscope for probing semiconductor surfaces. With this instrument it was possible to map regions of different doping levels on a silicon surface. The spatial resolution was found to be limited only by the laser beam spot size. In addition, Raman microprobe spectroscopy was used to profile locally doped regions in GaAs with micrometer-level resolution. This is an important in-situ diagnostic technique for compound semiconductors. Ways were investigated of making improved sources of silent light (also known as photon number squeezed light or sub-Poisson light), and determined how such light behaves when it impinges on simple optical elements such as dielectric beamsplitters. In addition, the novel ultrafast optical technique of time-delayed four-wavemixing (TDFWM) was used to measure optical dephasing phenomena in semiconductor doped glasses. Dephasing times as short as 18 fsec were observed at room temperature with no evidence of modulated structure. GRA

N90-20268# Sandia National Labs., Albuquerque, NM.
THE ADAPTIVE LINE ENHANCER APPLIED TO CHIRP DETECTION
Glenn R. Elliott and Samuel D. Stearns 1990 9 p Presented at the 1990 International Symposium on Circuits and Systems, New Orleans, LA, 1-3 May 1990
(Contract DE-AC04-76DP-00789)
(DE90-006772; SAND-90-0231C; CONF-9005116-1) Avail: NTIS HC A02/MF A01

This paper discusses the ability of an adaptive line enhancer (ALE) driven by the least-mean-squares (LMS) algorithm to track the frequency of a chirping signal in broadband noise. The dynamic behavior of the weights is described and a weight tracking error bound is derived in terms in chirp rate. Frequency tracking and weight behavior are illustrated in examples. DOE

N90-20269# Lawrence Livermore National Lab., CA.
MODELLING DOPPLER BROADENING IN RAMAN PROPAGATION
Richard Sacks 28 Feb. 1990 5 p
(Contract W-7405-eng-48)
(DE90-008042; UCID-21792) Avail: NTIS HC A01/MF A01

In December 1986, Karr described an elegant treatment for inhomogeneous broadening of Raman lines, within the context of an integral formulation of the Bloch equation. This formulation relied, for important simplifications, on the assumptions that the molecular population inversion be independent of velocity and that the velocity distribution be Maxwellian. An alternative description, a truncated velocity moment series for the differential Liouville equation, is derived. DOE

N90-20270*# Communications Satellite Corp., Clarksburg, MD.
ADVANCED MODULATION TECHNOLOGY DEVELOPMENT FOR EARTH STATION DEMODULATOR APPLICATIONS. CODED MODULATION SYSTEM DEVELOPMENT Final Report
Susan P. Miller, J. Mark Kappes, David H. Layer, and Peter N. Johnson Apr. 1990 95 p

(Contract NAS3-24680)
(NASA-CR-185149; NAS 1.26:185149; CTD-90/022) Avail: NTIS HC A05/MF A01 CSCL 17B

A jointly optimized coded modulation system is described which was designed, built, and tested by COMSAT Laboratories for NASA LeRC which provides a bandwidth efficiency of 2 bits/s/Hz at an information rate of 160 Mbit/s. A high speed rate 8/9 encoder with a Viterbi decoder and an Octal PSK modem are used to achieve this. The BER performance is approximately 1 dB from the theoretically calculated value for this system at a BER of 5 E-7 under nominal conditions. The system operates in burst mode for downlink applications and tests have demonstrated very little degradation in performance with frequency and level offset. Unique word miss rate measurements were conducted which demonstrate reliable acquisition at low values of Eb/No. Codec self tests have verified the performance of this subsystem in a stand alone mode. The codec is capable of operation at a 200 Mbit/s information rate as demonstrated using a codec test set which introduces noise digitally. The measured performance is within 0.2 dB of the computer simulated predictions. A gate array implementation of the most time critical element of the high speed Viterbi decoder was completed. This gate array add-compare-select chip significantly reduces the power consumption and improves the manufacturability of the decoder. This chip has general application in the implementation of high speed Viterbi decoders. Author

N90-20271*# Ohio State Univ., Columbus. ElectroScience Lab.
EFFECTS OF ADDITIONAL INTERFERING SIGNALS ON ADAPTIVE ARRAY PERFORMANCE
Randolph L. Moses Sep. 1989 29 p
(Grant NAG3-536)
(NASA-CR-186508; NAS 1.26:186508; OSU-TR-716111-8) Avail: NTIS HC A03/MF A01 CSCL 20N

The effects of additional interference signals on the performance of a fully adaptive array are considered. The case is considered when more interference signals than array degrees of freedom. It is shown how performance is affected as a function of the number of array elements, the number of interference signals, and the directivity of the array antennas. By using directive auxiliary elements, the performance of the array can be as good as the performance when the additional interference signals are not present. Author

N90-20272# Air Force Inst. of Tech., Wright-Patterson AFB, OH.
MULTIPLE VERSUS SINGLE SCATTERING OF TERRESTRIAL INFRARED LONGWAVE RADIATION IN AN AEROSOL-LADEN PLANETARY BOUNDARY LAYER M.S. Thesis
Spencer R. Chapman 1989 102 p
(AD-A217709; AFIT/CI/CIA-89-036) Avail: NTIS HC A06/MF A01 CSCL 20/4

The quantitative difference between multiply and singly scattered infrared terrestrial radiation in an aerosol-laden planetary boundary layer (PBL) is examined. The total net (scattering plus emission) flux densities are calculated at 11 levels. The model PBL is a summertime mid-latitude urban structure from LOWTRAN 7. The study prototype incorporates an inversion located at 2.00 km above a surface whose elevation is at sea level with a visual range of 4.0 km. The visual range and extinction coefficients decrease with height to minimums located just below the inversion to simulate a differentially mixed aerosol-laden PBL. GRA

N90-20273# Naval Research Lab., Washington, DC.
GENERAL FORMS AND PROPERTIES OF ZERO CROSS-CORRELATION RADAR WAVEFORMS Interim Report
Karl Gerlach and F. F. Kretschmer, Jr. 30 Jan. 1990 17 p
(AD-A217779; NRL-9120) Avail: NTIS HC A03/MF A01 CSCL 17/9

General forms for both the complementary and noncomplementary zero cross correlation waveform sets are developed. Various properties of these codes and their relationship to zero sidelobe periodic codes are stated and proved. Some radar applications and practical considerations of using these codes are presented. GRA

N90-20274# Massachusetts Inst. of Tech., Cambridge. Lab. for Information and Decision Systems.
ON OPTIMAL DISTRIBUTED DECISION ARCHITECTURES IN A HYPOTHESIS TESTING ENVIRONMENT
Jason D. Papastavrou and Michael Athans Jan. 1990 50 p
(Contract N00014-84-K-0519)
(AD-A217824; LIDS-P-1928) Avail: NTIS HC A03/MF A01 CSCL 05/9

A distributed detection problem was considered in which a set of decision makers (DMs) receive observations of the environment and transmit finite valued messages to other DMs according to prespecified communication protocols. A designated primary DM makes the final decision on one out of two alternative hypotheses. All DMs make decisions, in order to maximize a measure of organizational performance. Given the DMs and the communication resources, the problem is to find an architecture for the organization which remains optimal for a variety of operating conditions (if it exists). It is shown that even for very small organizations this problem is quite complex, because the optimal architecture depends on variables external to the team like the prior probabilities of the hypotheses and the misclassification costs, so that global conclusions on optimal organizational structures cannot be drawn. Suboptimal solutions are also considered and bounds were obtained on their performance. GRA

N90-20275# Texas Univ., Arlington. Dept. of Electrical Engineering.
SIMULATION OF RADAR SCATTERING FROM ROUGH SURFACES Final Report
A. K. Fung 3 Jan. 1990 13 p
(Contract N00014-87-K-0751)
(AD-A217841) Avail: NTIS HC A03/MF A01 CSCL 20/14

The project established computer simulation as a tool for studying scattering from randomly rough surfaces. The proposed methods to be investigated included the standard moment method and the integral equation method (IEM). The minimum size was investigated for the surface patch necessary to obtain the scattering cross section per unit area, which should be the same as obtained from an infinite surface patch when the method used was the standard moment method. Five points per wavelength, or per surface correlation length (whichever was the smaller), were needed and the minimum surface patch should be at least seven electric wavelengths, or surface correlation lengths (whichever was the larger). The minimum number of surface patches to be averaged to obtain a satisfactory estimate of the scattering coefficient was 25. This means that the smallest number of unknowns to be evaluated was (35 x 35) for a scaler problem and 2 times (35 x 35) for a vector problem. To determine this many unknowns for a scalar problem one needs to invert a matrix size of 35 sq by 35 sq in the moment method. In general, the size of the problem would be larger and hence the integral equation method was investigated. The IEM was a better method than the moment method in that it required much less memory. It required a much greater computational time. For this reason another method called the frequency domain method (FDM) was considered and judged to be the preferred method. GRA

N90-20276# Utah State Univ., Logan. Dept. of Soil and Biometeorology.
METEOR OBSERVATIONS USING THE 50 MHz MENTOR IMAGING DOPPLER INTERFEROMETER M.S. Thesis
Dennis Randall Thomas 1989 56 p Sponsored in part by Holodyne, Inc.
(Contract F49620-89-C-022; NSF ATM-86-08391; NSF ATM-87-19781; NSF ATM-88-13454)
(AD-A217908; AFIT/CI/CIA-89-039) Avail: NTIS HC A04/MF A01 CSCL 17/9

The MENTOR Imaging Doppler Interferometer radar operated at a frequency of approximately 50 MHz with a 50 kilowatt peak power output. It was used to collect data from a field site. An

algorithm was developed to detect meteor echoes in the Time Domain Averaged (TDA) data, separate these echoes from the rest of the data, and then determine which of these echoes were good enough to be included in wind calculations. The meteor detection rate for useable meteors in the approximately 9 minutes of data available was 120 per hour. The meteors, after being located in 3-D space, were subjected to another algorithm which calculated the u, v, and w wind components for a range of altitudes, usually less than 4 kilometers, using the Doppler shift of the meteor echoes. Reasonable values for the wind components were obtained but could not be verified since there were no collateral data to back up the results. GRA

N90-20277# Rockwell International Corp., Anaheim, CA. Autonetics Sensors and Aircraft Systems Div.
MODELING AND CLASSIFICATION OF ACOUSTIC TRANSIENTS BY SPEECH RECOGNITION TECHNIQUES
Jeffrey P. Woodard 1989 62 p
(Contract N00014-88-C-0481)
(AD-A218070) Avail: NTIS HC A04/MF A01 CSCL 25/4

Techniques from automatic speech recognition are applied to the problem of modeling and classifying acoustic transients. Linear Predictive Coding (LPC), Vector Quantization (VQ) and Hidden Markov Models (HMMs) are three popular techniques which when combined together are called the structural-parametric approach to the recognition of speech sounds. The same approach is applied first in modeling and then in identifying three classes of brief, wideband sounds, similar to underwater passive sonar transients. An LPC analysis synthesis system operating below 9000 bits per second can produce high quality synthetic transients. The data rate necessary to maintain high quality can be further reduced to about 1100 bits per second by LPC followed by VQ, using the Itakura Saito (IS) class of distortion measures. The high fidelity achievable at low rates is evidence that LPC is a good spectral representation and that the IS distortion measure is meaningful in the comparison of transient spectra. Classification decisions based solely on averaged VQ distortion or entropy result in a classification accuracy of over 97 percent. Classification decisions based on VQ followed by HMMS result in a classification performance of the HMMM structures. The product code HMM consists of two independent HMMS per class; a classification decision is made by combining the results of the two independent HMMs. GRA

N90-20278# Ohio State Univ., Columbus. ElectroScience Lab.
HIGH RESOLUTION RADAR TARGET MODELING USING ARMA (AUTOREGRESSIVE MOVING AVERAGE) MODELS
R. Carriere and R. L. Moses Apr. 1989 53 p
(Contract N00014-86-K-0202)
(AD-A218212; Rept-718048-11) Avail: NTIS HC A04/MF A01 CSCL 17/9

A method for characterizing radar signatures using autoregressive moving average (ARMA) models is developed based on the concept of scattering centers. A parameterization of the ARMA model specific to the radar target identification problem is chosen, and several key improvements to the algorithm, including the use of singular value decomposition and the removal of spurious scattering centers are presented and compared to earlier versions of the algorithm. The resulting algorithm is tested with data taken from a compact range. These tests include comparison of different targets, different aspect angles and frequency ranges, as well as robustness tests on the algorithm and evaluation of performance in noise. GRA

N90-20279# Autonomous Technologies, Orlando, FL.
MULTI-DIMENSIONAL LADAR TRACKING AND ADAPTIVE GRASPING FOR SPACEBORNE ASSEMBLY OF SDI (STRATEGIC DEFENSE INITIATIVE) PLATFORMS Final Report, 1 Jun. - 30 Nov. 1989
Randy W. Frey and John A. Bohlin 16 Feb. 1990 40 p
(Contract DASG60-89-C-0079)
(AD-A218236; AD-E501191) Avail: NTIS HC A03/MF A01 CSCL 12/9

The most successful approaches to both machine target recognition and robot arm manipulation have been those where tasks are completely pre-specified. In such systems there is little room for deviations in robot path motion or target location and orientation. A novel approach to robotic implementation such as spaceborne assembly of SDI platforms are too difficult for existing robots because random occurrences and large numbers of external variables preclude the complete specification of tasks off-line. The proposed system has strong adaptability due to the following innovations: Registered video and range laser radar sensing (i.e., a one-to-one correspondence between visual and range data). This allows fast, accurate 3D target recognition as part of an autonomous CAD model based recognition system for Phase 2, or as input to teleoperator control in Phase 1. Closed loop range and video feedback for grasper guidance using the pose matching concept where target and grasper are both in the field of view, and CAD derived track points are used for position and orientation error signals. GRA

N90-20280* National Aeronautics and Space Administration. Lyndon B. Johnson Space Center, Houston, TX.
DOPPLER RADAR WITH MULTIPHASE MODULATION OF TRANSMITTED AND REFLECTED SIGNAL Patent
Paul W. Shores, inventor (to NASA), John W. Griffin, inventor (to NASA), and Herbert S. Kobayashi, inventor (to NASA) 25 Nov. 1987 16 p Filed 25 Nov. 1987
(NASA-Case-MSC-18808-1; US-Patent-4,860,014; US-Patent-Appl-SN-125677; US-Patent-Class-342-105; US-Patent-Class-342-114; US-Patent-Class-342-195) Avail: US Patent and Trademark Office CSCL 17I

A microwave radar signal is generated and split by a circulator. A phase shifter introduces a series of phase shifts into a first part of the split signal which is then transmitted by antenna. A like number of phase shifts is introduced by the phase shifter into the return signal from the target. The circulator delivers the phase shifted return signal and the leakage signal from the circulator to a mixer which generates an IF signal output at the Doppler frequency. The IF signal is amplified, filtered, counted per unit of time, and the result displayed to provide indications of target sense and range rate. An oscillator controls rate of phase shift in the transmitted and received radar signals and provides a time base for the counter. The phase shift magnitude increases may be continuous and linear or discrete functions of time.
Official Gazette of the U.S. Patent and Trademark Office

33 ELECTRONICS AND ELECTRICAL ENGINEERING

Includes test equipment and maintainability; components, e.g., tunnel diodes and transistors; microminiaturization; and integrated circuitry.

For related information see also *60 Computer Operations and Hardware* and *76 Solid-State Physics.*

N90-20281*# Jet Propulsion Lab., California Inst. of Tech., Pasadena.
PRODUCT ASSURANCE TECHNOLOGY FOR PROCURING RELIABLE, RADIATION-HARD, CUSTOM LSI/VLSI ELECTRONICS Report, Oct. 1984 - Sep. 1986
M. G. Buehler, R. A. Allen, B. R. Blaes, K. A. Hicks, G. A. Jennings, Y.-S. Lin, C. A. Pina, H. R. Sayah, and N. Zamani Jan. 1989 236 p
(Contract NAS7-918)
(NASA-CR-185954; JPL-Publ-89-1; NAS 1.26:185954) Avail: NTIS HC A11/MF A02 CSCL 09A

Advanced measurement methods using microelectronic test chips are described. These chips are intended to be used in acquiring the data needed to qualify Application Specific Integrated Circuits (ASIC's) for space use. Efforts were focused on developing the technology for obtaining custom IC's from CMOS/bulk silicon foundries. A series of test chips were developed: a parametric test strip, a fault chip, a set of reliability chips, and the CRRES (Combined Release and Radiation Effects Satellite) chip, a test

circuit for monitoring space radiation effects. The technical accomplishments of the effort include: (1) development of a fault chip that contains a set of test structures used to evaluate the density of various process-induced defects; (2) development of new test structures and testing techniques for measuring gate-oxide capacitance, gate-overlap capacitance, and propagation delay; (3) development of a set of reliability chips that are used to evaluate failure mechanisms in CMOS/bulk: interconnect and contact electromigration and time-dependent dielectric breakdown; (4) development of MOSFET parameter extraction procedures for evaluating subthreshold characteristics; (5) evaluation of test chips and test strips on the second CRRES wafer run; (6) two dedicated fabrication runs for the CRRES chip flight parts; and (7) publication of two papers: one on the split-cross bridge resistor and another on asymmetrical SRAM (static random access memory) cells for single-event upset analysis. Author

N90-20282* National Aeronautics and Space Administration. Goddard Space Flight Center, Greenbelt, MD.
MICROWAVE FIELD EFFECT TRANSISTOR Patent
Ho-Chung Huang, inventor (to NASA) (Radio Corp. of America, Bethesda, MD.) 27 Jun. 1989 12 p Filed 29 Nov. 1984 Continuation of US-Patent-Appl-SN-327659, dated 4 Dec. 1981, abandoned
(NASA-Case-GSC-12442-2; US-Patent-4,843,440; US-Patent-Appl-SN-675471; US-Patent-Class-357-22; US-Patent-Class-357-68; US-Patent-Class-357-76; US-Patent-Class-357-81; US-Patent-Class-357-55) Avail: US Patent and Trademark Office CSCL 09A

Electrodes of a high power, microwave field effect transistor are substantially matched to external input and output networks. The field effect transistor includes a metal ground plane layer, a dielectric layer on the ground plane layer, a gallium arsenide active region on the dielectric layer, and substantially coplanar spaced source, gate, and drain electrodes having active segments covering the active region. The active segment of the gate electrode is located between edges of the active segments of the source and drain electrodes. The gate and drain electrodes include inactive pads remote from the active segments. The pads are connected directly to the input and output networks. The source electrode is connected to the ground plane layer. The space between the electrodes and the geometry of the electrodes extablish parasitic shunt capacitances and series inductances that provide substantial matches between the input network and the gate electrode and between the output network and the drain electrode. Many of the devices are connected in parallel and share a common active region, so that each pair of adjacent devices shares the same source electrodes and each pair of adjacent devices shares the same drain electrodes. The gate electrodes for the parallel devices are formed by a continuous stripe that extends between adjacent devices and is connected at different points to the common gate pad. Official Gazette of the U.S. Patent and Trademark Office

N90-20283# Los Alamos National Lab., NM.
MEASUREMENT OF PROTON INDUCED RADIATION DAMAGE TO CMOS TRANSISTORS AND PIN DIODES
J. Bacigalupi, N. Cartiglia, J. DeWitt, P. Ferguson, P. Giubellino, C. M. Hoffman, D. Holtkamp, A. Kaluzniacki, W. W. Kinnison, and H. Kolanoski (California Univ., Santa Cruz.) et al 1990 4 p Presented at the IEEE 1989 Nuclear Science Symposium, San Francisco, CA, 22-26 Jan. 1990
(Contract W-7405-eng-36)
(DE90-007836; LA-UR-90-16; CONF-900143-23) Avail: NTIS HC A01/MF A01

As part of the program to develop a silicon tracking device for the SSC radiation-hard CMOS transistors and PIN diodes were exposed to the 800 MeV LAMPF proton beam. The fluences accumulated in a week corresponded to the expected radiation levels of about 10 SSC years. The leakage current constants for PIN diodes and threshold voltage shifts for CMOS transistors under different biasing conditions were determined. One of the main requirements for detectors and front-end electronics at the SSC is to be radiation resistant. The SSC Workshop on Radiation Levels in the SSC found that, for example, a silicon tracking device at a radius of 10 cm has to survive a yearly dose of about 0.3 MRad due to charged particles and a yearly neutron fluence of a few times 10(exp 12) neutrons/sq cm at the design luminosity of 10(exp 33)/sq cm/sec. DOE

N90-20284*# Old Dominion Univ., Norfolk, VA. Dept. of Electrical Engineering Technology.
ANALYSIS OF RADIOMETER CALIBRATION EFFECTS WITH TOUCHSTONE Final Report, 22 Jun. - 31 Dec. 1989
William D. Stanley Mar. 1990 36 p
(Contract NAS1-18584)
(NASA-CR-186476; NAS 1.26:186476) Avail: NTIS HC A03/MF A01 CSCL 09A

The microwave circuit analysis program TOUCHSTONE is used to study two effects of importance in radiometer calibration. The two effects are impedance mismatches at the antenna-air and cold load-air interfaces and dissipatives losses, which radiate thermal noise into the system. The results predicted by TOUCHSTONE are shown to be in very close agreement with earlier results obtained by purely analytical methods. The techniques used in establishing the circuit models and in processing the resulting data are described in detail. Author

N90-20285# Sandia National Labs., Albuquerque, NM.
THE INVERSE TRIAX X RAY DIODE: AN ALTERNATE REDUCED-ENDPOINT-ENERGY BREMSSTRAHLUNG SOURCE
V. J. Harper-Slaboszewicz, J. W. Poukey, W. A. Stygar, W. E. Fowler, and B. Peyton (Ktech Corp., Albuquerque, NM.) Feb. 1990 32 p
(Contract DE-AC04-76DP-00789)
(DE90-006366; SAND-89-1890) Avail: NTIS HC A03/MF A01

The inverse triax diode is a high power, low impedance electron diode which offers significant advantages over conventional electron diodes on short-pulse (less than 30 ns FWHM) high power x ray simulators. Parametric calculations show that the radiation efficiency of the inverse triax is competitive with standard diodes for mean photon energies below about 120 keV, and sometimes up to 150 keV. Particle-in-cell code simulations show the impedance behavior and flow pattern in the inverse triax with and without the presence of an anode plasma. The simulation results are used to suggest design rules for inverse triax diodes. Experimental results show good agreement with calculations of the impedance behavior and electron beam dynamics. Using inverse triax diodes, we have produced peak doses of 1.4 x 10(exp 11) rad(TLD)/s over 840 sq cm with a mean photon energy of 120 keV on SPEED and 3.1 x 10(exp 11) rad(TLD)/s over 3700 sq cm with a mean photon energy of 140 keV on Saturn. DOE

N90-20286*# National Aeronautics and Space Administration. Lewis Research Center, Cleveland, OH.
EXPERIMENTAL INVESTIGATIONS ON CHANNELIZED COPLANAR WAVEGUIDE
Rainee N. Simons, George E. Ponchak, Konstantinas S. Martzaklis (Akron Univ., OH.), and Robert R. Romanofsky Apr. 1990 17 p
(Grant NAG3-816)
(NASA-TM-102494; E-5285; NAS 1.15:102494) Avail: NTIS HC A03/MF A01 CSCL 09A

A new variant of coplanar waveguide (CPW) which was termed channelized coplanar waveguide (CCPW) is presented. Measured propagation characteristics for CCPW such as epsilon(eff) and unloaded Q as a function of geometrical parameters and frequency are presented. The measured and modeled epsilon(eff) are also compared. Equivalent circuit model element values are presented for a CCPW open circuit and a CCPW right angle bend. A CCPW matched T-junction, matched 1:3 junction, and a novel coax-to-CCPW in-phase, N-way, radial power divider are also demonstrated. Author

N90-20287# Massachusetts Inst. of Tech., Cambridge. Lab. for Computer Science.
EXPRESS CUBES: IMPROVING THE PERFORMANCE OF k-ary n-CUBE INTERCONNECTION NETWORKS
William J. Dally Oct. 1989 16 p Sponsored in part by NSF, General Electric Corp., and by IBM Corp.
(Contracts N00014-88-K-0738; N00014-87-K-0825)
(AD-A217117; VLSI-MEMO-89-564) Avail: NTIS HC A03/MF A01 CSCL 12/7

Interconnection networks are used to pass messages containing data and synchronization information between the nodes of concurrent computers. The messages may be sent between the processing nodes of a message-passing multicomputer or between the processors and memories of a shared-memory multiprocessor. Express cubes are k-ary n-cube interconnection networks augmented by express channels that provide a short path for non-local messages. An express cube combines the logarithmic diameter of an indirect network with the wire-efficiency and ability to exploit locality of a direct network. The insertion of express channels reduces the network diameter and thus the distance component of network latency. Wire length is increased allowing networks to operate with latencies that approach the physical speed-of-light limitation rather than being limited by node delays. Express channels increase wire bisection in a manner that allows the bisection to be controlled independent of the choice of radix, dimension, and channel width. By increasing wire bisection to saturate the available wiring media, throughput can be substantially increased. With an express cube both latency and throughput are wire-limited and within a small factor of the physical limit on performance. Express channels may be inserted into existing interconnection networks using interchanges. No changes to the local communication controllers are required. GRA

N90-20288# Old Dominion Univ., Norfolk, VA. Dept. of Electrical and Computer Engineering.
AN ELECTRON-BEAM CONTROLLED SEMICONDUCTOR SWITCH Final Report, 15 Jun. 1986 - 30 Sep. 1989
Karl H. Schoenbach and Vishnu K. Lakdawala Nov. 1989 153 p
(Contract DAAL03-86-K-0078)
(AD-A217181; ARO-24001.6-PH) Avail: NTIS HC A08/MF A01 CSCL 09/1

The objective of this work was to study the feasibility of using electron-beam controlled semiconductors as closing and opening switches. An electron-beam with electron energies in the range from 20 keV to 150 keV was used to generate an electron-hole plasma in the cathode region of a GaAs switch. The band-edge radiation provided by the radiatively recombining electron-hole pairs this region serves as the source function for electron-hole generation in the bulk of the switch. This self-pumping effect allows to overcome the space charge limitation of the current flow through the switch and therefore makes it suitable for high power applications. Switch current gains of more than 2000 have been obtained experimentally in semi-insulating GaAs. It was also demonstrated experimentally that doping of the cathodeluminescence region of switch with high concentrations of a shallow acceptor improves the radiative efficiency of the cathodoluminescence. Modeling results show that improvements by one order of magnitude over the previously reached current gain can be obtained by proper doping of the cathode region of the GaAs switch. The dark current in these devices can be kept in the range of 10 micro-A/sq cm by using a p-i-n structure. GRA

N90-20289# Dayton Univ., OH.
AN ELECTROCHEMICAL AND SPECTROSCOPIC STUDY OF ELECTRODE PROCESSES Final Report, May 1987 - Mar. 1989
Robert G. Keil Jun. 1989 55 p
(Contract F33615-87-C-2712; AF Proj. 2303)
(AD-A217261; UDR-TR-89-33; WRDC-TR-89-2065) Avail: NTIS HC A04/MF A01 CSCL 10/3

Research on the chloroaluminate melt, methyl-ethyl-imidazolium chloride-aluminum chloride was conducted to elucidate the structural properties of the melt. The melt was studied by obtaining its fluorescence spectra, NMR spectra and its conductance properties. In addition, ab-initio calculations (Extended Huckel M.O.) on the dichloro-hydrogen species were made. In other solution studies, proton NMR, infrared and Raman spectroscopic studies of the lithium-water interactions in acetonitrile were continued. The hydration number for lithium ion (four and the oxygen symmetry, Td, were determined. A gas chromatographic study of the reactivity of lithium with acetonitrile was conducted. GRA

N90-20290# Massachusetts Inst. of Tech., Lexington. Lincoln Lab.
RADIATION-HARDENED WAFER SCALE INTEGRATION
Allan H. Anderson, James A. Burns, Chenson K. Chen, Gregory J. Dunn, Kenneth H. Konkle, Bor-Yeu Tsaur, Charles E. Woodward, and P. W. Wyatt 25 Oct. 1989 137 p
(Contract F19628-90-C-0002)
(AD-A217332; TR-860; ESD-TR-89-164) Avail: NTIS HC A07/MF A01 CSCL 09/1

The logical and physical design of a prototype focal plane processor to be built as a wafer-scale circuit in a radiation-hard CMOS process is described. Design details and test results are presented for the five circuits which were fabricated in bulk CMOS through the MOSIS fabrication service. The floor plan of the wafer is described. This project was terminated before the wafer-scale circuit could be fabricated. New methods and equipment for fabrication of SOI wafers by zone-melting-recrystallization are described, as well as experience in fabricating CMOS circuits on these wafers. A summary is given of results in related work on fabrication of rad-hard gate dielectrics. GRA

N90-20291# Georgia Inst. of Tech., Atlanta.
CONFERENCE DIGEST: THIRTEENTH INTERNATIONAL CONFERENCE ON INFRARED AND MILLIMETER WAVES, VOLUME 1039 Final Report, 22 Aug. 1988 - 21 Aug. 1989
James C. Wiltse, ed. 9 Dec. 1989 505 p Conference held at Honolulu, HI, 5-9 Dec. 1988 Submitted for publication Sponsored in part by SPIE
(Contract DAAL03-88-G-0044)
(AD-A217343; ARO-26304.1-EL-CF-Vol-1039; LC-88-63146; ISBN-0-8194-0074-2) Avail: NTIS HC A22/MF A03 CSCL 09/1

When this conference is held in North America, it is essentially The Millimeter Wave Conference. Thirty of the thirty-six sessions lie exclusively in the realm of millimeter waves, 35 to 300 GHz. Measures are being devised by the Program Chair to increase the submillimeter component, but his appeal to the submillimeter scientists remains his strongest measure. A glance at the program shows that we have our usual Millimeter Wave Week and our usual Free Electron Laser and Gyrotron Week. But we now have another symposium on millimeter wave measurement techniques applied to the characterization of materials and the tabulation of their millimeter wave properties. Another new, and growing, component is the Microwave-Optical Interactions. GRA

N90-20292# Illinois Univ., Urbana. Coordinated Science Lab.
ISITE: AUTOMATIC CIRCUIT SYNTHESIS FOR DOUBLE-METAL CMOS VLSI (VERY LARGE SCALE INTEGRATED) CIRCUITS Ph.D. Thesis
Perry Gee Dec. 1989 141 p
(Contract N00014-84-C-0149)
(AD-A217459; UILU-ENG-89-2243) Avail: NTIS HC A07/MF A01 CSCL 09/1

Very large scale integrated (VLSI) circuit technology allows one to manufacture chips with several million devices. Designing such large circuits cannot be accomplished without design automation tools and computer aided design tools. The problem of automatic circuit synthesis for double-metal Complementary Metal Oxide Semiconductors technology is addressed. Large circuits are partitioned into cells and represented as incidence matrices. The rows and columns of these matrices are folded to minimize the area. A symbolic layout is then generated for each matrix. This

symbolic layout is then used to generate the physical mask layers necessary for fabrication in the metal-metal matrix methodology. GRA

N90-20293# Ohio State Univ., Columbus.
RECENT IMPROVEMENTS TO THE ELECTROMAGNETIC SURFACE PATCH CODE Final Report, May - Sep. 1987
Edward H. Newman Nov. 1989 57 p
(Contract F30602-81-C-0206)
(AD-A217479; RADC-TR-89-239) Avail: NTIS HC A04/MF A01 CSCL 09/1

Two improvements to the Electromagnetic Surface Patch or ESP code are described. ESP is a user oriented computer code, based upon the method of moments (MM), for the analysis of thin wires and polygonal plates. The two improvements to ESP are: (1) The ability to compute near zone fields, and (2) the ability to analyze thin dielectric plates through the use of a sheet impedance approximation. These two modifications are described and numerical data validating the accuracy of the code are presented. GRA

N90-20294# Defence Research Establishment, Ottawa (Ontario).
AN INVESTIGATION OF THE EXTENT OF THE FRESNEL REGION OF APERTURE ANTENNAS WITH ATTENTION TO SUPERDIRECTIVITY
Shawn Charland Aug. 1989 99 p
(AD-A217518; DREO-TN-89-20) Avail: NTIS HC A05/MF A01 CSCL 09/1

The principles governing superdirective antennas and the factors limiting their realization are described. A criterion for determining the minimum distance to the far field of aperture antennas, including superdirective antennas, is presented. Under this condition it is shown that, at least for the marginally superdirective case, such antennas do not exhibit large fresnel regions as compared with minimum distance to the far field in a given direction. Under this criterion it is shown that for the uniform distribution, the antenna pattern near nulls requires a large distance to converge to the far field form. This work has applications in determining antenna test range requirements. GRA

N90-20295# Rome Air Development Center, Griffiss AFB, NY.
WIDEBAND S BAND TRANSMITTER Report, Dec. 1980 - Jun. 1989
James M. VanDamme Oct. 1989 82 p
(AD-A217620; AD-E501190; RADC-TR-89-265) Avail: NTIS HC A05/MF A01 CSCL 09/1

Two high power radar transmitters were designed and constructed for the RADC Surveillance Laboratory. The first transmitter is an S band, 180 KW, 6 percent duty unit which was added to the existing vertical channel transmitter of the S band tracking radar to provide horizontal polarization coverage. The second is a 180 KW, 2 percent duty unit which powers the C band Advanced Mainbeam ECCM antenna. The S band transmitter was studied and covers maintenance, operation, design philosophy, and theory of operation, as well as being expository of novel technologies used and recommendations for further research. GRA

N90-20296# Sandia National Labs., Albuquerque, NM. Ground Motion and Seismic Div.
A LINEAR FILTERING TECHNIQUE FOR REMOVAL OF LOW-FREQUENCY NOISE
J. W. Long and S. D. Stearns 1990 5 p Presented at the 36th ISA International Instrumentation Symposium, Denver, CO, 6-10 May 1990
(Contract DE-AC04-76DP-00789)
(DE90-006183; SAND-89-2293C; CONF-900599-1) Avail: NTIS HC A01/MF A01

In an analog recording of an electronic pulse, the baseline of the recording can shift during the test. Before accurate processing can be performed on the recorded pulse, the baseline must be identified and adjusted so deflections may be measured from a zero baseline. A simple high-pass filtering method to identify and remove the baseline deviations has been devised and implemented. The primary advantages of this method are that little or no lead time is needed to initialize the filter, and data which cannot be processed with standard filters because of problems caused by filter response, may be successfully processed with this method. This paper explains how the baseline is identified and removed and provides examples using ground-motion accelerations recorded during underground nuclear tests at Nevada Test Site. DOE

N90-20297# Sandia National Labs., Albuquerque, NM. Power Sources Dept.
EXPLORATORY BATTERY TECHNOLOGY DEVELOPMENT AND TESTING REPORT FOR 1988
Nicholas J. Magnani, Ronald B. Ditzel, Jeffrey W. Braithwaite, Donald M. Bush, Paul C. Butler, James M. Freese, Kenneth R. Grothaus, and Kevin D. Murphy Oct. 1989 92 p
(Contract DE-AC04-76DP-00789)
(DE90-007996; SAND-89-3039) Avail: NTIS HC A06/MF A01

Sandia National Laboratories, Albuquerque, has been designated as Lead Center for the Exploratory Battery Technology Development and Testing Project. In this capacity, Sandia is responsible for the engineering development of advanced rechargeable batteries for both mobile and stationary energy storage applications. The technical achievements realized in pursuit of the Lead Center's goals during calendar year 1988 are detailed. DOE

N90-20298# Pacific Northwest Lab., Richland, WA.
LIFE-CYCLE COST COMPARISONS OF ADVANCED STORAGE BATTERIES AND FUEL CELLS FOR UTILITY, STAND-ALONE, AND ELECTRIC VEHICLE APPLICATIONS
K. K. Humphreys and D. R. Brown Jan. 1990 422 p
(Contract DE-AC06-76RL-01830)
(DE90-008090; PNL-7203) Avail: NTIS HC A18/MF A03

A comparison is presented of battery and fuel cell economics for ten different technologies. To develop an equitable economic comparison, the technologies were evaluated on a life cycle cost (LCC) basis. The LCC comparison involved normalizing source estimates to a standard set of assumptions and preparing a lifetime cost scenario for each technology, including the initial capital cost, replacement costs, operating and maintenance (O and M) costs, auxiliary energy costs, costs due to system inefficiencies, the cost of energy stored, and salvage costs or credits. By considering all the costs associated with each technology over its respective lifetime, the technology that is most economical to operate over any given period of time can be determined. An analysis of this type indicates whether paying a high initial capital cost for a technology with low O and M costs is more or less economical on a lifetime basis than purchasing a technology with a low initial capital cost and high O and M costs. It is important to realize that while minimizing cost is important, the customer will not always purchase the least expensive technology. The customer may identify benefits associated with a more expensive option that make it the more attractive over all (e.g., reduced construction lead times, modularity, environmental benefits, spinning reserve, etc.). The LCC estimates presented in this report represent three end-use applications: utility load-leveling, stand-alone power systems, and electric vehicles. DOE

N90-20299# Lawrence Livermore National Lab., CA.
A PROGRESS REPORT ON THE LIVERMORE MINIATURE VACUUM TUBE PROJECT
W. J. Orvis, D. R. Ciarlo, C. F. McConaghty, J. H. Yee, E. Hee, C. Hunt, and J. Trujillo (California Univ., Davis.) Sep. 1989 5 p Presented at the IEEE International Electron Devices Meeting, Washington, DC, 3-6 Dec. 1989 Submitted for publication
(Contract W-7405-eng-48)
(DE90-008302; UCRL-101479; CONF-891205-4) Avail: NTIS HC A01/MF A01

Using the sacrificial layer process, micron-sized vacuum diodes and triodes are being designed and built. The devices use silicon field emitters etched into the surface of a silicon wafer. The field

emitters are then buried in layers of glass and conductive polysilicon to produce the grid and anode. The last step is to remove the glass layers, leaving the free standing anode and grid with 1 to 2 micron separations. Vacuum microelectronics are expected to be hard to more than 10(exp 17) neutrons/sq cm and 10(exp 8) Rad(Si) of gammas without sustaining permanent damage. Note that this is three to four orders of magnitude greater than the radiation levels that comparable silicon devices can withstand. Upset is expected to be on the order of 10(exp 11) Rad(Si)/s, compared to 10(exp 8) Rad(Si)/s for silicon devices. Vacuum microelectronics should also be able to withstand in excess of 775 K, compared to a maximum of 650 K for the best silicon devices. The current work involves enhancing the sharpness of the field emitters, so that they can operate at lower voltages. Recent applications of an oxidation sharpening method has created tips with a radius of curvature on the tip of less than 10 A. DOE

N90-20300# Lawrence Livermore National Lab., CA.
CORE COOLING STUDIES AT LLNL (LAWRENCE LIVERMORE NATIONAL LABORATORY) AND SANDIA
R. Stone, J. VanSant, S. Bahowick, K. Reed, and S. Kempka (Sandia National Labs., Albuquerque, NM.) Feb. 1990 12 p Presented at the International Workshop on Magnetic Pulse Compression, Lake Tahoe, CA, 12-14 Feb. 1990
(Contract W-7405-eng-48)
(DE90-008303; UCRL-102620; CONF-900280-2) Avail: NTIS HC A03/MF A01

We are conducting numerical studies and experimental tests at Lawrence Livermore National Laboratory (LLNL) and Sandia National Laboratory (SNL) to determine a method of cooling pulse compression cores that use saturating magnetic material. We anticipate that for high average power throughput compressors, cores will have cooling channels wound at intervals to maintain the maximum temperature below 125 C. We have calculated, for a range of volumetric heating rates, the expected distance between channels using bulk core properties and laminar flow for the cooling fluid. We have completed Freon-113 flow tests on possible cooling-channel materials. We have found that, in tests using ohmically heated cores without cooling channels, we can achieve good agreement between calculated and measured performance by use of the bulk ore properties and assumed film coefficients. A two-dimensional code has been developed to determine core performance using both edge and channel cooling. We are planning additional ohmic heating tests of wound cores to further investigate the performance of the cores, both with and without cooling channels. We will then compare the measured values of temperature, flow rate, and pressure drop with code results.
DOE

N90-20301*# National Aeronautics and Space Administration. Lewis Research Center, Cleveland, OH.
POWER CONDITIONING TECHNIQUES
E. D. Baumann 1989 7 p Presented at the Neutral Particle Beam Technology Symposium, Monterey, CA, 18-21 Jul. 1989; sponsored by Strategic Defense Initiative Organization
(Contract MIPR-FY1455-89-N0655)
(NASA-TM-102577; E-5408; NAS 1.15:102577) Avail: NTIS HC A02/MF A01 CSCL 09C

The technological developments required to reduce the electrical power system component weights from the state-of-the-art 2.0 kg/kW to the range of 0.1 to 0.2 kg/kW are discussed. Power level requirements and their trends in aerospace applications are identified and presented. The projected weight and launch costs for a 1MW power converter built using state-of-the-art technology are established to illustrate the need for reliable, ultralightweight advanced power components. The key factors affecting converter weight are given and some of the tradeoffs between component ratings and circuit topology are identified. The weight and launch costs for a 1MW converter using 0.1 kg/kW technology are presented. Finally, the objectives and goals of the Multi-Megawatt Program at the NASA Lewis Research Center, which is funded by the SDIO through the Air Force, are given. Author

N90-20302*# National Aeronautics and Space Administration. Goddard Space Flight Center, Greenbelt, MD.
PERFORMANCE OF A 300 Mbps 1:16 SERIAL/PARALLEL OPTOELECTRONIC RECEIVER MODULE
M. A. Richard, P. C. Claspy, K. B. Bhasin, and M. B. Bendett (Honeywell, Inc., Bloomington, MN.) Apr. 1990 9 p Presented at the Technical Symposium on Optical Engineering and Photonics in Aerospace Sensing, Orlando, FL, 16-20 Apr. 1990; sponsored by the Society of Photo-Optical Instrumentation Engineers
(NASA-TM-103110; E-5434; NAS 1.15:103110) Avail: NTIS HC A02/MF A01 CSCL 09C

Optical interconnects are being considered for the high speed distribution of multiplexed control signals in GaAs monolithic microwave integrated circuit (MMIC) based phased array antennas. The performance of a hybrid GaAs optoelectronic integrated circuit (OEIC) is described, as well as its design and fabrication. The OEIC converts a 16-bit serial optical input to a 16 parallel line electrical output using an on-board 1:16 demultiplexer and operates at data rates as high as 30b Mbps. The performance characteristics and potential applications of the device are presented. Author

N90-20303# California Univ., Berkeley. Dept. of Materials Science and Engineering.
MODELING STUDIES OF ELECTROLYTE FLOW AND BUBBLE BEHAVIOR IN ADVANCED HALL CELLS
R. Shekhar and J. W. Evans 1990 7 p Presented at the 119th TMS (The Minerals, Metals and Metallurgical Society) Annual Meeting and Exhibit, Anaheim, CA, 18-22 Feb. 1990 Prepared for Edgerton, Germeshausen and Grier, Inc., Idaho Falls, ID
(Contract DE-AC07-76ID-01570)
(DE90-007013; EGG-M-89453; CONF-900206-5) Avail: NTIS HC A02/MF A01

Much research was performed in recent years by corporations and university/government labs on materials for use in advanced Hall-Heroult cells. Attention has focussed on materials for use as wettable cathodes and inert anodes and much was achieved in terms of material development. Comparatively less attention was devoted to how these materials might be incorporated in new or existing cells, i.e., to how the cells should be designed and redesigned, to take full advantage of these materials. The effort, supported by the U.S. Department of Energy, to address this issue, is described. The primary objectives are cell design where electrolyte flow can be managed to promote both the removal of the anode gas bubbles and the convection of dissolved alumina in the inter-electrode region, under conditions where the anode-cathode distance is small. The principal experimental tool was a water model consisting of a large tank in which simulated anodes can be suspended in either the horizontal or vertical configurations. Gas generation was by forcing compressed air through porous graphite and the fine bubbles characteristic of inert anodes were produced by adding butanol to the water. Velocities were measured using a laser Doppler velocimeter. Velocity measurements with two different anode designs (one that is flat and the other that has grooves) are presented. The results show that the electrode configuration has a significant effect on the fluid flow pattern in the inter-electrode region. Furthermore, it is shown that rapid fluid flow is obtained when the cell is operated with a submerged anode. DOE

N90-20304# California Univ., Berkeley. Dept. of Electrical Engineering and Computer Sciences.
STATISTICAL EQUIPMENT MODELING FOR VLSI MANUFACTURING
Oct. 1989 2 p Presented at the Symposium on Automated Semiconductor Manufacturing, 176th Electrochemical Society Meeting, Hollywood, CA, 15-20 Oct. 1989 Prepared in cooperation with Lawrence Livermore National Lab., CA
(Contract W-7405-eng-48)
(DE90-008527; UCRL-21264; CONF-8910107-10) Avail: NTIS HC A01/MF A01

The systematic methodology presented here aims at building and calibrating equipment-specific process models. These models describe the nominal equipment response and also the inherent

process variations. D-Optimal experiment design, combined with statistical modeling, is employed for the characterization and representation of the equipment and its associated processes. The methodology has been successfully applied for modeling a furnace used for low pressure chemical vapor deposition (LPCVD) of undoped polysilicon. A 2-stage D-Optimal design with 24 experiments was used to refine and calibrate physically-derived LPCVD models for the specific furnace. Statistical models have been built for two equipment responses, namely the polysilicon deposition rate and the built-in wafer stress. These models agree well with the experiment data, and account correctly for the observed variations. DOE

N90-20305# Lawrence Livermore National Lab., CA.
RELATIVISTIC KLYSTRON AFTERBURNER SIMULATION TECHNIQUES
R. D. Ryne, R. A. Jong, G. A. Westenskow, and S. S. Yu 24 Jan. 1990 6 p Presented at the SPIE Optics, Electro-Optics and Laser Applications in Science and Engineering Conference and Exhibition, Los Angeles, CA, 15-19 Jan. 1990
(Contract W-7405-eng-48)
(DE90-008539; UCRL-102538; CONF-900140-14) Avail: NTIS HC A02/MF A01

Computer codes are being developed for the numerical simulations of relativistic klystrons and relativistic klystron afterburners. The purpose is to discuss the main features of the numerical model. A relativistic klystron afterburner is a scheme to extract power from a spent FEL electron beam. Power is extracted from the beam by passing it through klystron output cavities. DOE

N90-20306# California Univ., Berkeley. Lawrence Berkeley Lab. Materials and Chemical Sciences Div.
ALL-SOLID-STATE THIN-FILM RECHARGEABLE LITHIUM BATTERIES USING SOLID REDOX POLYMERIZATION ELECTRODES
Meilin Liu, Steven J. Visco, and Lutgard C. DeJonghe Oct. 1989 8 p Presented at the Electrochemical Society Fall Meeting, Hollywood, FL, 15-20 Oct. 1989
(Contract DE-AC03-76SF-00098)
(DE90-008665; LBL-27964; CONF-8910107-11) Avail: NTIS HC A03/MF A01

Lithium batteries using solid redox polymerization electrodes maintain the advantages of all-solid-state thin-film systems while overcoming the limitations of using intercalation compounds as cathodes (i.e., insufficient rate capability and unsatisfactory cathode utilization). Laboratory Li/PEO/SRPE cells have already demonstrated much higher power capability, energy density, and cathode utilization than analogous Li/PEO/TiS2 cells. One of the Li/PEO/SRPE cells has achieved 350 cycles from 50 C to 93 C with a sustained energy density of 264 Wh/kg (241 Wh/1), power density of 160 W/kg (144 W/1), and 38 to 75 percent of cathode utilization at 90 percent voltage efficiency. At 100 C, power densities of over 2400 W/kg and energy density of 200 W/kg were achieved with up to 96 percent utilization of cathode capacity. At ambient temperatures, the cells can be discharged at a current density of 250 microA/sq cm, achieving a film capacity of 0.5 coulombs/sq cm. DOE

N90-20307# University of Southern California, Los Angeles. Electronic Sciences Lab.
JOINT SERVICES ELECTRONICS PROGRAM RESEARCH IN ELECTRONICS Annual Report No. 2, 1 Jan. - 31 Dec. 1989
W. H. Steier 5 Jan. 1990 59 p
(Contract F49620-88-C-0067)
(AD-A217745) Avail: NTIS HC A04/MF A01 CSCL 09/5

Reviews are presented in several areas of electronic science. Some topics of discussion are: Selective Area Epitaxial Growth of Photonic Structures by Metalorganic Chemical Vapor Deposition; Strain Induced Metastability in Heterostructures: Some Investigations of Molecular Beam Epitaxial Growth and Interconversion of Metastable States; Electrooptic Devices for Optical Information Processing and Computing Applications; Optoelectronic and Quantum Structures Using Pristine and Irradiated Organic Compounds; Research to Improve Long Wavelength Infrared Semiconductor Opto-Electronic Devices; A Spectroscopic Study of Basic Processes in Electrically Excited Materials; Nonlinear Optical Waveguiding in Compound Semiconductors; Parallel Optical Processing in Photorefractive Materials; Spread Spectrum Receiver Design for Intense Jamming Environments; Basic Research in C3 Distributed Databases; Segmentation and 2-D Motion Estimation of Noisy Image Sequences; Mathematical Modelling and Control of Complex Systems - Application to Piezoelectrically Coated Large Space Structures; and Knowledge-Based Interpretation of Aerial Images. GRA

N90-20308# University of South Florida, Tampa. Dept. of Computer Science and Engineering.
FAULT SIMULATOR EVALUATION Final Report, Apr. 1987 - Sep. 1988
Sami A. Al-Arian, Nordenso Martin, Hari Kunmenini, Hasam Abujbara, and Jerry Wang Nov. 1989 124 p
(Contract F30602-81-C-0202)
(AD-A217782; RADC-TR-89-230) Avail: NTIS HC A06/MF A01 CSCL 09/1

From the viewpoint of LSI/VLSI product-test preparation, simulation, at least a good circuit (fault-free) simulation, has become an absolute necessity simply because there can be no assurance that a design is structurally or functionally fault-free. Hence, as the system becomes more complex, and more parameters interact, then simulation is used to study relationships between the parameters. Rules are provided for relating commercially available fault simulators to a common baseline for calculation of fault coverage. It is known that drastic differences in fault coverage can be obtained from different commercial simulators, yet each bases its calculations on a justifiable and consistent set of rules. The objective was to develop a baseline method of fault simulation and associated rules such that essentially identical results can be obtained by using any commercial simulator product. Four simulators were initially chosen to help develop these guidelines; no simulator among these four is to be considered better than any other. The results have already been put into practice in the form draft MIL-STD-883 Test Method 5012, Fault Coverage Measurement Digital Microcircuits. GRA

N90-20309# Massachusetts Inst. of Tech., Cambridge. Research Lab. of Electronics.
THE DESIGN OF HIGH-PERFORMANCE CIRCUITS FOR DIGITAL SIGNAL PROCESSING Final Report, 1 May 1986 - 31 May 1989
Jonathan Allen Jan. 1990 11 p
(Grant AF-AFOSR-0164-86; AF Proj. 2305)
(AD-A217786; AFOSR-90-0012TR) Avail: NTIS HC A02/MF A01 CSCL 09/1

In order to place the research done under this contract in perspective, we start by describing the view of integrated circuit design that motivates our work. Our goal is to provide CAD design tools that enable the production of high-performance chips quickly, correctly, and economically, with particular emphasis on digital signal processing. It is the high-performance aspect of the design that has been our particular emphasis. We consider performance to have two aspects. Aspects of performance associated with circuit style and technology are extremely important, since there is continuing improvement in integrated circuit technology, and also because of the constant invention of new circuit forms that provide for faster performance without excessive demands on power. An additional goal at the circuit and layout level is the minimization of area, since this leads to small circuits with minimum length interconnect. In addition to circuit-oriented performance, however, there is also another aspect of performance that we call architectural performance. By this factor, we refer to the parallelism that is contained in a variety of different algorithms. Parallelism can be exploited through the use of pipelining, multiprocessing, and a variety of other architectural schemes. GRA

N90-20310# Illinois Univ., Urbana-Champaign. Dept. of Electrical and Computer Engineering.
INVESTIGATION OF TAPERED MULTIPLE MICROSTRIP LINES FOR VLSI CIRCUITS Ph.D. Thesis
Mark Andrew Mehalic 1989 83 p Sponsored by AFIT, Wright-Patterson AFB, OH
(AD-A217855; AFIT/CI/CIA-89-138D) Avail: NTIS HC A05/MF A01 CSCL 09/1

Tapered, coupled, microstrip transmission lines are an increasingly important part of high speed digital circuits. These lines, used as interconnects between integrated circuit devices, are modeled using an iteration-perturbation approach applied in the spatial domain. The approach is used first to solve the static problem, and then to iterate on the static solution to obtain the charge and current distributions on the lines at different frequencies. From this model, a frequency-dependent scattering parameter characterization is determined. Results for typical geometries are presented and are compared with those published by other authors. A time-domain simulation of pulse propagation through the tapered, coupled, microstrip lines is performed. The frequency-domain scattering parameters are inverse Fourier transformed to obtain the time-domain Green's function. The input pulse is convolved with the Green's function, and a Newton-Raphson algorithm is applied to account for nonlinear loads. Good agreement is found with other published results. Finally, some experimental results are shown and an equivalent circuit is proposed. The experimental results verify the model, while the equivalent circuit allows the time-domain simulation to be performed in less time with a negligible loss in accuracy. Results show that the equivalent circuit gives essentially the same time-domain response in about one-tenth of the simulation time. GRA

N90-20311# California Univ., Berkeley. Electronics Research Lab.
JOINT SERVICES ELECTRONICS PROGRAM Annual Progress Report, 1 Jan. - 31 Dec. 1989
W. G. Oldham 31 Jan. 1990 57 p
(Contract F49620-87-C-0041; AF Proj. 2305)
(AD-A217961; UCB/ERL-89/1) Avail: NTIS HC A04/MF A01 CSCL 20/3

The research is organized under two theme areas: High speed wide band elements for high frequency electronics and new architectures for parallel computation. The former has 5 work units and one supplement ranging from optoelectronic, Gunn-effect, ultra-short-channel Si and superconductive devices to new techniques for electromagnetic scattering computation. The second theme area has 3 work units which cover research projects ranging from CAD techniques for the synthesis of very large circuits and investigations of alternative architectures for parallel computation to devices for use in neural networks. One project is concerned with biologically-based neural networks. Included are four descriptions of especially significant accomplishments: (1) the discovery of hot electron effects in devices which occur at voltages less than the bandgap potential, (2) new designs for Gunn-effect oscillators which have unprecedented power and efficiency, (3) achievement of three unique guided wave devices, and (4) a technique to achieve fault tolerance in artificial neural networks. GRA

N90-20312# Wright State Univ., Dayton, OH. Dept. of Electrical Engineering.
INTEGRATED CIRCUITS FOR AVIONICS Final Report, Jul. 1985 - Jun. 1989
Raymond Siferd Oct. 1989 123 p
(Contract F33615-85-C-1718; AF Proj. 7662)
(AD-A217964; WRDC-TR-89-1118) Avail: NTIS HC A06/MF A01 CSCL 09/1

The main thrust of the Integrated Circuits for Avionics Program is to calibrate the chip area requirements and performance that can be obtained from custom VLSI circuits which were designed to accomplish a specific communication signal processing task. The two primary areas of investigation were stringent narrow band filtering based on highly parallel VLSI systolic array architectures and vector processors based on the residue number theory and highly parallel VLSI pipelined architectures. Designs are included for custom VLSI programmable filters in both NMOS and CMOS technologies along with measured performance of higher order filters resulting from cascading the custom prototype chips. A unique multirate sampling scheme is presented for improving filter response. A unique custom VLSI design is included for a high performance pipelined residue processor using 16-bit operands and providing 32-bit results. Measured performance of this architecture is also included based upon testing of a prototype custom VLSI circuit. GRA

N90-20313# North Carolina State Univ., Raleigh. Dept. of Electrical and Computer Engineering.
TRANSIENT RADIATION HARDENED CMOS (COMPLEMENTARY METAL OXIDE SEMICONDUCTOR) OPERATIONAL AMPLIFIERS M.S. Thesis
Gerald J. Trombley 1989 64 p Sponsored by AFIT, Wright-Patterson AFB, OH
(AD-A217972; AFIT/CI/CIA-89-102) Avail: NTIS HC A04/MF A01 CSCL 09/1

General strategies are developed for designing radiation hardened bulk and silicon on insulator (SOI) complementary metal oxide semiconductor (CMOS) operational amplifiers. Comparisons are made between each technology concerning photocurrent mechanisms and the inherent advantages of SOI CMOS. Methods are presented for analyzing circuit designs and minimizing the net photocurrent responses. Analysis is performed on standard operational amplifier circuits and subcircuits to demonstrate the usefulness of these methods. Radiation hardening topics discussed include superior radiation hardened topologies, photocurrent compensation and its limitations, and methods to ensure a preferred direction of photocurrent response. Several operational amplifier subcircuits are compared for their hardness characteristics. Folded cascade and three-stage operational amplifiers were fabricated on an SOI CMOS test chip supported by Texas Instruments, Incorporated. At the time of publication, the circuit operation was verified but radiation data were not yet available. GRA

N90-20314# Boeing Aerospace Co., Seattle, WA.
COMPUTED TOMOGRAPHY OF ELECTRONICS Interim Report, Aug. 1988 - May 1989
Richard H. Bossi, Robert J. Kruse, and Benjamin W. Knutson Dec. 1989 64 p
(Contract F33615-88-C-5404; AF Proj. 3153)
(AD-A217976; WRDC-TR-89-4112) Avail: NTIS HC A04/MF A01 CSCL 14/2

The application of Computed Tomography (CT) and laminography was tested on a variety of electronic components. The effort was performed as a preliminary testing task assignment in the Advanced Development of X ray Computed Tomography Application program. A key area for testing was printed circuit boards for the inspection of solder bonds and in particular for leadless chip carrier devices. During the course of the task assignment several other categories of electronic devices were examined including transformers, connectors, switches from solution and contrast sensitivity phantoms developed for the programs were used to establish quantitative measures of capability used to generate images. This preliminary testing of electronics lead to the conclusion that higher resolution CT scanning is needed to resolve details of interest. CT testing on commercially available system could resolve high contrast details in the range of 2 to 4 lp/mm; however, in many electronic components finer resolution is needed to detect microcracking, voiding and other features. Further testing on high resolution system is recommended. Two areas of immediate potential economic payback for electronics inspection were identified; the inspection of high volume printed circuit board production using high speed laminography and nondestructive failure analysis studies components using high-resolution CT. GRA

N90-20315# Chemical Research and Development Center, Aberdeen Proving Ground, MD.
OPTIMIZATION OF DIGITAL FILTERS FOR A SHORT-SCAN INTERFEROMETER Technical Report, Oct. 1987 - Jun. 1988
Ronald B. Crosier May 1989 28 p
(DA Proj. 1C1-62706-A-553-C)
(AD-A217997; CRDEC-TR-067) Avail: NTIS HC A03/MF A01 CSCL 07/1

It is shown how statistical methods can be used to optimize the performance of digital filters. Digital filters may be used in place of Fourier transform methods for detecting chemical agents by a short-scan interferometer. The variables to be optimized are the width of the Gaussian peak for the target compound, the number of filter coefficients, the number of filtered points obtained, and the location of the data points in the interferogram used as filter input. The methodology for optimizing these variables is general and can be used to optimize other variables and types of filters. GRA

N90-20316# Naval Research Lab., Washington, DC. Beam Physics Branch.
COMMON-MODE REJECTOR FOR PULSE POWER DIAGNOSTICS Interim Report
Joseph Mathew 15 Feb. 1990 30 p
(AD-A218096; NRL-MR-6607) Avail: NTIS HC A03/MF A01 CSCL 20/3

Pulse power diagnostics are usually prone to common-mode noise pickup. A sure way of suppressing this noise is to introduce a common-mode rejector in each suspected signal line. Two types of rejector were developed. One handles signals with risetimes exceeding 10 ns, or equivalently with frequencies less than 35 MHz. The other is suitable even for signals with subnanosecond risetime. Both were optimized to yield the highest rejection achievable. The method of winding employed and the inter lead separation were found to be quite important for proper operation of the common-mode rejector. Some of the underlying mechanisms of ground noise generation are also briefly investigated. GRA

N90-20317# Harry Diamond Labs., Adelphi, MD.
TRANSISTOR AND SOLID-STATE TECHNOLOGY: A HISTORICAL DEVELOPMENT Final Report, 7 Mar. - 25 Mar. 1988
Kelly W. Bennett Dec. 1989 17 p
(AD-A218141; HDL-SR-89-4) Avail: NTIS HC A03/MF A01 CSCL 09/1

From the invention of the first transistor in 1947 to solid-state advances leading up to the 21st century, this paper presents the historical developments of solid-state devices. Along with individual solid-state milestones, the paper relates the solid-state accomplishments to advances in the computer industry, military, and the commercial world. GRA

N90-20318# Colorado State Univ., Fort Collins. Dept. of Electrical Engineering.
ELECTRON BEAM GENERATION BY ELECTRON BOMBARDMENT INDUCED CATHODE EMISSION Final Report, Apr. 1988 - Jul. 1989
J. J. Rocca, B. Szapiro, and C. Murray 7 Jul. 1989 40 p
Sponsored in part by NSF
(Contract F33615-86-C-2723; AF Proj. 1D01)
(AD-A218203; WRDC-TR-89-2079) Avail: NTIS HC A03/MF A01 CSCL 09/1

It was demonstrated that pulsed electron beams can be created by multiplication of a lower current density primary beam impinging on high electron yield targets, similar to those used in photomultiplier tubes. The main results obtained are the generation of: a 17 ampere, 1 microsecond duration beam from a 2.5 cm diameter Ag-Mg polycrystalline alloy target by multiplication of a 2.5 ampere primary beam; implementation of a surface activation technique for Ag-Mg targets that allows reproducible yields up 5. GRA

N90-20319# Department of National Defence, Ottawa (Ontario). Research and Development Branch.
INVESTIGATION OF A PHOTOVOLTAIC/BATTERY HYBRID SYSTEM FOR POWERING THE HIGH ARCTIC DATA COMMUNICATIONS SYSTEM Final Report
C. L. Gardner Aug. 1989 63 p
(AD-A218353; CRAD-2/89) Avail: NTIS HC A04/MF A01 CSCL 10/3

The High Arctic Data Communications System (HADCS) was established to provide reliable communication between CFS Alert and Ottawa. This system includes a ground link from Alert to Eureka and a satellite link from Eureka to Ottawa. The ground link is necessary because Alert is over the horizon with respect to suitable satellites in stationary orbit. HADCS includes six unmanned microwave repeaters that are located on the top of mountains between Alert and Eureka. Typical power requirements for these sites are given. These repeater stations are powered at the present time using SAFT 608Z 2000 Ah air depolarized (zinc-air) primary cells. Each repeater has two banks of batteries; one prime and one backup with 8 to 10 battery boxes of 14 cells in each box. Cell and battery data are given. Annual battery maintenance is required. Each summer the prime battery bank is removed, the existing back-up bank is taken into active service (i.e., becomes the prime bank) and a fresh set of batteries is installed as the back-up bank. The old set of batteries has to be removed for disposal. Because of the remoteness of the HADCS sites and the weight of the battery system (about 2 tons per site), replacement of the batteries is a major operation. GRA

N90-20320* National Aeronautics and Space Administration. Langley Research Center, Hampton, VA.
ELECTRONIC PRECIPITATOR CONTROL Patent
David F. Johnston, inventor (to NASA) 22 Aug. 1989 8 p
Filed 14 May 1986 Division of US Patent-4,605,424, US-Patent-Appl-SN-625436, filed 28 Jun. 1984
(NASA-Case-LAR-13273-2; US-Patent-4,860,149; US-Patent-Appl-SN-862942; US-Patent-Class-361-79; US-Patent-Class-361-65; US-Patent-Class-323-903; US-Patent-Class-55-105; US-Patent-Class-55-139; US-Patent-Appl-SN-625436; US-Patent-4,605,424) Avail: US Patent and Trademark Office CSCL 09A

A method and apparatus for controlling power to a precipitator are disclosed. After each spark the power to the precipitator is reduced to zero, increased along a fast ramp for a fixed period of time and then increased along a slow ramp until a spark occurs. The fast and slow ramp data is computed and stored (memory) and then retrieved after each spark. The data retrieved is the data corresponding to the firing angle at the last spark. Apparatus is provided (selector and memory) for dividing (frequency divider) the retrieved slow ramp data by a number to select the number of sparks per minute. Also the ac current and the ac voltage in the power to the precipitator are detected and the RMS values are obtained and compared and if the difference is above a predetermined value the power is disconnected.
Official Gazette of the U.S. Patent and Trademark Office

34 FLUID MECHANICS AND HEAT TRANSFER

Includes boundary layers; hydrodynamics; fluidics; mass transfer; and ablation cooling.

For related information see also *02 Aerodynamics* and *77 Thermodynamics and Statistical Physics.*

N90-20321 Cornell Univ., Ithaca, NY.
A STUDY OF LOW-DIMENSIONAL MODELS FOR THE WALL REGION OF A TURBULENT BOUNDARY LAYER Ph.D. Thesis
Emily Foster Stone 1989 171 p
Avail: Univ. Microfilms Order No. DA8924648

Fluid flow turbulence has been a subject of intensive research over the past 100 years or more. There has been no work

conclusively linking fully developed turbulent flows and low order dynamical systems. The application of the proper orthogonal decomposition to the wall region is addressed. The effect of the addition of both streamwise and spanwise modes on the dynamics of the model is documented and analyzed, while, in particular, the presence of symmetry induced structurally stable heteroclinic cycles is qualified. The connection of these deterministic cycles to turbulent bursting in the wall layer is further elucidated by the derivation of a scaling law for burst frequency on inner and outer variables from the properties of the model, as well as an expression for the probability distribution of these time intervals.

Dissert. Abstr.

N90-20322 California Univ., San Diego.

NONINTRUSIVE OPTICAL MEASUREMENTS OF TURBULENCE AND MIXING IN A STABLY STRATIFIED FLUID Ph.D. Thesis

Todd Kent Barrett 1989 259 p

Avail: Univ. Microfilms Order No. DA8925083

The decay of turbulence generated by a biplanar grid towed horizontally through a stably stratified fluid was studied for three different constant density gradients. Experiments were performed in a closed rectangular test section. Two solutes (MgSO4 and sucrose) were used to allow for the creation of a solution with mean density gradients but uniform index of refraction. Fluid velocities are measured with a laser Doppler anemometer. Density was measured by adding a florescent dye to the working fluid in such a way that the light florescent by the dye when excited by a laser was proportional to the local density of the solution. Simultaneous single-point measurements of the vertical velocity, the horizontal velocity in the direction of grid motion, and the density were obtained at a fixed point in the center of the test section. Density profiles of the quiescent fluid before and after the grid was towed through the test section were measured. Instantaneous measurements of tile density field in a two-dimensional plane were also obtained. Immediately behind the grid the turbulence was unaffected by the stable stratifications. Measurements of the convective mass flux indicate that the vertical transport of mass due to turbulence was significantly reduced by buoyancy forces, while integral estimates of the mixing indicate that the ability of the turbulent eddies to homogenize the stratified fluid decreases significantly with increasing density gradients.

Dissert. Abstr.

N90-20323* National Aeronautics and Space Administration. Langley Research Center, Hampton, VA.

REUSABLE HIGH-TEMPERATURE HEAT PIPES AND HEAT PIPE PANELS Patent

Charles J. Camarda, inventor (to NASA) and Philip O. Ransone, inventor (to NASA) 13 Jun. 1989 7 p Filed 29 Aug. 1988

(NASA-Case-LAR-13761-1; US-Patent-4,838,346; US-Patent-Appl-SN-237036; US-Patent-Class-165-104; US-Patent-Class-165-41; US-Patent-Class-165-133; US-Patent-Class-165-180; US-Patent-Class-165-905) Avail: US Patent and Trademark Office CSCL 20D

A reusable, durable heat pipe which is capable of operating at temperatures up to about 3000 F in an oxidizing environment and at temperatures above 3000 F in an inert or vacuum environment is produced by embedding a refractory metal pipe within a carbon-carbon composite structure. A reusable, durable heat pipe panel is made from an array of refractory-metal pipes spaced from each other. The reusable, durable, heat-pipe is employed to fabricate a hypersonic vehicle leading edge and nose cap.

Official Gazette of the U.S. Patent and Trademark Office

N90-20324*# Alabama Univ., Huntsville. Dept. of Mechanical Engineering.

CHARACTERIZATION OF FLUID FLOW BY DIGITAL CORRELATION OF SCATTERED LIGHT

John A. Gilbert and Donald R. Matthys (Marquette Univ., Milwaukee, WI.) 22 May 1989 113 p

(Contract NCC8-15)

(NASA-CR-186403; NAS 1.26:186403) Avail: NTIS HC A06/MF A01 CSCL 20D

The objective is to produce a physical system suitable for a space environment that can measure fluid velocities in a three-dimensional volume by the development of a particle correlation velocimetry technique. Experimental studies were conducted on a field test cell to demonstrate the suitability and accuracy of digital correlation techniques for measuring two-dimensional fluid flows. This objective was satisfied by: (1) the design of an appropriate illumination and detection system for making velocity measurements within a test cell; (2) the design and construction of a test cell; (3) the preliminary evaluations on fluid and seeding requirements; and (4) the performance of controlled tests using a multiple exposure correlation technique. This presentation is represented by viewgraphs with very little text.

B.G.

N90-20325*# National Aeronautics and Space Administration. Ames Research Center, Moffett Field, CA.

ANALYSIS OF SMALL-SCALE ROTOR HOVER PERFORMANCE DATA

Cahit Kitaplioglu Mar. 1990 27 p

(NASA-TM-102271; A-90046; NAS 1.15:102271) Avail: NTIS HC A03/MF A01 CSCL 20D

Rotor hover-performance data from a 1/6-scale helicopter rotor are analyzed and the data sets compared for the effects of ambient wind, test stand configuration, differing test facilities, and scaling. The data are also compared to full scale hover data. The data exhibited high scatter, not entirely due to ambient wind conditions. Effects of download on the test stand proved to be the most significant influence on the measured data. Small-scale data correlated resonably well with full scale data; the correlation did not improve with Reynolds number corrections.

Author

N90-20326*# National Aeronautics and Space Administration. Lewis Research Center, Cleveland, OH.

AMPLITUDE-DEPENDENT NEUTRAL MODES IN COMPRESSIBLE BOUNDARY LAYER FLOWS

J. S. B. Gajjar Mar. 1990 19 p

(NASA Order C-99066-G)

(NASA-TM-102524; ICOMP-90-06; E-5331; NAS 1.15:102524)

Avail: NTIS HC A03/MF A01 CSCL 20D

The ideas of Benney and Bergeron (1969) and Davies (1970) on nonlinear critical layers are extended, and some new nonlinear neutral modes are computed for compressible boundary layer flow. A special case of the work is when the generalized inflexion point criterion holds. Neutral modes are found for a range of phase-speeds, dependent on the Mach number, and the properties of these are discussed. As in the linear case when the flow is relatively supersonic, multiple neutral modes exist. The behavior of the neutral amplitude in some limiting cases is also considered, and it is found that the results are significantly different from that in incompressible flow when the flow is locally supersonic.

Author

N90-20327# Purdue Univ., West Lafayette, IN. School of Mechanical Engineering.

THE EFFECT OF ADVERSE PRESSURE GRADIENT ON TURBULENT BURST STRUCTURE IN LOW-REYNOLDS NUMBER EQUILIBRIUM BOUNDARY LAYERS Technical Report, 1 Dec. 1988 - 30 Nov. 1989

Jack B. White and William G. Tiederman Jan. 1990 81 p

(Contract N00014-83-K-0183)

(AD-A217308; PME-FM-90-2) Avail: NTIS HC A05/MF A01 CSCL 20/4

This study is an investigation of low Reynolds number, zero and adverse pressure gradient, equilibrium boundary layers. Two adverse pressure gradient boundary layers and one zero pressure gradient boundary layer were studied with the zero pressure gradient case serving as a comparative standard for the non-zero pressure gradient boundary layers. The non-zero cases included a mild pressure gradient and a strong (relative to the mild case) pressure gradient. The study determined the effect of pressure gradient on the turbulent burst structure for these flows. The Reynolds number (based on momentum thickness), varied from

1120 to 2500 and the pressure gradient parameter, varied from 0.0 to 1.8. Single component laser Doppler velocimeter measurements were made of the streamwise velocity to determine the various boundary layer integral parameters and to create velocity records needed to calculate the period of the bursting cycle. Over the range of Reynolds numbers studied, the results indicate that the burst period (normalized with inner variables) is not a function of Reynolds number. The burst period appears to be solely a function of the pressure gradient and upstream history of the boundary layer. Although the period of the burst cycle is reduced by the adverse pressure gradient, the ensemble averaged velocity signature of the bursts do not change. GRA

N90-20328# Stanford Univ., CA. Center for Large Scale Scientific Computation.
COMPOSITE-GRID TECHNIQUES AND ADAPTIVE MESH REFINEMENT IN COMPUTATIONAL FLUID DYNAMICS Ph.D. Thesis
Robertus Franciscus vanderWijngaart Jan. 1990 239 p
(Contract N00014-86-K-0565)
(AD-A217383; SU-CLASSIC-90-07) Avail: NTIS HC A11/MF A02 CSCL 11/4

Viscous fluid flow is often smooth in most of the domain, with regions of rapid variation confined to some rather narrow zones in the field. These zones (boundary layers, shocks, etc.) cause problems during numerical solution of the equations governing the flow. The patched adaptive mesh refinement technique copes with these sources of error efficiently by refining the computational grid locally. This is done by creating separate fine grids for every region of large error. Because of the success of this approach, a project was started to extend its applicability to geometrically complex domains. As patched adaptive mesh refinement already entails multiple grids, it was decided that geometrical complexity would also be tackled using several grids. An arbitrarily shaped domain typically cannot be covered by a single grid without severe distortion, but a covering can be established with only mildly curved grids if more than one grid is allowed. Communication between these grids then becomes an issue, as well as their creation. In this project various types of communications between grids, based on the Schwarz Alternating Procedure (SWAP), are examined for solving steady, 2-D incompressible flow problems. Of these, the traditional SWAP on sets of overlapping grids works best and gives accurate results, despite the use of nonconservative interpolation procedures between grids. When reentrant problems occur, the pressures between grids may not match. A pressure communication scheme is devised which solves this difficulty. GRA

N90-20329# Purdue Univ., West Lafayette, IN. School of Mechanical Engineering.
INVESTIGATION INTO THE MECHANISM OF POLYMER THREAD DRAG REDUCTION Technical Report, 1 Dec. 1988 - 30 Nov. 1989
Ronald E. Smith and William G. Tiederman Jan. 1990 70 p
(Contract N00014-83-K-0183)
(AD-A217492; PME-FM-90-1) Avail: NTIS HC A04/MF A01 CSCL 20/4

The mechanism of drag reduction is investigated that occurs when a long chain, high molecular weight polymer is injected along the centerline of a pipe with a concentration high enough to form a coherent unbroken thread. The objective was to test the hypothesis that drag reduction is caused by the diffusion of polymer molecules from the thread into the near wall region of the pipe. The objective was realized through the measurement of the polymer concentration in the near wall region, the drag reduction and the radial location of the thread. The concentration was measured using a laser induced fluorescence technique where the polymer was marked with fluorescein dye. The experiments were conducted in a 3.18 cm diameter, clear acrylic pipe at Re = 40,000 using a 5000 ppm concentration solution of Separan AP 273 as the injectant. The drag reduction increased from zero at the point of injection to a maximum value about 200 diameters downstream of the injector. GRA

N90-20330# Ohio State Univ., Columbus. Chemical Research, Development and Engineering Center.
INTERIOR FLUID DYNAMICS OF LIQUID-FILLED PROJECTILES Report, Jul. 1985 - Dec. 1988
Thorwald Herbert Dec. 1989 120 p
(Contract DAAA15-85-K-0012)
(AD-A217630; CRDEC-CR-058) Avail: NTIS HC A06/MF A01 CSCL 20/4

Theoretical and numerical studies were conducted to analyze the flow in spinning and coning liquid-filled payload cylinders and to provide efficient tools for estimating and calculating the liquid moments as input data for flight simulations. Earlier analytical studies for cylinders of large aspect ratio were extended to the nonlinear problem to provide estimates for all moments. This perturbation analysis is currently used to investigate the influence of partial liquid fills, central rods, and two-fluid fills on the moments. A new method was developed to obtain the moments from volume integrals rather than surface integrals and thus increase the accuracy of the results at fixed numerical approximation. An efficient spectral code was developed for routine application to solve the three-dimensional Navier-Stokes equations. Utility of this code for efficient flight simulations was demonstrated. The code was applied to investigate liquid moments, velocity field, and pressure field in situations of pure forcing as well as resonance with inertial waves at Reynolds numbers up to 2000. For the linearized problem, a simplified set of equations was developed that permits closed form solutions for spatial eigenfunctions and highly efficient solution by spectral methods. GRA

N90-20331# Calspan Corp., Arnold AFS, TN.
INVESTIGATION OF THE DEVELOPMENT OF LAMINAR BOUNDARY-LAYER INSTABILITIES ALONG A COOLED-WALL HOLLOW CYLINDER AT MACH NUMBER 8 Final Report, 3-14 Aug. 1989
J. C. Donaldson and D. W. Sinclair Jan. 1990 44 p Prepared in cooperation with AEDC, Arnold AFS, TN
(AD-A217672; AEDC-TSR-89-V25) Avail: NTIS HC A03/MF A01 CSCL 20/4

Measurements of fluctuating flow and mean flow parameters were made in the boundary layer on a cooled wall hollow cylinder model in an investigation of the stability of laminar boundary layers in hypersonic flow. The flow fluctuation measurements were made using constant current hot wire anemometry techniques. Boundary layer profile and model surface conditions were measured to supplement the hot wire data. Testing was done at Mach 8 with free stream unit Reynolds numbers of 1.0 and 1.5 million per foot. The test equipment, test techniques, and the data acquisition and reduction procedures are described. Analysis of the hot wire anemometer data is beyond the scope. GRA

N90-20332# Institute of Gas Technology, Chicago, IL.
DETERMINATION OF FLOW-REGIME BOUNDARIES FOR COHESIVE PARTICLES Quarterly Report, 20 Mar. - 19 Jun. 1989
T. M. Knowlton Jan. 1990 32 p
(Contract DE-AC22-88PC-88951)
(DE90-007425; DOE/PC-88951/3) Avail: NTIS HC A03/MF A01

The overall objective of this program is the development of a hydrodynamic model to predict the choking/non-choking flow regime boundary of fine, cohesive (i.e., Geldart Group C) powders. Specific objectives are: (1) to develop a two-dimensional hydrodynamic model which can be applied to cohesive solids; and (2) to generate large-scale, solids-flow data which will be used to verify the model. Results are discussed. DOE

N90-20333*# National Aeronautics and Space Administration. Ames Research Center, Moffett Field, CA.
NUMERICAL SIMULATION METHODS OF INCOMPRESSIBLE FLOWS AND AN APPLICATION TO THE SPACE SHUTTLE MAIN ENGINE
J. L. C. Chang, D. Kwak, S. E. Rogers, and R.-J. Yang (Rockwell International Corp., Canoga Park, CA.) Mar. 1988 48 p

Previously announced in IAA as A89-17458
(NASA-TM-100038; A-88017; NAS 1.15:100038) Avail: NTIS HC A03/MF A01 CSCL 20D

Incompressible Navier-Stokes solution methods are discussed with an emphasis on the pseudocompressibility method. A steady-state flow solver based on the pseudocompressibility approach is then described. This flow-solver code was used to analyze the internal flow in the Space Shuttle main engine hot-gas manifold. Salient features associated with this three-dimensional realistic flow simulation are discussed. Numerical solutions relevant to the current engine analysis and the redesign effort are discussed along with experimental results. This example demonstrates the potential of computational fluid dynamics as a design tool for aerospace applications. Author

N90-20334# Sandia National Labs., Albuquerque, NM.
A SIMPLE MULTICOMPONENT FLUID THEORY WITH ACCURATE PHYSICS
Stephen L. Passman and Donald A. Drew (Rensselaer Polytechnic Inst., Troy, NY.) 24 Jan. 1990 10 p Presented at the Symposium on Structured Continua, Sherbrooke, Quebec, 22-25 May 1990 Sponsored in part by ARO
(Contract DE-AC04-76DP-00789)
(DE90-006537; SAND-89-3040C; CONF-9005108-1) Avail: NTIS HC A02/MF A01

Generally multicomponent mixtures can exhibit a rich collection of phenomena. Thus it is to be expected that they will be described by complicated theories. In this paper we describe a relatively simple theory that is still theoretically correct, and discuss some of the phenomena that it exhibits. DOE

N90-20335# Oak Ridge Gaseous Diffusion Plant, TN. Computing and Telecommunications Div.
AREA OVER LENGTH (AOL): A PROGRAM FOR THE CALCULATION OF EFFECTIVE TWO-DIMENSIONAL THERMAL CONDUCTANCE THROUGH AN ARBITRARILY SHAPED REGION
M. W. Wendel Feb. 1990 31 p
(Contract DE-AC05-84OT-21400)
(DE90-008005; K/CSD/TM-90) Avail: NTIS HC A03/MF A01

A computer program, Area Over Length (AOL), has been developed to solve for the effective thermal conductance between two isothermal surfaces through a region or arbitrary shape. It is based on a boundary integral method that is derived using complex variables. It is especially useful as an aid to finite-difference and finite-element modeling of irregularly shaped regions. The theory behind AOL applies to the linear solution of any two-dimensional, steady state heat conduction problem without holes in the computational domain. However, AOL has been developed for the specific case in which the boundary consists of four pieces: two opposing isothermal pieces and two opposing adiabatic pieces. This case applies when the effective thermal conductance of a heat flow path between two nodes in a discretization of a larger domain is desired. The program requires that the user supply a boundary discretization of the region across which heat transfer occurs. Also, the points in the boundary discretization that separate the pieces of the boundary must be indicated. A sample problem is discussed. DOE

N90-20336# Lawrence Livermore National Lab., CA.
HYDRODYNAMIC INTERACTIONS AND TRANSPORT COEFFICIENTS IN A SUSPENSION OF SPHERICAL PARTICLES
Anthony J. C. Ladd Feb. 1990 8 p Presented at the Conference on Microscopic Simulation of Complex Flows, Brussels, Belgium, 21-25 Aug. 1989
(Contract W-7405-eng-48)
(DE90-008301; UCRL-102966; CONF-8908158-3) Avail: NTIS HC A02/MF A01

Particulate suspensions of solids in liquids can be understood in terms of the microstructure of the solid phase by using the well-known techniques of numerical statistical mechanics. The major problem with such an approach has been the incorporation of the long-range, many-body hydrodynamic forces between the suspended particles. In this paper a general computational method for calculating the forces and torques exerted by slowly moving spheres suspended in an incompressible fluid are described. The method can be used to determine bulk constitutive properties of solid-fluid suspensions or particulate porous media. Numerical results for the sedimentation velocity and high frequency viscosity of monodisperse suspensions have been obtained, and the results are shown to compare very well with experimental measurement. DOE

N90-20337*# National Aeronautics and Space Administration. Lewis Research Center, Cleveland, OH.
UNSTEADY THREE-DIMENSIONAL MARGINAL SEPARATION, INCLUDING BREAKDOWN
Peter W. Duck (Manchester Univ., England) Feb. 1990 31 p
(NASA Order C-99066-G)
(NASA-TM-102525; ICOMP-90-07; E-5333; NAS 1.15:102525)
Avail: NTIS HC A03/MF A01 CSCL 20D

A situation involving a three-dimensional marginal separation is considered, where a (steady) boundary layer flow is on the verge of separating at a point (located along a line of symmetry/centerline). At this point, a triple-deck is included, thereby permitting a small amount of interaction to occur. Unsteadiness is included within this interaction region through some external means. It is shown that the problem reduces to the solution of a nonlinear, unsteady, partial-integro system, which is solved numerically by means of time-marching together with a pseudo-spectral method spatially. A number of solutions to this system are presented which strongly suggest a breakdown of this system may occur, at a finite spatial position, at a finite time. The structure and details of this breakdown are then described. Author

N90-20338*# National Aeronautics and Space Administration. Lewis Research Center, Cleveland, OH.
MASS TRANSFER FROM A SPHERE IN AN OSCILLATING FLOW WITH ZERO MEAN VELOCITY
Colin K. Drummond and Frederic A. Lyman (Syracuse Univ., Utica, NY.) Apr. 1990 21 p
(NASA-TM-102566; E-5202; NAS 1.15:102566) Avail: NTIS HC A03/MF A01 CSCL 20D

A pseudospectral numerical method is used for the solution of the Navier-Stokes and mass transport equations for a sphere in a sinusoidally oscillating flow with zero mean velocity. The flow is assumed laminar and axisymmetric about the sphere's polar axis. Oscillating flow results were obtained for Reynolds numbers (based on the free-stream oscillatory flow amplitude) between 1 and 150, and Strouhal numbers between 1 and 1000. Sherwood numbers were computed and their dependency on the flow frequency and amplitude discussed. An assessment of the validity of the quasi-steady assumption for mass transfer is based on these results. Author

N90-20339# Department of Energy, Pittsburgh, PA. Technology Center.
A METHOD FOR MEASURING THE MATERIAL MODULI OF GRANULAR MATERIALS: FLOW IN AN ORTHOGONAL RHEOMETER
K. R. Rajagopai (Pittsburgh Univ., PA.) and M. Massoudi Jan. 1990 24 p
(DE90-007160; DOE/PETC-TR/90/3) Avail: NTIS HC A03/MF A01

In this report, a theoretical approach that leads to the experimental characterization of the material moduli of granular media is discussed. A general constitutive model that predicts the possibility of both of the normal stress-differences and is properly frame invariant is derived. As a result of this generalization, there are many material properties which appear in the model and it is essential to devise experiments that will help measure these material moduli. Simple shear and Couette flows would provide some information for some of these material properties. If these simple flows are used in conjunction with the flow in an orthogonal rheometer, which has been used to characterize the material moduli

of viscoelastic fluids, many of the material properties of granular materials, in principle, can be measured. Analysis for simple shear flow and flow in an orthogonal rheometer is provided and a detailed discussion as to the advantages of using an orthogonal rheometer to measure these properties is also presented. DOE

N90-20340# Oak Ridge Gaseous Diffusion Plant, TN. Computing and Telecommunications Div.
FLUID DYNAMICS ANALYSIS OF A ROTATING AXISYMMETRIC PART USING FIDAP
G. E. Giles, J. R. Kirkpatrick, M. W. Wendel, and J. S. Bullock, IV (Oak Ridge Y-12 Plant, TN.) Mar. 1990 32 p
(Contract DE-AC05-84OT-21400)
(DE90-008733; K/CSD/INF-88/23) Avail: NTIS HC A03/MF A01

The effect of fluid flow on electrochemical plating on a rotating axisymmetric part was investigated by using a finite element computer code, FIDAP. The results from these investigations compare well with analytical results for laminar flow conditions. The addition of a nonrotating shield was also investigated for laminar flow conditions. An attempt to extend these analyses to turbulent conditions was unsuccessful. DOE

N90-20341# Virginia Polytechnic Inst. and State Univ., Blacksburg. Dept. of Mathematics.
PARALLEL ALGORITHMS IN THE FINITE ELEMENT APPROXIMATION OF FLOW PROBLEMS Final Report, 1 May 1988 - 31 Oct. 1989
Max D. Gunzburger 30 Oct. 1989 10 p
(Grant AF-AFOSR-0197-88; AF Proj. 2304)
(AD-A217729; AFOSR-90-0078TR) Avail: NTIS HC A02/MF A01 CSCL 20/4

The numerical simulation of viscous incompressible flows, the numerical approximation of certain control problems, the analysis and application of centroidal Voronoi grids, and a book on finite element methods for viscous incompressible flows are topics of discussion. Further information concerning these topics can be gained from the appropriate references. GRA

N90-20342# Michigan Univ., Ann Arbor. Lab. for Scientific Computation.
MASSIVELY-PARALLEL COMPUTATIONAL FLUID DYNAMICS Final Report, 1 May 1988 - 30 Sep. 1989
D. A. Calahan 30 Oct. 1989 5 p
(Grant AF-AFOSR-0212-88; AF Proj. 2304)
(AD-A217732; AFOSR-90-0079TR) Avail: NTIS HC A01/MF A01 CSCL 12/1

Algorithm development: Implementation of a 3-D Navier Stokes implicit research code for AFFDL was initiated. This required the parallel solution of block-tridiagonal system and so was more challenging than the explicit code. Connection Machine experiments: To keep abreast of SIMD architecture performance, a series of FORTRAN and C kerrels were studies on the Argonne Laboratory CM-2. It was concluded that the available FORTRAN 8X implementation of the CM-2 was too inefficient to warrant continued at that time. GRA

N90-20343# Stanford Univ., CA. Thermosciences Div.
A NUMERICAL INVESTIGATION OF THE COMPRESSIBLE MIXING LAYER
N. D. Sandham and W. C. Reynolds 22 Sep. 1989 245 p
(Contract F49620-86-K-0022)
(AD-A217738; TF-45; AFOSR-90-0001TR) Avail: NTIS HC A11/MF A02 CSCL 20/4

The effect of Mach number on the plane mixing layer was investigated by means of linear stability theory and 2-D and 3-D direct numerical simulations of the compressible Navier Stokes equations. The objective was to identify the effects of compressibility on a building block fluid flow, with applications to supersonic mixing and combustion. Results from linear stability theory show that the amplification rate is reduced as Mach number is increased. Above a convective Mach number of 0.6 it is found that 3-D waves are more amplified than 2-D waves and a simple relation is found to give the orientation of the most amplified waves. It is also shown that the linear stability theory can be used to predict the mixing layer growth rate as a function of velocity ratio, density ratio and Mach number. Three-dimensional simulations with random initial conditions confirm the linear stability result that oblique waves become the most amplified waves at high Mach numbers, with no evidence for any other modes of instability. Simulations beginning with a 2-D wave and a pair of equal and opposite oblique waves show a change in the evolved large scale structure as Mach number is increased. Above a convection Mach number of 0.6 the oblique modes have most of the energy in the developed structure, and above a convective Mach number of 1 the 2-D instability wave has little effect on flow structure. Similar organized structure was found in s simulation with random initial conditions. GRA

N90-20344# Aerospace Corp., El Segundo, CA. Aerophysics Lab.
GEOMETRIC SCALE OF INTERACTION BETWEEN MOVING SHOCK AND STATIONARY THERMAL LAYER
H. Mirels 1 Nov. 1989 33 p
(Contract F04701-88-C-0089)
(AD-A217769; ATR-89(4785)-1) Avail: NTIS HC A03/MF A01 CSCL 20/4

An analytical model is presented for estimating the streamwise length of the steady state separation bubble induced by the interaction of a shock moving with constant speed over a thin thermal (high sound speed) layer. In the case of a thermal layer of semi-infinite extent, the steady solution represents the asymptotic limit of an initially unsteady interaction. The streamwise length of the separation bubble is found by equating mass flow into the bubble to the mass flow removed by the wall boundary layer. Numerical results are presented for a variety of shock speeds, thermal layer heights, and thermal layer sound speeds. The present study indicates the importance of viscous effects on precursor development and provides a method for modifying the wall boundary condition in inviscid numerical codes in order to include the effect of the wall boundary layer on the inviscid flow field. GRA

N90-20345# Pennsylvania State Univ., University Park. Dept. of Mechanical Engineering.
DURIP OPTICAL EQUIPMENT FOR HIGH-SPEED VISCOUS-INVISCID INTERACTION RESEARCH Final Report, 1 Dec. 1988 - 30 Nov. 1989
Gary S. Settles 5 Jan. 1990 9 p
(Grant AF-AFOSR-0140-89; AF Proj. 2307)
(AD-A217772; AFOSR-90-0074TR) Avail: NTIS HC A02/MF A01 CSCL 20/4

The Penn State Gas Dynamics Lab has an active, ongoing program in experimental high speed fluid dynamics research. The current research of the Laboratory concerns supersonic viscous/inviscid interactions, compressible turbulent mixing, and high speed vortex dynamics pertaining to external and internal aerodynamics and propulsion. The Laboratory specializes in development and use of advanced, non-intrusive optical flow diagnostics in such research studies. These optical instruments and techniques are brought to bear on basic fluid dynamic experiments in the Penn State Supersonic Wind Tunnel, which has a high Reynolds number capability and continuously-variable Mach number range of Mach 1.5 to 4.0. GRA

N90-20346# Colorado Univ., Boulder. Dept. of Aerospace Engineering Sciences.
EXPERIMENTAL INVESTIGATION OF THE MECHANISMS UNDERLYING VORTEX KINEMATICS IN UNSTEADY SEPARATED FLOWS Ph.D. Thesis
Scott Jeffrey Schreck 1989 157 p Sponsored by AFIT, Wright-Patterson AFB, OH
(AD-A217889; AFIT/CI/CIA-89-149) Avail: NTIS HC A08/MF A01 CSCL 20/4

Unsteady separated flow fields in the vicinity of a flat plate oscillating sinusoidally in pitch about the quarterchord were

investigated for a broad range of pitching parameters. Phase locked photography of smoke flow visualization was employed in conjunction with hotwire anemometry to quantify vortex development as well as some of the primary boundary layer interactions contributing to the observed vortex kinematics. Leading edge vortex development was strongly influenced by both the freestream and boundary layer flows. These and other observations facilitated formulation of an conceptual model which accounts for many of these observations. Quantitative refinement of such a model is one methodology through which unsteady separation may eventually be understood, predicted and controlled for employment in future air vehicles. GRA

N90-20347# Science Applications International Corp., McLean, VA.
NUMERICAL MODELING OF AIRBLAST Annual Report No. 3, 10 Mar. 1988 - 9 Sep. 1987
Ellis Hyman, Richard Leighton, Ravi Ramamurti, and Mike Zuniga Nov. 1989 65 p
(Contract N00014-86-C-2197)
(AD-A217993; SAIC 89/1732) Avail: NTIS HC A04/MF A01 CSCL 20/4

The accomplishments of the program cover three major areas. They include the development of computer codes to numerically simulate turbulent flow at a free surface and inviscid/viscous flows over complex geometries. The third area concerns the development of numerical algorithms for multitarget tracking. GRA

N90-20348# Naval Postgraduate School, Monterey, CA. Dept. of Mechanical Engineering.
FLOW VISUALIZATION STUDIES IN A CURVED RECTANGULAR CHANNEL WITH 40 TO 1 ASPECT RATIO AND A STRAIGHT CHANNEL WITH BULK FLOW UNSTEADINESS M.S. Thesis
Jerry Mark Longest Jun. 1989 115 p Sponsored in part by ONR
(Grant C-80019-F)
(AD-A218020) Avail: NTIS HC A06/MF A01 CSCL 20/4

Flow visualization results are presented which were obtained in a curved channel with mild curvature and 40 to 1 aspect ratio. Inside channel dimensions are 1.27 x 50.80 cm. For Dean numbers from 60 to 200 and angular positions from 85 to 175 degs. measured from the start of curvature, video movies and photographic sequences of patterns in spanwise/radial planes show unsteady Dean vortex pair behavior. In particular, information is provided on mechanisms by which vortex pairs appear and disappear. Videos and still photographs of visualized flow in a straight channel with 40 to 1 aspect ratio and imposed bulk flow unsteadiness show different stages of transition, including; (1) 3-D Tollmien-Schlichting waves, (2) Lambda waves, (3) Lambda vortices, (4) vortex type motion, (5) turbulent spots, and (6) fully turbulent flow. Instantaneous velocity traces from hot-wire probes are presented for Reynolds numbers from 1400 to 8400 and Strouhal numbers from 0.004 to 0.047. These data, without unsteadiness, show that transition occurs at a Reynolds number of approx. 3000. With imposed sinusoidal unsteadiness at a Strouhal number of 0.028 and 7 percent peak to peak amplitude (relative to mean velocity), transition occurs at a Reynolds number of approx. 2300. GRA

N90-20349# Air Force Inst. of Tech., Wright-Patterson AFB, OH.
A MATRIX-FREE LOCALLY-IMPLICIT SCHEME FOR NAVIER-STOKES EQUATIONS M.S. Thesis - Tennessee Univ., Knoxville
Matthew C. Towne May 1989 53 p
(AD-A218298; AFIT/CI/CIA-89-050) Avail: NTIS HC A04/MF A01 CSCL 20/4

A locally-implicit scheme for steady-state solution of the thin-layer Navier Stokes Equations is simplified by elimination of coefficient matrices. This reduces both arithmetic computation and computer storage requirements. An added benefit is the simplification of the algorithm which eases the coding task. The locally-implicit scheme uses finite-volume spatial discretization, locally implicit time integration, Jameson-type artificial dissipation terms and a modified Gauss Seidel iteration. The modified method is tested for subsonic and transonic flows over an RAE 2822 airfoil. GRA

35 INSTRUMENTATION AND PHOTOGRAPHY

Includes remote sensors; measuring instruments and gages; detectors; cameras and photographic supplies; and holography.

For aerial photography see *43 Earth Resources and Remote Sensing*. For related information see also *06 Aircraft Instrumentation*, and *19 Spacecraft Instrumentation*.

N90-20350# National Aerospace Lab., Tokyo (Japan).
DESIGN AND TESTING OF A NONINTERACTING CONTROL LOOP FOR THE DYNAMICALLY TUNED DRY GYRO
H. Shingu and M. Otsuki 1989 36 p In JAPANESE; ENGLISH summary
(NAL-TR-1017; ISSN-0389-4010) Avail: NTIS HC A03/MF A01

A method of reducing the interaction effect between the input and output peculiar to the Dynamically Tuned Dry Gyro (TDG), and the possibility of measuring angular accelerations about two axes, through improvements of the Rebalance Control Circuit (RCC) installed on the TDG are reported. First, the design procedure and manufacture of the improved RCC which is necessary for noninteracting control are shown. Then, transfer functions of the TDG are derived, taking into consideration the manufacturing accuracy of the RCC, and each element of the RCC is examined analytically to see how relationships between inputs and outputs, and the reduction of the interaction effect, are affected by its accuracy. Next, the frequency characteristics of direct and cross transfer functions are measured experimentally by applying electrical inputs to the TDG, and their characteristics are transformed into values equivalent to those for applied mechanical inputs. It became evident after these experiments that the gain characteristics in cross transfer function, which correspond to the degree of reduction of the interaction effect, can be decreased remarkably without influencing the frequency characteristics of the direct transfer function, which prescribe the system performance of the TDG. Third, it is clarified that measurement of two-axis angular accretions is realizable by scaling the outputs of the sub-torquers which are newly introduced for noninteracting control. Finally, it is concluded from the analyses and experiments performed in this study that a fundamental concept of design and manufacture of the hardware of a noninteracting control system necessary for the development of future TDG's with excellent performance has been established. Author

N90-20351* National Aeronautics and Space Administration. Pasadena Office, CA.
DUAL CATHODE SYSTEM FOR ELECTRON BEAM INSTRUMENTS Patent
James G. Bradley, inventor (to NASA), Joseph M. Conley, inventor (to NASA), and David B. Wittry, inventor (to NASA) (California Inst. of Tech., Pasadena.) 11 Jul. 1989 9 p Filed 11 Aug. 1987
(NASA-Case-NPO-16878-1-CU; US-Patent-4,847,502; US-Patent-Appl-SN-084062; US-Patent-Class-250-396-ML; US-Patent-Class-250-396-R; US-Patent-Class-250-310; US-Patent-Class-219-121.28) Avail: US Patent and Trademark Office CSCL 14B

An electron beam source having a single electron optical axis is provided with two coplanar cathodes equally spaced on opposite sides from the electron optical axis. A switch permits selecting either cathode, and a deflection system comprised of electromagnets, each with separate pole pieces equally spaced from the plane of the cathodes and electron optical axis, first deflects the electron beam from a selected cathode toward the electron optical axis, and then in an opposite direction into

convergence with the electron optical axis. The result is that the electron beam from one selected cathode undergoes a sigmoid deflection in two opposite directions, like the letter S, with the sigmoid deflection of each being a mirror image of the other.
Official Gazette of the U.S. Patent and Trademark Office

N90-20352*# National Aeronautics and Space Administration. Lewis Research Center, Cleveland, OH.
SPACELAB QUALIFIED INFRARED IMAGER FOR MICROGRAVITY SCIENCE EXPERIMENTS
Alexander D. Pline and Robert L. Butcher 1990 11 p Presented at the Technical Symposium on Optical Engineering and Photonics in Aerospace Sensing, Orlando, FL, 16-20 Apr. 1990; sponsored by Society of Photo-Optical Instrumentation Engineers
(NASA-TM-102503; E-5304; NAS 1.15:102503) Avail: NTIS HC A03/MF A01 CSCL 14B

The Lewis Research Center is developing, under contract, a Spacelab (manned module in the Space Shuttle payload bay) qualified infrared imager for noncontact surface temperature measurement in the Surface Tension Driven Convection Experiment, a microgravity fluid physics experiment. A versatile design philosophy was used in order to provide other experiments with essentially an off the shelf Shuttle qualified instrument, eliminating the duplication of the rigorous development and flight qualification processes. An Inframetrics Model 600 Scanning Infrared Radiometer is being modified to satisfy both experimental and flight requirements, while maintaining the basic performance parameters of the commercial instrument. The modifications include an efficient, low power closed cycle cryogenic cooler to cool the detector, a ruggedized scanner mechanism, 8 bit A/D conversion, Mil-STD components (where possible), size and weight optimization, and the addition of a microprocessor to perform automatic gain control. Features such as detector spectral response, the addition of spectral filters, and target temperature ranges could easily be changed to make this instrument useful as both a qualitative and quantitative diagnostic tool for Spacelab microgravity experiments, in combustion and fluid physics. Author

N90-20353*# National Aeronautics and Space Administration. Lewis Research Center, Cleveland, OH.
DESIGN AND CALIBRATION OF A VACUUM COMPATIBLE SCANNING TUNNELING MICROSCOPE
Phillip B. Abel Mar. 1990 13 p
(NASA-TM-102514; E-5317; NAS 1.15:102514) Avail: NTIS HC A03/MF A01 CSCL 14B

A vacuum compatible scanning tunneling microscope was designed and built, capable of imaging solid surfaces with atomic resolution. The single piezoelectric tube design is compact, and makes use of sample mounting stubs standard to a commercially available surface analysis system. Image collection and display is computer controlled, allowing storage of images for further analysis. Calibration results from atomic scale images are presented.
Author

N90-20354# Sandia National Labs., Albuquerque, NM.
ESTIMATION OF MODELED OBJECT POSE FROM MONOCULAR IMAGES
L. P. Ray 1989 13 p Presented at the IEEE Robotics and Automation Conference, Cincinnati, OH, 13-18 May 1990
(Contract DE-AC04-76DP-00789)
(DE90-001678; SAND-89-2527C; CONF-900559-4) Avail: NTIS HC A03/MF A01

The application of one or more monocular images to estimate the three-dimensional position of objects in investigated. The identities of the objects are known, and geometric models are assumed to be available. Linear features extracted from sensor data are interpreted as corresponding with model features by search of an interpretation tree built using prior position estimates. Object positions are updated by maximum-likelihood estimation. Position estimation results from an implemented system are presented, demonstrating location of partially occluded objects in a cluttered scene. DOE

N90-20355# Oak Ridge National Lab., TN.
A NONINTRUSIVE METHOD FOR MEASURING THE OPERATING TEMPERATURE OF A SOLENOID-OPERATED VALVE
Robert C. Kryter 1990 15 p Presented at the Workshop on Monitoring Equipment Environments During Nuclear Plant Operation, Baltimore, MD, 10-11 Apr. 1990
(Contracts DE-AC05-84OR-21400; NRC-1886-8082-8B)
(DE90-007576; CONF-9004140-1) Avail: NTIS HC A03/MF A01

Experimental data are presented to show that the in-service operating temperature of a solenoid operated valve (SOV) can be inferred simply and nondisruptively by using the copper winding of the solenoid coil as a self-indicating, permanently available resistance thermometer. The principal merits of this approach include: (1) there is no need for an add-on temperature sensor, (2) the true temperature of a critical and likely the hottest, part of the SOV (namely, the electrical coil) is measured directly, (3) temperature readout can be provided at any location at which the SOV electrical lead wires are accessible (even though remote from the valve), (4) the SOV need not be disturbed (whether normally energized or deenergized) to measure its temperature in situ, and (5) the method is applicable to all types of SOVs, large and small, ac- and dc-powered. Laboratory tests comparing temperatures measured both by coil resistance and by a conventional thermometer placed in contact with the external surface of the potted solenoid coil indicate that temperature within the coil may be on the order of 40 C higher than that measured externally, a fact that is important to life-expectancy calculations made on the basis of Arrhenius theory. Field practicality is illustrated with temperature measurements made using this method on a SOV controlling the flow of refrigerant in a large chilled-water air-conditioning system. DOE

N90-20356# State Univ. of New York, Albany. Research Foundation.
X RAY MICROIMAGING BY DIFFRACTIVE TECHNIQUES
Progress Report
1990 7 p
(Contract DE-FG02-89ER-60858)
(DE90-008444; DOE/ER-60858/T1) Avail: NTIS HC A02/MF A01

The first year of the research program resulted in significant progress on several fronts. The soft x ray undulator beamline, X1A, at the National Synchrotron Light Source became operational shortly before the start of the grant period. In microimaging by diffraction, Dr. David Sayre was successful in recording moderately large angle diffraction patterns from single diatom specimens. The patterns correspond to information down to the 70A level, and are by far the best achieved to date. To obtain these, a new diffraction camera was constructed and commissioned. It features a multiple pinhole collimator to define a 10 micron diameter beam, and an alignment system to position the 2 micron specimen within it. DOE

N90-20357*# National Aeronautics and Space Administration, Washington, DC.
MERCURIC IODIDE ROOM TEMPERATURE GAMMA-RAY DETECTORS
Bradley E. Patt, Jeffrey M. Markakis, Vernon M. Gerrish, Robert C. Haymes, and Jacob I. Trombka (National Aeronautics and Space Administration. Goddard Space Flight Center, Greenbelt, MD.) 1989 4 p Presented at the Workshop on High Energy Astrophysics in the 21st Century, Taos, NM, 10-14 Dec. 1989
(Contract DE-AC08-88NV-10617)
(NASA-TM-103318; NAS 1.15:103318; DE90-008751; EGG-10617-2051; CONF-891276-5) Avail: NTIS HC A01/MF A01 CSCL 14B

High resolution mercuric iodide room temperature gamma-ray detectors have excellent potential as an essential component of space instruments to be used for high energy astrophysics. Mercuric iodide detectors are being developed both as photodetectors used in combination with scintillation crystals to detect gamma-rays,

and as direct gamma-ray detectors. These detectors are highly radiation damage resistant. The list of applications includes gamma-ray burst detection, gamma-ray line astronomy, solar flare studies, and elemental analysis. DOE

N90-20358*# National Aeronautics and Space Administration. Lewis Research Center, Cleveland, OH.
TiCl4 AS A SOURCE OF TiO2 PARTICLES FOR LASER ANEMOMETRY MEASUREMENTS IN HOT GAS
Donald H. Weikle, Richard G. Seasholtz, and Lawrence G. Oberle Apr. 1990 6 p
(NASA-TM-102581; E-5412; NAS 1.15:102581) Avail: NTIS HC A02/MF A01 CSCL 14B

A method of reacting TiCl4 with water saturated gaseous nitrogen (GN2) at the entrance into a high temperature gas flow is described. The TiO2 particles formed are then entrained in the gas flow and used as seed particles for making laser anemometry (LA) measurements of the flow velocity distribution in the hot gas. Scanning electron microscope photographs of the TiO2 particles are shown. Data rate of the LA processor was measured to determine the amount of TiO2 formed. The TiCl4 and mixing gas flow diagram is shown. This work was performed in an open jet burner. Author

N90-20359# Lawrence Livermore National Lab., CA.
SIMPLE REFLECTION HOLOGRAPHY
John Toeppen 29 Mar. 1990 11 p Presented at the Spring Optical Show of the Optical Society of Northern California, Palo Alto, CA, 29 Mar. 1990
(Contract W-7405-eng-48)
(DE90-008309; UCRL-102996; CONF-9003106-1) Avail: NTIS HC A03/MF A01

White light reflection holography is a good starting point for the first time holographer. The building of an inexpensive holographic camera offers an approach that has many distinct advantages. Not only can such a device be constructed by the average craftsman at a minimum cost but the monolithic design helps assure good results. The finished images are reasonably bright and easy to view in sunlight. The building of the camera itself is instructional as a design task which considers practical problems and scientific principles. The convenience of the finished device avoids many of the difficulties in setting up a dedicated optics lab. Further, the satisfaction of producing quality holograms is reinforced by a tangible reward for successful efforts. Methods, rather than theory, are the essence of this paper. It is intended that this project is not only an end in itself but that it serves as a basis for an outlook towards practical science. DOE

N90-20360# Lawrence Livermore National Lab., CA. Lab. for Experimental Astrophysics.
A NEW THERMAL SENSOR FOR X RAY MICROCALORIMETRY
E. Silver, S. Labov, T. Pfafman, F. Goulding, D. Landis, N. Madden, and J. Beeman (California Univ., Berkeley. Lawrence Berkeley Lab.) 2 Feb. 1990 6 p Presented at the Workshop on High Energy Astrophysics in the 21st Century, Taos, NM, 10-14 Dec. 1989
(Contract W-7405-eng-48)
(DE90-008547; UCRL-102559; CONF-891276-6) Avail: NTIS HC A02/MF A01

Photon counting x ray spectroscopy using microcalorimeters combines the high resolution power of a Bragg crystal with the broad bandwidth capability and high efficiency of charge sensitive detectors. To date, the developers of microcalorimeters take advantage of the strong temperature dependence of resistance in doped semiconductor crystals for converting the calorimeter temperature changes into useful voltage signals. Resistive sensors limit the ultimate sensitivity of microcalorimeters because they dissipate heat and add Johnson noise to the electronic conversion circuit. Potentially, these detrimental properties can be eliminated by exploiting the temperature dependence of the dielectric constant in ferroelectric materials. A mixed crystal quantum ferroelectric shows great promise for a dielectric thermal sensor. Results are presented from the most recent measurements which include the first detection of individual 6 MeV alpha particles with a dielectric calorimeter operating at 1.2 K. DOE

N90-20361# Physical Dynamics, Inc., La Jolla, CA.
SUPERCONDUCTIVE MICROPROBES FOR EDDY CURRENT EVALUATION OF MATERIALS Final Report, 1 Aug. 1988 - 31 Jan. 1989
Walter N. Podney Jul. 1989 46 p
(Contract F49620-88-C-0091)
(AD-A217776; AFOSR-90-0011TR) Avail: NTIS HC A03/MF A01 CSCL 20/3

Superconductive quantum interference devices (SQUIDS) offer new technology for locating materials flaws electromagnetically that promises to increase sensitivity, depth of magnetic flux enables use of microscopic pickup loops in a gradiometer configuration to give high resolution. A cryogenic umbilical connects pickup loops to a remote cryostat housing SQUID sensors to ease scanning. A pair of drive coils a few millimeters in radius that encircle pickup loops forming a coplanar gradiometer 1 mm or less in radius comprise a superconductive microprobe. It provides a depth of field of several millimeters to a 0.1 mm flaw in an aluminum plate, when operating with a drive current a 1 A oscillating at a frequency of 1kHz. Its field of view ranges to several millimeters, for flaws a few millimeters deep, and its horizontal resolution is 1 mm or so, for flaw depths out to its depth of field. An array of microprobes form receptors much like rods in the retina of a magnetic eye. The eye leads to an electromagnetic microscope for imaging internal flaws in aluminum plates. It gives multiple images that enable resolving depth of a 0.1 mm flaw to a few tenths of a millimeter with a horizontal resolution of one millimeter or so. GRA

N90-20362# Naval Postgraduate School, Monterey, CA.
THE DESIGN AND IMPLEMENTATION OF A POSITION MEASURING SYSTEM FOR A REMOTELY CONTROLLED VIDEO CAMERA M.S. Thesis
Peter D. Lloyd Jun. 1989 133 p
(AD-A218077) Avail: NTIS HC A07/MF A01 CSCL 17/5

A position measuring system for a remotely controlled video camera was designed and built. The camera is intended to be used with the modified Advance Development Model of the AN/SAR-8 Infrared Search and Target Designation System (IRSTD) in use at the Naval Postgraduate School. The video data collected by the camera will be correlated with the infrared data from the IRSTD to develop a background data base that will be used in the development of signal processing algorithms. The measurement system uses two Hewlett Packard HEDS-6000 incremental optical encoders, two Motorola MC68705U3 microprocessors and two digital display devices to measure and present the camera's azimuth and elevation angles to an operator at a remote location. The azimuth can be measured over a range of 360 deg with a resolution of + or - 0.0213 deg and the elevation can be measured over 24 deg with a resolution of + or - 0.138 deg. The resolution is limited primarily by hysteresis, which is due to the backlash in the gears between the transducers and the axes of interest. GRA

36 LASERS AND MASERS

Includes parametric amplifiers.
For related information see also *76 Solid-State Physics.*

N90-20363 Illinois Univ., Urbana-Champaign.
HIGH POWER SEMICONDUCTOR LASER ARRAYS BY METALORGANIC CHEMICAL VAPOR DEPOSITION Ph.D. Thesis
Charles Alan Zmudzinski 1989 110 p
Avail: Univ. Microfilms Order No. DA8924976

Semiconductor injection lasers have the capability of producing very high output powers if a large array of diodes can be fabricated. The development of useful high power semiconductor lasers

depends on fabrication processes which overcome the problems associated with high power laser operation. Developments in semiconductor fabrication processes which have led to the fabrication of large linear arrays capable of high power operation are described. Much of this work has been devoted to the fabrication of low threshold current, high efficiency laser diodes using the graded barrier quantum well (GBQW) structure grown by metalorganic chemical vapor deposition (MOCVD). The effects of various processing methods in the optical properties of the laser, such as the threshold current, efficiency, emission wavelength, and near- and far-field radiation patterns, are described and explained. Low threshold current operation with stable radiation patterns have been observed in several types of laser devices. One problem which has prevented high power semiconductor laser operation is lateral lasing and amplified spontaneous emission processes which limit the width of most semiconductor lasers to less than approximately 200 microns. This problem has been solved through the use of a non-planar active region, which allows the width of the laser array to be increased to at least several millimeters. The characteristics of these non-planar laser arrays are presented. Dissert. Abstr.

N90-20364# Maschinenfabrik Augsburg-Nuernberg A.G., Munich (Germany, F.R.).
DEVELOPMENT AND CONSTRUCTION OF EXTERNAL LASER COMPONENTS FOR HARDENING AND COATING [ENTWICKLUNG UND BAU VON EXTERNEN LASERKOMPONENTEN ZUM HAERTEN UND BESCHICHTEN]
Welf Amende 22 Jun. 1987 69 p In GERMAN
(MT-15/87; ETN-90-95325) Avail: NTIS HC A04/MF A01

The design, construction, and testing of several laser components for the treatment of materials with high power infrared radiation are presented. The following components are examined: metallic plane mirrors for beam guidance, facet mirrors for the formation of focal points with adjusted beam intensity, the splitting of laser beams into two partial beams with the possibility of changing the splitting ratio, and a continuous supply of powder for coatings. These components are designed for mass production. ESA

N90-20365# Los Alamos National Lab., NM.
ENERGY DEPOSITION MEASUREMENTS FOR E-BEAM PUMPED EXCIMER LASERS
Michael C. Cates, Karen L. Robertson, Paul C. Melcher (Maxwell Labs., Inc., San Diego, CA.), Dennis P. Greene, and Victor O. Romero 1989 7 p Presented at the International Conference on Lasers '89, New Orleans, LA, 3-8 Dec. 1989
(Contract W-7405-eng-36)
(DE90-007545; LA-UR-90-599; CONF-891261-8) Avail: NTIS HC A02/MF A01

The energy deposition of the E-beam pumped Maxwell Laboratories, Inc. (MLI) Two-Meter Laser was measured and compared using dosimetry films, electron calorimetry, current measurements, and pressure rise measurements. The measurements agreed within their uncertainties. DOE

N90-20366# San Diego State Univ., CA. Dept. of Electrical and Computer Engineering.
ELECTRON-IMPACT IONIZATION AND ELECTRON ATTACHMENT CROSS SECTIONS OF RADICALS IMPORTANT IN TRANSIENT GASEOUS DISCHARGES Final Technical Report, 1 Sep. 1986 - 31 Dec. 1989
Long C. Lee and Santosh K. Srivastava (Jet Propulsion Lab., California Inst. of Tech., Pasadena.) 25 Jan. 1990 67 p
(Contract N00014-86-K-0558)
(AD-A217510) Avail: NTIS HC A04/MF A01 CSCL 20/5

Electron-impact ionization and electron attachment cross sections of radicals and excited molecules were measured using an apparatus that consists of an electron beam, a molecular beam and a laser beam. The information obtained is needed for the pulse power applications in the areas of high power gaseous discharge switches, high energy lasers, particle beam experiments, and electromagnetic pulse systems. The basic data needed for the development of optically-controlled discharge switches were also investigated. Transient current pulses induced by laser irradiation of discharge media were observed and applied for the study of electron-molecule reaction kinetics in gaseous discharges. GRA

N90-20367# Unified Industries, Inc., Springfield, VA.
HIGH EFFICIENCY FLASHLAMP-PUMPED TITANIUM: SAPPHIRE LASER
Philip Lacovara, Leon Esterowitz, and Roger Allen 1989 6 p
(Contract N00014-85-C-2143)
(AD-A217598) Avail: NTIS HC A02/MF A01 CSCL 09/3

A flashlamp pumped titanium sapphire laser has been operated with efficiencies approaching 1 percent using a fluorescent converter. Performance of specific fluorescent converters is described, and ways to further increase the efficiency at the titanium sapphire laser are discussed. GRA

N90-20368# Unified Industries, Inc., Springfield, VA.
FLASH-PUMPED TITANIUM LASER
Leon Esterowitz, Roger Allen, and P. Lacovara 1989 4 p
(Contract N00014-85-C-2143)
(AD-A217599) Avail: NTIS HC A01/MF A01 CSCL 09/3

A flashlamp pumped titanium sapphire laser was operated with efficiencies approaching 1 percent using a fluorescent converter. Performance of specific fluorescent converters is described, and ways to further increase the efficiency at the titanium sapphire laser are discussed. GRA

N90-20369# Los Alamos National Lab., NM. Chemistry and Laser Science Div.
AMPLIFIED SPONTANEOUS EMISSION MEASUREMENTS ON THE AURORA LARGE-APERTURE MODULE
J. A. Oertel, S. J. Czuchlewski, W. T. Leland, and T. P. Turner 1989 5 p Presented at the Conference on Lasers and Electro-Optics, Anaheim, CA, 21-25 May 1990
(Contract W-7405-eng-36)
(DE90-004841; LA-UR-89-4110; CONF-900530-1) Avail: NTIS HC A01/MF A01

Amplified Spontaneous Emission is measured on the large-aperture module (1 x 1 x 2 cu m) of the Aurora KrF laser. Values are compared to the predictions of a 3-D code. DOE

N90-20370# Sandia National Labs., Albuquerque, NM.
STRATEGIES FOR HIGH EFFICIENCY OPERATION OF THE E-BEAM EXCITED ATOMIC XENON LASER USING HIGH-POWER AND HIGH-ENERGY LOADING
Mieko Ohwa, Mark J. Kushner, Peter J. Peters (Technische Hogeschool Twente, Enschede, Netherlands), Edward L. Patterson, and P. Jerry Brannon 1989 4 p Presented at the Conference on Lasers and Electro-Optics, Anaheim, CA, 21-25 May 1990
(Contract DE-AC04-76DP-00789)
(DE90-005196; SAND-89-3025C; CONF-900530-2) Avail: NTIS HC A01/MF A01

E-beam excitation of the atomic xenon laser is theoretically and experimentally investigated using short-pulse high-power deposition (1 to 10 MW/cu cm-atm) and low-power high-energy loading (less than or equal to 1 kJ/l-atm). Scaling laws are derived to maximize laser power and energy efficiency. DOE

N90-20371# Lawrence Livermore National Lab., CA.
PERFORMANCE OF ZIG-ZAG SLAB REGENERATIVE RING AMPLIFIER LASER SYSTEM
Lloyd A. Hackel, Mark A. Summers, Robert Boyd, and Mary Norton 13 Dec. 1989 2 p Presented at the Conference on Lasers and Electro-Optics, Anaheim, CA, 21-25 May 1990
(Contract W-7405-eng-48; DARPA Order 5358)
(DE90-006995; UCRL-102645; CONF-900530-4) Avail: NTIS HC A01/MF A01

We report on a zig-zag slab laser system operated in a burst mode at 300 W at 1.05 microns and 100 W at 0.53 microns. The laser was operated at pulse energies up to 20 Joules/pulse and

1 GW peak power and repetition rates from 1 to 30 Hz. Output in continuous operation exceeded 50 W at 1.05 microns and doubling efficiency of greater than 32 percent. DOE

N90-20372# Lawrence Livermore National Lab., CA.
IMPROVED ENERGY AND POWER BALANCE AT NOVA TARGETS
D. R. Speck, C. Bibeau, R. B. Ehrlich, M. A. Henesian, G. L. Hermes, C. W. Laumann, J. K. Lawson, H. T. Powell, J. E. Murray, and P. J. Wegner et al Dec. 1989 6 p Presented at the Conference on Lasers and Electro-optics, Anaheim, CA, 21-25 May 1990
(Contract W-7405-eng-48)
(DE90-007260; UCRL-102536; CONF-900530-5) Avail: NTIS HC A02/MF A01

Nova can now provide more than 40 kJ of energy and shaped laser pulses onto targets at 0.35 micron. The power balance at 0.35 micron is being improved as required for optimum target performance. DOE

N90-20373# Lawrence Livermore National Lab., CA.
SHAPED PULSES FROM NOVA FOR INERTIAL CONFINEMENT FUSION EXPERIMENTS
S. C. Burkhart, E. H. Padilla, T. L. Weiland, and R. B. Wilcox Dec. 1989 6 p Presented at the Conference on Lasers and Electro-Optics, Anaheim, CA, 21-25 May 1990
(Contract W-7405-eng-48)
(DE90-007261; UCRL-102537; CONF-900530-6) Avail: NTIS HC A02/MF A01

Temporally shaping the target irradiation pulse is crucial for the realization of inertial confinement fusion. We have developed a versatile electrooptic technique for making shaped pulses at 0.35 microns on Nova. DOE

N90-20374# Los Alamos National Lab., NM.
HARMONIC GENERATION MECHANISMS IN SHORT-WAVELENGTH FREE-ELECTRON LASERS
Mark J. Schmitt 1990 9 p Presented at the Free-Electron Lasers and Applications Conference, Los Angeles, CA, 15-19 Jan. 1990 Sponsored in part by Army Strategic Defense Command
(Contract W-7405-eng-36)
(DE90-007622; LA-UR-90-413; CONF-900140-13) Avail: NTIS HC A02/MF A01

The physical mechanisms that contribute to harmonic radiation in free-electron laser systems are examined. Mathematical models for the spontaneous and coherent-spontaneous emission in plane-polarized wigglers are given. How these models are used to perform numerical simulations is discussed. Modifications of the models to incorporate non-ideal free-electron laser effects are reviewed. DOE

N90-20375# Oak Ridge National Lab., TN. Solid State Div.
Y1Ba2Cu3O(7-x) LASER-ABLATION PLUME DYNAMICS MEASUREMENT BY NANOSECOND RESPONSE ION PROBE: COMPARISON WITH OPTICAL MEASUREMENTS
D. N. Mashburn and D. B. Geohegan Nov. 1989 11 p Presented at the SPIE Symposium on Microelectronic Integrated Processing: Growth, Monitoring, and Control, Santa Clara, CA, 8-13 Oct. 1989 Revised Submitted for publication
(Contract DE-AC05-84OR-21400)
(DE90-007658; CONF-8910197-3) Avail: NTIS HC A03/MF A01

A family of fast time response ion probes was developed to study the laser-ablation plume dynamics under Y1Ba2Cu3O(7-x) film-growth conditions. These probes are useful over a wide range of pressures, distances, laser energies, and energy densities. The ion probe measurements are complemented and corroborated by measurements using spatially and temporally resolved optical emission and absorption spectroscopy. The results confirm a long lived ionized component to the plume and a marked slowing of the plasma front at film deposition pressures and distances. Both the ion probe and spectroscopic techniques show promise as sensitive process monitors for film deposition by laser ablation. DOE

N90-20376# Lawrence Livermore National Lab., CA.
MEASUREMENT OF THE STIMULATED THERMAL RAYLEIGH SCATTERING INSTABILITY
T. J. Karr, M. C. Rushford, J. R. Murray, and J. R. Morris Jan. 1990 14 p Presented at the SPIE Optics, Electro-Optics and Laser Applications in Science and Engineering Conference and Exhibition, Los Angeles, CA, 15-19 Jan. 1990
(Contract W-7405-eng-48)
(DE90-007849; UCRL-99967-Rev-1; CONF-900140-12-Rev-1)
Avail: NTIS HC A03/MF A01

The first clear experimental demonstration is reported of large amplification of small scale spatial perturbations by stimulated thermal Rayleigh scattering (STRS) of a CW laser beam propagating through an absorbing medium in a context normally associated with thermal blooming. A single-mode argon-ion laser beam with lambda = 488 nm was propagated vertically downward through a 1.2 m cell filled with CCl4 that was doped with an absorber to have optical depths in the range 0.5 to 2.3. A shear plate interferometer near the cell input generated the perturbation. Fringe growth was rapid and visually obvious, as was competing growth from dust specks, etc. The measured growth rate is in good agreement with the asymptotic rate from analytic STRS theory. DOE

N90-20377# Columbia Univ., New York, NY.
LASER ENHANCED CHEMICAL REACTIONS Technical Report, 1 Mar. 1989 - 28 Feb. 1990
1990 10 p
(Contract DE-FG02-88ER-13937)
(DE90-008273; DOE/ER-13937/2) Avail: NTIS HC A02/MF A01

Included is the discussion of infrared diode lasers used to study time dependent dynamic events. Also, hot atom excitation of vibrational states of polyatomic molecules, bimolecular quenching and reactions of O(sup 1)D, bimolecular reaction studies of the OH + CO yields H + CO2 system, and the chemical dynamics of the reaction between chlorine atoms and deuterated cyclohexane are covered briefly. DOE

N90-20378# Lawrence Livermore National Lab., CA.
SPATIAL IMAGING USING CONFOCAL FABRY-PEROT INTERFEROMETERS
D. W. Myers, D. E. Decker, M. A. Johnson, and S. D. Mostek 1990 6 p Presented at the Conference on Lasers and Electro-Optics, Anaheim, CA, 21-25 May 1990
(Contract W-7405-eng-48)
(DE90-008363; UCRL-102525; CONF-900530-8) Avail: NTIS HC A02/MF A01

A diagnostic imaging package containing confocal Fabry-Perot interferometers is used to provide spatial intensity information for each of several closely spaced wavelength components of a single laser beam. DOE

N90-20379# Los Alamos National Lab., NM.
LASER-INDUCED SHOCK WAVES EFFECTS IN MATERIALS
R. S. Dingus and B. P. Shafer 1990 11 p Presented at Biomedical Optics '90, Los Angeles, CA, 14-19 Jan. 1990
(Contract W-7405-eng-36)
(DE90-007626; LA-UR-90-445; CONF-900178-1) Avail: NTIS HC A03/MF A01

A review of the effects of pressure pulses on materials is presented with an orientation toward laser-induced shock wave effects in biological tissue. The behavior is first discussed for small amplitudes, namely sound waves, since many important features in this region are also applicable at large amplitudes. The generation of pressure pulses by lasers is discussed along with amplitudes. The origin and characteristic properties of shock waves are discussed along with the different types of effects they can produce. The hydrodynamic code techniques required for shock wave

calculations are discussed along with the necessary empirical data base and methods for generating that data base. DOE

N90-20380# Utah Univ., Salt Lake City.
PULSED LASER PHOTOTHERMAL SPECTROSCOPY OF LIQUIDS AND SOLIDS Progress Report, 1 Apr. 1987 - 25 Sep. 1989
Edward M. Eyring 25 Sep. 1989 16 p Sponsored in part by ONR, Washington, DC
(Contract DE-FG02-84ER-13227)
(DE90-008642; DOE/ER-13227/6) Avail: NTIS HC A03/MF A01

Published papers have compared the advantages of piezoelectric and optical detection of photoacoustic signals in sample liquids and have demonstrated the superior capabilities of thermal lens measurements on time scales as short as a few hundred nanoseconds. Computer programs were developed to compare theoretical and experimental photoacoustic pulse shapes in liquids with a view to determining triplet state quantum yields and radiationless decay lifetimes with greater accuracy. Non-radiative quantum yields of 1.0, 0.9 and 0.5 were measured for nonaqueous solutions of Crystal Violet, Evan's Blue and Nile Blue A respectively. Pulsed photothermal radiometry experiments have yielded thermal diffusivity data for a room temperature molten salt system. Microphonic photoacoustic signals obtained by illuminating solid samples with synchrotron x rays were enhanced with volatile liquids, and the results were compared with theory. DOE

N90-20381# State Univ. of New York, Buffalo. Dept. of Electrical and Computer Engineering.
PICOSECOND LASER STUDY OF POLYATOMIC MOLECULES Progress Report
Hoi S. Kwok 10 Mar. 1990 5 p
(Contract DE-FG02-85ER-13405)
(DE90-008647; DOE/ER-13405/T3) Avail: NTIS HC A01/MF A01

The photodissociation of NO2 by lasers and the improvement to femtosecond spectroscopy measurement is discussed. DOE

N90-20382# Lawrence Livermore National Lab., CA.
LASER LINE TRANSPORT WITH REFRACTION Final Report
Paul Kunasz Aug. 1989 6 p
(Contract W-7405-eng-48)
(DE90-008683; UCRL-21275) Avail: NTIS HC A02/MF A01

Extensive studies were completed of numerical methods for the treatment of refraction in laser line transport. A stable method which provides acceptable accuracy now resides in the three dimensional laser transport code BEAM3. By way of review, the numerical method employed by BEAM3 is an extension to three dimensions of a technique tested extensively in a one-dimensional model of a laser rod. At each time step, this method involves sweeping back and forth along the rod axis z, solving for the forward propagating intensity while holding the back-propagating beam fixed. The sweeps continue until convergence is achieved. On each sweep, the nonlinear transport equation is solved by the method of Newton Raphson, for the intensity J(sub k), at each slice z(sub k) along the rod. At slice z(sub k), on a sweep over increasing values of k, the upwind intensity value is known at z(sub k-1), z(sub k-2), ..., z(sub 2), z(sub 1). To solve the transport equation at z(sub k) the ray of propagation is extended upwind until it intersects either the coordinate boundary z(sub k-1), or the previous time value, ct(sub n-1). Therefore, for sub-Courant time steps, the upwind conditions couple to the unknown slice as well as the upwind slice. DOE

N90-20383# Colorado Univ., Boulder.
DURIP THEORETICAL/EXPERIMENTAL INVESTIGATIONS OF HIGHLY ENERGETIC DICATION SPECIES Final Report, 1 Dec. 1988 - 30 Nov. 1989
W. C. Lineberger and Stephen R. Leone 15 Dec. 1989 5 p
(Grant AF-AFOSR-0087-89; AF Proj. 3842)
(AD-A217771; AFOSR-90-0125TR) Avail: NTIS HC A01/MF A01 CSCL 07/5

The titanium sapphire laser was modified with a thick etalon to achieve single frequency scanning capability. The Neodymium:YAG laser and dye laser were modified with a home-built scanning system. Preliminary investigations using a medium pressure electrical discharge ion source gave reasonable quantities of NO(++) and several other dications. These ions survived the rather severe collisional environment of the ion source. The nature of this source, however, did not permit very controlled formation conditions. Consequently, the ion source was replaced with an electron impact ionized supersonic expansion source. Construction of this source was completed, and the first mass spectra of dications were just obtained. A new ion source was devised to optimize the production of doubly charged molecular cations. Using the NF3 precursor, the species NF2(++) and NF(++) are observed. With HCL and DCL precursors, both HCL(++) and DCL(++) species are observed. Using CCl4, a wide variety of species are formed, including CCL(++), HCCL(++), and H2CCL(++), several of which may be previously unreported. With CF4, CF(++), CF2(++) and CF3(++) was observed. The readily made species, NO(++) and CO(++), starting from their parent neutrals were also observed. An eight-photon double ionization process in NO and a ten-photon process for N2 (to produce NO(++) and N2(++), respectively), is in the works. GRA

N90-20384# Rome Air Development Center, Griffiss AFB, NY.
PICOSECOND LASER FACILITY Report, Mar. 1987 - Aug. 1988
Dorothy Jackson and Michael Ward Nov. 1989 36 p
(AD-A217784; RADC-TR-89-290) Avail: NTIS HC A03/MF A01 CSCL 09/3

This report contains the results of our work in setting up, aligning, and characterizing the picosecond pulse laser facility in the Photonics Laboratory. It explains the theory of production of picosecond pulses using a dye laser pumped by a mode locked argon laser. It also briefly describes our suggested uses of this facility. These include degenerate four wave mixing for the measurement of nonlinear optical effects in optical materials and electro-optic sampling for the characterization of ultrafast electronic and optoelectronic devices. GRA

N90-20385# Medical Coll. of Virginia, Richmond.
BIOLOGICAL APPLICATIONS AND EFFECTS OF OPTICAL MASERS Final Report, 1 Sep. 1987 - 31 Aug. 1989
William T. Ham, Jr., Harold A. Mueller, R. Kennon Guerry, Dupont Guerry, III, and Stephen F. Cleary 31 Oct. 1989 18 p
(Contract DAMD17-87-C-7186; DA Proj. 3M1-62787-A-878)
(AD-A217910) Avail: NTIS HC A02/MF A01 CSCL 09/3

Research was continued on basic mechanisms involving photochemical events in mammalian retina by injecting superoxide dismutase (SOD) and catalase (CAT) into vitreous of monkey eye before and after exposure to blue light. Intravitreal injection plus exposure to blue light proved toxic to the eye and no information on oxygen radicals was obtained. The argon krypton laser line at 488 nm was acoustically modulated at 1, 10, and 20 MHz for 1000s exposures of the monkey retina. Threshold radiant exposures at 20 MHz were 3 times lower than those at 1 MHz. The oxygen effect (high PO2 arterial blood-oxygen) on retinal damage was investigated at 3 wavelengths (540, 640, 840 nm). Lack of an appreciable O2 effect at 640 nm and none at 840 nm provides evidence that photochemical toxicity is confined primarily to wavelengths below 640 nm. GRA

N90-20386# Laser Applications Research Center, The Woodlands, TX.
SHORT WAVELENGTH LASER/MATERIALS INTERACTIONS Final Technical Report, 1 Sep. 1985 - 30 Sep. 1988
Leif G. Fredin, David T. Halligan, Brendan D. Krenek, Terry D. Kunz, Richard F. Menefee, and Michael J. Berry 20 Dec. 1989 206 p

(Grant AF-AFOSR-0365-85; AF Proj. 2306)
(AD-A218015; AFOSR-90-0049TR) Avail: NTIS HC A10/MF A02 CSCL 09/3

The overall objective of the program is to understand the nature of laser interactions with materials, with special emphasis on the phenomenology and effects associated with short wavelength laser interactions with spacecraft materials. HARC/Rice personnel have completed the following projects: (1) development of new diagnostic instrumentation and testing methods for evaluation of laser effects and high temperature performance; (2) fundamental studies of laser/materials interactions; (3) determination of short wavelength laser/materials interaction phenomena and effects; and (4) materials evaluation. The program has led to major advances in science-based understanding of materials performance under extreme conditions for two applications: enhancement of spacecraft survivability, and development of high and ultrahigh temperature oxidation resistant materials. GRA

N90-20387# Stanford Univ., CA. Dept. of Chemistry.
PICOSECOND NONLINEAR STUDIES OF COMPLEX MATERIALS USING THE FREE ELECTRON LASER Final Report, 15 Sep. 1986 - 31 Mar. 1989
Michael David Fayer 8 Feb. 1990 11 p
(Contract N00014-86-K-0825)
(AD-A218215) Avail: NTIS HC A03/MF A01 CSCL 09/3

This project involves the use of the Stanford Free Electron Laser (FEL) to conduct picosecond optical nonlinear experiments to study complex materials. The theoretical foundation for the work was established. A new four time correlation function approach for the analysis of optical nonlinear line narrowing experiments was developed. The method explains previous experiments and will allow the FEL experiments to be analyzed to extract important dynamical information about complex materials. A full nonlinear optics laboratory was established at the Stanford FEL. This includes necessary beam diagnostic equipment, optical components, computerized delay lines, liquid helium equipment, and detection equipment. The laboratory has the capability of performing photon echo and other nonlinear experiments. GRA

37 MECHANICAL ENGINEERING

Includes auxiliary systems (nonpower); machine elements and processes; and mechanical equipment.

N90-20388# Carnegie-Mellon Univ., Pittsburgh, PA. Robotics Inst.
THE CMU RECONFIGURABLE MODULAR MANIPULATOR SYSTEM
Donald Schmitz, Pradeep Khosla, and Takeo Kanade May 1988 21 p
(CMU-RI-TR-88-7) Avail: NTIS HC A03/MF A01

Modular manipulator designs have long been considered for use as research tools, and as the basis for easily modified industrial manipulators. In these manipulators the links and joints are discrete and modular components can be assembled into a desired manipulator configuration. As hardware advances have made actual modular manipulators practical, various capabilities of such manipulators have gained interest. Particularly desirable is the ability to rapidly reconfigure such a manipulator in order to custom tailor it to specific tasks. This reconfiguration greatly enhances the capacity of a given amount of manipulator hardware. The development of a prototype modular manipulator and the implementation of a configuration independent manipulator kinematics algorithm used for path planning in the prototype are discussed. Author

N90-20389 Pennsylvania State Univ., University Park.
DEVELOPMENT OF A PASSIVE ROBOT-CONTROLLED REACTION ARM Ph.D. Thesis
Curtis Harvey Reed 1989 207 p
Avail: Univ. Microfilms Order No. DA8922108

A robot controlled reaction arm is developed to increase the load capacity and task capability of an industrial robot. The reaction arm serves as a positionable cool platform that can be locked in place to absorb the reaction forces generated by a tool's operation. The arm is passive in the sense that its motion, and the tool's operation, are controlled by the robot. The reaction arm concept is discussed and design objectives are established for a reaction arm that is to be installed on the table framework of a six axis IBM model RS-1 assembly robot equipped with a two fingered general purpose gripper. The mechanical structure of the constructed prototype arm comprises a mounting base with a vertically travelling shoulder, a horizontally flexible arm assembly of three links with lockable revolute joints, and a unique tool holding end effector. The robot's gripper engages a guide tab on the end effector for direct horizontal manipulation of the tool. The guide tab and tool slide vertically within the body of the end effector, the tab's relative vertical position sensed to control a shoulder actuator that regulates the end effector's elevation. Leveraged tool advancement is obtained through gearing between the vertical travel mechanisms of the guide tab and the tool carriage.
Dissert. Abstr.

N90-20390# Instituto de Pesquisas Espaciais, Sao Jose dos Campos (Brazil).
SPACE MECHANISM OF LOW VELOCITY FOR AN ARRAY OF SOLAR PANELS: ANALYSIS AND DESIGN OF AN EXPERIMENTAL MODEL; DIMENSIONS OF BEARINGS M.S. Thesis [MECANISMOS ESPACIAIS DE BAIXA VELOCIDADE PARA ACIONAMENTO DE PAINEIS SOLARES: ANALISE E PROJETO DE UM MODELO EXPERIMENTAL; DIMENSIONAMENTO DE MANCAIS]
Mario Cesar Ricci Aug. 1989 173 p In PORTUGUESE; ENGLISH summary
(INPE-4859-TDL/370) Avail: NTIS HC A08/MF A01

The analysis and the design of a solar array drive mechanism (SADM) experimental model are presented. Emphasis is put on the design aspects relative to SADM drive and bearing units, although almost every component present in a space mechanism is described. SADM generates friction torques. Specifically angular contact ball bearing generated torques are analyzed in details since a prime requirement is to avoid possible interferences with the satellite attitude control system. A computer program which allows estimation of the dry friction torque generated by ball bearings running at low speeds is developed. Simulation results show good agreement with the experimental results available in the literature. Concerning the drive unit, the hybrid step motor characteristics are discussed, as well as, a driver control technique that minimizes vehicle interaction. Finally, the main aspects relative to the construction of the SADM experimental model, as gearing trains and bearing lubrication, are also proposed and discussed.
Author

N90-20391*# National Aeronautics and Space Administration. Lewis Research Center, Cleveland, OH.
BEARING AND GEAR STEELS FOR AEROSPACE APPLICATIONS
Erwin V. Zaretsky Mar. 1990 30 p Submitted for publication
(NASA-TM-102529; E-5300; NAS 1.15:102529) Avail: NTIS HC A03/MF A01 CSCL 13I

Research in metallurgy and processing for bearing and gear steels has resulted in improvements in rolling-element bearing and gear life for aerospace application by a factor of approximately 200 over that obtained in the early 1940's. The selection and specification of a bearing or gear steel is dependent on the integration of multiple metallurgical and physical variables. For most aerospace bearings, through-hardened VIM-VAR AISI M-50 steel is the material of preference. For gears, the preferential material is case-carburized VAR AISI 9310. However, the VAR processing for this material is being replaced by VIM-VAR processing. Since case-carburized VIM-VAR M-50NiL incorporates the desirable qualities of both the AISI M-50 and AISI 9310 materials, optimal life and reliability can be achieved in both bearings and gears

with a single steel. Hence, this material offers the promise of a common steel for both bearings and gears for future aerospace applications. Author

N90-20392*# National Aeronautics and Space Administration. Lewis Research Center, Cleveland, OH.
AN APPLICATIONAL PROCESS FOR DYNAMIC BALANCING OF TURBOMACHINERY SHAFTING
Vincent G. Verhoff Mar. 1990 36 p
(NASA-TM-102537; E-4768; NAS 1.15:102537) Avail: NTIS HC A03/MF A01 CSCL 13I

The NASA Lewis Research Center has developed and implemented a time-efficient methodology for dynamically balancing turbomachinery shafting. This methodology minimizes costly facility downtime by using a balancing arbor (mandrel) that simulates the turbomachinery (rig) shafting. The need for precision dynamic balancing of turbomachinery shafting and for a dynamic balancing methodology is discussed in detail. Additionally, the inherent problems (and their causes and effects) associated with unbalanced turbomachinery shafting as a function of increasing shaft rotational speeds are discussed. Included are the design criteria concerning rotor weight differentials for rotors made of different materials that have similar parameters and shafting. The balancing methodology for applications where rotor replaceability is a requirement is also covered. This report is intended for use as a reference when designing, fabricating, and troubleshooting turbomachinery shafting. Author

N90-20393*# National Aeronautics and Space Administration. Lewis Research Center, Cleveland, OH.
ELECTRON BEAM INDUCED DAMAGE IN PECVD Si3N4 AND SiO2 FILMS ON InP
Dragan M. Pantic, Vik J. Kapoor, Paul G. Young (Cincinnati Univ., OH.), Wallace D. Williams, and John E. Dickman Mar. 1990 17 p Presented at the Dielectric Films on Compound Semiconductors Symposium, Honolulu, HI, 18-23 Oct. 1987; sponsored by The Electrochemical Society
(NASA-TM-102544; E-5356; NAS 1.15:102544) Avail: NTIS HC A03/MF A01 CSCL 13I

Phosphorus rich plasma enhanced chemical vapor deposition (PECVD) of silicon nitride and silicon dioxide films on n-type indium phosphide (InP) substrates were exposed to electron beam irradiation in the 5 to 40 keV range for the purpose of characterizing the damage induced in the dielectic. The electron beam exposure was on the range of 10(exp -7) to 10(exp -3) C/sq cm. The damage to the devices was characterized by capacitance-voltage (C-V) measurements of the metal insulator semiconductor (MIS) capacitors. These results were compared to results obtained for radiation damage of thermal silicon dioxide on silicon (Si) MOS capacitors with similar exposures. The radiation induced damage in the PECVD silicon nitride films on InP was successfully annealed out in an hydrogen/nitrogen (H2/N2) ambient at 400 C for 15 min. The PECVD silicon dioxide films on InP had the least radiation damage, while the thermal silicon dioxide films on Si had the most radiation damage. Author

N90-20394# Argonne National Lab., IL. Industrial Cogeneration Program.
A TECHNICAL AND ECONOMIC EVALUATION OF OXYGEN-ENRICHED COMBUSTION IN DIESEL ENGINES USING WATER-EMULSIFIED FUELS
R. L. Cole, T. J. Marciniak, R. R. Sekar, and F. Stodolsky Jan. 1990 75 p
(Contract W-31-109-eng-38)
(DE90-008095; ANL/ESD/TM-2) Avail: NTIS HC A05/MF A01

The technical and economic feasibility of using oxygen-enriched air and low-grade fuels in diesel cogeneration systems is reported. The effects of oxygen enrichment, low-grade fuels, and water addition on the combustion process were studied using first principles of combustion theory; the effects of oxygen enrichment and water addition on diesel engine performance were analyzed with a computer model; air separation technologies were evaluated; the coupling of the oxygen plant to the diesel engine was studied; and the internal rate of return for several system options was determined. The greatest improvement in economic benefits is obtained primarily from fuel switching, and the optimal oxygen enrichment is the minimum that will enable medium- and high-speed diesel engines to use low-grade fuels. Two oxygen-enrichment technologies, selective membranes and pressure-swing adsorption, were identified as being both technically and economically feasible. Oxygen enrichment increases the power of the diesel engine by allowing an increased fueling rate, although increased pressures and temperatures may decrease engine life. Oxygen enrichment decreases CO, smoke, and particulate emissions from the engine but increases NO sub x emissions. However, the NO sub x emissions, pressures, and temperatures can be controlled by water addition and fuel-injection timing adjustments. DOE

N90-20395# Oak Ridge National Lab., TN. Center for Engineering Systems Advanced Research.
CONCEPT FORMATION AND GENERALIZATION BASED ON EXPERIMENTATION BY AN AUTONOMOUS MOBILE ROBOT
P. F. Spelt, G. deSaussure, E. Lyness, G. Oliver, and M. Silliman 1989 15 p Presented at the IEEE Robotics and Automation Conference, Cincinnati, OH, 13-18 May 1990
(Contract DE-AC05-84OR-21400)
(DE90-001731; CONF-900559-5; CESAR-89/41) Avail: NTIS HC A03/MF A01

The Center for Engineering Systems Advanced Research (CESAR) conducts basic research in the area of intelligent machines. In this paper, we describe our approach to a class of machine learning problems which involves autonomous concept formation using feedback from trial-and-error learning. Our formulation was experimentally validated on an autonomous mobile robot, which learned the task of control panel monitoring and manipulation for effective process control. Conclusions are drawn concerning the applicability of the system to a more general class of learning problems, and implications for the use of autonomous mobile robots in hostile and unknown environments are discussed. DOE

N90-20396# Oak Ridge National Lab., TN. Center for Engineering Systems Advanced Research.
ROBOT NAVIGATION RESEARCH USING THE HERMIES MOBILE ROBOT
Deanna L. Barnett 1989 18 p Presented at the IEEE Robotics and Automation Conference, Cincinnati, OH, 13-18 May 1990
(Contract DE-AC05-84OR-21400)
(DE90-001952; CONF-900559-7) Avail: NTIS HC A03/MF A01

In recent years robot navigation has attracted much attention from researchers around the world. Not only are theoretical studies being simulated on sophisticated computers, but many mobile robots are now used as test vehicles for these theoretical studies. Various algorithms have been perfected for navigation in a known static environment; but navigation in an unknown and dynamic environment poses a much more challenging problem for researchers. Many different methodologies have been developed for autonomous robot navigation, but each methodology is usually restricted to a particular type of environment. One important research focus of the Center for Engineering Systems Advanced research (CESAR) at Oak Ridge National Laboratory, is autonomous navigation in unknown and dynamic environments using the series of HERMIES mobile robots. The research uses an expert system for high-level planning interfaced with C-coded routines for implementing the plans, and for quick processing of data requested by the expert system. In using this approach, the navigation is not restricted to one methodology since the expert system can activate a rule module for the methodology best suited for the current situation. Rule modules can be added the rule base as they are developed and tested. This paper will report on the various rule modules and methods of navigation in use, or under development at CESAR, using the HERMIES-IIB robot as a testbed. DOE

N90-20397# Oak Ridge National Lab., TN. Engineering Physics and Mathematics Div.
ROBUST PERFORMANCE OF MULTIPLE TASKS BY A MOBILE ROBOT
Martin Beckerman, Deanna L. Barnett, Mike Dickens, and Charles R. Weisbin (Jet Propulsion Lab., California Inst. of Tech., Pasadena.) 1989 14 p Presented at the IEEE Robotics and Automation Conference, Cincinnati, OH, 13-18 May 1990
(Contract DE-AC05-84OR-21400)
(DE90-001953; CONF-900559-8) Avail: NTIS HC A03/MF A01

While there have been many successful mobile robot experiments, only a few papers have addressed issues pertaining to the range of applicability, or robustness, of robotic systems. The purpose of this paper is to report results of a series of benchmark experiments done to determine and quantify the robustness of an integrated hardware and software system of a mobile robot. DOE

N90-20398# Sandia National Labs., Albuquerque, NM.
SWING-FREE MOVEMENT OF SIMPLY SUSPENDED OBJECTS EMPLOYING PARAMETER ESTIMATION
Jill C. Werner, Rush D. Robinett, and Ben J. Petterson 1989 7 p Presented at the IEEE Robotics and Automation Conference, Cincinnati, OH, 13-18 May 1990
(Contract DE-AC04-76DP-00789)
(DE90-002238; SAND-89-2511C; CONF-900559-3) Avail: NTIS HC A02/MF A01

An adaptive, swing-free trajetory planner for a gantry robot has been analytically developed and experimentally implemented on a commercial robot. A batch, nonlinear least square estimator (differential correction) is used to predict the initial conditions, mass, and frequency of the simply suspended object from a set of force sensor measurements. These parameters, in turn, are supplied to the swing-free trajectory planner to perform the maneuver. These algorithms have been implemented on a CIMCORP XR6100 gantry robot, and swing-free trajectories have been performed by the robot using the adaptive trajectory planner. DOE

N90-20399# Sandia National Labs., Albuquerque, NM.
RESOLVED MOTION RATE AND RESOLVED ACCELERATION SERVO-CONTROL OF WHEELED MOBILE ROBOTS
Patrick F. Muir and Charles P. Neuman (Carnegie-Mellon Univ., Pittsburgh, PA.) 1989 20 p Presented at the IEEE Robotics and Automation Conference, Cincinnati, OH, 13-18 May 1990 Sponsored in part by Dept. of Electrical and Computer Engineering, Carnegie-Mellon Univ., Pittsburgh, PA
(Contracts DE-AC04-76DP-00789; N00014-81-K-0503)
(DE90-002585; SAND-89-2414C; CONF-900559-1) Avail: NTIS HC A03/MF A01

Accurate motion control of wheeled mobile robots (WMRs) is required for their application to autonomous, semi-autonomous and teleoperated tasks. The similarities between WMRs and stationary manipulators suggest that current, successful, model-based manipulator control algorithms may be applied to WMRs. Special characteristics of WMRs including higher-pairs, closed-chains, friction and unactuated and unsensed joints require innovative modeling methodologies. The WMR modeling challenge has been recently overcome, thus enabling the application of manipulator control algorithms to WMRs. This realization lays the foundation for significant technology transfer from manipulator control to WMR control. We apply two Cartesian-space manipulator control algorithms: resolved motion rate (kinematics-based) and resolved acceleration (dynamics-based) control to WMR servo-control. We evaluate simulation studies of two exemplary WMRs: Uranus (a three degree-of-freedom WMR constructed at Carnegie Mellon University), and Bicsun-Bicas (a two degree-of-freedom WMR being constructed at Sandia National Laboratories) under the control of these algorithms. Although resolved motion rate servo-control is adequate for the control of Uranus, resolved acceleration servo-control is required for the control of the mechanically simpler Bicsun-Bicas. DOE

N90-20400# Argonne National Lab., IL. Tribology Section.
TRIBOLOGICAL PROPERTIES OF BORIC ACID AND BORIC-ACID-FORMING SURFACES. PART 2: FORMATION AND SELF-LUBRICATION MECHANISMS OF BORIC ACID FILMS ON BORON- AND BORIC-OXIDE-CONTAINING SURFACES
A. Erdemir, G. R. Fenske, R. A. Erck, F. A. Nichols, and D. Busch 1990 23 p Presented at the 45th Annual Meeting of the Society of Tribologists and Lubrication Engineers, Denver, CO, 7-10 May 1990
(Contract W-31-109-eng-38)
(DE90-005632; CONF-900588-2) Avail: NTIS HC A03/MF A01

This paper describes the formation and self-lubricating mechanisms of boric acid films on boron- and boric oxide-containing surfaces. As reported in part 1, boric acid, owing to a layered triclinic crystal structure and weak interlayer bonds, enjoys an unusual lubrication capability. RF-magnetron sputtering and vacuum evaporation techniques were used to produce thin coatings of boron and boric oxides on steel substrates. The results of tribological experiments indicate that the room temperature friction coefficient of tribosystems that include boron and/or boric oxide coatings ranges from 0.05 to 0.07, depending on the coating type. Laser-Raman spectroscopy of these surfaces revealed that this low friction is associated with a thin boric acid film that forms on the surfaces of these coatings. The fabrication and potential importance of boric acid and boric acid-forming surfaces for practical applications are enumerated. Surface engineering of tribomaterials, such as these demonstrated in this paper, is suggested as a new lubrication concept for use in present and future tribological industries. DOE

N90-20401# Argonne National Lab., IL. Tribology Section.
TRIBOLOGICAL PROPERTIES OF BORIC ACID AND BORIC ACID FORMING SURFACES. PART 1: CRYSTAL CHEMISTRY AND SELF-LUBRICATING MECHANISM OF BORIC ACID
Ali Erdemir 1990 18 p Presented at the 45th Annual Meeting of the Society of Tribologists and Lubrication Engineers, Denver, CO, 7-10 May 1990
(Contract W-31-109-eng-38)
(DE90-005665; CONF-900588-1) Avail: NTIS HC A03/MF A01

An in-depth understanding of the atomic-scale structure and chemistry of self-lubricating solids and how they relate to the efficiency and endurance of large-scale tribosystems is critically important. Of particular interest is the utilization of this understanding for the development of mechanistic models that can increase our ability to assess and predict the capabilities of self-lubricating solids. Accordingly, a comprehensive investigation was made of the crystal chemistry and self-lubrication mechanisms of boric acid and boric acid-forming surfaces. In this paper, the fundamentals of the crystal chemistry and the proposed lubrication mechanism of boric acid are described. Pin-on-disk tests performed on cold-pressed boric-acid pins and AISI 52100 steel disks, showed that the friction coefficient of this tribosystem is approximately 0.1. The results of this investigation indicate that boric acid, owing to its unique crystal structure and bond characteristics, is a promising solid lubricant for a wide range of tribological applications. DOE

N90-20402# Sandia National Labs., Albuquerque, NM.
KNOWLEDGE-BASED ROBOTIC GRASPING
S. A. Stansfield 1989 6 p Presented at the IEEE Robotics and Automation Conference, Cincinnati, OH, 13-18 May 1990
(Contract DE-AC04-76DP-00789)
(DE90-007216; SAND-89-2044C; CONF-900559-9) Avail: NTIS HC A02/MF A01

In this paper, we describe a general-purpose robotic grasping system for use in unstructured environments. Using computer vision and a compact set of heuristics, the system automatically generates the robot arm and hand motions required for grasping an unmodeled object. The utility of such a system is most evident in environments where the robot will have to grasp and manipulate a variety of unknown objects, but where many of the manipulation tasks may be relatively simple. Examples of such domains are

planetary exploration and astronaut assistance, undersea salvage and rescue, and nuclear waste site clean-up. This work implements a two-stage model of grasping: stage one is an orientation of the hand and wrist and a ballistic reach toward the object; stage two is hand preshaping and adjustment. Visual features are first extracted from the unmodeled object. These features and their relations are used by an expert system to generate a set of valid reach/grasps for the object. These grasps are then used in driving the robot hand and arm to bring the fingers into contact with the object in the desired configuration. DOE

N90-20403# Sandia National Labs., Albuquerque, NM.
DYNAMIC DAMPING CONTROL: IMPLEMENTATION ISSUES AND SIMULATION RESULTS
Robert J. Anderson 1989 22 p Presented at the IEEE Robotics and Automation Conference, Cincinnati, OH, 13-18 May 1990
(Contract DE-AC04-76DP-00789)
(DE90-007687; SAND-89-2506C; CONF-900559-10) Avail: NTIS HC A03/MF A01

Computed torque algorithms are used to compensate for the changing dynamics of robot manipulators in order to ensure that a constant level of damping is maintained for all configurations. Unfortunately, there are three significant problems with existing computed torque algorithms. First, they are nonpassive and can lead to unstable behavior; second, they make inefficient use of actuator capability; and third, they cannot be used to maintain a constant end-effector stiffness for force control tasks. Recently, we introduced a new control algorithm for robots which, like computed torque, uses a model of the manipulator's dynamics to maintain a constant level of damping in the system, but does so passively. This new class of passive control algorithms has guaranteed stability properties, utilizes actuators more effectively, and can also be used to maintain constant end-effector stiffness. In this paper, this approach is described in detail, implementation issues are discussed, and simulation results are given. DOE

N90-20404# Oak Ridge National Lab., TN. Instrumentation and Controls Div.
DESIGN OF A TELEROBOTIC CONTROLLER WITH JOINT TORQUE SENSORS
J. F. Jansen and J. N. Herndon 1990 8 p Presented at the IEEE Robotics and Automation Conference, Cincinnati, OH, 13-18 May 1990
(Contract DE-AC05-84OR-21400)
(DE90-008753; CONF-900559-12) Avail: NTIS HC A02/MF A01

The purpose was to analytically show how to design a joint controller for a telerobotic system when joint torque sensors are available. Other sensors such as actuator position, actuator velocity, joint position, and joint velocity are assumed to be accessible; however, the results will also be useful when only partial measurements are available. The controller presented can be applied to either mode of operation of a manipulator (i.e., teleoperation or robotic). Mechanical manipulators with high levels of friction are assumed. Finally, the results are applied to a telerobotic system built for NASA. Very high levels of friction have been reduced using high-grain feedback while avoiding limit cycles. DOE

N90-20405# Naval Postgraduate School, Monterey, CA. Dept. of Mechanical Engineering.
CONTROL SYSTEM DESIGN OF THE THIRD FLEXIBLE JOINT OF PUMA 560 ROBOT M.S. Thesis
Robby Lee Knight Jun. 1989 141 p
(AD-A218075) Avail: NTIS HC A07/MF A01 CSCL 12/9

With the increased demands for higher productivity in industry and the military, control of robot manipulators with flexible joints is needed. The difficulties associated with the control of flexible joint robots include: (1) Nonlinearity of the arm motion; (2) Coupled large motion (motion of the motor) and small motion (mechanical vibration); and (3) Measurements of feedback signals. A controller designed to handle the difficulties related to flexible joint robots is presented. The third joint of the PUMA 560 Robot was selected as an example. A control algorithm for flexible-body control was devised and an observer was designed with the use of MATRIX sub x to control tip motion of the single-link single-joint system. Computer simulation results are discussed, and a comparison between rigid-body controllers and the flexible-body control is conducted. GRA

N90-20406# Aeronautical Research Labs., Melbourne (Australia).
ANALYSES OF POWER CONSUMPTION FOR TWO SLIDING VANE TYPE COMPRESSORS
A. A. Mabanta Jul. 1989 37 p
(AD-A218366; ARL-PROP-TM-464; DODA-AR-005-643) Avail: NTIS HC A03/MF A01 CSCL 21/7

An outline is given of the theoretical analyses carried out for estimating the power requirements of two sliding vane compressor designs, adapted for high speed operation, to determine if advantages exist over a trailing vane compressor, previously used for air scavenging in an experimental two stroke piston engine. GRA

N90-20407# Aeronautical Research Labs., Melbourne (Australia).
COMPLEX DEMODULATION FOR BEARING FAULT DETECTION
I. M. Howard Oct. 1989 29 p
(AD-A218367; ARL-PROP-TM-468; DODA-AR-006-058) Avail: NTIS HC A03/MF A01 CSCL 13/9

Vibration analysis using the high frequency resonance technique has been used successfully to detect incipient failure in rolling element bearings. This memo outlines a new method of obtaining the demodulated narrow band envelope of a bearing vibration signal from the high frequency resonant response. Previous techniques have used an analogue envelope where the raw analogue signal is bandpass filtered and enveloped before digitizing. The method outlined in this document first digitizes the vibration signal, performs a complex demodulation operation, then computes the envelope followed by its spectrum. Fault repetition frequencies can be identified in the demodulated spectrum of the high frequency resonant response. GRA

N90-20408* National Aeronautics and Space Administration. Lyndon B. Johnson Space Center, Houston, TX.
GRIPPING DEVICE Patent
George F. Parma, inventor (to NASA) 22 Aug. 1989 11 p Filed 19 Jul. 1988
(NASA-Case-MSC-21365-1; US-Patent-4,858,979;
US-Patent-Appl-SN-221388; US-Patent-Class-294-106;
US-Patent-Class-294-86.4; US-Patent-Class-901-38;
US-Patent-Class-901-39) Avail: US Patent and Trademark Office CSCL 13I

This invention relates to a gripping device, and more particularly to one with a large moment carrying capability for handling long workpieces of various diameters and which can be particularly used as an end effector on a robotic arm.
Official Gazette of the U.S. Patent and Trademark Office

N90-20409* National Aeronautics and Space Administration. Langley Research Center, Hampton, VA.
TENSILE FILM CLAMPS AND MOUNTING BLOCK FOR THE RHEOVIBRON AND AUTOVIBRON VISCOELASTOMETER Patent
Diane M. Stoakley, inventor (to NASA), Anne K. St.Clair, inventor (to NASA), and Bruce D. Little, inventor (to NASA) 4 Nov. 1988 8 p Filed 4 Nov. 1988
(NASA-Case-LAR-13696-1; US-Patent-4,864,865;
US-Patent-Appl-SN-267146; US-Patent-Class-73-831;
US-Patent-Class-73-860) Avail: US Patent and Trademark Office CSCL 13I

A set of film clamps and a mounting block for use in the determination of tensile modulus and damping properties of films in a manually operated or automated Rheovibron is diagrammed.

These clamps and mounting block provide uniformity of sample gripping and alignment in the instrument. Operator dependence and data variability are greatly reduced.
Official Gazette of the U.S. Patent and Trademark Office

38 QUALITY ASSURANCE AND RELIABILITY

Includes product sampling procedures and techniques; and quality control.

N90-20410# United Kingdom Atomic Energy Authority, Harwell (England). National NDT Centre.
THE DIFFRACTION OF ULTRASOUND BY CRACKS: COMPARISON OF EXPERIMENT WITH THEORY
F. A. Ravenscroft, K. Newton, and C. B. Scruby Aug. 1989 37 p
(AERE-R-13334) Avail: NTIS HC A03/MF A01

The full potential of the ultrasonic time-of-flight diffraction technique for characterizing defects can only be realized if the amplitude and phase of the diffracted ultrasound can be reliably interpreted. Published theoretical models lay a foundation for interpretation of the diffracted ultrasound by ideal cracks, but experimental studies on simulated and real cracks have to date not confirmed all the predictions of the theory, in particular, amplitude minima and phase reversals at small diffraction angles. The use of short-pulse transducers and laser-generated ultrasound to study diffraction by machined defects and fatigue cracks is reported. Good agreement was found between experiment and theory for an open fatigue crack. However, a tight fatigue crack did not exhibit the predicted amplitude minimum at small angles, due to interactions between the crack faces. There were discrepancies between experiment and theory for artificial defects which can be explained in terms of diffraction and mode conversion at the corners of the slots used to simulate cracks. Author

N90-20411# Oxford Univ. (England). Dept. of Metallurgy and Science of Materials.
NONDESTRUCTIVE TESTING OF CERAMICS BY ACOUSTIC MICROSCOPY
C. B. Scruby, C. W. Lawrence, D. G. P. Fatkin, G. A. D. Briggs, A. Dunhill, A. E. Gee, and C.-L. Chao (Cranfield Inst. of Tech., Bedford, England) Jun. 1989 26 p Prepared in cooperation with United Kingdom Atomic Energy Authority, Harwell, England
(AERE-R-13350) Avail: NTIS HC A03/MF A01

The application of acoustic microscopy to the nondestructive testing of ceramics and ceramic composites are described. The technique can be used to detect surface-breaking defects whose depth is 5 to 30 micrometers, which is beyond the resolution limit of conventional ultrasonic testing. Examples are given of the detection of critical defects both in a test block and in a finished ball bearing component, manufactured from silicon nitride, in addition to the detection of sub-surface machining damage. The potential of the line-focus beam microscope for quantifying variations in microstructure, by making accurate measurements of ultrasonic velocity and attenuation, is demonstrated for a range of ceramics and a ceramic matrix composite. Finally, the application of acoustic microscopy to the characterization of the fiber-matrix interface in advanced composites is discussed. Author

N90-20412# General Electric Co., Largo, FL. Quartz Devices Engineering.
NINE-YEAR AGING BEHAVIOR OF THE CERAMIC FLATPACK RESONATOR
Dale E. Beetley Mar. 1990 13 p
(Contract DE-AC04-76DP-00656)
(DE90-008044; GEPP-TIS-1168) Avail: NTIS HC A03/MF A01

A multichannel, high precision aging measurement facility capable of high volume testing of resonators was developed. Features of the facility considered unique for production aging systems test include: (1) Loran-C/disciplined time-frequency (DTF) oscillator frequency standard, (2) direct current power bus design, (3) measurement and switching techniques, and (4) high volume automatic precision resonator aging. Computer-controlled data acquisition is used for unattended operation. Facility requirements included frequency measurement with sufficient precision to allow 20 year extrapolation of resonator frequency shift using 30 data points. The frequency reference is traceable to the National Institute of Standards and Technology (NIST). Long-term extrapolation required selection of a model which would most accurately reflect the major processes involved in aging. In order to verify the accuracy of model extrapolation, a group of resonators was maintained in test for more than nine years. DOE

N90-20413# Oak Ridge National Lab., TN.
RESEARCH AND DEVELOPMENT QUALITY ASSURANCE PLANNING
Paul B. Hoke 14 May 1990 6 p Presented at the 1990 American Society for Quality Control Congress, San Francisco, CA, 14 May 1990
(Contract DE-AC05-84OR-21400)
(DE90-003687; CONF-900566-1) Avail: NTIS HC A02/MF A01

Planning for quality assurance (QA) in research and development (R and D) is like stealing eggs without waking up the chickens. The QA program should be as unobtrusive as possible. Researchers require a QA program that affords them an environment capable of supporting repeatable experiments with accurate data without unduly stifling their creative abilities. Careful advance planning ensures that the intensity of control provided by quality-related systems is commensurate with the importance and scope of the activities being performed. Good scientific practices applied to small bench-scale projects may require minimal additional controls. As projects increase in size and complexity the controls imposed through planning must, by necessity, be increased. Research and development QA planning, just like any other planning, involves all affected individuals. The application of control systems is determined by factors such as customer or sponsor requirements, the importance of an item or activity to the experiment's success, and the organizational complexity of the project. Many larger experiments are highly dependent on quality-related support activities such as calibration, engineering design, and inspection provided by organizations outside the R and D group. DOE

N90-20414# Westinghouse Savannah River Co., Aiken, SC.
TRANSACTION PROCESSING IN A QUALITY CONTROL LABORATORY
John E. Aull 1990 20 p Presented at the 1990 Digital Equipment Corporation User's Society Meeting, New Orleans, LA, 7-11 May 1990
(Contract DE-AC09-89SR-18035)
(DE90-004655; WSRC-RP-89-1100; CONF-900580-1) Avail: NTIS HC A03/MF A01

Sample receiving data is received from VAX 8700 process computer via Ethernet and saved in RDB database on VAX 11/750 lab computer for transmission of results. Data entry pretests include technician qualification and instrument verification by analysis of blind standards. Raw data are transmitted by instruments that talk to ADACS 1200 systems via microprocessors to lab computer which confirms storage to instrument operator. Results are transmitted to process computer by batch job submitted by approving supervisor. Results are archived as samples are disposed. Daily reports of sample load and results are printed. Weekly reports of technician qualification are printed. Scientist and managers retrieve results, sample status, and technician qualification reports via heirarchical menu system. DOE

N90-20415# North Carolina Univ., Chapel Hill. Dept. of Operations Research.
RESEARCH IN RELIABILITY, AVAILABILITY AND MAINTAINABILITY FOR COMPLEX FAILURE SYSTEMS Final Report
G. S. Fishman, V. G. Kulkarni, and J. S. Provan Jan. 1990 34 p

(Grant AF-AFOSR-0140-84; AF Proj. 2304)
(AD-A217744; AFOSR-90-0002TR) Avail: NTIS HC A03/MF A01 CSCL 12/3

This report presents an overview of work performed on AFOSR Grant 84-0140 by G. S. Fishman, V. G. Kulkarni and J. S. Provan during the period June 1, 1984 through November 30, 1989 in the Department of Operations Research at the University of North Carolina at Chapel Hill. This grant was awarded to the three principal investigators in response to their submitted proposal to AFOSR's 1983 initiative in reliability. The work performed on this grant has focused on developing efficient methods of evaluating reliability. This topic is approached through medium of Monte Carlo experimentation, the exploitation of special probabilistic structure and special network structure. Parts 1, 2 and 3 describe the contributions of each principal investigator separately. GRA

N90-20416# Ohio State Univ., Columbus. Dept. of Statistics.
THEORY SYSTEM RELIABILITY DEMONSTRATION AND BURN-IN DESIGN Final Report, 1 Aug. 1987 - 30 Jun. 1989
Saul Blumenthal Jul. 1989 5 p
(Grant AF-AFOSR-0306-87; AF Proj. 2304)
(AD-A217775; AFOSR-90-0118TR) Avail: NTIS HC A01/MF A01 CSCL 12/3

Research accomplishments were registered in three areas. The first is lifetime estimation with truncated data. Maximum likelihood estimators and their asymptotic properties were studied. A Monte Carlo comparison of several estimators was performed when only interval data on lifetimes is available. The second area is under what conditions a burn-in was developed and tested using sequential estimation. Thirdly, distributions other than Poisson were tried, and it was found that in some cases a binomial approximation provides a more robust testing scheme for series systems with aging components. GRA

N90-20417# Cincinnati Univ., OH. Dept. of Aerospace Engineering and Engineering Mechanics.
APPROXIMATE EVALUATION OF RELIABILITY AND RELATED QUANTITIES VIA PERTURBATION TECHNIQUES Final Report, 15 Feb. 1988 - 14 Feb. 1989
Bruce K. Walker and Ramaswamy Srichander Jul. 1989 41 p
(Grant AF-AFOSR-0131-88; AF Proj. 2304)
(AD-A218340; AFOSR-90-0268TR) Avail: NTIS HC A03/MF A01 CSCL 12/3

Reliability evaluation of fault tolerant control systems (FTCS) that include sequential tests for failure detection and identification involve the transient analysis of finite-state semi-Markov chains of very large dimension. Such models for the time horizons of interest are intractable even for simple architectures. This has motivated the work summarized herein. The basis for the work is the idea of asymptotic aggregation of semi-Markov chains that include slow and fast transitions. The extension of earlier asymptotic aggregation results (primarily due to Korolyuk) to models that include decomposed classes that are non-ergodic and the subsequent application of these results to FTCS models was the subject of studies conducted under the previous grant. The research efforts reported here concentrate on the application of the results from the previous study to more general FTCS architectures. GRA

39 STRUCTURAL MECHANICS

Includes structural element design and weight analysis; fatigue; and thermal stress.

For applications see *05 Aircraft Design, Testing and Performance* and *18 Spacecraft Design, Testing and Performance.*

N90-20418 Virginia Polytechnic Inst. and State Univ., Blacksburg.
MODAL INTERACTIONS IN SHELL DYNAMICS Ph.D. Thesis
Raouf Ali Raouf 1989 168 p
Avail: Univ. Microfilms Order No. DA8921163

A numerical-perturbation approach is used to study modal interactions in the dynamic response of infinitely long circular cylindrical shells to a harmonic excitation. The excitation frequency is near the linear natural frequency of the breathing mode which is approximately twice that of a flexural mode. The method of multiple-time scales is used to derive a set of autonomous first-order nonlinear differential equations that describe the modulation of the amplitudes and phases of the interacting modes. The same approach is used to study the axisymmetric dynamic response of spherical shells to radial harmonic excitations having a frequency near one of the linear natural frequencies of a flexural mode and in the presence of two-to-one internal resonance between the excited mode and a lower flexural mode. The two sets of modulation equations derived above are scaled to the same form and their fixed points, limit cycles, and chaotic solutions are studied as the amplitude or the frequency of excitation varies. The force-response curve exhibits the jump and saturation phenomena. The frequency-response curve exhibits Hopf bifurcations. Between the Hopf-bifurcation frequencies, fixed points are unstable and limit cycles exist. Limit cycles become chaotic either through an infinite cascade of period-doubling bifurcations or through cyclic-fold bifurcations. Dissert. Abstr.

N90-20419 Rensselaer Polytechnic Inst., Troy, NY.
PERTURBATION SOLUTIONS IN D* FOR BUCKLING, VIBRATION, AND STATIC LOADING OF SPECIALLY ORTHOTROPIC PLATES Ph.D. Thesis
David Bomkyu O 1989 178 p
Avail: Univ. Microfilms Order No. DA8926588

It is proposed to find perturbation solutions in Generalized Rigidity Ratio, D*, for rectangular plates that are specially orthotropic. Solutions include static deflections under uniform lateral load, buckling loads under uniaxial compression and natural frequencies. Using the affine transformation, partial differential equations and boundary conditions of the specially orthotropic plate can be put in a neater form. It also reduces the number of parameters (elastic constants) to two. These affinely transformed parameters are the Generalized Rigidity Ratio, D*, and the Generalized Poisson's Ratio. The resulting equation, containing parameter D*, will be solved by the perturbation method for a variety of boundary conditions. The perturbation technique presented herein stems from the need for new, unified and more rapid methods for problems in the theory of orthotropic plates. In order to get more coherent insight into the orthotropic behavior and to eliminate the computational difficulties encountered in the use of other analytical solutions, the present method reduces the analysis of an orthotropic structure to the solution of a corresponding basic plate equation. Since the solutions for the basic plate equation are exact, the perturbation process can be accomplished with a minimum of difficulty. Dissert. Abstr.

N90-20420 Rensselaer Polytechnic Inst., Troy, NY.
POSTBUCKLING BEHAVIOR OF LAMINATED SPECIALLY ORTHOTROPIC PLATES BY AFFINE TRANSFORMATION Ph.D. Thesis
Kyung-Soo Shin 1989 206 p
Avail: Univ. Microfilms Order No. DA8926595

The postbuckling behavior of rectangular orthotropic plates is addressed. The analysis is based on the nonlinear large deflection equations of von Karman, written for specially orthotropic plates which have been transformed into the affine space, and the solution is obtained using the perturbation method. The combinations of three standard boundary conditions are considered. The plates are simply supported on two loaded edges and the two unloaded side edges are either simply supported-simply supported, or clamped-clamped, or simply supported-clamped, or simply supported-free, or clamped-free. The application of an affine transformation produces generic material constants, D* and epsilon, which concisely describe whole classes of plates for buckling and postbuckling problems. This form of solution, being generic, allows one to abstract a physical intuition about the postbuckling process for any material or any cross ply material combination. Furthermore, it is found that the postbuckling behavior is primarily described by only one additional parameter beyond

the required for buckling, the generalized rigidity ratio, is only a weak parameter if the boundary condition doesn't have a free edge. This means that the free edge boundary condition is affected by the Generalized Poisson's Ratio. Also, regardless of what analysis techniques are used, the results can be cast in terms of material parameters, D* and epsilon. Thus these problems never need be recalculated, no matter what new materials become available in the future. Dissert. Abstr.

N90-20421*# Lockheed Missiles and Space Co., Palo Alto, CA.
COMPARISON OF TWO MATRIX DATA STRUCTURES FOR ADVANCED CSM TESTBED APPLICATIONS
M. E. Regelbrugge, F. A. Brogan, B. Nour-Omid, C. C. Rankin, and M. A. Wright Dec. 1989 50 p
(Contract NAS1-18444)
(NASA-CR-181951; NAS 1.26:181951) Avail: NTIS HC A03/MF A01 CSCL 20K

The first section describes data storage schemes presently used by the Computational Structural Mechanics (CSM) testbed sparse matrix facilities and similar skyline (profile) matrix facilities. The second section contains a discussion of certain features required for the implementation of particular advanced CSM algorithms, and how these features might be incorporated into the data storage schemes described previously. The third section presents recommendations, based on the discussions of the prior sections, for directing future CSM testbed development to provide necessary matrix facilities for advanced algorithm implementation and use. The objective is to lend insight into the matrix structures discussed and to help explain the process of evaluating alternative matrix data structures and utilities for subsequent use in the CSM testbed. Author

N90-20422*# Analytical Services and Materials, Inc., Hampton, VA.
A 4-NODE ASSUMED-STRESS HYBRID SHELL ELEMENT WITH ROTATIONAL DEGREES OF FREEDOM
Mohammad A. Aminpour Washington NASA Apr. 1990 30 p
(Contract NAS1-18599)
(NASA-CR-4279; NAS 1.26:4279) Avail: NTIS HC A03/MF A01 CSCL 20K

An assumed-stress hybrid/mixed 4-node quadrilateral shell element is introduced that alleviates most of the deficiencies associated with such elements. The formulation of the element is based on the assumed-stress hybrid/mixed method using the Hellinger-Reissner variational principle. The membrane part of the element has 12 degrees of freedom including rotational or drilling degrees of freedom at the nodes. The bending part of the element also has 12 degrees of freedom. The bending part of the element uses the Reissner-Mindlin plate theory which takes into account the transverse shear contributions. The element formulation is derived from an 8-node isoparametric element. This process is accomplished by assuming quadratic variations for both in-plane and out-of-plane displacement fields and linear variations for both in-plane and out-of-plane rotation fields along the edges of the element. In addition, the degrees of freedom at midside nodes are approximated in terms of the degrees of freedom at corner nodes. During this process the rotational degrees of freedom at the corner nodes enter into the formulation of the element. The stress field are expressed in the element natural-coordinate system such that the element remains invariant with respect to node numbering. Author

N90-20423# United Kingdom Atomic Energy Authority, Harwell (England). Materials Development Div.
RESIDUAL STRESSES: A REVIEW OF THEIR MEASUREMENT AND INTERPRETATION USING X RAY DIFFRACTION
A. M. Jones May 1989 118 p
(AERE-R-13005) Avail: NTIS HC A03/MF A01

The importance of residual stresses is illustrated by the fact that they are present to some degree in practically every manufactured component and assembled structure. Thus, during service the stress distribution will be a combination of the applied and residual stresses, and the residual stress will affect the performance, or lifetime to failure of the workpiece under investigation. A review of the different techniques available to measure residual stresses is presented including mechanical (semi-destructive) and the variety of non-destructive methods (x ray and neutron diffraction, ultrasonic velocity, Barkhausen noise analysis, and optical techniques). The methods of stress generation, modification, and elimination are discussed. The x ray diffraction (XRD) method of residual stress measurement is considered in greater detail with emphasis on problems originating from the x ray optics, equipment, materials, data reduction, analysis, and interpretation of results. Finally, some of the major advances in the XRD technique during the last five years or so are described and evaluated. Some future opportunities are outlined, focusing on areas such as energy-dispersive (instead of angle-dispersive) analysis, use of high intensity beams (e.g., from a synchrotron source), advances in both equipment and analysis, and applications to specific materials of interest. Author

N90-20424# United Kingdom Atomic Energy Authority, Harwell (England). Materials Development Div.
THE STRESS-DRIVEN REDISTRIBUTION OF POINT DEFECTS IN THE VICINITY OF CRACK-LIKE SINGULARITIES
H. Rauh and R. Bullough Dec. 1988 55 p
(AERE-R-12898) Avail: NTIS HC A04/MF A01

The relevant energy of the elastic interaction is presented and used to estimate the kinetics of redistribution of point defects in the stress field of an isolated crack under mode 2 load and a slip band impinging against a grain boundary sink. Analyses show that the point defects should migrate only to the tip of the crack, whereas they should enter both into the slip band tip and along the adjacent boundary interface. Explicit results are obtained for the concentrations, the number, and the flux distribution as well as the total numbers segregated in the transient depletion and the steady-state irradiation situation and serve to reinforce previous conclusions regarding the importance of such stress-driven processes in the fracture of materials. Author

N90-20425# United Kingdom Atomic Energy Authority, Harwell (England). Theoretical Physics Div.
LIMITATIONS AND APPLICATIONS OF FRACTURE ASSESSMENT WITH R6
J. A. G. Temple Mar. 1988 33 p
(AERE-R-13012) Avail: NTIS HC A03/MF A01

A description and critical review of the Central Electricity Board's (Great Britain) R6 revision 3 fracture assessment procedure to determine the defect tolerances of structures operating at low temperatures is presented. The procedure is designed to assess the structural integrity of both brittle and ductile materials, using semi-empirical rules to determine whether or not the defects are to be assessed as acceptable for the loads applied. The basis of the procedure is to plot an assessment point on a failure assessment diagram having two axes: the plotted point on the vertical axis is a measure of the propensity to failure by rapid brittle fracture; the plotted point on the second axis is a measure of the propensity to failure by plastic collapse. The following areas within the R6 procedure are examined: the basis for the general and specific options of the failure assessment diagrams; the basis for J-controlled crack growth limit and the validity of assessing growth beyond this limit; the treatment of residual and thermal stresses; the procedure for dealing with fracture of a multiaxially loaded crack; the kind of structures and materials to which the procedure may be applied; and the determination of whether upper or lower bound properties produce the most conservative assessments in complex cases. Areas for further research or validation are highlighted. Author

N90-20426*# National Aeronautics and Space Administration. Langley Research Center, Hampton, VA.
EVALUATION OF AN ADAPTIVE UNSTRUCTURED REMESHING TECHNIQUE FOR INTEGRATED FLUID-THERMAL-STRUCTURAL ANALYSIS
Pramote Dechaumphai Feb. 1990 13 p Presented at the

AIAA 28th Aerospace Sciences Meeting, Reno, NV, 8-11 Jan. 1990 Previously announced in IAA as A90-19911
(NASA-TM-102611; NAS 1.15:102611) Avail: NTIS HC A03/MF A01 CSCL 20K

An adaptive unstructured remeshing technique is evaluated for integrated fluid-thermal-structural analysis. The technique is combined with the finite element method to solve: (1) the Navier-Stokes equations for high-speed compressible flow; (2) the energy equation for the structural-thermal response; and (3) the quasi-static equilibrium equations for the structural response. The remeshing technique and the analysis solution procedure are described. The effectiveness of the approach is evaluated with two application studies. The flow analysis of Mach 8 shock-shock interference on a three-inch-diameter cylinder is used as the first application study to demonstrate the capability of the remeshing technique and to examine proper remeshing indicators for the inviscid and boundary layer regions. The applicability of the approach for the thermal and structural analyses of the structure is evaluated in the second application study of a 0.25-inch-diameter convectively cooled leading edge subjected to intense aerodynamic heating. Issues associated with remeshing indicators for thermal stress problems are identified. Author

N90-20427*# National Aeronautics and Space Administration. Langley Research Center, Hampton, VA.
THROUGH-THE-THICKNESS FATIGUE CRACK CLOSURE BEHAVIOR IN AN ALUMINUM ALLOY
D. S. Dawicke, J. C. Newman, Jr., and A. F. Grandt, Jr. (Purdue Univ., West Lafayette, IN.) Jan. 1990 8 p
(NASA-TM-102590; NAS 1.15:102590) Avail: NTIS HC A02/MF A01 CSCL 20K

The variation in fatigue crack closure behavior across the thickness of aluminum alloy specimens was investigated. The specimen geometries examined were the middle crack tension M(T) and compact tension C(T). The fatigue crack closure behavior was determined using remote displacement and strain gages, near tip strain gages, and fatigue striations. A hybrid experimental/numerical method was also used to infer the crack opening loads. The results indicate a variation in crack opening load, of 0.2 in the specimen interior to 0.4 to 0.5 at the surface. Author

N90-20428*# National Aeronautics and Space Administration. Lewis Research Center, Cleveland, OH.
COMPUTER SIMULATION OF THE MATHEMATICAL MODELING INVOLVED IN CONSTITUTIVE EQUATION DEVELOPMENT: VIA SYMBOLIC COMPUTATIONS
S. M. Arnold, H. Q. Tan, and X. Dong (Akron Univ., OH.) 1989 13 p Presented at the 7th International Conference on Mathematical and Computer Modeling, Chicago, IL, 2-5 Aug. 1989; cosponsored by IAMCM and IMACS
(NASA-TM-102532; E-5276; NAS 1.15:102532) Avail: NTIS HC A03/MF A01 CSCL 20K

Development of new material models for describing the high temperature constitutive behavior of real materials represents an important area of research in engineering disciplines. Derivation of mathematical expressions (constitutive equations) which describe this high temperature material behavior can be quite time consuming, involved and error prone; thus intelligent application of symbolic systems to facilitate this tedious process can be of significant benefit. A computerized procedure (SDICE) capable of efficiently deriving potential based constitutive models, in analytical form is presented. This package, running under MACSYMA, has the following features: partial differentiation, tensor computations, automatic grouping and labeling of common factors, expression substitution and simplification, back substitution of invariant and tensorial relations and a relational data base. Also limited aspects of invariant theory were incorporated into SDICE due to the utilization of potentials as a starting point and the desire for these potentials to be frame invariant (objective). Finally not only calculation of flow and/or evolutionary laws were accomplished but also the determination of history independent nonphysical coefficients in terms of physically measurable parameters, e.g., Young's modulus, was achieved. The uniqueness of SDICE resides in its ability to manipulate expressions in a general yet predefined order and simplify expressions so as to limit expression growth. Results are displayed when applicable utilizing index notation. Author

N90-20429# Technische Univ., Brunswick (Germany, F.R.). Fakultaet fuer Maschinenbau und Elektrotechnik.
EXPERIMENTS ON BUCKLING AND CRITICAL BUCKLING. BEHAVIOR OF CARBON FIBER REINFORCED PLASTIC SHELLS SUBMITTED TO TENSILE STRESSES Ph.D. Thesis [UNTERSUCHUNGEN ZUM BEUL- UND NACHBEULVERHALTEN SCHUBBEANSPRUCHTER TEILSCHALEN AUS KOHLENSTOFFASERVERSTAERKTEM KUNSTSTOFF]
Klaus Wolf 1989 161 p In GERMAN
(ETN-90-95382) Avail: NTIS HC A08/MF A01

A digital calculation process is developed, which is based on a combined finite element method and realizes linear static stability analyses and the search for geometrical nonlinear stress behavior of shells in the buckling area. By use of special algorithms, puncture and ramification problems are addressed. The resolution of the linear eigen value problem of the classical stability theory shows a strong dependence on the curvature for cylindrical shells. There are only two types of deformation: a symmetric in relation to the shell middle point and an antisymmetric buckling form. The longitudinal axes of local bucklings are directed to the tensile diagonal of the buckling. ESA

N90-20430*# Joint Inst. for Advancement of Flight Sciences, Hampton, VA.
ACTIVE CONTROL OF THE FORCED AND TRANSIENT RESPONSE OF A FINITE BEAM M.S. Thesis
John T. Post Jan. 1990 92 p
(Contract NCC1-14)
(NASA-CR-181957; NAS 1.26:181957) Avail: NTIS HC A05/MF A01 CSCL 20K

Structural vibrations from a point force are modelled on a finite beam. This research explores the theoretical limit on controlling beam vibrations utilizing another point source as an active controller. Three different types of excitation are considered, harmonic, random, and transient. For harmonic excitation, control over the entire beam length is possible only when the excitation frequency is near a resonant frequency of the beam. Control over a subregion may be obtained even between resonant frequencies at the cost of increasing the vibration outside of the control region. For random excitation, integrating the expected value of the displacement squared over the required interval, is shown to yield the identical cost function as obtained by integrating the cost function for harmonic excitation over all excitation frequencies. As a result, it is always possible to reduce the cost function for random excitation whether controlling the entire beam or just a subregion, without ever increasing the vibration outside the region in which control is desired. The last type of excitation considered is a single, transient pulse. The form of the controller is specified as either one or two delayed pulses, thus constraining the controller to be casual. The best possible control is examined while varying the region of control and the controller location. It is found that control is always possible using either one or two control pulses. Author

N90-20431*# National Aeronautics and Space Administration. Lewis Research Center, Cleveland, OH.
MODEL DEVELOPMENT IN VISCOPLASTIC RATCHETTING
Alan D. Freed and Kevin P. Walker (Engineering Science Software, Inc., Smithfield, RI.) Apr. 1990 32 p
(NASA-TM-102509; E-5311; NAS 1.15:102509) Avail: NTIS HC A03/MF A01 CSCL 20K

Space Station Freedom's solar dynamic power modules, like all power plants, contain components that are subjected to conditions which favor thermally driven ratchetting. Existing viscoplastic models tend to overpredict ratchetting behavior, because their back stress (the kinematic variable) seems to stick

more than it should during unloading. For this reason, a study was undertaken to compare a variety of possible modifications to the evolution equation for back stress. All models considered herein have a hardening vs. dynamic-recovery format. To remove the stickiness of the back stress, a linear dependence on stress rate is introduced into the evolution equation for back stress in a variety of ways. Several favorable models were screened out of the field of candidates by qualitatively determining their relative ability to fit experimentally observed behavior through six numerical experiments. A final selection must be made by quantitatively correlating the proposed models with experimental data, and then seeing which candidate does the best job of predicting observed ratchetting behavior. This is a subject of future work. Author

N90-20432*# National Aeronautics and Space Administration. Lewis Research Center, Cleveland, OH.
COMPUTATIONAL SIMULATION OF DAMPING IN COMPOSITE STRUCTURES
D. A. Saravanos and C. C. Chamis Jul. 1989 26 p Presented at the 2nd National Congress in Mechanics, Athens, Greece, 29 Jun. - 1 Jul. 1989
(NASA-TM-102567; E-5143; NAS 1.15:102567) Avail: NTIS HC A03/MF A01 CSCL 20K

A computational methodology is developed for the prediction of passive damping in composite structures. The method involves multiple levels of damping modeling by integrating micromechanics, laminate, and structural damping theories. The effects of temperature and moisture on structural damping are included. The simulation of damping in the structural level is accomplished with finite-element discretization. Applications are performed on graphite/epoxy composite beams, plates, and shells to illustrate the methodology. Additional parametric studies demonstrate the variation of structural modal damping with respect to ply angles, fiber volume ratio, and temperature. Author

N90-20433# Massachusetts Inst. of Tech., Cambridge. Dept. of Aeronautics and Astronautics.
SENSOR AND ACTUATOR SELECTION FOR FAULT-TOLERANT CONTROL OF FLEXIBLE STRUCTURES Ph.D. Thesis
William Neil McCasland Feb. 1989 194 p Sponsored by AFIT Prepared in cooperation with Draper (Charles Stark) Lab., Inc., Cambridge, MA
(AD-A217384; AFIT/CI/CIA-88-227; CSDL-T-1010) Avail: NTIS HC A09/MF A01 CSCL 20/11

Control system design for structural dynamics requires instrumenting the structure with sensors and actuators, the effectiveness of which depends strongly on spatial position. For the long duration missions typical of spacecraft, the possibility of failures must be considered and coverage provided for with redundancy and a reconfiguration strategy. To support these, it is mandatory that sensors and actuators be located such that sufficient controllability and observability of the flexible dynamics is assured in the presence of failures. A systematic procedure is developed for finding such configurations of sensors and actuators for large scale systems. Norms on the controllability and observability open loop Gramian are taken as an index for optimization. The control objectives are reflected by truncating the time interval over which the Gramian is defined, and by scaling the state basis with respect to a normalizing, or reference, signal path. GRA

N90-20434# Air Force Inst. of Tech., Wright-Patterson AFB, OH.
ROTORDYNAMIC ANALYSIS WITH SHELL ELEMENTS FOR THE TRANSFER MATRIX METHOD M.S. Thesis
Edward A. LAntigua Aug. 1989 179 p
(AD-A217455; AFIT/CI/CIA-89-111) Avail: NTIS HC A09/MF A01 CSCL 20/11

Shell finite elements were used to model conical sections with a range in parameters; axial length, radius, wall thickness, cone angle and Young's modulus. The parameters were chosen to cover the complete range of rotors, casings, and housings used throughout the turbomachinery industry. Flexibility coefficients were generated for these structures. The need for these flexibilities to be used in the current day rotor dynamics transfer matrix computer programs is demonstrated. The flexibility coefficients are presented in nondimensional tables and plots for ease in use by turbomachinery design engineers and analysts in industry. GRA

N90-20435# Sandia National Labs., Albuquerque, NM.
PARAMETER-SCHEDULED TRAJECTORY PLANNING FOR SUPPRESSION OF COUPLED HORIZONTAL AND VERTICAL VIBRATIONS IN A FLEXIBLE ROD
Ben J. Petterson, Rush D. Robinett, and Jill C. Werner 1989 11 p Presented at the IEEE Robotics and Automation Conference, Cincinnati, OH, 13-18 May 1990
(Contract DE-AC04-76DP-00789)
(DE90-002313; SAND-89-2522C; CONF-900559-2) Avail: NTIS HC A03/MF A01

Angularly accelerating a cantilevered rod which sags under gravity couples the out-of-plane dynamics of the flexible rod and causes oscillation in both the horizontal and vertical planes. A parameter-scheduled trajectory planner has been analytically developed and experimentally implemented on a commercial robot to suppress the first mode of these vibrations during a horizontal angular move. A load was attached to the tip of the rod and the resulting static, out-of-plane, hub torque was measured with a force-torque sensor. This torque was used to predict the period of the horizontal first mode of vibration of the payload (rod and attached load) from a nonlinear function in order to calculate (schedule) the appropriate control parameters for the angular move. This system has been implemented on a Cincinnati Milacron T3-786 robot, and vibration suppressed trajectories (which reduce the coupled residual vibrations by over 90 percent) have been performed by the robot for various payloads. DOE

N90-20436# Los Alamos National Lab., NM.
FINITE ELEMENT MODELS TO PREDICT THE STRUCTURAL RESPONSE OF 120-MM SABOT/RODS DURING LAUNCH
D. A. Rabern and K. A. Bannister (Ballistic Research Labs., Aberdeen Proving Ground, MD.) 1990 22 p Presented at the US Army Symposium on Gun Dynamics, Tamiment, PA, 14-17 May 1990 Sponsored in part by Dept. of the Army and BRL
(Contract W-7405-eng-36)
(DE90-007497; LA-UR-90-650; CONF-9005118-1) Avail: NTIS HC A03/MF A01

Numerical modeling techniques in two- and three-dimensions were used to predict the structural and mechanical behavior of sabot/rod systems while inbore and just after muzzle exit. Three-dimensional transient numerical simulations were used to predict the rod deformations and states of stress and strain caused by axial and lateral accelerations during launch. The numerical models include the launch tube, recoil motion, and sabot/rod system modeled as it transits the launch tube and exits. The simulated rod leaves the muzzle of the gun, and exit parameters, including transverse displacement, transverse velocity, pitch, and pitch rate are extracted from the analysis results. Results from the inbore numerical simulations were compared with previous full-scale experiments. The results of the comparisons indicated a predictive capability to model inbore three-dimensional phenomena. Two-dimensional analyses were used to model details of the structural behavior caused by the axial load environment. Methodology and results are presented for several launch environments. DOE

N90-20437# Lawrence Livermore National Lab., CA.
COMPUTER SIMULATIONS AND EXPERIMENTS TO STUDY THE FRACTURE OF RODS BY FLYING PLATES
John E. Reaugh and Mark L. Wilkins Feb. 1990 8 p Presented at the 1990 Conference on the Application of 3-D Hydrocodes To Armor/Anti-Armor Problems, Aberdeen Proving Ground, MD, 7-11 May 1990
(Contract W-7405-eng-48)
(DE90-008308; UCRL-102995; CONF-9005122-1) Avail: NTIS HC A02/MF A01

HEMP3D was used to study the interaction of flying plates with a tungsten-alloy rod. HEMP3D is a three-dimensional elastic-plastic-hydrodynamic Lagrangian finite-difference computer simulation program with sliding interfaces. A fracture model was implemented that treats both the initiation and growth of fractures. This model does not require the prespecification of fracture surfaces. Comparison of the results of computer simulations with a limited number of experiments indicated that the computer simulations were in good agreement with experiment as to the number and size of the broken pieces. A number of computer simulations were subsequently performed varying the mass and velocity of the flying plates. The results of these simulations at a fixed time after impact were compared to obtain the relative effectiveness of a given flying plate configuration. A configuration that produces many fragments and rotates them all out of alignment is given high ranking. It is intuitively likely that bigger and faster plates would rank higher than smaller, slower ones. In the experiments, the plates are accelerated by explosive. A constraint was imposed on the flying plates that corresponds to a fixed amount of explosive, so the more massive plates move more slowly. DOE

N90-20438*# National Aeronautics and Space Administration. Lewis Research Center, Cleveland, OH.
COMGEN: A COMPUTER PROGRAM FOR GENERATING FINITE ELEMENT MODELS OF COMPOSITE MATERIALS AT THE MICRO LEVEL
Matthew E. Melis Apr. 1990 24 p
(NASA-TM-102556; E-5372; NAS 1.15:102556) Avail: NTIS HC A03/MF A01 CSCL 20K

COMGEN (Composite Model Generator) is an interactive FORTRAN program which can be used to create a wide variety of finite element models of continuous fiber composite materials at the micro level. It quickly generates batch or session files to be submitted to the finite element pre- and postprocessor PATRAN based on a few simple user inputs such as fiber diameter and percent fiber volume fraction of the composite to be analyzed. In addition, various mesh densities, boundary conditions, and loads can be assigned easily to the models within COMGEN. PATRAN uses a session file to generate finite element models and their associated loads which can then be translated to virtually any finite element analysis code such as NASTRAN or MARC. Author

N90-20439*# Sikorsky Aircraft, Stratford, CT.
PLAN, FORMULATE, AND DISCUSS A NASTRAN FINITE ELEMENT MODEL OF THE UH-60A HELICOPTER AIRFRAME Final Report
P. Dinyovszky and W. J. Twomey Feb. 1990 248 p
(Contract NAS1-17499)
(NASA-CR-181975; NAS 1.26:181975) Avail: NTIS HC A11/MF A02 CSCL 20K

Under a rotorcraft structural dynamics program sponsored by the NASA Langley Research Center, Sikorsky Aircraft, together with the other major helicopter airframe manufacturers, is engaged in a study to improve the use of finite element analysis to predict the dynamic behavior of helicopter airframes. This program, which was designated DAMVIBS (Design Analysis Methods for VIBrationS), includes activities in the areas of: planning, creating, and documenting finite element models of helicopter airframes; the performance of ground vibration tests; and the correlation of test and analysis. The work performed at Sikorsky Aircraft for planning, creating, and documenting a finite element model of the UH-60A BLACK HAWK helicopter airframe is summarized. A complete description of the components of the helicopter which are to be represented in the model is presented and includes: the structural arrangement, the identification of primary and secondary structure, the components of the drive and power trains, and the attachment of large weight items to the structure. Also presented are the techniques which were used to formulate the structural finite element model for static analysis, for forming the mass and vibration models for dynamic analysis, and the procedures which were used to check out and verify the integrity of the model. Initial predictions for the vibration modes for the helicopter are included. Author

N90-20440# Lawrence Livermore National Lab., CA.
TIME-DEPENDENT FAILURE OF SILVER INTERLAYER WELDS Ph.D. Thesis
Robert S. Rosen Feb. 1990 204 p
(Contract W-7405-eng-48)
(DE90-008015; UCRL-53945) Avail: NTIS HC A10/MF A02

Silver interlayer diffusion welds exhibit very high tensile strengths, despite the soft interlayer, because of the constraint provided by the stronger base metals. However, despite the high tensile strength, diffusion-welded-silver joints undergo time-dependent failure, or creep rupture at relatively low tensile stresses at ambient temperature, apparently by a ductile microvoid-coalescence mechanism at the coated and welded interfaces. Two classes of time-dependent tensile failure were investigated. In the first case, the applied stress does not produce any plastic deformation in the base metal, and rupture appears to be controlled by time-dependent plasticity within the silver interlayer as a result of the effective stress in the interlayer. The plasticity causes cavity nucleation and, eventually, coalescence and rupture. In the second case, time-dependent plasticity is observed in the base metals, and concomitant shear occurs within the soft silver interlayer under a high triaxial stress state. Here, the time-dependent plasticity of the base metal accelerates rupture. These models were substantiated by analyses of the stress and temperature dependence of the rupture times, finite-element analysis of the stress state within the interlayer, and microscopy of the fracture surfaces and interfaces loaded to various fractions of the expected rupture times. The procedures for preparing silver interlayers by planar-magnetron sputtering were developed in this research. This process was preferred over other interlayer fabrication methods, such as brazing, electrodeposition, and other physical vapor deposition processes, because of the more reproducible results obtained using planar-magnetron sputtering. The findings of this research, however, are applicable to joints in which the interlayers are prepared by these and other processes. DOE

N90-20441# Houston Univ., TX. Dept. of Mechanical Engineering.
STRESS FIELD NEAR CRACK TIP: AN EXPERIMENTAL EVALUATION OF THE THREE DIMENSIONAL VARIATION Final Technical Report, 1 May 1987 - 31 Aug. 1989
K. Ravi-Chandar 30 Nov. 1989 35 p
(Grant AF-AFOSR-0183-87; AF Proj. 2302)
(AD-A217878; AFOSR-90-0088TR) Avail: NTIS HC A03/MF A01 CSCL 20/6

A new special purpose laboratory equipment called the Scattered Light Polariscope was designed and constructed. The Polariscope system consists of a device for loading the specimen, optical alignment devices for precise positioning of the specimen with respect to the incident light and an imaging system with a video camera, digitizing frame grabber and image processing software. The systems were all assembled and tested for proper operation. Certain limitations of the current photoelastic equations were performed. Calibration experiments were performed to determine the reliability of the technique as well as the data interpretation procedures. Results were obtained on the nature of the stress variation near the tip of a rounded notch and a crack. Significant differences were demonstrated between the 2-D and 3-D stress fields. GRA

42 GEOSCIENCES (GENERAL)

No abstracts in this category.

43 EARTH RESOURCES AND REMOTE SENSING

Includes remote sensing of earth resources by aircraft and spacecraft; photogrammetry; and aerial photography.

For instrumentation see *35 Instrumentation and Photography.*

N90-20442# Instituto de Pesquisas Espaciais, Sao Jose dos Campos (Brazil).

EVALUATION OF TM/LANDSAT AND HRV/SPOT DATA IN THE IDENTIFICATION OF REFORESTED AREAS IN THE MOGI-GUACU (SP) REGION [AVALIACAO DE DADOS TM/LANDSAT E HRV/SPOT NA IDENTIFICACAO DE AREAS REFLORESTADAS NA REGIAO DE MOGI-GUACU-SP]

Pedro HernandezFilho, David Chung Liang Lee, Sergio Alberto deOliveiraAlmeida, and Facundo Salomon RecaldeRamos (Universidad Nacional de Asuncion, Paraguay) Aug. 1989 8 p In PORTUGUESE; ENGLISH summary Presented at the 5th Brazilian Symposium on Remote Sensing, Natal, Brazil, 11-15 Oct. 1988

(INPE-4874-PRE/1485) Avail: NTIS HC A02/MF A01

The objective is to evaluate the TM/LANDSAT and HRV/SPOT data. This study area, Mogi-Guacu, Sao Paulo State, is located at 44 deg 00 to 47 deg 15 min W and 22 deg 05 min to 22 deg 15 min S. This area includes pine and eucalyptus plantions, with different ages and density canopy. Based on visual and digital analysis of TM/LANDSAT and HRV/SPOT data, the Pinus-1, Pinus-2 and Euca classes were defined. The interpretation and mapping accuracy of the classes were estimated. The combination bands were selected by JM distance algorithm. Author

N90-20443# Instituto de Pesquisas Espaciais, Sao Jose dos Campos (Brazil).

RELATIONSHIP OF RADIOMETRIC FIELD MEASUREMENTS OF WHEAT IN THE ASSIS-SAFRA REGION, 1988 [RELATORIO DA CAMPANHA DE MEDIDAS RADIOMETRICAS DO TRIGO NA REGIAO DE ASSIS-SAFRA, 1988]

Bernardo F. T. Rudorff, Getulio T. Batista, Moacir GodayJunior, Carlos A. Steffen, Lelio RibeirodeSa, Antonio F. P. Oviedo, Eduardo SdeFreitas, Cesar Luiz Bertolucci, Celia R. Zimback, and Eduardo PissiliateJunior et al Aug. 1989 85 p In PORTUGUESE; ENGLISH summary Presented at the Meeting with the Banco de Brasil and financed through Fundacao Banco de Brasil

(INPE-4949-RPE/598) Avail: NTIS HC A05/MF A01

The activities concerning the obtaining of radiometric data throughout the growing cycle of three varieties of wheat in the 1988 crop year, in the region of Assis, SP are described. A preliminary analysis is presented for the relationship between the spectral data and agronomic variables. The radiometric measurements were obtained with a spectroradiometer which measures the reflected energy from the crop in the visible and near infrared portion of the electromagnetic spectrum. The data were collected over 30 sampled plots distributed in commercially planted fields of four farms. The radiometric data were then transformed into vegetation indices which are expected to represent crop growing conditions and development. These indices were related to agronomic variables (grain yield, green phytomass, dry phytomass, canopy height) obtained in ten measurement campaigns carried out weekly beginning at initial stages of growing (30 days after planting approximately) until harvesting. It was observed that the vegetation index obtained at booting to begin of flowering stages was quite well related to the final grain yield and correlation coefficients of 0.82 to 0.93 were obtained. Results obtained clearly indicated that the reflected energy at certain stages of the crop development and at certain wavelength bands are well related to the final grain yield. Therefore, spectral data, transformed into vegetation indices have great potential to be used in yield predicting models. Author

N90-20444# Instituto de Pesquisas Espaciais, Sao Jose dos Campos (Brazil).

LANDSAT-5 DATA IN THE STUDY OF WHEAT AND BEAN CROPS Ph.D. Thesis - Sao Paulo Univ. [DADOS TM LANDSAT-5 NO ESTUDO DAS CULTURAS DE TRIGO E FEIJAO]

Jose Carlos NevesEpiphanio Dec. 1988 163 p In PORTUGUESE; ENGLISH summary

(INPE-4746-RPE/580) Avail: NTIS HC A08/MF A01

The objective was to study wheat and bean spectral behavior during their vital cycle using digitalized TM/LANDSAT-5 data recorded on computer compatible tapes (CCT). Samples of digital numbers were extracted from CCT previously corrected for atmospheric effects, and these values were graphically and quantitatively analyzed. The graphic analysis allows the visualization of crops development and their spectral alterations along time and TM bands. The influence of each crop typic parameter (row spacing, stand density, soil cover, foliar architecture) on its spectral behavior was discussed. To quantitatively evaluate the potentiality of each TM band to differentiate wheat areas from beam areas, an analysis of variance was performed followed by Student-Newman-Keuls test to test the null hypothesis of equality among the areas. After this, an index, called efficiency of correct acceptation was created that allows the evaluation of each band potential to maximize the correct Ho acceptation and to minimize the incorrect Ho acceptation. These analysis showed the effect of general crop developing stage on the band potentiality for distinguishing areas, and allowed a fundamental discussion about chlorophyll content and its effect on spectral response of each crop. This analysis of fundamental processes can be useful as a support to digital processing of color composites to be used in routine photointerpretation tasks. Various ratio indices were tested to evaluate their potential to distinguish wheat from bean. Another analysis was performed to test the correlation between remote sensing parameters (single bands and ratio indices) and crop parameters (leaf area index and percent soil cover). Author

N90-20445# Instituto de Pesquisas Espaciais, Sao Jose dos Campos (Brazil).

UTILIZATION OF LANDSAT-5 AND NOAA-9 SATELLITE IMAGERY IN THE IDENTIFICATION OF PHYSICAL-CHEMICAL PARAMETERS OF THE WATER IN THE GUANABARA BAY M.S. Thesis [UTILIZACAO DE IMAGENS DOS SATELITES LANDSAT-5 E NOAA-9 NA IDENTIFICACAO DE PARAMETROS FISICO-QUIMICOS DA AGUA NA BAIA DE GUANABARA]

Claudia ZuccariFernandesBraga Dec. 1988 116 p In PORTUGUESE; ENGLISH summary

(INPE-4761-TDL/349) Avail: NTIS HC A06/MF A01

The purpose was the development of an orbital remote sensing method to monitor water in coastal areas. Physical, chemical and biological parameters were measured in the waters of the Guanabara Bay, RJ, Brazil, and its vicinity, simultaneously with the imaging of the region by the satellites LANDSAT-5 and NOAA-9. Surface water temperature and Secchi depth were measured during the sampling. Chlorophyll-a, total suspended solids (TSS) and their iron and manganese contents, and salinity were subsequently measured in laboratories. The TM/LANDSAT images were digitally processed with distinct algorithms and were statistically correlated with the water parameters. The results showed a strong effect of high and low tides in the correlations. During the high tide marine characteristics prevailed in the Bay, while low tides showed continental ones; both cases were well correlated with the satellite products. TM/LANDSAT digital products showed to be adequate tools to monitor temperature, Secchi depth, TSS, and iron and manganese in the TSS. Author

N90-20446# Instituto de Pesquisas Espaciais, Sao Jose dos Campos (Brazil).

SYNTHESIS AND ANALYSIS OF 25 YEARS (1961-1986) OF INPE/SRE ACTIVITIES RELATED TO THE VEGETATION/FOREST AREA [SINTESE E ANALISE DOS 25 ANOS (1961-1986) DE ATIVIDADES DO INPE/SRE VOLTADAS PARA A AREA DE VEGETACAO/FLORESTA]

Vitor CelsodeCarvalho Oct. 1989 85 p In PORTUGUESE; ENGLISH summary
(INPE-4969-RPE/604) Avail: NTIS HC A05/MF A01

Brazil, with a territorial extension of 8.5 million square kilometers, scarce economic resources and an unequal and concentrated populational distribution, presents operational difficulties to the knowledge and evaluation of its natural resources. Analyzing this problem, the Federal Government decided to start, in the sixtieth decade, the development of researches related to the spatial area, having as one of its objectives the utilization of orbital data to the execution of the natural resources survey. The Institute for Space Research (INPE) is the main civilian organ responsible for the development of these researches through its Research and Applications Department (DPA) in the Remote Sensing area. This work presents the studies realized by the Vegetation and Forest Program of the DPA, that has as its main purpose the study of the vegetal cover using the remote sensing techniques, including its characterization and/or mapping, its evaluation and/or inventory, and its management and/or monitoring, in natural environments, in forest plantation areas, or in ecological conservation areas.
Author

N90-20447# Instituto de Pesquisas Espaciais, Sao Jose dos Campos (Brazil).
ANALYSIS OF METHODS TO DETERMINE EMISSIVITY FOR GROUND SURFACE TARGETS IN THE SPECTRAL BAND 8 TO 14 MICRONS M.S. Thesis [ANALISE DE METODOS DE DETERMINACAO DE EMISSIVIDADE PARA ALVOS DA SUPERFICIE TERRESTRE, NA FAIXA ESPECTRAL DE 8 A 14 MICRON]
Admilson PenhaPacheco Nov. 1989 172 p In PORTUGUESE; ENGLISH summary
(INPE-4984-TDL/394) Avail: NTIS HC A08/MF A01

Emissivity is a physical parameter which is indispensable to the correction of ground temperatures surveyed by orbital sensors which operate in the thermal infrared. In the laboratory, under controlled conditions, the determination of emissivity is facilitated; however, in the field, it is more difficult, since alterations in environmental radiation can greatly influence the detection of radiances coming up from the investigated target. Different (passive) methods of determination of natural targets emissivity are presented based on the analysis of classical methods which utilize: portable radiometers which operate in the thermal band; approximations of blackbodies as auxiliary devices to the determination of the thermodynamic temperature of the test target; reference surfaces as auxiliar supports to the determination of the environmental irradiance, and supposition of the existence of infinite parallel plans as a theoretical basis to the emissivity determination. A theoretical formulation, an experimental procedure and an error analysis are presented for each method. For this, a theoretical basis is used, which is based on the study of the blackbody radiation, on the conceptual emissivity and on emissivity data found in the literature. In experimental terms, the methods utilize, in laboratory and in the field, the infrared radiometer model PRT-5 from Barnes, the contact thermometer SPG-40, approximation of blackbodies in form of cones and cylinders and some reference surfaces of high or low emissivity. Samples of soils, rocks, water and artificial reference surfaces are tested. The experimental results obtained are compared, subsequently, taking into account the emissivity data found in literature. Author

N90-20448# Instituto de Pesquisas Espaciais, Sao Jose dos Campos (Brazil).
UNDERWATER PHYSIOGRAPHY OF THE CONTINENTAL SHELF OF RIO GRANDE DO NORTE VISIBLE THROUGH SATELLITE IMAGERY M.S. Thesis [FEICOES FISIOGRAFICAS SUBMARINAS DA PLATAFORMA CONTINENTAL DO RIO GRANDE DO NORTE VISIVEIS POR IMAGENS DE SATELITE]
Reynaldo Solewicz 5 Oct. 1989 152 p In PORTUGUESE; ENGLISH summary
(INPE-4964-TDL/392) Avail: NTIS HC A08/MF A01

Visible TM-LANDSAT imagery is introduced as an effective tool for the investigation of underwater physiography on a regional scale, down to 35 m depth, with a resolution of 30 m, on highly reflective seabed on continental shelves with highly transparent waters. The choice of the State of Rio Grande do Norte, Brazil, as the main survey area was dictated by the richness in geomorphological units and benthic ecosystems not recorded on charts or previous literature, which could be seen in the imagery. Most of the large-scale physiography could be recognized by comparing these images with digital charts obtained from smooth sheets, and nautical charts, while some of the geomorphology was only recognized by image assisted in-situ work. Field work involved echosounder profiling, sediment sampling by diving, and underwater photography. Four important geomorphological units, related to holocene sedimentation processes are reported: the discovery of a great lineament limiting a terrace at 20 m depth, shown to correspond to an ancient shore-face; the location and field study of a beach-rock reef over this lineament; the identification and field study of large-scale transverse bedforms (dunes), and the location of a large field of longitudinal bedforms. The occurrence of ancient submerged river-beds, tidal bedforms, and a conspicuous lineament, probably related to a tectonic event are also reported.
Author

N90-20449# Center for Naval Analyses, Alexandria, VA. Advanced Systems Div.
SMALL AND GREAT CIRCLE ROUTINES Final Report
Victoria Booth Jul. 1989 25 p
(Contract N00014-87-C-0001; R0148)
(AD-A217652; CIM-48) Avail: NTIS HC A03/MF A01 CSCL 08/2

This information manual documents routines in the CNA mapping software library that calculate the points of small and great circles on the earth. The equations upon which the routines are based are described and a user's walk-through of the programs is given.
GRA

N90-20450# Pennsylvania State Univ., University Park. Environmental Resources Research Inst.
HYPOTHESES TESTING OF WATERSHED/LANDSCAPE DYNAMICS IN NORTHERN ALASKA USING DIGITAL ANALYSIS Final Report, 15 Jul. 1986 - 14 Jul. 1989
Barry M. Evans, Gary W. Petersen, and Kathryn F. Connors Sep. 1989 113 p
(Contract DE-FG02-86ER-60470)
(DE90-006721; DOE/ER-60470/1) Avail: NTIS HC A06/MF A01

Since July of 1985, Penn State scientists have been cooperating with investigators from other universities in several ecosystem studies at an existing Department of Energy (DOE) study site on the North Slope of Alaska. The primary focus of the REFLEX program is to test new applications of remote sensing systems and allied digital database processing techniques for studying hydrologic/ecologic interactions. One of the goals of this particular REFLEX project was to complement ongoing R4D studies near Toolik Lake. Since their initial cooperative efforts with R4D investigators at the R4D study site in Phase 1, scientists (primarily G. Petersen and B. Evans), have been intimately involved with the Landscape Ecology Working Group, one of several such groups established within the R4D program. As part of the R4D program, the Landscape Ecology Working Group is focusing on landscape-scale patterns and interactions that have applications to long slopes, watersheds, and large regions of the Alaskan North Slope.
DOE

N90-20451# Geological Survey of Japan, Ibaraki.
GEOLOGY, DISTRIBUTION OF HOT SPRINGS AND HYDROTHERMAL ALTERATION ZONES OF MAJOR GEOTHERMAL AREAS IN JAPAN
K. Kimbara and K. Sakaguchi 24 Mar. 1989 489 p In JAPANESE
(DE90-753026; GSJ-8902-270) Avail: NTIS (US Sales Only) HC A21/MF A03

With the intention to evaluate the hydrothermal convective system geothermal resource, the existing research data in 28 major

geothermal areas were prepared by the compilation works. The results of the works were collected in each area to following figures and tables, such as: (1) simplified geologic map, (2) distribution map of mineral and hot springs together with quality of spring, (3) metamorphic belts distribution map, (4) zonal distribution map of alteration zones, (5) correlation table between geologic map and compilation data, (6) catalog for hot and mineral springs, and (7) catalog for hydrothermal alteration alteration haloes. These figures and tables showed the outline of the distribution of the geology and hot springs and metamophic belts distribution map of major geothermal areas in Japan. DOE

N90-20452# National Academy of Sciences - National Research Council, Washington, DC.
COMMITTEE ON GEODESY - NATIONAL RESEARCH COUNCIL Final Report, 1 Jun. - 31 Aug. 1989
Robert S. Long 1990 25 p
(Grant AF-AFOSR-0124-89; AF Proj. 2309)
(AD-A217770; AFOSR-90-0124TR) Avail: NTIS HC A03/MF A01 CSCL 08/5

The focus was on the applications of geodesy to oceanography, geophysics, space science, surveying, mapping and instrumentation. A report, Geodesy in the Year 2000, is under review and will be published during the winter 1989 to 1990. The Committee plans to continue to review the activities and research in geodesy; identify basic research opportunities and applied research needs; and recommend actions to meet future national, societal, scientific and technological demands on geodetic science, including surveying, mapping, and photogrammetry. A panel was set up to: (1) evaluate the scientific impact of a global network of fiducial sites; (2) examine strategies for implementing and operating such a network in the light of anticipated scientific return using existing capabilities where possible; and (3) assess whether such a network would provide a suitable global infrastructure for geodetic and other geophysical system of the next century. GRA

N90-20453# Naval Postgraduate School, Monterey, CA.
A SPLIT-AND-MERGE METHOD FOR CREATING POLYGONAL HOMOGENEOUS-VEGETATION REGIONS FROM DIGITIZED TERRAIN DATA M.S. Thesis
Roderick K. Wade Jun. 1989 89 p
(AD-A218080) Avail: NTIS HC A05/MF A01 CSCL 12/9

Providing a simplified representation of terrain characteristics has applications to optimal-path-planning programs using spatial reasoning. Utilizing computer vision techniques, our program creates polygonal homogeneous-vegetation regions based on map vegetation data from a digitized Defense Mapping Agency Database. Boundary points for regions are identified from the vegetation codes in the database, and then the boundary contours of the regions are traced using a modified look-left boundary tracing algorithm. Each region is then represented by a polyline comprised of line segments that meet a minimum threshold for fit using the linear least-squares criterion. The segments are determined by first recursively splitting the region boundary until all segments meet the fit threshold, and then merging adjacent segments that meet the threshold. GRA

44 ENERGY PRODUCTION AND CONVERSION

Includes specific energy conversion systems, e.g., fuel cells; global sources of energy; geophysical conversion; and windpower.

For related information see also *07 Aircraft Propulsion and Power, 20 Spacecraft Propulsion and Power,* and *28 Propellants and Fuels.*

N90-20454*# National Aeronautics and Space Administration. Lewis Research Center, Cleveland, OH.
SPACE ELECTROCHEMICAL RESEARCH AND TECHNOLOGY (SERT), 1989
Richard S. Baldwin, ed. Washington Dec. 1989 351 p
Conference held in Cleveland, OH, 11-13 Apr. 1989
(NASA-CP-3056; E-4708; NAS 1.55:3056) Avail: NTIS HC A16/MF A02 CSCL 10A

The proceedings of NASA's second Space Electrochemical Research and Technology Conference are presented. The objectives of the conference were to examine current technologies, research efforts, and advanced ideas, and to identify technical barriers which affect the advancement of electrochemical energy storage systems for space applications. The conference provided a forum for the exchange of ideas and opinions of those actively involved in the field, with the intention of coalescing views and findings into conclusions on progress in the field, prospects for future advances, areas overlooked, and the directions of future efforts. Related overviews were presented in the areas of NASA advanced mission models. Papers were presented and workshops conducted in four technical areas: advanced concepts, hydrogen-oxygen fuel cells and electrolyzers, the nickel electrode, and advanced rechargable batteries. For individual titles, see N90-20455 through N90-20481.

N90-20455*# National Aeronautics and Space Administration. Goddard Space Flight Center, Greenbelt, MD.
OVERVIEW OF BATTERY USAGE IN NASA/GSFC LEO AND GEOSPACECRAFTS
Thomas Y. Yi *In* NASA, Lewis Research Center, Space Electrochemical Research and Technology (SERT), 1989 Dec. 1989 p 1-3 (For primary document see N90-20454 13-44)
Avail: NTIS HC A16/MF A02 CSCL 10A

A survey of the batteries used in the low earth orbit (LEO) and geosynchronous earth orbit (GEO) missions at the Goddard Space Flight Center is described. For each spacecraft, tentative launch date is given, along with relevant battery parameters including battery size and description, depth-of-discharge, predicted mission temperature, and life requirement. Author

N90-20456*# Jet Propulsion Lab., California Inst. of Tech., Pasadena.
THE IMPORTANCE OF BATTERIES IN UNMANNED MISSIONS
John W. Klein *In* NASA, Lewis Research Center, Space Electrochemical Research and Technology (SERT), 1989 Dec. 1989 p 5-8 (For primary document see N90-20454 13-44)
Avail: NTIS HC A16/MF A02 CSCL 10C

The planetary program has historically used batteries to supply peak power needs for mission specific applications. Any time that additional power has been required in order to meet peak power demands or those applications where only limited amounts of power were required, batteries have always been used. Up until the mid to late 70's they have performed their task admirably. Recently, however, we have all become aware of the growing problem of developing reliable NiCd batteries for long mission and high cycle life applications. Here, the role rechargeable batteries will play for future planetary and earth observing spacecraft is discussed. In conclusion, NiCds have been and will continue to be the mainstay of the power system engineers tools for peak power production. Recent experience has tarnished its once sterling reputation. However, the industry has stood up to this challenge and implemented wide ranging plans to rectify the situation. These efforts should be applauded and supported as new designs and materials become available. In addition, project managers must become aware of their responsibility to test their batteries and insure quality and mission operating characteristics. Without this teamwork, the role of NiCds in the future will diminish, and other batteries, not as optimum for high performance applications (low mass and volume) will take their place. Author

N90-20457*# National Aeronautics and Space Administration. Lewis Research Center, Cleveland, OH.
HUMAN EXPLORATION MISSION STUDIES **c12**
Robert L. Cataldo *In its* Space Electrochemical Research and Technology (SERT), 1989 Dec. 1989 p 9-15 (For primary document see N90-20454 13-44)
Avail: NTIS HC A16/MF A02 CSCL 22A

The nation's efforts to expand human presence and activity

beyond Earth orbit into the solar system was given renewed emphasis in January of 1988 when the Presidential Directive on National Space Policy was signed into effect. The expansion of human presence into the solar system has particular significance, in that it defines long-range goals for NASA's future missions. To embark and achieve such ambitious ventures is a significant undertaking, particularly compared to past space activities. Missions to Mars, the Moon, and Phobos, as well as an observatory based on the dark side of the Moon are discussed. Author

N90-20458*# Jet Propulsion Lab., California Inst. of Tech., Pasadena.
A SURVEY OF ADVANCED BATTERY SYSTEMS FOR SPACE APPLICATIONS
Alan I. Attia *In* NASA, Lewis Research Center, Space Electrochemical Research and Technology (SERT), 1989 Dec. 1989 p 17-32 (For primary document see N90-20454 13-44)
Avail: NTIS HC A16/MF A02 CSCL 10C

The results of a survey on advanced secondary battery systems for space applications are presented. Fifty-five battery experts from government, industry and universities participated in the survey by providing their opinions on the use of several battery types for six space missions, and their predictions of likely technological advances that would impact the development of these batteries. The results of the survey predict that only four battery types are likely to exceed a specific energy of 150 Wh/kg and meet the safety and reliability requirements for space applications within the next 15 years. Author

N90-20459*# Jet Propulsion Lab., California Inst. of Tech., Pasadena.
ADVANCED RECHARGEABLE SODIUM BATTERIES WITH NOVEL CATHODES
S. DiStefano, B. V. Ratnakumar, and C. P. Bankston *In* NASA, Lewis Research Center, Space Electrochemical Research and Technology (SERT), 1989 Dec. 1989 p 33-39 (For primary document see N90-20454 13-44)
Avail: NTIS HC A16/MF A02 CSCL 10C

Various high energy density rechargeable batteries are being considered for future space applications. Of these, the sodium sulfur battery is one of the leading candidates. The primary advantage is the high energy density (760 Wh/kg theoretical). Energy densities in excess of 180 Wh/kg have been realized in practical batteries. More recently, cathodes other than sulfur are being evaluated. Researchers at JPL are evaluating various new cathode materials for use in high energy density sodium batteries for advanced space applications. The approach is to carry out basic electrochemical studies of these materials in a sodium cell configuration in order to understand their fundamental behaviors. Thus far studies have focused on alternate metal chlorides such as CuCl2 and organic cathode materials such as tetracyanoethylene (TCNE). Author

N90-20460*# Argonne National Lab., IL.
MONOLITHIC SOLID OXIDE FUEL CELL DEVELOPMENT
K. M. Myles and C. C. McPheeters *In* NASA, Lewis Research Center, Space Electrochemical Research and Technology (SERT), 1989 Dec. 1989 p 41-49 Previously announced as N89-25511 (For primary document see N90-20454 13-44)
(Contract W-31-109-eng-38; ARPA Order 4850)
Avail: NTIS HC A16/MF A02 CSCL 10C

The feasibility of the monolithic solid oxide fuel cell (MSOFC) concept has been proven, and the performance has been dramatically improved. The differences in thermal expansion coefficients and firing shrinkages among the fuel cell materials have been minimized, thus allowing successful fabrication of the MSOFC with few defects. The MSOFC shows excellent promise for development into a practical power source for many applications from stationary power, to automobile propulsion, to space pulsed power. Author

N90-20461*# Eltron Research, Inc., Aurora, IL.
THE ELECTROCHEMICAL GENERATION OF USEFUL CHEMICAL SPECIES FROM LUNAR MATERIALS
Kan J. Tsai, Daniel J. Kuchynka, and Anthony F. Sammells *In* NASA, Lewis Research Center, Space Electrochemical Research and Technology (SERT), 1989 Dec. 1989 p 51-60 (For primary document see N90-20454 13-44)
(Contract NAS9-17991)
Avail: NTIS HC A16/MF A02 CSCL 10C

Electrochemical cells have been fabricated for the simultaneous generation of oxygen and lithium from a Li2O containing molten salt (Li2O-LiCl-LiF). The cell utilizes an oxygen vacancy conducting solid electrolyte, yttria-stabilized zirconia (YSZ), to effect separation between oxygen evolving and lithium reduction half-cell reactions. The ceil, which operates at 700 to 850 C, possesses rapid electrode kinetics at the lithium-alloy electrode with exchange current density (i sub o) values being greater than 60mA sq cm. When used in the electrolytic mode, lithium produced at the negative electrode would be continuously removed from the cell for later use (under lunar conditions) as an easily storable reducing agent (compared to H2) for the chemical refining of lunar ores. Because of the high reversibility of this electrochemical system, it has also formed tha basis for the lithium oxygen secondary battery system which possesses the highest theoretical energy density yet investigated. Author

N90-20462*# Texas A&M Univ., College Station. Center for Electrochemical Systems and Hydrogen Research.
A NEW CONCEPT FOR HIGH-CYCLE-LIFE LEO: RECHARGEABLE MnO2-HYDROGEN
A. J. Appleby, H. P. Dhar, Y. J. Kim, and O. J. Murphy *In* NASA, Lewis Research Center, Space Electrochemical Research and Technology (SERT), 1989 Dec. 1989 p 61-68 (For primary document see N90-20454 13-44)
Avail: NTIS HC A16/MF A02 CSCL 10C

The nickel-hydrogen secondary battery system, developed in the early 1970s, has become the system of choice for geostationary earth orbit (GEO) applications. However, for low earth orbit (LEO) satellites with long expected lifetimes the nickel positive limits performance. This requires derating of the cell to achieve very long cycle life. A new system, rechargeable MnO2-Hydrogen, which does not require derating, is described here. For LEO applications, it promises to have longer cycle life, high rate capability, a higher effective energy density, and much lower self-discharge behavior than those of the nickel-hydrogen system. Author

N90-20463*# National Aeronautics and Space Administration. Lewis Research Center, Cleveland, OH.
CHARACTERIZATION TESTING OF A 40 AHR BIPOLAR NICKEL-HYDROGEN BATTERY
Jeffrey C. Brewer (National Aeronautics and Space Administration. Marshall Space Flight Center, Huntsville, AL.), Michelle A. Manzo, and Russel P. Gemeiner *In its* Space Electrochemical Research and Technology (SERT), 1989 Dec. 1989 p 69-82 (For primary document see N90-20454 13-44)
Avail: NTIS HC A16/MF A02 CSCL 10C

Extensive characterization testing has been done on a second 40 amp-hour (Ahr), 10-cell bipolar nickel-hydrogen (Ni-H2) battery to study the effects of such operating parameters as charge and discharge rates, temperature, and pressure, on capacity, Ahr and watt-hour (Whr) efficiencies, end-of-charge (EOC) and mid-point discharge voltages. Testing to date has produced many interesting results, with the battery performing well throughout all of the test matrix except during the high-rate (5C and 10C) discharges, where poorer than expected results were observed. The exact cause of this poor performance is, as yet, unknown. Small scale 2 x 2 inch battery tests are to be used in studying this problem. Low earth orbit (LEO) cycle life testing at a 40 percent depth of discharge (DOD) and 10 C is scheduled to follow the characterization testing. Author

N90-20464*# Giner, Inc., Waltham, MA.
ADVANCED DOUBLE LAYER CAPACITORS

S. Sarangapani, P. Lessner, J. Forchione, A. Griffith, and A. B. LaConti *In* NASA, Lewis Research Center, Space Electrochemical Research and Technology (SERT), 1989 Dec. 1989 p 83-94 (For primary document see N90-20454 13-44)
(Contract N00014-88-C-0391)
Avail: NTIS HC A16/MF A02 CSCL 10C

Work was conducted that could lead to a high energy density electrochemical capacitor, completely free of liquid electrolyte. A three-dimensional RuO sub x-ionomer composite structure has been successfully formed and appears to provide an ionomer ionic linkage throughout the composite structure. Capacitance values of approximately 0.6 F/sq cm were obtained compared with 1 F/sq cm when a liquid electrolyte is used with the same configuration. Author

N90-20465*# Texas A&M Univ., College Station. Center for Electrochemical Systems and Hydrogen Research.
RECENT ADVANCES IN SOLID POLYMER ELECTROLYTE FUEL CELL TECHNOLOGY WITH LOW PLATINUM LOADING ELECTRODES
Supramaniam Srinivasan, David J. Manko, Hermann Koch (Ruhr Univ., Bochum, Germany, F.R.), Mohammad A. Enayetullah, and A. John Appleby *In* NASA, Lewis Research Center, Space Electrochemical Research and Technology (SERT), 1989 Dec. 1989 p 95-113 Sponsored in part by Navy (For primary document see N90-20454 13-44)
Avail: NTIS HC A16/MF A02 CSCL 10C

Of all the fuel cell systems only alkaline and solid polymer electrolyte fuel cells are capable of achieving high power densities (greater than 1 W/sq cm) required for terrestrial and extraterrestrial applications. Electrode kinetic criteria for attaining such high power densities are discussed. Attainment of high power densities in solid polymer electrolyte fuel cells has been demonstrated earlier by different groups using high platinum loading electrodes (4 mg/sq cm). Recent works at Los Alamos National Laboratory and at Texas A and M University (TAMU) demonstrated similar performance for solid polymer electrolyte fuel cells with ten times lower platinum loading (0.45 mg/sq cm) in the electrodes. Some of the results obtained are discussed in terms of the effects of type and thickness of membrane and of the methods platinum localization in the electrodes on the performance of a single cell. Author

N90-20466*# Dow Chemical Co., Freeport, TX.
THE APPLICATION OF DOW CHEMICAL'S PERFLUORINATED MEMBRANES IN PROTON-EXCHANGE MEMBRANE FUEL CELLS
G. A. Eisman *In* NASA, Lewis Research Center, Space Electrochemical Research and Technology (SERT), 1989 Dec. 1989 p 115-12 (For primary document see N90-20454 13-44)
Avail: NTIS HC A16/MF A02 CSCL 10C

Dow Chemical's research activities in fuel cells revolve around the development of perfluorosulfonic acid membranes useful as the proton transport medium and separator. Some of the performance characteristics which are typical for such membranes are outlined. The results of tests utilizing a new experimental membrane useful in proton-exchange membrane fuel cells are presented. The high voltage at low current densities can lead to higher system efficiencies while, at the same time, not sacrificing other critical properties pertinent to membrane fuel cell operation. A series of tests to determine response times indicated that on-off cycles are on the order of 80 milliseconds to reach 90 percent of full power. The IR free voltage at 100 amps/sq ft was determined and the results indicating a membrane/electrode package resistance to be .15 ohm-sq cm at 100 amps/sq ft. Author

N90-20467*# National Aeronautics and Space Administration. Lewis Research Center, Cleveland, OH.
HYDROGEN-OXYGEN PROTON-EXCHANGE MEMBRANE FUEL CELLS AND ELECTROLYZERS
R. Baldwin, M. Pham, A. Leonida, J. McElroy, and T. Nalette (Hamilton Standard, Windsor Locks, CT.) *In its* Space Electrochemical Research and Technology (SERT), 1989 Dec. 1989 p 127-136 (For primary document see N90-20454 13-44)
Avail: NTIS HC A16/MF A02 CSCL 10C

Hydrogen-oxygen solid polymer electrolyte (SPE) fuel cells and SPE electrolyzers (products of Hamilton Standard) both use a Proton-Exchange Membrane (PEM) as the sole electrolyte. These solid electrolyte devices have been under continuous development for over 30 years. This experience has resulted in a demonstrated ten-year SPE cell life capability under load conditions. Ultimate life of PEM fuel cells and electrolyzers is primarily related to the chemical stability of the membrane. For perfluorocarbon proton exchange membranes an accurate measure of the membrane stability is the fluoride loss rate. Millions of cell hours have contributed to establishing a relationship between fluoride loss rates and average expected ultimate cell life. This relationship is shown. Several features have been introduced into SPE fuel cells and SPE electrolyzers such that applications requiring greater than or equal to 100,000 hours of life can be considered. Equally important as the ultimate life is the voltage stability of hydrogen-oxygen fuel cells and electrolyzers. Here again the features of SPE fuel cells and SPE electrolyzers have shown a cell voltage stability in the order of 1 microvolt per hour. That level of stability has been demonstrated for tens of thousands of hours in SPE fuel cells at up to 500 amps per square foot (ASF) current density. Author

N90-20468*# Case Western Reserve Univ., Cleveland, OH. Dept. of Chemistry.
ELECTROCATALYSIS FOR OXYGEN ELECTRODES IN FUEL CELLS AND WATER ELECTROLYZERS FOR SPACE APPLICATIONS
Jai Prakash, Donald Tryk, and Ernest Yeager *In* NASA, Lewis Research Center, Space Electrochemical Research and Technology (SERT), 1989 Dec. 1989 p 137-14 Previously announced at N89-22997 (For primary document see N90-20454 13-44)
(Grant NAG3-964)
Avail: NTIS HC A16/MF A02 CSCL 10C

In most instances separate electrocatalysts are needed to promote the reduction of O2 in the fuel cell mode and to generate O2 in the energy storage-water electrolysis mode in aqueous electrochemical systems operating at low and moderate temperatures (T greater than or equal to 200 C). Interesting exceptions are the lead and bismuth ruthenate pyrochlores in alkaline electrolytes. These catalysts on high area carbon supports have high catalytic activity for both O2 reduction and generation. Rotating ring-disk electrode measurements provide evidence that the O2 reduction proceeds by a parallel four-electron pathway. The ruthenates can also be used as self-supported catalysts to avoid the problems associated with carbon oxidation, but the electrode performance so far achieved in the research at Case Western Reserve University (CWRU) is considerably less. At the potentials involved in the anodic mode the ruthenate pyrochlores have substantial equilibrium solubility in concentrated alkaline electrolyte. This results in the loss of catalyst into the bulk solution and a decline in catalytic activity. Furthermore, the hydrogen generation counter electrode may become contaminated with reduction products from the pyrochlores (lead, ruthenium).
Author

N90-20469*# Giner, Inc., Waltham, MA.
OXYGEN ELECTRODES FOR RECHARGEABLE ALKALINE FUEL CELLS-II
L. Swette and N. Kackley *In* NASA, Lewis Research Center, Space Electrochemical Research and Technology (SERT), 1989 Dec. 1989 p 149-16 (For primary document see N90-20454 13-44)
(Contract NAS3-24635)
Avail: NTIS HC A16/MF A02 CSCL 10C

The primary objective of this program is the investigation and development of electrocatalysts and supports for the positive electrode of moderate temperature single-unit rechargeable alkaline

fuel cells. Approximately six support materials and five catalyst materials have been identified to date for further development.
Author

N90-20470*# Giner, Inc., Waltham, MA.
NON-NOBLE ELECTROCATALYSTS FOR ALKALINE FUEL CELLS
S. Sarangapani, P. Lessner, M. Manoukian, and J. Giner *In* NASA, Lewis Research Center, Space Electrochemical Research and Technology (SERT), 1989 Dec. 1989 p 165-17 (For primary document see N90-20454 13-44)
(Contract DE-AC02-87ER-80500)
Avail: NTIS HC A16/MF A02 CSCL 10C

The doping of solid phase precursors followed by pyrolysis or the copyrolysis of gas phase precursors has allowed us to produce catalysts with good activity toward oxygen reduction. Efforts are currently underway to better understand the reasons for the catalytic activity of the bulk doped catalysts with a view toward further improving their activity.
Author

N90-20471*# National Aeronautics and Space Administration. Lewis Research Center, Cleveland, OH.
CORROSION TESTING OF CANDIDATES FOR THE ALKALINE FUEL CELL CATHODE
Joseph Singer and William L. Fielder *In its* Space Electrochemical Research and Technology (SERT), 1989 Dec. 1989 p 171-180 (For primary document see N90-20454 13-44)
(Contract NAS3-25199)
Avail: NTIS HC A16/MF A02 CSCL 10C

Current/voltage data was obtained for specially made corrosion electrodes of some oxides and of gold materials for the purpose of developing a screening test of catalysts and supports for use at the cathode of the alkaline fuel cell. The data consists of measurements of current at fixed potentials and cyclic voltammograms. These data will have to be correlated with longtime performance data in order to fully evaluate this approach to corrosion screening. Corrosion test screening of candidates for the oxygen reduction electrode of the alkaline fuel cell was applied to two substances, the pyrochlore Pb2Ru2O6.5 and the spinel NiCo2O4. The substrate gold screen and a sample of the IFC Orbiter Pt-Au performance electrode were included as blanks. The pyrochlore data indicate relative stability, although nothing yet can be said about long term stability. The spinel was plainly unstable. For this type of testing to be validated, comparisons will have to be made with long term performance tests.
Author

N90-20472*# Michigan Technological Univ., Houghton.
STRUCTURAL COMPARISON OF NICKEL ELECTRODES AND PRECURSOR PHASES
Bahne C. Cornilsen, Xiaoyin Shan, and Patricia Loyselle *In* NASA, Lewis Research Center, Space Electrochemical Research and Technology (SERT), 1989 Dec. 1989 p 181-19 (For primary document see N90-20454 13-44)
(Grant NAG3-519)
Avail: NTIS HC A16/MF A02 CSCL 10C

Researchers summarize previous Raman spectroscopic results and discuss important structural differences in the various phases of active mass and active mass precursors. Raman spectra provide unique signatures for these phases, and allow one to distinguish each phase, even when the compound is amorphous to x rays (i.e., does not scatter x rays because of a lack of order and/or small particle size). The structural changes incurred during formation, charge and discharge, cobalt addition, and aging are discussed. The oxidation states and dopant contents are explained in terms of the nonstoichiometric structures.
Author

N90-20473*# National Aeronautics and Space Administration. Lewis Research Center, Cleveland, OH.
IMPEDANCE STUDIES OF Ni/Cd AND Ni/H2 CELLS USING THE CELL CASE AS A REFERENCE ELECTRODE
Margaret A. Reid *In its* Space Electrochemical Research and Technology (SERT), 1989 Dec. 1989 p 197-209 (For primary document see N90-20454 13-44)
Avail: NTIS HC A16/MF A02 CSCL 10C

Impedance measurements have been made on several Ni/Cd and Ni/H2 flightweight cells using the case as a reference electrode. For these measurements the voltage of the case with respect to the anode or cathode is unimportant provided that it remains stable during the measurement of the impedance. In the cells measured so far, the voltages of the cell cases with respect to the individual electrodes differ from cell to cell even at the same overall cell voltage, but they remains stable with time. The measurements can thus be used to separate the cell impedance into the contributions of each electrode, allowing improved diagnosis of cell problems.
Author

N90-20474*# SRI International Corp., Menlo Park, CA.
THE APPLICATION OF ELECTROCHEMICAL IMPEDANCE SPECTROSCOPY FOR CHARACTERIZING THE DEGRADATION OF Ni(OH)2/NiOOH ELECTRODES
D. D. Macdonald, B. G. Pound, and S. J. Lenhart (Ford Aerospace and Communications Corp., Palo Alto, CA.) *In* NASA, Lewis Research Center, Space Electrochemical Research and Technology (SERT), 1989 Dec. 1989 p 311-24 Sponsored in part by DOE (For primary document see N90-20454 13-44)
Avail: NTIS HC A16/MF A02 CSCL 10C

Electrochemical impedance spectra of rolled and bonded and sintered porous nickel battery electrodes were recorded periodically during charge/discharge cycling in concentrated KOH solution at various temperatures. A transmission line model (TLM) was adopted to represent the impedance of the porous electrodes, and various model parameters were adjusted in a curve fitting routine to reproduce the experimental impedances. Degradation processes for rolled and bonded electrodes were deduced from changes in model parameters with electrode cycling time. In developing the TLM, impedance spectra of planar (non-porous) electrodes were used to represent the pore wall and backing plate interfacial impedances. These data were measured over a range of potentials and temperatures, and an equivalent circuit model was adopted to represent the planar electrode data. Cyclic voltammetry was used to study the characteristics of the oxygen evolution reaction on planar nickel electrodes during charging, since oxygen evolution can affect battery electrode charging efficiency and ultimately electrode cycle life if the overpotential for oxygen evolution is sufficiently low. Transmission line modeling results suggest that porous rolled and bonded nickel electrodes undergo restructuring during charge/discharge cycling prior to failure.
Author

N90-20475*# Hughes Aircraft Co., Los Angeles, CA.
KOH CONCENTRATION EFFECT ON THE CYCLE LIFE OF NICKEL-HYDROGEN CELLS. PART 4: RESULTS OF FAILURE ANALYSES
H. S. Lim and S. A. Verzwyvelt *In* NASA, Lewis Research Center, Space Electrochemical Research and Technology (SERT), 1989 Dec. 1989 p 243-25 (For primary document see N90-20454 13-44)
Avail: NTIS HC A16/MF A02 CSCL 10C

KOH concentration effects on cycle life of a Ni/H2 cell have been studied by carrying out a cycle life test of ten Ni/H2 boiler plate cells which contain electrolytes of various KOH concentrations. Failure analyses of these cells were carried out after completion of the life test which accumulated up to 40,000 cycles at an 80 percent depth of discharge over a period of 3.7 years. These failure analyses included studies on changes of electrical characteristics of test cells and component analyses after disassembly of the cell. The component analyses included visual inspections, dimensional changes, capacity measurements of nickel electrodes, scanning electron microscopy, BET surface area measurements, and chemical analyses. Results have indicated that failure mode and change in the nickel electrode varied as the concentration was varied, especially, when the concentration was changed from 31 percent or higher to 26 percent or lower.
Author

N90-20476*# Eagle-Picher Industries, Inc., Joplin, MO. Electronics Div.
ADVANCES IN LIGHTWEIGHT NICKEL ELECTRODE TECHNOLOGY
Dwaine Coates, Gary Paul, and Paul Daugherty *In* NASA, Lewis Research Center, Space Electrochemical Research and Technology (SERT), 1989 Dec. 1989 p 259-26 (For primary document see N90-20454 13-44)
Avail: NTIS HC A16/MF A02 CSCL 10C

Studies are currently underway to further the development of lightweight nickel electrode technology. Work is focused primarily on the space nickel-hydrogen system and nickel-iron system but is also applicable to the nickel-cadmium and nickel-zinc systems. The goal is to reduce electrode weight while maintaining or improving performance, thereby increasing electrode energy density. Two basic electrode structures are being investigated. The first is the traditional nickel sponge produced from sintered nickel-carbonyl powder. The second is a new material for this application which consists of a non-woven mat of nickel fiber. Electrodes are being manufactured, tested, and evaluated at the electrode and cell level. Author

N90-20477*# Eagle-Picher Industries, Inc., Joplin, MO.
MULTI-MISSION Ni-H2 BATTERY CELLS FOR THE 1990'S
Lee Miller, Jack Brill, and Gary Dodson *In* NASA, Lewis Research Center, Space Electrochemical Research and Technology (SERT), 1989 Dec. 1989 p 269-27 (For primary document see N90-20454 13-44)
Avail: NTIS HC A16/MF A02 CSCL 10C

A sufficient production, test and operational database is now available to permit design technology optimization for the next decade. The evolved battery cell design features standardized technology intended to support multiple type missions (e.g., both GEO and LEO). Design analysis and validation test cells demonstrate that improved performance plus attractive specific-energy characteristics will be achieved. Author

N90-20478*# National Aeronautics and Space Administration. Lewis Research Center, Cleveland, OH.
NICKEL-HYDROGEN CAPACITY LOSS ON STORAGE
Michelle A. Manzo *In its* Space Electrochemical Research and Technology (SERT), 1989 Dec. 1989 p 279-295 (For primary document see N90-20454 13-44)
Avail: NTIS HC A16/MF A02 CSCL 10C

A controlled experiment evaluating the capacity loss experienced by nickel electrodes stored under various conditions of temperature, hydrogen pressure, and electrolyte concentration was conducted using nickel electrodes from four different manufacturers. It was found that capacity loss varied with respect to hydrogen pressure, and storage temperature as well as with respect to electrode manufacturing processes. Impedance characteristics were monitored and found to be indicative of electrode manufacturing processes and capacity loss. Cell testing to evaluate state-of-charge effects on capacity loss were inconclusive as no loss was sustained by the cells tested in this experiment. Author

N90-20479*# Ford Aerospace and Communications Corp., Palo Alto, CA. Space Systems Div.
SODIUM-SULFUR BATTERY FLIGHT EXPERIMENT DEFINITION STUDY
Rebecca Chang and Robert Minck (Ford Aerospace Corp., Newport Beach, CA.) *In* NASA, Lewis Research Center, Space Electrochemical Research and Technology (SERT), 1989 Dec. 1989 p 297-30 (For primary document see N90-20454 13-44)
(Contract NAS3-25355)
Avail: NTIS HC A16/MF A02 CSCL 10C

NaS batteries have been identified as the most likely successor to space Ni-H2 or Ni-Cd batteries, primarily due to a mass reduction by a factor 2 to 3 over Ni-H2 and by a factor of 4 over Ni-Cd. This yields major launch cost reductions or payload mass improvements. NaS batteries support NASA OAST's proposed Civil Space Technology Initiative goal of a factor of two improvement in spacecraft 2000 initiative. Since Ni-H2 and Ni-Cd batteries have been space flight proven, it is essential to have the flight experiment to establish a national space technology base to demonstrate the operation of the NaS battery for space applications. Author

N90-20480*# Argonne National Lab., IL.
ADVANCED HIGH-TEMPERATURE BATTERIES
P. A. Nelson *In* NASA, Lewis Research Center, Space Electrochemical Research and Technology (SERT), 1989 Dec. 1989 p 307-32 Previously announced as N89-25390 (For primary document see N90-20454 13-44)
(Contract W-31-109-eng-38)
Avail: NTIS HC A16/MF A02 CSCL 10C

Recent results for Li-Al/FeS2 cells and bipolar battery design have shown the possibility of achieving high specific energy (210 Wh/kg) and high specific power (239 W/kg) at the cell level for an electric vehicle application. Outstanding performance is also projected for sodium/metal chloride cells having large electrolyte areas and thin positive electrodes. Author

N90-20481*# Jet Propulsion Lab., California Inst. of Tech., Pasadena.
ADVANCES IN AMBIENT TEMPERATURE SECONDARY LITHIUM CELLS
S. Subbarao, D. H. Shen, F. Deligiannis, C-K. Huang, and G. Halpert *In* NASA, Lewis Research Center, Space Electrochemical Research and Technology (SERT), 1989 Dec. 1989 p 325-33 (For primary document see N90-20454 13-44)
Avail: NTIS HC A16/MF A02 CSCL 10C

The goal is to develop secondary lithium cells with a 100 Wh/kg specific energy capable of 1000 cycles at 50 percent DOD. The approach towards meeting this goal initially focused on several basic issues related to the cell chemistry, selection of cathode materials and electrolytes and component development. The performance potential of Li-TiS2, Li-MoS3, Li-V6O13 and Li-NbSe3 electrochemical systems was examined. Among these four, the Li-TiS2 system was found to be the most promising system in terms of achievable specific energy and cycle life. Major advancements to date in the development of Li-TiS2 cells are in the areas of cathode processing technology, mixed solvent electrolytes, and cell assembly. A summary is given of these advances. Author

N90-20482# Tel-Aviv Univ. (Israel). School of Chemistry.
ADVANCED CALCIUM THIONYL CHLORIDE HIGH POWER BATTERY Periodic Report, No. 2, 15 Jul. - 15 Nov. 1989
Emanuel Peled 15 Nov. 1989 23 p
(Contract DAJA45-89-C-0013)
(AD-A216685; R/D-5899A-CH-01) Avail: NTIS HC A03/MF A01 CSCL 10/3

In this phase we have demonstrated that an improved c-size Ca/TC A type cell can deliver at RT up to 5.5 Ah at low rates and 4.4 Ah at 0.9A rate. It has 10 to 80 percent more capacity than have commercial Li-TC and Li-SO2 wound C-size cells. The improved Ca-TC cell lost almost no capacity after 4 to 5 weeks of storage at 70 C. It generates less heat at 20 C under OCV conditions than equivalent Li/TC cells, having the same electrode area, i.e., it has a longer shelf life. The improved shelf-life of calcium in BaX2/TC solutions as compared to CaX2/TC solutions results mainly from the difference in the solubility or reactivity of the CaO film in those two solutions. In CaX2/TC solutions the oxide dissolves leaving the calcium with a CaCl2 layer which does not provide the metal with good protection. In BaX2/TC solutions, on the native CaO layer a BaCl2 and AlCl3 or Al2O3 layer is formed. This BaCl3, AlCl3, and Al2O3 layer does not form when the oxide is missing from the surface. Therefore cleaned calcium in BaX2/TC solution corrodes at the same rate as does calcium in CaX2/TC solutions. GRA

N90-20483# Stirling Power Systems Corp., Ann Arbor, MI.
PHASE 1 SUPPLEMENTAL DEVELOPMENT OF A KINEMATIC STIRLING/RANKINE COMMERCIAL GAS-FIRED HEAT PUMP SYSTEM Final Report, Jan. - Jun. 1989

Russell E. Monahan Jun. 1989 50 p
(Contract GRI-5089-242-1776)
(PB90-129974; GRI-89/0133) Avail: NTIS HC A03/MF A01
CSCL 10B

The Kinematic Stirling/Rankine gas heat pump concept is based on the application of a Stirling engine that was under development for over a decade. The engine was converted to natural gas and is characterized with many thousand hours of operating experience. The goal is to develop a commercial size Stirling engine-driven gas heat pump with a cooling capacity of 10-tons, a COP (heating) of 1.8 and a COP (cooling) of 1.1. The project is a multi-phase development with commercialization planned for the mid-1990's. In previous phases, an HVAC systems manufacturer was working with SPS to develop a prototype gas heat pump system. To date, two generations of prototype GHP systems were built and tested and have demonstrated significant operating cost savings over the conventional electric heat pump. Under the program a number of design and manufacturing process changes were made to the engine to reduce costs and improve endurance and shaft efficiency and are described. The adaptation and operation of a computer optimization code was accomplished under the program and is reported. Author

N90-20484# International Fuel Cells Corp., South Windsor, CT.
ADVANCED ON-SITE POWER PLANT DEVELOPMENT TECHNOLOGY PROGRAM Final Report
Sep. 1989 251 p
(Contract DE-AC21-82MC-24222)
(DE90-000443; DOE/MC-24222/2790) Avail: NTIS HC A12/MF A02

The purpose of the technical effort was to establish a technology base for 200-kW on-site fuel cell power plants. It was conducted in two phases: (1) Component evaluation; and (2) Full-scale system verification. This contract was supplemented by a Gas Research Institute (GRI) contract which was conducted in the 1981 to 1986 time period. This GRI contract concentrated on 200-kW scale component design, thermal management/water treatment system analysis and redesign and advanced DC/AC inverter development. The component evaluation phase generally included subscale component tests, scale-up to full-size 200-kW hardware and full-size hardware tests of the cell stack (in Tasks 1 and 2), the power conditioner (in Task 3), the heat exchangers and ancillary components (in Task 4), and the fuel processor (in Task 5). The full-size cell stack, fuel processor, heat exchangers, and ancillary components from the component development tasks were integrated into a dc system called the Verification Test Article (VTA). The VTA which was fabricated and tested under Task 7 allowed for system integration issues associated with the cell stack, fuel processor, thermal management, and water treatment subsystems to be explored under conditions similar to an actual fuel cell power plant. Key accomplishments of this contract are described. DOE

N90-20485# Los Alamos National Lab., NM. Earth and Environmental Sciences Div.
HOT DRY ROCK GEOTHERMAL ENERGY: A RENEWABLE ENERGY RESOURCE THAT IS READY FOR DEVELOPMENT NOW
D. W. Brown, R. M. Potter, and C. W. Myers 1990 20 p
Presented at the Energy and the Environment in the 21st Century, Cambridge, MA, 26-28 Mar. 1990
(Contract W-7405-eng-36)
(DE90-007509; LA-UR-90-698; CONF-900377-2) Avail: NTIS HC A03/MF A01

Hot dry rock (HDR) geothermal energy, which utilizes the natural heat contained in the earth's crust, is a very large and well-distributed resource of nonpolluting, and essentially renewable, energy that is available globally. Its use could help mitigate climatic change and reduce acid rain, two of the major environmental consequences of our ever-increasing use of fossil fuels for heating and power generation. In addition, HDR, as a readily available source of indigenous energy, can reduce our nations's dependence on imported oil, enhancing national security and reducing our trade deficit. On a national scale we can begin to develop this new source, using it directly for power generation or for direct-heat applications, or indirectly in hybrid geothermal/fossil-fuel power plants. In the HDR concept, which has been demonstrated in the field in two different applications and flow-tested for periods up to one year, heat is recovered from the earth by pressurized water in a closed-loop circulation system. As a consequence, minimal effluents are released to the atmosphere, and no wastes are produced. This paper describes the nature of the HDR resource and the technology required to implement the heat-mining concept. An assessment of the requirements for establishing HDR feasibility is presented in the context of providing a commercially competitive energy source. DOE

N90-20486# Midwest Research Inst., Golden, CO.
PHOTOVOLTAIC ENERGY Program Summary
Jan. 1990 20 p
(Contract DE-AC02-83CH-10093)
(DE89-009473; DOE/CH-10093/58) Avail: NTIS HC A03/MF A01

In 1989, the U.S. photovoltaic industry enjoyed a growth rate of 30 percent in sales for the second year in a row. This sends a message that the way we think about electricity is changing. Instead of big energy projects that perpetuate environmental and economic damage, there is a growing trend toward small renewable technologies that are well matched to end-user needs and operating conditions. As demand grows and markets expand, investment capital will be drawn to the industry and new growth trends will emerge. The photovoltaic industry around the world achieved record shipments also. Worldwide shipments of photovoltaic (PV) modules for 1989 totaled more than 40 megawatts (MW), nearly a 20 percent increase over last year's shipments. The previous two years showed increases in worldwide shipments of 23 and 25 percent, respectively. If this growth rate continues through the 1990s, as industry back orders would indicate, 300 to 1000 MW of PV-supplied power could be on line by 2000. Photovoltaic systems have low environmental impact and they are inexpensive to operate and maintain. Using solid-state technology, PV systems directly convert sunlight to electricity without high-temperature fluids or moving parts that could cause mechanical failure. This makes the technology very reliable. DOE

N90-20487# Midwest Research Inst., Golden, CO.
SOLAR THERMAL PROGRAM SUMMARY, FISCAL YEAR 1989
Jan. 1990 20 p
(Contract DE-AC02-83CH-10093)
(DE89-009475; DOE/CH-10093/60) Avail: NTIS HC A03/MF A01

The nation faces many difficult challenges in energy supply and use. These challenges involve numerous national issues, including energy security, energy cost, international balance-of-trade, and international competitiveness. Energy use directly affects environmental quality as well. Growing, pervasive problems with atmospheric pollution, water resources, acid rain, and the greenhouse effect may ultimately limit the burning of fossil fuels. We need to find ways to ameliorate these environmental problems while maintaining assured access to the energy resources our nation requires. Concentrated sunlight is a versatile and high-quality form of energy that can help us meet our energy needs. Solar thermal energy systems concentrate the sun's radiation to generate electricity, produce high-temperature heat for industrial and commercial uses, and carry out various chemical reactions that take advantage of the unique attributes of highly concentrated sunlight. Solar thermal technology has many applications, including electrical power generation, hazardous waste destruction, and other advanced applications such as materials processing and the pumping of lasers using very high concentration. Solar thermal technology is a desirable energy supply option for several reasons. DOE

N90-20488# Midwest Research Inst., Golden, CO.
ENERGY STORAGE AND DISTRIBUTION Program Summary
Jan. 1990 20 p

(Contract DE-AC02-83CH-10093)
(DE89-009487; DOE/CH-10093/72) Avail: NTIS HC A03/MF A01

The United States consumes more electricity today than ever before, despite increases in energy efficiency during the past 35 years. Historically, there has been a direct correlation between energy consumption and the gross national product (GNP). The association is logical, because GNP influences several of the factors that determine electricity consumption. This complex relationship between economic growth and electricity use ties success in the economy to an increase in electricity demand and requires the supply of electricity to be stable and dependable. Projections of both GNP and electricity demand estimate that between now and 2000, the average annual growth rates will be 2 to 3 percent. Providing an adequate supply of electricity could be a problem, however. Projections of electricity supply indicate that by 2000, many regions of the country will experience electrical generating capacity shortages. DOE

N90-20489# Midwest Research Inst., Golden, CO.
CuInSe2 AND CdTe: SCALE-UP FOR MANUFACTURING
Ken Zweibel and Richard Mitchell Dec. 1989 109 p
(Contract DE-AC02-83CH-10093)
(DE89-009503; SERI/TR-211-3571) Avail: NTIS HC A06/MF A01

The information in this report was originally compiled to serve as a chapter in a photovoltaic reference book. The particular focus of this chapter was on the development of low-cost photovoltaic materials, namely CuInSe2 and CdTe, two leading polycrystalline thin film materials exhibiting high efficiencies and low production costs. Both materials demonstrate significant potential as usable technologies in the commercial market. While the primary focus of this review is on the characteristics of these materials, the authors also provide a look at key methods for making these materials as well as for making added layers that are required for completing a device. In addition, the authors discuss related issues to specific materials (e.g., availability, stability, toxicity) and to each approach (e.g., advantages and drawbacks). DOE

N90-20490# Sandia National Labs., Albuquerque, NM.
HIGH-EFFICIENCY SILICON CONCENTRATOR SOLAR CELL RESEARCH
M. A. Greene, A. W. Blakers, Jianhua Zhao, Ahua Wang, A. M. Milne, Dai Ximing, and C. M. Chong Dec. 1989 64 p Prepared in cooperation with New South Wales Univ., Kensington (Australia)
(Contract DE-AC04-76DP-00789)
(DE90-008040; SAND-89-7041) Avail: NTIS HC A04/MF A01

This project continued the development of high efficiency silicon concentrator solar cells with the goal of achieving a 24% efficient module ready cell. This target was comfortably achieved with efficiencies as high as 25.2% at 125 suns concentration measured at Sandia National Laboratories. In outdoor testing at Sandia, cells of this type but of more modest performance resulted in lens/cell efficiency above 20% for the first time. Exciting results were obtained with a new cell structure, the PERC cell (passivated emitter and rear cell) which demonstrated an efficiency of 21.8% for a nonconcentrating cell and creditable performance out to 20 suns for concentrator cells. Progress was also reported for cells fabricated on n-type substrates and for plasma grooved, buried contact solar cells. DOE

N90-20491# Midwest Research Inst., Golden, CO. Solar Energy Research Inst.
WIND ENERGY PROGRAM SUMMARY. VOLUME 1: OVERVIEW Report, fiscal year 1989
Jan. 1990 16 p
(Contract DE-AC02-83CH-10093)
(DE89-009479; DOE/CH-10093/64-Vol-1) Avail: NTIS HC A03/MF A01

A new wind is sweeping our country. It's a shared desire, both public and private, to preserve our environment. To manage our technology and our resources in the most efficient manner possible. To ensure our standard of living, yet allow for growth and prosperity. Wind power is already helping the United States to meet these challenges, with about 1400 megawatts (MW) of installed wind turbine capacity on-line to utilities primarily in California and Hawaii. And according to a recent report by the Electric Power Research Institute (EPRI), the best of today's wind turbines are performing well. When located in sites with good wind resources, today's superior designs have energy costs of about 8(cents)/kilowatt-hour (kWh), a price competitive with some forms of conventional power. The EPRI report also found that operation and maintenance costs for the best machines can be as low as 0.5(cents)/kWh, comparable to that of conventional power-producing technologies, if on-site maintenance facilities are available. These achievements are remarkable for a technology that began generating utility-scale power just a decade ago, after oil embargoes first imperiled U.S. energy security in 1973. Today's wind turbines can produce cost-competitive electricity only in areas where wind speeds annually average an energetic 18 mph or more. DOE

N90-20492# Midwest Research Inst., Golden, CO. Solar Energy Research Inst.
A COMPARISON OF TWO-AND THREE-DIMENSIONAL S809 AIRFOIL PROPERTIES FOR ROUGH AND SMOOTH HAWT (HORIZONTAL-AXIS WIND TUNNEL) ROTOR OPERATION
W. D. Musial, C. P. Butterfield, and M. D. Jenks Feb. 1990 8 p Presented at the 9th ASME Wind Energy Symposium, New Orleans, LA, 14-17 Jan. 1990
(Contract DE-AC02-83CH-10093)
(DE89-009512; SERI/TP-257-3603; CONF-900136-8) Avail: NTIS HC A02/MF A01

At the Solar Energy Research Institute (SERI), we carried out tests to measure the effects of leading-edge roughness on an S809 airfoil using a 10-m, three-bladed, horizontal-axis wind turbine (HAWT). The rotor employed a constant-chord (.457 m) blade geometry with zero twist. Blade structural loads were measured with strain gages mounted at 9 spanwise locations. Airfoil pressure measurements were taken at the 80 percent spanwise station using 32 pressure taps distributed around the airfoil surface. Detailed inflow measurements were taken using nine R.M. Young Model 8002 propvane anemometers on a vertical plane array (VPA) located 10 m upwind of the test turbine in the prevailing wind direction. The major objective of this test was to determine the sensitivity of the S809 airfoil to roughness on a rotating wind turbine blade. We examined this effect by comparing several parameters. We compared power curves to show the sensitivity of whole rotor performance to roughness. We used pressure measurements to generate pressure distributions at the 80 percent span which operates at a Reynolds number (Re) of 800,000. We then integrated these distributions to determine the effect of roughness on the section's lift and pressure-drag coefficients. DOE

N90-20493# Massachusetts Inst. of Tech., Cambridge.
INNOVATIVE TURBINE CONCEPTS FOR OPEN-CYCLE OTEC (OCEAN THERMAL ENERGY CONVERSION)
Dec. 1989 70 p Prepared in cooperation with Texas A and M Univ., College Station and Pennsylvania Univ., Philadelphia
(Contract DE-AC02-83CH-10093)
(DE90-000315; SERI/TR-253-3549) Avail: NTIS HC A04/MF A01

The results are summarized of preliminary studies conducted to identify and evaluate three innovative concepts for an open cycle ocean thermal energy conversion (OTEC) steam turbine that could significantly reduce the cost of OTEC electrical power plants. The three concepts are: (1) a crossflow turbine, (2) a vertical axis, axial flow turbine, and (3) a double flow, radial inflow turbine with mixed flow blading. In all cases, the innovation involves the use of lightweight, composite plastic blading and a physical geometry that facilitates efficient fluid flow to and from the other major system components and reduces the structural requirements for both the turbine or the system vacuum enclosure, or both. The performance, mechanical design, and cost of each of the

concepts are developed to varying degrees but in sufficient detail to show that the potential exists for cost reductions to the goals established in the U.S. Department of Energy's planning documents. Specifically, results showed that an axial turbine operating with 33 percent higher steam throughput and 7 percent lower efficiency than the most efficient configuration provides the most cost effective open-cycle OTEC system. The vacuum enclosure can be significantly modified to reduce costs by establishing better interfaces with the system. DOE

N90-20494# Sandia National Labs., Albuquerque, NM.
PERSPECTIVES ON SOLAR ENERGY AND THE ENVIRONMENT
Dan L. Hartley and D. G. Schueler 1990 14 p Presented at the Energy and the Environment in the 21st Century, Cambridge, MA, 26-38 Mar. 1990
(Contract DE-AC04-76DP-00789)
(DE90-007680; SAND-90-0438C; CONF-900377-3) Avail: NTIS HC A03/MF A01

Over the next several decades, it is expected that the use of renewable energy technologies will greatly expand as these technologies mature, as the cost of conventional energy supply increases, and as the environmental impact of fossil fuel usage is better understood. A critical question is whether the impact of renewables, in terms of displaced fossil fuel use and reduced environmental effects, can be significant. Certainly, public policy will have dramatic effects on this question. Given a positive policy environment, renewables have the potential to displace a significant fraction of projected energy use within 30 to 40 years. For the United States, renewables could contribute as much as 25 to 55 exajoules of energy annually by the year 2030, or 15 to 35 percent of the projected total U.S. energy consumption. DOE

N90-20495# Science Applications International Corp., San Diego, CA. Energy Projects Div.
SELECTION AND DESIGN OF A STRETCHED-MEMBRANE HELIOSTAT FOR TODAY'S MARKETS
Kelly Beninga, Roger Davenport, and Jeffrey Sandubrae Jan. 1990 178 p Prepared for Sandia National Labs., Albuquerque, NM
(Contract DE-AC04-76DP-00789)
(DE90-007997; SAND-89-7040) Avail: NTIS HC A09/MF A01

Science Applications International Corporation has designed a complete, integrated stretched membrane heliostat. The present state-of-the-art is a single pedestal that does not take advantage of the unique characteristics of stretched membrane mirror modules and does not allow face down stow. It was desired to seek more cost effective designs for use with stretched membrane mirrors. Many stretched membrane heliostat drive system designs were generated and evaluated relative to the pedestal design. The two most promising alternate designs were determined to be a dual module design and a shared support design. Further refinement and cost analysis led to the selection of the dual module heliostat as the preferred design. The dual module design was estimated to cost about 18 percent less than a pedestal heliostat over its lifetime, and was determined to have the best near-term development potential of all the designs studied. This design incorporates long sought features such as face down stow as well as proven technology such as the single pedestal mounted drive unit. A 100 sq m dual module heliostat was designed. Detailed design studies and manufacturing cost estimates were performed. The SAIC dual module heliostat is structurally optimized and cost efficient. At a production rate of 5000 heliostats per year, the installed cost of the dual module heliostat is estimated to be $107/sq m ($10/sq ft) and the total lifetime cost (including O and M costs) is estimated to be $139/sq n ($13/sq ft). DOE

N90-20496# California Univ., Berkeley. Lawrence Berkeley Lab. Materials and Chemical Sciences Div.
NOVEL ELECTRODES FOR ADVANCED ENERGY STORAGE SYSTEMS Ph.D. Thesis
Meilin Liu Sep. 1989 163 p
(Contract DE-AC03-76SF-00098)
(DE90-008667; LBL-28083) Avail: NTIS HC A08/MF A01

The objective was to explore advanced cathode materials and the corresponding energy storage systems based on these materials. A diverse group of organodisulfides (RSSR) and solid redox polymerization electrodes (SRPE) were developed in this laboratory. The attractive features of these materials include low operating temperatures (ambient to 150 C), high energy densities, low cost, passive behavior to many materials, and low toxicity (biodegradable). Furthermore, their properties can easily be tailored for various applications by appropriate selection of the organic groups, while their reversibility with respect to many metals allows for a great choice of negative electrodes. The discovery of redox polymerization electrodes may revolutionize energy storage systems. A number of publications regarding electrochemical properties of these materials and the performance of the cells based on them are summarized. Detailed descriptions of impedance spectroscopy studies, 4-probe polarization measurements, and ambient temperature lithium batteries based on redox polymerization electrodes are not covered and will be addressed in subsequent communications. DOE

N90-20497# Ceramic Binder Systems, Inc., Butte, MT.
THERMOELECTRIC CONVERSION WITH ION CONDUCTORS Final Report
Ashok V. Joshi Jan. 1990 40 p
(Contract N00014-86-C-0827)
(AD-A217822; CERAMATEC-90610/55001) Avail: NTIS HC A03/MF A01 CSCL 10/2

A theoretical and experimental investigation of an oxygen thermoelectric generator based on oxygen ion-conducting solid electrolyte was carried out. In this thermoelectric generator concept, oxygen is electrochemically expanded at a higher temperature T and compressed at T1 (T1 less than T2). The purpose of this program was to establish the theoretical and experimental foundation necessary for assessment of feasibility of this concept for potential application to space power systems. GRA

N90-20498# International Fuel Cells Corp., South Windsor, CT.
ENHANCED CERIA SOLID ELECTROLYTE FUEL CELL DEVELOPMENT. REDUCTION OF ELECTRONIC CONDUCTIVITY PERMITS USE OF A SOLID CERIA ELECTROLYTE IN HIGH EFFICIENCY HIGH POWER DENSITY FUEL CELLS AT TEMPERATURES COMPATIBLE WITH METALLIC CELL HARDWARE Final Technical Report
D. L. Maricle Jan. 1990 61 p
(Contract N00014-88-C-0390; DARPA Order 9526)
(AD-A217640; FCR-10824) Avail: NTIS HC A04/MF A01 CSCL 10/3

The primary obstacle to the use of ceria as a high power density solid oxide fuel cell electrolyte has been a low level electronic short. This develops under reducing (anode) conditions as a result of partial reduction of the CeO2 lattice. The result is a decrease in cell voltage, useful external current, efficiency, power density. A dopant concept was shown to lower the anode PO2 below which the short becomes detrimental (electrolytic domain boundary) by two orders of magnitude. Two dopants, A and B were shown to be effective. The optimum dopant A level was shown to be 1 to 3 metal atom percent. This reduction in the electronic short current is the primary achievement of this program. Analysis of the activation energies for electronic and ionic conduction indicate that the dopant is effective in reducing the short by trapping the electronic charge carriers rather than preventing partial reduction of the ceria. Measurement of the grain boundary and bulk conductivities show the overall ionic conductivity is limited by grain boundary resistance. If lower grain boundary resistance can be achieved by processing changes, another two orders of magnitude improvement in electrolytic domain boundary is possible. An attempt to limit the short by establishing an electronically resistive grain boundary barrier layer was abandoned. A separate grain boundary phase was difficult to maintain during the sinter densification step. GRA

45 ENVIRONMENT POLLUTION

Includes atmospheric, noise, thermal, and water pollution.

N90-20499# Oldenburg Univ. (Germany, F.R.). Fachbereich Physik.
DEVELOPMENT OF A LASER FLUOROSENSOR FOR THE AIRCRAFT SUPPORTED ANALYSIS OF MARITIME TOXIC AGENTS LOADS: DEFINITION PHASE Final Report, 1 Sep. 1987 - 31 Mar. 1988 [ENTWICKLUNG EINES LASERFLUOROSENSORS FUER DIE FLUGZEUGGESTUETZTE ANALYSE MARINER SCHADSTOFFBELASTUNGEN: DEFINITIONSPHASE]
Rainer Reuter 31 Mar. 1989 11 p In GERMAN
(Contract BMFT-01-ZV-8705-0)
(ETN-90-95320) Avail: NTIS HC A03/MF A01

Technical components for an aircraft supported laser fluorosensor (based on laser fluorescence) for monitoring maritime pollution are defined. The emphasis is on the specifications of the excimer laser and the detector system, as well as on the suitability of some essential components. The optical signature of a large number of mineral oil samples and toxic chemicals are measured as a basis for a data interpretation with prediction capability. ESA

N90-20500# Federal Aviation Administration, Atlantic City, NJ.
ANALYSIS OF HELIPORT ENVIRONMENTAL DATA: INDIANAPOLIS DOWNTOWN HELIPORT, WALL STREET HELIPORT. VOLUME 3: INDIANAPOLIS DOWNTOWN HELIPORT DATA PLOTS
Rosanne M. Weiss, John G. Morrow, Donald Gallagher, Mark DiMeo, and Scott Erlichman Oct. 1989 436 p Sponsored by FAA, Washington, DC
(AD-A217412; DOT/FAA/CT-TN87/54-Vol-3) Avail: NTIS HC A19/MF A03 CSCL 01/5

During the summer of 1987 heliport environmental data were collected at the Indianapolis Downtown Heliport and at New York's Wall Street Heliport. The purpose of this data collection activity was to obtain measures of rotorwash in the heliport environment due to maneuvering helicopters, and to obtain pilot perceptions and observations concerning maneuvering and parking separation criteria. Ten wind vector transmitters were situated at various locations around the heliport in order to gather information to describe the rotorwash induced wind speed and direction changes. Pilot interviews were also conducted at these heliports. This volume provides the plots generated from the wind sensor data collected at the Indianapolis Downtown Heliport. The results will be considered in future modifications of the Federal Aviation Administration Heliport Design Advisory Circular. GRA

N90-20501# Oregon State Univ., Corvallis. Dept. of General Science.
AIR POLLUTION-CAUSED CHANGES IN PHOTOSYNTHESIS: EFFECTS ON PLANT GROWTH AND RHIZOSPHERE FUNCTIONS Final Report
William E. Winner, R. K. Antibus, and A. E. Linkins (Clarkson Univ., Potsdam, NY.) Feb. 1990 70 p
(Contract DE-FG05-85ER-60312)
(DE90-007184; DOE/ER-60312/3) Avail: NTIS HC A04/MF A01

The relationships between plants, soil nutrient status, and rhizosphere symbionts were probed using ozone (O3), a commonly occurring air pollutant, as an above-ground stress to alter carbon gain. Laboratory experiments were designed to examine O3 effects on: (1) tree species grown at varying nutrient levels, (2) plants in symbiosis with a dinitrogen-fixing symbiont, (3) plants in symbiosis with mycorrhizal fungi, and (4) plants having both a dinitrogen-fixing symbiont and mycorrhizae. Photosynthesis measurements and growth analysis were applied to detect O3 effects on plant carbon gain and allocation, respectively. Stable carbon isotope ratios were analyzed as a means of integrating effects of O3 on gas exchange of leaves over the life of the plant. Transmission electron microscopy detected alterations in plant root cells symbiotic with dinitrogen-fixing bacteria caused by ozone. To better understand the relationship between host plant and mycorrhizal fungi, studies were conducted on utilization of carbohydrate by ectomycorrhizal fungi and metabolism of ectomycorrhizal fungi and roots. Taken together, these studies provide new information on metabolic relationships of plants and symbionts and the effect of O3 on these relationships. DOE

N90-20502# Rockwell International Corp., Golden, CO.
THE TERRAIN-RESPONSIVE ATMOSPHERIC CODE (TRAC) PROJECT PLAN: DEVELOPMENT OF A HAZARDOUS MATERIALS DISPERSION MODELING CAPABILITY WITH APPLICATION TO AMBIENT AIR MONITORING NETWORK DESIGN
C. Reed Hodgin 7 Jul. 1989 31 p Revised
(Contract DE-AC04-90DP-6234)
(DE90-007293; RFP-4406) Avail: NTIS HC A03/MF A01

The Rocky Flats Plant is applying the Terrain-Responsive Atmospheric Code (TRAC) for developing a monitoring network design for airborne hazardous materials around the Rocky Flats site. This project is being implemented in response to a recent agreement between the State of Colorado and the Department of Energy. The Hazardous Materials version of TRAC (and resulting monitor sitting plan) will be developed in a series of 63 tasks which will involve modification of the TRAC model to account for continuous emissions, source configuration and hazardous materials. After testing these modifications, a long-term archival meteorological data base will be implemented and used to produce the monitoring design. DOE

N90-20503# Kansas Univ., Lawrence. Dept. of Geography.
SIMULATION OF LANDSCAPE DISTURBANCES AND THE EFFECT OF CLIMATIC CHANGE Technical Progress Report No. 1, Jul. 1989 - Feb. 1990
William L. Baker, Stephen L. Egbert, and George F. Frazier 1 Mar. 1990 109 p
(Contract DE-FG02-89ER-60883)
(DE90-007565; DOE/ER-60883/1) Avail: NTIS HC A08/MF A01

This first progress report covers the seven month period from July 1989 through February 1990, during which the primary achievements have been in developing the conceptual framework for the model and in writing code. This project is the first to attempt to directly model the effects of changing atmospheric conditions on the decadal and century scale, and on landscapes whose structure is influenced by atmospherically-controlled natural disturbances. The model has a landscape ecological emphasis, meaning that the primary concern is with the patchy structure present in landscapes on the kilometers scale. A central feature of this model, in addition to the tie to atmospheric conditions, is that it contains an analytical tool, the program STRUCT, for monitoring a variety of quantitative changes in landscape structure at several scales as the model runs. DOE

N90-20504# Department of Energy, Washington, DC. Atmospheric and Climate Research Div.
ATMOSPHERIC RADIATION MEASUREMENT PROGRAM PLAN
Feb. 1990 116 p
(DE90-008108; DOE/ER-0441) Avail: NTIS HC A07/MF A01

In order to understand energy's role in anthropogenic global climate change, significant reliance is being placed on General Circulation Models (GCMs). A major goal of the Department is to foster the development of GCMs capable of predicting the timing and magnitude of greenhouse gas-induced global warming and the regional effects of such warming. DOE research has revealed that cloud radiative feedback is the single most important effect determining the magnitude of possible climate responses to human activity. However, cloud radiative forcing and feedbacks are not understood at the levels needed for reliable climate prediction. The Atmospheric Radiation Measurement (ARM) Program will contribute to the DOE goal by improving the treatment of cloud radiative forcing and feedbacks in GCMs. Two issues will be addressed: the radiation budget and its spectral dependence and

the radiative and other properties of clouds. Understanding cloud properties and how to predict them is critical because cloud properties may very well change as climate changes. The experimental objective of the ARM Program is to characterize empirically the radiative processes in the Earth's atmosphere with improved resolution and accuracy. A key to this characterization is the effective treatment of cloud formation and cloud properties in GCMs. Through this characterization of radiative properties, it will be possible to understand both the forcing and feedback effects. GCM modelers will then be able to better identify the best approaches to improved parameterizations of radiative transfer effects. This is expected to greatly improve the accuracy of long-term, GCM predictions and the efficacy of those predictions at the important regional scale, as the research community and DOE attempt to understand the effects of greenhouse gas emissions on the Earth's climate. DOE

N90-20505# Pacific Northwest Lab., Richland, WA.
GLOBAL WARMING: A NORTHWEST PERSPECTIVE
M. J. Scott, ed. and C. A. Counts, ed. Feb. 1990 103 p Symposium held in Olympia, WA, 9 Feb. 1989; sponsored by Oregon Department of Energy, Pacific Northwest Lab. and Washington State Energy Office
(Contract DE-AC06-76RL-01830)
(DE90-008140; PNL-SA-17905; CONF-8902158-1) Avail: NTIS HC A06/MF A01

The Northwest Power Planning Council convened a symposium on the subject of global climate change (the greenhouse effect) and its potential for affecting the Pacific Northwest. The symposium was organized in response to a need by the Power Council to understand global climate change and its potential impacts on resource planning and fish and wildlife planning for the region, as well as a need to understand national policy developing toward climate change and the Pacific Northwest's role in it. DOE

N90-20506# Oak Ridge National Lab., TN.
UNITED STATES HISTORICAL CLIMATOLOGY NETWORK (HCN) SERIAL TEMPERATURE AND PRECIPITATION DATA
Jan. 1990 381 p
(Contract DE-AC05-84OR-21400)
(DE90-008029; ORNL/CDIAC-30; NDP-019/R1) Avail: NTIS HC A17/MF A02

This document describes a data base containing monthly temperature and precipitation data for 1219 U.S. stations. This network of stations, known as the Historical Climatology Network (HCN), and the resulting data base were compiled by the National Climatic Data Center. These data represent the best available data from the United States for analyzing long-term climate trends on a regional scale and may be used for studies attempting to determine the climatic impacts of increased concentrations of greenhouse gases. Unlike most data sets that have been used in past climate studies, these station data have been adjusted to remove biases introduced by station moves, instrument changes, time-of-observation differences, and urbanization effects. These monthly data, along with supporting data, including station inventories, station histories, temperature corrections for time-of-observation bias, and data quality assessments, are available free of charge as a numeric data package (NDP) from the Carbon Dioxide Information Analysis Center. The NDP consists of this document and magnetic tapes containing machine-readable data files, supporting data files, a descriptive file, and computer access codes. This document describes how the stations in the HCN were selected and how the data were processed. DOE

N90-20507# Department of Energy, Portland, OR.
DRAFT GLOBAL WARMING STUDY
Jan. 1990 35 p
(DE90-008446; DOE/BP-1327) Avail: NTIS HC A03/MF A01

The 1990 Resource Program Global Warming Study examines potential Bonneville Power Administration (BPA) resource alternatives related to the risk of global warming. The study evaluates strategies for reducing net carbon emissions, and identifies the net carbon contribution of certain resource strategies designed to reduce those emissions. Carbon dioxide (CO2) is the greenhouse gas most associated with electricity production. The main purpose of the global warming study is to identify possible courses of action that BPA might take to reduce its contributions to the risk of global warming and to estimate the efficacy and costs of each approach. The principal measure of effectiveness is the reduction in total atmospheric carbon emissions compared to a base case. DOE

N90-20508# California Univ., Berkeley. Lawrence Berkeley Lab. Energy Analysis Program.
CONTROLLING SUMMER HEAT ISLANDS: PROCEEDINGS
Karina Garbesi, ed., Hashem Akbari, ed., and Phil Martien, ed. Nov. 1989 351 p Proceedings of the Workshop on Saving Energy and Reducing Atmospheric Pollution by Controlling Summer Heat Islands, Berkeley, CA, 23-24 Feb. 1989
(Contract DE-AC03-76SF-00098)
(DE90-008075; LBL-27872; CONF-8902142) Avail: NTIS HC A16/MF A02

A workshop was held on the energy and pollution implications of summertime urban heat islands and the potential to control them. The presentations, papers, and discussions fell into four broad categories: the potential to conserve energy, reduce atmospheric pollution, and slow global warming by reducing summer heat islands; the use of computer models to understand and simulate the heat island phenomenon; measurements of heat islands; and the design and implementation of heat island mitigation strategies. On the afternoon of the second day of the workshop, the participants divided into workgroups. Group 1 discussed research needs to better quantify the effect of heat island mitigation on energy use. Group 2 discussed future research on the characterization and modeling of heat islands. And Group 3 discussed the development of a manual that would present to policy makers the current knowledge of techniques to mitigate heat islands and thereby save energy. DOE

N90-20509# Brookhaven National Lab., Upton, NY. Atmospheric Sciences Div.
OVERVIEW OF THE METHODOLOGIES USED TO COMPILE LARGE SCALE EMISSIONS INVENTORIES
Carmen M. Benkovitz 1989 13 p Presented at the 82nd Annual Meeting of Association of Air Pollution Control and Hazardous Waste Management, Anaheim, CA, 25-30 Jun. 1988
(Contract DE-AC02-76CH-00016)
(DE90-008518; BNL-42102; CONF-8806460-1) Avail: NTIS HC A03/MF A01

Development of emissions inventories for large geographic areas is currently based on the use of mass balance equations to estimate the emissions from each source. The general equation used states that the emissions (E) from a particular source for a specific pollutant in a specified time frame are equal to the product of the activity rate of the source (A) in the selected time frame, an emission factor (EF) which estimates the amount of pollutant emitted per unit activity, and additional parameters which vary according to the type of source whose emissions are being estimated. Emissions for large stationary sources (point sources) are calculated on an individual basis; for smaller sources and for mobile sources methodologies currently in use estimate emissions as area aggregates. Values for the parameters and disaggregation factors used in emissions calculations can be estimated in two different ways. Individual estimates can be made for the parameters by estimating a value for each source. Averaged estimates can be made for some parameters; in this case, the set of all sources is divided into categories that are thought to be internally more homogeneous than the general population. For each of these categories, a value is estimated for the parameter and used to calculate the emissions from all the sources in the category. The objective is to present an overview of the methodologies currently used to estimate the values of the parameters needed to compile large scale inventories of anthropogenic emissions, to discuss the major approximations used and to offer recommendations for future refinement of the inventory data. DOE

N90-20510# Pacific Northwest Lab., Richland, WA.
USE OF ENVIRONMENTAL MONITORING DATA IN EVALUATION OF ATMOSPHERIC MODELING RESULTS
James Garnet Droppo, Jr. Oct. 1989 10 p Presented at the 28th Hanford Life Sciences Symposium on Environmental Monitoring, Restoration and Assessment, What Have We Learned, Richland, WA, 16-19 Oct. 1989
(Contract DE-AC06-76RL-01830)
(DE90-008607; PNL-SA-16909; CONF-891053-18) Avail: NTIS HC A02/MF A01

Modeling results are often used to conduct assessments of exposures resulting from releases to the atmosphere. Routine air monitoring was conducted at many of the U.S. Department of Energy's (DOE's) major facilities. In the application of the Multimedia Environmental Pollutant Assessment System (MEPAS) to DOE environmental issues as part of DOE's Environmental Survey, these monitoring data were found to be very useful in evaluation of modeling results. An illustrative example is given of the comparison of monitoring and modeled data at DOE sites. DOE

N90-20511# Pacific Northwest Lab., Richland, WA.
INFORMATION MANAGEMENT SYSTEMS FOR INTEGRATING THE TECHNICAL DATA AND REGULATORY REQUIREMENTS OF ENVIRONMENTAL RESTORATION ACTIVITIES
C. A. Geffen, B. A. Garrett, and M. B. Walter Mar. 1990 11 p Presented at the 16th Annual Waste Management Symposium: Working Towards a Cleaner Environment, Tucson, AZ, 25 Feb. - 1 Mar. 1990
(Contract DE-AC06-76RL-01830)
(DE90-008622; PNL-SA-17283; CONF-900210-29) Avail: NTIS HC A03/MF A01

Current environmental regulations require that comprehensive planning be conducted before remediating a hazardous waste site to characterize the nature and extent of site contamination, calculate the risk to the public, and assess the effectiveness of various remediation technologies. Remediation of Department of Energy (DOE) sites contaminated with hazardous or mixed wastes will require the effective integration of scientific and engineering data with regulatory and institutional requirements. The information management challenge presented by waste site cleanup activities goes beyond merely dealing with the large quantity of data that will be generated. The information must be stored, managed, and presented in a way that provides some consistency in approach across sites, avoids duplication of effort, and facilitates responses to requests for information from the regulators and the public. Background information is provided on the regulatory requirements for data gathering and analysis for environmental restoration activities, and outlines the data and information management requirements for completing the pre-remediation phases of an environmental restoration project. Information management systems for integrating the regulatory and institutional requirements of the environmental restoration process with the technical data and analysis requirements are also described. DOE

N90-20512# Colorado State Univ., Fort Collins. Dept. of Range Science.
PROCESSES OF COMMUNITY DEVELOPMENT AND RESPONSES OF ECOSYSTEMS TO CLIMATE CHANGE
Progress Report, 28 Sep. 1989 - 27 Sep. 1990
Edward F. Redente, H. W. Hunt, D. A. Klein, T. Mclendon, J. C. Moore, and F. B. Reeves 1990 44 p
(Contract DE-FG02-87ER-60612)
(DE90-008640; DOE/ER-60612/3) Avail: NTIS HC A03/MF A01

Plant community development is a dynamic process that results from the responses of those organisms present at the site to a constantly fluctuating environment created by the interaction of variations in climatic, edaphic, and biotic factors imposed on the physio-geographic matrix of the site. Too often, this process of community development is studied only in relation to primary producers. The studies are based on the premise that plant community development is closely linked to the coupling of decomposers with primary producers through direct and indirect mutualistic interactions. Therefore, plant community development is a process that can be explained only by understanding the simultaneous and closely interdependent development of primary producer and decomposer subsystem. To increase understanding of these development relationships, the studies are investigating changes in composition, structure, and activity of soil microflora and fauna; quantity, quality, and decomposition rate of litter; and nutrient availability levels in the soil, and relating these changes to plant community development patterns within a semiarid shrubland ecosystem. DOE

46 GEOPHYSICS

Includes aeronomy; upper and lower atmosphere studies; ionospheric and magnetospheric physics; and geomagnetism.

For space radiation see *93 Space Radiation.*

N90-20513*# Ohio State Univ., Columbus. Dept. of Geodetic Science and Surveying.
PROGRESS IN THE DETERMINATION OF THE EARTH'S GRAVITY FIELD Extended Abstracts
Richard H. Rapp, ed. Jun. 1989 207 p Meeting held in Fort Lauderdale, FL, 13-16 Sep. 1988; sponsored by the American Geophysical Union and the International Association of Geodesy Sponsored in cooperation with AFGL
(Grant NGR-36-008-161)
(NASA-CR-185721; NAS 1.26:185721; Rept-397) Avail: NTIS HC A10/MF A02 CSCL 08G

Topics addressed include: global gravity model development; methods for approximation of the gravity field; gravity field measuring techniques; global gravity field applications and requirements in geophysics and oceanography; and future gravity missions. For individual titles, see N90-20514 through N90-20561.

N90-20514*# National Aeronautics and Space Administration. Goddard Space Flight Center, Greenbelt, MD.
GRAVITATIONAL MODEL IMPROVEMENT AT THE GODDARD SPACE FLIGHT CENTER
J. G. Marsh, F. J. Lerch, B. H. Putney, T. L. Felsentreger, B. V. Sanchez, D. E. Smith, S. M. Klosko, E. C. Pavlis, J. W. Robbins, and R. G. Williamson (EG and G Washington Analytical Services Center, Inc., Lanham, MD.) et al *In* Ohio State Univ., Progress in the Determination of the Earth's Gravity Field Jun. 1989 p 3-7 Prepared in cooperation with Science Applications Research, Lanham, MD (For primary document see N90-20513 13-46)
Avail: NTIS HC A10/MF A02 CSCL 08G

Major new computations of terrestrial gravitational field models were performed by the Geodynamics Branch of Goddard Space Flight Center (GSFC). This development has incorporated the present state of the art results in satellite geodesy and have relied upon a more consistent set of reference constants than was heretofore utilized in GSFC's GEM models. The solutions are complete in spherical harmonic coefficients out to degree 50 for the gravity field parameters. These models include adjustment for a subset of 66 ocean tidal coefficients for the long wavelength components of 12 major ocean tides. This tidal adjustment was made in the presence of 550 other fixed ocean tidal terms representing 32 major and minor ocean tides and the Wahr frequency dependent solid earth tidal model. In addition 5-day averaged values for Earth rotation and polar motion were derived for the time period of 1980 onward. Two types of models were computed. These are satellite only models relying exclusively on tracking data and combination models which have incorporated satellite altimetry and surface gravity data. The satellite observational data base consists of over 1100 orbital arcs of data on 31 satellites. A large percentage of these observations were provided by third generation laser stations (less than 5 cm). A calibration of the model accuracy of the GEM-T2 satellite only solution indicated that it was a significant improvement over

previous models based solely upon tracking data. The rms geoid error for this field is 110 cm to degree and order 36. This is a major advancement over GEM-T1 whose errors were estimated to be 160 cm. An error propagation using the covariances of the GEM-T2 model for the TOPEX radial orbit component indicates that the rms radial errors are expected to be 12 cm. The combination solution, PGS-3337, is a preliminary effort leading to the development of GEM-T3. PGS-3337 has incorporated global sets of surface gravity data and the Seasat altimetry to produce a model complete to (50,50). A solution for the dynamic ocean topography to degree and order 10 was included as part of this adjustment. Author

N90-20515*# Texas Univ., Austin. Center for Space Research.
AN IMPROVED MODEL FOR THE EARTH'S GRAVITY FIELD
B. D. Tapley, C. K. Shum, D. N. Yuan, J. C. Ries, and B. E. Schutz *In* Ohio State Univ., Progress in the Determination of the Earth's Gravity Field Jun. 1989 p 8-11 (For primary document see N90-20513 13-46)
(Contract JPL-956689)
Avail: NTIS HC A10/MF A02 CSCL 08G

An improved model for the Earth's gravity field, TEG-1, was determined using data sets from fourteen satellites, spanning the inclination ranges from 15 to 115 deg, and global surface gravity anomaly data. The satellite measurements include laser ranging data, Doppler range-rate data, and satellite-to-ocean radar altimeter data measurements, which include the direct height measurement and the differenced measurements at ground track crossings (crossover measurements). Also determined was another gravity field model, TEG-1S, which included all the data sets in TEG-1 with the exception of direct altimeter data. The effort has included an intense scrutiny of the gravity field solution methodology. The estimated parameters included geopotential coefficients complete to degree and order 50 with selected higher order coefficients, ocean and solid Earth tide parameters, Doppler tracking station coordinates and the quasi-stationary sea surface topography. Extensive error analysis and calibration of the formal covariance matrix indicate that the gravity field model is a significant improvement over previous models and can be used for general applications in geodesy. Author

N90-20516*# Ohio State Univ., Columbus. Dept. of Geodetic Science and Surveying.
PROGRESS IN THE DEVELOPMENT OF HIGH DEGREE POTENTIAL COEFFICIENT MODELS
Richard H. Rapp *In its* Progress in the Determination of the Earth's Gravity Field Jun. 1989 p 12-14 (For primary document see N90-20513 13-46)
Avail: NTIS HC A10/MF A02 CSCL 08G

A natural extension of the recent satellite derived potential coefficient models is the development of high degree (maximum 180 or 360) expansions. Such expansions are based on the combination of the satellite derived models with terrestrial gravity data and satellite altimeter data. Such models are useful for more precise geoid undulation computations, for simulation studies involving different typed of future missions (e.g., gradiometry), and as reference fields for different types of gravimetric computations. The attention is to the effect of the terrain, ellipsoidal terms, and weighting. The basic methods used for the high degree solutions are reviewed. Various correction terms are described and recent models are discussed and compared. Author

N90-20517*# Texas Univ., Austin. Center for Space Research.
GRAVITY FIELD DETERMINATION AND ERROR ASSESSMENT TECHNIQUES
D. N. Yuan, C. K. Shum, and B. D. Tapley *In* Ohio State Univ., Progress in the Determination of the Earth's Gravity Field Jun. 1989 p 15-18 (For primary document see N90-20513 13-46)
Avail: NTIS HC A10/MF A02 CSCL 08G

Linear estimation theory, along with a new technique to compute relative data weights, was applied to the determination of the Earth's geopotential field and other geophysical model parameters using a combination of satellite ground-based tracking data, satellite altimetry data, and the surface gravimetry data. The relative data weights for the inhomogeneous data sets are estimated simultaneously with the gravity field and other geophysical and orbit parameters in a least squares approach to produce the University of Texas gravity field models. New techniques to perform calibration of the formal covariance matrix for the geopotential solution were developed to obtain a reliable gravity field error estimate. Different techniques, which include orbit residual analysis, surface gravity anomaly residual analysis, subset gravity solution comparisons and consider covariance analysis, were applied to investigate the reliability of the calibration. Author

N90-20518*# National Aeronautics and Space Administration. Goddard Space Flight Center, Greenbelt, MD.
AN IMPROVED ERROR ASSESSMENT FOR THE GEM-T1 GRAVITATIONAL MODEL
F. J. Lerch, J. G. Marsh, S. M. Klosko, E. C. Pavlis, G. B. Patel, D. S. Chinn, and C. A. Wagner (National Geodetic Survey, Rockville, MD.) *In* Ohio State Univ., Progress in the Determination of the Earth's Gravity Field Jun. 1989 p 19-22 (For primary document see N90-20513 13-46)
Avail: NTIS HC A10/MF A02 CSCL 08G

Several tests were designed to determine the correct error variances for the GEM-T1 gravitational solution which was derived exclusively from satellite tracking data. The basic method employs both wholly independent and dependent subset data solutions and produces a full field coefficient by coefficient estimate of the model uncertainties. The GEM-T1 errors were further analyzed using a method based upon eigenvalue-eigenvector analysis which calibrates the entire covariance matrix. Dependent satellite and independent altimetric and surface gravity data sets, as well as independent satellite deep resonance information, confirm essentially the same error assessment. Author

N90-20519*# New South Wales Univ., Kensington (Australia). School of Surveying.
GEOPOTENTIAL MODELS IN THE AUSTRALIAN REGION
A. H. W. Kearsley and R. D. Holloway *In* Ohio State Univ., Progress in the Determination of the Earth's Gravity Field Jun. 1989 p 23-26 (For primary document see N90-20513 13-46)
Avail: NTIS HC A10/MF A02 CSCL 08G

The ability of three high-order geopotential models (OSU81, GPM2 and OSU86E) to recover the gravity anomaly field (delta g) in the Australian region was tested. The region was divided into 2 x 2 deg blocks, and the mean and rms of the residual gravity (delta g measured - delta g modeled) was found to estimate the fit of the model to the point gravity data. The results showed that OSU81 and GPM2 performed similarly, recovering the delta g with a mean value of less than plus or minus 5 mGal in 63 and 70 percent of the blocks, respectively. However, both these models achieved a fit of worse that was plus or minus 13 mGal in 6 to 7 percent of cases. These were in areas either on or near the coast, or in the Central Australian region, inferring that for a precise geoid slope determination in these regions, a detailed analysis of delta g in region is needed. On the other hand, OSU86E produced a very good result, having a mean fit of less than plus or minus 5 mGal in 80 percent of the blocks, and worse than plus or minus 13 mGal in only 1 percent of cases. The rms values for this model were also improved over the other two models, indicating that for applications requiring highest precision, the preferred model is OSU86E. Author

N90-20520*# Stuttgart Univ. (Germany, F.R.). Dept. of Geodetic Science.
STABILIZED DETERMINATION OF GEOPOTENTIAL COEFFICIENTS BY THE MIXED HOM-BLUP APPROACH
B. Middel and B. Schaffrin *In* Ohio State Univ., Progress in the Determination of the Earth's Gravity Field Jun. 1989 p 27-30 (For primary document see N90-20513 13-46)
Avail: NTIS HC A10/MF A02 CSCL 08G

For the determination of geopotential coefficients, data can be used from rather different sources, e.g., satellite tracking, gravimetry, or altimetry. As each data type is particularly sensitive

to certain wavelengths of the spherical harmonic coefficients it is of essential importance how they are treated in a combination solution. For example the longer wavelengths are well described by the coefficients of a model derived by satellite tracking, while other observation types such as gravity anomalies, delta g, and geoid heights, N, from altimetry contain only poor information for these long wavelengths. Therefore, the lower coefficients of the satellite model should be treated as being superior in the combination. In the combination a new method is presented which turns out to be highly suitable for this purpose due to its great flexibility combined with robustness. Author

N90-20521*# Royal Inst. of Tech., Stockholm (Sweden). Dept. of Geodesy.

GEOPOTENTIAL COEFFICIENT DETERMINATION AND THE GRAVIMETRIC BOUNDARY VALUE PROBLEM: A NEW APPROACH

Lars E. Sjoeberg *In* Ohio State Univ., Progress in the Determination of the Earth's Gravity Field Jun. 1989 p 31-34 Sponsored in part by the Swedish Natural Science Research Council (For primary document see N90-20513 13-46)

Avail: NTIS HC A10/MF A02 CSCL 08G

New integral formulas to determine geopotential coefficients from terrestrial gravity and satellite altimetry data are given. The formulas are based on the integration of data over the non-spherical surface of the Earth. The effect of the topography to low degrees and orders of coefficients is estimated numerically. Formulas for the solution of the gravimetric boundary value problem are derived. Author

N90-20522*# Johns Hopkins Univ., Laurel, MD. Applied Physics Lab.

PRECISE SOLUTION FOR A FINITE SET OF SPHERICAL COEFFICIENTS FROM EQUIANGULAR GRIDDED DATA

Paul A. Zucker *In* Ohio State Univ., Progress in the Determination of the Earth's Gravity Field Jun. 1989 p 35-38 (For primary document see N90-20513 13-46)

Avail: NTIS HC A10/MF A02 CSCL 08G

An important goal of geodesy is to determine the anomalous potential and its derivatives outside of the earth. Representing the surface anomalies by a series of spherical harmonics is useful since it is then possible to do a term by term solution of Laplace's equation and upward continuation. The problem of finding such a spherical harmonic series for anomaly values given on an equiangular surface grid is addressed. (This is a first step toward the more complicated problem of finding a function such that locally averaged values fit a grid of mean anomalies.) Three approaches to this fitting problem are discussed and compared: the discrete Fourier technique, the discrete integral technique, and a new approach. The peculiar nature of the equiangular grid, with its increasing density of (noisy) data toward the poles, causes each method to exhibit a different type of difficulty. The new method is shown to be practical as well as precise since the numerical conditioning problems which appear can be successfully handled by such well-known techniques as a (simple) Kalman filter.

Author

N90-20523*# Purdue Univ., West Lafayette, IN. Dept. of Physics.

MODELING OF THE EARTH'S GRAVITY FIELD USING THE NEW GLOBAL EARTH MODEL (NEWGEM)

Yeong E. Kim and W. Danny Braswell (Nichols Research Corp., Huntsville, AL.) *In* Ohio State Univ., Progress in the Determination of the Earth's Gravity Field Jun. 1989 p 39-42 (For primary document see N90-20513 13-46)

Avail: NTIS HC A10/MF A02 CSCL 08G

Traditionally, the global gravity field was described by representations based on the spherical harmonics (SH) expansion of the geopotential. The SH expansion coefficients were determined by fitting the Earth's gravity data as measured by many different methods including the use of artificial satellites. As gravity data have accumulated with increasingly better accuracies, more of the higher order SH expansion coefficients were determined. The SH representation is useful for describing the gravity field exterior to the Earth but is theoretically invalid on the Earth's surface and in the Earth's interior. A new global Earth model (NEWGEM) (KIM, 1987 and 1988a) was recently proposed to provide a unified description of the Earth's gravity field inside, on, and outside the Earth's surface using the Earth's mass density profile as deduced from seismic studies, elevation and bathymetric information, and local and global gravity data. Using NEWGEM, it is possible to determine the constraints on the mass distribution of the Earth imposed by gravity, topography, and seismic data. NEWGEM is useful in investigating a variety of geophysical phenomena. It is currently being utilized to develop a geophysical interpretation of Kaula's rule. The zeroth order NEWGEM is being used to numerically integrate spherical harmonic expansion coefficients and simultaneously determine the contribution of each layer in the model to a given coefficient. The numerically determined SH expansion coefficients are also being used to test the validity of SH expansions at the surface of the Earth by comparing the resulting SH expansion gravity model with exact calculations of the gravity at the Earth's surface. Author

N90-20524*# Calgary Univ. (Alberta). Dept. of Surveying Engineering.

A FRAMEWORK FOR MODELLING KINEMATIC MEASUREMENTS IN GRAVITY FIELD APPLICATIONS

K. P. Schwarz and M. Wei *In* Ohio State Univ., Progress in the Determination of the Earth's Gravity Field Jun. 1989 p 44-47 Sponsored in part by NSERC (For primary document see N90-20513 13-46)

Avail: NTIS HC A10/MF A02 CSCL 08G

To assess the resolution of the local gravity field from kinematic measurements, a state model for motion in the gravity field of the earth is formulated. The resulting set of equations can accommodate gravity gradients, specific force, acceleration, velocity and position as input data and can take into account approximation errors as well as sensor errors. Author

N90-20525*# Analytic Sciences Corp., Reading, MA.

SYNOPSIS OF EARLY FIELD TEST RESULTS FROM THE GRAVITY GRADIOMETER SURVEY SYSTEM

S. Brzezowski, D. Gleason, J. Goldstein, W. Heller, Christopher Jekeli (Air Force Geophysics Lab., Hanscom AFB, MA.), and J. White *In* Ohio State Univ., Progress in the Determination of the Earth's Gravity Field Jun. 1989 p 48-51 (For primary document see N90-20513 13-46)

Avail: NTIS HC A10/MF A02 CSCL 08G

Although the amount of data yielded by the initial airborne and surface tests was modest, it was sufficient to demonstrate that the full gravity gradient tensor was successfully measured from moving platforms both in the air and on the surface. The measurements were effectively continuous with spatial along-track resolution limited only by choice of integration lengths taken to reduce noise. The airborne data were less noisy (800 E squared/Hz typical) than were the Gravity Gradiometer Survey System (GGSS) measurements taken at the surface (5000 E squared/Hz typical). Single tracks of surface gravity disturbances recovered from airborne data were accurate to 3 to 4 mgal in each component of gravity when compared to 5 x 5 mean gravity anomalies over a 90 km track. Multitrack processing yielded 2 to 3 mgal when compared to 5 x 5 mean anomalies. Deflection of the vertical recovery over a distance of 150 km was about one arcsecond.

Author

N90-20526*# Lamont-Doherty Geological Inst., Palisades, NY.

GRAVITY FIELD OF THE WESTERN WEDDELL SEA: COMPARISON OF AIRBORNE GRAVITY AND GEOSAT DERIVED GRAVITY

R. E. Bell, J. M. Brozena (Naval Research Lab., Washington, DC.), W. F. Haxby, and J. L. LaBrecque *In* Ohio State Univ., Progress in the Determination of the Earth's Gravity Field Jun. 1989 p 52-55 (For primary document see N90-20513 13-46)

(Grant NSF DPP-87-19147)

Avail: NTIS HC A10/MF A02 CSCL 08G

Marine gravity surveying in polar regions was typically difficult and costly, requiring expensive long range research vessels and ice-breakers. Satellite altimetry can recover the gravity field in these regions where it is feasible to survey with a surface vessel. Unfortunately, the data collected by the first global altimetry mission, Seasat, was collected only during the austral winter, producing a very poor quality gravitational filed for the southern oceans, particularly in the circum-Antarctic regions. The advent of high quality airborne gravity (Brozena, 1984; Brozena and Peters, 1988; Bell, 1988) and the availability of satellite altimetry data during the austral summer (Sandwell and McAdoo, 1988) has allowed the recovery of a free air gravity field for most of the Weddell Sea. The derivation of the gravity field from both aircraft and satellite measurements are briefly reviewed, before presenting along track comparisons and shaded relief maps of the Weddell Sea gravity field based on these two data sets. Author

N90-20527*# LaCoste and Romberg Gravity Meters, Inc., Austin, TX.

TERRESTRIAL GRAVITY INSTRUMENTATION IN THE 20TH CENTURY: A BRIEF REVIEW

H. D. Valliant *In* Ohio State Univ., Progress in the Determination of the Earth's Gravity Field Jun. 1989 p 56-59 (For primary document see N90-20513 13-46)

Avail: NTIS HC A10/MF A02 CSCL 08G

At the turn of the century, only pendulum apparatuses and torsion balances were available for general exploration work. Both of these early techniques were cumbersome and time-consuming. It was no wonder that the development of the gravity meter was welcomed with a universal sigh of relief. By 1935 potential field measurements with gravity meters supplanted gradient measurements with torsion balances. Potential field measurements are generally characterized by three types: absolute - measurements are made in fundamental units, traceable to national standards of length and time at each observation site; relative with absolute scale - differences in gravity are measured in fundamental units traceable to national standards of length and time; and relative - differences in gravity are measured with arbitrary scale. Improvements in the design of gravity meters since their introduction has led to a significant reduction in size and greatly increased precision. As the precision increased, applications expanded to include the measurement of crustal motion, the search for non-Newtonian forces, archeology, and civil engineering. Apart from enhancements to the astatic gravity meter, few developments in hardware were achieved. One of these was the vibrating string gravity meter which was developed in the 1950s and was employed briefly for marine and borehole applications. Another is the cryogenic gravity meter which utilizes the stability of superconducting current to achieve a relative instrument with extremely low drift suitable for tidal and secular gravity measurements. An advance in performing measurements from a moving platform was achieved with the development of the straight-line gravity meter. The latter part of the century also saw the rebirth of gradient measurements which offers advantages for observations from a moving platform. Definitive testing of the Bell gradiometer was recently reported. Author

N90-20528*# Litton Guidance and Control Systems, Woodland Hills, CA.

THE RAPID GEODETIC SURVEY SYSTEM (RGSS)

J. R. Huddle *In* Ohio State Univ., Progress in the Determination of the Earth's Gravity Field Jun. 1989 p 60-63 (For primary document see N90-20513 13-46)

Avail: NTIS HC A10/MF A02 CSCL 08G

The Rapid Geodetic Survey System (RGSS) is a system employing a high-accuracy gimbaled inertial platform. It provides a cost-effective capability for accurate direct measurement of the change in position, elevation, gravity intensity and deflection of the vertical from an initial point. The RGSS is an adaptation of the production version of the U.S. Army Position and Azimuth Determining System (PADS). Several hardware and software enhancements to improve the performance of the system, primarily for gravity vector survey, have occurred over the last few years. The basic principles for the control of error in the survey measurements due to noise and systematic error are discussed below. Actual acceptance test results for the RGSS which indicate an inherent capability of the system to measure change in the deflection of the vertical to a few-tenths of an arcsecond over survey periods of one to two hours using careful survey techniques are also presented. Finally a simple method to extend the capability of the system for longer duration surveys is indicated. Author

N90-20529*# National Oceanic and Atmospheric Administration, Rockville, MD. Charting and Geodetic Services.

FIRST YEAR'S RESULTS AND FIELD EXPERIENCE WITH THE LATEST JILA ABSOLUTE GRAVIMETER

G. Peter, R. E. Moose, and C. W. Wessells *In* Ohio State Univ., Progress in the Determination of the Earth's Gravity Field Jun. 1989 p 64-67 (For primary document see N90-20513 13-46)

Avail: NTIS HC A10/MF A02 CSCL 08G

One of the six absolute gravity instruments developed and built by the Joint Institute for Laboratory Astrophysics (JILA) between 1982 and 1985 was tested under a variety of environmental conditions between May 1987 and 1988. Of the 30 sites visited during this period, 10 were occupied more than once. These reobservations indicate repeatability between 1 and 4 microgals. Author

N90-20530*# Air Force Geophysics Lab., Hanscom AFB, MA.

GPS-AIDED GRAVIMETRY AT 30 km ALTITUDE FROM A BALLOON-BORNE PLATFORM

Andrew R. Lazarewicz and Alan G. Evans (Naval Surface Weapons Center, Dahlgren, VA.) *In* Ohio State Univ., Progress in the Determination of the Earth's Gravity Field Jun. 1989 p 68-71 (For primary document see N90-20513 13-46)

Avail: NTIS HC A10/MF A02 CSCL 08G

A balloon-borne experiment, flown at 30 km altitude over New Mexico, was used to test dynamic differential Global Positioning System (GPS) tracking in support of gravimetry at high-altitudes. The experiment package contained a gravimeter (Vibrating String Accelerometer), a full complement of inertial instruments, a TI-4100 GPS receiver and a radar transponder. The flight was supported by two GPS receivers on the ground near the flight path. From the 8 hour flight, about a forty minute period was selected for analysis. Differential GPS phase measurements were used to estimate changes in position over the sample time interval, or average velocity. In addition to average velocity, differential positions and numerical averages of acceleration were obtained in three components. Gravitational acceleration was estimated by correcting for accelerations due to translational motion, ignoring all rotational effects. Author

N90-20531*# Wisconsin Univ., Madison. Dept. of Geology and Geophysics.

CRITIQUE OF THE VERTICAL GRADIENT OF GRAVITY

Sigmund Hammer *In* Ohio State Univ., Progress in the Determination of the Earth's Gravity Field Jun. 1989 p 72-75 (For primary document see N90-20513 13-46)

Avail: NTIS HC A10/MF A02 CSCL 08G

Growing interest in high precision studies of the Earth's gravitational field warrant a critical review of precision requirements to yield useful results. Several problems are now under consideration. All of these problems involve, more or less, the precise value of the vertical gradients of gravity. The principle conclusion from this review is that the essential absence of Free Air Vertical Gravity Gradient control and actual values of gravimeter calibrations require serious attention. Large errors in high topography on official published gravity maps also cannot be ignored. Author

N90-20532*# Analytic Sciences Corp., Reading, MA.

METHODS FOR LOCAL GRAVITY FIELD APPROXIMATION

R. V. Sailor, K. S. Tait, and A. R. Leschack *In* Ohio State Univ., Progress in the Determination of the Earth's Gravity Field Jun. 1989 p 77-80 (For primary document see N90-20513 13-46)

Avail: NTIS HC A10/MF A02 CSCL 08G

The most widely known modern method for estimating gravity field values from observed data is least-squares collocation. Its advantages are that it can make estimates at arbitrary locations based on irregularly spaced observations, and that it makes use of statistical information about errors in the input data while providing corresponding information about the quality of the output estimates. Disadvantages of collocation include the necessity of inverting square matrices of dimension equal to the number of data values and the need to assume covariance models for the gravity field and the data errors. Fourier methods are an important alternative to collocation; having the advantage of greater computational efficiency, but requiring data estimates to be on a regular grid and not using or providing statistical accuracy information. The GEOFAST algorithm is an implementation of collocation that achieves high computational efficiency by transforming the estimation equations into the frequency domain where an accurate approximation may be made to reduce the workload. The forward and inverse Fast Fourier Transforms (FFTs) are utilized. The accuracy and computational efficiency of the GEOFAST algorithm is demonstrated using two sets of synthetic gravity data: marine gravity for an ocean trench region including wavelengths longer than 200 km; and local land gravity containing wavelengths as short as 5 km. These results are discussed along with issues such as the advantages of first removing reference field models before carrying out the estimation algorithm. Author

N90-20533*# Technische Hochschule, Darmstadt (Germany, F.R.). Inst. fuer Physikalische Geodaesie.

THE USE OF HIGH-RESOLUTION TERRAIN DATA IN GRAVITY FIELD PREDICTION

E. Groten, M. Becker, H.-J. Euler, W. Hausch, and Th. Kling *In* Ohio State Univ., Progress in the Determination of the Earth's Gravity Field Jun. 1989 p 81-84 (For primary document see N90-20513 13-46)

Avail: NTIS HC A10/MF A02 CSCL 08G

Different types of gravity prediction methods for local and regional gravity evaluation are developed, tested, and compared. Four different test areas were particularly selected in view of different prediction requirements. Also different parts of the spectrum of the gravity field were considered. Author

N90-20534*# Geodetic Inst., Charlottenlund (Denmark).

THE ROLE OF TOPOGRAPHY IN GEODETIC GRAVITY FIELD MODELLING

R. Forsberg and M. G. Sideris (Calgary Univ., Alberta) *In* Ohio State Univ., Progress in the Determination of the Earth's Gravity Field Jun. 1989 p 85-88 (For primary document see N90-20513 13-46)

Avail: NTIS HC A10/MF A02 CSCL 08G

Masses associated with the topography, bathymetry, and its isostatic compensation are a dominant source of gravity field variations, especially at shorter wavelengths. On global scales the topographic/isostatic effects are also significant, except for the lowest harmonics. In practice, though, global effects need not be taken into account as such effects are included in the coefficients of the geopotential reference fields. On local scales, the short-wavelength gravity variations due to the topography may, in rugged terrain, be an order of magnitude larger than other effects. In such cases, explicit or implicit terrain reduction procedures are mandatory in order to obtain good prediction results. Such effects may be computed by space-domain integration or by fast Fourier transformation (FFT) methods. Numerical examples are given for areas of the Canadian Rockies. In principle, good knowledge of the topographic densities is required to produce the smoothest residual field. Densities may be determined from sample measurements or by gravimetric means, but both are somewhat troublesome methods in practice. The use of a standard density, e.g., 2.67 g/cu cm, may often yield satisfactory results and may be put within a consistent theoretical framework. The independence of density assumptions is the key point of the classical Molodensky approach to the geodetic boundary value problem. The Molodensky solutions take into account that land gravity field observations are done on a non-level surface. Molodensky's problem may be solved by integral expansions or more effective FFT methods, but the solution should not be intermixed with the use of terrain reductions. The methods are actually complimentary and may both be required in order to obtain the smoothest possible signal, least prone to aliasing and other effects coming from sparse data coverage, typical of rugged topography. Author

N90-20535*# Politecnico di Milano (Italy). Ist. di Topografia Fotogrammetria e Geofisica.

THE INVERSE GRAVIMETRIC PROBLEM IN GRAVITY MODELLING

F. Sanso and C. C. Tscherning *In* Ohio State Univ., Progress in the Determination of the Earth's Gravity Field Jun. 1989 p 89-91 (For primary document see N90-20513 13-46)

Avail: NTIS HC A10/MF A02 CSCL 08G

One of the main purposes of geodesy is to determine the gravity field of the Earth in the space outside its physical surface. This purpose can be pursued without any particular knowledge of the internal density even if the exact shape of the physical surface of the Earth is not known, though this seems to entangle the two domains, as it was in the old Stoke's theory before the appearance of Molodensky's approach. Nevertheless, even when large, dense and homogeneous data sets are available, it was always recognized that subtracting from the gravity field the effect of the outer layer of the masses (topographic effect) yields a much smoother field. This is obviously more important when a sparse data set is bad so that any smoothing of the gravity field heips in interpolating between the data without raising the modeling error, this approach is generally followed because it has become very cheap in terms of computing time since the appearance of spectral techniques. The mathematical description of the Inverse Gravimetric Problem (IGP) is dominated mainly by two principles, which in loose terms can be formulated as follows: the knowledge of the external gravity field determines mainly the lateral variations of the density; and the deeper the density anomaly giving rise to a gravity anomaly, the more improperly posed is the problem of recovering the former from the latter. The statistical relation between rho and n (and its inverse) is also investigated in its general form, proving that degree cross-covariances have to be introduced to describe the behavior of rho. The problem of the simultaneous estimate of a spherical anomalous potential and of the external, topographic masses is addressed criticizing the choice of the mixed collection approach. Author

N90-20536*# Geological Survey of Canada, Ottawa (Ontario). Geophysics Div.

FFT-LOCAL GRAVIMETRIC GEOID COMPUTATION

Dezso Nagy and Rudolf J. Fury (National Geodetic Survey, Rockville, MD.) *In* Ohio State Univ., Progress in the Determination of the Earth's Gravity Field Jun. 1989 p 92-99 (For primary document see N90-20513 13-46)

Avail: NTIS HC A10/MF A02 CSCL 08G

Model computations show that changes of sampling interval introduce only 0.3 cm changes, whereas zero padding provides an improvement of more than 5 cm in the fast Fourier transformation (FFT) generated geoid. For the Global Positioning System (GPS) survey of Franklin County, Ohio, the parameters selected as a result of model computations, allow large reduction in local data requirements while still retaining the cm accuracy when tapering and padding is applied. The results are shown in tables. Author

N90-20537*# Geodetic Inst., Charlottenlund (Denmark).

PERFORMANCE OF FFT METHODS IN LOCAL GRAVITY FIELD MODELLING

Rene Forsberg and Dag Solheim (Statens Kartverk, Honefoss, Norway) *In* Ohio State Univ., Progress in the Determination of the Earth's Gravity Field Jun. 1989 p 100-103 (For primary document see N90-20513 13-46)

Avail: NTIS HC A10/MF A02 CSCL 08G

Fast Fourier transform (FFT) methods provide a fast and efficient means of processing large amounts of gravity or geoid data in local gravity field modelling. The FFT methods, however,

has a number of theoretical and practical limitations, especially the use of flat-earth approximation, and the requirements for gridded data. In spite of this the method often yields excellent results in practice when compared to other more rigorous (and computationally expensive) methods, such as least-squares collocation. The good performance of the FFT methods illustrate that the theoretical approximations are offset by the capability of taking into account more data in larger areas, especially important for geoid predictions. For best results good data gridding algorithms are essential. In practice truncated collocation approaches may be used. For large areas at high latitudes the gridding must be done using suitable map projections such as UTM, to avoid trivial errors caused by the meridian convergence. The FFT methods are compared to ground truth data in New Mexico (xi, eta from delta g), Scandinavia (N from delta g, the geoid fits to 15 cm over 2000 km), and areas of the Atlantic (delta g from satellite altimetry using Wiener filtering). In all cases the FFT methods yields results comparable or superior to other methods. Author

N90-20538*# Geodynamics Corp., Santa Barbara, CA.
FOURIER TRANSFORM METHODS IN LOCAL GRAVITY MODELING Abstract Only
J. C. Harrison and M. Dickinson *In* Ohio State Univ., Progress in the Determination of the Earth's Gravity Field Jun. 1989 p 104 (For primary document see N90-20513 13-46)
Avail: NTIS HC A10/MF A02 CSCL 08G

New algorithms were derived for computing terrain corrections, all components of the attraction of the topography at the topographic surface and the gradients of these attractions. These algoriithms utilize fast Fourier transforms, but, in contrast to methods currently in use, all divergences of the integrals are removed during the analysis. Sequential methods employing a smooth intermediate reference surface were developed to avoid the very large transforms necessary when making computations at high resolution over a wide area. A new method for the numerical solution of Molodensky's problem was developed to mitigate the convergence difficulties that occur at short wavelengths with methods based on a Taylor series expansion. A trial field on a level surface is continued analytically to the topographic surface, and compared with that predicted from gravity observations. The difference is used to compute a correction to the trial field and the process iterated. Special techniques are employed to speed convergence and prevent oscillations. Three different spectral methods for fitting a point-mass set to a gravity field given on a regular grid at constant elevation are described. Two of the methods differ in the way that the spectrum of the point-mass set, which extends to infinite wave number, is matched to that of the gravity field which is band-limited. The third method is essentially a space-domain technique in which Fourier methods are used to solve a set of simultaneous equations. Author

N90-20539*# Natal Univ., Durban (South Africa). Dept. of Surveying and Mapping.
THIN-PLATE SPLINE QUADRATURE OF GEODETIC INTEGRALS
Herman vanGysen *In* Ohio State Univ., Progress in the Determination of the Earth's Gravity Field Jun. 1989 p 105-106 (For primary document see N90-20513 13-46)
Avail: NTIS HC A10/MF A02 CSCL 08G

Thin-plate spline functions (known for their flexibility and fidelity in representing experimental data) are especially well-suited for the numerical integration of geodetic integrals in the area where the integration is most sensitive to the data, i.e., in the immediate vicinity of the evaluation point. Spline quadrature rules are derived for the contribution of a circular innermost zone to Stoke's formula, to the formulae of Vening Meinesz, and to the recursively evaluated operator L(n) in the analytical continuation solution of Molodensky's problem. These rules are exact for interpolating thin-plate splines. In cases where the integration data are distributed irregularly, a system of linear equations needs to be solved for the quadrature coefficients. Formulae are given for the terms appearing in these equations. In case the data are regularly distributed, the coefficients may be determined once-and-for-all. Examples are given of some fixed-point rules. With such rules successive evaluation, within a circular disk, of the terms in Molodensky's series becomes relatively easy. The spline quadrature technique presented complements other techniques such as ring integration for intermediate integration zones. Author

N90-20540*# Geodynamics Corp., Santa Barbara, CA.
THE REDUCTION CORRECTION IN NORTH AMERICA Abstract Only
P. D. Martzen and J. C. Harrison *In* Ohio State Univ., Progress in the Determination of the Earth's Gravity Field Jun. 1989 p 107 Submitted for publication (For primary document see N90-20513 13-46)
Avail: NTIS HC A10/MF A02 CSCL 08G

An inverse Poisson integral technique was used to determine a gravity field on the geoid which, when continued by analytic free space methods to the topographic surface, agrees with the observed field. The computation is performed in three stages, each stage refining the previous solution using data at progressively increasing resolution (1 x 1 deg, 5 x 5', 5/8 x 5/8') from a decreasing area of integration. Reduction corrections are computed at 5/8 x 5/8' granularity by differencing the geoidal and surface values, smoothed by low-pass filtering and sub-sampled at 5' intervals. The 1 x 1 deg averages of the reduction corrections thus obtained for 172 1 x 1 deg squares in western North America are discussed. The 1 x 1 deg mean reduction corrections are predominantly positive, varying from -3 to +15 mgal, with values in excess of 5 mgal for 26 squares. Their mean and rms values are +2.4 and 3.6 mgal respectively and they correlate well with the mean terrain corrections. The mean and rms contributions from the three stages of computation are: 1 x 1 deg stage +0.15 and 0.7 mgal; 5 x 5' stage + 1.0 and 1.6 mgal; and 5/8 x 5/8' stage +1.3 and 1.8 mgal. These results reflect a tendency for the contributions to become larger and more systematically positive as the wavelengths involved become shorter. The results are discussed in terms of two mechanisms; the first is a tendency for the absolute values of both positive and negative anomalies to become larger when continued downwards and, the second, a non-linear rectification, due to the correlation between gravity anomaly and topographic height, which results in the values continued to a level surface being systematically more positive than those on the topography. Author

N90-20541*# Ohio State Univ., Columbus. Dept. of Geodetic Science and Surveying.
DOWNWARD CONTINUATION OF THE FREE-AIR GRAVITY ANOMALIES TO THE ELLIPSOID USING THE GRADIENT SOLUTION AND TERRAIN CORRECTION: AN ATTEMPT OF GLOBAL NUMERICAL COMPUTATIONS
Y. M. Wang *In its* Progress in the Determination of the Earth's Gravity Field Jun. 1989 p 108-111 (For primary document see N90-20513 13-46)
(Contract F19628-86-K-0016)
Avail: NTIS HC A10/MF A02 CSCL 08G

The formulas for the determination of the coefficients of the spherical harmonic expansion of the disturbing potential of the earth are defined for data given on a sphere. In order to determine the spherical harmonic coefficients, the gravity anomalies have to be analytically downward continued from the earth's surface to a sphere-at least to the ellipsoid. The goal is to continue the gravity anomalies from the earth's surface downward to the ellipsoid using recent elevation models. The basic method for the downward continuation is the gradient solution (the g sub 1 term). The terrain correction was also computed because of the role it can play as a correction term when calculating harmonic coefficients from surface gravity data. The fast Fourier transformation was applied to the computations. Author

N90-20542*# Nairobi Univ. (Kenya). Dept. of Surveying and Photogrammetry.
THE GEOID IN KENYA
Alphonse S. Lwangasi *In* Ohio State Univ., Progress in the

Determination of the Earth's Gravity Field Jun. 1989 p 112-116 (For primary document see N90-20513 13-46)
Avail: NTIS HC A10/MF A02 CSCL 08G

The definition of geoidal undulations is given and after summarizing the methods of determination of the geoid, computed geoidal undulations by some of the methods for several points in Kenya are compared to the results obtained by the satellite gravimetric solutions. Results from astrogeodetic levelling and satellite altimetry show some reasonable agreement with the satellite gravimetric geoids while results by Doppler satellite positioning indicate that good agreement can be obtained if the orthometric heights for the points are adjusted to a uniform system. Author

N90-20543*# Geological Survey of Canada, Ottawa (Ontario). Geophysics Div.
GEOID '88: A GRAVIMETRIC GEOID FOR CANADA
Dezso Nagy *In* Ohio State Univ., Progress in the Determination of the Earth's Gravity Field Jun. 1989 p 117-120 (For primary document see N90-20513 13-46)
Avail: NTIS HC A10/MF A02 CSCL 08G

Using Stokes' formula, a gravimetric geoid was calculated for Canada. The input data are as follows: 15 x 15' block averages were used for Canada and the USA and 1 x 1 deg block averages and satellite model (GEM-T1) provided values for the remaining part of the Earth. The geoid was calculated at 6398 points covering the area within the points rho(sub i)(phi sub i; lambda sub i) (lambda is + west): rho sub 1(40,125); rho sub 2(75,184); rho sub 3(75,10); and rho sub 4(40,60). The computed geoid refers to the GRS1980 and reaches a local minimum of -47.3 meters around the western part of Hudson Bay. A contour map of the geoid is shown. Author

N90-20544*# Technische Univ., Hanover (Germany, F.R.). Inst. fuer Erdmessung.
REGIONAL QUASIGEOID DETERMINATION IN NORTHERN GERMANY AND COMPARISON WITH GPS
Heiner Denker *In* Ohio State Univ., Progress in the Determination of the Earth's Gravity Field Jun. 1989 p 121-124 (For primary document see N90-20513 13-46)
Avail: NTIS HC A10/MF A02 CSCL 08G

For the northern part of the Federal Republic of Germany, new quasigeoid solutions were computed by least squares collocation and fast Fourier transformation (FFT) techniques using point and mean gravity data, a digital terrain model, and a global geopotential model. As severe accuracy limitations for precise regional quasigeoid determination come from global model uncertainties, different geopotential models were investigated by combining them with gravimetric data and comparing the quasigeoid heights with GPS and leveling. Optimum results were obtained by a global model tailored to gravity data in Europe. Collocation and FFT results based on this model agree well. The comparison with GPS and leveling yields rms discrepancies of + or - 2 cm over approximately 400 km range. Author

N90-20545*# Technische Univ., Hanover (Germany, F.R.). Inst. fuer Erdmessung.
LONG RANGE GEOID CONTROL THROUGH THE EUROPEAN GPS TRAVERSE: FINAL RESULTS Abstract Only
W. Torge, T. Basic, H. Denker, J. Doliff, and H.-G. Wenzel *In* Ohio State Univ., Progress in the Determination of the Earth's Gravity Field Jun. 1989 p 125 (For primary document see N90-20513 13-46)
Avail: NTIS HC A10/MF A02 CSCL 08G

The European north-south Global Positioning System (GPS)-traverse proposed by IAG SSG 3.88, should control and improve the European geoid. This traverse follows first order leveling lines, included in the United European Leveling Network. From May to August 1986 and in July 1987, the central and northern part of this traverse (approx. 3000 km) was observed using up to four TI 4100 receivers, covering Austria, Federal Republic of Germany, Denmark, Sweden and Norway. Both traverse parts contain 71 stations with distances of about 50 km. In addition, 8 stations have been occupied for overlapping connections, and traverse links were established for connecting the fundamental stations Wettzell (VLBI and SLR) and Onsala (VLBI). Final results show a GPS observation precision of a few cm for loops of some 100 km circumference. After transformation of the GPS results to geoid heights using the leveled heights, comparisons with different existing gravimetric geoid determinations including geopotential models were performed. In addition, new geopotential models complete to degree and order 360 tailored to gravity data in Europe, and gravimetric geoid solutions using 6 x 10' mean gravity anomalies were investigated. The comparison with GPS and leveling yields rms discrepancies of + or - 0.1...0.2 m over 1000 km traverse sections for the best solutions, but a strong slope is existing in Sweden and southern Norway in almost all solutions, which is probably caused by systematic errors in the available gravity data for Scandinavia. This is confirmed by a new geoid computation at the Danish Geodetic Institute where the slope has disappeared. If this new solution is taken for the northern traverse section and the best solution for the central part, the rms discrepancy reduces to approximately + or - 0.2 m over 3000 km. Thus, a + or - 10 (exp 7) relative height accuracy seems to be achievable over long distances with the GPS/leveling and the gravimetric geoid calculation techniques, applied in this experiment. Author

N90-20546*# National Oceanic and Atmospheric Administration, Rockville, MD. Geodetic Research and Development Lab.
TREATMENT OF GEODETIC LEVELING IN THE INTEGRATED GEODESY APPROACH
Dennis G. Milbert *In* Ohio State Univ., Progress in the Determination of the Earth's Gravity Field Jun. 1989 p 126-129 (For primary document see N90-20513 13-46)
Avail: NTIS HC A10/MF A02 CSCL 08G

Integrated geodesy is a method in which a wide variety of surveying measurements are modeled in terms of geometric positions and the earth's geopotential. Using heterogeneous data, both geometric and gravimetric quantities are simultaneously estimated by a least-squares procedure. Heretofore, geodetic leveling differences were reduced into pseudo-observables using assumed values of gravity prior to their inclusion into integrated geodesy least-squares adjustments. The errors in estimates of geometric and gravimetric quantities obtained from integrated geodesy adjustments of geodetic leveling difference, potential differences and Helmert height differences are compared. Author

N90-20547*# Chung Cheng Inst. of Tech. (Taiwan). Dept. of Surveying Mapping Engineering.
DETERMINATION OF MEAN GRAVITY ANOMALIES IN THE TAIWAN ISLAND
Ruey-Gang Chang *In* Ohio State Univ., Progress in the Determination of the Earth's Gravity Field Jun. 1989 p 130-133 (For primary document see N90-20513 13-46)
(Contract NSC78-0410-E014-02)
Avail: NTIS HC A10/MF A02 CSCL 08G

The fitting and proper regression coefficients were made of one hundred seventeen 10 x 10' blocks with observed gravity data and corresponding elevation in the Taiwan Island. To compare five different predicted models, and the proper one for the mean gravity anomalies were determined. The predicted gravity anomalies of the non-observed gravity blocks were decided when the coefficients obtained through the model with the weighted mean method. It was suggested that the mean gravity anomalies of 10 x 10' blocks should be made when comprehensive the observed and predicted data. Author

N90-20548*# Air Force Geophysics Lab., Hanscom AFB, MA.
VERY ACCURATE UPWARD CONTINUATION TO LOW HEIGHTS IN A TEST OF NON-NEWTONIAN THEORY
Anestis J. Romaides and Christopher Jekeli *In* Ohio State Univ., Progress in the Determination of the Earth's Gravity Field Jun. 1989 p 134-137 (For primary document see N90-20513

13-46)
Avail: NTIS HC A10/MF A02 CSCL 08G

Recently, gravity measurements were made on a tall, very stable television transmitting tower in order to detect a non-Newtonian gravitational force. This experiment required the upward continuation of gravity from the Earth's surface to points as high as only 600 m above ground. The upward continuation was based on a set of gravity anomalies in the vicinity of the tower whose data distribution exhibits essential circular symmetry and appropriate radial attenuation. Two methods were applied to perform the upward continuation - least-squares solution of a local harmonic expansion and least-squares collocation. Both methods yield comparable results, and have estimated accuracies on the order of 50 microGal or better (1 microGal = 10(exp -8) m/sq s). This order of accuracy is commensurate with the tower gravity measurments (which have an estimated accuracy of 20 microGal), and enabled a definitive detection of non-Newtonian gravity. As expected, such precise upward continuations require very dense data near the tower. Less expected was the requirement of data (though sparse) up to 220 km away from the tower (in the case that only an ellipsoidal reference gravity is applied). Author

N90-20549*# National Oceanic and Atmospheric Administration, Rockville, MD. Charting and Geodetic Services.
GEODYNAMICS AND TEMPORAL VARIATIONS IN THE GRAVITY FIELD
D. C. McAdoo and C. A. Wagner *In* Ohio State Univ., Progress in the Determination of the Earth's Gravity Field Jun. 1989 p 138-141 (For primary document see N90-20513 13-46)
Avail: NTIS HC A10/MF A02 CSCL 08G

Just as the Earth's surface deforms tectonically, so too does the gravity field evolve with time. Now that precise geodesy is yielding observations of these deformations it is important that concomitant, temporal changes in the gravity field be monitored. Although these temporal changes are minute they are observable: changes in the J2 component of the gravity field were inferred from satellite (LAGEOS) tracking data; changes in other components of the gravity field would likely be detected by Geopotential Research Mission (GRM), a proposed but unapproved NASA gravity field mission. Satellite gradiometers were also proposed for high-precision gravity field mapping. Using simple models of geodynamic processes such as viscous postglacial rebound of the solid Earth, great subduction zone earthquakes and seasonal glacial mass fluctuations, we predict temporal changes in gravity gradients at spacecraft altitudes. It was found that these proposed gravity gradient satellite missions should have sensitivities equal to or better than 10(exp -4) E in order to reliably detect these changes. It was also found that satellite altimetry yields little promise of useful detection of time variations in gravity. Author

N90-20550*# Texas Univ., Austin. Center for Space Research.
A MODEL OF THE GENERAL OCEAN CIRCULATION DETERMINED FROM A JOINT SOLUTION FOR THE EARTH'S GRAVITY FIELD
R. S. Nerem, B. D. Tapley, C. K. Shum, and D. N. Yuan *In* Ohio State Univ., Progress in the Determination of the Earth's Gravity Field Jun. 1989 p 142-145 (For primary document see N90-20513 13-46)
(Contract JPL-958122)
Avail: NTIS HC A10/MF A02 CSCL 08G

If the geoid and the satellite position are known accurately, satellite altimetry can be used to determine the geostrophic velocity of the surface ocean currents. The purpose of this investigation is to simultaneously estimate the sea surface topography, zeta, the model for the gravity field, and the satellite orbit. Satellite tracking data from fourteen satellites were used; along with Seasat and Geosat altimeter data as well as surface gravity data for the solution. The estimated model of zeta compares well at long wavelengths with the hydrographic model of zeta. Covariance studies show that the geoid is separable from zeta up to degree 9, at which point geoid error becomes comparable to the signal of zeta. Author

N90-20551*# Colorado Univ., Boulder. Dept. of Aerospace Engineering Sciences.
GEOGRAPHICALLY CORRELATED ORBIT ERROR
G. W. Rosborough *In* Ohio State Univ., Progress in the Determination of the Earth's Gravity Field Jun. 1989 p 146-149 (For primary document see N90-20513 13-46)
Avail: NTIS HC A10/MF A02 CSCL 08G

The dominant error source in estimating the orbital position of a satellite from ground based tracking data is the modeling of the Earth's gravity field. The resulting orbit error due to gravity field model errors are predominantly long wavelength in nature. This results in an orbit error signature that is strongly correlated over distances on the size of ocean basins. Anderle and Hoskin (1977) have shown that the orbit error along a given ground track also is correlated to some degree with the orbit error along adjacent ground tracks. This cross track correlation is verified here and is found to be significant out to nearly 1000 kilometers in the case of TOPEX/POSEIDON when using the GEM-T1 gravity model. Finally, it was determined that even the orbit error at points where ascending and descending ground traces cross is somewhat correlated. The implication of these various correlations is that the orbit error due to gravity error is geographically correlated. Such correlations have direct implications when using altimetry to recover oceanographic signals. Author

N90-20552*# Naval Research Lab., Washington, DC.
SPECTRAL ANALYSES OF SATELLITE GEOPOTENTIAL MISSIONS
Peter J. Melvin *In* Ohio State Univ., Progress in the Determination of the Earth's Gravity Field Jun. 1989 p 151-154 (For primary document see N90-20513 13-46)
Avail: NTIS HC A10/MF A02 CSCL 08G

A new, geometrical, first order, nonresonant, frozen orbit theory was developed based on Orlov's uniformly rotating plane of constant inclination. Perturbation spectra generated from a 90th order subset of OSU86F are shown for the ill-fated 1984 JHU/APL SAGE proposal for a pair of TRANSIT satellites at 400 km altitude with a 93.5 deg inclination. Author

N90-20553*# Jet Propulsion Lab., California Inst. of Tech., Pasadena.
REFINEMENT OF EARTH'S GRAVITY FIELD WITH TOPEX GPS MEASUREMENTS
Sien-Chong Wu and Jiun-Tsong Wu *In* Ohio State Univ., Progress in the Determination of the Earth's Gravity Field Jun. 1989 p 155-158 (For primary document see N90-20513 13-46)
Avail: NTIS HC A10/MF A02 CSCL 08G

The NASA Ocean Topography Experiment satellite TOPEX will carry a microwave altimeter accurate to a few centimeters for the measurement of ocean height. The capability can be fully exploited only if TOPEX altitude can be independently determined to 15 cm or better. This in turn requires an accurate gravity model. The gravity will be tuned with selected nine 10-day arcs of laser ranging, which will be the baseline tracking data type, collected in the first six months of TOPEX flight. TOPEX will also carry onboard an experimental Global Positioning System (GPS) flight receiver capable of simultaneously observing six GPS satellites above its horizon to demonstrate the capability of GPS carrier phase and P-code pseudorange for precise determination of the TOPEX orbit. It was found that subdecimeter orbit accuracy can be achieved with a mere two-hour arc of GPS tracking data, provided that simultaneous measurements are also made at six of more ground tracking sites. The precision GPS data from TOPEX are also valuable for refining the gravity model. An efficient technique is presented for gravity tuning using GPS measurements. Unlike conventional global gravity tuning, this technique solves for far fewer gravity parameters in each filter run. These gravity parameters yield local gravity anomalies which can later be combined with the solutions over other parts of the earth to generate a global gravity map. No supercomputing power will be needed for such combining. The approaches used in this study are described and preliminary results of a covariance analysis presented. Author

N90-20554*# National Aeronautics and Space Administration. Goddard Space Flight Center, Greenbelt, MD.
GRAVITY FIELD INFORMATION FROM GRAVITY PROBE-B
D. E. Smith, F. J. Lerch, O. L. Colombo, and C. W. F. Everitt (Stanford Univ., CA.) *In* Ohio State Univ., Progress in the Determination of the Earth's Gravity Field Jun. 1989 p 159-163 (For primary document see N90-20513 13-46)
(Contract NAS5-28067)
Avail: NTIS HC A10/MF A02 CSCL 08G

The Gravity Probe-B Mission will carry the Stanford Gyroscope relativity experiment into orbit in the mid 1990's, as well as a Global Positioning System (GPS) receiver whose tracking data will be used to study the earth gravity field. Estimates of the likely quality of a gravity field model to be derived from the GPS data are presented, and the significance of this experiment to geodesy and geophysics are discussed. Author

N90-20555*# Air Force Geophysics Lab., Hanscom AFB, MA.
LOCAL GRAVITY DISTURBANCE ESTIMATION FROM MULTIPLE-HIGH-SINGLE-LOW SATELLITE-TO-SATELLITE TRACKING
Christopher Jekeli *In* Ohio State Univ., Progress in the Determination of the Earth's Gravity Field Jun. 1989 p 164-167 (For primary document see N90-20513 13-46)
Avail: NTIS HC A10/MF A02 CSCL 08G

The idea of satellite-to-satellite tracking in the high-low mode has received renewed attention in light of the uncertain future of NASA's proposed low-low mission, Geopotential Research Mission (GRM). The principal disadvantage with a high-low system is the increased time interval required to obtain global coverage since the intersatellite visibility is often obscured by Earth. The U.S. Air Force has begun to investigate high-low satellite-to-satellite tracking between the Global Positioning System (GPS) of satellites (high component) and NASA's Space Transportation System (STS), the shuttle (low component). Because the GPS satellites form, or will form, a constellation enabling continuous three-dimensional tracking of a low-altitude orbiter, there will be no data gaps due to lack of intervisibility. Furthermore, all three components of the gravitation vector are estimable at altitude, a given grid of which gives a stronger estimate of gravity on Earth's surface than a similar grid of line-of-sight gravitation components. The proposed Air Force mission is STAGE (Shuttle-GPS Tracking for Anomalous Gravitation Estimation) and is designed for local gravity field determinations since the shuttle will likely not achieve polar orbits. The motivation for STAGE was the feasibility to obtain reasonable accuracies with absolutely minimal cost. Instead of simulating drag-free orbits, STAGE uses direct measurements of the nongravitational forces obtained by an inertial package onboard the shuttle. The sort of accuracies that would be achievable from STAGE vis-a-vis other satellite tracking missions such as GRM and European Space Agency's POPSAT-GRM are analyzed.
Author

N90-20556*# Mayflower Communications Co., Inc., Reading, MA.
SATELLITE-TO-SATELLITE TRACKING EXPERIMENT FOR GLOBAL GRAVITY FIELD MAPPING
Triveni N. Upadhyay and Christopher Jekeli (Air Force Geophysics Lab., Hanscom AFB, MA.) *In* Ohio State Univ., Progress in the Determination of the Earth's Gravity Field Jun. 1989 p 168-171 (For primary document see N90-20513 13-46)
(Contract F19628-86-C-0136)
Avail: NTIS HC A10/MF A02 CSCL 08G

The satellite-to-satellite (STS) tracking concept for estimating gravitational parameters offers an attractive means to improve on regional and global gravity models in areas where data availability is limited. The extent to which the STS tracking measurements can be effectively utilized in global field models depends primarily on the satellite's altitude, number of satellites, and their orbit constellation. The estimation accuracy of the gravity field recovery also depends on the measurement accuracy of the sensors employed in the STS tracking concept. A comparison of the obtainable accuracies in the gravity field recovery using various STS tracking concepts was presented by Jekeli. The results of a feasibility study for a specific realization of the STS high-low tracking concept are summarized. In this realization, the high altitude satellites are the GPS satellites, and the low orbit satellite is the space shuttle. The GPS satellite constellation consists of 18 satellites in 6 orbital planes inclined at 55 deg. The shuttle orbit is at approximately 300 km, with an inclination of 30 deg. This specific configuration of high-low satellites for measuring perturbation in the gravity field is named the Air Foce STAGE (Shuttle GPS Tracking for Anomalous Gravitation Estimation) mission. The STAGE mission objective is to estimate the perturbations in gravity vector at the shuttle altitude to an accuracy of 1 mgal or better. Recent simulation studies have confirmed that the 1 mgal accuracy objective is near optimum for the STAGE mission. Author

N90-20557*# Technische Hogeschool, Delft (Netherlands). Faculty of Geodesy.
A DISCUSSION OF OBSERVATION MODEL, ERROR SOURCES AND SIGNAL SIZE FOR SPACEBORNE GRAVITATIONAL GRADIOMETRY
R. Rummel, R. Koop, and E. J. O. Schrama *In* Ohio State Univ., Progress in the Determination of the Earth's Gravity Field Jun. 1989 p 172-175 (For primary document see N90-20513 13-46)
(Contract ESA-7521/87/F/FL)
Avail: NTIS HC A10/MF A02 CSCL 08G

Various space concepts were discussed during the past 20 years for a global improvement of the knowledge of the earth's gravity field. The concepts reach from high-low and low-low satellite-to-satellite tracking via tethered satellite gradiometers to sophisticated superconducting gradiometers. The purpose is to show that starting from one basic equation three criteria are sufficient to typify the various concepts and define the underlying observation model. Furthermore the different error sources, in particular, the time varying part of self-gravitation, and the expected signal size of all six gravity gradient components shall be discussed. Author

N90-20558*# Texas Univ., Austin. Center for Space Research.
STUDIES OF AN ORBITAL GRADIOMETER MISSION
B. E. Schutz, J. B. Lundberg, S. Bettadpur, and B. D. Tapley *In* Ohio State Univ., Progress in the Determination of the Earth's Gravity Field Jun. 1989 p 176-179 (For primary document see N90-20513 13-46)
(Grant NAG5-528)
Avail: NTIS HC A10/MF A02 CSCL 08G

The goal of using an orbital gradiometer mission to provide an accurate (1 to 2 mgal), high resolution (1 by 1 deg), global map of the earth's geopotential is currently being investigated. This investigation involves the simulation of the satellite ephemeris and the corresponding gradiometer measurements which can be used in the study of various techniques and methodologies that were proposed to recover the parameters used in modeling the geopotential. Also, the effects on the mission of various time varying forces acting on the spacecraft were included in the studies.
Author

N90-20559*# Dornier-Werke G.m.b.H., Friedrichshafen (Germany, F.R.).
ARISTOTELES: A EUROPEAN APPROACH FOR AN EARTH GRAVITY FIELD RECOVERY MISSION
R. Benz, H. Faulks, and M. Langemann *In* Ohio State Univ., Progress in the Determination of the Earth's Gravity Field Jun. 1989 p 180-183 (For primary document see N90-20513 13-46)
Avail: NTIS HC A10/MF A02 CSCL 08G

Under contract of the European Space Agency a system study for a spaceborne gravity field recovery mission was performed, covering as a secondary mission objective geodetic point positioning in the cm range as well. It was demonstrated that under the given programmatic constraints including dual launch and a very tight development schedule, a six months gravity field

mission in a 200 km near polar, dawn-dusk orbit is adequate to determine gravity anomalies to better than 5 mgal with a spatial resolution of 100 x 100 km half wavelength. This will enable scientists to determine improved spherical harmonic coefficients of the Earth gravity field equation to the order and degree of 180 or better. Author

N90-20560*# Office National d'Etudes et de Recherches Aerospatiales, Paris (France).
THE GRADIO SPACEBORNE GRAVITY GRADIOMETER: DEVELOPMENT AND ACCOMMODATION
A. Bernard *In* Ohio State Univ., Progress in the Determination of the Earth's Gravity Field Jun. 1989 p 184-187 (For primary document see N90-20513 13-46)
Avail: NTIS HC A10/MF A02 CSCL 08G

The European ARISTOTELES mission aims at the determination of the Earth's gravity field at short wavelength with a global coverage. Gravity gradient measurements will be achieved during six months by the GRADIO instrument onboard a dedicated satellite in a near dawn-dusk sun-synchronous orbit at an altitude of 200 km. The objective is an accuracy of better than 5 mgals for gravity anomalies, at ground level for blocks of 1 x 1 deg. According to present knowledge of the potential, the recovery of higher spherical harmonics (degree and order greater than 30) is of main importance. This leads to focus on the variations of the measured components T(sub ij) of the gravity gradient tensor, at frequencies greater than 5 x 10(exp -3) Hz. The resolution, required for the gradiometer is 10(exp -2) Eotvos (i.e., 10(exp -11)/s squared) with an averaging time of 4 s. Author

N90-20561*# EG and G Washington Analytical Services Center, Inc., Lanham, MD.
HIGH RESOLUTION ANALYSIS OF SATELLITE GRADIOMETRY
O. L. Colombo *In* Ohio State Univ., Progress in the Determination of the Earth's Gravity Field Jun. 1989 p 188-192 (For primary document see N90-20513 13-46)
(Contract NAS5-28067)
Avail: NTIS HC A10/MF A02 CSCL 08G

Satellite gravity gradiometry is a technique now under development which, by the middle of the next decade, may be used for the high resolution charting from space of the gravity field of the earth and, afterwards, of other planets. Some data analysis schemes are reviewed for getting detailed gravity maps from gradiometry on both a global and a local basis. It also presents estimates of the likely accuracies of such maps, in terms of normalized spherical harmonics expansions, both using gradiometry alone and in combination with data from a Global Positioning System (GPS) receiver carried on the same spacecraft. It compares these accuracies with those of current and future maps obtained from other data (conventional tracking, satellite-satellite tracking, etc.), and also with the spectra of various signals of geophysical interest. Author

N90-20562*# National Aeronautics and Space Administration. Goddard Space Flight Center, Greenbelt, MD.
SATELLITE RADAR ALTIMETRY OVER ICE. VOLUME 1: PROCESSING AND CORRECTIONS OF SEASAT DATA OVER GREENLAND
H. Jay Zwally, Anita C. Brenner, Judith A. Major, Thomas V. Martin (Van Martin Consulting, Inc., Rockville, MD.), and Robert A. Bindschadler Jan. 1990 147 p
(NASA-RP-1233-Vol-1; Rept-89B00239; NAS 1.61:1233-Vol-1)
Avail: NTIS HC A07/MF A01 CSCL 08C

The data-processing methods and ice data products derived from Seasat radar altimeter measurements over the Greenland ice sheet and surrounding sea ice are documented. The corrections derived and applied to the Seasat radar altimeter data over ice are described in detail, including the editing and retracking algorithm to correct for height errors caused by lags in the automatic range tracking circuit. The methods for radial adjustment of the orbits and estimation of the slope-induced errors are given. Author

N90-20563*# National Aeronautics and Space Administration. Goddard Space Flight Center, Greenbelt, MD.
SATELLITE RADAR ALTIMETRY OVER ICE. VOLUME 2: USERS' GUIDE FOR GREENLAND ELEVATION DATA FROM SEASAT
H. Jay Zwally, Judith A. Major, Anita C. Brenner, Robert A. Bindschadler, and Thomas V. Martin (Van Martin Consulting, Inc., Rockville, MD.) Jan. 1990 84 p
(NASA-RP-1233-Vol-2; Rept-89B00240; NAS 1.61:1233-Vol-2)
Avail: NTIS HC A05/MF A01 CSCL 08C

A gridded surface-elevation data set and a geo-referenced data base for the Seasat radar altimeter data over Antarctica are described. It is intended to be a user's guide to accompany the data provided to data centers and other users. The grid points are on a polar stereographic projection with a nominal spacing of 20 km. The gridded elevations are derived from the elevation data in the geo-referenced data base by a weighted fitting of a surface in the neighborhood of each grid point. The gridded elevations are useful for the creating smaller-scale contour maps, and examining individual elevation measurements in specific geographic areas. Tape formats are described, and a FORTRAN program for reading the data tape is listed and provided on the tape. Author

N90-20564*# National Aeronautics and Space Administration. Goddard Space Flight Center, Greenbelt, MD.
SATELLITE RADAR ALTIMETRY OVER ICE. VOLUME 4: USERS' GUIDE FOR ANTARCTICA ELEVATION DATA FROM SEASAT
H. Jay Zwally, Judith A. Major, Anita C. Brenner, Robert A. Bindschadler, and Thomas V. Martin (Van Martin Consulting, Inc., Rockville, MD.) Jan. 1990 57 p
(NASA-RP-1233-Vol-4; Rept-89B00241; NAS 1.61:1233-Vol-4)
Avail: NTIS HC A04/MF A01 CSCL 08C

A gridded surface-elevation data set and a geo-referenced data base for the Seasat radar altimeter data over Greenland are described. This is a user guide to accompany the data provided to data centers and other users. The grid points are on a polar stereographic projection with a nominal spacing of 20 km. The gridded elevations are derived from the elevation data in the geo-referenced data base by a weighted fitting of a surface in the neighborhood of each grid point. The gridded elevations are useful for the creating of large-scale contour maps, and the geo-referenced data base is useful for regridding, creating smaller-scale contour maps, and examinating individual elevation measurements in specific geographic areas. Tape formats are described, and a FORTRAN program for reading the data tape is listed and provided on the tape. Author

N90-20565# Instituto de Pesquisas Espaciais, Sao Jose dos Campos (Brazil).
A SYSTEM FOR ANALYSIS AND INTERPRETATION OF LINEAMENTS IN REMOTE SENSING IMAGES
Paulo OuveraSimoni, Valter Rodrigues, and Pedro Paulo BalbiOliveira Aug. 1989 10 p Presented at the 6th Scandinavian Conference on Image Analysis, Oulu, Finland, 19-22 Jun. 1989
(INPE-4893-PRE/1494) Avail: NTIS HC A02/MF A01

An interactive knowledge-based vision system for structural geology under development, aimed at helping the extraction of lineations and lineaments, is described. Many factors (e.g., sensor type, position of the observer, shadowing, knowledge about dominant structures) that act over the detection of linear features, and over the inference of relief convexity and the type of feature are considered. The stored knowledge allows reinforcing image processing algorithm parameters, choosing the region under focus, and generating and confirming hypotheses about the geologic significance of an extracted linear element. Author

N90-20566*# National Aeronautics and Space Administration. Goddard Space Flight Center, Greenbelt, MD.
ANALYSIS OF ALTIMETRY OVER INLAND SEAS
A. Y. Au, R. D. Brown (ST Systems Corp., Lanham, MD.), and J.

E. Welker Washington Apr. 1990 80 p
(NASA-TM-100729; NAS 1.15:100729; Rept-89B00107) Avail: NTIS HC A05/MF A01 CSCL 08B

Satellite-based altimetric data taken by GEOS-3 and SEASAT over the Black Sea and Caspian Sea are analyzed and a least squares collocation technique is used to predict the geoid undulation on a .25-degree by .25-degree grid and to transform these geoid undulations to free air gravity anomalies. This project entailed processing satellite altimeter data over inland seas for recovery of area mean gravity information. Gravity information in this area of the world is not readily available, so the possibility of obtaining it from the processing of altimeter observations is attractive. The principal objective was to complete and extend analyses done in a previous study, verify those results, and document the results and techniques. A secondary objective was to improve the algorithms and results, if possible. The approach used involved editing geoid height data to remove overland data; evaluating geoid height differences at crossover points; removing orbit errors from geoid heights using crossover differences; gridding geoid height data at .25-degree by .25-degree intervals; and estimating the gravity anomalies from gridded geoid heights using the collocation technique. Author

N90-20567# Colorado State Univ., Fort Collins. Dept. of Atmospheric Science.
THEORETICAL MODELING STUDIES OF THE MARINE PLANETARY Annual Report, 1 Jan. - 31 Dec. 1989
David A. Randall 31 Dec. 1989 3 p
(Contract N00014-89-J-1364)
(AD-A217200) Avail: NTIS HC A01/MF A01 CSCL 04/2

A new type of boundary-layer model is developed to combine second-order closure with a bulk presentation of the verticle structure. The boundary layer depth and turbulence kinetic energy (TKE) are prognostically determined. The large turbulent eddies that are primarily responsible for the fluxes are modeled as convective circulations, with ascending and descending branches. The upper part of the attached figure illustrates the structure of the PBL as represented in the model. The interior of the boundary layer is bounded above by a thin entrainment layer and below by a thin ventilation layer. Conservative variables such as the equivalent potential temperature have quadratic profiles in the interior. Convective circulations occur, with rising branches occupying fractional area sigma, which is predicted by the model. The lower panel is a plot of the fractional area covered by rising motion, sigma, as a function of the ratio of the entrainment rate to the ventilation rate. As indicated in the figure, the model predicts that as the entrainment rate increases the fractional area covered by rising motion decreases; rapid entrainment is associated with small sigma. It is hoped that an improved theoretical understanding of and predictive capability for partly cloudy boundary layers may be gained, and these ideas will be tested against data acquired in the field. Also, the role of air-sea interactions in regulating cloud amount in the marine boundary layer will be investigated. GRA

N90-20568# Utah State Univ., Logan. Center for Atmospheric and Space Sciences.
SOLAR CYCLICAL TREND STUDY OF THE MID-LATITUDE, QUIET-TIME, MERIDIONAL, NEUTRAL WINDS AT WINTER SOLSTICE CONDITIONS M.S. Thesis
Ronald Lee Breninger 1989 84 p Sponsored by AFIT
(AD-A217398; AFIT/CI/CIA-89-031) Avail: NTIS HC A05/MF A01 CSCL 04/1

Located within the region of the thermosphere is the major portion of the ionosphere. Distribution of the ionospheric plasma within this region is a function of atmospheric mass and energy transport. For the current study, the component of the neutral wind along the magnetic meridian is derived from ground-based ionosonde measurements of the F2 peak layer height. Meridional wind variations with respect to location, universal time, and level of solar activity are the focal points on this investigation. The primary timescale of interest covers a period of one solar cycle, from 1977 to 1987. Data from one station have been extended to 1965 to study the repetitive nature of solar activity on the meridional winds. Results indicate a definite variation of wind speed and direction, which correlates with changing levels of solar activity. It is hoped that the results will aid current efforts to develop ionospheric models and enhance their forecasting capabilities. GRA

N90-20569# R and D Associates, Marina Del Rey, CA.
FIRST-ORDER INTENSITY STATISTICS FOR NON-RAYLEIGH FADING Technical Report, 1 Jan. - 31 Dec. 1988
Lester L. DeRaad, Jr. and Morgan K. Grover 1 Feb. 1990 331 p
(Contract DNA001-88-C-0046; DNA Proj. P99-GMXD)
(AD-A217572; RDA-TR-022618902-002; DNA-TR-89-150) Avail: NTIS HC A15/MF A02 CSCL 04/1

First-order intensity statistics under multipath scintillation conditions which are not sufficiently severe to lead to fully developed Rayleigh fading are examined. It is shown that neither Rice nor Nakagami-m statistics are accurate in general. Actual signal intensity statistics can be systematically characterized in terms of the refractive index spatial power spectrum and the signal Fresnel length. Numerous calculated results are provided for signal intensity distributions and channel symbols bit error rates in non-Rayleigh fading. GRA

N90-20570# California Univ., Berkeley. Lawrence Berkeley Lab. Earth Sciences Div.
SEISMIC CHARACTERIZATION OF FRACTURE PROPERTIES
L. R. Myer, L. J. Pyrak-Nolte, D. Hopkins, and N. G. W. Cook (California Univ., Berkeley.) Jan. 1990 7 p Presented at the International Conference for High-Level Radioactive Waste Management, Las Vegas, NV, 8-12 Apr. 1990
(Contract DE-AC03-76SF-00098)
(DE90-007759; LBL-28333; CONF-900406-36) Avail: NTIS HC A02/MF A01

The purpose is to show that there is a relationship, both empirical and theoretical, between the measured seismic response, the mechanical stiffness (also referred to as specific stiffness) of fractures and their hydraulic conductivity. Laboratory measurements of the mechanical stiffness, hydraulic conductivity and seismic properties of natural fractures are summarized. A theoretical model for the amplitude and group time delay for compressional and shear waves transmitted across a single fracture is presented. Predictions based on this model are compared with laboratory measurements. Finally, the results for a single fracture are extended to multiple parallel fractures. DOE

N90-20571# Midwest Research Inst., Golden, CO.
SPECTRAL SOLAR RADIATION DATA BASE DOCUMENTATION, VOLUME 1
Carol J. Riordan, Daryl R. Myers, and Roland L. Hulstrom Jan. 1990 62 p
(Contract DE-AC02-83CH-10093)
(DE89-009447; SERI/TR-215-3513A-Vol-1) Avail: NTIS HC A04/MF A01

The Solar Energy Research Institute (SERI), Electric Power Research Institute, Florida Solar Energy Center, and Pacific Gas and Electric Company cooperated to produce a spectral solar radiation data base representing a range of atmospheric conditions. These data will help to characterize the natural variability in the spectral (color) content of outdoor solar radiation so that the sensitivity of spectrally selective solar devices (such as photovoltaics) to these variations can be studied quantitatively. Volume 1 of this report documents the history, approach, content and format of the data base. DOE

N90-20572*# National Aeronautics and Space Administration. Goddard Space Flight Center, Greenbelt, MD.
USER'S GUIDE: PROGRAMS FOR PROCESSING ALTIMETER DATA OVER INLAND SEAS
A. Y. Au, R. D. Brown (ST Systems Corp., Lanham, MD.), and J. E. Welker Apr. 1989 113 p
(NASA-TM-100730; Rept-89B00106; NAS 1.15:100730) Avail: NTIS HC A06/MF A01 CSCL 04A

The programs described were developed to process GEODYN-formatted satellite altimeter data, and to apply the processed results to predict geoid undulations and gravity anomalies of inland sea areas. These programs are written in standard FORTRAN 77 and are designed to run on the NSESCC IBM 3081(MVS) computer. Because of the experimental nature of these programs they are tailored to the geographical area analyzed. The attached program listings are customized for processing the altimeter data over the Black Sea. Users interested in the Caspian Sea data are expected to modify each program, although the required modifications are generally minor. Program control parameters are defined in the programs via PARAMETER statements and/or DATA statements. Other auxiliary parameters, such as labels, are hard-wired into the programs. Large data files are read in or written out through different input or output units. The program listings of these programs are accompanied by sample IBM job control language (JCL) images. Familiarity with IBM JCL and the TEMPLATE graphic package is assumed. Author

N90-20573# California Univ., Irvine. Dept. of Civil Engineering.
DAMAGE CHARACTERISTICS OF TIME DOMAIN HISTORIES
John Thomas Nov. 1989 71 p
(Contract W-7405-eng-48)
(DE90-008787; UCRL-21274) Avail: NTIS HC A04/MF A01

It is possible to create nomographs to characterize damage potential of candidate time histories, provided there exists extensive records of earlier time-histories and the damage that they have caused. Thus in order to create such nomographs, the correlated documentation between the input to the structure and the resulting damage is needed. In order to use the Response-Spectra approach, good statistical description of the input to the system is needed. Extensive literature exists on both these methods. The MAC method that has being developed for the present research has yet to be validated. However, if it is successful, it would provide a valuable link between the SEA method and the rational method. DOE

N90-20574# Air Force Geophysics Lab., Hanscom AFB, MA. Atmospheric Science Div.
RADAR DETECTION OF LIGHTNING AND ELECTRIC FIELDS Air Force Surveys In Geophysics
James I. Metcalf 16 Aug. 1989 34 p
(AD-A217894; GL-TR-89-0223; GL-AFSG-453) Avail: NTIS HC A03/MF A01 CSCL 04/1

In recent years, there has been increased interest in the use of radars to identify electrified clouds and to quantify electrification processes. The use of radars to observe lightning and to observe the effects of electrical fields on the orientations of hydrometeors is surveyed. Observations of lightning channels, conducted with increasing sophistication since the 1940's, have revealed the wavelength dependence of the reflectivity of lightning, the distribution of lightning echoes in storms, and the differential reflectivity of lightning. Observations of electrified clouds with polarization diversity radars during the 1970's and early 1980's revealed changes of orientations of ice crystals due to varying electric fields. These techniques can now be used in coordination with measurements of electrical fields and radio frequency emissions from lightning discharges to gain valuable new knowledge of the structure and evolution of electric fields in clouds. Several approaches to the continued investigations of electrical fields in clouds by radars are suggested. GRA

N90-20575# National Aeronautical Establishment, Ottawa (Ontario).
AN IMPROVED AIRBORNE WIND MEASUREMENT TECHNIQUE FOR THE NAE (NATIONAL AERONAUTICAL ESTABLISHMENT) TWIN OTTER
B. W. Leach and J. I. MacPherson Nov. 1989 46 p
(AD-A217978; NAE-AN-61; NRC-31023) Avail: NTIS HC A03/MF A01 CSCL 04/1

Airborne wind measurement techniques currently being used onboard the NAE Twin Otter Atmospheric Research Aircraft are described and their fundamental limitations are discussed. In particular, a recently acquired LTN-90-100 strapdown inertial reference system (IRS) demonstrates significant low frequency Schuler oscillations in its velocity components (attaining peak errors of 2 to 3 mps), actually degrading wind computation accuracy compared with older techniques. A new wind measurement technique, based on Kalman filter integration navigation approach, is described which solves this problem and provides wind computation accuracy superior to previous methods. Preliminary results, based on applying the Kalman filter to Twin Otter flight test data, indicate that inertial velocity accuracies of 0.3 mps RMS (per channel) are attainable, with a corresponding improvement in the accuracy of earth-referenced wind components. GRA

N90-20576# Naval Postgraduate School, Monterey, CA. Dept. of Meteorology.
CORRELATION OF ATMOSPHERIC OPTICAL TURBULENCE AND METEOROLOGICAL MEASUREMENTS M.S. Thesis
Gail M. Tirrell Vaucher Jun. 1989 158 p
(AD-A218019) Avail: NTIS HC A08/MF A01 CSCL 04/1

The correlation of meteorological events such as the jet stream, gravity waves and boundary layer circulation with the optical turbulence parameters, the transverse coherence length r sub o and the isoplanatic angle is essential for interpreting and forecasting imaging and laser systems performance. In support of the United States Air Force Relay Mirror Experiment, the Naval Postgraduate School performed a series of six site characterization measurements near Kihei, Maui, during August 1987 to July 1988. Spatial and temporal summaries of atmospheric events corresponding to the optical remote sensor data are presented using meteorological data from the National Weather Service Radiosonde Observation stations, synoptic charts, GOES-WEST infrared satellite images, and four Kihei, Maui rawinsonde datasets. To quantify the correlation between optical turbulence measurements and meteorological phenomena, four methods of calculating C square (T) from rawinsonde data were investigated. Results show that existing rawinsonde systems are inadequate for direct C square (T) calculation. However, moderate improvements in the vertical resolution, the temperature resolution and probe response time, will allow direct calculations of optical turbulence parameters from rawinsonde data. GRA

N90-20577# California Univ., Los Angeles.
QUANTIFYING AND REDUCING UNCERTAINTY IN THE ASSIMILATIVE MAPPING OF IONOSPHERIC ELECTRODYNAMICS Ph.D. Thesis
Delores J. Knipp 1989 192 p Sponsored by AFIT, Wright-Patterson AFB, OH
(AD-A218057; AFIT/CI/CIA-89-144) Avail: NTIS HC A09/MF A01 CSCL 04/1

The AMIE procedure, developed by Richmond and Kamide was applied to three periods: 23 to 24 July 1983, 18 to 19 Jan. 1984 and 19 Sep. 1984. The mapping procedure obtains optimal estimates of electrodynamic patterns from basis functions multiplied by an appropriate set of coefficients which are determined from a constrained least squares fit to the data. The impact of several additions to the procedure is shown and some of the geophysics implied by the results are analyzed. New estimates of auroral conductance are incorporated from satellite particle detectors and a satellite x ray imager. This new information is used to produce global estimates of conductance and to study the effect of uncertainty in those estimates on the estimates of the polar electric field structure. New (but somewhat indirect) observations relating to the electric field were incorporated: satellite magnetometer data and the vertical component of the ground magnetometer data. Addition of these data, as well as, increasing the number of estimated coefficients tend to reduce the uncertainty in the electric field estimates. The results demonstrate the ability of the AMIE procedure to define the temporal and spatial development of several important solar-wind magnetosphere-ionospheric interactions. Mappings of ionospheric response to the interplanetary Magnetic Field (IMF) east-west component is in excellent agreement with currently accepted theory. Enhancements of DP1 and DP2 current systems were observed. GRA

N90-20578# Air Force Geophysics Lab., Hanscom AFB, MA.
ATMOSPHERIC CHEMILUMINESCENCE: COCHISE AND FACELIF EXPERIMENTS Interim Scientific Report
Steven M. Miller, D. R. Sinclair, Jeffrey I. Steinfeld, C. Fell, Charles M. Phillips, I. Winkler, W. T. Rawlins, M. E. Fraser, H. C. Murphy, and G. E. Caledonia (Physical Sciences, Inc., Andover, MA.) 24 Feb. 1989 172 p
(AF Proj. 2310)
(AD-A218121; AFGL-TR-89-0070; ERP-1023) Avail: NTIS HC A08/MF A01 CSCL 04/1

During the last four years, many experiments have been performed in the COCHISE facility. Each of these experiments has measured a fundamental chemical quantity such as a radiative branching ratio, a quenching rate coefficient or a product vibrational energy distribution. These measurements are then provided for incorporation into the various atmospheric radiation codes such as NORSE, ARC, and AARC, where they provide a solid experimental footing for modeling the complex chemical system of the upper atmosphere. GRA

N90-20579# Arizona Univ., Tucson. Dept. of Geosciences.
THE EFFECTS OF STRUCTURE AND SOURCE COMPLEXITY ON WAVEFORMS: CRUSTAL STRUCTURE OF TIBET AND THE RECOVERY OF COMPLEX SEISMIC SOURCES Final Report, May 1987 - May 1989
Terry C. Wallace 7 Sep. 1989 198 p
(Contract F19628-87-K-0046; AF Proj. 2309; ARPA Order 5299)
(AD-A218202; GL-TR-89-0259) Avail: NTIS HC A09/MF A02 CSCL 08/11

In an attempt to better understand the effects of both source and path on regional distance waveforms, the crustal structure of Eurasia was investigated and an algorithm was developed for investigating complex seismic sources. Part 1 is a study based on the inversion of 130 regional distance waveforms for average crustal thickness and upper mantle Pn velocity beneath Tibet. Results indicate an increase in Pn velocity, coincident with the increase in crustal thickness, of about 0.2 km/s beneath the Plateau. Impulsive Pn arrivals from paths that cross the Tibetan Plateau can be modeled with a positive upper mantle gradient, indicating an upper mantle lid approx. 100 km thick beneath southern Tibet. This shield-like structure has important consequences for the propagation of regional phases Pg, Pn and Sn. Part 2 discusses an algorithm for time dependent moment tensor (TDMT) inversion. The algorithm was developed to investigate complex seismic sources, such as multiple earthquakes and, ultimately, explosions with tectonic release contamination. The TDMT inversion algorithm was tested with 3 synthetic data examples with varying degrees of complexity. It was also tested on the long period body waves for 3 earthquakes: the 1982 Yemen, the 1971 San Fernando, and the 1952 Kern County earthquakes. Preliminary modeling in the nearfield of nuclear explosions yielded mixed results. GRA

N90-20580# Air Force Inst. of Tech., Wright-Patterson AFB, OH.
MEASUREMENTS OF THE INTERACTION OF HIGH-VOLTAGE BIASSED CONDUCTORS WITH THE IONOSPHERE M.S. Thesis - Utah State Univ.
Jon Alan Roberts 1989 128 p
(AD-A218285; AFIT/CI/CIA-89-064) Avail: NTIS HC A07/MF A01 CSCL 22/2

The Space Power Experiments Aboard Rockets program was developed to study the interaction of high-voltage biassed conductors with the low earth orbit environment. The experiment utilized two spherical conductors, which were biassed to potentials as high as 45,000 volts, and the steady-state current-voltage characteristics were analyzed. The spheres were flown in three different orientations with respect to the earth's magnetic field. At times, only one sphere was biassed so that the current collection characteristics of a single spherical conductor could be studied. At other times, both spheres were biassed to approximately the same voltage, or to greatly differing voltages so that the interactions between charge sheaths could be studied. The failure of the plasma contactor allowed the rocket body to charge to up to several kilovolts negative during sphere biassing, resulting in the establishment of an unplanned positive ion sheath around the rocket body, thereby complicating the interpretation of the current-voltage characteristics of the spheres. GRA

N90-20581# Air Force Inst. of Tech., Wright-Patterson AFB, OH.
THE RECEIVING SYSTEM OF A DUAL DYE LIDAR TO STUDY MOLECULAR AND AEROSOL DENSITIES AT THE BASE OF THE STRATOSPHERE M.S. Thesis - Arizona Univ.
John Dexter Davidson, Jr. 1989 62 p
(AD-A218286; AFIT/CI/CIA-89-073) Avail: NTIS HC A04/MF A01 CSCL 04/1

The measurement of atmospheric constituents and their motion plays an integral part in the understanding of the Earth-Biosphere interaction. This circumstance has resulted in rapid growth within the field of remote sensing. Remote sensing systems may passively collect electromagnetic or acoustic waves transmitted from a distant point, or they may illuminate a volume of the atmosphere with radiation and observe the backscattered signal. These instruments operate over the entire spectrum from gamma waves to extremely low frequency radio waves. This thesis is concerned with the design and the construction of the optical receiver of a remote sensing instrument called a LIDAR, for light detection and ranging. The operating principles and design of an optical receiver for a Light Detection and Ranging (LIDAR) remote sensing instrument are addressed. The performance and limitations of a biaxial monostatic LIDAR system utilizing this design are investigated. The complete optical and structural design of the receiver, including specifications of components are outlined. The thermal stabilization of the detector assembly and the integration of control electronics are described. A detailed discussion of alignment procedures and possible improvements are made. A sample observation is presented with suggestions for fully automating the system. GRA

47 METEOROLOGY AND CLIMATOLOGY

Includes weather forecasting and modification.

N90-20582*# District of Columbia Univ., Washington, DC.
CLOUD TYPES AND THE TROPICAL EARTH RADIATION BUDGET, REVISED
Harbans L. Dhuria and H. Lee Kyle (National Aeronautics and Space Administration. Goddard Space Flight Center, Greenbelt, MD.) Dec. 1989 79 p Revised Submitted for publication
(Grant NAG5-1012)
(NASA-CR-180475; NAS 1.26:180475) Avail: NTIS HC A05/MF A01 CSCL 04A

Nimbus-7 cloud and Earth radiation budget data are compared in a study of the effects of clouds on the tropical radiation budget. The data consist of daily averages over fixed 500 sq km target areas, and the months of July 1979 and January 1980 were chosen to show the effect of seasonal changes. Six climate regions, consisting of 14 to 24 target areas each, were picked for intensive analysis because they exemplified the range in the tropical cloud/net radiation interactions. The normal analysis was to consider net radiation as the independent variable and examine how cloud cover, cloud type, albedo and emitted radiation varied with the net radiation. Two recurring themes keep repeating on a local, regional, and zonal basis: the net radiation is strongly influenced by the average cloud type and amount present, but most net radiation values could be produced by several combinations of cloud types and amount. The regions of highest net radiation (greater than 125 W/sq m) tend to have medium to heavy cloud cover. In these cases, thin medium altitude clouds predominate. Their cloud tops are normally too warm to be classified as cirrus by the Nimbus cloud algorithm. A common feature in the tropical oceans are large regions where the total regional cloud cover varies from 20 to 90 percent, but with little

regional difference in the net radiation. The monsoon and rain areas are high net radiation regions. Author

N90-20583*# National Aeronautics and Space Administration. Langley Research Center, Hampton, VA.
DOWNWARD SHORTWAVE SURFACE IRRADIANCE FROM 17 SITES FOR THE FIRE/SRB WISCONSIN EXPERIMENT Technical Memorandum, 12 Oct. - 2 Nov. 1986
Charles H. Whitlock, John E. Hay, David A. Robinson, Stephen K. Cox, David I. Wardle, and Stuart R. LeCroy (Lockheed Engineering and Sciences Co., Hampton, VA.) Feb. 1990 275 p
(NASA-TM-102596; NAS 1.15:102596) Avail: NTIS HC A12/MF A02 CSCL 04B

A field experiment was conducted in Wisconsin during Oct. to Nov. 1986 for purposes of both intensive cirrus cloud measurments and SRB algorithm validation activities. The cirrus cloud measurements were part of the FIRE. Tables are presented which show data from 17 sites in the First ISCCP (International Satellite Cloud Climatology Project) Regional Experiment/Surface Radiation Budget (FIRE/SRB) Wisconsin experiment region. A discussion of intercomparison results and calibration inconsistencies is also included. Author

N90-20584# Science Applications International Corp., McLean, VA.
ANALYSIS OF GALE (GENESIS OF ATLANTIC LOWS EXPERIMENT) DATA Final Report, 11 Aug. 1986 - 30 Sep. 1989
Ellis Hyman, Keith Sashegyi, Darrell Strobel, John Hardgrove, and Sethu Raman Dec. 1989 392 p Prepared in cooperation with North Carolina State University
(Contract N00014-86-C-2365)
(AD-A217182; SAIC-89/1746) Avail: NTIS HC A17/MF A01 CSCL 04/2

The Limited Area Numerical Weather Prediction system is being developed to accurately simulate and study the development of extratropical cyclones, which rapidly develop off the east coast of the U.S. and the North Atlantic Ocean. Data collected during the Genesis of Atlantic Lows Experiment (GALE) and the Experiment on Rapidly Intensifying Cyclones in Atlantic (ERICA) are being used for model simulations and studies and for testing of the software developed. Simulations were run for the case of cold air damming and coastal front formation and the subsequent offshore cyclogenesis during the second intensive observing period of GALE. Software is developed to read and unpack the special packed binary data for the analyses and forecasts on the National Meteorological Center (NMC) history tapes, and for the preprocessing of GALE data on the VAX computers. A dry convective adjustment scheme was developed to parameterize sub-grid scale dry convection and incorporated a lateral boundary formulation for use in the model for the simulation of GALE storms. A vertical mode initialization scheme was developed and extensively tested with analyses for the GALE period from the NMC. For use with the initialization procedures, the solver for partial differential equations was also modified as described. For the analysis of the GALE data, an efficient analysis scheme was developed. GRA

N90-20585# Massachusetts Inst. of Tech., Lexington. Lincoln Lab.
A CLOUD CLIMATOLOGY FOR THE NORTH PACIFIC AREA CENTERED AT SHEMYA, ALASKA
J. C. Barnes, H. K. Burke, and T. M. Joss 22 Nov. 1989 124 p
(Contract F19628-90-C-0002)
(AD-A217334; TR-864; ESD-TR-89-203) Avail: NTIS HC A06/MF A01 CSCL 04/2

A cloud climatology data set for the North Pacific area is presented based on monthly statistics of mean cloud percent and frequency of occurrence of cloud amount for 18 grid-point locations within approximately 1000 km of Shemya, Alaska. The cloud statistics are derived from the Air Force 3D-Nephanalysis Global Cloud Archive (3D-NEPH Model) for the period 1977 to 1983. These cloud statistics, together with atmospheric temperature profiles derived from the Air Force Summarized Analysis Data Set, are used to determine estimates of cloud top heights and temperatures for representative months at the various locations. GRA

N90-20586# Arizona Univ., Tucson. Dept. of Atmospheric Sciences.
STRUCTURE AND DYNAMICS OF THE ARIZONA MONSOON BOUNDARY Ph.D. Thesis
Thomas Charles Adang 1989 123 p Sponsored by AFIT
(AD-A217378; AFIT/CI/CIA-89-035) Avail: NTIS HC A06/MF A01 CSCL 04/1

The Arizona Monsoon Boundary is defined as the boundary separating two distinctly different air masses over Mexico, the southwestern U.S. and the adjacent Pacific during the summer. Its structure and dynamics are examined by cross sectional analysis using 3 different data sources: (1) a time height cross section, constructed using radiosonde observations, at the time the boundary initially passed through Tucson in 1984; (2) a composite cross section through the boundary, constructed from FNOC analysis; and (3) a cross section through the boundary using high resolution fields of temperature, moisture, and geopotential height obtained from the VISSR Atmospheric Sounder (VAS). All 3 cross sections showed similar structure. This boundary resembles a mid-latitude front with a distinct and relatively sharp air mass change across the boundary, forced almost entirely by confluence. A direct ageostrophic circulation is produced by this forcing, giving weak ascent on the warm, moist side of the boundary. Gradients and flow associated with the composite boundary are weaker, by a factor of 4, than those associated with strong mid-latitude fronts. However, the VAS cross section suggests that, at times, the strength of the boundary approaches that of middle-latitude fronts. The wind shear suggested by the composite boundary ought to be unstable to baroclinic or barotropic processes. Disturbances developing along the boundary were observed. GRA

N90-20587# National Climatic Center, Asheville, NC.
US NAVY REGIONAL CLIMATIC STUDY OF THE CENTRAL EAST ASIAN COAST AND ASSOCIATED WATERS Final Report
Joe D. Elms Nov. 1989 327 p Sponsored by Naval Oceanography Command Center, Stennis Space Center, MS
(AD-A217448; NAVAIR-50-1C-556) Avail: NTIS HC A15/MF A02 CSCL 04/2

This marine study covers the region off the Pacific Coast of Asia from the equator to 45 deg N and from 105 deg E to 140 deg E, encompassing the South China Sea, Philippine Sea, East China Sea, Yellow Sea, and the southern portion of the Sea of Japan. The data came mostly from the observations collected by ships of opportunity of many different nations. This climatic study of marine environment consists of monthly charts and tables of: (1) Clouds; (2) Atmospheric precipitation; (3) Visibility tables; (4) Ceiling visibility (mid-range/low range); (5) Wind visibility cloudiness; (6) Scalar mean wind speed; (7) Wind speed less than 11 and greater or equal to 34 knots; (8) Wind speed 11 to 21 and 22 to 33 knots; (9) Surface wind roses; (10) Air and sea temperature; (11) Wave height isopleths; (12) Wave height tables; (13) Ocean surface currents (seasonal). GRA

N90-20588# Lawrence Livermore National Lab., CA.
SOUTHERN OSCILLATION IN THE OSU COUPLED UPPER OCEAN/ATMOSPHERE GCM
Kenneth R. Sperber, Sultan Hameed (State Univ. of New York, Stony Brook.), W. Lawrence Gates, and Gerald L. Potter Jan. 1990 9 p Presented at the 14th Annual Climate Diagnostics Workshop, San Diego, CA, 16-20 Oct. 1989
(Contract W-7405-eng-48)
(DE90-008415; UCRL-102861; CONF-8910338-2) Avail: NTIS HC A02/MF A01

With the advent of coupled ocean/atmosphere global climate models it has become possible to study their inherent natural variability. This natural variability arises as a consequence of the encoded physics and dynamics since the only imposed constraint

on the simulation is the diurnal and annual cycle of solar radiation. One of the dominant modes of interannual variability is the Southern Oscillation (SO). The Oregon State University coupled upper ocean/atmosphere global climate model has been shown to qualitatively simulate many aspects of the SO. Sea-level pressure (SLP), sea-surface temperature (SST), thermocline layer temperature, surface air temperature, precipitation, and mixed layer currents are among the simulated fields which reproduce SO characteristics. Thus the nature of ocean/atmosphere feedback processes can be investigated. DOE

N90-20589# Lawrence Livermore National Lab., CA. Atmospheric and Geophysical Sciences Div.
AN INTERCOMPARISON OF GENERAL CIRCULATION MODEL PREDICTIONS OF REGIONAL CLIMATE CHANGE
Stanley L. Grotch Nov. 1989 25 p Presented at the International Conference on Modeling of Global Climate Change and Variability, Hamburg, Fed. Republic of Germany, Sep. 1989
(Contract W-7405-eng-48)
(DE90-008325; UCRL-102793; CONF-8909308-1) Avail: NTIS HC A03/MF A01

Simulations using the best-available general circulation models (GCMs) to estimate the sensitivity of the climate to a doubling of the atmospheric carbon dioxide concentration are in broad general agreement that, at equilibrium, the global annual average surface air temperature would increase about 2 to 5 K. Because of considerable public interest in potential climate changes due to greenhouse gases, there is pressure to use the predictions of these GCM simulations for regional climate assessments. In this work, statistical intercomparisons were made of the estimates for both the control and the equilibrium changes in surface air temperature and precipitation after a doubling of atmospheric CO(sub 2) as predicted by five GCMs. Intercomparisons were also made with historical data for the simulations of current climate. Two data fields which are of particular importance in regional impact studies are examined here: surface air temperature and precipitation. The seasonally averaged results predicted by five GCMs are intercompared among models and with observational data for the control climate over different scales. Intercomparisons are also made among the models for predictions of the change at equilibrium in these two variables after a doubling of atmospheric carbon dioxide. DOE

N90-20590# Air Force Inst. of Tech., Wright-Patterson AFB, OH.
COASTAL FRONTOGENESIS AND ASSOCIATED SEVERE WEATHER ON 13 MARCH 1986 (GALE IOP 13) M.S. Thesis
William H. Bauman, III 1989 126 p
(AD-A217708; AFIT/CI/CIA-89-037) Avail: NTIS HC A07/MF A01 CSCL 04/2

An investigation of the mesoscale structure of coastal frontogenesis and associated severe weather on 13 March 1986 occurring in North Carolina was conducted. A case study focused on the development of a coastal front and subsequent occurrence of severe weather during the GALE (Genesis of Atlantic Lows Experiment) field project. The GALE surface and upper-air data network was used to describe the kinematic and thermodynamic processes in the vicinity of the coastal front and severe weather. The presence of a mesoscale circulation conducive to frontogenesis was found from surface analyses of standard operational and special GALE data plus time-averaged divergence fields. The mesoscale divergence patterns plus numerical calculations of frontogenesis implied the coastal front developed in discontinuous sections as several convergence lines apparently formed independent of each other. The three-dimensional atmospheric structure in the vicinity of the frontogenesis was examined by means of divergence fields. Vertical velocities were calculated using the kinematic, thermodynamic, and quasi-geostrophic methods. Three types of mesoscale rainbands were observed and analyzed using 15 minute digitized radar data. Warm-sector rainbands developed south of the coastal front while convective cold-frontal and narrow cold-frontal rainbands developed along the coastal front as it moved southeast as a cold front. Severe weather mechanisms were investigated to determine why this unusual weather occurred during a late winter coastal front. Analysis of the K-index, lifted index, and dynamic ingredients conducive to severe weather indicated conditions did in fact exist for severe weather to form. GRA

N90-20591# Purdue Univ., West Lafayette, IN.
AN ESTIMATION OF RAINFALL AMOUNTS USING RADAR-DERIVED Z-R RELATIONSHIPS M.S. Thesis
Richard M. Harter Aug. 1989 69 p Sponsored by AFIT, Wright-Patterson AFB, OH
(AD-A217950; AFIT/CI/CIA-89-122) Avail: NTIS HC A04/MF A01 CSCL 04/2

Directly measured reflectivity values (Z) by radar and rainfall values (R) by rain gages are correlated over five minutes intervals to a maximum of one hour for 260 rain gage points. A nonlinear regression of the expression R = aZ sub b is performed, with Z the independent variable. This expression is solved for Z to obtain Z-R relationships of the form Z = AR sub B for each five minute period. A median value of the coefficient A and the exponent B is computed to represent the complete hour. Z-R relationships are then used to calculate estimates of average rainfall amount over a rain gage area. These radar-estimated values of average rainfall amount are then compared to the average rainfall amounts measured by the rain gages for dependent as well as independent data sets. The significant effect of hail is also examined. Results indicate that directly measured Z-R relationships derived from data containing shallow precipitation gradients were the most accurate in estimating the average water amount for the rain gage network area. In contrast, Z-R relationships derived from data containing steeper gradients of precipitation were not as accurate in estimating the average rainfall amount. The Z-R relationships of Marshall-Palmer, Jones, and the NEXRAD relationship underestimated the average rainfall amount by almost 30 percent for the data set containing shallow gradients of precipitation. GRA

N90-20592# Oklahoma Univ., Norman. School of Meteorology.
DERIVATION OF KINEMATIC FIELDS USING WIND PROFILER DATA FROM THE 1985 PRE-STORM EXPERIMENT M.S. Thesis
Jeffrey Douglas Powell 1989 151 p Sponsored by AFIT, Wright-Patterson AFB, OH
(AD-A217952; AFIT/CI/CIA-89-024) Avail: NTIS HC A08/MF A01 CSCL 04/2

During the May and June 1985 PRE-STORM experiment, three 50 MHz wind profilers were installed for the first time on the Great Plains to enhance the understanding of mesoscale system development and evolution. In order to utilize these profiler data for the computation of kinematic quantities, many instances of poor or missing data must be dealt with. Often, this requires the performance of separate screening, filling, interpolation, and filtering steps. The accomplishment of the latter three steps at once through the adaption of a Barnes objective analysis technique is proposed. Using wind covariance statistics from a Colorado profiler, a weight function is designed which assigns equal weight to equally correlated data in time and in the vertical. Features within vertical motion fields derived after application of this technique corresponds well with features seen in satellite imagery and contain detail unobtainable via analysis of rawinsonde data. The development of clear air wind observation systems through advances in Doppler radar technology has provided the meteorologist with a new generation measuring device, the wind profiler. Wind profilers can provide tropospheric wind profiles every few minutes at height intervals of 200 meters or less. It has long been known, via satellite imagery, that small scale upper air features exist and could partially be responsible for poor forecasts. GRA

N90-20593# Naval Postgraduate School, Monterey, CA. Dept. of Meteorology.
A PROTOTYPE EXPERT SYSTEM TO FORECAST SEVERE WINDS IN THE WESTERN MEDITERRANEAN SEA M.S. Thesis

Marcia L. Jones Jun. 1989 136 p
(AD-A218017) Avail: NTIS HC A07/MF A01 CSCL 04/2

A prototype expert system is designed to forecast severe winds in the western Mediterranean Sea. The first version of the expert system is to nowcast levante conditions in the Strait of Gibraltar and to nowcast/forecast mistral conditions in the Gulf of Lion. Rules of thumb for these events from the Handbook for Forecasters in the Mediterranean (Brody and Nestor 1980) are tested with observations during the period September 1988 through February 1989. Of the 19 rules listed in the Handbook for levante, five are used in the expert system without modification, six are modified and eight are discarded. Of the 41 rules for the mistral, 14 are used without modification, two are slightly modified and 25 are eliminated. The first step in each case is to select adjacent land stations whose observations best infer the presence of the gale wind conditions over the open seas, where in situ observations are not available. The basic approach in the expert system is to provide an ordered sequence of rules (based on the verifications during the six month period) that the forecaster can continue to test until a forecast decision can be made with confidence. Operational testing is needed to refine the severe wind algorithm, which can be easily modified to include more empirical rules from forecasters in the future. GRA

N90-20594# Air Force Inst. of Tech., Wright-Patterson AFB, OH. Dept. of Atmospheric Science.
A MODELING STUDY OF THE CLOUD-TOPPED MARINE BOUNDARY LAYER M.S. Thesis - Colorado State Univ.
Thomas A. Guinn 1989 72 p
(AD-A218103; AFIT/CI/CIA-89-172) Avail: NTIS HC A04/MF A01 CSCL 04/2

A coupled convective-radiative, boundary layer model of marine stratocumulus clouds is presented. The model, which slightly generalized Lilly's (1968) cloud-topped mixed layer model, has as dependent variables the cloud-top height, the cloud-base height, mixed layer equivalent potential temperature and total water mixing ratio, the turbulent fluxes of equivalent potential temperature, total water mixing ratio, and virtual potential temperature, the cloud-top jumps of equivalent potential temperature and total water mixing ratio, the cloud-top temperature, and the net radiative flux divergence at cloud top and in the mixed layer. GRA

N90-20595# Air Force Geophysics Lab., Hanscom AFB, MA.
ADIABATIC AND DIABATIC INITIALIZATION OF THE AFGL (AIR FORCE GEOPHYSICS LABORATORY) GLOBAL SPECTRAL MODEL USING DYNAMIC NORMAL MODE AND NONLINEAR NORMAL MODE METHODS Final Report, Oct. 1987 - Sep. 1988
Larry Knowlton, Donald Norquist, and Ross Hoffman (Atmospheric and Environmental Research, Inc., Cambridge, MA.) 16 Feb. 1989 46 p
(AD-A218120; AFGL-TR-89-0044; ERP-1022) Avail: NTIS HC A03/MF A01 CSCL 04/2

Dynamic normal mode initialization (DNI) is applied to low and high resolution versions of the AFGL global spectral mode. This scheme is tested against the operational nonlinear normal mode initialization (NMI) procedure using both adiabatic and diabatic forms of the model tendencies. The DNI-based forecasts are comparable in accuracy to the NMI-based forecasts, with small differences between the adiabatic and diabatic versions of each. DNI initial conditions were somewhat more damped in the divergence fields than were the NMI fields. This is believed to be due to the frequency response characteristics of the DNI's forward-backward time scheme, which tended to partially damp resolvable wavelengths. GRA

N90-20596# Air Force Inst. of Tech., Wright-Patterson AFB, OH.
A METHOD FOR CORRECTING AND REDUCING THE PRESSURE DATA RECORDED AT THE PAM 2 STATIONS DURING GALE M.S. Thesis - North Carolina State Univ., Raleigh
Ronald L. Dunic 1989 78 p
(AD-A218165; AFIT/CI/CIA-89-087) Avail: NTIS HC A05/MF A01 CSCL 04/2

The data recorded at the PAM II stations during GALE (Genesis of Atlantic Lows Experiment) will enable researchers to gain a better understanding of the mesoscale processes involved in the various phenomena, however, the recorded pressure cannot be directly analyzed because it has not been corrected or reduced to sea level. A method for correcting and reducing the pressure data is presented. The Barnes objective analysis scheme was employed to determine the pressure correction for each PAM II station. The corrected pressures are reduced to sea level using the standard NWS reduction procedure outlined in the Manual of Barometry (1963), which was rather involved and included a number of assumptions to obtain the sea level pressures. An empirical formula was derived for the GALE dataset to calculate the sea level pressures for the PAM II stations. Pressure analyses involving the corrected and reduced PAM II pressures for two cases were in good agreement with the NMC analyses for the same times. Another method for representing the surface geostrophic wind field and the horizontal pressure field, is explored to determine the true ageostrophic wind components in a cold air damming situation and to produce a horizontal pressure field that would eliminate the arbitrariness of the standard pressure reduction procedure. The result is an improvement over the geostrophic wind, but the observed winds are still highly ageostrophic in this cold air damming situation. GRA

N90-20597# Air Force Inst. of Tech., Wright-Patterson AFB, OH.
FORECASTING 24 AND 48 HOUR INTENSITY CHANGES, FOR NORTHWESTERN PACIFIC TROPICAL CYCLONES, USING SATELLITE IMAGERY M.S. Thesis - Hawaii Univ.
Richard W. Hartman May 1989 58 p
(AD-A218174; AFIT/CI/CIA-89-060) Avail: NTIS HC A04/MF A01 CSCL 04/2

Sixteen years of typhoon data were studied, in an effort to develop a technique for forecasting tropical cyclone intensity changes in the Northwestern Pacific. The data base provided average changes for 24 and 48 hour periods along with the average duration of each phase (intensifying and dissipating). Further study revealed that the upper-level outflow patterns provide a means to adjust these average changes so a more realistic forecast could be generated for the individual storms. Forecasts were further improved by studying how land and other environmental features effect the life cycle of tropical cyclones. Results from the research were compiled and incorporated into a series of flow charts. These charts were created to enable individuals to quickly determine future intensities of cyclones given the storm's history and a current satellite picture. GRA

N90-20598# Air Force Inst. of Tech., Wright-Patterson AFB, OH.
AN AIRCRAFT INVESTIGATION OF A CONVECTIVE BOUNDARY LAYER OVER LAKE MICHIGAN M.S. Thesis - Purdue Univ.
Mary L. Hart 1989 125 p
(AD-A218175; AFIT/CI/CIA-89-052) Avail: NTIS HC A06/MF A01 CSCL 04/2

Meteorological data from research flights have been used to study the structure of a Type 1 Cloud-Topped Boundary Layer (CTBL) that formed as a result of air mass modification by a Cold Air Outbreak (CAO) over Lake Michigan on 10 January 1984. Surface and upper air data were used as a source of information to describe the synoptic scale conditions that accompanied the CAO event. Vertical cross-sections of the CTBL were constructed using the aircraft data and assuming a steady-state in the north-south direction (parallel to the cloud streets) during the 1 hour and 50 minute time period covered by the flights. The cross-sections show a complex CTBL structure with off-shore flow from both Wisconsin and Michigan imposing lateral boundary conditions on the convection. Spectral representations of the convective well-mixed boundary layer contained length scales of

approximately 3, 10, and 30 km. These length scales correspond to the basic convective mode (BCM), a higher convective mode (HCM) which relates to organization within the 2-D cloud streets, and the length scale associated with Mesoscale Cellular Convection (MCC). The temperature, specific humidity, and vertical velocity spectra also indicated the presence of strong turbulence in the lower CTBL. This turbulence is a result of strong thermal forcing caused by a large temperature difference between lake and atmosphere. GRA

N90-20599# Air Force Inst. of Tech., Wright-Patterson AFB, OH.

A SUB-CLOUD LAYER VORTICITY BUDGET ANALYSIS FOR TWO MICROBURST-PRODUCING STORMS FROM JAWS DUAL-DOPPLER DATA M.S. Thesis - St. Louis Univ.

Paul G. Lapointe 1989 101 p

(AD-A218180; AFIT/CI/CIA-89-018) Avail: NTIS HC A06/MF A01 CSCL 04/2

A vorticity component and budget analysis in three-dimensions is conducted for the subcloud layer of two microburst-producing storms using dual-Doppler derived winds. This research examines the vorticity associated with a single microburst-producing storm which occurred on 14 July 1982 and a multiple microburst-producing storm which occurred on 5 August 1982. The calculated vorticity data are examined over the storm domain (10 km x 10 km for the 14 July case and 15 km x 15 km for the 5 August case) and the microburst domain (5 km x 5 km) including two analysis times for the first case and three for the latter case. Results indicate that horizontal vorticity centers are coincident with strong horizontal gradients of vertical velocity and with areas of strong vertical shear. A vorticity budget analysis of the advection, divergence, and tilting terms, comprising the vorticity component equations, shows the magnitude of these terms to be greater in the microburst domain than in the storm domain. The difference in storm structure allow examination of the vorticity of a simple, nearly circular-symmetric microburst and that of a microburst within a complicated flow field. This leads to different vorticity distributions and budgets. GRA

N90-20600# Saint Louis Univ., MO.

APPLICATIONS OF MICROWAVE RADIOMETRIC MEASUREMENTS TO INFER TROPICAL CYCLONE INTENSITY AND STRENGTH M.S. Thesis

Don Kenneth Rhudy 1989 93 p Sponsored by AFIT, Wright-Patterson AFB, OH

(AD-A218273; AFIT/CI/CIA-89-063) Avail: NTIS HC A05/MF A01 CSCL 04/2

Microwave radiometric data from the Special Sensor Microwave Imager (SSM/I) are available in the form of Environmental Data Records (EDR's) and Sensor Data Records (SDR's). The EDR's provide meteorological parameters such as rain rates and surface wind speeds over the oceans, while the SDR's provide the measured brightness temperatures (TB's). In this study, the EDR's were used to compute latent heat released (LHR) in tropical cyclones. The TB's at 85 GHz were used to diagnose the current intensity of the tropical cyclone. GRA

N90-20601# Air Force Inst. of Tech., Wright-Patterson AFB, OH.

ATMOSPHERIC WIND MEASUREMENTS USING A 50 MHz IMAGING DOPPLER INTERFEROMETER RADAR M.S. Thesis - Utah State Univ.

Michael Jerome Volek 1989 102 p

(AD-A218277; AFIT/CI/CIA-89-049) Avail: NTIS HC A06/MF A01 CSCL 04/2

The 50 megahertz radar located near LaSalle, Colorado, also known as MENTOR, was operated as an Imaging Doppler Interferometer (IDI) in order to collect radar data. These data were collected from 18:25 Universal Time to 20:15 Universal Time on 14 October 1988. The data were used to measure winds in the lower atmosphere from less than 1 kilometer up to approximately 11.25 kilometers. The raw data wre transformed from time domain to frequency domain so that the IDI technique could be employed. The number of returns decreased with altitude, as did their radial distance off-zenith. Filters were developed to reject points that did not meet certain criteria, and then algorithms were developed to derive wind speeds and directions. GRA

N90-20602# Air Force Inst. of Tech., Wright-Patterson AFB, OH.

FORECASTING THE TORNADIC INTENSITIES OF THUNDERSTORMS BY MULTIVARIATE TECHNIQUES M.S. Thesis - North Carolina State Univ.

Dale Robert Perry 1989 152 p

(AD-A218284; AFIT/CI/CIA-89-085) Avail: NTIS HC A08/MF A01 CSCL 04/2

An investigation on the feasibility of statistically characterizing tornadic and non-tornadic thunderstorms after cells develop is the basis of this research. Nine tornado outbreak cases during the years 1984 through 1988 were studied. The intensity of each tornado producing thunderstorm cell was obtained. Satellite as well as radiosonde data were used to determine the meteorological parameters describing thunderstorm behavior. One of these parameters was the downstream mass flux of an anvil outflow plume (called UMAX) and the other was the rightward deviation angle of the anvil from the storm-relative flow (called MDA). These parameters were used in a two-dimensional kinematic anvil plume model implemented on an interactive computer data system which simulated the actual anvil plume as seen in satellite imagery. A modified Fujita scale rating system was employed to characterize each outbreak cell as a weighted mean called Fw and a weighted mean square called Fw-sq. Fw was a better indicator of tornadic intensity than UMAX and MDA were used as predictors in a bivariate regression model (two-variables) to predict the tornadic intensity of a given observed cell. Linear regression yielded promising results in correlating the data, and described a rising-ridge surface that related UMAX to MDA for both F sub -w. GRA

N90-20603# Air Force Inst. of Tech., Wright-Patterson AFB, OH.

MICROWAVE BRIGHTNESS TEMPERATURE AND ITS RELATION TO ATMOSPHERIC GENERAL CIRCULATION FEATURES M.S. Thesis - Colorado State Univ.

Theodore T. Vroman May 1989 171 p

(AD-A218312; AFIT/CI/CIA-89-066) Avail: NTIS HC A08/MF A01 CSCL 20/13

Microwave Sounding Unit (MSU) global brightness temperature fields are compared with observed atmospheric general circulation features for the purpose of determining the extent to which MSU brightness temperature relates to observed atmospheric circulation. A six-week MSU data set covering 8 Jan. 1987 to 18 Feb. 1987 is analyzed. Global and hemispheric projections of MSU Channel 2 (53.74 GHz), Channel 3 (54.96 GHz), and Channel 4 (57.95 GHz) brightness temperature fields are presented in two divisions; 8 to 31 Jan. and 1 to 18 Feb. 1987. Complementary data sets of temperature, zonal wind, geopotential height, and streamfunction are developed using model analyses from the European Centre for Medium Range Weather Forecasts (ECMWF) and the National Meteorological Center (NMC) for the purpose of a comparative study. MSU thermal fields may be considered an estimate of atmospheric mean-layer temperature through levels determined by each channel's weighting function. GRA

N90-20604# Air Force Inst. of Tech., Wright-Patterson AFB, OH.

A CASE STUDY OF A QUASI-STATIONARY TROPICAL CONVECTIVE LINE M.S. Thesis - Pennsylvania State Univ.

Jeffrey Lynn Peters Aug. 1989 95 p

(AD-A218325; AFIT/CI/CIA-89-075) Avail: NTIS HC A05/MF A01 CSCL 04/2

An extreme case of a convectively dominated tropical convective system was investigated. Of particular interest is the observation that the nimbostratus anvil produced by the convective line was an order of magnitude smaller than most of the nimbostratus anvils. Flight level data from the NCAR Electra was composited to examine the thermodynamic and kinematic structure

of the convective line, of the environment, and of the wake. The boundary layer structure was studied using bulk aerodynamic surface fluxes and eddy correlation turbulence statistics. The review of the environmental thermodynamics showed that these factors did not control the velocity of the convective line or the production of nimbostratus anvil. The study of the kinematic structure and a review of previous studies determined that the ability of a convective line to produce nimbostratus anvil is a function of horizontal moisture advection from the convective region into the mesoscale stratiform anvil region. The advection of moisture into the mesoscale stratiform anvil region is controlled both directly and indirectly via across line shear and line speed. The bulk aerodynamic surface fluxes gave a wake recovery time on the order of 10 hours, and eddy correlation turbulence statistics were found to provide insight into the boundary layer forcing and turbulence structure. GRA

N90-20605# Air Force Inst. of Tech., Wright-Patterson AFB, OH.
THE INVERTIBILITY PRINCIPLE FOR A SIMPLE HURRICANE MODEL M.S. Thesis
Robert M. Fogarty 1989 76 p
(AD-A218344; AFIT/CI/CIA-89-068) Avail: NTIS HC A05/MF A01 CSCL 04/2

A reinterpretation of Ooyama's classic tropical cyclone model is presented in terms of the more recent theoretical notions of the potential thickness equation, the potential radius coordinate and the invertibility principle. This helps place tropical cyclone theory in a theoretical framework closer to that of midlatitude theory. A shallow water model of axisymmetric, frictionless flow of homogeneous incompressible fluid on an f-plane is presented. The potential thickness, the inverse of potential vorticity, is introduced and the equation for its evolution written. The system is transformed from physical space to absolute angular momentum or potential radius space. This eliminates the radial component of the wind from the problem and provides better resolution in areas of large vorticity. The invertibility principle is derived and solved using five different methods, solving for a potential function using the shooting method, the fluid depth using the same method, the fluid depth using a nonlinear equation solving black box, a transformed velocity using a tridiagonal matrix equation solver, and the transformed velocity with the nonlinear equation solver. The first four methods can not be generalized to two layers. A short review of Ooyama's model shows how the wind field is determined from the radial mass flux. The concepts of the shallow water case is generalized to a two layer model using the nonlinear equation solver to solve the invertibility for the transformed velocity. GRA

48 OCEANOGRAPHY

Includes biological, dynamic, and physical oceanography; and marine resources.

For related information see also *43 Earth Resources and Remote Sensing.*

N90-20606# Old Dominion Univ., Norfolk, VA. Dept. of Oceanography.
CONTINENTAL SHELF PROCESSES AFFECTING THE OCEANOGRAPHY OF THE SOUTH ATLANTIC BIGHT Progress Report, Jun. 1989 - May 1990
Larry P. Atkinson Feb. 1990 6 p
(Contract DE-FG05-85ER-60348)
(DE90-008439; DOE/ER-60348/12) Avail: NTIS HC A02/MF A01

During the past year research activities have focused on analysis and synthesis of existing data from the GALE, FLEX and SPREX experiments and preparation for the WINTER-90 field experiment. Some time was spent assisting DOE in planning for the restructuring of the marine program. DOE

N90-20607# Naval Postgraduate School, Monterey, CA.
CORRELATION OF AVHRR IMAGERY WITH SUB-SURFACE FEATURES IN CALIFORNIA CURRENT M.S. Thesis
Jeffrey S. Best Jun. 1989 67 p
(AD-A218184) Avail: NTIS HC A04/MF A01 CSCL 08/3

SST fields derived from AVHRR imagery are compared with subsurface temperature and surface dynamic height fields. The in-situ data collection was part of the Coastal Transition Zone (CTZ) cold filament experiments of 1987 and 1988. The results of the 1987 cruise show a subsurface maximum in the correlation coefficient between AVHRR SST and in-situ temperature at depth for all three phases of the cruise which is attributed to the temporal offset between the satellite image and the data collection. The results of the 1988 cruise show maximum correlations at the surface with significant correlations at the 95 percent level of confidence to about 130 to 150 m depth, with positive correlations to 310 to 350 m depth. Comparing the results of the 1987 and 1988 cruises shows that the offshore filament was much stronger both horizontally and vertically for the latter cruise. GRA

51 LIFE SCIENCES (GENERAL)

N90-20608# Microbial Products, Inc., Vacaville, CA.
DESIGN AND OPERATION OF AN OUTDOOR MICROALGAE TEST FACILITY Final Report
J. C. Weissman, D. M. Tillett, and R. P. Goebel Oct. 1989 56 p Prepared in cooperation with Midwest Research Inst. Sponsored in part by New Mexico Research and Development Inst.
(Contract DE-AC02-83CH-10093)
(DE89-009493; SERI/STR-232-3569) Avail: NTIS HC A04/MF A01

The objective of the project covered in this report is to establish and operate a facility in the American Southwest to test the concept of producing microalgae on a large scale. This microalgae would then be used as a feedstock for producing liquid fuels. The site chosen for this project was an existing water research station in Roswell, New Mexico; the climate and water resources are representative of those in the Southwest. For this project, researchers tested specific designs, modes of operation, and strains of microalgae; proposed and evaluated modifications to technological concepts; and assessed the progress toward meeting cost objectives. DOE

N90-20609# Letterman Army Inst. of Research, San Francisco, CA.
ACUTE ORAL TOXICITY OF JA-2 SOLID PROPELLANT IN ICR MICE Report, 17 Dec. 1985 - 17 Jan. 1986
Earl W. Morgan, Denzil F. Frost, Conrad R. Wheller, and Don W. Korte, Jr. Dec. 1989 73 p
(AD-A217264; LAIR-414; TOXICOLOGY-SER-177) Avail: NTIS HC A04/MF A01 CSCL 06/11

The acute oral toxicity of JA-2 Solid Propellant was determined in male and female ICR mice by using an oral gavage, split-dose method. The minimum lethal dose (MLD) was 3774.6 + or - 150.5 mg/kg for male mice and 3528.8 + or - 133.8 mg/kg for female mice. JA-2 produced component, diethyleneglycol dinitrate and nitroglycerin. These signs included tremors, inactivity, depression of reflexes, loss of equilibrium, opisthotonus, and increased respiratory activity. Other clinical signs observed were associated with the general malaise of the animals following dosing and included perianal staining, hunched posture, squinting, and rough coat. Most animals exhibited signs by 2 hours after dosing and either had died or the signs had cleared within 5 days of dosing. According to the classification scheme of Hodge and Sterner, these results place JA-2 in the slightly toxic class. GRA

N90-20610# California Univ., Berkeley. Lawrence Berkeley Lab. Center for X Ray Optics.

BIOLOGICAL SOFT X RAY CONTACT MICROSCOPY: IMAGING LIVING CHO-SC1 CELLS AND OTHER BIOLOGICAL MATERIALS Ph.D. Thesis

Geoffrey David Guttmann Aug. 1989 223 p

(Contracts DE-AC03-76SF-00098; F49620-87-K-0001)

(DE90-007560; LBL-28042) Avail: NTIS HC A11/MF A02

This dissertation is a description of soft x ray contact microscopy and the successful efforts to expand this technique to image at high resolution, living mammalian cells. Soft x ray contact microscopy (SXCM) is a form of x ray lithography. However, the biological cell is imaged instead of an electron-cut microcircuit mask. The contrast mechanism is based upon the x ray absorption lengths of carbon and nitrogen. The soft x rays were generated by a conventional laboratory source or a laser-induced plasma x ray source. The conventional laboratory soft x ray source was a converted electron evaporator. The target materials were vanadium and carbon. The laser-induced plasma x ray source was the Lawrence Livermore National Laboratory (LLNL) JANUS laser facility. The target material was tantalum. A radiachromic nylon film was used to calibrate the exposure dose. The imaging detector was an x ray sensitive resist or a copolymer. A wet cell chamber (WCC) was designed to keep a biological sample alive at atmospheric pressure yet permit imaging by soft x rays. The limits of resolution required an understanding of the interaction of soft x rays with matter, Fresnel diffraction, penumbral blurring and secondary electron travel within a resist. DOE

N90-20611# California Univ., Berkeley. Lawrence Berkeley Lab.

LIFE SCIENCES: LAWRENCE BERKELEY LABORATORY, 1988

Jul. 1989 76 p

(Contract DE-AC03-76SF-00098)

(DE90-008061; LBL-27460) Avail: NTIS HC A05/MF A01

Life Sciences Research at the Lawrence Berkeley Laboratory (LBL) has both a long history and a new visibility. The physics technologies pioneered in the days of Ernest O. Lawrence found almost immediate application in the medical research conducted by Ernest's brother, John Lawrence. And the tradition of nuclear medicine continues today, largely uninterrupted for more than 50 years. Until recently, though, life sciences research has been a secondary force at LBL. Today, a true multi-program laboratory has emerged, in which the life sciences participate as a full partner. The LBL Human Genome Center is a contribution to the growing international effort to map the human genome. Its achievements represent LBL divisions, including Engineering, Materials and Chemical Sciences, and Information and Computing Sciences, along with Cell and Molecular Biology and Chemical Biodynamics. The Advanced Light Source Life Sciences Center will comprise not only beamlines and experimental end stations, but also supporting laboratories and office space for scientists from across the U.S. This effort reflects a confluence of scientific disciplines --- this time represented by individuals from the life sciences divisions and by engineers and physicists associated with the Advanced Light Source project. And finally, this report itself, the first summarizing the efforts of all four life sciences divisions, suggests a new spirit of cooperation. DOE

N90-20612# Brandeis Univ., Waltham, MA.

CARBON AND HYDROGEN METABOLISM OF GREEN ALGAE IN LIGHT AND DARK

1990 7 p

(Contract DE-FG02-86ER-13486)

(DE90-008648; DOE/ER-13486/T1) Avail: NTIS HC A02/MF A01

After adaptation to a hydrogen metabolism, Chlamydomonas reinhardtii can photoanaerobically metabolize acetate with the evolution of H2 and CO2. An enzyme profile of the chloroplastic, cytoplasmic, and mitochondrial fractions were obtained with a cellular fractionation procedure that incorporated cell wall removal by autolysine, digestion of the plasmalemma with digitonin and fractionation by differential centrifugation on a Percoll step gradient. The sequence of events leading to the photo-evolution of H2 from acetate includes the conversion of acetate into succinate via the extraplastidic glyoxylate cycle, the oxidation of succinate to fumarate by chloroplastic succinic dehydrogenase and the oxidation of malate to oxaloacetate in the chloroplast by NAD dependent malate dehydrogenase. The level of potential activity of the enzymes was sufficient to accommodate the observed rate of gas evolution. The isolated darkened chloroplast evolves aerobically CO2 from glucose indicating a chloroplastic respiratory pathway. Evolution of CO2 is blocked by mitochondrial inhibitors. DOE

N90-20613# Letterman Army Inst. of Research, San Francisco, CA.

ACUTE ORAL TOXICITY OF DIGL-RP SOLID PROPELLANT IN ICR MICE Report, 7 Feb. - 3 Jul. 1986

Larry D. Brown, Conrad R. Wheeler, Yvonne C. LeTellier, and Don W. Korte, Jr. Dec. 1989 68 p

(AD-A217711; LAIR-410; TOXICOLOGY-SER-178) Avail: NTIS HC A04/MF A01 CSCL 06/11

The acute oral toxicity of DIGL-RP solid propellant was determined in male and female ICR mice by using an oral gavage split-dose method. The MLD was 4176.1 + or - 116.6 mg/kg for male mice and 3447.5 + or - 42.1 mg/kg for female mice. DIGL-RP produced clinical signs that were attributed to its nitrate ester component, diethyleneglycol dinitrate. These signs included tremors, depression of reflexes, and inactivity. Other clinical signs observed were associated with the general malaise of the animals following dosing and included urine staining (males), hunched posture, squinting, and rough coat. Most animals exhibited signs by 2 to 3 hours after dosing and either had died or the signs had cleared by 96 hours after dosing. According to the classification scheme of Hodge and Sterner, these results place DIGL-RP in the slightly toxic class. GRA

N90-20614# Letterman Army Inst. of Research, San Francisco, CA.

ACUTE ORAL TOXICITY OF DIGL-RP SOLID PROPELLANT IN SPRAGUE-DAWLEY RATS Report, 30 Dec. 1985 - 1 Jun. 1986

Larry D. Brown, Conrad R. Wheeler, and Don W. Korte, Jr. Nov. 1989 82 p

(AD-A217712; LAIR-409; TOXICOLOGY-SER-167) Avail: NTIS HC A05/MF A01 CSCL 06/11

The DOD is considering the use of diethyleneglycol dinitrate (DEGDN), triethyleneglycol dinitrate; or trimethylolethane trinitrate as a replacement for nitroglycerin in munition formulations. A health effects review identified numerous gaps in the toxicology database of these compounds. Consequently, an initial health effects evaluation of DEGDN, TMETN, TEGDN, and two DEGDN-based propellants, JA-2 and DIGL-RP was conducted. The acute oral toxicity of DIGL-RP solid propellant was determined in male and female Sprague-Dawley rats by using an oral gavage split-dose method. The medium lethal dosage was 2946.1 + or - 39.2 mg/kg for male rats and 2636.4 + or - 117.8 mg/kg for female rats. DIGL-RP produced clinical signs that were attributed to its nitrate ester component, DEGDN. These signs included tremors, depression of reflexes, cyanosis, increases in respiratory rate and depth, and decreased body temperature. Other clinical signs observed were associated with the general malaise of the animals and dosing and included hunched posture, squinting, reddish stains around the eyes and nose, and perianal staining. Most animals exhibited signs by 4 hours after dosing and either had died or the signs had cleared by 96 hours after dosing. According to the classification scheme of Hodge and Sterner, these results placed DIGL-RP in the slightly toxic class. GRA

N90-20615# Army Research Inst. of Environmental Medicine, Natick, MA.

HYPOBARIC HYPOXIA (380 TORR) DECREASES INTRACELLULAR AND TOTAL BODY WATER IN GOATS

R. W. Hoyt, M. J. Durkot, V. A. Forte, Jr., L. J. Hubbard, L. A. Trad, and A. Cymerman 1989 24 p

(AD-A218192; USARIEM-M7-90) Avail: NTIS HC A03/MF A01 CSCL 06/10

The effect of 16 days of hypobaric hypoxia on body fluid distribution was studied in four unanesthetized adult goats (Capra lircus). Total body water (TBW), extracellular fluid volume (ECF), and plasma volume (PV) were determined with (3)H2O, (14C)-inulin, and indocyanine green, respectively. Blood volume (BV = PV x 100/100 - HEMATOCRIT), red cell volume (RCV = BV - PV), intracellular fluid (ICF = TBW - ECF) and interstitial fluid (ISF = ECF - PV) volumes were calculated. Body mass (-7.1 percent), TBW (-9.1 percent), and ICF volume (-14.4 percent) decreased, while ECF (+11.7 percent), and ISF (+27.7 percent) volumes increased with exposure (p less than 0.05). The decrease in TBW accounts for 89 percent of the loss of body mass. Hematocrit increased from 24.0 + or - 1.0 percent SEM to 34.2 + or - 2.2 percent (p less than 0.05). BV was unchanged; an increase in RCV (+39.5 percent) counterbalanced the decrease in PV (-15.3 percent) (p less than 0.05). Goats were similar to humans in that prolonged hypobaric hypoxia resulted in decreases in TBW volume, ICF volume, and PV. GRA

52 AEROSPACE MEDICINE

Includes physiological factors; biological effects of radiation; and effects of weightlessness on man and animals.

N90-20616* National Aeronautics and Space Administration. Marshall Space Flight Center, Huntsville, AL.

HUMAN SERUM ALBUMIN CRYSTALS AND METHOD OF PREPARATION Patent

Daniel C. Carter, inventer (to NASA) 23 May 1989 8 p Filed 20 Aug. 1987

(NASA-Case-MFS-28234-1; US-Patent-4,833,233; US-Patent-Appl-SN-087281; US-Patent-Class-530-363; US-Patent-Class-530-362; US-Patent-Class-530-364; US-Patent-Class-530-387; US-Patent-Class-530-422; US-Patent-Class-427-2; US-Patent-Class-428-408) Avail: US Patent and Trademark Office CSCL 06E

Human serum albumin (HSA) crystals are provided in the form of tetragonal plates having the space groups P42(sub 1)2, the crystals being grown to sizes in excess of 0.5 mm in two dimensions and a thickness of 0.1 mm. Growth of the crystals is carried out by a hanging drop method wherein a precipitant solution containing polyethylene glycol (PEG) and a phosphate buffer is mixed with an HSA solution, and a droplet of mixed solution is suspended over a well of precipitant solution. Crystals grow to the desired size in 3 to 7 days. Concentration of reagents, pH and other parameters are controlled within prescribed limits. The resulting crystals exhibit a size and quality such as to allow performance of x ray diffraction studies and enable the conduct of drug binding studies as well as genetic engineering studies.

Official Gazette of the U.S. Patent and Trademark Office

N90-20617*# National Aeronautics and Space Administration. John F. Kennedy Space Center, Cocoa Beach, FL.

ELEVATED CENTRAL VENOUS PRESSURE: A CONSEQUENCE OF EXERCISE TRAINING-INDUCED HYPERVOLEMIA

Victor A. Convertino, Gary W. Mack, and Ethan R. Nadel 1990 22 p

(NASA-TM-102965; NAS 1.15:102965) Avail: NTIS HC A03/MF A01 CSCL 06P

Resting plasma volumes, and arterial and central venous pressures (CVP) were measured in 16 men before and after exercise training to determine if training-induced hypervolemia could be explained by a change in total vascular capacitance. In addition, resting levels of plasma vasopressin (AVP), atrial natriuretic peptide (ANP), aldosterone (ALD), and norepinephrine (NE) were measured before and after training. The same measurements of vacular volume, pressures, and plasma hormones were measured in 8 subjects who did not undergo exercise and acted as controls. The exercise training program consisted of 10 weeks of controlled cycle exercise for 30 min/d, 4 d/wk at 75 to 80 percent of maximal oxygen uptake (VO2max). A training effect was verified by a 20 percent increase in VO2max, a resting bradycardia, and a 370 ml (9 percent) increase in blood volume. Mean arterial blood pressure was unaltered by exercise training, but resting CVP increased. The percent change in blood volume from before to after training was linearly related to the percent change in CVP. As a consequence of elevations in both blood volume and CVP, the volume-to-pressure ratio was essentially unchanged following exercise training. Plasma AVP, ANP, ALD, and NE were unaltered. Results indicate that elevated CVP is a consequence of training-induced hypervolemia without alteration in total effective venous capacitance. This may represent a resetting of the pressure-volume stimulus-response relation for regulation of blood volume. Author

N90-20618# Defence and Civil Inst. of Environmental Medicine, Downsview (Ontario).

INFLUENCE OF THEOBROMINE ON HEAT PRODUCTION AND BODY TEMPERATURES IN COLD-EXPOSED HUMANS: A PRELIMINARY REPORT

Andre L. Vallerand, Lawrence C. H. Wang, and Ira Jacobs Nov. 1989 34 p Prepared in cooperation with Alberta Univ., Edmonton

(AD-A217203; DCIEM-89-RR-50) Avail: NTIS HC A03/MF A01 CSCL 06/15

One of the most successful classes of drugs employed to enhance cold tolerance in animals appears to be the methylxanthines. Indeed, methylxanthines such as caffeine, theophylline and theobromine have been shown to increase heat production, delay hypothermia and thus improve cold tolerance in animals. In humans, theophylline and caffeine (taken in combination with ephedrine) have similarly been shown to improve cold tolerance. Whether theobromine could enhance tolerance to cold in humans, is not known. The influence of theobromine was thus investigated in eight healthy young male subjects during two semi-nude exposures to cold air (3h, 7C, 1 m/s wind speed). The ingestion of theobromine produced two different types of responses, as shown by a significant interaction between the effect of group and the effect of drug treatment on the rate of decrease in mean body temperatures. The present results are interpreted as indicating that the ingestion of theobromine in subjects capable of producing a relatively high metabolic response to the cold, significantly improves cold tolerance by increasing heat production, mainly from a greater lipid utilization. GRA

N90-20619# Defence and Civil Inst. of Environmental Medicine, Downsview (Ontario).

PHYSICAL PERFORMANCE AND CARBOHYDRATE CONSUMPTION IN CF COMMANDOS DURING A 5-DAY FIELD TRIAL

I. Jacobs, D. VanLoon, L. Pasut, J. Pope, and D. Bell Dec. 1989 45 p

(AD-A217204; DCIEM-89-RR-48) Avail: NTIS HC A03/MF A01 CSCL 06/10

This study evaluated the capacity of military personnel to perform maximal exercise before and after 5 days of sustained physical activity. An additional goal was to evaluate whether a carbohydrate supplement to the regular field rations would reduce the extent of any performance impairments. Subjects (Ss) were 29 male volunteers from the Canadian Forces Airborne Regiment. They were allowed 4 to 5 h sleep each 24h and 45 min per meal, but were otherwise continuously occupied with physically demanding missions in a field environment. Performance tests administered 2 days before and at the end of a the 5-day field trial included evaluations of maximal aerobic power during cycle exercise, anaerobic power, muscular strength and endurance, rate of maximal force development and reaction time. Muscle and blood tissue samples were obtained before and after the trial to clarify the relative contribution of fat and carbohydrate energy stores to meeting the metabolic cost of the field trial. The results demonstrated that the Ss were in a marked negative caloric balance by the end of the field trial. Skeletal muscle glycogen stores were markedly depleted. There were impairments maximal aerobic power, maximal dynamic strength, and anaerobic power of large

muscle groups. These observations have direct implications for mission planning and physical performance expectations of military units involved in sustained operation GRA

N90-20620# Lawrence Livermore National Lab., CA.
A REVIEW OF THE LITERATURE ON THE TOXICITY OF RARE-EARTH METALS AS IT PERTAINS TO THE ENGINEERING DEMONSTRATION SYSTEM SURROGATE TESTING
P. H. Wald and V. Alan Mode Jan. 1990 32 p
(Contract W-7405-eng-48)
(DE90-008049; UCID-21823-Rev-1) Avail: NTIS HC A03/MF A01

Considerable data on the toxicology of the rare-earth metals and their compounds via oral ingestion or injection have been collected from animal studies at relatively high exposure levels. This report includes a general introduction to the rare-earth elements, data reviews on the toxicity of the rare earths from animal studies and the relatively rare occurrences of harmful human exposure, precautions for worker protection that should be taken with use of these materials, and scientific data with Engineering Demonstration System (EDS) operations. DOE

N90-20621# George Washington Univ., Washington, DC.
DEVELOPMENT OF GAMMA-EMITTING, RECEPTOR-BINDING RADIOTRACERS FOR IMAGING THE BRAIN AND PANCREAS
R. C. Reba 1989 11 p
(Contract DE-FG05-88ER-60649)
(DE90-008314; DOE/ER-60649/T2) Avail: NTIS HC A03/MF A01

The objectives were to: (1) synthesize analogues of 4-IQNB which exhibit lower lipophilicity, preferably similar to that of QNB; (2) prepare F-18 analogues of QNB; and (3) prepare analogues of 3-quinuclidinyl benzilate (QNB) containing a lipophilic chelate Tc-99m. DOE

N90-20622# School of Aerospace Medicine, Brooks AFB, TX. Human Systems Div.
THE UNITED STATES AIR FORCE SCHOOL OF AEROSPACE MEDICINE: SPECIAL REPORT Final Report, period ending 1989
Terry A. Benline Nov. 1989 28 p
(AD-A217740; USAFSAM-SR-89-6) Avail: NTIS HC A03/MF A01 CSCL 06/5

Our business is conducted in three functional areas: science and technology, operational support, and aeromedical education and training. Although we are called the USAF School of Aerospace Medicine (USAFSAM), most of what we do is science and technology--about 70 percent of our manpower and about 85 percent of our budget are invested in science and technology. We do have an operational support role for the U.S. Air Force (USAF), and that role is primarily in aerospace medical education, hyperbarics, and epidemiology. And, of course, we have an educational facility, which is here to provide training in aeromedical specialties and subspecialties, rather than general medical education per se. The medical training for the USAF is provided at Sheppard Air Force Base in Wichita Falls, Texas--training, for example, the pharmacy technicians, laboratory technicians, and corpsmen who work on the wards. The flight surgeons, their technicians, the aerospace physiologists, the bioenvironmental engineers, and the medical support people who are more related to the operational USAF, are trained here at USAFSAM. GRA

N90-20623# Defence and Civil Inst. of Environmental Medicine, Downsview (Ontario).
THE +Gz PROTECTION IN THE FUTURE: REVIEW OF SCIENTIFIC LITERATURE
Fred Buick Nov. 1989 25 p
(AD-A217887; DCIEM-89-RR-47) Avail: NTIS HC A03/MF A01 CSCL 06/5

To reduce the incidence of G-induced loss of consciousness and enable pilots to operate their aircraft at higher levels of performance, anti-G protection must be improved. A G-suit and the anti-G straining maneuver will likely remain essential components of any anti-G system, but several methods potentially increasing G-tolerance were investigated that could supplement the protection afforded by these traditional techniques. Pharmacological agents are of no benefit, while breathing carbon dioxide, shown to improve G tolerance, is impractical. Positive pressure breathing has so convincingly improved G-protection that it will become an operational procedure in the immediate future. The benefits of the G-suit were augmented through greater coverage of the lower body and efforts are also aimed at more responsive G-valves. Altering body position to shorten the heart to head hydrostatic distance adds directly to the protection offered by the other procedures but can impair vision and must wait until the cockpit is redesigned. GRA

N90-20624# Army Research Inst. of Environmental Medicine, Natick, MA.
NIACIN INGESTED AT NIGHT CAUSES SEVERE HYPOTENSION
Lou A. Stephenson and Margaret A. Kolka Nov. 1989 30 p
(DA Proj. 3E1-62787-A-879)
(AD-A217896; USARIEM-M8-90) Avail: NTIS HC A03/MF A01 CSCL 06/5

Four healthy subjects were studied during rest while in a seated posture in a moderately warm environment (T(a) = 30 C, rh = 23 percent) at 0800 h and again between 1800 and 2100 h. Evening experiments were done approximately 4 h before each subject went to bed. Esophageal temperature (T(es)), mean weighted skin temperature (T bar (sK)), forearm blood flow (FBF, venous occlusion plethesmography), skin blood flow (SkBF, laser Doppler velocimetry), mean arterial pressure (MAP) and heart rate (HR) were measured twice each minute. After instrumentation, a 15 minute control period was initiated. T(es) and T bar (sK) were 0.4 (p less than or = 0.05) and 0.6 C higher at 1800 h than 0800 h. SkBF was 47 percent higher (p less than or = 0.05) and cutaneous vascular conductance (CVC) was 43 percent greater (p less than or = 0.05) at 1800 h. Five mg niacin per kg body weight was ingested after the control period. Since onset time for niacin effects showed individual variability, the data were compared during pretreatment, the time of maximal vasodilation, and when T(es) was minimal. Niacin treatment during the morning and evening resulted in decreased T(es) and MAP and increased T bar (sK), SkBF, FBF, heart rate, and CVC (p less than or = 0.05). Peak HR at 1800 h was 25 b min higher than at 0800 h (p less than or = 0.05). MAP decreased an average of 12 Torr in the morning experiments and nearly 16 Torr in the evening experiments. Two of the subjects experienced severe hypotension after niacin treatment at 1800 h. A diurnal factor, presumably influencing the responsiveness of the cardiovascular system, may play a role in the hypotensive effect of niacin at night. GRA

N90-20625# Army Research Inst. of Environmental Medicine, Natick, MA. Health and Performance Div.
EFFECTS OF DEXAMETHASONE AND HIGH TERRESTRIAL ALTITUDE ON COGNITIVE PERFORMANCE AND AFFECT
Jared B. Jobe, Barbara Shukitt-Hale, Louis E. Banderet, and Paul B. Rock Dec. 1989 25 p
(DA Proj. 3E1-62787-A-879)
(AD-A217897; USARIEM-M13-90) Avail: NTIS HC A02/MF A01 CSCL 06/15

The effects were examined of dexamethasone (a potent corticosteroid) to high terrestrial altitude on cognitive performance, affect, and personality traits. Cognitive performance was evaluated by 5 cognitive tasks, affect was evaluated by the Clyde Mood Scale and the Multiple Affect Adjective Check List, and personality traits were examined using the Minnesota Multiphasic Personality Inventory. Sixteen healthy young men received either dexamethasone (4 mg every 6 h) or placebo for 48 h prior to and after ascent to 4300 m. Subjects treated with dexamethasone correctly performed more computer interaction and addition problems than did placebo-treated subjects. They also were less sleepy, dizzy, depressed, and anxious than placebo-treated subjects on the first day at altitude. No adverse effects on cognitive

performance, affect, or personality traits were noted after dexamethasone was discontinued on the third day at altitude. Results indicated that dexamethasone at the present dose positively influences cognitive performance and mood states at altitude, but it does not affect personality traits. GRA

N90-20626# Institute for Perception RVO-TNO, Soesterberg (Netherlands).
THE EFFECT OF MOISTURE ABSORPTION IN CLOTHING ON THE HUMAN HEAT BALANCE Final Report
W. A. Lotens and G. Havenith 6 Oct. 1989 36 p Sponsored by Organisation voor Toegepast Natuurwetenschappelijk Onderzoek, The Hague, Netherlands
(AD-A217899; IZF-1989-32) Avail: NTIS HC A03/MF A01 CSCL 11/5

A theory of moisture absorption in clothing, with the associated effects of heat transfer, was developed based on the assumption that clothing can be regarded as a moisture buffering capacitor enclosed between heat and vapor resistances, and covered with the adjacent air layer. The theory was checked with an experiment involving four subjects. They wore heavy woolen clothing, which was either initially dried or wetted, in both a warm and a cool environment. The experimental results confirmed satisfactorily the theoretical predictions that: (1) the dry and evaporative heat loss will change in time and will both converge for the dry and moist garments to the equilibrium condition, (2) the clothing surface temperature and humidity are bound to a straight line on the psychrometric chart, (3) dry garments cause higher heat strain than wet garments, (4) the time course is predictable from the buffering capacity of the clothing and the heat transfer coefficient, and (5) the apparent heat and moisture transfer coefficients are bound to a linear relationship, revealing the true values only during equilibrium. Contrary to the expectation the observed vapor resistance is lower in the heat than in the cold, probably due to differences in sweat distribution. GRA

N90-20627# Medical Coll. of Virginia, Richmond. Dept. of Physical Therapy.
THE RELIABILITY OF CLINICAL MEASUREMENTS OF FORWARD BENDING OBTAINED BY THE USE OF THE MODIFIED FINGERTIP-TO-FLOOR METHOD M.S. Thesis
Michael George Gauvin 18 Aug. 1989 121 p Sponsored by AFIT, Wright-Patterson AFB, OH
(AD-A217907; AFIT/CI/CIA-89-154) Avail: NTIS HC A06/MF A01 CSCL 06/5

The purpose was to examine the intra- and inter-tester reliability of measurements obtained using a modified version of the fingertip-to-floor (FTF) method of assessing forward bending. With the modified FTF (MFTF) method patients stand on a stool and forward bend so that measurements can be taken on patients who are able to reach beyond the floor. Randomly paired physical therapists took repeated MFTF measurements on 73 patients with low back pain. Intraclass correlation coefficients (ICC) were calculated for intra- and inter-tester reliability. The ICC value for intra-tester reliability was 0.98 and the ICC value for inter-tester reliability was 0.95. The results suggest that measurements of forward bending obtained on patients with low back pain using the MFTF method are highly reliable. GRA

N90-20628# Army Research Inst. of Environmental Medicine, Natick, MA. Exercise Physiology Div.
THE EFFECTS OF HIGH INTENSITY CYCLE EXERCISE ON SYMPATHO-ADRENAL-MEDULLARY RESPONSE PATTERNS
William J. Kraemer, John F. Patton, Howard G. Knuttgen, Charles J. Hannan, Thomas Kettler, Scott E. Gordon, Joseph E. Dziados, Andrew C. Fry, Peter N. Frykman, and Everett A. Harman 1989 33 p Prepared in cooperation with Madigan Army Medical Center, Takoma, WA and Pennsylvania State Univ., University Park.
(AD-A217962) Avail: NTIS HC A03/MF A01 CSCL 06/5

Plasma proenkephalin Peptide F immunoreactivity (ir) and catecholamines were examined before and after maximal exercise to exhaustion at four intensities 36, 55, 73 and 100 percent maximal leg power (MLP) by means of a high resistance cycle ergometer. All intensities were greater than those eliciting peak O2 uptake for the individual subjects. Blood samples were obtained immediately after exercise and at 5 and 15 main post-exercise. Data suggest that exercise-induced increases may be the result of non-colinear storage and release mechanisms in the adrenal medulla. GRA

N90-20629# Army Research Inst. of Environmental Medicine, Natick, MA.
HYDRATION EFFECTS ON HUMAN PHYSIOLOGY AND EXERCISE-HEAT PERFORMANCE
Michael N. Sawka, Andrew J. Young, William A. Latzka, P. Darrell Neufer, and Kent B. Pandolf Nov. 1989 72 p
(DA Proj. 3E1-162787-A-879)
(AD-A217969; USARIEM-T7-90) Avail: NTIS HC A04/MF A01 CSCL 06/10

During exercise in the heat, sweat output often exceeds water intake resulting in hypohydration, which defined as body fluid deficit. This fluid deficit is comprised of water loss from both the intracellular and extracellular fluid compartments. There is no evidence that hypohydration can benefit exercise performance; in addition, man cannot adapt to chronic dehydration. Exercise tasks that primarily require aerobic metabolism and that are prolonged will more likely be adversely influenced by hypohydration than exercise tasks that require anaerobic metabolism as well as muscular strength and power. Likewise, the warmer the environmental temperature, the greater the potential for hypohydration to cause decrements in all types of exercise performance. Hypohydration causes a greater heat storage and reduces endurance as well as maximal effort exercise performance in comparison to euhydration levels. The greater heat storage is mediated by a decreased sweating rate (evaporative heat loss) as well as by a decreased cutaneous blood flow (dry heat loss). These response decrements were attributed to both a plasma hyperosmolality and a reduced blood volume. The reduced blood volume also makes it difficult to maintain an adequate cardiac output during exercise-heat stress. Finally, preliminary data indicate that hypohydration does not alter muscle glycogen utilization during exercise or the glycogen resynthesis during recovery from exercise. GRA

N90-20630# Michigan Univ., Ann Arbor.
THREE-DIMENSIONAL MEDICAL IMAGE ANALYSIS USING LOCAL DYNAMIC ALGORITHM SELECTION ON A MULTIPLE-INSTRUCTION, MULTIPLE-DATA ARCHITECTURE Ph.D. Thesis
Martin Robert Stytz 1989 493 p Sponsored by AFIT, Wright-Patterson AFB, OH
(AD-A218024; AFIT/CI/CIA-89-158) Avail: NTIS HC A21/MF A03 CSCL 06/4

The dissertation outlines development of a medical imaging machine which renders 3D images from voxel data within a MIMD multiprocessor architecture at interactive rates. Interactive performance is achieved using local dynamic selection of the optimum adaptive recursive hidden-surface removal algorithm. A survey of the medical imaging, graphics, and medical imaging modality literature is provided. A description of Computerized Technology, Magnetic Resonance Imaging, Positron Emission Tomography, Single Photon Emission Computed Tomography, and Ultrasound imaging modalities is presented Previous work in 3D volume rendering graphics techniques and data models is introduced. Eleven medical imaging machines are examined with emphasis on characterization of the major innovation(s) and performance of each machine. A five stage image processing pipeline is described. GRA

N90-20631# Naval Aerospace Medical Research Lab., Pensacola, FL.
A COMPARISON OF THE MECHANISMS OF COLD- AND MICROGRAVITY-INDUCED FLUID LOSS
D. J. Horrigan, Jr. and W. G. Lotz 10 Aug. 1989 13 p
(AD-A218098; NAMRL-TM-89-3) Avail: NTIS HC A03/MF A01 CSCL 06/10

The physiological mechanisms involved in the diuresis and overall fluid loss associated with exposure to cold or microgravity environments are compared. Although the data available to thoroughly describe these responses are yet unavailable, some similarities in the changes caused by these different stimuli are apparent. The central mechanism common to the physiological responses to both these environments is an increase in central blood volume. The common endpoint of a net loss in body fluids and electrolytes is also clear. Differences in the response patterns also exist. The differences are evaluated, and the value of additional research in both areas, with potentially mutually beneficial results, is considered. GRA

N90-20632# Air Force Inst. of Tech., Wright-Patterson AFB, OH.

DETECTION ACUITY IN THE PERIPHERAL RETINA M.S. Thesis - Indiana Univ.

Frank E. Cheney, Jr. 1989 164 p

(AD-A218183; AFIT/CI/CIA-89-166) Avail: NTIS HC A08/MF A01 CSCL 06/4

One of the goals in exploring vision is to isolate the role each successive part of the visual system plays in transforming an external visual stimulus into a visual percept. This requires that methods be used which can separately test the pre-retinal, retinal and post-retinal contributions. New electrophysiological and psychophysical techniques are enabling us to probe more accurately these individual components. By integrating and correlating these findings with known anatomical and psychophysical findings, investigators attempt to form a consistent model which can describe how the visual system functions. However, the information gained from investigating separate components, though essential to our total understanding of the system, will frequently seem misleading until the interactions of all the other components have been determined. This certainly has been true for this experiment. GRA

N90-20633# Army Research Inst. of Environmental Medicine, Natick, MA. Exercise Physiology Div.

THE EFFECTS OF GRADED EXERCISE AT SEA LEVEL ON PLASMA PROENKEPHALIN PEPTIDE F AND CATECHOLAMINE RESPONSES

William J. Kraemer, Joseph E. Dziados, Scott E. Gordon, Andrew C. Fry, and Katy L. Reynolds 1989 22 p Prepared in cooperation with Pennsylvania State Univ., University Park

(AD-A218195; USARIEM-M5-90) Avail: NTIS HC A03/MF A01 CSCL 06/10

The effects were evaluated of graded treadmill exercise on plasma proenkephalin Peptide F immunoreactivity (ir) and catecholamine responses. Little data exists regarding the sea level responses of plasma Peptide F ir to exercise. Thirty-five healthy male subjects performed a graded exercise test on a motor-driven treadmill at the exercise intensities of 25, 50, 75, and 100 percent of VO2max. Significant increases above rest were observed for plasma Peptide F ir and norepinephrine at 75 and 100 percent of VO2max and at 5 min into recovery. Significant increases in plasma epinephrine were observed at 75 and 100 percent of VO2max. Whole blood lactate significantly increased above resting values at 50, 75 and 100 percent of the VO2max and at 5 min into recovery. These data demonstrate that exercise increases plasma Peptide F ir levels at sea level. While the exercise response patterns of Peptide F ir are similar to catecholamines and blood lactate responses, no bi-variate relationships were observed. These data show that sea level response patterns to graded exercise are similar to those previously observed at moderate altitude (2200 m). GRA

N90-20634# Army Aeromedical Research Unit, Fort Rucker, AL. Biodynamics Research Div.

SIMULATOR SICKNESS IN THE CH-47 (CHINOOK) FLIGHT SIMULATOR

Daniel J. Gower, Jr., Jennifer Fowlkes, and Dennis R. Baltzley (Essex Corp., Orlando, FL.) Sep. 1989 72 p

(AD-A218214; USAARL-89-28) Avail: NTIS HC A04/MF A01 CSCL 06/10

The principal goal in this field study was to assess the incidence of simulator sickness in the CH-47 flight simulator. The results show that this simulator produces a lower incidence of simulator sickness than the three other Army visually coupled flight simulators. Eighteen percent of the sample may be at risk for simulator-induced posteffects. Eyestrain and headache were leading symptoms of asthenopia, while fatigue and sweating were leading symptoms associated with motion sickness. Of possible impact on the results are the sample of aviators surveyed and the scenarios flown. None of the aviators sampled were in a training/qualification status. All were rated in the CH-47 and flying for continuation and proficiency. Therefore, it could be assumed the scenarios flown were less structured and flown by aviators familiar with both the aircraft that does not fly a large amount of high maneuver content missions. This could lead to lower amounts of provocative scene variables such as low-level flight, maneuvering in close proximity to the ground, and high speed turns. Forty-eight percent of the pilots' and thirty-seven percent of the copilots' missions were under instrument conditions. Such a large percentage of time spent with no scene content could account for some of the lower SSQ scores. The use of NVGs in the CH-47 simulator is associated with higher scores on the SSQ. GRA

N90-20635# Army Research Inst. of Environmental Medicine, Natick, MA.

FIELD ASSESSMENT OF WET BULB GLOBE TEMPERATURE: PRESENT AND FUTURE Final Report, Jun. 1986 - Aug. 1989

Robert Whang, William T. Matthew, John Christiansen, Billie Brown, Glenn Thomas, Madeleine S. Rose, Patricia C. Szlyk, Lawrence Armstrong, and Frank J. Schatzle (Gulf Weather Corp., Bay Saint Louis, MS.) 29 Aug. 1989 17 p

(AD-A218224) Avail: NTIS HC A03/MF A01 CSCL 06/10

Existing doctrinal guidance for preventing heat injury in military settings is based on measurements of the Wet Bulb Globe Temperature (WBGT) index. An existing military WBGT measurement device (NSN 6665-00-159-2218) was employed by a U.S. Army Reserve unit during field training exercises at Fort Bliss, TX in 1986, Tinker AFB, OK in 1987, and Fort Hood, TX in 1988. The majority of heat casualties seen in these three exercises (31 out of 35) occurred when the daily maximum WBGT index exceeded 85 F. Experiences of this unit suggest that a strictly enforced, WBGT-based, heat injury prevention program was effective in minimizing both the number and severity of heat-related injuries. During the exercises at Fort Hood in 1988, a preliminary evaluation of methods to obtain WBGT information from polar orbiting weather satellites was conducted. Data from 11 satellite passes were obtained and the average error, or bias, of the satellite-derived WBGT values was found to be -1.8 F (too low) with a variation (standard deviation) of + or - 3.7 F around that bias. Work is in progress to improve this future heat stress assessment technology. GRA

N90-20636# Army Research Inst. of Environmental Medicine, Natick, MA.

EFFECTIVE CALIBRATION OF HEAT FLUX TRANSDUCERS FOR EXPERIMENTAL USE

Stephen KW. Chang, Thomas L. Endrusick, James E. Bogart, and Richard R. Gonzalez Jan. 1990 24 p

(DA Proj. 3E1-62787-A-878)

(AD-A218262; USARIEM-T8-90) Avail: NTIS HC A03/MF A01 CSCL 06/12

Cutaneous heat flux data provide important information when evaluating the effectiveness of chemical protective antidotal drugs and assessing physiological responses during heat and cold environmental stress. A method of calibrating heat flux transducers (HFTs) using the USARIEM Hohenstein skin model system is described. A representative sample of the currently available types of HFTs were tested and their results confirmed that the factory supplied calibration constants should not be used for collecting experimental data. The HFT application procedure described must

also be subscribed to for attaching the HFT on human subjects. The adherence to a standard procedure ensures that the newly recalibrated constants are applicable, and avoids as much as possible any extraneous steps where error could be introduced. Employing this standard attachment method, the newly calibrated HFT constants were found to deviate from the factory supplied values by as much as 24 percent. It is recommended that heat flux transducers be recalibrated before each protocol study using techniques described with the Hohenstein skin model. GRA

N90-20637# Army Research Inst. of Environmental Medicine, Natick, MA.
WHAT SHOULD ATHLETES KNOW ABOUT LOW BODY TEMPERATURE (HYPOTHERMIA)
Lawrence E. Armstrong 30 Oct. 1989 4 p
(AD-A218316) Avail: NTIS HC A01/MF A01 CSCL 06/10

Athletes exposed to cold, wet environmental conditions for a long period of time are susceptible to hypothermia. This brief article is written in an ask the expert format per request of the journal editor. This article outlines the signs of hypothermia, recommended first aid, predisposing factors, and preventative measures that can be taken. GRA

53 BEHAVIORAL SCIENCES

Includes psychological factors; individual and group behavior; crew training and evaluation; and psychiatric research.

N90-20638# Navy Personnel Research and Development Center, San Diego, CA.
BRAIN ACTIVITY DURING TACTICAL DECISION-MAKING. PART 3: RELATIONSHIPS BETWEEN PROBE-EVOKED POTENTIALS, SIMULATION PERFORMANCE, AND ON-JOB PERFORMANCE Interim Report No. 3, Sep. 1988 - Oct. 1989
Leonard J. Trejo, Gregory W. Lewis, and Mark H. Blankenship Jan. 1990 25 p
(AD-A217207; NPRDC-TN-90-9) Avail: NTIS HC A03/MF A01 CSCL 05/8

This report, the third in a series, addresses the use of event related potentials (ERPs) to predict the decision making performance of combat system operators. We describe the relationships between individual measures of probe-ERP amplitude, and both task and on-job performance in 30 military subjects. GRA

N90-20639# Aerospace Medical Research Labs., Wright-Patterson AFB, OH.
THE ROLE OF CHAOS IN HEMISPHERIC PROCESS AND ATTENTION Technical Report, Nov. 1987 - Nov. 1989
Michael D. McNeese Nov. 1989 27 p
(AD-A217674; AAMRL-TR-89-043) Avail: NTIS HC A03/MF A01 CSCL 05/8

The recent application of chaos theory to interpret various brain functions suggests it's usefulness for understanding potentially confusing and often conflictual results in the area of hemispheric processing. There appears to be inherent relationships between elements of chaos theory and the nature of hemispheric processes especially when viewed from an attentional resources perspective. The goal is to elucidate these relations by interpreting some data on hemispheric pattern recognition in a chaos theory framework. In order to interpret such data, theoretical models as well as specific concepts in attention, hemispheric processing, and chaos is reviewed. A chaos-attentional model is proposed along with certain rules of determination that predict the appearance of chaos in hemispheric processes. In conclusion, some recent metaphors for Hofstadter (1979, 1985) that are supportive of this view of cognitive process are addressed. GRA

N90-20640# Aerospace Medical Research Labs., Wright-Patterson AFB, OH.
THE BOUNDARIES OF HEMISPHERIC PROCESSING IN VISUAL PATTERN RECOGNITION Final Report, Jan. 1987 - Nov. 1989
Michael D. McNeese Nov. 1989 26 p
(AD-A217675; AAMRL-TR-89-042) Avail: NTIS HC A03/MF A01 CSCL 05/8

Some of the positions, theories, and experiments which compose the adaptive hemispheric processing area are discussed. This discussion addresses some of the basic questions of human learning and relates some of the assumptions that are critical for interpreting research findings. Some theoretical perspectives are examined, then some of the author's own research application in hemispheric processing within the area of face recognition and attentional processes is studied. A neuro-cognitive systems model of results is proposed to interpret findings. GRA

N90-20641# Aerospace Medical Research Labs., Wright-Patterson AFB, OH.
LATERAL ASYMMETRY IN PATTERN RECOGNITION: UNDERSTANDING THE EFFECTS OF FAMILIARITY, DISTINCTION, AND PERSPECTIVE CHANGE Technical Report, Jan. 1987 - Nov. 1989
Michael D. McNeese Nov. 1989 25 p
(AD-A217739; AAMRL-TR-89-049) Avail: NTIS HC A03/MF A01 CSCL 05/8

The effects of perspective change and familiarity upon lateral asymmetry for a face recognition task are analyzed based on the results of several experiments. A four choice match-to-sample procedure involved frontal target perspective faces and choice sets which contained faces in either front perspective, 3/4 perspective, or side perspective faces. The study assesses the effects of stimulus familiarity and distinctiveness. Results taken from analysis of variance, multidimensional scaling, and hierarchical cluster analysis suggests complex relationships between the sensitivity of faces and the ensuing development of familiarity. Conclusions are drawn in terms of implications for interpreting higher order cognition in laterality studies. GRA

N90-20642# Air Force Human Resources Lab., Brooks AFB, TX. Manpower and Personnel Div.
ROLE OF COGNITIVE FACTORS IN THE ACQUISITION OF COGNITIVE SKILL Interim Report, Nov. 1986 - Jan. 1989
Patrick C. Kyllonen and Dan J. Woltz Jan. 1990 36 p Submitted for publication
(AD-A218069; AFHRL-TP-89-5) Avail: NTIS HC A03/MF A01 CSCL 05/8

Recent studies are reviewed and a theoretical framework is provided for examining the relationships between individual differences in basic cognitive abilities and performance on tasks involving the acquisition of cognitive skill. A claim made is that much of cognitive skill can be characterized as knowledge of how operators (symbols denoting an operation to be performed) in a skill domain actually work, and knowledge of when to apply operators to achieve problem solving goals. Studies of declarative learning, assumed to be the initial stage in skill acquisition, show that background knowledge and working memory capacity are primary determinants of success. Studies of cognitive skill learning per se make use of a distinction between attention capacity, which refers to how much information can be held in working memory at one time, and activation capacity, which refers to how long activation can be maintained. The success of learning by proceduralization is shown to depend on attention capacity, whereas the success of learning by composition is shown to depend additionally on activation capacity. Future research and the benefits of an individual differences approach to analyzing cognitive skill acquisition are discussed. GRA

N90-20643# Alphatech, Inc., Burlington, MA.
INFORMATION GATHERING AND DECISIONMAKING UNDER STRESS
Elliot E. Entin and Daniel Serfaty Jan. 1990 83 p

(Contract N00014-88-K-0545)
(AD-A218233; AD-E501191; TR-454) Avail: NTIS HC A05/MF A01 CSCL 05/8

An experiment to investigate the effects of cognitive stress on decisionmaking performance is described. The paradigm involves a single decisionmaker (DM) whose job is to classify a submarine sonar return as coming from a friendly or enemy boat, on the basis of difference in average pump noise frequency between the two classes. After being given the value of the unknown submarine's measured pump frequency, the subject may classify the submarine or (for a cost) ask for more information. This information is chosen to be either another raw measurement (probe) or the opinion of an automated consultant. Cognitive stress is operationalized through time pressure and an intrusive secondary task. Two distinct subject populations are used: civilian (engineering firm employees and college students) and military (grade 0 to 4 or above). Four independent variables manipulated: stress level, discrimination difficulty, relative information cost between measurement and opinion, and consultant expertise relative to the subject's measurement. GRA

N90-20644# Colorado Univ., Boulder. Dept. of Psychology.
A LONG-TERM RETENTION ADVANTAGE FOR SPATIAL INFORMATION LEARNED NATURALLY AND IN THE LABORATORY Ph.D. Thesis
William Thomas Wittman 1989 202 p
(Contract MDA903-86-K-0155)
(AD-A218268; AFIT/CI/CIA-89-128) Avail: NTIS HC A10/MF A02 CSCL 05/8

The long-term retention characteristics of three memory components learned both naturally and in the laboratory were investigated. Using a cued recall procedure, 48 college students were asked to recall the spatial, temporal, and item components of their own semester schedules (Experiment 2), or a fictitious schedule (Experiment 2). In completing class schedule questionnaires, students were both cued with and asked to recall these three components. GRA

54 MAN/SYSTEM TECHNOLOGY AND LIFE SUPPORT

Includes human engineering; biotechnology; and space suits and protective clothing.

For related information see also *16 Space Transportation.*

N90-20645*# National Aeronautics and Space Administration. Lyndon B. Johnson Space Center, Houston, TX.
DEVELOPMENT AND APPLICATION OF NONFLAMMABLE, HIGH-TEMPERATURE BETA FIBERS
Frederic S. Dawn Dec. 1989 40 p
(NASA-TM-102158; NAS 1.15:102158) Avail: NTIS HC A03/MF A01 CSCL 06K

Recent advances in fiber technology have contributed to the success of the U.S. space program. The inorganic fiber Beta, developed as a result of efforts begun in the early 1960's and heightened following the January 27, 1967 Apollo fire is unique among inorganic and organic fibers. It has been developed into woven, nonwoven, knitted, braided, coated and printed structures. All of these were used extensively for the Apollo, Skylab, Apollo-Soyuz test project, space shuttle, Spacelab, and satellite programs. In addition to being used successfully in the space program, Beta fibers are being used commercially as firesafe fabrics in homes, hospitals, institutions, public buildings, aircraft, and public transportation, wherever total nonflammability is required. One of the most unique applications of the Beta composite structure is the roofing material for the 80,000-seat Detroit Lion's Silverdome and 5 square miles of the Jeddah International Airport in Saudi Arabia. This fiber has been successfully incorporated into 165 major public construction projects around the globe. The United States alone has used more than 12 million square yards of the material. Beta fiber has been used successfully to date and has a promising future with unlimited potential for both space and commercial application. Efforts are currently underway to improve Beta fiber to meet the requirements of extended service life for the Space Station Freedom, lunar outpost, and Mars exploration missions. Author

N90-20646# Human Engineering Labs., Aberdeen Proving Ground, MD.
COMPARISON OF OCULOMETER AND HEAD-FIXED RETICLE WITH VOICE OR SWITCH AND TOUCH PANEL FOR DATA ENTRY ON A GENERIC TACTICAL AIR COMBAT DISPLAY Final Report
Christopher C. Smyth and Mary E. Dominessy Nov. 1989 82 p
(AD-A217231; HEL-TM-21-89) Avail: NTIS HC A05/MF A01 CSCL 01/3

An experiment with 15 U.S. Army enlisted military subjects was conducted to compare the use of a head-mounted oculometer, a head-fixed reticle, and a touch panel for data entry tasks on a generic tactical air combat display. The oculometer and the fixed reticle were operated in a head-free mode and were used with either switch or voice. The fixed reticle with switch, the oculometer with switch, and the touch panel are significantly faster than the fixed reticle with voice and the oculometer with voice. The fixed reticle methods are faster than the oculometer methods of the same modality. The switch methods are faster than the voice methods. The ocular pointing methods (whether oculometer of fixed reticle, voice or switch input) require a larger display activation window (+ or - 1.1 inches at 27 inches' viewing distance) than does the touch panel, thereby limiting the number of selections that can be shown on the display. This is especially true for the oculometer with voice method which generated significantly more selection errors and may therefore require a still larger display activation window for proper operation. GRA

N90-20647# Douglas Aircraft Co., Inc., Long Beach, CA.
ASSESSMENT OF CREW WORKLOAD MEASUREMENT METHODS, TECHNIQUES AND PROCEDURES. VOLUME 1: PROCESS, METHODS AND RESULTS Final Report, Jul. 1986 - Feb. 1989
William H. Corwin, Diane L. Sandry-Garza, Michael H. Biferno, George P. Boucek, Jr., and Aileen L. Logan Sep. 1989 237 p
Prepared in cooperation with Boeing Commercial Airplane Co., Seattle, WA
(Contract F33615-86-C-3600)
(AD-A217699; WRDC-TR-89-7006-Vol-1) Avail: NTIS HC A11/MF A02 CSCL 05/9

The primary goal was to identify assessment techniques which demonstrate evidence of validity and reliability and are suitable as measures of flightcrew workload for aircraft certification. To use a workload assessment technique with confidence for the certification of an aircraft flightdeck, the validity and reliability of the technique must be well established. Validity is the capability of the assessment technique to measure the abstract construct it is proposed to measure. Reliability is the capability of the measure to produce the same results with repeated testing. A comprehensive literature review was conducted to identify workload measures which have an empirical record of validity and reliability. All candidate workload assessment techniques had to be applicable for evaluating workload in an aircraft environment. Two workshops were conducted to bring together experts in the workload assessment field to determine candidate measures for simulation testing (aided by the literature search), and make recommendations for testing in a high fidelity simulation. Two separate simulation tests were conducted at the Man Vehicle System Research Facility at NASA-Ames Research Center using a Phase 2 B-727 motion-base simulator. GRA

N90-20648# Human Engineering Labs., Aberdeen Proving Ground, MD.
AIDING THE DECISION MAKER: PERCEPTUAL AND COGNITIVE ISSUES AT THE HUMAN-MACHINE INTERFACE Final Report
James D. Walrath Dec. 1989 22 p

(DA Proj. 1L1-162716-AH-70)
(AD-A217862; HEL-TN-15-89) Avail: NTIS HC A02/MF A01 CSCL 05/8

Advances in weapon and sensor technologies have given rise to very complex military systems. The soldier-machine interface, typical of such systems, is often characterized by elevated task loadings and speed stress. These conditions can combine to produce increased operator errors and degraded decision making performance. These operator performance problems are acknowledged and a general review is provided of the human judgement and decision making literature (specifically focusing on perceptual and attentional mechanisms). An abridged history of the psychological study of human decision making is provided to illuminate the domain, and four methods are discussed for improving the performance of systems that suffer because of poor human judgement and decision making. A special plea is made to consider aiding harassed decision makers by paying careful attention to principles of human perception and attention, because these mechanisms form the foundation of our ability to acquire relevant and timely problem data. GRA

N90-20649# Army Research Inst. of Environmental Medicine, Natick, MA.
COMPARISON OF LIGHT DUTY GLOVES WITH NATURAL AND SYNTHETIC MATERIALS UNDER WET AND DRY CONDITIONS
W. R. Santee, T. L. Endrusick, and L. S. Pensotti Jan. 1990 9 p
(AD-A218119) Avail: NTIS HC A02/MF A01 CSCL 15/5

The performance of five volunteer test subjects wearing a standard cold weather military uniform and three different gloves was compared during treadmill walking (120 minutes), sitting (125 minutes) and hand conductance or contact (60 minutes). Chamber conditions were -6.7 C (20 F) Ta and 1.1 m.s-1 wind speed. The sitting tests were repeated at 0 C (32 F). Contact tests were repeated with wet gloves. Rectal and finger temperatures, heart rate, and endurance times were measured. The results indicate that the new leather shell is more affected by external moisture than the standard shell. GRA

N90-20055# Aerospace Medical Research Labs., Wright-Patterson AFB, OH. Human Systems Div.
DEVELOPMENT OF ACCELERATION EXPOSURE LIMITS FOR ADVANCED ESCAPE SYSTEMS
James W. Brinkley, Lawrence J. Specker, and Stephen E. Mosher (DynCorp., Wright-Patterson AFB, OH.) *In* AGARD, Implications of Advanced Technologies for Air and Spacecraft Escape Feb. 1990 14 p (For primary document see N90-20054 13-03)
Copyright Avail: NTIS HC A06/MF A01; Non-NATO Nationals requests available only from AGARD/Scientific Publications Executive

N90-20062# Aerospace Medical Research Labs., Wright-Patterson AFB, OH. Biodynamics and Bioengineering Div.
THE USAF ADVANCED DYNAMIC ANTHROPOMORPHIC MANIKIN (ADAM)
Roy R. Rasmussen and Ints Kaleps *In* AGARD, Implications of Advanced Technologies for Air and Spacecraft Escape Feb. 1990 7 p (For primary document see N90-20054 13-03)
Copyright Avail: NTIS HC A06/MF A01; Non-NATO Nationals requests available only from AGARD/Scientific Publications Executive

55 SPACE BIOLOGY

Includes exobiology; planetary biology; and extraterrestrial life.

No abstracts in this category.

59 MATHEMATICAL AND COMPUTER SCIENCES (GENERAL)

N90-20650*# Institute for Computer Applications in Science and Engineering, Hampton, VA.
HIGH ORDER FILTERING METHODS FOR APPROXIMATING HYBERBOLIC SYSTEMS OF CONSERVATION LAWS Final Report
F. Lafon and S. Osher (California Univ., Los Angeles.) Mar. 1990 37 p Submitted for publication Sponsored in part by DARPA
(Contracts NAS1-18605; NAG1-270; N00014-86-K-0691; NSF DMS-88-11863)
(NASA-CR-182016; NAS 1.26:182016; ICASE-90-25) Avail: NTIS HC A03/MF A01 CSCL 12A

In the computation of discontinuous solutions of hyperbolic systems of conservation laws, the recently developed essentially non-oscillatory (ENO) schemes appear to be very useful. However, they are computationally costly compared to simple central difference methods. A filtering method which is developed uses simple central differencing of arbitrarily high order accuracy, except when a novel local test indicates the development of spurious oscillations. At these points, the full ENO apparatus is used, maintaining the high order of accuracy, but removing spurious oscillations. Numerical results indicate the success of the method. High order of accuracy was obtained in regions of smooth flow without spurious oscillations for a wide range of problems and a significant speed up of generally a factor of almost three over the full ENO method. Author

60 COMPUTER OPERATIONS AND HARDWARE

Includes hardware for computer graphics, firmware, and data processing.

For components see *33 Electronics and Electrical Engineering.*

N90-20651*# National Aeronautics and Space Administration. Lyndon B. Johnson Space Center, Houston, TX.
GRAPHICS TECHNOLOGY IN SPACE APPLICATIONS (GTSA 1989)
Sandy Griffin, ed. Aug. 1989 247 p Workshop held in Houston, TX, 12-14 Apr. 1989; sponsored by NASA, Washington and Houston Univ., Clear Lake
(NASA-CP-3045; S-594; NAS 1.55:3045) Avail: NTIS HC A11/MF A02 CSCL 09B

This document represents the proceedings of the Graphics Technology in Space Applications, which was held at NASA Lyndon B. Johnson Space Center on April 12 to 14, 1989 in Houston, Texas. The papers included in these proceedings were published in general as received from the authors with minimum modifications and editing. Information contained in the individual papers is not to be construed as being officially endorsed by NASA. For individual titles, see N90-20652 through N90-20684.

N90-20652*# National Aeronautics and Space Administration. Goddard Space Flight Center, Greenbelt, MD.
TAE PLUS: TRANSPORTABLE APPLICATIONS ENVIRONMENT PLUS TOOLS FOR BUILDING GRAPHIC-ORIENTED APPLICATIONS
Martha R. Szczur *In* NASA, Lyndon B. Johnson Space Center, Graphics Technology in Space Applications (GTSA 1989) Aug. 1989 p 1- (For primary document see N90-20651 13-60)
Avail: NTIS HC A11/MF A02 CSCL 09B

The Transportable Applications Environment Plus (TAE Plus), developed by NASA's Goddard Space Flight Center, is a portable User Interface Management System (UIMS), which provides an intuitive WYSIWYG WorkBench for prototyping and designing an application's user interface, integrated with tools for efficiently

implementing the designed user interface and effective management of the user interface during an application's active domain. During the development of TAE Plus, many design and implementation decisions were based on the state-of-the-art within graphics workstations, windowing system and object-oriented programming languages. Some of the problems and issues experienced during implementation are discussed. A description of the next development steps planned for TAE Plus is also given. Author

N90-20653*# Pixar Corp., San Rafael, CA.
RENDERMAN DESIGN PRINCIPLES
Tony Apodaca and Tom Porter *In* NASA, Lyndon B. Johnson Space Center, Graphics Technology in Space Applications (GTSA 1989) Aug. 1989 p 9-11 (For primary document see N90-20651 13-60)
Avail: NTIS HC A11/MF A02 CSCL 09B

The two worlds of interactive graphics and realistic graphics have remained separate. Fast graphics hardware runs simple algorithms and generates simple looking images. Photorealistic image synthesis software runs slowly on large expensive computers. The time has come for these two branches of computer graphics to merge. The speed and expense of graphics hardware is no longer the barrier to the wide acceptance of photorealism. There is every reason to believe that high quality image synthesis will become a standard capability of every graphics machine, from superworkstation to personal computer. The significant barrier has been the lack of a common language, an agreed-upon set of terms and conditions, for 3-D modeling systems to talk to 3-D rendering systems for computing an accurate rendition of that scene. Pixar has introduced RenderMan to serve as that common language. RenderMan, specifically the extensibility it offers in shading calculations, is discussed. Author

N90-20654*# Rockwell Shuttle Operations Co., Houston, TX.
THE REAL TIME INTERACTIVE DISPLAY ENVIRONMENT (RTIDE), A DISPLAY BUILDING TOOL DEVELOPED BY SPACE SHUTTLE FLIGHT CONTROLLERS
Thomas A. Kalvelage *In* NASA, Lyndon B. Johnson Space Center, Graphics Technology in Space Applications (GTSA 1989) Aug. 1989 p 17-23 (For primary document see N90-20651 13-60)
Avail: NTIS HC A11/MF A02 CSCL 09B

NASA's Mission Control Center, located at Johnson Space Center, is incrementally moving from a centralized architecture to a distributed architecture. Starting with STS-29, some host-driven console screens will be replaced with graphics terminals driven by workstations. These workstations will be supplied realtime data first by the Real Time Data System (RTDS), a system developed inhouse, and then months later (in parallel with RTDS) by interim and subsequently operational versions of the Mission Control Center Upgrade (MCCU) software package. The Real Time Interactive Display Environment (RTIDE) was built by Space Shuttle flight controllers to support the rapid development of multiple new displays to support Shuttle flights. RTIDE is a display building tool that allows non-programmers to define object-oriented, event-driven, mouseable displays. Particular emphasis was placed on upward compatibility between RTIDE versions, ability to acquire data from different data sources, realtime performance, ability to modularly upgrade RTIDE, machine portability, and a clean, powerful user interface. The operational and organizational factors that drove RTIDE to its present form, the actual design itself, simulation and flight performance, and lessons learned in the process are discussed. Author

N90-20655*# Jet Propulsion Lab., California Inst. of Tech., Pasadena.
KNOWLEDGE REPRESENTATION IN SPACE FLIGHT OPERATIONS
Carl Busse *In* NASA, Lyndon B. Johnson Space Center, Graphics Technology in Space Applications (GTSA 1989) Aug. 1989 p 25-31 (For primary document see N90-20651 13-60)
Avail: NTIS HC A11/MF A02 CSCL 09B

In space flight operations rapid understanding of the state of the space vehicle is essential. Representation of knowledge depicting space vehicle status in a dynamic environment presents a difficult challenge. The NASA Jet Propulsion Laboratory has pursued areas of technology associated with the advancement of spacecraft operations environment. This has led to the development of several advanced mission systems which incorporate enhanced graphics capabilities. These systems include: (1) Spacecraft Health Automated Reasoning Prototype (SHARP); (2) Spacecraft Monitoring Environment (SME); (3) Electrical Power Data Monitor (EPDM); (4) Generic Payload Operations Control Center (GPOCC); and (5) Telemetry System Monitor Prototype (TSM). Knowledge representation in these systems provides a direct representation of the intrinsic images associated with the instrument and satellite telemetry and telecommunications systems. The man-machine interface includes easily interpreted contextual graphic displays. These interactive video displays contain multiple display screens with pop-up windows and intelligent, high resolution graphics linked through context and mouse-sensitive icons and text. Author

N90-20656*# Dual and Associates, Houston, TX.
THE REAL TIME DISPLAY BUILDER (RTDB)
Erick D. Kindred and Samuel A. Bailey, Jr. *In* NASA, Lyndon B. Johnson Space Center, Graphics Technology in Space Applications (GTSA 1989) Aug. 1989 p 33-38 (For primary document see N90-20651 13-60)
Avail: NTIS HC A11/MF A02 CSCL 09B

The Real Time Display Builder (RTDB) is a prototype interactive graphics tool that builds logic-driven displays. These displays reflect current system status, implement fault detection algorithms in real time, and incorporate the operational knowledge of experienced flight controllers. RTDB utilizes an object-oriented approach that integrates the display symbols with the underlying operational logic. This approach allows the user to specify the screen layout and the driving logic as the display is being built. RTDB is being developed under UNIX in C utilizing the MASSCOMP graphics environment with appropriate functional separation to ease portability to other graphics environments. RTDB grew from the need to develop customized real-time data-driven Space Shuttle systems displays. One display, using initial functionality of the tool, was operational during the orbit phase of STS-26 Discovery. RTDB is being used to produce subsequent displays for the Real Time Data System project currently under development within the Mission Operations Directorate at NASA/JSC. The features of the tool, its current state of development, and its applications are discussed. Author

N90-20657*# Barrios Technology, Inc., Houston, TX.
BINARY SPACE PARTITIONING TREES AND THEIR USES
Bradley N. Bell *In* NASA, Lyndon B. Johnson Space Center, Graphics Technology in Space Applications (GTSA 1989) Aug. 1989 p 39-42 (For primary document see N90-20651 13-60)
Avail: NTIS HC A11/MF A02 CSCL 09B

Binary Space Partitioning (BSP) trees have some qualities that make them useful in solving many graphics related problems. The purpose is to describe what a BSP tree is, and how it can be used to solve the problem of hidden surface removal, and constructive solid geometry. The BSP tree is based on the idea that a plane acting as a divider subdivides space into two parts with one being on the positive side and the other on the negative. A polygonal solid is then represented as the volume defined by the collective interior half spaces of the solid's bounding surfaces. The nature of how the tree is organized lends itself well for sorting polygons relative to an arbitrary point in 3 space. The speed at which the tree can be traversed for depth sorting is fast enough to provide hidden surface removal at interactive speeds. The fact that a BSP tree actually represents a polygonal solid as a bounded volume also makes it quite useful in performing the boolean operations used in constructive solid geometry. Due to the nature of the BSP tree, polygons can be classified as they are subdivided. The ability to classify polygons as they are subdivided can enhance the simplicity of implementing constructive solid geometry.

Author

N90-20658*# International Business Machines Corp., Houston, TX.

ONBOARD SHUTTLE ON-LINE SOFTWARE REQUIREMENTS SYSTEM: PROTOTYPE c61

Barbara Kolkhorst and Barry Ogletree (International Business Machines Corp., Armonk, NY.) *In* NASA, Lyndon B. Johnson Space Center, Graphics Technology in Space Applications (GTSA 1989) Aug. 1989 p 43-48 (For primary document see N90-20651 13-60)

Avail: NTIS HC A11/MF A02 CSCL 09B

The prototype discussed here was developed as proof of a concept for a system which could support high volumes of requirements documents with integrated text and graphics; the solution proposed here could be extended to other projects whose goal is to place paper documents in an electronic system for viewing and printing purposes. The technical problems (such as conversion of documentation between word processors, management of a variety of graphics file formats, and difficulties involved in scanning integrated text and graphics) would be very similar for other systems of this type. Indeed, technological advances in areas such as scanning hardware and software and display terminals insure that some of the problems encountered here will be solved in the near-term (less than five years). Examples of these solvable problems include automated input of integrated text and graphics, errors in the recognition process, and the loss of image information which results from the digitization process. The solution developed for the Online Software Requirements System is modular and allows hardware and software components to be upgraded or replaced as industry solutions mature. The extensive commercial software content allows the NASA customer to apply resources to solving the problem and maintaining documents. Author

N90-20659*# Evans and Sutherland Computer Corp., Salt Lake City, UT.

DESIGN CONSIDERATIONS FOR A SPACE DATABASE c82

Lance M. Moss *In* NASA, Lyndon B. Johnson Space Center, Graphics Technology in Space Applications (GTSA 1989) Aug. 1989 p 49-53 (For primary document see N90-20651 13-60)

Avail: NTIS HC A11/MF A02 CSCL 05B

Part of the information used in a real-time simulator is stored in the visual database. This information is processed by an image generator and displayed as a real-time visual image. The database must be constructed in a specific format, and it should efficiently utilize the capacities of the image generator that is was created for. A visual simulation is crucially dependent upon the success with which the database provides visual cues and recognizable scenes. For this reason, more and more attention is being paid to the art and science of creating effective real-time visual databases. Investigated here are the database design considerations required for a space-oriented real-time simulator. Space applications often require unique designs that correspond closely to the particular image-generator hardware and visual-database-management software. Specific examples from the databases constructed for NASA and its Evans and Sutherland CT6 image generator illustrate the various design strategies used in a space-simulation environment. These database design considerations are essential for all who would create a space database. Author

N90-20660*# National Aeronautics and Space Administration. Ames Research Center, Moffett Field, CA.

TOOLS FOR 3D SCIENTIFIC VISUALIZATION IN COMPUTATIONAL AERODYNAMICS

Gordon Bancroft, Todd Plessel, Fergus Merritt (Sterling Software, Moffett Field, CA.), and Val Watson *In* NASA, Lyndon B. Johnson Space Center, Graphics Technology in Space Applications (GTSA 1989) Aug. 1989 p 55-64 (For primary document see N90-20651 13-60)

Avail: NTIS HC A11/MF A02 CSCL 09B

The purpose is to describe the tools and techniques in use at the NASA Ames Research Center for performing visualization of computational aerodynamics, for example visualization of flow fields from computer simulations of fluid dynamics about vehicles such as the Space Shuttle. The hardware used for visualization is a high-performance graphics workstation connected to a super computer with a high speed channel. At present, the workstation is a Silicon Graphics IRIS 3130, the supercomputer is a CRAY2, and the high speed channel is a hyperchannel. The three techniques used for visualization are post-processing, tracking, and steering. Post-processing analysis is done after the simulation. Tracking analysis is done during a simulation but is not interactive, whereas steering analysis involves modifying the simulation interactively during the simulation. Using post-processing methods, a flow simulation is executed on a supercomputer and, after the simulation is complete, the results of the simulation are processed for viewing. The software in use and under development at NASA Ames Research Center for performing these types of tasks in computational aerodynamics is described. Workstation performance issues, benchmarking, and high-performance networks for this purpose are also discussed as well as descriptions of other hardware for digital video and film recording. Author

N90-20661*# McDonnell-Douglas Space Systems Co., Houston, TX.

APPLICATIONS OF GRAPHICS TO SUPPORT A TESTBED FOR AUTONOMOUS SPACE VEHICLE OPERATIONS c61

K. R. Schmeckpeper, J. P. Aldridge, S. Benson, S. Horner, A. Kullman, T. Mulder, W. Parrott, D. Roman, G. Watts, and Daniel C. Bochsler (LinCom Corp., Houston, TX.) *In* NASA, Lyndon B. Johnson Space Center, Graphics Technology in Space Applications (GTSA 1989) Aug. 1989 p 65-71 (For primary document see N90-20651 13-60)

Avail: NTIS HC A11/MF A02 CSCL 09B

Researchers describe their experience using graphics tools and utilities while building an application, AUTOPS, that uses a graphical Machintosh (TM)-like interface for the input and display of data, and animation graphics to enhance the presentation of results of autonomous space vehicle operations simulations. AUTOPS is a test bed for evaluating decisions for intelligent control systems for autonomous vehicles. Decisions made by an intelligent control system, e.g., a revised mission plan, might be displayed to the user in textual format or he can witness the effects of those decisions via out of window graphics animations. Although a textual description conveys essentials, a graphics animation conveys the replanning results in a more convincing way. Similarily, iconic and menu-driven screen interfaces provide the user with more meaningful options and displays. Presented here are experiences with the SunView and TAE Plus graphics tools used for interface design, and the Johnson Space Center Interactive Graphics Laboratory animation graphics tools used for generating out out of the window graphics. Author

N90-20662*# Ford Aerospace and Communications Corp., Houston, TX. Space Information Systems Operation.

LARGE SCREEN DISPLAY FOR THE MISSION CONTROL CENTER

Martin J. Skudlarek *In* NASA, Lyndon B. Johnson Space Center, Graphics Technology in Space Applications (GTSA 1989) Aug. 1989 p 75-80 Sponsored in part by Hughes Aircraft Co. (For primary document see N90-20651 13-60)

(Contract NAS9-15014)

Avail: NTIS HC A11/MF A02 CSCL 09B

The Mission Control Center (MCC), located at the Johnson Space Center near Houston, Texas, is the primary point of control and monitoring for National Space Transportation System (NSTS) flight activities. NSTS flight managers monitor and command spacecraft from one of two Flight Control Rooms (FCR). Each FCR is equipped with five large screen displays for group dissemination of spacecraft system status and vehicle position relative to Earth geography. The primary or center screen display is ten feet in height and twenty feet in width. The secondary or side screens are seven and one-hald feet high and ten feet wide. The center screen projection system is exhibiting high maintenance costs and is considered to be in wear-out phase. The replacement of the large center screen displays at the MCC is complicated by the unique requirements of the Flight Controller user. These

requirements demand a very high performance, multiple color projection system capable of the display of high resolution text, graphics and images produced in near real time. The current system to be replaced, the replacement system requirements, the efforts necessary to procure the major element of this system (the projector) for the government, and how the new capabilities are to be integrated into the existing MCC operational configuration are discussed. Author

N90-20663*# Rockwell International Corp., Downey, CA. REGIS Computer Animation Lab.
EFFICIENT UTILIZATION OF GRAPHICS TECHNOLOGY FOR SPACE ANIMATION **c61**
Gregory Peter Panos *In* NASA, Lyndon B. Johnson Space Center, Graphics Technology in Space Applications (GTSA 1989) Aug. 1989 p 81-91 (For primary document see N90-20651 13-60)
Avail: NTIS HC A11/MF A02 CSCL 09B

Efficient utilization of computer graphics technology has become a major investment in the work of aerospace engineers and mission designers. These new tools are having a significant impact in the development and analysis of complex tasks and procedures which must be prepared prior to actual space flight. Design and implementation of useful methods in applying these tools has evolved into a complex interaction of hardware, software, network, video and various user interfaces. Because few people can understand every aspect of this broad mix of technology, many specialists are required to build, train, maintain and adapt these tools to changing user needs. Researchers have set out to create systems where an engineering designer can easily work to achieve goals with a minimum of technological distraction. This was accomplished with high-performance flight simulation visual systems and supercomputer computational horsepower. Control throughout the creative process is judiciously applied while maintaining generality and ease of use to accommodate a wide variety of engineering needs. Author

N90-20664*# National Aeronautics and Space Administration. Lyndon B. Johnson Space Center, Houston, TX.
ENGINEERING VISUALIZATION UTILIZING ADVANCED ANIMATION **c61**
Gunter R. Sabionski and Thomas L. Robinson, Jr. (Barrios Technology, Inc., Houston, TX.) *In its* Graphics Technology in Space Applications (GTSA 1989) Aug. 1989 p 93-102 (For primary document see N90-20651 13-60)
Avail: NTIS HC A11/MF A02 CSCL 09B

Engineering visualization is the use of computer graphics to depict engineering analysis and simulation in visual form from project planning through documentation. Graphics displays let engineers see data represented dynamically which permits the quick evaluation of results. The current state of graphics hardware and software generally allows the creation of two types of 3D graphics. The use of animated video as an engineering visualization tool is presented. The engineering, animation, and videography aspects of animated video production are each discussed. Specific issues include the integration of staffing expertise, hardware, software, and the various production processes. A detailed explanation of the animation process reveals the capabilities of this unique engineering visualization method. Automation of animation and video production processes are covered and future directions are proposed. Author

N90-20665*# National Aeronautics and Space Administration. Lyndon B. Johnson Space Center, Houston, TX.
MULTI-TASKING COMPUTER CONTROL OF VIDEO RELATED EQUIPMENT
Rod Molina and Bob Gilbert *In its* Graphics Technology in Space Applications (GTSA 1989) Aug. 1989 p 103-105 (For primary document see N90-20651 13-60)
Avail: NTIS HC A11/MF A02 CSCL 09B

The flexibility, cost-effectiveness and widespread availability of personal computers now makes it possible to completely integrate the previously separate elements of video post-production into a single device. Specifically, a personal computer, such as the Commodore-Amiga, can perform multiple and simultaneous tasks from an individual unit. Relatively low cost, minimal space requirements and user-friendliness, provides the most favorable environment for the many phases of video post-production. Computers are well known for their basic abilities to process numbers, text and graphics and to reliably perform repetitive and tedious functions efficiently. These capabilities can now apply as either additions or alternatives to existing video post-production methods. A present example of computer-based video post-production technology is the RGB CVC (Computer and Video Creations) WorkSystem. A wide variety of integrated functions are made possible with an Amiga computer existing at the heart of the system. Author

N90-20666*# Microexpert, Calabasas, CA.
BROADENING THE INTERFACE BANDWIDTH IN SIMULATION BASED TRAINING **c61**
Larry E. Somers *In* NASA, Lyndon B. Johnson Space Center, Graphics Technology in Space Applications (GTSA 1989) Aug. 1989 p 107-114 (For primary document see N90-20651 13-60)
Avail: NTIS HC A11/MF A02 CSCL 09B

Currently most computer based simulations rely exclusively on computer generated graphics to create the simulation. When training is involved, the method almost exclusively used to display information to the learner is text displayed on the cathode ray tube. MICROEXPERT Systems is concentrating on broadening the communications bandwidth between the computer and user by employing a novel approach to video image storage combined with sound and voice output. An expert system is used to combine and control the presentation of analog video, sound, and voice output with computer based graphics and text. Researchers are currently involved in the development of several graphics based user interfaces for NASA, the U.S. Army, and the U.S. Navy. Here, the focus is on the human factors considerations, software modules, and hardware components being used to develop these interfaces. Author

N90-20667*# Microexpert, Calabasas, CA.
ANIMATION GRAPHIC INTERFACE FOR THE SPACE SHUTTLE ONBOARD COMPUTER **c61**
Jeffrey Wike and Paul Griffith *In* NASA, Lyndon B. Johnson Space Center, Graphics Technology in Space Applications (GTSA 1989) Aug. 1989 p 115-119 (For primary document see N90-20651 13-60)
Avail: NTIS HC A11/MF A02 CSCL 09B

Graphics interfaces designed to operate on space qualified hardware challenge software designers to display complex information under processing power and physical size constraints. Under contract to Johnson Space Center, MICROEXPERT Systems is currently constructing an intelligent interface for the LASER DOCKING SENSOR (LDS) flight experiment. Part of this interface is a graphic animation display for Rendezvous and Proximity Operations. The displays have been designed in consultation with Shuttle astronauts. The displays show multiple views of a satellite relative to the shuttle, coupled with numeric attitude information. The graphics are generated using position data received by the Shuttle Payload and General Support Computer (PGSC) from the Laser Docking Sensor. Some of the design considerations include crew member preferences in graphic data representation, single versus multiple window displays, mission tailoring of graphic displays, realistic 3D images versus generic icon representations of real objects, the physical relationship of the observers to the graphic display, how numeric or textual information should interface with graphic data, in what frame of reference objects should be portrayed, recognizing conditions of display information-overload, and screen format and placement consistency. Author

N90-20668*# National Aeronautics and Space Administration. Goddard Space Flight Center, Greenbelt, MD.
OPERATIONAL COMPUTER GRAPHICS IN THE FLIGHT DYNAMICS ENVIRONMENT **c61**

James F. Jeletic *In* NASA, Lyndon B. Johnson Space Center, Graphics Technology in Space Applications (GTSA 1989) Aug. 1989 p 121-128 (For primary document see N90-20651 13-60)
Avail: NTIS HC A11/MF A02 CSCL 09B

Over the past five years, the Flight Dynamics Division of the National Aeronautics and Space Administration's (NASA's) Goddard Space Flight Center has incorporated computer graphics technology into its operational environment. In an attempt to increase the effectiveness and productivity of the Division, computer graphics software systems have been developed that display spacecraft tracking and telemetry data in 2-d and 3-d graphic formats that are more comprehensible than the alphanumeric tables of the past. These systems vary in functionality from real-time mission monitoring system, to mission planning utilities, to system development tools. Here, the capabilities and architecture of these systems are discussed. Author

N90-20669*# TRW Defense Systems Group, Redondo Beach, CA.
OMV MISSION SIMULATOR
Keith E. Cok *In* NASA, Lyndon B. Johnson Space Center, Graphics Technology in Space Applications (GTSA 1989) Aug. 1989 p 129-134 (For primary document see N90-20651 13-60)
Avail: NTIS HC A11/MF A02 CSCL 09B

The Orbital Maneuvering Vehicle (OMV) will be remotely piloted during rendezvous, docking, or proximity operations with target spacecraft from a ground control console (GCC). The real-time mission simulator and graphics being used to design a console pilot-machine interface are discussed. A real-time orbital dynamics simulator drives the visual displays. The dynamics simulator includes a J2 oblate earth gravity model and a generalized 1962 rotating atmospheric and drag model. The simulator also provides a variable-length communication delay to represent use of the Tracking and Data Relay Satellite System (TDRSS) and NASA Communications (NASCOM). Input parameter files determine the graphics display. This feature allows rapid prototyping since displays can be easily modified from pilot recommendations. A series of pilot reviews are being held to determine an effective pilot-machine interface. Pilots fly missions with nominal to 3-sigma dispersions in translational or rotational axes. Console dimensions, switch type and layout, hand controllers, and graphic interfaces are evaluated by the pilots and the GCC simulator is modified for subsequent runs. Initial results indicate a pilot preference for analog versus digital displays and for two 3-degree-of-freedom hand controllers. Author

N90-20670*# Lockheed Engineering and Sciences Co., Houston, TX.
THE USE OF GRAPHICS IN THE DESIGN OF THE HUMAN-TELEROBOT INTERFACE **c61**
Mark A. Stuart and Randy L. Smith *In* NASA, Lyndon B. Johnson Space Center, Graphics Technology in Space Applications (GTSA 1989) Aug. 1989 p 135-142 (For primary document see N90-20651 13-60)
(Contract NAS9-17900)
Avail: NTIS HC A11/MF A02 CSCL 09B

The Man-Systems Telerobotics Laboratory (MSTL) of NASA's Johnson Space Center employs computer graphics tools in their design and evaluation of the Flight Telerobotic Servicer (FTS) human/telerobot interface on the Shuttle and on the Space Station. It has been determined by the MSTL that the use of computer graphics can promote more expedient and less costly design endeavors. Several specific examples of computer graphics applied to the FTS user interface by the MSTL are described. Author

N90-20671*# National Aeronautics and Space Administration. Lyndon B. Johnson Space Center, Houston, TX.
DISTRIBUTED EARTH MODEL/ORBITER SIMULATION **c61**
Erik Geisler, Scott McClanahan, and Gary Smith (International Business Machines Corp., Houston, TX.) *In its* Graphics Technology in Space Applications (GTSA 1989) Aug. 1989 p 143-150 (For primary document see N90-20651 13-60)
Avail: NTIS HC A11/MF A02 CSCL 09B

Distributed Earth Model/Orbiter Simulation (DEMOS) is a network based application developed for the UNIX environment that visually monitors or simulates the Earth and any number of orbiting vehicles. Its purpose is to provide Mission Control Center (MCC) flight controllers with a visually accurate three dimensional (3D) model of the Earth, Sun, Moon and orbiters, driven by real time or simulated data. The project incorporates a graphical user interface, 3D modelling employing state-of-the art hardware, and simulation of orbital mechanics in a networked/distributed environment. The user interface is based on the X Window System and the X Ray toolbox. The 3D modelling utilizes the Programmer's Hierarchical Interactive Graphics System (PHIGS) standard and Raster Technologies hardware for rendering/display performance. The simulation of orbiting vehicles uses two methods of vector propagation implemented with standard UNIX/C for portability. Each part is a distinct process that can run on separate nodes of a network, exploiting each node's unique hardware capabilities. The client/server communication architecture of the application can be reused for a variety of distributed applications. Author

N90-20672*# Barrios Technology, Inc., Houston, TX.
PROTOTYPE PART TASK TRAINER: A REMOTE MANIPULATOR SYSTEM SIMULATOR
David Shores *In* NASA, Lyndon B. Johnson Space Center, Graphics Technology in Space Applications (GTSA 1989) Aug. 1989 p 151-153 (For primary document see N90-20651 13-60)
Avail: NTIS HC A11/MF A02 CSCL 09B

The Part Task Trainer program (PTT) is a kinematic simulation of the Remote Manipulator System (RMS) for the orbiter. The purpose of the PTT is to supply a low cost man-in-the-loop simulator, allowing the student to learn operational procedures which then can be used in the more expensive full scale simulators. PTT will allow the crew members to work on their arm operation skills without the need for other people running the simulation. The controlling algorithms for the arm were coded out of the Functional Subsystem Requirements Document to ensure realistic operation of the simulation. Relying on the hardware of the workstation to provide fast refresh rates for full shaded images allows the simulation to be run on small low cost stand alone work stations, removing the need to be tied into a multi-million dollar computer for the simulation. PTT will allow the student to make errors which in full scale mock up simulators might cause failures or damage hardware. On the screen the user is shown a graphical representation of the RMS control panel in the aft cockpit of the orbiter, along with a main view window and up to six trunion and guide windows. The dials drawn on the panel may be turned to select the desired mode of operation. The inputs controlling the arm are read from a chair with a Translational Hand Controller (THC) and a Rotational Hand Controller (RHC) attached to it. Author

N90-20673*# Lockheed Engineering and Sciences Co., Houston, TX.
SPACE STATION FREEDOM INTEGRATED FAULT MODEL **c61**
Fred J. Becker *In* NASA, Lyndon B. Johnson Space Center, Graphics Technology in Space Applications (GTSA 1989) Aug. 1989 p 155-163 (For primary document see N90-20651 13-60)
Avail: NTIS HC A11/MF A02 CSCL 09B

A demonstration of an integrated fault propagation model for Space Station Freedom is described. The demonstration uses a HyperCard graphical interface to show how failures can propagate from one component to another, both within a system and between systems. It also shows how hardware failures can impact certain defined functions like reboost, atmosphere maintenance or collision avoidance. The demonstration enables the user to view block diagrams for the various space station systems using an overview screen, and interactively choose a component and see what single

or dual failure combinations can cause it to fail. It also allows the user to directly view the fault model, which is a collection of drawing and text listings accessible from a guide screen. Fault modeling provides a useful technique for analyzing individual systems and also interactions between systems in the presence of multiple failures so that a complete picture of failure tolerance and component criticality can be achieved. Author

N90-20674*# Mitre Corp., Houston, TX.
GRAPHICAL PROGRAMMING AND THE USE OF SIMULATION FOR SPACE-BASED MANIPULATORS **c61**
Debra S. McGrath and James C. Reynolds *In* NASA, Lyndon B. Johnson Space Center, Graphics Technology in Space Applications (GTSA 1989) Aug. 1989 p 165-170 (For primary document see N90-20651 13-60)
Avail: NTIS HC A11/MF A02 CSCL 09B

Robotic manipulators are difficult to program even without the special requirements of a zero-gravity environment. While attention should be paid to investigating the usefulness of industrial application programming methods to space manipulators, new methods with potential application to both environments need to be invented. These methods should allow various levels of autonomy and human-in-the-loop interaction and simple, rapid switching among them. For all methods simulation must be integrated to provide reliability and safety. Graphical programming of manipulators is a candidate for an effective robot programming method despite current limitations in input devices and displays. A research project in task-level robot programming has built an innovative interface to a state-of-the-art commercial simulation and robot programming platform. The prototype demonstrates simple augmented methods for graphical programming and simulation which may be of particular interest to those concerned with Space Station applications; its development has also raised important issues for the development of more sophisticated robot programming tools. Both aspects of the project are discussed. Author

N90-20675*# National Aeronautics and Space Administration. Lyndon B. Johnson Space Center, Houston, TX.
USING AN INSTRUMENTED MANIKIN FOR SPACE STATION FREEDOM ANALYSIS **c61**
Linda Orr and Richard Hill (Lockheed Missiles and Space Co., Huntsville, AL.) *In its* Graphics Technology in Space Applications (GTSA 1989) Aug. 1989 p 171-175 (For primary document see N90-20651 13-60)
Avail: NTIS HC A11/MF A02 CSCL 09B

One of the most intriguing and complex areas of current computer graphics research is animating human figures to behave in a realistic manner. Believable, accurate human models are desirable for many everyday uses including industrial and architectural design, medical applications, and human factors evaluations. For zero-gravity (0-g) spacecraft design and mission planning scenarios, they are particularly valuable since 0-g conditions are difficult to simulate in a one-gravity Earth environment. At NASA/JSC, an in-house human modeling package called PLAID is currently being used to produce animations for human factors evaluation of Space Station Freedom design issues. Presented here is an introductory background discussion of problems encountered in existing techniques for animating human models and how an instrumented manikin can help improve the realism of these models. Author

N90-20676*# CAE Electronics Ltd., Montreal (Quebec).
THE DEVELOPMENT OF THE CANADIAN MOBILE SERVICING SYSTEM KINEMATIC SIMULATION FACILITY
G. Beyer, B. Diebold, W. Brimley, and H. Kleinberg (Spar Aerospace Ltd., Weston, Ontario) *In* NASA, Lyndon B. Johnson Space Center, Graphics Technology in Space Applications (GTSA 1989) Aug. 1989 p 177-186 Sponsored by National Research Council of Canada (For primary document see N90-20651 13-60)
Avail: NTIS HC A11/MF A02 CSCL 09B

Canada will develop a Mobile Servicing System (MSS) as its contribution to the U.S./International Space Station Freedom. Components of the MSS will include a remote manipulator (SSRMS), a Special Purpose Dexterous Manipulator (SPDM), and a mobile base (MRS). In order to support requirements analysis and the evaluation of operational concepts related to the use of the MSS, a graphics based kinematic simulation/human-computer interface facility has been created. The facility consists of the following elements: (1) A two-dimensional graphics editor allowing the rapid development of virtual control stations; (2) Kinematic simulations of the space station remote manipulators (SSRMS and SPDM), and mobile base; and (3) A three-dimensional graphics model of the space station, MSS, orbiter, and payloads. These software elements combined with state of the art computer graphics hardware provide the capability to prototype MSS workstations, evaluate MSS operational capabilities, and investigate the human-computer interface in an interactive simulation environment. The graphics technology involved in the development and use of this facility is described. Author

N90-20677*# Pennsylvania Univ., Philadelphia. Computer Graphics Research Lab.
SOFTWARE SYSTEMS FOR MODELING ARTICULATED FIGURES **c61**
Cary B. Phillips *In* NASA, Lyndon B. Johnson Space Center, Graphics Technology in Space Applications (GTSA 1989) Aug. 1989 p 187-193 (For primary document see N90-20651 13-60)
Avail: NTIS HC A11/MF A02 CSCL 09B

Research in computer animation and simulation of human task performance requires sophisticated geometric modeling and user interface tools. The software for a research environment should present the programmer with a powerful but flexible substrate of facilities for displaying and manipulating geometric objects, yet insure that future tools have a consistent and friendly user interface. Jack is a system which provides a flexible and extensible programmer and user interface for displaying and manipulating complex geometric figures, particularly human figures in a 3D working environment. It is a basic software framework for high-performance Silicon Graphics IRIS workstations for modeling and manipulating geometric objects in a general but powerful way. It provides a consistent and user-friendly interface across various applications in computer animation and simulation of human task performance. Currently, Jack provides input and control for applications including lighting specification and image rendering, anthropometric modeling, figure positioning, inverse kinematics, dynamic simulation, and keyframe animation. Author

N90-20678*# Pennsylvania Univ., Philadelphia. Dept. of Computer and Information Science.
HUMAN TASK ANIMATION FROM PERFORMANCE MODELS AND NATURAL LANGUAGE INPUT **c61**
Jeffrey Esakov, Norman I. Badler, and Moon Jung *In* NASA, Lyndon B. Johnson Space Center, Graphics Technology in Space Applications (GTSA 1989) Aug. 1989 p 195-203 Sponsored in part by Lockheed Engineering and Managment Services, Pacific Northwest Laboratories B-U0072-A-N and Pennsylvania Benjamin Franklin Partnership (For primary document see N90-20651 13-60)
(Contract NAG2-426; NGT-50063; NSF MCS-82-19196; NSF IST-86-12984; NSF DMC-85-16114; DAAG29-84-K-0061)
Avail: NTIS HC A11/MF A02 CSCL 09B

Graphical manipulation of human figures is essential for certain types of human factors analyses such as reach, clearance, fit, and view. In many situations, however, the animation of simulated people performing various tasks may be based on more complicated functions involving multiple simultaneous reaches, critical timing, resource availability, and human performance capabilities. One rather effective means for creating such a simulation is through a natural language description of the tasks to be carried out. Given an anthropometrically-sized figure and a geometric workplace environment, various simple actions such as reach, turn, and view can be effectively controlled from language commands or standard NASA checklist procedures. The commands may also be generated by external simulation tools. Task timing

is determined from actual performance models, if available, such as strength models or Fitts' Law. The resulting action specification are animated on a Silicon Graphics Iris workstation in real-time.
Author

N90-20679*# Lockheed Missiles and Space Co., Huntsville, AL.
SES CUPOLA INTERACTIVE DISPLAY DESIGN ENVIRONMENT
Bang Q. Vu and Kevin R. Kirkhoff *In* NASA, Lyndon B. Johnson Space Center, Graphics Technology in Space Applications (GTSA 1989) Aug. 1989 p 205-214 (For primary document see N90-20651 13-60)
Avail: NTIS HC A11/MF A02 CSCL 09B

The Systems Engineering Simulator, located at the Lyndon B. Johnson Space Center in Houston, Texas, is tasked with providing a real-time simulator for developing displays and controls targeted for the Space Station Freedom. These displays and controls will exist inside an enclosed workstation located on the space station. The simulation is currently providing the engineering analysis environment for NASA and contractor personnel to design, prototype, and test alternatives for graphical presentation of data to an astronaut while he performs specified tasks. A highly desirable aspect of this environment is to have the capability to rapidly develop and bring on-line a number of different displays for use in determining the best utilization of graphics techniques in achieving maximum efficiency of the test subject fulfilling his task. The Systems Engineering Simulator now has available a tool which assists in the rapid development of displays for these graphic workstations. The Display Builder was developed in-house to provide an environment which allows easy construction and modification of displays within minutes of receiving requirements for specific tests.
Author

N90-20680*# Lockheed Engineering and Sciences Co., Houston, TX.
ISSUES IN VISUAL SUPPORT TO REAL-TIME SPACE SYSTEM SIMULATION SOLVED IN THE SYSTEMS ENGINEERING SIMULATOR
Vincent K. Yuen *In* NASA, Lyndon B. Johnson Space Center, Graphics Technology in Space Applications (GTSA 1989) Aug. 1989 p 215-218 (For primary document see N90-20651 13-60)
Avail: NTIS HC A11/MF A02 CSCL 09B

The Systems Engineering Simulator has addressed the major issues in providing visual data to its real-time man-in-the-loop simulations. Out-the-window views and CCTV views are provided by three scene systems to give the astronauts their real-world views. To expand the window coverage for the Space Station Freedom workstation a rotating optics system is used to provide the widest field of view possible. To provide video signals to as many viewpoints as possible, windows and CCTVs, with a limited amount of hardware, a video distribution system has been developed to time-share the video channels among viewpoints at the selection of the simulation users. These solutions have provided the visual simulation facility for real-time man-in-the-loop simulations for the NASA space program.
Author

N90-20681*# National Aeronautics and Space Administration. Lyndon B. Johnson Space Center, Houston, TX.
HISTORY OF VISUAL SYSTEMS IN THE SYSTEMS ENGINEERING SIMULATOR
David C. Christianson *In its* Graphics Technology in Space Applications (GTSA 1989) Aug. 1989 p 219-228 (For primary document see N90-20651 13-60)
Avail: NTIS HC A11/MF A02 CSCL 09B

The Systems Engineering Simulator (SES) houses a variety of real-time computer generated visual systems. The earliest machine dates from the mid-1960's and is one of the first real-time graphics systems in the world. The latest acquisition is the state-of-the-art Evans and Sutherland CT6. Between the span of time from the mid-1960's to the late 1980's, tremendous strides have been made in the real-time graphics world. These strides include advances in both software and hardware engineering. The purpose is to explore the history of the development of these real-time computer generated image systems from the first machine to the present. Hardware advances as well as software algorithm changes are presented. This history is not only quite interesting but also provides us with a perspective with which we can look backward and forward.
Author

N90-20682*# Evans and Sutherland Computer Corp., Salt Lake City, UT.
COMPUTER IMAGE GENERATION: RECONFIGURABILITY AS A STRATEGY IN HIGH FIDELITY SPACE APPLICATIONS c61
Michael J. Bartholomew *In* NASA, Lyndon B. Johnson Space Center, Graphics Technology in Space Applications (GTSA 1989) Aug. 1989 p 229-233 (For primary document see N90-20651 13-60)
Avail: NTIS HC A11/MF A02 CSCL 09B

The demand for realistic, high fidelity, computer image generation systems to support space simulation is well established. However, as the number and diversity of space applications increase, the complexity and cost of computer image generation systems also increase. One strategy used to harmonize cost with varied requirements is establishment of a reconfigurable image generation system that can be adapted rapidly and easily to meet new and changing requirements. The reconfigurability strategy through the life cycle of system conception, specification, design, implementation, operation, and support for high fidelity computer image generation systems are discussed. The discussion is limited to those issues directly associated with reconfigurability and adaptability of a specialized scene generation system in a multi-faceted space applications environment. Examples and insights gained through the recent development and installation of the Improved Multi-function Scene Generation System at Johnson Space Center, System's Engineering Simulator are reviewed and compared with current simulator industry practices. The results are clear; the strategy of reconfigurability applied to space simulation requirements provides a viable path to supporting diverse applications with an adaptable computer image generation system.
Author

N90-20683*# National Aeronautics and Space Administration. Lyndon B. Johnson Space Center, Houston, TX.
REAL-TIME GRAPHICS FOR THE SPACE STATION FREEDOM CUPOLA, DEVELOPED IN THE SYSTEMS ENGINEERING SIMULATOR c61
Michael T. Red and Philip W. Hess (Lockheed Missiles and Space Co., Huntsville, AL.) *In its* Graphics Technology in Space Applications (GTSA 1989) Aug. 1989 p 235-247 (For primary document see N90-20651 13-60)
Avail: NTIS HC A11/MF A02 CSCL 09B

Among the Lyndon B. Johnson Space Center's responsibilities for Space Station Freedom is the cupola. Attached to the resource node, the cupola is a windowed structure that will serve as the space station's secondary control center. From the cupola, operations involving the mobile service center and orbital maneuvering vehicle will be conducted. The Systems Engineering Simulator (SES), located in building 16, activated a real-time man-in-the-loop cupola simulator in November 1987. The SES cupola is an engineering tool with the flexibility to evolve in both hardware and software as the final cupola design matures. Two workstations are simulated with closed-circuit television monitors, rotational and translational hand controllers, programmable display pushbuttons, and graphics display with trackball and keyboard. The displays and controls of the SES cupola are driven by a Silicon Graphics Integrated Raster Imaging System (IRIS) 4D/70 GT computer. Through the use of an interactive display builder program, SES, cupola display pages consisting of two dimensional and three dimensional graphics are constructed. These display pages interact with the SES via the IRIS real-time graphics interface. The focus is on the real-time graphics interface applications software developed on the IRIS.
Author

N90-20684*# CAE-Link Corp., Houston, TX. Link Flight Simulation Div.

THE ORBITAL MANEUVERING VEHICLE TRAINING FACILITY VISUAL SYSTEM CONCEPT

Keith Williams *In* NASA, Lyndon B. Johnson Space Center, Graphics Technology in Space Applications (GTSA 1989) Aug. 1989 p 249-254 (For primary document see N90-20651 13-60)

Avail: NTIS HC A11/MF A02 CSCL 09B

The purpose of the Orbital Maneuvering Vehicle (OMV) Training Facility (OTF) is to provide effective training for OMV pilots. A critical part of the training environment is the Visual System, which will simulate the video scenes produced by the OMV Closed-Circuit Television (CCTV) system. The simulation will include camera models, dynamic target models, moving appendages, and scene degradation due to the compression/decompression of video signal. Video system malfunctions will also be provided to ensure that the pilot is ready to meet all challenges the real-world might provide. One possible visual system configuration for the training facility that will meet existing requirements is described. Author

N90-20685 Department of the Navy, Washington, DC.

ADAPTIVE ASSOCIATIVE-PROCESSING OPTICAL COMPUTING ARCHITECTURES Patent

Arthur D. Fisher, inventor (to Navy) 29 Aug. 1989 15 p Filed 29 Jan. 1986 Supersedes N86-33034 (24 - 24, 3780), AD-D012305

(AD-D014317; US-Patent-4,862,406; US-Patent-Appl-SN-823719)

Avail: US Patent and Trademark Office CSCL 12/6

Accordingly, one object of the present invention is to provide a novel associative processing module which adapts in real-time as it is exposed to associated information patterns, so, at a later time presentation of one pattern results in recall of the other. Another object of the present invention is to provide a novel associative processing module which adaptively learns in real-time, even while simultaneously recalling associations. Another object of the present invention is to provide novel associative processing modules which may be interconnected and cascaded in order to obtain sophisticated processing capabilities.

N90-20686*# Illinois Univ., Urbana-Champaign. Coordinated Science Lab.

MEASURE: AN INTEGRATED DATA-ANALYSIS AND MODEL IDENTIFICATION FACILITY

Jaidip Singh and Ravi K. Iyer Jan. 1990 45 p

(Contract NCA2-301; NAG1-613)

(NASA-CR-186452; NAS 1.26:186452; UILU-ENG-90-2207; CSG-121) Avail: NTIS HC A03/MF A01 CSCL 09B

The first phase of the development of MEASURE, an integrated data analysis and model identification facility is described. The facility takes system activity data as input and produces as output representative behavioral models of the system in near real time. In addition a wide range of statistical characteristics of the measured system are also available. The usage of the system is illustrated on data collected via software instrumentation of a network of SUN workstations at the University of Illinois. Initially, statistical clustering is used to identify high density regions of resource-usage in a given environment. The identified regions form the states for building a state-transition model to evaluate system and program performance in real time. The model is then solved to obtain useful parameters such as the response-time distribution and the mean waiting time in each state. A graphical interface which displays the identified models and their characteristics (with real time updates) was also developed. The results provide an understanding of the resource-usage in the system under various workload conditions. This work is targeted for a testbed of UNIX workstations with the initial phase ported to SUN workstations on the NASA, Ames Research Center Advanced Automation Testbed. Author

N90-20687# Massachusetts Inst. of Tech., Cambridge. Lab. for Computer Science

A UNIFIED APPROACH TO THE SYNTHESIS OF FULLY TESTABLE SEQUENTIAL MACHINES

Srinivas Devadas and Kurt Keutzer Oct. 1989 11 p

(Contract N00014-87-K-0825)

(AD-A217120; VLSI-MEMO-89-570) Avail: NTIS HC A03/MF A01 CSCL 12/7

In this paper we attempt to unify and extend the various approaches to synthesizing fully testable sequential circuits that can be modeled as finite state machines (FSMs). We first identify classes of redundancies and isolate equivalent-state redundancies as those most difficult to eliminate. We then show that the essential problem behind equivalent-state redundancies is the creation of valid/invalid state pairs. We devote the remainder of the paper to techniques for developing differentiating sequences for valid/invalid state pairs created by a fault, as well as to techniques for retaining these sequences in the presence of that fault. A variety of techniques have been proposed to address this problem. At one end of the spectrum there are optimal synthesis procedures that ensure full testability by eliminating redundancies via the use of appropriate don't care sets. At the other end of the spectrum there are constrained synthesis procedures that produce fully and easily testable sequential circuits by restricting the implementation of the logic. The optimal synthesis procedures require fewer constraints on the logic but increase the expense of logic optimization to the point that CPU time requirements may be unacceptable. The constrained synthesis procedures require relatively simple logic optimization procedures but constrain the logic to the point that the area penalty may be unacceptable. GRA

N90-20688# New York Univ., New York. Inst. of Mathematical Sciences.

NYU (NEW YORK UNIVERSITY) ULTRACOMPUTER Final Report, 1 Sep. 1986 - 30 Sep. 1989

Allan Gottlieb 8 Jan. 1990 3 p

(Contract DAAL03-86-G-0023)

(AD-A217167; ARO-237781.1-MA-F) Avail: NTIS HC A01/MF A01 CSCL 12/5

Overall accomplishments include the architectural innovations, numerous algorithms and algorithmic analyses, the construction of fully functional multiprocessors, two generations of highly parallel operating systems and other system software, the production of parallel programs for several significant (mostly scientific) applications, and the design and implementation of full-custom VLSI chips for combining memory references. GRA

N90-20689# Illinois Univ., Urbana. Center for Supercomputing Research and Development.

SUPERCOMPUTER ENVIRONMENTS Final Technical Report, Oct. 1986 - Oct. 1989

Vincent A. Guarna, Jr. 9 Jan. 1990 35 p

(Contract F49620-86-C-0136)

(AD-A217682) Avail: NTIS HC A03/MF A01 CSCL 12/5

The objective of the Faust project is to provide users of high performance parallel and vector machines with an environment that makes the task of programming easier. This includes tools that are used in the process of developing, testing, tuning, and using scientific and engineering programs. Many of these tools are specific to the problem of parallel programming such as restructuring compilers, parallel debuggers, and parallel program performance evaluation tools, as well as tools that are useful in any program development environment such as text editors, program management assistants, on-line documentation systems, and graphic visualization tools. The first major goal is the design and implementation of a set of new tools aimed specifically at the problem of developing efficient scientific programs for supercomputers. The second goal is portability. Although the Faust environment assumes the existence of a bitmapped workstation running Unix as a basic platform, Faust is expected to run a variety of hardware. To accomplish this goal, all user interface

libraries have been layered on top of the X window system developed at MIT. The third goal is integration. GRA

N90-20690# National Academy of Sciences - National Research Council, Washington, DC.
COMPUTER SCIENCE AND TECHNOLOGY BOARD Progress Report, 15 Mar. 1989 - 14 Mar. 1990
Marjory S. Blumenthal 1990 5 p
(Contract DE-FG05-87ER-25029)
(DE90-008292; DOE/ER-25029/2) Avail: NTIS HC A01/MF A01

The Computer Science and Technology Board (CSTB) meets three times a year to consider scientific and policy issues in computer science as well as relevant problems in associated technologies. The objectives of the Board include: initiating studies involving computer science and technology as a critical national resource; responding to requests from the government, nonprofit foundations, and industry for advice on computer science and technology; promoting the health of the technology and other fields of pure and applied science and technology; and providing a base of expertise within the NRC in the area of computer science and technology. DOE

N90-20691# Lawrence Livermore National Lab., CA.
A REAL-TIME PARALLEL PIPELINED DATA-FLOW IMAGE-PROCESSING SYSTEM
G. J. Priatko and R. W. Andersen 1 May 1989 7 p Presented at the IEEE Nuclear Science Symposium and Exhibits, San Francisco, CA, 25-27 Oct. 1989
(Contract W-7405-eng-48)
(DE90-008324; UCRL-100992; CONF-891087-14) Avail: NTIS HC A02/MF A01

Until recently, using real-time image processing has been limited because of the expense and complexity of the processing systems. In general, image processing requires both high processor and communications bandwidths. This is particularly true when designing a real-time system that must be capable of handling multiple simultaneous images. Recent developments in both digital technology and system architecture have resulted in the potential for creating low-cost high-performance systems. In this paper we present a system that incorporates a highly modular task-specific hardware and software architecture. This architecture enables us to divide the tasks between high bandwidth processing elements and general-purpose workstations. An I/O bottleneck is avoided by including both high- and low-level processing elements and multiple high bandwidth buses within the image processor. This architecture produces a system that enables us to perform most of the imaging tasks within the image processor. In addition, our architecture provides efficient task partitioning. By separating the processing, display, and user interface functions, we can use different hardware and software platforms in different sections of the system. This enhances our ability to optimize, maintain, and upgrade the overall system. DOE

N90-20692# North Carolina State Univ., Raleigh.
(DURIP) TWO-PROCESSOR ALLIANT FX/4 SYSTEM Final Report, 1 Dec. 1988 - 30 Nov. 1989
C. T. Kelly 16 Jan. 1990 9 p
(Grant AF-AFOSR-0124-89; AF Proj. 3842)
(AD-A217810; AFOSR-90-0075TR) Avail: NTIS HC A02/MF A01 CSCL 12/7

This proposal requested a two-processor Alliant FX/4 system with disk drives, tape backup, operator's console, and local line printer. This computer offers vector processing capability, a high speed cache memory, and a shared memory multiprocessing architecture. When the project was funded, Alliant was willing to sell a two processor FX/40 for the same amount. This system supports research in control and optimization, nonlinear least squared problems, partial differential equations, integral equations, parameter identification problems, and signal processing. The equipment is being used for design and testing of algorithms that take advantage of multiprocessing and vector architectures for large scale problems in these areas, for training of graduate students, and as a high speed computing resource for problems, such as partial differential equations and large scale optimization problems that are too large to fit on other local facilities presently available. GRA

61 COMPUTER PROGRAMMING AND SOFTWARE

Includes computer programs, routines, alogorithms, and specific applications, e.g., CAD/CAM.

N90-20693# Princeton Univ., NJ. Dept. of Computer Science.
SIMPLIFIED LINEAR-TIME JORDAN SORTING AND POLYGON CLIPPING
Khun Yee Fung, Tina M. Nicholl, Robert E. Tarjan, and Christopher J. VanWyk (Bell Telephone Labs., Inc., Murray Hill, NJ.) Jul. 1988 17 p Sponsored in part by National Sciences and Engineering Council
(Contract N00014-87-K-0467; NSF DCR-86-05962)
(AD-A215110; CS-TR-189-88) Avail: NTIS HC A03/MF A01 CSCL 12/4

The Jordan sorting problem is, given the intersection points of a Jordan curve with the x-axis in the order in which they occur along the x-axis. This problem arises in clipping a simple polygon against a rectangle (a window) and in efficient algorithms for triangulating a simple polygon. Hoffman, Mehlhorn, Rosentiehl, and Tarjan proposed an algorithm that solves the Jordan sorting problem in time linear in the number of intersection points, but their algorithm requires the use of a sophisticated data structure, the level-linked search tree. A variant of the algorithm of Hoffman et al. is proposed that retains the linear time bound but simplifies both the operations required on the key data structure and the data structure itself. GRA

N90-20694*# Research Triangle Inst., Research Triangle Park, NC.
GCS PLAN FOR SOFTWARE ASPECTS OF CERTIFICATION
Anita M. Shagnea, Douglas S. Lowman, and B. Edward Withers Feb. 1990 36 p
(Contract NAS1-17964)
(NASA-CR-181972; NAS 1.26:181972) Avail: NTIS HC A03/MF A01 CSCL 09B

As part of the Guidance and Control Software (GCS) research project being sponsored by NASA to evaluate the failure processes of software, standard industry software development procedures are being employed. To ensure that these procedures are authentic, the guidelines outlined in the Radio Technical Commission for Aeronautics (RTCA/DO-178A document entitled, software considerations in airborne systems and equipment certification, were adopted. A major aspect of these guidelines is proper documentation. As such, this report, the plan for software aspects of certification, was produced in accordance with DO-178A. An overview is given of the GCS research project, including the goals of the project, project organization, and project schedules. It also specifies the plans for all aspects of the project which relate to the certification of the GCS implementations developed under a NASA contract. These plans include decisions made regarding the software specification, accuracy requirements, configuration management, implementation development and verification, and the development of the GCS simulator. Author

N90-20695# Technische Univ., Brunswick (Germany, F.R.). Fakultaet fuer Maschinenbau und Elektrotechnik.
A LEARNING REGULATOR FOR THE PLANE LONGITUDINAL MOVEMENT Ph.D. Thesis [EIN LERNENDER REGLER FUER DIE FLUGZEUGLAENGSBEWEGUNG]
Manfred Haverland 1988 151 p In GERMAN
(ETN-90-95381) Avail: NTIS HC A08/MF A01

The regulator of nonlinear large systems with a pure sequential regulation is often inadequate because of the calculation cost and the utilization attractiveness. The direct calculation of regulators

in time area is possible with very elegant algorithms. By identifying a simplified model and the transient state for the closed regulation device, a regulator is conceived as a transverse filter. The obtained system permits a piloting which is immediately adaptable to the trajectory changes. By means of the regression process, an inverse, quasi stationary model of the nonlinear trajectory is estimated; the model estimation a stability proof is possible. The flexibility of the learning piloting process permits a simple adaptation to other technical regulation operations. ESA

N90-20696# Nationaal Inst. voor Kernfysica en Hoge Energiefysica, Amsterdam (Netherlands).
THE HS6000/20 DEVELOPMENT SYSTEM [HET HS6000/20 ONTWIKKELINGSSYSTEEM]
Fred Schimmel and Sandra Pool (HTS Amsterdam, Netherlands) Apr. 1989 18 p In DUTCH
(LINO-1989-6; ETN-90-95407) Avail: NTIS HC A03/MF A01

The Syntel HS6000 software development system was tested with a view to the improvement of the three color displays for the graphical representation of the status information of the linear electron accelerator MEA (Medium Energy Accelerator). The software developed on the HS6000 has to be run on a target module which then locally controls the color display. The HS6000 system uses the OS-9 multi-user and multi-tasking operating system. The OS-9 uses modular software techniques based on memory modules. The interface between the user and the internal functions of the operating system is the OS-9 command interpreter program. The software is written using the MMACS screen editor, the draw program and the MEDIT editor. ESA

N90-20697# New Mexico State Univ., Las Cruces.
THE CONTOUR MODEL ARCHITECTURE AND ASSEMBLY LANGUAGE
John B. Johnston Jun. 1989 51 p
(Contract DAAL03-87-K-0106)
(AD-A217114; NMSU-ECE-89-005; ARO-25173.23-EL) Avail: NTIS HC A04/MF A01 CSCL 12/5

The purpose is limited to presenting the tagged record structure of the Contour Model Architecture (CMA), the static structure of individual snapshots of a nested module computation as realized in CMA, and the Contour Model Assembly Language (CMAL). Pedagogic illustrations of the CMAL-level evolution of a nested module computation are given in a separate report. The Contour Model (CM) as it currently exists can account for most of the semantic features of a broad spectrum of nested module computations; CM does not yet contain specific features for input/output, interrupts, or selectively restricted memory access. The architecture CMA and the assembly language CMAL together constitute a detailed operational mechanism which realized CM as it currently exists. SMA is a relatively conventional, fully tagged, stack-oriented architecture whose tagged record structure and assembly language are intended to be implemented in microcode. GRA

N90-20698# Pennsylvania State Univ., University Park. Center for Multivariate Analysis.
AN ALGORITHM FOR EFFICIENT ESTIMATION OF SUPERIMPOSED EXPONENTIAL SIGNALS
Z. D. Bai, C. Radhakrishna Rao, and Mosuk Chow Oct. 1989 20 p
(Contract DAAL03-89-K-0139)
(AD-A217218; TR-89-48; ARO-26792.1-MA-SDI) Avail: NTIS HC A03/MF A01 CSCL 12/3

A computational algorithm is given for obtaining asymptotically efficient estimates of the unknown complex amplitudes and frequencies in a superimposed exponential model for signals. It is shown that the variance covariance matrix of these estimates are asymptotically the same as that for the maximum likelihood estimates and thus attain the Cramer-Rao lower bound. GRA

N90-20699# Naval Ocean Systems Center, San Diego, CA.
FRACTAL-BASED IMAGE COMPRESSION
S. M. Kocsis Jan. 1990 6 p Submitted for publication
(AD-A217302) Avail: NTIS HC A02/MF A01 CSCL 12/9

Iterated Function Systems (IFS) offers a method of describing complicated digital files with a small set of functions exhibiting fractal properties. In coding an image, first cover it with contractive affine transformations of itself and then save the coefficients of the transformations. Decoding is performed by generating a dynamical system whose attractor is suitably close to the original image. The amount of distortion is dependent on the quality of the initial covering. This paper will describe the mathematics of IFS, the coding and decoding of a digital image with IFS, error analysis of IFS compression, and comparison to other compression techniques. Mandelbrot coined the term fractal to describe sets that demonstrate detail under any arbitrary magnification. Mandelbrot described the properties of sets with non-integer dimension, fractal sets, and produced many examples from nature: coastlines, clouds, brownian motion, trees, etc... Human-made mechanisms also display fractal behavior: the stock market, bouncing balls, dripping faucets, etc... Mandelbrot, made it clear that in nature fractal action has a limit while pure mathematical fractals have structure at all scales, but both have in common statistical invariance under transformation of a scale. An IFS generates a set with fractal properties. GRA

N90-20700# Center for Naval Analyses, Alexandria, VA.
COMPUTING MEAN RESPONSES IN NONLINEAR MODELS Final Report
Edward S. Cavin Dec. 1989 15 p
(Contract N00014-87-C-0001; DA Proj. C00-31)
(AD-A217642; CRM-89-292) Avail: NTIS HC A03/MF A01 CSCL 12/4

It is common in empirical studies using nonlinear models to estimate the mean response by evaluating the nonlinear response function at the mean value of its argument(s). However, this procedure conceptually is flawed if the response function has significant curvature in the neighborhood of the mean. Ideally, one should evaluate the estimated response function for each of the estimated responses. In general, there will be some nonzero approximation error if one instead simply evaluates the response function at the mean of the independent variable(s). Furthermore, if the variability is significant in the independent variable(s) of interest, the approximation error of using the evaluate at the mean procedure increases. The magnitude of the approximation error is examined, and situations are identified in which somewhat more computationally intensive procedures should be used. GRA

N90-20701# Illinois Univ., Urbana. Coordinated Science Lab.
COMPUTATIONAL COMPLEXITY OF RANDOM ACCESS MODELS Ph.D. Thesis
David Ralph Luginbuhl Jan. 1990 105 p Sponsored by Air Force Inst. of Tech., Wright-Patterson AFB, OH
(AD-A217685; UILI-ENG-90-2201; ACT-110) Avail: NTIS HC A06/MF A01 CSCL 12/5

The relative power of several computational models is considered in this thesis. These models are the Turing machine and its multidimensional variant, the random access machine (RAM), the tree machine, and the pointer machine. The basic computational properties of the pointer machine are examined in more detail. For example, time and space hierarchy theorems for pointer machines are presented. Every Turing machine of time complexity t and space complexity s can be simulated by a pointer machine of time complexity O(t) using O(s/log s) nodes. This strengthens a similar result by van Emde Boas (1989). Every alternating pointer machine of time complexity t can be simulated by a deterministic pointer machine using O(t/log t) nodes. Other results concerning nondeterministic and alternating pointer machines are presented. Every tree machine of time complexity t can be simulated on-line by a log-cost RAM of time complexity O((t log t)/log log t). GRA

N90-20702# Los Alamos National Lab., NM.
EXPERIMENTS IN FINDING NEURAL NETWORK WEIGHTS

Timothy R. Thomas and Tony L. Brewster Apr. 1990 10 p
(Contract W-7405-eng-36)
(DE90-007696; LA-11772-MS) Avail: NTIS HC A02/MF A01

The speed with which back-propagation, conjugate gradient, and Quickprop algorithms find the neural network weights that solve: a small-scale nonlinear classification problem and a mapping from a vector-valued time series to a one-dimensional signal, are compared. The problem of tuning each algorithm for these problems (i.e., selecting a good set of control parameters) is also discussed. The most efficient algorithm was found to be an enhanced form of back-propagation using large momentum and learning rates, with weight updates after each pattern presentation and a small constant added to the error derivatives. DOE

N90-20703# Argonne National Lab., IL. Experimental Breeder Reactor No. 2 Div.
USING FORMAL METHODS TO DEVELOP A PARADIGM FOR SOFTWARE DESIGN
G. H. Chisholm, B. T. Smith, and A. S. Wojcik (Michigan State Univ., East Lansing.) 1990 5 p Presented at the International Workshop on Formal Methods in Software Development, Napa, CA, 9-11 May 1990
(Contract W-31-109-eng-38)
(DE90-005633; CONF-900597-1) Avail: NTIS HC A01/MF A01

Formal methods have been used to analyze the properties of many kinds of systems. Over the past several years, a group at Argonne National Laboratory has been investigating the use of formal analysis techniques to study the behavior of fault tolerance in reactor control systems. This investigation has revealed that the key issue in modeling and qualifying fault tolerance properties is independence. Traditional verification tools (including formal analysis) deal with the issue of independence implicitly. For example, fault-injection testing may discover an instance where independence is not maintained when a system crash results from the injection of a single fault. However, this discovery is an effect of the method, in contrast to being a behavior for which the analysis is explicit. In contrast, the approach we describe here is based on the determination of essential system properties and the development of an analysis strategy that facilitates a formalization of that property within the context of the design. DOE

N90-20704# Lawrence Livermore National Lab., CA.
RECENT ADVANCES IN 3D FINITE DIFFERENCE MESH GENERATION USING THE BRL-CAD PACKAGE
Gary Laguna Sep. 1989 16 p Presented at the BRL-CAD Symposium '89, Aberdeen, MD, 24-25 Oct. 1989
(Contracts W-7405-eng-48; AFWL-87-217)
(DE90-007854; UCRL-102046; CONF-8910366-1) Avail: NTIS HC A03/MF A01

For the past three years Lawrence Livermore National Laboratory has been developing methods for generating 3D finite difference (FD) meshes directly from solid models. During the past year, the solid modeling platform was changed for FD mesh generation from the TIPS-1 solid modeler to the BRL-CAD package. In addition to the basic changes required by the differences between these two modelers and their application interfaces, a new strategy was also developed for generating the mesh from the sample data. This new approach has dramatically improved the correspondence between generated meshes and the originating geometries. The new approach also generates mesh elements which are more appropriate for the FD analysis code, TSAR, which calculates edge based vector unknowns. In the past, edge (wire) mesh elements were approximated from mesh cells, however, true edge mesh elements can now be generated in a direct and straightforward manner. The basis of this new approach is a two step process of sampling and filtering which require that each FD mesh cell be subdivided into eight equal-sized octants. By using octants, the mesh generator can sense the configuration of the geometry contained by a cell and assign only those mesh elements which are appropriate to the given configuration. In addition to the above changes, several new features and capabilities have been added which together form a very flexible tool for generating FD meshes. The mesh generator is currently undergoing internal testing further development. Nonetheless, it has already been used to generate meshes for several projects at LLNL, and users of these meshes have obtained acceptable results. DOE

N90-20705# Lawrence Livermore National Lab., CA. Engineering Research Div.
ISLE (IMAGE AND SIGNAL PROCESSING LISP ENVIRONMENT) REFERENCE MANUAL
R. J. Sherwood and R. M. Searfus Jan. 1990 97 p
(Contract W-7405-eng-48)
(DE90-007858; M-285) Avail: NTIS HC A05/MF A01

ISLE is a rapid prototyping system for performing image and signal processing. It is designed to meet the needs of a person doing development of image and signal processing algorithms in a research environment. The image and signal processing modules in ISLE form a very capable package in themselves. They also provide a rich environment for quickly and easily integrating user-written software modules into the package. ISLE is well suited to applications in which there is a need to develop a processing algorithm in an interactive manner. It is straightforward to develop the algorithms, load it into ISLE, apply the algorithm to an image or signal, display the results, then modify the algorithm and repeat the develop-load-apply-display cycle. ISLE consists of a collection of image and signal processing modules integrated into a cohesive package through a standard command interpreter. ISLE developer elected to concentrate their effort on developing image and signal processing software rather than developing a command interpreter. A COMMON LISP interpreter was selected for the command interpreter because it already has the features desired in a command interpreter, it supports dynamic loading of modules for customization purposes, it supports run-time parameter and argument type checking, it is very well documented, and it is a commercially supported product. This manual is intended to be a reference manual for the ISLE functions. The functions are grouped into a number of categories and briefly discussed in the Function Summary chapter. The full descriptions of the functions and all their arguments are given in the Function Descriptions chapter. DOE

N90-20706# California Univ., Berkeley. Lawrence Berkeley Lab.
SOFTWARE QUALITY ASSURANCE AND SOFTWARE SAFETY IN THE BIOMED CONTROL SYSTEM
R. P. Singh, William T. Chu, Bernhard A. Ludewigt, Krista M. Marks, Mark A. Nyman, Tim R. Renner, and Ronald Stradtner 31 Oct. 1989 16 p
(Contract DE-AC03-76SF-00098)
(DE90-008072; LBL-27948) Avail: NTIS HC A03/MF A01

The Biomed Control System is a hardware/software system used for the delivery, measurement and monitoring of heavy-ion beams in the patient treatment and biology experiment rooms in the Bevalac at the Lawrence Berkeley Laboratory (LBL). This paper describes some aspects of this system including historical background philosophy, configuration management, hardware features that facilitate software testing, software testing procedures, the release of new software quality assurance, safety and operator monitoring. DOE

N90-20707# Sandia National Labs., Albuquerque, NM.
RIPE: AN OBJECT-ORIENTED ROBOT INDEPENDENT PROGRAMMING ENVIRONMENT
David J. Miller and R. Charleene Lennox 1990 10 p Presented at the USENIX C++ Conference, San Francisco, CA, 9-11 Apr. 1990
(Contract DE-AC04-76DP-00789)
(DE90-008501; SAND-90-0052C; CONF-9004148-1) Avail: NTIS HC A02/MF A01

An object-oriented Robot Independent Programming Environment (RIPE) developed at Sandia National Laboratories is being used for rapid design and implementation of a variety of applications. A system architecture based on hierarchies of distributed multiprocessors provides the computing platform for a layered programming structure that models the application as a

set of software objects. These objects are designed to support model-based automated planning and programming, real-time sensor-based activity, error handling, and robust communication. The object-oriented paradigm provides mechanisms such as inheritance and polymorphism which allow the implementation of the system to satisfy the goals of software, reusability, extensibility, reliability, and portability. By designing a hierarchy of generic parent classes and device-specific subclasses which inherit the same interface, a Robot Independent Programming Language (RIPL) is realized. Work cell tasks demonstrating robotic cask handling operations for nuclear waste facilities are successfully implemented using this object-oriented software environment. DOE

N90-20708*# National Aeronautics and Space Administration. Lewis Research Center, Cleveland, OH.
GRID2D/3D: A COMPUTER PROGRAM FOR GENERATING GRID SYSTEMS IN COMPLEX-SHAPED TWO- AND THREE-DIMENSIONAL SPATIAL DOMAINS. PART 2: USER'S MANUAL AND PROGRAM LISTING
R. T. Bailey, T. I.-P. Shih (Carnegie-Mellon Univ., Pittsburgh, PA.), H. L. Nguyen, and R. J. Roelke Apr. 1990 73 p
(Grant NAG3-828)
(NASA-TM-102454; E-5242; NAS 1.15:102454) Avail: NTIS HC A04/MF A01 CSCL 09B

An efficient computer program, called GRID2D/3D, was developed to generate single and composite grid systems within geometrically complex two- and three-dimensional (2- and 3-D) spatial domains that can deform with time. GRID2D/3D generates single grid systems by using algebraic grid generation methods based on transfinite interpolation in which the distribution of grid points within the spatial domain is controlled by stretching functions. All single grid systems generated by GRID2D/3D can have grid lines that are continuous and differentiable everywhere up to the second-order. Also, grid lines can intersect boundaries of the spatial domain orthogonally. GRID2D/3D generates composite grid systems by patching together two or more single grid systems. The patching can be discontinuous or continuous. For continuous composite grid systems, the grid lines are continuous and differentiable everywhere up to the second-order except at interfaces where different single grid systems meet. At interfaces where different single grid systems meet, the grid lines are only differentiable up to the first-order. For 2-D spatial domains, the boundary curves are described by using either cubic or tension spline interpolation. For 3-D spatial domains, the boundary surfaces are described by using either linear Coon's interpolation, bi-hyperbolic spline interpolation, or a new technique referred to as 3-D bi-directional Hermite interpolation. Since grid systems generated by algebraic methods can have grid lines that overlap one another, GRID2D/3D contains a graphics package for evaluating the grid systems generated. With the graphics package, the user can generate grid systems in an interactive manner with the grid generation part of GRID2D/3D. GRID2D/3D is written in FORTRAN 77 and can be run on any IBM PC, XT, or AT compatible computer. In order to use GRID2D/3D on workstations or mainframe computers, some minor modifications must be made in the graphics part of the program; no modifications are needed in the grid generation part of the program. The theory and method used in GRID2D/3D is described. Author

N90-20709# Argonne National Lab., IL. Mathematics and Computer Science Div.
JOINT JAPANESE-AMERICAN WORKSHOP ON FUTURE TRENDS IN LOGIC PROGRAMMING
G. W. Pieper, ed. Dec. 1989 284 p Workshop held in Argonne, IL, 11-13 Oct. 1989
(Contract W-31-109-eng-38)
(DE90-008343; ANL-89/43; CONF-8910372) Avail: NTIS HC A13/MF A02

The objective of the workshop was to review developments and discuss the goals of logic programming. Four main areas were considered: multiprocessing, constraint logic programming, logical foundation of programming, and knowledge representation and database. Abstracts are presented for the sixteen presentations; Section 10 includes more detailed papers on each topic. Also summarized are the group discussions that were held informally during the three-day workshop, and the question-and-answer sessions that addressed pertinent issues, such as how logic programming addresses the needs of the software community. An important part of the workshop was the demonstration of the Japanese computer, the Multi-PSI. A summary of that demonstration is included; in Section 11 is a detailed Guide to the Japanese demonstrations. DOE

N90-20710# Sandia National Labs., Albuquerque, NM.
A PARADOXICAL RESULT IN UNCONDITIONALLY SECURE AUTHENTICATION CODES, AND AN EXPLANATION
Gustavus J. Simmons and Ben Smeets (Lund Univ., Sweden) 1989 29 p Presented at the IMA Conference on Cryptography and Coding, Cirencester, England, 18-20 Dec. 1989
(Contract DE-AC04-76DP-00789)
(DE90-008529; SAND-89-2783C; CONF-891282-1) Avail: NTIS HC A03/MF A01

Simmons defined an authentication code to be perfect if all of the information involved in the secret key exchange between the transmitter and receiver is used to either provide perfect secrecy (in the sense of Shannon) for the information being communicated or else to confound the opponent; i.e., to detect and prevent deception of the receiver. Numerous unconditionally secure and perfect authentication codes have been devised by Brickell, Simmons, Stinson and others that use the k bits of equivocation (uncertainty) to an opponent about the authentication key to provide perfect secrecy for a q bit source, q less than k, i.e., an opponent who knows the encoding scheme but not the encoding rule upon observing the encoding of a source state, cannot do better at identifying that state than to randomly guess at it using the a priori probability distribution on the source states and to provide 2(sup minus k+q) security against the first round of impersonation and substitution attacks. Intuitively, this would appear to have used up the k bits of equivocation about the key. The paradox referred to in the title is that this isn't true and that some security against deception may still be achievable for successive rounds of communication and authentication. In this paper, we will discuss this apparent paradox and show how its explanation forces a reexamination of the basic authentication channel bounds. DOE

N90-20711# Lawrence Livermore National Lab., CA.
SCATTERING SOURCES: A SPHERICAL HARMONICS EXPANSION
E. Garelis 19 Jul. 1989 8 p Presented at the International Conference on the Physics of Reactors: Operation, Design and Computation, Marseilles, France, 23-26 Apr. 1990
(Contract W-7405-eng-48)
(DE90-008724; UCRL-101560; CONF-900418-8) Avail: NTIS HC A02/MF A01

The Glam code solves the two dimensional azimuthally symmetric steady equation of transfer for the energy density, flux, and the pressure tensor. The code calculates the intensity along a given ray and then using a numerical quadrature scheme calculates the various moments. For problems with isotropic scattering it is a simple matter to include the scattering. The precise dependence of the flux and the pressure tensor on the anisotropic scattering are derived. With these relationships established these scattering sources are then included in the Glam code to account for the anisotropic scattering. DOE

N90-20712# Massachusetts Inst. of Tech., Cambridge.
TECHNICAL SPECIFICATIONS REQUIREMENTS: AUTOMATED REASONING APPLICATIONS
L. M. Lidsky and A. B. Dobrzeniecki Mar. 1990 13 p
(Contract DE-AC02-85NE-37944)
(DE90-008799; DOE/NE-37944/1) Avail: NTIS HC A03/MF A01

Several software systems were developed and tested to determine what advantages could be gained from explicitly translating complicated regulatory requirements into computerized relationships. The Technical Specifications for U.S. nuclear power

plants were chosen as the test-bed application domain, and two analysis systems were developed to monitor plant compliance with operational limits, and track and schedule equipment test and maintenance activities mandated by Technical Specifications. Choosing PROLOG as the computer language to represent these regulatory requirements resulted in a natural match between the semantic structure of the written specifications and the corollary coded rules. Additional research results affirmed the utility of declarative programming styles, explicit management of problem complexity, and attention to the robustness and flexibility of the overall software systems. DOE

N90-20713*# Lockheed Missiles and Space Co., Sunnyvale, CA.
VAPEPS USER'S REFERENCE MANUAL, VERSION 5.0 Final Report
D. M. Park Jul. 1988 808 p
(Contract NAS5-29452)
(NASA-CR-180781; NAS 1.26:180781; LMSC/F186312/SSV-2167) Avail: NTIS HC A99/MF E06 CSCL 09B

This is the reference manual for the VibroAcoustic Payload Environment Prediction System (VAPEPS). The system consists of a computer program and a vibroacoustic database. The purpose of the system is to collect measurements of vibroacoustic data taken from flight events and ground tests, and to retrieve this data and provide a means of using the data to predict future payload environments. This manual describes the operating language of the program. Topics covered include database commands, Statistical Energy Analysis (SEA) prediction commands, stress prediction command, and general computational commands. Author

N90-20714# Massachusetts Inst. of Tech., Cambridge. Dept. of Brain and Cognitive Sciences.
PARTS OF RECOGNITION Report, Jul. 1983 - Sep. 1989
Whitman Richards Oct. 1989 33 p
(Contract F49620-83-C-0135)
(AD-A217694; AFOSR-90-0070TR) Avail: NTIS HC A03/MF A01 CSCL 06/4

It is proposed that, for the task of object recognition, the visual system decomposes shapes into parts, that it does so using a rule defining part boundaries rather than part shapes, that the rule exploits a uniformity of nature transversality, and that parts with their descriptions and spatial relations provide a first index into a memory of shapes. This rule allows an explanation of several visual illusions. We stress the role of inductive inference in the theory and conclude with a precis of unsolved problems. GRA

N90-20715# Maryland Univ., College Park. Dept. of Computer Science.
RESEARCH IN PROGRAMMING LANGUAGES AND SOFTWARE ENGINEERING Final Report, 1 Mar. 1987 - 31 Oct. 1989
Victor R. Basili, John D. Gannon, and Marvin V. Zelkowitz 15 Jan. 1990 33 p
(Grant AF-AFOSR-0130-87; AF Proj. 2304)
(AD-A217765; AFOSR-90-0077TR) Avail: NTIS HC A03/MF A01 CSCL 12/5

The projects presented in this report encompass developing and integrating the concepts and models used in the TAME measurement environment, using syntax-editing technology to develop formal specifications, investigating the impact of functional specification and development on software construction, designing and evaluating a new exception handling mechanism, and transforming computations for single processors to execute efficiently on non-shared memory multiprocessors. GRA

N90-20716# Indiana Univ., Bloomington. Dept. of Computer Science.
PROBABILISTIC ANALYSIS OF ALGORITHMS FOR NP-COMPLETE PROBLEMS Final Report, 30 Sep. 1984 - 29 Sep. 1989
John Franco 29 Sep. 1989 35 p
(Grant AF-AFOSR-0372-84; AF Proj. 2304)
(AD-A217880; AFOSR-90-0119TR) Avail: NTIS HC A03/MF A01 CSCL 12/3

The main objective was the probabilistic sense, it is easy to find a satisfying truth assignment to an instance of satisfiability but it is hard to verify that an unsatisfiable instance has a solution. A side issue was the analysis of probabilistic models used to obtain the main results. GRA

N90-20717# Oklahoma Univ., Norman. School of Aerospace and Mechanical Engineering.
DEVELOPMENT OF COMPUTER SOFTWARE FOR THE ANALYSIS AND DESIGN OF MODERN CONTROL SYSTEMS M.S. Thesis
Carl Fred Adams 1989 124 p Sponsored by AFIT, Wright-Patterson AFB, OH
(AD-A217924; AFIT/CI/CIA-89-028) Avail: NTIS HC A06/MF A01 CSCL 12/5

With the wide spread availability of the personal computers to the control systems engineer, is would only make sense to supplement the time honored techniques of using root locus and bode plots in the analysis and design of control systems with one that involves computer aided support. Using the computer to do the mundane task of generating the graphs allows the designer to spend more time analyzing the system. This could also allow a student in a controls course the opportunity to learn more of the theory behind control systems analysis instead of spending all their time learning the tedious process of generating the graphs by hand. Computer algorithms were developed to automate this task in a easy to use format. This software is called the Control Systems Software Package (CSSP). GRA

N90-20718# Naval Postgraduate School, Monterey, CA. Dept. of Computer Science.
IMPLEMENTATION OF A HYPERTEXT HELP SYSTEM FOR GLAD (GRAPHICS LANGUAGE FOR DATABASE) M.S. Thesis
Lon M. Yeary Jun. 1989 63 p
(AD-A217936) Avail: NTIS HC A04/MF A01 CSCL 12/5

The design and implementation of a help system for a graphical user interface named GLAD (Graphic LAnguage for Database) is explored. Help system design alternatives are examined. Emphasis is on the implementation of a hypertext help system for GLAD using the Windows utility GUIDANCE and the object-oriented programming language ACTOR. Discussion includes the advantages of hypertext for on-line help systems. GRA

N90-20719# Wright Research Development Center, Wright-Patterson AFB, OH. Design Branch.
VHSIC HARDWARE DESCRIPTION LANGUAGE (VHDL) BENCHMARK SUITE Final Report, Mar. - Oct. 1989
Karen M. Serafino Oct. 1989 713 p
(AF Proj. 6096)
(AD-A217947; WRDC-TR-89-5046) Avail: NTIS HC A99/MF A04 CSCL 12/5

The development of a VHDL Benchmark Suite system is documented. Each benchmark is designed to test one or more of a set of 71 VHDL language features in terms of the limitations of user's of vendor's system architecture, operating system, and VHDL toolset. These limitations could include CPU time and amount of memory required to analyze, model generate, build and simulate a test. Examples of language feature tests are the maximum number of signal declarations allowed in an architecture or the number of input ports allowed in the port clause of a component before errors are caused. GRA

N90-20720# Louisville Univ., KY.
THE PERCEPTUAL INTERACTION OF GRAPHICAL ATTRIBUTES IN THIRTEEN BIVARIATE DISPLAYS Final Report
C. Melody Carswell and Christopher D. Wickens (Illinois Univ., Urbana-Champaign.) Dec. 1989 44 p

(DA Proj. 1L1-62716-AH-70)
(AD-A217980; HEL-TM-22-89) Avail: NTIS HC A03/MF A01
CSCL 12/6

Thirteen bivariate graphical displays were used to perform the speeded classification tasks necessary to diagnose dimensional integrality configurality, and separability. The nine classification tasks were performed by a different group of nine subjects for each of the graphs. Results from 9 of the 13 graphs clearly fit the pattern indicative of integrality. Instead, graphs varied on a continuum from highly configural to separable displays. A principal components analysis was used to derive a composite measure of configurality, and this measure was found to be correlated with the homogeneity of the various graphs. Greater homogeneity among graphical attributes was associated with higher performance based configurality scores. GRA

N90-20721# Houston Univ., TX. Coll. of Business Administration.
DESIGN DECISION MAKING WITH MULTIPLE INTERACTING CRITERIA AND VARYING RELATIVE WEIGHTS Ph.D. Thesis
Jacob VanVranken Simons, Jr. Jul. 1989 349 p Sponsored by AFIT, Wright-Patterson AFB, OH
(AD-A218027; AFIT/CI/CIA-89-124) Avail: NTIS HC A15/MF A02 CSCL 12/4

The design environment is typically characterized by conflicting objectives and numerous design alternatives, making selection of a specific system design problematic. The broad goal of this research is the development of a prescriptive decision making approach which facilitates the comparison of a large number of design alternatives with respect to multiple criteria. The approach developed considers both objective and subjective factors, yet strives for optimization rather than satisfying of the decision criteria. Each criterion is considered in light of perceived relative weights which are permitted to vary in response to the performance achieved for that objective. Finally, the decision technique described provides a means of treating potential interactions among the multiple criteria. A design methodology framework is presented, containing state-of-the-art features stemming from the dramatic influence of systems theory. These characteristics include a broad, macro view of the system being designed, an expansionist, deductive perspective in the evaluation of design alternatives, and explicit consideration of system life cycle phases. Within the context of this framework methodology, major decision making approaches frequently suggested as alternatives for the design decision problem are reviewed and critiqued with respect to the desired features. GRA

N90-20722# Naval Research Lab., Washington, DC.
TEXTURE SEGMENTATION USING LOCALIZED SPATIAL FILTERING Final Report
Li-Jen Du 26 Jan. 1990 46 p Sponsored by ONR, Arlington, VA
(AD-A218064; NRL-MR-6586) Avail: NTIS HC A03/MF A01
CSCL 12/9

Spatial filters based on 2-D Gabor functions are applied to the image segmentation problem using textural differences for discrimination. In order to provide class separability, the textural content of a scene must have spatial variations which exhibit characteristic differences in frequency and/or directional bandwidths. This idea stems from discoveries in vision research that the Gabor functions model effectively the architecture of the neural receptive fields in the striate visual cortex and in the belief that such functions can play an important role in the analytical study of machine vision, pattern recognition and image processing. This new technique in image segmentation does not require burdensome machine data processing as compared with other techniques based on pixel classification. The technique is applied to some SAR images of the open ocean surface and of some ice fields. The results are very encouraging. GRA

N90-20723# Mission Research Corp., Nashua, NH.
MATHEMATICS AND PHYSICS STUDIES: MULTI-PROJECT SUPPORT Final Report, 31 Aug. 1987 - 2 Sep. 1989
Richard R. Babcock, John R. Kennealy, Barbara T. Bancroft, Robert D. Geiger, Rose C. Korte, Dennis Delorey, and Brian Sullivan 2 Sep. 1989 81 p
(Contract F19628-87-C-0230; AF Proj. 9993)
(AD-A218208; GL-TR-89-0242) Avail: NTIS HC A05/MF A01
CSCL 12/9

The initial effort was the refinement of a maximum entropy-based image restoration technique for use in digital image processing and image enhancement using Weiner filters. The technique provides a fast and stable-to-convergence routine that can be applied to numerous distortion functions. A majority of the effort was developing and implementing a data management program for the SDIO's Infrared Background Signature Survey (IBSS) Shuttle-based experiments. The contract produced a Data Management Plan, an Interface Control Document for data distribution formats, and data access and display software programs for calibrating and surveying the data. An indepth survey was performed of the state of the art of scientific workstation technology. A report provided different concepts on the utilization of scientific workstations in the Geophysics Laboratory, the different hardware and software systems available, and the issues involved in designing and acquiring a workstation. Data from the Infrared Astronomical Satellite (IRAS) were processed using available image enhancement techniques to update the sky catalogs of infrared sources. Results from this analysis were applied to developing data processing and analysis concepts for the SDIO's Midcourse Space Experiment that will have similar instrumentation. GRA

N90-20724# Massachusetts Inst. of Tech., Cambridge. Artificial Intelligence Lab.
FREE INDEXATION: COMBINATORIAL ANALYSIS AND A COMPOSITIONAL ALGORITHM
Sandiway Fong Dec. 1989 12 p
(Contract N00014-85-K-0124; NSF DCR-85-552543)
(AD-A218219; AI-M-1156) Avail: NTIS HC A03/MF A01
CSCL 12/9

In the principles-and-parameters model of language, the principle known as free indexation plays an important part in the process of determining the referential properties of elements such as anaphors and pronominals. Two issues are addressed. The combinatorics of free indexation was investigated. By relating the problem to the n-set partitioning problem, it was shown that free indexation must produce an exponential number of referentially distinct phrase structures given a structure with n (independent) noun phrases. An algorithm was introduced for free indexation that is defined compositionally on phrase structures. It was shown how the compositional nature of the algorithm makes it possible to incrementally interleave the computation of free indexation with phrase structure construction. Additionally, the algorithm was proven to be an optimal procedure for free indexation. More precisely, by relating the compositional structure of the formulation to the combinatorial analysis, it was shown that the algorithm enumerates precisely all possible indexings, without duplicates. GRA

N90-20725# Massachusetts Inst. of Tech., Cambridge. Artificial Intelligence Lab.
OPTIMIZATION OF SERIES EXPRESSIONS. PART 1: USER'S MANUAL FOR THE SERIES MACRO PACKAGE
Richard C. Waters Dec. 1989 73 p
(Contract N00014-88-K-0487; NSF IRI-86-16644)
(AD-A218220; AI-M-1082) Avail: NTIS HC A04/MF A01
CSCL 12/5

The benefits of programming in a functional style are well known. In particular, algorithms that are expressed as compositions of functions operating on series/vectors/streams of data elements are much easier to understand and modify than equivalent algorithms expressed as loops. Unfortunately, many programmers hesitate to use series expressions. In part, this is due to the fact that series expressions are typically implemented very inefficiently. A Common Lisp macro package (called Series) was implemented that can evaluate a wide class of series expressions very efficiently by transforming them into iterative loops. When using this class

of series expressions, programmers can obtain the advantages of expressing computations as series expressions without incurring any run-time overhead. GRA

N90-20726# Air Force Inst. of Tech., Wright-Patterson AFB, OH.
A REVIEW OF THE SUITABILITY OF AVAILABLE COMPUTER AIDED SOFTWARE ENGINEERING (CASE) TOOLS FOR THE SMALL SOFTWARE DEVELOPMENT ENVIRONMENT M.S. Thesis - Univ. of South Florida
Marc L. Sims 11 Jul. 1989 123 p
(AD-A218276; AFIT/CI/CIA-89-077) Avail: NTIS HC A06/MF A01 CSCL 12/5

This research informally investigates the use of Computer Aided Software Engineering (CASE) tools by a small software development organization. These tools are heralded as being productivity enhancers for software development personnel. Most of the literature discusses the generic use of this new generation of software development tools. This research effort focuses on the appropriateness of using these tools by the small software development organizations consisting of less than seven personnel. Provided in this thesis is a brief presentation of the software engineering discipline and descriptions of the CASE family of tools along with a discussion of 33 specific tools. A small software development organization model is provided and its areas of concerns are discussed. This research also performed a survey of users of current CASE products and the results from the 76 respondents are presented. GRA

N90-20727# Air Force Inst. of Tech., Wright-Patterson AFB, OH.
PERFORMANCE OF CONCURRENCY CONTROL ALGORITHMS IN DISTRIBUTED SYSTEMS Ph.D. Thesis - Texas Univ., Austin
Samuel Lycurgus Grier, Jr. Aug. 1989 190 p
(AD-A218280; AFIT/CI/CIA-89-076) Avail: NTIS HC A09/MF A01 CSCL 12/7

The performance of concurrency control algorithms is explored in the context of pessimistic distributed mutual exclusion algorithms. A detailed model of the underlying asynchronous distributed system and its parameters are defined for fail-free systems and systems where processes may fail. New performance metrics are proposed as a means to measure the efficiency of distributed mutual exclusion algorithms. A model of distributed mutual exclusion algorithms and analytical approximations of their performance are developed. Simulation results of five selected distributed mutual exclusion algorithms on fully-connected, star and ring topologies are cataloged. Finally, simulation results of four selected distributed mutual exclusion algorithms on a fully-connected topology where processes may fail are cataloged. Conclusions are drawn as to which algorithm is most appropriate for particular environments. GRA

N90-20658*# International Business Machines Corp., Houston, TX.
ONBOARD SHUTTLE ON-LINE SOFTWARE REQUIREMENTS SYSTEM: PROTOTYPE
Barbara Kolkhorst and Barry Ogletree (International Business Machines Corp., Armonk, NY.) *In* NASA, Lyndon B. Johnson Space Center, Graphics Technology in Space Applications (GTSA 1989) Aug. 1989 p 43-48 (For primary document see N90-20651 13-60)
Avail: NTIS HC A11/MF A02 CSCL 09B

N90-20661*# McDonnell-Douglas Space Systems Co., Houston, TX.
APPLICATIONS OF GRAPHICS TO SUPPORT A TESTBED FOR AUTONOMOUS SPACE VEHICLE OPERATIONS
K. R. Schmeckpeper, J. P. Aldridge, S. Benson, S. Horner, A. Kullman, T. Mulder, W. Parrott, D. Roman, G. Watts, and Daniel C. Bochsler (LinCom Corp., Houston, TX.) *In* NASA, Lyndon B. Johnson Space Center, Graphics Technology in Space Applications (GTSA 1989) Aug. 1989 p 65-71 (For primary document see N90-20651 13-60)
Avail: NTIS HC A11/MF A02 CSCL 09B

N90-20663*# Rockwell International Corp., Downey, CA. REGIS Computer Animation Lab.
EFFICIENT UTILIZATION OF GRAPHICS TECHNOLOGY FOR SPACE ANIMATION
Gregory Peter Panos *In* NASA, Lyndon B. Johnson Space Center, Graphics Technology in Space Applications (GTSA 1989) Aug. 1989 p 81-91 (For primary document see N90-20651 13-60)
Avail: NTIS HC A11/MF A02 CSCL 09B

N90-20664*# National Aeronautics and Space Administration. Lyndon B. Johnson Space Center, Houston, TX.
ENGINEERING VISUALIZATION UTILIZING ADVANCED ANIMATION
Gunter R. Sabionski and Thomas L. Robinson, Jr. (Barrios Technology, Inc., Houston, TX.) *In its* Graphics Technology in Space Applications (GTSA 1989) Aug. 1989 p 93-102 (For primary document see N90-20651 13-60)
Avail: NTIS HC A11/MF A02 CSCL 09B

N90-20666*# Microexpert, Calabasas, CA.
BROADENING THE INTERFACE BANDWIDTH IN SIMULATION BASED TRAINING
Larry E. Somers *In* NASA, Lyndon B. Johnson Space Center, Graphics Technology in Space Applications (GTSA 1989) Aug. 1989 p 107-114 (For primary document see N90-20651 13-60)
Avail: NTIS HC A11/MF A02 CSCL 09B

N90-20667*# Microexpert, Calabasas, CA.
ANIMATION GRAPHIC INTERFACE FOR THE SPACE SHUTTLE ONBOARD COMPUTER
Jeffrey Wike and Paul Griffith *In* NASA, Lyndon B. Johnson Space Center, Graphics Technology in Space Applications (GTSA 1989) Aug. 1989 p 115-119 (For primary document see N90-20651 13-60)
Avail: NTIS HC A11/MF A02 CSCL 09B

N90-20668*# National Aeronautics and Space Administration. Goddard Space Flight Center, Greenbelt, MD.
OPERATIONAL COMPUTER GRAPHICS IN THE FLIGHT DYNAMICS ENVIRONMENT
James F. Jeletic *In* NASA, Lyndon B. Johnson Space Center, Graphics Technology in Space Applications (GTSA 1989) Aug. 1989 p 121-128 (For primary document see N90-20651 13-60)
Avail: NTIS HC A11/MF A02 CSCL 09B

N90-20670*# Lockheed Engineering and Sciences Co., Houston, TX.
THE USE OF GRAPHICS IN THE DESIGN OF THE HUMAN-TELEROBOT INTERFACE
Mark A. Stuart and Randy L. Smith *In* NASA, Lyndon B. Johnson Space Center, Graphics Technology in Space Applications (GTSA 1989) Aug. 1989 p 135-142 (For primary document see N90-20651 13-60)
(Contract NAS9-17900)
Avail: NTIS HC A11/MF A02 CSCL 09B

N90-20671*# National Aeronautics and Space Administration. Lyndon B. Johnson Space Center, Houston, TX.
DISTRIBUTED EARTH MODEL/ORBITER SIMULATION
Erik Geisler, Scott McClanahan, and Gary Smith (International Business Machines Corp., Houston, TX.) *In its* Graphics Technology in Space Applications (GTSA 1989) Aug. 1989 p 143-150 (For primary document see N90-20651 13-60)
Avail: NTIS HC A11/MF A02 CSCL 09B

N90-20673*# Lockheed Engineering and Sciences Co., Houston, TX.
SPACE STATION FREEDOM INTEGRATED FAULT MODEL

Fred J. Becker *In* NASA, Lyndon B. Johnson Space Center, Graphics Technology in Space Applications (GTSA 1989) Aug. 1989 p 155-163 (For primary document see N90-20651 13-60)
Avail: NTIS HC A11/MF A02 CSCL 09B

N90-20674*# Mitre Corp., Houston, TX.
GRAPHICAL PROGRAMMING AND THE USE OF SIMULATION FOR SPACE-BASED MANIPULATORS
Debra S. McGrath and James C. Reynolds *In* NASA, Lyndon B. Johnson Space Center, Graphics Technology in Space Applications (GTSA 1989) Aug. 1989 p 165-170 (For primary document see N90-20651 13-60)
Avail: NTIS HC A11/MF A02 CSCL 09B

N90-20675*# National Aeronautics and Space Administration. Lyndon B. Johnson Space Center, Houston, TX.
USING AN INSTRUMENTED MANIKIN FOR SPACE STATION FREEDOM ANALYSIS
Linda Orr and Richard Hill (Lockheed Missiles and Space Co., Huntsville, AL.) *In its* Graphics Technology in Space Applications (GTSA 1989) Aug. 1989 p 171-175 (For primary document see N90-20651 13-60)
Avail: NTIS HC A11/MF A02 CSCL 09B

N90-20677*# Pennsylvania Univ., Philadelphia. Computer Graphics Research Lab.
SOFTWARE SYSTEMS FOR MODELING ARTICULATED FIGURES
Cary B. Phillips *In* NASA, Lyndon B. Johnson Space Center, Graphics Technology in Space Applications (GTSA 1989) Aug. 1989 p 187-193 (For primary document see N90-20651 13-60)
Avail: NTIS HC A11/MF A02 CSCL 09B

N90-20678*# Pennsylvania Univ., Philadelphia. Dept. of Computer and Information Science.
HUMAN TASK ANIMATION FROM PERFORMANCE MODELS AND NATURAL LANGUAGE INPUT
Jeffrey Esakov, Norman I. Badler, and Moon Jung *In* NASA, Lyndon B. Johnson Space Center, Graphics Technology in Space Applications (GTSA 1989) Aug. 1989 p 195-203 Sponsored in part by Lockheed Engineering and Managment Services, Pacific Northwest Laboratories B-U0072-A-N and Pennsylvania Benjamin Franklin Partnership (For primary document see N90-20651 13-60)
(Contract NAG2-426; NGT-50063; NSF MCS-82-19196; NSF IST-86-12984; NSF DMC-85-16114; DAAG29-84-K-0061)
Avail: NTIS HC A11/MF A02 CSCL 09B

N90-20682*# Evans and Sutherland Computer Corp., Salt Lake City, UT.
COMPUTER IMAGE GENERATION: RECONFIGURABILITY AS A STRATEGY IN HIGH FIDELITY SPACE APPLICATIONS
Michael J. Bartholomew *In* NASA, Lyndon B. Johnson Space Center, Graphics Technology in Space Applications (GTSA 1989) Aug. 1989 p 229-233 (For primary document see N90-20651 13-60)
Avail: NTIS HC A11/MF A02 CSCL 09B

N90-20683*# National Aeronautics and Space Administration. Lyndon B. Johnson Space Center, Houston, TX.
REAL-TIME GRAPHICS FOR THE SPACE STATION FREEDOM CUPOLA, DEVELOPED IN THE SYSTEMS ENGINEERING SIMULATOR
Michael T. Red and Philip W. Hess (Lockheed Missiles and Space Co., Huntsville, AL.) *In its* Graphics Technology in Space Applications (GTSA 1989) Aug. 1989 p 235-247 (For primary document see N90-20651 13-60)
Avail: NTIS HC A11/MF A02 CSCL 09B

62 COMPUTER SYSTEMS

Includes computer networks and special application computer systems.

N90-20728# Princeton Univ., NJ. Dept. of Computer Science.
ALMOST-OPTIMUM PARALLEL SPEED-UPS OF ALGORITHMS FOR BIPARTITE MATCHING AND RELATED PROBLEMS
Harold N. Gabow and Robert E. Tarjan (Bell Telephone Labs., Inc., Murray Hill, NJ.) 18 Jan. 1989 33 p Sponsored in part by Bell Telephone Labs., Inc., Murray Hill, NJ
(Contract N00014-87-K-0467; NSF DCR-85-1191; NSF DCR-86-05962)
(AD-A215111; CS-TR-223-89) Avail: NTIS HC A03/MF A01 CSCL 12/4

Algorithms for matching problems that run on an EREW PRAM with p processors are examined. Given is a bipartite graph with n vertices, m edges, and integral edge costs at most N in magnitude. This bound is within a factor of log p of optimum speed-up of the best known sequential algorithm, which in turn is within a factor of log (nN) of the best known bound for the problem without costs (maximum cardinality matching). Extensions of the algorithm are given, including an algorithm for maximum cardinality bipartite matching with slightly better processor bounds, and similar results for bipartite degree-constrained subgraph problems (with and without costs). GRA

N90-20729# Massachusetts Inst. of Tech., Cambridge. Lab. for Computer Science.
PERFORMANCE TRADEOFFS IN MULTITHREADED PROCESSORS
Anant Agarwal Oct. 1989 32 p Sponsored in part by Sloan Foundation and by IBM Corp.
(Contract N00014-87-K-0825)
(AD-A217123; VLSI-MEMO-89-566) Avail: NTIS HC A03/MF A01 CSCL 12/7

High network and memory latencies in large-scale multiprocessors can cause a significant drop in processor utilization. Overlapping computation from alternate processes with memory accesses in multithreaded processors can reduce processor idle time. A multithreaded processor maintains multiple process contexts in hardware and can switch between them in a few (say, zero to 16) cycles. This paper proposes an analytical performance model for multithreaded processors that includes cache interference, network contention, and context-switching overhead effects. The model is validated through our own simulations and by comparison with previously published simulation results. Our results indicate that processors can substantially benefit from multithreading, even on systems with small caches. Large caches yield close to full processor utilization with as few as 2 to 4 processes, while small caches require two to four times more processes. Increased network contention due to multithreading has a negligible effect on performance, and the context switching overhead sets a limit on the best possible utilization. GRA

N90-20730# Massachusetts Inst. of Tech., Cambridge. Lab. for Computer Science.
A LOCALITY-BASED MULTIPROCESSOR CACHE INTERFERENCE MODEL
Anant Agarwal Oct. 1989 10 p Sponsored in part by Sloan Foundation and IBM Corp.
(AD-A217126; VLSI-MEMO-89-565) Avail: NTIS HC A02/MF A01 CSCL 12/6

Keeping data consistent in cache-coherent multiprocessors often requires the invalidation of cached blocks and results in higher miss rates. The increase in the cache miss rate due to invalidations is related to the number of processors and to the level of sharing. Analytically modeling this increase is important for the accurate performance evaluation of cache-based multiprocessors. Previous modeling efforts assumed a uniform probability of access to shared blocks. However, applications that we have studied show significant temporal locality of access to shared blocks, which substantially alters the magnitude of sharing related misses. This paper develops a multiprocessor cache

interference model using temporal locality information measured from address traces of parallel applications. The model is very simple and yields reasonable predictions. GRA

N90-20731# Purdue Univ., West Lafayette, IN.
ADVANCED PARALLEL SYSTEMS Final Report
John Rice Nov. 1989 8 p
(Contract DAAL03-86-K-0106)
(AD-A217175; ARO-24369.39-MA-SDI) Avail: NTIS HC A02/MF A01 CSCL 12/6

The objective of this work was to explore algorithms and their implementation for future advanced parallel systems. These systems are assumed to have hundreds or even thousands of processors and to be able to concentrate their computing power on one or a small number of tasks. The three principal questions to be explored were: (1) are there algorithms for the crucial applications which have enough parallelism to allow the power of the advanced parallel systems to be fully exploited; (2) what languages and implementation tools are needed for efficient programming of these algorithms; and (3) what are the relative performances of different algorithm types; of different architecture types; and of different implementation languages. The research results obtained appear in this report. GRA

N90-20732# New Hampshire Univ., Durham. Robotics Lab.
ROBUST PLANNING AND CONTROL USING NEURAL NETWORKS Progress Report
W. Thomas Miller, III, Filson H. Glanz, L. Gordon Kraft, III, and Michael J. Carter 31 Dec. 1989 6 p
(Contract N00014-89-J-3100)
(AD-A217216) Avail: NTIS HC A02/MF A01 CSCL 12/9

During the past five years, the Robotics Laboratory of the Department of Electrical and Computer Engineering at the University of New Hampshire has been studying the application of locally generalizing neural networks to difficult problems in control. In a series of theoretical and real time experimental studies, learning control approaches have been shown to be effective for controlling the dynamics of multidimensional, nonlinear robotic systems during repetitive and nonrepetitive operations. This project involves the extension of our work in learning control, with the combined goals of expanding our theoretical understanding of neural network based learning control systems and of extending our experimental work to include hierarchical learning control structures. Our work will consider the efficacy of locally generalizing versus globally generalizing neural network architectures in control applications, as well as developing and analyzing learning control paradigms which are not restricted to specific network architectures. Various robotic systems within the laboratory will form the basis for the real time experimental portions of the research. The concepts explored, however, will be applicable to a wide variety of control problems in addition to robotics. GRA

N90-20733# Naval Ocean Systems Center, San Diego, CA.
PARALLEL COMPUTER GRAPHICS ALGORITHMS FOR THE CONNECTION MACHINE
John F. Richardson Jan. 1990 26 p Submitted for publication
(AD-A217300) Avail: NTIS HC A03/MF A01 CSCL 12/5

Many of the classes of computer graphics algorithms and polygon storage schemes can be adapted for parallel execution on various parallel architectures. The connection machine is one such architecture that should be thought of as a multiprocessor grid that can be reconfigured into standard 2-dimensional mesh and n-dimensional hypercube architectures. The classes of algorithms considered in this paper are SPLINES; POLYGON STORAGE; TRIANGULARIZATION; and SYMBOLIC INPUT. The target Connection Machine (hereafter designated as CM) for the algorithms of this paper has 8192 physical processors. Each physical processor has 8 kilobytes of local memory plus an arithmetic-logic unit. All processors can communicate with any other processor through a router. Thus this CM has a shared memory of 64 megabytes when used as a standard multiprocessor (MIMD) architecture. In addition, the CM interconnection structure can simulate a 2-dimensional mesh and n-dimensional hypercube (SIMD) architecture with the mesh being the default architecture. The front end for the CM is a Symbolics and the high level language is LISP or FORTRAN. GRA

N90-20734# Stanford Univ., CA.
ASYNCHRONOUS DESIGN FOR PARALLEL PROCESSING ARCHITECTURES Semiannual Report, Jul. 1989 - Dec. 1989
Teresa H.-Y. Meng Dec. 1989 2 p
(Contract N00014-89-J-3036)
(AD-A217421) Avail: NTIS HC A01/MF A01 CSCL 12/6

The objective of this research is to provide an interconnect design synthesis methodology which facilitates a modular design approach without compromising the global performance. The main tasks of this effort will be the development of the theory for optimal interconnect synthesis from a high level specification, with emphasis on testability and fault tolerance asynchronous interface among parallel computing hardware objects, and the application of this design methodology to physical implementations of multi-processing systems. GRA

N90-20735# Lawrence Livermore National Lab., CA.
THE LIVERMORE DISTRIBUTED STORAGE SYSTEM: IMPLEMENTATION AND EXPERIENCES
Joy Foglesong, George Richmond, Loellyn Cassell, Carole Hogan, John Kordas, and Michael Nemanic Jan. 1990 10 p Presented at the 10th IEEE Symposium on Mass Storage Systems, Monterey, CA, 7-10 May 1990
(Contract W-7405-eng-48)
(DE90-007257; UCRL-102663; CONF-9005105-4) Avail: NTIS HC A02/MF A01

The LINCS Storage System (LSS) has been in production at Lawrence Livermore National Laboratory since January, 1988. In the development of the LSS, the designers made key architectural decisions which included the separation of data and control messages, a network-wide locking mechanism, and the separation of the naming mechanism from other object managers. Other important issues of the system deal with space management, descriptor management, and system administration. This paper outlines the LSS software system and then focuses on these key design decisions and issues with the intent of providing some insight into the types of difficulties designers face in developing a distributed storage system. DOE

N90-20736# Oak Ridge National Lab., TN.
IMPLEMENTATION OF A CONTROL SYSTEM TEST ENVIRONMENT IN UNIX
C. R. Brittain, L. A. Rovere (Tennessee Univ., Oak Ridge.), and P. J. Otaduy 1990 20 p Presented at the 3rd Canadian Nuclear Society International Conference on Simulation Methods in Nuclear Engineering, Montreal, Quebec, 18-20 Apr. 1990
(Contract DE-AC05-84OR-21400)
(DE90-007485; CONF-9004138-2) Avail: NTIS HC A03/MF A01

How UNIX features such as shared memory, remote procedure calls, and signalling were used to implement a distributed computational environment ideal for the development and testing of digital control systems are discussed. The resulting environment, based on features commonly available in commercial workstations, is flexible, allows process simulation and controller development to proceed in parallel, and provides for testing and validation in a realistic environment. In addition, the use of shared memory to exchange data allows other tasks such as user interfaces and recorders to be added without affecting the process simulation or controllers. A library of functions is presented which provides a simple interface to using the features described. These functions can be used in either C or FORTRAN programs and have been tested on a network of Sun workstations and an ENCORE parallel computer. DOE

N90-20737# Oak Ridge National Lab., TN. Mathematical Sciences Div.
DESIGN OF A SIMULATION INTERFACE FOR A PARELLEL COMPUTING ENVIRONMENT
Hira Narang (Tuskegee Inst., AL.), Ray Flanery, and John Drake 1990 19 p Presented at the Annual ACM South Eastern Region Conference, Atlanta, GA, 13 Apr. 1990
(Contract DE-AC05-84OR-21400)
(DE90-008497; CONF-9004144-1) Avail: NTIS HC A03/MF A01

A user interface for simulation of contaminant transport in groundwater flow using a distributed memory parallel processor is described. The user interface is a menu-mouse driven presentation using the X-Windows software. To facilitate the division and distribution of data among processors and to develop a data structure capable of manipulation for a variety of functions, graphics, remeshing, input and retrieval of auxiliary information, an object oriented programming style is used. The parallel computational model for the update of contaminant concentrations is organized around objects and an explicit time marching algorithm implemented on an IPSC2 Hypercube multiprocessor. DOE

N90-20738# Sandia National Labs., Albuquerque, NM.
A TIME STEPPING ALGORITHM FOR PARALLEL COMPUTERS
David E. Womble Feb. 1990 21 p
(Contract DE-AC04-76DP-00789)
(DE90-008163; SAND-88-3291) Avail: NTIS HC A03/MF A01

Parabolic and hyperbolic differential equations are often solved numerically by time stepping algorithms. These algorithms have been regarded as sequential in time; that is, the solution on a time level must be known before the computation of the solution at subsequent time levels can start. While this remains true in principle, we demonstrate that it is possible for processors to perform useful work on many time levels simultaneously. Specifically, it is possible for processors assigned to later time levels to compute a very good initial guess for the solution based on partial solutions from previous time levels, thus reducing the time required for solution. The reduction in the solution time can be measured as parallel speed up. We demonstrate this algorithm for both linear and nonlinear problems. In addition, we discuss the convergence properties of the method based on the convergence properties of the underlying iterative method, and we present an accurate performance model from which the speedup and other quantities can be estimated. DOE

N90-20739# Sandia National Labs., Albuquerque, NM.
A MODEL AND IMPLEMENTATION OF MULTIGRID FOR MASSIVELY PARALLEL COMPUTERS
David E. Womble and Brenton C. Young (Stanford Univ., CA.) Feb. 1990 19 p
(Contract DE-AC04-76DP-00789)
(DE90-008165; SAND-89-2781) Avail: NTIS HC A03/MF A01

Multigrid is a fast and popular iterative method used to solve linear partial differential equations. However, because the solution of very small problems is inherent in the multigrid iteration, it is difficult to implement efficiently on a massively parallel computer. In this paper, we present a model for the efficiency of multigrid on a parallel computer that depends only on the efficiency of the smoother at each level. This model can be used to verify that it is indeed difficult to obtain extremely high efficiencies (greater than 95 percent), but that it is relatively easy to obtain moderately high efficiencies (70 to 85 percent). The model also indicates that moderately high efficiencies can still be achieved as the number of dimensions in the partial differential equation increases. We also present an implementation of the multigrid v-cycle that has achieved 84 percent efficiency on the 1,024 processor NCUBE/ten. DOE

N90-20740# Sandia National Labs., Albuquerque, NM. Advanced Systems Development Div.
IMPLEMENTATION OF MIDCOURSE TRACKING AND CORRELATION ON MASSIVELY PARALLEL COMPUTERS
Report, fiscal year 1989
Ronald D. Halbgewachs, James L. Tomkins, and John P. VanDyke Jan. 1990 27 p
(Contract DE-AC04-76DP-00789)
(DE90-008166; SAND-89-2534) Avail: NTIS HC A03/MF A01

Sandia National Laboratories joined with two other laboratories, Los Alamos National Laboratory and Naval Research Laboratory, to study and implement a highly parallelized tracker/correlator algorithm. Significant progress was made at Sandia on a specific algorithm and code. This report summarizes the accomplishments by Sandia during FY '89 on this project. DOE

N90-20741# Air Force Inst. of Tech., Wright-Patterson AFB, OH.
A PARALLEL ARCHITECTURE FOR REAL-TIME SIMULATION
M.S. Thesis - Alabama Univ., Tuscaloosa
Clayton Dale Cockrell 1989 72 p
(AD-A218321; AFIT/CI/CIA-89-041) Avail: NTIS HC A04/MF A01 CSCL 12/6

This thesis is concerned with the development of a very fast and highly efficient parallel computer architecture for real-time simulation of continuous systems. Currently, several parallel processing systems exist that may be capable of executing a complex simulation in real-time. These systems are examined and the pros and cons of each system discussed. The thesis then introduced a custom-designed parallel architecture based upon The University of Alabama's OPERA architecture. Each component of this system is discussed and rationale presented for its selection. The problem selected, real-time simulation of the Space Shuttle Main Engine for the test and evaluation of the proposed architecture, is explored, identifying the areas where parallelism can be exploited and parallel processing applied. Results from the test and evaluation phase are presented and compared with the results of the same problem that has been processed on a uniprocessor system. GRA

63 CYBERNETICS

Includes feedback and control theory, artificial intelligence, robotics and expert systems.

For related information see also *54 Man/System Technology and Life Support.*

N90-20742# Massachusetts Inst. of Tech., Cambridge. Lab. for Computer Science.
IRREDUNDANT SEQUENTIAL MACHINES VIA OPTIMAL LOGIC SYNTHESIS
Srinivas Devadas, Hi-Keung T. Ma, A. R. Newton, and A. Sangiovanni-Vincentelli Oct. 1989 12 p Sponsored in part by AT and T Bell Labs.
(Contract N00014-87-K-0825)
(AD-A217119; VLSI-MEMO-89-571) Avail: NTIS HC A03/MF A01 CSCL 12/6

It is well known that optimal logic synthesis can ensure fully testable combinational logic design. In this paper we show that optimal sequential logic synthesis can produce irredundant, fully testable finite state machines. Test generation algorithms can be used to remove all the redundancies in sequential machines resulting in a fully testable design. However, this method may require exorbitant amounts of CPU time. The optimal synthesis procedure presented in this paper represents a more efficient approach to achieve 100 percent testability. Synthesizing a sequential circuit from a State Transition Graph description involves the steps of state minimization, state assignment and logic optimization. Previous approaches to producing fully and easily testable sequential circuits have involved the use of extra logic and constraints on state assignment and logic optimization. In this paper we show that 100 percent testability can be ensured without the addition of extra logic and without constraints on the state assignment and logic optimization. Unlike previous synthesis approaches to ensuring fully testable machines, there is no area/performance penalty associated with this approach. This

technique can be used in conjunction with previous approaches to ensure that the synthesized machine is easily testable. GRA

N90-20743# Pennsylvania State Univ., University Park. Dept. of Computer and Information Science.
ARTIFICIAL INTELLIGENCE (AI) CENTER OF EXCELLENCE AT THE UNIVERSITY OF PENNSYLVANIA Final Report, Jul. 1984 - Sep. 1989
Aravind Joshi, Ruzena Bajcsy, Norman Badler, Peter Buneman, and Bonnie Webber Oct. 1989 83 p
(Contract DAAG29-84-K-0061)
(AD-A217393; ARO-21684.204-EL-AI) Avail: NTIS HC A05/MF A01 CSCL 12/9

The five major research thrusts are: Natural language processing; Machine perception and robotics; Task oriented computer animation; Programming structures for databases and knowledge bases; and Parallel processing in AI. These capabilities are described by combining some past work and directions of new work under progress. GRA

N90-20744# Illinois Univ., Urbana. Coordinated Science Lab.
ROBUST ADAPTIVE NONLINEAR CONTROL UNDER EXTENDED MATCHING CONDITIONS
Ioannis Kanellakopoulos, Petar V. Kokotovic, and Richard Marino Jan. 1990 25 p
(Grants AF-AFOSR-0011-90; NSF ECS-87-15811)
(AD-A217684; UILU-ENG-90-2202; DC-115) Avail: NTIS HC A03/MF A01 CSCL 12/2

A new direct adaptive regulation scheme is proposed for nonlinear systems satisfying extended matching conditions. Two sets of additional conditions are given: first, for the regulation to be global, and second, for asymptotic parameter convergence. It is also shown that the new scheme is robust with respect to unmodeled dynamics. GRA

N90-20745# Sandia National Labs., Albuquerque, NM.
BOUNDARY EQUATIONS OF CONFIGURATION OBSTACLES FOR MANIPULATORS
Yong K. Hwang 1989 10 p Presented at the IEEE Robotics and Automation Conference, Cincinnati, OH, 13-18 May 1990
(Contract DE-AC04-76DP-00789)
(DE90-002101; SAND-89-2510C; CONF-900559-6) Avail: NTIS HC A02/MF A01

Configuration obstacle is an important idea for motion planning. Explicit expressions of configuration obstacles have been available for rigid polyhedral robots and planar polygonal manipulators. In this paper, such expressions are derived for arbitrary manipulators in three-dimensional polyhedral environments. The expressions can be used to compute configuration obstacles or to analyze the geometry of contacts between manipulators and obstacles. DOE

N90-20746# Oak Ridge National Lab., TN. Center for Engineering Systems Advanced Research.
HYBRID INTELLIGENT PERCEPTION SYSTEM: INTELLIGENT PERCEPTION THROUGH COMBINING ARTIFICIAL NEURAL NETWORKS AND AN EXPERT SYSTEM
C. W. Glover and P. F. Spelt 1990 13 p Presented at the 1st Workshop on Neural Networks: Academic/Industrial/NASA/ Defense, Auburn, AL, 5-6 Feb. 1990
(Contract DE-AC05-84OR-21400)
(DE90-007483; CONF-900290-2) Avail: NTIS HC A03/MF A01

This paper presents a report of work-in-progress on a project to combine Artificial Neural Networks (ANNs) and Expert Systems (ESs) into a hybrid, self-improving pattern recognition system. The purpose of this project is to explore methods of combining multiple classifiers into a Hybrid Intelligent Perception (HIP) System. The central research issue to be addressed for a multiclassifier hybrid system is whether such a system can perform better than the two classifiers taken by themselves. ANNs and ESs have different strengths and weaknesses, which are being exploited in this project in such a way that they are complementary to each other: Strengths in one system make up for weaknesses in the other, and vice versa. There is presently considerable interest in the AI community in ways to exploit the strengths of these methodologies to produce an intelligent system which is more robust and flexible than one using either technology alone. Perception, which involves both data-driven (bottom-up) and concept-driven (top-down) processing, is a process which seems especially well-suited to displaying the capabilities of such a hybrid system. Here we report on the efforts to develop the low-level ANNs and a graphic representation of their knowledge, and discuss ways of using an ES to integrate and supervise the entire system. DOE

N90-20747# Maryland Univ., Baltimore. Dept. of Computer Science.
A LOCALLY CONSTRAINED PARALLEL ACTIVATION MODEL FOR DIAGNOSTIC REASONING Final Report, 17 Aug. 1987 - 16 Aug. 1989
Sanjeev B. Ahuja Oct. 1989 5 p
(Grant AF-AFOSR-0335-87; AF Proj. 2304)
(AD-A217808; AFOSR-90-0076TR) Avail: NTIS HC A01/MF A01 CSCL 12/9

A general purpose competition-based parallel activation paradigm for diagnostic reasoning was formulated. To facilitate the task of formulating and testing this paradigm, a parallel activation model generator had also to be developed. Using the network specification language provided by this generator, a knowledge base for diagnosing faults in a prototype chemical processing plant was built to test the viability of the proposed approach as a practical diagnostic paradigm. Diagnosis of failures in process plants has been attempted in the past using conventional AI methodologies, which have raised several practical issues which need to be resolved before a viable automated tool can be built. GRA

N90-20748# Environmental Research Inst. of Michigan, Ann Arbor. Sensor Systems Div.
ROBOTIC MOBILITY SYSTEM: ROAD FOLLOWING ALGORITHMS Final Report, Sep. 1984 - Dec. 1988
Robert Franklin, Dwayne C. Carmer, F. Pont, N. Finzel, and L. Harmon Jan. 1990 132 p
(Contract DAAE07-84-C-R138)
(AD-A218107; ERIM-179100-40-F; TACOM-TR-13463) Avail: NTIS HC A07/MF A01 CSCL 12/9

Image processing algorithms were developed to permit use of a laser-based vision device for autonomous navigation of a wheeled vehicle. Imagery and processing results are given. Operation of the laser-based vision device (ERIM's Autonomous Land Vehicle sensor) is described, including a new output signal that is sensitive to scene texture or vertical structure; other signals provide range and reflectance information. Simulation software packages were developed to model a robotic vehicle's performance and to study advanced planner concepts required for flexible vehicle behavior. Plans to develop a demonstration vehicle are given. GRA

N90-20749# Aerospace Medical Research Labs., Wright-Patterson AFB, OH.
CEREBRAL WEEVIL: A MACHINE LEARNING MODEL FOR HEMISPHERIC CATEGORIZATION OF COMPLEX VISUAL PATTERNS Technical Report, Jan. 1987 - Nov. 1989
Michael D. McNeese Nov. 1989 29 p
(AF Proj. 7184)
(AD-A218143; AAMRL-TR-89-045) Avail: NTIS HC A03/MF A01 CSCL 12/9

The role is established of machine learning as a new human performance modeling technique. Learning mechanisms are modeled based on an empirical analysis of psychological reality and are subsequently tested empirically for their demonstration of that reality. Any variations in differences are considered in terms of changes to both future experimental studies of humans, and new evolvements in the programs used to model the reality. The reality used involved hemispheric processing in learning visual patterns. The factors which influence hemispheric processing are modelled using the ID3 inductive machine learning technique. Various subsets of training data were used to assess the point of convergence between the research data and the model. The model

successfully simulates the experimental data when it approaches a subset containing 90 percent of the examples. Conclusions look at ways to improve the model's convergence at a much lower percentage of examples induced. GRA

N90-20750# Air Force Inst. of Tech., Wright-Patterson AFB, OH.
AN INVESTIGATION OF THE LOCALITY OF MEMORY ACCESSES DURING SYMBOLIC PROGRAM EXECUTION Ph.D. Thesis - Texas Univ., Austin
William C. Hobart, Jr. Aug. 1989 163 p
(AD-A218168; AFIT/CI/CIA-89-081) Avail: NTIS HC A08/MF A01 CSCL 12/5

This research focused on the low level virtual address memory referencing behavior of symbolic programs. The virtual address traces of six artificial intelligence applications and two conventional workloads executed on the Texas Instruments Explorer II were used to characterize the locality of virtual memory accesses during symbolic program execution and to compare these characteristics with the locality characteristics of conventional workloads. By using this approach, this research accomplished three overall objectives: first, it enhanced the basic understanding of symbolic program memory referencing behavior; second, it found new ways in which the architecture can be tailored for these low-level memory referencing locality characteristics; and third, it laid the foundation for developing a symbolic program workload generator model that can be used to drive memory system design tools. This research was the first systematic effort to characterize symbolic program behavior through the investigation of symbolic workloads' temporal, spatial, and structural locality. Its specific contributions are the development of new measures and methods for the analysis of program locality, an extension of Denning's model of page referencing behavior to virtual address word-level memory referencing behavior, the identification of a low level virtual memory referencing structural locality, the identification of significant differences in the low level virtual memory referencing behavior of symbolic and conventional workloads, and a memory system design for exploiting the structural locality characteristics of symbolic workloads. GRA

N90-20751# Massachusetts Inst. of Tech., Cambridge. Artificial Intelligence Lab.
STEREO FEATURE MATCHING IN DISPARITY SPACE
David J. Braunegg Sep. 1989 22 p
(Contracts N00014-85-K-0124; DACA76-85-C-0010)
(AD-A218170; AI-M-1184) Avail: NTIS HC A03/MF A01 CSCL 12/9

A new method for matching, validating, and disambiguating features for stereo vision is described. It is based on the Marr-Poggio-Grimson stereo matching algorithm which uses zero-crossing contours in difference of Gaussian filtered images as features. The matched contours are represented in disparity space, which makes the information needed for matched contour validation and disambiguation easily accessible. The use of disparity space also makes the algorithm conceptually cleaner than previous implementations of the Marr-Poggio-Grimson algorithm and yields a more efficient matching process. GRA

N90-20752# Massachusetts Inst. of Tech., Cambridge. Artificial Intelligence Lab.
LOCATION RECOGNITION USING STEREO VISION
David J. Braunegg Oct. 1989 24 p
(Contracts N00014-85-K-0124; DACA76-85-C-0010; N00014-86-K-0685)
(AD-A218218; AI-M-1186) Avail: NTIS HC A03/MF A01 CSCL 12/9

A mobile robot must be able to determine its own position in the world. To support truly autonomous navigation, a system is presented that builds and maintains its own models of world locations and uses these models to recognize its world position from stereo vision input. The system is designed to be robust with respect to input errors and to respond to a gradually changing world by updating the world locations models. Results are presented from tests of the system that demonstrate its reliability. The model builder and recognizer system fit into a planned world modeling system that was described. GRA

64 NUMERICAL ANALYSIS

Includes iteration, difference equations, and numerical approximation.

N90-20753 Rensselaer Polytechnic Inst., Troy, NY.
AUTOMATED FINITE ELEMENT MODELING AND SIMULATION Ph.D. Thesis
Peggy L. Baehmann 1989 237 p
Avail: Univ Microfilms Order No. DA8926564

An automated, adaptive finite element modelling system is described which includes geometric modelling, automatic mesh generation, finite element analysis, error estimation and indication, and adaptive geometry and mesh updates. The problems considered are two-dimensional linear elasticity and nonlinear large deformation forging simulations. The automatic mesh generator interrogates the geometric information defined by the geometric modeler and automatically creates a valid mesh. The model is first represented as a set of cells in a quadtree. Finite elements are then created from the cells. Mesh gradations are controlled by changing the levels of the tree, and therefore the size of the cells, in the area needing further refinement. Adaptive finite element procedures determine the solution error, and use the magnitude of the error within an element to guide the multiple level refinement procedures of the mesh generator. After a linear elastic finite element analysis on 6-noded elements, the error estimator captures the residual error within an element by employing a basis consisting of cubic and quartic shape functions. The higher order shape functions are zero on the element edges, allowing the error to be solved for on the local element level. Important benefits of an automated analysis system are shown to be the added efficiency, accuracy, and reliability that can be achieved from adaptive program control. A forging simulation demonstrates the benefits that result when the analysis of an evolving geometry problem is automated. Dissert. Abstr.

N90-20754# Princeton Univ., NJ. Dept. of Computer Science.
MAINTAINING BRIDGE-CONNECTED AND BICONNECTED COMPONENTS ON-LINE
Jeffrey Westbrook and Robert E. Tarjan (Bell Telephone Labs., Inc., Murray Hill, NJ.) Aug. 1989 41 p
(Contract N00014-87-K-0467; NSF DCR-86-05962)
(AD-A215107; CS-TR-228-89) Avail: NTIS HC A03/MF A01 CSCL 12/4

The twin problems are considered of maintaining the bridge-connected components and the biconnected components of a dynamic undirected graph. The allowed changes to the graph are vertex and edge insertions. An algorithm is given for each problem. With simple data structures, each algorithm runs in O (n log n + m) time, where n is the number of vertices and m is the number of operations. A modified version is developed of the dynamic trees of Sleator and Tarjan that is suitable for efficient recursive algorithms, and it is used to reduce the running time of the algorithms for both problems to O(m alpha(m,n), where alpha is a functional inverse of Ackermann's function. This time bound is optimal. All of the algorithms use O(n) space. GRA

N90-20755# Stanford Univ., CA. Systems Optimization Lab.
GENERALIZED QUASI-VARIATIONAL INEQUALITY AND IMPLICIT COMPLEMENTARITY PROBLEMS
Jen-Chih Yao Oct. 1989 52 p
(Contract N00014-89-J-1659; NSF DMS-89-13089)
(AD-A215191; SOL-89-15) Avail: NTIS HC A04/MF A01 CSCL 12/4

A new problem called the generalized quasi-variational inequality problem is introduced. This new formulation extends all kinds of variational inequality problem formulations that have been introduced and enlarges the class of problems that can be

approached by the variational inequality problem formulation. Existence results without convexity assumptions are established and topological properties of the solution set are investigated. A new problem called the generalized implicit complementarity problem is also introduced which generalizes all the complementarity problem formulations that have been introduced. Applications of generalized quasi-variational inequality and implicit complementarity problems are given. GRA

N90-20756# Massachusetts Inst. of Tech., Cambridge. Lab. for Computer Science.
EXACT ALGORITHMS FOR OUTPUT ENCODING, STATE ASSIGNMENT AND FOUR-LEVEL BOOLEAN MINIMIZATION
Srinivas Devadas and A. R. Newton Oct. 1989 12 p
(Contract N00014-87-K-0825)
(AD-A217121; VLSI-MEMO-89-569) Avail: NTIS HC A03/MF A01 CSCL 12/1

Efficient, exact algorithms are presented for the problems of output encoding, state assignment and four-level Boolean minimization. All previous automatic approaches to encoding problems have involved the use of heuristic techniques. Other than the straightforward, exhaustive search procedure, no exact solution methods were proposed. The problems of output encoding and state assignment targeting two-level logic implementations involve finding appropriate binary codes for the symbolic outputs of states so a minimum number of product terms results after two-level Boolean minimization. A straightforward, exhaustive search procedure requires O(N) exact Boolean minimization, where N is the number of symbolic outputs or states. A minimization procedure of prime implicant generation and covering that operates symbolic outputs, rather than binary-valued outputs, for solving the output encoding problem is presented. An exact solution to this minimization problem is also an exact solution to the encoding problem. While the covering problem is more complex than the classic unate covering problem, a single logic minimization step replaces O(N) minimization. The input encoding problem can be exactly solved using multiple-valued Boolean minimization. An exact algorithm is presented for state assignment by generalizing the output encoding approach to the multiple-valued input case. GRA

N90-20757# Pennsylvania State Univ., University Park. Center for Multivariate Analysis
SPECTRAL ANALYTIC METHODS FOR THE ESTIMATION OF NUMBER OF SIGNALS AND DIRECTIONS OF ARRIVAL
Z. D. Bai and C. Radhakrisna Rao Nov. 1989 22 p
(Contract DAAL03-89-K-0139)
(AD-A217219; TR-89-49; ARO-26792.2-MA-SDI) Avail: NTIS HC A03/MF A01 CSCL 12/3

Consider the model x(t) = As(t) + n(t), t = 1,...,N where at time t, x(t) is a p-complex vector of observations, s(t) is a q-complex vector of unobservable signals emitted from q sources and n(t) is a noise p-complex vector variable. The matrix A has a special structure with its k-th column a sub k of the form a' sub k = (1, exp(j;(omega sub 0)(Tau sub k)),..., exp(-j;(omega sub 0)(p-10 (tau sub K) where j = sr rt(-1), rk = 1/c Delta is theta k, theta sub k being the direction of arrival of the signal from the k-th source. The problem is the estimation of q (the number of sources) and Theta sub i's (the direction of arrival). An information theoretic criterion is presented to decide on q, the number of sources, and a spectral analytic method to estimate the tau sub i's. The proposed method is straight forward and has some advantages over the search methods proposed in the literature for the latter problem. For instance, the method works even when the signals are coherent, i.e., the covariance matrix Gamma of signal is singular, whereas the MUSIC algorithm generally used in searching for the estimates of tau sub k is not applicable. GRA

N90-20758# Massachusetts Inst. of Tech., Lexington. Lincoln Lab.
ALGORITHMS FOR OPTIMAL PROCESSING OF POLARIMETRIC RADAR DATA
Leslie M. Novak, Michael B. Sechtin, and Michael C. Burl 6 Nov. 1989 99 p
(Contract F19628-90-C-0002; ARPA Order 3391)
(AD-A217330; TT-73; ESD-TR-89-236) Avail: NTIS HC A05/MF A01 CSCL 17/9

This report describes algorithms that make optimal use of polarimetric radar information to detect and classify targets in a ground clutter background. The optimal polarimetric detector (OPD) is derived; this algorithm processes the complete polarization scattering matrix (PSM) and provides the best possible detection performance from polarimetric radar data. Also derived is the best linear polarimetric detector, the polarimetric matched filter (PMF); the structure of this detector is shown to be related to simple polarimetric target types. Finally, the polarimetric whitening filter (PWF) is derived; this constant false alarm rate (CFAR) detector provides a simple alternative to the OPD for detecting targets in clutter. New K-distributed polarimetric target and clutter models are described; these models are used to predict the performance of the OPD, the PMF, and the PWF. The performance of these three algorithms is compared with that of simpler detectors that use only amplitude information to detect targets. The ability to classify target types by exploiting differences in polarimetric scattering properties is also discussed. GRA

N90-20759# Massachusetts Inst. of Tech., Lexington. Lincoln Lab.
ON METRIC ENTROPY, VAPNIK-CHERVONENKIS DIMENSION, AND LEARNABILITY FOR A CLASS OF DISTRIBUTIONS
Sanjeev R. Kulkarni 14 Dec. 1989 25 p
(Contracts F19628-90-C-0002; DAAL03-86-K-0171)
(AD-A217331; TR-868; ESD-TR-89-186) Avail: NTIS HC A02/MF A01 CSCL 12/3

A formal framework for distribution-free concept known as Valiant's learning framework has generated a great deal of interest. A fundamental result regarding this framework characterizes those concept classes which are learnable in terms of their Vapnik-Chervonenkis (VC) dimension. More recently, learnability in this case was shown. Also a conjecture regarding learnability for a class of distributions was stated. It is pointed out that the condition for learnability for a fixed distribution is equivalent to the notion of finite metric entropy (which has been studied in other contexts). Some relationships between the VC dimension of a concept class and its metric entropy with respect to various distributions are then discussed. Finally, some indication of when the set of learnable concept classes is enlarged by requiring learnability for only a class of distributions is pointed out. GRA

N90-20760# California Univ., Davis. Dept. of Mathematics.
OBSERVER BASED COMPENSATORS FOR NONLINEAR SYSTEMS Final Technical Report, 1 Oct. 1986 - 31 Mar. 1989
Arthur J. Krener, Mont Hubbard, Sinan Karahan, Andrew R. Phelps, Ruggero Frezza, Wei Kang, and J. Martin Clark 31 Mar. 1989 402 p
(Grant AF-AFOSR-0267-85; AF Proj. 2304)
(AD-A217426; AFOSR-89-1689TR) Avail: NTIS HC A18/MF A03 CSCL 12/1

A new method for obtaining higher degree linear approximations of a certain class of nonlinear control systems was developed. The standard approach in the analysis and synthesis of nonlinear systems is a first order approximation by a linear model. An approximation is sought for a nonlinear system by a linear model up to higher degrees than one. This is achieved by finding an appropriate nonlinear coordinate transformation-nonlinear feedback pair to perform the higher degree linearization. With the proposed method, one can improve the accuracy of the approximation up to arbitrarily higher degrees, provided certain solvability conditions are satisfied. The Hunt-Su linearizability theorem makes these conditions precise. The approach to the solution of this linearization problem is similar to Poincare's Normal Form Theorem in formulation, but different in its solution method. The Homological Equations are based on the goal of obtaining a model accurate to a higher degree in the series expansion. A solution to this system of linear equations is equivalent to the solution to the

problem of linearization up to higher degrees by coordinate change and feedback. GRA

N90-20761# Maryland Univ. Baltimore County, Catonsville. Dept. of Mathematics.
NONLINEAR SYSTEMS OF PARTIAL DIFFERENTIAL EQUATIONS Final Report, 25 Apr. 1987 - 24 Sep. 1989
Thomas I. Seidman 24 Sep. 1989 15 p
(Grant AF-AFOSR-0190-87; AF Proj. 2304)
(AD-A217581; AFOSR-90-0117TR) Avail: NTIS HC A03/MF A01 CSCL 12/1

Listed in the bibliography are some 40 items. These have been listed in roughly the order in which the work was done. The most significant accomplishments have been those specifically related to systems of nonlinear partial differential equations with a particular emphasis on semiconductor device models. These are discussed at some length. Considerable mathematical activity, especially the work on switching systems, is also noted. GRA

N90-20762# Lawrence Livermore National Lab., CA.
DOMAIN DECOMPOSITION FOR A BOUNDARY-VALUE PROBLEM WITH A SHOCK LAYER
G. W. Hedstrom and F. A. Howes (National Science Foundation, Washington, DC.) Mar. 1989 14 p Presented at the 3rd Society for Industrial and Applied Mathematics (SIAM) Conference on Domain Decomposition Methods, Houston, TX, 20-22 Mar. 1989
(Contract W-7405-eng-48)
(DE90-007857; UCRL-99707; CONF-8903169-3) Avail: NTIS HC A03/MF A01

We propose a domain decomposition method for a singularly perturbed elliptic partial differential equation for problems in which the solution has a shock layer interior to the domain. This method is designed for situations in which it is desired to resolve the behavior within the shock layer. DOE

N90-20763# Oak Ridge National Lab., TN. Physics Div.
THE BASIS SPLINE METHOD AND ASSOCIATED TECHNIQUES
C. Bottcher and M. R. Strayer 1989 25 p Presented at the Summer School of Computational Atomic and Nuclear Physics, Sewanee, TN, 26 Jun. - 7 Jul. 1989
(Contract DE-AC05-84OR-21400)
(DE90-008403; CONF-8906270-2) Avail: NTIS HC A03/MF A01

We outline the Basis Spline and Collocation methods for the solution of Partial Differential Equations. Particular attention is paid to the theory of errors, and the handling of non-self-adjoint problems which are generated by the collocation method. We discuss applications to Poisson's equation, the Dirac equation, and the calculation of bound and continuum states of atomic and nuclear systems. DOE

N90-20764*# Institute for Computer Applications in Science and Engineering, Hampton, VA.
AN APPROXIMATION THEORY FOR THE IDENTIFICATION OF LINEAR THERMOELASTIC SYSTEMS Final Report
I. G. Rosen and Chien-Hua Frank Su (University of Southern California, Los Angeles.) Mar. 1990 32 p Submitted for publication Sponsored in part by NSF
(Contract NAS1-18107; AF-AFOSR-0356-87)
(NASA-CR-182015; NAS 1.26:182015; ICASE-90-24) Avail: NTIS HC A03/MF A01 CSCL 12A

An abstract approximation framework and convergence theory for the identification of thermoelastic systems is developed. Starting from an abstract operator formulation consisting of a coupled second order hyperbolic equation of elasticity and first order parabolic equation for heat conduction, well-posedness is established using linear semigroup theory in Hilbert space, and a class of parameter estimation problems is then defined involving mild solutions. The approximation framework is based upon generic Galerkin approximation of the mild solutions, and convergence of solutions of the resulting sequence of approximating finite dimensional parameter identification problems to a solution of the original infinite dimensional inverse problem is established using approximation results for operator semigroups. An example involving the basic equations of one dimensional linear thermoelasticity and a linear spline based scheme are discussed. Numerical results indicate how the approach might be used in a study of damping mechanisms in flexible structures. Author

N90-20765# Oak Ridge National Lab., TN.
PERIODIC TRAJECTORIES FOR TWO-DIMENSIONAL NONINTEGRABLE HAMILTONIANS
K. T. R. Davies Feb. 1990 75 p Presented at the ORNL Chaos Workshop, Oak Ridge, TN, 10-11 Jan. 1990
(Contract DE-AC05-84OR-21400)
(DE90-008082; ORNL/TM-11468; CONF-900176-1) Avail: NTIS HC A04/MF A01

Some calculations are reported of classical periodic trajectories in a 2-D nonintegrable potential. After a brief introduction, some details are presented of the theory, pictures of the various families of trajectories are shown, and the topology and branching behavior of these families is discussed. The connection between periodic trajectories and nearby nonperiodic trajectories are shown, which nicely illustrates the relationship of this work to chaos. Finally, how periodic trajectories can be used to calculate tori is briefly discussed. DOE

N90-20766# Massachusetts Univ., Amherst.
COMPUTATION AND GRAPHICS IN MATHEMATICAL RESEARCH Progress Report, 1 Jun. 1989 - 31 May 1990
D. A. Hoffman and J. Spruck Jan. 1990 22 p
(Contract DE-FG02-86ER-25015)
(DE90-008429; DOE/ER-25015/29) Avail: NTIS HC A03/MF A01

Interactive graphics software and numerical computation are actively being developed and used to study problems in global differential geometry and calculus of variations, the structure and motion of interfaces, and the simulation of plasma equilibrium and evolution. The hardware, software and design of the video animation facility was improved and have begun to document the graphics software packages. DOE

N90-20767# Joint Inst. for Nuclear Research, Dubna (USSR). Lab. of Computing Techniques and Automation.
MAGNETOSTATIC BOUNDARY-VALUE PROBLEMS IN THE INCOMPLETE-NONLINEAR FORMULATION AND METHODS OF THEIR SOLUTION
B. N. Khoromsky 1988 29 p In RUSSIAN; ENGLISH summary
(DE90-615185; JINR-R-11-88-784) Avail: NTIS (US Sales Only) HC A03/MF A01

A new class preconditioners for one class of 2-D or 3-D elliptic operators with highly varying coefficients is developed. The construction is based on domain decomposition method when the substructure contains internal cross points. The approximation of the initial equation is based on the Galerkin method for special subspaces of Sobolev's spaces H(exp 1). The general estimates of the condition number for the preconditioned operator are given. This number does not depend on the variation range of the coefficient of the initial operator and slightly (logarithmically) depends on a step of the domain triangulation. The preconditioner operators provide means for constructing the cost effective methods for solution of magnetostatic equations in incomplete-nonlinear formulation as well as in formulation of the Maxwell equation for the scale potential representation. These operators are easily inverible both for parallel and for traditional computing architectures. DOE

N90-20768*# Institute for Computer Applications in Science and Engineering, Hampton, VA.
CELL AVERAGING CHEBYSHEV METHODS FOR HYPERBOLIC PROBLEMS Final Report
Cai Wei, David Gottlieb, and Ami Harten (Tel-Aviv Univ., Israel) Mar. 1990 23 p Submitted for publication

(Contracts NAS1-18605; N00014-86-K-0754; AF-AFOSR-0303-85; NSF DMS-88-10150)
(NASA-CR-182028; ICASE-90-27; NAS 1.26:182028) Avail: NTIS HC A03/MF A01 CSCL 12A

A cell averaging method for the Chebyshev approximations of first order hyperbolic equations in conservation form is described. Formulas are presented for transforming between pointwise data at the collocation points and cell averaged quantities, and vice-versa. This step, trivial for the finite difference and Fourier methods, is nontrivial for the global polynomials used in spectral methods. The cell averaging methods presented are proven stable for linear scalar hyperbolic equations and present numerical simulations of shock-density wave interaction using the new cell averaging Chebyshev methods. Author

N90-20769*# National Aeronautics and Space Administration. Lewis Research Center, Cleveland, OH.
INSTITUTE FOR COMPUTATIONAL MECHANICS IN PROPULSION (ICOMP) FOURTH ANNUAL REVIEW, 1989
Mar. 1990 59 p
(NASA Order C-99066-G)
(NASA-TM-102519; ICOMP-90-01; E-5323; NAS 1.15:102519)
Avail: NTIS HC A04/MF A01 CSCL 12A

The Institute for Computational Mechanics in Propulsion (ICOMP) is operated jointly by Case Western Reserve University and the NASA Lewis Research Center. The purpose of ICOMP is to develop techniques to improve problem solving capabilities in all aspects of computational mechanics related to propulsion. The activities at ICOMP during 1989 are described. Author

N90-20770# Pittsburgh Univ., PA. Dept. of Mathematics and Statistics.
A GENERAL EXISTENCE AND UNIQUENESS THEOREM FOR IMPLICIT DIFFERENTIAL-ALGEBRAIC EQUATIONS
Patrick J. Rabier and Werner C. Rheinboldt Jan. 1990 28 p
(Contract N00014-90-J-1025; NSF CCR-89-07654)
(AD-A217965; ICMA-90-145) Avail: NTIS HC A03/MF A01 CSCL 12/1

A general existence and uniqueness theory for differential-algebraic equation extending the well known ODE theory is presented. Both local and global aspects are considered, and the definition of the index for nonlinear problems is elucidated. For the case of linear problems with constant coefficients the results are shown to provide an alternate treatment equivalent to the standard approach in terms of matrix pencils. Also, it is proved that general differential-algebraic equations carry a geometric content, in that they are locally equivalent to ODEs on a constraint manifold. A simple example from particle dynamics is given to illustrate the approach. GRA

N90-20771# Naval Research Lab., Washington, DC.
SOME REMARKS ON SOLUTIONS OF FERMATS LAST EQUATION IN TERMS OF WRIGHT'S HYPERGEOMETRIC FUNCTION Final Report
Allen R. Miller, Emanuel Vegh, and William P. Wardlaw (Naval Academy, Annapolis, MD.) 16 Feb. 1990 10 p Sponsored by Naval Air Systems Command, Washington, DC
(AD-A218066; NRL-MR-6601) Avail: NTIS HC A02/MF A01 CSCL 12/1

Solutions of Fermats last equation are expressed in terms of Wright's generalized hypergeometric function. Some of the properties of these solutions are discussed and an equivalent form of Fermats conjecture is given in terms of them. GRA

N90-20772# Naval Aerospace Medical Research Lab., Pensacola, FL.
MICRO SAINT PROGRAMS FOR NUMERICAL METHODS OF INTEGRATION AND DIFFERENTIAL EQUATIONS Interim Report, Jan. - Mar. 1989
Shawky E. Shamma, Efrain A. Molina, and Robert R. Stanny 9 Sep. 1989 42 p
(AD-A218097; NAMRL-MONOGRAPH-39) Avail: NTIS HC A03/MF A01 CSCL 12/7

The Micro SAINT computational networks was developed for numerical integration and solving initial value problems for linear and nonlinear first- and second-order ordinary differential equations, as well as for systems of differential equations. These Micro SAINT computer programs are written with a user friendly approach where the user will be required to supply the input information and the functional form(s) of the function(s) in the function library section of Micro SAINT without any changes in the main programs. These computational modules could be used as subnetworks in modeling psychophysiological and biomedical problems of interest in naval aerospace medical research. For example, Micro SAINT developed models can be used by staff medical officers to predict psychophysiological performance of naval aircrew personnel under sustained operational work schedules. GRA

N90-20773# Naval Research Lab., Washington, DC. Identification Systems Branch.
ON FREE PRODUCTS OF TORSION FREE ABELIAN GROUPS Final Report, Jul. 1988 - Jul. 1989
A. M. Gaglione 23 Feb. 1990 15 p
(AD-A218146; NRL-MR-6606) Avail: NTIS HC A03/MF A01 CSCL 12/3

Let G be a group. For x,y epsilon G the commutator of x and y is (x,y) = x to the minus 1st power y to the minus 1st power x y. The lower central series of G is a sequence of normal subgroups of G defined inductively as follows: G sub 1 = G, and having defined G sub n (for n a positive integar), G sub n+1 is defined as the group generated by all commutators of (x,y) where x epsilon Gn and y epsilon G. The lower central series is studied for a group J which is a free product of a finite number of torsion free Abelian groups. In particular, the quotient groups J sub n/Jn sub n+1 are completely determined. GRA

N90-20774# Naval Research Lab., Washington, DC.
EULER'S THEOREM FOR POLYNOMIALS Final Report, Aug. 1988 - Aug. 1989
William P. Wardlaw 9 Feb. 1990 14 p
(AD-A218148; NRL-MR-6605) Avail: NTIS HC A03/MF A01 CSCL 12/1

The similarity of the arithmetic of the integers and the arithmetic of polynomials suggests that an analog of Euler's Totient theorem for integers also holds of polynomials over a finite field. This theorem is stated and proved, and then some properties of the totient function for polynomials are derived. The related notions of the order of one polynomials modulo another relatively prime polynomial, and of the exponent of a polynomial, are investigated. Finally, examples are given which show how to apply these ideas to the factorization of polynomials over finite fields. GRA

N90-20775# Oklahoma State Univ., Stillwater.
TECHNIQUES FOR ACCELERATING ITERATIVE METHODS FOR THE SOLUTION OF MATHEMATICAL PROBLEMS Ph.D. Thesis
Steven Russell Capehart Jul. 1989 145 p Sponsored by AFIT, Wright-Patterson AFB, OH
(AD-A218272; AFIT/CI/CIA-89-108) Avail: NTIS HC A07/MF A01 CSCL 12/1

Mathematical problems can be solved numerically by deriving an iteration scheme that generates a sequence, the limit of which is the solution of the problem. However, quite often the generated sequence converges very slowly or even diverges. This study describes and compares methods designed to accelerate a slowly convergent sequence or to obtain the solution of the problem from a divergent sequence. The methods studied are Aitken's Delta-Squared method, Wynn's epsilon and modified epsilon methods, the minimal polynomial extrapolation method, the reduced rank extrapolation method, and Anderson's generalized secant algorithms. The derivation of these methods, as applied to both linear and nonlinear problems, are presented. In addition, the acceleration methods are compared theoretically and numerically. Results are presented from extensive numerical testing of problems in an m-dimensional vector space. GRA

N90-20776# North Carolina Univ., Chapel Hill. Center for Stochastic Processes.
ON THE EXISTENCE OF LOCAL TIMES: A GEOMETRIC STUDY
J. M. Anderson, Joseph Horowitz, and L. D. Pitt (Virginia Univ., Charlottesville.) Jan. 1990 63 p
(Contract F49620-85-C-0144; NSF DMS-87-01212)
(AD-A218337; TR-281; AFOSR-90-0280TR) Avail: NTIS HC A04/MF A01 CSCL 12/3

A general study is presented relating the geometry of the graphs of a real function to the existence of local times for the function. The general results obtained are applied to Gaussian processes, and it is shown that with probability the sample functions of a non-differentiable stationary Gaussian process with local times will be Jarnik functions. This extends earlier works of Lifshitz and Pitt, which gave examples of Gaussian process without local times. An example is given of a Jarnik function without local times thus answering negatively a question raised by Geman and Horowitz. GRA

N90-20777# North Carolina Univ., Chapel Hill. Center for Stochastic Processes.
HOMOGENEOUS CHAOS, P-FORMS, SCALING AND THE FEYNMAN INTEGRAL
G. W. Johnson (Nebraska Univ., Lincoln.) and G. Kallianpur Sep. 1989 72 p
(Contract F49620-85-C-0144)
(AD-A218339; TR-274; AFOSR-90-0277TR) Avail: NTIS HC A04/MF A01 CSCL 12/3

Interesting questions concerning homogeneous chaos, scaling and the Feynman integral have been brought to light in a recent largely heuristic but fascinating paper of Hu and Meyer. A way is indicated of resolving these questions as well as others which have arisen in the course of the research. GRA

65 STATISTICS AND PROBABILITY

Includes data sampling and smoothing; Monte Carlo method; and stochastic processes.

N90-20778# North Carolina Univ., Chapel Hill. Center for Stochastic Processes.
LOCAL MODULI OF CONTINUITY OF SOME CLASSES OF GAUSSIAN PROCESSES
Gennady Samorodnitsky 1989 25 p
(Contract F49620-85-C-0144)
(AD-A217692; AFOSR-90-0058TR) Avail: NTIS HC A03/MF A01 CSCL 12/3

The local behavior of sample paths of Gaussian process was studied. The purpose is to find a connection between local sample moduli of a Gaussian process at a certain point of the parameter space and metric entropy of the set generated by the process in the corresponding Hilbert space. For certain classes of Gaussian processes, the results provide a unifying approach to finding local moduli of continuity. GRA

N90-20779# North Carolina Univ., Chapel Hill. Center for Stochastic Processes.
SLEPIAN MODELS AND REGRESSION APPROXIMATIONS IN CROSSING AND EXTREME VALUE THEORY
Georg Lindgren and Igor Rychlik (Colorado State Univ., Fort Collins.) Jan. 1990 54 p
(Contract F49620-85-C-0144)
(AD-A218338; TR-282; AFOSR-90-0276TR) Avail: NTIS HC A04/MF A01 CSCL 12/3

In crossing theory for stochastic processes the distribution of quantities such as distances between level crossing, maximum height of an excursion between level crossing, amplitude and wavelength, etc., can only be written in the form of infinite dimensional integrals, which are difficult to evaluate numerically. A Slepian model is an explicit random function representation of the process after a level crossing and it consists of one regression term and one residual process. The regression approximation of a crossing variable is defined as the corresponding variable in the regression term of the Slepian model, and its distribution can be evaluated numerically as a finite-dimensional integral. The use and structure of the Slepian model with the regression method is reviewed and it is shown how they can be used to obtain good numerical approximations to various crossing variables. It gives a detailed account of the regression method for Gaussian processes with auxilliary variables chosen in a recursive way. GRA

66 SYSTEMS ANALYSIS

Includes mathematical modeling; network analysis; and operations research.

N90-20780# Air War Coll., Maxwell AFB, AL.
ASSESSING THE MORALITY OF USING THE SPACE ENVIRONMENT AS A PLATFORM FOR WEAPONS
William E. Caffall and Russell G. Stafford May 1989 74 p
(AD-A217348) Avail: NTIS HC A04/MF A01 CSCL 15/6

Remarks about President Ronald Reagan's hope of developing a system of national defense which does not rest on the reliance on nuclear weapons introduce the discussion on how U.S. citizens expect their military to conduct war. A description of the Just War Theory and the Law of Armed Conflict completes the background for the authors' views of how space weapons could significantly change U.S. employment of the Principles of War. The dramatic enhancements to the Principles of War available through space weapons apply to the full spectrum of conflict and promote the very real possibility of truly limiting war. The analysis of the Just War Theory, the Law of Armed Conflict, and the space-enhanced Principles of War resulted in the conclusion that a more moral means of warfighting does exist than reliance on weapons of mass destruction and indiscriminate killing. The space environment offers that hopeful solution. GRA

N90-20781# Air War Coll., Maxwell AFB, AL.
THE ESSENCE OF SPACEPOWER: IMPORTANT INFLUENCES ON THE EVOLUTION OF NATIONAL SPACEPOWER
Craig P. Weston May 1989 79 p
(AD-A217498) Avail: NTIS HC A05/MF A01 CSCL 15/6

The concept of spacepower is scoped, the arenas in which it must be forged are identified, and the factors that strongly influence its evolution are outlined. These insights are drawn from the history of land, sea, and air power. Broad parallels in the formation of national power in these mediums suggest that spacepower is composed of three components and will evolve in five separate but interdependent arenas. Within each of these arenas there appear to be several factors that are a key to the evolution of national power in any medium. One obvious conclusion is that a number of nations could become spacepowers. Another conclusion is that the United States must come to grips with several shortfalls if it is to remain a preeminent spacepower for the long term. The reader with limited time may wish to focus on Chapter 2, the Integration of Arenas section in Chapter 4, and Chapter 6. They comprise a more detailed executive summary. GRA

N90-20782# Air War Coll., Maxwell AFB, AL.
SPACE IN WARFARE
Julian W. Shattuck May 1989 29 p
(AD-A217527) Avail: NTIS HC A03/MF A01 CSCL 15/6

An application of the Principles of War with space as the primary focus illustrates the contributions that space can make to the battlefield of today and tommorrow. Beginning with its birth in 1947, the United States Air Force has laid claim to the realms of space. Although officially given the space charter by Secretary of Defense Robert S. McNamarra in 1960, the United States Air Force as a whole has not been an articulate and knowledgeable advocate of space systems. This lack of advocacy is caused by a lack of understanding of the role of space in modern warfare.

Once this understanding is gained, the warfighter will not only be able to use what space systems are available, but demand systems to better fulfill his needs. GRA

N90-20783# Institute for Defense Analyses, Alexandria, VA.
TOWARDS SDS (STRATEGIC DEFENSE SYSTEM) TESTING AND EVALUATION: A COLLECTION OF RELEVANT TOPICS Final Report
Bill R. Brykczynski and Christine Youngblut Jul. 1989 160 p
(Contract MDA903-89-C-0003)
(AD-A217610; AD-E501189; IDA-M-513; IDA/HQ-88-33759)
Avail: NTIS HC A08/MF A01 CSCL 15/3

A compendium of position statements received at a two day invitational workshop hosted by the Institute for Defense Analyses (IDA) in September 1988 is presented. The purpose of the workshop was to determine the critical gaps in software testing and evaluation technology and to assess current research efforts toward resolving these deficiencies. The specific focus of the workshop was technology for the testing and evaluation of the Strategic Defense System (SDS) software. The workshop was designed to bring together leading researchers in the field of software testing and evaluation and government agencies involved in major software development efforts. The participants were divided into four groups, respectively addressing the areas of testing and analysis, formal verification, measurement, and reliability assessment. GRA

N90-20784# Air War Coll., Maxwell AFB, AL.
THE THRUST AND PARRY OF THE SIOP (SINGLE INTEGRATED OPERATIONAL PLAN) AND SDI
Gary D. Zank May 1989 64 p
(AD-A217617; AD-E501190) Avail: NTIS HC A04/MF A01 CSCL 15/6

The relationship between strategic offensive capabilities (reflected in the SIOP) and emerging strategic defensive capabilities (reflected by SDI) is not being adequately addressed. A summary of the existing nuclear war planning process is provided, and an analagous defensive process is postulated. Parallels and differences between the two processes are discussed. Potential areas for information exchange and cooperation are identified to enhance deterrence and improve war fighting potential. Operational, technical and political issues requiring resolution are raised and recommendations to resolve these issues are made. GRA

N90-20785# Los Alamos National Lab., NM.
SDI (STRATEGIC DEFENSE INITIATIVE): IS ITS FUTURE PAST
Gregory H. Canavan Mar. 1990 23 p
(Contract W-7405-eng-36)
(DE90-008016; LA-11782-MS) Avail: NTIS HC A03/MF A01

This paper reviews likely threats and the ability of known defenses to address them, concluding that initial deployments should be affordable and development appears to be a prudent hedge against an uncertain future. Effective defenses would provide a positive incentive for the reduction of offensive forces and hence a direct, stabilizing influence that could shift the threat in directions in which they could be more effective and mutually useful. DOE

N90-20786# Los Alamos National Lab., NM.
ROLE OF FREE-ELECTRON LASERS IN STRATEGIC DEFENSE
Gregory H. Canavan Mar. 1990 17 p
(Contract W-7405-eng-36)
(DE90-008028; LA-11774-MS) Avail: NTIS HC A03/MF A01

Directed-energy defenses could provide the performance, growth, and cost essential for effectiveness against progressively larger and more competent threats. Because they are less sensitive to modernization rates and can grow in performance, directed-energy defenses could provide significant margin against uncertain costs and improve the effectiveness of combined defenses by factors of 2 to 3. Delays in development could cause much larger cost growths. Thus, directed-energy, generally, and free-electron lasers, specifically, are critical in bounding the threat throughout the transition. DOE

N90-20787# Naval Postgraduate School, Monterey, CA.
THREE-DIMENSIONAL ROUTE PLANNING FOR A CRUISE MISSILE FOR MINIMAL DETECTION BY OBSERVER M.S. Thesis
Lawrence R. Wrenn, II Jun. 1989 221 p
(AD-A218336) Avail: NTIS HC A10/MF A02 CSCL 16/2

An algorithm is presented for finding optimal 3-D paths above polyhedral models of terrain using a technique referred to as random-ray. Contiguous sequences of homogeneous airspace volumes are generated using constraints of probability-of-detection and aerodynamic flight models. The flight costs are calculated as in actual mission planning using time, distance, airspeed, and fuel flow. Semi-random directions (rays) from the starting point are then tried, turning in accordance with Snell's Law at maneuver points (points between volumes). If the previously specified next volume is ever not entered, random adjustments are made to the ray (in, out, up, or down) with respect to the center of the facet between the two volumes, until either the path will enter the correct next volume or it is determined that it is impossible. The performance of random-ray technique is an improvement over an earlier approach using local optimization. A moveable display was implemented on a graphics workstation, to allow the user the ability to view the terrain and paths from any angle. GRA

67 THEORETICAL MATHEMATICS

Includes topology and number theory.

N90-20788# International Centre for Theoretical Physics, Trieste (Italy).
PROJECTIVE COHOMOLOGY OVER A CHAIN COMPLEX
Abd El-Sattar A. Dabbour and T. M. Salama (Ain Shams Univ., Cairo, Egypt) Jul. 1989 8 p Submitted for publication
(DE90-606958; IC-89/206) Avail: NTIS (US Sales Only) HC A02/MF A01

Some topics of spectrums with morphisms are examined and then a cohomology construction is defined for compact Hausdorff spaces over a chain complex as the coefficient group. It is proved that this construction is delta-functor. DOE

70 PHYSICS (GENERAL)

For precision time and time interval (PTTI) see *35 Instrumentation and Photography;* for geophysics, astrophysics or solar physics see *46 Geophysics, 90 Astrophysics,* or *92 Solar Physics.*

N90-20789# California Univ., Berkeley. Lawrence Berkeley Lab. Materials and Chemical Sciences Div.
MAGNETIC PROPERTIES OF SURFACES AND INTERFACES Ph.D. Thesis
Daryl C. Chrzan Nov. 1989 200 p Prepared in cooperation with California Univ., Berkeley
(Contract DE-AC03-76SF-00098)
(DE90-007348; LBL-28170) Avail: NTIS HC A09/MF A02

A survey of the magnetic properties of three types of planar defects is presented: a model interface in an Ising antiferromagnet, a model of the surface of an antiferromagnet, and a realistic calculation of the magnetic properties of stacking defects in a bulk ferromagnet. The simplest interface studied is the antiphase boundary in the nearest-neighbor face-centered-cubic Ising antiferromagnet. The properties of this defect are understood by means of the construction and solution of an exactly solvable thermodynamic model which mimics the boundary's properties. The implications for further calculations using the nearest-neighbor face-centered-cubic Ising model are explored. The effects of introducing a free surface in a real antiferromagnetic semiconductor, EuTe, are examined. The complex magnetic structures of the (001) faces of this material, which include spin structures incommensurable with the underlying lattice, are understood in terms of a classical Heisenberg Hamiltonian. Finally, the magnetic

properties of (111) stacking faults in nickel are investigated utilizing a self consistent, layered Korringa-Kohn-Rostoker formalism based on the local-density approximation to density functional theory. Very simple expressions for the spin polarization and internal energy are developed. The range of behaviors displayed by these three systems is remarkable in its diversity, and yet the underlying mechanisms are all similar. This similarity suggests that many of the tools necessary for understanding the magnetic properties of surfaces and interfaces are readily available. DOE

N90-20790# Kansas State Univ., Manhattan. Dept. of Physics.
MAGNETIC HARDENING STUDIES AND NOVEL TECHNIQUES FOR PREPARATION OF HIGH PERFORMANCE MAGNETS Final Progress Report, 1 Jul. 1988 - 31 Aug. 1989
George C. Hadjipanayis 15 Nov. 1989 9 p
(Contract DAAL03-88-K-0092)
(AD-A217737; ARO-25047.1-MS) Avail: NTIS HC A02/MF A01 CSCL 20/3

Our research efforts have been focused on the magnetic hardening behavior of R-Fe-B magnets, the development of processing techniques for improved magnetic properties and the search for new phases with better magnetic properties. The origin of magnetic hardening was examined by correlating the microstructure, microchemistry and magnetic domain structure with the magnetic properties. This was done on powders, ribbons and sintered magnets where the effects of Co, Al and Dy were examined. High coercivities have been obtained in as-cast Nd(Pr)Fe-B alloys with impurity additions (Cu,Al,Ga,Ag) indicating the potential of these materials for hot extruded magnets. New anisotropic magnetic phases have been found in Nd-Fe-O alloys and in rare-earth carbides. Both of these systems have the potential for permanent magnet development. GRA

N90-20791# Rockwell International Science Center, Thousand Oaks, CA.
DIELECTRIC COMPOSITE THIN FILMS Final Report, 15 Jan. 1988 - 14 Sep. 1989
H. O. Sankur Nov. 1989 64 p
(Contract F49620-88-C-0034; AF Proj. 2306)
(AD-A217940; SC5537.FR; AFOSR-90-0072TR) Avail: NTIS HC A04/MF A01 CSCL 20/3

Mixed composition films are widely used in gradient index and in discrete optical coatings. This study addressed the composition dependent properties of these films with special emphasis on the effect of composition on the film microstructure and structure-property relationships. One visible, Titanium dioxide-Silicon dioxide, and two potential infrared, ZnSe-SrF2 and Si-YF3, material systems were studied. The effect of composition, deposition and post-deposition treatment conditions on film properties such as intrinsic stress, moisture penetration, refractive index, optical scatter, morphology and crystallization have been investigated. The macroscopic film properties were observed to strongly depend on composition. This is not only due to averaging of the properties of the pure constituents in the mixture but also because of unique film microstructures engendered by the composite chemical environment during film growth. In general many of the microstructure dependent properties (e.g., stress) vary nonlinearly with composition and cannot be predicted on the basis of the properties of the pure constituents. In this study the process conditions and compositions that produce films with low stress, smooth morphology, dense microstructure and low or no water content have been established in three material systems studied. GRA

N90-20792# Army Materials Technology Lab., Watertown, MA. Material Technology Lab.
BARKHAUSEN NOISE ANALYSIS AND FERROMAGNETIC MATERIALS Final Report
Douglas J. Strand Dec. 1989 48 p
(DA Proj. 1L1-62105-AH-84)
(AD-A217989; MTL-TR-89-108) Avail: NTIS HC A03/MF A01 CSCL 20/3

At its foundations (ferromagnetic domains), the Barkhausen effect has a rich theory. An introduction to this theory is first given. The Barkhausen effect is defined and a description of how it comes about is given. Barkhausen Noise Analysis (BNA) is used as a nondestructive evaluation method. Completed applications of this are cited and explained. BNA is applicable only to ferromagnetic materials, so its use has primarily focused on armor applications. The parameters which affect the method were also sought and the results given. GRA

71 ACOUSTICS

Includes sound generation, transmission and attenuation. For noise pollution see *45 Environmental Pollution.*

N90-20793 Pennsylvania State Univ., University Park.
HIGH-RESOLUTION ACOUSTICAL IMAGING Ph.D. Thesis
Kent Edward Eschenberg 1989 256 p
Avail: Univ. Microfilms Order No. DA8922048

Pressure waves, detected by an array of receivers, can be analyzed to determine the location of the acoustic source, or the location of objects which the waves encountered along their path. High resolution methods which use a linear array to locate stationary objects which have scattered the pressure waves are examined. Several methods are explored through simulations in air. A theoretical examination of all of the basic and high resolution accoustical imaging methods is first conducted. These methods include holographic reconstruction, beamforming, a correlation method, autoregressive-moving average (ARMA) spectral estimators and minimum energy methods. One of the methods which was examined used the concept of a fictious source. This concept is developed to yield an imaging approach called the pattern-match method which is similiar to the temporal signal processing technique called the matched filter. In addition, a technique for comparing signals is used to develop a variation of the pattern-match method called the mismatch method. A series of simulations is used to examine the ability of both methods to locate either one or two acoustic sources. Each simulation is also conducted using the well-known holographic method which thus serves as a point of reference. One new feature of some of these simulations is the introduction of a barrier which diffracts and reflects the pressure wave. While some imaging methods have used multiple frequencies, it was found that none exploited the fact that an object's scattering pattern can have a characteristic frequency dependence. This characteristic is used for the first time in a method called swept-frequency imaging. Dissert. Abstr.

N90-20794*# National Aeronautics and Space Administration. Lewis Research Center, Cleveland, OH.
NOISE OF A SIMULATED INSTALLED MODEL COUNTERROTATION PROPELLER AT ANGLE-OF-ATTACK AND TAKEOFF/APPROACH CONDITIONS
Richard P. Woodward 1990 25 p Presented at the 28th Aerospace Sciences Meeting, Reno, NV, 8-11 Jan. 1990; sponsored by AIAA
(NASA-TM-102440; E-5210; NAS 1.15:102440; AIAA-90-0283)
Avail: NTIS HC A03/MF A01 CSCL 20A

Two modern high-speed advanced counterrotation propellers, F7/A7 and F7/A3 were tested in the NASA Lewis Research Center's 9- by 15-Foot Anechoic Wind Tunnel at simulated takeoff/approach conditions of 0.2 Mach. Both rotors were of similar diameter on the F7/A7 propeller, while the aft diameter of the F7/A3 propeller was 85 percent of the forward propeller to reduce tip vortex-aft rotor interaction. The two propellers were designed for similar performance. The propellers were tested in both the baseline configuration and installed configuration consisting of a simulated upstream nacelle support pylon and fuselage section. Acoustic measurements were made with a polar microphone probe which recorded sideline directivities at various azimuthal locations. Aerodynamic measurements were also made to establish propeller operating conditions. The propellers were run at initial blade setting angles adjusted to achieve equal forward/aft torque ratios at angle of attack with the pylon and

fuselage simulation in place. Data are presented for propeller operation at 80 and 90 percent of design speed (the forward rotor design tip speed was 238 m/sec (780 ft/sec). Both propellers were tested at the maximum rotor-rotor spacing of 14.99 cm (5.90 in.) based on the pitch change axis separation. Author

N90-20795*# National Aeronautics and Space Administration. Langley Research Center, Hampton, VA.
EXPERIMENTAL FEASIBILITY OF INVESTIGATING ACOUSTIC WAVES IN COUETTE FLOW WITH ENTROPY AND PRESSURE GRADIENTS
Tony L. Parrott, William E. Zorumski, and John W. Rawls, Jr. (Lockheed Engineering and Sciences Co., Hampton, VA.) Feb. 1990 52 p
(NASA-TM-102621; NAS 1.15:102621) Avail: NTIS HC A04/MF A01 CSCL 20A

The feasibility is discussed for an experimental program for studying the behavior of acoustic wave propagation in the presence of strong gradients of pressure, temperature, and flow. Theory suggests that gradients effects can be experimentally observed as resonant frequency shifts and mode shape changes in a waveguide. A convenient experimental geometry for such experiments is the annular region between two co-rotating cylinders. Radial temperature gradients in a spinning annulus can be generated by differentially heating the two cylinders via electromagnetic induction. Radial pressure gradients can be controlled by varying the cylinder spin rates. Present technology appears adequate to construct an apparatus to allow independent control of temperature and pressure gradients. A complicating feature of a more advanced experiment, involving flow gradients, is the requirement for independently controlled cylinder spin rates. Also, the boundary condition at annulus terminations must be such that flow gradients are minimally disturbed. The design and construction of an advanced apparatus to include flow gradients will require additional technology development. Author

N90-20796# Mississippi Univ., University. Physical Acoustics Research Lab.
A CONTINUED STUDY OF OPTICAL SOUND GENERATION AND AMPLIFICATION Final Technical Report, 1 Jan. 1987 - 31 Dec. 1989
Henry E. Bass and F. D. Shields 31 Dec. 1989 86 p
(Contract N00014-84-C-0193)
(AD-A217640; PARGUM-89-06) Avail: NTIS HC A05/MF A01 CSCL 20/1

The general thrust of the research described report is acoustics of systems far from the equilibrium. This topic is subdivided into sound amplification and sound generation though the two are very much intertwined. In the case of sound amplification, research is focused on the propagation of sound through a gas which has internal states far from equilibrium. Sound generation as discussed, results from depositing energy in an internal state. Calculations show that some very stringent conditions must be met if sound amplification is to be experimentally observed. For the magnitude of the gain to be appreciable, the v-t relaxation time can only be about one order of magnitude longer than the sound period. A number of experimental configurations were tried to meet these conditions. The effect was observed and measured in N2/H2, N2/He, N2/H2O, and N2/CH4 mixtures. Although the basic principles governing optoacoustic generation of sound have been well established for many years, the goal here was to use this technique to study energy transfer at the molecular level. This required that all factors influencing the acoustic waveform including vaporization be accurately considered. GRA

N90-20797# Naval Ship Research and Development Center, Bethesda, MD. Propulsion and Auxiliary Systems Dept.
LOCALIZATION AND DELOCALIZATION IN PERIODIC ONE-DIMENSIONAL DYNAMIC SYSTEMS
G. Maidanik and J. Dickey Dec. 1989 32 p
(AD-A217939; DTRC-PAS-90/2) Avail: NTIS HC A03/MF A01 CSCL 20/1

The impulse response function of ribbed membrane-like panels is derived. A model of such a panel in which certain interactions among the ribs are removed is constructed. The removed interactions are those that allow a rib to identify the dispositions of the other ribs. It is argued that the impulse response function describing this model just fails, by definition, to account for the phenomena associated with pass and stop bands. The characteristics of this model are then used to explain the phenomenon of localization that occurs, at frequencies that lie within the pass bands, when the periodicity of the ribs is disturbed. Similarly, this model is used to explain the phenomenon of delocalization that occurs, at frequencies that lie within the stop bands, when the periodicity of the ribs is disturbed. The results of computer experiments that exhibit these types of localization are cited. GRA

N90-20798# Naval Postgraduate School, Monterey, CA.
THE MEASUREMENTS OF THERMOACOUSTIC PHENOMENA USING THERMOACOUSTIC COUPLES M.S. Thesis
Chia-Ning Ao Jun. 1989 68 p
(AD-A218018) Avail: NTIS HC A04/MF A01 CSCL 20/13

Thermoacoustic heat transport and its applications, such as thermoacoustic engines and refrigerators, have been discussed in a number of articles over the past several years. However, lacking from these articles is a thorough, quantitative experimental investigation of the basic theory underlying thermoacoustic heat transport. Such an investigation is the purpose of this thesis. A logical starting point for such a study is to investigate the simplest class of thermoacoustic engine - a stack of short plates referred to as a ThermoAcoustic Couple, or TAC. The utility of this choice is that the theory can be reduced to its simplest form for analysis of the results. The results of measurements of thermoacoustically generated temperature gradients in TACs subjected to acoustic standing waves are reported. The value of the temperature gradient, which results from an acoustically generated entropy flow in the gas in thermal contact with the plate, is a function of the acoustic pressure amplitude, the mean gas pressure, the Prandtl number of the gas, the configuration of the TAC, and its position in the standing wave. Measurements were made with a computer controlled apparatus for drive ratios (the ratio of the acoustic pressure amplitude to the mean pressure of the gas) from approximately 0.1 to 2 percent, in argon and helium having mean standing wave. GRA

N90-20799# Aerospace Medical Research Labs., Wright-Patterson AFB, OH. Biodynamic Environment Branch.
LATERAL ATTENUATION OF MILITARY AIRCRAFT FLIGHT NOISE Final Report, Apr. 1984 - Sep. 1988
Jerry D. Speakman Jul. 1989 63 p
(AF Proj. 7231)
(AD-A218041; AAMRL-TR-89-034) Avail: NTIS HC A04/MF A01 CSCL 20/1

The results are presented of measurements on the noise propagated to the side of military aircraft during a series of controlled level flyovers. Data were acquired on attack/fighter aircraft (A-10A, F4D, F-5E, F-15, F-16, and F-18); bomber aircraft (B-52G and FB-111); cargo/tanker aircraft (C-18, C-141, KC-10A, KC-135A, and KC-135R); and special purpose aircraft (C-21 and E-3A). In addition to the normal attenuation provided by wave divergence (spherical spreading) and atmospheric absorption, noise propagated laterally to the ground from aircraft during flight is further reduced by the combination of several other frequency dependent phenomena such as ground, meteorological, forward flight, and engine/airplane installation effects. Airbase/airport noise models typically define this extra lateral attenuation for single event measures such as the Sound Exposure Level as a function of the elevation angle as viewed from a given location on the ground. Based on the results of these data, a new algorithm was developed and incorporated in the Air Force NOISEMAP model. GRA

N90-20800# Aerospace Medical Research Labs., Wright-Patterson AFB, OH. Biodynamic Environment Branch.
AIR FORCE BOOM EVENT ANALYZER RECORDER (BEAR): SYSSTEM DESCRIPTION Final Report, Oct. 1985 - Aug. 1989

Robert A. Lee, Monty Crabill, Doug Mazurek, Barbara Palmer, Dale Price, and Doug Mazurek Aug. 1989 179 p
(AF Proj. 7231; AF Proj. 3037)
(AD-A218048; AAMRL-TR-89-035) Avail: NTIS HC A09/MF A01 CSCL 20/1

Developed, tested, built and used in field studies were several Boom Event Analyzer Recorders (BEARs). These BEAR's operate unattended to capture the wave form of Impulsive Acoustic Events (e.g., Sonic Booms) and their time of occurrance while excluding all other acoustic events. These BEARs are designed to operate unattended for up to 10 days and can store over 50 normal (less than 250 miliseconds in duration) sonic booms. These BEAR systems were used successfully to capture the sonic boom signature from all U.S. supersonic aircraft. A complete system description of the BEAR is presented covering data collection, theory of operation, data storage and retrieval, operation and complete hardware and software description. The comparison test done in cooperation with NASA and field studies using these BEARs are detailed in companion reports. GRA

72 ATOMIC AND MOLECULAR PHYSICS

Includes atomic structure, electron properties, and molecular spectra.

N90-20801# United Kingdom Atomic Energy Authority, Harwell (England). Materials Physics and Metallurgy Div.
ENERGY TRANSFER BETWEEN ELECTRONS AND IONS IN COLLISION CASCADES IN SOLIDS
A. M. Stoneham Oct. 1989 24 p
(AERE-R-13662) Avail: NTIS HC A03/MF A01

An overview of the mechanisms, rates, and, characteristics of the several processes by which electronic and ionic energy exchange can occur is presented. This energy exchange raises questions about widely-accepted assumptions, and the circumstances in which those assumptions must be questioned. The situations where the problems are most easily seen concern low energies, and especially topics like whether there is a threshold associated with a bandgap or situations where structural or chemical features can be affected by the energy transfer. Yet there are other cases in which ion/electron energy transfer could be important, such as in the highly-excited centre of a cascade. In such situations, the observable consequences may be harder to relate to the energy exchange. The issue is therefore one of the final state achieved (and hence affected by annealling of defects and various thermal processes) as opposed to the higher-energy phenomena themselves. The role of the electronic system in metals is discussed as an energy sink and a means of energy transport, drawing analogies with the better-understood insulators. There are strong hints of electronic effects in collision cascades but their status is still not clear. Author

N90-20802# Vanderbilt Univ., Nashville, TN. Dept. of Physics and Astronomy.
THEORETICAL INVESTIGATIONS IN ELEMENTARY PARTICLE PHYSICS Progress Report, 1 Jun. 1989 - 31 May 1990
Thomas J. Weiler and Thomas W. Kephart Jan. 1990 8 p
(Contract DE-FG05-85ER-40226)
(DE90-007178; DOE/ER-40226/5) Avail: NTIS HC A02/MF A01

Progress is reported on the following topics: Isoflipped SU(5) models; Critical temperature and primordial neutrino abundancies; Production and decay of minimal SUSY Higgses at LEP and beyond; Neutrino magnetic moment in N = 1 minimal supergravity; and Theory of matter in Weyl spacetime. DOE

N90-20803# Max-Planck-Inst. fuer Kernphysik, Heidelberg (Germany, F.R.).
[ACTIVITIES REPORT IN NUCLEAR PHYSICS] Annual Report, 1988 [JAHRESBERICHT 1988]
H. V. Klapdor, ed. and E. K. Jessberger, ed. 1988 200 p Partly in ENGLISH and GERMAN Original contains color illustrations
(ETN-90-95322) Avail: NTIS HC A09/MF A02

In the field of nuclear physics, accelerators and ion sources, detectors, the study of solids and microstructures by nuclear methods, giant resonances and continuum excitations, nuclear spectroscopy items, mechanisms of nuclear reactions, the interaction of charged particles with matter, medium and high energy physics items, a statistical model of nuclei, reactions and solids, and theoretical items of hadron physics, deep-inelastic scattering, collective motion and nuclear beta and double beta decay were investigated. In the field of cosmophysics, meteorites and lunar rocks, the gallium-solar-neutrino experiment, comets, the project PHOBOS, interplanetary and interstellar dust, planetary atmospheres, interstellar medium and cosmic rays, molecular collision processes, in the gas phase, technological developments, and items in nuclear geology and chemistry and archeometry were investigated. ESA

N90-20804# Max-Planck-Inst. fuer Stroemungsforschung, Goettingen (Germany, F.R.).
REACTIVE AND ANISOTROPIC ELASTIC SCATTERING OF HIGHLY LASER-VIBRATION-EXCITED DIATOMIC MOLECULES Thesis [REAKTIVE UND ANISOTROPE ELASTISCHE STREUUNG HOCH LASER-SCHWINGUNGSANGEREGTER ZWEIATOMIGER MOLEKUELE]
H.-G. Rubahn Nov. 1988 261 p In GERMAN Sponsored by Deutsche Forschungsgemeinschaft
(MPIS-19/1988; ISSN-0436-1199; ETN-90-95331) Avail: NTIS HC A12/MF A02

The effect of vibration excitation on the simple (reactive) anisotropic atom-molecule interaction systems under single collision conditions was investigated. The laser molecular beam apparatus allows a particle detection which is rotation and vibration selective and orientation dependent. The anisotropic, vibration dependent total integral cross sections of the systems Li2-He and Li2-Kr were determined. The measurements on the reactive system Li2-Na show a strong dependence of the cross section on the vibrational state. For a suitable choice of the parameters, in many cases general laws can be found for the alkali molecules and the alkali-molecule-atom systems, especially for extreme vibrational excitation. ESA

N90-20805# Georgia Inst. of Tech., Atlanta. School of Physics.
TERMOLECULAR ASSOCIATIONS OF IONS IN GASES, RECOMBINATION AND ELECTRON-ATOM COLLISIONS Final Report, 1 Jul. 1984 - 30 Jul. 1989
M. R. Flannery 30 Sep. 1989 174 p
(Grant AF-AFOSR-0233-84; AF Proj. 2301)
(AD-A217678; GIT-85-019; AFOSR-90-0121TR) Avail: NTIS HC A08/MF A01 CSCL 20/5

A list of publications of the research performed during the period 7/1/84 to 7/30/89 is provided. Theoretical research was conducted on: (1) Termolecular Association and Recombination, (2) electron- (excited) atom collisions, and on (3) analytical solutions of the Time-Dependent Debye-Smoluchowske equation for transport influenced reactions. The exact Master Equation Method, a Variational Principle discovered during the course of this research, and various approximate treatments are presented in Special Highlights of this research. In addition, the Appendixes include a major review of Recombination Process in General. GRA

N90-20806# Brown Univ., Providence, RI.
INTERACTIONS OF MOLECULES WITH SURFACES Progress Report, 1 Feb. 1989 - 1 Jan. 1990
E. F. Greene Jan. 1990 6 p
(Contract DE-FG02-85ER-13441)
(DE90-007555; DOE/ER-13441/6) Avail: NTIS HC A02/MF A01

This is a report of the progress made on four projects supported by DOE Grant FG02-85ER13441 in the period 1 February 1989 to 31 December 1989. A long term study of the rate of transfer of electrons between gas atoms and the surfaces of crystals,

using the technique of surface ionization, reached a point where it could be submitted for publication. Measurement of the energy dependence of the yields of Na(=), K(+), and Cs(+) ions formed when beams of the corresponding alkali atoms M hit a Si(111) surface and of Na(+) for Na striking a Pt surface at a temperature T are those expected for equilibrium for thermal kinetic energies of the incident atoms. Energy transfer to surfaces has been studied by measuring the temperature rises of thermocouple surfaces exposed to molecular beams. He diffraction has been used to follow structural phase transitions on the (111) and (100) surfaces of Si and Ge. Work is in progress to measure the effect of adsorbed atoms on the forces parallel to the surface of a crystal as they are revealed by changes in the curvature of the surface. The first experiments are being done with alkali atoms adsorbed on a Si(111) surface. DOE

N90-20807# Brookhaven National Lab., Upton, NY.
SURFACE-PLASMON ENHANCED NONLINEAR PHOTOELECTRIC EMISSION FROM THIN SILVER FILMS
T. Tsang, T. Srinivasan-Rao, and J. Fischer Dec. 1989 8 p Presented at the Conference on Lasers and Electro-Optics, Anaheim, CA, 21-25 May 1990
(Contract DE-AC02-76CH-00016)
(DE90-007676; BNL-43791; CONF-900530-7) Avail: NTIS HC A02/MF A01

We report a 10(4) enhancement and quantum yield of 1.7 times 10(minus 8) obtained from a 2--photon photoelectric emission of a thin silver film using surface plasmon excitation, which are resonantly pumped by femtosecond laser pulses in an attenuated-total-internal reflection configuration. DOE

N90-20808# Lawrence Livermore National Lab., CA.
PRECOMPOUND DECAY MODELS FOR MEDIUM ENERGY NUCLEAR REACTIONS
M. Blann Nov. 1989 20 p Presented at the Winter Meeting of the American Nuclear Society, San Francisco, CA, 26-30 Nov. 1989
(Contract W-7405-eng-48)
(DE90-008352; UCRL-101262; CONF-891103-67) Avail: NTIS HC A03/MF A01

The formulations used for precompound decay models are presented and explained in terms of the physics of the intranuclear cascade model. Several features of spectra of medium energy (10 to 1000 MeV) reactions are summarized. Results of precompound plus evaporation calculations from the code ALICE are compared with a wide body of proton, alpha, and heavy ion induced reaction data to illustrate both the power and deficiencies of predicting yield of these reactions in the medium energy regime. DOE

N90-20809# Los Alamos National Lab., NM.
PRESENT STATUS OF (mu)CF THEORY
Melvin Leon 1989 23 p Presented at the Symposium on Muon Catalyzed Fusion Phenomena, Tokyo, Japan, 2-4 Nov. 1989
(Contract W-7405-eng-36)
(DE90-007547; LA-UR-90-370; CONF-8911172-1) Avail: NTIS HC A03/MF A01

Most of these steps of the catalysis cycle for a dt target are very fast and therefore do not contribute significantly to the cycling time. Energy loss of the free muon is due to electron ejection from target hydrogen molecules, as is most of the deexcitation of the newly-formed muonic atom. This can be either t(mu) or d(mu); if the latter, the muon can transfer to a t during the deexcitation cascade, since the greater reduced mass means stronger binding for the same n. The mu(-) then is in either the d(mu) or t(mu) ground state; the waiting time in these states dominate the cycling time. Ground-state transfer from d(mu) to t(mu) is comparatively slow, as is the next step, resonant molecular formation. Once the dt(mu) mesomolecule is formed (in the loosely-bound J = 1, (nu) = 1 state), deexcitation to J = 0 via an Auger process and subsequent fusion are very rapid. Because of the large recoil velocity of the alpha liberated in the fusion reaction d + t yields n + alpha, the mu(-) is usually freed to go around the cycle again. These steps are discussed in detail. DOE

N90-20810# Oak Ridge National Lab., TN. Health and Safety Research Div.
STOPPING POWER FOR PROTONS IN Al FOR THE WHOLE RANGE OF VELOCITIES
F. Flores, A. Arnau, P. M. Echenique (Universidad del Pais Vasco, San Sebastian, Spain), and R. H. Ritchie 1989 15 p Presented at the 12th Werner Brandt International Workshop on Charged Particle Penetration Phenomena, San Sebastian, Spain, 4-7 Sep. 1989
(Contract DE-AC05-84OR-21400)
(DE90-008558; CONF-8909210-9) Avail: NTIS HC A03/MF A01

The electronic stopping power of aluminum metal for protons was calculated with explicit inclusions of the different proton charge states inside the medium. The total stopping power is obtained by adding to the calculated stopping power of each charge state, the energy loss associated with the electronic exchange processes. Good agreement is obtained between the first principles calculation and the available experimental data. DOE

N90-20811# California Univ., Berkeley. Lawrence Berkeley Lab. Materials and Molecular Research Div.
POLYATOMIC REACTION DYNAMICS Ph.D. Thesis
Beverly Ann Ruf Nov. 1989 145 p
(Contract DE-AC03-76SF-00098)
(DE90-008668; LBL-28104) Avail: NTIS HC A08/MF A01

Five theoretical methods are presented which describe chemical reactions such as hydrogen transfer in polyatomic systems, where it is necessary to describe how energy is transferred between vibrational modes. These methods combine a minimal amount of ab-initio computation with other theoretical tools. The first technique is accurately describing two important degrees of freedom by generating a 2-dimensional potential surface that is a function of these coordinates and coupling the latter to vibrational modes. The second technique is the formation of a simple cartesian Hamiltonian without any kinetic coupling. Another method for generating an expression without kinetic coupling is presented. This third method rigorously transforms the kinetic energy coupling terms of the linear reference Hamiltonian into potential energy coupling terms. As an alternative to using only ab initio data as input into the potential, a fourth method is described which uses empirical information as well as ab initio data. Finally, the last approach presented uses Monte Carlo path integral techniques with density matrices to abstract tunneling splittings of a hydrogen transfer process. DOE

N90-20812# Chemical Dynamics Corp., Upper Marlboro, MD.
DYNAMICS OF ELECTRONICALLY EXCITED SPECIES IN GASEOUS AND CONDENSED PHASE Final Report, Jul. 1986 - Jul. 1989
P. K. Swaminathan, M. J. Redmon, C. S. Murthy, B. C. Garrett, and G. A. Natanson Dec. 1989 158 p
(Contract F04611-86-C-0068)
(AD-A217696; CD-TR-89-003; AL-TR-89-051) Avail: NTIS HC A08/MF A01 CSCL 07/4

In order to assess the potential of energetic molecules to be advanced rocket propellants, the Air Force High Energy Density Materials Program requires theoretical methods to predict the lifetimes of energetic molecules in condensed phase. This research met this need by developing dynamical methods which can be used to elucidate the microscopic dynamics controlling lifetimes relevant to energy storage in isolated and matrix-embedded molecules. This has resulted in the capability to identify important quenching pathways in gas and condensed phases using computational methods. Research consisted of: (1) developing semiclassical methods and computer simulation technology, and (2) applications to thedynamics of electronically inelastic chemistry of light metastables, including helium and hydrogen in the gas and condensed phase. The key accomplishments include: (1)

development and validation of general and powerful semiclassical methods for energetic polyatomic species, (2) development of reduced heatbath models of condensed phase helium, (3) development of models of condensed phase hydrogen, and (4) development of simulation procedures for solution-phase reaction and cluster formation of high energy density materials (HEDMs) with solvents. GRA

N90-20813# State Univ. of New York at Buffalo, Amherst. Dept. of Chemistry.
MOLECULAR DYNAMICS AND SPECTROSCOPY AT GAS-SOLID INTERFACES Final Report No. 114, 1 Oct. 1985 - 30 Nov. 1989
Thomas F. George Jan. 1990 12 p
(Contract F49620-86-C-0009)
(AD-A217743; AFOSR-90-0120TR) Avail: NTIS HC A03/MF A01 CSCL 07/4

Progress was made in the development of theories and computational programs for the following topics: infrared-laser-excited adspecies, including energy and phase relaxation, and desorption; ultraviolet-laser-induced chemical vapor deposition; resonance fluorescence at flat surfaces; photochemistry at structured surfaces, including gratings and thin films; phase-conjugated surfaces; spectroscopy in solid matrices; and nonlinear optical process in polymeric systems. GRA

N90-20814# SRI International Corp., Menlo Park, CA.
ELECTRONICALLY METASTABLE MOLECULES OF HIGH SYMMETRY Interim Report, 1 Nov. 1986 - 1 Nov. 1989
Hanspeter Helm 1 Jan. 1990 72 p
(Contract F49620-87-K-0002; SRI Proj. 2915)
(AD-A217768; SRI-MP-90-001; AFOSR-90-0003TR) Avail: NTIS HC A04/MF A01 CSCL 07/4

In this research, we studied of the metastable electronic states of small molecules such as tritium. Our goal was to obtain precise information on the origin of metastability in molecular systems of high symmetry and on structural, spectroscopic, and dynamic properties of such species. The research was performed in two experimental setups, both using fast neutral molecular beams that we form by charge transfer of an electron from a suitable donar gas to a mass selected ion. In one set of experiments we illuminate the neutral species by using laser light and detect the appearance of photoions so that we can study photoionization events. In the other we photodissociate the molecule and detect the neutral photofragments by using a position- and time-sensitive detector. This study focused on photodissociation and photoionization processes of triatomic hydrogen. A detailed account of the results obtained on triatomic hydrogen is given below. We also obtained new experimental data on the metastable species of Diatomic hydrogen, Diatomic Helium, Hydronium, and D3O. GRA

N90-20815# Johns Hopkins Univ., Baltimore, MD. Dept. of Chemistry.
THEORETICAL STUDIES OF SPIN-FORBIDDEN PROCESSES WITHIN THE BREIT-PAULI APPROXIMATION Final Report, 1 Jul. 1986 - 31 Oct. 1989
David R. Yarkony 10 Jan. 1990 27 p
(Grant AF-AFOSR-0110-86; AF Proj. 2303)
(AD-A217778; AFOSR-90-0081TR) Avail: NTIS HC A03/MF A01 CSCL 20/5

This program considered the electronic structure aspects of radiative and radiationless decay processes related to the stability and formation of high energy density materials. To accomplish this goal a unique system of electronic structure algorithms, the BROOKLYN programs, was developed. These programs provide advanced capabilities for the study of the electronic structure aspects of spin-forbidden and electronically nonadiabatic processes. The methodology is based exclusively on large scale configuration state function expansions (100000 to 1000000 terms). These methods permit significant contributions to the understanding of radiative and radiationless decay processes. Problems of particular relevance to the high energy density materials program include: (1) a study of the possible stability of the energetic maximum ionicity state (HeH)+ to H-; (2) a study of the spin-forbidden decay mechanism of the model azide system N3H(1A') yields N2(1 Sigma (+) sub g) + NH(X 3Sigma(-)) and finally a study of the decay pathways for the metastable excited state of the helium atom, He(23S), resulting from collisions with other (ground state) helium atoms. Finally a new phase of program development has been initiated focusing on the efficient determination of regions of allowed and avoided crossings of potential energy surfaces using analytic gradient techniques. This program development will provide powerful new tools for the study of spin-forbidden and electronically nonadiabatic processes. GRA

N90-20816# Colorado State Univ., Fort Collins. Dept. of Radiology and Radiation Biology.
DETERMINATIONS OF PHOTON SPECTRA M.S. Thesis
David L. Wannigman 1989 60 p Sponsored by AFIT, Wright-Patterson AFB, OH
(AD-A218003; AFIT/CI/CIA-89-152) Avail: NTIS HC A04/MF A01 CSCL 20/5

A method is developed to unfold photon spectra from measurements obtained with a sodium iodide counting system. A response matrix is computed by combining photon cross sections with probability distributions of path lengths for incident and internally generated photons in the energy range 0 to 2.8 MeV. This matrix is inverted and multiplied by a measured pulse height spectrum to obtain the photon energy distribution incident upon the detector. This deconvolution procedure provides improved information about the energy continuum of incident photons and can enhance the identification of discrete gamma energies. Experiments were performed to verify the unfolding methodology and to evaluate the feasibility and accuracy of this technique. Measured spectra were acquired from indoor and outdoor environments and unfolded. The results show that measured spectra overestimate the number of photons below 240 keV by up to 30 percent. When the total exposure was calculated directly from the measured spectra, the low energy contribution was overestimated by a factor of two. This may have implications on the interpretation and calibration of energy dependent dosimeters used for occupational and environmental monitoring. GRA

N90-20817# Naval Research Lab., Washington, DC. Beam Physics Branch.
PRODUCTION RATES FOR ELECTRON BEAMS AND SWARMS IN NITROGEN
S. P. Slinker, A. W. Ali, and R. D. Taylor (Berkeley Research Association, Springfield, VA.) 24 Feb. 1990 24 p
(AD-A218145; NRL-MR-6610) Avail: NTIS HC A03/MF A01 CSCL 20/5

Detailed calculations of the deposition of electron energy in molecular nitrogen are presented. Two cases are considered. In the first one, the electrons are accelerated by a constant, uniform electric field as in a swarm experiment. The reduced electric field strength ranges from 1 to 300 Townsends. In the second case, deposition is initiated by electron beams with energies up to 10 MeV. Production rates for the various excitation channels are given. GRA

N90-20818# Air Force Inst. of Tech., Wright-Patterson AFB, OH.
LARGE-ANGLE ELASTIC AND INELASTIC SCATTERING OF PI+ AND PI- FROM SI28 AND Ca40 M.S. Thesis - Texas Univ., Austin
Michael Paul Snell May 1989 200 p
(AD-A218163; AFIT/CI/CIA-89-083) Avail: NTIS HC A09/MF A02 CSCL 20/8

Differential cross sections were measured for Pi(+) and Pi(-) elastic scattering of Calcium 40 and Silicon 28 at incident pion energies ranging from 100 to 260 MeV at a scattering angle of 175 degs. Differential cross sections were also measured for Pi(+) and Pi(-) inelastic scattering to the 2(+), 1.78 MeV, 4(+), 4.62 MeV, and 3(-) 6.88 MeV states of 28Si at incident pion energies of 130, 180, and 226 MeV and scattering angles between 115

degs. and 175 degs. in 6 degs. increments. The data are compared to previously obtained forward angle data thrcugh 120 degs. and agree quite well. The data show a generally flat angular dependence for angles greater than 100 degs. Several theoretical codes are reviewed for their ability to predict large angle scattering. Coordinate-space and momentum-space models generally thought to be sufficient for predicting forward angle scattering have proved to be inappropriate for use at large angles. A new phenomenological delta-hole model, currently under modification, shows a greatly enhanced ability to predict scattering at back angles. GRA

73 NUCLEAR AND HIGH-ENERGY PHYSICS

Includes elementary and nuclear particles; and reactor theory.

For space radiation see *93 Space Radiation.*

N90-20819# Oak Ridge National Lab., TN.
POPULATIONS OF EXCITED STATES AND REACTION MECHANISMS IN THE EMISSION OF COMPLEX FRAGMENTS
J. GomezdelCampo 1990 14 p Presented at the 13th Symposium on Nuclear Physics, Oaxtepec, Mexico, 3-6 Jan. 1990
(Contract DE-AC05-84OR-21400)
(DE90-007481; CONF-900147-2) Avail: NTIS HC A03/MF A01

Cross sections for emission of complex fragments (Z greater than 2) in their ground and excited states are presented for several heavy-ion reactions at bombarding energies above 10 MeV/nucleon. Data presented are mostly on the cross sections extracted by (gamma)-ray techniques. It is shown that a simple statistical approach to associate the ratio, of cross sections for excited states and ground states, to the temperature of the emitter fails to give the expected temperatures. However, it is shown that this is mostly due to the fact that the fragments that (gamma) decay are secondary fragments, produced by the particle decay of the primary emitted complex fragments. A Hauser-Feshbach analysis accounts well for the cross sections and extracted temperatures. DOE

N90-20820# University of Northern Illinois, De Kalb.
STUDIES OF HIGH ENERGY PHENOMENA USING MUONS
Progress Report
David Hedin, Daniel Kaplan, and James Green 1990 11 p
(Contract DE-AC02-87ER-40368)
(DE90-008272; DOE/ER-40368/3) Avail: NTIS HC A03/MF A01

The group has two primary efforts. The first is the D0 experiment at the Fermilab proton antiproton collider, with major emphasis on its muon system. The second is the involvement of a precision study of the A-dependence of massive muon pion production and a study of low multiplicity decay modes of charm. The design of detectors for the SSC is briefly examined. Finally, a minor effort is being given to analyzing data from Fermilab of particles with lifetime between 10(exp -12) and 10(exp -13) seconds. A more detailed description of the work of the NIU high energy physics group can be found in the narrative accompanying our grant renewal proposal. DOE

N90-20821# Cornell Univ., Ithaca, NY. Lab. of Plasma Studies.
COLLECTIVE ION ACCELERATION IN HIGH CURRENT RELATIVISTIC ELECTRON BEAMS
John A. Nation 1990 24 p
(Contract DE-AC02-80ER-10569)
(DE90-008328; DOE/ER-10569/T5) Avail: NTIS HC A03/MF A01

The use of high power relativistic electron beams for electron and ion acceleration was investigated. A summary is given of results from the relativistic klystron experiment and details our plans for a large diameter coaxial system. The efforts to generate upper hybrid waves on relativistic electron beams are summarized. Simulation work of the upper hybrid excitation process is reported. The experiment using high power microwaves for electron acceleration is discussed. Progress is reported on development of repetitive pulsed experimental and data acquisition systems. The future research plans are outlined, followed by a list of publications and presentations from the present work. DOE

N90-20822# Lawrence Livermore National Lab., CA.
POWER THRESHOLD FOR NEUTRAL BEAM CURRENT DRIVE
P. A. Politzer (General Atomics Technologies Corp., San Diego, CA.) and G. D. Porter 2 Oct. 1989 14 p
(Contracts W-7405-eng-48; DE-AC03-89ER-51114)
(DE90-008348; UCRL-21233) Avail: NTIS HC A03/MF A01

For fully noninductive current drive in tokamaks using neutral beams, there is a power and density threshold condition, setting a minimum value for P(sup 3/2)/n(sup 2). If this condition is not met, stationary state cannot occur, and a tokamak discharge will collapse. This is a consequence of the coupling between current and electron temperature, or between current drive efficiency and energy confinement time. DOE

N90-20823# Lawrence Livermore National Lab., CA.
THE n-p BREMSSTRAHLUNG IN HEAVY ION COLLISION PROCESSES
M. Blann 16 Jan. 1990 8 p Presented at the Los Alamos National Laboratory (LANL) Workshop on n-p Bremsstrahlung, Los Alamos, NM, 25-26 Jan. 1990
(Contract W-7405-eng-48)
(DE90-008542; UCRL-102806; CONF-900179-1) Avail: NTIS HC A02/MF A01

The goal is to summarize the current status of the interpretation of energetic gamma-rays in heavy ion collisions via the n-p-bremsstrahlung mechanism. An essential element of the topic is a transport equation to approximate the fast non-equilibrium nucleon-nucleon cascade/emission stage of the heavy ion reactions. It is during this stage that it was expected that the n-p-bremsstrahlung processes produced energetic photons. The Boltzmann master equation (BME) model which will be used as the transport code is briefly described, deferring to earlier works for a more complete description, and present but a single representative comparison with an experimental neutron emission spectrum. The status of the elementary n-p-gamma cross section needed to extend the transport code to photon emission in heavy ion reactions, and the status of these comparisons with data are summarized. DOE

N90-20824# New Mexico State Univ., Las Cruces. Arts and Sciences Research Center.
A NEW TECHNIQUE FOR GUIDING OF ELECTRON BEAMS
Final Report, 1 Oct. 1986 - 1 Mar. 1990
Leon J. Radziemski 1 Mar. 1990 29 p
(Contract DE-AC03-86SF-16496)
(DE90-008660; DOE/SF-16496/T1) Avail: NTIS HC A03/MF A01

The contract objective was to demonstrate the possibility of guiding of an electron beam through a low pressure excited working gas other than benzene. This experimental and modeling study resulted in the following conclusions: (1) Guiding of a 10 kA electron beam through krypton with a 2 + 1 ionization process excited by ArF is feasible with ArF energies of less than 10 J; (2) Guiding through a gas which requires a 2 (or more) photon excitation process will not provide significant savings in laser energy. This is independent of whether or not the excited state is a Rydberg state; (3) The ideal medium for propagation from an energetics point of view would be a working gas which could be excited to a state near the ionization energy by a single photon; (4) Guiding through gases with non-resonant ionization of a working gas (e.g., xenon by KrF) will be feasible at KrF irradiances on the order of 10(exp 10) W/cm(exp 2); (5) There is a three photon resonance in atomic argon which could be useful for exciting and photoionizing that species. The maximum excitation cross section has been calculated for the first time; (6) Guiding with Rydberg states remains experimentally untested; and (7) The IPROP code was modified to include collisional and field ionization effects, the first time such

a modification has been incorporated into a sophisticated electron beam propagation model. DOE

74 OPTICS

Includes light phenomena; and optical devices.
For lasers see *36 Lasers and Masers.*

N90-20825# Technische Univ., Munich (Germany, F.R.). Lehrstuhl fuer Technische Elektronik.
INVESTIGATION OF THE TECHNOLOGICAL EFFECTS ON THE COUPLING BEHAVIOR OF PARALLEL GaAlAs RIB WAVEGUIDE Final Report [UNTERSUCHUNG DER TECHNOLOGISCHEN EINFLUESSE AUF DAS KOPPELVERHALTEN PARALLELER GAALAS-RIPPENWELLENLEITER]
R. Rodemeier, R. Bauer, H.-W. Geiger, H. Rauch, and P. Unger (Technische Hochschule, Aachen, Germany, F.R.) 1988 119 p In GERMAN
(Contract DFG-Mu-247/72)
(ETN-90-95323) Avail: NTIS HC A06/MF A01

The realizability of optical directional couplets with modulation capability in the GaAlAs material system is examined. In agreement with theory, the experiments show that, depending on the technological structural parameters, coupling length of 3 mm with a 5 microns technology up to 0.8 mm with a 2 microns technology can be manufacturated using molecular beam epitaxy layer waveguides with lateral dimensions below 0.5 microns and etching depths larger than 2 microns can be structured using a combined splutter and/or reactive dry etching process. The absolute accuracy of the etching depth is critical for the production of directional couplers. The lowest optical damping measured is 0.25 dB per coupler, corresponding to a specific damping of 3 dB/cm. ESA

N90-20826# North Carolina Univ., Chapel Hill. Dept. of Chemistry.
OBSERVATION OF NONLINEAR REFLECTIVITY FROM InSb SURFACE AND OPTICAL SWITCHING APPLICATION Interim Technical Report No. 27
S. Feng, R. E. Thomas, R. C. Jarnagin, and E. A. Irene 18 Jan. 1990 13 p Presented at the SPIE, Celase '90 Conference, Los Angeles, CA, 14-19 Jan. 1990
(Contract N00014-89-J-1178)
(AD-A217184) Avail: NTIS HC A03/MF A01 CSCL 20/12

We report the observation of external switching of the reflectivity from the InSb surface by a plasma enhanced absorption mechanism. A HeNe laser and a pulsed CO2 laser were used as probe beam and switching beam respectively. We also reported reflective'y switching initiated as a result of a thermal effect in the InSb surface. GRA

N90-20827# North Carolina Univ., Chapel Hill. Dept. of Chemistry.
AN ELLIPSOMETRIC MEASUREMENT OF OPTICAL PROPERTIES FOR InP SURFACES Interim Technical Report, No. 28
X. Liu, E. A. Irene, S. Hattangady, and G. Fountain (Research Triangle Inst., Research Triangle Park, NC.) 18 Jan. 1990 24 p Submitted for publication
(Contract N00014-89-J-1178)
(AD-A217185) Avail: NTIS HC A03/MF A01 CSCL 20/12

Several chemical cleaning procedures for Indium Phosphide surfaces have been studied using ellipsometry. The strong influence of cleaning on the optical properties of InP surfaces suggests that the measurements involve the formation of surface films. In order to determine the complex index of reflection for InP, a novel method which employs ellipsometry measurements of a thin non-absorbing film on a substrate rather than measurements of a bare surface has been explored. From the knowledge of the refractive index for a series of thicknesses of films on a substrate, the complex refractive index value for the substrate can be determined. Plasma Enhanced Chemical Vapor Deposition (PECVD) Silicon dioxide and Silicon nitride films on InP have been used for this experiment, and the complex refractive index for InP has been determined to be 3.521+i0.300 at the wavelength of 632.8 nm. GRA

N90-20828# Massachusetts Inst. of Tech., Lexington. Lincoln Lab.
A SPACE-BASED OPTICAL COMMUNICATION SYSTEM UTILIZING FIBER OPTICS
Eric A. Swanson and Roy S. Bondurant 9 Nov. 1989 41 p
(Contract F19628-90-C-0002)
(AD-A217333; TR-865; ESD-TR-89-185) Avail: NTIS HC A03/MF A01 CSCL 20/6

The use of fiber optics to simplify the design of free-space laser communication systems is explored. The potential advantages of fiber optics within free-space optical communication systems are not widely recognized. The current generation of spaceborne optical communication systems relies on the use of bulk optics rigidly mounted to an optical bench to get light from the optical sources to the exit aperture or from the entrance aperture to the optical receiver. These designs are all very sensitive to thermal and mechanical perturbations as well as to the detailed dynamic characteristics of the host spacecraft. Optical fibers can provide the means to remotely locate the transmitter lasers, local oscillator (LO) lasers (in the case of a coherent system), and the receiver from the front-end optics. This allows flexibility in the mechanical design which can reduce the size, weight, and stability requirements of the overall system. This paper presents an overview of a fiber-based free-space lasercom system and contrasts this proposed technology to the present technology. Detailed design considerations concerning the issues of pointing, tracking, and receiver communication performance are presented. Other key areas such as efficient source-to-fiber coupling, isolation, transmitter power limitations, and acquisition are highlighted. Preliminary experimental results of our breadboard fiber-based coherent optical communication system are also presented. GRA

N90-20829# Arizona Univ., Tucson. Optical Sciences Center.
NONLINEAR OPTICS IN THIN FILMS Final Report, 15 Jul. 1987 - 15 Jan. 1988
G. I. Stegeman and C. T. Seaton Nov. 1989 17 p
(Contract F29601-87-C-0052; AF Proj. 2301)
(AD-A217336; WL-TR-89-47) Avail: NTIS HC A02/MF A01 CSCL 20/6

Two nonlinear phenomena with the potential for locking together two waveguides/lasers have been examined theoretically. Phase conjugation of a plane-wave incident field onto a waveguide supporting two guided pump beams is a potentially useful phenomenon. This process can be very power efficient because of the strong spatial confinement of the pump beams. Multi-reflection effects within the guiding film lead to oscillations in the signal with increasing waveguide thickness and incidence angle. Coupling between two waveguides can be achieved by the exchange of spatial solitons when a self-focusing medium is used between two parallel waveguides. Model calculations based on the powerful Beam Propagation Method have indicated transfer efficiencies as large as 80 percent. GRA

N90-20830# State Univ. of New York, Buffalo. Dept. of Electrical and Computer Engineering.
VELOCITY MATCHED OPTICAL TRANSMITTER Final Technical Report, Jan. - Dec. 1988
Pao Lo Liu Nov. 1989 88 p
(Contract F30602-81-C-0193; AF Proj. 2863)
(AD-A217413; RADC-TR-89-251) Avail: NTIS HC A05/MF A01 CSCL 20/6

The development is described of a 50 GHz optical modulator. The H-guide configuration of the lithium niobate based modulator, along with the desire to reduce the modulation voltage, necessitated substrate dimensions of 1 cm x 120 micron x 25 micron. These dimensions were not obtainable. Polishing even below 25 micron to reduce the modulation voltage proved unsuccessful. Obtaining

the 120 micron dimension after obtaining the 25 micron dimension was also not obtainable. A new material for the structure is required which does not need mechanical processing to obtain the desired dimensions. This is the indicated path to pursue for obtaining a velocity matched modulator. Additionally, data is presented on V-shaped microcracks observed in titanium diffused lithium niobate presumed due to the heavy titanium indiffusion. Microcrack production leads to increased scattering and premature electrical breakdown. Material is also presented on a computer aided design tool for optical waveguide devices. GRA

N90-20831# Texas A&M Univ., College Station. Dept. of Physics.
EXPERIMENTAL AND THEORETICAL STUDIES OF LIGHT SCATTERING BY SMALL PARTICLES Final Report, 15 Sep. 1986 - 14 Nov. 1989
Edward S. Fry, George W. Kattawar, and Chia-Ren Hu 1 Dec. 1989 15 p
(Contract DAAL03-86-K-0168)
(AD-A217432; ARO-23909.4-GS) Avail: NTIS HC A03/MF A01 CSCL 20/6

The following studies were made: (1) Scattering of ultrashort laser pulses by microscopic particles both experimentally and theoretically; (2) Plane wave scattering by small clusters of spheres in various configurations; (3) Symmetries of Mueller matrices for forward (0 deg) and backward (180 deg) scattering by dielectric particles of various shapes; and (4) Optical scattering at zero degrees, and measurements of adsorption in the presence of high densities of scatters. GRA

N90-20832# Arizona Univ., Tucson.
OPTICAL BISTABILITY, 1988 Final Technical Report, 1 Mar. 1988 - 30 Apr. 1989
N. Peyghambarian 30 Apr. 1989 257 p Meeting held in Aussois, France, 23-25 Mar. 1988; sponsored by CNRS, CNET, CGE, DRET, Kodak, NSF, Optical Society of America, European Physical Society, Societe Francaise d'Optique, ONR, Air Force, EOARD and AFOSR
(Grant AF-AFOSR-0128-88; AF Proj. 2305)
(AD-A217681; AFOSR-90-0073TR; ISBN-1-55752-062-3) Avail: NTIS HC A12/MF A02 CSCL 20/6

The proceedings of the conference are presented. Some areas of discussion are: Photonics; Optical bistability; Instabilities and chaos; Poster session 1: Nonlinear guided waves; Poster session 2: Instabilities and chaos; Poster session 3: Optical nonlinearities; Semiconductor nonlinearities; Optical switching and computing; Semiconductor switching and bistability; Poster session 1: Transverse Effects; Poster session 2: Optical bistability and switching dynamics; Poster session 3: Post deadline papers; Quantum confined nonlinearities; Nonlinear guided waves; Fundamental properties of systems with strong light-matter interactions. GRA

N90-20833# Lawrence Livermore National Lab., CA.
PLACEMENT OF MULTIPLE APERTURES FOR IMAGING TELESCOPES
J. P. Fitch and T. W. Lawrence Jan. 1990 10 p Presented at the SPIE Astronomical Telescopes and Instrumentation for the 21st Century Symposium, Tucson, AZ, 11-17 Feb. 1990 Submitted for publication
(Contract W-7405-eng-48)
(DE90-006991; UCRL-101574; CONF-900285-1) Avail: NTIS HC A02/MF A01

Two techniques we have used for determining mirror positions in multiple-aperture telescope arrays are described. Our design criteria is the maximization of the contiguous central core diameter of the optical transfer function for the telescope system. The first technique is applicable to arrays with a relatively small, O(10), number of apertures and is essentially an exhaustive search with a simple in-line test which allows the search space to be pruned by an order of magnitude. In the second technique, arrays of a large number of apertures are designed using a fractal approach by recursively combining the results from several array patterns with fewer apertures. Both techniques are demonstrated for one and two dimensional designs and can be extended for higher dimensions if needed. DOE

N90-20834# Los Alamos National Lab., NM. Center for Nonlinear Studies and T Div.
INTEGRABILITY AND CHAOS IN NONLINEARLY COUPLED OPTICAL BEAMS
D. David 1989 20 p Presented at the CRM Workshop on Hamiltonian Systems, Transformation Groups, and Spectral Transform Methods, Montreal, Quebec, 20-26 Oct. 1989
(Contract W-7405-eng-36)
(DE90-007540; LA-UR-90-537; CONF-8910365-1) Avail: NTIS HC A03/MF A01

Using dynamical systems methods, the equations describing the polarization behavior of two nonlinearly coupled optical beams counterpropagating in a nonlinear medium are studied. In the traveling-wave regime assumption, this system possesses a Lie-Poisson structure on the manifold C squared x C squared. In the case where the medium is assumed to be isotropic, this system exhibits invariance under the Hamiltonian action of two copies of the rotation group, S(sup 1), and actually reduces to a lower-dimensional system on the two-sphere, S squared. The dynamics on the reduced space were studied and the structure of the phase portrait examined by determining the fixed points and infinite-period homoclinic and heteroclinic orbits; the focus was on some exotic behavior that occurs when some parameters are varied, and special solutions associated with some of the above-mentioned orbits were also shown. Last, the existence of complex dynamics were demonstrated when the system is subject to certain classes of Hamiltonian perturbations. To this end, use was made of the Melnikov method to analytically show the occurrence of either horseshoe chaos, or Arnold diffusion. DOE

N90-20835# Texas Univ., Austin. Microwave Lab.
GaAs TRAVELING-WAVE OPTICAL MODULATORS USING MODULATED COPLANAR ELECTRODES WITH PERIODIC CROSS-TIE OVERLAYS
Hai-Young Lee and Tatsuo Itoh Dec. 1989 99 p
(Contract DAAL03-88-K-0005)
(AD-A217731; MW-89-P-5; ARO-25045.32-EL) Avail: NTIS HC A05/MF A01 CSCL 20/6

Traveling wave optical modulators using cross-tie slow wave electrodes on GaAs substrates as well as wideband feeding of a coplanar strip electrode are described. Periodic cross-tie conductors are overlaid on a modulated coplanar strip and a modulated coplanar waveguide electrode to make slow wave electrodes. In these structures, phase velocity matching between modulation and optical waves is satisfied over a very wide bandwidth by reducing the phase velocity of the modulation wave using the slow wave electrodes. Therefore, the modulation bandwidths are greatly increased while the dominant conductor losses are relatively high and limit the bandwidths. The coplanar strip slow wave structure was build on a semi-insulating GaAs substrate and measured using a microwave network analyzer. The measured phase velocity is much lower than those of conventional coplanar electrodes and agrees very well with the calculated one. GRA

N90-20836# Rochester Univ., NY. Dept. of Physics and Astronomy.
FUNDAMENTAL STUDIES OF PHOTON STATISTICS Final Technical Report, 1 Aug. 1983 - 30 Sep. 1989
Leonard Mandel Jan. 1990 23 p
(Contract N00014-83-K-0576; RR01107)
(AD-A217825) Avail: NTIS HC A03/MF A01 CSCL 20/6

The final technical report on research performed under the Office of Naval Research (ONR) Contract Fundamental Studies of Photon Statistics, emphasizes some of the most interesting results obtained. They deal with non-classical interference, violations of locality, and the determination of the time interval between two photons with femtosecond accuracy. Some possibilities for a new type of optical communication channel were explored. The research

resulted in 62 publications and 88 lectures or papers presented at scientific meetings and seminars. These are all listed. Seven graduate students completed Ph.D. degrees with support from the ONR contract. GRA

N90-20837# Naval Postgraduate School, Monterey, CA.
MODIFICATION, TESTING, AND CALIBRATION OF INFRARED SEARCH AND TARGET DESIGNATOR HARDWARE RECEIVED FROM NSWC Final Report, May 1986 - Feb. 1988
Eugene C. Crittenden, Jr. and A. W. Cooper May 1989 32 p
(Contracts N62271-7183-4768; N62271-6059-7873; N62271-87-M-0205; N62271-86-M-0213)
(AD-A217920; NPS61-89-011CR) Avail: NTIS HC A03/MF A01 CSCL 17/5

The detecting system of the IRST (Infrared Search and Track), as received at the NPG, was inoperative because of failure of the cooling engine and detector Dewar flask thermal insulation. This system has now been converted to liquid nitrogen cooling with foam thermal insulation and has been successfully operated with the scanning head rotating. All surfaces are now temperature controlled and the system is provided with automatic controls to prevent thermal runaway during cool-down or warm-up. The present system eliminates the inner germanium window of the former Dewar flask. Besides simplifying the structure, this permits imaging closer objects than was previously possible. The optical system of the Schmidt telescope was tested with a collimating system, and by imaging of real objects at finite distances. A system was provided for relative calibration and identification of the position of the 180 individual detector elements, and the relative response of each element measured at the detector and at the output of its preamplifier. Signals obtained from a heated Calrod source and from clouds and the surrounding terrain were recorded with the optical system rotating. GRA

N90-20838# Lockheed Missiles and Space Co., Palo Alto, CA.
SPACECRAFT OPTICAL CONTAMINATION ENVIRONMENT Scientific Report No. 2, Feb. 1988 - Feb. 1989
S. B. Mende 1 Apr. 1989 26 p
(Contract F19628-87-C-0097)
(AD-A218088; GL-TR-89-0110) Avail: NTIS HC A03/MF A01 CSCL 03/2

In the framework of this program the Lockheed Palo Alto Research Laboratories is performing a joint experiment with AFGL to make observations of shuttle induced emission effects such as shuttle glow and thruster induced effects. In addition, observations will be made of natural background phenomena such as the aurora and airglow. At very high latitude when the shuttle transits the auroral regions an attempt will be a made to observe the direct effects of precipitation and precipitation induced discharges. In this program the Air Force will be flying Lockheed instrumentation as secondary payload on the shuttle and the payload or mission specialists will make observations through the orbiter windows with the equipment. The hardware is essentially a re-flight of the Auroral Photography Experiment (APE) which was flown on mission 41-G augmented with the spectrometer and Fabry-Perot. The APE experiment will be reflown again in the near future with the expanded configuration, Configuration B which includes the spectrometer and the Fabry-Perot. GRA

N90-20839# Keo Consultants, Brookline, MA.
OPTICAL INSTRUMENTATION SUPPORT FOR THE AIRBORNE IONOSPHERIC OBSERVATORY Final Report, 12 Mar. 1986 - 30 Sep. 1989
Robert H. Eather and Cyril A. Lance 25 Oct. 1989 38 p
(Contract F19628-86-C-0028; AF Proj. 4643)
(AD-A218207; AFGL-TR-89-0290) Avail: NTIS HC A03/MF A01 CSCL 20/6

Included is a description of software development for instrument control and calibration, hardware modifications and improvements, mission support for field trips, optics improvements, instrument maintenance, and data analysis. GRA

75 PLASMA PHYSICS

Includes magnetohydrodynamics and plasma fusion.
For ionospheric plasmas see *46 Geophysics*. For space plasmas see *90 Astrophysics*.

N90-20840 California Univ., Irvine.
SPONTANEOUS MAGNETIC RECONNECTION IN A TURBULENT PLASMA Ph.D. Thesis
Dean Alan Deeds 1989 125 p
Avail: Univ. Microfilms Order No. DA8915435

The effects of turbulence are examined in a variety of forms and strengths, on the resistive tearing instability (spontaneous reconnection) in an unstable, sheared-field, resistive-MHD plasma. Both periodic and nonperiodic background fields are modeled. Calculational techniques include a true spectral, or Galerkin-type, algorithm, and a finite-grid alternating direction-implicit method with variable grid spacing. All calculations are fully nonlinear. The tearing mode is found to arise from an initial random turbulent, excitation of fairly general form. This has various implications for solar corona physics (where it increases the likelihood of tearing in situations such as active coronal loops) and for laboratory plasma physics (since it implies that large-scale disruptions can evolve from small-scale turbulence). It also demonstrates that tearing can grow to dominate other forms of reconnection. In studying the effects of ongoing turbulence, it is found that although brief disturbances have little of no effect on tearing modes, continual stirring of background turbulence results in a modest enhancement of the tearing-mode growth rate (by a factor of perhaps two or three). This enhancement is the correct direction, but great enough by itself, to help explain the observed short coronal-loop-to-flare conversion time scales. The simulations demonstrate the Alfven effect, an equipartition between magnetic and kinetic turbulence energy, and that there is a dynamic mechanism serving to maintain this balance. There are however notable exceptions to this condition. Dissert. Abstr.

N90-20841# Los Alamos National Lab., NM.
THE IMPEDANCE OF ENERGY EFFICIENCY OF A COAXIAL MAGNETIZED PLASMA SOURCE USED FOR SPHEROMAK FORMATION AND SUSTAINMENT
Cris W. Barnes, Thomas R. Jarboe, George J. Marklin, Stephen O. Knox, and Ivars Henins 1989 7 p Presented at the 11th US/Japan Workshop on Field-Reversed Configurations and Compact Toroids, Los Alamos, NM, 7-9 Nov. 1989
(Contract W-7405-eng-36)
(DE90-003220; LA-UR-89-3720; CONF-8911130-5) Avail: NTIS HC A02/MF A01

Electrostatic (dc) helicity injection was previously shown to successfully sustain the magnetic fields of spheromaks and tokamaks. The magnitude of the injected magnetic helicity balances (within experimental error) the flux lost by resistive decay of the toroidal equilibrium. The problem of optimizing this current drive scheme hence involves maximizing the injected helicity (the voltage-connecting-flux product) while minimizing the current (which multiplied by the voltage represents the energy input and also possible damage to the electrodes). The impedance (voltage-to-current ratio) and energy efficiency of a dc helicity injection experiment are studied on the CTX spheromak. Over several years changes were made in the physical geometry of the coaxial magnetized plasmas source as well as changes in the external electrical circuit. The source could be operated over a wide range of external charging voltage (and hence current), applied axial flux, and source gas flow rate. A database of resulting voltage, helicity injection, efficiency, electron density, and rotation has been created. These experimental results are compared to an ideal magnetohydrodynamic theory of magnetic flux flow. The theory is parameterized by the dimensionless Hall parameter, the ratio of electric to mass current. For a constant Hall parameter the theory explains why the voltage depends quadratically on the current at constant flux. The theory also explains the approximately linear dependence of the impedance-to-current ratio on the current-to-flux ratio of the source. DOE

N90-20842# Institute of Plasma Physics, Prague (Czechoslovakia).
COMPUTATION OF COUPLING ELEMENTS BETWEEN WAVEGUIDES AND MODES FOR LARGE LAUNCHING STRUCTURES
O. Hurtak and J. Preinhaelter May 1989 20 p
(IPPCZ-290) Avail: NTIS HC A03/MF A01

Optimization of the large launching structures - grills and multijunction grills which are intended to be used for lower hybrid current drive (LHCD) in big tokamaks calls for quick and sufficiently precise computation of the coupling elements between waveguides and modes. The original method of computation, efficient only for small structures and based on integration along the real axis, was described. For computation of the coupling elements between distant waveguides, another method of integration using the shift of the integration path into the complex plan was developed. The analytical continuation of the plasma surface impedance into the complex N(sub z) - plane was performed and the new numerical code was evolved. In the last section some numerical results are given to compare both methods. Combination of both methods speeds up the computation needed for the grill design. Author

N90-20843# Oak Ridge National Lab., TN.
THE ANU (AUSTRALIAN NATIONAL UNIVERSITY) HELIAC PROGRAM
R. L. Dewar, H. J. Gardner, G. J. Cooper, S. M. Hamberger, L. E. Sharp, B. D. Blackwell, T. Y. Tou, G. D. Conway, X.-H. Shi, and D.-F. Zhou (Australian National Univ., Canberra.) et al 1989 4 p Presented at the 1st International Toki Conference on Plasma Physics and Controlled Nuclear Fusion, Toki, Japan, 4-8 Dec. 1989
(Contract DE-AC05-84OR-21400)
(DE90-006620; CONF-891240-6) Avail: NTIS HC A01/MF A01

The history and current status of experimental and theoretical work on heliacs at the Australian National University are reviewed. DOE

N90-20844# Texas Univ., Austin. Inst. for Fusion Studies.
ENHANCED PINCH EFFECT DUE TO ELECTROSTATIC POTENTIAL
K. C. Shaing (Oak Ridge National Lab., TN.) and R. D. Hazeltine Jan. 1990 18 p
(Contracts DE-FG05-80ET-53088; DE-AC05-84OR-21400)
(DE90-007088; DOE/ET-53088/415; IFSR-415) Avail: NTIS HC A03/MF A01

An inward pinch appears necessary to explain experimental results in tokamaks. Neither the neoclassical pinch effect, which is too small, nor the off-diagonal quasilinear term, which is usually outward in the trapped particle regime, can account for the observations. A mechanism for an enhanced inward pinch is proposed, based on results for an asymmetric magnetic field bump. Because turbulent fluctuations also break toroidal symmetry, an enhanced inward pinch driven by the fluctuations and the Ohmic inductive field, E is expected. To demonstrate this effect, an inward particle flux is calculated for a model tokamak configuration that has an electrostatic potential bump Phi (sub 0) at toroidal angle zeta = 2(pi). For the parameter regime r/R less than e Phi (sub 0)/T(sub e) less than 1, the flux is found to be Gamma = -4.47K (q) (r/R) L (Phi (sub 0) upsilon (sub te)/R nu e)(sup 1/2)cN E/B, where r(R) is minor (major) radius, B is the magnetic field strength, upsilon (sub te) is the electron thermal speed, nu (sub e) is the electron-ion collision frequency, q is the safety factor, and K(q) and L Phi (sub 0) are functions of q and Phi (sub 0) respectively. The results are also applicable to an asymmetric potential bump created externally to enhance the inward pinch flux of high energy, collisionless particles. DOE

N90-20845# Mississippi State Univ., Mississippi State. Diagnostic Instrumentation and Analysis Lab.
DIAGNOSTIC DEVELOPMENT AND SUPPORT OF MHD (MAGNETOHYDRODYNAMICS) TEST FACILITIES Technical Progress Report, Oct. - Dec. 1988
Jan. 1989 62 p
(Contract DE-AC02-80ET-15601)
(DE90-004969; DOE/ET-15601/35) Avail: NTIS HC A04/MF A01

Mississippi State University (MSU) is developing diagnostic instruments for magnetohydrodynamic (MHD) power train data acquisition and for support of MHD component development test facilities. Microprocessor-controlled optical instruments are being refined, and new systems to measure temperatures and gas-seed-slag stream characteristics are being developed. To further data acquisition and analysis capabilities, the diagnostic systems are being interfaced with MHD Energy Center computers. Technical support for the diagnostic needs of the national MHD research effort is being provided. MSU personnel will also cooperate with government agencies and private industries to improve the transformation of research and development results into processes, products and services applicable to their needs. DOE

N90-20846# Oak Ridge National Lab., TN.
DIFFERENCE IN ELECTRON THERMAL DIFFUSIVITY AND PROFILE BETWEEN INTERIOR AND EXTERIOR OF TFTR L-MODE PLASMAS
S. Hiroe, D. W. Johnson, and R. J. Goldston (Princeton Univ., NJ.) 1990 32 p Presented at the 2nd Transport Task Force Workshop, Hilton Head, SC, 19-23 Feb. 1990
(Contract DE-AC05-84OR-21400)
(DE90-007479; CONF-900288-4) Avail: NTIS HC A03/MF A01

The local properties such as scale lengths of the electron density (L sub n(sub e)), temperature (L sub T(sub e)), and pressure (L sub p(sub e)), and the electron thermal diffusivity chi(sub e)(r) (sq m/2) for r/a is greater than 0.3 were studied for TFTR L-mode discharges under the assumption of chi(sub e) = chi(sub i). The scale lengths and the electron thermal diffusivity in the interior 0.3 is less than r/a is less than 0.55 are significantly different from those on the exterior 0.55 is less than r/a is less than 0.8. following are some examples (temperatures in keV, other quantities in MKS units). In the interior (0.3 is less than r/a is less than 0.55), most of the scale lengths were constant or a weakly dependent on radius, and chi(sub e) can be expressed as (with correlation coefficient R = 0.61), chi(sub e)(r) = 1.44 x 10(exp 18)(r/a)(sup 1.0) T(sub e) (r)(sup 0.1) q(r)(sup 0.1)/n(sub e)(sup 0.9) (r). In the exterior region (0.55 is less than r/a is less than 0.8), the scale lengths decrease monotonically, and chi(sub e) can be described as (with R = 0.68), chi(sub e)(r) = 2.3 x 10(exp 3) (r/a)(sup 1.7) T (sub e) (r)(sup 0.7) q(r)(sup 0.8)/n(sub e)(sup 0.2) (r). It is interesting to note the negative n(sub e) dependence of chi(sub e) in the interior and the positive T(sub e) dependence of chi(sub e) in the exterior. DOE

N90-20847# Los Alamos National Lab., NM. Applied Theoretical Physics Div.
NEW METHODS IN PLASMA SIMULATION
Rodney J. Mason 23 Feb. 1990 28 p Presented at the International Conference on Plasma Physics, New Delhi, India, 22-28 Nov. 1989
(Contract W-7405-eng-36)
(DE90-007507; LA-UR-90-692; CONF-891182-3) Avail: NTIS HC A03/MF A01

The development of implicit methods of particle-in-cell (PIC) computer simulation in recent years, and their merger with older hybrid methods have created a new arsenal of simulation techniques for the treatment of complex practical problems in plasma physics. The new implicit hybrid codes are aimed at transitional problems that lie somewhere between the long time scale, high density regime associated with MHD modeling, and the short time scale, low density regime appropriate to PIC particle-in-cell techniques. This transitional regime arises in ICF coronal plasmas, in pulsed power plasma switches, in Z-pinches, and in foil implosions. Here, we outline how such a merger of implicit and hybrid methods has been carried out, specifically in the ANTHEM computer code, and demonstrate the utility of implicit hybrid simulation in applications. DOE

N90-20848# Oak Ridge National Lab., TN.
HIGH ELONGATION PLASMAS
E. A. Lazarus 1990 11 p Presented at the CIT West Coast Physics Meeting, San Diego, CA, 29 Jan. 1990
(Contract DE-AC05-84OR-21400)
(DE90-007575; CONF-900174-1-Vugraphs) Avail: NTIS HC A03/MF A01

This paper contains viewgraphs on axisymmetric stability of doublet-3 tokamak. The information available on this stability is applied to the Compact Ignition Tokamak. DOE

N90-20849# Los Alamos National Lab., NM. Applied Theoretical Physics Div.
LASER-PRODUCED PLASMAS IN MEDICINE
S. J. Gitomer and R. D. Jones 1990 15 p Presented at the Biomedical Optics 1990 Conference, Los Angeles, CA, 14-19 Jan. 1990
(Contract W-7405-eng-36)
(DE90-007623; LA-UR-90-419; CONF-900178-2) Avail: NTIS HC A03/MF A01

The laser has found numerous applications in medicine, beginning with uses in ophthalmology in the 1960's. Today, lasers are used in tissue cutting, blood coagulation, photo-dynamic cancer therapy, arterial plaque removal, dental drilling, etc. Those areas of laser medicine are examined in which plasmas (ionized gases) are produced. In fact, the presence of a plasma is essential for the application at hand to succeed. Examples are examined for the plasmas produced in ophthalmology (e.g., lens membrane destruction following cataract surgery), in urology and gastro-enterology (e.g., kidney and gall stone ablation and fragmentation) and in cardiology and vascular surgery (e.g., laser ablation and removal of fibro-fatty and calcified arterial plaque). Experimental data are presented along with some results from computer simulations of the phenomena. Comments on future directions in these areas are included. DOE

N90-20850# Oak Ridge National Lab., TN. Applied Technology Div.
MATERIALS AND SELECTION CRITERIA ANALYSIS FOR THE COMPACT IGNITION TOKAMAK TOROIDAL FIELD COIL TURN-TO-TURN INSULATION SYSTEM: PHOTOGRAPHIC SUMMARY OFLABORATORY TESTING Interim Report
V. W. Campbell, J. B. Dooley, J. G. Hubrig, C. J. Janke, T. J. McManamy, and D. E. Welch Jan. 1990 38 p
(Contract DE-AC05-84OR-21400)
(DE90-008020; ORNL/ATD-28/V2) Avail: NTIS HC A03/MF A01

This document contains photographs showing the results of laboratory testing of the combinations of epoxy resins, hardeners, and cures undertaken as part of the Compact Ignition Tokamak Insulation Screening Program. Cryogenic shock and soak to equilibrium proved to be the most demanding condition for these materials. The degree of damage to the basic materials when a poor candidate is selected is shown to be quite dramatic. DOE

N90-20851# Oak Ridge National Lab., TN. Fusion Energy Div.
PARTICLE TRANSPORT IN PELLET FUELED JET (JET EUROPEAN TORUS) PLASMAS
L. R. Baylor Jan. 1990 180 p
(Contract DE-AC05-84OR-21400)
(DE90-008077; ORNL/TM-11420) Avail: NTIS HC A09/MF A01

Pellet fueling experiments were carried out on the Joint European Torus (JET) tokamak with a multi-pellet injector. The pellets are injected at speeds approaching 1400 m/s and penetrate deep into the JET plasma. Highly peaked electron density profiles are achieved when penetration of the pellets approaches or goes beyond the magnetic axis, and these peaked profiles persist for more than two seconds in ohmic discharges and over one second in ICRF heated discharges. Analysis of electron particle transport in multi-pellet fueled JET limiter plasmas under a variety of heating conditions is described. The analysis is carried out with a one and one-half dimensional radial particle transport code to model the experimental density evolution with various particle transport coefficients. These analyses are carried out in plasmas with ohmic heating, ICRF heating, and neural beam heating, in limiter configurations. Peaked density profile cases are generally characterized by diffusion coefficients with a central (r/a less than 0.5) diffusivity approx. 0.1 sq m/s that increases rapidly to approx. 0.3 sq m/s at r/a = 0.6 and then increases out to the plasma edge as (r/a) squared. These discharges can be satisfactorily modeled without any anomalous convective (pinch) flux. DOE

N90-20852# Wisconsin Univ., Madison. Dept. of Nuclear Engineering and Engineering Physics.
DESIGN OF D-3 He COMMERCIAL TOKAMAK
1989 31 p
(Contract DE-FG02-89ER-52158)
(DE90-008252; DOE/ER-52158/1) Avail: NTIS HC A03/MF A01

The Fusion Technology Institute of the University of Wisconsin is participating in the ARIES design study. The objective of this work was to contribute to the design of a D-He-3 fueled commercial tokamak fusion reactor, ARIES II. In this proposal, the work during the first phase is summarized and the plans for the second phase are outlined. DOE

N90-20853# Lawrence Livermore National Lab., CA.
SPECTRAL LINE SHAPE CODE FOR MULTIELECTRON EMITTERS Final Report
A. Calisti, F. Khelfaoui, R. Stamm, L. Sylvander, and B. Talin Mar. 1989 31 p Prepared in cooperation with Provence Univ., Marseille, France
(Contract W-7405-eng-48)
(DE90-008526; UCRL-21298) Avail: NTIS HC A03/MF A01

A computer code providing theoretical line profiles of multielectron radiators in plasmas is described. The line profiles are calculated for a selected spectral range, in the presence of natural broadening, Doppler and stark effect. The model used for the description of stark effect assumes that the plasma and atomic structure parameters are such that the static ion microfield approximation and the model of a binary collision electronic operator are valid. Whereas an electronic collision operator can usually safely be used, neglecting ion motion requires that the width of the line is much larger than the typical fluctuation frequency of the ion microfield (ion plasma frequency). A careful check for the validity of this approximation has to be done for hot and dense plasma conditions. Breakdown of the static approximation occur especially for hydrogenic emitters. For multielectron emitters a large validity domain of the static ion approximation is usually found. In this static ion model, an average is performed over a static microfield distribution. For this quantity, the APEX model is used, which allows for calculations in the coupled plasma domain. DOE

N90-20854# Rochester Univ., NY. Lab. for Laser Energetics.
TIME-RESOLVED SPECTROSCOPY OF NONEQUILIBRIUM IONIZATION IN LASER-PRODUCED PLASMAS Ph.D. Thesis
Robin Stewart Marjoribanks Mar. 1990 198 p
(Contract DE-FC03-85DP-40200)
(DE90-008663; DOE/DP-40200/120) Avail: NTIS HC A09/MF A02

The highly transient ionization characteristic of laser-produced plasmas at high energy densities has been investigated experimentally, using x ray spectroscopy with time resolution of less than 20 ps. Spectroscopic diagnostics of plasma density and temperature were used, including line ratios, line profile broadening and continuum emission, to characterize the plasma conditions without relying immediately on ionization modeling. The experimentally measured plasma parameters were used as independent variables, driving an ionization code, as a test of ionization modelling, divorced from hydrodynamic calculations. Several state-of-the-art streak spectrographs, each recording a fiducial of the laser peak along with the time-resolved spectrum, characterized the laser heating of thin signature layers of different atomic numbers imbedded in plastic targets. Spherical targets were

illuminated uniformly with the OMEGA 351 nm laser system, to approximate a one-dimensional homogeneous plasma. A novel design of crystal spectrograph, with a conically curved crystal, was developed. Coupled with a streak camera, it provided high resolution and a collection efficiency roughly 20 to 50 times that of planar crystal spectrographs, affording improved spectra for quantitative reduction and greater sensitivity for the diagnosis of weak emitters. DOE

N90-20855# Fermi National Accelerator Lab., Batavia, IL.
NONLINEAR PLASMA AND BEAM PHYSICS IN PLASMA WAKE-FIELDS
J. B. Rosenszweig 12 Feb. 1990 36 p Presented at the Topical Conference on Research Trends in Nonlinear and Relativistic Effects in Plasmas, La Jolla, CA, 5-8 Feb. 1990 Prepared in cooperation with Argonne National Lab., IL
(Contract DE-AC02-76CH-03000)
(DE90-008812; FNAL/C-90/40; CONF-900264-3) Avail: NTIS HC A03/MF A01

In experimental studies of the Plasma Wake-field Accelerator performed to date at the Argonne Advanced Accelerator Test Facility, significant nonlinearities in both plasma and beam behavior were observed. The plasma waves driven in the wake of the intense driving beam in these experiments exhibit three-dimensional nonlinear behavior which has as yet no quantitative theoretical explanation. This nonlinearity is due in part to the self-pinching of the driving beam in the plasma, as the denser self-focused beam can excite larger amplitude plasma waves. The self-pinching is a process with interesting nonlinear aspects: the initial evolution of the beam envelope and the subsequent approach to Bennett equilibrium through phase mixing. DOE

N90-20856# California Univ., Berkeley. Dept. of Mathematics.
NONLINEAR STABILITY IN FLUID AND PLASMA DYNAMICS Final Report, 30 Sep. 1987 - 29 Sep. 1989
J. E. Marsden and T. Ratiu 30 Nov. 1989 5 p
(Contract F49620-87-C-0118)
(AD-A217735; AFOSR-90-0065TR) Avail: NTIS HC A01/MF A01 CSCL 20/11

Major work on the dynamics of coupled rigid bodies was done. We studied both the case of three coupled rigid bodies in the plane, with a complete stability, bifurcation, and chaotic solutions analysis, but also studied the three-dimensional case. In the energy-momentum method, for mechanical systems with Hamiltonian H of the form kinetic energy (K) plus potential (V), a way was found to choose variables that makes the determination of stability conditions sharper and more computable. The Poisson brackets of free boundary fluid equations has been determined. In the homogeneous case, it has been shown already that the structure of the bracket is that of a Yang Mills theory for the principal bundle whose total space consists of the embeddings of a given domain in space; the base space is the space of unparametrized fluid shapes, and the group is the particle relabeling group. The geometric reasons for the integrability of the planar three point vortex motion in terms of dual pairs appearing in the study of the geometry of Poisson manifolds has been given. The study of the hydrodynamic bifurcations was begun on the example of a rigidly rotating incompressible homogeneous disk. GRA

76 SOLID-STATE PHYSICS

Includes superconductivity.

For related information, see also *33 Electronics and Electrical Engineering* and *36 Lasers and Masers.*

N90-20857# Brookhaven National Lab., Upton, NY. Materials Science Div.
A SYSTEMATIC STUDY OF THE EFFECTS OF METAL SUBSTITUTIONS FOR Cu IN YBa(SUB 2) (Cu(SUB 1-x) M(SUB x)3 O(SUB 7-RHO), M=Fe, Co, Al, Ga, Cr, Ni, AND Zn
Youwen Xu, A. R. Moodenbaugh, Y. L. Wang, M. Suenaga, and R. L. Sabatini 1989 9 p Presented at the Materials Research Society Fall Meeting, Boston, MA, 27 Nov. - 2 Dec. 1989
(Contract DE-AC02-76CH-00016)
(DE90-003957; BNL-43006; CONF-891119-37) Avail: NTIS HC A02/MF A01

A series of polycrystalline YBa(sub 2) (Cu(sub 1-x)M(sub x) (sub 3O(sub Cu sub 1-x), M sub x sub 3, O sub 7- delta (1:2:3) samples with a typical grain size greater than 10 microns was prepared using well controlled and reproducible procedures. This relatively large grain size allowed microprobe studies of individual grains to determine M content of the 1:2:3 phase. Solubility limits of substitutions for Cu in these samples are estimated. Superconducting transition temperatures and lattice parameters are presented. In the case of Ga, microprobe studies show no evidence for Ga content of 1:2:3 above x = 0.01. Preliminary studies show no evidence for solid solution above x = 0.01 when substituting Mn, Cr, Zr, and Ti for Cu in 1:2:3. DOE

N90-20858# Belmont Coll., Nashville, TN.
INTERACTION BETWEEN IMPLANTED IONS AND INTRINSIC DEFECTS IN SILICA
R. H. Magruder, D. L. Kinse, R. A. Weeks, and R. A. Zuhr (Oak Ridge National Lab., TN.) 1989 6 p Presented at the Materials Research Society Fall Meeting, Boston, MA, 27 Nov. - 2 Dec. 1989
(Contract DE-AC05-84OR-21400; NSF DMR-85-13731)
(DE90-006569; CONF-891119-91) Avail: NTIS HC A02/MF A01

High purity silica (Spectrosil) samples were implanted with Ti, Cr, Mn, Fe and Cu at doses ranging from 1.0 to 5.0 x 10(exp 15) ions/sq cm at 160 keV and 2.6 microA/sq cm. The optical absorption extinction coefficients per ion were measured from 1.8 to 6.0 eV. In all samples there was an increase in absorption over the unimplanted sample at energies greater than or = 4.6 eV. The increase in absorption at 5.1 eV and 5.7 eV is attributed to B2(E") centers and E(') centers respectively. The relative values of the extinction coefficients of these bands are attributed to the relative oxygen activities of the TMI relative to the SiO2 host substrate. DOE

N90-20859# Sandia National Labs., Albuquerque, NM.
CHEMICALLY PREPARED PZT FILMS DOPED WITH NIOBIUM
B. A. Tuttle, D. H. Doughty, R. Schwartz, T. J. Garino, S. L. Martinez, D. Goodnow, C. L. Hernandez, and R. G. Tissot 1989 15 p Presented at the 1st International Ceramic Science and Technology Congress, Anaheim, CA, 31 Oct. - 3 Nov. 1989
(Contract DE-AC04-76DP-00789)
(DE90-006811; SAND-89-1480C; CONF-8910120-7) Avail: NTIS HC A03/MF A01

The first ferroelectric measurements are reported of chemically prepared thin films of PZT containing niobium, (PNZT). Polycrystalline, perovskite PNZT thin films were fabricated by spin coating Pt coated SiO2/Si substrates with alkoxide solutions. The base composition, PZT 53/47, was systematically doped with niobium (0 to 10 at. percent). Further compositional modifications included the variation of Zr/Ti ratio for films containing 2 at. percent Nb. The dielectric constants measured for PNZT 2/56/44, 2/53/47 and 2/48/52 films were in good agreement with bulk values. Dielectric constants on the order of 700, 1000 and 500, respectively, were measured for these three films. Both linear and nonlinear current-voltage behavior was observed for our Pt/PNZT/Pt device structures, depending on the amplitude of the applied voltage and the temperature of measurement. Ferroelectric films were made of PNZT 2/53/47 (2 at. percent Nb doping) with spontaneous polarizations of 0.2 C/sq m and coercive fields of 2.5 MV/m. PNZT films containing larger niobium additions (5 and 10 at. percent) had inferior ferroelectric properties because of the presence of nonperovskite phases. DOE

N90-20860# United Kingdom Atomic Energy Authority, Harwell (England). Materials Physics and Metallurgy Div.
THEORY OF DEFECT PROCESS: BASIC ISSUES IN QUANTITATIVE UNDERSTANDING
A. M. Stoneham Sep. 1989 29 p Presented at the US-Japan

Joint Seminar on Atomic Processes Induced by Electronic Excitation in Non-Metallic Solids
(AERE-R-13661) Avail: NTIS HC A03/MF A01

Defect processes are those defect reactions, transition, or motions by which defect populations change with time. Such processes are often the basis of applications, or may limit usefulness of materials. The quantitative prediction of the rates of defect processes is especially important for very fast processes or very slow processes, where experiment alone is not convenient; moreover, theory is especially helpful in separating out contributions in complex situations. A broad classification of defect processes (adiabatic versus non-adiabatic; near thermal equilibrium or not) is given and some of the key problems of principle and technique in extending calculations from adiabatic energy surfaces to the complex dynamics of real system are identified. An example is the distinction between reaction coordinates and modes, and the implications for combining good ion dynamics with good electronic structure calculations. Author

N90-20861# United Kingdom Atomic Energy Authority, Harwell (England). Materials Development Div.
DIFFERENTIAL MEASUREMENTS OF THE LATERAL PHOTO EFFECT IN GaAs/AlGaAs HETEROSTRUCTURES
P. F. Fontein, P. Hendriks, J. H. Wolter (Technische Hogeschool, Eindhoven, Netherlands), A. Kucernak, R. Peat, and D. E. Williams Jul. 1989 15 p
(AERE-R-13557) Avail: NTIS HC A03/MF A01

A laser scan technique based on the lateral photo effect to image the local resistivity of the two-dimensional electron gas of GaAs/AlGaAs heterostructures is presented. A measurement of the spatial derivative of the lateral photo effect gives direct information about the local resistivity. Compared with conventional measurements of the lateral photoeffect the technique presented here is able to resolve much smaller variations in the resistivity. This is illustrated by the experimental results presented. Author

N90-20862# United Kingdom Atomic Energy Authority, Harwell (England). Materials Physics and Metallurgy Div.
IONIC DISORDER IN CRYSTALS AT HIGH TEMPERATURES WITH EMPHASIS ON FLUORITES
M. T. Hutchings and W. Hayes (Oxford Univ., England) Jun. 1989 116 p
(AERE-R-13544) Avail: NTIS HC A06/MF A01

Research into the thermally-induced cooperative buildup of anomalously large concentrations of ionic defects in crystals (primarily those with the fluorite structure) is made. The objective is to create a single point defect of ionic solids for use at high temperatures. An acceptable model of the high temperature disordered phase which would be able to account for, or predict, the complete range of physical properties of the crystal is sought. A variety of measurements on fluorite physical properties are made: specific heat; ionic conductivity; nuclear magnetic resonance; diffusion; and light scattering. Neutron and x ray scattering are described, with detailed emphasis on coherent and incoherent scattering. Conslusions are drawn on the nature of the fast-ion state. Author

N90-20863# Los Alamos National Lab., NM.
COPPER AND OXYGEN NMR STUDIES ON THE MAGNETIC PROPERTIES OF YBa2Cu3O(7-y)
Masashi Takigawa 1989 13 p Presented at the NATO Advanced Research Workshop on Dynamics of Magnetic Fluctuations in High Temperature Superconductors, Crete, Greece, 10-14 Oct. 1989
(Contract W-7405-eng-36)
(DE90-007889; LA-UR-90-112; CONF-8910350-2) Avail: NTIS HC A03/MF A01

Microscopic magnetic properties of the CuO2 layers in YBa2Cu3O(7-y) wave investigated from Cu and O NMR experiments on the y(approx =)0 (T(sub c)=92K) and y=0.37 (T(sub c)=62K) materials. The Knight shift at the planar Cu and the planar oxygen sites are found to be proportional to a common spin susceptibility chi (sub s) which depends on temperature and oxygen-content, strongly supporting a single component spin model for the CuO2 planes. In the y=0.37 material, chi (sub s) shows a significant reduction with decreasing temperature in the normal state. The nuclear relaxation rate (1/T(sub 1)) in the y(approx =)0 material, particularly different behaviors at Cu and O sites, can be accounted for by the hyperfine coupling of Cu and O nuclei to an antiferromagnetically correlated single spin system. Quite different behaviors of 1/T(sub 1) were observed in the y=0.37 material, which might be due to combined effects of antiferromagnetic correlations and a temperature-dependent spin susceptibility. DOE

N90-20864# North Carolina Univ., Chapel Hill. Dept. of Chemistry.
IN-SITU DIFFERENTIAL REFLECTANCE STUDY OF THE ETCHING OF SiO2 FILMS Interim Technical Report No. 29
Uean-Sin Pahk, S. Chongsawangvirod, and E. A. Irene 18 Jan. 1990 27 p Submitted for publication
(Contract N00014-89-J-1178)
(AD-A217186) Avail: NTIS HC A03/MF A01 CSCL 07/4

A differential reflectance technique has been applied to study the etching of silicon dioxide films on silicon substrates in-situ in the liquid hydrogen fluoride/Water environment as well as ex-situ. Essentially, the technique scans an incident optical beam in the spectral range of 200 to 800 nm across two adjacent samples at near normal incidence and the reflected beams are detected using lock-in amplification so as to measure only the difference in the reflectance spectra. This study demonstrates the great sensitivity of the technique to follow the etching experiment in-situ, and in conjunction with simulated spectra and ex-situ results, a new spectral feature is seen which may be evidence for an electric double layer at the Si surface in the etch solution. In microelectronics processing, the cleaning of silicon substrates prior to processing and the etching of SiO2 films on Si for various lithographic procedures often involves the use of aqueous HF solutions. Previous studies have shown that the use of HF alters the Si surface and the oxidation kinetics. More recent studies have confirmed these results and indicate that the major effect is at the Si surface. GRA

N90-20865# North Carolina Univ., Chapel Hill. Dept. of Chemistry.
REFRACTIVE INDEX PROFILES OF THERMALLY GROWN AND CHEMICALLY VAPOR DEPOSITED FILMS ON SILICON Interim Technical Report, No. 30
S. Chongsawangvirod, E. A. Irene, A. Kalnitsky, S. P. Tay, and J. P. Ellul (Northern Telecom Electronics Ltd., Ottawa, Ontario) 18 Jan. 1990 29 p Submitted for publication
(Contract N00014-89-J-1178)
(AD-A217187) Avail: NTIS HC A03/MF A01 CSCL 09/1

Ellipsometry, although used extensively in the microelectronics field for the measurement of film thicknesses and refractive indices, does not usually yield reliable refractive indices for dielectric films less than 50 nm thick due to instrumental errors and software limitations. Addressing this issue, we report ellipsometric procedures that enable a reliable assessment of refractive index profiles for a variety of thermally grown and chemically vapor deposited, CVD, dielectric films on Si substrates down to about 10 nm thickness and we compare the results in terms of the current understanding about the film-substrate interface. In all cases studied we find that the interfacial region is optically different than the thick film, and that the precise film processing substantively alters the nature of the interface region. GRA

N90-20866# Massachusetts Inst. of Tech., Cambridge. Dept. of Electrical Engineering and Computer Science.
CHEMICAL BEAM EPITAXY OF ZnSe Semiannual Report, 1 Aug. 1989 - 31 Jan. 1990
Leslie A. Kolodziejski 31 Jan. 1990 7 p
(Contract N00014-88-K-0564)
(AD-A217375) Avail: NTIS HC A02/MF A01 CSCL 20/2

The objective of the program is to determine optimum growth parameters for the chemical beam epitaxial of ZnSe. In addition

microstructural, optical, and electrical characterization of the material will be performed to assess the material's quality and potential; comparisons will be made with material grown by molecular beam epitaxy. GRA

N90-20867# Palisades Inst. for Research Services, Inc., NY.
WORKSHOP ON THE PHYSICS AND CHEMISTRY OF MERCURY CADMIUM TELLURIDE AND RELATED II-VI COMPOUNDS Final Report, 1 Sep. 1989 - 31 Jan. 1990
Mark Goldfarb Nov. 1989 143 p Workshop held in San Diego, CA, 3-5 Oct. 1989
(Contract DAAL03-89-G-0097)
(AD-A217496; ARO-26911.1-EL-CF) Avail: NTIS HC A07/MF A01 CSCL 20/12

The proceedings of the workshop are presented. Some areas of discussion are: Crystal Growth; Molecular Beam Epitaxy; MBE Doping; Metalloorganic Chemical Vapor Deposition; Liquid Phase Epitaxy; Defects and Impurities; Surfaces and Interfaces; Novel Materials and Structures; Electronic Properties. GRA

N90-20868# Air Force Weapons Lab., Kirtland AFB, NM.
PROTON RESPONSES ON MOS (METAL-OXIDE-SEMICONDUCTOR) ELECTRONICS OPERATING AT CRYOGENIC TEMPERATURES Final Report, Jun. 1987 - Dec. 1989
R. W. Tallon, A. H. Hoffland, W. T. Kemp, and J. W. Brouse Jan. 1990 35 p
(AD-A217622; WL-TR-89-80) Avail: NTIS HC A03/MF A01 CSCL 18/7

Proton proton radiation damage data is presented which demonstrates that Metal-Oxide-Semiconductor (MOS) electronics (P-Channel or N-Channel), operated under applied negative gate biases and irradiated by 10 MeV protons, will suffer greater radiation damage per dose at cryogenic temperatures than at room temperatures. This was true for both radiation hardened and nonradiation hardened MOS structures. However, the data also showed that this was not true for all MOS devices operating under positive gate biases. Nonradiation hardened MOS units operating under positive gate biases, suffered radiation damages that were approximately equal at both the cold and room temperatures. Final data showed if irradiated cold temperature MOS devices were allowed to heat to about -123 C or warmer, the radiation damage within the devices would anneal rapidly. GRA

N90-20869# Indiana Univ., Bloomington.
METAL ALKOXIDES: MODELS FOR METAL OXIDES. ALKOXIDE LIGANDS IN EARLY TRANSITION METAL ORGANOMETALLIC CHEMISTRY Progress Report
1990 9 p
(Contract DE-FG02-86ER-13570)
(DE90-007523; DOE/ER-13570/4) Avail: NTIS HC A02/MF A01

The two most important results during the last year have come from studies of the activation of carbon monoxide by tetranuclear tungsten alkoxides and the activation of carbon-carbon double bonds in reactions with dinuclear tungsten alkoxides. DOE

N90-20870# Brookhaven National Lab., Upton, NY.
MOLECULAR ORGANIZATION AND ELECTRICAL PROPERTIES OF MIXED LANGMUIR-BLODGETT MULTILAYER THIN FILMS OF POLYPYRROLE
J. Cheung, R. B. Rosner, M. F. Rubner (Massachusetts Inst. of Tech., Cambridge.), X. Q. Yang, J. Chen, and T. A. Skotheim 1989 9 p Presented at the NATO Advanced Research Workshop on Conjugated Polymeric Materials: Opportunities in Electronics, Optoelectronics, and Molecular Electronics, Mons, Belgium, 3-8 Sep. 1989 Sponsored in part by NSF; Center for Materials Science, MIT; and Army Electronics Technology and Devices Lab.
(Contract DE-AC02-76CH-00016)
(DE90-007627; BNL-43851; CONF-8909307-1) Avail: NTIS HC A02/MF A01

The molecular organization of Langmuir-Blodgett multilayer thin films containing electrically conductive polypyrrole chains dispersed throughout insulating domains of surface active pyrrole molecules was examined by several thin film spectroscopic techniques. Reflection-absorption spectroscopy revealed that the 3-ODOP (3-octadecanoyl pyrrole) surface active pyrrole molecules are highly oriented within the film with their fully extended hydrocarbon chains tilted away from the surface normal with an unusually large tilt angle of about 55 degrees. Evidence for preferred orientation of the polypyrrole chains was also found. The multilayer films were found to exhibit very large dielectric constants (greater than 100) at low frequencies and enormous conductivity anisotropies. These unusual electrical properties can be directly attributed to the molecular organization of the film which consists of polypyrrole chains sandwiched between well ordered layers of 3-ODOP molecules. DOE

N90-20871# California Univ., Berkeley. Lawrence Berkeley Lab.
CRYSTAL PREPARATION AT LBL, 1976 TO 1986
Wini Heppler May 1989 52 p
(Contract DE-AC03-76SF-00098)
(DE90-007754; LBL-PUB-3078) Avail: NTIS HC A04/MF A01

Soon after some progress had been made in understanding the structure of solids and the relation of structures to physical properties of solids, attention has turned to understanding the boundaries of bulk materials and their surfaces. Aside from the intrinsic interest of the subject, the motivations for this study are many because many chemical processes, such as corrosion, catalysis, and adhesion to name a few are limited to the surface of bulk materials. The natural starting point for such studies is oriented and polished single crystal surfaces, since these idealized terminations of the bulk are expected to present a minimal number of different surface atoms or chemical states to the outside world. This report is meant to be a quick guide for the uninitiated into the mysteries of crystal orienting, cutting and polishing. It is hoped that the worker can then avoid some of the many pitfalls along the way. DOE

N90-20872# California Univ., Berkeley. Lawrence Berkeley Lab. Center for Advanced Materials.
ABSOLUTE PRESSURE DEPENDENCE OF THE SECOND IONIZATION LEVEL OF EL2 IN GaAs
D. E. Bliss, W. Walukiewicz, D. D. Nolte (Purdue Univ., West Lafayette, IN.), and E. E. Haller Nov. 1989 5 p Presented at the Materials Research Society Fall Meeting, Boston, MA, 27 Nov. - 2 Dec. 1989 Prepared in cooperation with California Univ., Berkeley
(Contract DE-AC03-76SF-00098)
(DE90-007761; LBL-27522; CONF-891119-104) Avail: NTIS HC A01/MF A01

Results are reported for DLTS experiments under uniaxial stress on the second ionization level of EL2(++/+) in p-type GaAs. We measured the shift in the hole emission rate as a function of stress applied in the (100) and (110) directions. By modeling the valence band with two independently displacing bands and appropriately derived effective masses, a small absolute hydrostatic pressure derivative for the defect, 39 + or - 15 MeV/GPa was obtained. The shear contribution is negligible. This result is very different than for the first ionization level, EL2(+/o) with a emission energy pressure derivative of 90 + or - 15 MeV/GPa. The difference can be accounted for by the pressure dependence of the electron capture barrier of EL2(+/o), 49 + or - 15 MeV/GPa. The absolute pressure derivatives of the two levels are then comparable and in good agreement with simple theory for Ga site point defects. DOE

N90-20873# California Univ., Berkeley. Lawrence Berkeley Lab. Materials and Chemical Sciences.
HIGH RESOLUTION TRANSMISSION ELECTRON MICROSCOPY STUDY OF DEFECT STRUCTURES IN MIXED-PHASE YBaCuO
M. Fendorf, E. Kvam, and R. Gronsky Dec. 1989 4 p Presented at the Materials Research Society Fall Meeting, Boston, MA, 27 Nov. - 2 Dec. 1989

(Contracts DE-AC03-76SF-00098; MDA972-88-J-1002)
(DE90-007767; LBL-27461; CONF-891119-103) Avail: NTIS HC A01/MF A01

Mixed-phase superconducting YBaCuO is characterized by means of high-resolution transmission electron microscopy. This technique reveals that such material contains numerous crystallographic defects of various types. Several of these are described in detail, and their origins discussed. DOE

N90-20874# Sandia National Labs., Albuquerque, NM.
CCST (CENTER FOR COMPOUND SEMICONDUCTOR TECHNOLOGY) RESEARCH BRIEFS
Jun. 1989 38 p
(Contract DE-AC04-76DP-00789)
(DE90-007782; SAND-89-0773) Avail: NTIS HC A03/MF A01

The Center for Compound Semiconductor Technology (CCST) was formed within the Solid-State Sciences Directorate at Sandia National Laboratories in 1988, as the culmination of a long-term thrust into compound semiconductor research and technology that began about ten years ago. At that time, it was realized that electronic and optoelectronic devices based on compound semiconductors would be necessary for photonic applications, and that they could provide greater radiation hardness, higher speed, and higher operating temperatures than comparable silicon devices and circuits. It was also realized that a successful program would require the development and integration of materials growth and processing capability, solid-state physics research, and device engineering. The program at Sandia grew steadily from the purchase of the first Molecular Beam Epitaxy (MBE) system in 1981, and the discovery of strained-layer superlattices in 1982, to the completion of the Compound Semiconductor Research Laboratory in 1989. To more formally organize this effort, Sandia established the CCST in 1988. The CCST comprises most of the compound semiconductor research and development activities in the Solid-State Sciences Directorate. Ongoing programs are funded by the DOE Office of Military Applications, DOE Basic Energy Sciences, DOE Conservation and Renewable Energy, and the Department of Defense. DOE

N90-20875# Sandia National Labs., Albuquerque, NM.
HIGH TEMPERATURE CHEMISTRY OF OXIDE SUPERCONDUCTORS
Terry L. Aselage, Keith D. Keefer, and Jim A. Voigt 1989 24 p Presented at the 1st International Ceramic Science and Technology Congress, Anaheim, CA, 31 Oct. - 3 Nov. 1989
(Contract DE-AC04-76DP-00789)
(DE90-007821; SAND-89-1514C; CONF-8910120-8) Avail: NTIS HC A03/MF A01

A knowledge of the high temperature chemistry involved in the formation of the high-(Tc) superconductors is necessary in order to prepare materials with desired properties. The liquidus relations were studied in the YO(1.5)-BaO-CuO system and initial experiments were performed to understand equilibrium conditions in the Tl-Ca-Ba-Cu-O system. The liquid forming reactions that pertain to the processing of YBa2Cu3O(7-delta) were reviewed, and it was shown that the ternary peritectic reaction between CuO and YBa2Cu3O(7-delta) generates a liquid phase that promotes deleterious grain growth of the superconducting phase. It was also shown that very small deviations in stoichiometry can have a large effect on microstructure through the generation of such liquids. Finally, the approach to understanding the equilibrium conditions of the thallium-based superconductors is described. Under experimental conditions, none of the superconducting phases exists in equilibrium with thallium oxide at high temperatures; rather, thallium-rich oxides containing barium and/or calcium, but not copper, coexist with thallium oxide. DOE

N90-20876# Massachusetts Inst. of Tech., Cambridge. Dept. of Materials Science and Engineering.
AN INVESTIGATION OF THE DISLOCATION STRUCTURE OF THE Ni/Ag PHASE BOUNDARY
T. A. Bamford Dec. 1989 7 p
(Contract DE-FG02-87ER-45310)
(DE90-008428; DOE/ER-45310/20) Avail: NTIS HC A02/MF A01

The Ni/Ag interphase boundary structure in the parallel cube-on-cube orientation was studied for the boundary planes (001) and (011). Coarsely spaced dislocations were found in all annealed interfaces; the origin of these was apparently differential thermal expansion of the bicrystal film. A detailed search for intrinsic periodic structure consistent with the O-lattice construction was made using x ray diffraction, electron diffraction and transmission electron microscopy. No evidence for this could be found; such a relaxation, if present, is very weak. It is unlikely that such a small relaxation could account for relative energy minimum associated with the parallel cube-on-cube orientation. DOE

N90-20877# Utah Univ., Salt Lake City. Dept. of Materials Science and Engineering.
THEORETICAL AND EXPERIMENTAL STUDY OF SOLID PHASE MISCIBILITY GAPS IN III/V QUATERNARY ALLOYS Progress Report, 1 Apr. 1987 - 2 Jun. 1989
G. B. Stringfellow 2 Jun. 1989 8 p
(Contract DE-FG02-84ER-45061)
(DE90-008430; DOE/ER-45061/6) Avail: NTIS HC A02/MF A01

The first 8 years of this DOE supported research was directed toward understanding, for the first time, the thermodynamics of miscibility gaps and ordering in III/V alloys. This research has led to the publication of 32 papers in technical journals as well as 17 invited papers and national and international conferences. In addition, this work led directly to the invitation to organize the Joint U.S./Japan Workshop on Alloy Semiconductor Physics and Electronics. A brief project summary, a listing of papers and talks, and a section devoted to supported and graduated students are contained. DOE

N90-20878# Sandia National Labs., Albuquerque, NM.
SiO(x) PRECIPITATION: DEFECT DENSITY CORRELATION WITH THE n+ SUBSTRATE RESISTIVITY
John W. Medernach 1989 5 p Presented at the Meeting of the Electrochemical Society, Montreal, Quebec, 6-11 May 1990
(Contract DE-AC04-76DP-00789)
(DE90-005593; SAND-89-1930C; CONF-900562-1) Avail: NTIS HC A01/MF A01

The thermal budget of a CMOS process, which employs n/n(+) epitaxial silicon, can constrain the SiO(x) precipitation necessary for bulk gettering sites. This makes the control of both the precipitation and its distribution difficult. Little or no precipitation will occur when heat treatments are inadequate or the n(sup +) substrate O(2) concentration (O) is too low. Likewise, uncontrolled precipitation can lead to warpage, slip and the formation of surface stacking faults. Bulk precipitation is some CMOS processes using n/n(+) epitaxial silicon may not be feasible, because of the smaller thermal budgets. However; many CMOS processes using n/n(+) epitaxial silicon rely on some form of gettering. Extrinsic and intrinsic gettering techniques as well as pre-processed gettered wafers can be employed with CMOS processes to develop the necessary internal SiO(x) defects for effective gettering . An experimental strategy was designed to determine how the CMOS thermal budget interacts with the extrinsic gettering layers on n(+) substrates with different (O). Models for the defect densities and denuded zones developed from the strategy are reported for the polysilicon (Poly) and polysilicon/nitride (PN) extrinsic gettering layers. An unexpected correlation between the defect density and the n(+) substrate resistivity with (O) also is discussed. DOE

N90-20879# Sandia National Labs., Albuquerque, NM.
IDENTIFICATION OF DEFECTS IN SOI (SILICON-ON-INSULATOR) WAFERS
M. J. Kelly, T. R. Guilinger, J. W. Medernach, S. S. Tsao, H. D. T. Jones, and J. O. Stevenson 1989 9 p Presented at the 4th International Symposium on Silicon-On-Insulators Technology and Device, Montreal, Quebec, 6-11 May 1990

(Contract DE-AC04-76DP-00789)
(DE90-006020; SAND-89-2696C; CONF-900598-1) Avail: NTIS HC A02/MF A01

Defects and metal contamination in device areas of silicon integrated circuits (IC) can limit yield in IC fabrication. An electrochemical method is described for identification of structural defects and metal contamination in low-doped n-type silicon (dopant concentration of about 10(exp 15)/cu cm. Anodic etching in 5 wt percent hydrofluoric acid produces crystallographic etch pits which correlate with both structural and impurity defects. Etch pit densities also correlate well with reported values of defect densities calculated from gate oxide breakdown. We show that the method is particularly suited to defect delineation in thin-film silicon-on-insulator (SOI) wafers. The technique is superior to chemical decoration etches and to transmission electron microscopy for defect delineation in thin-film SOI wafers since it does not etch bulk silicon and it has a detection limit much lower than 10(exp 4)-10(exp 5) defects/sq cm. The procedure was used to demonstrate how defect levels are strongly affected by the process parameters used to synthesize Zone Melt Recrystallization (ZMR) and Separation by IMplanted OXygen (SIMOX) wafers. DOE

N90-20880# Lawrence Livermore National Lab., CA.
L SHELL XANES (X RAY ABSORPTION NEAR EDGE STRUCTURE) FOR SOLID METALS: Ti, V, Cr, Fe, Ni, Cu
N. K. DelGrande Jan. 1990 4 p
(Contract W-7405-eng-48)
(DE90-008043; UCID-21873) Avail: NTIS HC A01/MF A01

The L shell x ray absorption near edge structure (XANES) for the 3d transition metals Ca-Cu is dominated by atomic-like behavior which is poorly understood. It was studied by electron energy loss spectroscopy (EELS) and bremsstrahlung isochromat spectra (BIS). More and better photoabsorption cross-section measurements are needed over the sparsely studied 400 to 1500 eV region to test theoretical methodologies which fuse atomic and condensed matter theories. Progress was made reporting absolute photoabsorption cross sections taken with the spherical grating monochromator on beamline 8-2 at SSRL in 1989. DOE

N90-20881# Rensselaer Polytechnic Inst., Troy, NY.
STABILIZATION OF HIGH (Tc) SUPERCONDUCTIVITY IN CADMIUM SULFIDE Progress Report, Feb. 1989 - Feb. 1990
S. J. Nettel and R. K. MacCrone 1990 22 p
(Contract DE-FG02-88ER-45362)
(DE90-008249; DOE/ER-45362/2) Avail: NTIS HC A03/MF A01

For the past year and a half, the problem of stabilizing the anomalous magnetic properties of pressure quenched, chlorine doped, cadmium sulfide was addressed. The essence of the proposal was to develop a fully reproducible procedure for obtaining magnetically active samples. The experimental work to date has verified that the anomalous magnetism does exist. Both large diamagnetism and large paramagnetism was observed. In all cases the magnetization varies as a function of time. Further evidence that a phase transition occurs in chlorine doped cadmium sulfide at the critical concentration of 0.75 wt percent chlorine with x ray diffraction was obtained and confirmed. This evidence of instability is consistent with the observation of the difficulty of controlling the chlorine during the precipitation of cadmium sulfide near the critical chlorine concentration. All the experimental observations, in particular the slow variations in the anomalous magnetism, have influenced and support the theoretical approach taken. Thus, it is believed that the program is well established, and has had sufficient success to warrant the proposing its continuation through the third year. This would enable the completion of the systematic investigation and establish the procedures leading to superconductivity in cadmium sulfide, and possible, in related materials. Establishment of high (Tc) superconductivity in a material as different from the original high (Tc) superconductors as is cadmium sulfide would obviously be of the greatest scientific importance. It is felt that part of the success lies in having obtained significant insight into the nature of the difficulties with cadmium sulfide, and the features required for superconductivity, and the pathway by which these may be attained. DOE

N90-20882# Boston Univ., MA.
THE GEOMETRY OF DISORDER: REPORT 1987 TO 1990
1990 25 p Prepared in cooperation with Cornell Univ., Ithaca, NY
(Contracts DE-FG02-89ER-45405; DE-FG02-87ER-45323)
(DE90-008250; DOE/ER-45405/1) Avail: NTIS HC A03/MF A01

Work is reported on the geometry, i.e., how are structural units packed together in space, including the development of the random tiling picture of quasicrystal ordering. This is followed by quasicrystal atomic structure (including work on quasicrystal faceting). Random frustrated magnetic systems are then examined, where ground state selection, ordering due to disorder were worked out, in some 2D model systems, and are currently studying the Wolff Monte Carlo algorithm. Finally, results are summarized on a new self organized percolation model with a non-equilibrium dynamics representing epidemics, forest fires, or other self-catalytic reactions. DOE

N90-20883# Lawrence Livermore National Lab., CA.
THE ELECTRONIC PROPERTIES OF HIGH (Tc) SUPERCONDUCTORS PROBED BY POSITRON ANNIHILATION
C. S. Sundar, A. Bharathi, Y. C. Jean, D. G. Hinks, B. Dabrowski, Y. Zheng, A. W. Mitchell, J. C. Ho (Wichita State Univ., KS.), K. H. Howell, and A. L. Wachs et al 23 Jun. 1989 4 p Presented at the International Conference on Materials and Mechanisms of Superconductivity - High-Temperature Superconductors 2, Stanford, CA, 23-28 Jul. 1989
(Contract W-7405-eng-48)
(DE90-008354; UCRL-101287; CONF-890718-34) Avail: NTIS HC A01/MF A01

The discovery of superconductivity at 30 K in Ba(.6)K(.4) BiO3 has generated considerable excitement in view of the contrasting properties of the Ba-K-Bi-O system when compared to the well known Cu-O based high temperature superconductors. Positron annihilation spectroscopy, which is a sensitive local probe of the electronic and defect properties of a solid, was extensively applied in the study of Cu-O based superconductors. The results of positron lifetime as a function of temperature in Ba-K-Bi-O are presented and compared with the known results in the cuprate superconductors. Plausible reasons for the observed temperature dependence of positron lifetime are presented. DOE

N90-20884# Lawrence Livermore National Lab., CA.
SYSTEMATICS IN POSITRON ANNIHILATION LIFETIME ANALYSIS OF HIGH (Tc) SUPERCONDUCTING TRANSITIONS
R. H. Howell, H. B. Radousky, A. L. Wachs, M. J. Fluss, P. E. A. Turchi, Y. C. Jean, C. S. Sundar, C. W. Chu, R. N. Shelton, and D. G. Hinks (Argonne National Lab., IL.) 23 Jun. 1989 4 p Presented at the International Conference on Materials and Mechanisms of Superconductivity - High-Temperature Superconductors 2, Stanford, CA, 23-28 Jul. 1989
(Contract W-7405-eng-48)
(DE90-008361; UCRL-100480; CONF-890718-35) Avail: NTIS HC A01/MF A01

The lifetimes and momentum distributions of annihilating electron-positron pairs are changed in high Tc superconductors cooled below the superconducting transition. Since the initial observation of this phenomena is YBCO the observation of these effects was reproduced and extended to other high (Tc) systems. There is a general consistency of results in most families of superconductors. An exception to this is YBCO which shows strong sample dependence. These consistent features have led to a model relating the pairing of the positive charge carriers and the positron distribution as one explanation for the lifetime changes. DOE

N90-20885# Lawrence Livermore National Lab., CA.
ULTRA-HIGH BRIGHTNESS LASER RESEARCH AT LLNL (LAWRENCE LIVERMORE NATIONAL LABORATORY)

F. G. Patterson, M. D. Perry, and E. M. Campbell Mar. 1989 9 p Presented at the Symposium on Lasers and Optics, Los Angeles, CA, 15-20 Jan. 1989
(Contract W-7405-eng-48)
(DE90-008366; UCRL-99094; CONF-890142-6) Avail: NTIS HC A02/MF A01

New short-pulse laser technology has made possible the production of extremely bright (greater than 10(exp 18) W/sq cm-sr) laser sources. The use of these new techniques on large scale Nd:glass based laser systems would make it possible to produce 1000 TW (Petawatt) pulses. Such pulses would yield focused intensities exceeding 10(exp 21) W/sq cm corresponding to an electric field in excess of 100 e/a(sub 0)(sup 2) and an energy density equivalent to that of a 10 keV blackbody. The first step towards the realization of such a source is the development of a compact 10 TW laser. The design of a 10 TW table-top laser and some potential applications are described. DOE

N90-20886*# National Aeronautics and Space Administration. Lewis Research Center, Cleveland, OH.
MILLIMETER WAVE SURFACE RESISTANCE OF RBa2Cu3O(7-DELTA) (R=Y,Eu,Dy,Sm,Er) SUPERCONDUCTORS
F. A. Miranda, W. L. Gordon, T. G. Eck (Case Western Reserve Univ., Cleveland, OH.), K. B. Bhasin, J. D. Warner, and K. A. Jenkins 1990 9 p Presented at the March Meeting of the American Physical Society, Anaheim, CA, 12-16 Mar. 1990
(NASA-TM-102571; E-5395; NAS 1.15:102571) Avail: NTIS HC A02/MF A01 CSCL 20L

The measurements are reported of the millimeter wave surface resistance R(sub s) at 58.6 GHz of bulk samples of RBa2Cu3O(7-delta) (R = Y,Eu,Dy,Sm,Er) and of YBa2Cu3O-(7-delta) superconducting films, in the temperature range from 20 to 300 K. The bulk samples were prepared by cold pressing the powders of RBa2Cu3O(7-delta) into one in. disks. The powders were prepared by several sinterings in one atmosphere of oxygen at 925 C, with grindings between sinterings, to obtain the superconducting phase. The thin films were deposited on SrTiO3 and LaGaO3 substrates by pulsed laser ablation. Each sample was measured by replacing the end wall of a gold-plated Te sub 013 circular mode copper cavity with the sample and determining the cavity quality factor . From the difference in the Q-factor of the cavity, with and without the sample, the R(sub s) of the sample was determined. Author

N90-20887# Los Alamos National Lab., NM. Ceramics Science and Technology Group.
SYNTHESIS AND PROPERTIES OF POLYCRYSTALLINE Tl2Ba2CaCu2O(x) AND Tl2Ba2Ca2Cu3O(x)
Gerald J. Vogt and David S. Phillips 1990 24 p Presented at the TMS Symposium on High Temperature Superconducting Compounds, Anaheim, CA, 20-21 Feb. 1990
(Contract W-7405-eng-36)
(DE90-007528; LA-UR-90-449; CONF-900287-1) Avail: NTIS HC A03/MF A01

Polycrystalline samples of Tl2Ba2CaCu2O(x) and Tl2B2-Ca2Cu3O(x) superconductors with high (greater than 95 wt percent) phase purity were prepared by a solid state reaction of Tl2O3 with a mixture of BaCuO2, Ca2CuO3, and CuO. Starting compositions of Tl(1 + delta)BaCaCu2O(x) and Tl(2 + delta)Ba2Ca2Cu3O(x) were fired in semi-sealed reaction vessels for durations of 12 to 48 hours in flowing oxygen with low, reproducible thallium losses. Samples fired at temperatures below 870 C produced predominately the 2212 phase, while samples above 870 C yielded the 2223 phase. While pressed mixed oxides reacted in a single firing step produced low-density (less than or equal to 50 percent theoretical) material, samples prepared by a two-step sequence of reactive calcination, intermediate grinding, and sintering yielded higher density material (greater than 70 percent theoretical). The sintered polycrystalline superconductors were characterized by x ray diffraction, reflected light and electron microscopy, magnetic susceptibility, and dc transport resistivity. Critical current density measurements by direct transport and magnetic moment hysteresis methods are presented for the denser samples. Transport J(sub c) values up to 300 A/sq cm at 75 K were observed for moderately dense material (5.2 g/cu cm, 74 percent theoretical) in transverse H fields up to 10 kOe. DOE

N90-20888# Argonne National Lab., IL. Materials and Components Technology Div.
SYNTHESIS OF Bi-Sr-Ca-Cu OXIDE SUPERCONDUCTOR BY SOLUTION TECHNIQUE
Dayse I. dosSantos, U. Balachandran, M. T. Lanagan, Donglu Shi, M. A. Patel, and R. B. Poeppel 1990 10 p
(Contract W-31-109-eng-38)
(DE90-008707; ANL/PPRNT-90-204) Avail: NTIS HC A03/MF A01

Superconducting Bi2Sr2Ca2Cu3O(x) powders were synthesized using a solution technique in which bismuth nitrate, strontium hydroxide, calcium acetate and copper ethoxide were dissolved in a glacial acetic acid-ethanol mixture. The resulting solution was evaporated to dryness to obtain pale blue powder. This powder was calcined and pressed into pellets and sintered at 860 C in air. The resistance of these samples indicated an on-set of 110 K and reached zero electrical resistance state at about 70 K. DOE

N90-20889# Army Inst. for Research in Management Information and Computer Sciences, Atlanta, GA.
TECHNOLOGY ASSESSMENT OF SUPERCONDUCTIVITY
Winfred Y. Fong 13 Feb. 1989 11 p
(AD-A217697; ASQBG-I-89-013) Avail: NTIS HC A03/MF A01 CSCL 20/3

Superconductivity is the name given to an exceptional combination of electric and magnetic properties in certain materials when such materials are cooled to extremely low temperatures. The temperature at which a superconductor loses its resistance is called its superconducting transition temperature or critical temperature. While in the superconducting state, it has been demonstrated that a current can flow forever in a superconductor without loss of any form. An assessment of the current, near-term (1995), and long-term (2010) trends in Superconductivity is given. GRA

N90-20890# Army Lab. Command, Watertown, MA. Material Technology Lab.
PERFORMANCE OF Y-TZP MATERIALS BETWEEN 800 C AND 1200 C Final Report
Jeffrey J. Swab Jan. 1990 16 p
(AD-A217723; MTL-TR-90-3) Avail: NTIS HC A03/MF A01 CSCL 11/2

The performance of seven yttria-tetragonal zirconia polycrystal materials in the 800 C to 1200 C temperature range was examined using stepped-temperature stress-rupture tests. The strength in this temperature range was significantly lower than the room temperature strength. This is due to a decrease in the chemical driving force for the tetragonal-to-monoclinic transformation. As a result, these materials are not suitable for high temperature structural applications. At these temperatures the strength is controlled by microstructural parameters such as grain size, grain size distribution, and porosity. GRA

N90-20891# Harry Diamond Labs., Adelphi, MD.
CRYSTALLOGRAPHY, SPECTROSCOPIC ANALYSIS, AND LASING PROPERTIES OF Nd3+:Y3Sc2Al3O12 Final Report, Aug. - Dec. 1988
Toomas H. Allik, Clyde A. Morrison, John B. Gruber, and Milan R. Kokta Dec. 1989 24 p
(AD-A217792; HDL-TR-2169) Avail: NTIS HC A03/MF A01 CSCL 20/2

The crystallographic, optical, and spectroscopic properties of Neodymium(3+):Yttrium scandium aluminum garnet are reported from which an assessment can be made regarding the material's potential as a laser. Individual Stark levels for many of the (2S+1)Lj manifolds of Nd(3+) (4f3) in the crystal have been identified from emission and absorption data up to 17,600/cm at 14K. The observed crystal-field splitting and the measured cross sections

(intensities) associated with manifold-to-manifold transitions are compared with calculated splittings and calculated intensities. Branching ratios and diode-array-pumped laser slope efficiencies are also reported. We conclude that Nd(3+):YSAG has potential as a diode-pumped 1-micrometer laser material. GRA

N90-20892# Texas A&M Univ., College Station.
ELECTRONIC PROPERTIES OF HIGH-TEMPERATURE SUPERCONDUCTORS Ph.D. Thesis
Brent Armand Richert Aug. 1989 193 p Sponsored in part by AFIT, Wright-Patterson AFB, OH and ONR
(AD-A217953; AFIT/CI/CIA-89-099) Avail: NTIS HC A09/MF A01 CSCL 20/3

A semiempirical tight-binding model was developed for the electronic energy bands, the local and total densities of states, and the atomic valences in the high temperature superconductors La(1.85)Sr(0.15)CuO4, YBaCu307, Bi2Sr2CuO6, Bi2CaSr2Cu2O8, Tl2Ba2CuO6, Tl2CaBa2Cu2O8, Tl2Ca2Ba2Cu3O10, TlCa3-Ba2Cu4O11, BaPb(0.75)Bi(0.25)O3, and Ba(0.6)K(0.4)BiO3. Calculations of the changes in electronic properties associated with atomic substitutions in YBa2Cu3O7, Bi2CaSr2Cu2O8, and Tl2CaBa2Cu2O8 give results in agreement with expected chemical trends and consistent with observed changes in the superconducting properties. For example, substitution of Lead for Bismuth in BiMCaSr2Cu2O8 increases the concentration of hole carriers within the CuO2 planes. Similarly, doping with Mercury or Pb in TlMCaBa2Cu2O8 also affects the carrier concentration, with Hg creating holes and Pb destroying them. Oxygen vacancies in both La(1.85)Sr(0.15)CuO(4-y) and YBa2Cu3O(7-y) act as electron donors. This is consistent with the observations that oxygen vacancies degrade the superconductivity and metallic conductivity in these materials. Lanthanum vacancies in La2-xCuO4 donate holes, giving the same electronic effect as doping with divalent metal atoms or excess oxygen initially stoichiometric La2CuO4. A specific excitonic mechanism for high temperature superconductivity is proposed which requires insulating metal oxide layers adjacent to the superconducting planes. GRA

N90-20893# Santa Barbara Research Center, Goleta, CA.
NRL HYBRID RELIABILITY. PHYSICS OF FAILURE INITIAL STUDY Final Report, 1 Oct. 1986 - 30 Sep. 1988
Jan. 1990 71 p
(Contract N00014-86-C-2553)
(AD-A217986; SBRC-90-0045) Avail: NTIS HC A04/MF A01 CSCL 20/12

The objective of this program was to identify the failure mechanisms associated with the thermal cycling of HgCdTe hybrid infrared focal plane arrays from room temperatures to cryogenic temperature (typically 77K). This work included evaluating the possible occurrence of damage (increased dislocation density, fracturing, etc.) in the HgCdTe as a result of the hybridization process and/or cycling. Infrared focal plane arrays (IRFPAs) are hybrid structures consisting of a HgCdTe infrared-sensitive material subdivided into an array of photodiodes and connected, via a matrix of indium interconnects or bumps, to a silicon readout used to collect the charge generated in the HgCdTe as a result of the IR signal. The readout output can be used to generate an IR image. There is a concern in the IR community that the long term reliability of IRFPAs may be in question due to defects being formed as a result of the hybridization process and/or thermal cycling of the arrays from room to cryogenic temperatures. GRA

N90-20894# Massachusetts Inst. of Tech., Cambridge. Research Lab. of Electronics.
FOCUSED ION BEAM IMPLANTATION Progress Report, 1 Jul. - 31 Dec. 1989
John Melngailis 31 Dec. 1989 5 p
(Contract DAAL03-88-K-0108)
(AD-A217987; ARO-26051-EL) Avail: NTIS HC A01/MF A01 CSCL 20/12

During the latter half of 1989 the focused ion beam was used to implant new tunable Gunn diodes, CMOS transistors in circuits, and CCD's. Most of these devices were tested. Tunable Gunn diodes were fabricated in GaAs and InP. The channels CMOS transistors were implanted with both Boron and Arsenic in a variety of doses, dose gradients, and geometries. CCD's were implanted with gradients of doping under each of the gate electrodes. Previous simulations have indicated that this type of gradient results in a built in field which would tend to push carriers out of each channel increasing the speed. The channels of GaAs MESFET'S were implanted with various doses and dose geometries. Some of these MESFET'S will have submicron length gates fabricated by the focused ion beam. An SiN film is deposited over the channel to stop the ion penetration and lattice damage. GRA

N90-20895# North Carolina State Univ., Raleigh. Dept. of Materials Science and Engineering.
GROWTH, CHARACTERIZATION AND DEVICE DEVELOPMENT IN MONOCRYSTALLINE DIAMOND FILMS Annual Report, 1 Jun. 1988 - 31 May 1989
R. F. Davis, J. T. Glass, K. J. Bachmann, R. J. Trew, and R. J. Nemanich Feb. 1990 137 p
(Contract N00014-86-K-0666)
(AD-A218211) Avail: NTIS HC A07/MF A01 CSCL 20/12

Two chemical vapor deposition (CVD) systems (hot filament and microwave plasma) and a multitechnique analysis system were designed, constructed and characterized. The effects of surface steps, substrate material and substrate/filament bias were examined. Diamond films from outside sources were analyzed by a variety of techniques. Most notably, numerous defects, especially (111) twins, were identified by TEM and are similar to those found in natural diamond. Certain diamond particles were in a twinned epitaxial relationship with the Silicon substrate. It was also found that a thin Silicon carbide layer forms immediately (i.e., less than 5 min) upon exposure to the Methane + Hydrogen plasma, followed by the slow formation of the diamond crystallites. Large-Signal, nonlinear device models for both microwave diamond power MESFETs and mm-wave diamond IMPATT diodes were developed. Diamond power MESFETs operating in X band are found to be capable of producing approximately 25 W/unit gate width of RF power with a power-added efficiency of greater than 40 percent. A diamond IMPATT oscillator should produce about 2 W RF power with an efficiency of 10 percent at 100 GHz. GRA

N90-20896* National Aeronautics and Space Administration. Marshall Space Flight Center, Huntsville, AL.
METHOD OF PREPARING RADIALLY HOMOGENEOUS MERCURY CADMIUM TELLURIDE CRYSTALS Patent
Sandor L. Lehoczky, inventor (to NASA) and Frank R. Szofran, inventor (to NASA) 5 Sep. 1989 6 p Filed 17 Dec. 1985 Continuation of US Patent-Appl-SN-441896, filed 15 Nov. 1982, abandoned
(NASA-Case-MFS-25786-2; US-Patent-4,863,553;
US-Patent-Appl-SN-811309; US-Patent-Class-156-616.41;
US-Patent-Class-156-616.4; US-Patent-Class-422-249;
US-Patent-Appl-SN-441896) Avail: US Patent and Trademark Office CSCL 20L

Hg(1-x)Cd(x)Te is prepared in an improved directional solidification method in which a precast alloy sample containing predetermined amounts of Hg, Cd, and Te is disposed in a sealed ampule and a furnace providing two controlled temperature zones is translated upward past the ampule to provide melting and resolidification. The present improvement is directed to maintaining the zones at temperatures determined in accordance with a prescribed formula providing a thermal barrier between the zones with a maximum thickness and translating the furnace past the zones at a rate less the 0.31 micron/sec.

Official Gazette of the U.S. Patent and Trademark Office

77 THERMODYNAMICS AND STATISTICAL PHYSICS

Includes quantum mechanics; theoretical physics; and Bose and Fermi statistics.

For related information see also *25 Inorganic and Physical Chemistry* and *34 Fluid Mechanics and Heat Transfer.*

N90-20897# Florida Univ., Gainesville. Dept. of Physics.
SUPERSTRING FIELD THEORY
Christian R. Preitschopf, Charles B. Thorn, and Scott A. Yost 1989 14 p Presented at the 1989 Superstrings Workshop, Tuscaloosa, AL, 8-11 Nov. 1989
(Contract DE-FG05-86ER-40272)
(DE90-007694; DOE/ER-40272/94; UFIFT-HEP-90-3; CONF-8911164-2) Avail: NTIS HC A03/MF A01

The construction of a class of cubic gauge-invariant actions for superstring field theory, and the gauge-fixing of one representative are described. Fermion string fields are taken in the -1/2-picture and boson string fields in the 0-picture, which makes a picture-changing insertion carrying picture number -2 necessary. The construction of all such operators is outlined. The gauge b(sub 1) + b(sub -1) = 0 is discussed in which the action formally linearizes. Nontrivial scattering amplitudes are obtained by approaching this gauge as a limit. DOE

N90-20898# Joint Inst. for Nuclear Research, Dubna (USSR). Lab. of Theoretical Physics.
CONSERVED INTEGRAL CHARACTERISTICS OF THE GRAVITATIONAL FIELD
M. N. Tentyukov 1988 8 p In RUSSIAN; ENGLISH summary
(DE90-615205; JINR-R-2-88-851) Avail: NTIS (US Sales Only) HC A02/MF A01

The dynamics of the gravitational field is considered on the affinely connected space. It is shown that the presence of the r-parameter group of motions of the background connection leads to the r integral conservation laws. DOE

N90-20899# Air Force Inst. of Tech., Wright-Patterson AFB, OH.
AN EXPERIMENTAL INVESTIGATION OF THE THERMAL CONDUCTIVITY OF POROUS ADSORBENTS M.S. Thesis
Joseph J. Secary 1989 64 p
(AD-A217854; AFIT/CI/CIA-89-101) Avail: NTIS HC A04/MF A01 CSCL 20/13

The thermal conductivities of Praseodymium Cerium Oxide (PCO) and Saran Carbon were experimentally investigated using a steady state heat transfer technique. The investigated substances are used as adsorbents in adsorption compressors being developed for spaceborne refrigeration applications. The objectives of the investigation were to determine the thermal conductivities and establish their temperature dependency. Data were collected for the PCO over a temperature range of 300 to 600 C, and 0 to 200 C for the Saran Carbon. The thermal conductivities were found to have a strong temperature dependency. In particular, the results for the PCO showed a temperature dependency indicative of some thermal radiation effects. GRA

80 SOCIAL SCIENCES (GENERAL)

Includes educational matters.

N90-20900*# National Aeronautics and Space Administration, Washington, DC.
SEEING IN A NEW LIGHT: ASTRO-1 TEACHER'S GUIDE WITH ACTIVITIES
Jan. 1990 66 p
(NASA-EP-274; NAS 1.19:274) Avail: NTIS HC A04/MF A01 CSCL 05I

A teacher's guide that concentrates on the electromagnetic spectrum is presented. The subject was chosen because it is part of the middle school curriculum and because an understanding of the different ranges of energy is crucial to an understanding of the high energy astronomy performed by the Astro-1 telescopes to be carried on the Space Shuttle's first astrophysics mission. Various learning activities are outlined. R.J.F.

81 ADMINISTRATION AND MANAGEMENT

Includes management planning and research.

N90-20901*# National Aeronautics and Space Administration. Lewis Research Center, Cleveland, OH.
MIDDLE MANAGEMENT OF RESEARCH
Robert W. Graham Jan. 1990 14 p Submitted for publication
(NASA-TM-102417; E-5183; NAS 1.15:102417) Avail: NTIS HC A03/MF A01 CSCL 05A

The role of the middle manager in a research organization is discussed. The middle manager serves as a liaison between upper management and researchers to assure that individual research projects manifest the goals of the organization. The author draws on his long experience in this role to describe management practices that have proven successful. A general discussion is presented of the makeup of a research environment, derived from a study of a division involved in aerospace research and development (R and D). The study emphasized the importance of planning and management style in producing an attractive environment. Management practices are described, which include goal setting, planning, staffing, reviewing and evaluating, and rewarding. The importance of selecting and defining an appropriate research area is discussed. It is emphasized that in relating to the staff the middle manager must cultivate the human side of supervision, develop the art of delegating responsibility, judiciously select facilities, and provide recognition and meaningful rewards to develop a productive research staff. The development of the staff is probably the most important and challenging role of the manager. Author

N90-20902# Bundesministerium fuer Forschung und Technologie, Bonn (Germany, F.R.).
REORGANIZATION OF THE GERMAN SPACE ADMINISTRATION. FOUNDATION OF DARA [NEUORDNUNG DES DEUTSCHEN RAUMFAHRTMANAGEMENTS. GRUENDUNG DER DARA]
26 Apr. 1989 11 p In GERMAN
(Rept-16/89; ETN-90-95319) Avail: NTIS HC A03/MF A01

The concept of the reorganization of the German space administration is outlined. The structure of this reorganization is explained. The fundamentals of the organization of DARA (German Agency for Space Affairs) are given. DARA is compared with other space agencies. ESA

N90-20903# Air Force Inst. of Tech., Wright-Patterson AFB, OH.
AN INTEGRATIVE RESEARCH REVIEW OF THE RELATIONSHIP BETWEEN TECHNOLOGY AND STRUCTURE: A META-ANALYTIC SYNTHESIS Ph.D. Thesis
Clyde Curtis Caufield 1989 494 p
(AD-A218115; AFIT/CI/CIA-89-157) Avail: NTIS HC A21/MF A03 CSCL 05/1

Contingency theory is the dominant paradigm in organization research, and technology occupies a central role in that paradigm. However, 30 years of research into the relationship between technology and organization structure has generated inconsistent results and a body of literature in a general state of chaos. Narrative reviews of the literature have recently suggested that several situational factors may contribute to this condition. This thesis employs the techniques of meta-analysis to test these proposed moderators on an a priori basis. The noninteractive artifact distribution technique was used to correct the correlations obtained from past research for the effects of sampling error, in measurement reliability, and differences in the extent of range restriction. Both published and unpublished sources provided a

total of 833 correlations between four conceptual definitions of technology (i.e., workflow continuity, workflow integration and automation, task routineness, and information technology) and 30 structural variables. Five suspected moderators were tested: organization size, level of analysis, organization type, type of measure used, and the conceptual definition of technology employed. Contrary to the conclusions reached in previous research and narrative reviews neither organization size, level of analysis, nor the type of measure used had a significant moderating effect. GRA

82 DOCUMENTATION AND INFORMATION SCIENCE

Includes information management; information storage and retrieval technology; technical writing; graphic arts; and micrography.

For computer documentation see *61 Computer Programming and Software.*

N90-20904# Lawrence Livermore National Lab., CA.
CALS (COMPUTER-AIDED ACQUISITION AND LOGISTIC SUPPORT) TEST NETWORK INFORMATION EXCHANGE USER'S MANUAL, REVISION 1
22 Dec. 1989 18 p Revised
(Contract W-7405-eng-48)
(DE90-008119; UCID-21679-Rev-1; CTN-89-007) Avail: NTIS HC A03/MF A01

The DoD Computer-aided Acquisition and Logistic Support (CALS) Test Network is conducting tests of the military standard for the Automated Interchange of Technical Information (MIL-STD-1840A) and its companion suite of military specifications. The CTN is a DoD-sponsored confederation of voluntary participants from industry and government, managed jointly by a technical staff at Air Force Logistics Command (AFLC) and Lawrence Livermore National Laboratory (LLNL). The objective of CTN tests is to demonstrate and evaluate the interchange and functional use of digital data information between industry and government using the CALS standards. The CTN Information Exchange (CTN Info-X) is a combination of information services for participants and sponsors of the work of the CALS Test Network. This manual tells how to access and use the CALS Info-X. DOE

N90-20905# Virginia Univ., Charlottesville. Dept. of Computer Science.
IMPLEMENTATION OF A HYPERCUBE DATABASE SYSTEM Annual Report, Mar. 1989 - Feb. 1990
John L. Pfaltz, S. H. Son, and James C. French Feb. 1990 28 p
(Contract DE-FG05-88ER-25063)
(DE90-008440; DOE/ER-25063/2; UVA-527387/CS90/102)
Avail: NTIS HC A03/MF A01

This year can be fairly called one of implementation. A great many low-level modules that are needed for any database system, together with functional implementations of various syntactic constructs of ADAMS were coded and tested. Moreover, these were integrated into three basic system components: the language preprocessor, the persistent dictionary, and the run-time system, to create a complete working database system. Representative application programs using persistent ADAMS elements were written and executed using the system. To be sure, not all of the components work as effectively as perferred and the level of parallelism that was expected was not obtained. Because of this a fundamental redesign of the run-time system was begun and some of its component servers are described in later sections. DOE

N90-20906# EG and G Energy Measurements, Inc., Las Vegas, NV.
A MODEL RESEARCH ARCHIVE: ARCHIVE AND RESEARCH IMPLICATIONS FOR ORIGINAL RECORDS AND SUPPORT DOCUMENTS
William A. Fisher Dec. 1989 14 p Presented at the Scientific and Technical Information Coordinating Group Meeting, Washington, DC, 10 Dec. 1989
(Contract DE-AC08-88NV-10617)
(DE90-008246; EGG-10617-1066; CONF-891281-1) Avail: NTIS HC A03/MF A01

The Office of Scientific and Technical Information (OSTI) and the National Technical Information Service (NTIS) maintain a well organized system to classify, store and retrieve reports of DOE funded research. However, there is no practicable automated system that fully addresses the storage, maintenance, and retrieval of information contained in the original research data from which the reports were generated. These data are the records that record the conditions and limits of research projects and the data derived from experiments and tests. They include field notebooks, commentary, descriptions of instruments used, project officers reports and observations of the biota and the environment. These documents contain significant original research data, much of which cannot be reproduced in a laboratory and some, will never be attempted again. The data are priceless even in their present semi-organized state. However, depending upon the institution having custody, there is considerable danger that many of these records may be lost or deteriorate in time. Then, on increasing occasion, the researcher is often faced with an insurmountable volume of information. The very magnitude of the reports digested often results in a paucity of information in the midst of plenty. If specific information contained within these records can be preserved and made fully accessible to authorized researchers reflecting upon modern questions, the impact will have scientific, technology transfer, or commercial implications. The data, while priceless, will increase in value and be more likely to be preserved if they can be organized into an information retrievable format. DOE

N90-20907# Sandia National Labs., Albuquerque, NM. Diagnostics Theory Div.
DESIGNING AN EXPERIMENTERS DATABASE USING THE NIJSSEN INFORMATION ANALYSIS METHODOLOGY (NIAM)
Michael J. Eaton 1990 9 p Presented at the 1990 Digital Equipment Corporation User's Society Meeting, New Orleans, LA, 7-11 May 1990
(Contract DE-AC04-76DP-00789)
(DE90-008548; SAND-90-0746C; CONF-900580-2) Avail: NTIS HC A02/MF A01

This paper presents a discussion of the use of the Nijssen Information Analysis Methodology (NIAM) in the design of an experimenters database. This database is used by physicists and technicians to describe the configuration and diagnostic systems used on Sandia National Laboratories Particle Beam Fusion Accelerator II (PBFA II). The design of this database presented some unique challenges because of the large degree of flexibility required to enable timely response to changing experimental configurations. The NIAM user-oriented technique proved to be invaluable in translating experimenter's requirements into an information model and then to a normalized relational design. DOE

N90-20908# Air Force Inst. of Tech., Wright-Patterson AFB, OH. School of Systems and Logistics.
AN EMPIRICAL TEST OF A COMPREHENSIVE MODEL FOR PREDICTING SUCCESSFUL INFORMATION SYSTEMS IMPLEMENTATION M.S. Thesis
Brian J. Magers Dec. 1989 144 p
(AD-A218124; AFIT/GIR/LSR/89D-5) Avail: NTIS HC A07/MF A01 CSCL 05/2

An Empirical Test of a Comprehensive Model for Predicting Successful Information Systems Implementation is discussed. Management Information Systems, User Satisfaction, Information Systems, Successful Information Systems, and Systems Analysis is included. GRA

N90-20909# Air Force Inst. of Tech., Wright-Patterson AFB, OH.
REAL-TIME CONCURRENCY CONTROL AND TRANSACTION SCHEDULING M.S. Thesis - Florida Univ.
Ronnie Edge 1989 100 p
(AD-A218162; AFIT/CI/CIA-89-180) Avail: NTIS HC A05/MF A01 CSCL 12/5

Existing real time concurrency control and scheduling techniques are inadequate for controlling the execution of transactions in a real time database system. Some of these techniques place unnecessary restrictions of the concurrent execution of tasks in order to ensure they are executed correctly. Several of these mechanisms lack modularity, an important property in database concurrency control. Most of these real time scheduling mechanisms lack the flexibility necessary to schedule both periodic and event-driven transactions to meet their timing constraints. The desired properties of concurrency control and the desired properties and priority management issues of real time transaction scheduling are examined. A survey of some existing real time concurrency control and scheduling mechanisms are presented and evaluated. A new integrated real time concurrency control and transaction scheduling mechanism, teamed the dataflow scheduler, is presented. This scheduling technique meets all of the desired properties of concurrency control and provides more flexibility than existing real time techniques. A roll-forward approach to data item conflict resolution is used by the scheduler. Simulation results show that this method performs better in meeting transactions deadlines that restarting or rolling back a transaction. GRA

N90-20659*# Evans and Sutherland Computer Corp., Salt Lake City, UT.
DESIGN CONSIDERATIONS FOR A SPACE DATABASE
Lance M. Moss *In* NASA, Lyndon B. Johnson Space Center, Graphics Technology in Space Applications (GTSA 1989) Aug. 1989 p 49-53 (For primary document see N90-20651 13-60)
Avail: NTIS HC A11/MF A02 CSCL 05B

83 ECONOMICS AND COST ANALYSIS

Includes cost effectiveness studies.

No abstracts in this category.

84 LAW, POLITICAL SCIENCE AND SPACE POLICY

Includes NASA appropriation hearings; aviation law; space law and policy; international law; international cooperation; and patent policy.

No abstracts in this category.

85 URBAN TECHNOLOGY AND TRANSPORTATION

Includes applications of space technology to urban problems; technology transfer; technology assessment; and surface and mass transportation.

For related information see also *03 Air Transportation and Safety, 16 Space Transportation,* and *44 Energy Production and Conversion.*

No abstracts in this category.

88 SPACE SCIENCES (GENERAL)

No abstracts in this category.

89 ASTRONOMY

Includes radio, gamma-ray, and infrared astronomy, and astrometry.

N90-20910 Leicester Univ. (England).
EXOSAT OBSERVATIONS OF SEYFERT TYPE GALAXIES Ph.D. Thesis
Tracey Jane Turner 1988 213 p
Avail: Univ. Microfilms Order No. BRD-86041

Analysis and results are presented from EXOSAT observations of Seyfert type active galactic nuclei (AGN). The sample chosen for study are 48 hard x ray selected Seyfert type AGN including 29 of the emission line AGN in the Piccinotti sample, making this the largest such survey to date. EXOSAT, its detectors and methods of data analysis, are detailed with emphasis on background techniques. One of the most important results from EXOSAT data is the discovery that rapid variability (factor 2 over a few thousand seconds) is common in AGN. No evidence is found in the sample sources for any characteristic timescales of variability. Combining EXOSAT LE and ME data allowed broadband x ray spectra over the range 0.1 to 10 keV to be obtained. Spectra in the approximately 2 to 10 keV range are found to be well described by a simple power law. The distribution of spectral indices across the sample can be approximated by a Gaussian distribution of mean alpha = 0.70 and sigma = 0.17. The spectra are not all consistent with this mean at the 90 percent confidence level and there must be some intrinsic spread in AGN slopes. This spread can be constrained to less than 0.14. EXOSAT has also revealed a significant number of sources with complex soft x ray spectra. These include spectra with a second spectral component at soft x ray energies and sources with leaky absorbing columns. Evidence that soft excess components occur in at least 50 percent of Seyfert type AGN, together with detection of rapid variability in the soft component provides the strongest support to date for an accretion disk model for AGN. Dissert. Abstr.

N90-20911*# National Aeronautics and Space Administration. Goddard Space Flight Center, Greenbelt, MD.
BIBLIOGRAPHY OF SPATIAL INTERFEROMETRY IN OPTICAL ASTRONOMY
Daniel Y. Gezari, Francois Roddier, and Claude Roddier (National Optical Astronomy Lab. Tucson, AZ.) Feb. 1990 234 p
(NASA-TM-100754; Rept-90-068; NAS 1.15:100754) Avail: NTIS HC A11/MF A02 CSCL 03A

The Bibliography of Spatial Interferometry in Optical Astronomy is a guide to the published literature in applications of spatial interferometry techniques to astronomical observations, theory and

instrumentation at visible and infrared wavelengths. The key words spatial and optical define the scope of this discipline, distinguishing it from spatial interferometry at radio wavelengths, interferometry in the frequency domain applied to spectroscopy, or more general electro-optics theoretical and laboratory research. The main bibliography is a listing of all technical articles published in the international scientific literature and presented at the major international meetings and workshops attended by the spatial interferometry community. Section B summarizes publications dealing with the basic theoretical concepts and algorithms proposed and applied to optical spatial interferometry and imaging through a turbulent atmosphere. The section on experimental techniques is divided into twelve categories, representing the most clearly identified major areas of experimental research work. Section D, Observations, identifies publications dealing specifically with observations of astronomical sources, in which optical spatial interferometry techniques have been applied. Author

N90-20912# Massachusetts Inst. of Tech., Cambridge. Research Lab. of Electronics.
MARK 3 INTERFEROMETER Final Report, 1 Apr. 1988 - 30 Jun. 1989
David H. Staelin, John W. Barrett, Edward J. Kim, and Howard R. Stuart 22 Jan. 1990 8 p
(Contract N00014-88-K-2016)
(AD-A217188) Avail: NTIS HC A02/MF A01 CSCL 03/1

This work is a continuation of that begun under Naval Research Laboratory Contracts N00014-84-C-2082 and N00014-86-C-2114. All three of these contracts involved participation in the development and testing of the Mark-III stellar interferometer at the Mount Wilson Observatory in California. This instrument employs a two-color technique to reduce position errors due to atmospheric turbulence, and can operate with four possible baseline configurations ranging from 9 to 20 meters. Despite its function as a technology development platform, it is also capable of stellar separation and stellar diameter measurements with nearly unprecedented accuracy and sensitivity. The major contributions of this work are the development of a dispersed-fringe group delay measurement system which can boost the system sensitivity be several stellar magnitudes, and the initial stages of development of an infrared capability, which should increase the future scientific interest of the facility. GRA

N90-20913# Illinois Univ., Urbana-Champaign.
DESIGN AND PERFORMANCE ANALYSIS OF ADAPTIVE OPTICAL TELESCOPES USING LASER GUIDE STARS Ph.D. Thesis
Byron MacMaster Welsh 1989 287 p
(Grant NSF ATM-88-11771)
(AD-A218025; AFIT/CI/CIA-89-155) Avail: NTIS HC A13/MF A02 CSCL 03/1

Atmospheric turbulence severely limits the resolution of ground-based astronomical telescopes. In good seeing conditions at the best observatory sites, resolution at visible wavelengths is typically limited to approx. 1 sec of arc. During the past 15 years adaptive optical systems using electrically deformable mirrors have been developed to compensate for turbulence effects. Unfortunately, these systems require bright reference sources adjacent to the object of interest and can be used to observe only the brightest stars. Artificial guide stars suitable for controlling an adaptive imaging system can be created in the upper atmosphere by using a laser to excite either Rayleigh backscattering in the stratosphere or resonance backscattering in the mesospheric sodium layer. The design requirements of a laser-guided adaptive telescope, as well as the expected imaging performance, are discussed. Analytical expressions giving the performance of a class of adaptive optics systems using slope sensors are derived. We show that a two-meter, ground-based, laser-guided telescope can achieve imaging performance levels at visible wavelengths nearly matching those of the Hubble Space Telescope (HST). Design examples, including lidar systems for atmospheric research and laser-guided telescopes, are studied in detail. GRA

90 ASTROPHYSICS

Includes cosmology; celestial mechanics; space plasmas; and interstellar and interplanetary gases and dust.
For related information see also *75 Plasma Physics*.

N90-20914*# Washington Univ., Seattle. Dept. of Astronomy.
THE INTER-OUTBURST BEHAVIOR OF CATACLYSMIC VARIABLES
Paula Szkody, Janet A. Mattei, Elizabeth O. Waagen (American Association of Variable Star Observers, Cambridge, MA.), and Clay Stablein 1990 27 p
(Grant NsG-5395)
(NASA-CR-186374; NAS 1.26:186374) Avail: NTIS HC A03/MF A01 CSCL 03B

Existing International Ultraviolet Explorer (IUE) and American Association of Variable Star Observers (AAVSO) archive data was used to accomplish a large scale study of what happens to the ultraviolet flux of accretion disk systems during the quiescent intervals between outbursts and how it relates to the preceding outburst characteristics of amplitude and width. The data sample involved multiple IUE observations for 16 dwarf novae and 8 novae along with existing optical coverage. Results indicate that most systems show correlated ultraviolet (UV) flux behavior with interoutburst phase, with 60 percent of the dwarf novae and 50 percent of the novae having decreasing flux trends while 33 percent of the dwarf novae and 38 percent of the novae show rising UV flux during the quiescent interval. All of the dwarf novae with decreasing UV fluxes at 1475A have orbital periods longer than 4.4 hours, while all (except BV Cen) with flat or rising fluxes at 1475A have orbital periods less than two hours. There are not widespread correlations of the UV fluxes with the amplitude of the preceding outburst and no correlations with the width of the outburst. From a small sample (7) that have relatively large quiescent V magnitude changes between the IUE observations, most show a strong correlation between the UV and optical continuum. Interpretation of the results is complicated by not being able to determine how much the white dwarf contributes to the ultraviolet flux. However, it is now evident that noticeable changes are occurring in the hot zones in accreting systems long after the outburst, and not only for systems that are dominated by the white dwarf. Whether these differences are due to different outburst mechanisms or to changes on white dwarfs which provide varying contributions to the UV flux remains to be determined. Author

N90-20915# Stanford Linear Accelerator Center, CA.
THE INEVITABLE UNIVERSE: PARKER-RHODES' PECULIAR MIXTURE OF ONTOLOGY AND PHYSICS
H. Pierre Noyes Dec. 1989 21 p Presented at the 11th Annual International Meeting of the Alternative Natural Philosophy Association, Cambridge, England, 14-17 Sep. 1989
(Contract DE-AC03-76SF-00515)
(DE90-006453; SU-SLAC-PUB-5161; CONF-8909297-1) Avail: NTIS HC A03/MF A01

When asked to give a lecture on Parker-Rhodes' physics, I was somewhat non-plused. I almost replied, what physics --- a point of view that Frederick expresses himself more than once in the book he was working on when he died. But that would be unjust. Whatever his view, I assert that the discovery of the Combinational Hierarchy is one of the most important discoveries --- or whatever you want to call it --- in physics made in this century. His calculation of the proton-electron mass ratio is also a fantastic result that we are still trying to come to grips with. And his insight into early cosmology --- what he called a cold big bang --- which appeared in an early version of the Theory of Indistinguishables, also had merit. His early universe is a lot closer to my own views now than I realized when I first encountered it. We will mention other insights as I go along. But his views are so different from those of anyone I know or knew, that I have decided to let him speak for himself by reading passages from his manuscript The Inevitable Universe, or TIU, which was still unpublished at the time of his death, and add a few comments on them. DOE

N90-20916# Los Alamos National Lab., NM.
M51'S SPIRAL STRUCTURE
S. Howard and G. G. Byrd (Alabama Univ., Tuscaloosa.) 1989 6 p Presented at the Astrophysics Meeting, Tuscalosa, AL, 3-7 Dec. 1989 Sponsored in part by Cray Research, Inc.
(Contract W-7405-eng-36; NSF RII-86-10669)
(DE90-007624; LA-UR-90-432; CONF-891278-1) Avail: NTIS HC A02/MF A01

The M51 system (NGC 5194/5195) provides an excellent problem both in spiral structure and in galaxy interactions. We present an analytic study of a computer experiment on the excitation mechanisms for M51's spiral arms and whether or not a halo is important for these mechanisms. This work extends previous numerical studies of the M51 system by including self-gravitation in a two component disk: gas and stars, and a dark halo. The analytic study provides two new observational constraints: the time (approx. 70 to 84 million years ago) and position angle of perigalacticon (300 degrees). By using these constraints and a simple conic approximation, the search for the companion's possible orbit is greatly simplified. This requires fewer N-body simulations than a fully self-gravitating orbit search. DOE

N90-20917# Air Force Geophysics Lab., Hanscom AFB, MA.
STUDY OF POSSIBLE SOLAR HEATING EFFECTS ON THERMOSONDE PROBES: ERROR ANALYSIS Interim Scientific Report
James H. Brown, Edmond Dewan, Edmund Murphy, and Peter Thomas 10 Jul. 1989 73 p
(AF Proj. 7670)
(AD-A218116; GL-TR-89-0178; ERP-1034) Avail: NTIS HC A04/MF A01 CSCL 03/2

Thermosonde data reveals a diurnal daytime shift in measured levels of C square (n) in the free atmosphere. The shift is manifested in two ways. First, an apparent offset in the smallest measured values of C square (n) exists. Secondly, the curve of the average profile shows an enhancement over nighttime profiles. Related optical and radar measurements have indicated that differences between day and night probably exist, but because of limited instrumental resolution and altitude capabilities those results are inconclusive. Several hypotheses were put forward concerning possible instrumental or solar based sources of data contamination. The possibility was examined that solar radiation causes probe heating with subsequent instrumental effects. Calculation, computer simulation, and direct measurements have shown that the sun heats the body of the probe sensor a couple of degrees above the ambient and that the level of heating depends upon the solar aspect angle and magnitude and direction of air flow over the probe. A small but insignificant ac type effect can result from improper probe geometry or probe mismatch together with a coupling of solar heating with velocity turbulence. Transient and dc type effects can occur, but measured, processed, and transmitted root mean square C square (n) information is not likely to contain instrumental contamination. GRA

91 LUNAR AND PLANETARY EXPLORATION

Includes planetology; and manned and unmanned flights.

For spacecraft design or space stations see *18 Spacecraft Design, Testing and Performance.*

No abstracts in this category.

92 SOLAR PHYSICS

Includes solar activity, solar flares, solar radiation and sunspots.

For related information see *93 Space Radiation.*

No abstracts in this category.

93 SPACE RADIATION

Includes cosmic radiation; and inner and outer earth's radiation belts.

For biological effects of radiation see *52 Aerospace Medicine.* For theory see *73 Nuclear and High-Energy Physics.*

N90-20918*# Hawaii Univ., Honolulu. Inst. of Astronomy.
STUDIES OF THE EVOLUTION OF THE X RAY EMISSION OF CLUSTERS OF GALAXIES Final Technical Report, 1 Jul. 1988 - 31 Dec, 1989
J. Patrick Henry 6 Apr. 1990 21 p
(Grant NAG8-738)
(NASA-CR-186471; NAS 1.26:186471) Avail: NTIS HC A03/MF A01 CSCL 03B

The x ray luminosity function of clusters of galaxies was determined at different cosmic epoches using data from the Einstein Observatory Extended Medium Survey. The sample consisted of 67 x ray selected clusters that were grouped into three redshift shells. Evolution was detected in the x ray properties of clusters. The present volume density of high luminosity clusters was found to be greater than it was in the past. This result is the first convincing evidence for evolution in the x ray properties of clusters. Investigations into the constraints provided by these data on various Cold Dark Matter models are underway. Author

99 GENERAL

N90-20919# Rensselaer Polytechnic Inst., Troy, NY. Office of Minority Student Affairs.
ONR (OFFICE OF NAVAL RESEARCH) SUMMER SCHOLARS FOR THE 1989 PREFACE PROGRAM Final Technical Report, Apr. - Dec. 1989
Mark D. Smith 31 Dec. 1989 14 p
(Contract N00014-89-J-1857)
(AD-A217746) Avail: NTIS HC A03/MF A01 CSCL 05/5

PREFACE, a two-week residential program for disadvantaged students, women and members of ethnic minority groups historically underrepresented in scientific, technological and engineering professions, will celebrate its thirteenth summer program in 1990. PREFACE is designed to facilitate a broader and deeper understanding of engineering and related professional career options, and the kinds of competencies and expectations of engineering faculty and professionals on the collegiate and practioner levels. The most unique feature of PREFACE is its linking the development of engineering professionals (theoretical) and the practice and application of engineering and scientific principles (practical). Participants have the opportunity to learn what engineering is from experts in the various fields of engineering and observe how principles of engineering are applied in industrial and research settings. This summer experience serves to clarify the kinds of knowledge and skills essential to successfully complete and engineering degree. GRA

Typical Subject Index Listing

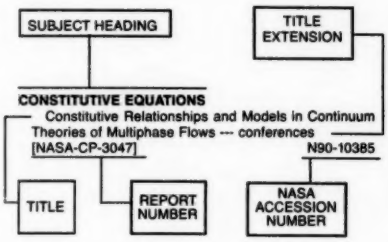

The subject heading is a key to the subject content of the document. Titles, report numbers, and accession numbers of pertinent documents are provided under each subject heading. When the title is insufficiently descriptive of the document content, a title extension has been added, separated from the title by three hyphens. The report number helps to indicate the type of document cited (e.g., NASA report, NASA translation, NASA contractor report). The NASA accession number is the number by which the document abstracts are arranged in this journal and by which the document is sold or requested. The titles, with title extensions if present, are arranged under each subject heading in ascending accession number order. The subject headings have been selected from the latest revision of the *NASA Thesaurus* (NASA SP-7064).

A

ABLATION
Y1Ba2Cu3O(7-x) laser-ablation plume dynamics measurement by nanosecond response ion probe: Comparison with optical measurements
[DE90-007658] N90-20375

ACCELERATION (PHYSICS)
Resolved motion rate and resolved acceleration servo-control of wheeled mobile robots
[DE90-002585] N90-20399
Collective ion acceleration in high current relativistic electron beams
[DE90-006328] N90-20821

ACCELERATION STRESSES (PHYSIOLOGY)
Parachute opening shocks during high speed ejections: Normalization N90-20056

ACCELERATION TOLERANCE
Development of acceleration exposure limits for advanced escape systems N90-20055
Parachute opening shocks during high speed ejections: Normalization N90-20056
The +Gz protection in the future: Review of scientific literature
[AD-A217887] N90-20623

ACCESS CONTROL
The contour model architecture and assembly language
[AD-A217114] N90-20697

ACCIDENTS
A guide to performing and documenting safety analyses
[DE90-008687] N90-20260

ACCRETION DISKS
The inter-outburst behavior of cataclysmic variables
[NASA-CR-186374] N90-20914

ACCURACY
An improved airborne wind measurement technique for the NAE (National Aeronautical Establishment) Twin Otter
[AD-A217978] N90-20575

ACIDS
Infrared and X ray photoelectron spectroscopy studies of the polyimide/metal interface
[AD-A218249] N90-20179

ACOUSTIC EMISSION
Spallation of oxide scales from 20 percent Cr/25 percent Ni/Nb stainless steel
[AERE-R-13464] N90-20189

ACOUSTIC MICROSCOPES
Nondestructive testing of ceramics by acoustic microscopy
[AERE-R-13350] N90-20411

ACOUSTIC PROPERTIES
Localization and delocalization in periodic one-dimensional dynamic systems
[AD-A217939] N90-20797
Air Force Boom Event Analyzer Recorder (BEAR): Sysstem description
[AD-A218048] N90-20800

ACOUSTIC VELOCITY
Geometric scale of interaction between moving shock and stationary thermal layer
[AD-A217769] N90-20344

ACOUSTICAL HOLOGRAPHY
High-resolution acoustical imaging N90-20793

ACOUSTICS
Modeling and classification of acoustic transients by speech recognition techniques
[AD-A218070] N90-20277
VAPEPS user's reference manual, version 5.0
[NASA-CR-180781] N90-20713

ACRYLIC RESINS
Investigation into the mechanism of polymer thread drag reduction
[AD-A217492] N90-20329

ACTIVATION ENERGY
Supercooling and germ formation N90-20242
Metal alkoxides: Models for metal oxides. Alkoxide ligands in early transition metal organometallic chemistry
[DE90-007523] N90-20869

ACTIVE CONTROL
The application of active controls technology to a generic hypersonic aircraft configuration
[NASA-TM-101689] N90-20071
Active control of the forced and transient response of a finite beam
[NASA-CR-181957] N90-20430

ACTIVE GALACTIC NUCLEI
EXOSAT observations of Seyfert type galaxies N90-20910

ACTIVITY (BIOLOGY)
Ceramic oxide thin film formation utilizing biological processes
[DE90-008599] N90-20225

ACTUATORS
Aerospace induction motor actuators driven from a 20-kHz power link
[NASA-TM-102482] N90-20085
Sensor and actuator selection for fault-tolerant control of flexible structures
[AD-A217384] N90-20433

ADAPTIVE CONTROL
Multi-dimensional LADAR tracking and adaptive grasping for spaceborne assembly of SDI (Strategic Defense Initiative) platforms
[AD-A218236] N90-20279
A learning regulator for the plane longitudinal movement
[ETN-90-95381] N90-20695
Robust adaptive nonlinear control under extended matching conditions
[AD-A217684] N90-20744

ADAPTIVE FILTERS
Evaluation of an adaptive unstructured remeshing technique for integrated fluid-thermal-structural analysis
[NASA-TM-102611] N90-20426

ADAPTIVE OPTICS
Design and performance analysis of adaptive optical telescopes using laser guide stars
[AD-A218025] N90-20913

ADDITIVES
Infrared absorption study of zinc-doped silicon
[DE90-007779] N90-20164
Non-noble electrocatalysts for alkaline fuel cells N90-20470

ADHESION
Oxygen concentrations on surfaces of carbon fibers
[AD-A217724] N90-20152
Determination of flow-regime boundaries for cohesive particles
[DE90-007425] N90-20332

ADRENAL GLAND
The effects of high intensity cycle exercise on sympatho-adrenal-medullary response patterns
[AD-A217962] N90-20628

ADSORBENTS
An experimental investigation of the thermal conductivity of porous adsorbents
[AD-A217854] N90-20899

ADVANCED LAUNCH SYSTEM (STS)
Aerospace induction motor actuators driven from a 20-kHz power link
[NASA-TM-102482] N90-20085

ADVANCED VERY HIGH RESOLUTION RADIOMETER
Correlation of AVHRR imagery with sub-surface features in California current
[AD-A218184] N90-20607

ADVECTION
A sub-cloud layer vorticity budget analysis for two microburst-producing storms from jaws dual-Doppler data
[AD-A218180] N90-20599
A case study of a quasi-stationary tropical convective line
[AD-A218325] N90-20604

AEROBRAKING
Use of random Martian atmosphere to evaluate potential entry guidance schemes
[NASA-TM-102606] N90-20122

AERODYNAMIC CHARACTERISTICS
Experimental and theoretical aerodynamic characteristics of a high-lift semispan wing model
[NASA-TP-2990] N90-20046
Unsteady free-wake viscous aerodynamic analysis of helicopter rotors
[AD-A217166] N90-20048
Windblast protection for advanced ejection seats N90-20063

AERODYNAMIC CONFIGURATIONS
Experimental and theoretical aerodynamic characteristics of a high-lift semispan wing model
[NASA-TP-2990] N90-20046

AERODYNAMIC FORCES
Windblast protection for advanced ejection seats N90-20063

AERODYNAMIC HEATING
Analysis of flow-, thermal-, and structural-interaction of hypersonic structures subjected to severe aerodynamic heating
[AD-A217882] N90-20053
The application of active controls technology to a generic hypersonic aircraft configuration
[NASA-TM-101689] N90-20071

AERODYNAMIC LOADS
Aeroelastic characteristics of aircraft with circulation control wings N90-20070

AERODYNAMIC NOISE
Air Force Boom Event Analyzer Recorder (BEAR): Sysstem description
[AD-A218048] N90-20800

AERODYNAMIC STABILITY
The application of active controls technology to a generic hypersonic aircraft configuration
[NASA-TM-101689] N90-20071

AERODYNAMICS
Unsteady free-wake viscous aerodynamic analysis of helicopter rotors
[AD-A217166] N90-20048

Aerodynamic analysis of a US Navy and Marine Corps unmanned air vehicle
[AD-A216282] N90-20077
ETO (Earth-To-Orbit): A trajectory program for aerospace vehicles
[AD-A218157] N90-20103
Aerodynamic and kinetic processes in flames
[AD-A217796] N90-20176
Analysis of small-scale rotor hover performance data
[NASA-TM-102271] N90-20325
A comparison of two-and three-dimensional S809 airfoil properties for rough and smooth HAWT (Horizontal-Axis Wind Tunnel) rotor operation
[DE89-009512] N90-20492
Operational computer graphics in the flight dynamics environment N90-20668

AEROELASTICITY
Using transonic small disturbance theory for predicting the aeroelastic stability of a flexible wind-tunnel model
[NASA-TM-102617] N90-20047
Aeroelastic characteristics of aircraft with circulation control wings N90-20070
Static aeroelastic analysis of a three-dimensional generic wing
[NASA-TM-102231] N90-20087

AEROSOLS
Multiple versus single scattering of terrestrial infrared longwave radiation in an aerosol-laden planetary boundary layer
[AD-A217709] N90-20272
The receiving system of a dual dye lidar to study molecular and aerosol densities at the base of the stratosphere
[AD-A218286] N90-20581

AEROSPACE ENGINEERING
Power conditioning techniques
[NASA-TM-102577] N90-20301
Numerical simulation methods of incompressible flows and an application to the space shuttle main engine
[NASA-TM-100038] N90-20333
Bearing and gear steels for aerospace applications
[NASA-TM-102529] N90-20391
Engineering visualization utilizing advanced animation N90-20664

AEROSPACE ENVIRONMENTS
Efficient utilization of graphics technology for space animation N90-20663

AEROSPACE MEDICINE
Ejection seat training of jet pilots and weapon system officers at the German Air Force School of Aviation Medicine N90-20061
The United States Air Force School of Aerospace Medicine: Special report
[AD-A217740] N90-20622

AEROSPACE SAFETY
Requirements for protective pressure suits for the Hermes spacecrew N90-20065

AEROSPACE SYSTEMS
Trajectory optimization in the presence of constraints
[AD-A218271] N90-20104
Measurements of the interaction of high-voltage biassed conductors with the ionosphere
[AD-A218285] N90-20580
Space in warfare
[AD-A217527] N90-20782

AEROSPACE VEHICLES
Development of acceleration exposure limits for advanced escape systems N90-20055

AEROTHERMODYNAMICS
Evaluation of an adaptive unstructured remeshing technique for integrated fluid-thermal-structural analysis
[NASA-TM-102611] N90-20426

AEROTHERMOELASTICITY
The application of active controls technology to a generic hypersonic aircraft configuration
[NASA-TM-101689] N90-20071

AFTERBURNING
Relativistic klystron afterburner simulation techniques
[DE90-008539] N90-20305

AGING (MATERIALS)
Hydrogen, thermal ageing and the role of carbides in fatigue of a high strength steel
[AERE-R-13599] N90-20183
Ageing effects in welded cast CF3 stainless steel
[AERE-R-13559] N90-20186
The ageing effect of the matrix-reinforcement interface on the ageing response of an aluminium 6061 alloy reinforced with 20vol percent SiC particulates
[AERE-R-13361] N90-20193
Positron annihilation spectroscopy: A nondestructive, submicroscopic characterization technique for structural polymers
[AD-A217748] N90-20226
Nine-year aging behavior of the ceramic flatpack resonator
[DE90-008044] N90-20412
Theory system reliability demonstration and burn-in design
[AD-A217775] N90-20416

AGRICULTURE
Relationship of radiometric field measurements of wheat in the Assis-Safra region, 1988
[INPE-4949-RPE/598] N90-20443

AIR
A technical and economic evaluation of oxygen-enriched combustion in diesel engines using water-emulsified fuels
[DE90-008095] N90-20394

AIR CONDITIONING EQUIPMENT
An expert system for the design of heating, ventilating, and air-conditioning systems
[AD-A218287] N90-20262

AIR COOLING
Transpiration cooling in hypersonic flight
[NASA-CR-186435] N90-20052

AIR DEFENSE
Comparison of oculometer and head-fixed reticle with voice or switch and touch panel for data entry on a generic tactical air combat display
[AD-A217231] N90-20646

AIR FLOW
Passive venting technique for shallow cavities
[NASA-CASE-LAR-14031-1] N90-20079
A comparison of two-and three-dimensional S809 airfoil properties for rough and smooth HAWT (Horizontal-Axis Wind Tunnel) rotor operation
[DE89-009512] N90-20492
Study of possible solar heating effects on thermosonde probes: Error analysis
[AD-A218116] N90-20917

AIR MASSES
Structure and dynamics of the Arizona monsoon boundary
[AD-A217378] N90-20586

AIR POLLUTION
Air pollution-caused changes in photosynthesis: Effects on plant growth and rhizosphere functions
[DE90-007184] N90-20501
The Terrain-Responsive Atmospheric Code (TRAC) project plan: Development of a hazardous materials dispersion modeling capability with application to ambient air monitoring network design
[DE90-007293] N90-20502

AIR QUALITY
Controlling Summer Heat Islands: Proceedings
[DE90-008075] N90-20508

AIR WATER INTERACTIONS
Theoretical modeling studies of the marine planetary
[AD-A217200] N90-20567
Southern oscillation in the OSU coupled upper ocean/atmosphere GCM
[DE90-008415] N90-20588
A modeling study of the cloud-topped marine boundary layer
[AD-A218103] N90-20594

AIRBORNE EQUIPMENT
An improved airborne wind measurement technique for the NAE (National Aeronautical Establishmant) Twin Otter
[AD-A217978] N90-20575

AIRBORNE/SPACEBORNE COMPUTERS
Space station Simulation Computer System (SCS) study for NASA/MSFC. Volume 1: Overview and summary
[NASA-CR-183840] N90-20113
Animation graphic interface for the space shuttle onboard computer N90-20667

AIRCRAFT ACCIDENTS
A review of the analytical simulation of aircraft crash dynamics
[NASA-TM-102595] N90-20068

AIRCRAFT COMPARTMENTS
Floor pull test of a transport airframe section
[DOT/FAA/CT-TN88/14] N90-20072

AIRCRAFT CONSTRUCTION MATERIALS
Compendium of abstracts and viewgraphs.
[AD-A217189] N90-20140

AIRCRAFT DESIGN
Implications of Advanced Technologies for Air and Spacecraft Escape
[AGARD-CP-472] N90-20054
Development of an ejection seat specification for a new fighter aircraft N90-20057
Compression pylon
[NASA-CASE-LAR-13777-1] N90-20078
The NASA digital VGH program. Exploration of methods and final results. Volume 1: Development of methods
[NASA-CR-181909-VOL-1] N90-20081
The NASA digital VGH program. Exploration of methods and final results. Volume 3: B 727 data 1978-1980: 1765 hours
[NASA-CR-181909-VOL-3] N90-20082
The NASA digital VGH program: Exploration of methods and final results. Volume 4: B 747 data 1978-1980, 1689 hours
[NASA-CR-181909-VOL-4] N90-20083
The NASA digital VGH program: Exploration of methods and final results. Volume 5: DC 10 data 1981-1982, 129 hours
[NASA-CR-181909-VOL-5] N90-20084

AIRCRAFT LANDING
Airplane takeoff and landing performance monitoring system
[NASA-CASE-LAR-13734-1-CU] N90-20096
Runaway rubber removal
[AD-A218349] N90-20100

AIRCRAFT NOISE
Noise of a simulated installed model counterrotation propeller at angle-of-attack and takeoff/approach conditions
[NASA-TM-102440] N90-20794
Lateral attenuation of military aircraft flight noise
[AD-A218041] N90-20799

AIRCRAFT PERFORMANCE
Potential role of avionics in escape systems N90-20060
The implementation and operation of a variable-response electronic throttle control system for a TF-104G aircraft
[NASA-TM-101696] N90-20086
Airplane takeoff and landing performance monitoring system
[NASA-CASE-LAR-13734-1-CU] N90-20096

AIRCRAFT RELIABILITY
Activities report in civil aviation
[ETN-90-95471] N90-20067
Airworthiness and flight characteristics evaluation of the McDonnell Douglas Helicopter Corporation (MDHC) 530FF helicopter
[AD-A218253] N90-20076
The NASA digital VGH program. Exploration of methods and final results. Volume 1: Development of methods
[NASA-CR-181909-VOL-1] N90-20081
The NASA digital VGH program. Exploration of methods and final results. Volume 3: B 727 data 1978-1980: 1765 hours
[NASA-CR-181909-VOL-3] N90-20082
The NASA digital VGH program: Exploration of methods and final results. Volume 4: B 747 data 1978-1980, 1689 hours
[NASA-CR-181909-VOL-4] N90-20083
The NASA digital VGH program: Exploration of methods and final results. Volume 5: DC 10 data 1981-1982, 129 hours
[NASA-CR-181909-VOL-5] N90-20084

AIRCRAFT TIRES
Runaway rubber removal
[AD-A218349] N90-20100

AIRFOIL PROFILES
Experimental and theoretical aerodynamic characteristics of a high-lift semispan wing model
[NASA-TP-2990] N90-20046

AIRFOILS
Numerical simulations of supersonic flow through oscillating cascade sections
[NASA-TM-103100] N90-20051
A comparison of two-and three-dimensional S809 airfoil properties for rough and smooth HAWT (Horizontal-Axis Wind Tunnel) rotor operation
[DE89-009512] N90-20492

AIRFRAMES
Floor pull test of a transport airframe section
[DOT/FAA/CT-TN88/14] N90-20072
Compendium of abstracts and viewgraphs.
[AD-A217189] N90-20140
Plan, formulate, and discuss a NASTRAN finite element model of the UH-60A helicopter airframe
[NASA-CR-181975] N90-20439

AIRGLOW
Spacecraft optical contamination environment
[AD-A218088] N90-20838
Optical instrumentation support for the airborne ionospheric observatory
[AD-A218207] N90-20839

AIRPORTS
Activities report in civil aviation
[ETN-90-95471] N90-20067
Airfields on antarctic glacier ice
[AD-A217638] N90-20097

ALASKA
Hypotheses testing of watershed/landscape dynamics in northern Alaska using digital analysis
[DE90-006721] N90-20450
A cloud climatology for the North Pacific area centered at Shemya, Alaska
[AD-A217334] N90-20585

ALBUMINS
Human serum albumin crystals and method of preparation
[NASA-CASE-MFS-28234-1] N90-20616
ALGAE
Design and operation of an outdoor microalgae test facility
[DE89-009493] N90-20608
Carbon and hydrogen metabolism of green algae in light and dark
[DE90-008648] N90-20612
ALGEBRA
Projective cohomology over a chain complex
[DE90-606958] N90-20788
ALGORITHMS
Viscous shock profiles and primitive formulations
[NASA-CR-182029] N90-20049
Experimental validation of extended image reconstruction using bispectral speckle interferometry
[DE90-008545] N90-20171
Numerical Arc Segmentation Algorithm for a Radio Conference-NASARC (version 4.0) technical manual
[NASA-TM-101453] N90-20264
Tomographic processing of synthetic aperture radar signals for enhanced resolution
[AD-A217178] N90-20265
Effects of additional interfering signals on adaptive array performance
[NASA-CR-186508] N90-20271
Meteor observations using the 50 MHz MENTOR imaging Doppler interferometer
[AD-A217908] N90-20276
High resolution radar target modeling using ARMA (Autoregressive Moving Average) models
[AD-A218212] N90-20278
Statistical equipment modeling for VLSI manufacturing
[DE90-008527] N90-20304
Parallel algorithms in the finite element approximation of flow problems
[AD-A217729] N90-20341
Massively-parallel computational fluid dynamics
[AD-A217732] N90-20342
Numerical modeling of airblast
[AD-A217993] N90-20347
The design and implementation of a position measuring system for a remotely controlled video camera
[AD-A218077] N90-20362
Control system design of the third flexible joint of PUMA 560 robot
[AD-A218075] N90-20405
Comparison of two matrix data structures for advanced CSM testbed applications
[NASA-CR-181951] N90-20421
Utilization of LANDSAT-5 and NOAA-9 satellite imagery in the identification of physical-chemical parameters of the water in the Guanabara Bay
[INPE-4761-TDL/349] N90-20445
Synopsis of early field test results from the gravity gradiometer survey system N90-20525
Methods for local gravity field approximation N90-20532
The effects of structure and source complexity on waveforms: Crustal structure of Tibet and the recovery of complex seismic sources
[AD-A218202] N90-20579
Downward shortwave surface irradiance from 17 sites for the FIRE/SRB Wisconsin experiment
[NASA-TM-102596] N90-20583
A prototype expert system to forecast severe winds in the western Mediterranean Sea
[AD-A218017] N90-20593
Three-dimensional medical image analysis using local dynamic algorithm selection on a multiple-instruction, multiple-data architecture
[AD-A218024] N90-20630
NYU (New York University) ultracomputer
[AD-A217167] N90-20688
(DURIP) Two-Processor Alliant FX/4 System
[AD-A217810] N90-20692
Simplified linear-time Jordan sorting and polygon clipping
[AD-A215110] N90-20693
An algorithm for efficient estimation of superimposed exponential signals
[AD-A217218] N90-20698
Experiments in finding neural network weights
[DE90-007696] N90-20702
ISLE (Image and Signal Processing LISP Environment) reference manual
[DE90-007858] N90-20705
Parts of recognition
[AD-A217694] N90-20714
Probabilistic analysis of algorithms for NP-complete problems
[AD-A217880] N90-20716
Development of computer software for the analysis and design of modern control systems
[AD-A217924] N90-20717
Free indexation: Combinatorial analysis and a compositional algorithm
[AD-A218219] N90-20724
Optimization of series expressions. Part 1: User's manual for the series macro package
[AD-A218220] N90-20725
Performance of concurrency control algorithms in distributed systems
[AD-A218280] N90-20727
Almost-optimum parallel speed-ups of algorithms for bipartite matching and related problems
[AD-A215111] N90-20728
Advanced parallel systems
[AD-A217175] N90-20731
Parallel computer graphics algorithms for the connection machine
[AD-A217300] N90-20733
Design of a simulation interface for a parellel computing environment
[DE90-008497] N90-20737
A time stepping algorithm for parallel computers
[DE90-008163] N90-20738
A model and implementation of multigrid for massively parallel computers
[DE90-008165] N90-20739
Implementation of midcourse tracking and correlation on massively parallel computers
[DE90-008166] N90-20740
Robotic mobility system: Road following algorithms
[AD-A218107] N90-20748
Stereo feature matching in disparity space
[AD-A218170] N90-20751
Maintaining bridge-connected and biconnected components on-line
[AD-A215107] N90-20754
Exact algorithms for output encoding, state assignment and four-level Boolean minimization
[AD-A217121] N90-20756
Algorithms for optimal processing of polarimetric radar data
[AD-A217330] N90-20758
Three-dimensional route planning for a cruise missile for minimal detection by observer
[AD-A218336] N90-20787
Lateral attenuation of military aircraft flight noise
[AD-A218041] N90-20799
Theoretical studies of spin-forbidden processes within the Breit-Pauli approximation
[AD-A217778] N90-20815
ALIGNMENT
Tensile film clamps and mounting block for the rheovibron and autovibron viscoelastometer
[NASA-CASE-LAR-13696-1] N90-20409
ALKALI METALS
Interactions of molecules with surfaces
[DE90-007555] N90-20806
ALKALINE BATTERIES
Oxygen electrodes for rechargeable alkaline fuel cells-II N90-20469
Non-noble electrocatalysts for alkaline fuel cells N90-20470
ALKYL COMPOUNDS
X ray specular reflection studies of silicon coated by organic monolayers (alkylsiloxanes)
[AD-A217418] N90-20213
ALTIMETERS
User's guide: Programs for processing altimeter data over inland seas
[NASA-TM-100730] N90-20572
ALTITUDE SICKNESS
Effects of dexamethasone and high terrestrial altitude on cognitive performance and affect
[AD-A217897] N90-20625
ALUMINIDES
An introduction to nickel aluminide alloy
[DE90-008565] N90-20207
Improved toughness alloys based on titanium aluminides
[AD-A218149] N90-20208
ALUMINUM
Advanced high-temperature batteries N90-20480
Stopping power for protons in Al for the whole range of velocities
[DE90-008558] N90-20810
ALUMINUM ALLOYS
Corrosion properties of Fe3Al in H2S-H2-H2O mixtures
[DE90-004936] N90-20167
The effect of the SiC/Al interface on matrix microstructure in 2xxx-SiCp metal matrix
[AERE-R-13591] N90-20184
Constitutive data acquisition and modelling in aluminium 2014 alloy
[AERE-R-13651] N90-20186
The ageing effect of the matrix-reinforcement interface on the ageing response of an aluminium 6061 alloy reinforced with 20vol percent SiC particulates
[AERE-R-13361] N90-20193
Evaluation of 2090-T8E48 aluminum-lithium plates
[AD-A217262] N90-20196
Through-the-thickness fatigue crack closure behavior in an aluminum alloy
[NASA-TM-102590] N90-20427
ALUMINUM GALLIUM ARSENIDES
Investigation of the technological effects on the coupling behavior of parallel GaAlAs rib waveguide
[ETN-90-95323] N90-20825
Differential measurements of the lateral photo effect in GaAs/AlGaAs heterostructures
[AERE-R-13557] N90-20861
ALUMINUM OXIDES
Experimentally determined wear behavior of an Al2O3-SiC composite from 25 to 1200 C
[NASA-TM-102549] N90-20130
Synthesis of alumina-coated SiC whiskers for production of SiC whisker-reinforced alumina composite materials
[DE90-007778] N90-20147
Techno-economic assessment of a carbothermic alumina reduction process
[DE90-007018] N90-20170
Tensile fracture toughness of ceramic materials: Effects of dynamic loading and elevated temperatures
[DE90-008329] N90-20223
AMBIENT TEMPERATURE
Advances in ambient temperature secondary lithium cells N90-20481
AMMUNITION
Evaluation of 2090-T8E48 aluminum-lithium plates
[AD-A217262] N90-20196
AMPLIFIERS
Performance of zig-zag slab regenerative ring amplifier laser system
[DE90-006995] N90-20371
AMPLITUDES
An algorithm for efficient estimation of superimposed exponential signals
[AD-A217218] N90-20698
AMPOULES
Method of preparing radially homogeneous mercury cadmium telluride crystals
[NASA-CASE-MFS-25786-2] N90-20896
ANALOGS
Condensed phase kinetic deuterium isotope effects in high energy phenomena: Mechanistic investigations and relationships
[AD-A217161] N90-20156
ANALYSIS (MATHEMATICS)
Institute for Computational Mechanics in Propulsion (ICOMP) fourth annual review, 1989
[NASA-TM-102519] N90-20769
ANALYZERS
A linear filtering technique for removal of low-frequency noise
[DE90-006183] N90-20296
ANGLE OF ATTACK
F-15B high angle-of-attack phenomena and spin prediction using bifurcation analysis
[AD-A217366] N90-20073
ANGULAR ACCELERATION
Design and testing of a noninteracting control loop for the dynamically tuned dry gyro
[NAL-TR-1017] N90-20350
ANISOTROPY
Shaping the insonifying pulse to optimise B-scans obtained in austenite
[AERE-R-13518] N90-20187
Scattering sources: A spherical harmonics expansion
[DE90-008724] N90-20711
ANNEALING
Systematics in positron annihilation lifetime analysis of high (Tc) superconducting transitions
[DE90-008361] N90-20884
ANNUAL VARIATIONS
US Navy regional climatic study of the Central East Asian coast and associated waters
[AD-A217448] N90-20587
ANODES
Impedance studies of Ni/Cd and Ni/H2 cells using the cell case as a reference electrode N90-20473
ANTARCTIC REGIONS
Gravity field of the Western Weddell Sea: Comparison of airborne gravity and Geosat derived gravity N90-20526
Satellite radar altimetry over ice. Volume 1: Processing and corrections of Seasat data over Greenland
[NASA-RP-1233-VOL-1] N90-20562

Satellite radar altimetry over ice. Volume 4: Users' guide for Antarctica elevation data from Seasat
[NASA-RP-1233-VOL-4] N90-20564

ANTENNA ARRAYS
Effects of additional interfering signals on adaptive array performance
[NASA-CR-186508] N90-20271
Performance of a 300 Mbps 1:16 serial/parallel optoelectronic receiver module
[NASA-TM-103110] N90-20302

ANTENNA RADIATION PATTERNS
An investigation of the extent of the fresnel region of aperture antennas with attention to superdirectivity
[AD-A217518] N90-20294

ANTHROPOMETRY
Software systems for modeling articulated figures N90-20677

ANTIFERROMAGNETISM
Magnetic properties of surfaces and interfaces
[DE90-007348] N90-20789

ANTIGRAVITY
The +Gz protection in the future: Review of scientific literature
[AD-A217887] N90-20623

ANTIMISSILE DEFENSE
Multi-dimensional LADAR tracking and adaptive grasping for spaceborne assembly of SDI (Strategic Defense Initiative) platforms
[AD-A218236] N90-20279
The thrust and parry of the SIOP (Single Integrated Operational Plan) and SDI
[AD-A217617] N90-20784

APERTURES
An investigation of the extent of the fresnel region of aperture antennas with attention to superdirectivity
[AD-A217518] N90-20294
Placement of multiple apertures for imaging telescopes
[DE90-006991] N90-20833

APPLICATION SPECIFIC INTEGRATED CIRCUITS
Product assurance technology for procuring reliable, radiation-hard, custom LSI/VLSI electronics
[NASA-CR-185854] N90-20281

APPLICATIONS PROGRAMS (COMPUTERS)
Satellite radar altimetry over ice. Volume 2: Users' guide for Greenland elevation data from Seasat
[NASA-RP-1233-VOL-2] N90-20563
TAE Plus: Transportable Applications Environment Plus tools for building graphic-oriented applications N90-20652
The Real Time Interactive Display Environment (RTIDE), a display building tool developed by Space Shuttle flight controllers N90-20654
Applications of graphics to support a testbed for autonomous space vehicle operations N90-20661

APPROXIMATION
Theory system reliability demonstration and burn-in design
[AD-A217775] N90-20416
Methods for local gravity field approximation N90-20532
High order filtering methods for approximating hyberbolic systems of conservation laws
[NASA-CR-182016] N90-20650
Computing mean responses in nonlinear models
[AD-A217642] N90-20700
Performance of concurrency control algorithms in distributed systems
[AD-A218280] N90-20727
Observer based compensators for nonlinear systems
[AD-A217426] N90-20760
An approximation theory for the identification of linear thermoelastic systems
[NASA-CR-182015] N90-20764
Spectral line shape code for multielectron emitters
[DE90-008526] N90-20853

ARCHITECTURE (COMPUTERS)
Space station Simulation Computer System (SCS) study for NASA/MSFC. Volume 3: Refined conceptual design report
[NASA-CR-183842] N90-20115
Space station Simulation Computer System (SCS) study for NASA/MSFC. Volume 4: Conceptual design report
[NASA-CR-183843] N90-20116
Joint services electronics program
[AD-A217961] N90-20311
Integrated circuits for avionics
[AD-A217964] N90-20312
Massively-parallel computational fluid dynamics
[AD-A217732] N90-20342
Robot navigation research using the HERMIES mobile robot
[DE90-001952] N90-20396
Robust performance of multiple tasks by a mobile robot
[DE90-001953] N90-20397
Swing-free movement of simply suspended objects employing parameter estimation
[DE90-002238] N90-20398
Transaction processing in a quality control laboratory
[DE90-004655] N90-20414
Approximate evaluation of reliability and related quantities via perturbation techniques
[AD-A218340] N90-20417
Three-dimensional medical image analysis using local dynamic algorithm selection on a multiple-instruction, multiple-data architecture
[AD-A218024] N90-20630
Adaptive associative-processing optical computing architectures
[AD-D014317] N90-20685
A unified approach to the synthesis of fully testable sequential machines
[AD-A217120] N90-20687
NYU (New York University) ultracomputer
[AD-A217167] N90-20688
Computer Science and Technology Board
[DE90-008292] N90-20690
A real-time parallel pipelined data-flow image-processing system
[DE90-008324] N90-20691
(DURIP) Two-Processor Alliant FX/4 System
[AD-A217810] N90-20692
The contour model architecture and assembly language
[AD-A217114] N90-20697
Using formal methods to develop a paradigm for software design
[DE90-005633] N90-20703
ISLE (Image and Signal Processing LISP Environment) reference manual
[DE90-007858] N90-20705
RIPE: An object-oriented Robot Independent Programming Environment
[DE90-008501] N90-20707
Joint Japanese-American Workshop on Future Trends in Logic Programming
[DE90-008343] N90-20709
A paradoxical result in unconditionally secure authentication codes, and an explanation
[DE90-008529] N90-20710
Technical specifications requirements: Automated reasoning applications
[DE90-008799] N90-20712
Advanced parallel systems
[AD-A217175] N90-20731
Robust planning and control using neural networks
[AD-A217216] N90-20732
Parallel computer graphics algorithms for the connection machine
[AD-A217300] N90-20733
Asynchronous design for parallel processing architectures
[AD-A217421] N90-20734
The Livermore distributed storage system: Implementation and experiences
[DE90-007257] N90-20735
Implementation of a control system test environment in UNIX
[DE90-007485] N90-20736
A parallel architecture for real-time simulation
[AD-A218321] N90-20741
Irredundant sequential machines via optimal logic synthesis
[AD-A217119] N90-20742
Hybrid intelligent perception system: Intelligent perception through combining artificial neural networks and an expert system
[DE90-007483] N90-20746
Computation and graphics in mathematical research
[DE90-008429] N90-20766
Towards SDS (Strategic Defense System) testing and evaluation: A collection of relevant topics
[AD-A217610] N90-20783

ARGON LASERS
Picosecond Laser Facility
[AD-A217784] N90-20384

ARITHMETIC
Euler's theorem for polynomials
[AD-A218148] N90-20774

ARMED FORCES (FOREIGN)
Physical performance and carbohydrate consumption in CF commandos during a 5-day field trial
[AD-A217204] N90-20619

ARMED FORCES (UNITED STATES)
Physical performance and carbohydrate consumption in CF commandos during a 5-day field trial
[AD-A217204] N90-20619

ARMOR
Evaluation of 2090-T8E48 aluminum-lithium plates
[AD-A217262] N90-20196

ARTIFICIAL INTELLIGENCE
Concept formation and generalization based on experimentation by an autonomous mobile robot
[DE90-001731] N90-20395
Parameter-scheduled trajectory planning for suppression of coupled horizontal and vertical vibrations in a flexible rod
[DE90-002313] N90-20435
Free indexation: Combinatorial analysis and a compositional algorithm
[AD-A218219] N90-20724
Artificial Intelligence (AI) Center of Excellence at the University of Pennsylvania
[AD-A217393] N90-20743
A locally constrained parallel activation model for diagnostic reasoning
[AD-A217808] N90-20747
CEREBRAL WEEVIL: A machine learning model for hemispheric categorization of complex visual patterns
[AD-A218143] N90-20749
An investigation of the locality of memory accesses during symbolic program execution
[AD-A218168] N90-20750
Stereo feature matching in disparity space
[AD-A218170] N90-20751
Location recognition using stereo vision
[AD-A218218] N90-20752
Three-dimensional route planning for a cruise missile for minimal detection by observer
[AD-A218336] N90-20787

ARTIFICIAL SATELLITES
A satellite simulation program
[AD-A218079] N90-20124
Distributed earth model/orbiter simulation N90-20671

ASCENT PROPULSION SYSTEMS
ETO (Earth-To-Orbit): A trajectory program for aerospace vehicles
[AD-A218157] N90-20103

ASSEMBLING
Component count and preliminary assembly considerations for large space truss structures
[NASA-TM-102604] N90-20121
Flexible automatic discrete parts assembly
[AD-A217401] N90-20256

ASSEMBLY LANGUAGE
The contour model architecture and assembly language
[AD-A217114] N90-20697

ASSOCIATIVE PROCESSING (COMPUTERS)
Adaptive associative-processing optical computing architectures
[AD-D014317] N90-20685

ASTRO MISSIONS (STS)
Seeing in a new light: Astro-1 teacher's guide with activities
[NASA-EP-274] N90-20900

ASTRO VEHICLE
Microgravity conditions of a space vehicle N90-20247

ASTRONAUTS
Animation graphic interface for the space shuttle onboard computer N90-20667
SES cupola interactive display design environment N90-20679
Issues in visual support to real-time space system simulation solved in the Systems Engineering Simulator N90-20680

ASTRONOMICAL CATALOGS
Mathematics and physics studies: Multi-project support
[AD-A218208] N90-20723

ASTRONOMICAL MODELS
Studies of the evolution of the x ray emission of clusters of galaxies
[NASA-CR-186471] N90-20918

ASTRONOMY
Experimental validation of extended image reconstruction using bispectral speckle interferometry
[DE90-008545] N90-20171
Bibliography of spatial interferometry in optical astronomy
[NASA-TM-100754] N90-20911
Design and performance analysis of adaptive optical telescopes using laser guide stars
[AD-A218025] N90-20913

ASTROPHYSICS
Mercuric iodide room temperature gamma-ray detectors
[NASA-TM-103318] N90-20357

ASYMMETRY
Lateral asymmetry in pattern recognition: Understanding the effects of familiarity, distinction, and perspective change
[AD-A217739] N90-20641

ATHLETES
What should athletes know about low body temperature (hypothermia)
[AD-A218316] N90-20637
ATLANTIC OCEAN
Analysis of GALE (Genesis of Atlantic Lows Experiment) data
[AD-A217182] N90-20584
ATMOSPHERIC BOUNDARY LAYER
A modeling study of the cloud-topped marine boundary layer
[AD-A218103] N90-20594
ATMOSPHERIC CHEMISTRY
Atmospheric chemiluminescence: COCHISE and FACELIF experiments
[AD-A218121] N90-20578
The receiving system of a dual dye lidar to study molecular and aerosol densities at the base of the stratosphere
[AD-A218286] N90-20581
ATMOSPHERIC CIRCULATION
Structure and dynamics of the Arizona monsoon boundary
[AD-A217378] N90-20586
Atmospheric wind measurements using a 50 MHz imaging Doppler Interferometer radar
[AD-A218277] N90-20601
Microwave brightness temperature and its relation to atmospheric general circulation features
[AD-A218312] N90-20603
Mark 3 interferometer
[AD-A217188] N90-20912
ATMOSPHERIC COMPOSITION
Draft global warming study
[DE90-008446] N90-20507
ATMOSPHERIC EFFECTS
LANDSAT-5 data in the study of wheat and bean crops
[INPE-4746-RPE/580] N90-20444
ATMOSPHERIC ELECTRICITY
Radar detection of lightning and electric fields
[AD-A217894] N90-20574
ATMOSPHERIC ENTRY
Use of random Martian atmosphere to evaluate potential entry guidance schemes
[NASA-TM-102606] N90-20122
ATMOSPHERIC GENERAL CIRCULATION MODELS
USU center of excellence in theory and analysis of the geo-plasma environment
[AD-A217736] N90-20101
Atmospheric Radiation Measurement Program Plan
[DE90-008108] N90-20504
An intercomparison of general circulation model predictions of regional climate change
[DE90-008325] N90-20589
ATMOSPHERIC LASERS
Design and performance analysis of adaptive optical telescopes using laser guide stars
[AD-A218025] N90-20913
ATMOSPHERIC MODELS
USU center of excellence in theory and analysis of the geo-plasma environment
[AD-A217736] N90-20101
Use of environmental monitoring data in evaluation of atmospheric modeling results
[DE90-008607] N90-20510
Analysis of GALE (Genesis of Atlantic Lows Experiment) data
[AD-A217182] N90-20584
Adiabatic and diabatic initialization of the AFGL (Air Force Geophysics Laboratory) global spectral model using dynamic normal mode and nonlinear normal mode methods
[AD-A218120] N90-20595
ATMOSPHERIC PHYSICS
Atmospheric chemiluminescence: COCHISE and FACELIF experiments
[AD-A218121] N90-20578
ATMOSPHERIC PRESSURE
A method for correcting and reducing the pressure data recorded at the PAM 2 stations during GALE
[AD-A218165] N90-20596
ATMOSPHERIC RADIATION
Cloud types and the tropical Earth radiation budget, revised
[NASA-CR-180475] N90-20582
ATMOSPHERIC TEMPERATURE
United States Historical Climatology Network (HCN) serial temperature and precipitation data
[DE90-008029] N90-20506
A cloud climatology for the North Pacific area centered at Shemya, Alaska
[AD-A217334] N90-20585
ATMOSPHERIC TURBULENCE
Correlation of atmospheric optical turbulence and meteorological measurements
[AD-A218019] N90-20576
ATOMIC EXCITATIONS
Laser enhanced chemical reactions
[DE90-008273] N90-20377
ATOMIC PHYSICS
Theoretical investigations in elementary particle physics
[DE90-007178] N90-20802
ATOMIC STRUCTURE
Electronic structure, alloy phase stability, and phase diagrams
[DE90-008306] N90-20203
The basis spline method and associated techniques
[DE90-008403] N90-20763
Theoretical studies of spin-forbidden processes within the Breit-Pauli approximation
[AD-A217778] N90-20815
Spectral line shape code for multielectron emitters
[DE90-008526] N90-20853
Theory of defect process: Basic issues in quantitative understanding
[AERE-R-13661] N90-20860
The geometry of disorder: Report 1987 to 1990
[DE90-008250] N90-20882
ATOMIZING
The glow discharge as an atomization and ionization source
[DE90-007693] N90-20163
A technical and economic evaluation of oxygen-enriched combustion in diesel engines using water-emulsified fuels
[DE90-008095] N90-20394
AURORAL ZONES
Quantifying and reducing uncertainty in the assimilative mapping of ionospheric electrodynamics
[AD-A218057] N90-20577
Spacecraft optical contamination environment
[AD-A218088] N90-20838
AURORAS
Amplified spontaneous emission measurements on the aurora large-aperture module
[DE90-004841] N90-20369
Optical instrumentation support for the airborne ionospheric observatory
[AD-A218207] N90-20839
AUSTENITIC STAINLESS STEELS
Shaping the insonifying pulse to optimise B-scans obtained in austenite
[AERE-R-13518] N90-20187
Stochastic approach to the initiation of pitting corrosion
[AERE-R-13348] N90-20190
AUSTRALIA
Geopotential models in the Australian region
N90-20519
AUTOCORRELATION
Picosecond Laser Facility
[AD-A217784] N90-20384
AUTOMATIC CONTROL
Development of a passive robot-controlled reaction arm N90-20389
AUTOMATIC PILOTS
The NASA digital VGH program: Exploration of methods and final results. Volume 2: L 1011 data 1978-1979: 1619 hours
[NASA-CR-181909-VOL-2] N90-20080
AUTONOMOUS NAVIGATION
Robotic mobility system: Road following algorithms
[AD-A218107] N90-20748
Location recognition using stereo vision
[AD-A218218] N90-20752
AVALANCHE DIODES
Growth, characterization and device development in monocrystalline diamond films
[AD-A218211] N90-20895
AVIONICS
Potential role of avionics in escape systems
N90-20060
Controllable propulsion for escape systems control
N90-20064
Integrated circuits for avionics
[AD-A217964] N90-20312
AXIAL FLOW TURBINES
Innovative turbine concepts for open-cycle OTEC (Ocean Thermal Energy Conversion)
[DE90-000315] N90-20493
AXISYMMETRIC FLOW
Fluid dynamics analysis of a rotating axisymmetric part using FIDAP
[DE90-008733] N90-20340

B

BAGS
Research and development on enhanced degradable plastics
[AD-A217180] N90-20212
BALANCE
Improved energy and power balance at Nova targets
[DE90-007260] N90-20372
BALANCING
An applicational process for dynamic balancing of turbomachinery shafting
[NASA-TM-102537] N90-20392
BALLOON-BORNE INSTRUMENTS
GPS-aided gravimetry at 30 km altitude from a balloon-borne platform N90-20530
BANDWIDTH
Broadening the interface bandwidth in simulation based training N90-20666
BARIUM OXIDES
Y1Ba2Cu3O(7-x) laser-ablation plume dynamics measurement by nanosecond response ion probe: Comparison with optical measurements
[DE90-007658] N90-20375
High resolution transmission electron microscopy study of defect structures in mixed-phase YBaCuO
[DE90-007767] N90-20873
Synthesis and properties of polycrystalline Tl2Ba2CaCu2O(x) and Tl2Ba2Ca2Cu3O(x)
[DE90-007528] N90-20887
BARKHAUSEN EFFECT
Barkhausen noise analysis and ferromagnetic materials
[AD-A217989] N90-20792
BARRIER LAYERS
System for venting gas from a liquid storage tank
[NASA-CASE-MSC-21253-1] N90-20254
Microwave field effect transistor
[NASA-CASE-GSC-12442-2] N90-20282
BATTERY CHARGERS
All-solid-state thin-film rechargeable lithium batteries using solid redox polymerization electrodes
[DE90-008665] N90-20306
BAYS (TOPOGRAPHIC FEATURES)
Continental shelf processes affecting the oceanography of the South Atlantic Bight
[DE90-008439] N90-20606
BEACON EXPLORER A
Satellite radar altimetry over ice. Volume 4: Users' guide for Antarctica elevation data from Seasat
[NASA-RP-1233-VOL-4] N90-20564
BEAM CURRENTS
Power threshold for neutral beam current drive
[DE90-008348] N90-20822
BEAM INJECTION
Power threshold for neutral beam current drive
[DE90-008348] N90-20822
BEAMS (RADIATION)
Nonlinear optics in thin films
[AD-A217336] N90-20829
BEAMS (SUPPORTS)
Active control of the forced and transient response of a finite beam
[NASA-CR-181957] N90-20430
BEARINGS
Bearing and gear steels for aerospace applications
[NASA-TM-102529] N90-20391
BEHAVIOR
Local moduli of continuity of some classes of Gaussian processes
[AD-A217692] N90-20778
BENDING
The reliability of clinical measurements of forward bending obtained by the use of the modified fingertip-to-floor method
[AD-A217907] N90-20627
BENZENE
The 1-(diorganooxyphosphonyl)-methyl)-2,4- and -2,6-diamido benzenes
[NASA-CASE-ARC-11425-4] N90-20133
BERYLLIUM OXIDES
The role of polarity on the stability of graphitic compounds
[DE90-006528] N90-20218
BIBLIOGRAPHIES
The NASA, Marshall Space Flight Center drop tube user's manual
[NASA-TM-100392] N90-20251
Bibliography of spatial interferometry in optical astronomy
[NASA-TM-100754] N90-20911
BINARY ALLOYS
Electronic structure, alloy phase stability, and phase diagrams
[DE90-008306] N90-20203

Dynamics of the solidification front N90-20243

BINARY CODES
Exact algorithms for output encoding, state assignment and four-level Boolean minimization
[AD-A217121] N90-20756

BINARY DATA
Binary space partitioning trees and their uses N90-20657

BIOCHEMISTRY
Assessment of biobased materials
[DE90-000300] N90-20220

BIODEGRADABILITY
Assessment of biobased materials
[DE90-000300] N90-20220

BIODEGRADATION
Research and development on enhanced degradable plastics
[AD-A217180] N90-20212

BIODYNAMICS
Escape systems research at RAE N90-20058

BIOELECTRICITY
Life sciences: Lawrence Berkeley Laboratory, 1988
[DE90-008061] N90-20611

BIOENGINEERING
The United States Air Force School of Aerospace Medicine: Special report
[AD-A217740] N90-20622

BIOLOGICAL EFFECTS
Biological applications and effects of optical masers
[AD-A217910] N90-20385

BIOMEDICAL DATA
Software quality assurance and software safety in the biomed control system
[DE90-008072] N90-20706

BIOPHYSICS
Life sciences: Lawrence Berkeley Laboratory, 1988
[DE90-008061] N90-20611

BIOSYNTHESIS
Assessment of biobased materials
[DE90-000300] N90-20220

BIPOLARITY
Characterization testing of a 40 AHR bipolar nickel-hydrogen battery N90-20463

BIRD-AIRCRAFT COLLISIONS
Full-scale birdstrike testing of in-service aged F-111 ADBIRT windshield transparencies
[AD-A218035] N90-20089

BISMUTH OXIDES
Synthesis of Bi-Sr-Ca-Cu oxide superconductor by solution technique
[DE90-008707] N90-20888

BIVARIATE ANALYSIS
Forecasting the tornadic intensities of thunderstorms by multivariate techniques
[AD-A218284] N90-20602
The perceptual interaction of graphical attributes in thirteen bivariate displays
[AD-A217960] N90-20720

BLACK BODY RADIATION
Analysis of methods to determine emissivity for ground surface targets in the spectral band 8 to 14 microns
[INPE-4984-TDL/394] N90-20447

BLACK SEA
Analysis of altimetry over inland seas
[NASA-TM-100729] N90-20566

BLOCK COPOLYMERS
CO2 diffusion and solubility in a Polystyrene/Polybutadiene block copolymer with highly oriented lamellar morphology
[AD-A217165] N90-20211

BLOOD PLASMA
Hypobaric hypoxia (380 torr) decreases intracellular and total body water in goats
[AD-A218192] N90-20615
The effects of graded exercise at sea level on plasma proenkephalin peptide F and catecholamine responses
[AD-A218195] N90-20633

BLOOD PRESSURE
Elevated central venous pressure: A consequence of exercise training-induced hypervolemia
[NASA-TM-102965] N90-20617

BLOOD VOLUME
Elevated central venous pressure: A consequence of exercise training-induced hypervolemia
[NASA-TM-102965] N90-20617
A comparison of the mechanisms of cold- and microgravity-induced fluid loss
[AD-A218098] N90-20631

BODY FLUIDS
Hypobaric hypoxia (380 torr) decreases intracellular and total body water in goats
[AD-A218192] N90-20615
A comparison of the mechanisms of cold- and microgravity-induced fluid loss
[AD-A218098] N90-20631

BODY TEMPERATURE
What should athletes know about low body temperature (hypothermia)
[AD-A218316] N90-20637
Comparison of light duty gloves with natural and synthetic materials under wet and dry conditions
[AD-A218119] N90-20649

BOEING 727 AIRCRAFT
The NASA digital VGH program. Exploration of methods and final results. Volume 3: B 727 data 1978-1980: 1765 hours
[NASA-CR-181909-VOL-3] N90-20082

BOEING 747 AIRCRAFT
The NASA digital VGH program: Exploration of methods and final results. Volume 4: B 747 data 1978-1980, 1689 hours
[NASA-CR-181909-VOL-4] N90-20083

BOILING
Process for making a noble metal on tin oxide catalyst
[NASA-CASE-LAR-13741-1-SB] N90-20180
Design and test of a compact optics system for the pool boiling experiment
[NASA-TM-102530] N90-20253

BOLTZMANN TRANSPORT EQUATION
The n-p bremsstrahlung in heavy ion collision processes
[DE90-006542] N90-20823

BOLTZMANN-VLASOV EQUATION
Nonlinear plasma and beam physics in plasma wake-fields
[DE90-008812] N90-20855

BOOLEAN ALGEBRA
Binary space partitioning trees and their uses N90-20657
Exact algorithms for output encoding, state assignment and four-level Boolean minimization
[AD-A217121] N90-20756

BORIC ACIDS
Tribological properties of boric acid and boric-acid-forming surfaces. Part 2: Formation and self-lubrication mechanisms of boric acid films on boron- and boric-oxide-containing surfaces
[DE90-005632] N90-20400
Tribological properties of boric acid and boric acid forming surfaces. Part 1: Crystal chemistry and self-lubricating mechanism of boric acid
[DE90-005665] N90-20401

BORON NITRIDES
Vibrational spectroscopy of boron nitride at high temperatures and pressures
[DE90-008633] N90-20172
The role of polarity on the stability of graphitic compounds
[DE90-006528] N90-20218

BOROSILICATE GLASS
Diffusion and germ formation in glasses N90-20250

BOUNDARY INTEGRAL METHOD
Area Over Length (AOL): A program for the calculation of effective two-dimensional thermal conductance through an arbitrarily shaped region
[DE90-008005] N90-20335

BOUNDARY LAYER CONTROL
Experimental and theoretical aerodynamic characteristics of a high-lift semispan wing model
[NASA-TP-2990] N90-20046

BOUNDARY LAYER EQUATIONS
Composite-grid techniques and adaptive mesh refinement in computational fluid dynamics
[AD-A217383] N90-20328

BOUNDARY LAYER FLOW
The effect of adverse pressure gradient on turbulent burst structure in low-Reynolds number equilibrium boundary layers
[AD-A217308] N90-20327
Experimental investigation of the mechanisms underlying vortex kinematics in unsteady separated flows
[AD-A217889] N90-20346

BOUNDARY LAYER SEPARATION
Unsteady three-dimensional marginal separation, including breakdown
[NASA-TM-102525] N90-20337

BOUNDARY LAYER STABILITY
Investigation of the development of laminar boundary-layer instabilities along a cooled-wall hollow cylinder at Mach number 8
[AD-A217672] N90-20331

BOUNDARY VALUE PROBLEMS
A unified integrated model for sputter coating uniformity
[DE90-008322] N90-20205
Amplitude-dependent neutral modes in compressible boundary layer flows
[NASA-TM-102524] N90-20326
A simple multicomponent fluid theory with accurate physics
[DE90-006537] N90-20334
Geopotential coefficient determination and the gravimetric boundary value problem: A new approach N90-20521
The role of topography in geodetic gravity field modelling N90-20534
Very accurate upward continuation to low heights in a test of non-Newtonian theory N90-20548
Domain decomposition for a boundary-value problem with a shock layer
[DE90-007857] N90-20762
Magnetostatic boundary-value problems in the incomplete-nonlinear formulation and methods of their solution
[DE90-615185] N90-20767
Micro SAINT programs for numerical methods of integration and differential equations
[AD-A218097] N90-20772

BRAIN
Development of gamma-emitting, receptor-binding radiotracers for imaging the brain and pancreas
[DE90-008314] N90-20621
Brain activity during tactical decision-making. Part 3: Relationships between probe-evoked potentials, simulation performance, and on-job performance
[AD-A217207] N90-20638

BRANCHING (MATHEMATICS)
F-15B high angle-of-attack phenomena and spin prediction using bifurcation analysis
[AD-A217366] N90-20073

BRAZIL
Evaluation of TM/LANDSAT and HRV/SPOT data in the identification of reforested areas in the Mogi-Guacu (SP) region
[INPE-4874-PRE/1485] N90-20442
Utilization of LANDSAT-5 and NOAA-9 satellite imagery in the identification of physical-chemical parameters of the water in the Guanabara Bay
[INPE-4761-TDL/349] N90-20445
Synthesis and analysis of 25 years (1961-1986) of INPE/SRE activities related to the vegetation/forest area
[INPE-4969-RPE/604] N90-20446
Underwater physiography of the continental shelf of Rio Grande do Norte visible through satellite imagery
[INPE-4964-TDL/392] N90-20448

BRAZILIAN SPACE PROGRAM
Experimental proposition aboard the second data collecting satellite-SCD 2 of the MECB
[INPE-4980-RPE/606] N90-20128

BREMSSTRAHLUNG
The inverse triax x ray diode: An alternate reduced-endpoint-energy bremsstrahlung source
[DE90-006366] N90-20285
The n-p bremsstrahlung in heavy ion collision processes
[DE90-008542] N90-20823

BRIGHTNESS TEMPERATURE
Microwave brightness temperature and its relation to atmospheric general circulation features
[AD-A218312] N90-20603

BRITTLENESS
Effect of heat treatment on the fracture toughness transition properties of an A508 class 3 steel
[AERE-R-13548] N90-20182
Strength and microstructure of ceramics
[AD-A217752] N90-20227

BROADBAND
Joint services electronics program
[AD-A217961] N90-20311

BUBBLES
Diffusion and germ formation in glasses N90-20250
Modeling studies of electrolyte flow and bubble behavior in advanced Hall cells
[DE90-007013] N90-20303

BUCKLING
Innovative design of composite structures: The use of curvilinear fiber format to improve buckling resistance of composite plates with central circular holes
[NASA-CR-186454] N90-20135
Innovative design of composite structures: The use of curvilinear fiber format in composite structure design
[NASA-CR-186453] N90-20136
Perturbation solutions in D* for buckling, vibration, and static loading of specially orthotropic plates N90-20419
Postbuckling behavior of laminated specially orthotropic plates by affine transformation N90-20420
Experiments on buckling and critical buckling. Behavior of carbon fiber reinforced plastic shells submitted to tensile stresses
[ETN-90-95382] N90-20429

BUOYANCY
Nonintrusive optical measurements of turbulence and mixing in a stably stratified fluid N90-20322

BURN-IN
Theory system reliability demonstration and burn-in design
[AD-A217775] N90-20416
BURNERS
Modification and improvement of software for modeling multidimensional reacting fuel flows
[AD-A217789] N90-20235
BUS CONDUCTORS
Laboratory implementation of the Continuously Reconfiguring Multi-Microprocessor Flight Control System (CRMMFCS)
[AD-A217730] N90-20094

C

CABLES
The effects of radiation on the mechanical properties of polymers used as electrical cable insulation and jacketing materials
[AERE-R-13286] N90-20209
CADMIUM
Impedance studies of Ni/Cd and Ni/H2 cells using the cell case as a reference electrode N90-20473
CADMIUM SULFIDES
Stabilization of high (Tc) superconductivity in cadmium sulfide
[DE90-008249] N90-20881
CADMIUM TELLURIDES
CuInSe2 and CdTe: Scale-up for manufacturing
[DE89-009503] N90-20489
CAFFEINE
Influence of theobromine on heat production and body temperatures in cold-exposed humans: A preliminary report
[AD-A217203] N90-20618
CALCIUM CHLORIDES
Advanced calcium thionyl chloride high power battery
[AD-A216685] N90-20482
CALCIUM ISOTOPES
Large-angle elastic and inelastic scattering of Pi+ and Pi- from Si28 and Ca40
[AD-A218163] N90-20818
CALCIUM OXIDES
Synthesis and properties of polycrystalline Tl2Ba2CaCu2O(x) and Tl2Ba2Ca2Cu3O(x)
[DE90-007528] N90-20887
Synthesis of Bi-Sr-Ca-Cu oxide superconductor by solution technique
[DE90-008707] N90-20888
CALIBRATING
Analysis of radiometer calibration effects with TOUCHSTONE
[NASA-CR-186476] N90-20284
Statistical equipment modeling for VLSI manufacturing
[DE90-008527] N90-20304
Design and calibration of a vacuum compatible scanning tunneling microscope
[NASA-TM-102514] N90-20353
Gravity field determination and error assessment techniques N90-20517
An improved error assessment for the GEM-T1 gravitational model N90-20518
Geopotential models in the Australian region N90-20519
First year's results and field experience with the latest JILA absolute gravimeter N90-20529
Effective calibration of heat flux transducers for experimental use
[AD-A218262] N90-20636
Modification, testing, and calibration of infrared search and target designator hardware received from NSWC
[AD-A217920] N90-20837
CALIFORNIA
Correlation of AVHRR imagery with sub-surface features in California current
[AD-A218184] N90-20607
CALORIMETERS
A new thermal sensor for x ray microcalorimetry
[DE90-008547] N90-20360
CAMERAS
Simple reflection holography
[DE90-008309] N90-20359
The design and implementation of a position measuring system for a remotely controlled video camera
[AD-A218077] N90-20362
CANADA
GEOID '88: A gravimetric geoid for Canada N90-20543
CANOPIES (VEGETATION)
Evaluation of TM/LANDSAT and HRV/SPOT data in the identification of reforested areas in the Mogi-Guacu (SP) region
[INPE-4874-PRE/1485] N90-20442
Relationship of radiometric field measurements of wheat in the Assis-Safra region, 1988
[INPE-4949-RPE/598] N90-20443
CAPACITANCE
Deep level transient spectroscopy in resistive layers
[DE90-008349] N90-20169
Advanced double layer capacitors N90-20464
CAPACITANCE-VOLTAGE CHARACTERISTICS
Electron beam induced damage in PECVD Si3N4 and SiO2 films on InP
[NASA-TM-102544] N90-20393
CAPACITORS
Advanced double layer capacitors N90-20464
CAPILLARY FLOW
Experimental investigation of the thermocapillary migration of water droplets in butylbenzoate
[MPIS-14/1988] N90-20155
CARBIDES
Wetting of metallic carbides by non-reactive liquid metals
[AERE-M-3759] N90-20185
The role of polarity on the stability of graphitic compounds
[DE90-006528] N90-20218
CARBOHYDRATES
Physical performance and carbohydrate consumption in CF commandos during a 5-day field trial
[AD-A217204] N90-20619
CARBON
Techno-economic assessment of a carbothermic alumina reduction process
[DE90-007018] N90-20170
Carbon and hydrogen metabolism of green algae in light and dark
[DE90-008648] N90-20612
CARBON DIOXIDE
CO2 diffusion and solubility in a Polystyrene/Polybutadiene block copolymer with highly oriented lamellar morphology
[AD-A217165] N90-20211
Global Warming: A Northwest Perspective
[DE90-008140] N90-20505
CARBON DIOXIDE CONCENTRATION
Draft global warming study
[DE90-008446] N90-20507
CARBON FIBER REINFORCED PLASTICS
Experiments on buckling and critical buckling. Behavior of carbon fiber reinforced plastic shells submitted to tensile stresses
[ETN-90-95382] N90-20429
CARBON FIBERS
Oxygen concentrations on surfaces of carbon fibers
[AD-A217724] N90-20152
CARBON MONOXIDE
Structure of model gas flames in nitramines
[AD-A217578] N90-20159
CARBON STEELS
Bearing and gear steels for aerospace applications
[NASA-TM-102529] N90-20391
CARBON-CARBON COMPOSITES
Reusable high-temperature heat pipes and heat pipe panels
[NASA-CASE-LAR-13761-1] N90-20323
CARDIOVASCULAR SYSTEM
Elevated central venous pressure: A consequence of exercise training-induced hypervolemia
[NASA-TM-102965] N90-20617
A comparison of the mechanisms of cold- and microgravity-induced fluid loss
[AD-A218098] N90-20631
CARRIER FREQUENCIES
Numerical Arc Segmentation Algorithm for a Radio Conference-NASARC (version 4.0) technical manual
[NASA-TM-101453] N90-20264
CASPIAN SEA
Analysis of altimetry over inland seas
[NASA-TM-100729] N90-20566
CAST ALLOYS
Ageing effects in welded cast CF3 stainless steel
[AERE-R-13559] N90-20188
CASTING
Dispersion reinforced materials N90-20244
Spray deposition: A fundamental study of droplet impingement, spreading and consolidation
[AD-A217202] N90-20255
CASUALTIES
Field assessment of wet bulb globe temperature: Present and future
[AD-A218224] N90-20635
CATACLYSMIC VARIABLES
The inter-outburst behavior of cataclysmic variables
[NASA-CR-186374] N90-20914
CATALASE
Biological applications and effects of optical masers
[AD-A217910] N90-20385
CATALYSIS
Ligand-centered electron-transfer redox processes for manganese, iron, and cobalt complexes in relation to selected catalytic systems
[AD-A217957] N90-20177
CATALYSTS
Isotope exchange in oxide-containing catalyst
[NASA-CASE-LAR-13542-2-SB] N90-20154
Hydrous metal oxide-supported catalysts. Part 1: Preparation chemistry and physical and chemical properties
[DE90-007607] N90-20161
Developments in solar photocatalysis for destruction of organics in water
[DE90-007685] N90-20162
Analytical electron microscopy of catalyst preparations
[DE90-008699] N90-20173
Process for making a noble metal on tin oxide catalyst
[NASA-CASE-LAR-13741-1-SB] N90-20180
CATALYTIC ACTIVITY
Non-noble electrocatalysts for alkaline fuel cells N90-20470
CATECHOLAMINE
The effects of high intensity cycle exercise on sympatho-adrenal-medullary response patterns
[AD-A217962] N90-20628
The effects of graded exercise at sea level on plasma proenkephalin peptide F and catecholamine responses
[AD-A218195] N90-20633
CATHODE GLOW
Electron beam generation by electron bombardment induced cathode emission
[AD-A218203] N90-20318
CATHODES
Dual cathode system for electron beam instruments
[NASA-CASE-NPO-16878-1-CU] N90-20351
Advanced rechargeable sodium batteries with novel cathodes N90-20459
Corrosion testing of candidates for the alkaline fuel cell cathode N90-20471
Impedance studies of Ni/Cd and Ni/H2 cells using the cell case as a reference electrode N90-20473
CATHODIC COATINGS
Advances in ambient temperature secondary lithium cells N90-20481
CATHODOLUMINESCENCE
An electron-beam controlled semiconductor switch
[AD-A217181] N90-20288
CATIONS
DURIP theoretical/experimental investigations of highly energetic dication species
[AD-A217771] N90-20383
CAVITIES
Passive venting technique for shallow cavities
[NASA-CASE-LAR-14031-1] N90-20079
CAVITY RESONATORS
High-temperature ceramic superconductors
[AD-A218347] N90-20233
CELESTIAL SPHERE
Mark 3 interferometer
[AD-A217188] N90-20912
CELL CATHODES
Corrosion testing of candidates for the alkaline fuel cell cathode N90-20471
Advances in ambient temperature secondary lithium cells N90-20481
CELLS (BIOLOGY)
Biological soft x ray contact microscopy: Imaging living CHO-SC1 cells and other biological materials
[DE90-007560] N90-20610
CENTRAL PROCESSING UNITS
Onboard shuttle on-line software requirements system: Prototype N90-20658
Performance tradeoffs in multithreaded processors
[AD-A217123] N90-20729
CENTRIFUGAL FORCE
Vortex motion phase separator for zero gravity liquid transfer
[NASA-CASE-KSC-11387-1] N90-20236
CERAMIC FIBERS
Processing, fabrication, characterization and device demonstration of high temperature superconducting ceramics
[AD-A218330] N90-20231
CERAMIC MATRIX COMPOSITES
Characterization of ceramic matrix composites fabricated by chemical vapor infiltration
[DE90-008409] N90-20149
Fundamental aspects of and failure modes in high-temperature composites
[NASA-TM-102558] N90-20151
CERAMICS
Materials Science Programs, fiscal year 1989
[DE90-008169] N90-20131

Summary report of the Summer Conference of the DARPA-Materials Research Council
[AD-A217380] N90-20143
Summary of the DoD Metal Matrix Composites (MMC) Steering Committee Meeting, hosted by the Institute for Defense Analysis
[AD-A217611] N90-20145
Interface science in deformation processing of ceramics
[DE90-008424] N90-20219
Radiation disorder and aperiodicity in irradiated ceramics
[DE90-008253] N90-20222
Tensile fracture toughness of ceramic materials: Effects of dynamic loading and elevated temperatures
[DE90-008329] N90-20223
Mechanical behavior of whisker reinforced ceramics
[DE90-008758] N90-20224
Ceramic oxide thin film formation utilizing biological processes
[DE90-008599] N90-20225
Strength and microstructure of ceramics
[AD-A217752] N90-20227
High-temperature ceramic superconductors
[AD-A218347] N90-20233
Nondestructive testing of ceramics by acoustic microscopy
[AERE-R-13350] N90-20411
Nine-year aging behavior of the ceramic flatpack resonator
[DE90-008044] N90-20412
Technology assessment of superconductivity
[AD-A217697] N90-20889
Performance of Y-TZP materials between 800 C and 1200 C
[AD-A217723] N90-20890

CEREBRAL CORTEX
The boundaries of hemispheric processing in visual pattern recognition
[AD-A217675] N90-20640
CEREBRAL WEEVIL: A machine learning model for hemispheric categorization of complex visual patterns
[AD-A218143] N90-20749

CERIUM OXIDES
Enhanced ceria solid electrolyte fuel cell development. Reduction of electronic conductivity permits use of a solid ceria electrolyte in high efficiency high power density fuel cells at temperatures compatible with metallic cell hardware
[AD-A217840] N90-20498

CERTIFICATION
GCS plan for software aspects of certification
[NASA-CR-181972] N90-20694

CESIUM
Tellurium embrittlement of type 316 steel
[AERE-R-13440] N90-20192

CH-47 HELICOPTER
Simulator sickness in the CH-47 (Chinook) flight simulator
[AD-A218214] N90-20634

CHANNEL FLOW
Experimental investigations on channelized coplanar waveguide
[NASA-TM-102494] N90-20286
Flow visualization studies in a curved rectangular channel with 40 to 1 aspect ratio and a straight channel with bulk flow unsteadiness
[AD-A218020] N90-20348

CHANNELS (DATA TRANSMISSION)
Error control techniques for satellite and space communications
[NASA-CR-186221] N90-20263

CHAOS
The role of chaos in hemispheric process and attention
[AD-A217674] N90-20639
Homogeneous chaos, p-forms, scaling and the feynman integral
[AD-A218339] N90-20777
Integrability and chaos in nonlinearly coupled optical beams
[DE90-007540] N90-20834

CHARACTERIZATION
Synthesis and analysis of 25 years (1961-1986) of INPE/SRE activities related to the vegetation/forest area
[INPE-4969-RPE/604] N90-20446
Growth, characterization and device development in monocrystalline diamond films
[AD-A218211] N90-20895

CHARGE CARRIERS
Electronic properties of high-temperature superconductors
[AD-A217953] N90-20892

CHARGED PARTICLES
Physical sputtering of metallic systems by charged-particle impact
[DE90-007803] N90-20201

CHARPY IMPACT TEST
Evaluation of material homogeneity as a function of thickness of low-alloy ferritic steel
[DE90-008069] N90-20202

CHEBYSHEV APPROXIMATION
Spectral simulation of unsteady compressible flow past a circular cylinder
[NASA-CR-182030] N90-20050
Cell averaging Chebyshev methods for hyperbolic problems
[NASA-CR-182028] N90-20768

CHEMICAL ANALYSIS
Corrosion properties of Fe3Al in H2S-H2-H2O mixtures
[DE90-004936] N90-20167
Techno-economic assessment of a carbothermic alumina reduction process
[DE90-007018] N90-20170
DURIP FTIR studies of solid state reaction dynamics
[AD-A217713] N90-20174
The effect of the SiC/Al interface on matrix microstructure in 2xxx-SiCp metal matrix
[AERE-R-13591] N90-20184
Evaluation of material homogeneity as a function of thickness of low-alloy ferritic steel
[DE90-008069] N90-20202
Pyrotechnic device technology
[DE90-007683] N90-20234
Tribological properties of boric acid and boric acid forming surfaces. Part 1: Crystal chemistry and self-lubricating mechanism of boric acid
[DE90-005665] N90-20401
High temperature chemistry of oxide superconductors
[DE90-007821] N90-20875

CHEMICAL BONDS
Quantum-theoretical methods and studies relating to properties of materials
[AD-A217843] N90-20132
The 1-(diorganooxyphosphonyl)-methyl)-2,4- and -2,6-diamido benzenes
[NASA-CASE-ARC-11425-4] N90-20133
Molecular organization and electrical properties of mixed Langmuir-Blodgett multilayer thin films of polypyrrole
[DE90-007627] N90-20870

CHEMICAL CLEANING
An ellipsometric measurement of optical properties for InP surfaces
[AD-A217185] N90-20827

CHEMICAL COMPOSITION
Oxygen concentrations on surfaces of carbon fibers
[AD-A217724] N90-20152
Design and processing of strong-tough microcomposite steels
[DE90-007764] N90-20197
A systematic study of the effects of metal substitutions for Cu in YBa(sub 2) (Cu(sub 1-x) M(sub x)3 O(sub 7-rho), M=Fe, Co, Al, Ga, Cr, Ni, and Zn
[DE90-003957] N90-20857

CHEMICAL EQUILIBRIUM
Aerodynamic and kinetic processes in flames
[AD-A217796] N90-20176

CHEMICAL FUELS
Electrochemical phase diagrams for aqueous redox systems
[AD-A217168] N90-20157

CHEMICAL PROPERTIES
Symposium on High Temperature and Materials Chemistry
[DE90-008047] N90-20148
Hydrous metal oxide-supported catalysts. Part 1: Preparation chemistry and physical and chemical properties
[DE90-007607] N90-20161
High temperature chemistry of oxide superconductors
[DE90-007821] N90-20875

CHEMICAL REACTIONS
Techno-economic assessment of a carbothermic alumina reduction process
[DE90-007018] N90-20170
The extinction and structure of counterflow premixed flames
[AD-A218106] N90-20178
Infrared and X ray photoelectron spectroscopy studies of the polyimide/metal interface
[AD-A218249] N90-20179
An investigation of the mechanisms of solid state powder reaction in the combustion synthesis and sintering of high temperature materials
[DE90-007860] N90-20198
Modification and improvement of software for modeling multidimensional reacting fuel flows
[AD-A217789] N90-20235
TiCl4 as a source of TiO2 particles for laser anemometry measurements in hot gas
[NASA-TM-102581] N90-20358
Laser enhanced chemical reactions
[DE90-008273] N90-20377
Reactive and anisotropic elastic scattering of highly laser-vibration-excited diatomic molecules
[MPIS-19/1988] N90-20804
Growth, characterization and device development in monocrystalline diamond films
[AD-A218211] N90-20895

CHEMICAL REACTORS
Developments in solar photocatalysis for destruction of organics in water
[DE90-007685] N90-20162

CHEMILUMINESCENCE
Atmospheric chemiluminescence: COCHISE and FACELIF experiments
[AD-A218121] N90-20578

CHIPS (ELECTRONICS)
Product assurance technology for procuring reliable, radiation-hard, custom LSI/VLSI electronics
[NASA-CR-185954] N90-20281
ISITE: Automatic circuit synthesis for double-metal CMOS VLSI (Very Large Scale Integrated) circuits
[AD-A217459] N90-20292
Fault simulator evaluation
[AD-A217782] N90-20308
The design of high-performance circuits for digital signal processing
[AD-A217786] N90-20309
Integrated circuits for avionics
[AD-A217964] N90-20312

CHIRP
The adaptive line enhancer applied to chirp detection
[DE90-006772] N90-20268

CHLOROPHYLLS
LANDSAT-5 data in the study of wheat and bean crops
[INPE-4746-RPE/580] N90-20444
Utilization of LANDSAT-5 and NOAA-9 satellite imagery in the identification of physical-chemical parameters of the water in the Guanabara Bay
[INPE-4761-TDL/349] N90-20445

CHLOROPLASTS
Carbon and hydrogen metabolism of green algae in light and dark
[DE90-008648] N90-20612

CHROMIUM
Infrared and X ray photoelectron spectroscopy studies of the polyimide/metal interface
[AD-A218249] N90-20179
The stress corrosion performance of diffusion bonded nickel base alloys
[DE90-008130] N90-20199
L shell XANES (X ray Absorption Near Edge Structure) for solid metals: Ti, V, Cr, Fe, Ni, Cu
[DE90-008043] N90-20880

CIRCUIT RELIABILITY
Product assurance technology for procuring reliable, radiation-hard, custom LSI/VLSI electronics
[NASA-CR-185954] N90-20281

CIRCUITS
Measurement of proton induced radiation damage to CMOS transistors and pin diodes
[DE90-007836] N90-20283

CIRCULAR CYLINDERS
Spectral simulation of unsteady compressible flow past a circular cylinder
[NASA-CR-182030] N90-20050

CIRCULATION CONTROL AIRFOILS
Aeroelastic characteristics of aircraft with circulation control wings N90-20070

CIRRUS CLOUDS
Downward shortwave surface irradiance from 17 sites for the FIRE/SRB Wisconsin experiment
[NASA-TM-102596] N90-20583

CITIES
Controlling Summer Heat Islands: Proceedings
[DE90-008075] N90-20508

CIVIL AVIATION
Activities report in civil aviation
[ETN-90-95471] N90-20067

CLADDING
Tellurium embrittlement of type 316 steel
[AERE-R-13440] N90-20192

CLAMPS
Tensile film clamps and mounting block for the rheovibron and autovibron viscoelastometer
[NASA-CASE-LAR-13696-1] N90-20409

CLASSIFICATIONS
Acute oral toxicity of DIGL-RP solid propellant in ICR mice
[AD-A217711] N90-20613

Acute oral toxicity of DIGL-RP solid propellant in Sprague-Dawley rats
[AD-A217712] N90-20614
Theory of defect process: Basic issues in quantitative understanding
[AERE-R-13661] N90-20860

CLEAVAGE
Effect of heat treatment on the fracture toughness transition properties of an A508 class 3 steel
[AERE-R-13548] N90-20182

CLIMATE
Global Warming: A Northwest Perspective
[DE90-008140] N90-20505
Cloud types and the tropical Earth radiation budget, revised
[NASA-CR-180475] N90-20582
Southern oscillation in the OSU coupled upper ocean/atmosphere GCM
[DE90-008415] N90-20588

CLIMATE CHANGE
Simulation of landscape disturbances and the effect of climatic change
[DE90-007565] N90-20503
Processes of community development and responses of ecosystems to climate change
[DE90-008640] N90-20512
An intercomparison of general circulation model predictions of regional climate change
[DE90-008325] N90-20589

CLIMATOLOGY
United States Historical Climatology Network (HCN) serial temperature and precipitation data
[DE90-008029] N90-20506
A cloud climatology for the North Pacific area centered at Shemya, Alaska
[AD-A217334] N90-20585
US Navy regional climatic study of the Central East Asian coast and associated waters
[AD-A217448] N90-20587

CLIMBING FLIGHT
Airplane takeoff and landing performance monitoring system
[NASA-CASE-LAR-13734-1-CU] N90-20096

CLINICAL MEDICINE
Acute oral toxicity of DIGL-RP solid propellant in ICR mice
[AD-A217711] N90-20613
Acute oral toxicity of DIGL-RP solid propellant in Sprague-Dawley rats
[AD-A217712] N90-20614
Laser-produced plasmas in medicine
[DE90-007623] N90-20849

CLOSED CIRCUIT TELEVISION
Issues in visual support to real-time space system simulation solved in the Systems Engineering Simulator N90-20680
Real-time graphics for the Space Station Freedom cupola, developed in the Systems Engineering Simulator N90-20683
The Orbital Maneuvering Vehicle Training Facility visual system concept N90-20684

CLOSURE LAW
Theoretical modeling studies of the marine planetary
[AD-A217200] N90-20567

CLOTHING
The effect of moisture absorption in clothing on the human heat balance
[AD-A217899] N90-20626

CLOUD COVER
Cloud types and the tropical Earth radiation budget, revised
[NASA-CR-180475] N90-20582
US Navy regional climatic study of the Central East Asian coast and associated waters
[AD-A217448] N90-20587

CLOUDS (METEOROLOGY)
Cloud types and the tropical Earth radiation budget, revised
[NASA-CR-180475] N90-20582
A cloud climatology for the North Pacific area centered at Shemya, Alaska
[AD-A217334] N90-20585
An aircraft investigation of a convective boundary layer over Lake Michigan
[AD-A218175] N90-20598

CLUTTER
Algorithms for optimal processing of polarimetric radar data
[AD-A217330] N90-20758

CMOS
Measurement of proton induced radiation damage to CMOS transistors and pin diodes
[DE90-007836] N90-20283
Radiation-hardened wafer scale integration
[AD-A217332] N90-20290
ISITE: Automatic circuit synthesis for double-metal CMOS VLSI (Very Large Scale Integrated) circuits
[AD-A217459] N90-20292
Transient radiation hardened CMOS (Complementary Metal Oxide Semiconductor) operational amplifiers
[AD-A217972] N90-20313
SiO(x) precipitation: Defect density correlation with the n+ substrate resistivity
[DE90-005593] N90-20878

COAL GASIFICATION
Corrosion properties of Fe3Al in H2S-H2-H2O mixtures
[DE90-004936] N90-20167

COASTAL WATER
US Navy regional climatic study of the Central East Asian coast and associated waters
[AD-A217448] N90-20587
Continental shelf processes affecting the oceanography of the South Atlantic Bight
[DE90-008439] N90-20606

COASTS
Utilization of LANDSAT-5 and NOAA-9 satellite imagery in the identification of physical-chemical parameters of the water in the Guanabara Bay
[INPE-4761-TDL/349] N90-20445
Analysis of GALE (Genesis of Atlantic Lows Experiment) data
[AD-A217182] N90-20584
Coastal frontogenesis and associated severe weather on 13 March 1986 (GALE IOP 13)
[AD-A217708] N90-20590
Correlation of AVHRR imagery with sub-surface feetures in California current
[AD-A218184] N90-20607

COATING
Fluid dynamics analysis of a rotating axisymmetric part using FIDAP
[DE90-008733] N90-20340

COATINGS
Synthesis of alumina-coated SiC whiskers for production of SiC whisker-reinforced alumina composite materials
[DE90-007778] N90-20147
Process for making a nobie metal on tin oxide catalyst
[NASA-CASE-LAR-13741-1-SB] N90-20180
A unified integrated model for sputter coating uniformity
[DE90-008322] N90-20205
Sol-gel derived polytitanosiloxane coatings
[DE90-004186] N90-20210
Development and construction of external laser components for hardening and coating
[MT-15/87] N90-20364
Tribological properties of boric acid and boric-acid-forming surfaces. Part 2: Formation and self-lubrication mechanisms of boric acid films on boron- and boric-oxide-containing surfaces
[DE90-005632] N90-20400
Development and application of nonflammable, high-temperature beta fibers
[NASA-TM-102158] N90-20645

COBALT
Ligand-centered electron-transfer redox processes for manganese, iron, and cobalt complexes in relation to selected catalytic systems
[AD-A217957] N90-20177

CODERS
Advanced modulation technology development for earth station demodulator applications. Coded modulation system development
[NASA-CR-185149] N90-20270

CODING
Error control techniques for satellite and space communications
[NASA-CR-186221] N90-20263
Fractal-based image compression
[AD-A217302] N90-20699
Exact algorithms for output encoding, state assignment and four-level Boolean minimization
[AD-A217121] N90-20756
Spectral line shape code for multielectron emitters
[DE90-008526] N90-20853

COEFFICIENTS
Geopotential coefficient determination and the gravimetric boundary value problem: A new approach N90-20521
Precise solution for a finite set of spherical coefficients from equiangular gridded data N90-20522

COGNITION
Effects of dexamethasone and high terrestrial altitude on cognitive performance and affect
[AD-A217897] N90-20625
The role of chaos in hemispheric process and attention
[AD-A217674] N90-20639
The boundaries of hemispheric processing in visual pattern recognition
[AD-A217675] N90-20640
Lateral asymmetry in pattern recognition: Understanding the effects of familiarity, distinction, and perspective change
[AD-A217739] N90-20641
Role of cognitive factors in the acquisition of cognitive skill
[AD-A218069] N90-20642
Information gathering and decisionmaking under stress
[AD-A218233] N90-20643
Aiding the decision maker: Perceptual and cognitive issues at the human-machine interface
[AD-A217862] N90-20648
CEREBRAL WEEVIL: A machine learning model for hemispheric categorization of complex visual patterns
[AD-A218143] N90-20749

COHESION
Determination of flow-regime boundaries for cohesive particles
[DE90-007425] N90-20332

COLD FRONTS
Coastal frontogenesis and associated severe weather on 13 March 1986 (GALE IOP 13)
[AD-A217708] N90-20590
A method for correcting and reducing the pressure data recorded at the PAM 2 stations during GALE
[AD-A218165] N90-20596

COLD PRESSING
Millimeter wave surface resistance of RBa2Cu3O(7-delta) (R=Y,Eu,Dy,Sm,Er) superconductors
[NASA-TM-102571] N90-20886

COLLISIONS
The n-p bremsstrahlung in heavy ion collision processes
[DE90-008542] N90-20823

COLLOCATION
Methods for local gravity field approximation N90-20532
Local gravity disturbance estimation from multiple-high-single-low satellite-to-satellite tracking N90-20555
Analysis of altimetry over inland seas
[NASA-TM-100729] N90-20566

COLOR
LANDSAT-5 data in the study of wheat and bean crops
[INPE-4746-RPE/580] N90-20444

COLORADO
Processes of community development and responses of ecosystems to climate change
[DE90-008640] N90-20512

COMBAT
Comparison of oculometer and head-fixed reticle with voice or switch and touch panel for data entry on a generic tactical air combat display
[AD-A217231] N90-20646

COMBINATORIAL ANALYSIS
Free indexation: Combinatorial analysis and a compositional algorithm
[AD-A218219] N90-20724

COMBUSTIBLE FLOW
Modification and improvement of software for modeling multidimensional reacting fuel flows
[AD-A217789] N90-20235

COMBUSTION
An investigation of the mechanisms of solid state powder reaction in the combustion synthesis and sintering of high temperature materials
[DE90-007880] N90-20198
A numerical investigation of the compressible mixing layer
[AD-A217738] N90-20343
A technical and economic evaluation of oxygen-enriched combustion in diesel engines using water-emulsified fuels
[DE90-008095] N90-20394

COMBUSTION EFFICIENCY
Overview of the methodologies used to compile large scale emissions inventories
[DE90-008518] N90-20509

COMBUSTION PHYSICS
Spacelab qualified infrared imager for microgravity science experiments
[NASA-TM-102503] N90-20352

COMMUNICATION NETWORKS
Express cubes: Improving the performance of k-ary n-cube interconnection networks
[AD-A217117] N90-20287

COMMUNICATION SATELLITES
Investigation of a photovoltaic/battery hybrid system for powering the high arctic data communications system
[AD-A218353] N90-20319

COMMUNITIES
Processes of community development and responses of ecosystems to climate change
[DE90-008640] N90-20512
COMPENSATORS
Design and testing of a noninteracting control loop for the dynamically tuned dry gyro
[NAL-TR-1017] N90-20350
Observer based compensators for nonlinear systems
[AD-A217426] N90-20760
COMPLEMENTS (MATHEMATICS)
Generalized quasi-variational inequality and implicit complementarity problems
[AD-A215191] N90-20755
COMPLEX COMPOUNDS
Ligand-centered electron-transfer redox processes for manganese, iron, and cobalt complexes in relation to selected catalytic systems
[AD-A217957] N90-20177
COMPLEX SYSTEMS
Research in reliability, availability and maintainability for complex failure systems
[AD-A217744] N90-20415
Theory of defect process: Basic issues in quantitative understanding
[AERE-R-13661] N90-20860
COMPONENT RELIABILITY
Space Station Freedom electric power system availability study
[NASA-CR-185181] N90-20120
Dual cathode system for electron beam instruments
[NASA-CASE-NPO-16878-1-CU] N90-20351
COMPOSITE MATERIALS
Symposium on High Temperature and Materials Chemistry
[DE90-008047] N90-20148
Extended x ray absorption fine structure analysis applied to composite materials
[DE90-008575] N90-20150
Determination of fundamental thermodynamic properties of constituent materials and performance screening of candidate systems
[AD-A218089] N90-20153
Assessment of biobased materials
[DE90-000300] N90-20220
Electronic and ionic transport in processable conducting polymers
[AD-A218093] N90-20229
Spray deposition: A fundamental study of droplet impingement, spreading and consolidation
[AD-A217202] N90-20255
Comparison of light duty gloves with natural and synthetic materials under wet and dry conditions
[AD-A218119] N90-20649
Dielectric composite thin films
[AD-A217940] N90-20791
COMPOSITE STRUCTURES
A review of the analytical simulation of aircraft crash dynamics
[NASA-TM-102595] N90-20068
Innovative design of composite structures: The use of curvilinear fiber format to improve buckling resistance of composite plates with central circular holes
[NASA-CR-186454] N90-20135
Innovative design of composite structures: The use of curvilinear fiber format in composite structure design
[NASA-CR-186453] N90-20136
Through-thickness strain response of thick composites in compression
[AD-A217233] N90-20141
Nondestructive testing of ceramics by acoustic microscopy
[AERE-R-13350] N90-20411
Computational simulation of damping in composite structures
[NASA-TM-102567] N90-20432
Advanced double layer capacitors N90-20464
Free indexation: Combinatorial analysis and a compositional algorithm
[AD-A218219] N90-20724
COMPRESSIBILITY
Compression pylon
[NASA-CASE-LAR-13777-1] N90-20078
Summary report of the Summer Conference of the DARPA-Materials Research Council
[AD-A217380] N90-20143
COMPRESSIBLE BOUNDARY LAYER
Amplitude-dependent neutral modes in compressible boundary layer flows
[NASA-TM-102524] N90-20326
COMPRESSIBLE FLOW
Spectral simulation of unsteady compressible flow past a circular cylinder
[NASA-CR-182030] N90-20050
Analysis of flow-, thermal-, and structural-interaction of hypersonic structures subjected to severe aerodynamic heating
[AD-A217882] N90-20053
A numerical investigation of the compressible mixing layer
[AD-A217738] N90-20343
COMPRESSION LOADS
Optimization of laminated composite plates
[AD-A217621] N90-20146
COMPRESSION TESTS
Compression testing of thick-section composite materials
[AD-A217234] N90-20142
COMPRESSIVE STRENGTH
Through-thickness strain response of thick composites in compression
[AD-A217233] N90-20141
Compression testing of thick-section composite materials
[AD-A217234] N90-20142
COMPRESSORS
Analyses of power consumption for two sliding vane type compressors
[AD-A218366] N90-20406
COMPUTATION
A matrix-free locally-implicit scheme for Navier-Stokes equations
[AD-A218298] N90-20349
Long range geoid control through the European GPS traverse: Final results N90-20545
Research in programming languages and software engineering
[AD-A217765] N90-20715
Optimization of series expressions. Part 1: User's manual for the series macro package
[AD-A218220] N90-20725
COMPUTATIONAL CHEMISTRY
Quantum-theoretical methods and studies relating to properties of materials
[AD-A217843] N90-20132
COMPUTATIONAL FLUID DYNAMICS
Viscous shock profiles and primitive formulations
[NASA-CR-182029] N90-20049
Numerical simulations of supersonic flow through oscillating cascade sections
[NASA-TM-103100] N90-20051
Comparison of 3-D viscous flow computations of Mach 5 inlet with experimental data
[NASA-TM-102518] N90-20090
Composite-grid techniques and adaptive mesh refinement in computational fluid dynamics
[AD-A217383] N90-20328
Interior fluid dynamics of liquid-filled projectiles
[AD-A217630] N90-20330
Numerical simulation methods of incompressible flows and an application to the space shuttle main engine
[NASA-TM-100038] N90-20333
Mass transfer from a sphere in an oscillating flow with zero mean velocity
[NASA-TM-102566] N90-20338
Fluid dynamics analysis of a rotating axisymmetric part using FIDAP
[DE90-008733] N90-20340
Massively-parallel computational fluid dynamics
[AD-A217732] N90-20342
Evaluation of an adaptive unstructured remeshing technique for integrated fluid-thermal-structural analysis
[NASA-TM-102611] N90-20426
Tools for 3D scientific visualization in computational aerodynamics N90-20660
GRID2D/3D: A computer program for generating grid systems in complex-shaped two- and three-dimensional spatial domains. Part 2: User's manual and program listing
[NASA-TM-102454] N90-20708
COMPUTATIONAL GRIDS
Composite-grid techniques and adaptive mesh refinement in computational fluid dynamics
[AD-A217383] N90-20328
Precise solution for a finite set of spherical coefficients from equiangular gridded data N90-20522
Satellite radar altimetry over ice. Volume 4: Users' guide for Antarctica elevation data from Seasat
[NASA-RP-1233-VOL-4] N90-20564
GRID2D/3D: A computer program for generating grid systems in complex-shaped two- and three-dimensional spatial domains. Part 2: User's manual and program listing
[NASA-TM-102454] N90-20708
Automated finite element modeling and simulation N90-20753
COMPUTER AIDED DESIGN
An expert system for the design of heating, ventilating, and air-conditioning systems
[AD-A218287] N90-20262
The design of high-performance circuits for digital signal processing
[AD-A217786] N90-20309
TAE Plus: Transportable Applications Environment Plus tools for building graphic-oriented applications N90-20652
RenderMan design principles N90-20653
Recent advances in 3D finite difference mesh generation using the BRL-CAD package
[DE90-007854] N90-20704
A review of the suitability of available Computer Aided Software Engineering (CASE) tools for the small software development environment
[AD-A218276] N90-20726
COMPUTER AIDED MANUFACTURING
Flexible automatic discrete parts assembly
[AD-A217401] N90-20256
COMPUTER AIDED TOMOGRAPHY
Computed tomography of electronics
[AD-A217976] N90-20314
COMPUTER ANIMATION
Graphics Technology in Space Applications (GTSA 1989)
[NASA-CP-3045] N90-20651
Using an instrumented manikin for Space Station Freedom analysis N90-20675
Software systems for modeling articulated figures N90-20677
Human task animation from performance models and natural language input N90-20678
COMPUTER GRAPHICS
Harmonic generation mechanisms in short-wavelength free-electron lasers
[DE90-007622] N90-20374
A split-and-merge method for creating polygonal homogeneous-vegetation regions from digitized terrain data
[AD-A218080] N90-20453
Graphics Technology in Space Applications (GTSA 1989)
[NASA-CP-3045] N90-20651
TAE Plus: Transportable Applications Environment Plus tools for building graphic-oriented applications N90-20652
RenderMan design principles N90-20653
Knowledge representation in space flight operations N90-20655
The Real Time Display Builder (RTDB) N90-20656
Applications of graphics to support a testbed for autonomous space vehicle operations N90-20661
Efficient utilization of graphics technology for space animation N90-20663
Engineering visualization utilizing advanced animation N90-20664
Animation graphic interface for the space shuttle onboard computer N90-20667
Operational computer graphics in the flight dynamics environment N90-20668
The use of graphics in the design of the human-telerobot interface N90-20670
Distributed earth model/orbiter simulation N90-20671
Space Station Freedom integrated fault model N90-20673
Using an instrumented manikin for Space Station Freedom analysis N90-20675
The development of the Canadian Mobile Servicing System Kinematic Simulation Facility N90-20676
History of visual systems in the Systems Engineering Simulator N90-20681
Computer image generation: Reconfigurability as a strategy in high fidelity space applications N90-20682
Real-time graphics for the Space Station Freedom cupola, developed in the Systems Engineering Simulator N90-20683
MEASURE: An integrated data-analysis and model identification facility
[NASA-CR-186452] N90-20686
The HS6000/20 development system
[LINO-1989-6] N90-20696
Implementation of a hypertext help system for GLAD (Graphics LAnguage for Database)
[AD-A217936] N90-20718
The perceptual interaction of graphical attributes in thirteen bivariate displays
[AD-A217980] N90-20720
Parallel computer graphics algorithms for the connection machine
[AD-A217300] N90-20733
Implementation of a control system test environment in UNIX
[DE90-007485] N90-20736
Computation and graphics in mathematical research
[DE90-006429] N90-20766
COMPUTER NETWORKS
Transaction processing in a quality control laboratory
[DE90-004655] N90-20414

Supercomputer environments
[AD-A217682] N90-20689
Robust planning and control using neural networks
[AD-A217216] N90-20732
The Livermore distributed storage system: Implementation and experiences
[DE90-007257] N90-20735
Design of a simulation interface for a parellel computing environment
[DE90-008497] N90-20737
Micro SAINT programs for numerical methods of integration and differential equations
[AD-A218097] N90-20772
CALS (Computer-aided Acquisition and Logistic Support) Test Network information exchange user's manual, revision 1
[DE90-008119] N90-20904

COMPUTER PROGRAMMING

A data acquisition parallel bus for wind tunnels at ARL (Aeronautical Research Laboratory)
[AD-A218052] N90-20098
Flexible automatic discrete parts assembly
[AD-A217401] N90-20256
Numerical Arc Segmentation Algorithm for a Radio Conference-NASARC (version 4.0) technical manual
[NASA-TM-101453] N90-20264
TAE Plus: Transportable Applications Environment Plus tools for building graphic-oriented applications
N90-20652
Onboard shuttle on-line software requirements system: Prototype N90-20658
GCS plan for software aspects of certification
[NASA-CR-181972] N90-20694
The contour model architecture and assembly language
[AD-A217114] N90-20697
RIPE: An object-oriented Robot Independent Programming Environment
[DE90-008501] N90-20707
Research in programming languages and software engineering
[AD-A217765] N90-20715
VHSIC Hardware Description Language (VHDL) benchmark suite
[AD-A217947] N90-20719
Optimization of series expressions. Part 1: User's manual for the series macro package
[AD-A218220] N90-20725
A review of the suitability of available Computer Aided Software Engineering (CASE) tools for the small software development environment
[AD-A218276] N90-20726
Towards SDS (Strategic Defense System) testing and evaluation: A collection of relevant topics
[AD-A217610] N90-20783

COMPUTER PROGRAMS

Experimental and theoretical aerodynamic characteristics of a high-lift semispan wing model
[NASA-TP-2990] N90-20046
The application of active controls technology to a generic hypersonic aircraft configuration
[NASA-TM-101689] N90-20071
Comparison of 3-D viscous flow computations of Mach 5 inlet with experimental data
[NASA-TM-102518] N90-20090
Laboratory implementation of the Continuously Reconfiguring Multi-Microprocessor Flight Control System (CRMMFCS)
[AD-A217730] N90-20094
A data acquisition parallel bus for wind tunnels at ARL (Aeronautical Research Laboratory)
[AD-A218052] N90-20098
ETO (Earth-To-Orbit): A trajectory program for aerospace vehicles
[AD-A218157] N90-20103
Component count and preliminary assembly considerations for large space truss structures
[NASA-TM-102604] N90-20121
Composite laminate tailoring with probabilistic constraints and loads
[NASA-TM-102515] N90-20136
Electrochemical phase diagrams for aqueous redox systems
[AD-A217168] N90-20157
Modification and improvement of software for modeling multidimensional reacting fuel flows
[AD-A217789] N90-20235
Analysis of radiometer calibration effects with TOUCHSTONE
[NASA-CR-186476] N90-20284
Recent improvements to the electromagnetic surface patch code
[AD-A217479] N90-20293
Area Over Length (AOL): A program for the calculation of effective two-dimensional thermal conductance through an arbitrarily shaped region
[DE90-008005] N90-20335
Numerical modeling of airblast
[AD-A217993] N90-20347
Space mechanism of low velocity for an array of solar panels: Analysis and design of an experimental model; dimensions of bearings
[INPE-4859-TDL/370] N90-20390
Robust performance of multiple tasks by a mobile robot
[DE90-001953] N90-20397
Comparison of two matrix data structures for advanced CSM testbed applications
[NASA-CR-181951] N90-20421
Computer simulation of the mathematical modeling involved in constitutive equation development: Via symbolic computations
[NASA-TM-102532] N90-20428
COMGEN: A computer program for generating finite element models of composite materials at the micro level
[NASA-TM-102556] N90-20438
Stress field near crack tip: An experimental evaluation of the three dimensional variation
[AD-A217878] N90-20441
Small and great circle routines
[AD-A217652] N90-20449
A split-and-merge method for creating polygonal homogeneous-vegetation regions from digitized terrain data
[AD-A218080] N90-20453
Phase 1 supplemental development of a kinematic Stirling/Rankine commercial gas-fired heat pump system
[PB90-129974] N90-20483
The Terrain-Responsive Atmospheric Code (TRAC) project plan: Development of a hazardous materials dispersion modeling capability with application to ambient air monitoring network design
[DE90-007293] N90-20502
GEOID '88: A gravimetric geoid for Canada
N90-20543
User's guide: Programs for processing altimeter data over inland seas
[NASA-TM-100730] N90-20572
A prototype expert system to forecast severe winds in the western Mediterranean Sea
[AD-A218017] N90-20593
RenderMan design principles N90-20653
Onboard shuttle on-line software requirements system: Prototype N90-20658
Engineering visualization utilizing advanced animation
N90-20664
GCS plan for software aspects of certification
[NASA-CR-181972] N90-20694
Recent advances in 3D finite difference mesh generation using the BRL-CAD package
[DE90-007854] N90-20704
ISLE (Image and Signal Processing LISP Environment) reference manual
[DE90-007858] N90-20705
Software quality assurance and software safety in the biomed control system
[DE90-008072] N90-20706
GRID2D/3D: A computer program for generating grid systems in complex-shaped two- and three-dimensional spatial domains. Part 2: User's manual and program listing
[NASA-TM-102454] N90-20708
Scattering sources: A spherical harmonics expansion
[DE90-008724] N90-20711
VAPEPS user's reference manual, version 5.0
[NASA-CR-180781] N90-20713
Research in programming languages and software engineering
[AD-A217765] N90-20715
Development of computer software for the analysis and design of modern control systems
[AD-A217924] N90-20717
Mathematics and physics studies: Multi-project support
[AD-A218208] N90-20723
Implementation of midcourse tracking and correlation on massively parallel computers
[DE90-008166] N90-20740
Computation and graphics in mathematical research
[DE90-008429] N90-20766
Towards SDS (Strategic Defense System) testing and evaluation: A collection of relevant topics
[AD-A217610] N90-20783
Air Force Boom Event Analyzer Recorder (BEAR): Sysstem description
[AD-A218048] N90-20800
Optical instrumentation support for the airborne ionospheric observatory
[AD-A218207] N90-20839
Theory of defect process: Basic issues in quantitative understanding
[AERE-R-13661] N90-20860

COMPUTER STORAGE DEVICES

Role of cognitive factors in the acquisition of cognitive skill
[AD-A218069] N90-20642
(DURIP) Two-Processor Alliant FX/4 System
[AD-A217810] N90-20692
The HS6000/20 development system
[LINO-1989-6] N90-20696
A Locality-based multiprocessor cache interference model
[AD-A217126] N90-20730
The Livermore distributed storage system: Implementation and experiences
[DE90-007257] N90-20735
An investigation of the locality of memory accesses during symbolic program execution
[AD-A218168] N90-20750

COMPUTER SYSTEMS DESIGN

Development of computer software for the analysis and design of modern control systems
[AD-A217924] N90-20717

COMPUTER SYSTEMS PERFORMANCE

Express cubes: Improving the performance of k-ary n-cube interconnection networks
[AD-A217117] N90-20287
Almost-optimum parallel speed-ups of algorithms for bipartite matching and related problems
[AD-A215111] N90-20728
An investigation of the locality of memory accesses during symbolic program execution
[AD-A218168] N90-20750

COMPUTER SYSTEMS SIMULATION

A satellite simulation program
[AD-A218079] N90-20124

COMPUTER TECHNIQUES

A matrix-free locally-implicit scheme for Navier-Stokes equations
[AD-A218298] N90-20349
Picosecond nonlinear studies of complex materials using the free electron laser
[AD-A218215] N90-20387
Approximate evaluation of reliability and related quantities via perturbation techniques
[AD-A218340] N90-20417
A split-and-merge method for creating polygonal homogeneous-vegetation regions from digitized terrain data
[AD-A218080] N90-20453
Three-dimensional medical image analysis using local dynamic algorithm selection on a multiple-instruction, multiple-data architecture
[AD-A218024] N90-20630
Role of cognitive factors in the acquisition of cognitive skill
[AD-A218069] N90-20642
Multi-tasking computer control of video related equipment N90-20665
Computer image generation: Reconfigurability as a strategy in high fidelity space applications N90-20682
A locally constrained parallel activation model for diagnostic reasoning
[AD-A217808] N90-20747
Institute for Computational Mechanics in Propulsion (ICOMP) fourth annual review, 1989
[NASA-TM-102519] N90-20769
CALS (Computer-aided Acquisition and Logistic Support) Test Network information exchange user's manual, revision 1
[DE90-008119] N90-20904

COMPUTER VISION

Flexible automatic discrete parts assembly
[AD-A217401] N90-20256
A system for analysis and interpretation of lineaments in remote sensing images
[INPE-4893-PRE/1494] N90-20565
Texture segmentation using localized spatial filtering
[AD-A218064] N90-20722
Robotic mobility system: Road following algorithms
[AD-A218107] N90-20748

COMPUTERIZED SIMULATION

Spectral simulation of unsteady compressible flow past a circular cylinder
[NASA-CR-182030] N90-20050
Escape systems research at RAE N90-20058
Design and performance of a multi-stage cylindrical reconnection launcher
[DE90-007820] N90-20108
Space station Simulation Computer System (SCS) study for NASA/MSFC. Volume 1: Overview and summary
[NASA-CR-183840] N90-20113

Space station Simulation Computer System (SCS) study for NASA/MSFC. Volume 2: Concept document
[NASA-CR-183841] N90-20114
Space station Simulation Computer System (SCS) study for NASA/MSFC. Volume 3: Refined conceptual design report
[NASA-CR-183842] N90-20115
Space station Simulation Computer System (SCS) study for NASA/MSFC. Volume 4: Conceptual design report
[NASA-CR-183843] N90-20116
Space station Simulation Computer System (SCS) study for NASA/MSFC. Volume 5: Study analysis report
[NASA-CR-183844] N90-20117
Space station Simulation Computer System (SCS) study for NASA/MSFC. Volume 6: Study issues report
[NASA-CR-183845] N90-20118
Shaping the insonifying pulse to optimise B-scans obtained in austenite
[AERE-R-13518] N90-20187
Physical sputtering of metallic systems by charged-particle impact
[DE90-007803] N90-20201
A unified integrated model for sputter coating uniformity
[DE90-008322] N90-20205
The thermal response of generic objects in JP-4 pool fires
[DE90-008503] N90-20259
Advanced modulation technology development for earth station demodulator applications. Coded modulation system development
[NASA-CR-185149] N90-20270
Simulation of radar scattering from rough surfaces
[AD-A217841] N90-20275
Analysis of radiometer calibration effects with TOUCHSTONE
[NASA-CR-186476] N90-20284
The inverse triax x ray diode: An alternate reduced-endpoint-energy bremsstrahlung source
[DE90-006366] N90-20285
Relativistic klystron afterburner simulation techniques
[DE90-008539] N90-20305
Fluid dynamics analysis of a rotating axisymmetric part using FIDAP
[DE90-008733] N90-20340
Amplified spontaneous emission measurements on the aurora large-aperture module
[DE90-004841] N90-20369
Harmonic generation mechanisms in short-wavelength free-electron lasers
[DE90-007622] N90-20374
Measurement of the stimulated thermal Rayleigh scattering instability
[DE90-007549] N90-20376
Laser line transport with refraction
[DE90-008683] N90-20382
Dynamic damping control: Implementation issues and simulation results
[DE90-007687] N90-20403
Computer simulation of the mathematical modeling involved in constitutive equation development: Via symbolic computations
[NASA-TM-102532] N90-20428
Finite element models to predict the structural response of 120-mm sabot/rods during launch
[DE90-007497] N90-20436
Computer simulations and experiments to study the fracture of rods by flying plates
[DE90-008308] N90-20437
Controlling Summer Heat Islands: Proceedings
[DE90-008075] N90-20508
Use of environmental monitoring data in evaluation of atmospheric modeling results
[DE90-008607] N90-20510
Studies of an orbital gradiometer mission N90-20558
Analysis of GALE (Genesis of Atlantic Lows Experiment) data
[AD-A217182] N90-20584
Southern oscillation in the OSU coupled upper ocean/atmosphere GCM
[DE90-008415] N90-20588
Tools for 3D scientific visualization in computational aerodynamics N90-20660
Engineering visualization utilizing advanced animation N90-20664
Broadening the interface bandwidth in simulation based training N90-20666
Distributed earth model/orbiter simulation N90-20671
Prototype part task trainer: A remote manipulator system simulator N90-20672
Graphical programming and the use of simulation for space-based manipulators N90-20674
Using an instrumented manikin for Space Station Freedom analysis N90-20675
The development of the Canadian Mobile Servicing System Kinematic Simulation Facility N90-20676
Software systems for modeling articulated figures N90-20677
Human task animation from performance models and natural language input N90-20678
Computational complexity of random access models
[AD-A217685] N90-20701
Performance of concurrency control algorithms in distributed systems
[AD-A218280] N90-20727
Implementation of a control system test environment in UNIX
[DE90-007485] N90-20736
Design of a simulation interface for a parallel computing environment
[DE90-008497] N90-20737
A parallel architecture for real-time simulation
[AD-A218321] N90-20741
Dynamics of electronically excited species in gaseous and condensed phase
[AD-A217696] N90-20812
A new technique for guiding of electron beams
[DE90-008660] N90-20824
Spontaneous magnetic reconnection in a turbulent plasma N90-20840
New methods in plasma simulation
[DE90-007507] N90-20847
M51's spiral structure
[DE90-007624] N90-20916
Study of possible solar heating effects on thermosonde probes: Error analysis
[AD-A218116] N90-20917

COMPUTERS
Space station Simulation Computer System (SCS) study for NASA/MSFC. Volume 4: Conceptual design report
[NASA-CR-183843] N90-20116
Space station Simulation Computer System (SCS) study for NASA/MSFC. Volume 6: Study issues report
[NASA-CR-183845] N90-20118

CONCENTRATION (COMPOSITION)
KOH concentration effect on the cycle life of nickel-hydrogen cells. Part 4: Results of failure analyses N90-20475

CONCURRENT PROCESSING
Real-time concurrency control and transaction scheduling
[AD-A218162] N90-20909

CONDUCTING POLYMERS
Electronic and ionic transport in processable conducting polymers
[AD-A218093] N90-20229

CONDUCTIVE HEAT TRANSFER
An approximation theory for the identification of linear thermoelastic systems
[NASA-CR-182015] N90-20764

CONDUCTORS
Measurements of the interaction of high-voltage biassed conductors with the ionosphere
[AD-A218285] N90-20580

CONFERENCES
Implications of Advanced Technologies for Air and Spacecraft Escape
[AGARD-CP-472] N90-20054
Summary report of the Summer Conference of the DARPA Materials Research Council
[AD-A217380] N90-20143
Symposium on High Temperature and Materials Chemistry
[DE90-006047] N90-20148
Center of Gravity: Metallic Solidification
[DFVLR-IB-333-89/3] N90-20238
Conference digest: Thirteenth International Conference on Infrared and Millimeter Waves, volume 1039
[AD-A217343] N90-20291
Space Electrochemical Research and Technology (SERT), 1989
[NASA-CP-3056] N90-20454
Assessment of crew workload measurement methods, techniques and procedures. Volume 1: Process, methods and results
[AD-A217699] N90-20647
Graphics Technology in Space Applications (GTSA 1989)
[NASA-CP-3045] N90-20651
Towards SDS (Strategic Defense System) testing and evaluation: A collection of relevant topics
[AD-A217610] N90-20783
Optical Bistability, 1988
[AD-A217681] N90-20832
Workshop on the Physics and Chemistry of Mercury Cadmium Telluride and Related II-VI compounds
[AD-A217496] N90-20867

CONFORMAL MAPPING
Small and great circle routines
[AD-A217652] N90-20449

CONIFERS
Evaluation of TM/LANDSAT and HRV/SPOT data in the identification of reforested areas in the Mogi-Guacu (SP) region
[INPE-4874-PRE/1485] N90-20442

CONNECTORS
Vortex motion phase separator for zero gravity liquid transfer
[NASA-CASE-KSC-11387-1] N90-20236

CONSCIOUSNESS
Development of an ejection seat specification for a new fighter aircraft N90-20057

CONSERVATION LAWS
Viscous shock profiles and primitive formulations
[NASA-CR-182029] N90-20049
High order filtering methods for approximating hyberbolic systems of conservation laws
[NASA-CR-182016] N90-20650
Conserved integral characteristics of the gravitational field
[DE90-615205] N90-20898

CONSOLES
The Real Time Interactive Display Environment (RTIDE), a display building tool developed by Space Shuttle flight controllers N90-20654

CONSOLIDATION
Spray deposition: A fundamental study of droplet impingement, spreading and consolidation
[AD-A217202] N90-20255

CONSTITUTIVE EQUATIONS
Computer simulation of the mathematical modeling involved in constitutive equation development: Via symbolic computations
[NASA-TM-102532] N90-20428

CONSTRAINTS
Trajectory optimization in the presence of constraints
[AD-A218271] N90-20104

CONSTRUCTION
Simple reflection holography
[DE90-008309] N90-20359

CONSUMPTION
Physical performance and carbohydrate consumption in CF commandos during a 5-day field trial
[AD-A217204] N90-20619

CONTAINERLESS MELTS
The NASA, Marshall Space Flight Center drop tube user's manual
[NASA-TM-100392] N90-20251

CONTAMINANTS
Overview of the methodologies used to compile large scale emissions inventories
[DE90-008518] N90-20509

CONTINENTAL SHELVES
Underwater physiography of the continental shelf of Rio Grande do Norte visible through satellite imagery
[INPE-4964-TDL/392] N90-20448
Continental shelf processes affecting the oceanography of the South Atlantic Bight
[DE90-008439] N90-20606

CONTINUITY
Local moduli of continuity of some classes of Gaussian processes
[AD-A217692] N90-20778

CONTINUOUS WAVE LASERS
Measurement of the stimulated thermal Rayleigh scattering instability
[DE90-007849] N90-20376

CONTOURS
The contour model architecture and assembly language
[AD-A217114] N90-20697

CONTROL SIMULATION
Performance of concurrency control algorithms in distributed systems
[AD-A218280] N90-20727
Robotic mobility system: Road following algorithms
[AD-A218107] N90-20748

CONTROL SYSTEMS DESIGN
Laboratory implementation of the Continuously Reconfiguring Multi-Microprocessor Flight Control System (CRMMFCS)
[AD-A217730] N90-20094
Discrete-time control of a spacecraft with retargetable flexible antennas N90-20119
Docking mechanism for spacecraft
[NASA-CASE-MSC-21386-1] N90-20126
Error control techniques for satellite and space communications
[NASA-CR-186221] N90-20263
Design and testing of a noninteracting control loop for the dynamically tuned dry gyro
[NAL-TR-1017] N90-20350
Design of a telerobotic controller with joint torque sensors
[DE90-008753] N90-20404

Control system design of the third flexible joint of PUMA 560 robot
[AD-A218075] N90-20405
The Rapid Geodetic Survey System (RGSS)
N90-20528
A learning regulator for the plane longitudinal movement
[ETN-90-95381] N90-20695
Development of computer software for the analysis and design of modern control systems
[AD-A217924] N90-20717
Observer based compensators for nonlinear systems
[AD-A217426] N90-20760

CONTROL THEORY
Digital-flutter-suppression-system investigations for the active flexible wing wind-tunnel model
[NASA-TM-102618] N90-20093
Optimal, impulsive, time-fixed orbital rendezvous and interception with path constraints N90-20102
Discrete-time control of a spacecraft with retargetable flexible antennas N90-20119
Aiming control: Theory and applications to dynamic control of space structures
[AD-A217877] N90-20123
Discrete-time control of a spacecraft with retargetable flexible antennas
[AD-A218345] N90-20125
Development of computer software for the analysis and design of modern control systems
[AD-A217924] N90-20717
Robust planning and control using neural networks
[AD-A217216] N90-20732

CONTROLLERS
Potential role of avionics in escape systems
N90-20060
The implementation and operation of a variable-response electronic throttle control system for a TF-104G aircraft
[NASA-TM-101696] N90-20086
Interaction of switch actuation on tracking with a four-axis flight control (cross-coupling)
[AD-A217981] N90-20095
Space station Simulation Computer System (SCS) study for NASA/MSFC. Volume 4: Conceptual design report
[NASA-CR-183843] N90-20116
Design and testing of a noninteracting control loop for the dynamically tuned dry gyro
[NAL-TR-1017] N90-20350
Prototype part task trainer: A remote manipulator system simulator N90-20672

CONVECTION
Spacelab qualified infrared imager for microgravity science experiments
[NASA-TM-102503] N90-20352
An aircraft investigation of a convective boundary layer over Lake Michigan
[AD-A218175] N90-20598
A case study of a quasi-stationary tropical convective line
[AD-A218325] N90-20604

CONVECTION CLOUDS
Theoretical modeling studies of the marine planetary
[AD-A217200] N90-20567

CONVECTIVE HEAT TRANSFER
Heat transfer near the entrance to a film cooling hole in a gas turbine blade
[AD-A217396] N90-20089

CONVERGENCE
Dual cathode system for electron beam instruments
[NASA-CASE-NPO-16878-1-CU] N90-20351
Techniques for accelerating iterative methods for the solution of mathematical problems
[AD-A218272] N90-20775

COOLING
Spallation of oxide scales from 20 percent Cr/25 percent Ni/Nb stainless steel
[AERE-R-13464] N90-20189
Core cooling studies at LLNL (Lawrence Livermore National Laboratory) and Sandia
[DE90-008303] N90-20300
Phase 1 supplemental development of a kinematic Stirling/Rankine commercial gas-fired heat pump system
[PB90-129974] N90-20483

COORDINATES
Estimation of modeled object pose from monocular images
[DE90-001678] N90-20354

COPOLYMERS
CO2 diffusion and solubility in a Polystyrene/Polybutadiene block copolymer with highly oriented lamellar morphology
[AD-A217165] N90-20211
Copolymer-like structures of nematic nitroimine dimers
[AD-A217574] N90-20215
Synthesis of new polyphosphazene elastomers
[AD-A217585] N90-20216
Assessment of biobased materials
[DE90-000300] N90-20220
Electronic and ionic transport in processable conducting polymers
[AD-A218093] N90-20229

COPPER
Infrared and X ray photoelectron spectroscopy studies of the polyimide/metal interface
[AD-A218249] N90-20179
CuInSe2 and CdTe: Scale-up for manufacturing
[DE89-009503] N90-20489
A systematic study of the effects of metal substitutions for Cu in YBa(sub 2) (Cu(sub 1-x) M(sub x)3 O(sub 7-rho), M=Fe, Co, Al, Ga, Cr, Ni, and Zn
[DE90-003957] N90-20857
Copper and oxygen NMR studies on the magnetic properties of YBa2Cu3O(7-y)
[DE90-007889] N90-20863
L shell XANES (X ray Absorption Near Edge Structure) for solid metals: Ti, V, Cr, Fe, Ni, Cu
[DE90-008043] N90-20880

COPPER OXIDES
Y1Ba2Cu3O(7-x) laser-ablation plume dynamics measurement by nanosecond response ion probe: Comparison with optical measurements
[DE90-007658] N90-20375
High resolution transmission electron microscopy study of defect structures in mixed-phase YBaCuO
[DE90-007767] N90-20873
Synthesis and properties of polycrystalline Tl2Ba2CaCu2O(x) and Tl2Ba2Ca2Cu3O(x)
[DE90-007528] N90-20887
Synthesis of Bi-Sr-Ca-Cu oxide superconductor by solution technique
[DE90-008707] N90-20888

CORK (MATERIALS)
Thiokol/Wasatch installation evaluation of the redesigned field joint protection system (concepts 1 and 3)
[NASA-CR-183860] N90-20127

CORRELATION
Implementation of midcourse tracking and correlation on massively parallel computers
[DE90-008166] N90-20740

CORROSION
Corrosion properties of Fe3Al in H2S-H2-H2O mixtures
[DE90-004936] N90-20167
Stochastic approach to the initiation of pitting corrosion
[AERE-R-13348] N90-20190
Corrosion testing of candidates for the alkaline fuel cell cathode N90-20471

CORROSION RESISTANCE
Corrosion properties of Fe3Al in H2S-H2-H2O mixtures
[DE90-004936] N90-20167
The stress corrosion performance of diffusion bonded nickel base alloys
[DE90-008130] N90-20199
Sol-gel derived polytitanosiloxane coatings
[DE90-004186] N90-20210

CORROSION TESTS
Corrosion testing of candidates for the alkaline fuel cell cathode N90-20471

CORTICOSTEROIDS
Effects of dexamethasone and high terrestrial altitude on cognitive performance and affect
[AD-A217897] N90-20625

COSMIC BACKGROUND EXPLORER SATELLITE
Overview of battery usage in NASA/GSFC LEO and GEOspacecrafts N90-20455

COSMIC X RAYS
EXOSAT observations of Seyfert type galaxies
N90-20910

COSMOLOGY
Activities report in nuclear physics
[ETN-90-95322] N90-20803
The Inevitable Universe: Parker-Rhodes' peculiar mixture of ontology and physics
[DE90-006453] N90-20915

COST ANALYSIS
Selection and design of a stretched-membrane heliostat for today's markets
[DE90-007997] N90-20495

COST REDUCTION
Phase 1 supplemental development of a kinematic Stirling/Rankine commercial gas-fired heat pump system
[PB90-129974] N90-20483

COUETTE FLOW
Experimental feasibility of investigating acoustic waves in Couette flow with entropy and pressure gradients
[NASA-TM-102621] N90-20795

COUNTER ROTATION
Noise of a simulated installed model counterrotation propeller at angle-of-attack and takeoff/approach conditions
[NASA-TM-102440] N90-20794

COUNTERFLOW
The extinction and structure of counterflow premixed flames
[AD-A216106] N90-20178

COUPLINGS
Docking mechanism for spacecraft
[NASA-CASE-MSC-21386-1] N90-20126

COVARIANCE
Derivation of kinematic fields using wind profiler data from the 1985 pre-storm experiment
[AD-A217952] N90-20592
Spectral analytic methods for the estimation of number of signals and directions of arrival
[AD-A217219] N90-20757

CRACK CLOSURE
Through-the-thickness fatigue crack closure behavior in an aluminum alloy
[NASA-TM-102590] N90-20427

CRACK GEOMETRY
Hydrogen, thermal ageing and the role of carbides in fatigue of a high strength steel
[AERE-R-13599] N90-20183

CRACK PROPAGATION
Hydrogen, thermal ageing and the role of carbides in fatigue of a high strength steel
[AERE-R-13599] N90-20183
Fatigue crack growth in martensitic 2 1/4Cr-1Mo steel at elevated temperatures
[AERE-R-13524] N90-20191
Strength and microstructure of ceramics
[AD-A217752] N90-20227
Limitations and applications of fracture assessment with R6
[AERE-R-13012] N90-20425
Through-the-thickness fatigue crack closure behavior in an aluminum alloy
[NASA-TM-102590] N90-20427

CRACK TIPS
Stress field near crack tip: An experimental evaluation of the three dimensional variation
[AD-A217878] N90-20441

CRACKING (FRACTURING)
Limitations and applications of fracture assessment with R6
[AERE-R-13012] N90-20425

CRACKS
Fatigue crack growth in martensitic 2 1/4Cr-1Mo steel at elevated temperatures
[AERE-R-13524] N90-20191
Strength and microstructure of ceramics
[AD-A217752] N90-20227
The diffraction of ultrasound by cracks: Comparison of experiment with theory
[AERE-R-13334] N90-20410
The stress-driven redistribution of point defects in the vicinity of crack-like singularities
[AERE-R-12898] N90-20424

CRASHES
A review of the analytical simulation of aircraft crash dynamics
[NASA-TM-102595] N90-20068

CRASHWORTHINESS
Floor pull test of a transport airframe section
[DOT/FAA/CT-TN88/14] N90-20072

CREEP RUPTURE STRENGTH
Mechanical properties of pure nickel alloys after long term exposures to LiOH and vacuum at 775 K
[NASA-TM-102403] N90-20181

CREWS
Assessment of crew workload measurement methods, techniques and procedures. Volume 1: Process, methods and results
[AD-A217699] N90-20647

CRITERIA
Amplitude-dependent neutral modes in compressible boundary layer flows
[NASA-TM-102524] N90-20326

CROP GROWTH
Relationship of radiometric field measurements of wheat in the Assis-Safra region, 1988
[INPE-4949-RPE/598] N90-20443

CROSS CORRELATION
General forms and properties of zero cross-correlation radar waveforms
[AD-A217779] N90-20273

CROSS FLOW
Application of a three-dimensional Navier-Stokes model for a subsonic jet in a crossflow N90-20045

CROSSLINKING
Rigid rod molecules as liquid crystal thermosets
[AD-A217573] N90-20158

CRYOGENIC TEMPERATURE
Proton responses on MOS (Metal-Oxide-Semiconductor) electronics operating at cryogenic temperatures
[AD-A217622] N90-20868
CRYOGENICS
Materials and selection criteria analysis for the compact ignition tokamak toroidal field coil turn-to-turn insulation system: Photographic summary oflaboratory testing
[DE90-008020] N90-20850
CRYPTOGRAPHY
A paradoxical result in unconditionally secure authentication codes, and an explanation
[DE90-008529] N90-20710
CRYSTAL DEFECTS
Research of the interaction between hydrogen and deuterium with atomic eigen defects and dislocations in nickel and iron
[ETN-90-95380] N90-20195
Magnetic properties of surfaces and interfaces
[DE90-007348] N90-20789
Workshop on the Physics and Chemistry of Mercury Cadmium Telluride and Related II-VI compounds
[AD-A217496] N90-20867
SiO(x) precipitation: Defect density correlation with the n+ substrate resistivity
[DE90-005593] N90-20878
Identification of defects in SOI (Silicon-On-Insulator) wafers
[DE90-006020] N90-20879
CRYSTAL DISLOCATIONS
Research of the interaction between hydrogen and deuterium with atomic eigen defects and dislocations in nickel and iron
[ETN-90-95380] N90-20195
An investigation of the dislocation structure of the Ni/Ag phase boundary
[DE90-008428] N90-20876
CRYSTAL GROWTH
Human serum albumin crystals and method of preparation
[NASA-CASE-MFS-28234-1] N90-20616
CRYSTAL LATTICES
Research of the interaction between hydrogen and deuterium with atomic eigen defects and dislocations in nickel and iron
[ETN-90-95380] N90-20195
A systematic study of the effects of metal substitutions for Cu in YBa(sub 2) (Cu(sub 1-x) M(sub x)3 O(sub 7-rho), M=Fe, Co, Al, Ga, Cr, Ni, and Zn
[DE90-003957] N90-20857
CRYSTAL STRUCTURE
Vibrational spectroscopy of boron nitride at high temperatures and pressures
[DE90-008633] N90-20172
Reactive sputtering of molybdenum
[DE90-008307] N90-20204
An introduction to nickel aluminide alloy
[DE90-008565] N90-20207
The role of polarity on the stability of graphitic compounds
[DE90-006528] N90-20218
Ultrastructure processing of ordered polymers
[AD-A218331] N90-20232
Ionic disorder in crystals at high temperatures with emphasis on fluorites
[AERE-R-13544] N90-20862
An investigation of the dislocation structure of the Ni/Ag phase boundary
[DE90-008428] N90-20876
Theoretical and experimental study of solid phase miscibility gaps in III/V quaternary alloys
[DE90-008430] N90-20877
The geometry of disorder: Report 1987 to 1990
[DE90-008250] N90-20882
Performance of Y-TZP materials between 800 C and 1200 C
[AD-A217723] N90-20890
CRYSTAL SURFACES
Interactions of molecules with surfaces
[DE90-007555] N90-20806
CRYSTALLIZATION
Principles of metallic solidification N90-20241
Dielectric composite thin films
[AD-A217940] N90-20791
CRYSTALLOGRAPHY
Techno-economic assessment of a carbothermic alumina reduction process
[DE90-007018] N90-20170
Crystallography, spectroscopic analysis, and lasing properties of Nd3+:Y3Sc2Al3O12
[AD-A217792] N90-20891
CRYSTALS
A new thermal sensor for x ray microcalorimetry
[DE90-008547] N90-20360
Tribological properties of boric acid and boric acid forming surfaces. Part 1: Crystal chemistry and self-lubricating mechanism of boric acid
[DE90-005665] N90-20401
Interactions of molecules with surfaces
[DE90-007555] N90-20806
Crystal preparation at LBL, 1976 to 1986
[DE90-007754] N90-20871
CCST (Center for Compound Semiconductor Technology) research briefs
[DE90-007782] N90-20874
High temperature chemistry of oxide superconductors
[DE90-007821] N90-20875
Method of preparing radially homogeneous mercury cadmium telluride crystals
[NASA-CASE-MFS-25786-2] N90-20896
CURING
The viscoelasticity of curing thermosets
[DE90-006535] N90-20221
CURRENT DENSITY
Electron beam generation by electron bombardment induced cathode emission
[AD-A218203] N90-20318
The application of Dow Chemical's perfluorinated membranes in proton-exchange membrane fuel cells N90-20466
Power threshold for neutral beam current drive
[DE90-008348] N90-20822
CYBERNETICS
An expert system for the design of heating, ventilating, and air-conditioning systems
[AD-A218287] N90-20262
CYCLONES
Analysis of GALE (Genesis of Atlantic Lows Experiment) data
[AD-A217182] N90-20584
Applications of microwave radiometric measurements to infer tropical cyclone intensity and strength
[AD-A218273] N90-20600
The invertibility principle for a simple hurricane model
[AD-A218344] N90-20605
CYLINDRICAL BODIES
Diagnostics and firing control for the cylindrical reconnection launcher
[DE90-007677] N90-20107
CYLINDRICAL SHELLS
Modal interactions in shell dynamics N90-20418
CYTOPLASM
Carbon and hydrogen metabolism of green algae in light and dark
[DE90-008648] N90-20612

D

DAMAGE
The NASA, Marshall Space Flight Center drop tube user's manual
[NASA-TM-100392] N90-20251
Nondestructive testing of ceramics by acoustic microscopy
[AERE-R-13350] N90-20411
Damage characteristics of time domain histories
[DE90-008787] N90-20573
DAMAGE ASSESSMENT
The effects of radiation on the mechanical properties of polymers used as electrical cable insulation and jacketing materials
[AERE-R-13286] N90-20209
DAMPING
Dynamic damping control: Implementation issues and simulation results
[DE90-007687] N90-20403
DARK MATTER
Studies of the evolution of the x ray emission of clusters of galaxies
[NASA-CR-186471] N90-20918
DATA ACQUISITION
The USAF Advanced Dynamic Anthropomorphic Manikin (ADAM) N90-20062
A data acquisition parallel bus for wind tunnels at ARL (Aeronautical Research Laboratory)
[AD-A218052] N90-20098
Diagnostics and firing control for the cylindrical reconnection launcher
[DE90-007677] N90-20107
PC-based PCM telemetry data reduction system software
[DE90-000317] N90-20111
Experimental proposition aboard the second data collecting satellite-SCD 2 of the MECB
[INPE-4980-RPE/606] N90-20128
Constitutive data acquisition and modelling in aluminium 2014 alloy
[AERE-R-13651] N90-20186
The NASA, Marshall Space Flight Center drop tube user's manual
[NASA-TM-100392] N90-20251
Spectral solar radiation data base documentation, volume 1
[DE89-009447] N90-20571
Correlation of AVHRR imagery with sub-surface features in California current
[AD-A218184] N90-20607
Diagnostic development and support of MHD (Magnetohydrodynamics) test facilities
[DE90-004969] N90-20845
CALS (Computer-aided Acquisition and Logistic Support) Test Network information exchange user's manual, revision 1
[DE90-008119] N90-20904
DATA BASE MANAGEMENT SYSTEMS
Hypotheses testing of watershed/landscape dynamics in northern Alaska using digital analysis
[DE90-006721] N90-20450
The Terrain-Responsive Atmospheric Code (TRAC) project plan: Development of a hazardous materials dispersion modeling capability with application to ambient air monitoring network design
[DE90-007293] N90-20502
Design considerations for a space database N90-20659
Software quality assurance and software safety in the biomed control system
[DE90-008072] N90-20706
Mathematics and physics studies: Multi-project support
[AD-A218208] N90-20723
A model research archive: Archive and research implications for original records and support documents
[DE90-008246] N90-20906
Designing an experimenters database using the Nijssen Information Analysis Methodology (NIAM)
[DE90-008548] N90-20907
DATA BASES
Satellite radar altimetry over ice. Volume 1: Processing and corrections of Seasat data over Greenland
[NASA-RP-1233-VOL-1] N90-20562
Satellite radar altimetry over ice. Volume 2: Users' guide for Greenland elevation data from Seasat
[NASA-RP-1233-VOL-2] N90-20563
Satellite radar altimetry over ice. Volume 4: Users' guide for Antarctica elevation data from Seasat
[NASA-RP-1233-VOL-4] N90-20564
Spectral solar radiation data base documentation, volume 1
[DE89-009447] N90-20571
Acute oral toxicity of DIGL-RP solid propellant in Sprague-Dawley rats
[AD-A217712] N90-20614
Design considerations for a space database N90-20659
Implementation of a hypertext help system for GLAD (Graphics LAnguage for Database)
[AD-A217936] N90-20718
Maintaining bridge-connected and biconnected components on-line
[AD-A215107] N90-20754
Implementation of a hypercube database system
[DE90-008440] N90-20905
Designing an experimenters database using the Nijssen Information Analysis Methodology (NIAM)
[DE90-008548] N90-20907
Real-time concurrency control and transaction scheduling
[AD-A218162] N90-20909
DATA COMPRESSION
Fractal-based image compression
[AD-A217302] N90-20699
DATA CORRELATION
Characterization of fluid flow by digital correlation of scattered light
[NASA-CR-186403] N90-20324
DATA LINKS
OMV mission simulator N90-20669
DATA MANAGEMENT
PC-based PCM telemetry data reduction system software
[DE90-000317] N90-20111
Three-dimensional medical image analysis using local dynamic algorithm selection on a multiple-instruction, multiple-data architecture
[AD-A218024] N90-20630
DATA PROCESSING
A guide to performing and documenting safety analyses
[DE90-008687] N90-20260
Laser line transport with refraction
[DE90-008683] N90-20382
Transaction processing in a quality control laboratory
[DE90-004655] N90-20414

Controlling Summer Heat Islands: Proceedings
[DE90-008075] N90-20508
Overview of the methodologies used to compile large scale emissions inventories
[DE90-008518] N90-20509
Performance of FFT methods in local gravity field modelling N90-20537
High resolution analysis of satellite gradiometry N90-20561
Satellite radar altimetry over ice. Volume 2: Users' guide for Greenland elevation data from Seasat
[NASA-RP-1233-VOL-2] N90-20563
User's guide: Programs for processing altimeter data over inland seas
[NASA-TM-100730] N90-20572
Comparison of oculometer and head-fixed reticle with voice or switch and touch panel for data entry on a generic tactical air combat display
[AD-A217231] N90-20646
Animation graphic interface for the space shuttle onboard computer N90-20667
MEASURE: An integrated data-analysis and model identification facility
[NASA-CR-186452] N90-20686
A paradoxical result in unconditionally secure authentication codes, and an explanation
[DE90-008529] N90-20710
Mathematics and physics studies: Multi-project support
[AD-A218208] N90-20723
Implementation of a control system test environment in UNIX
[DE90-007485] N90-20736

DATA RECORDERS
The NASA digital VGH program: Exploration of methods and final results. Volume 2: L 1011 data 1978-1979: 1619 hours
[NASA-CR-181909-VOL-2] N90-20080
The NASA digital VGH program. Exploration of methods and final results. Volume 1: Development of methods
[NASA-CR-181909-VOL-1] N90-20081
The NASA digital VGH program. Exploration of methods and final results. Volume 3: B 727 data 1978-1980: 1765 hours
[NASA-CR-181909-VOL-3] N90-20082
The NASA digital VGH program: Exploration of methods and final results. Volume 4: B 747 data 1978-1980, 1689 hours
[NASA-CR-181909-VOL-4] N90-20083
The NASA digital VGH program: Exploration of methods and final results. Volume 5: DC 10 data 1981-1982, 129 hours
[NASA-CR-181909-VOL-5] N90-20084

DATA REDUCTION
PC-based PCM telemetry data reduction system software
[DE90-000317] N90-20111
The reduction correction in North America N90-20540

DATA STORAGE
Comparison of two matrix data structures for advanced CSM testbed applications
[NASA-CR-181951] N90-20421
A Locality-based multiprocessor cache interference model
[AD-A217126] N90-20730
A model research archive: Archive and research implications for original records and support documents
[DE90-008246] N90-20906

DATA STRUCTURES
Comparison of two matrix data structures for advanced CSM testbed applications
[NASA-CR-181951] N90-20421
Binary space partitioning trees and their uses N90-20657

DATA SYSTEMS
Comparison of oculometer and head-fixed reticle with voice or switch and touch panel for data entry on a generic tactical air combat display
[AD-A217231] N90-20646
The Real Time Interactive Display Environment (RTIDE), a display building tool developed by Space Shuttle flight controllers N90-20654
The Real Time Display Builder (RTDB) N90-20656

DATA TRANSMISSION
Investigation of a photovoltaic/battery hybrid system for powering the high arctic data communications system
[AD-A218353] N90-20319
A real-time parallel pipelined data-flow image-processing system
[DE90-008324] N90-20691

DC 10 AIRCRAFT
The NASA digital VGH program: Exploration of methods and final results. Volume 5: DC 10 data 1981-1982, 129 hours
[NASA-CR-181909-VOL-5] N90-20084

DEBRIS
In-line wear monitor
[AD-A217799] N90-20091

DECISION MAKING
On optimal distributed decision architectures in a hypothesis testing environment
[AD-A217824] N90-20274
Controlling Summer Heat Islands: Proceedings
[DE90-008075] N90-20508
Brain activity during tactical decision-making. Part 3: Relationships between probe-evoked potentials, simulation performance, and on-job performance
[AD-A217207] N90-20638
Information gathering and decisionmaking under stress
[AD-A218233] N90-20643
Aiding the decision maker: Perceptual and cognitive issues at the human-machine interface
[AD-A217862] N90-20648
Design decision making with multiple interacting criteria and varying relative weights
[AD-A218027] N90-20721

DECISION THEORY
On optimal distributed decision architectures in a hypothesis testing environment
[AD-A217824] N90-20274
Design decision making with multiple interacting criteria and varying relative weights
[AD-A218027] N90-20721

DECODING
Fractal-based image compression
[AD-A217302] N90-20699

DECOMPOSITION
Condensed phase kinetic deuterium isotope effects in high energy phenomena: Mechanistic investigations and relationships
[AD-A217161] N90-20156
Developments in solar photocatalysis for destruction of organics in water
[DE90-007685] N90-20162
Domain decomposition for a boundary-value problem with a shock layer
[DE90-007857] N90-20762

DEFECTS
Interaction between implanted ions and intrinsic defects in silica
[DE90-006569] N90-20858
Theory of defect process: Basic issues in quantitative understanding
[AERE-R-13661] N90-20860

DEFENSE PROGRAM
Assessing the morality of using the space environment as a platform for weapons
[AD-A217348] N90-20780
The essence of spacepower: Important influences on the evolution of national spacepower
[AD-A217498] N90-20781
The thrust and parry of the SIOP (Single Integrated Operational Plan) and SDI
[AD-A217617] N90-20784

DEFORMATION
Interface science in deformation processing of ceramics
[DE90-008424] N90-20219
Design and performance analysis of adaptive optical telescopes using laser guide stars
[AD-A218025] N90-20913

DEGRADATION
Research and development on enhanced degradable plastics
[AD-A217180] N90-20212
Advanced modulation technology development for earth station demodulator applications. Coded modulation system development
[NASA-CR-185149] N90-20270
The application of electrochemical impedance spectroscopy for characterizing the degradation of Ni(OH)2/NiOOH electrodes N90-20474

DEHYDRATION
Hydration effects on human physiology and exercise-heat performance
[AD-A217969] N90-20629

DEIONIZATION
Process for making a noble metal on tin oxide catalyst
[NASA-CASE-LAR-13741-1-SB] N90-20180

DELTA WINGS
A video-based experimental investigation of wing rock
[AD-A218244] N90-20075

DEMODULATION
Complex demodulation for bearing fault detection
[AD-A218367] N90-20407

DEMODULATORS
Advanced modulation technology development for earth station demodulator applications. Coded modulation system development
[NASA-CR-185149] N90-20270

DENSITY (MASS/VOLUME)
Nonintrusive optical measurements of turbulence and mixing in a stably stratified fluid N90-20322

DEOXIDIZING
Isotope exchange in oxide-containing catalyst
[NASA-CASE-LAR-13542-2-SB] N90-20154

DEPOSITION
Characterization of ceramic matrix composites fabricated by chemical vapor infiltration
[DE90-008409] N90-20149
Spray deposition: A fundamental study of droplet impingement, spreading and consolidation
[AD-A217202] N90-20255
Tribological properties of boric acid and boric-acid-forming surfaces. Part 2: Formation and self-lubrication mechanisms of boric acid films on boron- and boric-oxide-containing surfaces
[DE90-005632] N90-20400
Dielectric composite thin films
[AD-A217940] N90-20791

DEPOSITS
Geology, distribution of hot springs and hydrothermal alteration zones of major geothermal areas in Japan
[DE90-753026] N90-20451

DESICCANTS
Moisture control in sealed electronic packages
[DE90-008136] N90-20166

DESIGN ANALYSIS
Aerodynamic analysis of a US Navy and Marine Corps unmanned air vehicle
[AD-A218282] N90-20077
The NASA digital VGH program: Exploration of methods and final results. Volume 4: B 747 data 1978-1980, 1689 hours
[NASA-CR-181909-VOL-4] N90-20083
Space station Simulation Computer System (SCS) study for NASA/MSFC. Volume 3: Refined conceptual design report
[NASA-CR-183842] N90-20115
Space station Simulation Computer System (SCS) study for NASA/MSFC. Volume 4: Conceptual design report
[NASA-CR-183843] N90-20116
Composite laminate tailoring with probabilistic constraints and loads
[NASA-TM-102515] N90-20138
Design and test of a compact optics system for the pool boiling experiment
[NASA-TM-102530] N90-20253
An applicational process for dynamic balancing of turbomachinery shafting
[NASA-TM-102537] N90-20392
Plan, formulate, and discuss a NASTRAN finite element model of the UH-60A helicopter airframe
[NASA-CR-181975] N90-20439
Multi-mission Ni-H2 battery cells for the 1990's N90-20477
RenderMan design principles N90-20653
Design decision making with multiple interacting criteria and varying relative weights
[AD-A218027] N90-20721

DESTRUCTION
Developments in solar photocatalysis for destruction of organics in water
[DE90-007685] N90-20162

DESTRUCTIVE TESTS
Floor pull test of a transport airframe section
[DOT/FAA/CT-TN88/14] N90-20072

DETECTION
The adaptive line enhancer applied to chirp detection
[DE90-006772] N90-20268
A linear filtering technique for removal of low-frequency noise
[DE90-006183] N90-20296
Algorithms for optimal processing of polarimetric radar data
[AD-A217330] N90-20758

DEUTERIUM
Research of the interaction between hydrogen and deuterium with atomic eigen defects and dislocations in nickel and iron
[ETN-90-95380] N90-20195

DIAGNOSIS
Common-mode rejector for pulse power diagnostics
[AD-A218096] N90-20316
A locally constrained parallel activation model for diagnostic reasoning
[AD-A217808] N90-20747

DIAMONDS
Fluorinated diamond thin films for tribological applications
[AD-A217452] N90-20214
Growth, characterization and device development in monocrystalline diamond films
[AD-A218211] N90-20895

DIATOMIC MOLECULES
DURIP FTIR studies of solid state reaction dynamics
[AD-A217713] N90-20174
Reactive and anisotropic elastic scattering of highly laser-vibration-excited diatomic molecules
[MPIS-19/1988] N90-20804
Electronically metastable molecules of high symmetry
[AD-A217768] N90-20814

DIELECTRIC PROPERTIES
Wetting of metallic carbides by non-reactive liquid metals
[AERE-M-3759] N90-20185
Molecular organization and electrical properties of mixed Langmuir-Blodgett multilayer thin films of polypyrrole
[DE90-007627] N90-20870

DIELECTRICS
Microwave field effect transistor
[NASA-CASE-GSC-12442-2] N90-20262
Dielectric composite thin films
[AD-A217940] N90-20791
Refractive index profiles of thermally grown and chemically vapor deposited films on silicon
[AD-A217187] N90-20865

DIESEL ENGINES
A technical and economic evaluation of oxygen-enriched combustion in diesel engines using water-emulsified fuels
[DE90-008095] N90-20394

DIESEL FUELS
A technical and economic evaluation of oxygen-enriched combustion in diesel engines using water-emulsified fuels
[DE90-008095] N90-20394

DIFFERENTIAL CALCULUS
Computation and graphics in mathematical research
[DE90-008429] N90-20766

DIFFERENTIAL EQUATIONS
A general existence and uniqueness theorem for implicit differential-algebraic equations
[AD-A217965] N90-20770
Micro SAINT programs for numerical methods of integration and differential equations
[AD-A218097] N90-20772

DIFFRACTION
The diffraction of ultrasound by cracks: Comparison of experiment with theory
[AERE-R-13334] N90-20410

DIFFRACTION PATTERNS
X ray microimaging by diffractive techniques
[DE90-008444] N90-20356

DIFFUSION
CO2 diffusion and solubility in a Polystyrene/Polybutadiene block copolymer with highly oriented lamellar morphology
[AD-A217165] N90-20211
Diffusion and germ formation in glasses N90-20250
Hydrodynamic interactions and transport coefficients in a suspension of spherical particles
[DE90-008301] N90-20336

DIFFUSION ELECTRODES
Electrocatalysis for oxygen electrodes in fuel cells and water electrolyzers for space applications N90-20468

DIFFUSION FLAMES
Structure of model gas flames in nitramines
[AD-A217578] N90-20159
Aerodynamic and kinetic processes in flames
[AD-A217796] N90-20176

DIFFUSION WELDING
Time-dependent failure of silver interlayer welds
[DE90-008015] N90-20440

DIGITAL DATA
A split-and-merge method for creating polygonal homogeneous-vegetation regions from digitized terrain data
[AD-A218080] N90-20453

DIGITAL FILTERS
Optimization of digital filters for a short-scan interferometer
[AD-A217997] N90-20315

DIGITAL SIMULATION
A numerical investigation of the compressible mixing layer
[AD-A217738] N90-20343

DIGITAL SYSTEMS
Digital-flutter-suppression-system investigations for the active flexible wing wind-tunnel model
[NASA-TM-102618] N90-20093
LANDSAT-5 data in the study of wheat and bean crops
[INPE-4746-RPE/580] N90-20444
A split-and-merge method for creating polygonal homogeneous-vegetation regions from digitized terrain data
[AD-A218080] N90-20453
Fractal-based image compression
[AD-A217302] N90-20699
Mathematics and physics studies: Multi-project support
[AD-A218208] N90-20723
Implementation of a control system test environment in UNIX
[DE90-007485] N90-20736

DIGITAL TECHNIQUES
Characterization of fluid flow by digital correlation of scattered light
[NASA-CR-186403] N90-20324
Onboard shuttle on-line software requirements system: Prototype N90-20658

DIMERS
Chemical and electrochemical studies in ionic liquids
[AD-A217742] N90-20175
Copolymer-like structures of nematic nitroimine dimers
[AD-A217574] N90-20215

DIODES
Measurement of proton induced radiation damage to CMOS transistors and pin diodes
[DE90-007836] N90-20283
The inverse triax x ray diode: An alternate reduced-endpoint-energy bremsstrahlung source
[DE90-006366] N90-20285
A progress report on the Livermore Miniature Vacuum Tube Project
[DE90-008302] N90-20299

DIRAC EQUATION
The basis spline method and associated techniques
[DE90-008403] N90-20763

DIRECTIONAL ANTENNAS
An investigation of the extent of the fresnel region of aperture antennas with attention to superdirectivity
[AD-A217518] N90-20294

DIRECTIONAL CONTROL
Development of a passive robot-controlled reaction arm N90-20389

DIRECTIVITY
An investigation of the extent of the fresnel region of aperture antennas with attention to superdirectivity
[AD-A217518] N90-20294

DISPLAY DEVICES
Comparison of oculometer and head-fixed reticle with voice or switch and touch panel for data entry on a generic tactical air combat display
[AD-A217231] N90-20646
Graphics Technology in Space Applications (GTSA 1989)
[NASA-CP-3045] N90-20651
The Real Time Interactive Display Environment (RTIDE), a display building tool developed by Space Shuttle flight controllers N90-20654
Knowledge representation in space flight operations N90-20655
The Real Time Display Builder (RTDB) N90-20656
Design considerations for a space database N90-20659
Applications of graphics to support a testbed for autonomous space vehicle operations N90-20661
Large screen display for the Mission Control Center N90-20662
Engineering visualization utilizing advanced animation N90-20664
Broadening the interface bandwidth in simulation based training N90-20666
Animation graphic interface for the space shuttle onboard computer N90-20667
OMV mission simulator N90-20669
Graphical programming and the use of simulation for space-based manipulators N90-20674
SES cupola interactive display design environment N90-20679
History of visual systems in the Systems Engineering Simulator N90-20681
Real-time graphics for the Space Station Freedom cupola, developed in the Systems Engineering Simulator N90-20683
The HS6000/20 development system
[LINO-1989-6] N90-20696
The perceptual interaction of graphical attributes in thirteen bivariate displays
[AD-A217980] N90-20720

DISTRIBUTED PROCESSING
RIPE: An object-oriented Robot Independent Programming Environment
[DE90-008501] N90-20707
Performance of concurrency control algorithms in distributed systems
[AD-A218280] N90-20727
The Livermore distributed storage system: Implementation and experiences
[DE90-007257] N90-20735

DISULFIDES
Advanced high-temperature batteries N90-20480

DIURESIS
A comparison of the mechanisms of cold- and microgravity-induced fluid loss
[AD-A218098] N90-20631

DIURNAL VARIATIONS
Niacin ingested at night causes severe hypotension
[AD-A217896] N90-20624

DOPED CRYSTALS
Chemically prepared PZT films doped with niobium
[DE90-006811] N90-20859

DOPPLER EFFECT
Modelling Doppler broadening in Raman propagation
[DE90-008042] N90-20269
Meteor observations using the 50 MHz MENTOR imaging Doppler interferometer
[AD-A217908] N90-20276

DOPPLER RADAR
Doppler radar with multiphase modulation of transmitted and reflected signal
[NASA-CASE-MSC-18808-1] N90-20280
Atmospheric wind measurements using a 50 MHz imaging Doppler interferometer radar
[AD-A218277] N90-20601

DOSAGE
Acute oral toxicity of JA-2 solid propellant in ICR mice
[AD-A217264] N90-20609
Acute oral toxicity of DIGL-RP solid propellant in ICR mice
[AD-A217711] N90-20613
Acute oral toxicity of DIGL-RP solid propellant in Sprague-Dawley rats
[AD-A217712] N90-20614

DOSIMETERS
Energy deposition measurements for E-beam pumped excimer lasers
[DE90-007545] N90-20365
Determinations of photon spectra
[AD-A218003] N90-20816

DOWNLINKING
Advanced modulation technology development for earth station demodulator applications. Coded modulation system development
[NASA-CR-185149] N90-20270

DOWNWASH
Analysis of heliport environmental data: Indianapolis downtown heliport, Wall Street heliport. Volume 3: Indianapolis downtown heliport data plots
[AD-A217412] N90-20500

DRAG REDUCTION
Aerodynamic analysis of a US Navy and Marine Corps unmanned air vehicle
[AD-A218282] N90-20077
Compression pylon
[NASA-CASE-LAR-13777-1] N90-20078
Passive venting technique for shallow cavities
[NASA-CASE-LAR-14031-1] N90-20079
Investigation into the mechanism of polymer thread drag reduction
[AD-A217492] N90-20329

DRILLING
Hot dry rock geothermal energy: A renewable energy resource that is ready for development now
[DE90-007509] N90-20485

DROP TOWERS
The NASA, Marshall Space Flight Center drop tube user's manual
[NASA-TM-100392] N90-20251

DROPS (LIQUIDS)
Experimental investigation of the thermocapillary migration of water droplets in butylbenzoate
[MPIS-14/1988] N90-20155
Spray deposition: A fundamental study of droplet impingement, spreading and consolidation
[AD-A217202] N90-20255

DRUGS
Human serum albumin crystals and method of preparation
[NASA-CASE-MFS-28234-1] N90-20616
Influence of theobromine on heat production and body temperatures in cold-exposed humans: A preliminary report
[AD-A217203] N90-20618

DRY FRICTION
Space mechanism of low velocity for an array of solar panels: Analysis and design of an experimental model; dimensions of bearings
[INPE-4859-TDL/370] N90-20390

DRYING
Process for making a noble metal on tin oxide catalyst
[NASA-CASE-LAR-13741-1-SB] N90-20180
Comparison of light duty gloves with natural and synthetic materials under wet and dry conditions
[AD-A218119] N90-20649

DUCTILITY
Evaluation of material homogeneity as a function of thickness of low-alloy ferritic steel
[DE90-008069] N90-20202
An introduction to nickel aluminide alloy
[DE90-008565] N90-20207
DUCTS
Vortex motion phase separator for zero gravity liquid transfer
[NASA-CASE-KSC-11387-1] N90-20236
DUMMIES
The USAF Advanced Dynamic Anthropomorphic Manikin (ADAM) N90-20062
DWARF NOVAE
The inter-outburst behavior of cataclysmic variables
[NASA-CR-186374] N90-20914
DYE LASERS
DURIP theoretical/experimental investigations of highly energetic dication species
[AD-A217771] N90-20383
Picosecond Laser Facility
[AD-A217784] N90-20384
The receiving system of a dual dye lidar to study molecular and aerosol densities at the base of the stratosphere
[AD-A218286] N90-20581
DYNAMIC CHARACTERISTICS
DURIP FTIR studies of solid state reaction dynamics
[AD-A217713] N90-20174
Y1Ba2Cu3O(7-x) laser-ablation plume dynamics measurement by nanosecond response ion probe: Comparison with optical measurements
[DE90-007658] N90-20375
An applicational process for dynamic balancing of turbomachinery shafting
[NASA-TM-102537] N90-20392
Plan, formulate, and discuss a NASTRAN finite element model of the UH-60A helicopter airframe
[NASA-CR-181975] N90-20439
Coastal frontogenesis and associated severe weather on 13 March 1986 (GALE IOP 13)
[AD-A217708] N90-20590
Correlation of AVHRR imagery with sub-surface features in California current
[AD-A218184] N90-20607
Implementation of a control system test environment in UNIX
[DE90-007485] N90-20736
Dynamics of electronically excited species in gaseous and condensed phase
[AD-A217696] N90-20812
DYNAMIC CONTROL
Discrete-time control of a spacecraft with retargetable flexible antennas N90-20119
Aiming control: Theory and applications to dynamic control of space structures
[AD-A217877] N90-20123
Dynamic damping control: Implementation issues and simulation results
[DE90-007687] N90-20403
Sensor and actuator selection for fault-tolerant control of flexible structures
[AD-A217384] N90-20433
Robust planning and control using neural networks
[AD-A217216] N90-20732
DYNAMIC LOADS
Tensile fracture toughness of ceramic materials: Effects of dynamic loading and elevated temperatures
[DE90-008329] N90-20223
DYNAMIC RESPONSE
Modal interactions in shell dynamics N90-20418
DYNAMIC STRUCTURAL ANALYSIS
A review of the analytical simulation of aircraft crash dynamics
[NASA-TM-102595] N90-20068
Computational simulation of damping in composite structures
[NASA-TM-102567] N90-20432
Plan, formulate, and discuss a NASTRAN finite element model of the UH-60A helicopter airframe
[NASA-CR-181975] N90-20439
Localization and delocalization in periodic one-dimensional dynamic systems
[AD-A217939] N90-20797
DYNAMICAL SYSTEMS
Localization and delocalization in periodic one-dimensional dynamic systems
[AD-A217939] N90-20797

E

EARTH (PLANET)
Distributed earth model/orbiter simulation N90-20671
EARTH ATMOSPHERE
Spectral solar radiation data base documentation, volume 1
[DE89-009447] N90-20571
Southern oscillation in the OSU coupled upper ocean/atmosphere GCM
[DE90-008415] N90-20588
EARTH CRUST
The effects of structure and source complexity on waveforms: Crustal structure of Tibet and the recovery of complex seismic sources
[AD-A218202] N90-20579
EARTH GRAVITATION
Modeling of the Earth's gravity field using the New Global Earth Model (NEWGEM) N90-20523
A framework for modelling kinematic measurements in gravity field applications N90-20524
Synopsis of early field test results from the gravity gradiometer survey system N90-20525
Terrestrial gravity instrumentation in the 20th Century: A brief review N90-20527
Critique of the vertical gradient of gravity N90-20531
The inverse gravimetric problem in gravity modelling N90-20535
GEOID '88: A gravimetric geoid for Canada N90-20543
Very accurate upward continuation to low heights in a test of non-Newtonian theory N90-20548
A model of the general ocean circulation determined from a joint solution for the Earth's gravity field N90-20550
Refinement of Earth's gravity field with Topex GPS measurements N90-20553
Gravity field information from Gravity Probe-B N90-20554
Satellite-to-satellite tracking experiment for global gravity field mapping N90-20556
ARISTOTELES: A European approach for an Earth gravity field recovery mission N90-20559
EARTH IONOSPHERE
USU center of excellence in theory and analysis of the geo-plasma environment
[AD-A217736] N90-20101
Quantifying and reducing uncertainty in the assimilative mapping of ionospheric electrodynamics
[AD-A218057] N90-20577
Measurements of the interaction of high-voltage biassed conductors with the ionosphere
[AD-A218285] N90-20580
Optical instrumentation support for the airborne ionospheric observatory
[AD-A218207] N90-20839
EARTH MAGNETOSPHERE
USU center of excellence in theory and analysis of the geo-plasma environment
[AD-A217736] N90-20101
Quantifying and reducing uncertainty in the assimilative mapping of ionospheric electrodynamics
[AD-A218057] N90-20577
EARTH ORBITS
ETO (Earth-To-Orbit): A trajectory program for aerospace vehicles
[AD-A218157] N90-20103
A satellite simulation program
[AD-A218079] N90-20124
Measurements of the interaction of high-voltage biassed conductors with the ionosphere
[AD-A218285] N90-20580
EARTH RADIATION BUDGET
Cloud types and the tropical Earth radiation budget, revised
[NASA-CR-180475] N90-20582
EARTHQUAKES
Damage characteristics of time domain histories
[DE90-008787] N90-20573
The effects of structure and source complexity on waveforms: Crustal structure of Tibet and the recovery of complex seismic sources
[AD-A218202] N90-20579
ECOLOGY
Hypotheses testing of watershed/landscape dynamics in northern Alaska using digital analysis
[DE90-006721] N90-20450
ECONOMETRICS
Computing mean responses in nonlinear models
[AD-A217642] N90-20700
ECONOMIC ANALYSIS
Techno-economic assessment of a carbothermic alumina reduction process
[DE90-007018] N90-20170
Photovoltaic energy
[DE89-009473] N90-20486
Wind Energy Program summary. Volume 1: Overview
[DE89-009479] N90-20491
ECONOMICS
Synthesis and analysis of 25 years (1961-1986) of INPE/SRE activities related to the vegetation/forest area
[INPE-4969-RPE/604] N90-20446
ECOSYSTEMS
Underwater physiography of the continental shelf of Rio Grande do Norte visible through satellite imagery
[INPE-4964-TDL/392] N90-20448
Hypotheses testing of watershed/landscape dynamics in northern Alaska using digital analysis
[DE90-006721] N90-20450
Processes of community development and responses of ecosystems to climate change
[DE90-008640] N90-20512
EDDY CURRENTS
Superconductive microprobes for eddy current evaluation of materials
[AD-A217776] N90-20361
EDITING
Multi-tasking computer control of video related equipment N90-20665
EDUCATION
The United States Air Force School of Aerospace Medicine: Special report
[AD-A217740] N90-20622
Broadening the interface bandwidth in simulation based training N90-20666
Seeing in a new light: Astro-1 teacher's guide with activities
[NASA-EP-274] N90-20900
ONR (Office of Naval Research) summer scholars for the 1989 PREFACE Program
[AD-A217746] N90-20919
EJECTION SEATS
Development of acceleration exposure limits for advanced escape systems N90-20055
Parachute opening shocks during high speed ejections: Normalization N90-20056
Development of an ejection seat specification for a new fighter aircraft N90-20057
Escape systems research at RAE N90-20058
Fighter escape system: The next step forward N90-20059
Ejection seat training of jet pilots and weapon system officers at the German Air Force School of Aviation Medicine N90-20061
The USAF Advanced Dynamic Anthropomorphic Manikin (ADAM) N90-20062
Windblast protection for advanced ejection seats N90-20063
Spacecraft escape N90-20066
EJECTION TRAINING
Ejection seat training of jet pilots and weapon system officers at the German Air Force School of Aviation Medicine N90-20061
ELASTIC DEFORMATION
Static aeroelastic analysis of a three-dimensional generic wing
[NASA-TM-102231] N90-20087
ELASTIC PLATES
Through-thickness strain response of thick composites in compression
[AD-A217233] N90-20141
ELASTIC PROPERTIES
Dynamics of electronically excited species in gaseous and condensed phase
[AD-A217696] N90-20812
ELASTIC SCATTERING
Reactive and anisotropic elastic scattering of highly laser-vibration-excited diatomic molecules
[MPIS-19/1988] N90-20804
Large-angle elastic and inelastic scattering of Pi+ and Pi- from Si28 and Ca40
[AD-A218163] N90-20818
ELASTOMERS
Synthesis of new polyphosphazene elastomers
[AD-A217585] N90-20216
ELASTOSTATICS
Ultrastructure processing of ordered polymers
[AD-A218331] N90-20232
ELECTRIC AUTOMOBILES
Advanced high-temperature batteries N90-20480
ELECTRIC BATTERIES
Flight termination system battery guidelines
[AD-A217310] N90-20092
All-solid-state thin-film rechargeable lithium batteries using solid redox polymerization electrodes
[DE90-008665] N90-20306
Space Electrochemical Research and Technology (SERT), 1989
[NASA-CP-3056] N90-20454
Overview of battery usage in NASA/GSFC LEO and GEOspacecrafts N90-20455

The application of electrochemical impedance spectroscopy for characterizing the degradation of Ni(OH)2/NiOOH electrodes N90-20474
Advanced high-temperature batteries N90-20480
Advanced calcium thionyl chloride high power battery [AD-A216685] N90-20482
Energy storage and distribution [DE89-009487] N90-20486

ELECTRIC CONDUCTORS
Thermoelectric conversion with ion conductors [AD-A217822] N90-20497

ELECTRIC CURRENT
Measurements of the interaction of high-voltage biassed conductors with the ionosphere [AD-A218285] N90-20580

ELECTRIC ENERGY STORAGE
Space Electrochemical Research and Technology (SERT), 1989 [NASA-CP-3056] N90-20454

ELECTRIC FIELDS
Modelling Doppler broadening in Raman propagation [DE90-008042] N90-20269
Radar detection of lightning and electric fields [AD-A217894] N90-20574
Quantifying and reducing uncertainty in the assimilative mapping of ionospheric electrodynamics [AD-A218057] N90-20577

ELECTRIC FILTERS
A linear filtering technique for removal of low-frequency noise [DE90-006183] N90-20296

ELECTRIC MOTOR VEHICLES
Life-cycle cost comparisons of advanced storage batteries and fuel cells for utility, stand-alone, and electric vehicle applications [DE90-008090] N90-20298

ELECTRIC POTENTIAL
Electronic precipitator control [NASA-CASE-LAR-13273-2] N90-20320
The application of Dow Chemical's perfluorinated membranes in proton-exchange membrane fuel cells N90-20466
Hydrogen-oxygen proton-exchange membrane fuel cells and electrolyzers N90-20467
Measurements of the interaction of high-voltage biassed conductors with the ionosphere [AD-A218285] N90-20580

ELECTRIC POWER PLANTS
Advanced on-site power plant development technology program [DE90-000443] N90-20484
Innovative turbine concepts for open-cycle OTEC (Ocean Thermal Energy Conversion) [DE90-000315] N90-20493

ELECTRIC POWER SUPPLIES
Flight termination system battery guidelines [AD-A217310] N90-20092
Space Station Freedom electric power system availability study [NASA-CR-185181] N90-20120
Power conditioning techniques [NASA-TM-102577] N90-20301

ELECTRICAL FAULTS
Velocity matched optical transmitter [AD-A217413] N90-20830

ELECTRICAL INSULATION
The effects of radiation on the mechanical properties of polymers used as electrical cable insulation and jacketing materials [AERE-R-13286] N90-20209
Materials and selection criteria analysis for the compact ignition tokamak toroidal field coil turn-to-turn insulation system: Photographic summary oflaboratory testing [DE90-006020] N90-20850

ELECTRICAL PROPERTIES
Modeling studies of electrolyte flow and bubble behavior in advanced Hall cells [DE90-007013] N90-20303
A nonintrusive method for measuring the operating temperature of a solenoid-operated valve [DE90-007576] N90-20355
The electronic properties of high (Tc) superconductors probed by positron annihilation [DE90-008354] N90-20883

ELECTRICAL RESISTANCE
Enhanced ceria solid electrolyte fuel cell development. Reduction of electronic conductivity permits use of a solid ceria electrolyte in high efficiency high power density fuel cells at temperatures compatible with metallic cell hardware [AD-A217840] N90-20498

ELECTRICAL RESISTIVITY
Deep level transient spectroscopy in resistive layers [DE90-008349] N90-20169
Electronic and ionic transport in processable conducting polymers [AD-A218093] N90-20229
High-temperature ceramic superconductors [AD-A218347] N90-20233
Differential measurements of the lateral photo effect in GaAs/AlGaAs heterostructures [AERE-R-13557] N90-20861
SiO(x) precipitation: Defect density correlation with the n+ substrate resistivity [DE90-005593] N90-20878

ELECTRICITY
Perspectives on solar energy and the environment [DE90-007680] N90-20494

ELECTRO-OPTICS
Performance of a 300 Mbps 1:16 serial/parallel optoelectronic receiver module [NASA-TM-103110] N90-20302
Joint Services Electronics Program research in electronics [AD-A217745] N90-20307
Joint services electronics program [AD-A217961] N90-20311
Picosecond Laser Facility [AD-A217784] N90-20384
Bibliography of spatial interferometry in optical astronomy [NASA-TM-100754] N90-20911

ELECTROCATALYSTS
Space Electrochemical Research and Technology (SERT), 1989 [NASA-CP-3056] N90-20454
Electrocatalysis for oxygen electrodes in fuel cells and water electrolyzers for space applications N90-20468
Non-noble electrocatalysts for alkaline fuel cells N90-20470

ELECTROCHEMICAL CELLS
The electrochemical generation of useful chemical species from lunar materials N90-20461
KOH concentration effect on the cycle life of nickel-hydrogen cells. Part 4: Results of failure analyses N90-20475
Advances in ambient temperature secondary lithium cells N90-20481

ELECTROCHEMICAL CORROSION
Electrochemical phase diagrams for aqueous redox systems [AD-A217168] N90-20157

ELECTROCHEMISTRY
Chemical and electrochemical studies in ionic liquids [AD-A217742] N90-20175
Electronic and ionic transport in processable conducting polymers [AD-A218093] N90-20229
An electrochemical and spectroscopic study of electrode processes [AD-A217261] N90-20289
Exploratory battery technology development and testing report for 1988 [DE90-007996] N90-20297
Fluid dynamics analysis of a rotating axisymmetric part using FIDAP [DE90-008733] N90-20340
Space Electrochemical Research and Technology (SERT), 1989 [NASA-CP-3056] N90-20454
Advanced double layer capacitors N90-20464
Novel electrodes for advanced energy storage systems [DE90-008667] N90-20496
Identification of defects in SOI (Silicon-On-Insulator) wafers [DE90-006020] N90-20879

ELECTRODE MATERIALS
Space Electrochemical Research and Technology (SERT), 1989 [NASA-CP-3056] N90-20454

ELECTRODES
Enhancement of mass transfer to a rotating cylinder electrode by inert particles suspended in the electrolyte [DE90-008054] N90-20165
Techno-economic assessment of a carbothermic alumina reduction process [DE90-007018] N90-20170
Microwave field effect transistor [NASA-CASE-GSC-12442-2] N90-20282
An electrochemical and spectroscopic study of electrode processes [AD-A217261] N90-20289
The electrochemical generation of useful chemical species from lunar materials N90-20461
Recent advances in solid polymer electrolyte fuel cell technology with low platinum loading electrodes N90-20465
Oxygen electrodes for rechargeable alkaline fuel cells-II N90-20469
Corrosion testing of candidates for the alkaline fuel cell cathode N90-20471
Structural comparison of nickel electrodes and precursor phases N90-20472
Impedance studies of Ni/Cd and Ni/H2 cells using the cell case as a reference electrode N90-20473
The application of electrochemical impedance spectroscopy for characterizing the degradation of Ni(OH)2/NiOOH electrodes N90-20474
KOH concentration effect on the cycle life of nickel-hydrogen cells. Part 4: Results of failure analyses N90-20475
Advances in lightweight nickel electrode technology N90-20476
Nickel-hydrogen capacity loss on storage N90-20478
Advanced high-temperature batteries N90-20480
Novel electrodes for advanced energy storage systems [DE90-008667] N90-20496
GaAs traveling-wave optical modulators using modulated coplanar electrodes with periodic cross-tie overlays [AD-A217731] N90-20835

ELECTRODYNAMICS
Quantifying and reducing uncertainty in the assimilative mapping of ionospheric electrodynamics [AD-A218057] N90-20577

ELECTROLYSIS
Electrocatalysis for oxygen electrodes in fuel cells and water electrolyzers for space applications N90-20468

ELECTROLYTES
Enhancement of mass transfer to a rotating cylinder electrode by inert particles suspended in the electrolyte [DE90-008054] N90-20165
Exploratory battery technology development and testing report for 1988 [DE90-007996] N90-20297
Monolithic solid oxide fuel cell development N90-20460
Advanced double layer capacitors N90-20464
KOH concentration effect on the cycle life of nickel-hydrogen cells. Part 4: Results of failure analyses N90-20475
Nickel-hydrogen capacity loss on storage N90-20478
Advanced high-temperature batteries N90-20480
Advances in ambient temperature secondary lithium cells N90-20481

ELECTROLYTIC CELLS
Modeling studies of electrolyte flow and bubble behavior in advanced Hall cells [DE90-007013] N90-20303
Recent advances in solid polymer electrolyte fuel cell technology with low platinum loading electrodes N90-20465
Impedance studies of Ni/Cd and Ni/H2 cells using the cell case as a reference electrode N90-20473
Enhanced ceria solid electrolyte fuel cell development. Reduction of electronic conductivity permits use of a solid ceria electrolyte in high efficiency high power density fuel cells at temperatures compatible with metallic cell hardware [AD-A217840] N90-20498

ELECTROMAGNETIC COUPLING
Computation of coupling elements between waveguides and modes for large launching structures [IPPCZ-290] N90-20842

ELECTROMAGNETIC FIELDS
Integrability and chaos in nonlinearly coupled optical beams [DE90-007540] N90-20834

ELECTROMAGNETIC INTERFERENCE
Effects of additional interfering signals on adaptive array performance [NASA-CR-186508] N90-20271

ELECTROMAGNETIC SPECTRA
Research investigation directed toward extending the useful range of the electromagnetic spectrum [AD-A217460] N90-20267
Seeing in a new light: Astro-1 teacher's guide with activities [NASA-EP-274] N90-20900

ELECTROMAGNETIC SURFACE WAVES
Recent improvements to the electromagnetic surface patch code [AD-A217479] N90-20293

ELECTROMAGNETISM
Superconductive microprobes for eddy current evaluation of materials [AD-A217776] N90-20361

ELECTROMECHANICS
Aerospace induction motor actuators driven from a 20-kHz power link [NASA-TM-102482] N90-20085

ELECTRON ATTACHMENT
Electron-impact ionization and electron attachment cross sections of radicals important in transient gaseous discharges
[AD-A217510] N90-20366
ELECTRON BEAMS
An electron-beam controlled semiconductor switch
[AD-A217181] N90-20288
Relativistic klystron afterburner simulation techniques
[DE90-008539] N90-20305
Electron beam generation by electron bombardment induced cathode emission
[AD-A218203] N90-20318
Dual cathode system for electron beam instruments
[NASA-CASE-NPO-16878-1-CU] N90-20351
Energy deposition measurements for E-beam pumped excimer lasers
[DE90-007545] N90-20365
Strategies for high efficiency operation of the E-beam excited atomic xenon laser using high-power and high-energy loading
[DE90-005196] N90-20370
Electron beam induced damage in PECVD Si3N4 and SiO2 films on InP
[NASA-TM-102544] N90-20393
Production rates for electron beams and swarms in nitrogen
[AD-A218145] N90-20817
A new technique for guiding of electron beams
[DE90-008660] N90-20824
Nonlinear plasma and beam physics in plasma wake-fields
[DE90-008812] N90-20855
ELECTRON BOMBARDMENT
Electron beam generation by electron bombardment induced cathode emission
[AD-A218203] N90-20318
ELECTRON CAPTURE
Absolute pressure dependence of the second ionization level of EL2 in GaAs
[DE90-007761] N90-20872
ELECTRON DENSITY (CONCENTRATION)
Wetting of metallic carbides by non-reactive liquid metals
[AERE-M-3759] N90-20185
Difference in electron thermal diffusivity and profile between interior and exterior of TFTR L-mode plasmas
[DE90-007479] N90-20846
Particle transport in pellet fueled JET (Jet European Torus) plasmas
[DE90-008077] N90-20851
ELECTRON ENERGY
Production rates for electron beams and swarms in nitrogen
[AD-A218145] N90-20817
Difference in electron thermal diffusivity and profile between interior and exterior of TFTR L-mode plasmas
[DE90-007479] N90-20846
Electronic properties of high-temperature superconductors
[AD-A217953] N90-20892
ELECTRON GUNS
The impedance of energy efficiency of a coaxial magnetized plasma source used for spheromak formation and sustainment
[DE90-003220] N90-20841
ELECTRON IMPACT
Electron-impact ionization and electron attachment cross sections of radicals important in transient gaseous discharges
[AD-A217510] N90-20366
ELECTRON MICROSCOPY
Analytical electron microscopy of catalyst preparations
[DE90-008699] N90-20173
High resolution transmission electron microscopy study of defect structures in mixed-phase YBaCuO
[DE90-007767] N90-20873
ELECTRON PLASMA
Difference in electron thermal diffusivity and profile between interior and exterior of TFTR L-mode plasmas
[DE90-007479] N90-20846
ELECTRON PUMPING
High efficiency flashlamp-pumped titanium: Sapphire laser
[AD-A217598] N90-20367
ELECTRON RADIATION
Research of the interaction between hydrogen and deuterium with atomic eigen defects and dislocations in nickel and iron
[ETN-90-95380] N90-20195
ELECTRON SPECTROSCOPY
Deep level transient spectroscopy in resistive layers
[DE90-008349] N90-20169
ELECTRON SPIN
Theoretical studies of spin-forbidden processes within the Breit-Pauli approximation
[AD-A217778] N90-20815
ELECTRON STATES
Dynamics of electronically excited species in gaseous and condensed phase
[AD-A217696] N90-20812
Electronically metastable molecules of high symmetry
[AD-A217768] N90-20814
ELECTRON TRANSFER
Ligand-centered electron-transfer redox processes for manganese, iron, and cobalt complexes in relation to selected catalytic systems
[AD-A217957] N90-20177
Interactions of molecules with surfaces
[DE90-007555] N90-20806
ELECTRON TUNNELING
Design and calibration of a vacuum compatible scanning tunneling microscope
[NASA-TM-102514] N90-20353
ELECTRONIC CONTROL
The implementation and operation of a variable-response electronic throttle control system for a TF-104G aircraft
[NASA-TM-101696] N90-20086
Electronic precipitator control
[NASA-CASE-LAR-13273-2] N90-20320
ELECTRONIC COUNTERMEASURES
Wideband S band transmitter
[AD-A217620] N90-20295
ELECTRONIC EQUIPMENT
Computed tomography of electronics
[AD-A217976] N90-20314
ELECTRONIC PACKAGING
Moisture control in sealed electronic packages
[DE90-008136] N90-20166
ELECTRONS
Energy transfer between electrons and ions in collision cascades in solids
[AERE-R-13662] N90-20801
Electronically metastable molecules of high symmetry
[AD-A217768] N90-20814
ELECTROSTATICS
The calculation of hydrogen-bonding properties
[DE90-007534] N90-20168
The GRADIO spaceborne gravity gradiometer: Development and accommodation N90-20560
The impedance of energy efficiency of a coaxial magnetized plasma source used for spheromak formation and sustainment
[DE90-003220] N90-20841
Enhanced pinch effect due to electrostatic potential
[DE90-007088] N90-20844
ELEVATION ANGLE
Lateral attenuation of military aircraft flight noise
[AD-A218041] N90-20799
ELLIPSES
Downward continuation of the free-air gravity anomalies to the ellipsoid using the gradient solution and terrain correction: An attempt of global numerical computations N90-20541
ELLIPSOMETERS
An ellipsometric measurement of optical properties for InP surfaces
[AD-A217185] N90-20827
Refractive index profiles of thermally grown and chemically vapor deposited films on silicon
[AD-A217187] N90-20865
EMBRITTLEMENT
Tellurium embrittlement of type 316 steel
[AERE-R-13440] N90-20192
EMISSION
Overview of the methodologies used to compile large scale emissions inventories
[DE90-008518] N90-20509
Populations of excited states and reaction mechanisms in the emission of complex fragments
[DE90-007481] N90-20819
EMISSION SPECTRA
Spectral solar radiation data base documentation, volume 1
[DE89-009447] N90-20571
EMISSIVITY
Analysis of methods to determine emissivity for ground surface targets in the spectral band 8 to 14 microns
[INPE-4984-TDL/394] N90-20447
EMITTERS
Spectral line shape code for multielectron emitters
[DE90-008526] N90-20853
END EFFECTORS
Development of a passive robot-controlled reaction arm N90-20389
Gripping device
[NASA-CASE-MSC-21365-1] N90-20408
ENERGY ABSORPTION
Optimization of fracture resistance in composites
[AD-A217431] N90-20144
ENERGY BANDS
Electronic properties of high-temperature superconductors
[AD-A217953] N90-20892
ENERGY BUDGETS
Improved energy and power balance at Nova targets
[DE90-007260] N90-20372
Cloud types and the tropical Earth radiation budget, revised
[NASA-CR-180475] N90-20582
ENERGY CONSERVATION
Modeling studies of electrolyte flow and bubble behavior in advanced Hall cells
[DE90-007013] N90-20303
Energy storage and distribution
[DE89-009487] N90-20488
Controlling Summer Heat Islands: Proceedings
[DE90-008075] N90-20508
The impedance of energy efficiency of a coaxial magnetized plasma source used for spheromak formation and sustainment
[DE90-003220] N90-20841
ENERGY CONSUMPTION
Analyses of power consumption for two sliding vane type compressors
[AD-A218366] N90-20406
Energy storage and distribution
[DE89-009487] N90-20488
Perspectives on solar energy and the environment
[DE90-007680] N90-20494
ENERGY CONVERSION EFFICIENCY
Strategies for high efficiency operation of the E-beam excited atomic xenon laser using high-power and high-energy loading
[DE90-005196] N90-20370
High-efficiency silicon concentrator solar cell research
[DE90-008040] N90-20490
ENERGY DISSIPATION
Present status of (mu)CF theory
[DE90-007547] N90-20809
ENERGY LEVELS
Precompound decay models for medium energy nuclear reactions
[DE90-008352] N90-20808
Determinations of photon spectra
[AD-A218003] N90-20816
ENERGY POLICY
Perspectives on solar energy and the environment
[DE90-007680] N90-20494
ENERGY SPECTRA
Determinations of photon spectra
[AD-A218003] N90-20816
ENERGY STORAGE
ARDEC (Armament Research, Development and Engineering Center) electric gun in-house test program
[AD-A217337] N90-20105
Exploratory battery technology development and testing report for 1988
[DE90-007996] N90-20297
Energy storage and distribution
[DE89-009487] N90-20488
Novel electrodes for advanced energy storage systems
[DE90-008667] N90-20496
Physical performance and carbohydrate consumption in CF commandos during a 5-day field trial
[AD-A217204] N90-20619
ENERGY TRANSFER
Energy deposition measurements for E-beam pumped excimer lasers
[DE90-007545] N90-20365
Solar cyclical trend study of the mid-latitude, quiet-time, meridional, neutral winds at winter solstice conditions
[AD-A217398] N90-20568
A continued study of optical sound generation and amplification
[AD-A217640] N90-20796
Energy transfer between electrons and ions in collision cascades in solids
[AERE-R-13662] N90-20801
Interactions of molecules with surfaces
[DE90-007555] N90-20806
ENGINE CONTROL
The implementation and operation of a variable-response electronic throttle control system for a TF-104G aircraft
[NASA-TM-101696] N90-20086
ENGINE DESIGN
Development and fabrication of structural components for a scramjet engine
[NASA-CR-181945] N90-20088

Analyses of power consumption for two sliding vane type compressors
[AD-A218366] N90-20406

ENGINE PARTS
Compendium of abstracts and viewgraphs.
[AD-A217189] N90-20140

ENTHALPY
Wetting of metallic carbides by non-reactive liquid metals
[AERE-M-3759] N90-20185

ENTROPY
On metric entropy, Vapnik-Chervonenkis dimension, and learnability for a class of distributions
[AD-A217331] N90-20759
Experimental feasibility of investigating acoustic waves in Couette flow with entropy and pressure gradients
[NASA-TM-102621] N90-20795
The measurements of thermoacoustic phenomena using thermoacoustic couples
[AD-A218018] N90-20796

ENVIRONMENT SIMULATION
Assessment of crew workload measurement methods, techniques and procedures. Volume 1: Process, methods and results
[AD-A217699] N90-20647

ENVIRONMENTAL MONITORING
Use of environmental monitoring data in evaluation of atmospheric modeling results
[DE90-008607] N90-20510

ENZYMES
Carbon and hydrogen metabolism of green algae in light and dark
[DE90-008648] N90-20612

EPHEMERIDES
A satellite simulation program
[AD-A218079] N90-20124

EPIDEMIOLOGY
The United States Air Force School of Aerospace Medicine: Special report
[AD-A217740] N90-20622

EPINEPHRINE
The effects of high intensity cycle exercise on sympatho-adrenal-medullary response patterns
[AD-A217962] N90-20628
The effects of graded exercise at sea level on plasma proenkephalin peptide F and catecholamine responses
[AD-A218195] N90-20633

EPITAXY
Growth, characterization and device development in monocrystalline diamond films
[AD-A218211] N90-20695

EPOXY RESINS
Compression testing of thick-section composite materials
[AD-A217234] N90-20142
Materials and selection criteria analysis for the compact ignition tokamak toroidal field coil turn-to-turn insulation system: Photographic summary oflaboratory testing
[DE90-008020] N90-20850

EQUATIONS OF MOTION
ETO (Earth-To-Orbit): A trajectory program for aerospace vehicles
[AD-A218157] N90-20103
Discrete-time control of a spacecraft with retargetable flexible antennas N90-20119
Discrete-time control of a spacecraft with retargetable flexible antennas
[AD-A218345] N90-20125
The invertibility principle for a simple hurricane model
[AD-A218344] N90-20605
Periodic trajectories for two-dimensional nonintegrable Hamiltonians
[DE90-008082] N90-20765
Integrability and chaos in nonlinearly coupled optical beams
[DE90-007540] N90-20834

EQUIVALENT CIRCUITS
Investigation of tapered multiple microstrip lines for VLSI circuits
[AD-A217855] N90-20310

EROSION
Magnetic vapor shield mechanism for protection of material surfaces exposed to high heat load
[AD-A217667] N90-20217

ERROR ANALYSIS
Error control techniques for satellite and space communications
[NASA-CR-186221] N90-20263
Analysis of methods to determine emissivity for ground surface targets in the spectral band 8 to 14 microns
[INPE-4984-TDL/394] N90-20447
Gravity field determination and error assessment techniques N90-20517
An improved error assessment for the GEM-T1 gravitational model N90-20518
Synopsis of early field test results from the gravity gradiometer survey system N90-20525
The Rapid Geodetic Survey System (RGSS) N90-20528
Geographically correlated orbit error N90-20551
Gravity field information from Gravity Probe-B N90-20554
Local gravity disturbance estimation from multiple-high-single-low satellite-to-satellite tracking N90-20555
A discussion of observation model, error sources and signal size for spaceborne gravitational gradiometry N90-20557
Satellite radar altimetry over ice. Volume 1: Processing and corrections of Seasat data over Greenland
[NASA-RP-1233-VOL-1] N90-20562
Study of possible solar heating effects on thermosonde probes: Error analysis
[AD-A218116] N90-20917

ERROR SIGNALS
The adaptive line enhancer applied to chirp detection
[DE90-006772] N90-20268
First-order intensity statistics for non-Rayleigh fading
[AD-A217572] N90-20569

ERRORS
Viscous shock profiles and primitive formulations
[NASA-CR-182029] N90-20049
A guide to performing and documenting safety analyses
[DE90-008687] N90-20260
Error control techniques for satellite and space communications
[NASA-CR-186221] N90-20263
Treatment of geodetic leveling in the integrated geodesy approach N90-20546

ESA SPACECRAFT
ARISTOTELES: A European approach for an Earth gravity field recovery mission N90-20559

ESCAPE CAPSULES
Requirements for protective pressure suits for the Hermes spacecrew N90-20065

ESCAPE SYSTEMS
Implications of Advanced Technologies for Air and Spacecraft Escape
[AGARD-CP-472] N90-20054
Development of acceleration exposure limits for advanced escape systems N90-20055
Development of an ejection seat specification for a new fighter aircraft N90-20057
Escape systems research at RAE N90-20058
Fighter escape system: The next step forward N90-20059
Potential role of avionics in escape systems N90-20060
Ejection seat training of jet pilots and weapon system officers at the German Air Force School of Aviation Medicine N90-20061
The USAF Advanced Dynamic Anthropomorphic Manikin (ADAM) N90-20062
Controllable propulsion for escape systems control N90-20064

ESTIMATES
Stochastic approach to the initiation of pitting corrosion
[AERE-R-13348] N90-20190

ESTIMATING
Evaluation of TM/LANDSAT and HRV/SPOT data in the identification of reforested areas in the Mogi-Guacu (SP) region
[INPE-4874-PRE/1485] N90-20442
Local gravity disturbance estimation from multiple-high-single-low satellite-to-satellite tracking N90-20555
Analysis of altimetry over inland seas
[NASA-TM-100729] N90-20566

ETCHING
Mechanisms of reactive etching
[AD-A217679] N90-20160
In-situ differential reflectance study of the etching of SiO2 films
[AD-A217186] N90-20864

ETHNIC FACTORS
ONR (Office of Naval Research) summer scholars for the 1989 PREFACE Program
[AD-A217746] N90-20919

EULER EQUATIONS OF MOTION
Numerical simulations of supersonic flow through oscillating cascade sections
[NASA-TM-103100] N90-20051

EUROPE
Long range geoid control through the European GPS traverse: Final results N90-20545

EUROPEAN SPACE PROGRAMS
Center of Gravity: Metallic Solidification
[DFVLR-IB-333-89/3] N90-20238
German microgravity program and flight opportunities N90-20239
User center and assitance N90-20240
Microgravity conditions of a space vehicle N90-20247

EVAPORATION RATE
Hydration effects on human physiology and exercise-heat performance
[AD-A217969] N90-20629

EVOKED RESPONSE (PSYCHOPHYSIOLOGY)
Brain activity during tactical decision-making. Part 3: Relationships between probe-evoked potentials, simulation performance, and on-job performance
[AD-A217207] N90-20638

EXCIMER LASERS
Energy deposition measurements for E-beam pumped excimer lasers
[DE90-007545] N90-20365
Development of a laser fluorosensor for the aircraft supported analysis of maritime toxic agents loads: Definition phase
[ETN-90-95320] N90-20499

EXCITATION
Strategies for high efficiency operation of the E-beam excited atomic xenon laser using high-power and high-energy loading
[DE90-005196] N90-20370
Energy transfer between electrons and ions in collision cascades in solids
[AERE-R-13662] N90-20801
Populations of excited states and reaction mechanisms in the emission of complex fragments
[DE90-007481] N90-20819

EXERCISE PHYSIOLOGY
Elevated central venous pressure: A consequence of exercise training-induced hypervolemia
[NASA-TM-102965] N90-20617

EXISTENCE THEOREMS
A general existence and uniqueness theorem for implicit differential-algebraic equations
[AD-A217965] N90-20770

EXOSAT SATELLITE
EXOSAT observations of Seyfert type galaxies N90-20910

EXPANSION
Ring expansion and equilibration in organophosphazenes, and the relationship to polymerization
[AD-A218234] N90-20230

EXPERIMENT DESIGN
Experimental proposition aboard the second data collecting satellite-SCD 2 of the MECB
[INPE-4980-RPE/606] N90-20128
ARISTOTELES: A European approach for an Earth gravity field recovery mission N90-20559
The GRADIO spaceborne gravity gradiometer: Development and accommodation N90-20560

EXPERIMENTATION
Microgravity Science and Application Program tasks, 1989 revision
[NASA-TM-4191] N90-20252

EXPERT SYSTEMS
An expert system for the design of heating, ventilating, and air-conditioning systems
[AD-A218287] N90-20262
Robot navigation research using the HERMIES mobile robot
[DE90-001952] N90-20396
Computer simulation of the mathematical modeling involved in constitutive equation development: Via symbolic computations
[NASA-TM-102532] N90-20428
A system for analysis and interpretation of lineaments in remote sensing images
[INPE-4893-PRE/1494] N90-20565
A prototype expert system to forecast severe winds in the western Mediterranean Sea
[AD-A218017] N90-20593
Broadening the interface bandwidth in simulation based training N90-20666
Hybrid intelligent perception system: Intelligent perception through combining artificial neural networks and an expert system
[DE90-007483] N90-20746

EXPLOSIVES
High-Explosives Applications Facility (HEAF)
[DE90-008122] N90-20257

EXPONENTIAL FUNCTIONS
An algorithm for efficient estimation of superimposed exponential signals
[AD-A217218] N90-20698

EXPOSURE
Development of acceleration exposure limits for advanced escape systems N90-20055

EXTINCTION
The extinction and structure of counterflow premixed flames
[AD-A218106] N90-20178
EXTRAPOLATION
Techniques for accelerating iterative methods for the solution of mathematical problems
[AD-A218272] N90-20775
EYE (ANATOMY)
Biological applications and effects of optical masers
[AD-A217910] N90-20385

F

FABRICATION
Development and fabrication of structural components for a scramjet engine
[NASA-CR-181945] N90-20088
Simple reflection holography
[DE90-008309] N90-20359
An applicational process for dynamic balancing of turbomachinery shafting
[NASA-TM-102537] N90-20392
Monolithic solid oxide fuel cell development
N90-20460
The electrochemical generation of useful chemical species from lunar materials N90-20461
CCST (Center for Compound Semiconductor Technology) research briefs
[DE90-007782] N90-20874
FABRICS
Development and application of nonflammable, high-temperature beta fibers
[NASA-TM-102158] N90-20645
FABRY-PEROT INTERFEROMETERS
Spatial imaging using confocal Fabry-Perot interferometers
[DE90-008363] N90-20378
FACTORIZATION
Euler's theorem for polynomials
[AD-A218148] N90-20774
FAILURE
Residual stresses: A review of their measurement and interpretation using x ray diffraction
[AERE-R-13005] N90-20423
Space Station Freedom integrated fault model
N90-20673
FAILURE ANALYSIS
Space Station Freedom electric power system availability study
[NASA-CR-185181] N90-20120
Innovative design of composite structures: The use of curvilinear fiber format in composite structure design
[NASA-CR-186453] N90-20136
Fundamental aspects of and failure modes in high-temperature composites
[NASA-TM-102558] N90-20151
Tellurium embrittlement of type 316 steel
[AERE-R-13440] N90-20192
Pyrotechnic device technology
[DE90-007683] N90-20234
A guide to performing and documenting safety analyses
[DE90-008688] N90-20261
Product assurance technology for procuring reliable, radiation-hard, custom LSI/VLSI electronics
[NASA-CR-185954] N90-20281
Time-dependent failure of silver interlayer welds
[DE90-008015] N90-20440
KOH concentration effect on the cycle life of nickel-hydrogen cells. Part 4: Results of failure analyses
N90-20475
GCS plan for software aspects of certification
[NASA-CR-181972] N90-20694
Using formal methods to develop a paradigm for software design
[DE90-005633] N90-20703
FAILURE MODES
Fundamental aspects of and failure modes in high-temperature composites
[NASA-TM-102558] N90-20151
Pyrotechnic device technology
[DE90-007683] N90-20234
Nine-year aging behavior of the ceramic flatpack resonator
[DE90-008044] N90-20412
KOH concentration effect on the cycle life of nickel-hydrogen cells. Part 4: Results of failure analyses
N90-20475
FARM CROPS
Relationship of radiometric field measurements of wheat in the Assis-Safra region, 1988
[INPE-4949-RPE/598] N90-20443
LANDSAT-5 data in the study of wheat and bean crops
[INPE-4746-RPE/580] N90-20444
FAST FOURIER TRANSFORMATIONS
FFT-local gravimetric geoid computation N90-20536
Performance of FFT methods in local gravity field modelling N90-20537
Downward continuation of the free-air gravity anomalies to the ellipsoid using the gradient solution and terrain correction: An attempt of global numerical computations
N90-20541
Regional quasigeoid determination in Northern Germany and comparison with GPS N90-20544
FATIGUE (MATERIALS)
Hydrogen, thermal ageing and the role of carbides in fatigue of a high strength steel
[AERE-R-13599] N90-20183
Fatigue crack growth in martensitic 2 1/4Cr-1Mo steel at elevated temperatures
[AERE-R-13524] N90-20191
The diffraction of ultrasound by cracks: Comparison of experiment with theory
[AERE-R-13334] N90-20410
Through-the-thickness fatigue crack closure behavior in an aluminum alloy
[NASA-TM-102590] N90-20427
FATIGUE TESTS
Rolling contact fatigue of surface modified 440C using a 'Ge-Polymet' type disc rod test rig
[NASA-TM-100390] N90-20200
Strength and microstructure of ceramics
[AD-A217752] N90-20227
FAULT TOLERANCE
Fault simulator evaluation
[AD-A217782] N90-20308
Approximate evaluation of reliability and related quantities via perturbation techniques
[AD-A218340] N90-20417
Sensor and actuator selection for fault-tolerant control of flexible structures
[AD-A217384] N90-20433
Space Station Freedom integrated fault model
N90-20673
Using formal methods to develop a paradigm for software design
[DE90-005633] N90-20703
Asynchronous design for parallel processing architectures
[AD-A217421] N90-20734
FEASIBILITY ANALYSIS
A technical and economic evaluation of oxygen-enriched combustion in diesel engines using water-emulsified fuels
[DE90-008095] N90-20394
FEEDBACK
Aiming control: Theory and applications to dynamic control of space structures
[AD-A217877] N90-20123
FEEDBACK CONTROL
Design of a telerobotic controller with joint torque sensors
[DE90-008753] N90-20404
FEMALES
ONR (Office of Naval Research) summer scholars for the 1989 PREFACE Program
[AD-A217746] N90-20919
FERMIONS
Superstring field theory
[DE90-007694] N90-20897
FERROELECTRICITY
A new thermal sensor for x ray microcalorimetry
[DE90-008547] N90-20360
FERROMAGNETIC MATERIALS
Barkhausen noise analysis and ferromagnetic materials
[AD-A217989] N90-20792
FEYNMAN DIAGRAMS
Homogeneous chaos, p-forms, scaling and the feynman integral
[AD-A218339] N90-20777
FIBER COMPOSITES
Infiltration mechanics in conventional and hybridised fibre reinforced metal matrix composites
[AERE-R-13330] N90-20134
Composite laminate tailoring with probabilistic constraints and loads
[NASA-TM-102515] N90-20138
Compression testing of thick-section composite materials
[AD-A217234] N90-20142
Optimization of fracture resistance in composites
[AD-A217431] N90-20144
Oxygen concentrations on surfaces of carbon fibers
[AD-A217724] N90-20152
COMGEN: A computer program for generating finite element models of composite materials at the micro level
[NASA-TM-102556] N90-20438
FIBER OPTICS
A space-based optical communication system utilizing fiber optics
[AD-A217333] N90-20828
FIBER ORIENTATION
Innovative design of composite structures: The use of curvilinear fiber format to improve buckling resistance of composite plates with central circular holes
[NASA-CR-186454] N90-20135
Innovative design of composite structures: The use of curvilinear fiber format in composite structure design
[NASA-CR-186453] N90-20136
Compression testing of thick-section composite materials
[AD-A217234] N90-20142
Optimization of laminated composite plates
[AD-A217621] N90-20146
FIELD EFFECT TRANSISTORS
Microwave field effect transistor
[NASA-CASE-GSC-12442-2] N90-20282
FIELD EMISSION
A progress report on the Livermore Miniature Vacuum Tube Project
[DE90-008302] N90-20299
Amplified spontaneous emission measurements on the aurora large-aperture module
[DE90-004841] N90-20369
FIELD THEORY (PHYSICS)
Superstring field theory
[DE90-007694] N90-20897
FIGHTER AIRCRAFT
Development of an ejection seat specification for a new fighter aircraft N90-20057
F-15B high angle-of-attack phenomena and spin prediction using bifurcation analysis
[AD-A217366] N90-20073
The implementation and operation of a variable-response electronic throttle control system for a TF-104G aircraft
[NASA-TM-101696] N90-20086
FILE MAINTENANCE (COMPUTERS)
A model research archive: Archive and research implications for original records and support documents
[DE90-008246] N90-20906
FILM COOLING
Heat transfer near the entrance to a film cooling hole in a gas turbine blade
[AD-A217396] N90-20089
FINE STRUCTURE
Extended x ray absorption fine structure analysis applied to composite materials
[DE90-008575] N90-20150
L shell XANES (X ray Absorption Near Edge Structure) for solid metals: Ti, V, Cr, Fe, Ni, Cu
[DE90-008043] N90-20880
FINITE DIFFERENCE THEORY
Computer simulations and experiments to study the fracture of rods by flying plates
[DE90-008308] N90-20437
Recent advances in 3D finite difference mesh generation using the BRL-CAD package
[DE90-007854] N90-20704
Cell averaging Chebyshev methods for hyperbolic problems
[NASA-CR-182028] N90-20768
FINITE ELEMENT METHOD
A review of the analytical simulation of aircraft crash dynamics
[NASA-TM-102595] N90-20068
Optimization of laminated composite plates
[AD-A217621] N90-20146
Fluid dynamics analysis of a rotating axisymmetric part using FIDAP
[DE90-008733] N90-20340
Parallel algorithms in the finite element approximation of flow problems
[AD-A217729] N90-20341
A 4-node assumed-stress hybrid shell element with rotational degrees of freedom
[NASA-CR-4279] N90-20422
Rotordynamic analysis with shell elements for the transfer matrix method
[AD-A217455] N90-20434
Finite element models to predict the structural response of 120-mm sabot/rods during launch
[DE90-007497] N90-20436
COMGEN: A computer program for generating finite element models of composite materials at the micro level
[NASA-TM-102556] N90-20438

Plan, formulate, and discuss a NASTRAN finite element model of the UH-60A helicopter airframe
[NASA-CR-181975] N90-20439
Time-dependent failure of silver interlayer welds
[DE90-008015] N90-20440
Automated finite element modeling and simulation N90-20753

FIRE CONTROL
Diagnostics and firing control for the cylindrical reconnection launcher
[DE90-007677] N90-20107

FIRES
The thermal response of generic objects in JP-4 pool fires
[DE90-008503] N90-20259

FIRST AID
What should athletes know about low body temperature (hypothermia)
[AD-A218316] N90-20637

FLAME PROPAGATION
Aerodynamic and kinetic processes in flames
[AD-A217796] N90-20176
The extinction and structure of counterflow premixed flames
[AD-A218106] N90-20178

FLAME RETARDANTS
Development and application of nonflammable, high-temperature beta fibers
[NASA-TM-102158] N90-20645

FLAPS (CONTROL SURFACES)
The NASA digital VGH program: Exploration of methods and final results. Volume 2: L 1011 data 1978-1979: 1619 hours
[NASA-CR-181909-VOL-2] N90-20080

FLASH LAMPS
High efficiency flashlamp-pumped titanium: Sapphire laser
[AD-A217598] N90-20367
Flash-pumped titanium laser
[AD-A217599] N90-20368

FLAT PLATES
Numerical simulations of supersonic flow through oscillating cascade sections
[NASA-TM-103100] N90-20051

FLEXIBILITY
Control system design of the third flexible joint of PUMA 560 robot
[AD-A218075] N90-20405
Stabilized determination of geopotential coefficients by the mixed hom-BLUP approach N90-20520

FLEXIBLE BODIES
Sensor and actuator selection for fault-tolerant control of flexible structures
[AD-A217384] N90-20433

FLEXIBLE WINGS
Using transonic small disturbance theory for predicting the aeroelastic stability of a flexible wind-tunnel model
[NASA-TM-102617] N90-20047
Static aeroelastic analysis of a three-dimensional generic wing
[NASA-TM-102231] N90-20087
Digital-flutter-suppression-system investigations for the active flexible wing wind-tunnel model
[NASA-TM-102618] N90-20093

FLIGHT ALTITUDE
Computation of hypersonic low density flows with thermochemical nonequilibrium N90-20044

FLIGHT CHARACTERISTICS
Airworthiness and flight characteristics evaluation of the McDonnell Douglas Helicopter Corporation (MDHC) 530FF helicopter
[AD-A218253] N90-20076
The Real Time Interactive Display Environment (RTIDE), a display building tool developed by Space Shuttle flight controllers N90-20654

FLIGHT CONTROL
F-15B high angle-of-attack phenomena and spin prediction using bifurcation analysis
[AD-A217366] N90-20073
Flight termination system battery guidelines
[AD-A217310] N90-20092
Laboratory implementation of the Continuously Reconfiguring Multi-Microprocessor Flight Control System (CRMMFCS)
[AD-A217730] N90-20094
Interaction of switch actuation on tracking with a four-axis flight control (cross-coupling)
[AD-A217981] N90-20095
The Real Time Interactive Display Environment (RTIDE), a display building tool developed by Space Shuttle flight controllers N90-20654
The Real Time Display Builder (RTDB) N90-20656
Large screen display for the Mission Control Center N90-20662
Distributed earth model/orbiter simulation N90-20671

FLIGHT CREWS
Development of acceleration exposure limits for advanced escape systems N90-20055

FLIGHT OPERATIONS
Knowledge representation in space flight operations N90-20655

FLIGHT PATHS
Three-dimensional route planning for a cruise missile for minimal detection by observer
[AD-A218336] N90-20787

FLIGHT RECORDERS
The NASA digital VGH program: Exploration of methods and final results. Volume 2: L 1011 data 1978-1979: 1619 hours
[NASA-CR-181909-VOL-2] N90-20080
The NASA digital VGH program. Exploration of methods and final results. Volume 1: Development of methods
[NASA-CR-181909-VOL-1] N90-20081
The NASA digital VGH program. Exploration of methods and final results. Volume 3: B 727 data 1978-1980: 1765 hours
[NASA-CR-181909-VOL-3] N90-20082
The NASA digital VGH program: Exploration of methods and final results. Volume 4: B 747 data 1978-1980, 1689 hours
[NASA-CR-181909-VOL-4] N90-20083
The NASA digital VGH program: Exploration of methods and final results. Volume 5: DC 10 data 1981-1982, 129 hours
[NASA-CR-181909-VOL-5] N90-20084

FLIGHT SAFETY
Activities report in civil aviation
[ETN-90-95471] N90-20067

FLIGHT SIMULATION
Simulator sickness in the CH-47 (Chinook) flight simulator
[AD-A218214] N90-20634
The Real Time Interactive Display Environment (RTIDE), a display building tool developed by Space Shuttle flight controllers N90-20654
Efficient utilization of graphics technology for space animation N90-20663

FLIGHT SIMULATORS
Simulator sickness in the CH-47 (Chinook) flight simulator
[AD-A218214] N90-20634

FLIGHT STABILITY TESTS
F-15B high angle-of-attack phenomena and spin prediction using bifurcation analysis
[AD-A217366] N90-20073

FLIGHT SURGEONS
The United States Air Force School of Aerospace Medicine: Special report
[AD-A217740] N90-20622

FLIGHT TESTS
Airworthiness and flight characteristics evaluation of the McDonnell Douglas Helicopter Corporation (MDHC) 530FF helicopter
[AD-A218253] N90-20076
Aerodynamic analysis of a US Navy and Marine Corps unmanned air vehicle
[AD-A218282] N90-20077
Design and performance of a multi-stage cylindrical reconnection launcher
[DE90-007820] N90-20108

FLOORS
Floor pull test of a transport airframe section
[DOT/FAA/CT-TN88/14] N90-20072

FLOW CHARACTERISTICS
A method for measuring the material moduli of granular materials: Flow in an orthogonal rheometer
[DE90-007160] N90-20339

FLOW DISTRIBUTION
Heat transfer near the entrance to a film cooling hole in a gas turbine blade
[AD-A217396] N90-20089
A study of low-dimensional models for the wall region of a turbulent boundary layer N90-20321
Geometric scale of interaction between moving shock and stationary thermal layer
[AD-A217769] N90-20344
Experimental investigation of the mechanisms underlying vortex kinematics in unsteady separated flows
[AD-A217889] N90-20346
A sub-cloud layer vorticity budget analysis for two microburst-producing storms from jaws dual-Doppler data
[AD-A218180] N90-20599
Tools for 3D scientific visualization in computational aerodynamics N90-20660

FLOW EQUATIONS
Spectral simulation of unsteady compressible flow past a circular cylinder
[NASA-CR-182030] N90-20050
Composite-grid techniques and adaptive mesh refinement in computational fluid dynamics
[AD-A217383] N90-20328

FLOW MEASUREMENT
Nonintrusive optical measurements of turbulence and mixing in a stably stratified fluid N90-20322
A method for measuring the material moduli of granular materials: Flow in an orthogonal rheometer
[DE90-007160] N90-20339

FLOW STABILITY
Amplitude-dependent neutral modes in compressible boundary layer flows
[NASA-TM-102524] N90-20326

FLOW VELOCITY
Nonintrusive optical measurements of turbulence and mixing in a stably stratified fluid N90-20322
Characterization of fluid flow by digital correlation of scattered light
[NASA-CR-186403] N90-20324

FLOW VISUALIZATION
Characterization of fluid flow by digital correlation of scattered light
[NASA-CR-186403] N90-20324
Flow visualization studies in a curved rectangular channel with 40 to 1 aspect ratio and a straight channel with bulk flow unsteadiness
[AD-A218020] N90-20348
Tools for 3D scientific visualization in computational aerodynamics N90-20660

FLUID DYNAMICS
Aerodynamic analysis of a US Navy and Marine Corps unmanned air vehicle
[AD-A218282] N90-20077
Modification and improvement of software for modeling multidimensional reacting fuel flows
[AD-A217789] N90-20235
A simple multicomponent fluid theory with accurate physics
[DE90-006537] N90-20334
DURIP optical equipment for high-speed viscous-inviscid interaction research
[AD-A217772] N90-20345
Spacelab qualified infrared imager for microgravity science experiments
[NASA-TM-102503] N90-20352
Nonlinear stability in fluid and plasma dynamics
[AD-A217735] N90-20856

FLUID FLOW
Modeling studies of electrolyte flow and bubble behavior in advanced Hall cells
[DE90-007013] N90-20303
Characterization of fluid flow by digital correlation of scattered light
[NASA-CR-186403] N90-20324
Interior fluid dynamics of liquid-filled projectiles
[AD-A217630] N90-20330
A simple multicomponent fluid theory with accurate physics
[DE90-006537] N90-20334
Hydrodynamic interactions and transport coefficients in a suspension of spherical particles
[DE90-008301] N90-20336
A nonintrusive method for measuring the operating temperature of a solenoid-operated valve
[DE90-007576] N90-20355
Seismic characterization of fracture properties
[DE90-007759] N90-20570

FLUID MECHANICS
Multiple versus single scattering of terrestrial infrared longwave radiation in an aerosol-laden planetary boundary layer
[AD-A217709] N90-20272
Fluid dynamics analysis of a rotating axisymmetric part using FIDAP
[DE90-008733] N90-20340

FLUORESCENCE
An electrochemical and spectroscopic study of electrode processes
[AD-A217261] N90-20289

FLUORINATION
Fluorinated diamond thin films for tribological applications
[AD-A217452] N90-20214

FLUORO COMPOUNDS
Ionic disorder in crystals at high temperatures with emphasis on fluorites
[AERE-R-13544] N90-20862

FLUTTER
Using transonic small disturbance theory for predicting the aeroelastic stability of a flexible wind-tunnel model
[NASA-TM-102617] N90-20047
Digital-flutter-suppression-system investigations for the active flexible wing wind-tunnel model
[NASA-TM-102618] N90-20093

FLUTTER ANALYSIS
Using transonic small disturbance theory for predicting the aeroelastic stability of a flexible wind-tunnel model
[NASA-TM-102617] N90-20047
The application of active controls technology to a generic hypersonic aircraft configuration
[NASA-TM-101689] N90-20071
FLUX (RATE)
The inter-outburst behavior of cataclysmic variables
[NASA-CR-186374] N90-20914
FLUX DENSITY
Multiple versus single scattering of terrestrial infrared longwave radiation in an aerosol-laden planetary boundary layer
[AD-A217709] N90-20272
FOAMING
Instantaneously generated foam and its applicability to reduced gravity
[NASA-CR-185208] N90-20237
FOAMS
Instantaneously generated foam and its applicability to reduced gravity
[NASA-CR-185208] N90-20237
FOCAL PLANE DEVICES
NRL hybrid reliability. Physics of failure initial study
[AD-A217986] N90-20893
FOCUSING
Focused ion beam implantation
[AD-A217987] N90-20894
FORECASTING
A guide to performing and documenting safety analyses
[DE90-008687] N90-20260
Energy storage and distribution
[DE89-009487] N90-20488
Wind Energy Program summary. Volume 1: Overview
[DE89-009479] N90-20491
Global Warming: A Northwest Perspective
[DE90-008140] N90-20505
Overview of the methodologies used to compile large scale emissions inventories
[DE90-008518] N90-20509
An intercomparison of general circulation model predictions of regional climate change
[DE90-008325] N90-20589
FORESTS
Synthesis and analysis of 25 years (1961-1986) of INPE/SRE activities related to the vegetation/forest area
[INPE-4969-RPE/604] N90-20446
FORGING
Evaluation of material homogeneity as a function of thickness of low-alloy ferritic steel
[DE90-008069] N90-20202
FORMALISM
Theory of defect process: Basic issues in quantitative understanding
[AERE-R-13661] N90-20860
FOURIER TRANSFORMATION
Fourier transform methods in local gravity modeling N90-20538
FRACTALS
Fractal-based image compression
[AD-A217302] N90-20699
FRACTURE MECHANICS
Mechanical behavior of whisker reinforced ceramics
[DE90-008758] N90-20224
Limitations and applications of fracture assessment with R6
[AERE-R-13012] N90-20425
Computer simulations and experiments to study the fracture of rods by flying plates
[DE90-008308] N90-20437
FRACTURE STRENGTH
Optimization of fracture resistance in composites
[AD-A217431] N90-20144
Effect of heat treatment on the fracture toughness transition properties of an A508 class 3 steel
[AERE-R-13548] N90-20182
Fatigue crack growth in martensitic 2 1/4Cr-1Mo steel at elevated temperatures
[AERE-R-13524] N90-20191
Improved toughness alloys based on titanium aluminides
[AD-A218149] N90-20208
Tensile fracture toughness of ceramic materials: Effects of dynamic loading and elevated temperatures
[DE90-008329] N90-20223
Strength and microstructure of ceramics
[AD-A217752] N90-20227
FRACTURES (MATERIALS)
Summary report of the Summer Conference of the DARPA-Materials Research Council
[AD-A217380] N90-20143
FRACTURING
Effect of heat treatment on the fracture toughness transition properties of an A508 class 3 steel
[AERE-R-13548] N90-20182
Ageing effects in welded cast CF3 stainless steel
[AERE-R-13559] N90-20188
The stress-driven redistribution of point defects in the vicinity of crack-like singularities
[AERE-R-12898] N90-20424
FRAGMENTS
Populations of excited states and reaction mechanisms in the emission of complex fragments
[DE90-007481] N90-20819
FREE ATMOSPHERE
Downward continuation of the free-air gravity anomalies to the ellipsoid using the gradient solution and terrain correction: An attempt of global numerical computations N90-20541
FREE ELECTRON LASERS
Conference digest: Thirteenth International Conference on Infrared and Millimeter Waves, volume 1039
[AD-A217343] N90-20291
Harmonic generation mechanisms in short-wavelength free-electron lasers
[DE90-007622] N90-20374
Picosecond nonlinear studies of complex materials using the free electron laser
[AD-A218215] N90-20387
SDI (Strategic Defense Initiative): Is its future past
[DE90-008016] N90-20785
Role of free-electron lasers in strategic defense
[DE90-008028] N90-20786
FREE ENERGY
Interaction between implanted ions and intrinsic defects in silica
[DE90-006569] N90-20858
FREQUENCIES
An algorithm for efficient estimation of superimposed exponential signals
[AD-A217218] N90-20698
FREQUENCY ASSIGNMENT
Numerical Arc Segmentation Algorithm for a Radio Conference-NASARC (version 4.0) technical manual
[NASA-TM-101453] N90-20264
FREQUENCY SCANNING
DURIP theoretical/experimental investigations of highly energetic dication species
[AD-A217771] N90-20383
FRESNEL REGION
An investigation of the extent of the fresnel region of aperture antennas with attention to superdirectivity
[AD-A217518] N90-20294
FRICTION
Runaway rubber removal
[AD-A218349] N90-20100
FRICTION FACTOR
Experimentally determined wear behavior of an Al2O3-SiC composite from 25 to 1200 C
[NASA-TM-102549] N90-20130
FRONTS (METEOROLOGY)
Structure and dynamics of the Arizona monsoon boundary
[AD-A217378] N90-20586
Coastal frontogenesis and associated severe weather on 13 March 1986 (GALE IOP 13)
[AD-A217708] N90-20590
FUEL CELLS
Life-cycle cost comparisons of advanced storage batteries and fuel cells for utility, stand-alone, and electric vehicle applications
[DE90-008090] N90-20298
Monolithic solid oxide fuel cell development N90-20460
Recent advances in solid polymer electrolyte fuel cell technology with low platinum loading electrodes N90-20465
The application of Dow Chemical's perfluorinated membranes in proton-exchange membrane fuel cells N90-20466
Hydrogen-oxygen proton-exchange membrane fuel cells and electrolyzers N90-20467
Electrocatalysis for oxygen electrodes in fuel cells and water electrolyzers for space applications N90-20468
Oxygen electrodes for rechargeable alkaline fuel cells-II N90-20469
Non-noble electrocatalysts for alkaline fuel cells N90-20470
Corrosion testing of candidates for the alkaline fuel cell cathode N90-20471
Advanced on-site power plant development technology program
[DE90-000443] N90-20484
Enhanced ceria solid electrolyte fuel cell development. Reduction of electronic conductivity permits use of a solid ceria electrolyte in high efficiency high power density fuel cells at temperatures compatible with metallic cell hardware
[AD-A217840] N90-20498
FUEL COMBUSTION
Structure of model gas flames in nitramines
[AD-A217578] N90-20159
FUELS
Modification and improvement of software for modeling multidimensional reacting fuel flows
[AD-A217789] N90-20235
FUNGI
Air pollution-caused changes in photosynthesis: Effects on plant growth and rhizosphere functions
[DE90-007184] N90-20501
FURNACES
Fusion furnaces for Spacelab N90-20248
Method of preparing radially homogeneous mercury cadmium telluride crystals
[NASA-CASE-MFS-25786-2] N90-20896
FUSELAGES
Floor pull test of a transport airframe section
[DOT/FAA/CT-TN88/14] N90-20072
FUSION (MELTING)
Center of Gravity: Metallic Solidification
[DFVLR-IB-333-89/3] N90-20238
Principles of metallic solidification N90-20241
Supercooling and germ formation N90-20242
Fusion furnaces for Spacelab N90-20248
Electromagnetic fusion process and position research N90-20249
Diffusion and germ formation in glasses N90-20250
FUSION REACTORS
Application of railgun principle to high-velocity hydrogen pellet injection for magnetic fusion reactor refueling
[DE90-008281] N90-20109
Design of D-3 He commercial tokamak
[DE90-008252] N90-20852

G

GALACTIC CLUSTERS
Studies of the evolution of the x ray emission of clusters of galaxies
[NASA-CR-186471] N90-20918
GALACTIC EVOLUTION
Studies of the evolution of the x ray emission of clusters of galaxies
[NASA-CR-186471] N90-20918
GALACTIC STRUCTURE
M51's spiral structure
[DE90-007624] N90-20916
GALERKIN METHOD
An approximation theory for the identification of linear thermoelastic systems
[NASA-CR-182015] N90-20764
Magnetostatic boundary-value problems in the incomplete-nonlinear formulation and methods of their solution
[DE90-615185] N90-20767
GALLIUM ARSENIDES
An electron-beam controlled semiconductor switch
[AD-A217181] N90-20288
GaAs traveling-wave optical modulators using modulated coplanar electrodes with periodic cross-tie overlays
[AD-A217731] N90-20835
Differential measurements of the lateral photo effect in GaAs/AlGaAs heterostructures
[AERE-R-13557] N90-20861
Absolute pressure dependence of the second ionization level of EL2 in GaAs
[DE90-007761] N90-20872
GAMMA RAY SPECTROMETERS
Mercuric iodide room temperature gamma-ray detectors
[NASA-TM-103318] N90-20357
GAMMA RAYS
Development of gamma-emitting, receptor-binding radiotracers for imaging the brain and pancreas
[DE90-008314] N90-20621
The n-p bremsstrahlung in heavy ion collision processes
[DE90-008542] N90-20823
GAS ATOMIZATION
Spray deposition: A fundamental study of droplet impingement, spreading and consolidation
[AD-A217202] N90-20255
GAS DENSITY
Computation of hypersonic low density flows with thermochemical nonequilibrium N90-20044

GAS DISCHARGES
Electron-impact ionization and electron attachment cross sections of radicals important in transient gaseous discharges
[AD-A217510] N90-20366

GAS DYNAMICS
Spectral simulation of unsteady compressible flow past a circular cylinder
[NASA-CR-182030] N90-20050

GAS FLOW
Determination of flow-regime boundaries for cohesive particles
[DE90-007425] N90-20332
TiCl4 as a source of TiO2 particles for laser anemometry measurements in hot gas
[NASA-TM-102581] N90-20358

GAS JETS
Application of a three-dimensional Navier-Stokes model for a subsonic jet in a crossflow N90-20045

GAS LASERS
Strategies for high efficiency operation of the E-beam excited atomic xenon laser using high-power and high-energy loading
[DE90-005196] N90-20370

GAS TURBINE ENGINES
Heat transfer near the entrance to a film cooling hole in a gas turbine blade
[AD-A217396] N90-20089

GAS-ION INTERACTIONS
Termolecular associations of ions in gases, recombination and electron-atom collisions
[AD-A217678] N90-20805

GAS-SOLID INTERACTIONS
Molecular dynamics and spectroscopy at gas-solid interfaces
[AD-A217743] N90-20813

GAS-SOLID INTERFACES
Molecular dynamics and spectroscopy at gas-solid interfaces
[AD-A217743] N90-20813

GASES
System for venting gas from a liquid storage tank
[NASA-CASE-MSC-21253-1] N90-20254

GAUGE INVARIANCE
Superstring field theory
[DE90-007694] N90-20897

GAUSS EQUATION
Local moduli of continuity of some classes of Gaussian processes
[AD-A217692] N90-20778

GEARS
Bearing and gear steels for aerospace applications
[NASA-TM-102529] N90-20391

GENETIC ENGINEERING
Human serum albumin crystals and method of preparation
[NASA-CASE-MFS-28234-1] N90-20616

GENETICS
Life sciences: Lawrence Berkeley Laboratory, 1988
[DE90-008061] N90-20611

GEOCHEMISTRY
Electrochemical phase diagrams for aqueous redox systems
[AD-A217168] N90-20157

GEODESY
Committee on Geodesy - National Research Council
[AD-A217770] N90-20452
Gravitational model improvement at the Goddard Space Flight Center N90-20514
An improved model for the Earth's gravity field N90-20515
Precise solution for a finite set of spherical coefficients from equiangular gridded data N90-20522
The Rapid Geodetic Survey System (RGSS) N90-20528
First year's results and field experience with the latest JILA absolute gravimeter N90-20529
The role of topography in geodetic gravity field modelling N90-20534
Performance of FFT methods in local gravity field modelling N90-20537
Thin-plate spline quadrature of geodetic integrals N90-20539
Treatment of geodetic leveling in the integrated geodesy approach N90-20546
Geodynamics and temporal variations in the gravity field N90-20549

GEODYNAMICS
Progress in the Determination of the Earth's Gravity Field
[NASA-CR-185721] N90-20513
Geodynamics and temporal variations in the gravity field N90-20549

GEOIDS
Progress in the Determination of the Earth's Gravity Field
[NASA-CR-185721] N90-20513
Progress in the development of high degree potential coefficient models N90-20516
Geopotential models in the Australian region N90-20519
FFT-local gravimetric geoid computation N90-20536
The reduction correction in North America N90-20540
The geoid in Kenya N90-20542
GEOID '88: A gravimetric geoid for Canada N90-20543
Long range geoid control through the European GPS traverse: Final results N90-20545
A model of the general ocean circulation determined from a joint solution for the Earth's gravity field N90-20550
Analysis of altimetry over inland seas
[NASA-TM-100729] N90-20566

GEOLOGICAL FAULTS
A system for analysis and interpretation of lineaments in remote sensing images
[INPE-4893-PRE/1494] N90-20565
Seismic characterization of fracture properties
[DE90-007759] N90-20570

GEOLOGY
Geology, distribution of hot springs and hydrothermal alteration zones of major geothermal areas in Japan
[DE90-753026] N90-20451
Damage characteristics of time domain histories
[DE90-008787] N90-20573

GEOMAGNETISM
Measurements of the interaction of high-voltage biassed conductors with the ionosphere
[AD-A218285] N90-20580

GEOMETRY
Study of possible solar heating effects on thermosonde probes: Error analysis
[AD-A218116] N90-20917

GEOMORPHOLOGY
Underwater physiography of the continental shelf of Rio Grande do Norte visible through satellite imagery
[INPE-4964-TDL/392] N90-20448

GEOPHYSICS
Committee on Geodesy - National Research Council
[AD-A217770] N90-20452
Progress in the Determination of the Earth's Gravity Field
[NASA-CR-185721] N90-20513
Gravity field determination and error assessment techniques N90-20517
Modeling of the Earth's gravity field using the New Global Earth Model (NEWGEM) N90-20523

GEOPOTENTIAL
Geopotential models in the Australian region N90-20519
Stabilized determination of geopotential coefficients by the mixed hom-BLUP approach N90-20520
Geopotential coefficient determination and the gravimetric boundary value problem: A new approach N90-20521
Regional quasigeoid determination in Northern Germany and comparison with GPS N90-20544
Treatment of geodetic leveling in the integrated geodesy approach N90-20546
Spectral analyses of satellite geopotential missions N90-20552
Gravity field information from Gravity Probe-B N90-20554
Studies of an orbital gradiometer mission N90-20558

GEOPOTENTIAL HEIGHT
Long range geoid control through the European GPS traverse: Final results N90-20545
Structure and dynamics of the Arizona monsoon boundary
[AD-A217378] N90-20586

GEOPOTENTIAL RESEARCH MISSION
Studies of an orbital gradiometer mission N90-20558

GEOSTROPHIC WIND
A method for correcting and reducing the pressure data recorded at the PAM 2 stations during GALE
[AD-A218165] N90-20596

GEOSYNCHRONOUS ORBITS
A new concept for high-cycle-life LEO: Rechargeable MnO2-hydrogen N90-20462

GEOTHERMAL ENERGY CONVERSION
Hot dry rock geothermal energy: A renewable energy resource that is ready for development now
[DE90-007509] N90-20485

GEOTHERMAL ENERGY UTILIZATION
Hot dry rock geothermal energy: A renewable energy resource that is ready for development now
[DE90-007509] N90-20485

GEOTHERMAL RESOURCES
Geology, distribution of hot springs and hydrothermal alteration zones of major geothermal areas in Japan
[DE90-753026] N90-20451
Hot dry rock geothermal energy: A renewable energy resource that is ready for development now
[DE90-007509] N90-20485

GET AWAY SPECIALS (STS)
Design and test of a compact optics system for the pool boiling experiment
[NASA-TM-102530] N90-20253

GLACIERS
Airfields on antarctic glacier ice
[AD-A217638] N90-20097

GLASS
Instantaneously generated foam and its applicability to reduced gravity
[NASA-CR-185208] N90-20237

GLOBAL POSITIONING SYSTEM
GPS-aided gravimetry at 30 km altitude from a balloon-borne platform N90-20530
Regional quasigeoid determination in Northern Germany and comparison with GPS N90-20544
Long range geoid control through the European GPS traverse: Final results N90-20545
Refinement of Earth's gravity field with Topex GPS measurements N90-20553
Local gravity disturbance estimation from multiple-high-single-low satellite-to-satellite tracking N90-20555
Satellite-to-satellite tracking experiment for global gravity field mapping N90-20556

GLOBAL WARMING
Atmospheric Radiation Measurement Program Plan
[DE90-008108] N90-20504
Global Warming: A Northwest Perspective
[DE90-008140] N90-20505
Draft global warming study
[DE90-008446] N90-20507

GLOVES
Comparison of light duty gloves with natural and synthetic materials under wet and dry conditions
[AD-A218119] N90-20649

GLOW DISCHARGES
The glow discharge as an atomization and ionization source
[DE90-007693] N90-20163

GOLD
Infrared and X ray photoelectron spectroscopy studies of the polyimide/metal interface
[AD-A218249] N90-20179

GOVERNMENTS
The essence of spacepower: Important influences on the evolution of national spacepower
[AD-A217498] N90-20781

GRADIOMETERS
Terrestrial gravity instrumentation in the 20th Century: A brief review N90-20527
A discussion of observation model, error sources and signal size for spaceborne gravitational gradiometry N90-20557
Studies of an orbital gradiometer mission N90-20558

GRAIN BOUNDARIES
Tellurium embrittlement of type 316 steel
[AERE-R-13440] N90-20192
Dynamics of the solidification front N90-20243
Enhanced ceria solid electrolyte fuel cell development. Reduction of electronic conductivity permits use of a solid ceria electrolyte in high efficiency high power density fuel cells at temperatures compatible with metallic cell hardware
[AD-A217840] N90-20498

GRAIN SIZE
Effect of heat treatment on the fracture toughness transition properties of an A508 class 3 steel
[AERE-R-13548] N90-20182
Processing, fabrication, characterization and device demonstration of high temperature superconducting ceramics
[AD-A218330] N90-20231
A systematic study of the effects of metal substitutions for Cu in YBa(sub 2) (Cu(sub 1-x) M(sub x)3 O(sub 7-rho), M=Fe, Co, Al, Ga, Cr, Ni, and Zn
[DE90-003957] N90-20857

GRANULAR MATERIALS
A method for measuring the material moduli of granular materials: Flow in an orthogonal rheometer
[DE90-007160] N90-20339

GRAPH THEORY
Almost-optimum parallel speed-ups of algorithms for bipartite matching and related problems
[AD-A215111] N90-20728
On the existence of local times: A geometric study
[AD-A218337] N90-20776

GRAPHITE
The role of polarity on the stability of graphitic compounds
[DE90-006528] N90-20218
GRAVIMETERS
Geopotential coefficient determination and the gravimetric boundary value problem: A new approach N90-20521
First year's results and field experience with the latest JILA absolute gravimeter N90-20529
GPS-aided gravimetry at 30 km altitude from a balloon-borne platform N90-20530
The inverse gravimetric problem in gravity modelling N90-20535
FFT-local gravimetric geoid computation N90-20536
The geoid in Kenya N90-20542
GEOID '88: A gravimetric geoid for Canada N90-20543
GRAVITATION
Progress in the Determination of the Earth's Gravity Field
[NASA-CR-185721] N90-20513
Gravitational model improvement at the Goddard Space Flight Center N90-20514
GRAVITATIONAL EFFECTS
Secondary arm coarsening and microsegregation in superalloy PWA-1480 single crystals: Effect of low gravity
[NASA-TM-102445] N90-20194
Instantaneously generated foam and its applicability to reduced gravity
[NASA-CR-185208] N90-20237
Spacelab qualified infrared imager for microgravity science experiments
[NASA-TM-102503] N90-20352
The +Gz protection in the future: Review of scientific literature
[AD-A217887] N90-20623
GRAVITATIONAL FIELDS
Progress in the Determination of the Earth's Gravity Field
[NASA-CR-185721] N90-20513
Gravitational model improvement at the Goddard Space Flight Center N90-20514
An improved model for the Earth's gravity field N90-20515
Progress in the development of high degree potential coefficient models N90-20516
Gravity field determination and error assessment techniques N90-20517
Modeling of the Earth's gravity field using the New Global Earth Model (NEWGEM) N90-20523
A framework for modelling kinematic measurements in gravity field applications N90-20524
Gravity field of the Western Weddell Sea: Comparison of airborne gravity and Geosat derived gravity N90-20526
Critique of the vertical gradient of gravity N90-20531
Methods for local gravity field approximation N90-20532
The use of high-resolution terrain data in gravity field prediction N90-20533
The role of topography in geodetic gravity field modelling N90-20534
The inverse gravimetric problem in gravity modelling N90-20535
Performance of FFT methods in local gravity field modelling N90-20537
Fourier transform methods in local gravity modeling N90-20538
The reduction correction in North America N90-20540
Geodynamics and temporal variations in the gravity field N90-20549
A model of the general ocean circulation determined from a joint solution for the Earth's gravity field N90-20550
Geographically correlated orbit error N90-20551
Refinement of Earth's gravity field with Topex GPS measurements N90-20553
Gravity field information from Gravity Probe-B N90-20554
ARISTOTELES: A European approach for an Earth gravity field recovery mission N90-20559
Conserved integral characteristics of the gravitational field
[DE90-615205] N90-20898
GRAVITY ANOMALIES
An improved model for the Earth's gravity field N90-20515
Progress in the development of high degree potential coefficient models N90-20516
Geopotential models in the Australian region N90-20519
Geopotential coefficient determination and the gravimetric boundary value problem: A new approach N90-20521
Precise solution for a finite set of spherical coefficients from equiangular gridded data N90-20522
Synopsis of early field test results from the gravity gradiometer survey system N90-20525
Downward continuation of the free-air gravity anomalies to the ellipsoid using the gradient solution and terrain correction: An attempt of global numerical computations N90-20541
Determination of mean gravity anomalies in the Taiwan Island N90-20547
Very accurate upward continuation to low heights in a test of non-Newtonian theory N90-20548
Refinement of Earth's gravity field with Topex GPS measurements N90-20553
ARISTOTELES: A European approach for an Earth gravity field recovery mission N90-20559
Analysis of altimetry over inland seas
[NASA-TM-100729] N90-20566
User's guide: Programs for processing altimeter data over inland seas
[NASA-TM-100730] N90-20572
GRAVITY GRADIOMETERS
Synopsis of early field test results from the gravity gradiometer survey system N90-20525
The GRADIO spaceborne gravity gradiometer: Development and accommodation N90-20560
High resolution analysis of satellite gradiometry N90-20561
GRAVITY PROBE B
Gravity field information from Gravity Probe-B N90-20554
GREAT CIRCLES
Small and great circle routines
[AD-A217652] N90-20449
GREEN'S FUNCTIONS
Investigation of tapered multiple microstrip lines for VLSI circuits
[AD-A217855] N90-20310
GREENHOUSE EFFECT
Atmospheric Radiation Measurement Program Plan
[DE90-008108] N90-20504
Global Warming: A Northwest Perspective
[DE90-008140] N90-20505
United States Historical Climatology Network (HCN) serial temperature and precipitation data
[DE90-008029] N90-20506
Draft global warming study
[DE90-008446] N90-20507
An intercomparison of general circulation model predictions of regional climate change
[DE90-008325] N90-20589
GREENLAND
Satellite radar altimetry over ice. Volume 1: Processing and corrections of Seasat data over Greenland
[NASA-RP-1233-VOL-1] N90-20562
Satellite radar altimetry over ice. Volume 2: Users' guide for Greenland elevation data from Seasat
[NASA-RP-1233-VOL-2] N90-20563
GRID GENERATION (MATHEMATICS)
Composite-grid techniques and adaptive mesh refinement in computational fluid dynamics
[AD-A217383] N90-20328
Evaluation of an adaptive unstructured remeshing technique for integrated fluid-thermal-structural analysis
[NASA-TM-102611] N90-20426
Recent advances in 3D finite difference mesh generation using the BRL-CAD package
[DE90-007854] N90-20704
GRID2D/3D: A computer program for generating grid systems in complex-shaped two- and three-dimensional spatial domains. Part 2: User's manual and program listing
[NASA-TM-102454] N90-20708
Automated finite element modeling and simulation N90-20753
GROUND BASED CONTROL
Large screen display for the Mission Control Center N90-20662
GROUND EFFECT (COMMUNICATIONS)
Algorithms for optimal processing of polarimetric radar data
[AD-A217330] N90-20758
GROUND OPERATIONAL SUPPORT SYSTEM
Space station Simulation Computer System (SCS) study for NASA/MSFC. Volume 2: Concept document
[NASA-CR-183841] N90-20114
GROUND STATE
Present status of (mu)CF theory
[DE90-007547] N90-20809
GROUND WIND
A method for correcting and reducing the pressure data recorded at the PAM 2 stations during GALE
[AD-A218165] N90-20596
GROUP THEORY
On free products of torsion free abelian groups
[AD-A218146] N90-20773
Projective cohomology over a chain complex
[DE90-606958] N90-20788
GUN PROPELLANTS
Acute oral toxicity of DIGL-RP solid propellant in Sprague-Dawley rats
[AD-A217712] N90-20614
GUNN DIODES
Focused ion beam implantation
[AD-A217987] N90-20894
GYROSCOPES
Design and testing of a noninteracting control loop for the dynamically tuned dry gyro
[NAL-TR-1017] N90-20350

H

HAIL
An estimation of rainfall amounts using radar-derived Z-R relationships
[AD-A217950] N90-20591
HALF SPACES
Binary space partitioning trees and their uses N90-20657
HAMILTONIAN FUNCTIONS
Periodic trajectories for two-dimensional nonintegrable Hamiltonians
[DE90-008082] N90-20765
Integrability and chaos in nonlinearly coupled optical beams
[DE90-007540] N90-20834
HANDLING EQUIPMENT
Knowledge-based robotic grasping
[DE90-007216] N90-20402
HARDENERS
Materials and selection criteria analysis for the compact ignition tokamak toroidal field coil turn-to-turn insulation system: Photographic summary oflaboratory testing
[DE90-008020] N90-20850
HARDENING (MATERIALS)
Development and construction of external laser components for hardening and coating
[MT-15/87] N90-20364
HARDNESS
Ageing effects in welded cast CF3 stainless steel
[AERE-R-13559] N90-20188
Time-dependent failure of silver interlayer welds
[DE90-008015] N90-20440
HARMONIC EXCITATION
Modal interactions in shell dynamics N90-20418
Active control of the forced and transient response of a finite beam
[NASA-CR-181957] N90-20430
HARMONIC GENERATIONS
Harmonic generation mechanisms in short-wavelength free-electron lasers
[DE90-007622] N90-20374
HARMONIC OSCILLATION
Vibrational spectroscopy of boron nitride at high temperatures and pressures
[DE90-008633] N90-20172
HAZARDS
High-Explosives Applications Facility (HEAF)
[DE90-008122] N90-20257
The Terrain-Responsive Atmospheric Code (TRAC) project plan: Development of a hazardous materials dispersion modeling capability with application to ambient air monitoring network design
[DE90-007293] N90-20502
HEALTH
A review of the literature on the toxicity of rare-earth metals as it pertains to the engineering demonstration system surrogate testing
[DE90-008049] N90-20620
HEAT
Field assessment of wet bulb globe temperature: Present and future
[AD-A218224] N90-20635
HEAT AFFECTED ZONE
Ageing effects in welded cast CF3 stainless steel
[AERE-R-13559] N90-20188
HEAT BALANCE
The effect of moisture absorption in clothing on the human heat balance
[AD-A217899] N90-20626
HEAT EXCHANGERS
Evaluation of industrial magnetic heat pump/refrigerator concepts that utilize superconducting magnets
[DE90-008093] N90-20258
Advanced on-site power plant development technology program
[DE90-000443] N90-20484

HEAT FLUX
Magnetic vapor shield mechanism for protection of material surfaces exposed to high heat load
[AD-A217667] N90-20217
Effective calibration of heat flux transducers for experimental use
[AD-A218262] N90-20636
HEAT GENERATION
Influence of theobromine on heat production and body temperatures in cold-exposed humans: A preliminary report
[AD-A217203] N90-20618
HEAT ISLANDS
Controlling Summer Heat Islands: Proceedings
[DE90-008075] N90-20508
HEAT PIPES
Reusable high-temperature heat pipes and heat pipe panels
[NASA-CASE-LAR-13761-1] N90-20323
HEAT PUMPS
Evaluation of industrial magnetic heat pump/refrigerator concepts that utilize superconducting magnets
[DE90-008093] N90-20258
Phase 1 supplemental development of a kinematic Stirling/Rankine commercial gas-fired heat pump system
[PB90-129974] N90-20483
HEAT RESISTANT ALLOYS
Secondary arm coarsening and microsegregation in superalloy PWA-1480 single crystals: Effect of low gravity
[NASA-TM-102445] N90-20194
HEAT SHIELDING
Magnetic vapor shield mechanism for protection of material surfaces exposed to high heat load
[AD-A217667] N90-20217
HEAT STORAGE
Mechanical properties of pure nickel alloys after long term exposures to LiOH and vacuum at 775 K
[NASA-TM-102403] N90-20181
HEAT TRANSFER
Design and test of a compact optics system for the pool boiling experiment
[NASA-TM-102530] N90-20253
The thermal response of generic objects in JP-4 pool fires
[DE90-008503] N90-20259
Core cooling studies at LLNL (Lawrence Livermore National Laboratory) and Sandia
[DE90-008303] N90-20300
Area Over Length (AOL): A program for the calculation of effective two-dimensional thermal conductance through an arbitrarily shaped region
[DE90-008005] N90-20335
The effect of moisture absorption in clothing on the human heat balance
[AD-A217899] N90-20626
The measurements of thermoacoustic phenomena using thermoacoustic couples
[AD-A218018] N90-20798
An experimental investigation of the thermal conductivity of porous adsorbents
[AD-A217854] N90-20899
HEAT TREATMENT
Effect of heat treatment on the fracture toughness transition properties of an A508 class 3 steel
[AERE-R-13548] N90-20182
The ageing effect of the matrix-reinforcement interface on the ageing response of an aluminium 6061 alloy reinforced with 20vol percent SiC particulates
[AERE-R-13361] N90-20193
Positron annihilation spectroscopy: A nondestructive, submicroscopic characterization technique for structural polymers
[AD-A217748] N90-20226
HEATERS
Determination of fundamental thermodynamic properties of constituent materials and performance screening of candidate systems
[AD-A218089] N90-20153
HEATING
An expert system for the design of heating, ventilating, and air-conditioning systems
[AD-A218287] N90-20262
HEAVY IONS
Software quality assurance and software safety in the biomed control system
[DE90-008072] N90-20706
The n-p bremsstrahlung in heavy ion collision processes
[DE90-008542] N90-20823
HEIGHT
The reduction correction in North America N90-20540
Analysis of altimetry over inland seas
[NASA-TM-100729] N90-20566
HELICAL WINDINGS
The ANU (Australian National University) Heliac Program
[DE90-006620] N90-20843
HELICOPTER CONTROL
Airworthiness and flight characteristics evaluation of the McDonnell Douglas Helicopter Corporation (MDHC) 530FF helicopter
[AD-A218253] N90-20076
Interaction of switch actuation on tracking with a four-axis flight control (cross-coupling)
[AD-A217981] N90-20095
HELICOPTER PERFORMANCE
Airworthiness and flight characteristics evaluation of the McDonnell Douglas Helicopter Corporation (MDHC) 530FF helicopter
[AD-A218253] N90-20076
HELICOPTER WAKES
Analysis of heliport environmental data: Indianapolis downtown heliport, Wall Street heliport. Volume 3: Indianapolis downtown heliport data plots
[AD-A217412] N90-20500
HELICOPTERS
Comparison of oculometer and head-fixed reticle with voice or switch and touch panel for data entry on a generic tactical air combat display
[AD-A217231] N90-20646
HELIOSTATS
Selection and design of a stretched-membrane heliostat for today's markets
[DE90-007997] N90-20495
HELIPORTS
Analysis of heliport environmental data: Indianapolis downtown heliport, Wall Street heliport. Volume 3: Indianapolis downtown heliport data plots
[AD-A217412] N90-20500
HELIUM ISOTOPES
Design of D-3 He commercial tokamak
[DE90-008252] N90-20852
HEMODYNAMIC RESPONSES
Hydration effects on human physiology and exercise-heat performance
[AD-A217969] N90-20629
HETEROJUNCTIONS
Workshop on the Physics and Chemistry of Mercury Cadmium Telluride and Related II-VI compounds
[AD-A217496] N90-20867
HEURISTIC METHODS
Trajectory optimization in the presence of constraints
[AD-A218271] N90-20104
HIGH ALTITUDE
GPS-aided gravimetry at 30 km altitude from a balloon-borne platform N90-20530
Hypobaric hypoxia (380 torr) decreases intracellular and total body water in goats
[AD-A218192] N90-20615
HIGH ASPECT RATIO
Aeroelastic characteristics of aircraft with circulation control wings N90-20070
HIGH CURRENT
Collective ion acceleration in high current relativistic electron beams
[DE90-008328] N90-20821
HIGH ENERGY INTERACTIONS
Studies of high energy phenomena using muons
[DE90-008272] N90-20820
HIGH FREQUENCIES
Joint services electronics program
[AD-A217961] N90-20311
HIGH POWER LASERS
High power semiconductor laser arrays by metalorganic chemical vapor deposition N90-20363
HIGH RESOLUTION
High resolution radar target modeling using ARMA (Autoregressive Moving Average) models
[AD-A218212] N90-20278
The use of high-resolution terrain data in gravity field prediction N90-20533
Studies of an orbital gradiometer mission N90-20558
High resolution analysis of satellite gradiometry N90-20561
Biological soft x ray contact microscopy: Imaging living CHO-SC1 cells and other biological materials
[DE90-007560] N90-20610
High resolution transmission electron microscopy study of defect structures in mixed-phase YBaCuO
[DE90-007767] N90-20873
HIGH STRENGTH STEELS
Effect of heat treatment on the fracture toughness transition properties of an A508 class 3 steel
[AERE-R-13548] N90-20182
Hydrogen, thermal ageing and the role of carbides in fatigue of a high strength steel
[AERE-R-13599] N90-20183
Spray deposition: A fundamental study of droplet impingement, spreading and consolidation
[AD-A217202] N90-20255
HIGH TEMPERATURE
Symposium on High Temperature and Materials Chemistry
[DE90-008047] N90-20148
Fundamental aspects of and failure modes in high-temperature composites
[NASA-TM-102558] N90-20151
Determination of fundamental thermodynamic properties of constituent materials and performance screening of candidate systems
[AD-A218089] N90-20153
Vibrational spectroscopy of boron nitride at high temperatures and pressures
[DE90-008633] N90-20172
Advanced high-temperature batteries N90-20480
Ionic disorder in crystals at high temperatures with emphasis on fluorites
[AERE-R-13544] N90-20862
HIGH TEMPERATURE ENVIRONMENTS
Reusable high-temperature heat pipes and heat pipe panels
[NASA-CASE-LAR-13761-1] N90-20323
HIGH TEMPERATURE GASES
TiCl4 as a source of TiO2 particles for laser anemometry measurements in hot gas
[NASA-TM-102581] N90-20358
HIGH TEMPERATURE SUPERCONDUCTORS
High-temperature ceramic superconductors
[AD-A218347] N90-20233
Copper and oxygen NMR studies on the magnetic properties of YBa2Cu3O(7-y)
[DE90-007889] N90-20863
High temperature chemistry of oxide superconductors
[DE90-007821] N90-20875
Stabilization of high (Tc) superconductivity in cadmium sulfide
[DE90-008249] N90-20881
The electronic properties of high (Tc) superconductors probed by positron annihilation
[DE90-008354] N90-20883
Systematics in positron annihilation lifetime analysis of high (Tc) superconducting transitions
[DE90-008361] N90-20884
Electronic properties of high-temperature superconductors
[AD-A217953] N90-20892
HIGH TEMPERATURE TESTS
Mechanical properties of pure nickel alloys after long term exposures to LiOH and vacuum at 775 K
[NASA-TM-102403] N90-20181
Performance of Y-TZP materials between 800 C and 1200 C
[AD-A217723] N90-20890
HIGH VOLTAGES
Measurements of the interaction of high-voltage biassed conductors with the ionosphere
[AD-A218285] N90-20580
HILBERT SPACE
An approximation theory for the identification of linear thermoelastic systems
[NASA-CR-182015] N90-20764
Local moduli of continuity of some classes of Gaussian processes
[AD-A217692] N90-20778
HISTORIES
Transistor and solid-state technology: A historical development
[AD-A218141] N90-20317
Terrestrial gravity instrumentation in the 20th Century: A brief review N90-20527
History of visual systems in the Systems Engineering Simulator N90-20681
HMX
Condensed phase kinetic deuterium isotope effects in high energy phenomena: Mechanistic investigations and relationships
[AD-A217161] N90-20156
HOLDERS
Gripping device
[NASA-CASE-MSC-21365-1] N90-20408
HOLES (MECHANICS)
Heat transfer near the entrance to a film cooling hole in a gas turbine blade
[AD-A217396] N90-20089
Innovative design of composite structures: The use of curvilinear fiber format to improve buckling resistance of composite plates with central circular holes
[NASA-CR-186454] N90-20135
Innovative design of composite structures: The use of curvilinear fiber format in composite structure design
[NASA-CR-186453] N90-20136

HOLOGRAPHY
X ray microimaging by diffractive techniques
[DE90-008444] N90-20356
Simple reflection holography
[DE90-008309] N90-20359
HOMOGENEITY
Evaluation of material homogeneity as a function of thickness of low-alloy ferritic steel
[DE90-008069] N90-20202
HOMOLOGY
Projective cohomology over a chain complex
[DE90-606958] N90-20788
HOMOPOLAR GENERATORS
ARDEC (Armament Research, Development and Engineering Center) electric gun in-house test program
[AD-A217337] N90-20105
HORMONES
The effects of high intensity cycle exercise on sympatho-adrenal-medullary response patterns
[AD-A217962] N90-20628
HOT WORKING
Constitutive data acquisition and modelling in aluminium 2014 alloy
[AERE-R-13651] N90-20186
HOVERING
Analysis of small-scale rotor hover performance data
[NASA-TM-102271] N90-20325
HUMAN BEINGS
Influence of theobromine on heat production and body temperatures in cold-exposed humans: A preliminary report
[AD-A217203] N90-20618
A review of the literature on the toxicity of rare-earth metals as it pertains to the engineering demonstration system surrogate testing
[DE90-008049] N90-20620
HUMAN BODY
The USAF Advanced Dynamic Anthropomorphic Manikin (ADAM) N90-20062
HUMAN FACTORS ENGINEERING
The USAF Advanced Dynamic Anthropomorphic Manikin (ADAM) N90-20062
Controllable propulsion for escape systems control N90-20064
Spacecraft escape N90-20066
A guide to performing and documenting safety analyses
[DE90-008687] N90-20260
A guide to performing and documenting safety analyses
[DE90-008688] N90-20261
Using an instrumented manikin for Space Station Freedom analysis N90-20675
Human task animation from performance models and natural language input N90-20678
HUMAN PERFORMANCE
Physical performance and carbohydrate consumption in CF commandos during a 5-day field trial
[AD-A217204] N90-20619
Hydration effects on human physiology and exercise-heat performance
[AD-A217969] N90-20629
Information gathering and decisionmaking under stress
[AD-A218233] N90-20643
Human task animation from performance models and natural language input N90-20678
HURRICANES
The invertibility principle for a simple hurricane model
[AD-A218344] N90-20605
HYBRID CIRCUITS
Performance of a 300 Mbps 1:16 serial/parallel optoelectronic receiver module
[NASA-TM-103110] N90-20302
HYBRID COMPUTERS
Hybrid intelligent perception system: Intelligent perception through combining artificial neural networks and an expert system
[DE90-007483] N90-20746
HYDRATION
An electrochemical and spectroscopic study of electrode processes
[AD-A217261] N90-20289
HYDROCARBONS
The calculation of hydrogen-bonding properties
[DE90-007534] N90-20168
HYDRODYNAMIC COEFFICIENTS
Hydrodynamic interactions and transport coefficients in a suspension of spherical particles
[DE90-008301] N90-20336
HYDRODYNAMICS
Enhancement of mass transfer to a rotating cylinder electrode by inert particles suspended in the electrolyte
[DE90-008054] N90-20165
The viscoelasticity of curing thermosets
[DE90-006535] N90-20221
Hydrodynamic interactions and transport coefficients in a suspension of spherical particles
[DE90-008301] N90-20336
Computer simulations and experiments to study the fracture of rods by flying plates
[DE90-008308] N90-20437
HYDROELECTRICITY
Draft global warming study
[DE90-008446] N90-20507
HYDROGEN
Application of railgun principle to high-velocity hydrogen pellet injection for magnetic fusion reactor refueling
[DE90-008281] N90-20109
The calculation of hydrogen-bonding properties
[DE90-007534] N90-20168
Research of the interaction between hydrogen and deuterium with atomic eigen defects and dislocations in nickel and iron
[ETN-90-95380] N90-20195
Evaluation of industrial magnetic heat pump/refrigerator concepts that utilize superconducting magnets
[DE90-008093] N90-20258
Impedance studies of Ni/Cd and Ni/H2 cells using the cell case as a reference electrode N90-20473
HYDROGEN BONDS
The calculation of hydrogen-bonding properties
[DE90-007534] N90-20168
HYDROGEN EMBRITTLEMENT
Hydrogen, thermal ageing and the role of carbides in fatigue of a high strength steel
[AERE-R-13599] N90-20183
HYDROGEN METABOLISM
Carbon and hydrogen metabolism of green algae in light and dark
[DE90-008648] N90-20612
HYDROGEN OXYGEN FUEL CELLS
Space Electrochemical Research and Technology (SERT), 1989
[NASA-CP-3056] N90-20454
Hydrogen-oxygen proton-exchange membrane fuel cells and electrolyzers N90-20467
HYDROGEN PLASMA
Growth, characterization and device development in monocrystalline diamond films
[AD-A218211] N90-20895
HYDROLOGY
Hypotheses testing of watershed/landscape dynamics in northern Alaska using digital analysis
[DE90-006721] N90-20450
HYDROLYSIS
Hydrous metal oxide-supported catalysts. Part 1: Preparation chemistry and physical and chemical properties
[DE90-007607] N90-20161
HYDROSTATICS
The +Gz protection in the future: Review of scientific literature
[AD-A217887] N90-20623
HYPERBOLIC DIFFERENTIAL EQUATIONS
Cell averaging Chebyshev methods for hyperbolic problems
[NASA-CR-182028] N90-20768
HYPERBOLIC FUNCTIONS
High order filtering methods for approximating hyberbolic systems of conservation laws
[NASA-CR-182016] N90-20650
HYPERCUBE MULTIPROCESSORS
Design of a simulation interface for a parellel computing environment
[DE90-008497] N90-20737
Implementation of a hypercube database system
[DE90-008440] N90-20905
HYPERGEOMETRIC FUNCTIONS
Some remarks on solutions of Fermats last equation in terms of Wright's hypergeometric function
[AD-A218066] N90-20771
HYPERSONIC AIRCRAFT
The application of active controls technology to a generic hypersonic aircraft configuration
[NASA-TM-101689] N90-20071
HYPERSONIC BOUNDARY LAYER
Investigation of the development of laminar boundary-layer instabilities along a cooled-wall hollow cylinder at Mach number 8
[AD-A217672] N90-20331
HYPERSONIC FLIGHT
Transpiration cooling in hypersonic flight
[NASA-CR-186435] N90-20052
Analysis of flow-, thermal-, and structural-interaction of hypersonic structures subjected to severe aerodynamic heating
[AD-A217882] N90-20053
HYPERSONIC FLOW
Computation of hypersonic low density flows with thermochemical nonequilibrium N90-20044
HYPERSONIC VEHICLES
Hypersonic waverider configurations for trans-atmospheric vehicles
[AD-A217925] N90-20074
HYPERVELOCITY GUNS
ARDEC (Armament Research, Development and Engineering Center) electric gun in-house test program
[AD-A217337] N90-20105
HYPERVOLEMIA
Elevated central venous pressure: A consequence of exercise training-induced hypervolemia
[NASA-TM-102965] N90-20617
HYPOBARIC ATMOSPHERES
Hypobaric hypoxia (380 torr) decreases intracellular and total body water in goats
[AD-A218192] N90-20615
HYPOTENSION
Niacin ingested at night causes severe hypotension
[AD-A217896] N90-20624
HYPOTHERMIA
Influence of theobromine on heat production and body temperatures in cold-exposed humans: A preliminary report
[AD-A217203] N90-20618
What should athletes know about low body temperature (hypothermia)
[AD-A218316] N90-20637
HYPOTHESES
On optimal distributed decision architectures in a hypothesis testing environment
[AD-A217824] N90-20274
HYPOXIA
Hypobaric hypoxia (380 torr) decreases intracellular and total body water in goats
[AD-A218192] N90-20615

I

ICE
Airfields on antarctic glacier ice
[AD-A217638] N90-20097
Satellite radar altimetry over ice. Volume 1: Processing and corrections of Seasat data over Greenland
[NASA-RP-1233-VOL-1] N90-20562
Satellite radar altimetry over ice. Volume 2: Users' guide for Greenland elevation data from Seasat
[NASA-RP-1233-VOL-2] N90-20563
Satellite radar altimetry over ice. Volume 4: Users' guide for Antarctica elevation data from Seasat
[NASA-RP-1233-VOL-4] N90-20564
IMAGE ANALYSIS
A system for analysis and interpretation of lineaments in remote sensing images
[INPE-4893-PRE/1494] N90-20565
Three-dimensional medical image analysis using local dynamic algorithm selection on a multiple-instruction, multiple-data architecture
[AD-A218024] N90-20630
Texture segmentation using localized spatial filtering
[AD-A218064] N90-20722
IMAGE PROCESSING
Experimental validation of extended image reconstruction using bispectral speckle interferometry
[DE90-008545] N90-20171
Characterization of fluid flow by digital correlation of scattered light
[NASA-CR-186403] N90-20324
Estimation of modeled object pose from monocular images
[DE90-001678] N90-20354
X ray microimaging by diffractive techniques
[DE90-008444] N90-20356
Simple reflection holography
[DE90-008309] N90-20359
Spatial imaging using confocal Fabry-Perot interferometers
[DE90-008363] N90-20378
Robust performance of multiple tasks by a mobile robot
[DE90-001953] N90-20397
Knowledge-based robotic grasping
[DE90-007216] N90-20402
Nine-year aging behavior of the ceramic flatpack resonator
[DE90-008044] N90-20412
Three-dimensional medical image analysis using local dynamic algorithm selection on a multiple-instruction, multiple-data architecture
[AD-A218024] N90-20630
A real-time parallel pipelined data-flow image-processing system
[DE90-008324] N90-20691
Fractal-based image compression
[AD-A217302] N90-20699

ISLE (Image and Signal Processing LISP Environment) reference manual
[DE90-007858] N90-20705
Mathematics and physics studies: Multi-project support
[AD-A218208] N90-20723
Robotic mobility system: Road following algorithms
[AD-A218107] N90-20748
Placement of multiple apertures for imaging telescopes
[DE90-006991] N90-20833

IMAGE RECONSTRUCTION
Experimental validation of extended image reconstruction using bispectral speckle interferometry
[DE90-008545] N90-20171
Tomographic processing of synthetic aperture radar signals for enhanced resolution
[AD-A217178] N90-20265

IMAGE RESOLUTION
Design and performance analysis of adaptive optical telescopes using laser guide stars
[AD-A218025] N90-20913

IMAGES
Computer image generation: Reconfigurability as a strategy in high fidelity space applications N90-20682
Fractal-based image compression
[AD-A217302] N90-20699

IMAGING RADAR
Atmospheric wind measurements using a 50 MHz imaging Doppler interferometer radar
[AD-A218277] N90-20601

IMAGING TECHNIQUES
Meteor observations using the 50 MHz MENTOR imaging Doppler interferometer
[AD-A217908] N90-20276
Design and calibration of a vacuum compatible scanning tunneling microscope
[NASA-TM-102514] N90-20353
Spatial imaging using confocal Fabry-Perot interferometers
[DE90-006363] N90-20378
Utilization of LANDSAT-5 and NOAA-9 satellite imagery in the identification of physical-chemical parameters of the water in the Guanabara Bay
[INPE-4761-TDL/349] N90-20445
Hypotheses testing of watershed/landscape dynamics in northern Alaska using digital analysis
[DE90-006721] N90-20450
Development of gamma-emitting, receptor-binding radiotracers for imaging the brain and pancreas
[DE90-008314] N90-20621
Real-time graphics for the Space Station Freedom cupola, developed in the Systems Engineering Simulator N90-20683
High-resolution acoustical imaging N90-20793
Placement of multiple apertures for imaging telescopes
[DE90-006991] N90-20833
Bibliography of spatial interferometry in optical astronomy
[NASA-TM-100754] N90-20911

IMINES
Copolymer-like structures of nematic nitroimine dimers
[AD-A217574] N90-20215

IMPACT DAMAGE
Optimization of fracture resistance in composites
[AD-A217431] N90-20144

IMPACT LOADS
A review of the analytical simulation of aircraft crash dynamics
[NASA-TM-102595] N90-20068
Full-scale birdstrike testing of in-service aged F-111 ADBIRT windshield transparencies
[AD-A218035] N90-20069
Runaway rubber removal
[AD-A218349] N90-20100

IMPACT STRENGTH
Improved toughness alloys based on titanium aluminides
[AD-A218149] N90-20208

IMPEDANCE
Microwave field effect transistor
[NASA-CASE-GSC-12442-2] N90-20282
Recent improvements to the electromagnetic surface patch code
[AD-A217479] N90-20293
Impedance studies of Ni/Cd and Ni/H2 cells using the cell case as a reference electrode N90-20473
Nickel-hydrogen capacity loss on storage N90-20478
The impedance of energy efficiency of a coaxial magnetized plasma source used for spheromak formation and sustainment
[DE90-003220] N90-20841

IMPEDANCE MEASUREMENT
Impedance studies of Ni/Cd and Ni/H2 cells using the cell case as a reference electrode N90-20473

IMPINGEMENT
Spray deposition: A fundamental study of droplet impingement, spreading and consolidation
[AD-A217202] N90-20255

INCOMPRESSIBILITY
Nonlinear stability in fluid and plasma dynamics
[AD-A217735] N90-20856

INCOMPRESSIBLE FLOW
Numerical simulation methods of incompressible flows and an application to the space shuttle main engine
[NASA-TM-100038] N90-20333
Parallel algorithms in the finite element approximation of flow problems
[AD-A217729] N90-20341

INCOMPRESSIBLE FLUIDS
The invertibility principle for a simple hurricane model
[AD-A218344] N90-20605

INDEXES (DOCUMENTATION)
Free indexation: Combinatorial analysis and a compositional algorithm
[AD-A218219] N90-20724
Bibliography of spatial interferometry in optical astronomy
[NASA-TM-100754] N90-20911

INDIUM
CuInSe2 and CdTe: Scale-up for manufacturing
[DE89-009503] N90-20489

INDIUM PHOSPHIDES
Electron beam induced damage in PECVD Si3N4 and SiO2 films on InP
[NASA-TM-102544] N90-20393
An ellipsometric measurement of optical properties for InP surfaces
[AD-A217185] N90-20827

INDUCTION HEATING
Electromagnetic fusion process and position research N90-20249

INDUCTION MOTORS
Aerospace induction motor actuators driven from a 20-kHz power link
[NASA-TM-102482] N90-20085

INDUSTRIAL SAFETY
A review of the literature on the toxicity of rare-earth metals as it pertains to the engineering demonstration system surrogate testing
[DE90-008049] N90-20620

INDUSTRIES
Microgravity Science and Application Program tasks, 1989 revision
[NASA-TM-4191] N90-20252
Photovoltaic energy
[DE89-009473] N90-20486

INELASTIC SCATTERING
Large-angle elastic and inelastic scattering of Pi+ and Pi- from Si28 and Ca40
[AD-A218163] N90-20818

INEQUALITIES
Generalized quasi-variational inequality and implicit complementarity problems
[AD-A215191] N90-20755

INERTIAL CONFINEMENT FUSION
Energy deposition measurements for E-beam pumped excimer lasers
[DE90-007545] N90-20365
Shaped pulses from Nova for inertial confinement fusion experiments
[DE90-007261] N90-20373

INERTIAL PLATFORMS
The Rapid Geodetic Survey System (RGSS) N90-20528

INFILTRATION
Infiltration mechanics in conventional and hybridised fibre reinforced metal matrix composites
[AERE-R-13330] N90-20134
Characterization of ceramic matrix composites fabricated by chemical vapor infiltration
[DE90-008409] N90-20149

INFORMATION MANAGEMENT
Information management systems for integrating the technical data and regulatory requirements of environmental restoration activities
[DE90-008622] N90-20511

INFORMATION PROCESSING (BIOLOGY)
The role of chaos in hemispheric process and attention
[AD-A217674] N90-20639
The boundaries of hemispheric processing in visual pattern recognition
[AD-A217675] N90-20640
The perceptual interaction of graphical attributes in thirteen bivariate displays
[AD-A217980] N90-20720
CEREBRAL WEEVIL: A machine learning model for hemispheric categorization of complex visual patterns
[AD-A218143] N90-20749

INFORMATION RETRIEVAL
Transaction processing in a quality control laboratory
[DE90-004655] N90-20414
A model research archive: Archive and research implications for original records and support documents
[DE90-008246] N90-20906

INFORMATION SYSTEMS
Information management systems for integrating the technical data and regulatory requirements of environmental restoration activities
[DE90-008622] N90-20511
Software quality assurance and software safety in the biomed control system
[DE90-008072] N90-20706
A model research archive: Archive and research implications for original records and support documents
[DE90-008246] N90-20906

INFORMATION THEORY
A paradoxical result in unconditionally secure authentication codes, and an explanation
[DE90-008529] N90-20710
Spectral analytic methods for the estimation of number of signals and directions of arrival
[AD-A217219] N90-20757

INFRARED ABSORPTION
Infrared absorption study of zinc-doped silicon
[DE90-007779] N90-20164

INFRARED ASTRONOMY
Mathematics and physics studies: Multi-project support
[AD-A218208] N90-20723
Mark 3 interferometer
[AD-A217188] N90-20912

INFRARED DETECTORS
Modification, testing, and calibration of infrared search and target designator hardware received from NSWC
[AD-A217920] N90-20837
NRL hybrid reliability. Physics of failure initial study
[AD-A217986] N90-20893

INFRARED IMAGERY
Correlation of AVHRR imagery with sub-surface features in California current
[AD-A218184] N90-20607

INFRARED INTERFEROMETERS
Mark 3 interferometer
[AD-A217188] N90-20912

INFRARED LASERS
Laser enhanced chemical reactions
[DE90-008273] N90-20377

INFRARED RADIATION
Conference digest: Thirteenth International Conference on Infrared and Millimeter Waves, volume 1039
[AD-A217343] N90-20291

INFRARED SIGNATURES
Mathematics and physics studies: Multi-project support
[AD-A218208] N90-20723

INFRARED SPECTRA
Infrared absorption study of zinc-doped silicon
[DE90-007779] N90-20164
Bibliography of spatial interferometry in optical astronomy
[NASA-TM-100754] N90-20911

INFRARED SPECTROSCOPY
Infrared and X ray photoelectron spectroscopy studies of the polyimide/metal interface
[AD-A218249] N90-20179

INFRARED TRACKING
The design and implementation of a position measuring system for a remotely controlled video camera
[AD-A218077] N90-20362
Modification, testing, and calibration of infrared search and target designator hardware received from NSWC
[AD-A217920] N90-20837

INGESTION (BIOLOGY)
Niacin ingested at night causes severe hypotension
[AD-A217896] N90-20624

INGOTS
Constitutive data acquisition and modelling in aluminium 2014 alloy
[AERE-R-13651] N90-20186

INJECTION
Application of railgun principle to high-velocity hydrogen pellet injection for magnetic fusion reactor refueling
[DE90-008281] N90-20109

INJECTION LASERS
High power semiconductor laser arrays by metalorganic chemical vapor deposition N90-20363

INJURIES
Windblast protection for advanced ejection seats N90-20063
Field assessment of wet bulb globe temperature: Present and future
[AD-A218224] N90-20635

INSPECTION
Shaping the insonifying pulse to optimise B-scans obtained in austenite
[AERE-R-13518] N90-20187
A guide to performing and documenting safety analyses
[DE90-008668] N90-20261
Research and development quality assurance planning
[DE90-003687] N90-20413
INSTALLING
Thiokol/Wasatch installation evaluation of the redesigned field joint protection system (concepts 1 and 3)
[NASA-CR-183860] N90-20127
INTEGRALS
Conserved integral characteristics of the gravitational field
[DE90-615205] N90-20898
INTEGRATED CIRCUITS
Processing, fabrication, characterization and device demonstration of high temperature superconducting ceramics
[AD-A218330] N90-20231
Radiation-hardened wafer scale integration
[AD-A217332] N90-20290
Fault simulator evaluation
[AD-A217782] N90-20308
The design of high-performance circuits for digital signal processing
[AD-A217786] N90-20309
Transistor and solid-state technology: A historical development
[AD-A218141] N90-20317
Identification of defects in SOI (Silicon-On-Insulator) wafers
[DE90-006020] N90-20879
INTEGRATED MISSION CONTROL CENTER
Large screen display for the Mission Control Center N90-20662
INTERACTIONAL AERODYNAMICS
Application of a three-dimensional Navier-Stokes model for a subsonic jet in a crossflow N90-20045
INTERCEPTION
Optimal, impulsive, time-fixed orbital rendezvous and interception with path constraints N90-20102
INTERFACES
Interface science in deformation processing of ceramics
[DE90-008424] N90-20219
Modeling studies of electrolyte flow and bubble behavior in advanced Hall cells
[DE90-007013] N90-20303
RenderMan design principles N90-20653
The use of graphics in the design of the human-telerobot interface N90-20670
Magnetic properties of surfaces and interfaces
[DE90-007348] N90-20789
An investigation of the dislocation structure of the Ni/Ag phase boundary
[DE90-008428] N90-20876
INTERFACIAL TENSION
Studies of the structure and properties of organic monolayers, multilayers and superlattices
[DE90-008330] N90-20129
Spacelab qualified infrared imager for microgravity science experiments
[NASA-TM-102503] N90-20352
INTERFEROMETERS
Meteor observations using the 50 MHz MENTOR imaging Doppler interferometer
[AD-A217908] N90-20276
Optimization of digital filters for a short-scan interferometer
[AD-A217997] N90-20315
Atmospheric wind measurements using a 50 MHz imaging Doppler Interferometer radar
[AD-A218277] N90-20601
INTERFEROMETRY
Bibliography of spatial interferometry in optical astronomy
[NASA-TM-100754] N90-20911
INTERLAYERS
Time-dependent failure of silver interlayer welds
[DE90-008015] N90-20440
INTERMETALLICS
An introduction to nickel aluminide alloy
[DE90-008565] N90-20207
INTERPLANETARY MAGNETIC FIELDS
Quantifying and reducing uncertainty in the assimilative mapping of ionospheric electrodynamics
[AD-A218057] N90-20577
INTERPLANETARY SPACECRAFT
The importance of batteries in unmanned missions N90-20456
INTERPOLATION
A linear filtering technique for removal of low-frequency noise
[DE90-006183] N90-20296
INTERPROCESSOR COMMUNICATION
Express cubes: Improving the performance of k-ary n-cube interconnection networks
[AD-A217117] N90-20287
INVARIANCE
Fractal-based image compression
[AD-A217302] N90-20699
INVENTORIES
Overview of the methodologies used to compile large scale emissions inventories
[DE90-008518] N90-20509
INVERSIONS
Multiple versus single scattering of terrestrial infrared longwave radiation in an aerosol-laden planetary boundary layer
[AD-A217709] N90-20272
INVISCID FLOW
DURIP optical equipment for high-speed viscous-inviscid interaction research
[AD-A217772] N90-20345
Numerical modeling of airblast
[AD-A217993] N90-20347
IODIDES
Mercuric iodide room temperature gamma-ray detectors
[NASA-TM-103318] N90-20357
Determinations of photon spectra
[AD-A218003] N90-20816
ION BEAMS
Physical sputtering of metallic systems by charged-particle impact
[DE90-007803] N90-20201
Software quality assurance and software safety in the biomed control system
[DE90-008072] N90-20706
Collective ion acceleration in high current relativistic electron beams
[DE90-008328] N90-20821
Focused ion beam implantation
[AD-A217987] N90-20894
ION CURRENTS
Electronic and ionic transport in processable conducting polymers
[AD-A218093] N90-20229
ION EXCHANGE MEMBRANE ELECTROLYTES
Electrocatalysis for oxygen electrodes in fuel cells and water electrolyzers for space applications N90-20468
ION IMPACT
Physical sputtering of metallic systems by charged-particle impact
[DE90-007803] N90-20201
ION IMPLANTATION
Rolling contact fatigue of surface modified 440C using a 'Ge-Polymet' type disc rod test rig
[NASA-TM-100390] N90-20200
Radiation disorder and aperiodicity in irradiated ceramics
[DE90-008253] N90-20222
Interaction between implanted ions and intrinsic defects in silica
[DE90-006569] N90-20858
Workshop on the Physics and Chemistry of Mercury Cadmium Telluride and Related II-VI compounds
[AD-A217496] N90-20867
Focused ion beam implantation
[AD-A217987] N90-20894
ION PROBES
Y1Ba2Cu3O(7-x) laser-ablation plume dynamics measurement by nanosecond response ion probe: Comparison with optical measurements
[DE90-007658] N90-20375
ION PROPULSION
Experimental proposition aboard the second data collecting satellite-SCD 2 of the MECB
[INPE-4980-RPE/606] N90-20128
IONIC COLLISIONS
DURIP theoretical/experimental investigations of highly energetic dication species
[AD-A217771] N90-20383
IONIZATION
The glow discharge as an atomization and ionization source
[DE90-007693] N90-20163
DURIP FTIR studies of solid state reaction dynamics
[AD-A217713] N90-20174
Interactions of molecules with surfaces
[DE90-007555] N90-20806
Time-resolved spectroscopy of nonequilibrium ionization in laser-produced plasmas
[DE90-008663] N90-20854
Absolute pressure dependence of the second ionization level of EL2 in GaAs
[DE90-007761] N90-20872
IONIZATION CROSS SECTIONS
Electron-impact ionization and electron attachment cross sections of radicals important in transient gaseous discharges
[AD-A217510] N90-20366
IONS
Energy transfer between electrons and ions in collision cascades in solids
[AERE-R-13662] N90-20801
IRON
Ligand-centered electron-transfer redox processes for manganese, iron, and cobalt complexes in relation to selected catalytic systems
[AD-A217957] N90-20177
L shell XANES (X ray Absorption Near Edge Structure) for solid metals: Ti, V, Cr, Fe, Ni, Cu
[DE90-008043] N90-20880
IRON ALLOYS
Corrosion properties of Fe3Al in H2S-H2-H2O mixtures
[DE90-004936] N90-20167
IRRADIANCE
Analysis of methods to determine emissivity for ground surface targets in the spectral band 8 to 14 microns
[INPE-4984-TDL/394] N90-20447
Downward shortwave surface irradiance from 17 sites for the FIRE/SRB Wisconsin experiment
[NASA-TM-102596] N90-20583
IRRADIATION
Electron beam induced damage in PECVD Si3N4 and SiO2 films on InP
[NASA-TM-102544] N90-20393
The stress-driven redistribution of point defects in the vicinity of crack-like singularities
[AERE-R-12898] N90-20424
ISING MODEL
Electronic structure, alloy phase stability, and phase diagrams
[DE90-008306] N90-20203
Magnetic properties of surfaces and interfaces
[DE90-007348] N90-20789
The geometry of disorder: Report 1987 to 1990
[DE90-008250] N90-20882
ISOTOPE EFFECT
Condensed phase kinetic deuterium isotope effects in high energy phenomena: Mechanistic investigations and relationships
[AD-A217161] N90-20156
ITERATION
Investigation of tapered multiple microstrip lines for VLSI circuits
[AD-A217855] N90-20310
A time stepping algorithm for parallel computers
[DE90-008163] N90-20738
A model and implementation of multigrid for massively parallel computers
[DE90-008165] N90-20739
Techniques for accelerating iterative methods for the solution of mathematical problems
[AD-A218272] N90-20775
ITERATIVE SOLUTION
Techniques for accelerating iterative methods for the solution of mathematical problems
[AD-A218272] N90-20775

J

J INTEGRAL
Limitations and applications of fracture assessment with R6
[AERE-R-13012] N90-20425
JAPAN
Geology, distribution of hot springs and hydrothermal alteration zones of major geothermal areas in Japan
[DE90-753026] N90-20451
JET FLOW
System for venting gas from a liquid storage tank
[NASA-CASE-MSC-21253-1] N90-20254
JET STREAMS (METEOROLOGY)
Correlation of atmospheric optical turbulence and meteorological measurements
[AD-A218019] N90-20576
JOINTS (JUNCTIONS)
Thiokol/Wasatch installation evaluation of the redesigned field joint protection system (concepts 1 and 3)
[NASA-CR-183860] N90-20127
The CMU Reconfigurable Modular Manipulator System
[CMU-RI-TR-88-7] N90-20388
Control system design of the third flexible joint of PUMA 560 robot
[AD-A218075] N90-20405

JORDAN FORM
Simplified linear-time Jordan sorting and polygon clipping
[AD-A215110] N90-20693
JP-4 JET FUEL
The thermal response of generic objects in JP-4 pool fires
[DE90-008503] N90-20259

K

KALMAN FILTERS
An improved airborne wind measurement technique for the NAE (National Aeronautical Establishment) Twin Otter
[AD-A217978] N90-20575
KAPTON (TRADEMARK)
A study of physical properties of ODPA-p-PDA polyimide films
[NASA-TM-102625] N90-20137
KENYA
The geoid in Kenya N90-20542
KINEMATICS
Experimental investigation of the mechanisms underlying vortex kinematics in unsteady separated flows
[AD-A217889] N90-20346
The CMU Reconfigurable Modular Manipulator System
[CMU-RI-TR-88-7] N90-20388
Model development in viscoplastic ratchetting
[NASA-TM-102509] N90-20431
Phase 1 supplemental development of a kinematic Stirling/Rankine commercial gas-fired heat pump system
[PB90-129974] N90-20483
A framework for modelling kinematic measurements in gravity field applications N90-20524
Coastal frontogenesis and associated severe weather on 13 March 1986 (GALE IOP 13)
[AD-A217708] N90-20590
Derivation of kinematic fields using wind profiler data from the 1985 pre-storm experiment
[AD-A217952] N90-20592
A case study of a quasi-stationary tropical convective line
[AD-A218325] N90-20604
The development of the Canadian Mobile Servicing System Kinematic Simulation Facility N90-20676
Software systems for modeling articulated figures N90-20677
KINETIC ENERGY
Theoretical modeling studies of the marine planetary
[AD-A217200] N90-20567
SDI (Strategic Defense Initiative): Is its future past
[DE90-008016] N90-20785
Role of free-electron lasers in strategic defense
[DE90-008028] N90-20786
Polyatomic reaction dynamics
[DE90-008668] N90-20811
KINETICS
Condensed phase kinetic deuterium isotope effects in high energy phenomena: Mechanistic investigations and relationships
[AD-A217161] N90-20156
Aerodynamic and kinetic processes in flames
[AD-A217796] N90-20176
Spallation of oxide scales from 20 percent Cr/25 percent Ni/Nb stainless steel
[AERE-R-13464] N90-20189
The stress-driven redistribution of point defects in the vicinity of crack-like singularities
[AERE-R-12898] N90-20424
The electrochemical generation of useful chemical species from lunar materials N90-20461
In-situ differential reflectance study of the etching of SiO2 films
[AD-A217186] N90-20864
KLYSTRONS
Relativistic klystron afterburner simulation techniques
[DE90-008539] N90-20305
KNOWLEDGE REPRESENTATION
Knowledge representation in space flight operations N90-20655
Joint Japanese-American Workshop on Future Trends in Logic Programming
[DE90-008343] N90-20709

L

L-1011 AIRCRAFT
The NASA digital VGH program: Exploration of methods and final results. Volume 2: L 1011 data 1978-1979: 1619 hours
[NASA-CR-181909-VOL-2] N90-20080
The NASA digital VGH program. Exploration of methods and final results. Volume 1: Development of methods
[NASA-CR-181909-VOL-1] N90-20081
LABORATORIES
Life sciences: Lawrence Berkeley Laboratory, 1988
[DE90-008061] N90-20611
The United States Air Force School of Aerospace Medicine: Special report
[AD-A217740] N90-20622
LACTATES
The effects of graded exercise at sea level on plasma proenkephalin peptide F and catecholamine responses
[AD-A218195] N90-20633
LAKE MICHIGAN
An aircraft investigation of a convective boundary layer over Lake Michigan
[AD-A218175] N90-20598
LAMINAR BOUNDARY LAYER
Experimental and theoretical aerodynamic characteristics of a high-lift semispan wing model
[NASA-TP-2990] N90-20046
Investigation of the development of laminar boundary-layer instabilities along a cooled-wall hollow cylinder at Mach number 8
[AD-A217672] N90-20331
LAMINAR FLOW
Modification and improvement of software for modeling multidimensional reacting fuel flows
[AD-A217789] N90-20235
LAMINAR MIXING
Aerodynamic and kinetic processes in flames
[AD-A217796] N90-20176
LAMINATES
Compendium of abstracts and viewgraphs.
[AD-A217189] N90-20140
Through-thickness strain response of thick composites in compression
[AD-A217233] N90-20141
Compression testing of thick-section composite materials
[AD-A217234] N90-20142
Optimization of laminated composite plates
[AD-A217621] N90-20146
Postbuckling behavior of laminated specially orthotropic plates by affine transformation N90-20420
LARGE SCALE INTEGRATION
Product assurance technology for procuring reliable, radiation-hard, custom LSI/VLSI electronics
[NASA-CR-185954] N90-20281
LARGE SPACE STRUCTURES
Component count and preliminary assembly considerations for large space truss structures
[NASA-TM-102604] N90-20121
Aiming control: Theory and applications to dynamic control of space structures
[AD-A217877] N90-20123
LASER ANEMOMETERS
TiCl4 as a source of TiO2 particles for laser anemometry measurements in hot gas
[NASA-TM-102581] N90-20358
LASER APPLICATIONS
Determination of fundamental thermodynamic properties of constituent materials and performance screening of candidate systems
[AD-A218089] N90-20153
Isotope exchange in oxide-containing catalyst
[NASA-CASE-LAR-13542-2-SB] N90-20154
Development and construction of external laser components for hardening and coating
[MT-15/87] N90-20364
Robotic mobility system: Road following algorithms
[AD-A218107] N90-20748
Laser-produced plasmas in medicine
[DE90-007623] N90-20849
Differential measurements of the lateral photo effect in GaAs/AlGaAs heterostructures
[AERE-R-13557] N90-20861
Ultra-high brightness laser research at LLNL (Lawrence Livermore National Laboratory)
[DE90-008366] N90-20885
LASER BEAMS
Multi-dimensional LADAR tracking and adaptive grasping for spaceborne assembly of SDI (Strategic Defense Initiative) platforms
[AD-A218236] N90-20279
Development and construction of external laser components for hardening and coating
[MT-15/87] N90-20364
Shaped pulses from Nova for inertial confinement fusion experiments
[DE90-007261] N90-20373
Measurement of the stimulated thermal Rayleigh scattering instability
[DE90-007849] N90-20376
Picosecond laser study of polyatomic molecules
[DE90-008647] N90-20381
Short wavelength laser/materials interactions
[AD-A218015] N90-20386
LASER GUIDANCE
A new technique for guiding of electron beams
[DE90-008660] N90-20824
Design and performance analysis of adaptive optical telescopes using laser guide stars
[AD-A218025] N90-20913
LASER INDUCED FLUORESCENCE
Development of a laser fluorosensor for the aircraft supported analysis of maritime toxic agents loads: Definition phase
[ETN-90-95320] N90-20499
Reactive and anisotropic elastic scattering of highly laser-vibration-excited diatomic molecules
[MPIS-19/1988] N90-20804
LASER MATERIALS
Performance of zig-zag slab regenerative ring amplifier laser system
[DE90-006995] N90-20371
LASER MODE LOCKING
Picosecond Laser Facility
[AD-A217784] N90-20384
LASER OUTPUTS
High power semiconductor laser arrays by metalorganic chemical vapor deposition N90-20363
Strategies for high efficiency operation of the E-beam excited atomic xenon laser using high-power and high-energy loading
[DE90-005196] N90-20370
Y1Ba2Cu3O(7-x) laser-ablation plume dynamics measurement by nanosecond response ion probe: Comparison with optical measurements
[DE90-007658] N90-20375
Spatial imaging using confocal Fabry-Perot interferometers
[DE90-008363] N90-20378
LASER PLASMAS
Laser-produced plasmas in medicine
[DE90-007623] N90-20849
Time-resolved spectroscopy of nonequilibrium ionization in laser-produced plasmas
[DE90-008663] N90-20854
LASER PUMPING
High efficiency flashlamp-pumped titanium: Sapphire laser
[AD-A217598] N90-20367
Flash-pumped titanium laser
[AD-A217599] N90-20368
Picosecond Laser Facility
[AD-A217784] N90-20384
Picosecond nonlinear studies of complex materials using the free electron laser
[AD-A218215] N90-20387
Crystallography, spectroscopic analysis, and lasing properties of Nd3+:Y3Sc2Al3O12
[AD-A217792] N90-20891
LASER SPECTROSCOPY
Pulsed laser photothermal spectroscopy of liquids and solids
[DE90-008642] N90-20380
Picosecond laser study of polyatomic molecules
[DE90-008647] N90-20381
LASER STABILITY
Electronic and ionic transport in processable conducting polymers
[AD-A218093] N90-20229
Measurement of the stimulated thermal Rayleigh scattering instability
[DE90-007849] N90-20376
Laser line transport with refraction
[DE90-008683] N90-20382
LASER TARGET INTERACTIONS
Short wavelength laser/materials interactions
[AD-A218015] N90-20386
LASER TARGETS
Improved energy and power balance at Nova targets
[DE90-007260] N90-20372
Shaped pulses from Nova for inertial confinement fusion experiments
[DE90-007261] N90-20373
LASERS
High efficiency flashlamp-pumped titanium: Sapphire laser
[AD-A217598] N90-20367
Laser line transport with refraction
[DE90-008683] N90-20382
Observation of nonlinear reflectivity from InSb surface and optical switching application
[AD-A217184] N90-20826
LATENT HEAT
Applications of microwave radiometric measurements to infer tropical cyclone intensity and strength
[AD-A218273] N90-20600

LATTICE VIBRATIONS
Ionic disorder in crystals at high temperatures with emphasis on fluorites
[AERE-R-13544] N90-20862
LAUNCH VEHICLES
Advanced launch vehicle propulsion at the NASA Lewis Research Center
[NASA-TM-103096] N90-20110
LAUNCHERS
A 10-stage reconnection demonstration launcher
[DE90-007653] N90-20106
Diagnostics and firing control for the cylindrical reconnection launcher
[DE90-007677] N90-20107
Design and performance of a multi-stage cylindrical reconnection launcher
[DE90-007820] N90-20108
LAUNCHING
Finite element models to predict the structural response of 120-mm sabot/rods during launch
[DE90-007497] N90-20436
LEAD ACID BATTERIES
Investigation of a photovoltaic/battery hybrid system for powering the high arctic data communications system
[AD-A218353] N90-20319
LEAD ALLOYS
The metallurgical mechanisms of solder fatigue
[DE90-008390] N90-20206
LEAD OXIDES
Chemically prepared PZT films doped with niobium
[DE90-006811] N90-20859
LEARNING
Role of cognitive factors in the acquisition of cognitive skill
[AD-A218069] N90-20642
A long-term retention advantage for spatial information learned naturally and in the laboratory
[AD-A218268] N90-20644
On metric entropy, Vapnik-Chervonenkis dimension, and learnability for a class of distributions
[AD-A217331] N90-20759
LEARNING THEORY
On metric entropy, Vapnik-Chervonenkis dimension, and learnability for a class of distributions
[AD-A217331] N90-20759
LEAST SQUARES METHOD
Swing-free movement of simply suspended objects employing parameter estimation
[DE90-002238] N90-20398
Methods for local gravity field approximation
N90-20532
Treatment of geodetic leveling in the integrated geodesy approach N90-20546
Quantifying and reducing uncertainty in the assimilative mapping of ionospheric electrodynamics
[AD-A218057] N90-20577
LEAVES
LANDSAT-5 data in the study of wheat and bean crops
[INPE-4746-RPE/580] N90-20444
LENSES
Simple reflection holography
[DE90-008309] N90-20359
LETHALITY
Acute oral toxicity of DIGL-RP solid propellant in Sprague-Dawley rats
[AD-A217712] N90-20614
LEVITATION
The NASA, Marshall Space Flight Center drop tube user's manual
[NASA-TM-100392] N90-20251
LEVITATION MELTING
Electromagnetic fusion process and position research
N90-20249
LEXAN (TRADEMARK)
Positron annihilation spectroscopy: A nondestructive, submicroscopic characterization technique for structural polymers
[AD-A217748] N90-20226
LIFE (DURABILITY)
Bearing and gear steels for aerospace applications
[NASA-TM-102529] N90-20391
The importance of batteries in unmanned missions
N90-20456
A new concept for high-cycle-life LEO: Rechargeable MnO2-hydrogen N90-20462
Characterization testing of a 40 AHR bipolar nickel-hydrogen battery N90-20463
The application of electrochemical impedance spectroscopy for characterizing the degradation of Ni(OH)2/NiOOH electrodes N90-20474
KOH concentration effect on the cycle life of nickel-hydrogen cells. Part 4: Results of failure analyses
N90-20475
LIFE CYCLE COSTS
Life-cycle cost comparisons of advanced storage batteries and fuel cells for utility, stand-alone, and electric vehicle applications
[DE90-008090] N90-20298
LIFE SCIENCES
Life sciences: Lawrence Berkeley Laboratory, 1988
[DE90-008061] N90-20611
LIFE SUPPORT SYSTEMS
Implications of Advanced Technologies for Air and Spacecraft Escape
[AGARD-CP-472] N90-20054
LIFT DRAG RATIO
Hypersonic waverider configurations for trans-atmospheric vehicles
[AD-A217925] N90-20074
LIGANDS
Ligand-centered electron-transfer redox processes for manganese, iron, and cobalt complexes in relation to selected catalytic systems
[AD-A217957] N90-20177
Metal alkoxides: Models for metal oxides. Alkoxide ligands in early transition metal organometallic chemistry
[DE90-007523] N90-20869
LIGHT (VISIBLE RADIATION)
Biological applications and effects of optical masers
[AD-A217910] N90-20385
LIGHT BEAMS
Integrability and chaos in nonlinearly coupled optical beams
[DE90-007540] N90-20834
LIGHT EMISSION
Spacecraft optical contamination environment
[AD-A218088] N90-20838
LIGHT SCATTERING
Electronic and ionic transport in processable conducting polymers
[AD-A218093] N90-20229
Characterization of fluid flow by digital correlation of scattered light
[NASA-CR-186403] N90-20324
Stress field near crack tip: An experimental evaluation of the three dimensional variation
[AD-A217878] N90-20441
Experimental and theoretical studies of light scattering by small particles
[AD-A217432] N90-20831
LIGHT SOURCES
Research investigation directed toward extending the useful range of the electromagnetic spectrum
[AD-A217460] N90-20267
LIGHTNING
Radar detection of lightning and electric fields
[AD-A217894] N90-20574
LIGNIN
Assessment of biobased materials
[DE90-000300] N90-20220
LIMITERS (FUSION REACTORS)
Particle transport in pellet fueled JET (Jet European Torus) plasmas
[DE90-008077] N90-20851
LINE SHAPE
Spectral line shape code for multielectron emitters
[DE90-008526] N90-20853
LINE SPECTRA
The adaptive line enhancer applied to chirp detection
[DE90-006772] N90-20268
Spectral line shape code for multielectron emitters
[DE90-008526] N90-20853
LINEAR EQUATIONS
Observer based compensators for nonlinear systems
[AD-A217426] N90-20760
LINEAR QUADRATIC REGULATOR
Discrete-time control of a spacecraft with retargetable flexible antennas N90-20119
Discrete-time control of a spacecraft with retargetable flexible antennas
[AD-A218345] N90-20125
LINEAR SYSTEMS
An approximation theory for the identification of linear thermoelastic systems
[NASA-CR-182015] N90-20764
LIOUVILLE EQUATIONS
Modelling Doppler broadening in Raman propagation
[DE90-008042] N90-20269
LIPIDS
Influence of theobromine on heat production and body temperatures in cold-exposed humans: A preliminary report
[AD-A217203] N90-20618
LIQUEFACTION
Evaluation of industrial magnetic heat pump/refrigerator concepts that utilize superconducting magnets
[DE90-008093] N90-20258
LIQUID COOLING
Modification, testing, and calibration of infrared search and target designator hardware received from NSWC
[AD-A217920] N90-20837
LIQUID CRYSTALS
Rigid rod molecules as liquid crystal thermosets
[AD-A217573] N90-20158
Copolymer-like structures of nematic nitroimine dimers
[AD-A217574] N90-20215
Polymer liquid crystals with side chain discogens
[AD-A218013] N90-20228
LIQUID FILLED SHELLS
Interior fluid dynamics of liquid-filled projectiles
[AD-A217630] N90-20330
LIQUID FUELS
Electrochemical phase diagrams for aqueous redox systems
[AD-A217168] N90-20157
LIQUID METALS
Wetting of metallic carbides by non-reactive liquid metals
[AERE-M-3759] N90-20185
LIQUID PHASES
Systems with a miscibility gap in the liquid state
N90-20245
Dynamics of electronically excited species in gaseous and condensed phase
[AD-A217696] N90-20812
LIQUID SURFACES
Interior fluid dynamics of liquid-filled projectiles
[AD-A217630] N90-20330
LIQUID-SOLID INTERFACES
Principles of metallic solidification N90-20241
Supercooling and germ formation N90-20242
Dynamics of the solidification front N90-20243
Dispersion reinforced materials N90-20244
LIQUIDS
Chemical and electrochemical studies in ionic liquids
[AD-A217742] N90-20175
Pulsed laser photothermal spectroscopy of liquids and solids
[DE90-008642] N90-20380
LITHIUM
Advanced high-temperature batteries N90-20480
Advances in ambient temperature secondary lithium cells N90-20481
LITHIUM ALLOYS
Evaluation of 2090-T8E48 aluminum-lithium plates
[AD-A217262] N90-20196
LITHIUM HYDROXIDES
Mechanical properties of pure nickel alloys after long term exposures to LiOH and vacuum at 775 K
[NASA-TM-102403] N90-20181
LITHIUM SULFUR BATTERIES
All-solid-state thin-film rechargeable lithium batteries using solid redox polymerization electrodes
[DE90-008665] N90-20306
Novel electrodes for advanced energy storage systems
[DE90-008667] N90-20496
LITHOGRAPHY
Biological soft x ray contact microscopy: Imaging living CHO-SC1 cells and other biological materials
[DE90-007560] N90-20610
In-situ differential reflectance study of the etching of SiO2 films
[AD-A217186] N90-20864
LOAD DISTRIBUTION (FORCES)
Innovative design of composite structures: The use of curvilinear fiber format to improve buckling resistance of composite plates with central circular holes
[NASA-CR-186454] N90-20135
LOAD TESTS
Floor pull test of a transport airframe section
[DOT/FAA/CT-TN88/14] N90-20072
LOADS (FORCES)
Floor pull test of a transport airframe section
[DOT/FAA/CT-TN88/14] N90-20072
Experimentally determined wear behavior of an Al2O3-SiC composite from 25 to 1200 C
[NASA-TM-102549] N90-20130
Innovative design of composite structures: The use of curvilinear fiber format in composite structure design
[NASA-CR-186453] N90-20136
Composite laminate tailoring with probabilistic constraints and loads
[NASA-TM-102515] N90-20138
COMGEN: A computer program for generating finite element models of composite materials at the micro level
[NASA-TM-102556] N90-20438
LOGIC CIRCUITS
A unified approach to the synthesis of fully testable sequential machines
[AD-A217120] N90-20687

Irredundant sequential machines via optimal logic synthesis
[AD-A217119] N90-20742
LOGIC PROGRAMMING
Joint Japanese-American Workshop on Future Trends in Logic Programming
[DE90-008343] N90-20709
Exact algorithms for output encoding, state assignment and four-level Boolean minimization
[AD-A217121] N90-20756
LOSSES
Nickel-hydrogen capacity loss on storage N90-20478
A comparison of the mechanisms of cold- and microgravity-induced fluid loss
[AD-A218098] N90-20631
LOW COST
Fighter escape system: The next step forward N90-20059
LOW DENSITY FLOW
Computation of hypersonic low density flows with thermochemical nonequilibrium N90-20044
LOW FREQUENCIES
A linear filtering technique for removal of low-frequency noise
[DE90-006183] N90-20296
LOW REYNOLDS NUMBER
The effect of adverse pressure gradient on turbulent burst structure in low-Reynolds number equilibrium boundary layers
[AD-A217308] N90-20327
LOW SPEED
Space mechanism of low velocity for an array of solar panels: Analysis and design of an experimental model; dimensions of bearings
[INPE-4859-TDL/370] N90-20390
LOW SPEED WIND TUNNELS
Design of a high angle of attack robotic sting mount for tests in a low speed wind tunnel
[AD-A218105] N90-20099
LOW TEMPERATURE
A comparison of the mechanisms of cold- and microgravity-induced fluid loss
[AD-A218098] N90-20631
LOW TEMPERATURE ENVIRONMENTS
Effective calibration of heat flux transducers for experimental use
[AD-A218262] N90-20636
What should athletes know about low body temperature (hypothermia)
[AD-A218316] N90-20637
LUBRICANTS
Tribological properties of boric acid and boric-acid-forming surfaces. Part 2: Formation and self-lubrication mechanisms of boric acid films on boron- and boric-oxide-containing surfaces
[DE90-005632] N90-20400
LUBRICATION
In-line wear monitor
[AD-A217799] N90-20091
Space mechanism of low velocity for an array of solar panels: Analysis and design of an experimental model; dimensions of bearings
[INPE-4859-TDL/370] N90-20390
LUMINOSITY
Studies of the evolution of the x ray emission of clusters of galaxies
[NASA-CR-186471] N90-20918
LUNAR OBSERVATORIES
Human exploration mission studies N90-20457
LUNAR SOIL
The electrochemical generation of useful chemical species from lunar materials N90-20451

M

MACH NUMBER
A numerical investigation of the compressible mixing layer
[AD-A217738] N90-20343
MACHINE LEARNING
Concept formation and generalization based on experimentation by an autonomous mobile robot
[DE90-001731] N90-20395
CEREBRAL WEEVIL: A machine learning model for hemispheric categorization of complex visual patterns
[AD-A218143] N90-20749
MACHINING
Nondestructive testing of ceramics by acoustic microscopy
[AERE-R-13350] N90-20411
MAGNET COILS
Materials and selection criteria analysis for the compact ignition tokamak toroidal field coil turn-to-turn insulation system: Photographic summary ofllaboratory testing
[DE90-008020] N90-20850
MAGNETIC CORES
Core cooling studies at LLNL (Lawrence Livermore National Laboratory) and Sandia
[DE90-008303] N90-20300
MAGNETIC FIELD RECONNECTION
Spontaneous magnetic reconnection in a turbulent plasma N90-20840
MAGNETIC FIELDS
Magnetic hardening studies and novel techniques for preparation of high performance magnets
[AD-A217737] N90-20790
Enhanced pinch effect due to electrostatic potential
[DE90-007088] N90-20844
MAGNETIC MOMENTS
Theoretical investigations in elementary particle physics
[DE90-007178] N90-20802
MAGNETIC PROPERTIES
Magnetic hardening studies and novel techniques for preparation of high performance magnets
[AD-A217737] N90-20790
Stabilization of high (Tc) superconductivity in cadmium sulfide
[DE90-008249] N90-20881
Technology assessment of superconductivity
[AD-A217697] N90-20889
MAGNETIC SHIELDING
Magnetic vapor shield mechanism for protection of material surfaces exposed to high heat load
[AD-A217667] N90-20217
MAGNETOHYDRODYNAMIC STABILITY
Spontaneous magnetic reconnection in a turbulent plasma N90-20840
High elongation plasmas
[DE90-007575] N90-20848
Nonlinear stability in fluid and plasma dynamics
[AD-A217735] N90-20856
MAGNETOHYDRODYNAMICS
Diagnostic development and support of MHD (Magnetohydrodynamics) test facilities
[DE90-004969] N90-20845
MAGNETOSTATICS
Magnetostatic boundary-value problems in the incomplete-nonlinear formulation and methods of their solution
[DE90-615185] N90-20767
MAINTAINABILITY
Space Station Freedom electric power system availability study
[NASA-CR-185181] N90-20120
MAN ENVIRONMENT INTERACTIONS
Overview of the methodologies used to compile large scale emissions inventories
[DE90-008518] N90-20509
MAN MACHINE SYSTEMS
Aiding the decision maker: Perceptual and cognitive issues at the human-machine interface
[AD-A217862] N90-20648
Graphics Technology in Space Applications (GTSA 1989)
[NASA-CP-3045] N90-20651
The use of graphics in the design of the human-telerobot interface N90-20670
MAN-COMPUTER INTERFACE
Comparison of oculometer and head-fixed reticle with voice or switch and touch panel for data entry on a generic tactical air combat display
[AD-A217231] N90-20646
The development of the Canadian Mobile Servicing System Kinematic Simulation Facility N90-20676
Design of a simulation interface for a parellel computing environment
[DE90-008497] N90-20737
MANAGEMENT ANALYSIS
Middle management of research
[NASA-TM-102417] N90-20901
MANAGEMENT INFORMATION SYSTEMS
An empirical test of a comprehensive model for predicting successful information systems implementation
[AD-A218124] N90-20908
MANAGEMENT METHODS
On optimal distributed decision architectures in a hypothesis testing environment
[AD-A217824] N90-20274
MANAGEMENT PLANNING
An integrative research review of the relationship between technology and structure: A meta-analytic synthesis
[AD-A218115] N90-20903
MANAGEMENT SYSTEMS
Information management systems for integrating the technical data and regulatory requirements of environmental restoration activities
[DE90-008622] N90-20511
MANEUVERS
Potential role of avionics in escape systems N90-20060
MANGANESE
Ligand-centered electron-transfer redox processes for manganese, iron, and cobalt complexes in relation to selected catalytic systems
[AD-A217957] N90-20177
MANIPULATORS
Multi-dimensional LADAR tracking and adaptive grasping for spaceborne assembly of SDI (Strategic Defense Initiative) platforms
[AD-A218236] N90-20279
The CMU Reconfigurable Modular Manipulator System
[CMU-RI-TR-88-7] N90-20388
Development of a passive robot-controlled reaction arm N90-20389
Resolved motion rate and resolved acceleretion servo-control of wheeled mobile robots
[DE90-002585] N90-20399
Knowledge-based robotic grasping
[DE90-007216] N90-20402
Dynamic damping control: Implementation issues and simulation results
[DE90-007687] N90-20403
Design of a telerobotic controller with joint torque sensors
[DE90-008753] N90-20404
Control system design of the third flexible joint of PUMA 560 robot
[AD-A218075] N90-20405
Gripping device
[NASA-CASE-MSC-21365-1] N90-20408
Graphical programming and the use of simulation for space-based manipulators N90-20674
Using an instrumented manikin for Space Station Freedom analysis N90-20675
Boundary equations of configuration obstacles for manipulators
[DE90-002101] N90-20745
MANUALS
The NASA, Marshall Space Flight Center drop tube user's manual
[NASA-TM-100392] N90-20251
MANUFACTURING
Statistical equipment modeling for VLSI manufacturing
[DE90-008527] N90-20304
Phase 1 supplemental development of a kinematic Stirling/Rankine commercial gas-fired heat pump system
[PB90-129974] N90-20483
CuInSe2 and CdTe: Scale-up for manufacturing
[DE89-009503] N90-20489
MANY BODY PROBLEM
Periodic trajectories for two-dimensional nonintegrable Hamiltonians
[DE90-008082] N90-20765
MAPPING
Synthesis and analysis of 25 years (1961-1986) of INPE/SRE activities related to the vegetation/forest area
[INPE-4969-RPE/604] N90-20446
Progress in the Determination of the Earth's Gravity Field
[NASA-CR-185721] N90-20513
Gravity field of the Western Weddell Sea: Comparison of airborne gravity and Geosat derived gravity N90-20526
Geodynamics and temporal variations in the gravity field N90-20549
Gravity field information from Gravity Probe-B N90-20554
Local gravity disturbance estimation from multiple-high-single-low satellite-to-satellite tracking N90-20555
MAPS
A split-and-merge method for creating polygonal homogeneous-vegetation regions from digitized terrain data
[AD-A218080] N90-20453
MARINE ENVIRONMENTS
Research and development on enhanced degradable plastics
[AD-A217180] N90-20212
Theoretical modeling studies of the marine planetary
[AD-A217200] N90-20567
US Navy regional climatic study of the Central East Asian coast and associated waters
[AD-A217448] N90-20587
MARINE METEOROLOGY
US Navy regional climatic study of the Central East Asian coast and associated waters
[AD-A217448] N90-20587
Coastal frontogenesis and associated severe weather on 13 March 1986 (GALE IOP 13)
[AD-A217708] N90-20590

A modeling study of the cloud-topped marine boundary layer
[AD-A218103] N90-20594

MARKOV PROCESSES
Modeling and classification of acoustic transients by speech recognition techniques
[AD-A218070] N90-20277
Approximate evaluation of reliability and related quantities via perturbation techniques
[AD-A218340] N90-20417

MARS ATMOSPHERE
Use of random Martian atmosphere to evaluate potential entry guidance schemes
[NASA-TM-102606] N90-20122

MARTENSITIC STAINLESS STEELS
Fatigue crack growth in martensitic 2 1/4Cr-1Mo steel at elevated temperatures
[AERE-R-13524] N90-20191
Rolling contact fatigue of surface modified 440C using a 'Ge-Polymet' type disc rod test rig
[NASA-TM-100390] N90-20200

MASERS
Biological applications and effects of optical masers
[AD-A217910] N90-20385

MASS FLOW
Geometric scale of interaction between moving shock and stationary thermal layer
[AD-A217769] N90-20344

MASS TRANSFER
Enhancement of mass transfer to a rotating cylinder electrode by inert particles suspended in the electrolyte
[DE90-008054] N90-20165
Mass transfer from a sphere in an oscillating flow with zero mean velocity
[NASA-TM-102566] N90-20338
Solar cyclical trend study of the mid-latitude, quiet-time, meridional, neutral winds at winter solstice conditions
[AD-A217398] N90-20568

MASSIVELY PARALLEL PROCESSORS
Massively-parallel computational fluid dynamics
[AD-A217732] N90-20342
Parallel computer graphics algorithms for the connection machine
[AD-A217300] N90-20733
A model and implementation of multigrid for massively parallel computers
[DE90-008165] N90-20739
Implementation of midcourse tracking and correlation on massively parallel computers
[DE90-008166] N90-20740

MATCHED FILTERS
High-resolution acoustical imaging N90-20793

MATCHING
Almost-optimum parallel speed-ups of algorithms for bipartite matching and related problems
[AD-A215111] N90-20728
Robust adaptive nonlinear control under extended matching conditions
[AD-A217684] N90-20744

MATERIALS HANDLING
Knowledge-based robotic grasping
[DE90-007216] N90-20402
RIPE: An object-oriented Robot Independent Programming Environment
[DE90-008501] N90-20707

MATHEMATICAL LOGIC
Joint Japanese-American Workshop on Future Trends in Logic Programming
[DE90-008343] N90-20709
A paradoxical result in unconditionally secure authentication codes, and an explanation
[DE90-008529] N90-20710

MATHEMATICAL MODELS
Using transonic small disturbance theory for predicting the aeroelastic stability of a flexible wind-tunnel model
[NASA-TM-102617] N90-20047
Development of acceleration exposure limits for advanced escape systems N90-20055
Aeroelastic characteristics of aircraft with circulation control wings N90-20070
A video-based experimental investigation of wing rock
[AD-A218244] N90-20075
Component count and preliminary assembly considerations for large space truss structures
[NASA-TM-102604] N90-20121
Use of random Martian atmosphere to evaluate potential entry guidance schemes
[NASA-TM-102606] N90-20122
Summary report of the Summer Conference of the DARPA-Materials Research Council
[AD-A217380] N90-20143
Structure of model gas flames in nitramines
[AD-A217578] N90-20159
Moisture control in sealed electronic packages
[DE90-008136] N90-20166
Spallation of oxide scales from 20 percent Cr/25 percent Ni/Nb stainless steel
[AERE-R-13464] N90-20189
Stochastic approach to the initiation of pitting corrosion
[AERE-R-13348] N90-20190
Secondary arm coarsening and microsegregation in superalloy PWA-1480 single crystals: Effect of low gravity
[NASA-TM-102445] N90-20194
A unified integrated model for sputter coating uniformity
[DE90-008322] N90-20205
Magnetic vapor shield mechanism for protection of material surfaces exposed to high heat load
[AD-A217667] N90-20217
Modification and improvement of software for modeling multidimensional reacting fuel flows
[AD-A217789] N90-20235
Modelling Doppler broadening in Raman propagation
[DE90-008042] N90-20269
High resolution radar target modeling using ARMA (Autoregressive Moving Average) models
[AD-A218212] N90-20278
Statistical equipment modeling for VLSI manufacturing
[DE90-008527] N90-20304
Amplitude-dependent neutral modes in compressible boundary layer flows
[NASA-TM-102524] N90-20326
Geometric scale of interaction between moving shock and stationary thermal layer
[AD-A217769] N90-20344
Harmonic generation mechanisms in short-wavelength free-electron lasers
[DE90-007622] N90-20374
Laser-induced shock waves effects in materials
[DE90-007626] N90-20379
Laser line transport with refraction
[DE90-008683] N90-20382
The diffraction of ultrasound by cracks: Comparison of experiment with theory
[AERE-R-13334] N90-20410
Computer simulation of the mathematical modeling involved in constitutive equation development: Via symbolic computations
[NASA-TM-102532] N90-20428
Model development in viscoplastic ratchetting
[NASA-TM-102509] N90-20431
Computational simulation of damping in composite structures
[NASA-TM-102567] N90-20432
COMGEN: A computer program for generating finite element models of composite materials at the micro level
[NASA-TM-102556] N90-20438
Plan, formulate, and discuss a NASTRAN finite element model of the UH-60A helicopter airframe
[NASA-CR-181975] N90-20439
Analysis of methods to determine emissivity for ground surface targets in the spectral band 8 to 14 microns
[INPE-4984-TDL/394] N90-20447
Simulation of landscape disturbances and the effect of climatic change
[DE90-007565] N90-20503
Atmospheric Radiation Measurement Program Plan
[DE90-008108] N90-20504
Overview of the methodologies used to compile large scale emissions inventories
[DE90-008518] N90-20509
Use of environmental monitoring data in evaluation of atmospheric modeling results
[DE90-008607] N90-20510
Processes of community development and responses of ecosystems to climate change
[DE90-008640] N90-20512
Progress in the Determination of the Earth's Gravity Field
[NASA-CR-185721] N90-20513
Gravitational model improvement at the Goddard Space Flight Center N90-20514
An improved model for the Earth's gravity field N90-20515
Progress in the development of high degree potential coefficient models N90-20516
Gravity field determination and error assessment techniques N90-20517
An improved error assessment for the GEM-T1 gravitational model N90-20518
Geopotential models in the Australian region N90-20519
Stabilized determination of geopotential coefficients by the mixed hom-BLUP approach N90-20520
Precise solution for a finite set of spherical coefficients from equiangular gridded data N90-20522
Modeling of the Earth's gravity field using the New Global Earth Model (NEWGEM) N90-20523
A framework for modelling kinematic measurements in gravity field applications N90-20524
The use of high-resolution terrain data in gravity field prediction N90-20533
The role of topography in geodetic gravity field modelling N90-20534
The inverse gravimetric problem in gravity modelling N90-20535
FFT-local gravimetric geoid computation N90-20536
Performance of FFT methods in local gravity field modelling N90-20537
Fourier transform methods in local gravity modeling N90-20538
Downward continuation of the free-air gravity anomalies to the ellipsoid using the gradient solution and terrain correction: An attempt of global numerical computations N90-20541
The geoid in Kenya N90-20542
GEOID '88: A gravimetric geoid for Canada N90-20543
Regional quasigeoid determination in Northern Germany and comparison with GPS N90-20544
Treatment of geodetic leveling in the integrated geodesy approach N90-20546
Determination of mean gravity anomalies in the Taiwan Island N90-20547
Very accurate upward continuation to low heights in a test of non-Newtonian theory N90-20548
Geodynamics and temporal variations in the gravity field N90-20549
Geographically correlated orbit error N90-20551
Spectral analyses of satellite geopotential missions N90-20552
Local gravity disturbance estimation from multiple-high-single-low satellite-to-satellite tracking N90-20555
Satellite-to-satellite tracking experiment for global gravity field mapping N90-20556
A discussion of observation model, error sources and signal size for spaceborne gravitational gradiometry N90-20557
Studies of an orbital gradiometer mission N90-20558
Theoretical modeling studies of the marine planetary
[AD-A217200] N90-20567
Seismic characterization of fracture properties
[DE90-007759] N90-20570
Damage characteristics of time domain histories
[DE90-008787] N90-20573
A modeling study of the cloud-topped marine boundary layer
[AD-A218103] N90-20594
The invertibility principle for a simple hurricane model
[AD-A218344] N90-20605
Space Station Freedom integrated fault model N90-20673
Computing mean responses in nonlinear models
[AD-A217642] N90-20700
Computational complexity of random access models
[AD-A217685] N90-20701
Automated finite element modeling and simulation N90-20753
Spectral analytic methods for the estimation of number of signals and directions of arrival
[AD-A217219] N90-20757
Observer based compensators for nonlinear systems
[AD-A217426] N90-20760
Micro SAINT programs for numerical methods of integration and differential equations
[AD-A218097] N90-20772
Slepian models and regression approximations in crossing and extreme value theory
[AD-A218338] N90-20779
The n-p bremsstrahlung in heavy ion collision processes
[DE90-008542] N90-20823
Spectral line shape code for multielectron emitters
[DE90-008526] N90-20853
The electronic properties of high (Tc) superconductors probed by positron annihilation
[DE90-008354] N90-20883
Systematics in positron annihilation lifetime analysis of high (Tc) superconducting transitions
[DE90-008361] N90-20884
Growth, characterization and device development in monocrystalline diamond films
[AD-A218211] N90-20895
An empirical test of a comprehensive model for predicting successful information systems implementation
[AD-A218124] N90-20908
EXOSAT observations of Seyfert type galaxies N90-20910

MATRICES (MATHEMATICS)
Comparison of two matrix data structures for advanced CSM testbed applications
[NASA-CR-181951] N90-20421

Progress in the development of high degree potential coefficient models N90-20516
An improved error assessment for the GEM-T1 gravitational model N90-20518
An algorithm for efficient estimation of superimposed exponential signals [AD-A217218] N90-20698

MATRIX MATERIALS
Composite laminate tailoring with probabilistic constraints and loads [NASA-TM-102515] N90-20138

MATRIX METHODS
Rotordynamic analysis with shell elements for the transfer matrix method [AD-A217455] N90-20434

MAXIMUM LIKELIHOOD ESTIMATES
An algorithm for efficient estimation of superimposed exponential signals [AD-A217218] N90-20698

MAXWELL EQUATION
Magnetostatic boundary-value problems in the incomplete-nonlinear formulation and methods of their solution [DE90-615185] N90-20767

MEAN SQUARE VALUES
Electronic precipitator control [NASA-CASE-LAR-13273-2] N90-20320

MEASURING INSTRUMENTS
Dual cathode system for electron beam instruments [NASA-CASE-NPO-16878-1-CU] N90-20351
Nine-year aging behavior of the ceramic flatpack resonator [DE90-008044] N90-20412

MECHANICAL PROPERTIES
Studies of the structure and properties of organic monolayers, multilayers and superlattices [DE90-008330] N90-20129
Tellurium embrittlement of type 316 steel [AERE-R-13440] N90-20192
Design and processing of strong-tough microcomposite steels [DE90-007764] N90-20197
The stress corrosion performance of diffusion bonded nickel base alloys [DE90-008130] N90-20199
An introduction to nickel aluminide alloy [DE90-008565] N90-20207
The effects of radiation on the mechanical properties of polymers used as electrical cable insulation and jacketing materials [AERE-R-13286] N90-20209
Interface science in deformation processing of ceramics [DE90-008424] N90-20219
Pyrotechnic device technology [DE90-007683] N90-20234
An electrochemical and spectroscopic study of electrode processes [AD-A217261] N90-20289
Seismic characterization of fracture properties [DE90-007759] N90-20570
Performance of Y-TZP materials between 800 C and 1200 C [AD-A217723] N90-20890

MEDICAL SCIENCE
Three-dimensional medical image analysis using local dynamic algorithm selection on a multiple-instruction, multiple-data architecture [AD-A218024] N90-20630
Micro SAINT programs for numerical methods of integration and differential equations [AD-A218097] N90-20772

MELTING
Techno-economic assessment of a carbothermic alumina reduction process [DE90-007018] N90-20170
High temperature chemistry of oxide superconductors [DE90-007821] N90-20875
Systematics in positron annihilation lifetime analysis of high (Tc) superconducting transitions [DE90-008361] N90-20884
Method of preparing radially homogeneous mercury cadmium telluride crystals [NASA-CASE-MFS-25786-2] N90-20896

MELTS (CRYSTAL GROWTH)
Infiltration mechanics in conventional and hybridised fibre reinforced metal matrix composites [AERE-R-13330] N90-20134

MEMBRANES
CO2 diffusion and solubility in a Polystyrene/Polybutadiene block copolymer with highly oriented lamellar morphology [AD-A217165] N90-20211
The application of Dow Chemical's perfluorinated membranes in proton-exchange membrane fuel cells N90-20466
Hydrogen-oxygen proton-exchange membrane fuel cells and electrolyzers N90-20467
Selection and design of a stretched-membrane heliostat for today's markets [DE90-007997] N90-20495

MEMORY
A long-term retention advantage for spatial information learned naturally and in the laboratory [AD-A218268] N90-20644

MEMORY (COMPUTERS)
The contour model architecture and assembly language [AD-A217114] N90-20697

MENISCI
Infiltration mechanics in conventional and hybridised fibre reinforced metal matrix composites [AERE-R-13330] N90-20134

MENTAL PERFORMANCE
Effects of dexamethasone and high terrestrial altitude on cognitive performance and affect [AD-A217897] N90-20625
Role of cognitive factors in the acquisition of cognitive skill [AD-A218069] N90-20642

MERCURY CADMIUM TELLURIDES
Workshop on the Physics and Chemistry of Mercury Cadmium Telluride and Related II-VI compounds [AD-A217496] N90-20867
NRL hybrid reliability. Physics of failure initial study [AD-A217986] N90-20893
Method of preparing radially homogeneous mercury cadmium telluride crystals [NASA-CASE-MFS-25786-2] N90-20896

MERCURY COMPOUNDS
Mercuric iodide room temperature gamma-ray detectors [NASA-TM-103318] N90-20357

MERIDIONAL FLOW
Solar cyclical trend study of the mid-latitude, quiet-time, meridional, neutral winds at winter solstice conditions [AD-A217398] N90-20568

MESOSCALE PHENOMENA
Derivation of kinematic fields using wind profiler data from the 1985 pre-storm experiment [AD-A217952] N90-20592
A method for correcting and reducing the pressure data recorded at the PAM 2 stations during GALE [AD-A218165] N90-20596
An aircraft investigation of a convective boundary layer over Lake Michigan [AD-A218175] N90-20598

MESSAGE PROCESSING
Express cubes: Improving the performance of k-ary n-cube interconnection networks [AD-A217117] N90-20287

METABOLISM
Influence of theobromine on heat production and body temperatures in cold-exposed humans: A preliminary report [AD-A217203] N90-20618
Physical performance and carbohydrate consumption in CF commandos during a 5-day field trial [AD-A217204] N90-20619

METAL AIR BATTERIES
Exploratory battery technology development and testing report for 1988 [DE90-007996] N90-20297
Investigation of a photovoltaic/battery hybrid system for powering the high arctic data communications system [AD-A218353] N90-20319

METAL FILMS
Surface-plasmon enhanced nonlinear photoelectric emission from thin silver films [DE90-007676] N90-20807

METAL FLUORIDES
Mechanisms of reactive etching [AD-A217679] N90-20160

METAL GRINDING
Crystal preparation at LBL, 1976 to 1986 [DE90-007754] N90-20871

METAL IONS
Interaction between implanted ions and intrinsic defects in silica [DE90-006569] N90-20858

METAL MATRIX COMPOSITES
Infiltration mechanics in conventional and hybridised fibre reinforced metal matrix composites [AERE-R-13330] N90-20134
Evaluation of thermal and mechanical loading effects on the structural behavior of a SiC/titanium composite [NASA-TM-102536] N90-20139
Compendium of abstracts and viewgraphs. [AD-A217189] N90-20140
Summary report of the Summer Conference of the DARPA-Materials Research Council [AD-A217380] N90-20143
Summary of the DoD Metal Matrix Composites (MMC) Steering Committee Meeting, hosted by the Institute for Defense Analysis [AD-A217611] N90-20145
Fundamental aspects of and failure modes in high-temperature composites [NASA-TM-102558] N90-20151
The effect of the SiC/Al interface on matrix microstructure in 2xxx-SiCp metal matrix [AERE-R-13591] N90-20184
The ageing effect of the matrix-reinforcement interface on the ageing response of an aluminium 6061 alloy reinforced with 20vol percent SiC particulates [AERE-R-13361] N90-20193

METAL OXIDE SEMICONDUCTORS
Proton responses on MOS (Metal-Oxide-Semiconductor) electronics operating at cryogenic temperatures [AD-A217622] N90-20868

METAL OXIDES
Metal alkoxides: Models for metal oxides. Alkoxide ligands in early transition metal organometallic chemistry [DE90-007523] N90-20869
Crystal preparation at LBL, 1976 to 1986 [DE90-007754] N90-20871
Electronic properties of high-temperature superconductors [AD-A217953] N90-20892

METAL PLATES
Evaluation of 2090-T8E48 aluminum-lithium plates [AD-A217262] N90-20196
Superconductive microprobes for eddy current evaluation of materials [AD-A217776] N90-20361

METALLIZING
Infrared and X ray photoelectron spectroscopy studies of the polyimide/metal interface [AD-A218249] N90-20179

METALS
Principles of metallic solidification N90-20241
Dynamics of the solidification front N90-20243

METASTABLE STATE
Joint Services Electronics Program research in electronics [AD-A217745] N90-20307
Electronically metastable molecules of high symmetry [AD-A217768] N90-20814
Theoretical studies of spin-forbidden processes within the Breit-Pauli approximation [AD-A217778] N90-20815

METEOROIDS
Meteor observations using the 50 MHz MENTOR imaging Doppler interferometer [AD-A217908] N90-20276

METEOROLOGICAL PARAMETERS
Forecasting the tornadic intensities of thunderstorms by multivariate techniques [AD-A218284] N90-20602

METEOROLOGICAL SATELLITES
Forecasting 24 and 48 hour intensity changes, for northwestern Pacific tropical cyclones, using satellite imagery [AD-A218174] N90-20597

METEOROLOGY
The Terrain-Responsive Atmospheric Code (TRAC) project plan: Development of a hazardous materials dispersion modeling capability with application to ambient air monitoring network design [DE90-007293] N90-20502

METHANE
The extinction and structure of counterflow premixed flames [AD-A218106] N90-20178

METHOD OF MOMENTS
Recent improvements to the electromagnetic surface patch code [AD-A217479] N90-20293

METHYL COMPOUNDS
The 1-(diorganooxyphosphonyl)-methyl)-2,4- and -2,6-diamido benzenes [NASA-CASE-ARC-11425-4] N90-20133

MICE
Acute oral toxicity of JA-2 solid propellant in ICR mice [AD-A217264] N90-20609
Acute oral toxicity of DIGL-RP solid propellant in ICR mice [AD-A217711] N90-20613

MICROANALYSIS
Oxygen concentrations on surfaces of carbon fibers [AD-A217724] N90-20152

MICROCRACKS
Computed tomography of electronics [AD-A217976] N90-20314
Velocity matched optical transmitter [AD-A217413] N90-20830

MICROELECTRONICS
Processing, fabrication, characterization and device demonstration of high temperature superconducting ceramics
[AD-A218330] N90-20231
A progress report on the Livermore Miniature Vacuum Tube Project
[DE90-008302] N90-20299
Fault simulator evaluation
[AD-A217782] N90-20308
In-situ differential reflectance study of the etching of SiO2 films
[AD-A217186] N90-20864
MICROGRAVITY APPLICATIONS
Microgravity Science and Application Program tasks, 1989 revision
[NASA-TM-4191] N90-20252
MICROMECHANICS
Composite laminate tailoring with probabilistic constraints and loads
[NASA-TM-102515] N90-20138
Computational simulation of damping in composite structures
[NASA-TM-102567] N90-20432
MICROORGANISMS
Design and operation of an outdoor microalgae test facility
[DE89-009493] N90-20608
MICROPROCESSORS
Laboratory implementation of the Continuously Reconfiguring Multi-Microprocessor Flight Control System (CRMMFCS)
[AD-A217730] N90-20094
X ray microimaging by diffractive techniques
[DE90-008444] N90-20356
Diagnostic development and support of MHD (Magnetohydrodynamics) test facilities
[DE90-004969] N90-20845
MICROSCOPY
Superconductive microprobes for eddy current evaluation of materials
[AD-A217776] N90-20361
Biological soft x ray contact microscopy: Imaging living CHO-SC1 cells and other biological materials
[DE90-007560] N90-20610
MICROSTRIP TRANSMISSION LINES
Investigation of tapered multiple microstrip lines for VLSI circuits
[AD-A217855] N90-20310
MICROSTRUCTURE
Synthesis of alumina-coated SiC whiskers for production of SiC whisker-reinforced alumina composite materials
[DE90-007778] N90-20147
Analytical electron microscopy of catalyst preparations
[DE90-008699] N90-20173
The effect of the SiC/Al interface on matrix microstructure in 2xxx-SiCp metal matrix
[AERE-R-13591] N90-20184
Ageing effects in welded cast CF3 stainless steel
[AERE-R-13559] N90-20188
Stochastic approach to the initiation of pitting corrosion
[AERE-R-13348] N90-20190
The ageing effect of the matrix-reinforcement interface on the ageing response of an aluminium 6061 alloy reinforced with 20vol percent SiC particulates
[AERE-R-13361] N90-20193
Design and processing of strong-tough microcomposite steels
[DE90-007764] N90-20197
The stress corrosion performance of diffusion bonded nickel base alloys
[DE90-008130] N90-20199
Physical sputtering of metallic systems by charged-particle impact
[DE90-007803] N90-20201
Evaluation of material homogeneity as a function of thickness of low-alloy ferritic steel
[DE90-008069] N90-20202
The metallurgical mechanisms of solder fatigue
[DE90-008390] N90-20206
Strength and microstructure of ceramics
[AD-A217752] N90-20227
Nondestructive testing of ceramics by acoustic microscopy
[AERE-R-13350] N90-20411
Time-dependent failure of silver interlayer welds
[DE90-008015] N90-20440
Dielectric composite thin films
[AD-A217940] N90-20791
Synthesis and properties of polycrystalline Tl2Ba2CaCu2O(x) and Tl2Ba2Ca2Cu3O(x)
[DE90-007528] N90-20887
Performance of Y-TZP materials between 800 C and 1200 C
[AD-A217723] N90-20890
MICROWAVE CIRCUITS
Analysis of radiometer calibration effects with TOUCHSTONE
[NASA-CR-186476] N90-20284
Performance of a 300 Mbps 1:16 serial/parallel optoelectronic receiver module
[NASA-TM-103110] N90-20302
MICROWAVE IMAGERY
Applications of microwave radiometric measurements to infer tropical cyclone intensity and strength
[AD-A218273] N90-20600
MICROWAVE RADIOMETERS
Applications of microwave radiometric measurements to infer tropical cyclone intensity and strength
[AD-A218273] N90-20600
Microwave brightness temperature and its relation to atmospheric general circulation features
[AD-A218312] N90-20603
MICROWAVE SOUNDING
Microwave brightness temperature and its relation to atmospheric general circulation features
[AD-A218312] N90-20603
MICROWAVES
Microwave field effect transistor
[NASA-CASE-GSC-12442-2] N90-20282
Growth, characterization and device development in monocrystalline diamond films
[AD-A218211] N90-20895
MILITARY AIR FACILITIES
The United States Air Force School of Aerospace Medicine: Special report
[AD-A217740] N90-20622
MILITARY OPERATIONS
Physical performance and carbohydrate consumption in CF commandos during a 5-day field trial
[AD-A217204] N90-20619
Field assessment of wet bulb globe temperature: Present and future
[AD-A218224] N90-20635
The thrust and parry of the SIOP (Single Integrated Operational Plan) and SDI
[AD-A217617] N90-20784
SDI (Strategic Defense Initiative): Is its future past
[DE90-008016] N90-20785
Role of free-electron lasers in strategic defense
[DE90-008028] N90-20786
MILLIMETER WAVES
Conference digest: Thirteenth International Conference on Infrared and Millimeter Waves, volume 1039
[AD-A217343] N90-20291
Superconductive microprobes for eddy current evaluation of materials
[AD-A217776] N90-20361
Millimeter wave surface resistance of RBa2Cu3O(7-delta) (R=Y,Eu,Dy,Sm,Er) superconductors
[NASA-TM-102571] N90-20886
Growth, characterization and device development in monocrystalline diamond films
[AD-A218211] N90-20895
MIMD (COMPUTERS)
Three-dimensional medical image analysis using local dynamic algorithm selection on a multiple-instruction, multiple-data architecture
[AD-A218024] N90-20630
MINIATURIZATION
A progress report on the Livermore Miniature Vacuum Tube Project
[DE90-008302] N90-20299
MINORITIES
ONR (Office of Naval Research) summer scholars for the 1989 PREFACE Program
[AD-A217746] N90-20919
MIRRORS
Placement of multiple apertures for imaging telescopes
[DE90-006991] N90-20833
Design and performance analysis of adaptive optical telescopes using laser guide stars
[AD-A218025] N90-20913
MISCIBILITY GAP
Systems with a miscibility gap in the liquid state
N90-20245
MISSILE DETECTION
Three-dimensional route planning for a cruise missile for minimal detection by observer
[AD-A218336] N90-20787
MISSION PLANNING
Proximity operations concept design study, task 6
[NASA-CR-181971] N90-20112
Gravity field information from Gravity Probe-B
N90-20554
Operational computer graphics in the flight dynamics environment N90-20668
Three-dimensional route planning for a cruise missile for minimal detection by observer
[AD-A218336] N90-20787
MITOCHONDRIA
Carbon and hydrogen metabolism of green algae in light and dark
[DE90-008648] N90-20612
MIXING LAYERS (FLUIDS)
A numerical investigation of the compressible mixing layer
[AD-A217738] N90-20343
MOBILITY
Concept formation and generalization based on experimentation by an autonomous mobile robot
[DE90-001731] N90-20395
Resolved motion rate and resolved acceleration servo-control of wheeled mobile robots
[DE90-002585] N90-20399
MODELS
Determination of fundamental thermodynamic properties of constituent materials and performance screening of candidate systems
[AD-A218089] N90-20153
MEASURE: An integrated data-analysis and model identification facility
[NASA-CR-186452] N90-20686
A locally constrained parallel activation model for diagnostic reasoning
[AD-A217808] N90-20747
MODULARITY
Selection and design of a stretched-membrane heliostat for today's markets
[DE90-007997] N90-20495
Real-time concurrency control and transaction scheduling
[AD-A218162] N90-20909
MODULATION
Error control techniques for satellite and space communications
[NASA-CR-186221] N90-20263
Advanced modulation technology development for earth station demodulator applications. Coded modulation system development
[NASA-CR-185149] N90-20270
Doppler radar with multiphase modulation of transmitted and reflected signal
[NASA-CASE-MSC-18808-1] N90-20280
MODULATORS
Velocity matched optical transmitter
[AD-A217413] N90-20830
GaAs traveling-wave optical modulators using modulated coplanar electrodes with periodic cross-tie overlays
[AD-A217731] N90-20835
MODULES
Amplified spontaneous emission measurements on the aurora large-aperture module
[DE90-004841] N90-20369
MODULUS OF ELASTICITY
Ultrastructure processing of ordered polymers
[AD-A218331] N90-20232
MOISTURE
Thiokol/Wasatch installation evaluation of the redesigned field joint protection system (concepts 1 and 3)
[NASA-CR-183860] N90-20127
Moisture control in sealed electronic packages
[DE90-008136] N90-20166
Structure and dynamics of the Arizona monsoon boundary
[AD-A217378] N90-20586
Comparison of light duty gloves with natural and synthetic materials under wet and dry conditions
[AD-A218119] N90-20649
MOISTURE CONTENT
The effect of moisture absorption in clothing on the human heat balance
[AD-A217899] N90-20626
MOLECULAR BEAM EPITAXY
Joint Services Electronics Program research in electronics
[AD-A217745] N90-20307
Investigation of the technological effects on the coupling behavior of parallel GaAlAs rib waveguide
[ETN-90-95323] N90-20825
Chemical beam epitaxy of ZnSe
[AD-A217375] N90-20866
CCST (Center for Compound Semiconductor Technology) research briefs
[DE90-007782] N90-20874
MOLECULAR BEAMS
Interactions of molecules with surfaces
[DE90-007555] N90-20806

MOLECULAR CHAINS
Investigation into the mechanism of polymer thread drag reduction
[AD-A217492] N90-20329
MOLECULAR COLLISIONS
Interactions of molecules with surfaces
[DE90-007555] N90-20806
MOLECULAR DIFFUSION
Investigation into the mechanism of polymer thread drag reduction
[AD-A217492] N90-20329
MOLECULAR EXCITATION
Reactive and anisotropic elastic scattering of highly laser-vibration-excited diatomic molecules
[MPIS-19/1988] N90-20804
Dynamics of electronically excited species in gaseous and condensed phase
[AD-A217696] N90-20812
MOLECULAR INTERACTIONS
Termolecular associations of ions in gases, recombination and electron-atom collisions
[AD-A217678] N90-20805
Interactions of molecules with surfaces
[DE90-007555] N90-20806
MOLECULAR OSCILLATIONS
Production rates for electron beams and swarms in nitrogen
[AD-A218145] N90-20817
MOLECULAR RELAXATION
A continued study of optical sound generation and amplification
[AD-A217640] N90-20796
Molecular dynamics and spectroscopy at gas-solid interfaces
[AD-A217743] N90-20813
MOLECULAR ROTATION
Production rates for electron beams and swarms in nitrogen
[AD-A218145] N90-20817
MOLECULAR SPECTROSCOPY
Quantum-theoretical methods and studies relating to properties of materials
[AD-A217843] N90-20132
Molecular dynamics and spectroscopy at gas-solid interfaces
[AD-A217743] N90-20813
MOLECULAR STRUCTURE
Quantum-theoretical methods and studies relating to properties of materials
[AD-A217843] N90-20132
The viscoelasticity of curing thermosets
[DE90-006535] N90-20221
Radiation disorder and aperiodicity in irradiated ceramics
[DE90-008253] N90-20222
Positron annihilation spectroscopy: A nondestructive, submicroscopic characterization technique for structural polymers
[AD-A217748] N90-20226
Development of gamma-emitting, receptor-binding radiotracers for imaging the brain and pancreas
[DE90-008314] N90-20621
Dielectric composite thin films
[AD-A217940] N90-20791
Electronically metastable molecules of high symmetry
[AD-A217768] N90-20814
Metal alkoxides: Models for metal oxides. Alkoxide ligands in early transition metal organometallic chemistry
[DE90-007523] N90-20869
MOLECULAR WEIGHT
A study of physical properties of ODPA-p-PDA polyimide films
[NASA-TM-102625] N90-20137
Investigation into the mechanism of polymer thread drag reduction
[AD-A217492] N90-20329
MOLECULES
The calculation of hydrogen-bonding properties
[DE90-007534] N90-20168
Interactions of molecules with surfaces
[DE90-007555] N90-20806
Molecular organization and electrical properties of mixed Langmuir-Blodgett multilayer thin films of polypyrrole
[DE90-007627] N90-20870
MOLTEN SALTS
Chemical and electrochemical studies in ionic liquids
[AD-A217742] N90-20175
Mechanical properties of pure nickel alloys after long term exposures to LiOH and vacuum at 775 K
[NASA-TM-102403] N90-20181
The electrochemical generation of useful chemical species from lunar materials N90-20461
MOLYBDENUM OXIDES
Reactive sputtering of molybdenum
[DE90-008307] N90-20204
MOMENTS
Interior fluid dynamics of liquid-filled projectiles
[AD-A217630] N90-20330
MONITORS
In-line wear monitor
[AD-A217799] N90-20091
Airplane takeoff and landing performance monitoring system
[NASA-CASE-LAR-13734-1-CU] N90-20096
The Terrain-Responsive Atmospheric Code (TRAC) project plan: Development of a hazardous materials dispersion modeling capability with application to ambient air monitoring network design
[DE90-007293] N90-20502
Large screen display for the Mission Control Center N90-20662
Distributed earth model/orbiter simulation N90-20671
MONOMERS
Rigid rod molecules as liquid crystal thermosets
[AD-A217573] N90-20158
MONSOONS
Cloud types and the tropical Earth radiation budget, revised
[NASA-CR-180475] N90-20582
Structure and dynamics of the Arizona monsoon boundary
[AD-A217378] N90-20586
MONTE CARLO METHOD
Theory system reliability demonstration and burn-in design
[AD-A217775] N90-20416
MOON
Distributed earth model/orbiter simulation N90-20671
MORPHOLOGY
Oxygen concentrations on surfaces of carbon fibers
[AD-A217724] N90-20152
Design and processing of strong-tough microcomposite steels
[DE90-007764] N90-20197
CO2 diffusion and solubility in a Polystyrene/Polybutadiene block copolymer with highly oriented lamellar morphology
[AD-A217165] N90-20211
The effects of high intensity cycle exercise on sympatho-adrenal-medullary response patterns
[AD-A217962] N90-20628
MOTION SICKNESS
Simulator sickness in the CH-47 (Chinook) flight simulator
[AD-A218214] N90-20634
MRCA AIRCRAFT
Fighter escape system: The next step forward N90-20059
MULTIPATH TRANSMISSION
First-order intensity statistics for non-Rayleigh fading
[AD-A217572] N90-20569
MULTIPLEXING
Performance of a 300 Mbps 1:16 serial/parallel optoelectronic receiver module
[NASA-TM-103110] N90-20302
MULTIPROCESSING (COMPUTERS)
Laboratory implementation of the Continuously Reconfiguring Multi-Microprocessor Flight Control System (CRMMFCS)
[AD-A217730] N90-20094
Express cubes: Improving the performance of k-ary n-cube interconnection networks
[AD-A217117] N90-20287
Three-dimensional medical image analysis using local dynamic algorithm selection on a multiple-instruction, multiple-data architecture
[AD-A218024] N90-20630
NYU (New York University) ultracomputer
[AD-A217167] N90-20688
(DURIP) Two-Processor Alliant FX/4 System
[AD-A217810] N90-20692
RIPE: An object-oriented Robot Independent Programming Environment
[DE90-008501] N90-20707
Joint Japanese-American Workshop on Future Trends in Logic Programming
[DE90-008343] N90-20709
Performance tradeoffs in multithreaded processors
[AD-A217123] N90-20729
A Locality-based multiprocessor cache interference model
[AD-A217126] N90-20730
Parallel computer graphics algorithms for the connection machine
[AD-A217300] N90-20733
MULTISTATIC RADAR
Tomographic processing of synthetic aperture radar signals for enhanced resolution
[AD-A217178] N90-20265
MULTIVARIATE STATISTICAL ANALYSIS
Forecasting the tornadic intensities of thunderstorms by multivariate techniques
[AD-A218284] N90-20602
MUONS
Present status of (mu)CF theory
[DE90-007547] N90-20809
Studies of high energy phenomena using muons
[DE90-008272] N90-20820
MUSCULAR STRENGTH
Physical performance and carbohydrate consumption in CF commandos during a 5-day field trial
[AD-A217204] N90-20619
MUSCULOSKELETAL SYSTEM
The effects of high intensity cycle exercise on sympatho-adrenal-medullary response patterns
[AD-A217962] N90-20628

N

NASA PROGRAMS
Microgravity Science and Application Program tasks, 1989 revision
[NASA-TM-4191] N90-20252
NASCOM NETWORK
OMV mission simulator N90-20669
NASTRAN
Static aeroelastic analysis of a three-dimensional generic wing
[NASA-TM-102231] N90-20087
COMGEN: A computer program for generating finite element models of composite materials at the micro level
[NASA-TM-102556] N90-20438
Plan, formulate, and discuss a NASTRAN finite element model of the UH-60A helicopter airframe
[NASA-CR-181975] N90-20439
NATIONS
The essence of spacepower: Important influences on the evolution of national spacepower
[AD-A217498] N90-20781
NATURAL GAS
Phase 1 supplemental development of a kinematic Stirling/Rankine commercial gas-fired heat pump system
[PB90-129974] N90-20483
NATURAL LANGUAGE (COMPUTERS)
Human task animation from performance models and natural language input N90-20678
Artificial Intelligence (AI) Center of Excellence at the University of Pennsylvania
[AD-A217393] N90-20743
NAVIER-STOKES EQUATION
Application of a three-dimensional Navier-Stokes model for a subsonic jet in a crossflow N90-20045
Comparison of 3-D viscous flow computations of Mach 5 inlet with experimental data
[NASA-TM-102518] N90-20090
Numerical simulation methods of incompressible flows and an application to the space shuttle main engine
[NASA-TM-100038] N90-20333
Mass transfer from a sphere in an oscillating flow with zero mean velocity
[NASA-TM-102566] N90-20338
A matrix-free locally-implicit scheme for Navier-Stokes equations
[AD-A218298] N90-20349
NAVIGATION
Estimation of modeled object pose from monocular images
[DE90-001678] N90-20354
Robot navigation research using the HERMIES mobile robot
[DE90-001952] N90-20396
Boundary equations of configuration obstacles for manipulators
[DE90-002101] N90-20745
NEODYMIUM LASERS
Performance of zig-zag slab regenerative ring amplifier laser system
[DE90-006995] N90-20371
Ultra-high brightness laser research at LLNL (Lawrence Livermore National Laboratory)
[DE90-006366] N90-20885
NEURAL NETS
Joint services electronics program
[AD-A217961] N90-20311
Experiments in finding neural network weights
[DE90-007696] N90-20702
Robust planning and control using neural networks
[AD-A217216] N90-20732
Hybrid intelligent perception system: Intelligent perception through combining artificial neural networks and an expert system
[DE90-007483] N90-20748

NEUTRAL BEAMS
Power threshold for neutral beam current drive
[DE90-008348] N90-20822
NICKEL
Structural comparison of nickel electrodes and precursor phases N90-20472
Impedance studies of Ni/Cd and Ni/H2 cells using the cell case as a reference electrode N90-20473
The application of electrochemical impedance spectroscopy for characterizing the degradation of Ni(OH)2/NiOOH electrodes N90-20474
KOH concentration effect on the cycle life of nickel-hydrogen cells. Part 4: Results of failure analyses N90-20475
Advances in lightweight nickel electrode technology N90-20476
An investigation of the dislocation structure of the Ni/Ag phase boundary
[DE90-008428] N90-20876
L shell XANES (X ray Absorption Near Edge Structure) for solid metals: Ti, V, Cr, Fe, Ni, Cu
[DE90-008043] N90-20880
NICKEL ALLOYS
Mechanical properties of pure nickel alloys after long term exposures to LiOH and vacuum at 775 K
[NASA-TM-102403] N90-20181
The stress corrosion performance of diffusion bonded nickel base alloys
[DE90-008130] N90-20199
An introduction to nickel aluminide alloy
[DE90-008565] N90-20207
NICKEL CADMIUM BATTERIES
The importance of batteries in unmanned missions N90-20456
NICKEL HYDROGEN BATTERIES
Space Electrochemical Research and Technology (SERT), 1989
[NASA-CP-3056] N90-20454
Characterization testing of a 40 AHR bipolar nickel-hydrogen battery N90-20463
Multi-mission Ni-H2 battery cells for the 1990's N90-20477
Nickel-hydrogen capacity loss on storage N90-20478
NICOTINIC ACID
Niacin ingested at night causes severe hypotension
[AD-A217896] N90-20624
NIGHT
Niacin ingested at night causes severe hypotension
[AD-A217896] N90-20624
NIMBOSTRATUS CLOUDS
A case study of a quasi-stationary tropical convective line
[AD-A218325] N90-20604
NIMBUS 7 SATELLITE
Cloud types and the tropical Earth radiation budget, revised
[NASA-CR-180475] N90-20582
NIOBIUM
Chemically prepared PZT films doped with niobium
[DE90-006811] N90-20859
NITRAMINE PROPELLANTS
Structure of model gas flames in nitramines
[AD-A217578] N90-20159
NITRATION
The 1-(diorganooxyphosphonyl)-methyl)-2,4- and -2,6-diamido benzenes
[NASA-CASE-ARC-11425-4] N90-20133
NITRIC OXIDE
Computation of hypersonic low density flows with thermochemical nonequilibrium N90-20044
NITROGEN ATOMS
Computation of hypersonic low density flows with thermochemical nonequilibrium N90-20044
NITROGEN COMPOUNDS
Copolymer-like structures of nematic nitroimine dimers
[AD-A217574] N90-20215
NITROGEN IONS
Production rates for electron beams and swarms in nitrogen
[AD-A218145] N90-20817
NOAA SATELLITES
Overview of battery usage in NASA/GSFC LEO and GEOspacecrafts N90-20455
NOBLE METALS
Process for making a noble metal on tin oxide catalyst
[NASA-CASE-LAR-13741-1-SB] N90-20180
NOISE INTENSITY
Lateral attenuation of military aircraft flight noise
[AD-A218041] N90-20799
NOISE REDUCTION
The adaptive line enhancer applied to chirp detection
[DE90-006772] N90-20268
Common-mode rejector for pulse power diagnostics
[AD-A218096] N90-20316
Synopsis of early field test results from the gravity gradiometer survey system N90-20525
Lateral attenuation of military aircraft flight noise
[AD-A218041] N90-20799
NONDESTRUCTIVE TESTS
Summary of the DoD Metal Matrix Composites (MMC) Steering Committee Meeting, hosted by the Institute for Defense Analysis
[AD-A217611] N90-20145
Nondestructive testing of ceramics by acoustic microscopy
[AERE-R-13350] N90-20411
Residual stresses: A review of their measurement and interpretation using x ray diffraction
[AERE-R-13005] N90-20423
Barkhausen noise analysis and ferromagnetic materials
[AD-A217969] N90-20792
NONEQUILIBRIUM IONIZATION
Time-resolved spectroscopy of nonequilibrium ionization in laser-produced plasmas
[DE90-008663] N90-20854
NONLINEAR EQUATIONS
Computing mean responses in nonlinear models
[AD-A217642] N90-20700
Experiments in finding neural network weights
[DE90-007686] N90-20702
NONLINEAR OPTICS
Picosecond nonlinear studies of complex materials using the free electron laser
[AD-A218215] N90-20387
Nonlinear optics in thin films
[AD-A217336] N90-20829
Integrability and chaos in nonlinearly coupled optical beams
[DE90-007540] N90-20834
NONLINEAR SYSTEMS
A learning regulator for the plane longitudinal movement
[ETN-90-95381] N90-20695
Computing mean responses in nonlinear models
[AD-A217642] N90-20700
Robust adaptive nonlinear control under extended matching conditions
[AD-A217684] N90-20744
Observer based compensators for nonlinear systems
[AD-A217426] N90-20760
Nonlinear systems of partial differential equations
[AD-A217581] N90-20761
Techniques for accelerating iterative methods for the solution of mathematical problems
[AD-A218272] N90-20775
Observation of nonlinear reflectivity from InSb surface and optical switching application
[AD-A217184] N90-20826
NONLINEARITY
Amplitude-dependent neutral modes in compressible boundary layer flows
[NASA-TM-102524] N90-20326
Observation of nonlinear reflectivity from InSb surface and optical switching application
[AD-A217184] N90-20826
Nonlinear plasma and beam physics in plasma wake-fields
[DE90-008812] N90-20855
Nonlinear stability in fluid and plasma dynamics
[AD-A217735] N90-20856
NORTH AMERICA
The reduction correction in North America N90-20540
NORTH CAROLINA
Coastal frontogenesis and associated severe weather on 13 March 1986 (GALE IOP 13)
[AD-A217708] N90-20590
NOVA LASER SYSTEM
Improved energy and power balance at Nova targets
[DE90-007260] N90-20372
NUCLEAR EXPLOSIONS
A linear filtering technique for removal of low-frequency noise
[DE90-006183] N90-20296
NUCLEAR FISSION
Populations of excited states and reaction mechanisms in the emission of complex fragments
[DE90-007481] N90-20819
NUCLEAR FUELS
Particle transport in pellet fueled JET (Jet European Torus) plasmas
[DE90-008077] N90-20851
NUCLEAR FUSION
Application of railgun principle to high-velocity hydrogen pellet injection for magnetic fusion reactor refueling
[DE90-008281] N90-20109
Present status of (mu)CF theory
[DE90-007547] N90-20809
Designing an experimenters database using the Nijssen Information Analysis Methodology (NIAM)
[DE90-008548] N90-20907
NUCLEAR MAGNETIC RESONANCE
Copper and oxygen NMR studies on the magnetic properties of YBa2Cu3O(7-y)
[DE90-007889] N90-20863
Metal alkoxides: Models for metal oxides. Alkoxide ligands in early transition metal organometallic chemistry
[DE90-007523] N90-20869
NUCLEAR MEDICINE
Software quality assurance and software safety in the biomed control system
[DE90-008072] N90-20706
NUCLEAR MODELS
Precompound decay models for medium energy nuclear reactions
[DE90-008352] N90-20808
NUCLEAR PHYSICS
Activities report in nuclear physics
[ETN-90-95322] N90-20803
NUCLEAR POWER PLANTS
Technical specifications requirements: Automated reasoning applications
[DE90-008799] N90-20712
NUCLEAR REACTIONS
Activities report in nuclear physics
[ETN-90-95322] N90-20803
Precompound decay models for medium energy nuclear reactions
[DE90-008352] N90-20808
Present status of (mu)CF theory
[DE90-007547] N90-20809
Populations of excited states and reaction mechanisms in the emission of complex fragments
[DE90-007481] N90-20819
NUCLEAR REACTORS
Activities report in nuclear physics
[ETN-90-95322] N90-20803
NUCLEAR SCATTERING
Multiple versus single scattering of terrestrial infrared longwave radiation in an aerosol-laden planetary boundary layer
[AD-A217709] N90-20272
NUCLEAR STRUCTURE
The basis spline method and associated techniques
[DE90-008403] N90-20763
NUCLEAR WARFARE
The thrust and parry of the SIOP (Single Integrated Operational Plan) and SDI
[AD-A217617] N90-20784
NUCLEAR WEAPONS
Assessing the morality of using the space environment as a platform for weapons
[AD-A217348] N90-20780
SDI (Strategic Defense Initiative): Is its future past
[DE90-008016] N90-20785
NUCLEATION
Ceramic oxide thin film formation utilizing biological processes
[DE90-008599] N90-20225
NUMERICAL ANALYSIS
Aerodynamic and kinetic processes in flames
[AD-A217796] N90-20176
Modification and improvement of software for modeling multidimensional reacting fuel flows
[AD-A217789] N90-20235
Micro SAINT programs for numerical methods of integration and differential equations
[AD-A218097] N90-20772
NUMERICAL CONTROL
Multi-tasking computer control of video related equipment N90-20665
NUMERICAL INTEGRATION
Micro SAINT programs for numerical methods of integration and differential equations
[AD-A218097] N90-20772
NUMERICAL WEATHER FORECASTING
Adiabatic and diabatic initialization of the AFGL (Air Force Geophysics Laboratory) global spectral model using dynamic normal mode and nonlinear normal mode methods
[AD-A218120] N90-20595
NUTRITION
Physical performance and carbohydrate consumption in CF commandos during a 5-day field trial
[AD-A217204] N90-20619

O

OBJECT PROGRAMS
Implementation of a hypertext help system for GLAD (Graphics LAnguage for Database)
[AD-A217936] N90-20718
OBLIQUE WINGS
Static aeroelastic analysis of a three-dimensional generic wing
[NASA-TM-102231] N90-20087

OBSERVATORIES
Design and performance analysis of adaptive optical telescopes using laser guide stars
[AD-A218025] N90-20913
OCEAN CURRENTS
A model of the general ocean circulation determined from a joint solution for the Earth's gravity field
N90-20550
Correlation of AVHRR imagery with sub-surface features in California current
[AD-A218184] N90-20607
OCEAN MODELS
A model of the general ocean circulation determined from a joint solution for the Earth's gravity field
N90-20550
OCEAN THERMAL ENERGY CONVERSION
Innovative turbine concepts for open-cycle OTEC (Ocean Thermal Energy Conversion)
[DE90-000315] N90-20493
Perspectives on solar energy and the environment
[DE90-007680] N90-20494
OCEANOGRAPHIC PARAMETERS
An improved model for the Earth's gravity field
N90-20515
US Navy regional climatic study of the Central East Asian coast and associated waters
[AD-A217448] N90-20587
OCEANOGRAPHY
Committee on Geodesy - National Research Council
[AD-A217770] N90-20452
Progress in the Determination of the Earth's Gravity Field
[NASA-CR-185721] N90-20513
Continental shelf processes affecting the oceanography of the South Atlantic Bight
[DE90-008439] N90-20606
OCEANS
Gravitational model improvement at the Goddard Space Flight Center N90-20514
OCULOMETERS
Comparison of oculometer and head-fixed reticle with voice or switch and touch panel for data entry on a generic tactical air combat display
[AD-A217231] N90-20646
OHIO
FFT-local gravimetric geoid computation N90-20536
OHMIC DISSIPATION
Electromagnetic fusion process and position research
N90-20249
ON-LINE SYSTEMS
Onboard shuttle on-line software requirements system: Prototype N90-20658
SES cupola interactive display design environment
N90-20679
Implementation of a hypertext help system for GLAD (Graphics LAnguage for Database)
[AD-A217936] N90-20718
Maintaining bridge-connected and biconnected components on-line
[AD-A215107] N90-20754
OPERATING COSTS
Phase 1 supplemental development of a kinematic Stirling/Rankine commercial gas-fired heat pump system
[PB90-129974] N90-20483
OPERATING SYSTEMS (COMPUTERS)
TAE Plus: Transportable Applications Environment Plus tools for building graphic-oriented applications
N90-20652
Applications of graphics to support a testbed for autonomous space vehicle operations N90-20661
MEASURE: An integrated data-analysis and model identification facility
[NASA-CR-186452] N90-20686
NYU (New York University) ultracomputer
[AD-A217167] N90-20688
The HS6000/20 development system
[LINO-1989-6] N90-20696
VHSIC Hardware Description Language (VHDL) benchmark suite
[AD-A217947] N90-20719
OPERATING TEMPERATURE
A nonintrusive method for measuring the operating temperature of a solenoid-operated valve
[DE90-007576] N90-20355
Proton responses on MOS (Metal-Oxide-Semiconductor) electronics operating at cryogenic temperatures
[AD-A217622] N90-20868
OPERATIONAL AMPLIFIERS
Transient radiation hardened CMOS (Complementary Metal Oxide Semiconductor) operational amplifiers
[AD-A217972] N90-20313
OPERATIONS RESEARCH
Research in reliability, availability and maintainability for complex failure systems
[AD-A217744] N90-20415
An integrative research review of the relationship between technology and structure: A meta-analytic synthesis
[AD-A218115] N90-20903
OPERATOR PERFORMANCE
Brain activity during tactical decision-making. Part 3: Relationships between probe-evoked potentials, simulation performance, and on-job performance
[AD-A217207] N90-20638
OPERATORS (MATHEMATICS)
Magnetostatic boundary-value problems in the incomplete-nonlinear formulation and methods of their solution
[DE90-615185] N90-20767
OPHTHALMOLOGY
Laser-produced plasmas in medicine
[DE90-007623] N90-20849
OPTICAL BISTABILITY
Optical Bistability, 1988
[AD-A217681] N90-20832
OPTICAL COMMUNICATION
A space-based optical communication system utilizing fiber optics
[AD-A217333] N90-20828
GaAs traveling-wave optical modulators using modulated coplanar electrodes with periodic cross-tie overlays
[AD-A217731] N90-20835
Fundamental studies of photon statistics
[AD-A217825] N90-20836
OPTICAL COMPUTERS
Adaptive associative-processing optical computing architectures
[AD-D014317] N90-20685
OPTICAL COUPLING
Investigation of the technological effects on the coupling behavior of parallel GaAlAs rib waveguide
[ETN-90-95323] N90-20825
OPTICAL DATA PROCESSING
Adaptive associative-processing optical computing architectures
[AD-D014317] N90-20685
OPTICAL DENSITY
The receiving system of a dual dye lidar to study molecular and aerosol densities at the base of the stratosphere
[AD-A218286] N90-20581
OPTICAL EQUIPMENT
Design and test of a compact optics system for the pool boiling experiment
[NASA-TM-102530] N90-20253
Simple reflection holography
[DE90-008309] N90-20359
Robotic mobility system: Road following algorithms
[AD-A218107] N90-20748
A space-based optical communication system utilizing fiber optics
[AD-A217333] N90-20828
Velocity matched optical transmitter
[AD-A217413] N90-20830
CCST (Center for Compound Semiconductor Technology) research briefs
[DE90-007782] N90-20874
OPTICAL MEASUREMENT
Correlation of atmospheric optical turbulence and meteorological measurements
[AD-A218019] N90-20576
An ellipsometric measurement of optical properties for InP surfaces
[AD-A217185] N90-20827
OPTICAL MEASURING INSTRUMENTS
Design and performance analysis of adaptive optical telescopes using laser guide stars
[AD-A218025] N90-20913
OPTICAL POLARIZATION
Polymer liquid crystals with side chain discogens
[AD-A218013] N90-20228
OPTICAL PROPERTIES
Performance of zig-zag slab regenerative ring amplifier laser system
[DE90-006995] N90-20371
Picosecond nonlinear studies of complex materials using the free electron laser
[AD-A218215] N90-20387
Theoretical and experimental study of solid phase miscibility gaps in III/V quaternary alloys
[DE90-008430] N90-20877
OPTICAL RADAR
Multi-dimensional LADAR tracking and adaptive grasping for spaceborne assembly of SDI (Strategic Defense Initiative) platforms
[AD-A218236] N90-20279
The receiving system of a dual dye lidar to study molecular and aerosol densities at the base of the stratosphere
[AD-A218286] N90-20581
Design and performance analysis of adaptive optical telescopes using laser guide stars
[AD-A218025] N90-20913
OPTICAL REFLECTION
An ellipsometric measurement of optical properties for InP surfaces
[AD-A217185] N90-20827
OPTICAL SWITCHING
Observation of nonlinear reflectivity from InSb surface and optical switching application
[AD-A217184] N90-20826
OPTICAL TRACKING
Multi-dimensional LADAR tracking and adaptive grasping for spaceborne assembly of SDI (Strategic Defense Initiative) platforms
[AD-A218236] N90-20279
OPTICAL WAVEGUIDES
Investigation of the technological effects on the coupling behavior of parallel GaAlAs rib waveguide
[ETN-90-95323] N90-20825
Nonlinear optics in thin films
[AD-A217336] N90-20829
Velocity matched optical transmitter
[AD-A217413] N90-20830
OPTIMAL CONTROL
Trajectory optimization in the presence of constraints
[AD-A218271] N90-20104
OPTIMIZATION
Design and performance of a multi-stage cylindrical reconnection launcher
[DE90-007820] N90-20108
Composite laminate tailoring with probabilistic constraints and loads
[NASA-TM-102515] N90-20138
Optimization of fracture resistance in composites
[AD-A217431] N90-20144
Optimization of laminated composite plates
[AD-A217621] N90-20146
On optimal distributed decision architectures in a hypothesis testing environment
[AD-A217824] N90-20274
Optimization of digital filters for a short-scan interferometer
[AD-A217997] N90-20315
Common-mode rejector for pulse power diagnostics
[AD-A218096] N90-20316
Multi-mission Ni-H2 battery cells for the 1990's
N90-20477
Phase 1 supplemental development of a kinematic Stirling/Rankine commercial gas-fired heat pump system
[PB90-129974] N90-20483
A unified approach to the synthesis of fully testable sequential machines
[AD-A217120] N90-20687
(DURIP) Two-Processor Alliant FX/4 System
[AD-A217810] N90-20692
Design decision making with multiple interacting criteria and varying relative weights
[AD-A218027] N90-20721
Irredundant sequential machines via optimal logic synthesis
[AD-A217119] N90-20742
Exact algorithms for output encoding, state assignment and four-level Boolean minimization
[AD-A217121] N90-20756
Chemical beam epitaxy of ZnSe
[AD-A217375] N90-20866
Study of possible solar heating effects on thermosonde probes: Error analysis
[AD-A218116] N90-20917
ORBITAL ASSEMBLY
Multi-dimensional LADAR tracking and adaptive grasping for spaceborne assembly of SDI (Strategic Defense Initiative) platforms
[AD-A218236] N90-20279
ORBITAL MANEUVERING VEHICLES
OMV mission simulator N90-20669
The Orbital Maneuvering Vehicle Training Facility visual system concept N90-20684
ORBITAL MECHANICS
Geographically correlated orbit error N90-20551
Distributed earth model/orbiter simulation N90-20671
ORBITAL RENDEZVOUS
Optimal, impulsive, time-fixed orbital rendezvous and interception with path constraints N90-20102
ORBITS
M51's spiral structure
[DE90-007624] N90-20916
ORDER-DISORDER TRANSFORMATIONS
Ionic disorder in crystals at high temperatures with emphasis on fluorites
[AERE-R-13544] N90-20862
The geometry of disorder: Report 1987 to 1990
[DE90-008250] N90-20882

ORGANIC COMPOUNDS
Studies of the structure and properties of organic monolayers, multilayers and superlattices
[DE90-008330] N90-20129
Developments in solar photocatalysis for destruction of organics in water
[DE90-007685] N90-20162
Ring expansion and equilibration in organophosphazenes, and the relationship to polymerization
[AD-A218234] N90-20230
ORGANIZATIONS
An integrative research review of the relationship between technology and structure: A meta-analytic synthesis
[AD-A218115] N90-20903
ORGANOMETALLIC COMPOUNDS
High power semiconductor laser arrays by metalorganic chemical vapor deposition N90-20363
Metal alkoxides: Models for metal oxides. Alkoxide ligands in early transition metal organometallic chemistry
[DE90-007523] N90-20869
ORTHOTROPIC PLATES
Through-thickness strain response of thick composites in compression
[AD-A217233] N90-20141
Perturbation solutions in D* for buckling, vibration, and static loading of specially orthotropic plates N90-20419
Postbuckling behavior of laminated specially orthotropic plates by affine transformation N90-20420
OSCILLATING FLOW
Mass transfer from a sphere in an oscillating flow with zero mean velocity
[NASA-TM-102566] N90-20338
OSCILLATIONS
Numerical simulations of supersonic flow through oscillating cascade sections
[NASA-TM-103100] N90-20051
A video-based experimental investigation of wing rock
[AD-A218244] N90-20075
OXIDATION
Determination of fundamental thermodynamic properties of constituent materials and performance screening of candidate systems
[AD-A218089] N90-20153
Structural comparison of nickel electrodes and precursor phases N90-20472
OXIDATION RESISTANCE
Short wavelength laser/materials interactions
[AD-A218015] N90-20386
OXIDATION-REDUCTION REACTIONS
Electrochemical phase diagrams for aqueous redox systems
[AD-A217168] N90-20157
Ligand-centered electron-transfer redox processes for manganese, iron, and cobalt complexes in relation to selected catalytic systems
[AD-A217957] N90-20177
All-solid-state thin-film rechargeable lithium batteries using solid redox polymerization electrodes
[DE90-008665] N90-20306
OXIDE FILMS
Ceramic oxide thin film formation utilizing biological processes
[DE90-008599] N90-20225
OXIDES
Spallation of oxide scales from 20 percent Cr/25 percent Ni/Nb stainless steel
[AERE-R-13464] N90-20189
High temperature chemistry of oxide superconductors
[DE90-007821] N90-20875
OXYGEN
Oxygen concentrations on surfaces of carbon fibers
[AD-A217724] N90-20152
A technical and economic evaluation of oxygen-enriched combustion in diesel engines using water-emulsified fuels
[DE90-008095] N90-20394
Oxygen electrodes for rechargeable alkaline fuel cells-II N90-20469
Copper and oxygen NMR studies on the magnetic properties of YBa2Cu3O(7-y)
[DE90-007889] N90-20863
OXYGEN ATOMS
Computation of hypersonic low density flows with thermochemical nonequilibrium N90-20044
OXYGEN IONS
Thermoelectric conversion with ion conductors
[AD-A217822] N90-20497
OXYGEN ISOTOPES
Isotope exchange in oxide-containing catalyst
[NASA-CASE-LAR-13542-2-SB] N90-20154
OZONE
Air poilution-caused changes in photosynthesis: Effects on plant growth and rhizosphere functions
[DE90-007184] N90-20501

P

P-I-N JUNCTIONS
An electron-beam controlled semiconductor switch
[AD-A217181] N90-20288
PACIFIC OCEAN
A cloud climatology for the North Pacific area centered at Shemya, Alaska
[AD-A217334] N90-20585
Forecasting 24 and 48 hour intensity changes, for northwestern Pacific tropical cyclones, using satellite imagery
[AD-A218174] N90-20597
PAIN
The reliability of clinical measurements of forward bending obtained by the use of the modified fingertip-to-floor method
[AD-A217907] N90-20627
PAIR PRODUCTION
Studies of high energy phenomena using muons
[DE90-008272] N90-20820
PANEL METHOD (FLUID DYNAMICS)
Experimental and theoretical aerodynamic characteristics of a high-lift semispan wing model
[NASA-TP-2990] N90-20046
PANELS
Reusable high-temperature heat pipes and heat pipe panels
[NASA-CASE-LAR-13761-1] N90-20323
Comparison of oculometer and head-fixed reticle with voice or switch and touch panel for data entry on a generic tactical air combat display
[AD-A217231] N90-20646
Localization and delocalization in periodic one-dimensional dynamic systems
[AD-A217939] N90-20797
PARACHUTING INJURY
Parachute opening shocks during high speed ejections: Normalization N90-20056
PARALLEL COMPUTERS
A time stepping algorithm for parallel computers
[DE90-008163] N90-20738
PARALLEL PROCESSING (COMPUTERS)
Joint services electronics program
[AD-A217961] N90-20311
Parallel algorithms in the finite element approximation of flow problems
[AD-A217729] N90-20341
Supercomputer environments
[AD-A217682] N90-20689
A real-time parallel pipelined data-flow image-processing system
[DE90-008324] N90-20691
Joint Japanese-American Workshop on Future Trends in Logic Programming
[DE90-008343] N90-20709
Almost-optimum parallel speed-ups of algorithms for bipartite matching and related problems
[AD-A215111] N90-20728
Advanced parallel systems
[AD-A217175] N90-20731
Asynchronous design for parallel processing architectures
[AD-A217421] N90-20734
Design of a simulation interface for a parellel computing environment
[DE90-008497] N90-20737
A time stepping algorithm for parallel computers
[DE90-008163] N90-20738
A model and implementation of multigrid for massively parallel computers
[DE90-008165] N90-20739
Implementation of midcourse tracking and correlation on massively parallel computers
[DE90-008166] N90-20740
A parallel architecture for real-time simulation
[AD-A218321] N90-20741
Artificial Intelligence (AI) Center of Excellence at the University of Pennsylvania
[AD-A217393] N90-20743
Implementation of a hypercube database system
[DE90-008440] N90-20905
PARALLEL PROGRAMMING
NYU (New York University) ultracomputer
[AD-A217167] N90-20688
PARAMETER IDENTIFICATION
Gravity field determination and error assessment techniques N90-20517
An approximation theory for the identification of linear thermoelastic systems
[NASA-CR-182015] N90-20764
PARTIAL DIFFERENTIAL EQUATIONS
A time stepping algorithm for parallel computers
[DE90-008163] N90-20738
A model and implementation of multigrid for massively parallel computers
[DE90-008165] N90-20739
Nonlinear systems of partial differential equations
[AD-A217581] N90-20761
PARTICLE ACCELERATORS
Designing an experimenters database using the Nijssen Information Analysis Methodology (NIAM)
[DE90-008548] N90-20907
PARTICLE BEAMS
Designing an experimenters database using the Nijssen Information Analysis Methodology (NIAM)
[DE90-008548] N90-20907
PARTICLE COLLISIONS
Energy transfer between electrons and ions in collision cascades in solids
[AERE-R-13662] N90-20801
Termolecular associations of ions in gases, recombination and electron-atom collisions
[AD-A217678] N90-20805
PARTICLE IN CELL TECHNIQUE
The inverse triax x ray diode: An alternate reduced-endpoint-energy bremsstrahlung source
[DE90-006366] N90-20285
PARTICLE PRODUCTION
Theoretical investigations in elementary particle physics
[DE90-007178] N90-20802
PARTICLE SIZE DISTRIBUTION
Experimental and theoretical studies of light scattering by small particles
[AD-A217432] N90-20831
PARTICLE THEORY
Particle transport in pellet fueled JET (Jet European Torus) plasmas
[DE90-008077] N90-20851
PARTICLES
Enhancement of mass transfer to a rotating cylinder electrode by inert particles suspended in the electrolyte
[DE90-008054] N90-20165
PARTICULATES
Hydrodynamic interactions and transport coefficients in a suspension of spherical particles
[DE90-008301] N90-20336
Overview of the methodologies used to compile large scale emissions inventories
[DE90-008518] N90-20509
PATTERN RECOGNITION
The role of chaos in hemispheric process and attention
[AD-A217674] N90-20639
The boundaries of hemispheric processing in visual pattern recognition
[AD-A217675] N90-20640
Lateral asymmetry in pattern recognition: Understanding the effects of familiarity, distinction, and perspective change
[AD-A217739] N90-20641
Parts of recognition
[AD-A217694] N90-20714
Texture segmentation using localized spatial filtering
[AD-A218064] N90-20722
Hybrid intelligent perception system: Intelligent perception through combining artificial neural networks and an expert system
[DE90-007483] N90-20746
PATTERN REGISTRATION
Stereo feature matching in disparity space
[AD-A218170] N90-20751
PAYLOAD STATIONS
Space station Simulation Computer System (SCS) study for NASA/MSFC. Volume 4: Conceptual design report
[NASA-CR-183843] N90-20116
Space station Simulation Computer System (SCS) study for NASA/MSFC. Volume 5: Study analysis report
[NASA-CR-183844] N90-20117
PAYLOADS
Space station Simulation Computer System (SCS) study for NASA/MSFC. Volume 2: Concept document
[NASA-CR-183841] N90-20114
Space station Simulation Computer System (SCS) study for NASA/MSFC. Volume 3: Refined conceptual design report
[NASA-CR-183842] N90-20115
Space station Simulation Computer System (SCS) study for NASA/MSFC. Volume 4: Conceptual design report
[NASA-CR-183843] N90-20116
Space station Simulation Computer System (SCS) study for NASA/MSFC. Volume 5: Study analysis report
[NASA-CR-183844] N90-20117
Space station Simulation Computer System (SCS) study for NASA/MSFC. Volume 6: Study issues report
[NASA-CR-183845] N90-20118

PCM TELEMETRY
PC-based PCM telemetry data reduction system software
[DE90-000317] N90-20111
PELLETS
Application of railgun principle to high-velocity hydrogen pellet injection for magnetic fusion reactor refueling
[DE90-008281] N90-20109
PENETRATION
Focused ion beam implantation
[AD-A217987] N90-20894
PEPTIDES
The effects of high intensity cycle exercise on sympatho-adrenal-medullary response patterns
[AD-A217962] N90-20628
The effects of graded exercise at sea level on plasma proenkephalin peptide F and catecholamine responses
[AD-A218195] N90-20633
PERCEPTUAL ERRORS
Aiding the decision maker: Perceptual and cognitive issues at the human-machine interface
[AD-A217862] N90-20648
PERCOLATION
The viscoelasticity of curing thermosets
[DE90-006535] N90-20221
PERFORATED PLATES
Innovative design of composite structures: The use of curvilinear fiber format to improve buckling resistance of composite plates with central circular holes
[NASA-CR-186454] N90-20135
PERFORMANCE PREDICTION
Using transonic small disturbance theory for predicting the aeroelastic stability of a flexible wind-tunnel model
[NASA-TM-102617] N90-20047
Airplane takeoff and landing performance monitoring system
[NASA-CASE-LAR-13734-1-CU] N90-20096
Model development in viscoplastic ratchetting
[NASA-TM-102509] N90-20431
PERFORMANCE TESTS
The USAF Advanced Dynamic Anthropomorphic Manikin (ADAM) N90-20062
In-line wear monitor
[AD-A217799] N90-20091
Flight termination system battery guidelines
[AD-A217310] N90-20092
ARDEC (Armament Research, Development and Engineering Center) electric gun in-house test program
[AD-A217337] N90-20105
Design and performance of a multi-stage cylindrical reconnection launcher
[DE90-007820] N90-20108
Characterization testing of a 40 AHR bipolar nickel-hydrogen battery N90-20463
Sodium-sulfur battery flight experiment definition study N90-20479
Advanced on-site power plant development technology program
[DE90-000443] N90-20484
First year's results and field experience with the latest JILA absolute gravimeter N90-20529
PERIPHERAL VISION
Detection acuity in the peripheral retina
[AD-A218183] N90-20632
PERMANENT MAGNETS
Magnetic hardening studies and novel techniques for preparation of high performance magnets
[AD-A217737] N90-20790
PERMITTIVITY
A study of physical properties of ODPA-p-PDA polyimide films
[NASA-TM-102625] N90-20137
PEROVSKITES
Chemically prepared PZT films doped with niobium
[DE90-006811] N90-20859
PERSONAL COMPUTERS
RenderMan design principles N90-20653
Multi-tasking computer control of video related equipment N90-20665
PERSONALITY
Effects of dexamethasone and high terrestrial altitude on cognitive performance and affect
[AD-A217897] N90-20625
PERSONNEL
Physical performance and carbohydrate consumption in CF commandos during a 5-day field trial
[AD-A217204] N90-20619
PERSONNEL MANAGEMENT
Middle management of research
[NASA-TM-102417] N90-20901
PERSPIRATION
The effect of moisture absorption in clothing on the human heat balance
[AD-A217899] N90-20626
Hydration effects on human physiology and exercise-heat performance
[AD-A217969] N90-20629
PERTURBATION
Aiming control: Theory and applications to dynamic control of space structures
[AD-A217877] N90-20123
PERTURBATION THEORY
Using transonic small disturbance theory for predicting the aeroelastic stability of a flexible wind-tunnel model
[NASA-TM-102617] N90-20047
Numerical simulations of supersonic flow through oscillating cascade sections
[NASA-TM-103100] N90-20051
Electronic structure, alloy phase stability, and phase diagrams
[DE90-008306] N90-20203
Measurement of the stimulated thermal Rayleigh scattering instability
[DE90-007849] N90-20376
Perturbation solutions in D* for buckling, vibration, and static loading of specially orthotropic plates N90-20419
Postbuckling behavior of laminated specially orthotropic plates by affine transformation N90-20420
PHARMACOLOGY
The United States Air Force School of Aerospace Medicine: Special report
[AD-A217740] N90-20622
PHASE DIAGRAMS
Electrochemical phase diagrams for aqueous redox systems
[AD-A217168] N90-20157
Electronic structure, alloy phase stability, and phase diagrams
[DE90-008306] N90-20203
PHASE LOCKED SYSTEMS
Experimental investigation of the mechanisms underlying vortex kinematics in unsteady separated flows
[AD-A217889] N90-20346
PHASE SHIFT
Doppler radar with multiphase modulation of transmitted and reflected signal
[NASA-CASE-MSC-18808-1] N90-20280
PHASE SHIFT KEYING
Advanced modulation technology development for earth station demodulator applications. Coded modulation system development
[NASA-CR-185149] N90-20270
PHASE TRANSFORMATIONS
Studies of the structure and properties of organic monolayers, multilayers and superlattices
[DE90-008330] N90-20129
Copolymer-like structures of nematic nitroimine dimers
[AD-A217574] N90-20215
PHASED ARRAYS
Performance of a 300 Mbps 1:16 serial/parallel optoelectronic receiver module
[NASA-TM-103110] N90-20302
PHOSPHAZENE
Synthesis of new polyphosphazene elastomers
[AD-A217585] N90-20216
Ring expansion and equilibration in organophosphazenes, and the relationship to polymerization
[AD-A218234] N90-20230
PHOSPHORUS
The 1-(diorganooxyphosphonyl)-methyl)-2,4- and -2,6-diamido benzenes
[NASA-CASE-ARC-11425-4] N90-20133
Electron beam induced damage in PECVD Si3N4 and SiO2 films on InP
[NASA-TM-102544] N90-20393
PHOTOCHEMICAL REACTIONS
Biological applications and effects of optical masers
[AD-A217910] N90-20385
Use of environmental monitoring data in evaluation of atmospheric modeling results
[DE90-008607] N90-20510
Molecular dynamics and spectroscopy at gas-solid interfaces
[AD-A217743] N90-20813
PHOTODIODES
NRL hybrid reliability. Physics of failure initial study
[AD-A217986] N90-20893
PHOTODISSOCIATION
DURIP FTIR studies of solid state reaction dynamics
[AD-A217713] N90-20174
DURIP theoretical/experimental investigations of highly energetic dication species
[AD-A217771] N90-20383
Electronically metastable molecules of high symmetry
[AD-A217768] N90-20814
PHOTOELASTICITY
Stress field near crack tip: An experimental evaluation of the three dimensional variation
[AD-A217878] N90-20441
PHOTOELECTRIC EMISSION
Research investigation directed toward extending the useful range of the electromagnetic spectrum
[AD-A217460] N90-20267
Surface-plasmon enhanced nonlinear photoelectric emission from thin silver films
[DE90-007676] N90-20807
PHOTOELECTRON SPECTROSCOPY
Infrared and X ray photoelectron spectroscopy studies of the polyimide/metal interface
[AD-A218249] N90-20179
PHOTOGRAMMETRY
Committee on Geodesy - National Research Council
[AD-A217770] N90-20452
PHOTOGRAPHY
Spacecraft optical contamination environment
[AD-A218088] N90-20838
PHOTOINTERPRETATION
LANDSAT-5 data in the study of wheat and bean crops
[INPE-4746-RPE/580] N90-20444
A system for analysis and interpretation of lineaments in remote sensing images
[INPE-4893-PRE/1494] N90-20565
PHOTOIONIZATION
DURIP FTIR studies of solid state reaction dynamics
[AD-A217713] N90-20174
Atmospheric chemiluminescence: COCHISE and FACELIF experiments
[AD-A218121] N90-20578
Electronically metastable molecules of high symmetry
[AD-A217768] N90-20814
PHOTOMETERS
Mercuric iodide room temperature gamma-ray detectors
[NASA-TM-103318] N90-20357
PHOTONICS
Optical Bistability, 1988
[AD-A217681] N90-20632
PHOTONS
Research investigation directed toward extending the useful range of the electromagnetic spectrum
[AD-A217460] N90-20267
Determinations of photon spectra
[AD-A218003] N90-20816
Fundamental studies of photon statistics
[AD-A217825] N90-20836
PHOTOSYNTHESIS
Air pollution-caused changes in photosynthesis: Effects on plant growth and rhizosphere functions
[DE90-007184] N90-20501
Carbon and hydrogen metabolism of green algae in light and dark
[DE90-008648] N90-20612
PHOTOVOLTAIC CELLS
Investigation of a photovoltaic/battery hybrid system for powering the high arctic data communications system
[AD-A218353] N90-20319
PHOTOVOLTAIC CONVERSION
Photovoltaic energy
[DE89-009473] N90-20486
PHOTOVOLTAIC EFFECT
CuInSe2 and CdTe: Scale-up for manufacturing
[DE89-009503] N90-20489
PHYSICAL EXERCISE
The reliability of clinical measurements of forward bending obtained by the use of the modified fingertip-to-floor method
[AD-A217907] N90-20627
The effects of high intensity cycle exercise on sympatho-adrenal-medullary response patterns
[AD-A217962] N90-20628
Hydration effects on human physiology and exercise-heat performance
[AD-A217969] N90-20629
The effects of graded exercise at sea level on plasma proenkephalin peptide F and catecholamine responses
[AD-A218195] N90-20633
PHYSIOLOGICAL EFFECTS
Windblast protection for advanced ejection seats N90-20063
PHYSIOLOGICAL RESPONSES
Influence of theobromine on heat production and body temperatures in cold-exposed humans: A preliminary report
[AD-A217203] N90-20618
A comparison of the mechanisms of cold- and microgravity-induced fluid loss
[AD-A218098] N90-20631
Effective calibration of heat flux transducers for experimental use
[AD-A218262] N90-20636

PICOSECOND PULSES
Picosecond Laser Facility
[AD-A217784] N90-20384
Picosecond nonlinear studies of complex materials using the free electron laser
[AD-A218215] N90-20387
PILOT PERFORMANCE
A learning regulator for the plane longitudinal movement
[ETN-90-95381] N90-20695
PINCH EFFECT
Enhanced pinch effect due to electrostatic potential
[DE90-007088] N90-20844
New methods in plasma simulation
[DE90-007507] N90-20847
PIPELINING (COMPUTERS)
A real-time parallel pipelined data-flow image-processing system
[DE90-008324] N90-20691
PIPES (TUBES)
Determination of flow-regime boundaries for cohesive particles
[DE90-007425] N90-20332
PITTING
Stochastic approach to the initiation of pitting corrosion
[AERE-R-13348] N90-20190
PLANAR STRUCTURES
Experimental investigations on channelized coplanar waveguide
[NASA-TM-102494] N90-20286
Dual cathode system for electron beam instruments
[NASA-CASE-NPO-16878-1-CU] N90-20351
PLANETARY BOUNDARY LAYER
Multiple versus single scattering of terrestrial infrared longwave radiation in an aerosol-laden planetary boundary layer
[AD-A217709] N90-20272
PLANETARY ORBITS
Use of random Martian atmosphere to evaluate potential entry guidance schemes
[NASA-TM-102606] N90-20122
PLANNING
Experimental validation of extended image reconstruction using bispectral speckle interferometry
[DE90-008545] N90-20171
Swing-free movement of simply suspended objects employing parameter estimation
[DE90-002238] N90-20398
Controlling Summer Heat Islands: Proceedings
[DE90-008075] N90-20508
Robust planning and control using neural networks
[AD-A217216] N90-20732
PLANT STRESS
Air pollution-caused changes in photosynthesis: Effects on plant growth and rhizosphere functions
[DE90-007184] N90-20501
PLANTING
Relationship of radiometric field measurements of wheat in the Assis-Safra region, 1988
[INPE-4949-RPE/598] N90-20443
PLASMA CONTROL
Improved energy and power balance at Nova targets
[DE90-007260] N90-20372
Power threshold for neutral beam current drive
[DE90-008348] N90-20822
The impedance of energy efficiency of a coaxial magnetized plasma source used for spheromak formation and sustainment
[DE90-003220] N90-20841
The ANU (Australian National University) Heliac Program
[DE90-006620] N90-20843
Difference in electron thermal diffusivity and profile between interior and exterior of TFTR L-mode plasmas
[DE90-007479] N90-20846
High elongation plasmas
[DE90-007575] N90-20848
PLASMA DIAGNOSTICS
Particle transport in pellet fueled JET (Jet European Torus) plasmas
[DE90-008077] N90-20851
Time-resolved spectroscopy of nonequilibrium ionization in laser-produced plasmas
[DE90-008663] N90-20854
PLASMA DYNAMICS
Nonlinear stability in fluid and plasma dynamics
[AD-A217735] N90-20856
PLASMA HEATING
Computation of coupling elements between waveguides and modes for large launching structures
[IPPCZ-290] N90-20842
PLASMA INTERACTIONS
USU center of excellence in theory and analysis of the geo-plasma environment
[AD-A217736] N90-20101
PLASMA PINCH
Nonlinear plasma and beam physics in plasma wake-fields
[DE90-008812] N90-20855
PLASMA RADIATION
An electron-beam controlled semiconductor switch
[AD-A217181] N90-20288
PLASMA TURBULENCE
Spontaneous magnetic reconnection in a turbulent plasma N90-20840
PLASMA WAVES
Nonlinear plasma and beam physics in plasma wake-fields
[DE90-008812] N90-20855
PLASMA-ELECTROMAGNETIC INTERACTION
Computation of coupling elements between waveguides and modes for large launching structures
[IPPCZ-290] N90-20842
PLASMAS (PHYSICS)
Electron beam induced damage in PECVD Si3N4 and SiO2 films on InP
[NASA-TM-102544] N90-20393
Solar cyclical trend study of the mid-latitude, quiet-time, meridional, neutral winds at winter solstice conditions
[AD-A217398] N90-20568
The impedance of energy efficiency of a coaxial magnetized plasma source used for spheromak formation and sustainment
[DE90-003220] N90-20841
New methods in plasma simulation
[DE90-007507] N90-20847
High elongation plasmas
[DE90-007575] N90-20848
PLASMASPHERE
USU center of excellence in theory and analysis of the geo-plasma environment
[AD-A217736] N90-20101
PLASMONS
Surface-plasmon enhanced nonlinear photoelectric emission from thin silver films
[DE90-007676] N90-20807
PLASTICS
Assessment of biobased materials
[DE90-000300] N90-20220
PLATES
Computer simulations and experiments to study the fracture of rods by flying plates
[DE90-008308] N90-20437
PLATES (STRUCTURAL MEMBERS)
Postbuckling behavior of laminated specially orthotropic plates by affine transformation N90-20420
PLATINUM
Recent advances in solid polymer electrolyte fuel cell technology with low platinum loading electrodes N90-20465
PLUMES
Y1Ba2Cu3O(7-x) laser-ablation plume dynamics measurement by nanosecond response ion probe: Comparison with optical measurements
[DE90-007658] N90-20375
POINT DEFECTS
The stress-driven redistribution of point defects in the vicinity of crack-like singularities
[AERE-R-12898] N90-20424
Ionic disorder in crystals at high temperatures with emphasis on fluorites
[AERE-R-13544] N90-20862
POINTING CONTROL SYSTEMS
Aiming control: Theory and applications to dynamic control of space structures
[AD-A217877] N90-20123
POISSON EQUATION
Experimental validation of extended image reconstruction using bispectral speckle interferometry
[DE90-008545] N90-20171
The reduction correction in North America N90-20540
POISSON RATIO
Postbuckling behavior of laminated specially orthotropic plates by affine transformation N90-20420
POLAR CAPS
Airfields on antarctic glacier ice
[AD-A217638] N90-20097
POLARIMETRY
Algorithms for optimal processing of polarimetric radar data
[AD-A217330] N90-20758
POLARISCOPES
Stress field near crack tip: An experimental evaluation of the three dimensional variation
[AD-A217878] N90-20441
POLARITY
The role of polarity on the stability of graphitic compounds
[DE90-006528] N90-20218
POLISHING
Stochastic approach to the initiation of pitting corrosion
[AERE-R-13348] N90-20190
Crystal preparation at LBL, 1976 to 1986
[DE90-007754] N90-20871
POLITICS
The essence of spacepower: Important influences on the evolution of national spacepower
[AD-A217498] N90-20781
POLLUTION MONITORING
Development of a laser fluorosensor for the aircraft supported analysis of maritime toxic agents loads: Definition phase
[ETN-90-95320] N90-20499
POLYATOMIC MOLECULES
DURIP FTIR studies of solid state reaction dynamics
[AD-A217713] N90-20174
Laser enhanced chemical reactions
[DE90-008273] N90-20377
Picosecond laser study of polyatomic molecules
[DE90-008647] N90-20381
Polyatomic reaction dynamics
[DE90-008868] N90-20811
Electronically metastable molecules of high symmetry
[AD-A217768] N90-20814
POLYBUTADIENE
CO2 diffusion and solubility in a Polystyrene/Polybutadiene block copolymer with highly oriented lamellar morphology
[AD-A217165] N90-20211
POLYCRYSTALS
Electron beam generation by electron bombardment induced cathode emission
[AD-A218203] N90-20318
Chemically prepared PZT films doped with niobium
[DE90-006811] N90-20859
Synthesis and properties of polycrystalline Tl2Ba2CaCu2O(x) and Tl2Ba2Ca2Cu3O(x)
[DE90-007528] N90-20887
POLYETHYLENES
Research and development on enhanced degradable plastics
[AD-A217180] N90-20212
POLYGONS
Binary space partitioning trees and their uses N90-20657
Simplified linear-time Jordan sorting and polygon clipping
[AD-A215110] N90-20693
POLYIMIDE RESINS
Infrared and X ray photoelectron spectroscopy studies of the polyimide/metal interface
[AD-A218249] N90-20179
POLYIMIDES
A study of physical properties of ODPA-p-PDA polyimide films
[NASA-TM-102625] N90-20137
POLYMER CHEMISTRY
Materials Science Programs, fiscal year 1989
[DE90-008169] N90-20131
Synthesis of new polyphosphazene elastomers
[AD-A217585] N90-20216
POLYMERIC FILMS
Infrared and X ray photoelectron spectroscopy studies of the polyimide/metal interface
[AD-A218249] N90-20179
Sol-gel derived polytitanosiloxane coatings
[DE90-004186] N90-20210
CO2 diffusion and solubility in a Polystyrene/Polybutadiene block copolymer with highly oriented lamellar morphology
[AD-A217165] N90-20211
Research and development on enhanced degradable plastics
[AD-A217180] N90-20212
Tensile film clamps and mounting block for the rheovibron and autovibron viscoelastometer
[NASA-CASE-LAR-13696-1] N90-20409
Molecular organization and electrical properties of mixed Langmuir-Blodgett multilayer thin films of polypyrrole
[DE90-007627] N90-20870
POLYMERIZATION
The 1-(diorganooxyphosphonyl)-methyl)-2,4- and -2,6-diamido benzenes
[NASA-CASE-ARC-11425-4] N90-20133
Rigid rod molecules as liquid crystal thermosets
[AD-A217573] N90-20158
Synthesis of new polyphosphazene elastomers
[AD-A217585] N90-20216
The viscoelasticity of curing thermosets
[DE90-006535] N90-20221
Ring expansion and equilibration in organophosphazenes, and the relationship to polymerization
[AD-A218234] N90-20230

Novel electrodes for advanced energy storage systems
[DE90-008667] N90-20496

POLYNOMIALS
Component count and preliminary assembly considerations for large space truss structures
[NASA-TM-102604] N90-20121
Cell averaging Chebyshev methods for hyperbolic problems
[NASA-CR-182028] N90-20768
Euler's theorem for polynomials
[AD-A218148] N90-20774
Techniques for accelerating iterative methods for the solution of mathematical problems
[AD-A218272] N90-20775

POLYSTYRENE
CO2 diffusion and solubility in a Polystyrene/Polybutadiene block copolymer with highly orientsd lamellar morphology
[AD-A217165] N90-20211

PONDS
Design and operation of an outdoor microalgae test facility
[DE89-009493] N90-20608

POPULATIONS
Populations of excited states and reaction mechanisms in the emission of complex fragments
[DE90-007481] N90-20819

POROUS MATERIALS
An experimental investigation of the thermal conductivity of porous adsorbents
[AD-A217854] N90-20899

POSITION (LOCATION)
Estimation of modeled object pose from monocular images
[DE90-001678] N90-20354
Localization and delocalization in periodic one-dimensional dynamic systems
[AD-A217939] N90-20797

POSITION ERRORS
Location recognition using stereo vision
[AD-A218218] N90-20752
Mark 3 interferometer
[AD-A217188] N90-20912

POSITIONING DEVICES (MACHINERY)
Gripping device
[NASA-CASE-MSC-21365-1] N90-20408

POSITRON ANNIHILATION
Positron annihilation spectroscopy: A nondestructive, submicroscopic characterization technique for structural polymers
[AD-A217748] N90-20226
The electronic properties of high (Tc) superconductors probed by positron annihilation
[DE90-008354] N90-20883
Systematics in positron annihilation lifetime analysis of high (Tc) superconducting transitions
[DE90-008361] N90-20884

POTASSIUM HYDROXIDES
The application of electrochemical impedance spectroscopy for characterizing the degradation of Ni(OH)2/NiOOH electrodes N90-20474
KOH concentration effect on the cycle life of nickel-hydrogen cells. Part 4: Results of failure analyses N90-20475

POTENTIAL
Precise solution for a finite set of spherical coefficients from equiangular gridded data N90-20522
Very accurate upward continuation to low heights in a test of non-Newtonian theory N90-20548

POTENTIAL ENERGY
Polyatomic reaction dynamics
[DE90-008668] N90-20811
Theoretical studies of spin-forbidden processes within the Breit-Pauli approximation
[AD-A217778] N90-20815

POWDER (PARTICLES)
An investigation of the mechanisms of solid state powder reaction in the combustion synthesis and sintering of high temperature materials
[DE90-007880] N90-20198
Determination of flow-regime boundaries for cohesive particles
[DE90-007425] N90-20332
Magnetic hardening studies and novel techniques for preparation of high performance magnets
[AD-A217737] N90-20790
Millimeter wave surface resistance of RBa2Cu3O(7-delta) (R=Y,Eu,Dy,Sm,Er) superconductors
[NASA-TM-102571] N90-20586

POWDER METALLURGY
Constitutive data acquisition and modelling in aluminium 2014 alloy
[AERE-R-13651] N90-20186
Improved toughness alloys based on titanium aluminides
[AD-A218149] N90-20208

POWER CONDITIONING
Power conditioning techniques
[NASA-TM-102577] N90-20301

POWER LIMITED SPACECRAFT
A space-based optical communication system utilizing fiber optics
[AD-A217333] N90-20828

PRASEODYMIUM
An experimental investigation of the thermal conductivity of porous adsorbents
[AD-A217854] N90-20899

PRECIPITATION (CHEMISTRY)
Human serum albumin crystals and method of preparation
[NASA-CASE-MFS-28234-1] N90-20616
SiO(x) precipitation: Defect density correlation with the n+ substrate resistivity
[DE90-005593] N90-20878

PRECIPITATION (METEOROLOGY)
United States Historical Climatology Network (HCN) serial temperature and precipitation data
[DE90-008029] N90-20506
An intercomparison of general circulation model predictions of regional climate change
[DE90-008325] N90-20589

PRECIPITATORS
Electronic precipitator control
[NASA-CASE-LAR-13273-2] N90-20320

PREDICTION ANALYSIS TECHNIQUES
Escape systems research at RAE N90-20058
Relationship of radiometric field measurements of wheat in the Assis-Safra region, 1988
[INPE-4949-RPE/598] N90-20443
Progress in the Determination of the Earth's Gravity Field
[NASA-CR-185721] N90-20513
Gravity field determination and error assessment techniques N90-20517
The use of high-resolution terrain data in gravity field prediction N90-20533
The role of topography in geodetic gravity field modelling N90-20534
Fourier transform methods in local gravity modeling N90-20538
Determination of mean gravity anomalies in the Taiwan Island N90-20547
Adiabatic and diabatic initialization of the AFGL (Air Force Geophysics Laboratory) global spectral model using dynamic normal mode and nonlinear normal mode methods
[AD-A218120] N90-20595
An algorithm for efficient estimation of superimposed exponential signals
[AD-A217218] N90-20698
VAPEPS user's reference manual, version 5.0
[NASA-CR-180781] N90-20713
Precompound decay models for medium energy nuclear reactions
[DE90-008352] N90-20808
The electronic properties of high (Tc) superconductors probed by positron annihilation
[DE90-008354] N90-20883

PREDICTIONS
F-15B high angle-of-attack phenomena and spin prediction using bifurcation analysis
[AD-A217366] N90-20073

PREMIXED FLAMES
The extinction and structure of counterflow premixed flames
[AD-A218106] N90-20178

PRESSURE
Difference in electron thermal diffusivity and profile between interior and exterior of TFTR L-mode plasmas
[DE90-007479] N90-20846

PRESSURE BREATHING
The +Gz protection in the future: Review of scientific literature
[AD-A217887] N90-20623

PRESSURE DEPENDENCE
Absolute pressure dependence of the second ionization level of EL2 in GaAs
[DE90-007761] N90-20872

PRESSURE EFFECTS
An investigation of the mechanisms of solid state powder reaction in the combustion synthesis and sintering of high temperature materials
[DE90-007680] N90-20198
The effect of adverse pressure gradient on turbulent burst structure in low-Reynolds number equilibrium boundary layers
[AD-A217308] N90-20327
Laser-induced shock waves effects in materials
[DE90-007626] N90-20379

PRESSURE GRADIENTS
The effect of adverse pressure gradient on turbulent burst structure in low-Reynolds number equilibrium boundary layers
[AD-A217308] N90-20327
Experimental feasibility of investigating acoustic waves in Couette flow with entropy and pressure gradients
[NASA-TM-102621] N90-20795

PRESSURE REDUCTION
System for venting gas from a liquid storage tank
[NASA-CASE-MSC-21253-1] N90-20254

PRESSURE SUITS
Requirements for protective pressure suits for the Hermes spacecrew N90-20065
The +Gz protection in the future: Review of scientific literature
[AD-A217887] N90-20623

PRESSURE VESSELS
High elongation plasmas
[DE90-007575] N90-20848

PRETREATMENT
Stochastic approach to the initiation of pitting corrosion
[AERE-R-13348] N90-20190

PRINTED CIRCUITS
Computed tomography of electronics
[AD-A217976] N90-20314

PROBABILITY DISTRIBUTION FUNCTIONS
Determinations of photon spectra
[AD-A218003] N90-20816

PROBABILITY THEORY
Development of acceleration exposure limits for advanced escape systems N90-20055
Determination of fundamental thermodynamic properties of constituent materials and performance screening of candidate systems
[AD-A218089] N90-20153
Error control techniques for satellite and space communications
[NASA-CR-186221] N90-20263
On optimal distributed decision architectures in a hypothesis testing environment
[AD-A217824] N90-20274
Research in reliability, availability and maintainability for complex failure systems
[AD-A217744] N90-20415
A paradoxical result in unconditionally secure authentication codes, and an explanation
[DE90-008529] N90-20710
Probabilistic analysis of algorithms for NP-complete problems
[AD-A217880] N90-20716
A Locality-based multiprocessor cache interference model
[AD-A217126] N90-20730

PROBLEM SOLVING
A matrix-free locally-implicit scheme for Navier-Stokes equations
[AD-A218298] N90-20349
The inverse gravimetric problem in gravity modelling N90-20535
Experiments in finding neural network weights
[DE90-007696] N90-20702
Institute for Computational Mechanics in Propulsion (ICOMP) fourth annual review, 1989
[NASA-TM-102519] N90-20769
Techniques for accelerating iterative methods for the solution of mathematical problems
[AD-A218272] N90-20775

PROCESS CONTROL (INDUSTRY)
Techno-economic assessment of a carbothermic alumina reduction process
[DE90-007018] N90-20170

PRODUCT DEVELOPMENT
Development and construction of external laser components for hardening and coating
[MT-15/87] N90-20364
A review of the suitability of available Computer Aided Software Engineering (CASE) tools for the small software development environment
[AD-A218276] N90-20726

PRODUCTION ENGINEERING
A locally constrained parallel activation model for diagnostic reasoning
[AD-A217808] N90-20747

PROGRAMMING LANGUAGES
Massively-parallel computational fluid dynamics
[AD-A217732] N90-20342
TAE Plus: Transportable Applications Environment Plus tools for building graphic-oriented applications N90-20652
Research in programming languages and software engineering
[AD-A217765] N90-20715

Implementation of a hypertext help system for GLAD (Graphics LAnguage for Database)
[AD-A217936] N90-20718
VHSIC Hardware Description Language (VHDL) benchmark suite
[AD-A217947] N90-20719
Implementation of a hypercube database system
[DE90-008440] N90-20905

PROJECT MANAGEMENT
Spacecraft escape N90-20066
Reorganization of the German space administration. Foundation of DARA
[REPT-16/89] N90-20902

PROJECT PLANNING
Research and development quality assurance planning
[DE90-003687] N90-20413
Atmospheric Radiation Measurement Program Plan
[DE90-008108] N90-20504
Middle management of research
[NASA-TM-102417] N90-20901

PROJECTILES
ARDEC (Armament Research, Development and Engineering Center) electric gun in-house test program
[AD-A217337] N90-20105
A 10-stage reconnection demonstration launcher
[DE90-007653] N90-20106
Diagnostics and firing control for the cylindrical reconnection launcher
[DE90-007677] N90-20107
Design and performance of a multi-stage cylindrical reconnection launcher
[DE90-007820] N90-20108
Evaluation of 2090-T8E48 aluminum-lithium plates
[AD-A217262] N90-20196
Interior fluid dynamics of liquid-filled projectiles
[AD-A217630] N90-20330

PROJECTORS
Large screen display for the Mission Control Center N90-20662

PROPAGATION MODES
Computation of coupling elements between waveguides and modes for large launching structures
[IPPCZ-290] N90-20842

PROPELLERS
Noise of a simulated installed model counterrotation propeller at angle-of-attack and takeoff/approach conditions
[NASA-TM-102440] N90-20794

PROPORTIONAL COUNTERS
In-line wear monitor
[AD-A217799] N90-20091

PROPULSION SYSTEM CONFIGURATIONS
Controllable propulsion for escape systems control N90-20064
Advanced launch vehicle propulsion at the NASA Lewis Research Center
[NASA-TM-103096] N90-20110

PROPULSION SYSTEM PERFORMANCE
Controllable propulsion for escape systems control N90-20064
Advanced launch vehicle propulsion at the NASA Lewis Research Center
[NASA-TM-103096] N90-20110

PROTECTION
The USAF Advanced Dynamic Anthropomorphic Manikin (ADAM) N90-20062
Windblast protection for advanced ejection seats N90-20063
Spacecraft escape N90-20066

PROTECTIVE COATINGS
Molding solidification N90-20246

PROTONS
The application of Dow Chemical's perfluorinated membranes in proton-exchange membrane fuel cells N90-20466
Stopping power for protons in Al for the whole range of velocities
[DE90-008558] N90-20810
Proton responses on MOS (Metal-Oxide-Semiconductor) electronics operating at cryogenic temperatures
[AD-A217622] N90-20868

PROTOTYPES
Phase 1 supplemental development of a kinematic Stirling/Rankine commercial gas-fired heat pump system
[PB90-129974] N90-20483

PROVING
Comparison of 3-D viscous flow computations of Mach 5 inlet with experimental data
[NASA-TM-102518] N90-20090

PROXIMITY
Proximity operations concept design study, task 6
[NASA-CR-181971] N90-20112

PSYCHOLOGICAL FACTORS
Aiding the decision maker: Perceptual and cognitive issues at the human-machine interface
[AD-A217862] N90-20648
The perceptual interaction of graphical attributes in thirteen bivariate displays
[AD-A217980] N90-20720

PSYCHOPHYSICS
Detection acuity in the peripheral retina
[AD-A218183] N90-20632
Parts of recognition
[AD-A217694] N90-20714

PULSE CODE MODULATION
General forms and properties of zero cross-correlation radar waveforms
[AD-A217779] N90-20273

PULSE COMPRESSION
General forms and properties of zero cross-correlation radar waveforms
[AD-A217779] N90-20273
Core cooling studies at LLNL (Lawrence Livermore National Laboratory) and Sandia
[DE90-008303] N90-20300

PULSE DURATION
Experimental and theoretical studies of light scattering by small particles
[AD-A217432] N90-20831

PULSED LASERS
Pulsed laser photothermal spectroscopy of liquids and solids
[DE90-008642] N90-20380
Picosecond Laser Facility
[AD-A217784] N90-20384
Ultra-high brightness laser research at LLNL (Lawrence Livermore National Laboratory)
[DE90-008366] N90-20885

PULSED RADIATION
Core cooling studies at LLNL (Lawrence Livermore National Laboratory) and Sandia
[DE90-008303] N90-20300

PULSES
Common-mode rejector for pulse power diagnostics
[AD-A218096] N90-20316
Determinations of photon spectra
[AD-A218003] N90-20816

PYLONS
Compression pylon
[NASA-CASE-LAR-13777-1] N90-20078

PYROLYSIS
Non-noble electrocatalysts for alkaline fuel cells N90-20470

PYROTECHNICS
Pyrotechnic device technology
[DE90-007683] N90-20234

PYRROLES
Chemical and electrochemical studies in ionic liquids
[AD-A217742] N90-20175
Molecular organization and electrical properties of mixed Langmuir-Blodgett multilayer thin films of polypyrrole
[DE90-007627] N90-20870

Q

QUADRATIC EQUATIONS
Theoretical modeling studies of the marine planetary
[AD-A217200] N90-20567

QUADRATURES
Thin-plate spline quadrature of geodetic integrals N90-20539

QUALIFICATIONS
Spacecraft escape N90-20066
Spacelab qualified infrared imager for microgravity science experiments
[NASA-TM-102503] N90-20352

QUALITY CONTROL
A guide to performing and documenting safety analyses
[DE90-008688] N90-20261
Product assurance technology for procuring reliable, radiation-hard, custom LSI/VLSI electronics
[NASA-CR-185954] N90-20281
Research and development quality assurance planning
[DE90-003687] N90-20413
Transaction processing in a quality control laboratory
[DE90-004655] N90-20414
Overview of the methodologies used to compile large scale emissions inventories
[DE90-008518] N90-20509
Software quality assurance and software safety in the biomed control system
[DE90-008072] N90-20706

QUANTUM EFFICIENCY
A new thermal sensor for x ray microcalorimetry
[DE90-008547] N90-20360

QUANTUM ELECTRONICS
Joint Services Electronics Program research in electronics
[AD-A217745] N90-20307
Superconductive microprobes for eddy current evaluation of materials
[AD-A217776] N90-20361

QUANTUM MECHANICS
Systematics in positron annihilation lifetime analysis of high (Tc) superconducting transitions
[DE90-008361] N90-20884

QUANTUM THEORY
Quantum-theoretical methods and studies relating to properties of materials
[AD-A217843] N90-20132
Optical Bistability, 1988
[AD-A217681] N90-20832

QUATERNARY ALLOYS
Theoretical and experimental study of solid phase miscibility gaps in III/V quaternary alloys
[DE90-008430] N90-20877

R

RADAR
Algorithms for optimal processing of polarimetric radar data
[AD-A217330] N90-20758

RADAR CROSS SECTIONS
Simulation of radar scattering from rough surfaces
[AD-A217841] N90-20275

RADAR DATA
Algorithms for optimal processing of polarimetric radar data
[AD-A217330] N90-20758

RADAR DETECTION
Radar detection of lightning and electric fields
[AD-A217894] N90-20574

RADAR ECHOES
Radar detection of lightning and electric fields
[AD-A217894] N90-20574

RADAR IMAGERY
Atmospheric wind measurements using a 50 MHz imaging Doppler interferometer radar
[AD-A218277] N90-20601

RADAR MEASUREMENT
Atmospheric wind measurements using a 50 MHz imaging Doppler interferometer radar
[AD-A218277] N90-20601

RADAR RESOLUTION
Tomographic processing of synthetic aperture radar signals for enhanced resolution
[AD-A217178] N90-20265

RADAR SCATTERING
Simulation of radar scattering from rough surfaces
[AD-A217841] N90-20275

RADAR TARGETS
High resolution radar target modeling using ARMA (Autoregressive Moving Average) models
[AD-A218212] N90-20278
Algorithms for optimal processing of polarimetric radar data
[AD-A217330] N90-20758

RADAR TRACKING
High resolution radar target modeling using ARMA (Autoregressive Moving Average) models
[AD-A218212] N90-20278
Wideband S band transmitter
[AD-A217620] N90-20295

RADAR TRANSMITTERS
Wideband S band transmitter
[AD-A217620] N90-20295

RADIATION DAMAGE
X ray specular reflection studies of silicon coated by organic monolayers (alkylsiloxanes)
[AD-A217418] N90-20213
Measurement of proton induced radiation damage to CMOS transistors and pin diodes
[DE90-007836] N90-20283
Electron beam induced damage in PECVD Si3N4 and SiO2 films on InP
[NASA-TM-102544] N90-20393
Proton responses on MOS (Metal-Oxide-Semiconductor) electronics operating at cryogenic temperatures
[AD-A217622] N90-20868

RADIATION EFFECTS
Physical sputtering of metallic systems by charged-particle impact
[DE90-007803] N90-20201
The effects of radiation on the mechanical properties of polymers used as electrical cable insulation and jacketing materials
[AERE-R-13286] N90-20209

Radiation disorder and aperiodicity in irradiated ceramics
[DE90-008253] N90-20222
Measurement of proton induced radiation damage to CMOS transistors and pin diodes
[DE90-007836] N90-20283
A progress report on the Livermore Miniature Vacuum Tube Project
[DE90-008302] N90-20299
Short wavelength laser/materials interactions
[AD-A218015] N90-20386
Software quality assurance and software safety in the biomed control system
[DE90-008072] N90-20706
Interaction between implanted ions and intrinsic defects in silica
[DE90-006569] N90-20858

RADIATION HARDENING
Product assurance technology for procuring reliable, radiation-hard, custom LSI/VLSI electronics
[NASA-CR-185954] N90-20281
Measurement of proton induced radiation damage to CMOS transistors and pin diodes
[DE90-007836] N90-20283
Radiation-hardened wafer scale integration
[AD-A217332] N90-20290
Transient radiation hardened CMOS (Complementary Metal Oxide Semiconductor) operational amplifiers
[AD-A217972] N90-20313

RADIATION MEASUREMENT
Atmospheric Radiation Measurement Program Plan
[DE90-008108] N90-20504

RADIATION PROTECTION
A guide to performing and documenting safety analyses
[DE90-008687] N90-20260

RADIATION THERAPY
Life sciences: Lawrence Berkeley Laboratory, 1988
[DE90-006061] N90-20611

RADICALS
Ring expansion and equilibration in organophosphazenes, and the relationship to polymerization
[AD-A218234] N90-20230
Electron-impact ionization and electron attachment cross sections of radicals important in transient gaseous discharges
[AD-A217510] N90-20366

RADIO ALTIMETERS
Satellite radar altimetry over ice. Volume 1: Processing and corrections of Seasat data over Greenland
[NASA-RP-1233-VOL-1] N90-20562
Satellite radar altimetry over ice. Volume 2: Users' guide for Greenland elevation data from Seasat
[NASA-RP-1233-VOL-2] N90-20563
Satellite radar altimetry over ice. Volume 4: Users' guide for Antarctica elevation data from Seasat
[NASA-RP-1233-VOL-4] N90-20564

RADIO EMISSION
Radar detection of lightning and electric fields
[AD-A217894] N90-20574

RADIO FREQUENCY HEATING
Computation of coupling elements between waveguides and modes for large launching structures
[IPPCZ-290] N90-20842

RADIO TRANSMITTERS
Wideband S band transmitter
[AD-A217620] N90-20295

RADIOACTIVE DECAY
Precompound decay models for medium energy nuclear reactions
[DE90-008352] N90-20808
Theoretical studies of spin-forbidden processes within the Breit-Pauli approximation
[AD-A217778] N90-20815
Populations of excited states and reaction mechanisms in the emission of complex fragments
[DE90-007481] N90-20819

RADIOACTIVE WASTES
RIPE: An object-oriented Robot Independent Programming Environment
[DE90-008501] N90-20707

RADIOMETERS
Analysis of radiometer calibration effects with TOUCHSTONE
[NASA-CR-186476] N90-20284
Relationship of radiometric field measurements of wheat in the Assis-Safra region, 1988
[INPE-4949-RPE/598] N90-20443

RAILGUN ACCELERATORS
A 10-stage reconnection demonstration launcher
[DE90-007653] N90-20106
Diagnostics and firing control for the cylindrical reconnection launcher
[DE90-007677] N90-20107
Application of railgun principle to high-velocity hydrogen pellet injection for magnetic fusion reactor refueling
[DE90-008261] N90-20109

RAIN
An estimation of rainfall amounts using radar-derived Z-R relationships
[AD-A217950] N90-20591

RAIN GAGES
An estimation of rainfall amounts using radar-derived Z-R relationships
[AD-A217950] N90-20591

RAMAN SPECTRA
Modelling Doppler broadening in Raman propagation
[DE90-008042] N90-20269
Structural comparison of nickel electrodes and precursor phases N90-20472

RAMAN SPECTROSCOPY
Research investigation directed toward extending the useful range of the electromagnetic spectrum
[AD-A217460] N90-20267

RAMJET ENGINES
Modification and improvement of software for modeling multidimensional reacting fuel flows
[AD-A217789] N90-20235

RANDOM ACCESS
Computational complexity of random access models
[AD-A217685] N90-20701

RANDOM ACCESS MEMORY
Computational complexity of random access models
[AD-A217685] N90-20701

RANGE AND RANGE RATE TRACKING
An improved model for the Earth's gravity field
N90-20515

RANGEFINDING
Multi-dimensional LADAR tracking and adaptive grasping for spaceborne assembly of SDI (Strategic Defense Initiative) platforms
[AD-A218236] N90-20279

RANKINE-HUGONIOT RELATION
Laser-induced shock waves effects in materials
[DE90-007626] N90-20379

RARE EARTH COMPOUNDS
Magnetic hardening studies and novel techniques for preparation of high performance magnets
[AD-A217737] N90-20790

RARE EARTH ELEMENTS
A review of the literature on the toxicity of rare-earth metals as it pertains to the engineering demonstration system surrogate testing
[DE90-008049] N90-20620

RATES (PER TIME)
Research and development on enhanced degradable plastics
[AD-A217180] N90-20212

RATIONS
Physical performance and carbohydrate consumption in CF commandos during a 5-day field trial
[AD-A217204] N90-20619

RATS
Acute oral toxicity of DIGL-RP solid propellant in Sprague-Dawley rats
[AD-A217712] N90-20614

RAYLEIGH DISTRIBUTION
First-order intensity statistics for non-Rayleigh fading
[AD-A217572] N90-20569

RAYLEIGH SCATTERING
Measurement of the stimulated thermal Rayleigh scattering instability
[DE90-007849] N90-20376

RAYLEIGH WAVES
Laser-induced shock waves effects in materials
[DE90-007626] N90-20379

RDX
Condensed phase kinetic deuterium isotope effects in high energy phenomena: Mechanistic investigations and relationships
[AD-A217161] N90-20156

REACTION KINETICS
Summary report of the Summer Conference of the DARPA-Materials Research Council
[AD-A217380] N90-20143
Structure of model gas flames in nitramines
[AD-A217578] N90-20159
Corrosion properties of Fe3Al in H2S-H2-H2O mixtures
[DE90-004936] N90-20167
DURIP FTIR studies of solid state reaction dynamics
[AD-A217713] N90-20174
Aerodynamic and kinetic processes in flames
[AD-A217796] N90-20176
The extinction and structure of counterflow premixed flames
[AD-A218106] N90-20178
Polyatomic reaction dynamics
[DE90-008668] N90-20811
Populations of excited states and reaction mechanisms in the emission of complex fragments
[DE90-007481] N90-20819

REACTIVITY
Mechanisms of reactive etching
[AD-A217679] N90-20160
Reactive sputtering of molybdenum
[DE90-008307] N90-20204
An electrochemical and spectroscopic study of electrode processes
[AD-A217261] N90-20289
Advanced calcium thionyl chloride high power battery
[AD-A216685] N90-20482

REACTOR SAFETY
A nonintrusive method for measuring the operating temperature of a solenoid-operated valve
[DE90-007576] N90-20355

REACTOR TECHNOLOGY
Using formal methods to develop a paradigm for software design
[DE90-005633] N90-20703

REAL TIME OPERATION
Potential role of avionics in escape systems
N90-20060
Airplane takeoff and landing performance monitoring system
[NASA-CASE-LAR-13734-1-CU] N90-20096
A data acquisition parallel bus for wind tunnels at ARL (Aeronautical Research Laboratory)
[AD-A218052] N90-20098
The Real Time Display Builder (RTDB) N90-20656
Design considerations for a space database
N90-20659
Operational computer graphics in the flight dynamics environment N90-20668
Real-time graphics for the Space Station Freedom cupola, developed in the Systems Engineering Simulator
N90-20683
MEASURE: An integrated data-analysis and model identification facility
[NASA-CR-186452] N90-20686
A real-time parallel pipelined data-flow image-processing system
[DE90-008324] N90-20691
A parallel architecture for real-time simulation
[AD-A218321] N90-20741
Real-time concurrency control and transaction scheduling
[AD-A218162] N90-20909

RECEIVERS
Performance of a 300 Mbps 1:16 serial/parallel optoelectronic receiver module
[NASA-TM-103110] N90-20302

RECEPTION DIVERSITY
Radar detection of lightning and electric fields
[AD-A217894] N90-20574

RECOMBINATION REACTIONS
Isotope exchange in oxide-containing catalyst
[NASA-CASE-LAR-13542-2-SB] N90-20154
Termolecular associations of ions in gases, recombination and electron-atom collisions
[AD-A217678] N90-20805

RECRYSTALLIZATION
Identification of defects in SOI (Silicon-On-Insulator) wafers
[DE90-006020] N90-20879

RECURSIVE FUNCTIONS
Maintaining bridge-connected and biconnected components on-line
[AD-A215107] N90-20754

REDUCED GRAVITY
Secondary arm coarsening and microsegregation in superalloy PWA-1480 single crystals: Effect of low gravity
[NASA-TM-102445] N90-20194
Instantaneously generated foam and its applicability to reduced gravity
[NASA-CR-185208] N90-20237
German microgravity program and flight opportunities
N90-20239
User center and assitance N90-20240
Systems with a miscibility gap in the liquid state
N90-20245
Molding solidification N90-20246
Microgravity conditions of a space vehicle
N90-20247
Diffusion and germ formation in glasses N90-20250
The NASA, Marshall Space Flight Center drop tube user's manual
[NASA-TM-100392] N90-20251
Microgravity Science and Application Program tasks, 1989 revision
[NASA-TM-4191] N90-20252
Design and test of a compact optics system for the pool boiling experiment
[NASA-TM-102530] N90-20253

REDUCTION (CHEMISTRY)
Techno-economic assessment of a carbothermic alumina reduction process
[DE90-007018] N90-20170
REFLECTANCE
Doppler radar with multiphase modulation of transmitted and reflected signal
[NASA-CASE-MSC-18808-1] N90-20280
Simple reflection holography
[DE90-008309] N90-20359
High-efficiency silicon concentrator solar cell research
[DE90-008040] N90-20490
An estimation of rainfall amounts using radar-derived Z-R relationships
[AD-A217950] N90-20591
Observation of nonlinear reflectivity from InSb surface and optical switching application
[AD-A217184] N90-20826
REFORESTATION
Evaluation of TM/LANDSAT and HRV/SPOT data in the identification of reforested areas in the Mogi-Guacu (SP) region
[INPE-4874-PRE/1485] N90-20442
REFRACTION
Laser line transport with refraction
[DE90-008683] N90-20382
REFRACTIVITY
An ellipsometric measurement of optical properties for InP surfaces
[AD-A217185] N90-20827
Refractive index profiles of thermally grown and chemically vapor deposited films on silicon
[AD-A217187] N90-20865
Crystallography, spectroscopic analysis, and lasing properties of Nd3+:Y3Sc2Al3O12
[AD-A217792] N90-20891
REFRACTORY MATERIALS
Symposium on High Temperature and Materials Chemistry
[DE90-008047] N90-20148
Determination of fundamental thermodynamic properties of constituent materials and performance screening of candidate systems
[AD-A218089] N90-20153
An investigation of the mechanisms of solid state powder reaction in the combustion synthesis and sintering of high temperature materials
[DE90-007880] N90-20198
REFRIGERATORS
Evaluation of industrial magnetic heat pump/refrigerator concepts that utilize superconducting magnets
[DE90-008093] N90-20258
REFUELING
Application of railgun principle to high-velocity hydrogen pellet injection for magnetic fusion reactor refueling
[DE90-008281] N90-20109
REGENERATIVE COOLING
Development and fabrication of structural components for a scramjet engine
[NASA-CR-181945] N90-20088
REGRESSION ANALYSIS
High resolution radar target modeling using ARMA (Autoregressive Moving Average) models
[AD-A218212] N90-20278
Slepian models and regression approximations in crossing and extreme value theory
[AD-A218338] N90-20779
REGRESSION COEFFICIENTS
An estimation of rainfall amounts using radar-derived Z-R relationships
[AD-A217950] N90-20591
REGULATIONS
High-Explosives Applications Facility (HEAF)
[DE90-008122] N90-20257
A guide to performing and documenting safety analyses
[DE90-008688] N90-20261
Information management systems for integrating the technical data and regulatory requirements of environmental restoration activities
[DE90-008622] N90-20511
REGULATORS
A learning regulator for the plane longitudinal movement
[ETN-90-95381] N90-20695
REGULATORY MECHANISMS (BIOLOGY)
Elevated central venous pressure: A consequence of exercise training-induced hypervolemia
[NASA-TM-102965] N90-20617
REINFORCING FIBERS
Mechanical behavior of whisker reinforced ceramics
[DE90-008758] N90-20224
RELATIVISTIC ELECTRON BEAMS
Collective ion acceleration in high current relativistic electron beams
[DE90-008328] N90-20821
RELIABILITY
Fault simulator evaluation
[AD-A217782] N90-20308
Research in reliability, availability and maintainability for complex failure systems
[AD-A217744] N90-20415
RELIABILITY ANALYSIS
Product assurance technology for procuring reliable, radiation-hard, custom LSI/VLSI electronics
[NASA-CR-185954] N90-20281
RELIABILITY ENGINEERING
Approximate evaluation of reliability and related quantities via perturbation techniques
[AD-A218340] N90-20417
RELIEF MAPS
Satellite radar altimetry over ice. Volume 4: Users' guide for Antarctica elevation data from Seasat
[NASA-RP-1233-VOL-4] N90-20564
REMOTE CONTROL
The design and implementation of a position measuring system for a remotely controlled video camera
[AD-A218077] N90-20362
REMOTE MANIPULATOR SYSTEM
Prototype part task trainer: A remote manipulator system simulator N90-20672
The development of the Canadian Mobile Servicing System Kinematic Simulation Facility N90-20676
REMOTE SENSING
Hypotheses testing of watershed/landscape dynamics in northern Alaska using digital analysis
[DE90-006721] N90-20450
Progress in the Determination of the Earth's Gravity Field
[NASA-CR-185721] N90-20513
A system for analysis and interpretation of lineaments in remote sensing images
[INPE-4893-PRE/1494] N90-20565
REMOTE SENSORS
Correlation of atmospheric optical turbulence and meteorological measurements
[AD-A218019] N90-20576
The receiving system of a dual dye lidar to study molecular and aerosol densities at the base of the stratosphere
[AD-A218286] N90-20581
REMOTELY PILOTED VEHICLES
Aerodynamic analysis of a US Navy and Marine Corps unmanned air vehicle
[AD-A218282] N90-20077
RESEARCH
Materials Science Programs, fiscal year 1989
[DE90-008169] N90-20131
Micro SAINT programs for numerical methods of integration and differential equations
[AD-A218097] N90-20772
RESEARCH AIRCRAFT
An improved airborne wind measurement technique for the NAE (National Aeronautical Establishment) Twin Otter
[AD-A217978] N90-20575
RESEARCH AND DEVELOPMENT
Research and development quality assurance planning
[DE90-003687] N90-20413
Ultra-high brightness laser research at LLNL (Lawrence Livermore National Laboratory)
[DE90-008366] N90-20885
Middle management of research
[NASA-TM-102417] N90-20901
RESEARCH FACILITIES
Microgravity Science and Application Program tasks, 1989 revision
[NASA-TM-4191] N90-20252
RESEARCH MANAGEMENT
Research in reliability, availability and maintainability for complex failure systems
[AD-A217744] N90-20415
Middle management of research
[NASA-TM-102417] N90-20901
Reorganization of the German space administration. Foundation of DARA
[REPT-16/89] N90-20902
RESIDUAL STRESS
Residual stresses: A review of their measurement and interpretation using x ray diffraction
[AERE-R-13005] N90-20423
Barkhausen noise analysis and ferromagnetic materials
[AD-A217989] N90-20792
RESONANCE FLUORESCENCE
Molecular dynamics and spectroscopy at gas-solid interfaces
[AD-A217743] N90-20813
RESONANT FREQUENCIES
Complex demodulation for bearing fault detection
[AD-A218367] N90-20407
Modal interactions in shell dynamics N90-20418
Perturbation solutions in D* for buckling, vibration, and static loading of specially orthotropic plates N90-20419
Active control of the forced and transient response of a finite beam
[NASA-CR-181957] N90-20430
Experimental feasibility of investigating acoustic waves in Couette flow with entropy and pressure gradients
[NASA-TM-102621] N90-20795
RESONATORS
Nine-year aging behavior of the ceramic flatpack resonator
[DE90-008044] N90-20412
RESOURCES MANAGEMENT
Synthesis and analysis of 25 years (1961-1986) of INPE/SRE activities related to the vegetation/forest area
[INPE-4969-RPE/604] N90-20446
Global Warming: A Northwest Perspective
[DE90-008140] N90-20505
RESPIRATION
A review of the literature on the toxicity of rare-earth metals as it pertains to the engineering demonstration system surrogate testing
[DE90-008049] N90-20620
RESTORATION
Information management systems for integrating the technical data and regulatory requirements of environmental restoration activities
[DE90-008622] N90-20511
RETENTION (PSYCHOLOGY)
A long-term retention advantage for spatial information learned naturally and in the laboratory
[AD-A218268] N90-20644
RETICLES
Comparison of oculometer and head-fixed reticle with voice or switch and touch panel for data entry on a generic tactical air combat display
[AD-A217231] N90-20646
RETINA
Biological applications and effects of optical masers
[AD-A217910] N90-20385
Detection acuity in the peripheral retina
[AD-A218183] N90-20632
REUSE
Reusable high-temperature heat pipes and heat pipe panels
[NASA-CASE-LAR-13761-1] N90-20323
RHEOLOGY
Determination of flow-regime boundaries for cohesive particles
[DE90-007425] N90-20332
A method for measuring the material moduli of granular materials: Flow in an orthogonal rheometer
[DE90-007160] N90-20339
Tribological properties of boric acid and boric acid forming surfaces. Part 1: Crystal chemistry and self-lubricating mechanism of boric acid
[DE90-005665] N90-20401
RHEOMETERS
A method for measuring the material moduli of granular materials: Flow in an orthogonal rheometer
[DE90-007160] N90-20339
RING LASERS
Performance of zig-zag slab regenerative ring amplifier laser system
[DE90-006995] N90-20371
RISK
Simulator sickness in the CH-47 (Chinook) flight simulator
[AD-A218214] N90-20634
ROBOT ARMS
Development of a passive robot-controlled reaction arm N90-20389
Graphical programming and the use of simulation for space-based manipulators N90-20674
ROBOTICS
Design of a high angle of attack robotic sting mount for tests in a low speed wind tunnel
[AD-A218105] N90-20099
The CMU Reconfigurable Modular Manipulator System
[CMU-RI-TR-88-7] N90-20388
Knowledge-based robotic grasping
[DE90-007216] N90-20402
Gripping device
[NASA-CASE-MSC-21365-1] N90-20408
The use of graphics in the design of the human-telerobot interface N90-20670
Robust planning and control using neural networks
[AD-A217216] N90-20732
Artificial Intelligence (AI) Center of Excellence at the University of Pennsylvania
[AD-A217393] N90-20743
Robotic mobility system: Road following algorithms
[AD-A218107] N90-20748

ROBOTS
Multi-dimensional LADAR tracking and adaptive grasping for spaceborne assembly of SDI (Strategic Defense Initiative) platforms
[AD-A218236] N90-20279
Estimation of modeled object pose from monocular images
[DE90-001678] N90-20354
The CMU Reconfigurable Modular Manipulator System
[CMU-RI-TR-88-7] N90-20388
Concept formation and generalization based on experimentation by an autonomous mobile robot
[DE90-001731] N90-20395
Robot navigation research using the HERMIES mobile robot
[DE90-001952] N90-20396
Robust performance of multiple tasks by a mobile robot
[DE90-001953] N90-20397
Swing-free movement of simply suspended objects employing parameter estimation
[DE90-002238] N90-20398
Resolved motion rate and resolved acceleration servo-control of wheeled mobile robots
[DE90-002585] N90-20399
Knowledge-based robotic grasping
[DE90-007216] N90-20402
Dynamic damping control: Implementation issues and simulation results
[DE90-007687] N90-20403
Design of a telerobotic controller with joint torque sensors
[DE90-008753] N90-20404
Control system design of the third flexible joint of PUMA 560 robot
[AD-A218075] N90-20405
Parameter-scheduled trajectory planning for suppression of coupled horizontal and vertical vibrations in a flexible rod
[DE90-002313] N90-20435
Graphical programming and the use of simulation for space-based manipulators N90-20674
Using an instrumented manikin for Space Station Freedom analysis N90-20675
RIPE: An object-oriented Robot Independent Programming Environment
[DE90-008501] N90-20707
Robust planning and control using neural networks
[AD-A217216] N90-20732
Boundary equations of configuration obstacles for manipulators
[DE90-002101] N90-20745
Location recognition using stereo vision
[AD-A218218] N90-20752
ROBUSTNESS (MATHEMATICS)
Stabilized determination of geopotential coefficients by the mixed hom-BLUP approach N90-20520
Robust adaptive nonlinear control under extended matching conditions
[AD-A217684] N90-20744
ROCKET ENGINES
Spacecraft escape N90-20066
ROCKET EXHAUST
Spacecraft optical contamination environment
[AD-A218088] N90-20838
ROCKS
Hot dry rock geothermal energy: A renewable energy resource that is ready for development now
[DE90-007509] N90-20485
RODS
Finite element models to predict the structural response of 120-mm sabot/rods during launch
[DE90-007497] N90-20436
Computer simulations and experiments to study the fracture of rods by flying plates
[DE90-008308] N90-20437
ROLLING CONTACT LOADS
Rolling contact fatigue of surface modified 440C using a 'Ge-Polymet' type disc rod test rig
[NASA-TM-100390] N90-20200
ROLLING MOMENTS
A video-based experimental investigation of wing rock
[AD-A218244] N90-20075
ROSS ICE SHELF
Airfields on antarctic glacier ice
[AD-A217638] N90-20097
ROTARY WING AIRCRAFT
Compendium of abstracts and viewgraphs.
[AD-A217189] N90-20140
ROTARY WINGS
Unsteady free-wake viscous aerodynamic analysis of helicopter rotors
[AD-A217166] N90-20048
Analysis of small-scale rotor hover performance data
[NASA-TM-102271] N90-20325
ROTATING CYLINDERS
Enhancement of mass transfer to a rotating cylinder electrode by inert particles suspended in the electrolyte
[DE90-008054] N90-20165
ROTATION
Fluid dynamics analysis of a rotating axisymmetric part using FIDAP
[DE90-008733] N90-20340
ROTOR DYNAMICS
Rotordynamic analysis with shell elements for the transfer matrix method
[AD-A217455] N90-20434
ROTORS
Analysis of small-scale rotor hover performance data
[NASA-TM-102271] N90-20325
A comparison of two-and three-dimensional S809 airfoil properties for rough and smooth HAWT (Horizontal-Axis Wind Tunnel) rotor operation
[DE89-009512] N90-20492
Noise of a simulated installed model counterrotation propeller at angle-of-attack and takeoff/approach conditions
[NASA-TM-102440] N90-20794
ROUTES
Three-dimensional route planning for a cruise missile for minimal detection by observer
[AD-A218336] N90-20787
RUBBER
Runaway rubber removal
[AD-A218349] N90-20100
RUNGE-KUTTA METHOD
A video-based experimental investigation of wing rock
[AD-A218244] N90-20075
RUNWAYS
Airfields on antarctic glacier ice
[AD-A217638] N90-20097
Runaway rubber removal
[AD-A218349] N90-20100

S

SABOT PROJECTILES
Finite element models to predict the structural response of 120-mm sabot/rods during launch
[DE90-007497] N90-20436
SAFETY
High-Explosives Applications Facility (HEAF)
[DE90-008122] N90-20257
A guide to performing and documenting safety analyses
[DE90-008687] N90-20260
A guide to performing and documenting safety analyses
[DE90-008688] N90-20261
Software quality assurance and software safety in the biomed control system
[DE90-008072] N90-20706
SALINITY
Utilization of LANDSAT-5 and NOAA-9 satellite imagery in the identification of physical-chemical parameters of the water in the Guanabara Bay
[INPE-4761-TDL/349] N90-20445
SAMPLES
Analysis of methods to determine emissivity for ground surface targets in the spectral band 8 to 14 microns
[INPE-4984-TDL/394] N90-20447
SAMPLING
Spatial imaging using confocal Fabry-Perot interferometers
[DE90-008363] N90-20378
Utilization of LANDSAT-5 and NOAA-9 satellite imagery in the identification of physical-chemical parameters of the water in the Guanabara Bay
[INPE-4761-TDL/349] N90-20445
Underwater physiography of the continental shelf of Rio Grande do Norte visible through satellite imagery
[INPE-4964-TDL/392] N90-20448
The electronic properties of high (Tc) superconductors probed by positron annihilation
[DE90-008354] N90-20883
SAPPHIRE
High efficiency flashlamp-pumped titanium: Sapphire laser
[AD-A217598] N90-20367
Flash-pumped titanium laser
[AD-A217599] N90-20368
SATELLITE ALTIMETRY
Progress in the development of high degree potential coefficient models N90-20516
Gravity field of the Western Weddell Sea: Comparison of airborne gravity and Geosat derived gravity N90-20526
Performance of FFT methods in local gravity field modelling N90-20537
The geoid in Kenya N90-20542
Analysis of altimetry over inland seas
[NASA-TM-100729] N90-20566
SATELLITE COMMUNICATION
Error control techniques for satellite and space communications
[NASA-CR-186221] N90-20263
First-order intensity statistics for non-Rayleigh fading
[AD-A217572] N90-20569
SATELLITE IMAGERY
Utilization of LANDSAT-5 and NOAA-9 satellite imagery in the identification of physical-chemical parameters of the water in the Guanabara Bay
[INPE-4761-TDL/349] N90-20445
Underwater physiography of the continental shelf of Rio Grande do Norte visible through satellite imagery
[INPE-4964-TDL/392] N90-20448
Methods for local gravity field approximation N90-20532
Derivation of kinematic fields using wind profiler data from the 1985 pre-storm experiment
[AD-A217952] N90-20592
Forecasting 24 and 48 hour intensity changes, for northwestern Pacific tropical cyclones, using satellite imagery
[AD-A218174] N90-20597
Correlation of AVHRR imagery with sub-surface features in California current
[AD-A218184] N90-20607
SATELLITE OBSERVATION
An improved model for the Earth's gravity field N90-20515
FFT-local gravimetric geoid computation N90-20536
A discussion of observation model, error sources and signal size for spaceborne gravitational gradiometry N90-20557
EXOSAT observations of Seyfert type galaxies N90-20910
SATELLITE TRACKING
A satellite simulation program
[AD-A218079] N90-20124
Gravity field determination and error assessment techniques N90-20517
An improved error assessment for the GEM-T1 gravitational model N90-20518
GPS-aided gravimetry at 30 km altitude from a balloon-borne platform N90-20530
Geographically correlated orbit error N90-20551
Local gravity disturbance estimation from multiple-high-single-low satellite-to-satellite tracking N90-20555
Satellite-to-satellite tracking experiment for global gravity field mapping N90-20556
SATELLITE TRANSMISSION
Numerical Arc Segmentation Algorithm for a Radio Conference-NASARC (version 4.0) technical manual
[NASA-TM-101453] N90-20264
SATELLITE-BORNE INSTRUMENTS
High resolution analysis of satellite gradiometry N90-20561
SATELLITE-BORNE PHOTOGRAPHY
Forecasting 24 and 48 hour intensity changes, for northwestern Pacific tropical cyclones, using satellite imagery
[AD-A218174] N90-20597
SCALARS
Simulation of radar scattering from rough surfaces
[AD-A217841] N90-20275
Cell averaging Chebyshev methods for hyperbolic problems
[NASA-CR-182028] N90-20768
SCANNING TUNNELING MICROSCOPY
Design and calibration of a vacuum compatible scanning tunneling microscope
[NASA-TM-102514] N90-20353
SCATTER PROPAGATION
First-order intensity statistics for non-Rayleigh fading
[AD-A217572] N90-20569
SCATTERING
Multiple versus single scattering of terrestrial infrared longwave radiation in an aerosol-laden planetary boundary layer
[AD-A217709] N90-20272
Laser-induced shock waves effects in materials
[DE90-007626] N90-20379
Laser line transport with refraction
[DE90-008683] N90-20382
Scattering sources: A spherical harmonics expansion
[DE90-008724] N90-20711
SCATTERING CROSS SECTIONS
Large-angle elastic and inelastic scattering of Pi+ and Pi- from Si28 and Ca40
[AD-A218163] N90-20818
SCHEDULING
Real-time concurrency control and transaction scheduling
[AD-A218162] N90-20909

SCHOOLS
The United States Air Force School of Aerospace Medicine: Special report
[AD-A217740] N90-20622
ONR (Office of Naval Research) summer scholars for the 1989 PREFACE Program
[AD-A217746] N90-20919
SCHOTTKY DIODES
Deep level transient spectroscopy in resistive layers
[DE90-008349] N90-20169
SCINTILLATION
First-order intensity statistics for non-Rayleigh fading
[AD-A217572] N90-20569
SCINTILLATION COUNTERS
Mercuric iodide room temperature gamma-ray detectors
[NASA-TM-103318] N90-20357
SEA ICE
Satellite radar altimetry over ice. Volume 1: Processing and corrections of Seasat data over Greenland
[NASA-RP-1233-VOL-1] N90-20562
SEALS (STOPPERS)
Thiokol/Wasatch installation evaluation of the redesigned field joint protection system (concepts 1 and 3)
[NASA-CR-183860] N90-20127
SEAS
User's guide: Programs for processing altimeter data over inland seas
[NASA-TM-100730] N90-20572
SEASAT SATELLITES
Satellite radar altimetry over ice. Volume 1: Processing and corrections of Seasat data over Greenland
[NASA-RP-1233-VOL-1] N90-20562
Satellite radar altimetry over ice. Volume 2: Users' guide for Greenland elevation data from Seasat
[NASA-RP-1233-VOL-2] N90-20563
Satellite radar altimetry over ice. Volume 4: Users' guide for Antarctica elevation data from Seasat
[NASA-RP-1233-VOL-4] N90-20564
SECURITY
A paradoxical result in unconditionally secure authentication codes, and an explanation
[DE90-008529] N90-20710
SEDIMENTS
Hydrodynamic interactions and transport coefficients in a suspension of spherical particles
[DE90-008301] N90-20336
SEGMENTS
Numerical Arc Segmentation Algorithm for a Radio Conference-NASARC (version 4.0) technical manual
[NASA-TM-101453] N90-20264
SEISMOLOGY
Seismic characterization of fracture properties
[DE90-007759] N90-20570
Damage characteristics of time domain histories
[DE90-008787] N90-20573
The effects of structure and source complexity on waveforms: Crustal structure of Tibet and the recovery of complex seismic sources
[AD-A218202] N90-20579
SELENIUM
CuInSe2 and CdTe: Scale-up for manufacturing
[DE89-009503] N90-20489
SELF TESTS
Advanced modulation technology development for earth station demodulator applications. Coded modulation system development
[NASA-CR-185149] N90-20270
SEMICONDUCTOR DEVICES
Summary report of the Summer Conference of the DARPA-Materials Research Council
[AD-A217380] N90-20143
An electron-beam controlled semiconductor switch
[AD-A217181] N90-20288
A new thermal sensor for x ray microcalorimetry
[DE90-008547] N90-20360
Nonlinear systems of partial differential equations
[AD-A217581] N90-20761
CCST (Center for Compound Semiconductor Technology) research briefs
[DE90-007782] N90-20874
SEMICONDUCTOR DIODES
High power semiconductor laser arrays by metalorganic chemical vapor deposition N90-20363
Crystallography, spectroscopic analysis, and lasing properties of Nd3+:Y3Sc2Al3O12
[AD-A217792] N90-20891
SEMICONDUCTOR LASERS
High power semiconductor laser arrays by metalorganic chemical vapor deposition N90-20363
SEMICONDUCTORS (MATERIALS)
Polymer liquid crystals with side chain discogens
[AD-A218013] N90-20228
Research investigation directed toward extending the useful range of the electromagnetic spectrum
[AD-A217460] N90-20267
An electron-beam controlled semiconductor switch
[AD-A217181] N90-20288
Joint Services Electronics Program research in electronics
[AD-A217745] N90-20307
An ellipsometric measurement of optical properties for InP surfaces
[AD-A217185] N90-20827
Workshop on the Physics and Chemistry of Mercury Cadmium Telluride and Related II-VI compounds
[AD-A217496] N90-20867
CCST (Center for Compound Semiconductor Technology) research briefs
[DE90-007782] N90-20874
Theoretical and experimental study of solid phase miscibility gaps in III/V quaternary alloys
[DE90-008430] N90-20877
SEMISPAN MODELS
Experimental and theoretical aerodynamic characteristics of a high-lift semispan wing model
[NASA-TP-2990] N90-20046
SEPARATED FLOW
Unsteady three-dimensional marginal separation, including breakdown
[NASA-TM-102525] N90-20337
Experimental investigation of the mechanisms underlying vortex kinematics in unsteady separated flows
[AD-A217889] N90-20346
SEPARATORS
Vortex motion phase separator for zero gravity liquid transfer
[NASA-CASE-KSC-11387-1] N90-20236
The application of Dow Chemical's perfluorinated membranes in proton-exchange membrane fuel cells N90-20466
SEQUENCING
A unified approach to the synthesis of fully testable sequential machines
[AD-A217120] N90-20687
Irredundant sequential machines via optimal logic synthesis
[AD-A217119] N90-20742
SERIES EXPANSION
Very accurate upward continuation to low heights in a test of non-Newtonian theory N90-20548
Observer based compensators for nonlinear systems
[AD-A217426] N90-20760
SERUMS
Human serum albumin crystals and method of preparation
[NASA-CASE-MFS-28234-1] N90-20616
SERVICE LIFE
Full-scale birdstrike testing of in-service aged F-111 ADBIRT windshield transparencies
[AD-A218035] N90-20069
Theory system reliability demonstration and burn-in design
[AD-A217775] N90-20416
SERVOMECHANISMS
Resolved motion rate and resolved acceleration servo-control of wheeled mobile robots
[DE90-002585] N90-20399
Design of a telerobotic controller with joint torque sensors
[DE90-008753] N90-20404
SEYFERT GALAXIES
EXOSAT observations of Seyfert type galaxies N90-20910
SHAFTS (MACHINE ELEMENTS)
An applicational process for dynamic balancing of turbomachinery shafting
[NASA-TM-102537] N90-20392
SHALE OIL
Determination of flow-regime boundaries for cohesive particles
[DE90-007425] N90-20332
SHAPES
Parts of recognition
[AD-A217694] N90-20714
SHARP LEADING EDGES
A video-based experimental investigation of wing rock
[AD-A218244] N90-20075
SHEAR FLOW
A method for measuring the material moduli of granular materials: Flow in an orthogonal rheometer
[DE90-007160] N90-20339
SHELL STABILITY
Experiments on buckling and critical buckling. Behavior of carbon fiber reinforced plastic shells submitted to tensile stresses
[ETN-90-95382] N90-20429
SHELL THEORY
Modal interactions in shell dynamics N90-20418
SHOCK (PHYSIOLOGY)
Parachute opening shocks during high speed ejections: Normalization N90-20056
SHOCK LAYERS
Geometric scale of interaction between moving shock and stationary thermal layer
[AD-A217769] N90-20344
Domain decomposition for a boundary-value problem with a shock layer
[DE90-007857] N90-20762
SHOCK WAVE PROPAGATION
Laser-induced shock waves effects in materials
[DE90-007626] N90-20379
SHOCK WAVES
Viscous shock profiles and primitive formulations
[NASA-CR-182029] N90-20049
Numerical modeling of airblast
[AD-A217993] N90-20347
Domain decomposition for a boundary-value problem with a shock layer
[DE90-007857] N90-20762
SHORT WAVE RADIATION
Short wavelength laser/materials interactions
[AD-A218015] N90-20386
Downward shortwave surface irradiance from 17 sites for the FIRE/SRB Wisconsin experiment
[NASA-TM-102596] N90-20583
SIDELOBES
Effects of additional interfering signals on adaptive array performance
[NASA-CR-186508] N90-20271
SIGNAL ANALYZERS
Air Force Boom Event Analyzer Recorder (BEAR): Sysstem description
[AD-A218048] N90-20800
SIGNAL DETECTION
Complex demodulation for bearing fault detection
[AD-A218367] N90-20407
SIGNAL FADING
First-order intensity statistics for non-Rayleigh fading
[AD-A217572] N90-20569
SIGNAL PROCESSING
Proximity operations concept design study, task 6
[NASA-CR-181971] N90-20112
Tomographic processing of synthetic aperture radar signals for enhanced resolution
[AD-A217178] N90-20265
The adaptive line enhancer applied to chirp detection
[DE90-006772] N90-20268
Doppler radar with multiphase modulation of transmitted and reflected signal
[NASA-CASE-MSC-18808-1] N90-20280
The design of high-performance circuits for digital signal processing
[AD-A217786] N90-20309
Common-mode rejector for pulse power diagnostics
[AD-A218096] N90-20316
The design and implementation of a position measuring system for a remotely controlled video camera
[AD-A218077] N90-20362
A discussion of observation model, error sources and signal size for spaceborne gravitational gradiometry N90-20557
(DURIP) Two-Processor Alliant FX/4 System
[AD-A217810] N90-20692
An algorithm for efficient estimation of superimposed exponential signals
[AD-A217218] N90-20698
ISLE (Image and Signal Processing LISP Environment) reference manual
[DE90-007858] N90-20705
Spectral analytic methods for the estimation of number of signals and directions of arrival
[AD-A217219] N90-20757
GaAs traveling-wave optical modulators using modulated coplanar electrodes with periodic cross-tie overlays
[AD-A217731] N90-20835
SIGNAL TRANSMISSION
Doppler radar with multiphase modulation of transmitted and reflected signal
[NASA-CASE-MSC-18808-1] N90-20280
SIGNS AND SYMPTOMS
Acute oral toxicity of JA-2 solid propellant in ICR mice
[AD-A217264] N90-20609
Acute oral toxicity of DIGL-RP solid propellant in ICR mice
[AD-A217711] N90-20613
Acute oral toxicity of DIGL-RP solid propellant in Sprague-Dawley rats
[AD-A217712] N90-20614
Simulator sickness in the CH-47 (Chinook) flight simulator
[AD-A218214] N90-20634

What should athletes know about low body temperature (hypothermia)
[AD-A218316] N90-20637

SILICON
Mechanisms of reactive etching
[AD-A217679] N90-20160
Infrared absorption study of zinc-doped silicon
[DE90-007779] N90-20164
Refractive index profiles of thermally grown and chemically vapor deposited films on silicon
[AD-A217187] N90-20865

SILICON CARBIDES
Evaluation of thermal and mechanical loading effects on the structural behavior of a SiC/titanium composite
[NASA-TM-102536] N90-20139
Synthesis of alumina-coated SiC whiskers for production of SiC whisker-reinforced alumina composite materials
[DE90-007778] N90-20147
Characterization of ceramic matrix composites fabricated by chemical vapor infiltration
[DE90-008409] N90-20149
The effect of the SiC/Al interface on matrix microstructure in 2xxx-SiCp metal matrix
[AERE-R-13591] N90-20184
The ageing effect of the matrix-reinforcement interface on the ageing response of an aluminium 6061 alloy reinforced with 20vol percent SiC particulates
[AERE-R-13361] N90-20193

SILICON DIOXIDE
Mechanisms of reactive etching
[AD-A217679] N90-20160
Hydrous metal oxide-supported catalysts. Part 1: Preparation chemistry and physical and chemical properties
[DE90-007607] N90-20161
Interaction between implanted ions and intrinsic defects in silica
[DE90-006569] N90-20858
In-situ differential reflectance study of the etching of SiO2 films
[AD-A217186] N90-20864

SILICON FILMS
In-situ differential reflectance study of the etching of SiO2 films
[AD-A217186] N90-20864

SILICON ISOTOPES
Large-angle elastic and inelastic scattering of Pi+ and Pi- from Si28 and Ca40
[AD-A218163] N90-20618

SILICON OXIDES
Experimentally determined wear behavior of an Al2O3-SiC composite from 25 to 1200 C
[NASA-TM-102549] N90-20130
SiO(x) precipitation: Defect density correlation with the n+ substrate resistivity
[DE90-005593] N90-20878

SILOXANES
Sol-gel derived polytitanosiloxane coatings
[DE90-004186] N90-20210
X ray specular reflection studies of silicon coated by organic monolayers (alkylsiloxanes)
[AD-A217418] N90-20213

SILVER
Time-dependent failure of silver interlayer welds
[DE90-008015] N90-20440
Surface-plasmon enhanced nonlinear photoelectric emission from thin silver films
[DE90-007676] N90-20807
An investigation of the dislocation structure of the Ni/Ag phase boundary
[DE90-008428] N90-20876

SIMD (COMPUTERS)
Massively-parallel computational fluid dynamics
[AD-A217732] N90-20342

SIMULATION
Evaluation of 2090-T8E48 aluminum-lithium plates
[AD-A217262] N90-20196
Computational simulation of damping in composite structures
[NASA-TM-102567] N90-20432
Simulation of landscape disturbances and the effect of climatic change
[DE90-007565] N90-20503
Design considerations for a space database N90-20659
The Orbital Maneuvering Vehicle Training Facility visual system concept N90-20684
Performance tradeoffs in multithreaded processors
[AD-A217123] N90-20729
High-resolution acoustical imaging N90-20793

SIMULATORS
Ejection seat training of jet pilots and weapon system officers at the German Air Force School of Aviation Medicine N90-20061
Fault simulator evaluation
[AD-A217782] N90-20308
Design considerations for a space database N90-20659
Prototype part task trainer: A remote manipulator system simulator N90-20672
SES cupola interactive display design environment N90-20679
Issues in visual support to real-time space system simulation solved in the Systems Engineering Simulator N90-20680
History of visual systems in the Systems Engineering Simulator N90-20681
Computer image generation: Reconfigurability as a strategy in high fidelity space applications N90-20682
Real-time graphics for the Space Station Freedom cupola, developed in the Systems Engineering Simulator N90-20683

SINGLE CRYSTALS
Secondary arm coarsening and microsegregation in superalloy PWA-1480 single crystals: Effect of low gravity
[NASA-TM-102445] N90-20194

SINGULARITY (MATHEMATICS)
The stress-driven redistribution of point defects in the vicinity of crack-like singularities
[AERE-R-12898] N90-20424

SINTERING
Magnetic hardening studies and novel techniques for preparation of high performance magnets
[AD-A217737] N90-20790
Synthesis and properties of polycrystalline Tl2Ba2CaCu2O(x) and Tl2Ba2Ca2Cu3O(x)
[DE90-007528] N90-20887

SKIN FRICTION
Hypersonic waverider configurations for trans-atmospheric vehicles
[AD-A217925] N90-20074

SKIN TEMPERATURE (BIOLOGY)
Effective calibration of heat flux transducers for experimental use
[AD-A218262] N90-20636

SMOKE
Experimental investigation of the mechanisms underlying vortex kinematics in unsteady separated flows
[AD-A217889] N90-20346

SODIUM
Determinations of photon spectra
[AD-A218003] N90-20816

SODIUM COMPOUNDS
Hydrous metal oxide-supported catalysts. Part 1: Preparation chemistry and physical and chemical properties
[DE90-007607] N90-20161

SODIUM SULFUR BATTERIES
Advanced rechargeable sodium batteries with novel cathodes N90-20459
Sodium-sulfur battery flight experiment definition study N90-20479

SOFTWARE ENGINEERING
The Rapid Geodetic Survey System (RGSS) N90-20528
Operational computer graphics in the flight dynamics environment N90-20688
Software systems for modeling articulated figures N90-20677
GCS plan for software aspects of certification
[NASA-CR-181972] N90-20694
The HS6000/20 development system
[LINO-1989-6] N90-20696
Using formal methods to develop a paradigm for software design
[DE90-005633] N90-20703
Technical specifications requirements: Automated reasoning applications
[DE90-008799] N90-20712
Research in programming languages and software engineering
[AD-A217765] N90-20715
A review of the suitability of available Computer Aided Software Engineering (CASE) tools for the small software development environment
[AD-A218276] N90-20726

SOFTWARE TOOLS
TAE Plus: Transportable Applications Environment Plus tools for building graphic-oriented applications N90-20652
Applications of graphics to support a testbed for autonomous space vehicle operations N90-20661
The use of graphics in the design of the human-telerobot interface N90-20670
Graphical programming and the use of simulation for space-based manipulators N90-20674
Supercomputer environments
[AD-A217882] N90-20689
A review of the suitability of available Computer Aided Software Engineering (CASE) tools for the small software development environment
[AD-A218276] N90-20726

SOI (SEMICONDUCTORS)
Radiation-hardened wafer scale integration
[AD-A217332] N90-20290
Transient radiation hardened CMOS (Complementary Metal Oxide Semiconductor) operational amplifiers
[AD-A217972] N90-20313
Identification of defects in SOI (Silicon-On-Insulator) wafers
[DE90-006020] N90-20879

SOIL SCIENCE
Relationship of radiometric field measurements of wheat in the Assis-Safra region, 1988
[INPE-4949-RPE/598] N90-20443

SOILS
LANDSAT-5 data in the study of wheat and bean crops
[INPE-4746-RPE/580] N90-20444
Analysis of methods to determine emissivity for ground surface targets in the spectral band 8 to 14 microns
[INPE-4984-TDL/394] N90-20447
Air pollution-caused changes in photosynthesis: Effects on plant growth and rhizosphere functions
[DE90-007184] N90-20501

SOL-GEL PROCESSES
Sol-gel derived polytitanosiloxane coatings
[DE90-004186] N90-20210

SOLAR ACTIVITY
Solar cyclical trend study of the mid-latitude, quiet-time, meridional, neutral winds at winter solstice conditions
[AD-A217398] N90-20568

SOLAR ARRAYS
Space mechanism of low velocity for an array of solar panels: Analysis and design of an experimental model; dimensions of bearings
[INPE-4859-TDL/370] N90-20390

SOLAR CELLS
Space mechanism of low velocity for an array of solar panels: Analysis and design of an experimental model; dimensions of bearings
[INPE-4859-TDL/370] N90-20390
Photovoltaic energy
[DE89-009473] N90-20486
CuInSe2 and CdTe: Scale-up for manufacturing
[DE89-009503] N90-20489
High-efficiency silicon concentrator solar cell research
[DE90-008040] N90-20490
Perspectives on solar energy and the environment
[DE90-007680] N90-20494
Enhanced ceria solid electrolyte fuel cell development. Reduction of electronic conductivity permits use of a solid ceria electrolyte in high efficiency high power density fuel cells at temperatures compatible with metallic cell hardware
[AD-A217840] N90-20498

SOLAR COLLECTORS
Solar thermal program summary, fiscal year 1989
[DE89-009475] N90-20487

SOLAR CORONA
Spontaneous magnetic reconnection in a turbulent plasma N90-20840

SOLAR CYCLES
Solar cyclical trend study of the mid-latitude, quiet-time, meridional, neutral winds at winter solstice conditions
[AD-A217398] N90-20568

SOLAR DYNAMIC POWER SYSTEMS
Mechanical properties of pure nickel alloys after long term exposures to LiOH and vacuum at 775 K
[NASA-TM-102403] N90-20181
Model development in viscoplastic ratchetting
[NASA-TM-102509] N90-20431

SOLAR ENERGY
Photovoltaic energy
[DE89-009473] N90-20486
Solar thermal program summary, fiscal year 1989
[DE89-009475] N90-20487

SOLAR ENERGY CONVERSION
High-efficiency silicon concentrator solar cell research
[DE90-008040] N90-20490
Perspectives on solar energy and the environment
[DE90-007680] N90-20494

SOLAR GENERATORS
Photovoltaic energy
[DE89-009473] N90-20486

SOLAR HEATING
Study of possible solar heating effects on thermosonde probes: Error analysis
[AD-A218116] N90-20917

SOLAR RADIATION
Developments in solar photocatalysis for destruction of organics in water
[DE90-007685] N90-20162

Spectral solar radiation data base documentation, volume 1
[DE89-009447] N90-20571

SOLAR SENSORS
Study of possible solar heating effects on thermosonde probes: Error analysis
[AD-A218116] N90-20917

SOLAR SYSTEM
Human exploration mission studies N90-20457

SOLAR THERMAL ELECTRIC POWER PLANTS
Solar thermal program summary, fiscal year 1989
[DE89-009475] N90-20487

SOLDERED JOINTS
The metallurgical mechanisms of solder fatigue
[DE90-008390] N90-20206
Computed tomography of electronics
[AD-A217976] N90-20314

SOLDERS
The metallurgical mechanisms of solder fatigue
[DE90-008390] N90-20206

SOLENOIDS
A nonintrusive method for measuring the operating temperature of a solenoid-operated valve
[DE90-007576] N90-20355

SOLID ELECTROLYTES
The electrochemical generation of useful chemical species from lunar materials N90-20461
Recent advances in solid polymer electrolyte fuel cell technology with low platinum loading electrodes N90-20465
Hydrogen-oxygen proton-exchange membrane fuel cells and electrolyzers N90-20467
Thermoelectric conversion with ion conductors
[AD-A217822] N90-20497
Enhanced ceria solid electrolyte fuel cell development. Reduction of electronic conductivity permits use of a solid ceria electrolyte in high efficiency high power density fuel cells at temperatures compatible with metallic cell hardware
[AD-A217840] N90-20498

SOLID PHASES
Theoretical and experimental study of solid phase miscibility gaps in III/V quaternary alloys
[DE90-008430] N90-20877

SOLID PROPELLANT ROCKET ENGINES
Thiokol/Wasatch installation evaluation of the redesigned field joint protection system (concepts 1 and 3)
[NASA-CR-183860] N90-20127

SOLID PROPELLANTS
Acute oral toxicity of JA-2 solid propellant in ICR mice
[AD-A217264] N90-20609
Acute oral toxicity of DIGL-RP solid propellant in ICR mice
[AD-A217711] N90-20613
Acute oral toxicity of DIGL-RP solid propellant in Sprague-Dawley rats
[AD-A217712] N90-20614

SOLID STATE
Materials Science Programs, fiscal year 1989
[DE90-008169] N90-20131
DURIP FTIR studies of solid state reaction dynamics
[AD-A217713] N90-20174
An investigation of the mechanisms of solid state powder reaction in the combustion synthesis and sintering of high temperature materials
[DE90-007880] N90-20198
Transistor and solid-state technology: A historical development
[AD-A218141] N90-20317

SOLID STATE DEVICES
Transistor and solid-state technology: A historical development
[AD-A218141] N90-20317

SOLID STATE LASERS
Laser enhanced chemical reactions
[DE90-008273] N90-20377

SOLID-SOLID INTERFACES
Molecular dynamics and spectroscopy at gas-solid interfaces
[AD-A217743] N90-20813

SOLIDIFICATION
Rigid rod molecules as liquid crystal thermosets
[AD-A217573] N90-20158
Secondary arm coarsening and microsegregation in superalloy PWA-1480 single crystals: Effect of low gravity
[NASA-TM-102445] N90-20194
Center of Gravity: Metallic Solidification
[DFVLR-IB-333-89/3] N90-20238
Principles of metallic solidification N90-20241
Dynamics of the solidification front N90-20243
Dispersion reinforced materials N90-20244
Molding solidification N90-20246
Method of preparing radially homogeneous mercury cadmium telluride crystals
[NASA-CASE-MFS-25786-2] N90-20896

SOLIDS
A method for measuring the material moduli of granular materials: Flow in an orthogonal rheometer
[DE90-007160] N90-20339
Pulsed laser photothermal spectroscopy of liquids and solids
[DE90-008642] N90-20380
Utilization of LANDSAT-5 and NOAA-9 satellite imagery in the identification of physical-chemical parameters of the water in the Guanabara Bay
[INPE-4761-TDL/349] N90-20445
Energy transfer between electrons and ions in collision cascades in solids
[AERE-R-13662] N90-20801

SOLSTICES
Solar cyclical trend study of the mid-latitude, quiet-time, meridional, neutral winds at winter solstice conditions
[AD-A217398] N90-20568

SOLUBILITY
Systems with a miscibility gap in the liquid state N90-20245
Advanced calcium thionyl chloride high power battery
[AD-A216685] N90-20482
A systematic study of the effects of metal substitutions for Cu in YBa(sub 2) (Cu(sub 1-x) M(sub x)3 O(sub 7-rho), M=Fe, Co, Al, Ga, Cr, Ni, and Zn
[DE90-003957] N90-20857
Theoretical and experimental study of solid phase miscibility gaps in III/V quaternary alloys
[DE90-008430] N90-20877

SONIC BOOMS
Air Force Boom Event Analyzer Recorder (BEAR): Sysstem description
[AD-A218048] N90-20800

SORPTION
CO2 diffusion and solubility in a Polystyrene/Polybutadiene block copolymer with highly oriented lamellar morphology
[AD-A217165] N90-20211

SOUND AMPLIFICATION
A continued study of optical sound generation and amplification
[AD-A217640] N90-20796

SOUND GENERATORS
A continued study of optical sound generation and amplification
[AD-A217640] N90-20796

SOUND WAVES
Modeling and classification of acoustic transients by speech recognition techniques
[AD-A218070] N90-20277
Laser-induced shock waves effects in materials
[DE90-007626] N90-20379
High-resolution acoustical imaging N90-20793
Experimental feasibility of investigating acoustic waves in Couette flow with entropy and pressure gradients
[NASA-TM-102621] N90-20795
A continued study of optical sound generation and amplification
[AD-A217640] N90-20796
The measurements of thermoacoustic phenomena using thermoacoustic couples
[AD-A218018] N90-20798

SOUTHERN OSCILLATION
Southern oscillation in the OSU coupled upper ocean/atmosphere GCM
[DE90-008415] N90-20588

SPACE EXPLORATION
Human exploration mission studies N90-20457

SPACE MISSIONS
A survey of advanced battery systems for space applications N90-20458
Advanced rechargeable sodium batteries with novel cathodes N90-20459

SPACE NAVIGATION
Microgravity conditions of a space vehicle N90-20247

SPACE PROGRAMS
Development and application of nonflammable, high-temperature beta fibers
[NASA-TM-102158] N90-20645
Reorganization of the German space administration. Foundation of DARA
[REPT-16/89] N90-20902

SPACE SHUTTLE MAIN ENGINE
Numerical simulation methods of incompressible flows and an application to the space shuttle main engine
[NASA-TM-100038] N90-20333
A parallel architecture for real-time simulation
[AD-A218321] N90-20741

SPACE SHUTTLE MISSIONS
Seeing in a new light: Astro-1 teacher's guide with activities
[NASA-EP-274] N90-20900

SPACE SHUTTLE PAYLOADS
Spacelab qualified infrared imager for microgravity science experiments
[NASA-TM-102503] N90-20352
Animation graphic interface for the space shuttle onboard computer N90-20667
VAPEPS user's reference manual, version 5.0
[NASA-CR-180781] N90-20713
Spacecraft optical contamination environment
[AD-A218088] N90-20838

SPACE SHUTTLES
Docking mechanism for spacecraft
[NASA-CASE-MSC-21386-1] N90-20126
Graphics Technology in Space Applications (GTSA 1989)
[NASA-CP-3045] N90-20651
The Real Time Display Builder (RTDB) N90-20656
Onboard shuttle on-line software requirements system: Prototype N90-20658
Tools for 3D scientific visualization in computational aerodynamics N90-20660
Animation graphic interface for the space shuttle onboard computer N90-20667
Seeing in a new light: Astro-1 teacher's guide with activities
[NASA-EP-274] N90-20900

SPACE SIMULATORS
OMV mission simulator N90-20669

SPACE STATION PAYLOADS
Space station Simulation Computer System (SCS) study for NASA/MSFC. Volume 1: Overview and summary
[NASA-CR-183840] N90-20113

SPACE STATION POWER SUPPLIES
Space Station Freedom electric power system availability study
[NASA-CR-185181] N90-20120
Model development in viscoplastic ratchetting
[NASA-TM-102509] N90-20431

SPACE STATIONS
Aerospace induction motor actuators driven from a 20-kHz power link
[NASA-TM-102482] N90-20085
Proximity operations concept design study, task 6
[NASA-CR-181971] N90-20112
Space station Simulation Computer System (SCS) study for NASA/MSFC. Volume 1: Overview and summary
[NASA-CR-183840] N90-20113
Space station Simulation Computer System (SCS) study for NASA/MSFC. Volume 2: Concept document
[NASA-CR-183841] N90-20114
Space station Simulation Computer System (SCS) study for NASA/MSFC. Volume 3: Refined conceptual design report
[NASA-CR-183842] N90-20115
Space station Simulation Computer System (SCS) study for NASA/MSFC. Volume 4: Conceptual design report
[NASA-CR-183843] N90-20116
Space station Simulation Computer System (SCS) study for NASA/MSFC. Volume 5: Study analysis report
[NASA-CR-183844] N90-20117
Space station Simulation Computer System (SCS) study for NASA/MSFC. Volume 6: Study issues report
[NASA-CR-183845] N90-20118
Space Station Freedom electric power system availability study
[NASA-CR-185181] N90-20120
Docking mechanism for spacecraft
[NASA-CASE-MSC-21386-1] N90-20126
Graphics Technology in Space Applications (GTSA 1989)
[NASA-CP-3045] N90-20651
Space Station Freedom integrated fault model N90-20673
Graphical programming and the use of simulation for space-based manipulators N90-20674
Using an instrumented manikin for Space Station Freedom analysis N90-20675
The development of the Canadian Mobile Servicing System Kinematic Simulation Facility N90-20676
SES cupola interactive display design environment N90-20679
Issues in visual support to real-time space system simulation solved in the Systems Engineering Simulator N90-20680
Real-time graphics for the Space Station Freedom cupola, developed in the Systems Engineering Simulator N90-20683

SPACE TRANSPORTATION SYSTEM FLIGHTS
Large screen display for the Mission Control Center N90-20662

SPACE WEAPONS
Assessing the morality of using the space environment as a platform for weapons
[AD-A217348] N90-20780
The thrust and parry of the SIOP (Single Integrated Operational Plan) and SDI
[AD-A217617] N90-20784
SDI (Strategic Defense Initiative): Is its future past
[DE90-008016] N90-20785
Role of free-electron lasers in strategic defense
[DE90-008028] N90-20786
SPACE-TIME FUNCTIONS
Theoretical investigations in elementary particle physics
[DE90-007178] N90-20802
SPACEBORNE ASTRONOMY
Seeing in a new light: Astro-1 teacher's guide with activities
[NASA-EP-274] N90-20900
SPACEBORNE EXPERIMENTS
A discussion of observation model, error sources and signal size for spaceborne gravitational gradiometry N90-20557
The GRADIO spaceborne gravity gradiometer: Development and accommodation N90-20560
SPACECRAFT ANTENNAS
Discrete-time control of a spacecraft with retargetable flexible antennas N90-20119
Discrete-time control of a spacecraft with retargetable flexible antennas
[AD-A218345] N90-20125
SPACECRAFT COMMUNICATION
A space-based optical communication system utilizing fiber optics
[AD-A217333] N90-20828
SPACECRAFT COMPONENTS
Short wavelength laser/materials interactions
[AD-A218015] N90-20386
SPACECRAFT CONFIGURATIONS
Sensor and actuator selection for fault-tolerant control of flexible structures
[AD-A217384] N90-20433
SPACECRAFT CONTAMINATION
Spacecraft optical contamination environment
[AD-A218088] N90-20838
SPACECRAFT CONTROL
Discrete-time control of a spacecraft with retargetable flexible antennas
[AD-A218345] N90-20125
Sensor and actuator selection for fault-tolerant control of flexible structures
[AD-A217384] N90-20433
Applications of graphics to support a testbed for autonomous space vehicle operations N90-20661
GCS plan for software aspects of certification
[NASA-CR-181972] N90-20694
SPACECRAFT DESIGN
Implications of Advanced Technologies for Air and Spacecraft Escape
[AGARD-CP-472] N90-20054
Using an instrumented manikin for Space Station Freedom analysis N90-20675
SPACECRAFT DOCKING
Docking mechanism for spacecraft
[NASA-CASE-MSC-21366-1] N90-20126
Animation graphic interface for the space shuttle onboard computer N90-20667
OMV mission simulator N90-20669
SPACECRAFT ENVIRONMENTS
Knowledge representation in space flight operations N90-20655
Spacecraft optical contamination environment
[AD-A218088] N90-20838
SPACECRAFT GUIDANCE
GCS plan for software aspects of certification
[NASA-CR-181972] N90-20694
SPACECRAFT MAINTENANCE
The development of the Canadian Mobile Servicing System Kinematic Simulation Facility N90-20676
SPACECRAFT MANEUVERS
Use of random Martian atmosphere to evaluate potential entry guidance schemes
[NASA-TM-102606] N90-20122
SPACECRAFT POWER SUPPLIES
Space Electrochemical Research and Technology (SERT), 1989
[NASA-CP-3056] N90-20454
Overview of battery usage in NASA/GSFC LEO and GEOspacecrafts N90-20455
The importance of batteries in unmanned missions N90-20456
Monolithic solid oxide fuel cell development N90-20460
A new concept for high-cycle-life LEO: Rechargeable MnO2-hydrogen N90-20462
Multi-mission Ni-H2 battery cells for the 1990's N90-20477
Sodium-sulfur battery flight experiment definition study N90-20479
SPACECRAFT PROPULSION
Advanced launch vehicle propulsion at the NASA Lewis Research Center
[NASA-TM-103096] N90-20110
Experimental proposition aboard the second data collecting satellite-SCD 2 of the MECB
[INPE-4980-RPE/606] N90-20128
SPACECRAFT STRUCTURES
Aiming control: Theory and applications to dynamic control of space structures
[AD-A217877] N90-20123
SPACECRAFT TRAJECTORIES
A satellite simulation program
[AD-A218079] N90-20124
SPACECREWS
Requirements for protective pressure suits for the Hermes spacecrew N90-20065
Space station Simulation Computer System (SCS) study for NASA/MSFC. Volume 6: Study issues report
[NASA-CR-183845] N90-20118
SPACELAB
Fusion furnaces for Spacelab N90-20248
Spacelab qualified infrared imager for microgravity science experiments
[NASA-TM-102503] N90-20352
SPALLATION
Spallation of oxide scales from 20 percent Cr/25 percent Ni/Nb stainless steel
[AERE-R-13464] N90-20189
SPARKS
Electronic precipitator control
[NASA-CASE-LAR-13273-2] N90-20320
SPATIAL DISTRIBUTION
Use of environmental monitoring data in evaluation of atmospheric modeling results
[DE90-008607] N90-20510
Parts of recognition
[AD-A217694] N90-20714
SPATIAL FILTERING
Texture segmentation using localized spatial filtering
[AD-A218064] N90-20722
SPECIFICATIONS
Pyrotechnic device technology
[DE90-007683] N90-20234
Technical specifications requirements: Automated reasoning applications
[DE90-008799] N90-20712
A locally constrained parallel activation model for diagnostic reasoning
[AD-A217808] N90-20747
CCST (Center for Compound Semiconductor Technology) research briefs
[DE90-007782] N90-20874
SPECKLE INTERFEROMETRY
Experimental validation of extended image reconstruction using bispectral speckle interferometry
[DE90-008545] N90-20171
SPECTRA
Metal alkoxides: Models for metal oxides. Alkoxide ligands in early transition metal organometallic chemistry
[DE90-007523] N90-20869
SPECTRAL BANDS
Analysis of methods to determine emisaivity for ground surface targets in the spectral band 8 to 14 microns
[INPE-4984-TDL/394] N90-20447
SPECTRAL METHODS
Spectral simulation of unsteady compressible flow past a circular cylinder
[NASA-CR-182030] N90-20050
Unsteady three-dimensional marginal separation, including breakdown
[NASA-TM-102525] N90-20337
Spectral analytic methods for the estimation of number of signals and directions of arrival
[AD-A217219] N90-20757
SPECTRAL REFLECTANCE
In-situ differential reflectance study of the etching of SiO2 films
[AD-A217186] N90-20864
SPECTRAL SENSITIVITY
In-situ differential reflectance study of the etching of SiO2 films
[AD-A217186] N90-20864
SPECTROMETERS
Optimization of digital filters for a short-scan interferometer
[AD-A217997] N90-20315
SPECTROPHOTOMETERS
Optical instrumentation support for the airborne ionospheric observatory
[AD-A218207] N90-20839
SPECTROSCOPIC ANALYSIS
Crystallography, spectroscopic analysis, and lasing properties of Nd3+:Y3Sc2Al3O12
[AD-A217792] N90-20891
SPECTROSCOPY
Chemical and electrochemical studies in ionic liquids
[AD-A217742] N90-20175
Positron annihilation spectroscopy: A nondestructive, submicroscopic characterization technique for structural polymers
[AD-A217748] N90-20226
An electrochemical and spectroscopic study of electrode processes
[AD-A217261] N90-20289
Structural comparison of nickel electrodes and precursor phases N90-20472
The application of electrochemical impedance spectroscopy for characterizing the degradation of Ni(OH)2/NiOOH electrodes N90-20474
Time-resolved spectroscopy of nonequilibrium ionization in laser-produced plasmas
[DE90-008663] N90-20854
SPECTRUM ANALYSIS
Spectral simulation of unsteady compressible flow past a circular cylinder
[NASA-CR-182030] N90-20050
Modeling and classification of acoustic transients by speech recognition techniques
[AD-A218070] N90-20277
Spectral analyses of satellite geopotential missions N90-20552
Spectral analytic methods for the estimation of number of signals and directions of arrival
[AD-A217219] N90-20757
SPECULAR REFLECTION
X ray specular reflection studies of silicon coated by organic monolayers (alkylsiloxanes)
[AD-A217418] N90-20213
Simple reflection holography
[DE90-008309] N90-20359
SPEECH RECOGNITION
Modeling and classification of acoustic transients by speech recognition techniques
[AD-A218070] N90-20277
SPHERES
Process for making a noble metal on tin oxide catalyst
[NASA-CASE-LAR-13741-1-SB] N90-20180
Mass transfer from a sphere in an oscillating flow with zero mean velocity
[NASA-TM-102566] N90-20338
SPHERICAL HARMONICS
Gravitational model improvement at the Goddard Space Flight Center N90-20514
Stabilized determination of geopotential coefficients by the mixed hom-BLUP approach N90-20520
Precise solution for a finite set of spherical coefficients from equiangular gridded data N90-20522
Modeling of the Earth's gravity field using the New Global Earth Model (NEWGEM) N90-20523
Downward continuation of the free-air gravity anomalies to the ellipsoid using the gradient solution and terrain correction: An attempt of global numerical computations N90-20541
Spectral analyses of satellite geopotential missions N90-20552
The GRADIO spaceborne gravity gradiometer: Development and accommodation N90-20560
High resolution analysis of satellite gradiometry N90-20561
Scattering sources: A spherical harmonics expansion
[DE90-008724] N90-20711
SPHEROMAKS
The impedance of energy efficiency of a coaxial magnetized plasma source used for spheromak formation and sustainment
[DE90-003220] N90-20841
SPIN DYNAMICS
F-15B high angle-of-attack phenomena and spin prediction using bifurcation analysis
[AD-A217366] N90-20073
Interior fluid dynamics of liquid-filled projectiles
[AD-A217630] N90-20330
SPIN-LATTICE RELAXATION
Copper and oxygen NMR studies on the magnetic properties of YBa2Cu3O(7-y)
[DE90-007889] N90-20863
SPINEL
Corrosion testing of candidates for the alkaline fuel cell cathode N90-20471
SPIRAL GALAXIES
M51's spiral structure
[DE90-007624] N90-20916
SPLINE FUNCTIONS
The basis spline method and associated techniques
[DE90-008403] N90-20763

SPLINES
Thin-plate spline quadrature of geodetic integrals
N90-20539
SPONTANEOUS EMISSION
Amplified spontaneous emission measurements on the aurora large-aperture module
[DE90-004841] N90-20369
SPRAYERS
Spray deposition: A fundamental study of droplet impingement, spreading and consolidation
[AD-A217202] N90-20255
SPREAD SPECTRUM TRANSMISSION
Joint Services Electronics Program research in electronics
[AD-A217745] N90-20307
SPREADING
Spray deposition: A fundamental study of droplet impingement, spreading and consolidation
[AD-A217202] N90-20255
SPUTTERING
Rolling contact fatigue of surface modified 440C using a 'Ge-Polymet' type disc rod test rig
[NASA-TM-100390] N90-20200
Physical sputtering of metallic systems by charged-particle impact
[DE90-007803] N90-20201
Reactive sputtering of molybdenum
[DE90-008307] N90-20204
A unified integrated model for sputter coating uniformity
[DE90-008322] N90-20205
STABILITY
Development of an ejection seat specification for a new fighter aircraft N90-20057
Electronic structure, alloy phase stability, and phase diagrams
[DE90-008306] N90-20203
STABILITY TESTS
A learning regulator for the plane longitudinal movement
[ETN-90-95381] N90-20695
STABILIZATION
Escape systems research at RAE N90-20058
Controllable propulsion for escape systems control N90-20064
Spacecraft escape N90-20066
Digital-flutter-suppression-system investigations for the active flexible wing wind-tunnel model
[NASA-TM-102618] N90-20093
Stabilized determination of geopotential coefficients by the mixed hom-BLUP approach N90-20520
Stabilization of high (Tc) superconductivity in cadmium sulfide
[DE90-008249] N90-20881
STAINLESS STEELS
Ageing effects in welded cast CF3 stainless steel
[AERE-R-13559] N90-20188
Spallation of oxide scales from 20 percent Cr/25 percent Ni/Nb stainless steel
[AERE-R-13464] N90-20189
STANDARDS
Nine-year aging behavior of the ceramic flatpack resonator
[DE90-008044] N90-20412
Terrestrial gravity instrumentation in the 20th Century: A brief review N90-20527
STANDING WAVES
The measurements of thermoacoustic phenomena using thermoacoustic couples
[AD-A218018] N90-20798
STARCHES
Research and development on enhanced degradable plastics
[AD-A217180] N90-20212
STATIC LOADS
Perturbation solutions in D* for buckling, vibration, and static loading of specially orthotropic plates N90-20419
STATIC MODELS
The contour model architecture and assembly language
[AD-A217114] N90-20697
STATIC TESTS
Floor pull test of a transport airframe section
[DOT/FAA/CT-TN88/14] N90-20072
Thiokol/Wasatch installation evaluation of the redesigned field joint protection system (concepts 1 and 3)
[NASA-CR-183860] N90-20127
STATISTICAL ANALYSIS
The NASA digital VGH program. Exploration of methods and final results. Volume 3: B 727 data 1978-1980: 1765 hours
[NASA-CR-181909-VOL-3] N90-20082
The NASA digital VGH program: Exploration of methods and final results. Volume 4: B 747 data 1978-1980, 1689 hours
[NASA-CR-181909-VOL-4] N90-20083
The NASA digital VGH program: Exploration of methods and final results. Volume 5: DC 10 data 1981-1982, 129 hours
[NASA-CR-181909-VOL-5] N90-20084
Statistical equipment modeling for VLSI manufacturing
[DE90-008527] N90-20304
Optimization of digital filters for a short-scan interferometer
[AD-A217997] N90-20315
Methods for local gravity field approximation N90-20532
VAPEPS user's reference manual, version 5.0
[NASA-CR-180781] N90-20713
Local moduli of continuity of some classes of Gaussian processes
[AD-A217692] N90-20778
Slepian models and regression approximations in crossing and extreme value theory
[AD-A218338] N90-20779
Fundamental studies of photon statistics
[AD-A217825] N90-20836
STATISTICAL DISTRIBUTIONS
Geology, distribution of hot springs and hydrothermal alteration zones of major geothermal areas in Japan
[DE90-753026] N90-20451
On metric entropy, Vapnik-Chervonenkis dimension, and learnability for a class of distributions
[AD-A217331] N90-20759
STEADY FLOW
Unsteady three-dimensional marginal separation, including breakdown
[NASA-TM-102525] N90-20337
STEAM TURBINES
Innovative turbine concepts for open-cycle OTEC (Ocean Thermal Energy Conversion)
[DE90-000315] N90-20493
STEELS
Tellurium embrittlement of type 316 steel
[AERE-R-13440] N90-20192
Design and processing of strong-tough microcomposite steels
[DE90-007764] N90-20197
Evaluation of material homogeneity as a function of thickness of low-alloy ferritic steel
[DE90-008069] N90-20202
STEERABLE ANTENNAS
Discrete-time control of a spacecraft with retargetable flexible antennas N90-20119
Effects of additional interfering signals on adaptive array performance
[NASA-CR-186508] N90-20271
STELLAR RADIATION
The inter-outburst behavior of cataclysmic variables
[NASA-CR-186374] N90-20914
STELLARATORS
The ANU (Australian National University) Heliac Program
[DE90-006620] N90-20843
STEREOSCOPIC VISION
Stereo feature matching in disparity space
[AD-A218170] N90-20751
Location recognition using stereo vision
[AD-A218218] N90-20752
STILBENE
Polymer liquid crystals with side chain discogens
[AD-A218013] N90-20228
STIRLING CYCLE
Phase 1 supplemental development of a kinematic Stirling/Rankine commercial gas-fired heat pump system
[PB90-129974] N90-20483
STOCHASTIC PROCESSES
Stochastic approach to the initiation of pitting corrosion
[AERE-R-13348] N90-20190
On the existence of local times: A geometric study
[AD-A218337] N90-20776
Homogeneous chaos, p-forms, scaling and the feynman integral
[AD-A218339] N90-20777
Slepian models and regression approximations in crossing and extreme value theory
[AD-A218338] N90-20779
STOICHIOMETRY
High temperature chemistry of oxide superconductors
[DE90-007821] N90-20875
STOPPING POWER
Stopping power for protons in Al for the whole range of velocities
[DE90-008558] N90-20810
STORAGE BATTERIES
Life-cycle cost comparisons of advanced storage batteries and fuel cells for utility, stand-alone, and electric vehicle applications
[DE90-008090] N90-20298
A survey of advanced battery systems for space applications N90-20458
The electrochemical generation of useful chemical species from lunar materials N90-20461
A new concept for high-cycle-life LEO: Rechargeable MnO2-hydrogen N90-20462
STORAGE STABILITY
Nickel-hydrogen capacity loss on storage N90-20478
STORAGE TANKS
System for venting gas from a liquid storage tank
[NASA-CASE-MSC-21253-1] N90-20254
STORMS
Coastal frontogenesis and associated severe weather on 13 March 1986 (GALE IOP 13)
[AD-A217708] N90-20590
A sub-cloud layer vorticity budget analysis for two microburst-producing storms from jaws dual-Doppler data
[AD-A218180] N90-20599
STORMS (METEOROLOGY)
Analysis of GALE (Genesis of Atlantic Lows Experiment) data
[AD-A217182] N90-20584
STRAIN DISTRIBUTION
A 4-node assumed-stress hybrid shell element with rotational degrees of freedom
[NASA-CR-4279] N90-20422
STRAIN ENERGY METHODS
Spallation of oxide scales from 20 percent Cr/25 percent Ni/Nb stainless steel
[AERE-R-13464] N90-20189
STRATEGY
Strategies for high efficiency operation of the E-beam excited atomic xenon laser using high-power and high-energy loading
[DE90-005196] N90-20370
Space in warfare
[AD-A217527] N90-20782
STRATOCUMULUS CLOUDS
A modeling study of the cloud-topped marine boundary layer
[AD-A218103] N90-20594
STRATOSPHERE
The receiving system of a dual dye lidar to study molecular and aerosol densities at the base of the stratosphere
[AD-A218286] N90-20581
STRESS (PHYSIOLOGY)
Windblast protection for advanced ejection seats N90-20063
Field assessment of wet bulb globe temperature: Present and future
[AD-A218224] N90-20635
Effective calibration of heat flux transducers for experimental use
[AD-A218262] N90-20636
Comparison of light duty gloves with natural and synthetic materials under wet and dry conditions
[AD-A218119] N90-20649
STRESS (PSYCHOLOGY)
Information gathering and decisionmaking under stress
[AD-A218233] N90-20643
STRESS ANALYSIS
Through-thickness strain response of thick composites in compression
[AD-A217233] N90-20141
Optimization of laminated composite plates
[AD-A217621] N90-20146
Model development in viscoplastic ratchetting
[NASA-TM-102509] N90-20431
Innovative turbine concepts for open-cycle OTEC (Ocean Thermal Energy Conversion)
[DE90-000315] N90-20493
STRESS CONCENTRATION
Oxygen concentrations on surfaces of carbon fibers
[AD-A217724] N90-20152
STRESS CORROSION
Evaluation of 2090-T8E48 aluminum-lithium plates
[AD-A217262] N90-20196
The stress corrosion performance of diffusion bonded nickel base alloys
[DE90-008130] N90-20199
STRESS CORROSION CRACKING
Evaluation of 2090-T8E48 aluminum-lithium plates
[AD-A217262] N90-20196
The stress corrosion performance of diffusion bonded nickel base alloys
[DE90-008130] N90-20199

STRESS DISTRIBUTION
A 4-node assumed-stress hybrid shell element with rotational degrees of freedom
[NASA-CR-4279] N90-20422
Residual stresses: A review of their measurement and interpretation using x ray diffraction
[AERE-R-13005] N90-20423
The stress-driven redistribution of point defects in the vicinity of crack-like singularities
[AERE-R-12898] N90-20424
Stress field near crack tip: An experimental evaluation of the three dimensional variation
[AD-A217878] N90-20441
STRESS INTENSITY FACTORS
Fatigue crack growth in martensitic 2 1/4Cr-1Mo steel at elevated temperatures
[AERE-R-13524] N90-20191
Through-the-thickness fatigue crack closure behavior in an aluminum alloy
[NASA-TM-102590] N90-20427
STRESS-STRAIN RELATIONSHIPS
Optimization of fracture resistance in composites
[AD-A217431] N90-20144
STRESSES
A method for measuring the material moduli of granular materials: Flow in an orthogonal rheometer
[DE90-007160] N90-20339
Seismic characterization of fracture properties
[DE90-007759] N90-20570
STRING THEORY
Superstring field theory
[DE90-007694] N90-20897
STRIP TRANSMISSION LINES
Experimental investigations on channelized coplanar waveguide
[NASA-TM-102494] N90-20286
STRONGLY COUPLED PLASMAS
Nonlinear stability in fluid and plasma dynamics
[AD-A217735] N90-20856
STRONTIUM COMPOUNDS
Synthesis of Bi-Sr-Ca-Cu oxide superconductor by solution technique
[DE90-008707] N90-20888
STRUCTURAL ANALYSIS
Analysis of flow-, thermal-, and structural-interaction of hypersonic structures subjected to severe aerodynamic heating
[AD-A217882] N90-20053
Extended x ray absorption fine structure analysis applied to composite materials
[DE90-008575] N90-20150
An electrochemical and spectroscopic study of electrode processes
[AD-A217261] N90-20289
Comparison of two matrix data structures for advanced CSM testbed applications
[NASA-CR-181951] N90-20421
A 4-node assumed-stress hybrid shell element with rotational degrees of freedom
[NASA-CR-4279] N90-20422
Limitations and applications of fracture assessment with R6
[AERE-R-13012] N90-20425
Evaluation of an adaptive unstructured remeshing technique for integrated fluid-thermal-structural analysis
[NASA-TM-102611] N90-20426
Automated finite element modeling and simulation N90-20753
STRUCTURAL DESIGN
Development and fabrication of structural components for a scramjet engine
[NASA-CR-181945] N90-20088
Design and performance of a multi-stage cylindrical reconnection launcher
[DE90-007820] N90-20108
A progress report on the Livermore Miniature Vacuum Tube Project
[DE90-008302] N90-20299
Space mechanism of low velocity for an array of solar panels: Analysis and design of an experimental model; dimensions of bearings
[INPE-4859-TDL/370] N90-20390
STRUCTURAL FAILURE
Limitations and applications of fracture assessment with R6
[AERE-R-13012] N90-20425
STRUCTURAL PROPERTIES (GEOLOGY)
Underwater physiography of the continental shelf of Rio Grande do Norte visible through satellite imagery
[INPE-4964-TDL/392] N90-20448
A system for analysis and interpretation of lineaments in remote sensing images
[INPE-4893-PRE/1494] N90-20565
The effects of structure and source complexity on waveforms: Crustal structure of Tibet and the recovery of complex seismic sources
[AD-A218202] N90-20579
STRUCTURAL STABILITY
Floor pull test of a transport airframe section
[DOT/FAA/CT-TN88/14] N90-20072
Limitations and applications of fracture assessment with R6
[AERE-R-13012] N90-20425
STRUCTURAL STRAIN
Through-thickness strain response of thick composites in compression
[AD-A217233] N90-20141
STRUCTURAL VIBRATION
Active control of the forced and transient response of a finite beam
[NASA-CR-181957] N90-20430
Computational simulation of damping in composite structures
[NASA-TM-102567] N90-20432
STUDENTS
A long-term retention advantage for spatial information learned naturally and in the laboratory
[AD-A218268] N90-20644
SUBMILLIMETER WAVES
Conference digest: Thirteenth International Conference on Infrared and Millimeter Waves, volume 1039
[AD-A217343] N90-20291
SUBSONIC FLOW
Application of a three-dimensional Navier-Stokes model for a subsonic jet in a crossflow N90-20045
A matrix-free locally-implicit scheme for Navier-Stokes equations
[AD-A218298] N90-20349
SUBSONIC WIND TUNNELS
A data acquisition parallel bus for wind tunnels at ARL (Aeronautical Research Laboratory)
[AD-A218052] N90-20098
SUBSTITUTES
A systematic study of the effects of metal substitutions for Cu in YBa(sub 2) (Cu(sub 1-x) M(sub x)3 O(sub 7-rho), M=Fe, Co, Al, Ga, Cr, Ni, and Zn
[DE90-003957] N90-20857
SUBSTRATES
Process for making a noble metal on tin oxide catalyst
[NASA-CASE-LAR-13741-1-SB] N90-20180
Wetting of metallic carbides by non-reactive liquid metals
[AERE-M-3759] N90-20185
Refractive index profiles of thermally grown and chemically vapor deposited films on silicon
[AD-A217187] N90-20865
SUMMER
Controlling Summer Heat Islands: Proceedings
[DE90-008075] N90-20508
SUN
Distributed earth model/orbiter simulation N90-20671
SUPERCOMPUTERS
An improved error assessment for the GEM-T1 gravitational model N90-20518
Tools for 3D scientific visualization in computational aerodynamics N90-20660
Efficient utilization of graphics technology for space animation N90-20663
Supercomputer environments
[AD-A217682] N90-20689
Computer Science and Technology Board
[DE90-008292] N90-20690
SUPERCONDUCTING FILMS
Millimeter wave surface resistance of RBa2Cu3O(7-delta) (R=Y,Eu,Dy,Sm,Er) superconductors
[NASA-TM-102571] N90-20886
SUPERCONDUCTING MAGNETS
Evaluation of industrial magnetic heat pump/refrigerator concepts that utilize superconducting magnets
[DE90-008093] N90-20258
SUPERCONDUCTIVITY
Materials Science Programs, fiscal year 1989
[DE90-008169] N90-20131
Processing, fabrication, characterization and device demonstration of high temperature superconducting ceramics
[AD-A218330] N90-20231
Superconductive microprobes for eddy current evaluation of materials
[AD-A217776] N90-20361
High resolution transmission electron microscopy study of defect structures in mixed-phase YBaCuO
[DE90-007767] N90-20873
Stabilization of high (Tc) superconductivity in cadmium sulfide
[DE90-008249] N90-20881
Millimeter wave surface resistance of RBa2Cu3O(7-delta) (R=Y,Eu,Dy,Sm,Er) superconductors
[NASA-TM-102571] N90-20886
Technology assessment of superconductivity
[AD-A217697] N90-20889
SUPERCONDUCTORS
Symposium on High Temperature and Materials Chemistry
[DE90-008047] N90-20148
Processing, fabrication, characterization and device demonstration of high temperature superconducting ceramics
[AD-A218330] N90-20231
Superconductive microprobes for eddy current evaluation of materials
[AD-A217776] N90-20361
Ultra-high brightness laser research at LLNL (Lawrence Livermore National Laboratory)
[DE90-008366] N90-20885
Millimeter wave surface resistance of RBa2Cu3O(7-delta) (R=Y,Eu,Dy,Sm,Er) superconductors
[NASA-TM-102571] N90-20886
Synthesis and properties of polycrystalline Tl2Ba2CaCu2O(x) and Tl2Ba2Ca2Cu3O(x)
[DE90-007528] N90-20887
Synthesis of Bi-Sr-Ca-Cu oxide superconductor by solution technique
[DE90-008707] N90-20888
Technology assessment of superconductivity
[AD-A217697] N90-20889
SUPERCOOLING
Principles of metallic solidification N90-20241
Supercooling and germ formation N90-20242
SUPERGRAVITY
Theoretical investigations in elementary particle physics
[DE90-007178] N90-20802
SUPERHIGH FREQUENCIES
Wideband S band transmitter
[AD-A217620] N90-20295
SUPERLATTICES
Studies of the structure and properties of organic monolayers, multilayers and superlattices
[DE90-008330] N90-20129
CCST (Center for Compound Semiconductor Technology) research briefs
[DE90-007782] N90-20874
SUPERSONIC AIRCRAFT
Passive venting technique for shallow cavities
[NASA-CASE-LAR-14031-1] N90-20079
SUPERSONIC COMBUSTION RAMJET ENGINES
Development and fabrication of structural components for a scramjet engine
[NASA-CR-181945] N90-20088
SUPERSONIC FLOW
Numerical simulations of supersonic flow through oscillating cascade sections
[NASA-TM-103100] N90-20051
Compression pylon
[NASA-CASE-LAR-13777-1] N90-20078
SUPERSONIC INLETS
Comparison of 3-D viscous flow computations of Mach 5 inlet with experimental data
[NASA-TM-102518] N90-20090
SUPERSONIC WIND TUNNELS
Comparison of 3-D viscous flow computations of Mach 5 inlet with experimental data
[NASA-TM-102518] N90-20090
DURIP optical equipment for high-speed viscous-inviscid interaction research
[AD-A217772] N90-20345
SUPPORTS
Design of a high angle of attack robotic sting mount for tests in a low speed wind tunnel
[AD-A218105] N90-20099
Tensile film clamps and mounting block for the rheovibron and autovibron viscoelastometer
[NASA-CASE-LAR-13696-1] N90-20409
SURFACE FINISHING
Crystal preparation at LBL, 1976 to 1986
[DE90-007754] N90-20871
SURFACE PROPERTIES
Studies of the structure and properties of organic monolayers, multilayers and superlattices
[DE90-008330] N90-20129
Oxygen concentrations on surfaces of carbon fibers
[AD-A217724] N90-20152
Rolling contact fatigue of surface modified 440C using a 'Ge-Polymet' type disc rod test rig
[NASA-TM-100390] N90-20200
Ceramic oxide thin film formation utilizing biological processes
[DE90-008599] N90-20225

Design and calibration of a vacuum compatible scanning tunneling microscope
[NASA-TM-102514] N90-20353
Magnetic properties of surfaces and interfaces
[DE90-007348] N90-20789
An ellipsometric measurement of optical properties for InP surfaces
[AD-A217185] N90-20827

SURFACE ROUGHNESS
Simulation of radar scattering from rough surfaces
[AD-A217841] N90-20275

SURFACE TEMPERATURE
Design and test of a compact optics system for the pool boiling experiment
[NASA-TM-102530] N90-20253
Analysis of methods to determine emissivity for ground surface targets in the spectral band 8 to 14 microns
[INPE-4984-TDL/394] N90-20447
An intercomparison of general circulation model predictions of regional climate change
[DE90-008325] N90-20589

SURFACE VEHICLES
Robotic mobility system: Road following algorithms
[AD-A218107] N90-20748

SURFACE WATER
Utilization of LANDSAT-5 and NOAA-9 satellite imagery in the identification of physical-chemical parameters of the water in the Guanabara Bay
[INPE-4761-TDL/349] N90-20445

SURGERY
Laser-produced plasmas in medicine
[DE90-007623] N90-20849

SURGES
Deep level transient spectroscopy in resistive layers
[DE90-008349] N90-20169

SURVEILLANCE
Tomographic processing of synthetic aperture radar signals for enhanced resolution
[AD-A217178] N90-20265

SURVEYS
Synthesis and analysis of 25 years (1961-1986) of INPE/SRE activities related to the vegetation/forest area
[INPE-4969-RPE/604] N90-20446
A survey of advanced battery systems for space applications N90-20458
Synopsis of early field test results from the gravity gradiometer survey system N90-20525
The Rapid Geodetic Survey System (RGSS) N90-20528
First year's results and field experience with the latest JILA absolute gravimeter N90-20529
Treatment of geodetic leveling in the integrated geodesy approach N90-20546

SURVIVAL
Implications of Advanced Technologies for Air and Spacecraft Escape
[AGARD-CP-472] N90-20054

SUSPENDING (HANGING)
Swing-free movement of simply suspended objects employing parameter estimation
[DE90-002238] N90-20398

SUSPENDING (MIXING)
Enhancement of mass transfer to a rotating cylinder electrode by inert particles suspended in the electrolyte
[DE90-008054] N90-20165
A simple multicomponent fluid theory with accurate physics
[DE90-006537] N90-20334
Hydrodynamic interactions and transport coefficients in a suspension of spherical particles
[DE90-008301] N90-20336

SWEPTBACK WINGS
Aeroelastic characteristics of aircraft with circulation control wings N90-20070

SWIRLING
Vortex motion phase separator for zero gravity liquid transfer
[NASA-CASE-KSC-11387-1] N90-20236

SWITCHES
Interaction of switch actuation on tracking with a four-axis flight control (cross-coupling)
[AD-A217981] N90-20095
Electron-impact ionization and electron attachment cross sections of radicals important in transient gaseous discharges
[AD-A217510] N90-20366
New methods in plasma simulation
[DE90-007507] N90-20847

SWITCHING
Optical Bistability, 1988
[AD-A217681] N90-20832

SWITCHING CIRCUITS
An electron-beam controlled semiconductor switch
[AD-A217181] N90-20288

SYMBOLIC PROGRAMMING
An investigation of the locality of memory accesses during symbolic program execution
[AD-A218168] N90-20750

SYNCHROTRON RADIATION
X ray microimaging by diffractive techniques
[DE90-008444] N90-20356
Design of D-3 He commercial tokamak
[DE90-008252] N90-20852

SYNTHESIS (CHEMISTRY)
The 1-(diorganooxyphosphonyl)-methyl)-2,4- and -2,6-diamido benzenes
[NASA-CASE-ARC-11425-4] N90-20133
Analytical electron microscopy of catalyst preparations
[DE90-008699] N90-20173
Process for making a noble metal on tin oxide catalyst
[NASA-CASE-LAR-13741-1-SB] N90-20180
An investigation of the mechanisms of solid state powder reaction in the combustion synthesis and sintering of high temperature materials
[DE90-007880] N90-20198
Human serum albumin crystals and method of preparation
[NASA-CASE-MFS-28234-1] N90-20616
Development of gamma-emitting, receptor-binding radiotracers for imaging the brain and pancreas
[DE90-008314] N90-20621
Synthesis and properties of polycrystalline Tl2Ba2CaCu2O(x) and Tl2Ba2Ca2Cu3O(x)
[DE90-007528] N90-20887
Synthesis of Bi-Sr-Ca-Cu oxide superconductor by solution technique
[DE90-008707] N90-20888

SYNTHETIC APERTURE RADAR
Tomographic processing of synthetic aperture radar signals for enhanced resolution
[AD-A217178] N90-20265

SYNTHETIC APERTURES
Shaping the insonifying pulse to optimise B-scans obtained in austenite
[AERE-R-13518] N90-20187

SYNTHETIC FUELS
Design and operation of an outdoor microalgae test facility
[DE89-009493] N90-20608

SYSTEMS ANALYSIS
A guide to performing and documenting safety analyses
[DE90-008688] N90-20261
Using formal methods to develop a paradigm for software design
[DE90-005633] N90-20703

SYSTEMS ENGINEERING
Potential role of avionics in escape systems N90-20060
Proximity operations concept design study, task 6
[NASA-CR-181971] N90-20112
Space station Simulation Computer System (SCS) study for NASA/MSFC. Volume 2: Concept document
[NASA-CR-183841] N90-20114
A linear filtering technique for removal of low-frequency noise
[DE90-006183] N90-20296
The CMU Reconfigurable Modular Manipulator System
[CMU-RI-TR-88-7] N90-20388
Operational computer graphics in the flight dynamics environment N90-20668
Space Station Freedom integrated fault model N90-20673
SES cupola interactive display design environment N90-20679
Issues in visual support to real-time space system simulation solved in the Systems Engineering Simulator N90-20680
History of visual systems in the Systems Engineering Simulator N90-20681
Computer image generation: Reconfigurability as a strategy in high fidelity space applications N90-20682
Real-time graphics for the Space Station Freedom cupola, developed in the Systems Engineering Simulator N90-20683
The Orbital Maneuvering Vehicle Training Facility visual system concept N90-20684
Design decision making with multiple interacting criteria and varying relative weights
[AD-A218027] N90-20721
Towards SDS (Strategic Defense System) testing and evaluation: A collection of relevant topics
[AD-A217610] N90-20783

SYSTEMS INTEGRATION
Experimental proposition aboard the second data collecting satellite-SCD 2 of the MECB
[INPE-4980-RPE/606] N90-20128
Flexible automatic discrete parts assembly
[AD-A217401] N90-20256
The Real Time Display Builder (RTDB) N90-20656

SYSTEMS SIMULATION
Graphics Technology in Space Applications (GTSA 1989)
[NASA-CP-3045] N90-20651
Issues in visual support to real-time space system simulation solved in the Systems Engineering Simulator N90-20680
History of visual systems in the Systems Engineering Simulator N90-20681
Computer image generation: Reconfigurability as a strategy in high fidelity space applications N90-20682

T

TACTICS
Brain activity during tactical decision-making. Part 3: Relationships between probe-evoked potentials, simulation performance, and on-job performance
[AD-A217207] N90-20638

TAIWAN
Determination of mean gravity anomalies in the Taiwan Island N90-20547

TAKEOFF
Airplane takeoff and landing performance monitoring system
[NASA-CASE-LAR-13734-1-CU] N90-20096

TARGET RECOGNITION
Multi-dimensional LADAR tracking and adaptive grasping for spaceborne assembly of SDI (Strategic Defense Initiative) platforms
[AD-A218236] N90-20279
Algorithms for optimal processing of polarimetric radar data
[AD-A217330] N90-20758
Modification, testing, and calibration of infrared search and target designator hardware received from NSWC
[AD-A217920] N90-20837

TARGETS
Analysis of methods to determine emissivity for ground surface targets in the spectral band 8 to 14 microns
[INPE-4984-TDL/394] N90-20447

TASK COMPLEXITY
Aiding the decision maker: Perceptual and cognitive issues at the human-machine interface
[AD-A217862] N90-20648

TASKS
Human task animation from performance models and natural language input N90-20678

TATB
Condensed phase kinetic deuterium isotope effects in high energy phenomena: Mechanistic investigations and relationships
[AD-A217161] N90-20156

TDR SATELLITES
OMV mission simulator N90-20669

TEARING MODES (PLASMAS)
Spontaneous magnetic reconnection in a turbulent plasma N90-20840

TECHNOLOGICAL FORECASTING
An integrative research review of the relationship between technology and structure: A meta-analytic synthesis
[AD-A218115] N90-20903

TECHNOLOGIES
An integrative research review of the relationship between technology and structure: A meta-analytic synthesis
[AD-A218115] N90-20903
ONR (Office of Naval Research) summer scholars for the 1989 PREFACE Program
[AD-A217746] N90-20919

TECHNOLOGY ASSESSMENT
Pyrotechnic device technology
[DE90-007663] N90-20234
Technology assessment of video teleconferencing
[AD-A217318] N90-20266
Exploratory battery technology development and testing report for 1988
[DE90-007996] N90-20297
Solar thermal program summary, fiscal year 1989
[DE89-009475] N90-20487
Assessment of crew workload measurement methods, techniques and procedures. Volume 1: Process, methods and results
[AD-A217699] N90-20647
Technology assessment of superconductivity
[AD-A217697] N90-20889

TECTONICS
The effects of structure and source complexity on waveforms: Crustal structure of Tibet and the recovery of complex seismic sources
[AD-A218202] N90-20579

TELECONFERENCING
Technology assessment of video teleconferencing
[AD-A217318] N90-20266

TELEMETRY
The Real Time Display Builder (RTDB) N90-20656
Operational computer graphics in the flight dynamics environment N90-20668
TELEOPERATORS
Multi-dimensional LADAR tracking and adaptive grasping for spaceborne assembly of SDI (Strategic Defense Initiative) platforms
[AD-A218236] N90-20279
Design of a telerobotic controller with joint torque sensors
[DE90-008753] N90-20404
Graphics Technology in Space Applications (GTSA 1989)
[NASA-CP-3045] N90-20651
The use of graphics in the design of the human-telerobot interface N90-20670
TELESCOPES
Placement of multiple apertures for imaging telescopes
[DE90-006991] N90-20833
Design and performance analysis of adaptive optical telescopes using laser guide stars
[AD-A218025] N90-20913
TELLURIUM
Tellurium embrittlement of type 316 steel
[AERE-R-13440] N90-20192
TEMPERATURE CONTROL
Modification, testing, and calibration of infrared search and target designator hardware received from NSWC
[AD-A217920] N90-20837
TEMPERATURE DEPENDENCE
Ultrastructure processing of ordered polymers
[AD-A218331] N90-20232
TEMPERATURE DISTRIBUTION
Design and test of a compact optics system for the pool boiling experiment
[NASA-TM-102530] N90-20253
Structure and dynamics of the Arizona monsoon boundary
[AD-A217378] N90-20586
TEMPERATURE EFFECTS
Evaluation of thermal and mechanical loading effects on the structural behavior of a SiC/titanium composite
[NASA-TM-102536] N90-20139
Fundamental aspects of and failure modes in high-temperature composites
[NASA-TM-102558] N90-20151
Experimental investigation of the thermocapillary migration of water droplets in butylbenzoate
[MPIS-14/1988] N90-20155
Effect of heat treatment on the fracture toughness transition properties of an A508 class 3 steel
[AERE-R-13548] N90-20182
Hydrogen, thermal ageing and the role of carbides in fatigue of a high strength steel
[AERE-R-13599] N90-20183
Fluorinated diamond thin films for tribological applications
[AD-A217452] N90-20214
Tensile fracture toughness of ceramic materials: Effects of dynamic loading and elevated temperatures
[DE90-008329] N90-20223
The effect of moisture absorption in clothing on the human heat balance
[AD-A217899] N90-20626
Study of possible solar heating effects on thermosonde probes: Error analysis
[AD-A218116] N90-20917
TEMPERATURE GRADIENTS
Experimental feasibility of investigating acoustic waves in Couette flow with entropy and pressure gradients
[NASA-TM-102621] N90-20795
The measurements of thermoacoustic phenomena using thermoacoustic couples
[AD-A218018] N90-20798
TEMPERATURE INVERSIONS
An aircraft investigation of a convective boundary layer over Lake Michigan
[AD-A218175] N90-20598
TEMPERATURE MEASUREMENT
Spacelab qualified infrared imager for microgravity science experiments
[NASA-TM-102503] N90-20352
A nonintrusive method for measuring the operating temperature of a solenoid-operated valve
[DE90-007576] N90-20355
Applications of microwave radiometric measurements to infer tropical cyclone intensity and strength
[AD-A218273] N90-20600
TEMPERATURE PROFILES
Microwave brightness temperature and its relation to atmospheric general circulation features
[AD-A218312] N90-20603
TENSILE CREEP
Improved toughness alloys based on titanium aluminides
[AD-A218149] N90-20208
TENSILE DEFORMATION
Laser-induced shock waves effects in materials
[DE90-007626] N90-20379
TENSILE PROPERTIES
Ageing effects in welded cast CF3 stainless steel
[AERE-R-13559] N90-20188
The ageing effect of the matrix-reinforcement interface on the ageing response of an aluminium 6061 alloy reinforced with 20vol percent SiC particulates
[AERE-R-13361] N90-20193
Evaluation of 2090-T8E48 aluminum-lithium plates
[AD-A217262] N90-20196
Tensile film clamps and mounting block for the rheovibron and autovibron viscoelastometer
[NASA-CASE-LAR-13696-1] N90-20409
TENSILE STRENGTH
Mechanical properties of pure nickel alloys after long term exposures to LiOH and vacuum at 775 K
[NASA-TM-102403] N90-20181
Tensile fracture toughness of ceramic materials: Effects of dynamic loading and elevated temperatures
[DE90-008329] N90-20223
TENSILE STRESS
Ultrastructure processing of ordered polymers
[AD-A218331] N90-20232
Experiments on buckling and critical buckling. Behavior of carbon fiber reinforced plastic shells submitted to tensile stresses
[ETN-90-95382] N90-20429
TERMINAL BALLISTICS
Evaluation of 2090-T8E48 aluminum-lithium plates
[AD-A217262] N90-20196
TERRAIN
A split-and-merge method for creating polygonal homogeneous-vegetation regions from digitized terrain data
[AD-A218080] N90-20453
Simulation of landscape disturbances and the effect of climatic change
[DE90-007565] N90-20503
The use of high-resolution terrain data in gravity field prediction N90-20533
TERRAIN ANALYSIS
Fourier transform methods in local gravity modeling N90-20538
Three-dimensional route planning for a cruise missile for minimal detection by observer
[AD-A218336] N90-20787
TEST FACILITIES
High-Explosives Applications Facility (HEAF)
[DE90-008122] N90-20257
Nine-year aging behavior of the ceramic flatpack resonator
[DE90-008044] N90-20412
Diagnostic development and support of MHD (Magnetohydrodynamics) test facilities
[DE90-004969] N90-20845
TEST STANDS
Analysis of small-scale rotor hover performance data
[NASA-TM-102271] N90-20325
TETRAHEDRONS
Component count and preliminary assembly considerations for large space truss structures
[NASA-TM-102604] N90-20121
TEXTURES
Texture segmentation using localized spatial filtering
[AD-A218064] N90-20722
THEMATIC MAPPING
Evaluation of TM/LANDSAT and HRV/SPOT data in the identification of reforested areas in the Mogi-Guacu (SP) region
[INPE-4874-PRE/1485] N90-20442
Utilization of LANDSAT-5 and NOAA-9 satellite imagery in the identification of physical-chemical parameters of the water in the Guanabara Bay
[INPE-4761-TDL/349] N90-20445
THEOREMS
Euler's theorem for polynomials
[AD-A218148] N90-20774
THEORETICAL PHYSICS
Studies of high energy phenomena using muons
[DE90-008272] N90-20820
The Inevitable Universe: Parker-Rhodes' peculiar mixture of ontology and physics
[DE90-006453] N90-20915
THERMAL ANALYSIS
Evaluation of an adaptive unstructured remeshing technique for integrated fluid-thermal-structural analysis
[NASA-TM-102611] N90-20426
THERMAL BLOOMING
Nonlinear optics in thin films
[AD-A217336] N90-20829
THERMAL BOUNDARY LAYER
Geometric scale of interaction between moving shock and stationary thermal layer
[AD-A217769] N90-20344
THERMAL CONDUCTIVITY
The thermal response of generic objects in JP-4 pool fires
[DE90-008503] N90-20259
Core cooling studies at LLNL (Lawrence Livermore National Laboratory) and Sandia
[DE90-008303] N90-20300
Area Over Length (AOL): A program for the calculation of effective two-dimensional thermal conductance through an arbitrarily shaped region
[DE90-008005] N90-20335
A nonintrusive method for measuring the operating temperature of a solenoid-operated valve
[DE90-007576] N90-20355
High temperature chemistry of oxide superconductors
[DE90-007821] N90-20875
An experimental investigation of the thermal conductivity of porous adsorbents
[AD-A217854] N90-20899
THERMAL CYCLING TESTS
NRL hybrid reliability. Physics of failure initial study
[AD-A217986] N90-20893
THERMAL DEGRADATION
Study of possible solar heating effects on thermosonde probes: Error analysis
[AD-A218116] N90-20917
THERMAL DIFFUSIVITY
Difference in electron thermal diffusivity and profile between interior and exterior of TFTR L-mode plasmas
[DE90-007479] N90-20846
THERMAL ENVIRONMENTS
Hydrogen, thermal ageing and the role of carbides in fatigue of a high strength steel
[AERE-R-13599] N90-20183
THERMAL FATIGUE
The metallurgical mechanisms of solder fatigue
[DE90-008390] N90-20206
THERMAL INSTABILITY
Measurement of the stimulated thermal Rayleigh scattering instability
[DE90-007849] N90-20376
THERMAL NOISE
Analysis of radiometer calibration effects with TOUCHSTONE
[NASA-CR-186476] N90-20284
THERMAL PROTECTION
Development and fabrication of structural components for a scramjet engine
[NASA-CR-181945] N90-20088
THERMAL RADIATION
An experimental investigation of the thermal conductivity of porous adsorbents
[AD-A217854] N90-20899
THERMAL STABILITY
Ring expansion and equilibration in organophosphazenes, and the relationship to polymerization
[AD-A218234] N90-20230
THERMAL STRESSES
Optimization of fracture resistance in composites
[AD-A217431] N90-20144
Magnetic vapor shield mechanism for protection of material surfaces exposed to high heat load
[AD-A217667] N90-20217
THERMOCHEMISTRY
Determination of fundamental thermodynamic properties of constituent materials and performance screening of candidate systems
[AD-A218089] N90-20153
Condensed phase kinetic deuterium isotope effects in high energy phenomena: Mechanistic investigations and relationships
[AD-A217161] N90-20156
THERMODYNAMIC COUPLING
The measurements of thermoacoustic phenomena using thermoacoustic couples
[AD-A218018] N90-20798
THERMODYNAMIC EQUILIBRIUM
Theory of defect process: Basic issues in quantitative understanding
[AERE-R-13661] N90-20860
THERMODYNAMIC PROPERTIES
Determination of fundamental thermodynamic properties of constituent materials and performance screening of candidate systems
[AD-A218089] N90-20153
Condensed phase kinetic deuterium isotope effects in high energy phenomena: Mechanistic investigations and relationships
[AD-A217161] N90-20156

Electronic structure, alloy phase stability, and phase diagrams
[DE90-008306] N90-20203
The measurements of thermoacoustic phenomena using thermoacoustic couples
[AD-A218018] N90-20798

THERMODYNAMICS
Evaluation of thermal and mechanical loading effects on the structural behavior of a SiC/titanium composite
[NASA-TM-102536] N90-20139
Techno-economic assessment of a carbothermic alumina reduction process
[DE90-007018] N90-20170
A unified integrated model for sputter coating uniformity
[DE90-008322] N90-20205
Core cooling studies at LLNL (Lawrence Livermore National Laboratory) and Sandia
[DE90-008303] N90-20300
A nonintrusive method for measuring the operating temperature of a solenoid-operated valve
[DE90-007576] N90-20355
A technical and economic evaluation of oxygen-enriched combustion in diesel engines using water-emulsified fuels
[DE90-008095] N90-20394
Analysis of methods to determine emissivity for ground surface targets in the spectral band 8 to 14 microns
[INPE-4984-TDL/394] N90-20447
Coastal frontogenesis and associated severe weather on 13 March 1986 (GALE IOP 13)
[AD-A217708] N90-20590
A case study of a quasi-stationary tropical convective line
[AD-A218325] N90-20604
Theoretical and experimental study of solid phase miscibility gaps in III/V quaternary alloys
[DE90-008430] N90-20877

THERMOELASTICITY
An approximation theory for the identification of linear thermoelastic systems
[NASA-CR-182015] N90-20764

THERMOELECTRIC POWER GENERATION
Thermoelectric conversion with ion conductors
[AD-A217822] N90-20497

THERMOREGULATION
Influence of theobromine on heat production and body temperatures in cold-exposed humans: A preliminary report
[AD-A217203] N90-20618
The effect of moisture absorption in clothing on the human heat balance
[AD-A217899] N90-20626
Hydration effects on human physiology and exercise-heat performance
[AD-A217969] N90-20629

THERMOSPHERE
USU center of excellence in theory and analysis of the geo-plasma environment
[AD-A217736] N90-20101

THICK PLATES
Through-thickness strain response of thick composites in compression
[AD-A217233] N90-20141

THICKNESS
Optimization of laminated composite plates
[AD-A217621] N90-20146
Evaluation of material homogeneity as a function of thickness of low-alloy ferritic steel
[DE90-008069] N90-20202
Through-the-thickness fatigue crack closure behavior in an aluminum alloy
[NASA-TM-102590] N90-20427

THIN FILMS
Studies of the structure and properties of organic monolayers, multilayers and superlattices
[DE90-008330] N90-20129
Symposium on High Temperature and Materials Chemistry
[DE90-008047] N90-20148
Mechanisms of reactive etching
[AD-A217679] N90-20160
Hydrous metal oxide-supported catalysts. Part 1: Preparation chemistry and physical and chemical properties
[DE90-007607] N90-20161
Deep level transient spectroscopy in resistive layers
[DE90-008349] N90-20169
Infrared and X ray photoelectron spectroscopy studies of the polyimide/metal interface
[AD-A218249] N90-20179
Reactive sputtering of molybdenum
[DE90-008307] N90-20204
X ray specular reflection studies of silicon coated by organic monolayers (alkylsiloxanes)
[AD-A217418] N90-20213
Fluorinated diamond thin films for tribological applications
[AD-A217452] N90-20214
Ceramic oxide thin film formation utilizing biological processes
[DE90-008599] N90-20225
Polymer liquid crystals with side chain discogens
[AD-A218013] N90-20228
All-solid-state thin-film rechargeable lithium batteries using solid redox polymerization electrodes
[DE90-008665] N90-20306
CuInSe2 and CdTe: Scale-up for manufacturing
[DE89-009503] N90-20489
Dielectric composite thin films
[AD-A217940] N90-20791
Surface-plasmon enhanced nonlinear photoelectric emission from thin silver films
[DE90-007676] N90-20807
An ellipsometric measurement of optical properties for InP surfaces
[AD-A217185] N90-20827
Nonlinear optics in thin films
[AD-A217336] N90-20829
Chemically prepared PZT films doped with niobium
[DE90-006811] N90-20859
Refractive index profiles of thermally grown and chemically vapor deposited films on silicon
[AD-A217187] N90-20865
Molecular organization and electrical properties of mixed Langmuir-Blodgett multilayer thin films of polypyrrole
[DE90-007627] N90-20870
Millimeter wave surface resistance of RBa2Cu3O(7-delta) (R=Y,Eu,Dy,Sm,Er) superconductors
[NASA-TM-102571] N90-20886
Growth, characterization and device development in monocrystalline diamond films
[AD-A218211] N90-20895

THIN PLATES
Thin-plate spline quadrature of geodetic integrals N90-20539

THREADS
Investigation into the mechanism of polymer thread drag reduction
[AD-A217492] N90-20329

THREE DIMENSIONAL COMPOSITES
Through-thickness strain response of thick composites in compression
[AD-A217233] N90-20141

THREE DIMENSIONAL MODELS
Application of a three-dimensional Navier-Stokes model for a subsonic jet in a crossflow N90-20045
Unsteady three-dimensional marginal separation, including breakdown
[NASA-TM-102525] N90-20337
Finite element models to predict the structural response of 120-mm sabot/rods during launch
[DE90-007497] N90-20436
Distributed earth model/orbiter simulation N90-20671
Recent advances in 3D finite difference mesh generation using the BRL-CAD package
[DE90-007854] N90-20704

THRUST VECTOR CONTROL
Spacecraft escape N90-20066

THUNDERSTORMS
Forecasting the tornadic intensities of thunderstorms by multivariate techniques
[AD-A218284] N90-20602
A case study of a quasi-stationary tropical convective line
[AD-A218325] N90-20604

TIME DEPENDENCE
Time-dependent failure of silver interlayer welds
[DE90-008015] N90-20440

TIME SERIES ANALYSIS
Damage characteristics of time domain histories
[DE90-008787] N90-20573

TIME SHARING
A data acquisition parallel bus for wind tunnels at ARL (Aeronautical Research Laboratory)
[AD-A218052] N90-20098

TIN OXIDES
Process for making a noble metal on tin oxide catalyst
[NASA-CASE-LAR-13741-1-SB] N90-20180

TITANIUM
High efficiency flashlamp-pumped titanium: Sapphire laser
[AD-A217598] N90-20367
Flash-pumped titanium laser
[AD-A217599] N90-20368
L shell XANES (X ray Absorption Near Edge Structure) for solid metals: Ti, V, Cr, Fe, Ni, Cu
[DE90-008043] N90-20880

TITANIUM ALLOYS
Improved toughness alloys based on titanium aluminides
[AD-A218149] N90-20208

TITANIUM CHLORIDES
TiCl4 as a source of TiO2 particles for laser anemometry measurements in hot gas
[NASA-TM-102581] N90-20358

TITANIUM COMPOUNDS
Sol-gel derived polytitanosiloxane coatings
[DE90-004186] N90-20210

TITANIUM OXIDES
TiCl4 as a source of TiO2 particles for laser anemometry measurements in hot gas
[NASA-TM-102581] N90-20358

TOKAMAK DEVICES
Computation of coupling elements between waveguides and modes for large launching structures
[IPPCZ-290] N90-20842
Enhanced pinch effect due to electrostatic potential
[DE90-007088] N90-20844
High elongation plasmas
[DE90-007575] N90-20848
Materials and selection criteria analysis for the compact ignition tokamak toroidal field coil turn-to-turn insulation system: Photographic summary oflaboratory testing
[DE90-008020] N90-20850
Particle transport in pellet fueled JET (Jet European Torus) plasmas
[DE90-008077] N90-20851
Design of D-3 He commercial tokamak
[DE90-008252] N90-20852

TOLERANCES (PHYSIOLOGY)
A comparison of the mechanisms of cold- and microgravity-induced fluid loss
[AD-A218098] N90-20631

TOMOGRAPHY
Tomographic processing of synthetic aperture radar signals for enhanced resolution
[AD-A217178] N90-20265
Three-dimensional medical image analysis using local dynamic algorithm selection on a multiple-instruction, multiple-data architecture
[AD-A218024] N90-20630

TOOLING
Development and fabrication of structural components for a scramjet engine
[NASA-CR-181945] N90-20088

TOPEX
Refinement of Earth's gravity field with Topex GPS measurements N90-20553

TOPOGRAPHY
Design and calibration of a vacuum compatible scanning tunneling microscope
[NASA-TM-102514] N90-20353
Simulation of landscape disturbances and the effect of climatic change
[DE90-007565] N90-20503
Gravitational model improvement at the Goddard Space Flight Center N90-20514
Geopotential coefficient determination and the gravimetric boundary value problem: A new approach N90-20521
First year's results and field experience with the latest JILA absolute gravimeter N90-20529
Critique of the vertical gradient of gravity N90-20531
The role of topography in geodetic gravity field modelling N90-20534
High resolution analysis of satellite gradiometry N90-20561

TORNADOES
Forecasting the tornadic intensities of thunderstorms by multivariate techniques
[AD-A218284] N90-20602

TOROIDAL PLASMAS
Materials and selection criteria analysis for the compact ignition tokamak toroidal field coil turn-to-turn insulation system: Photographic summary oflaboratory testing
[DE90-008020] N90-20850

TORQUE
Space mechanism of low velocity for an array of solar panels: Analysis and design of an experimental model; dimensions of bearings
[INPE-4859-TDL/370] N90-20390
Design of a telerobotic controller with joint torque sensors
[DE90-008753] N90-20404

TORSION
Constitutive data acquisition and modelling in aluminium 2014 alloy
[AERE-R-13651] N90-20186
On free products of torsion free abelian groups
[AD-A218146] N90-20773

TOXICITY
Development of a laser fluorosensor for the aircraft supported analysis of maritime toxic agents loads: Definition phase
[ETN-90-95320] N90-20499
Acute oral toxicity of JA-2 solid propellant in ICR mice
[AD-A217264] N90-20609
Acute oral toxicity of DIGL-RP solid propellant in ICR mice
[AD-A217711] N90-20613
Acute oral toxicity of DIGL-RP solid propellant in Sprague-Dawley rats
[AD-A217712] N90-20614
A review of the literature on the toxicity of rare-earth metals as it pertains to the engineering demonstration system surrogate testing
[DE90-008049] N90-20620
TOXICOLOGY
Acute oral toxicity of JA-2 solid propellant in ICR mice
[AD-A217264] N90-20609
TRACE ELEMENTS
Development of gamma-emitting, receptor-binding radiotracers for imaging the brain and pancreas
[DE90-008314] N90-20621
TRACKING (POSITION)
Interaction of switch actuation on tracking with a four-axis flight control (cross-coupling)
[AD-A217981] N90-20095
High resolution analysis of satellite gradiometry N90-20561
Implementation of midcourse tracking and correlation on massively parallel computers
[DE90-008166] N90-20740
TRADEOFFS
Performance tradeoffs in multithreaded processors
[AD-A217123] N90-20729
TRAINING DEVICES
Ejection seat training of jet pilots and weapon system officers at the German Air Force School of Aviation Medicine N90-20061
Prototype part task trainer: A remote manipulator system simulator N90-20672
TRAINING SIMULATORS
Space station Simulation Computer System (SCS) study for NASA/MSFC. Volume 1: Overview and summary
[NASA-CR-183840] N90-20113
Space station Simulation Computer System (SCS) study for NASA/MSFC. Volume 2: Concept document
[NASA-CR-183841] N90-20114
Space station Simulation Computer System (SCS) study for NASA/MSFC. Volume 4: Conceptual design report
[NASA-CR-183843] N90-20116
Space station Simulation Computer System (SCS) study for NASA/MSFC. Volume 5: Study analysis report
[NASA-CR-183844] N90-20117
Space station Simulation Computer System (SCS) study for NASA/MSFC. Volume 6: Study issues report
[NASA-CR-183845] N90-20118
Graphics Technology in Space Applications (GTSA 1989)
[NASA-CP-3045] N90-20651
The Orbital Maneuvering Vehicle Training Facility visual system concept N90-20684
TRAJECTORIES
Escape systems research at RAE N90-20058
Swing-free movement of simply suspended objects employing parameter estimation
[DE90-002238] N90-20398
Parameter-scheduled trajectory planning for suppression of coupled horizontal and vertical vibrations in a flexible rod
[DE90-002313] N90-20435
Periodic trajectories for two-dimensional nonintegrable Hamiltonians
[DE90-008082] N90-20765
TRAJECTORY ANALYSIS
Use of random Martian atmosphere to evaluate potential entry guidance schemes
[NASA-TM-102606] N90-20122
TRAJECTORY CONTROL
The CMU Reconfigurable Modular Manipulator System
[CMU-RI-TR-88-7] N90-20388
Parameter-scheduled trajectory planning for suppression of coupled horizontal and vertical vibrations in a flexible rod
[DE90-002313] N90-20435
TRAJECTORY OPTIMIZATION
Optimal, impulsive, time-fixed orbital rendezvous and interception with path constraints N90-20102
ETO (Earth-To-Orbit): A trajectory program for aerospace vehicles
[AD-A218157] N90-20103
Trajectory optimization in the presence of constraints
[AD-A218271] N90-20104
Three-dimensional route planning for a cruise missile for minimal detection by observer
[AD-A218336] N90-20787
TRANSATMOSPHERIC VEHICLES
Hypersonic waverider configurations for trans-atmospheric vehicles
[AD-A217925] N90-20074
TRANSCENDENTAL FUNCTIONS
Some remarks on solutions of Fermats last equation in terms of Wright's hypergeometric function
[AD-A218066] N90-20771
TRANSDUCERS
Effective calibration of heat flux transducers for experimental use
[AD-A218262] N90-20636
TRANSFER FUNCTIONS
Shaping the insonifying pulse to optimise B-scans obtained in austenite
[AERE-R-13518] N90-20187
Design and testing of a noninteracting control loop for the dynamically tuned dry gyro
[NAL-TR-1017] N90-20350
TRANSIENT RESPONSE
Active control of the forced and transient response of a finite beam
[NASA-CR-181957] N90-20430
TRANSISTORS
Measurement of proton induced radiation damage to CMOS transistors and pin diodes
[DE90-007836] N90-20283
Transistor and solid-state technology: A historical development
[AD-A218141] N90-20317
TRANSMISSION CIRCUITS
Investigation of tapered multiple microstrip lines for VLSI circuits
[AD-A217855] N90-20310
TRANSMISSION LINES
Technology assessment of video teleconferencing
[AD-A217318] N90-20266
TRANSMITTERS
Velocity matched optical transmitter
[AD-A217413] N90-20830
TRANSONIC FLOW
A matrix-free locally-implicit scheme for Navier-Stokes equations
[AD-A218298] N90-20349
TRANSPIRATION
Transpiration cooling in hypersonic flight
[NASA-CR-186435] N90-20052
TRANSPORT PROPERTIES
Electronic and ionic transport in processable conducting polymers
[AD-A218093] N90-20229
Hydrodynamic interactions and transport coefficients in a suspension of spherical particles
[DE90-008301] N90-20336
TRAVELING WAVE MODULATION
GaAs traveling-wave optical modulators using modulated coplanar electrodes with periodic cross-tie overlays
[AD-A217731] N90-20835
TREES (MATHEMATICS)
Binary space partitioning trees and their uses N90-20657
TRENDS
Fighter escape system: The next step forward N90-20059
Power conditioning techniques
[NASA-TM-102577] N90-20301
Joint Japanese-American Workshop on Future Trends in Logic Programming
[DE90-008343] N90-20709
TRIBOLOGY
Experimentally determined wear behavior of an Al2O3-SiC composite from 25 to 1200 C
[NASA-TM-102549] N90-20130
Fluorinated diamond thin films for tribological applications
[AD-A217452] N90-20214
Tribological properties of boric acid and boric-acid-forming surfaces. Part 2: Formation and self-lubrication mechanisms of boric acid films on boron- and boric-oxide-containing surfaces
[DE90-005632] N90-20400
Tribological properties of boric acid and boric acid forming surfaces. Part 1: Crystal chemistry and self-lubricating mechanism of boric acid
[DE90-005665] N90-20401
TRINITROTOLUENE
Condensed phase kinetic deuterium isotope effects in high energy phenomena: Mechanistic investigations and relationships
[AD-A217161] N90-20156
TRIODES
A progress report on the Livermore Miniature Vacuum Tube Project
[DE90-008302] N90-20299
TROPICAL REGIONS
Cloud types and the tropical Earth radiation budget, revised
[NASA-CR-180475] N90-20582
A case study of a quasi-stationary tropical convective line
[AD-A218325] N90-20604
TROPICAL STORMS
The invertibility principle for a simple hurricane model
[AD-A218344] N90-20605
TRUSSES
Component count and preliminary assembly considerations for large space truss structures
[NASA-TM-102604] N90-20121
TURBINE BLADES
Heat transfer near the entrance to a film cooling hole in a gas turbine blade
[AD-A217396] N90-20089
A comparison of two-and three-dimensional S809 airfoil properties for rough and smooth HAWT (Horizontal-Axis Wind Tunnel) rotor operation
[DE89-009512] N90-20492
Innovative turbine concepts for open-cycle OTEC (Ocean Thermal Energy Conversion)
[DE90-000315] N90-20493
TURBOFAN ENGINES
In-line wear monitor
[AD-A217799] N90-20091
TURBOJET ENGINES
The implementation and operation of a variable-response electronic throttle control system for a TF-104G aircraft
[NASA-TM-101696] N90-20086
TURBOMACHINERY
An applicational process for dynamic balancing of turbomachinery shafting
[NASA-TM-102537] N90-20392
Rotordynamic analysis with shell elements for the transfer matrix method
[AD-A217455] N90-20434
GRID2D/3D: A computer program for generating grid systems in complex-shaped two- and three-dimensional spatial domains. Part 2: User's manual and program listing
[NASA-TM-102454] N90-20708
TURBOPROP AIRCRAFT
Noise of a simulated installed model counterrotation propeller at angle-of-attack and takeoff/approach conditions
[NASA-TM-102440] N90-20794
TURBULENCE
Mark 3 interferometer
[AD-A217188] N90-20912
TURBULENCE EFFECTS
Spontaneous magnetic reconnection in a turbulent plasma N90-20840
TURBULENCE MODELS
Comparison of 3-D viscous flow computations of Mach 5 inlet with experimental data
[NASA-TM-102518] N90-20090
A study of low-dimensional models for the wall region of a turbulent boundary layer N90-20321
TURBULENT BOUNDARY LAYER
A study of low-dimensional models for the wall region of a turbulent boundary layer N90-20321
The effect of adverse pressure gradient on turbulent burst structure in low-Reynolds number equilibrium boundary layers
[AD-A217308] N90-20327
Theoretical modeling studies of the marine planetary
[AD-A217200] N90-20567
Correlation of atmospheric optical turbulence and meteorological measurements
[AD-A218019] N90-20576
A modeling study of the cloud-topped marine boundary layer
[AD-A218103] N90-20594
An aircraft investigation of a convective boundary layer over Lake Michigan
[AD-A218175] N90-20598
A case study of a quasi-stationary tropical convective line
[AD-A218325] N90-20604
TURBULENT FLOW
A study of low-dimensional models for the wall region of a turbulent boundary layer N90-20321
Nonintrusive optical measurements of turbulence and mixing in a stably stratified fluid N90-20322
A numerical investigation of the compressible mixing layer
[AD-A217738] N90-20343

Numerical modeling of airblast
[AD-A217993] N90-20347
Flow visualization studies in a curved rectangular channel with 40 to 1 aspect ratio and a straight channel with bulk flow unsteadiness
[AD-A218020] N90-20348
Correlation of atmospheric optical turbulence and meteorological measurements
[AD-A218019] N90-20576
An aircraft investigation of a convective boundary layer over Lake Michigan
[AD-A218175] N90-20598
The role of chaos in hemispheric process and attention
[AD-A217674] N90-20639

TURBULENT MIXING
Nonintrusive optical measurements of turbulence and mixing in a stably stratified fluid N90-20322
DURIP optical equipment for high-speed viscous-inviscid interaction research
[AD-A217772] N90-20345

TURING MACHINES
Computational complexity of random access models
[AD-A217685] N90-20701

TWO DIMENSIONAL BOUNDARY LAYER
Heat transfer near the entrance to a film cooling hole in a gas turbine blade
[AD-A217396] N90-20089

TWO DIMENSIONAL FLOW
Characterization of fluid flow by digital correlation of scattered light
[NASA-CR-186403] N90-20324

TWO DIMENSIONAL MODELS
Finite element models to predict the structural response of 120-mm sabot/rods during launch
[DE90-007497] N90-20436

TYPHOONS
Forecasting 24 and 48 hour intensity changes, for northwestern Pacific tropical cyclones, using satellite imagery
[AD-A218174] N90-20597

U

UH-60A HELICOPTER
Plan, formulate, and discuss a NASTRAN finite element model of the UH-60A helicopter airframe
[NASA-CR-181975] N90-20439

ULTRAHIGH FREQUENCIES
Wideband S band transmitter
[AD-A217620] N90-20295

ULTRASONIC FLAW DETECTION
The diffraction of ultrasound by cracks: Comparison of experiment with theory
[AERE-R-13334] N90-20410

ULTRASONIC TESTS
Residual stresses: A review of their measurement and interpretation using x ray diffraction
[AERE-R-13005] N90-20423

ULTRASONICS
Shaping the insonifying pulse to optimise B-scans obtained in austenite
[AERE-R-13518] N90-20187
Three-dimensional medical image analysis using local dynamic algorithm selection on a multiple-instruction, multiple-data architecture
[AD-A218024] N90-20630

ULTRAVIOLET RADIATION
The inter-outburst behavior of cataclysmic variables
[NASA-CR-186374] N90-20914

UNDERGROUND EXPLOSIONS
A linear filtering technique for removal of low-frequency noise
[DE90-006183] N90-20296

UNDERWATER PHOTOGRAPHY
Underwater physiography of the continental shelf of Rio Grande do Norte visible through satellite imagery
[INPE-4964-TDL/392] N90-20448

UNIQUENESS THEOREM
A general existence and uniqueness theorem for implicit differential-algebraic equations
[AD-A217965] N90-20770

UNITED STATES
United States Historical Climatology Network (HCN) serial temperature and precipitation data
[DE90-008029] N90-20506

UNIVERSAL TIME
Discrete-time control of a spacecraft with retargetable flexible antennas
[AD-A218345] N90-20125

UNIVERSITIES
Microgravity Science and Application Program tasks, 1989 revision
[NASA-TM-4191] N90-20252

UNIX (OPERATING SYSTEM)
Implementation of a control system test environment in UNIX
[DE90-007485] N90-20736

UNSTEADY AERODYNAMICS
Unsteady free-wake viscous aerodynamic analysis of helicopter rotors
[AD-A217166] N90-20048
Aeroelastic characteristics of aircraft with circulation control wings N90-20070
Numerical simulation methods of incompressible flows and an application to the space shuttle main engine
[NASA-TM-100038] N90-20333

UNSTEADY FLOW
Spectral simulation of unsteady compressible flow past a circular cylinder
[NASA-CR-182030] N90-20050
Mass transfer from a sphere in an oscillating flow with zero mean velocity
[NASA-TM-102566] N90-20338
Experimental investigation of the mechanisms underlying vortex kinematics in unsteady separated flows
[AD-A217889] N90-20346
Flow visualization studies in a curved rectangular channel with 40 to 1 aspect ratio and a straight channel with bulk flow unsteadiness
[AD-A218020] N90-20348

UPPER ATMOSPHERE
An aircraft investigation of a convective boundary layer over Lake Michigan
[AD-A218175] N90-20598

URBAN DEVELOPMENT
Processes of community development and responses of ecosystems to climate change
[DE90-008640] N90-20512

USER MANUALS (COMPUTER PROGRAMS)
ETO (Earth-To-Orbit): A trajectory program for aerospace vehicles
[AD-A218157] N90-20103
Numerical Arc Segmentation Algorithm for a Radio Conference-NASARC (version 4.0) technical manual
[NASA-TM-101453] N90-20264
Small and great circle routines
[AD-A217652] N90-20449
User's guide: Programs for processing altimeter data over inland seas
[NASA-TM-100730] N90-20572
GRID2D/3D: A computer program for generating grid systems in complex-shaped two- and three-dimensional spatial domains. Part 2: User's manual and program listing
[NASA-TM-102454] N90-20708
VAPEPS user's reference manual, version 5.0
[NASA-CR-180781] N90-20713
Optimization of series expressions. Part 1: User's manual for the series macro package
[AD-A218220] N90-20725

USER REQUIREMENTS
Proximity operations concept design study, task 6
[NASA-CR-181971] N90-20112
ARISTOTELES: A European approach for an Earth gravity field recovery mission N90-20559

V

VACUUM
Design and calibration of a vacuum compatible scanning tunneling microscope
[NASA-TM-102514] N90-20353

VACUUM MELTING
Bearing and gear steels for aerospace applications
[NASA-TM-102529] N90-20391

VACUUM TUBES
A progress report on the Livermore Miniature Vacuum Tube Project
[DE90-008302] N90-20299

VALVES
A nonintrusive method for measuring the operating temperature of a solenoid-operated valve
[DE90-007576] N90-20355
Analyses of power consumption for two sliding vane type compressors
[AD-A218366] N90-20406

VANADIUM
L shell XANES (X ray Absorption Near Edge Structure) for solid metals: Ti, V, Cr, Fe, Ni, Cu
[DE90-008043] N90-20880

VAPOR DEPOSITION
Interface science in deformation processing of ceramics
[DE90-008424] N90-20219
High power semiconductor laser arrays by metalorganic chemical vapor deposition N90-20363
Electron beam induced damage in PECVD Si3N4 and SiO2 films on InP
[NASA-TM-102544] N90-20393
Molecular dynamics and spectroscopy at gas-solid interfaces
[AD-A217743] N90-20813
An ellipsometric measurement of optical properties for InP surfaces
[AD-A217185] N90-20827
Refractive index profiles of thermally grown and chemically vapor deposited films on silicon
[AD-A217187] N90-20865
Growth, characterization and device development in monocrystalline diamond films
[AD-A218211] N90-20895

VAPOR PHASES
Structure of model gas flames in nitramines
[AD-A217578] N90-20159
Dynamics of electronically excited species in gaseous and condensed phase
[AD-A217696] N90-20812

VAPORS
Characterization of ceramic matrix composites fabricated by chemical vapor infiltration
[DE90-008409] N90-20149
Magnetic vapor shield mechanism for protection of material surfaces exposed to high heat load
[AD-A217667] N90-20217

VARIATIONAL PRINCIPLES
A 4-node assumed-stress hybrid shell element with rotational degrees of freedom
[NASA-CR-4279] N90-20422
Generalized quasi-variational inequality and implicit complementarity problems
[AD-A215191] N90-20755
Termolecular associations of ions in gases, recombination and electron-atom collisions
[AD-A217678] N90-20805

VECTOR ANALYSIS
Simulation of radar scattering from rough surfaces
[AD-A217841] N90-20275
Modeling and classification of acoustic transients by speech recognition techniques
[AD-A218070] N90-20277
Analysis of heliport environmental data: Indianapolis downtown heliport, Wall Street heliport. Volume 3: Indianapolis downtown heliport data plots
[AD-A217412] N90-20500

VECTOR PROCESSING (COMPUTERS)
Supercomputer environments
[AD-A217682] N90-20689
(DURIP) Two-Processor Alliant FX/4 System
[AD-A217810] N90-20692

VEGETATION
Synthesis and analysis of 25 years (1961-1986) of INPE/SRE activities related to the vegetation/forest area
[INPE-4969-RPE/604] N90-20446
A split-and-merge method for creating polygonal homogeneous-vegetation regions from digitized terrain data
[AD-A218080] N90-20453

VELOCITY
Stopping power for protons in Al for the whole range of velocities
[DE90-008558] N90-20810

VELOCITY DISTRIBUTION
Nonintrusive optical measurements of turbulence and mixing in a stably stratified fluid N90-20322
TiCl4 as a source of TiO2 particles for laser anemometry measurements in hot gas
[NASA-TM-102581] N90-20358

VELOCITY MEASUREMENT
Nonintrusive optical measurements of turbulence and mixing in a stably stratified fluid N90-20322
The effect of adverse pressure gradient on turbulent burst structure in low-Reynolds number equilibrium boundary layers
[AD-A217308] N90-20327

VENTILATION
An expert system for the design of heating, ventilating, and air-conditioning systems
[AD-A218287] N90-20262

VENTING
Passive venting technique for shallow cavities
[NASA-CASE-LAR-14031-1] N90-20079
System for venting gas from a liquid storage tank
[NASA-CASE-MSC-21253-1] N90-20254

VERTICAL ORIENTATION
Critique of the vertical gradient of gravity N90-20531

VERY LARGE SCALE INTEGRATION
Product assurance technology for procuring reliable, radiation-hard, custom LSI/VLSI electronics
[NASA-CR-185954] N90-20281

ISITE: Automatic circuit synthesis for double-metal CMOS VLSI (Very Large Scale Integrated) circuits
[AD-A217459] N90-20292
Statistical equipment modeling for VLSI manufacturing
[DE90-008527] N90-20304
Investigation of tapered multiple microstrip lines for VLSI circuits
[AD-A217855] N90-20310
Integrated circuits for avionics
[AD-A217964] N90-20312

VHSIC (CIRCUITS)
VHSIC Hardware Description Language (VHDL) benchmark suite
[AD-A217947] N90-20719

VIBRATION
Evaluation of thermal and mechanical loading effects on the structural behavior of a SiC/titanium composite
[NASA-TM-102536] N90-20139
Perturbation solutions in D* for buckling, vibration, and static loading of specially orthotropic plates N90-20419
Parameter-scheduled trajectory planning for suppression of coupled horizontal and vertical vibrations in a flexible rod
[DE90-002313] N90-20435

VIBRATION DAMPING
Digital-flutter-suppression-system investigations for the active flexible wing wind-tunnel model
[NASA-TM-102618] N90-20093
Tensile film clamps and mounting block for the rheovibron and autovibron viscoelastometer
[NASA-CASE-LAR-13696-1] N90-20409
Active control of the forced and transient response of a finite beam
[NASA-CR-181957] N90-20430
Computational simulation of damping in composite structures
[NASA-TM-102567] N90-20432

VIBRATION EFFECTS
Ionic disorder in crystals at high temperatures with emphasis on fluorites
[AERE-R-13544] N90-20862

VIBRATION MODE
Experimental feasibility of investigating acoustic waves in Couette flow with entropy and pressure gradients
[NASA-TM-102621] N90-20795

VIBRATION TESTS
Complex demodulation for bearing fault detection
[AD-A218367] N90-20407

VIBRATIONAL SPECTRA
Vibrational spectroscopy of boron nitride at high temperatures and pressures
[DE90-008633] N90-20172
Laser enhanced chemical reactions
[DE90-008273] N90-20377
Reactive and anisotropic elastic scattering of highly laser-vibration-excited diatomic molecules
[MPIS-19/1988] N90-20804

VIBRATIONAL STRESS
Complex demodulation for bearing fault detection
[AD-A218367] N90-20407
VAPEPS user's reference manual, version 5.0
[NASA-CR-180781] N90-20713

VIDEO COMMUNICATION
Technology assessment of video teleconferencing
[AD-A217318] N90-20266

VIDEO EQUIPMENT
The design and implementation of a position measuring system for a remotely controlled video camera
[AD-A218077] N90-20362
Engineering visualization utilizing advanced animation N90-20664
Multi-tasking computer control of video related equipment N90-20665

VIDEO SIGNALS
Issues in visual support to real-time space system simulation solved in the Systems Engineering Simulator N90-20680
The Orbital Maneuvering Vehicle Training Facility visual system concept N90-20684

VIRTUAL MEMORY SYSTEMS
An investigation of the locality of memory accesses during symbolic program execution
[AD-A218168] N90-20750

VISCOELASTICITY
The viscoelasticity of curing thermosets
[DE90-006535] N90-20221
Tensile film clamps and mounting block for the rheovibron and autovibron viscoelastometer
[NASA-CASE-LAR-13696-1] N90-20409

VISCOPLASTICITY
Model development in viscoplastic ratchetting
[NASA-TM-102509] N90-20431

VISCOSITY
Hydrodynamic interactions and transport coefficients in a suspension of spherical particles
[DE90-008301] N90-20336

VISCOUS DRAG
Hypersonic waverider configurations for trans-atmospheric vehicles
[AD-A217925] N90-20074

VISCOUS FLOW
Viscous shock profiles and primitive formulations
[NASA-CR-182029] N90-20049
Analysis of flow-, thermal-, and structural-interaction of hypersonic structures subjected to severe aerodynamic heating
[AD-A217882] N90-20053
Comparison of 3-D viscous flow computations of Mach 5 inlet with experimental data
[NASA-TM-102518] N90-20090
Parallel algorithms in the finite element approximation of flow problems
[AD-A217729] N90-20341
DURIP optical equipment for high-speed viscous-inviscid interaction research
[AD-A217772] N90-20345
Numerical modeling of airblast
[AD-A217993] N90-20347

VISUAL ACUITY
Detection acuity in the peripheral retina
[AD-A218183] N90-20632

VISUAL PERCEPTION
Multi-dimensional LADAR tracking and adaptive grasping for spaceborne assembly of SDI (Strategic Defense Initiative) platforms
[AD-A218236] N90-20279
The role of chaos in hemispheric process and attention
[AD-A217674] N90-20639
The boundaries of hemispheric processing in visual pattern recognition
[AD-A217675] N90-20640
Lateral asymmetry in pattern recognition: Understanding the effects of familiarity, distinction, and perspective change
[AD-A217739] N90-20641
Parts of recognition
[AD-A217694] N90-20714

VISUAL STIMULI
Detection acuity in the peripheral retina
[AD-A218183] N90-20632

VITERBI DECODERS
Advanced modulation technology development for earth station demodulator applications. Coded modulation system development
[NASA-CR-185149] N90-20270

VOICE COMMUNICATION
Technology assessment of video teleconferencing
[AD-A217318] N90-20266
Comparison of oculometer and head-fixed reticle with voice or switch and touch panel for data entry on a generic tactical air combat display
[AD-A217231] N90-20646

VOLUME
A study of physical properties of ODPA-p-PDA polyimide films
[NASA-TM-102625] N90-20137

VORTICES
A video-based experimental investigation of wing rock
[AD-A218244] N90-20075
Vortex motion phase separator for zero gravity liquid transfer
[NASA-CASE-KSC-11387-1] N90-20236
Experimental investigation of the mechanisms underlying vortex kinematics in unsteady separated flows
[AD-A217889] N90-20346
Flow visualization studies in a curved rectangular channel with 40 to 1 aspect ratio and a straight channel with bulk flow unsteadiness
[AD-A218020] N90-20348

VORTICITY
A sub-cloud layer vorticity budget analysis for two microburst-producing storms from jaws dual-Doppler data
[AD-A218180] N90-20599

VULNERABILITY
A paradoxical result in unconditionally secure authentication codes, and an explanation
[DE90-008529] N90-20710

W

WAFERS
Radiation-hardened wafer scale integration
[AD-A217332] N90-20290
Identification of defects in SOI (Silicon-On-Insulator) wafers
[DE90-006020] N90-20879

WAKES
Unsteady free-wake viscous aerodynamic analysis of helicopter rotors
[AD-A217166] N90-20048
Spectral simulation of unsteady compressible flow past a circular cylinder
[NASA-CR-182030] N90-20050

WALL FLOW
A study of low-dimensional models for the wall region of a turbulent boundary layer N90-20321

WARFARE
Assessing the morality of using the space environment as a platform for weapons
[AD-A217348] N90-20780
Space in warfare
[AD-A217527] N90-20782

WASTE DISPOSAL
Information management systems for integrating the technical data and regulatory requirements of environmental restoration activities
[DE90-008622] N90-20511

WATER
Experimental investigation of the thermocapillary migration of water droplets in butylbenzoate
[MPIS-14/1988] N90-20155
Developments in solar photocatalysis for destruction of organics in water
[DE90-007685] N90-20162
A technical and economic evaluation of oxygen-enriched combustion in diesel engines using water-emulsified fuels
[DE90-008095] N90-20394

WATER BALANCE
Hypobaric hypoxia (380 torr) decreases intracellular and total body water in goats
[AD-A218192] N90-20615

WATER POLLUTION
Development of a laser fluorosensor for the aircraft supported analysis of maritime toxic agents loads: Definition phase
[ETN-90-95320] N90-20499

WATER TREATMENT
Advanced on-site power plant development technology program
[DE90-000443] N90-20484

WATERSHEDS
Hypotheses testing of watershed/landscape dynamics in northern Alaska using digital analysis
[DE90-006721] N90-20450

WAVE FUNCTIONS
The basis spline method and associated techniques
[DE90-008403] N90-20763

WAVE INTERACTION
Cell averaging Chebyshev methods for hyperbolic problems
[NASA-CR-182028] N90-20768

WAVE PROPAGATION
Nonlinear optics in thin films
[AD-A217336] N90-20829

WAVE RESISTANCE
Millimeter wave surface resistance of RBa2Cu3O(7-delta) (R=Y,Eu,Dy,Sm,Er) superconductors
[NASA-TM-102571] N90-20886

WAVEFORMS
The effects of structure and source complexity on waveforms: Crustal structure of Tibet and the recovery of complex seismic sources
[AD-A218202] N90-20579
Air Force Boom Event Analyzer Recorder (BEAR): Sysstem description
[AD-A218048] N90-20800

WAVEGUIDES
Experimental investigations on channelized coplanar waveguide
[NASA-TM-102494] N90-20286
Computation of coupling elements between waveguides and modes for large launching structures
[IPPCZ-290] N90-20842

WAVELENGTHS
Stabilized determination of geopotential coefficients by the mixed hom-BLUP approach N90-20520

WAVERIDERS
Hypersonic waverider configurations for trans-atmospheric vehicles
[AD-A217925] N90-20074

WEAPON SYSTEMS
Ejection seat training of jet pilots and weapon system officers at the German Air Force School of Aviation Medicine N90-20061
Brain activity during tactical decision-making. Part 3: Relationships between probe-evoked potentials, simulation performance, and on-job performance
[AD-A217207] N90-20638

WEAR
In-line wear monitor
[AD-A217799] N90-20091
Experimentally determined wear behavior of an Al2O3-SiC composite from 25 to 1200 C
[NASA-TM-102549] N90-20130
Tribological properties of boric acid and boric-acid-forming surfaces. Part 2: Formation and self-lubrication mechanisms of boric acid films on boron- and boric-oxide-containing surfaces
[DE90-005632] N90-20400
WEATHER
Spectral solar radiation data base documentation, volume 1
[DE89-009447] N90-20571
Coastal frontogenesis and associated severe weather on 13 March 1986 (GALE IOP 13)
[AD-A217708] N90-20590
Continental shelf processes affecting the oceanography of the South Atlantic Bight
[DE90-008439] N90-20606
WEATHER FORECASTING
Analysis of GALE (Genesis of Atlantic Lows Experiment) data
[AD-A217182] N90-20584
Derivation of kinematic fields using wind profiler data from the 1985 pre-storm experiment
[AD-A217952] N90-20592
A prototype expert system to forecast severe winds in the western Mediterranean Sea
[AD-A218017] N90-20593
Forecasting 24 and 48 hour intensity changes, for northwestern Pacific tropical cyclones, using satellite imagery
[AD-A218174] N90-20597
Forecasting the tornadic intensities of thunderstorms by multivariate techniques
[AD-A218284] N90-20602
Microwave brightness temperature and its relation to atmospheric general circulation features
[AD-A218312] N90-20603
WEIGHT REDUCTION
Advances in lightweight nickel electrode technology
N90-20476
WEIGHTLESSNESS
Vortex motion phase separator for zero gravity liquid transfer
[NASA-CASE-KSC-11387-1] N90-20236
Center of Gravity: Metallic Solidification
[DFVLR-IB-333-89/3] N90-20238
German microgravity program and flight opportunities
N90-20239
User center and assitance N90-20240
Microgravity conditions of a space vehicle
N90-20247
A comparison of the mechanisms of cold- and microgravity-induced fluid loss
[AD-A218098] N90-20631
WELDED JOINTS
Evaluation of material homogeneity as a function of thickness of low-alloy ferritic steel
[DE90-008069] N90-20202
Time-dependent failure of silver interlayer welds
[DE90-008015] N90-20440
WEST GERMANY
German microgravity program and flight opportunities
N90-20239
Regional quasigeoid determination in Northern Germany and comparison with GPS N90-20544
WETTING
Wetting of metallic carbides by non-reactive liquid metals
[AERE-M-3759] N90-20185
WHEAT
Relationship of radiometric field measurements of wheat in the Assis-Safra region, 1988
[INPE-4949-RPE/598] N90-20443
LANDSAT-5 data in the study of wheat and bean crops
[INPE-4746-RPE/580] N90-20444
WHISKER COMPOSITES
Experimentally determined wear behavior of an Al2O3-SiC composite from 25 to 1200 C
[NASA-TM-102549] N90-20130
Synthesis of alumina-coated SiC whiskers for production of SiC whisker-reinforced alumina composite materials
[DE90-007778] N90-20147
Mechanical behavior of whisker reinforced ceramics
[DE90-008758] N90-20224
WIND (METEOROLOGY)
Meteor observations using the 50 MHz MENTOR imaging Doppler interferometer
[AD-A217908] N90-20276
An improved airborne wind measurement technique for the NAE (National Aeronautical Establishment) Twin Otter
[AD-A217978] N90-20575
Atmospheric wind measurements using a 50 MHz imaging Doppler interferometer radar
[AD-A218277] N90-20601
Microwave brightness temperature and its relation to atmospheric general circulation features
[AD-A218312] N90-20603
The invertibility principle for a simple hurricane model
[AD-A218344] N90-20605
WIND EFFECTS
Aerodynamic analysis of a US Navy and Marine Corps unmanned air vehicle
[AD-A218282] N90-20077
Analysis of small-scale rotor hover performance data
[NASA-TM-102271] N90-20325
WIND MEASUREMENT
Atmospheric wind measurements using a 50 MHz imaging Doppler interferometer radar
[AD-A218277] N90-20601
WIND PROFILES
Derivation of kinematic fields using wind profiler data from the 1985 pre-storm experiment
[AD-A217952] N90-20592
A prototype expert system to forecast severe winds in the western Mediterranean Sea
[AD-A218017] N90-20593
WIND SHEAR
Structure and dynamics of the Arizona monsoon boundary
[AD-A217378] N90-20586
A sub-cloud layer vorticity budget analysis for two microburst-producing storms from jaws dual-Doppler data
[AD-A218180] N90-20599
WIND TUNNEL APPARATUS
Design of a high angle of attack robotic sting mount for tests in a low speed wind tunnel
[AD-A218105] N90-20099
WIND TUNNEL MODELS
Using transonic small disturbance theory for predicting the aeroelastic stability of a flexible wind-tunnel model
[NASA-TM-102617] N90-20047
Digital-flutter-suppression-system investigations for the active flexible wing wind-tunnel model
[NASA-TM-102618] N90-20093
Design of a high angle of attack robotic sting mount for tests in a low speed wind tunnel
[AD-A218105] N90-20099
WIND TUNNEL TESTS
Windblast protection for advanced ejection seats
N90-20063
Aerodynamic analysis of a US Navy and Marine Corps unmanned air vehicle
[AD-A218282] N90-20077
Digital-flutter-suppression-system investigations for the active flexible wing wind-tunnel model
[NASA-TM-102618] N90-20093
A data acquisition parallel bus for wind tunnels at ARL (Aeronautical Research Laboratory)
[AD-A218052] N90-20098
Noise of a simulated installed model counterrotation propeller at angle-of-attack and takeoff/approach conditions
[NASA-TM-102440] N90-20794
WIND TUNNEL WALLS
Investigation of the development of laminar boundary-layer instabilities along a cooled-wall hollow cylinder at Mach number 8
[AD-A217672] N90-20331
WIND TURBINES
PC-based PCM telemetry data reduction system software
[DE90-000317] N90-20111
A comparison of two-and three-dimensional S809 airfoil properties for rough and smooth HAWT (Horizontal-Axis Wind Tunnel) rotor operation
[DE89-009512] N90-20492
WIND VARIATIONS
A comparison of two-and three-dimensional S809 airfoil properties for rough and smooth HAWT (Horizontal-Axis Wind Tunnel) rotor operation
[DE89-009512] N90-20492
WIND VELOCITY
Analysis of heliport environmental data: Indianapolis downtown heliport, Wall Street heliport. Volume 3: Indianapolis downtown heliport data plots
[AD-A217412] N90-20500
US Navy regional climatic study of the Central East Asian coast and associated waters
[AD-A217448] N90-20587
Atmospheric wind measurements using a 50 MHz imaging Doppler interferometer radar
[AD-A218277] N90-20601
WIND VELOCITY MEASUREMENT
An improved airborne wind measurement technique for the NAE (National Aeronautical Establishment) Twin Otter
[AD-A217978] N90-20575
WINDPOWER UTILIZATION
Wind Energy Program summary. Volume 1: Overview
[DE89-009479] N90-20491
A comparison of two-and three-dimensional S809 airfoil properties for rough and smooth HAWT (Horizontal-Axis Wind Tunnel) rotor operation
[DE89-009512] N90-20492
WINDS ALOFT
Solar cyclical trend study of the mid-latitude, quiet-time, meridional, neutral winds at winter solstice conditions
[AD-A217398] N90-20568
WINDSHIELDS
Full-scale birdstrike testing of in-service aged F-111 ADBIRT windshield transparencies
[AD-A218035] N90-20069
WING PROFILES
Static aeroelastic analysis of a three-dimensional generic wing
[NASA-TM-102231] N90-20087
WIRE
Recent improvements to the electromagnetic surface patch code
[AD-A217479] N90-20293
WORKLOADS (PSYCHOPHYSIOLOGY)
Assessment of crew workload measurement methods, techniques and procedures. Volume 1: Process, methods and results
[AD-A217699] N90-20647
WORKSTATIONS
Space station Simulation Computer System (SCS) study for NASA/MSFC. Volume 4: Conceptual design report
[NASA-CR-183843] N90-20116
Space station Simulation Computer System (SCS) study for NASA/MSFC. Volume 5: Study analysis report
[NASA-CR-183844] N90-20117
Space station Simulation Computer System (SCS) study for NASA/MSFC. Volume 6: Study issues report
[NASA-CR-183845] N90-20118
The Real Time Interactive Display Environment (RTIDE), a display building tool developed by Space Shuttle flight controllers N90-20654
Tools for 3D scientific visualization in computational aerodynamics N90-20660
Software systems for modeling articulated figures
N90-20677
SES cupola interactive display design environment
N90-20679
Issues in visual support to real-time space system simulation solved in the Systems Engineering Simulator
N90-20680
Real-time graphics for the Space Station Freedom cupola, developed in the Systems Engineering Simulator
N90-20683

X

X RAY ABSORPTION
Extended x ray absorption fine structure analysis applied to composite materials
[DE90-008575] N90-20150
L shell XANES (X ray Absorption Near Edge Structure) for solid metals: Ti, V, Cr, Fe, Ni, Cu
[DE90-008043] N90-20880
X RAY ANALYSIS
X ray specular reflection studies of silicon coated by organic monolayers (alkylsiloxanes)
[AD-A217418] N90-20213
X RAY DIFFRACTION
X ray microimaging by diffractive techniques
[DE90-008444] N90-20356
Residual stresses: A review of their measurement and interpretation using x ray diffraction
[AERE-R-13005] N90-20423
X RAY FLUORESCENCE
In-line wear monitor
[AD-A217799] N90-20091
X RAY SOURCES
The inverse triax x ray diode: An alternate reduced-endpoint-energy bremsstrahlung source
[DE90-006366] N90-20285
EXOSAT observations of Seyfert type galaxies
N90-20910
X RAY SPECTROSCOPY
Infrared and X ray photoelectron spectroscopy studies of the polyimide/metal interface
[AD-A218249] N90-20179
X RAYS
Studies of the evolution of the x ray emission of clusters of galaxies
[NASA-CR-186471] N90-20918

Y

YAG LASERS
DURIP theoretical/experimental investigations of highly energetic dication species
[AD-A217771] N90-20383
YTTRIUM COMPOUNDS
Performance of Y-TZP materials between 800 C and 1200 C
[AD-A217723] N90-20890
YTTRIUM OXIDES
Processing, fabrication, characterization and device demonstration of high temperature superconducting ceramics
[AD-A218330] N90-20231
Y1Ba2Cu3O(7-x) laser-ablation plume dynamics measurement by nanosecond response ion probe: Comparison with optical measurements
[DE90-007658] N90-20375
High resolution tranamission electron microscopy study of defect structures in mixed-phase YBaCuO
[DE90-007767] N90-20873
YTTRIUM-ALUMINUM GARNET
Crystallography, spectroscopic analysis, and lasing properties of Nd3+:Y3Sc2Al3O12
[AD-A217792] N90-20891

Z

ZINC
Infrared absorption study of zinc-doped silicon
[DE90-007779] N90-20164
ZINC SELENIDES
Chemical beam epitaxy of ZnSe
[AD-A217375] N90-20866
ZIRCONIUM OXIDES
Hydrous metal oxide-supported catalysts. Part 1: Preparation chemistry and physical and chemical properties
[DE90-007607] N90-20161
Performance of Y-TZP materials between 800 C and 1200 C
[AD-A217723] N90-20890
ZONE MELTING
Identification of defects in SOI (Silicon-On-Insulator) wafers
[DE90-006020] N90-20879

Typical Personal Author Index Listing

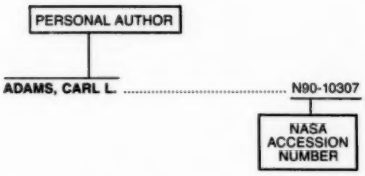

Listings in this index are arranged alphabetically by personal author. The NASA accession number denotes the number by which the citation is identified.

A

ABBOTT, WILLIAM Y. N90-20076
ABEL, PHILLIP B. N90-20353
ABUJBARA, HASAM N90-20308
ADAMS, CARL FRED N90-20717
ADANG, THOMAS CHARLES N90-20586
ADOLF, DOUGLAS N90-20221
AGARWAL, ANANT N90-20729
N90-20730
AHUJA, SANJEEV B. N90-20747
AKBARI, HASHEM N90-20508
AKSAY, ILHAN N90-20231
AL-ARIAN, SAMI A. N90-20308
ALDRIDGE, E. E. N90-20187
ALDRIDGE, J. P. N90-20661
ALI, A. W. N90-20817
ALLCOCK, HARRY R. N90-20216
N90-20230
ALLEN, JONATHAN N90-20309
ALLEN, R. A. N90-20281
ALLEN, ROGER N90-20367
N90-20368
ALLIK, TOOMAS H. N90-20891
ALPERT, C. J. N90-20227
AMENDE, WELF N90-20364
AMENDT, R. O. N90-20061
AMINPOUR, MOHAMMAD A. N90-20422
ANDERSEN, R. W. N90-20691
ANDERSON, ALLAN H. N90-20290
ANDERSON, J. M. N90-20776
ANDERSON, ROBERT J. N90-20403
ANDERSON, T. L. N90-20202
ANDRADY, ANTHONY L. N90-20212
ANGUS, JOHN C. N90-20157
ANTIBUS, R. K. N90-20501
ANTON, D. J. N90-20057
AO, CHIA-NING N90-20798
APELIAN, D. N90-20255
APODACA, TONY N90-20653
APPLEBY, A. J. N90-20462
APPLEBY, A. JOHN N90-20465
APPLIN, ZACHARY T. N90-20046
ARMSTRONG, LAWRENCE N90-20635
ARMSTRONG, LAWRENCE E. N90-20637
ARNAU, A. N90-20810
ARNOLD, S. M. N90-20428
ASELAGE, TERRY L. N90-20875
ATHANS, MICHAEL N90-20274
ATKINS, D. E. N90-20256
ATKINSON, LARRY P. N90-20606
ATTIA, ALAN I. N90-20458
AU, A. Y. N90-20566
N90-20572
AULL, JOHN E. N90-20414
AXE, J. D. N90-20213
AZAROFF, L. V. N90-20215

B

BABCOCK, RICHARD R. N90-20723
BACHMANN, K. J. N90-20895
BACIGALUPI, J. N90-20283
BADDOUR, R. F. N90-20211
BADLER, NORMAN N90-20743
BADLER, NORMAN I. N90-20678
BAEHMANN, PEGGY L. N90-20753
BAHOWICK, S. N90-20300
BAI, Z. D. N90-20698
N90-20757
BAILEY, R. T. N90-20708
BAILEY, SAMUEL A., JR. N90-20656
BAJCSY, RUZENA N90-20743
BAKER, WILLIAM L. N90-20503
BALACHANDRAN, U. N90-20888
BALBIOLIVEIRA, PEDRO PAULO N90-20565
BALDWIN, R. N90-20467
BALDWIN, RICHARD S. N90-20454
BALKWILL, P. H. N90-20190
BALTZLEY, DENNIS R. N90-20634
BAMFORD, T. A. N90-20876
BANCROFT, BARBARA T. N90-20723
BANCROFT, GORDON N90-20660
BANDERET, LOUIS E. N90-20625
BANKSTON, C. P. N90-20459
BANNISTER, K. A. N90-20436
BARCLAY, J. A. N90-20258
BARNES, CRIS W. N90-20841
BARNES, J. C. N90-20585
BARNETT, DEANNA L. N90-20396
N90-20397
BARRERA, ENRIQUE V. N90-20150
BARRETT, JOHN W. N90-20912
BARRETT, TODD KENT N90-20322
BARTHOLOMEW, MICHAEL J. N90-20682
BASIC, T. N90-20545
BASILI, VICTOR R. N90-20715
BASS, HENRY E. N90-20796
BATISTA, GETULIO T. N90-20443
BAUCK, JERALD LEE N90-20265
BAUER, R. N90-20825
BAUMAN, WILLIAM H., III N90-20590
BAUMANN, DANIEL D. N90-20073
BAUMANN, E. D. N90-20301
BAYLOR, L. R. N90-20851
BEAUDOUIN, P. N90-20056
BECHER, PAUL F. N90-20224
BECKER, FRED J. N90-20673
BECKER, M. N90-20533
BECKERMAN, MARTIN N90-20397
BEEMAN, J. N90-20360
BEETLEY, DALE E. N90-20412
BELL, BRADLEY N. N90-20657
BELL, D. N90-20619
BELL, R. E. N90-20526
BENDETT, M. B. N90-20302
BENICEWICZ, BRIAN N90-20158
BENINGA, KELLY N90-20495
BENKOVITZ, CARMEN M. N90-20509
BENLINE, TERRY A. N90-20622
BENNETT, KELLY W. N90-20317
BENNETT, M. J. N90-20189
BENNETT, ROBERT M. N90-20047
BENNISON, S. J. N90-20227
BENSON, S. N90-20661
BENSON, T. J. N90-20090
BENZ, R. N90-20559
BERNARD, A. N90-20560
BERNASEK, STEVEN L. N90-20160
BERRY, MICHAEL J. N90-20386
BERTOLUCCI, CESAR LUIZ N90-20443
BESMANN, T. M. N90-20149
BEST, JEFFREY S. N90-20607
BETTADPUR, S. N90-20558
BEYER, G. N90-20676
BHARATHI, A. N90-20883
BHASIN, K. B. N90-20302
N90-20886
BIBEAU, C. N90-20372
BIFERNO, MICHAEL H. N90-20647
BINDSCHADLER, ROBERT A. N90-20562
N90-20563
N90-20564
BINNENBRUCK, H. N90-20239
BLACKBURN, MARTIN J. N90-20208
BLACKWELL, B. D. N90-20843
BLAES, B. R. N90-20281
BLAKERS, A. W. N90-20490
BLANKENSHIP, MARK H. N90-20638
BLANN, M. N90-20808
N90-20823
BLISS, D. E. N90-20872
BLUMENTHAL, MARJORY S. N90-20690
BLUMENTHAL, SAUL N90-20416
BOCHSLER, DANIEL C. N90-20661
BOGART, JAMES E. N90-20636
BOHLIN, JOHN A. N90-20279
BOITNOTT, RICHARD L. N90-20068
BONDURANT, ROY S. N90-20828
BOOK, PATRICIA O. N90-20130
BOOTH, VICTORIA N90-20449
BORTNER, RAY N90-20094
BOSSI, RICHARD H. N90-20314
BOTTCHER, C. N90-20763
BOUCEK, GEORGE P., JR. N90-20647
BOWEN, P. N90-20191
BOWMAN, DANIEL R. N90-20069
BOYD, ROBERT N90-20371
BRADLEY, JAMES G. N90-20351
BRAITHWAITE, JEFFREY W. N90-20297
BRANCH, MELVYN C. N90-20159
BRANNON, P. JERRY N90-20370
BRASWELL, W. DANNY N90-20523
BRAUNEGG, DAVID J. N90-20751
N90-20752
BRAWLEY, EDWIN L. N90-20108
BRENINGER, RONALD LEE N90-20568
BRENNER, ANITA C. N90-20562
N90-20563
N90-20564
BREWER, JEFFREY C. N90-20463
BREWSTER, TONY L. N90-20702
BRIGGS, G. A. D. N90-20411
BRILL, JACK N90-20477
BRIMLEY, W. N90-20676
BRINKLEY, JAMES W. N90-20055
N90-20063
BRITTAIN, C. R. N90-20736
BROGAN, F. A. N90-20421
BROUSE, J. W. N90-20868
BROWN, BILLIE N90-20635
BROWN, D. R. N90-20298
BROWN, D. W. N90-20485
BROWN, JAMES H. N90-20917
BROWN, KENNETH G. N90-20154
BROWN, LARRY D. N90-20613
N90-20614
BROWN, R. D. N90-20566
N90-20572
BROZENA, J. M. N90-20526
BRYKCZYNSKI, BILL R. N90-20783
BRZEZOWSKI, S. N90-20525
BUCHMANN, O. A. N90-20088
BUEHLER, M. G. N90-20281
BUICK, FRED N90-20623
BULLOCK, J. S., IV N90-20340
BULLOUGH, R. N90-20424
BUNEMAN, PETER N90-20743
BUNKER, B. C. N90-20161
BURKE, H. K. N90-20585
BURKHART, S. C. N90-20373
BURL, MICHAEL C. N90-20758
BURNS, JAMES A. N90-20290
BUSCH, D. N90-20400
BUSH, DONALD M. N90-20297
BUSSE, CARL N90-20655
BUTCHER, ROBERT L. N90-20352
BUTLER, PAUL C. N90-20297
BUTTERFIELD, C. P. N90-20492
BUTTLE, D. J. N90-20189
BUTTRILL, CAREY S. N90-20093
BYERLEY, AARON R. N90-20089
BYRD, G. G. N90-20916

C

CAFFALL, WILLIAM E. N90-20780
CALAHAN, D. A. N90-20342
CALEDONIA, G. E. N90-20578
CALISTI, A. N90-20653
CAMARDA, CHARLES J. N90-20323
CAMEJO, PEDRO JOSE N90-20262
CAMPBELL, E. M. N90-20885
CAMPBELL, V. W. N90-20850
CAMPONESCHI, E. T., JR. N90-20142
CAMPONESCHI, EUGENE T., JR. N90-20141
CANAVAN, GREGORY H. N90-20785
N90-20786
CAPEHART, STEVEN RUSSELL N90-20775
CAPEL, M. N90-20182
CAPPUCCI, MARIETTA R. N90-20196
CARDEN, HUEY D. N90-20068
CARMER, DWAYNE C. N90-20748
CARREIRO, LOUIS R. N90-20103
CARRIERE, R. N90-20278
CARSWELL, C. MELODY N90-20720
CARTER, DANIEL C. N90-20616
CARTER, MICHAEL J. N90-20732
CARTIGLIA, N. N90-20283
CARWILE, CLIFF N90-20162
CASSELL, LOELLYN N90-20735
CATALDO, ROBERT L. N90-20457
CATES, MICHAEL C. N90-20365
CAUFIELD, CLYDE CURTIS N90-20903
CAVIN, EDWARD S. N90-20700
CELSODECARVALHO, VITOR N90-20446
CHAMIS, C. C. N90-20138
N90-20432
CHAMIS, CHRISTOS C. N90-20151
CHAN, H. M. N90-20227
CHANG, DUK IN N90-20105
CHANG, J. L. C. N90-20333
CHANG, REBECCA N90-20479
CHANG, RUEY-GANG N90-20547
CHANG, STEPHEN KW. N90-20636
CHAO, C.-L. N90-20411
CHAPMAN, SPENCER R. N90-20272
CHARETTE, R. F. N90-20136
CHARLAND, SHAWN N90-20294
CHEN, A. N90-20233
CHEN, CHENSON K. N90-20290
CHEN, J. N90-20870
CHEN, K. C. N90-20233
CHENEY, FRANK E., JR. N90-20632
CHEUNG, J. N90-20870
CHIN, ERNEST S. N90-20196
CHIN, ING WCO N90-20105
CHINN, D. S. N90-20518
CHISHOLM, G. H. N90-20703
CHO, S.-J. N90-20227
CHONG, C. M. N90-20490
CHONGSAWANGVIROD, S. N90-20864
N90-20865
CHOW, MOSUK N90-20698
CHRISTIANSEN, JOHN N90-20635
CHRISTIANSON, DAVID C. N90-20681
CHRZAN, DARYL C. N90-20789
CHU, C. W. N90-20884
CHU, WILLIAM T. N90-20706
CHUM, HELENA L. N90-20220
CIARLO, D. R. N90-20299
CLAASEN, F. N90-20248
CLARK, J. MARTIN N90-20760
CLASPY, P. C. N90-20302
CLEARY, STEPHEN F. N90-20385
CNARE, EUGENE C. N90-20106
N90-20108
COATES, DWAINE N90-20476
COCKRELL, CLAYTON DALE N90-20741
COHEN, R. E. N90-20211
COK, KEITH E. N90-20669
COLE, R. L. N90-20394
COLE, STANLEY R. N90-20093
COLLEDGE, P. D. N90-20189
COLOMBO, GREGORY N90-20105
COLOMBO, O. L. N90-20554
N90-20561
CONLEY, JOSEPH M. N90-20351
CONNORS, KATHRYN F. N90-20450
CONTINENZA, ALESSANDRA N90-20218
CONVERTINO, VICTOR A. N90-20617
CONWAY, G. D. N90-20843
COOK, M. N90-20127
COOK, N. G. W. N90-20570
COOK, R. F. N90-20227
COOPER, A. W. N90-20837
COOPER, G. J. N90-20843
CORADESCHI, THOMAS N90-20105
CORNILSEN, BAHNE C. N90-20472
CORWIN, WILLIAM H. N90-20647
COSTELLO, DANIEL J., JR. N90-20263
COUNTS, C. A. N90-20505
COX, STEPHEN K. N90-20583
CRABILL, MONTY N90-20800
CRABILL, NORMAN L. N90-20080
N90-20081
N90-20082
N90-20083
N90-20084
CRISPIN, R. M. N90-20192
CRITTENDEN, EUGENE C., JR. N90-20837
CROSIER, RONALD B. N90-20315
CRUMP, JESSE KEITH N90-20178
CSERNICA, J. J. N90-20211
CURRERI, P. A. N90-20194
CYMERMAN, A. N90-20615
CZUCHLEWSKI, S. J. N90-20369

D

DABBOUR, ABD EL-SATTAR A. N90-20788
DABROWSKI, B. N90-20883
DALLY, WILLIAM J. N90-20267
DAUGHERTY, PAUL N90-20478
DAVENPORT, ROGER N90-20495
DAVID, D. N90-20834
DAVIDSON, JOHN DEXTER, JR. N90-20581
DAVIES, K. T. R. N90-20765
DAVIS, PATRICIA A. N90-20180
DAVIS, R. F. N90-20895
DAWICKE, D. S. N90-20427
DAWN, FREDERIC S. N90-20645
DEBELLIS, WILLIAM B. N90-20095
DECHAUMPHAI, PRAMOTE N90-20426
DECKER, D. E. N90-20378
DEEDS, DEAN ALAN N90-20840
DEGREGORIA, A. J. N90-20258
DEJONGHE, LUTGARD C. N90-20306
DELGRANDE, N. K. N90-20680
DELIGIANNIS, F. N90-20481
DELLACORTE, CHRISTOPHER N90-20130
DELOREY, DENNIS N90-20723
DENKER, H. N90-20545
DENKER, HEINER N90-20544
DEOLIVEIRAALMEIDA, SERGIO ALBERTO N90-20442
DERAAD, LESTER L., JR. N90-20569
DESAUSSURE, G. N90-20395
DESORCIE, JAMES L. N90-20216
N90-20230
DEVADAS, SRINIVAS N90-20687
N90-20742
N90-20756
DEVAN, J. H. N90-20167
DEWAN, EDMOND N90-20917
DEWAR, R. L. N90-20843
DEWITT, J. N90-20283
DHAR, H. P. N90-20482
DHURIA, HARBANS L. N90-20582
DICKENS, MIKE N90-20397
DICKEY, J. N90-20797
DICKINSON, M. N90-20538
DICKMAN, JOHN E. N90-20393
DIEBOLD, B. N90-20676
DIEFENDORF, R. J. N90-20140
DIMEO, MARK N90-20500
DINGUS, R. S. N90-20379
DINYOVSZKY, P. N90-20439
DISTEFANO, S. N90-20459
DITZEL, RONALD B. N90-20297
DOBRZENIECKI, A. B. N90-20712
DODSON, GARY N90-20477
DOLIFF, J. N90-20545
DOLOU, P. N90-20056
DOMINESSY, MARY E. N90-20646
DON, WAI-SUN N90-20050
DONALDSON, J. C. N90-20331
DONALDSON, WAYNE A. N90-20103
DONG, X. N90-20428
DOOLEY, J. B. N90-20850
DOSCH, R. G. N90-20161
DOSSANTOS, DAYSE I. N90-20888
DOUGHTY, D. H. N90-20859
DOWNEY, MARK N90-20048
DRAKE, JOHN N90-20737
DREW, DONALD A. N90-20334
DROPPO, JAMES GARNET, JR. N90-20510
DRUCE, S. G. N90-20182
N90-20188
DRUMMOND, COLIN K. N90-20338
DU, LI-JEN N90-20722
DUCK, PETER W. N90-20337
DUFFY, J. N90-20223
DUGAN, REGINA E. N90-20254
DUGGAN, D. M. N90-20233
DUGGIN, BILLY W. N90-20106
N90-20107
N90-20108
DUNHAM, CURTIS N90-20105
DUNHILL, A. N90-20411
DUNIC, RONALD L. N90-20596
DUNN, GREGORY J. N90-20290
DUNN, H. J. N90-20071
DURKOT, M. J. N90-20615
DUTTA, P. N90-20129
DZIADOS, JOSEPH E. N90-20628
N90-20633

E

EATHER, ROBERT H. N90-20839
EATON, MICHAEL J. N90-20907
EBY, RONALD K. N90-20232
ECHENIQUE, P. M. N90-20810
ECK, T. G. N90-20886
EDGE, RONNIE N90-20909
EFTEKHARI, ABE N90-20137
EGBERT, STEPHEN L. N90-20503
EGRY, I. N90-20249
EHRLICH, R. B. N90-20372
EISMAN, G. A. N90-20466
ELLIOTT, GLENN R. N90-20268
ELLUL, J. P. N90-20865
ELMS, JOE D. N90-20587
ENAYETULLAH, MOHAMMAD A. N90-20485
ENDRUSICK, T. L. N90-20649
ENDRUSICK, THOMAS L. N90-20636
ENTIN, ELLIOT E. N90-20643
ERCK, R. A. N90-20400
ERDEMIR, A. N90-20400
ERDEMIR, ALI N90-20401
ERLICHMAN, SCOTT N90-20500
ESAKOV, JEFFREY N90-20678
ESCHENBERG, KENT EDWARD N90-20793
ESTEROWITZ, LEON N90-20367
N90-20368
EULER, H.-J. N90-20533
EVANS, ALAN G. N90-20530
EVANS, BARRY M. N90-20450
EVANS, J. W. N90-20303
EVERETT, RICHARD K. N90-20150
EVERITT, C. W. F. N90-20554
EWIG, CARI S. N90-20132
EXARHOS, GREGORY J. N90-20172
EYRING, EDWARD M. N90-20380

F

FAGOT, C. N90-20065
FAIRBANKS, C. J. N90-20227
FALOONA, IAN C. N90-20168
FARMER, SERENE C. N90-20130
FASANELLA, EDWIN L. N90-20068
FATKIN, D. G. P. N90-20411
FAULKS, H. N90-20559
FAYER, MICHAEL DAVID N90-20387
FELL, C. N90-20578
FELSENTREGER, T. L. N90-20514
FENDORF, M. N90-20873
FENG, S. N90-20826
FENSKE, G. R. N90-20400
FERGUSON, P. N90-20283
FERREIRA, JOSE LEONARDO N90-20128
FEUERBACHER, B. N90-20241
FICHTER, W. B. N90-20121
FIELDER, WILLIAM L. N90-20471
FINZEL, N. N90-20748
FISCHER, J. N90-20807
FISHER, ARTHUR D. N90-20685
FISHER, WILLIAM A. N90-20906
FISHMAN, G. S. N90-20415
FITCH, J. P. N90-20833
FITCH, J. PATRICK N90-20171
FLANERY, RAY N90-20737
FLANNERY, M. R. N90-20805
FLEMINGS, MERTON C. N90-20222
FLORES, F. N90-20810
FLUSS, M. J. N90-20884
FLYNN, GEORGE W. N90-20267
FOGARTY, ROBERT M. N90-20605
FOGLESONG, JOY N90-20735
FONG, SANDIWAY N90-20724
FONG, WINFRED Y. N90-20889
FONTEIN, P. F. N90-20861
FORCHIONE, J. N90-20464
FORD, WARREN T. N90-20228
FORSBERG, R. N90-20534
FORSBERG, RENE N90-20537
FORTE, V. A., JR. N90-20615

FOSTER, R. W. N90-20258
FOUNTAIN, G. N90-20827
FOWLER, W. E. N90-20285
FOWLKES, JENNIFER N90-20634
FRANCE, MARTIN E. N90-20125
FRANCE, MARTIN ERNEST BARTEAU N90-20119
FRANCO, JOHN N90-20716
FRANKLIN, ROBERT N90-20748
FRASER, M. E. N90-20578
FRASER, WILSON M., JR. N90-20236
FRAZIER, GEORGE F. N90-20503
FREDIN, LEIF G. N90-20386
FREDRIKSSON, H. N90-20245
FREED, ALAN D. N90-20431
FREEDMAN, ANDREW N90-20214
FREEMAN, A. J. N90-20218
FREESE, JAMES M. N90-20297
FRENCH, JAMES C. N90-20905
FREY, RANDY W. N90-20279
FREZZA, RUGGERO N90-20760
FRISCHAT, G. N90-20250
FROST, DENZIL F. N90-20609
FRY, ANDREW C. N90-20628
N90-20633
FRY, EDWARD S. N90-20831
FRYKMAN, PETER N. N90-20628
FUNG, A. K. N90-20275
FUNG, KHUN YEE N90-20693
FURY, RUDOLF J. N90-20536

G

GABOW, HAROLD N. N90-20728
GAGLIONE, A. M. N90-20773
GAJJAR, J. S. B. N90-20326
GALLAGHER, DONALD N90-20500
GANNON, JOHN D. N90-20715
GARBESI, KARINA N90-20508
GARDNER, C. L. N90-20319
GARDNER, H. J. N90-20843
GARELIS, E. N90-20711
GARINO, T. J. N90-20859
GARRETT, B. A. N90-20511
GARRETT, B. C. N90-20812
GATES, W. LAWRENCE N90-20588
GAUVIN, MICHAEL GEORGE N90-20627
GEE, A. E. N90-20411
GEE, PERRY N90-20292
GEFFEN, C. A. N90-20511
GEIGER, H.-W. N90-20625
GEIGER, ROBERT D. N90-20723
GEISLER, ERIK N90-20671
GEMEINER, RUSSEL P. N90-20463
GENTRY, GARL L., JR. N90-20046
GEOHEGAN, D. B. N90-20375
GEORGE, THOMAS F. N90-20813
GERLACH, KARL N90-20273
GERRISH, VERNON M. N90-20357
GEZARI, DANIEL Y. N90-20911
GIBSON, G. P. N90-20182
GILBERT, BOB N90-20665
GILBERT, JOHN A. N90-20324
GILBERT, M. G. N90-20071
GILES, G. E. N90-20340
GILL, W. N90-20259
GILLIGAN, J. G. N90-20217
GILSON, D. J. N90-20058
GINER, J. N90-20470
GINTY, CAROL A. N90-20151
GITOMER, S. J. N90-20849
GIUBELLINO, P. N90-20283
GLANZ, FILSON H. N90-20732
GLASS, J. T. N90-20895
GLATTER, E. I. N90-20233
GLEASON, D. N90-20525
GLOVER, C. W. N90-20746
GODAYJUNIOR, MOACIR N90-20443
GOEBEL, R. P. N90-20608
GOEKCEN, TAHIR N90-20044
GOLDFARB, MARK N90-20867
GOLDSTEIN, J. N90-20525
GOLDSTON, R. J. N90-20846
GOMEZDELCAMPO, J. N90-20819
GONIS, A. N90-20203
GONZALEZ, RICHARD R. N90-20636
GOODMAN, DENNIS M. N90-20171
GOODNOW, D. N90-20859
GORDON, SCOTT E. N90-20628
N90-20633
GORDON, W. L. N90-20886
GOTTLIEB, ALLAN N90-20688
GOTTLIEB, DAVID N90-20050
N90-20768
GOULD, WARREN N90-20076
GOULDING, F. N90-20360
GOWER, DANIEL J., JR. N90-20634
GRADY, JOSEPH E. N90-20139
GRAHAM, ROBERT W. N90-20901
GRANDT, A. F., JR. N90-20427
GREEN, JAMES N90-20820
GREEN, JOHN A. N90-20087
GREENE, DENNIS P. N90-20365
GREENE, E. F. N90-20806
GREENE, M. A. N90-20490
GRIER, SAMUEL LYCURGUS, JR. N90-20727
GRIFFIN, ANSELM C. N90-20215
GRIFFIN, JOHN W. N90-20280
GRIFFIN, SANDY N90-20651
GRIFFITH, A. N90-20464
GRIFFITH, PAUL N90-20667
GRIVAS, D. N90-20206
GROMEK, JACK M. N90-20215
GRONSKY, R. N90-20873
GROTCH, STANLEY L. N90-20589
GROTEN, E. N90-20533
GROTHAUS, KENNETH R. N90-20297
GROVER, MORGAN K. N90-20569
GROVES, DONALD N90-20145
GRUBER, JOHN B. N90-20891
GUARNA, VINCENT A., JR. N90-20689
GUERRY, DUPONT, III N90-20385
GUERRY, R. KENNON N90-20385
GUILINGER, T. R. N90-20879
GUIMARAESFERREIRA, JULIO N90-20128
GUINN, THOMAS A. N90-20594
GUNZBURGER, MAX D. N90-20341
GUTTMANN, GEOFFREY DAVID N90-20610

H

HAAS, DAVID JOSEPH N90-20070
HACKEL, LLOYD A. N90-20371
HADJIPANAYIS, GEORGE C. N90-20790
HAEHNEL, M. N90-20155
HALBGEWACHS, RONALD D. N90-20740
HALLER, E. E. N90-20164
N90-20872
HALLIGAN, DAVID T. N90-20386
HALLINAN, EDWARD J. N90-20260
N90-20261
HALPERT, G. N90-20481
HAM, WILLIAM T., JR. N90-20385
HAMACHER, H. N90-20247
HAMBERGER, S. M. N90-20843
HAMEED, SULTAN N90-20588
HAMMER, SIGMUND N90-20531
HANNAN, CHARLES J. N90-20628
HANSEN, IRVING G. N90-20085
HARDGROVE, JOHN N90-20584
HARMAN, EVERETT A. N90-20628
HARMER, M. P. N90-20227
HARMON, L. N90-20748
HARPER-SLABOSZEWICZ, V. J. N90-20285
HARRIGAN, DAVID J. N90-20222
HARRISON, J. C. N90-20538
N90-20540
HART, MARY L. N90-20598
HARTEN, AMI N90-20768
HARTER, RICHARD M. N90-20591
HARTLEY, DAN L. N90-20494
HARTMAN, RICHARD W. N90-20597
HARVEY, J. F. N90-20098
HATTANGADY, S. N90-20827
HAUSCH, W. N90-20533
HAVENITH, G. N90-20826
HAVERLAND, MANFRED N90-20695
HAWKER, B. M. N90-20187
HAXBY, W. F. N90-20526
HAY, JOHN E. N90-20583
HAYDUK, ROBERT J. N90-20068
HAYES, W. N90-20862
HAYMES, ROBERT C. N90-20357
HAZELTINE, R. D. N90-20844
HEALD, STEVE M. N90-20150
HEDIN, DAVID N90-20820
HEDSTROM, G. W. N90-20762
HEE, E. N90-20299
HEEG, J. N90-20071
HELLER, W. N90-20525
HELM, HANSPETER N90-20814
HEMBREE, D. M., JR. N90-20149
HEMSWORTH, J. A. N90-20192
HENDRIKS, P. N90-20861
HENESIAN, M. A. N90-20372
HENINS, IVARS N90-20841
HENRY, J. PATRICK N90-20918
HEPPLER, WINI N90-20871
HERBERT, THORWALD N90-20330
HERLACH, D. M. N90-20242
HERMES, G. L. N90-20372
HERNANDEZ, C. L. N90-20859
HERNANDEZFILHO, PEDRO N90-20442
HERNDON, J. N. N90-20404
HESS, NANCY J. N90-20172
HESS, PHILIP W. N90-20683
HESS, ROBERT V. N90-20154
HEYMAN, J. N90-20164
HEYWARD, ANN O. N90-20264
HICKS, K. A. N90-20281
HILL, RICHARD N90-20675
HINKS, D. G. N90-20883
N90-20884
HIPPSLEY, C. A. N90-20183
N90-20191
N90-20193
HIROE, S. N90-20846
HIRSCHER, MICHAEL N90-20195
HO, J. C. N90-20883
HOADLEY, SHERWOOD T. N90-20093
HOBART, WILLIAM C., JR. N90-20750
HOBBS, LINN W. N90-20222
HOCKEY, B. J. N90-20227
HODGIN, C. REED N90-20502
HOFFLAND, A. H. N90-20868
HOFFMAN, C. M. N90-20283
HOFFMAN, D. A. N90-20766
HOFFMAN, ROSS N90-20595
HOGAN, CAROLE N90-20735
HOKE, PAUL B. N90-20413
HOLLOWAY, R. D. N90-20519
HOLMES, M. J. N90-20186
HOLTKAMP, D. N90-20283
HOPKINS, D. N90-20570
HORNER, S. N90-20861
HOROWITZ, JOSEPH N90-20776
HORRIGAN, D. J., JR. N90-20631
HOUCK, JACOB A. N90-20093
HOWARD, FRANK S. N90-20236
HOWARD, I. M. N90-20407
HOWARD, S. N90-20916
HOWELL, K. H. N90-20883
HOWELL, R. H. N90-20884
HOWES, F. A. N90-20762
HOYT, ANDREA E. N90-20158
HOYT, R. W. N90-20615
HOYT, RONALD F. N90-20154
HRMA, PAVEL N90-20237
HSIEH, E. J. N90-20205
HU, CHIA-REN N90-20831
HUANG, C-K. N90-20481
HUANG, HO-CHUNG N90-20282
HUANG, SAMUEL J. N90-20158
HUBBARD, L. J. N90-20615
HUBBARD, MONT N90-20760
HUBRIG, J. G. N90-20850
HUDDLE, J. R. N90-20528
HUFF, DENNIS L. N90-20051
HUIE, ROBERT M. N90-20196
HULSTROM, ROLAND L. N90-20571
HUMPHREYS, K. K. N90-20298
HUNT, C. N90-20299
HUNT, CHARLES E. N90-20169
HUNT, H. W. N90-20512
HURTAK, O. N90-20842
HUTCHINGS, M. T. N90-20862
HWANG, YONG K. N90-20745
HYER, M. W. N90-20135
N90-20136
HYMAN, ELLIS N90-20347
N90-20584

I

ILHAN, ALI N90-20237
IRENE, E. A. N90-20826
N90-20827
N90-20864
N90-20865
ITOH, TATSUO N90-20835
IYER, RAVI K. N90-20686

J

JACKSON, DOROTHY N90-20384
JACOBS, I. N90-20619
JACOBS, IRA N90-20618
JANG, BOR Z. N90-20144
JANKE, C. J. N90-20850
JANKOWSKI, A. F. N90-20204
JANSEN, J. F. N90-20404
JARBOE, THOMAS R. N90-20841
JARNAGIN, R. C. N90-20826
JEAN, Y. C. N90-20883
N90-20884

JEKELI, CHRISTOPHER N90-20525
N90-20548
N90-20555
N90-20556
JELETIC, JAMES F. N90-20668
JENKINS, K. A. N90-20886
JENKS, M. D. N90-20492
JENNINGS, G. A. N90-20281
JESSBERGER, E. K. N90-20803
N90-20247
JILG, R. N90-20625
JOBE, JARED B. N90-20209
JOHNSON, D. I. N90-20846
JOHNSON, D. W. N90-20072
JOHNSON, DICK N90-20777
JOHNSON, G. W. N90-20376
JOHNSON, M. A. N90-20270
JOHNSON, PETER N. N90-20320
JOHNSTON, DAVID F. N90-20697
JOHNSTON, JOHN B. N90-20423
JONES, A. M. N90-20879
JONES, H. D. T. N90-20593
JONES, MARCIA L. N90-20226
JONES, PHILLIP L. N90-20849
JONES, R. D. N90-20305
JONG, R. A. N90-20743
JOSHI, ARAVIND N90-20497
JOSHI, ASHOK V. N90-20585
JOSS, T. M. N90-20105
JUHASZ, WILLIAM N90-20678
JUNG, MOON N90-20678

K

KACKLEY, N. N90-20469
KALEPS, INTS N90-20062
KALLIANPUR, G. N90-20777
KALNITSKY, A. N90-20865
KALUZNIACKI, A. N90-20283
KALVELAGE, THOMAS A. N90-20654
KANADE, TAKEO N90-20386
KANELLAKOPOULOS, IOANNIS N90-20744
KANG, WEI N90-20760
KAPLAN, DANIEL N90-20820
KAPOLNEK, DAVID N90-20147
KAPOOR, VIK J. N90-20393
KAPPES, J. MARK N90-20270
KARAHAN, SINAN N90-20760
KARNI, S. N90-20049
KARR, T. J. N90-20376
KATTAWAR, GEORGE W. N90-20831
KAYE, RONALD J. N90-20108
KEARSLEY, A. H. W. N90-20519
KEEFER, KEITH D. N90-20875
KEENAN, M. R. N90-20166
KEIL, ROBERT G. N90-20289
KELLY, C. T. N90-20692
KELLY, M. J. N90-20879
KELTNER, N. R. N90-20259
KEMP, W. T. N90-20868
KEMPKA, S. N90-20300
KENNEALY, JOHN R. N90-20723
KENNER, W. SCOTT N90-20121
KEPHART, THOMAS W. N90-20802
KETTERSON, J. B. N90-20129
KETTLER, THOMAS N90-20628
KEUTZER, KURT N90-20687
KEYES, DAVID E. N90-20235
KHELFAOUI, F. N90-20853
KHOROMSKY, B. N. N90-20767
KHOSLA, PRADEEP N90-20388
KIM, DONG-SANG N90-20237
KIM, EDWARD J. N90-20912
KIM, KYEKYOON N90-20109
KIM, L. H. N90-20165
KIM, Y. J. N90-20462
KIM, YEONG E. N90-20523
KIMBARA, K. N90-20451
KINDRED, ERICK D. N90-20656
KINNISON, W. W. N90-20283
KINSE, D. L. N90-20858
KIRKHOFF, KEVIN R. N90-20679
KIRKPATRICK, J. R. N90-20340
KITAPLIOGLU, CAHIT N90-20325
KLAPDOR, H. V. N90-20803
KLEIN, D. A. N90-20512
KLEIN, JOHN W. N90-20456
KLEINBERG, H. N90-20676
KLING, TH. N90-20533
KLOSKO, S. M. N90-20514
N90-20518
KNIGHT, ROBBY LEE N90-20405
KNIPP, DELORES J. N90-20577
KNOTT, J. F. N90-20191
KNOWLTON, LARRY N90-20595
KNOWLTON, T. M. N90-20332
KNOX, STEPHEN O. N90-20841
KNUTSON, BENJAMIN W. N90-20314
KNUTTGEN, HOWARD G. N90-20626
KOBAYASHI, HERBERT S. N90-20280
KOBER, EDWARD M. N90-20168
KOCH, HERMANN N90-20465
KOCSIS, S. M. N90-20699
KOKOTOVIC, PETAR V. N90-20744
KOKTA, MILAN R. N90-20891
KOLANOSKI, H. N90-20283
KOLKA, MARGARET A. N90-20624
KOLKHORST, BARBARA N90-20658
KOLODZIEJSKI, LESLIE A. N90-20866
KONKLE, KENNETH H. N90-20290
KOOP, R. N90-20557
KORDAS, JOHN N90-20735
KORTE, DON W., JR. N90-20609
N90-20613
N90-20614
KORTE, ROSE C. N90-20723
KOURTIDES, DEMETRIUS A. N90-20133
KRAEMER, WILLIAM J. N90-20628
N90-20633
KRAFT, L. GORDON, III N90-20732
KRENEK, BRENDAN D. N90-20386
KRENER, ARTHUR J. N90-20760
KRETSCHMER, F. F., JR. N90-20273
KRUSE, ROBERT J. N90-20314
KRYTER, ROBERT C. N90-20355
KUBLER, TOMMY JACK N90-20099
KUCERNAK, A. N90-20861
KUCHYNKA, DANIEL J. N90-20461
KULKARNI, SANJEEV R. N90-20759
KULKARNI, V. G. N90-20415
KULLMAN, A. N90-20661
KUNASZ, PAUL N90-20382
KUNMENINI, HARI N90-20308
KUNZ, TERRY D. N90-20386
KUSHNER, MARK J. N90-20370
KUSIK, C. L. N90-20170
KVAM, E. N90-20873
KWAK, D. N90-20333
KWOK, HOI S. N90-20381
KYLE, H. LEE N90-20582
KYLLONEN, PATRICK C. N90-20642

L

LABOV, S. N90-20360
LABRECQUE, J. L. N90-20526
LACONTI, A. B. N90-20464
LACOVARA, P. N90-20368
LACOVARA, PHILIP N90-20367
LADD, ANTHONY J. C. N90-20336
LAFON, F. N90-20650
LAGUNA, GARY N90-20704
LAKDAWALA, VISHNU K. N90-20288
LAM, NGHI Q. N90-20201
LAMBERT, M. A. N90-20202
LANAGAN, M. T. N90-20888
LANCE, CYRIL A. N90-20839
LANDIS, D. N90-20360
LANE, C. E. N90-20183
LANGE, GREGORY A. N90-20126
LANGEMANN, M. N90-20559
LANTIGUA, EDWARD A. N90-20434
LAPOINTE, PAUL G. N90-20599
LATZKA, WILLIAM A. N90-20629
LAUBENTHAL, JAMES R. N90-20253
LAUMANN, C. W. N90-20372
LAW, CHUNG K. N90-20176
LAWLEY, A. N90-20255
LAWN, BRIAN R. N90-20227
LAWRENCE, C. W. N90-20411
LAWRENCE, T. W. N90-20833
LAWRENCE, TAYLOR W. N90-20171
LAWSON, J. K. N90-20372
LAYER, DAVID H. N90-20270
LAZAREWICZ, ANDREW R. N90-20530
LAZARUS, E. A. N90-20848
LEACH, B. W. N90-20575
LECROY, STUART R. N90-20583
LEE, DAVID CHUNG LIANG N90-20442
LEE, H. H. N90-20135
LEE, HAI-YOUNG N90-20835
LEE, IN N90-20087
LEE, J. E. N90-20194
LEE, LONG C. N90-20366
LEE, ROBERT A. N90-20800
LEGER, A. N90-20056
LEHOCZKY, SANDOR L. N90-20896
LEIGHTON, RICHARD N90-20347
LEINGANG, JOHN L. N90-20103
LELAND, W. T. N90-20369
LENHART, S. J. N90-20474
LENNOX, R. CHARLEENE N90-20707
LEON, MELVIN N90-20809
LEONE, STEPHEN R. N90-20383
LEONIDA, A. N90-20467
LERCH, BRADLEY A. N90-20139
LERCH, F. J. N90-20514
N90-20518
N90-20554
LESCHACK, A. R. N90-20532
LESSNER, P. N90-20464
N90-20470
LETELLIER, YVONNE C. N90-20613
LEWIS, GREGORY W. N90-20638
LIDSKY, L. M. N90-20712
LIM, H. S. N90-20475
LIN, H. T. N90-20224
LIN, SIN-SHONG N90-20152
LIN, Y.-S. N90-20281
LINDGREN, GEORG N90-20779
LINEBERGER, W. C. N90-20383
LING, JERRI S. N90-20253
LINKINS, A. E. N90-20501
LITTLE, BRUCE D. N90-20409
LIU, MEILIN N90-20306
N90-20496
LIU, PAO LO N90-20830
LIU, X. N90-20827
LLOYD, PETER D. N90-20362
LOGAN, AILEEN L. N90-20647
LONG, J. W. N90-20296
LONG, ROBERT S. N90-20452
LONGEST, JERRY MARK N90-20348
LOTENS, W. A. N90-20626
LOTZ, W. G. N90-20631
LOWMAN, DOUGLAS S. N90-20694
LOYSELLE, PATRICIA N90-20472
LUDEWIGT, BERNHARD A. N90-20706
LUDWIG, GERSON OTTO N90-20128
LUGINBUHL, DAVID RALPH N90-20701
LUHMAN, THOMAS S. N90-20231
LUNDBERG, J. B. N90-20558
LWANGASI, ALPHONSE S. N90-20542
LYMAN, CHARLES E. N90-20173
LYMAN, FREDERIC A. N90-20338
LYNESS, E. N90-20395
LYONS, DANIEL F. N90-20077

M

MA, HI-KEUNG T. N90-20742
MABANTA, A. A. N90-20406
MACCRONE, R. K. N90-20881
MACDONALD, D. D. N90-20474
MACK, GARY W. N90-20617
MACPHERSON, J. I. N90-20575
MADDEN, N. N90-20360
MAGERS, BRIAN J. N90-20908
MAGNANI, NICHOLAS J. N90-20297
MAGRINI, KIMBERLY A. N90-20162
MAGRUDER, R. H. N90-20858
MAIDANIK, G. N90-20797
MAJOR, JUDITH A. N90-20562
N90-20563
N90-20564
MANDEL, LEONARD N90-20836
MANKO, DAVID J. N90-20465
MANOUKIAN, M. N90-20470
MANZO, MICHELLE A. N90-20463
N90-20478
MAPLE, M. B. N90-20233
MARCINIAK, T. J. N90-20394
MARICLE, D. L. N90-20498
MARINO, RICHARD N90-20744
MARJORIBANKS, ROBIN STEWART N90-20854
MARKAKIS, JEFFREY M. N90-20357
MARKLIN, GEORGE J. N90-20841
MARKS, KRISTA M. N90-20706
MARREGASANDONATO, GILBERTO N90-20128
MARSDEN, J. E. N90-20856
MARSH, J. G. N90-20514
N90-20518
MARSHALL, D. B. N90-20227
MARTIEN, PHIL N90-20508
MARTIN, JAMES E. N90-20221
MARTIN, NORDENSO N90-20308
MARTIN, THOMAS V. N90-20562
N90-20563
N90-20564
MARTIN, WILLIAM P. N90-20074
MARTINEZ, S. L. N90-20859
MARTZAKLIS, KONSTANTINAS S. N90-20286
MARTZEN, P. D. N90-20540
MARUYAMA, BENJI N90-20150
MARYNICK, DENNIS S. N90-20229
MASHBURN, D. N. N90-20375

MASON, RODNEY J. N90-20847
MASSIE, NORBERT A. N90-20171
MASSOUDI, M. N90-20339
MATHEW, JOSEPH N90-20316
MATHUR, P. N90-20255
MATTEI, JANET A. N90-20914
MATTHEW, WILLIAM T. N90-20635
MATTHYS, DONALD R. N90-20324
MAZDIYASNI, K. S. N90-20233
MAZUREK, DOUG N90-20800
N90-20800
MCADOO, D. C. N90-20549
MCCASLAND, WILLIAM NEIL N90-20433
MCCLANAHAN, SCOTT N90-20671
MCCONAGHTY, C. F. N90-20299
MCDONALD, A. BLAIR N90-20064
MCDONNELL, GAYANN S. N90-20216
N90-20230
MCELROY, J. N90-20467
MCGRATH, DEBRA S. N90-20674
MCLENDON, T. N90-20512
MCMANAMEN, JOHN P. N90-20126
MCMANAMY, T. J. N90-20850
MCNEESE, MICHAEL D. N90-20639
N90-20640
N90-20641
N90-20749
MCPHEETERS, C. C. N90-20460
MCQUADE, TIMOTHY E. N90-20104
MEARS, MARK N90-20094
MEDERNACH, J. W. N90-20879
MEDERNACH, JOHN W. N90-20878
MEERKOV, SEMYON M. N90-20123
MEHALIC, MARK ANDREW N90-20310
MEHOS, MARK N90-20162
MELCHER, PAUL C. N90-20365
MELIS, MATTHEW E. N90-20438
MELLOR, MALCOLM N90-20097
MELNGAILIS, JOHN N90-20894
MELVIN, PETER J. N90-20552
MENDE, S. B. N90-20838
MENEFEE, RICHARD F. N90-20386
MENG, TERESA H.-Y. N90-20734
MERK, E. N90-20164
MERRITT, FERGUS N90-20660
METCALF, JAMES I. N90-20574
MIDDEL, B. N90-20520
MIDDLETON, DAVID B. N90-20096
MIKROYANNIDIS, JOHN A. N90-20133
MILBERT, DENNIS G. N90-20546
MILLER, ALLEN R. N90-20771
MILLER, B. A. N90-20059
N90-20066
MILLER, DAVID J. N90-20707
MILLER, IRVIN M. N90-20154
N90-20180
MILLER, LEE N90-20477
MILLER, STEVEN M. N90-20578
MILLER, SUSAN P. N90-20270
MILLER, W. THOMAS, III N90-20732
MILNE, A. M. N90-20490
MINCK, ROBERT N90-20479
MIRANDA, F. A. N90-20886
MIRAVETE, ANTONIO N90-20146
MIRELS, H. N90-20344
MITCHELL, A. W. N90-20883
MITCHELL, RICHARD N90-20489
MIURA, HIROKAZU N90-20087
MODE, V. ALAN N90-20620
MOLINA, EFRAIN A. N90-20772
MOLINA, ROD N90-20665
MONAHAN, RUSSELL E. N90-20483
MONTESFILHO, ANTONIO N90-20128
MONTGOMERY, F. C. N90-20233
MOODENBAUGH, A. R. N90-20857
MOORE, J. C. N90-20512
MOOSE, R. E. N90-20529
MORE, K. L. N90-20149
MORGAN, EARL W. N90-20609
MORINO, LUIGI N90-20048
MORRIS, J. R. N90-20376
MORRIS, J. W., JR. N90-20206
MORRIS, STEVEN LYNN N90-20075
MORRISON, CLYDE A. N90-20891
MORROW, JOHN G. N90-20500
MORSE, J. L. N90-20257
MOSES, R. L. N90-20278
MOSES, RANDOLPH L. N90-20271
MOSHER, STEPHEN E. N90-20055
MOSS, LANCE M. N90-20659
MOSTEK, S. D. N90-20378
MUELLER, HAROLD A. N90-20385
MUIR, PATRICK F. N90-20399
MUKHOPADHYAY, VIVEK N90-20093
MULDER, T. N90-20661
MULLER, R. H. N90-20165
MULLINS, JOHN N90-20170
MUNIR, ZUHAIR A. N90-20198
MURPHY, EDMUND N90-20917
MURPHY, H. C. N90-20578
MURPHY, KEVIN D. N90-20297
MURPHY, O. J. N90-20462
MURRAY, C. N90-20318
MURRAY, J. E. N90-20372
MURRAY, J. R. N90-20376
MURTHY, C. S. N90-20812
MUSIAL, W. D. N90-20492
MYER, L. R. N90-20570
MYERS, C. W. N90-20485
MYERS, D. W. N90-20378
MYERS, DARYL R. N90-20571
MYLES, K. M. N90-20460

N

NADEL, ETHAN R. N90-20617
NAGY, DEZSO N90-20536
N90-20543
NAKAMURA, T. N90-20223
NAKOS, J. T. N90-20259
NALETTE, T. N90-20467
NARANG, HIRA N90-20737
NATANSON, G. A. N90-20812
NATION, JOHN A. N90-20821
NEAL, BRADFORD N90-20086
NELSON, P. A. N90-20480
NEMANIC, MICHAEL N90-20735
NEMANICH, R. J. N90-20895
NEREM, R. S. N90-20550
NETTEL, S. J. N90-20881
NEUFER, P. DARRELL N90-20629
NEUMAN, CHARLES P. N90-20399
NEVESEPIPHANIO, JOSE CARLOS N90-20444
NEWMAN, EDWARD H. N90-20293
NEWMAN, J. C., JR. N90-20427
NEWTON, A. R. N90-20742
N90-20756
NEWTON, K. N90-20410
NG, KIM N90-20169
NGUYEN, H. L. N90-20708
NICHOLAS, M. G. N90-20192
NICHOLL, TINA M. N90-20693
NICHOLS, F. A. N90-20400
NICHOLSON, D. M. N90-20203
NOLTE, D. D. N90-20872
NORQUIST, DONALD N90-20595
NORTON, MARY N90-20371
NOUR-OMID, B. N90-20421
NOVAK, LESLIE M. N90-20758
NOYES, H. PIERRE N90-20915
NYMAN, MARK A. N90-20706

O

O, DAVID BOMKYU N90-20419
OBERLE, LAWRENCE G. N90-20358
OCKO, B. M. N90-20213
OERTEL, J. A. N90-20369
OGLETREE, BARRY N90-20658
OHWA, MIEKO N90-20370
OLDHAM, W. G. N90-20311
OLIVER, G. N90-20395
OLSON, TODD M. N90-20212
ORR, LINDA N90-20675
ORVIS, W. J. N90-20299
OSGOOD, RICHARD M., JR. N90-20267
OSHER, S. N90-20650
OSTERYOUNG, ROBERT A. N90-20175
OTADUY, P. J. N90-20736
OTSUKI, M. N90-20350
OTTO, G. N90-20238
OUVERASIMONI, PAULO N90-20565
OVIEDO, ANTONIO F. P. N90-20443

P

PACHECO, JAMES E. N90-20162
PADILLA, E. H. N90-20373
PAHK, UEAN-SIN N90-20864
PAK, S. S. N90-20233
PALASZEWSKI, BRYAN A. N90-20110
PALMER, BARBARA N90-20800
PANDOLF, KENT B. N90-20629
PANOS, GREGORY PETER N90-20663
PANTIC, DRAGAN M. N90-20393
PAPASTAVROU, JASON D. N90-20274
PARK, D. M. N90-20713
PARMA, GEORGE F. N90-20408
PARROTT, TONY L. N90-20795
PARROTT, W. N90-20661
PASSMAN, STEPHEN L. N90-20334
PASTERNAK, ROBERT E. N90-20196
PASUT, L. N90-20619
PATEL, G. B. N90-20518
PATEL, M. A. N90-20888
PATT, BRADLEY E. N90-20357
PATTERSON, EDWARD L. N90-20370
PATTERSON, F. G. N90-20885
PATTERSON, JAMES C., JR. N90-20078
PATTON, JOHN F. N90-20628
PAUL, GARY N90-20476
PAULIUS, L. N90-20233
PAVLIS, E. C. N90-20514
N90-20518
PEAT, R. N90-20861
PEDEN, C. H. N90-20161
PELED, EMANUEL N90-20482
PENHAPACHECO, ADMILSON N90-20447
PENSOTTI, L. S. N90-20649
PERRY, BOYD, III N90-20093
PERRY, DALE ROBERT N90-20602
PERRY, M. D. N90-20885
PERSHAN, P. S. N90-20213
PERSON, LEE H. N90-20096
PETER, G. N90-20529
PETERS, JEFFREY LYNN N90-20604
PETERS, PETER J. N90-20370
PETERSEN, GARY W. N90-20450
PETTERSON, BEN J. N90-20398
N90-20435
PEYGHAMBARIAN, N. N90-20832
PEYTON, B. N90-20285
PFAFMAN, T. N90-20360
PFALTZ, JOHN L. N90-20905
PHAM, M. N90-20467
PHELPS, ANDREW R. N90-20760
PHILBIN, DENNIS J. N90-20235
PHILLIPS, CARY B. N90-20677
PHILLIPS, CHARLES M. N90-20578
PHILLIPS, DAVID S. N90-20887
PIEPER, G. W. N90-20709
PIEPER, KEITH A. N90-20091
PINA, C. A. N90-20281
PISSILIATEJUNIOR, EDUARDO N90-20443
PITT, L. D. N90-20776
PLESSEL, TODD N90-20660
PLINE, ALEXANDER D. N90-20352
PODNEY, WALTER N. N90-20361
POEPPEL, R. B. N90-20888
POETSCHKE, JUERGEN N90-20244
POLITZER, P. A. N90-20822
POMERANTZ, MARTIN N90-20229
PONCHAK, DENISE S. N90-20264
PONCHAK, GEORGE E. N90-20286
PONT, F. N90-20748
POOL, SANDRA N90-20696
POPE, J. N90-20619
PORTER, G. D. N90-20822
PORTER, JOHN T. N90-20153
PORTER, TOM N90-20653
POST, JOHN T. N90-20430
POTOTZKY, A. S. N90-20071
POTTER, GERALD L. N90-20588
POTTER, R. M. N90-20485
POUKEY, J. W. N90-20285
POUND, B. G. N90-20474
POWELL, H. T. N90-20372
POWELL, JEFFREY DOUGLAS N90-20592
PRAKASH, JAI N90-20468
PREDEL, B. N90-20245
PREINHAELTER, J. N90-20842
PREITSCHOPF, CHRISTIAN R. N90-20897
PRIATKO, G. J. N90-20691
PRICE, DALE N90-20800
PRICE, J. B. N90-20189
PROVAN, J. S. N90-20415
PRUETT, STAN N90-20094
PUTNEY, B. H. N90-20514
PYRAK-NOLTE, L. J. N90-20570

R

RABERN, D. A. N90-20436
RABIER, PATRICK J. N90-20770
RADOUSKY, H. B. N90-20884
RADZIEMSKI, LEON J. N90-20824
RAJ, RISHI N90-20219
RAJAGOPAL, K. R. N90-20339
RAJESHWAR, KRISHNAN N90-20229
RAMAMURTI, RAVI N90-20347
RAMAN, SETHU N90-20584
RANDALL, DAVID A. N90-20567
RANKIN, C. C. N90-20421
RANSONE, PHILIP O. N90-20323
RAO, C. RADHAKRISHNA N90-20698

RAO, C. RADHAKRISNA N90-20757
RAOUF, RAOUF ALI N90-20418
RAPP, RICHARD H. N90-20513
N90-20516
RASMUSSEN, ROY R. N90-20062
RATHZ, THOMAS J. N90-20251
RATIU, T. N90-20856
RATKE, L. N90-20245
RATNAKUMAR, B. V. N90-20459
RAUCH, H. N90-20825
RAUH, H. N90-20424
RAVENSCROFT, F. A. N90-20410
RAVI-CHANDAR, K. N90-20441
RAWLINS, W. T. N90-20578
RAWLS, JOHN W., JR. N90-20795
RAY, L. P. N90-20354
REAUGH, JOHN E. N90-20437
REBA, R. C. N90-20621
RECALDERAMOS, FACUNDO SALOMON N90-20442
RED, MICHAEL T. N90-20683
REDDY, D. R. N90-20090
REDDY, T. S. R. N90-20051
REDENTE, EDWARD F. N90-20512
REDMON, M. J. N90-20812
REED, CURTIS HARVEY N90-20389
REED, K. N90-20300
REEVES, F. B. N90-20512
REGELBRUGGE, M. E. N90-20421
REID, MARGARET A. N90-20473
REIN, D. H. N90-20211
RENNER, TIM R. N90-20706
REUTER, RAINER N90-20499
REX, S. N90-20243
REYNOLDS, G. H. N90-20153
REYNOLDS, JAMES C. N90-20674
REYNOLDS, JOHN R. N90-20229
REYNOLDS, KATY L. N90-20633
REYNOLDS, W. C. N90-20343
RHEINBOLDT, WERNER C. N90-20770
RHODES, MARVIN D. N90-20121
RHUDY, DON KENNETH N90-20600
RIBEIRODESA, LELIO N90-20443
RICCI, MARIO CESAR N90-20390
RICE, JOHN N90-20731
RICHARD, M. A. N90-20302
RICHARDS, WHITMAN N90-20714
RICHARDSON, JOHN F. N90-20733
RICHERT, BRENT ARMAND N90-20892
RICHERT, SILVIA ANN N90-20177
RICHMOND, GEORGE N90-20735
RIEKE, P. C. N90-20225
RIES, J. C. N90-20515
RIGDON, MICHAEL A. N90-20145
RIORDAN, CAROL J. N90-20571
RITCHIE, JAMES P. N90-20168
RITCHIE, R. H. N90-20810
ROBBINS, J. W. N90-20514
ROBERTS, JON ALAN N90-20580
ROBERTS, LEONARD N90-20052
ROBERTSON, KAREN L. N90-20365
ROBINETT, RUSH D. N90-20398
N90-20435
ROBINSON, DAVID A. N90-20583
ROBINSON, MICHAEL B. N90-20251
ROBINSON, THOMAS L., JR. N90-20664
ROCCA, J. J. N90-20318
ROCK, PAUL B. N90-20625
RODDIER, CLAUDE N90-20911
RODDIER, FRANCOIS N90-20911
RODEMEIER, R. N90-20825
RODRIGUES, VALTER N90-20565
ROELKE, R. J. N90-20708
ROGERS, S. E. N90-20333
ROLLISON, BILL N90-20094
ROMAIDES, ANESTIS J. N90-20548
ROMAN, D. N90-20661
ROMANOFSKY, ROBERT R. N90-20286
ROMERO, VICTOR O. N90-20365
ROSBOROUGH, G. W. N90-20551
ROSE, MADELEINE S. N90-20635
ROSEN, I. G. N90-20764
ROSEN, ROBERT S. N90-20440
ROSENBLATT, GERD M. N90-20148
ROSENSZWEIG, J. B. N90-20855
ROSNER, R. B. N90-20870
ROTH, KARLIN RENEE N90-20045
ROVANG, DEAN C. N90-20108
ROVERE, L. A. N90-20736
RUBAHN, H.-G. N90-20804
RUBNER, M. F. N90-20870
RUDORFF, BERNARDO F. T. N90-20443
RUF, BEVERLY ANN N90-20811
RUMMEL, R. N90-20557
RUSHFORD, M. C. N90-20376
RYCHLIK, IGOR N90-20779
RYNE, R. D. N90-20305

S

SABATINI, R. L. N90-20857
SABIONSKI, GUNTER R. N90-20664
SACKS, RICHARD N90-20269
SAILOR, R. V. N90-20532
SAINI, AGYA R. N90-20215
SAKAGUCHI, K. N90-20451
SALAMA, T. M. N90-20788
SAMMELLS, ANTHONY F. N90-20461
SAMORODNITSKY, GENNADY N90-20778
SANCHEZ, B. V. N90-20514
SANDHAM, N. D. N90-20343
SANDOR, P. N90-20056
SANDRY-GARZA, DIANE L. N90-20647
SANDUBRAE, JEFFREY N90-20495
SANGIOVANNI-VINCENTELLI, A. N90-20742
SANKUR, H. O. N90-20791
SANSO, F. N90-20535
SANTEE, W. R. N90-20649
SARANGAPANI, S. N90-20464
N90-20470
SARAVANOS, D. A. N90-20432
SASHEGYI, KEITH N90-20584
SAWKA, MICHAEL N. N90-20629
SAYAH, H. R. N90-20281
SCHAFFRIN, B. N90-20520
SCHATZLE, FRANK J. N90-20635
SCHIMMEL, FRED N90-20696
SCHLIESING, JOHN A. N90-20126
SCHMECKPEPER, K. R. N90-20661
SCHMITT, MARK J. N90-20374
SCHMITZ, DONALD N90-20388
SCHOEN, JAMES J. N90-20060
SCHOENBACH, KARL H. N90-20288
SCHRAMA, E. J. O. N90-20557
SCHRAWYER, L. R. N90-20204
SCHRECK, SCOTT JEFFREY N90-20346
SCHRYER, DAVID R. N90-20154
SCHUELER, D. G. N90-20494
SCHUNK, ROBERT W. N90-20101
SCHUTZ, B. E. N90-20515
N90-20558
SCHWARTZ, R. N90-20859
SCHWARZ, K. P. N90-20524
SCOTT, M. J. N90-20505
SCRUBY, C. B. N90-20189
N90-20410
N90-20411
SDEFREITAS, EDUARDO N90-20443
SEARFUS, R. M. N90-20705
SEASHOLTZ, RICHARD G. N90-20358
SEATON, C. T. N90-20829
SECARY, JOSEPH J. N90-20899
SECHTIN, MICHAEL B. N90-20758
SEIDMAN, THOMAS I. N90-20761
SEKAR, R. R. N90-20394
SENGUPTA, UPAL N90-20086
SERAFINO, KAREN M. N90-20719
SERFATY, DANIEL N90-20643
SETTLES, GARY S. N90-20345
SHACKELFORD, SCOTT A. N90-20156
SHAFER, B. P. N90-20379
SHAGNEA, ANITA M. N90-20694
SHAING, K. C. N90-20844
SHAMMA, SHAWKY E. N90-20772
SHAN, XIAOYIN N90-20472
SHARP, L. E. N90-20843
SHATTUCK, JULIAN W. N90-20782
SHEKHAR, R. N90-20303
SHELDON, B. W. N90-20149
SHELTON, R. N. N90-20884
SHEN, D. H. N90-20481
SHERWOOD, R. J. N90-20705
SHERWOOD, ROBERT J. N90-20171
SHI, DONGLU N90-20888
SHI, X.-H. N90-20843
SHIELDS, F. D. N90-20796
SHIH, T. I.-P. N90-20708
SHIN, KYUNG-SOO N90-20420
SHINGU, H. N90-20350
SHORES, DAVID N90-20672
SHORES, PAUL W. N90-20280
SHUDDE, REX H. N90-20124
SHUKITT-HALE, BARBARA N90-20625
SHUM, C. K. N90-20515
N90-20517
N90-20550
SIDERIS, M. G. N90-20534
SIDNEY, BARRY D. N90-20154
SIFERD, RAYMOND N90-20312
SILLIMAN, M. N90-20395
SILVA, WALTER A. N90-20047
SILVER, E. N90-20360
SIMIONESCO, I. N90-20065
SIMMONS, GUSTAVUS J. N90-20710
SIMMS, D. A. N90-20111
SIMONS, JACOB VANVRANKEN, JR. N90-20721
SIMONS, RAINEE N. N90-20286
SIMPSON, DEAN W. N90-20100
SIMS, MARC L. N90-20726
SINCLAIR, D. R. N90-20578
SINCLAIR, D. W. N90-20331
SINGER, JOSEPH N90-20471
SINGH, JAG J. N90-20137
SINGH, JAIDIP N90-20686
SINGH, R. P. N90-20706
SINNOTT, M. J. N90-20143
SIPCIC, SLOBODAN N90-20048
SJOEBERG, LARS E. N90-20521
SKOTHEIM, T. A. N90-20870
SKUDLAREK, MARTIN J. N90-20662
SLINKER, S. P. N90-20817
SLUITER, M. N90-20203
SMEETS, BEN N90-20710
SMITH, B. T. N90-20703
SMITH, D. E. N90-20514
N90-20554
SMITH, GARY N90-20671
SMITH, MARK D. N90-20919
SMITH, MICHAEL P. N90-20208
SMITH, RANDY L. N90-20670
SMITH, RONALD E. N90-20329
SMOOKE, MITCHELL D. N90-20235
SMYTH, CHRISTOPHER C. N90-20646
SNELL, MICHAEL PAUL N90-20818
SOISTMANN, D. L. N90-20071
SOLEWICZ, REYNALDO N90-20448
SOLHEIM, DAG N90-20537
SOMERS, LARRY E. N90-20666
SON, S. H. N90-20905
SPAIN, C. V. N90-20071
SPEAKMAN, JERRY D. N90-20799
SPECK, D. R. N90-20372
SPECKER, LAWRENCE J. N90-20055
N90-20063
SPELT, P. F. N90-20395
N90-20746
SPENCE, RODNEY L. N90-20264
SPERBER, KENNETH R. N90-20588
SPRENGER, H. J. N90-20246
SPRUCK, J. N90-20766
SRICHANDER, RAMASWAMY N90-20417
SRINIVASAN-RAO, T. N90-20807
SRINIVASAN, SUPRAMANIAM N90-20465
SRIVASTAVA, SANTOSH K. N90-20366
SRIVATSAN, RAGHAVACHARI N90-20096
ST.CLAIR, ANNE K. N90-20409
ST.CLAIR, TERRY L. N90-20137
STABLEIN, CLAY N90-20914
STACEY, K. A. N90-20189
STAELIN, DAVID H. N90-20912
STAFFORD, RUSSELL G. N90-20780
STALLINGS, ROBERT L., JR. N90-20079
STAMM, R. N90-20853
STANLEY, WILLIAM D. N90-20284
STANNY, ROBERT R. N90-20772
STANSFIELD, S. A. N90-20402
STEARNS, S. D. N90-20296
STEARNS, SAMUEL D. N90-20268
STEFFEN, CARLOS A. N90-20443
STEGEMAN, G. I. N90-20829
STEIER, W. H. N90-20307
STEINFELD, JEFFREY I. N90-20578
STENGER, GREGORY J. N90-20089
STEPHENS, H. P. N90-20161
STEPHENSON, LOU A. N90-20624
STEVENSON, J. O. N90-20879
STEWART, WILLIAM CREED N90-20179
STINESPRING, CHARTER N90-20214
STINTON, D. P. N90-20149
STOAKLEY, DIANE M. N90-20409
STOCKS, G. M. N90-20203
STODOLSKY, F. N90-20394
STOHL, F. V. N90-20161
STONE, EMILY FOSTER N90-20321
STONE, R. N90-20300
STONEHAM, A. M. N90-20185
N90-20801
N90-20860
STORMER, WILLIAM N90-20076
STRADTNER, RONALD N90-20706
STRAND, DOUGLAS J. N90-20792
STRANGWOOD, M. N90-20184
N90-20188
N90-20193
STRAYER, M. R. N90-20763
STRINGFELLOW, G. B. N90-20877
STROBEL, DARRELL N90-20584
STUART, HOWARD R. N90-20912
STUART, MARK A. N90-20670

STYGAR, W. A. N90-20285
STYTZ, MARTIN ROBERT N90-20630
SU, CHIEN-HUA FRANK N90-20764
SUBBARAO, S. N90-20481
SUENAGA, M. N90-20857
SUGAMA, TOSHIFUMI N90-20210
SUHLING, JEFF N90-20144
SUIT, WILLIAM T. N90-20122
SULLIVAN, BRIAN N90-20723
SUMMERS, MARK A. N90-20371
SUMMERS, T. S. E. N90-20206
SUNDAR, C. S. N90-20883
N90-20884
SURESH, S. N90-20223
SWAB, JEFFREY J. N90-20890
SWAMINATHAN, P. K. N90-20812
SWANSON, ERIC A. N90-20828
SWETTE, L. N90-20469
SWITHINBANK, CHARLES N90-20097
SYLVANDER, L. N90-20853
SYSKA, ANDREW N90-20170
SZAPIRO, B. N90-20318
SZCZUR, MARTHA R. N90-20652
SZKODY, PAULA N90-20914
SZLYK, PATRICIA C. N90-20635
SZOFRAN, FRANK R. N90-20896

T

TAIT, K. S. N90-20532
TAKIGAWA, MASASHI N90-20863
TALIN, B. N90-20853
TALLON, R. W. N90-20868
TAN, H. Q. N90-20428
TAPLEY, B. D. N90-20515
N90-20517
N90-20550
N90-20558
TARASEVICH, B. J. N90-20225
TARJAN, ROBERT E. N90-20693
N90-20728
N90-20754
TASAI, P. K. N90-20233
TASKER, P. W. N90-20185
TAUR, DER-REN N90-20102
TAVELLA, DOMINGO N90-20052
TAY, S. P. N90-20865
TAYLOR, IVOR J. N90-20091
TAYLOR, N. J. N90-20193
TAYLOR, R. D. N90-20817
TEMPLE, J. A. G. N90-20425
TENTYUKOV, M. N. N90-20898
TEWARI, S. N. N90-20194
THANEDAR, P. B. N90-20138
THOM, ROBERT L. N90-20200
THOMAS, DENNIS RANDALL N90-20276
THOMAS, GARETH N90-20197
THOMAS, GLENN N90-20635
THOMAS, JOHN N90-20573
THOMAS, PETER N90-20917
THOMAS, R. E. N90-20826
THOMAS, TIMOTHY R. N90-20702
THOMPSON, DAN N90-20094
THORN, CHARLES B. N90-20897
TIDSWELL, I. M. N90-20213
TIEDERMAN, WILLIAM G. N90-20327
N90-20329
TILLETT, D. M. N90-20608
TISSOT, R. G. N90-20859
TOBIAS, C. W. N90-20165
TOEPPEN, JOHN N90-20359
TOMKINS, JAMES L. N90-20740
TOMLINSON, BARBARA S. N90-20122
TORGE, W. N90-20545
TOU, T. Y. N90-20843
TOWNE, MATTHEW C. N90-20349
TRAD, L. A. N90-20615
TREJO, LEONARD J. N90-20638
TREW, R. J. N90-20895
TRIBULA, D. N90-20206
TROMBKA, JACOB I. N90-20357
TROMBLEY, GERALD J. N90-20313
TRUJILLO, J. N90-20299
TRYK, DONALD N90-20468
TSAI, KAN J. N90-20461
TSANG, T. N90-20807
TSAO, S. S. N90-20879
TSAUR, BOR-YEU N90-20290
TSCHERNING, C. C. N90-20535
TURCHI, P. E. A. N90-20203
N90-20884
TURNER, T. P. N90-20369
TURNER, TRACEY JANE N90-20910
TURNQUIST, SCOTT R. N90-20120
TUTTLE, B. A. N90-20859
TWOMEY, W. J. N90-20439

U

UNGER, P. N90-20825
UPADHYAY, TRIVENI N. N90-20556
UPADHYE, R. S. N90-20205
UPCHURCH, BILLY T. N90-20154
N90-20180

V

VALAIRE, BRUCE N90-20144
VALLERAND, ANDRE L. N90-20618
VALLIANT, H. D. N90-20527
VANCAMP, KENNETH N90-20105
VANDAMME, JAMES M. N90-20295
VANDERWIJNGAART, ROBERTUS FRANCISCUS
N90-20328
VANDYKE, JOHN P. N90-20740
VANGYSEN, HERMAN N90-20539
VANLOON, D. N90-20619
VANSANT, J. N90-20300
VANWYK, CHRISTOPHER J. N90-20693
VAUCHER, GAIL M. TIRRELL N90-20576
VEGH, EMANUEL N90-20771
VEJINS, V. N90-20170
VERHOFF, VINCENT G. N90-20392
VERZWYVELT, S. A. N90-20475
VESELY, E. J., JR. N90-20181
VIJAYAKUMAR, M. N90-20194
VISCO, STEVEN J. N90-20306
VOGT, GERALD J. N90-20887
VOIGT, JIM A. N90-20875
VOLEK, MICHAEL JEROME N90-20601
VOLZ, R. A. N90-20256
VROMAN, THEODORE T. N90-20603
VU, BANG Q. N90-20679

W

WAAGEN, ELIZABETH O. N90-20914
WACHS, A. L. N90-20883
N90-20884
WADE, RODERICK K. N90-20453
WAGNER, C. A. N90-20518
N90-20549
WALD, P. H. N90-20620
WALKER, BRUCE K. N90-20417
WALKER, KEVIN P. N90-20431
WALLACE, TERRY C. N90-20579
WALRATH, JAMES D. N90-20648
WALTER, M. B. N90-20511
WALUKIEWICZ, W. N90-20872
WANG, AHUA N90-20490
WANG, JERRY N90-20308
WANG, LAWRENCE C. H. N90-20618
WANG, Y. L. N90-20857
WANG, Y. M. N90-20541
WANNIGMAN, DAVID L. N90-20816
WARD, MICHAEL N90-20384
WARDLAW, WILLIAM P. N90-20771
N90-20774
WARDLE, DAVID I. N90-20583
WARNER, J. D. N90-20886
WASSERMAN, S. R. N90-20213
WATERS, RICHARD C. N90-20725
WATSON, KENNETH A. N90-20103
WATSON, VAL N90-20660
WATTS, G. N90-20661
WAYNERT, J. A. N90-20258
WEBBER, BONNIE N90-20743
WEBRE, JAMES L. N90-20076
WEEKS, R. A. N90-20858
WEGNER, P. J. N90-20372
WEI, CAI N90-20768
WEI, M. N90-20524
WEIKLE, DONALD H. N90-20358
WEILAND, T. L. N90-20373
WEILER, THOMAS J. N90-20802
WEINGART, R. C. N90-20257
WEIR, J. R., JR. N90-20207
WEIR, L. J. N90-20090
WEISBIN, CHARLES R. N90-20397
WEISS, ROSANNE M. N90-20500
WEISSMAN, J. C. N90-20608
WELCH, D. E. N90-20850
WELKER, J. E. N90-20566
N90-20572
WELSH, BYRON MACMASTER N90-20913
WENDEL, M. W. N90-20335
N90-20340
WENTZCOVITCH, RENATA M. N90-20218
WENZEL, H.-G. N90-20545
WERNER, JILL C. N90-20398
N90-20435
WESSELLS, C. W. N90-20529
WEST, BLAINE S. N90-20069
WESTBROOK, JEFFREY N90-20754
WESTCOTT, C. N90-20190
WESTENSKOW, G. A. N90-20305
WESTON, CRAIG P. N90-20781
WHANG, ROBERT N90-20635
WHEELER, CONRAD R. N90-20613
N90-20614
WHELLER, CONRAD R. N90-20609
WHITE, J. N90-20525
WHITE, JACK B. N90-20327
WHITE, MICHAEL N90-20076
WHITESIDES, G. M. N90-20213
WHITLOCK, CHARLES H. N90-20583
WHITTENBERGER, J. DANIEL N90-20181
WHYTE, WAYNE A., JR. N90-20264
WICKENS, CHRISTOPHER D. N90-20720
WIDNER, MELVIN M. N90-20106
N90-20108
WIE, MICHAEL N90-20105
WIGHT, CHARLES A. N90-20174
WIKE, JEFFREY N90-20667
WILCOX, FLOYD J., JR. N90-20079
WILCOX, P. D. N90-20234
WILCOX, R. B. N90-20373
WILKINS, MARK L. N90-20437
WILLIAMS, A. N. N90-20112
WILLIAMS, D. E. N90-20190
N90-20861
WILLIAMS, KEITH N90-20684
WILLIAMS, WALLACE D. N90-20393
WILLIAMSON, R. G. N90-20514
WILSON, ANTHONY N90-20072
WILTSE, JAMES C. N90-20291
WINKLER, I. N90-20578
WINNER, WILLIAM E. N90-20501
WITHERS, B. EDWARD N90-20694
WITTMAN, WILLIAM THOMAS N90-20644
WITTMANN, K. N90-20240
WITTRY, DAVID B. N90-20351
WOJCIK, A. S. N90-20703
WOLF, KLAUS N90-20429
WOLTER, J. H. N90-20861
WOLTZ, DAN J. N90-20642
WOMBLE, DAVID E. N90-20738
N90-20739
WOOD, GEORGE M. N90-20154
WOODARD, JEFFREY P. N90-20277
WOODWARD, CHARLES E. N90-20290
WOODWARD, RICHARD P. N90-20794
WRENN, LAWRENCE R., II N90-20787
WRIGHT, M. A. N90-20421
WU, JIUN-TSONG N90-20553
WU, SIEN-CHONG N90-20553
WYATT, P. W. N90-20290

X

XIMING, DAI N90-20490
XU, YOUWEN N90-20857

Y

YANG, K. N90-20223
YANG, R.-J. N90-20333
YANG, X. Q. N90-20870
YAO, JEN-CHIH N90-20755
YARKONY, DAVID R. N90-20815
YEAGER, ERNEST N90-20468
YEARY, LON M. N90-20718
YEE, J. H. N90-20299
YI, THOMAS Y. N90-20455
YOST, SCOTT A. N90-20897
YOUNG, ANDREW J. N90-20629
YOUNG, BRENTON C. N90-20739
YOUNG, PAUL G. N90-20393
YOUNG, R. M. K. N90-20134
N90-20186
YOUNGBLUT, CHRISTINE N90-20783
YU, S. S. N90-20305
YUAN, D. N. N90-20515
N90-20517
N90-20550
YUEN, VINCENT K. N90-20680
YUNG, REBECCA C. N90-20157

Z

ZAMANI, N. N90-20281
ZANK, GARY D. N90-20784
ZAPPIA, MICHAEL J. N90-20157

ZARETSKY, ERWIN V. N90-20391
ZEE, RALPH H. N90-20144
ZELKOWITZ, MARVIN V. N90-20715
ZHAO, JIANHUA N90-20490
ZHENG, Y. N90-20883
ZHOU, D.-F. N90-20843
ZIMBACK, CELIA R. N90-20443
ZMUDZINSKI, CHARLES ALAN N90-20363
ZORUMSKI, WILLIAM E. N90-20795
ZUCCARIFERNANDESBRAGA, CLAUDIA N90-20445
ZUCKER, PAUL A. N90-20522
ZUHR, R. A. N90-20858
ZUNIGA, MIKE N90-20347
ZUZEK, JOHN E. N90-20264
ZWALLY, H. JAY N90-20562
N90-20563
N90-20564
ZWEIBEL, KEN N90-20489

Typical Corporate Source Index Listing

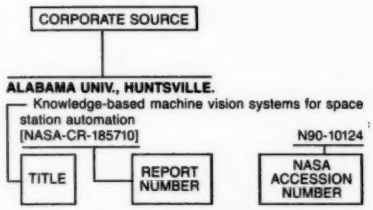

Listings in this index are arranged alphabetically by corporate source. The title of the document provides the user with a brief description of the subject matter. The report number helps to indicate the type of document cited (e.g., NASA report, translation, NASA contractor report). The NASA accession number denotes the number by which the citation is identified. The titles are arranged under each corporate source in ascending accession number order.

A

AACHENER CENTRUM FUER ERSTARRUNG UNTER SCHWERELOSIGKEIT E.V. (GERMANY, F.R.).
Dynamics of the solidification front N90-20243

ADVISORY GROUP FOR AEROSPACE RESEARCH AND DEVELOPMENT, NEUILLY-SUR-SEINE (FRANCE).
Implications of Advanced Technologies for Air and Spacecraft Escape
[AGARD-CP-472] N90-20054

AERODYNE RESEARCH, INC., BILLERICA, MA.
Fluorinated diamond thin films for tribological applications
[AD-A217452] N90-20214

AERONAUTICAL RESEARCH LABS., MELBOURNE (AUSTRALIA).
A data acquisition parallel bus for wind tunnels at ARL (Aeronautical Research Laboratory)
[AD-A218052] N90-20098
Analyses of power consumption for two sliding vane type compressors
[AD-A218366] N90-20406
Complex demodulation for bearing fault detection
[AD-A218367] N90-20407

AEROSPACE CORP., EL SEGUNDO, CA.
Geometric scale of interaction between moving shock and stationary thermal layer
[AD-A217769] N90-20344

AEROSPACE MEDICAL RESEARCH LABS., WRIGHT-PATTERSON AFB, OH.
Development of acceleration exposure limits for advanced escape systems N90-20055
The USAF Advanced Dynamic Anthropomorphic Manikin (ADAM) N90-20062
Windblast protection for advanced ejection seats N90-20063
The role of chaos in hemispheric process and attention
[AD-A217674] N90-20639
The boundaries of hemispheric processing in visual pattern recognition
[AD-A217675] N90-20640
Lateral asymmetry in pattern recognition: Understanding the effects of familiarity, distinction, and perspective change
[AD-A217739] N90-20641
CEREBRAL WEEVIL: A machine learning model for hemispheric categorization of complex visual patterns
[AD-A218143] N90-20749
Lateral attenuation of military aircraft flight noise
[AD-A218041] N90-20799
Air Force Boom Event Analyzer Recorder (BEAR): Sysstem description
[AD-A218048] N90-20800

AIR FORCE ACADEMY, CO.
Condensed phase kinetic deuterium isotope effects in high energy phenomena: Mechanistic investigations and relationships
[AD-A217161] N90-20156

AIR FORCE GEOPHYSICS LAB., HANSCOM AFB, MA.
GPS-aided gravimetry at 30 km altitude from a balloon-borne platform N90-20530
Very accurate upward continuation to low heights in a test of non-Newtonian theory N90-20548
Local gravity disturbance estimation from multiple-high-single-low satellite-to-satellite tracking N90-20555
Radar detection of lightning and electric fields
[AD-A217894] N90-20574
Atmospheric chemiluminescence: COCHISE and FACELIF experiments
[AD-A218121] N90-20578
Adiabatic and diabatic initialization of the AFGL (Air Force Geophysics Laboratory) global spectral model using dynamic normal mode and nonlinear normal mode methods
[AD-A218120] N90-20595
Study of possible solar heating effects on thermosonde probes: Error analysis
[AD-A218116] N90-20917

AIR FORCE HUMAN RESOURCES LAB., BROOKS AFB, TX.
Role of cognitive factors in the acquisition of cognitive skill
[AD-A218069] N90-20642

AIR FORCE INST. OF TECH., WRIGHT-PATTERSON AFB, OH.
F-15B high angle-of-attack phenomena and spin prediction using bifurcation analysis
[AD-A217366] N90-20073
Design of a high angle of attack robotic sting mount for tests in a low speed wind tunnel
[AD-A218105] N90-20099
Runaway rubber removal
[AD-A218349] N90-20100
Discrete-time control of a spacecraft with retargetable flexible antennas
[AD-A218345] N90-20125
The extinction and structure of counterflow premixed flames
[AD-A218106] N90-20178
An expert system for the design of heating, ventilating, and air-conditioning systems
[AD-A218287] N90-20262
Multiple versus single scattering of terrestrial infrared longwave radiation in an aerosol-laden planetary boundary layer
[AD-A217709] N90-20272
A matrix-free locally-implicit scheme for Navier-Stokes equations
[AD-A218298] N90-20349
Rotordynamic analysis with shell elements for the transfer matrix method
[AD-A217455] N90-20434
Measurements of the interaction of high-voltage biassed conductors with the ionosphere
[AD-A218285] N90-20580
The receiving system of a dual dye lidar to study molecular and aerosol densities at the base of the stratosphere
[AD-A218286] N90-20581
Coastal frontogenesis and associated severe weather on 13 March 1986 (GALE IOP 13)
[AD-A217708] N90-20590
A modeling study of the cloud-topped marine boundary layer
[AD-A218103] N90-20594
A method for correcting and reducing the pressure data recorded at the PAM 2 stations during GALE
[AD-A218165] N90-20596
Forecasting 24 and 48 hour intensity changes, for northwestern Pacific tropical cyclones, using satellite imagery
[AD-A218174] N90-20597
An aircraft investigation of a convective boundary layer over Lake Michigan
[AD-A218175] N90-20598
A sub-cloud layer vorticity budget analysis for two microburst-producing storms from jaws dual-Doppler data
[AD-A218180] N90-20599
Atmospheric wind measurements using a 50 MHz imaging Doppler interferometer radar
[AD-A218277] N90-20601
Forecasting the tornadic intensities of thunderstorms by multivariate techniques
[AD-A218284] N90-20602
Microwave brightness temperature and its relation to atmospheric general circulation features
[AD-A218312] N90-20603
A case study of a quasi-stationary tropical convective line
[AD-A218325] N90-20604
The invertibility principle for a simple hurricane model
[AD-A218344] N90-20605
Detection acuity in the peripheral retina
[AD-A218183] N90-20632
A review of the suitability of available Computer Aided Software Engineering (CASE) tools for the small software development environment
[AD-A218276] N90-20726
Performance of concurrency control algorithms in distributed systems
[AD-A218280] N90-20727
A parallel architecture for real-time simulation
[AD-A218321] N90-20741
An investigation of the locality of memory accesses during symbolic program execution
[AD-A218168] N90-20750
Large-angle elastic and inelastic scattering of Pi+ and Pi- from Si28 and Ca40
[AD-A218163] N90-20818
An experimental investigation of the thermal conductivity of porous adsorbents
[AD-A217854] N90-20899
An integrative research review of the relationship between technology and structure: A meta-analytic synthesis
[AD-A218115] N90-20903
An empirical test of a comprehensive model for predicting successful information systems implementation
[AD-A218124] N90-20908
Real-time concurrency control and transaction scheduling
[AD-A218162] N90-20909

AIR FORCE WEAPONS LAB., KIRTLAND AFB, NM.
Proton responses on MOS (Metal-Oxide-Semiconductor) electronics operating at cryogenic temperatures
[AD-A217622] N90-20868

AIR FORCE WRIGHT RESEARCH AND DEVELOPMENT CENTER, WRIGHT-PATTERSON AFB, OH.
ETO (Earth-To-Orbit): A trajectory program for aerospace vehicles
[AD-A218157] N90-20103

AIR WAR COLL., MAXWELL AFB, AL.
Assessing the morality of using the space environment as a platform for weapons
[AD-A217348] N90-20780
The essence of spacepower: Important influences on the evolution of national spacepower
[AD-A217498] N90-20781
Space in warfare
[AD-A217527] N90-20782
The thrust and parry of the SIOP (Single Integrated Operational Plan) and SDI
[AD-A217617] N90-20784

ALABAMA UNIV., HUNTSVILLE.
Characterization of fluid flow by digital correlation of scattered light
[NASA-CR-186403] N90-20324

ALBERTA UNIV., EDMONTON.
Influence of theobromine on heat production and body temperatures in cold-exposed humans: A preliminary report
[AD-A217203] N90-20618
ALLIED-SIGNAL AEROSPACE CO., TORRANCE, CA.
Development and fabrication of structural components for a scramjet engine
[NASA-CR-181945] N90-20088
ALPHATECH, INC., BURLINGTON, MA.
Information gathering and decisionmaking under stress
[AD-A218233] N90-20643
ANALEX CORP., CLEVELAND, OH.
Space Station Freedom electric power system availability study
[NASA-CR-185181] N90-20120
ANALYTIC SCIENCES CORP., READING, MA.
Synopsis of early field test results from the gravity gradiometer survey system N90-20525
Methods for local gravity field approximation N90-20532
ANALYTICAL SERVICES AND MATERIALS, INC., HAMPTON, VA.
A 4-node assumed-stress hybrid shell element with rotational degrees of freedom
[NASA-CR-4279] N90-20422
ARGONNE NATIONAL LAB., IL.
Physical sputtering of metallic systems by charged-particle impact
[DE90-007803] N90-20201
Evaluation of industrial magnetic heat pump/refrigerator concepts that utilize superconducting magnets
[DE90-008093] N90-20258
A technical and economic evaluation of oxygen-enriched combustion in diesel engines using water-emulsified fuels
[DE90-008095] N90-20394
Tribological properties of boric acid and boric-acid-forming surfaces. Part 2: Formation and self-lubrication mechanisms of boric acid films on boron- and boric-oxide-containing surfaces
[DE90-005632] N90-20400
Tribological properties of boric acid and boric acid forming surfaces. Part 1: Crystal chemistry and self-lubricating mechanism of boric acid
[DE90-005665] N90-20401
Monolithic solid oxide fuel cell development N90-20460
Advanced high-temperature batteries N90-20480
Using formal methods to develop a paradigm for software design
[DE90-005633] N90-20703
Joint Japanese-American Workshop on Future Trends in Logic Programming
[DE90-008343] N90-20709
Nonlinear plasma and beam physics in plasma wake-fields
[DE90-008812] N90-20855
Synthesis of Bi-Sr-Ca-Cu oxide superconductor by solution technique
[DE90-008707] N90-20888
ARINC RESEARCH CORP., ANNAPOLIS, MD.
Space Station Freedom electric power system availability study
[NASA-CR-185181] N90-20120
ARIZONA UNIV., TUCSON.
The effects of structure and source complexity on waveforms: Crustal structure of Tibet and the recovery of complex seismic sources
[AD-A218202] N90-20579
Structure and dynamics of the Arizona monsoon boundary
[AD-A217378] N90-20586
Nonlinear optics in thin films
[AD-A217336] N90-20829
Optical Bistability, 1988
[AD-A217681] N90-20832
ARMY AEROMEDICAL RESEARCH UNIT, FORT RUCKER, AL.
Simulator sickness in the CH-47 (Chinook) flight simulator
[AD-A218214] N90-20634
ARMY ARMAMENT RESEARCH AND DEVELOPMENT COMMAND, DOVER, NJ.
ARDEC (Armament Research, Development and Engineering Center) electric gun in-house test program
[AD-A217337] N90-20105
ARMY AVIATION ENGINEERING FLIGHT ACTIVITY, EDWARDS AFB, CA.
Airworthiness and flight characteristics evaluation of the McDonnell Douglas Helicopter Corporation (MDHC) 530FF helicopter
[AD-A218253] N90-20076
ARMY COLD REGIONS RESEARCH AND ENGINEERING LAB., HANOVER, NH.
Airfields on antarctic glacier ice
[AD-A217638] N90-20097
ARMY INST. FOR RESEARCH IN MANAGEMENT INFORMATION AND COMPUTER SCIENCES, ATLANTA, GA.
Technology assessment of video teleconferencing
[AD-A217318] N90-20266
Technology assessment of superconductivity
[AD-A217697] N90-20889
ARMY LAB. COMMAND, WATERTOWN, MA.
Oxygen concentrations on surfaces of carbon fibers
[AD-A217724] N90-20152
Evaluation of 2090-T8E48 aluminum-lithium plates
[AD-A217262] N90-20196
Performance of Y-TZP materials between 800 C and 1200 C
[AD-A217723] N90-20890
ARMY MATERIALS TECHNOLOGY LAB., WATERTOWN, MA.
Barkhausen noise analysis and ferromagnetic materials
[AD-A217989] N90-20792
ARMY RESEARCH INST. OF ENVIRONMENTAL MEDICINE, NATICK, MA.
Hypobaric hypoxia (380 torr) decreases intracellular and total body water in goats
[AD-A218192] N90-20615
Niacin ingested at night causes severe hypotension
[AD-A217896] N90-20624
Effects of dexamethasone and high terrestrial altitude on cognitive performance and affect
[AD-A217897] N90-20625
The effects of high intensity cycle exercise on sympatho-adrenal-medullary response patterns
[AD-A217962] N90-20628
Hydration effects on human physiology and exercise-heat performance
[AD-A217969] N90-20629
The effects of graded exercise at sea level on plasma proenkephalin peptide F and catecholamine responses
[AD-A218195] N90-20633
Field assessment of wet bulb globe temperature: Present and future
[AD-A218224] N90-20635
Effective calibration of heat flux transducers for experimental use
[AD-A218262] N90-20636
What should athletes know about low body temperature (hypothermia)
[AD-A218316] N90-20637
Comparison of light duty gloves with natural and synthetic materials under wet and dry conditions
[AD-A218119] N90-20649
ARNOLD ENGINEERING DEVELOPMENT CENTER, ARNOLD AIR FORCE STATION, TN.
Investigation of the development of laminar boundary-layer instabilities along a cooled-wall hollow cylinder at Mach number 8
[AD-A217672] N90-20331
ASTRONAUTICS CORP. OF AMERICA, MADISON, WI.
Evaluation of industrial magnetic heat pump/refrigerator concepts that utilize superconducting magnets
[DE90-008093] N90-20258
AUBURN UNIV., AL.
Optimization of fracture resistance in composites
[AD-A217431] N90-20144
AUTONOMOUS TECHNOLOGIES, ORLANDO, FL.
Multi-dimensional LADAR tracking and adaptive grasping for spaceborne assembly of SDI (Strategic Defense Initiative) platforms
[AD-A218236] N90-20279
AVIONS MARCEL DASSAULT-BREGUET AVIATION, SAINT-CLOUD (FRANCE).
Requirements for protective pressure suits for the Hermes spacecrew N90-20065

B

BARRIOS TECHNOLOGY, INC., HOUSTON, TX.
Binary space partitioning trees and their uses N90-20657
Prototype part task trainer: A remote manipulator system simulator N90-20672
BELMONT COLL., NASHVILLE, TN.
Interaction between implanted ions and intrinsic defects in silica
[DE90-006569] N90-20858
BOEING AEROSPACE CO., SEATTLE, WA.
Processing, fabrication, characterization and device demonstration of high temperature superconducting ceramics
[AD-A218330] N90-20231
Computed tomography of electronics
[AD-A217976] N90-20314
BOEING COMMERCIAL AIRPLANE CO., SEATTLE, WA.
Assessment of crew workload measurement methods, techniques and procedures. Volume 1: Process, methods and results
[AD-A217699] N90-20647
BOSTON UNIV., MA.
Unsteady free-wake viscous aerodynamic analysis of helicopter rotors
[AD-A217166] N90-20048
The geometry of disorder: Report 1987 to 1990
[DE90-008250] N90-20882
BRANDEIS UNIV., WALTHAM, MA.
Carbon and hydrogen metabolism of green algae in light and dark
[DE90-008648] N90-20612
BROOKHAVEN NATIONAL LAB., UPTON, NY.
Extended x ray absorption fine structure analysis applied to composite materials
[DE90-008575] N90-20150
Sol-gel derived polytitanosiloxane coatings
[DE90-004186] N90-20210
The role of polarity on the stability of graphitic compounds
[DE90-006528] N90-20218
Overview of the methodologies used to compile large scale emissions inventories
[DE90-008518] N90-20509
Surface-plasmon enhanced nonlinear photoelectric emission from thin silver films
[DE90-007676] N90-20807
A systematic study of the effects of metal substitutions for Cu in YBa(sub 2) (Cu(sub 1-x) M(sub x)3 O(sub 7-rho), M=Fe, Co, Al, Ga, Cr, Ni, and Zn
[DE90-003957] N90-20857
Molecular organization and electrical properties of mixed Langmuir-Blodgett multilayer thin films of polypyrrole
[DE90-007627] N90-20870
BROWN UNIV., PROVIDENCE, RI.
Tensile fracture toughness of ceramic materials: Effects of dynamic loading and elevated temperatures
[DE90-008329] N90-20223
Interactions of molecules with surfaces
[DE90-007555] N90-20806
BUNDESMINISTERIUM FUER FORSCHUNG UND TECHNOLOGIE, BONN (GERMANY, F.R.).
Reorganization of the German space administration. Foundation of DARA
[REPT-16/89] N90-20902

C

CAE ELECTRONICS LTD., MONTREAL (QUEBEC).
The development of the Canadian Mobile Servicing System Kinematic Simulation Facility N90-20676
CAE-LINK CORP., HOUSTON, TX.
The Orbital Maneuvering Vehicle Training Facility visual system concept N90-20684
CALGARY UNIV. (ALBERTA).
A framework for modelling kinematic measurements in gravity field applications N90-20524
CALIFORNIA UNIV., BERKELEY.
Synthesis of alumina-coated SiC whiskers for production of SiC whisker-reinforced alumina composite materials
[DE90-007778] N90-20147
The metallurgical mechanisms of solder fatigue
[DE90-008390] N90-20206
Modeling studies of electrolyte flow and bubble behavior in advanced Hall cells
[DE90-007013] N90-20303
Statistical equipment modeling for VLSI manufacturing
[DE90-008527] N90-20304
Joint services electronics program
[AD-A217961] N90-20311
Magnetic properties of surfaces and interfaces
[DE90-007348] N90-20789
Nonlinear stability in fluid and plasma dynamics
[AD-A217735] N90-20856
Absolute pressure dependence of the second ionization level of EL2 in GaAs
[DE90-007761] N90-20872
CALIFORNIA UNIV., BERKELEY. LAWRENCE BERKELEY LAB.
Synthesis of alumina-coated SiC whiskers for production of SiC whisker-reinforced alumina composite materials
[DE90-007778] N90-20147
Symposium on High Temperature and Materials Chemistry
[DE90-008047] N90-20148
Infrared absorption study of zinc-doped silicon
[DE90-007779] N90-20164
Enhancement of mass transfer to a rotating cylinder electrode by inert particles suspended in the electrolyte
[DE90-008054] N90-20165

The metallurgical mechanisms of solder fatigue
[DE90-008390] N90-20206
All-solid-state thin-film rechargeable lithium batteries using solid redox polymerization electrodes
[DE90-008665] N90-20306
Novel electrodes for advanced energy storage systems
[DE90-008667] N90-20496
Controlling Summer Heat Islands: Proceedings
[DE90-008075] N90-20508
Seismic characterization of fracture properties
[DE90-007759] N90-20570
Biological soft x ray contact microscopy: Imaging living CHO-SC1 cells and other biological materials
[DE90-007560] N90-20610
Life sciences: Lawrence Berkeley Laboratory, 1988
[DE90-008061] N90-20611
Software quality assurance and software safety in the biomed control system
[DE90-008072] N90-20706
Magnetic properties of surfaces and interfaces
[DE90-007348] N90-20789
Polyatomic reaction dynamics
[DE90-008668] N90-20811
Crystal preparation at LBL, 1976 to 1986
[DE90-007754] N90-20871
Absolute pressure dependence of the second ionization level of EL2 in GaAs
[DE90-007761] N90-20872
High resolution transmission electron microscopy study of defect structures in mixed-phase YBaCuO
[DE90-007767] N90-20873

CALIFORNIA UNIV., DAVIS.
Deep level transient spectroscopy in resistive layers
[DE90-008349] N90-20169
Aerodynamic and kinetic processes in flames
[AD-A217796] N90-20176
An investigation of the mechanisms of solid state powder reaction in the combustion synthesis and sintering of high temperature materials
[DE90-007880] N90-20198
Observer based compensators for nonlinear systems
[AD-A217426] N90-20760

CALIFORNIA UNIV., IRVINE.
Damage characteristics of time domain histories
[DE90-008787] N90-20573
Spontaneous magnetic reconnection in a turbulent plasma N90-20840

CALIFORNIA UNIV., LOS ANGELES.
Quantifying and reducing uncertainty in the assimilative mapping of ionospheric electrodynamics
[AD-A218057] N90-20577

CALIFORNIA UNIV., SAN DIEGO.
Nonintrusive optical measurements of turbulence and mixing in a stably stratified fluid N90-20322

CALSPAN CORP., ARNOLD AFS, TN.
Investigation of the development of laminar boundary-layer instabilities along a cooled-wall hollow cylinder at Mach number 8
[AD-A217672] N90-20331

CARNEGIE-MELLON UNIV., PITTSBURGH, PA.
The CMU Reconfigurable Modular Manipulator System
[CMU-RI-TR-88-7] N90-20388

CASE WESTERN RESERVE UNIV., CLEVELAND, OH.
Electrochemical phase diagrams for aqueous redox systems
[AD-A217168] N90-20157
Instantaneously generated foam and its applicability to reduced gravity
[NASA-CR-185208] N90-20237
Electrocatalysis for oxygen electrodes in fuel cells and water electrolyzers for space applications N90-20468

CENTER FOR NAVAL ANALYSES, ALEXANDRIA, VA.
Small and great circle routines
[AD-A217652] N90-20449
Computing mean responses in nonlinear models
[AD-A217642] N90-20700

CERAMIC BINDER SYSTEMS, INC., BUTTE, MT.
Thermoelectric conversion with ion conductors
[AD-A217822] N90-20497

CHEMICAL DYNAMICS CORP., UPPER MARLBORO, MD.
Dynamics of electronically excited species in gaseous and condensed phase
[AD-A217696] N90-20812

CHEMICAL RESEARCH AND DEVELOPMENT CENTER, ABERDEEN PROVING GROUND, MD.
Optimization of digital filters for a short-scan interferometer
[AD-A217997] N90-20315

CHUNG CHENG INST. OF TECH. (TAIWAN).
Determination of mean gravity anomalies in the Taiwan Island N90-20547

CINCINNATI UNIV., OH.
Approximate evaluation of reliability and related quantities via perturbation techniques
[AD-A218340] N90-20417

COLORADO STATE UNIV., FORT COLLINS.
Structure of model gas flames in nitramines
[AD-A217578] N90-20159
Electron beam generation by electron bombardment induced cathode emission
[AD-A218203] N90-20318
Processes of community development and responses of ecosystems to climate change
[DE90-008640] N90-20512
Theoretical modeling studies of the marine planetary
[AD-A217200] N90-20567
Determinations of photon spectra
[AD-A218003] N90-20816

COLORADO UNIV., BOULDER.
Experimental investigation of the mechanisms underlying vortex kinematics in unsteady separated flows
[AD-A217889] N90-20346
DURIP theoretical/experimental investigations of highly energetic dication species
[AD-A217771] N90-20383
Geographically correlated orbit error N90-20551
A long-term retention advantage for spatial information learned naturally and in the laboratory
[AD-A218268] N90-20644

COLUMBIA UNIV., NEW YORK, NY.
Research investigation directed toward extending the useful range of the electromagnetic spectrum
[AD-A217460] N90-20267
Laser enhanced chemical reactions
[DE90-008273] N90-20377

COMMUNICATIONS SATELLITE CORP., CLARKSBURG, MD.
Advanced modulation technology development for earth station demodulator applications. Coded modulation system development
[NASA-CR-185149] N90-20270

COMPUTATIONAL MECHANICS CO., AUSTIN, TX.
Analysis of flow-, thermal-, and structural-interaction of hypersonic structures subjected to severe aerodynamic heating
[AD-A217882] N90-20053

CONNECTICUT UNIV., STORRS.
Rigid rod molecules as liquid crystal thermosets
[AD-A217573] N90-20158
Copolymer-like structures of nematic nitroimine dimers
[AD-A217574] N90-20215

CORNELL UNIV., ITHACA, NY.
Interface science in deformation processing of ceramics
[DE90-008424] N90-20219
A study of low-dimensional models for the wall region of a turbulent boundary layer N90-20321
Collective ion acceleration in high current relativistic electron beams
[DE90-008328] N90-20821
The geometry of disorder: Report 1987 to 1990
[DE90-008250] N90-20882

D

DAYTON UNIV., OH.
Full-scale birdstrike testing of in-service aged F-111 ADBIRT windshield transparencies
[AD-A218035] N90-20069
An electrochemical and spectroscopic study of electrode processes
[AD-A217261] N90-20289

DEFENCE AND CIVIL INST. OF ENVIRONMENTAL MEDICINE, DOWNSVIEW (ONTARIO).
Influence of theobromine on heat production and body temperatures in cold-exposed humans: A preliminary report
[AD-A217203] N90-20618
Physical performance and carbohydrate consumption in CF commandos during a 5-day field trial
[AD-A217204] N90-20619
The +Gz protection in the future: Review of scientific literature
[AD-A217887] N90-20623

DEFENCE RESEARCH ESTABLISHMENT, OTTAWA (ONTARIO).
An investigation of the extent of the fresnel region of aperture antennas with attention to superdirectivity
[AD-A217518] N90-20294

DEPARTMENT OF ENERGY, PITTSBURGH, PA.
A method for measuring the material moduli of granular materials: Flow in an orthogonal rheometer
[DE90-007160] N90-20339

DEPARTMENT OF ENERGY, PORTLAND, OR.
Draft global warming study
[DE90-008446] N90-20507

DEPARTMENT OF ENERGY, WASHINGTON, DC.
Materials Science Programs, fiscal year 1989
[DE90-008169] N90-20131
Atmospheric Radiation Measurement Program Plan
[DE90-008108] N90-20504

DEPARTMENT OF NATIONAL DEFENCE, OTTAWA (ONTARIO).
Investigation of a photovoltaic/battery hybrid system for powering the high arctic data communications system
[AD-A218353] N90-20319

DEPARTMENT OF THE NAVY, WASHINGTON, DC.
Adaptive associative-processing optical computing architectures
[AD-D014317] N90-20685

DEUTSCHE FORSCHUNGSANSTALT FUER LUFT- UND RAUMFAHRT, COLOGNE (GERMANY, F.R.).
Center of Gravity: Metallic Solidification
[DFVLR-IB-333-89/3] N90-20238
German microgravity program and flight opportunities N90-20239
User center and assitance N90-20240
Principles of metallic solidification N90-20241
Supercooling and germ formation N90-20242
Microgravity conditions of a space vehicle N90-20247
Fusion furnaces for Spacelab N90-20248
Electromagnetic fusion process and position research N90-20249

DISTRICT OF COLUMBIA UNIV., WASHINGTON, DC.
Cloud types and the tropical Earth radiation budget, revised
[NASA-CR-180475] N90-20582

DORNIER-WERKE G.M.B.H., FRIEDRICHSHAFEN (GERMANY, F.R.).
ARISTOTELES: A European approach for an Earth gravity field recovery mission N90-20559

DOUGLAS AIRCRAFT CO., INC., LONG BEACH, CA.
Potential role of avionics in escape systems N90-20060
Controllable propulsion for escape systems control N90-20064
Assessment of crew workload measurement methods, techniques and procedures. Volume 1: Process, methods and results
[AD-A217699] N90-20647

DOW CHEMICAL CO., FREEPORT, TX.
The application of Dow Chemical's perfluorinated membranes in proton-exchange membrane fuel cells N90-20466

DRAPER (CHARLES STARK) LAB., INC., CAMBRIDGE, MA.
Trajectory optimization in the presence of constraints
[AD-A218271] N90-20104
Sensor and actuator selection for fault-tolerant control of flexible structures
[AD-A217384] N90-20433

DREXEL UNIV., PHILADELPHIA, PA.
Spray deposition: A fundamental study of droplet impingement, spreading and consolidation
[AD-A217202] N90-20255

DUAL AND ASSOCIATES, HOUSTON, TX.
The Real Time Display Builder (RTDB) N90-20656

DUKE UNIV., DURHAM, NC.
Positron annihilation spectroscopy: A nondestructive, submicroscopic characterization technique for structural polymers
[AD-A217748] N90-20226

E

EAGLE ENGINEERING, INC., HAMPTON, VA.
The NASA digital VGH program: Exploration of methods and final results. Volume 2: L 1011 data 1978-1979: 1619 hours
[NASA-CR-181909-VOL-2] N90-20080
The NASA digital VGH program. Exploration of methods and final results. Volume 1: Development of methods
[NASA-CR-181909-VOL-1] N90-20081
The NASA digital VGH program. Exploration of methods and final results. Volume 3: B 727 data 1978-1980: 1765 hours
[NASA-CR-181909-VOL-3] N90-20082
The NASA digital VGH program: Exploration of methods and final results. Volume 4: B 747 data 1978-1980, 1689 hours
[NASA-CR-181909-VOL-4] N90-20083
The NASA digital VGH program: Exploration of methods and final results. Volume 5: DC 10 data 1981-1982, 129 hours
[NASA-CR-181909-VOL-5] N90-20084

EAGLE-PICHER INDUSTRIES, INC., JOPLIN, MO.
Advances in lightweight nickel electrode technology N90-20476
Multi-mission Ni-H2 battery cells for the 1990's N90-20477

EDGERTON, GERMESHAUSEN AND GRIER, INC., IDAHO FALLS, ID.
Modeling studies of electrolyte flow and bubble behavior in advanced Hall cells
[DE90-007013] N90-20303

EG AND G ENERGY MEASUREMENTS, INC., LAS VEGAS, NV.
A model research archive: Archive and research implications for original records and support documents
[DE90-008246] N90-20906

EG AND G WASHINGTON ANALYTICAL SERVICES CENTER, INC., LANHAM, MD.
High resolution analysis of satellite gradiometry N90-20561

ELTRON RESEARCH, INC., AURORA, IL.
The electrochemical generation of useful chemical species from lunar materials N90-20461

ENVIRONMENTAL RESEARCH INST. OF MICHIGAN, ANN ARBOR.
Robotic mobility system: Road following algorithms
[AD-A218107] N90-20748

ESSEX CORP., HUNTSVILLE, AL.
Space station Simulation Computer System (SCS) study for NASA/MSFC. Volume 1: Overview and summary
[NASA-CR-183840] N90-20113
Space station Simulation Computer System (SCS) study for NASA/MSFC. Volume 2: Concept document
[NASA-CR-183841] N90-20114
Space station Simulation Computer System (SCS) study for NASA/MSFC. Volume 3: Refined conceptual design report
[NASA-CR-183842] N90-20115
Space station Simulation Computer System (SCS) study for NASA/MSFC. Volume 4: Conceptual design report
[NASA-CR-183843] N90-20116
Space station Simulation Computer System (SCS) study for NASA/MSFC. Volume 5: Study analysis report
[NASA-CR-183844] N90-20117
Space station Simulation Computer System (SCS) study for NASA/MSFC. Volume 6: Study issues report
[NASA-CR-183845] N90-20118

EVANS AND SUTHERLAND COMPUTER CORP., SALT LAKE CITY, UT.
Design considerations for a space database N90-20659
Computer image generation: Reconfigurability as a strategy in high fidelity space applications N90-20682

EXETER UNIV. (ENGLAND).
Amplitude-dependent neutral modes in compressible boundary layer flows
[NASA-TM-102524] N90-20326

F

FEDERAL AVIATION ADMINISTRATION, ATLANTIC CITY, NJ.
Floor pull test of a transport airframe section
[DOT/FAA/CT-TN88/14] N90-20072
Analysis of heliport environmental data: Indianapolis downtown heliport, Wall Street heliport. Volume 3: Indianapolis downtown heliport data plots
[AD-A217412] N90-20500

FERMI NATIONAL ACCELERATOR LAB., BATAVIA, IL.
Nonlinear plasma and beam physics in plasma wake-fields
[DE90-008812] N90-20855

FLORIDA UNIV., GAINESVILLE.
Application of a three-dimensional Navier-Stokes model for a subsonic jet in a crossflow N90-20045
The glow discharge as an atomization and ionization source
[DE90-007693] N90-20163
Superstring field theory
[DE90-007694] N90-20897

FORD AEROSPACE AND COMMUNICATIONS CORP., HOUSTON, TX.
Large screen display for the Mission Control Center N90-20682

FORD AEROSPACE AND COMMUNICATIONS CORP., PALO ALTO, CA.
Sodium-sulfur battery flight experiment definition study N90-20479

G

GENERAL ATOMIC CO., SAN DIEGO, CA.
High-temperature ceramic superconductors
[AD-A218347] N90-20233

GENERAL ELECTRIC CO., LARGO, FL.
Nine-year aging behavior of the ceramic flatpack resonator
[DE90-008044] N90-20412

GENERAL ELECTRIC CO., SCHENECTADY, NY.
The stress corrosion performance of diffusion bonded nickel base alloys
[DE90-008130] N90-20199

GENERAL MOTORS CORP., INDIANAPOLIS, IN.
In-line wear monitor
[AD-A217799] N90-20091

GEODETIC INST., CHARLOTTENLUND (DENMARK).
The role of topography in geodetic gravity field modelling N90-20534
Performance of FFT methods in local gravity field modelling N90-20537

GEODYNAMICS CORP., SANTA BARBARA, CA.
Fourier transform methods in local gravity modeling N90-20538
The reduction correction in North America N90-20540

GEOLOGICAL SURVEY OF CANADA, OTTAWA (ONTARIO).
FFT-local gravimetric geoid computation N90-20536
GEOID '88: A gravimetric geoid for Canada N90-20543

GEOLOGICAL SURVEY OF JAPAN, IBARAKI.
Geology, distribution of hot springs and hydrothermal alteration zones of major geothermal areas in Japan
[DE90-753026] N90-20451

GEORGE WASHINGTON UNIV., WASHINGTON, DC.
Development of gamma-emitting, receptor-binding radiotracers for imaging the brain and pancreas
[DE90-008314] N90-20621

GEORGIA INST. OF TECH., ATLANTA.
Conference digest: Thirteenth International Conference on Infrared and Millimeter Waves, volume 1039
[AD-A217343] N90-20291
Termolecular associations of ions in gases, recombination and electron-atom collisions
[AD-A217678] N90-20805

GERMAN AIR FORCE, FUERSTENFELDBRUK (GERMANY, F.R.).
Ejection seat training of jet pilots and weapon system officers at the German Air Force School of Aviation Medicine N90-20061

GINER, INC., WALTHAM, MA.
Advanced double layer capacitors N90-20464
Oxygen electrodes for rechargeable alkaline fuel cells-II N90-20469
Non-noble electrocatalysts for alkaline fuel cells N90-20470

GRUMMAN DATA SYSTEMS CORP., WOODBURY, NY.
Space station Simulation Computer System (SCS) study for NASA/MSFC. Volume 1: Overview and summary
[NASA-CR-183840] N90-20113
Space station Simulation Computer System (SCS) study for NASA/MSFC. Volume 2: Concept document
[NASA-CR-183841] N90-20114
Space station Simulation Computer System (SCS) study for NASA/MSFC. Volume 3: Refined conceptual design report
[NASA-CR-183842] N90-20115
Space station Simulation Computer System (SCS) study for NASA/MSFC. Volume 4: Conceptual design report
[NASA-CR-183843] N90-20116
Space station Simulation Computer System (SCS) study for NASA/MSFC. Volume 5: Study analysis report
[NASA-CR-183844] N90-20117
Space station Simulation Computer System (SCS) study for NASA/MSFC. Volume 6: Study issues report
[NASA-CR-183845] N90-20118

H

HARRIS CORP., PALM BAY, FL.
Proximity operations concept design study, task 6
[NASA-CR-181971] N90-20112

HARRY DIAMOND LABS., ADELPHI, MD.
Transistor and solid-state technology: A historical development
[AD-A218141] N90-20317
Crystallography, spectroscopic analysis, and lasing properties of Nd3+:Y3Sc2Al3O12
[AD-A217792] N90-20891

HARVARD UNIV., CAMBRIDGE, MA.
X ray specular reflection studies of silicon coated by organic monolayers (alkylsiloxanes)
[AD-A217418] N90-20213

HAWAII UNIV., HONOLULU.
Studies of the evolution of the x ray emission of clusters of galaxies
[NASA-CR-186471] N90-20918

HOUSTON UNIV., TX.
Stress field near crack tip: An experimental evaluation of the three dimensional variation
[AD-A217878] N90-20441
Design decision making with multiple interacting criteria and varying relative weights
[AD-A218027] N90-20721
The electronic properties of high (Tc) superconductors probed by positron annihilation
[DE90-008354] N90-20883

HUGHES AIRCRAFT CO., LOS ANGELES, CA.
KOH concentration effect on the cycle life of nickel-hydrogen cells. Part 4: Results of failure analyses N90-20475

HUMAN ENGINEERING LABS., ABERDEEN PROVING GROUND, MD.
Interaction of switch actuation on tracking with a four-axis flight control (cross-coupling)
[AD-A217981] N90-20095
Comparison of oculometer and head-fixed reticle with voice or switch and touch panel for data entry on a generic tactical air combat display
[AD-A217231] N90-20646
Aiding the decision maker: Perceptual and cognitive issues at the human-machine interface
[AD-A217862] N90-20648

I

ILLINOIS UNIV., URBANA.
Application of railgun principle to high-velocity hydrogen pellet injection for magnetic fusion reactor refueling
[DE90-008281] N90-20109
ISITE: Automatic circuit synthesis for double-metal CMOS VLSI (Very Large Scale Integrated) circuits
[AD-A217459] N90-20292
Supercomputer environments
[AD-A217682] N90-20689
Computational complexity of random access models
[AD-A217685] N90-20701
Robust adaptive nonlinear control under extended matching conditions
[AD-A217684] N90-20744

ILLINOIS UNIV., URBANA-CHAMPAIGN.
Optimal, impulsive, time-fixed orbital rendezvous and interception with path constraints N90-20102
Tomographic processing of synthetic aperture radar signals for enhanced resolution
[AD-A217178] N90-20265
Investigation of tapered multiple microstrip lines for VLSI circuits
[AD-A217855] N90-20310
High power semiconductor laser arrays by metalorganic chemical vapor deposition N90-20363
MEASURE: An integrated data-analysis and model identification facility
[NASA-CR-186452] N90-20686
Design and performance analysis of adaptive optical telescopes using laser guide stars
[AD-A218025] N90-20913

INDIANA UNIV., BLOOMINGTON.
Probabilistic analysis of algorithms for NP-complete problems
[AD-A217880] N90-20716
Metal alkoxides: Models for metal oxides. Alkoxide ligands in early transition metal organometallic chemistry
[DE90-007523] N90-20869

INSTITUTE FOR COMPUTER APPLICATIONS IN SCIENCE AND ENGINEERING, HAMPTON, VA.
Viscous shock profiles and primitive formulations
[NASA-CR-182029] N90-20049
Spectral simulation of unsteady compressible flow past a circular cylinder
[NASA-CR-182030] N90-20050
High order filtering methods for approximating hyperbolic systems of conservation laws
[NASA-CR-182016] N90-20650
An approximation theory for the identification of linear thermoelastic systems
[NASA-CR-182015] N90-20764
Cell averaging Chebyshev methods for hyperbolic problems
[NASA-CR-182028] N90-20768

INSTITUTE FOR DEFENSE ANALYSES, ALEXANDRIA, VA.
Summary of the DoD Metal Matrix Composites (MMC) Steering Committee Meeting, hosted by the Institute for Defense Analysis
[AD-A217611] N90-20145
Towards SDS (Strategic Defense System) testing and evaluation: A collection of relevant topics
[AD-A217610] N90-20783

INSTITUTE FOR PERCEPTION RVO-TNO, SOESTERBERG (NETHERLANDS).
The effect of moisture absorption in clothing on the human heat balance
[AD-A217899] N90-20626
INSTITUTE OF AVIATION MEDICINE, FARNBOROUGH (ENGLAND).
Development of an ejection seat specification for a new fighter aircraft N90-20057
INSTITUTE OF GAS TECHNOLOGY, CHICAGO, IL.
Determination of flow-regime boundaries for cohesive particles
[DE90-007425] N90-20332
INSTITUTE OF PLASMA PHYSICS, PRAGUE (CZECHOSLOVAKIA).
Computation of coupling elements between waveguides and modes for large launching structures
[IPPCZ-290] N90-20842
INSTITUTO DE PESQUISAS ESPACIAIS, SAO JOSE DOS CAMPOS (BRAZIL).
Experimental proposition aboard the second data collecting satellite-SCD 2 of the MECB
[INPE-4980-RPE/606] N90-20128
Space mechanism of low velocity for an array of solar panels: Analysis and design of an experimental model; dimensions of bearings
[INPE-4859-TDL/370] N90-20390
Evaluation of TM/LANDSAT and HRV/SPOT data in the identification of reforested areas in the Mogi-Guacu (SP) region
[INPE-4874-PRE/1485] N90-20442
Relationship of radiometric field measurements of wheat in the Assis-Safra region, 1988
[INPE-4949-RPE/598] N90-20443
LANDSAT-5 data in the study of wheat and bean crops
[INPE-4746-RPE/580] N90-20444
Utilization of LANDSAT-5 and NOAA-9 satellite imagery in the identification of physical-chemical parameters of the water in the Guanabara Bay
[INPE-4761-TDL/349] N90-20445
Synthesis and analysis of 25 years (1961-1986) of INPE/SRE activities related to the vegetation/forest area
[INPE-4969-RPE/604] N90-20446
Analysis of methods to determine emissivity for ground surface targets in the spectral band 8 to 14 microns
[INPE-4984-TDL/394] N90-20447
Underwater physiography of the continental shelf of Rio Grande do Norte visible through satellite imagery
[INPE-4964-TDL/392] N90-20448
A system for analysis and interpretation of lineaments in remote sensing images
[INPE-4893-PRE/1494] N90-20565
INTERNATIONAL BUSINESS MACHINES CORP., HOUSTON, TX.
Onboard shuttle on-line software requirements system: Prototype N90-20658
INTERNATIONAL CENTRE FOR THEORETICAL PHYSICS, TRIESTE (ITALY).
Projective cohomology over a chain complex
[DE90-606958] N90-20788
INTERNATIONAL FUEL CELLS CORP., SOUTH WINDSOR, CT.
Advanced on-site power plant development technology program
[DE90-000443] N90-20484
Enhanced ceria solid electrolyte fuel cell development. Reduction of electronic conductivity permits use of a solid ceria electrolyte in high efficiency high power density fuel cells at temperatures compatible with metallic cell hardware
[AD-A217840] N90-20498
INTOSPACE G.M.B.H., HANOVER (GERMANY, F.R.).
Molding solidification N90-20246

J

JET PROPULSION LAB., CALIFORNIA INST. OF TECH., PASADENA.
Product assurance technology for procuring reliable, radiation-hard, custom LSI/VLSI electronics
[NASA-CR-185954] N90-20281
The importance of batteries in unmanned missions N90-20456
A survey of advanced battery systems for space applications N90-20458
Advanced rechargeable sodium batteries with novel cathodes N90-20459
Advances in ambient temperature secondary lithium cells N90-20481
Refinement of Earth's gravity field with Topex GPS measurements N90-20553
Knowledge representation in space flight operations N90-20655
JOHNS HOPKINS UNIV., BALTIMORE, MD.
Ultrastructure processing of ordered polymers
[AD-A218331] N90-20232
Theoretical studies of spin-forbidden processes within the Breit-Pauli approximation
[AD-A217778] N90-20815
JOHNS HOPKINS UNIV., LAUREL, MD.
Precise solution for a finite set of spherical coefficients from equiangular gridded data N90-20522
JOINT INST. FOR ADVANCEMENT OF FLIGHT SCIENCES, HAMPTON, VA.
Active control of the forced and transient response of a finite beam
[NASA-CR-181957] N90-20430
JOINT INST. FOR NUCLEAR RESEARCH, DUBNA (USSR).
Magnetostatic boundary-value problems in the incomplete-nonlinear formulation and methods of their solution
[DE90-615185] N90-20767
Conserved integral characteristics of the gravitational field
[DE90-615205] N90-20898

K

KANSAS STATE UNIV., MANHATTAN.
Magnetic hardening studies and novel techniques for preparation of high performance magnets
[AD-A217737] N90-20790
KANSAS UNIV., LAWRENCE.
Airplane takeoff and landing performance monitoring system
[NASA-CASE-LAR-13734-1-CU] N90-20096
Simulation of landscape disturbances and the effect of climatic change
[DE90-007565] N90-20503
KEO CONSULTANTS, BROOKLINE, MA.
Optical instrumentation support for the airborne ionospheric observatory
[AD-A218207] N90-20839
KRUPP (FRIED.) G.M.B.H., ESSEN (GERMANY, F.R.).
Dispersion reinforced materials N90-20244

L

LABORATOIRE DE MEDECINE AEROSPATIALE, BRETIGNY-SUR-ORGE (FRANCE).
Parachute opening shocks during high speed ejections: Normalization N90-20056
LACOSTE AND ROMBERG GRAVITY METERS, INC., AUSTIN, TX.
Terrestrial gravity instrumentation in the 20th Century: A brief review N90-20527
LAMONT-DOHERTY GEOLOGICAL INST., PALISADES, NY.
Gravity field of the Western Weddell Sea: Comparison of airborne gravity and Geosat derived gravity N90-20526
LASER APPLICATIONS RESEARCH CENTER, THE WOODLANDS, TX.
Short wavelength laser/materials interactions
[AD-A218015] N90-20386
LAWRENCE LIVERMORE NATIONAL LAB., CA.
Experimental validation of extended image reconstruction using bispectral speckle interferometry
[DE90-008545] N90-20171
Design and processing of strong-tough microcomposite steels
[DE90-007764] N90-20197
Electronic structure, alloy phase stability, and phase diagrams
[DE90-008306] N90-20203
Reactive sputtering of molybdenum
[DE90-008307] N90-20204
A unified integrated model for sputter coating uniformity
[DE90-008322] N90-20205
High-Explosives Applications Facility (HEAF)
[DE90-008122] N90-20257
A guide to performing and documenting safety analyses
[DE90-008687] N90-20260
A guide to performing and documenting safety analyses
[DE90-008688] N90-20261
Modelling Doppler broadening in Raman propagation
[DE90-008042] N90-20269
A progress report on the Livermore Miniature Vacuum Tube Project
[DE90-008302] N90-20299
Core cooling studies at LLNL (Lawrence Livermore National Laboratory) and Sandia
[DE90-008303] N90-20300
Statistical equipment modeling for VLSI manufacturing
[DE90-008527] N90-20304
Relativistic klystron afterburner simulation techniques
[DE90-008539] N90-20305
Hydrodynamic interactions and transport coefficients in a suspension of spherical particles
[DE90-008301] N90-20336
Simple reflection holography
[DE90-008309] N90-20359
A new thermal sensor for x ray microcalorimetry
[DE90-008547] N90-20360
Performance of zig-zag slab regenerative ring amplifier laser system
[DE90-006995] N90-20371
Improved energy and power balance at Nova targets
[DE90-007260] N90-20372
Shaped pulses from Nova for inertial confinement fusion experiments
[DE90-007261] N90-20373
Measurement of the stimulated thermal Rayleigh scattering instability
[DE90-007849] N90-20376
Spatial imaging using confocal Fabry-Perot interferometers
[DE90-008363] N90-20378
Laser line transport with refraction
[DE90-008683] N90-20382
Computer simulations and experiments to study the fracture of rods by flying plates
[DE90-008308] N90-20437
Time-dependent failure of silver interlayer welds
[DE90-008015] N90-20440
Southern oscillation in the OSU coupled upper ocean/atmosphere GCM
[DE90-008415] N90-20588
An intercomparison of general circulation model predictions of regional climate change
[DE90-008325] N90-20589
A review of the literature on the toxicity of rare-earth metals as it pertains to the engineering demonstration system surrogate testing
[DE90-008049] N90-20620
A real-time parallel pipelined data-flow image-processing system
[DE90-008324] N90-20691
Recent advances in 3D finite difference mesh generation using the BRL-CAD package
[DE90-007854] N90-20704
ISLE (Image and Signal Processing LISP Environment) reference manual
[DE90-007858] N90-20705
Scattering sources: A spherical harmonics expansion
[DE90-008724] N90-20711
The Livermore distributed storage system: Implementation and experiences
[DE90-007257] N90-20735
Domain decomposition for a boundary-value problem with a shock layer
[DE90-007857] N90-20762
Precompound decay models for medium energy nuclear reactions
[DE90-008352] N90-20808
Power threshold for neutral beam current drive
[DE90-008348] N90-20822
The n-p bremsstrahlung in heavy ion collision processes
[DE90-008542] N90-20823
Placement of multiple apertures for imaging telescopes
[DE90-006991] N90-20833
Spectral line shape code for multielectron emitters
[DE90-008526] N90-20853
L shell XANES (X ray Absorption Near Edge Structure) for solid metals: Ti, V, Cr, Fe, Ni, Cu
[DE90-008043] N90-20880
The electronic properties of high (Tc) superconductors probed by positron annihilation
[DE90-008354] N90-20883
Systematics in positron annihilation lifetime analysis of high (Tc) superconducting transitions
[DE90-008361] N90-20884
Ultra-high brightness laser research at LLNL (Lawrence Livermore National Laboratory)
[DE90-008366] N90-20885
CALS (Computer-aided Acquisition and Logistic Support) Test Network information exchange user's manual, revision 1
[DE90-008119] N90-20904
LEHIGH UNIV., BETHLEHEM, PA.
Analytical electron microscopy of catalyst preparations
[DE90-008699] N90-20173
LEICESTER UNIV. (ENGLAND).
EXOSAT observations of Seyfert type galaxies N90-20910

LETTERMAN ARMY INST. OF RESEARCH, SAN FRANCISCO, CA.
Acute oral toxicity of JA-2 solid propellant in ICR mice
[AD-A217264] N90-20609
Acute oral toxicity of DIGL-RP solid propellant in ICR mice
[AD-A217711] N90-20613
Acute oral toxicity of DIGL-RP solid propellant in Sprague-Dawley rats
[AD-A217712] N90-20614
LITTLE (ARTHUR D.), INC., CAMBRIDGE, MA.
Techno-economic assessment of a carbothermic alumina reduction process
[DE90-007018] N90-20170
LITTON GUIDANCE AND CONTROL SYSTEMS, WOODLAND HILLS, CA.
The Rapid Geodetic Survey System (RGSS) N90-20528
LOCKHEED ENGINEERING AND SCIENCES CO., HOUSTON, TX.
The use of graphics in the design of the human-telerobot interface N90-20670
Space Station Freedom integrated fault model N90-20673
Issues in visual support to real-time space system simulation solved in the Systems Engineering Simulator N90-20680
LOCKHEED MISSILES AND SPACE CO., HUNTSVILLE, AL.
SES cupola interactive display design environment N90-20679
LOCKHEED MISSILES AND SPACE CO., PALO ALTO, CA.
Comparison of two matrix data structures for advanced CSM testbed applications
[NASA-CR-181951] N90-20421
Spacecraft optical contamination environment
[AD-A218088] N90-20638
LOCKHEED MISSILES AND SPACE CO., SUNNYVALE, CA.
VAPEPS user's reference manual, version 5.0
[NASA-CR-180781] N90-20713
LOS ALAMOS NATIONAL LAB., NM.
The calculation of hydrogen-bonding properties
[DE90-007534] N90-20168
Measurement of proton induced radiation damage to CMOS transistors and pin diodes
[DE90-007836] N90-20283
Energy deposition measurements for E-beam pumped excimer lasers
[DE90-007545] N90-20365
Amplified spontaneous emission measurements on the aurora large-aperture module
[DE90-004841] N90-20369
Harmonic generation mechanisms in short-wavelength free-electron lasers
[DE90-007622] N90-20374
Laser-induced shock waves effects in materials
[DE90-007626] N90-20379
Finite element models to predict the structural response of 120-mm sabot/rods during launch
[DE90-007497] N90-20436
Hot dry rock geothermal energy: A renewable energy resource that is ready for development now
[DE90-007509] N90-20485
Experiments in finding neural network weights
[DE90-007696] N90-20702
SDI (Strategic Defense Initiative): Is its future past
[DE90-008016] N90-20785
Role of free-electron lasers in strategic defense
[DE90-008028] N90-20786
Present status of (mu)CF theory
[DE90-007547] N90-20809
Integrability and chaos in nonlinearly coupled optical beams
[DE90-007540] N90-20834
The impedance of energy efficiency of a coaxial magnetized plasma source used for spheromak formation and sustainment
[DE90-003220] N90-20841
New methods in plasma simulation
[DE90-007507] N90-20847
Laser-produced plasmas in medicine
[DE90-007623] N90-20849
Copper and oxygen NMR studies on the magnetic properties of YBa2Cu3O(7-y)
[DE90-007889] N90-20863
Synthesis and properties of polycrystalline Tl2Ba2CaCu2O(x) and Tl2Ba2Ca2Cu3O(x)
[DE90-007526] N90-20887
M51's spiral structure
[DE90-007624] N90-20916
LOUISVILLE UNIV., KY.
The perceptual interaction of graphical attributes in thirteen bivariate displays
[AD-A217980] N90-20720

M

MADIGAN ARMY MEDICAL CENTER, TAKOMA, WA.
The effects of high intensity cycle exercise on sympatho-adrenal-medullary response patterns
[AD-A217962] N90-20628
MARTIN-BAKER AIRCRAFT CO. LTD., DENHAM (ENGLAND).
Fighter escape system: The next step forward N90-20059
Spacecraft escape N90-20066
MARYLAND UNIV., BALTIMORE.
A locally constrained parallel activation model for diagnostic reasoning
[AD-A217808] N90-20747
MARYLAND UNIV., COLLEGE PARK.
Aeroelastic characteristics of aircraft with circulation control wings N90-20070
Research in programming languages and software engineering
[AD-A217765] N90-20715
MARYLAND UNIV. BALTIMORE COUNTY, CATONSVILLE.
Nonlinear systems of partial differential equations
[AD-A217581] N90-20761
MASCHINENFABRIK AUGSBURG-NUERNBERG A.G., MUNICH (GERMANY, F.R.).
Development and construction of external laser components for hardening and coating
[MT-15/87] N90-20364
MASSACHUSETTS INST. OF TECH., CAMBRIDGE.
CO2 diffusion and solubility in a Polystyrene/Polybutadiene block copolymer with highly oriented lamellar morphology
[AD-A217165] N90-20211
Radiation disorder and aperiodicity in irradiated ceramics
[DE90-008253] N90-20222
On optimal distributed decision architectures in a hypothesis testing environment
[AD-A217824] N90-20274
Express cubes: Improving the performance of k-ary n-cube interconnection networks
[AD-A217117] N90-20287
The design of high-performance circuits for digital signal processing
[AD-A217786] N90-20309
Sensor and actuator selection for fault-tolerant control of flexible structures
[AD-A217384] N90-20433
Innovative turbine concepts for open-cycle OTEC (Ocean Thermal Energy Conversion)
[DE90-000315] N90-20493
A unified approach to the synthesis of fully testable sequential machines
[AD-A217120] N90-20687
Technical specifications requirements: Automated reasoning applications
[DE90-008799] N90-20712
Parts of recognition
[AD-A217694] N90-20714
Free indexation: Combinatorial analysis and a compositional algorithm
[AD-A218219] N90-20724
Optimization of series expressions. Part 1: User's manual for the series macro package
[AD-A218220] N90-20725
Performance tradeoffs in multithreaded processors
[AD-A217123] N90-20729
A Locality-based multiprocessor cache interference model
[AD-A217126] N90-20730
Irredundant sequential machines via optimal logic synthesis
[AD-A217119] N90-20742
Stereo feature matching in disparity space
[AD-A218170] N90-20751
Location recognition using stereo vision
[AD-A218218] N90-20752
Exact algorithms for output encoding, state assignment and four-level Boolean minimization
[AD-A217121] N90-20756
Chemical beam epitaxy of ZnSe
[AD-A217375] N90-20866
An investigation of the dislocation structure of the Ni/Ag phase boundary
[DE90-008428] N90-20876
Focused ion beam implantation
[AD-A217987] N90-20894
Mark 3 interferometer
[AD-A217188] N90-20912
MASSACHUSETTS INST. OF TECH., LEXINGTON.
Radiation-hardened wafer scale integration
[AD-A217332] N90-20290
A cloud climatology for the North Pacific area centered at Shemya, Alaska
[AD-A217334] N90-20585
Algorithms for optimal processing of polarimetric radar data
[AD-A217330] N90-20758
On metric entropy, Vapnik-Chervonenkis dimension, and learnability for a class of distributions
[AD-A217331] N90-20759
A space-based optical communication system utilizing fiber optics
[AD-A217333] N90-20828
MASSACHUSETTS UNIV., AMHERST.
Computation and graphics in mathematical research
[DE90-008429] N90-20766
MAX-PLANCK-INST. FUER KERNPHYSIK, HEIDELBERG (GERMANY, F.R.).
Activities report in nuclear physics
[ETN-90-95322] N90-20803
MAX-PLANCK-INST. FUER METALLFORSCHUNG, STUTTGART (GERMANY, F.R.).
Systems with a miscibility gap in the liquid state N90-20245
MAX-PLANCK-INST. FUER STROEMUNGSFORSCHUNG, GOETTINGEN (GERMANY, F.R.).
Experimental investigation of the thermocapillary migration of water droplets in butylbenzoate
[MPIS-14/1988] N90-20155
Reactive and anisotropic elastic scattering of highly laser-vibration-excited diatomic molecules
[MPIS-19/1988] N90-20804
MAYFLOWER COMMUNICATIONS CO., INC., READING, MA.
Satellite-to-satellite tracking experiment for global gravity field mapping N90-20556
MCDONNELL-DOUGLAS SPACE SYSTEMS CO., HOUSTON, TX.
Applications of graphics to support a testbed for autonomous space vehicle operations N90-20661
MEDICAL COLL. OF VIRGINIA, RICHMOND.
Biological applications and effects of optical masers
[AD-A217910] N90-20385
The reliability of clinical measurements of forward bending obtained by the use of the modified fingertip-to-floor method
[AD-A217907] N90-20627
MICHIGAN TECHNOLOGICAL UNIV., HOUGHTON.
Structural comparison of nickel electrodes and precursor phases N90-20472
MICHIGAN UNIV., ANN ARBOR.
Aiming control: Theory and applications to dynamic control of space structures
[AD-A217877] N90-20123
Summary report of the Summer Conference of the DARPA-Materials Research Council
[AD-A217380] N90-20143
Flexible automatic discrete parts assembly
[AD-A217401] N90-20256
Massively-parallel computational fluid dynamics
[AD-A217732] N90-20342
Three-dimensional medical image analysis using local dynamic algorithm selection on a multiple-instruction, multiple-data architecture
[AD-A218024] N90-20630
MICROBIAL PRODUCTS, INC., VACAVILLE, CA.
Design and operation of an outdoor microalgae test facility
[DE89-009493] N90-20608
MICROEXPERT, CALABASAS, CA.
Broadening the interface bandwidth in simulation based training N90-20666
Animation graphic interface for the space shuttle onboard computer N90-20667
MIDWEST RESEARCH INST., GOLDEN, CO.
PC-based PCM telemetry data reduction system software
[DE90-000317] N90-20111
Assessment of biobased materials
[DE90-000300] N90-20220
Photovoltaic energy
[DE89-009473] N90-20486
Solar thermal program summary, fiscal year 1989
[DE89-009475] N90-20487
Energy storage and distribution
[DE89-009487] N90-20488
CuInSe2 and CdTe: Scale-up for manufacturing
[DE89-009503] N90-20489
Wind Energy Program summary. Volume 1: Overview
[DE89-009479] N90-20491
A comparison of two-and three-dimensional S809 airfoil properties for rough and smooth HAWT (Horizontal-Axis Wind Tunnel) rotor operation
[DE89-009512] N90-20492
Spectral solar radiation data base documentation, volume 1
[DE89-009447] N90-20571

Design and operation of an outdoor microalgae test facility
[DE89-009493] N90-20608

MINISTERIE VAN VERKEER EN WATERSTAAT, 'S-GRAVENHAGE (NETHERLANDS).
Activities report in civil aviation
[ETN-90-95471] N90-20067

MINNESOTA UNIV., MINNEAPOLIS.
Infrared and X ray photoelectron spectroscopy studies of the polyimide/metal interface
[AD-A218249] N90-20179

MISSION RESEARCH CORP., NASHUA, NH.
Mathematics and physics studies: Multi-project support
[AD-A218208] N90-20723

MISSISSIPPI STATE UNIV., MISSISSIPPI STATE.
Diagnostic development and support of MHD (Magnetohydrodynamics) test facilities
[DE90-004969] N90-20845

MISSISSIPPI UNIV., UNIVERSITY.
A continued study of optical sound generation and amplification
[AD-A217640] N90-20796

MITRE CORP., HOUSTON, TX.
Graphical programming and the use of simulation for space-based manipulators N90-20674

MSNW, INC., SAN MARCOS, CA.
Determination of fundamental thermodynamic properties of constituent materials and performance screening of candidate systems
[AD-A218089] N90-20153

N

NAIROBI UNIV. (KENYA).
The geoid in Kenya N90-20542

NATAL UNIV., DURBAN (SOUTH AFRICA).
Thin-plate spline quadrature of geodetic integrals N90-20539

NATIONAAL INST. VOOR KERNFYSICA EN HOGE ENERGIEFYSICA, AMSTERDAM (NETHERLANDS).
The HS6000/20 development system
[LINO-1989-6] N90-20696

NATIONAL ACADEMY OF SCIENCES - NATIONAL RESEARCH COUNCIL, WASHINGTON, DC.
Committee on Geodesy - National Research Council
[AD-A217770] N90-20452
Computer Science and Technology Board
[DE90-008292] N90-20690

NATIONAL AERONAUTICAL ESTABLISHMENT, OTTAWA (ONTARIO).
An improved airborne wind measurement technique for the NAE (National Aeronautical Establishment) Twin Otter
[AD-A217978] N90-20575

NATIONAL AERONAUTICS AND SPACE ADMINISTRATION, WASHINGTON, DC.
Microgravity Science and Application Program tasks, 1989 revision
[NASA-TM-4191] N90-20252
Mercuric iodide room temperature gamma-ray detectors
[NASA-TM-103318] N90-20357
Seeing in a new light: Astro-1 teacher's guide with activities
[NASA-EP-274] N90-20900

NATIONAL AERONAUTICS AND SPACE ADMINISTRATION. AMES RESEARCH CENTER, MOFFETT FIELD, CA.
Static aeroelastic analysis of a three-dimensional generic wing
[NASA-TM-102231] N90-20087
The 1-(diorganooxyphosphonyl)-methyl)-2,4- and -2,6-diamido benzenes
[NASA-CASE-ARC-11425-4] N90-20133
Analysis of small-scale rotor hover performance data
[NASA-TM-102271] N90-20325
Numerical simulation methods of incompressible flows and an application to the space shuttle main engine
[NASA-TM-100038] N90-20333
Tools for 3D scientific visualization in computational aerodynamics N90-20660

NATIONAL AERONAUTICS AND SPACE ADMINISTRATION. GODDARD SPACE FLIGHT CENTER, GREENBELT, MD.
Microwave field effect transistor
[NASA-CASE-GSC-12442-2] N90-20282
Performance of a 300 Mbps 1:16 serial/parallel optoelectronic receiver module
[NASA-TM-103110] N90-20302
Overview of battery usage in NASA/GSFC LEO and GEOspacecrafts N90-20455
Gravitational model improvement at the Goddard Space Flight Center N90-20514
An improved error assessment for the GEM-T1 gravitational model N90-20518
Gravity field information from Gravity Probe-B N90-20554
Satellite radar altimetry over ice. Volume 1: Processing and corrections of Seasat data over Greenland
[NASA-RP-1233-VOL-1] N90-20562
Satellite radar altimetry over ice. Volume 2: Users' guide for Greenland elevation data from Seasat
[NASA-RP-1233-VOL-2] N90-20563
Satellite radar altimetry over ice. Volume 4: Users' guide for Antarctica elevation data from Seasat
[NASA-RP-1233-VOL-4] N90-20564
Analysis of altimetry over inland seas
[NASA-TM-100729] N90-20566
User's guide: Programs for processing altimeter data over inland seas
[NASA-TM-100730] N90-20572
TAE Plus: Transportable Applications Environment Plus tools for building graphic-oriented applications N90-20652
Operational computer graphics in the flight dynamics environment N90-20668
Bibliography of spatial interferometry in optical astronomy
[NASA-TM-100754] N90-20911

NATIONAL AERONAUTICS AND SPACE ADMINISTRATION. HUGH L. DRYDEN FLIGHT RESEARCH FACILITY, EDWARDS, CA.
The implementation and operation of a variable-response electronic throttle control system for a TF-104G aircraft
[NASA-TM-101696] N90-20086

NATIONAL AERONAUTICS AND SPACE ADMINISTRATION. JOHN F. KENNEDY SPACE CENTER, COCOA BEACH, FL.
Vortex motion phase separator for zero gravity liquid transfer
[NASA-CASE-KSC-11387-1] N90-20236
Elevated central venous pressure: A consequence of exercise training-induced hypervolemia
[NASA-TM-102965] N90-20617

NATIONAL AERONAUTICS AND SPACE ADMINISTRATION. LYNDON B. JOHNSON SPACE CENTER, HOUSTON, TX.
Docking mechanism for spacecraft
[NASA-CASE-MSC-21386-1] N90-20126
System for venting gas from a liquid storage tank
[NASA-CASE-MSC-21253-1] N90-20254
Doppler radar with multiphase modulation of transmitted and reflected signal
[NASA-CASE-MSC-18808-1] N90-20280
Gripping device
[NASA-CASE-MSC-21365-1] N90-20408
Development and application of nonflammable, high-temperature beta fibers
[NASA-TM-102158] N90-20645
Graphics Technology in Space Applications (GTSA 1989)
[NASA-CP-3045] N90-20651
Engineering visualization utilizing advanced animation N90-20664
Multi-tasking computer control of video related equipment N90-20665
Distributed earth model/orbiter simulation N90-20671
Using an instrumented manikin for Space Station Freedom analysis N90-20675
History of visual systems in the Systems Engineering Simulator N90-20681
Real-time graphics for the Space Station Freedom cupola, developed in the Systems Engineering Simulator N90-20683

NATIONAL AERONAUTICS AND SPACE ADMINISTRATION. LANGLEY RESEARCH CENTER, HAMPTON, VA.
Experimental and theoretical aerodynamic characteristics of a high-lift semispan wing model
[NASA-TP-2990] N90-20046
Using transonic small disturbance theory for predicting the aeroelastic stability of a flexible wind-tunnel model
[NASA-TM-102617] N90-20047
A review of the analytical simulation of aircraft crash dynamics
[NASA-TM-102595] N90-20068
The application of active controls technology to a generic hypersonic aircraft configuration
[NASA-TM-101689] N90-20071
Compression pylon
[NASA-CASE-LAR-13777-1] N90-20078
Passive venting technique for shallow cavities
[NASA-CASE-LAR-14031-1] N90-20079
Digital-flutter-suppression-system investigations for the active flexible wing wind-tunnel model
[NASA-TM-102618] N90-20093
Airplane takeoff and landing performance monitoring system
[NASA-CASE-LAR-13734-1-CU] N90-20096
Component count and preliminary assembly considerations for large space truss structures
[NASA-TM-102604] N90-20121
Use of random Martian atmosphere to evaluate potential entry guidance schemes
[NASA-TM-102606] N90-20122
A study of physical properties of ODPA-p-PDA polyimide films
[NASA-TM-102625] N90-20137
Isotope exchange in oxide-containing catalyst
[NASA-CASE-LAR-13542-2-SB] N90-20154
Process for making a noble metal on tin oxide catalyst
[NASA-CASE-LAR-13741-1-SB] N90-20180
Electronic precipitator control
[NASA-CASE-LAR-13273-2] N90-20320
Reusable high-temperature heat pipes and heat pipe panels
[NASA-CASE-LAR-13761-1] N90-20323
Tensile film clamps and mounting block for the rheovibron and autovibron viscoelastometer
[NASA-CASE-LAR-13696-1] N90-20409
Evaluation of an adaptive unstructured remeshing technique for integrated fluid-thermal-structural analysis
[NASA-TM-102611] N90-20426
Through-the-thickness fatigue crack closure behavior in an aluminum alloy
[NASA-TM-102590] N90-20427
Downward shortwave surface irradiance from 17 sites for the FIRE/SRB Wisconsin experiment
[NASA-TM-102596] N90-20583
Experimental feasibility of investigating acoustic waves in Couette flow with entropy and pressure gradients
[NASA-TM-102621] N90-20795

NATIONAL AERONAUTICS AND SPACE ADMINISTRATION. LEWIS RESEARCH CENTER, CLEVELAND, OH.
Numerical simulations of supersonic flow through oscillating cascade sections
[NASA-TM-103100] N90-20051
Aerospace induction motor actuators driven from a 20-kHz power link
[NASA-TM-102482] N90-20085
Comparison of 3-D viscous flow computations of Mach 5 inlet with experimental data
[NASA-TM-102518] N90-20090
Advanced launch vehicle propulsion at the NASA Lewis Research Center
[NASA-TM-103096] N90-20110
Experimentally determined wear behavior of an Al2O3-SiC composite from 25 to 1200 C
[NASA-TM-102549] N90-20130
Composite laminate tailoring with probabilistic constraints and loads
[NASA-TM-102515] N90-20138
Evaluation of thermal and mechanical loading effects on the structural behavior of a SiC/titanium composite
[NASA-TM-102536] N90-20139
Fundamental aspects of and failure modes in high-temperature composites
[NASA-TM-102558] N90-20151
Mechanical properties of pure nickel alloys after long term exposures to LiOH and vacuum at 775 K
[NASA-TM-102403] N90-20181
Design and test of a compact optics system for the pool boiling experiment
[NASA-TM-102530] N90-20253
Numerical Arc Segmentation Algorithm for a Radio Conference-NASARC (version 4.0) technical manual
[NASA-TM-101453] N90-20264
Experimental investigations on channelized coplanar waveguide
[NASA-TM-102494] N90-20286
Power conditioning techniques
[NASA-TM-102577] N90-20301
Amplitude-dependent neutral modes in compressible boundary layer flows
[NASA-TM-102524] N90-20326
Unsteady three-dimensional marginal separation, including breakdown
[NASA-TM-102525] N90-20337
Mass transfer from a sphere in an oscillating flow with zero mean velocity
[NASA-TM-102566] N90-20338
Spacelab qualified infrared imager for microgravity science experiments
[NASA-TM-102503] N90-20352
Design and calibration of a vacuum compatible scanning tunneling microscope
[NASA-TM-102514] N90-20353
TiCl4 as a source of TiO2 particles for laser anemometry measurements in hot gas
[NASA-TM-102581] N90-20358

Bearing and gear steels for aerospace applications
[NASA-TM-102529] N90-20391
An applicational process for dynamic balancing of turbomachinery shafting
[NASA-TM-102537] N90-20392
Electron beam induced damage in PECVD Si3N4 and SiO2 films on InP
[NASA-TM-102544] N90-20393
Computer simulation of the mathematical modeling involved in constitutive equation development: Via symbolic computations
[NASA-TM-102532] N90-20428
Model development in viscoplastic ratchetting
[NASA-TM-102509] N90-20431
Computational simulation of damping in composite structures
[NASA-TM-102567] N90-20432
COMGEN: A computer program for generating finite element models of composite materials at the micro level
[NASA-TM-102556] N90-20438
Space Electrochemical Research and Technology (SERT), 1989
[NASA-CP-3056] N90-20454
Human exploration mission studies N90-20457
Characterization testing of a 40 AHR bipolar nickel-hydrogen battery N90-20463
Hydrogen-oxygen proton-exchange membrane fuel cells and electrolyzers N90-20467
Corrosion testing of candidates for the alkaline fuel cell cathode N90-20471
Impedance studies of Ni/Cd and Ni/H2 cells using the cell case as a reference electrode N90-20473
Nickel-hydrogen capacity loss on storage N90-20478
GRID2D/3D: A computer program for generating grid systems in complex-shaped two- and three-dimensional spatial domains. Part 2: User's manual and program listing
[NASA-TM-102454] N90-20708
Institute for Computational Mechanics in Propulsion (ICOMP) fourth annual review, 1989
[NASA-TM-102519] N90-20769
Noise of a simulated installed model counterrotation propeller at angle-of-attack and takeoff/approach conditions
[NASA-TM-102440] N90-20794
Milimeter wave surface resistance of RBa2Cu3O(7-delta) (R=Y,Eu,Dy,Sm,Er) superconductors
[NASA-TM-102571] N90-20886
Middle management of research
[NASA-TM-102417] N90-20901

NATIONAL AERONAUTICS AND SPACE ADMINISTRATION. MARSHALL SPACE FLIGHT CENTER, HUNTSVILLE, AL.

Secondary arm coarsening and microsegregation in superalloy PWA-1480 single crystals: Effect of low gravity
[NASA-TM-102445] N90-20194
Rolling contact fatigue of surface modified 440C using a 'Ge-Polymet' type disc rod test rig
[NASA-TM-100390] N90-20200
The NASA, Marshall Space Flight Center drop tube user's manual
[NASA-TM-100392] N90-20251
Human serum albumin crystals and method of preparation
[NASA-CASE-MFS-28234-1] N90-20616
Method of preparing radially homogeneous mercury cadmium telluride crystals
[NASA-CASE-MFS-25786-2] N90-20896

NATIONAL AERONAUTICS AND SPACE ADMINISTRATION. PASADENA OFFICE, CA.

Dual cathode system for electron beam instruments
[NASA-CASE-NPO-16878-1-CU] N90-20351

NATIONAL AEROSPACE LAB., TOKYO (JAPAN).

Design and testing of a noninteracting control loop for the dynamically tuned dry gyro
[NAL-TR-1017] N90-20350

NATIONAL CLIMATIC CENTER, ASHEVILLE, NC.

US Navy regional climatic study of the Central East Asian coast and associated waters
[AD-A217448] N90-20587

NATIONAL INST. OF STANDARDS AND TECHNOLOGY, GAITHERSBURG, MD.

Strength and microstructure of ceramics
[AD-A217752] N90-20227

NATIONAL OCEANIC AND ATMOSPHERIC ADMINISTRATION, ROCKVILLE, MD.

First year's results and field experience with the latest JILA absolute gravimeter N90-20529
Treatment of geodetic leveling in the integrated geodesy approach N90-20546
Geodynamics and temporal variations in the gravity field N90-20549

NAVAL AEROSPACE MEDICAL RESEARCH LAB., PENSACOLA, FL.

A comparison of the mechanisms of cold- and microgravity-induced fluid loss
[AD-A218098] N90-20631
Micro SAINT programs for numerical methods of integration and differential equations
[AD-A218097] N90-20772

NAVAL OCEAN SYSTEMS CENTER, SAN DIEGO, CA.

Fractal-based image compression
[AD-A217302] N90-20699
Parallel computer graphics algorithms for the connection machine
[AD-A217300] N90-20733

NAVAL POSTGRADUATE SCHOOL, MONTEREY, CA.

Aerodynamic analysis of a US Navy and Marine Corps unmanned air vehicle
[AD-A218282] N90-20077
A satellite simulation program
[AD-A218079] N90-20124
Flow visualization studies in a curved rectangular channel with 40 to 1 aspect ratio and a straight channel with bulk flow unsteadiness
[AD-A218020] N90-20348
The design and implementation of a position measuring system for a remotely controlled video camera
[AD-A218077] N90-20362
Control system design of the third flexible joint of PUMA 560 robot
[AD-A218075] N90-20405
A split-and-merge method for creating polygonal homogeneous-vegetation regions from digitized terrain data
[AD-A218080] N90-20453
Correlation of atmospheric optical turbulence and meteorological measurements
[AD-A218019] N90-20576
A prototype expert system to forecast severe winds in the western Mediterranean Sea
[AD-A218017] N90-20593
Correlation of AVHRR imagery with sub-surface features in California current
[AD-A218184] N90-20607
Implementation of a hypertext help system for GLAD (Graphics LAnguage for Database)
[AD-A217936] N90-20718
Three-dimensional route planning for a cruise missile for minimal detection by observer
[AD-A218336] N90-20787
The measurements of thermoacoustic phenomena using thermoacoustic couples
[AD-A218018] N90-20798
Modification, testing, and calibration of infrared search and target designator hardware received from NSWC
[AD-A217920] N90-20837

NAVAL RESEARCH LAB., WASHINGTON, DC.

General forms and properties of zero cross-correlation radar waveforms
[AD-A217779] N90-20273
Common-mode rejector for pulse power diagnostics
[AD-A218096] N90-20316
Spectral analyses of satellite geopotential missions N90-20552
Texture segmentation using localized spatial filtering
[AD-A218064] N90-20722
Some remarks on solutions of Fermats last equation in terms of Wright's hypergeometric function
[AD-A218066] N90-20771
On free products of torsion free abelian groups
[AD-A218146] N90-20773
Euler's theorem for polynomials
[AD-A218148] N90-20774
Production rates for electron beams and swarms in nitrogen
[AD-A218145] N90-20817

NAVAL SHIP RESEARCH AND DEVELOPMENT CENTER, BETHESDA, MD.

Through-thickness strain response of thick composites in compression
[AD-A217233] N90-20141
Compression testing of thick-section composite materials
[AD-A217234] N90-20142
Localization and delocalization in periodic one-dimensional dynamic systems
[AD-A217939] N90-20797

NAVY PERSONNEL RESEARCH AND DEVELOPMENT CENTER, SAN DIEGO, CA.

Brain activity during tactical decision-making. Part 3: Relationships between probe-evoked potentials, simulation performance, and on-job performance
[AD-A217207] N90-20638

NEW HAMPSHIRE UNIV., DURHAM.

Robust planning and control using neural networks
[AD-A217216] N90-20732

NEW MEXICO STATE UNIV., LAS CRUCES.

The contour model architecture and assembly language
[AD-A217114] N90-20697
A new technique for guiding of electron beams
[DE90-008660] N90-20824

NEW SOUTH WALES UNIV., KENSINGTON (AUSTRALIA).

High-efficiency silicon concentrator solar cell research
[DE90-008040] N90-20490
Geopotential models in the Australian region N90-20519

NEW YORK UNIV., NEW YORK.

NYU (New York University) ultracomputer
[AD-A217167] N90-20688

NORTH CAROLINA STATE UNIV., RALEIGH.

Magnetic vapor shield mechanism for protection of material surfaces exposed to high heat load
[AD-A217667] N90-20217
Transient radiation hardened CMOS (Complementary Metal Oxide Semiconductor) operational amplifiers
[AD-A217972] N90-20313
Analysis of GALE (Genesis of Atlantic Lows Experiment) data
[AD-A217182] N90-20584
(DURIP) Two-Processor Alliant FX/4 System
[AD-A217810] N90-20692
Growth, characterization and device development in monocrystalline diamond films
[AD-A218211] N90-20895

NORTH CAROLINA UNIV., CHAPEL HILL.

Research in reliability, availability and maintainability for complex failure systems
[AD-A217744] N90-20415
On the existence of local times: A geometric study
[AD-A218337] N90-20776
Homogeneous chaos, p-forms, scaling and the feynman integral
[AD-A218339] N90-20777
Local moduli of continuity of some classes of Gaussian processes
[AD-A217692] N90-20778
Slepian models and regression approximations in crossing and extreme value theory
[AD-A218338] N90-20779
Observation of nonlinear reflectivity from InSb surface and optical switching application
[AD-A217184] N90-20826
An ellipsometric measurement of optical properties for InP surfaces
[AD-A217185] N90-20827
In-situ differential reflectance study of the etching of SiO2 films
[AD-A217186] N90-20864
Refractive index profiles of thermally grown and chemically vapor deposited films on silicon
[AD-A217187] N90-20865

NORTHWESTERN UNIV., EVANSTON, IL.

Studies of the structure and properties of organic monolayers, multilayers and superlattices
[DE90-008330] N90-20129

NOTRE DAME UNIV., IN.

Error control techniques for satellite and space communications
[NASA-CR-186221] N90-20263

O

OAK RIDGE GASEOUS DIFFUSION PLANT, TN.

Area Over Length (AOL): A program for the calculation of effective two-dimensional thermal conductance through an arbitrarily shaped region
[DE90-008005] N90-20335
Fluid dynamics analysis of a rotating axisymmetric part using FIDAP
[DE90-008733] N90-20340

OAK RIDGE NATIONAL LAB., TN.

Characterization of ceramic matrix composites fabricated by chemical vapor infiltration
[DE90-008409] N90-20149
Corrosion properties of Fe3Al in H2S-H2-H2O mixtures
[DE90-004936] N90-20167
An introduction to nickel aluminide alloy
[DE90-008565] N90-20207
Mechanical behavior of whisker reinforced ceramics
[DE90-008758] N90-20224
A nonintrusive method for measuring the operating temperature of a solenoid-operated valve
[DE90-007576] N90-20355
Y1Ba2Cu3O(7-x) laser-ablation plume dynamics measurement by nanosecond response ion probe: Comparison with optical measurements
[DE90-007658] N90-20375

Concept formation and generalization based on experimentation by an autonomous mobile robot
[DE90-001731] N90-20395
Robot navigation research using the HERMIES mobile robot
[DE90-001952] N90-20396
Robust performance of multiple tasks by a mobile robot
[DE90-001953] N90-20397
Design of a telerobotic controller with joint torque sensors
[DE90-008753] N90-20404
Research and development quality assurance planning
[DE90-003687] N90-20413
United States Historical Climatology Network (HCN) serial temperature and precipitation data
[DE90-008029] N90-20506
Implementation of a control system test environment in UNIX
[DE90-007485] N90-20736
Design of a simulation interface for a parellel computing environment
[DE90-008497] N90-20737
Hybrid intelligent perception system: Intelligent perception through combining artificial neural networks and an expert system
[DE90-007483] N90-20746
The basis spline method and associated techniques
[DE90-008403] N90-20763
Periodic trajectories for two-dimensional nonintegrable Hamiltonians
[DE90-008082] N90-20765
Stopping power for protons in Al for the whole range of velocities
[DE90-008558] N90-20810
Populations of excited states and reaction mechanisms in the emission of complex fragments
[DE90-007481] N90-20819
The ANU (Australian National University) Heliac Program
[DE90-006620] N90-20843
Difference in electron thermal diffusivity and profile between interior and exterior of TFTR L-mode plasmas
[DE90-007479] N90-20846
High elongation plasmas
[DE90-007575] N90-20848
Materials and selection criteria analysis for the compact ignition tokamak toroidal field coil turn-to-turn insulation system: Photographic summary oflaboratory testing
[DE90-008020] N90-20850
Particle transport in pellet fueled JET (Jet European Torus) plasmas
[DE90-008077] N90-20851

OFFICE NATIONAL D'ETUDES ET DE RECHERCHES AEROSPATIALES, PARIS (FRANCE).
The GRADIO spaceborne gravity gradiometer: Development and accommodation N90-20560

OHIO STATE UNIV., COLUMBUS.
Effects of additional interfering signals on adaptive array performance
[NASA-CR-186508] N90-20271
High resolution radar target modeling using ARMA (Autoregressive Moving Average) models
[AD-A218212] N90-20278
Recent improvements to the electromagnetic surface patch code
[AD-A217479] N90-20293
Interior fluid dynamics of liquid-filled projectiles
[AD-A217630] N90-20330
Theory system reliability demonstration and burn-in design
[AD-A217775] N90-20416
Progress in the Determination of the Earth's Gravity Field
[NASA-CR-185721] N90-20513
Progress in the development of high degree potential coefficient models N90-20516
Downward continuation of the free-air gravity anomalies to the ellipsoid using the gradient solution and terrain correction: An attempt of global numerical computations N90-20541

OKLAHOMA STATE UNIV., STILLWATER.
Polymer liquid crystals with side chain discogens
[AD-A218013] N90-20228
Techniques for accelerating iterative methods for the solution of mathematical problems
[AD-A218272] N90-20775

OKLAHOMA UNIV., NORMAN.
Hypersonic waverider configurations for trans-atmospheric vehicles
[AD-A217925] N90-20074
Derivation of kinematic fields using wind profiler data from the 1985 pre-storm experiment
[AD-A217952] N90-20592
Development of computer software for the analysis and design of modern control systems
[AD-A217924] N90-20717

OLD DOMINION UNIV., NORFOLK, VA.
Analysis of radiometer calibration effects with TOUCHSTONE
[NASA-CR-186476] N90-20284
An electron-beam controlled semiconductor switch
[AD-A217181] N90-20288
Continental shelf processes affecting the oceanography of the South Atlantic Bight
[DE90-008439] N90-20606

OLDENBURG UNIV. (GERMANY, F.R.).
Development of a laser fluorosensor for the aircraft supported analysis of maritime toxic agents loads: Definition phase
[ETN-90-95320] N90-20499

OREGON STATE UNIV., CORVALLIS.
Air pollution-caused changes in photosynthesis: Effects on plant growth and rhizosphere functions
[DE90-007184] N90-20501

OXFORD UNIV. (ENGLAND).
Heat transfer near the entrance to a film cooling hole in a gas turbine blade
[AD-A217396] N90-20089
Nondestructive testing of ceramics by acoustic microscopy
[AERE-R-13350] N90-20411

P

PACIFIC NORTHWEST LAB., RICHLAND, WA.
Vibrational spectroscopy of boron nitride at high temperatures and pressures
[DE90-008633] N90-20172
Ceramic oxide thin film formation utilizing biological processes
[DE90-008599] N90-20225
Life-cycle cost comparisons of advanced storage batteries and fuel cells for utility, stand-alone, and electric vehicle applications
[DE90-008090] N90-20298
Global Warming: A Northwest Perspective
[DE90-008140] N90-20505
Use of environmental monitoring data in evaluation of atmospheric modeling results
[DE90-008607] N90-20510
Information management systems for integrating the technical data and regulatory requirements of environmental restoration activities
[DE90-008622] N90-20511

PALISADES INST. FOR RESEARCH SERVICES, INC., NY.
Workshop on the Physics and Chemistry of Mercury Cadmium Telluride and Related II-VI compounds
[AD-A217496] N90-20867

PENNSYLVANIA STATE UNIV., UNIVERSITY PARK.
Synthesis of new polyphosphazene elastomers
[AD-A217585] N90-20216
Ring expansion and equilibration in organophosphazenes, and the relationship to polymerization
[AD-A218234] N90-20230
DURIP optical equipment for high-speed viscous-inviscid interaction research
[AD-A217772] N90-20345
Development of a passive robot-controlled reaction arm N90-20389
Hypotheses testing of watershed/landscape dynamics in northern Alaska using digital analysis
[DE90-006721] N90-20450
The effects of high intensity cycle exercise on sympatho-adrenal-medullary response patterns
[AD-A217962] N90-20628
The effects of graded exercise at sea level on plasma proenkephalin peptide F and catecholamine responses
[AD-A218195] N90-20633
An algorithm for efficient estimation of superimposed exponential signals
[AD-A217218] N90-20698
Artificial Intelligence (AI) Center of Excellence at the University of Pennsylvania
[AD-A217393] N90-20743
Spectral analytic methods for the estimation of number of signals and directions of arrival
[AD-A217219] N90-20757
High-resolution acoustical imaging N90-20793

PENNSYLVANIA UNIV., PHILADELPHIA.
Innovative turbine concepts for open-cycle OTEC (Ocean Thermal Energy Conversion)
[DE90-000315] N90-20493
Software systems for modeling articulated figures N90-20677
Human task animation from performance models and natural language input N90-20678

PHYSICAL DYNAMICS, INC., LA JOLLA, CA.
Superconductive microprobes for eddy current evaluation of materials
[AD-A217776] N90-20361

PITTSBURGH UNIV., PA.
A general existence and uniqueness theorem for implicit differential-algebraic equations
[AD-A217965] N90-20770

PIXAR CORP., SAN RAFAEL, CA.
RenderMan design principles N90-20653

POLITECNICO DI MILANO (ITALY).
The inverse gravimetric problem in gravity modelling N90-20535

PRATT AND WHITNEY AIRCRAFT, WEST PALM BEACH, FL.
Improved toughness alloys based on titanium aluminides
[AD-A218149] N90-20208

PRINCETON UNIV., NJ.
Mechanisms of reactive etching
[AD-A217679] N90-20160
Simplified linear-time Jordan sorting and polygon clipping
[AD-A215110] N90-20693
Almost-optimum parallel speed-ups of algorithms for bipartite matching and related problems
[AD-A215111] N90-20728
Maintaining bridge-connected and biconnected components on-line
[AD-A215107] N90-20754

PROVENCE UNIV., MARSEILLE (FRANCE).
Spectral line shape code for multielectron emitters
[DE90-008526] N90-20853

PURDUE UNIV., WEST LAFAYETTE, IN.
The effect of adverse pressure gradient on turbulent burst structure in low-Reynolds number equilibrium boundary layers
[AD-A217308] N90-20327
Investigation into the mechanism of polymer thread drag reduction
[AD-A217492] N90-20329
Modeling of the Earth's gravity field using the New Global Earth Model (NEWGEM) N90-20523
An estimation of rainfall amounts using radar-derived Z-R relationships
[AD-A217950] N90-20591
Advanced parallel systems
[AD-A217175] N90-20731

R

R AND D ASSOCIATES, MARINA DEL REY, CA.
First-order intensity statistics for non-Rayleigh fading
[AD-A217572] N90-20569

RANGE COMMANDERS COUNCIL, WHITE SANDS MISSILE RANGE, NM.
Flight termination system battery guidelines
[AD-A217310] N90-20092

RENSSELAER POLYTECHNIC INST., TROY, NY.
Compendium of abstracts and viewgraphs.
[AD-A217189] N90-20140
Perturbation solutions in D* for buckling, vibration, and static loading of specially orthotropic plates N90-20419
Postbuckling behavior of laminated specially orthotropic plates by affine transformation N90-20420
Automated finite element modeling and simulation N90-20753
Stabilization of high (Tc) superconductivity in cadmium sulfide
[DE90-008249] N90-20881
ONR (Office of Naval Research) summer scholars for the 1989 PREFACE Program
[AD-A217746] N90-20919

RESEARCH TRIANGLE INST., RESEARCH TRIANGLE PARK, NC.
Research and development on enhanced degradable plastics
[AD-A217180] N90-20212
GCS plan for software aspects of certification
[NASA-CR-181972] N90-20694

ROCHESTER UNIV., NY.
Fundamental studies of photon statistics
[AD-A217825] N90-20836
Time-resolved spectroscopy of nonequilibrium ionization in laser-produced plasmas
[DE90-008663] N90-20854

ROCKWELL INTERNATIONAL CORP., ANAHEIM, CA.
Modeling and classification of acoustic transients by speech recognition techniques
[AD-A218070] N90-20277

ROCKWELL INTERNATIONAL CORP., DOWNEY, CA.
Efficient utilization of graphics technology for space animation N90-20663

ROCKWELL INTERNATIONAL CORP., GOLDEN, CO.
The Terrain-Responsive Atmospheric Code (TRAC) project plan: Development of a hazardous materials dispersion modeling capability with application to ambient air monitoring network design
[DE90-007293] N90-20502
ROCKWELL INTERNATIONAL SCIENCE CENTER, THOUSAND OAKS, CA.
Dielectric composite thin films
[AD-A217940] N90-20791
ROCKWELL SHUTTLE OPERATIONS CO., HOUSTON, TX.
The Real Time Interactive Display Environment (RTIDE), a display building tool developed by Space Shuttle flight controllers N90-20654
ROME AIR DEVELOPMENT CENTER, GRIFFISS AFB, NY.
Wideband S band transmitter
[AD-A217620] N90-20295
Picosecond Laser Facility
[AD-A217784] N90-20384
ROYAL AEROSPACE ESTABLISHMENT, FARNBOROUGH (ENGLAND).
Escape systems research at RAE N90-20058
ROYAL INST. OF TECH., STOCKHOLM (SWEDEN).
Geopotential coefficient determination and the gravimetric boundary value problem: A new approach N90-20521

S

SAINT LOUIS UNIV., MO.
Applications of microwave radiometric measurements to infer tropical cyclone intensity and strength
[AD-A218273] N90-20600
SAN DIEGO STATE UNIV., CA.
Electron-impact ionization and electron attachment cross sections of radicals important in transient gaseous discharges
[AD-A217510] N90-20366
SANDIA NATIONAL LABS., ALBUQUERQUE, NM.
A 10-stage reconnection demonstration launcher
[DE90-007653] N90-20106
Diagnostics and firing control for the cylindrical reconnection launcher
[DE90-007677] N90-20107
Design and performance of a multi-stage cylindrical reconnection launcher
[DE90-007820] N90-20108
Hydrous metal oxide-supported catalysts. Part 1: Preparation chemistry and physical and chemical properties
[DE90-007607] N90-20161
Developments in solar photocatalysis for destruction of organics in water
[DE90-007685] N90-20162
Moisture control in sealed electronic packages
[DE90-008136] N90-20166
Evaluation of material homogeneity as a function of thickness of low-alloy ferritic steel
[DE90-008069] N90-20202
The viscoelasticity of curing thermosets
[DE90-006535] N90-20221
Pyrotechnic device technology
[DE90-007683] N90-20234
The thermal response of generic objects in JP-4 pool fires
[DE90-008503] N90-20259
The adaptive line enhancer applied to chirp detection
[DE90-006772] N90-20268
The inverse triax x ray diode: An alternate reduced-endpoint-energy bremsstrahlung source
[DE90-006366] N90-20285
A linear filtering technique for removal of low-frequency noise
[DE90-006183] N90-20296
Exploratory battery technology development and testing report for 1988
[DE90-007996] N90-20297
A simple multicomponent fluid theory with accurate physics
[DE90-006537] N90-20334
Estimation of modeled object pose from monocular images
[DE90-001678] N90-20354
Strategies for high efficiency operation of the E-beam excited atomic xenon laser using high-power and high-energy loading
[DE90-005198] N90-20370
Swing-free movement of simply suspended objects employing parameter estimation
[DE90-002238] N90-20398
Resolved motion rate and resolved acceleration servo-control of wheeled mobile robots
[DE90-002585] N90-20399
Knowledge-based robotic grasping
[DE90-007216] N90-20402
Dynamic damping control: Implementation issues and simulation results
[DE90-007687] N90-20403
Parameter-scheduled trajectory planning for suppression of coupled horizontal and vertical vibrations in a flexible rod
[DE90-002313] N90-20435
High-efficiency silicon concentrator solar cell research
[DE90-006040] N90-20490
Perspectives on solar energy and the environment
[DE90-007680] N90-20494
Selection and design of a stretched-membrane heliostat for today's markets
[DE90-007997] N90-20495
RIPE: An object-oriented Robot Independent Programming Environment
[DE90-008501] N90-20707
A paradoxical result in unconditionally secure authentication codes, and an explanation
[DE90-008529] N90-20710
A time stepping algorithm for parallel computers
[DE90-008163] N90-20738
A model and implementation of multigrid for massively parallel computers
[DE90-008165] N90-20739
Implementation of midcourse tracking and correlation on massively parallel computers
[DE90-008166] N90-20740
Boundary equations of configuration obstacles for manipulators
[DE90-002101] N90-20745
Chemically prepared PZT films doped with niobium
[DE90-006811] N90-20859
CCST (Center for Compound Semiconductor Technology) research briefs
[DE90-007782] N90-20874
High temperature chemistry of oxide superconductors
[DE90-007821] N90-20875
SiO(x) precipitation: Defect density correlation with the n+ substrate resistivity
[DE90-005593] N90-20878
Identification of defects in SOI (Silicon-On-Insulator) wafers
[DE90-006020] N90-20879
Designing an experimenters database using the Nijssen Information Analysis Methodology (NIAM)
[DE90-008548] N90-20907
SANTA BARBARA RESEARCH CENTER, GOLETA, CA.
NRL hybrid reliability. Physics of failure initial study
[AD-A217986] N90-20893
SCHOOL OF AEROSPACE MEDICINE, BROOKS AFB, TX.
The United States Air Force School of Aerospace Medicine: Special report
[AD-A217740] N90-20622
SCIENCE APPLICATIONS INTERNATIONAL CORP., MCLEAN, VA.
Numerical modeling of airblast
[AD-A217993] N90-20347
Analysis of GALE (Genesis of Atlantic Lows Experiment) data
[AD-A217182] N90-20584
SCIENCE APPLICATIONS INTERNATIONAL CORP., SAN DIEGO, CA.
Selection and design of a stretched-membrane heliostat for today's markets
[DE90-007997] N90-20495
SCIENCE APPLICATIONS RESEARCH, LANHAM, MD.
Gravitational model improvement at the Goddard Space Flight Center N90-20514
SCIENTIFIC COMPUTING ASSOCIATES, INC., NEW HAVEN, CT.
Modification and improvement of software for modeling multidimensional reacting fuel flows
[AD-A217789] N90-20235
SIKORSKY AIRCRAFT, STRATFORD, CT.
Plan, formulate, and discuss a NASTRAN finite element model of the UH-60A helicopter airframe
[NASA-CR-181975] N90-20439
SRI INTERNATIONAL CORP., MENLO PARK, CA.
The application of electrochemical impedance spectroscopy for characterizing the degradation of Ni(OH)2/NiOOH electrodes N90-20474
Electronically metastable molecules of high symmetry
[AD-A217768] N90-20814
STANFORD LINEAR ACCELERATOR CENTER, CA.
The Inevitable Universe: Parker-Rhodes' peculiar mixture of ontology and physics
[DE90-006453] N90-20915
STANFORD UNIV., CA.
Computation of hypersonic low density flows with thermochemical nonequilibrium N90-20044
Transpiration cooling in hypersonic flight
[NASA-CR-186435] N90-20052
Composite-grid techniques and adaptive mesh refinement in computational fluid dynamics
[AD-A217383] N90-20328
A numerical investigation of the compressible mixing layer
[AD-A217738] N90-20343
Picosecond nonlinear studies of complex materials using the free electron laser
[AD-A218215] N90-20387
Asynchronous design for parallel processing architectures
[AD-A217421] N90-20734
Generalized quasi-variational inequality and implicit complementarity problems
[AD-A215191] N90-20755
STATE UNIV. OF NEW YORK, ALBANY.
X ray microimaging by diffractive techniques
[DE90-008444] N90-20356
STATE UNIV. OF NEW YORK, BUFFALO.
Chemical and electrochemical studies in ionic liquids
[AD-A217742] N90-20175
Picosecond laser study of polyatomic molecules
[DE90-008647] N90-20381
Velocity matched optical transmitter
[AD-A217413] N90-20830
STATE UNIV. OF NEW YORK AT BUFFALO, AMHERST.
Molecular dynamics and spectroscopy at gas-solid interfaces
[AD-A217743] N90-20813
STIRLING POWER SYSTEMS CORP., ANN ARBOR, MI.
Phase 1 supplemental development of a kinematic Stirling/Rankine commercial gas-fired heat pump system
[PB90-129974] N90-20483
STUTTGART UNIV. (GERMANY, F.R.).
Research of the interaction between hydrogen and deuterium with atomic eigen defects and dislocations in nickel and iron
[ETN-90-95380] N90-20195
Stabilized determination of geopotential coefficients by the mixed hom-BLUP approach N90-20520
SYSTRAN CORP., DAYTON, OH.
Optimization of laminated composite plates
[AD-A217621] N90-20146

T

TECHNISCHE HOCHSCHULE, DARMSTADT (GERMANY, F.R.).
The use of high-resolution terrain data in gravity field prediction N90-20533
TECHNISCHE HOGESCHOOL, DELFT (NETHERLANDS).
A discussion of observation model, error sources and signal size for spaceborne gravitational gradiometry N90-20557
TECHNISCHE UNIV., BRUNSWICK (GERMANY, F.R.).
Experiments on buckling and critical buckling. Behavior of carbon fiber reinforced plastic shells submitted to tensile stresses
[ETN-90-95382] N90-20429
A learning regulator for the plane longitudinal movement
[ETN-90-95381] N90-20695
TECHNISCHE UNIV., CLAUSTHAL-ZELLERFELD (GERMANY, F.R.).
Diffusion and germ formation in glasses N90-20250
TECHNISCHE UNIV., HANOVER (GERMANY, F.R.).
Regional quasigeoid determination in Northern Germany and comparison with GPS N90-20544
Long range geoid control through the European GPS traverse: Final results N90-20545
TECHNISCHE UNIV., MUNICH (GERMANY, F.R.).
Investigation of the technological effects on the coupling behavior of parallel GaAlAs rib waveguide
[ETN-90-95323] N90-20825
TEL-AVIV UNIV. (ISRAEL).
Advanced calcium thionyl chloride high power battery
[AD-A216685] N90-20482
TEXAS A&M UNIV., COLLEGE STATION.
A video-based experimental investigation of wing rock
[AD-A218244] N90-20075
Ligand-centered electron-transfer redox processes for manganese, iron, and cobalt complexes in relation to selected catalytic systems
[AD-A217957] N90-20177
A new concept for high-cycle-life LEO: Rechargeable MnO2-hydrogen N90-20462
Recent advances in solid polymer electrolyte fuel cell technology with low platinum loading electrodes N90-20465
Innovative turbine concepts for open-cycle OTEC (Ocean Thermal Energy Conversion)
[DE90-000315] N90-20493
Experimental and theoretical studies of light scattering by small particles
[AD-A217432] N90-20831

Electronic properties of high-temperature superconductors
[AD-A217953] N90-20892

TEXAS UNIV., ARLINGTON.
Electronic and ionic transport in processable conducting polymers
[AD-A218093] N90-20229
Simulation of radar scattering from rough surfaces
[AD-A217841] N90-20275

TEXAS UNIV., AUSTIN.
An improved model for the Earth's gravity field N90-20515
Gravity field determination and error assessment techniques N90-20517
A model of the general ocean circulation determined from a joint solution for the Earth's gravity field N90-20550
Studies of an orbital gradiometer mission N90-20558
GaAs traveling-wave optical modulators using modulated coplanar electrodes with periodic cross-tie overlays
[AD-A217731] N90-20835
Enhanced pinch effect due to electrostatic potential
[DE90-007088] N90-20844

THIOKOL CORP., BRIGHAM CITY, UT.
Thiokol/Wasatch installation evaluation of the redesigned field joint protection system (concepts 1 and 3)
[NASA-CR-183860] N90-20127

TRW, INC., HUNTSVILLE, AL.
Space station Simulation Computer System (SCS) study for NASA/MSFC. Volume 1: Overview and summary
[NASA-CR-183840] N90-20113
Space station Simulation Computer System (SCS) study for NASA/MSFC. Volume 2: Concept document
[NASA-CR-183841] N90-20114
Space station Simulation Computer System (SCS) study for NASA/MSFC. Volume 3: Refined conceptual design report
[NASA-CR-183842] N90-20115
Space station Simulation Computer System (SCS) study for NASA/MSFC. Volume 4: Conceptual design report
[NASA-CR-183843] N90-20116
Space station Simulation Computer System (SCS) study for NASA/MSFC. Volume 5: Study analysis report
[NASA-CR-183844] N90-20117
Space station Simulation Computer System (SCS) study for NASA/MSFC. Volume 6: Study issues report
[NASA-CR-183845] N90-20118

TRW DEFENSE SYSTEMS GROUP, REDONDO BEACH, CA.
OMV mission simulator N90-20669

U

UNIFIED INDUSTRIES, INC., SPRINGFIELD, VA.
High efficiency flashlamp-pumped titanium: Sapphire laser
[AD-A217598] N90-20367
Flash-pumped titanium laser
[AD-A217599] N90-20368

UNITED KINGDOM ATOMIC ENERGY AUTHORITY, HARWELL (ENGLAND).
Infiltration mechanics in conventional and hybridised fibre reinforced metal matrix composites
[AERE-R-13330] N90-20134
Effect of heat treatment on the fracture toughness transition properties of an A508 class 3 steel
[AERE-R-13548] N90-20182
Hydrogen, thermal ageing and the role of carbides in fatigue of a high strength steel
[AERE-R-13599] N90-20183
The effect of the SiC/Al interface on matrix microstructure in 2xxx-SiCp metal matrix
[AERE-R-13591] N90-20184
Wetting of metallic carbides by non-reactive liquid metals
[AERE-M-3759] N90-20185
Constitutive data acquisition and modelling in aluminium 2014 alloy
[AERE-R-13651] N90-20186
Shaping the insonifying pulse to optimise B-scans obtained in austenite
[AERE-R-13518] N90-20187
Ageing effects in welded cast CF3 stainless steel
[AERE-R-13559] N90-20188
Spallation of oxide scales from 20 percent Cr/25 percent Ni/Nb stainless steel
[AERE-R-13464] N90-20189
Stochastic approach to the initiation of pitting corrosion
[AERE-R-13348] N90-20190
Fatigue crack growth in martensitic 2 1/4Cr-1Mo steel at elevated temperatures
[AERE-R-13524] N90-20191
Tellurium embrittlement of type 316 steel
[AERE-R-13440] N90-20192
The ageing effect of the matrix-reinforcement interface on the ageing response of an aluminium 6061 alloy reinforced with 20vol percent SiC particulates
[AERE-R-13361] N90-20193
The effects of radiation on the mechanical properties of polymers used as electrical cable insulation and jacketing materials
[AERE-R-13286] N90-20209
The diffraction of ultrasound by cracks: Comparison of experiment with theory
[AERE-R-13334] N90-20410
Nondestructive testing of ceramics by acoustic microscopy
[AERE-R-13350] N90-20411
Residual stresses: A review of their measurement and interpretation using x ray diffraction
[AERE-R-13005] N90-20423
The stress-driven redistribution of point defects in the vicinity of crack-like singularities
[AERE-R-12898] N90-20424
Limitations and applications of fracture assessment with R6
[AERE-R-13012] N90-20425
Energy transfer between electrons and ions in collision cascades in solids
[AERE-R-13662] N90-20801
Theory of defect process: Basic issues in quantitative understanding
[AERE-R-13661] N90-20860
Differential measurements of the lateral photo effect in GaAs/AlGaAs heterostructures
[AERE-R-13557] N90-20861
Ionic disorder in crystals at high temperatures with emphasis on fluorites
[AERE-R-13544] N90-20862

UNIVERSITY OF NORTHERN ILLINOIS, DE KALB.
Studies of high energy phenomena using muons
[DE90-008272] N90-20820

UNIVERSITY OF SOUTH FLORIDA, TAMPA.
Fault simulator evaluation
[AD-A217782] N90-20308

UNIVERSITY OF SOUTHERN CALIFORNIA, LOS ANGELES.
Joint Services Electronics Program research in electronics
[AD-A217745] N90-20307

UTAH STATE UNIV., LOGAN.
USU center of excellence in theory and analysis of the geo-plasma environment
[AD-A217736] N90-20101
Meteor observations using the 50 MHz MENTOR imaging Doppler interferometer
[AD-A217908] N90-20276
Solar cyclical trend study of the mid-latitude, quiet-time, meridional, neutral winds at winter solstice conditions
[AD-A217398] N90-20568

UTAH UNIV., SALT LAKE CITY.
DURIP FTIR studies of solid state reaction dynamics
[AD-A217713] N90-20174
Pulsed laser photothermal spectroscopy of liquids and solids
[DE90-008642] N90-20380
Theoretical and experimental study of solid phase miscibility gaps in III/V quaternary alloys
[DE90-008430] N90-20877

V

VANDERBILT UNIV., NASHVILLE, TN.
Quantum-theoretical methods and studies relating to properties of materials
[AD-A217843] N90-20132
Theoretical investigations in elementary particle physics
[DE90-007178] N90-20802

VIRGINIA POLYTECHNIC INST. AND STATE UNIV., BLACKSBURG.
Discrete-time control of a spacecraft with retargetable flexible antennas N90-20119
Innovative design of composite structures: The use of curvilinear fiber format to improve buckling resistance of composite plates with central circular holes
[NASA-CR-186454] N90-20135
Innovative design of composite structures: The use of curvilinear fiber format in composite structure design
[NASA-CR-186453] N90-20136
Parallel algorithms in the finite element approximation of flow problems
[AD-A217729] N90-20341
Modal interactions in shell dynamics N90-20418

VIRGINIA UNIV., CHARLOTTESVILLE.
Implementation of a hypercube database system
[DE90-008440] N90-20905

W

WASHINGTON UNIV., SEATTLE.
The inter-outburst behavior of cataclysmic variables
[NASA-CR-186374] N90-20914

WESTINGHOUSE SAVANNAH RIVER CO., AIKEN, SC.
Transaction processing in a quality control laboratory
[DE90-004655] N90-20414

WISCONSIN UNIV., MADISON.
Critique of the vertical gradient of gravity N90-20531
Design of D-3 He commercial tokamak
[DE90-008252] N90-20852

WRIGHT RESEARCH DEVELOPMENT CENTER, WRIGHT-PATTERSON AFB, OH.
Laboratory implementation of the Continuously Reconfiguring Multi-Microprocessor Flight Control System (CRMMFCS)
[AD-A217730] N90-20094
VHSIC Hardware Description Language (VHDL) benchmark suite
[AD-A217947] N90-20719

WRIGHT STATE UNIV., DAYTON, OH.
Integrated circuits for avionics
[AD-A217964] N90-20312

Typical Contract Number Index Listing

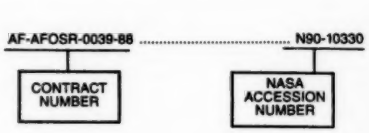

Listings in this index are arranged alphanumerically by contract number. Under each contract number the NASA accession numbers denoting documents that have been produced as a result of research done under that contract are arranged in ascending order. The NASA accession number denotes the number by which the citation is identified.

AF PROJ. 1D01 ..... N90-20318
AF PROJ. 1926 ..... N90-20069
AF PROJ. 2301 ..... N90-20805
N90-20829
AF PROJ. 2302 ..... N90-20053
N90-20441
AF PROJ. 2303 ..... N90-20132
N90-20156
N90-20160
N90-20175
N90-20232
N90-20289
N90-20815
AF PROJ. 2304 ..... N90-20123
N90-20341
N90-20342
N90-20415
N90-20416
N90-20417
N90-20715
N90-20716
N90-20747
N90-20760
N90-20761
AF PROJ. 2305 ..... N90-20309
N90-20311
N90-20832
AF PROJ. 2306 ..... N90-20227
N90-20256
N90-20386
N90-20791
AF PROJ. 2307 ..... N90-20345
AF PROJ. 2308 ..... N90-20159
N90-20176
AF PROJ. 2309 ..... N90-20452
N90-20579
AF PROJ. 2310 ..... N90-20578
AF PROJ. 2420 ..... N90-20153
AF PROJ. 2863 ..... N90-20830
AF PROJ. 3037 ..... N90-20800
AF PROJ. 3153 ..... N90-20314
AF PROJ. 3842 ..... N90-20174
N90-20383
N90-20692
AF PROJ. 4643 ..... N90-20639
AF PROJ. 6096 ..... N90-20719
AF PROJ. 7184 ..... N90-20749
AF PROJ. 7231 ..... N90-20799
N90-20800
AF PROJ. 7662 ..... N90-20312
AF PROJ. 7670 ..... N90-20917
AF PROJ. 9993 ..... N90-20723
AF-AFOSR-0011-90 ..... N90-20744
AF-AFOSR-0087-89 ..... N90-20383
AF-AFOSR-0088-87 ..... N90-20175
AF-AFOSR-0108-89 ..... N90-20174
AF-AFOSR-0110-86 ..... N90-20815
AF-AFOSR-0124-89 ..... N90-20452
N90-20692
AF-AFOSR-0128-88 ..... N90-20832
AF-AFOSR-0130-87 ..... N90-20715
AF-AFOSR-0131-88 ..... N90-20417
AF-AFOSR-0140-84 ..... N90-20415
AF-AFOSR-0140-89 ..... N90-20345
AF-AFOSR-0146-86 ..... N90-20132
AF-AFOSR-0147-85 ..... N90-20176
AF-AFOSR-0164-86 ..... N90-20309
AF-AFOSR-0183-87 ..... N90-20441
AF-AFOSR-0190-87 ..... N90-20761
AF-AFOSR-0197-88 ..... N90-20341
AF-AFOSR-0209G-85 ..... N90-20160
AF-AFOSR-0212-88 ..... N90-20342
AF-AFOSR-0233-84 ..... N90-20805
AF-AFOSR-0267-85 ..... N90-20760
AF-AFOSR-0303-85 ..... N90-20050
N90-20768
AF-AFOSR-0306-87 ..... N90-20416
AF-AFOSR-0320-87 ..... N90-20232
AF-AFOSR-0331-88 ..... N90-20159
AF-AFOSR-0335-87 ..... N90-20747
AF-AFOSR-0356-87 ..... N90-20764
AF-AFOSR-0365-85 ..... N90-20386
AF-AFOSR-0372-84 ..... N90-20716
AFOSR-ISSA-87-0034 ..... N90-20227
AFOSR-ISSA-88-0005 ..... N90-20227
AFWL-87-217 ..... N90-20704
ARO PROJ. P-24025-EG N90-20048
ARPA ORDER 3391 ..... N90-20758
ARPA ORDER 4850 ..... N90-20460
ARPA ORDER 5299 ..... N90-20579
BMFT-01-ZV-8705-0 ..... N90-20499
C-80019-F N90-20348
DA PROJ. C00-31 ..... N90-20700
DA PROJ. 1C1-62706-A-553-C N90-20315
DA PROJ. 1L1-62105-AH-84 ..... N90-20196
N90-20792
DA PROJ. 1L1-62716-AH-70 ..... N90-20095
N90-20720
DA PROJ. 1L1-162716-AH-70 ..... N90-20648
DA PROJ. 3E1-62787-A-878 ..... N90-20636
DA PROJ. 3E1-62787-A-879 ..... N90-20624
N90-20625
DA PROJ. 3E1-162787-A-879 ..... N90-20629
DA PROJ. 3M1-62787-A-878 ..... N90-20385
DAAA15-85-K-0012 ..... N90-20330
DAAE07-84-C-R138 ..... N90-20748
DAAG29-84-K-0061 ..... N90-20678
N90-20743
DAAL03-86-G-0023 ..... N90-20688
DAAL03-86-G-0046 ..... N90-20226
DAAL03-86-G-0211 ..... N90-20144
DAAL03-86-K-0029 ..... N90-20217
DAAL03-86-K-0062 ..... N90-20157
DAAL03-86-K-0078 ..... N90-20288
DAAL03-86-K-0106 ..... N90-20731
DAAL03-86-K-0111 ..... N90-20265
DAAL03-86-K-0168 ..... N90-20831
DAAL03-86-K-0171 ..... N90-20759
DAAL03-87-K-0022 ..... N90-20048
DAAL03-87-K-0106 ..... N90-20697
DAAL03-88-C-0009 ..... N90-20267
DAAL03-88-G-0044 ..... N90-20291
DAAL03-88-K-0005 ..... N90-20835
DAAL03-88-K-0092 ..... N90-20790
DAAL03-88-K-0108 ..... N90-20894
DAAL03-89-G-0003 ..... N90-20140
DAAL03-89-G-0097 ..... N90-20867
DAAL03-89-K-0028 ..... N90-20267
DAAL03-89-K-0139 ..... N90-20698
N90-20757
DACA76-85-C-0010 ..... N90-20751
N90-20752
DAJA45-89-C-0013 ..... N90-20482
DAMD17-87-C-7186 ..... N90-20385
DARPA ORDER 5358 ..... N90-20371
DARPA ORDER 6029 ..... N90-20143
DARPA ORDER 9526 ..... N90-20498
DASG60-89-C-0079 ..... N90-20279
DE-AC02-76CH-00016 ..... N90-20150
N90-20210
N90-20218
N90-20509
N90-20807
N90-20857
N90-20870
DE-AC02-76CH-03000 ..... N90-20855
DE-AC02-80ER-10569 ..... N90-20821
DE-AC02-80ET-15601 ..... N90-20845
DE-AC02-83CH-10093 ..... N90-20111
N90-20220
N90-20486
N90-20487
N90-20488
N90-20489
N90-20491
N90-20492
N90-20493
N90-20571
N90-20608
DE-AC02-85NE-37944 ..... N90-20712
DE-AC02-87ER-40368 ..... N90-20820
DE-AC02-87ER-80500 ..... N90-20470
DE-AC03-76SF-00098 ..... N90-20147
N90-20148
N90-20164
N90-20165
N90-20197
N90-20206
N90-20306
N90-20496
N90-20508
N90-20570
N90-20610
N90-20611
N90-20706
N90-20789
N90-20811
N90-20871
N90-20872
N90-20873
DE-AC03-76SF-00515 ..... N90-20915
DE-AC03-86SF-16496 ..... N90-20824
DE-AC03-89ER-51114 ..... N90-20822
DE-AC04-76DP-00656 ..... N90-20412
DE-AC04-76DP-00789 ..... N90-20106
N90-20107
N90-20108
N90-20161
N90-20162
N90-20166
N90-20202
N90-20221
N90-20234
N90-20259
N90-20268
N90-20285
N90-20296
N90-20297
N90-20334
N90-20354
N90-20370
N90-20398
N90-20399
N90-20402
N90-20403
N90-20435
N90-20490
N90-20494
N90-20495
N90-20707
N90-20710
N90-20738
N90-20739
N90-20740
N90-20745
N90-20859
N90-20874
N90-20875
N90-20878
N90-20879
N90-20907
DE-AC04-90DP-6234 ..... N90-20502
DE-AC05-80ER-10742 ..... N90-20150
DE-AC05-84OR-21400 ..... N90-20149
N90-20167
N90-20207
N90-20224

N90-20355
N90-20375
N90-20395
N90-20396
N90-20397
N90-20404
N90-20413
N90-20506
N90-20736
N90-20737
N90-20746
N90-20763
N90-20765
N90-20810
N90-20819
N90-20843
N90-20844
N90-20846
N90-20848
N90-20850
N90-20851
N90-20858
DE-AC05-84OT-21400 ..... N90-20335
N90-20340
DE-AC06-78RL-01830 ..... N90-20172
N90-20225
N90-20298
N90-20505
N90-20510
N90-20511
DE-AC07-76ID-01570 ..... N90-20170
N90-20303
DE-AC08-88NV-10617 ..... N90-20357
N90-20906
DE-AC09-89SR-18035 ..... N90-20414
DE-AC12-76SN-00052 ..... N90-20199
DE-AC21-82MC-24222 ..... N90-20484
DE-AC22-88PC-88951 ..... N90-20332
DE-FC03-85DP-40200 ..... N90-20854
DE-FG02-84ER-13227 ..... N90-20380
DE-FG02-84ER-45061 ..... N90-20877
DE-FG02-84ER-45125 ..... N90-20129
DE-FG02-84ER-45167 ..... N90-20223
DE-FG02-84ER-52111 ..... N90-20109
DE-FG02-85ER-13405 ..... N90-20381
DE-FG02-85ER-13441 ..... N90-20806
DE-FG02-86ER-13486 ..... N90-20612
DE-FG02-86ER-13570 ..... N90-20869
DE-FG02-86ER-25015 ..... N90-20766
DE-FG02-86ER-45269 ..... N90-20173
DE-FG02-86ER-60470 ..... N90-20450
DE-FG02-87ER-45303 ..... N90-20219
DE-FG02-87ER-45310 ..... N90-20876
DE-FG02-87ER-45323 ..... N90-20882
DE-FG02-87ER-60612 ..... N90-20512
DE-FG02-88ER-13937 ..... N90-20267
N90-20377
DE-FG02-88ER-45362 ..... N90-20681
DE-FG02-89ER-45396 ..... N90-20222
DE-FG02-89ER-45405 ..... N90-20882
DE-FG02-89ER-52158 ..... N90-20852
DE-FG02-89ER-60858 ..... N90-20356
DE-FG02-89ER-60883 ..... N90-20503
DE-FG03-86ER-45249 ..... N90-20198
DE-FG05-80ET-53088 ..... N90-20844
DE-FG05-85ER-40226 ..... N90-20802
DE-FG05-85ER-60312 ..... N90-20501
DE-FG05-85ER-60348 ..... N90-20606
DE-FG05-86ER-40272 ..... N90-20897
DE-FG05-87ER-25029 ..... N90-20690
DE-FG05-88ER-25063 ..... N90-20905
DE-FG05-88ER-60649 ..... N90-20621
DE-FG05-89ER-14018 ..... N90-20163
DE-FG07-83ID-12467 ..... N90-20170
DFG-MU-247/72 ..... N90-20625
DNA PROJ. P99-GMXD N90-20569
DNA001-88-C-0046 ..... N90-20569
DTFA03-89O-A-00019 ..... N90-20080
ESA-7521/87/F/FL N90-20557
F04611-86-C-0068 ..... N90-20812
F04701-88-C-0089 ..... N90-20344
F19628-86-C-0028 ..... N90-20839
F19628-86-C-0136 ..... N90-20556
F19628-86-K-0016 ..... N90-20541
F19628-87-C-0097 ..... N90-20838
F19628-87-C-0230 ..... N90-20723
F19628-87-K-0046 ..... N90-20579
F19628-90-C-0002 ..... N90-20290
N90-20585
N90-20758
N90-20759
N90-20828
F29601-87-C-0052 ..... N90-20829
F30602-81-C-0193 ..... N90-20830
F30602-81-C-0202 ..... N90-20308
F30602-81-C-0206 ..... N90-20293
F33615-84-C-3404 ..... N90-20069
F33615-85-C-1718 ..... N90-20312
F33615-85-C-2537 ..... N90-20091
F33615-85-C-5030 ..... N90-20208
F33615-85-C-5105 ..... N90-20256
F33615-86-C-2694 ..... N90-20235
F33615-86-C-2723 ..... N90-20318
F33615-86-C-3600 ..... N90-20647
F33615-87-C-2712 ..... N90-20289
F33615-88-C-5401 ..... N90-20153
F33615-88-C-5402 ..... N90-20146
F33615-88-C-5404 ..... N90-20314
F49620-83-C-0135 ..... N90-20714
F49620-85-C-0144 ..... N90-20776
N90-20777
N90-20778
N90-20779
F49620-86-C-0009 ..... N90-20813
F49620-86-C-0067 ..... N90-20267
F49620-86-C-0109 ..... N90-20101
F49620-86-C-0136 ..... N90-20689
F49620-86-K-0022 ..... N90-20343
F49620-87-C-0041 ..... N90-20311
F49620-87-C-0069 ..... N90-20075
F49620-87-C-0079 ..... N90-20123
F49620-87-C-0118 ..... N90-20856
F49620-87-K-0001 ..... N90-20610
F49620-87-K-0002 ..... N90-20814
F49620-88-C-0034 ..... N90-20791
F49620-88-C-0067 ..... N90-20307
F49620-88-C-0091 ..... N90-20361
F49620-88-C-0143 ..... N90-20231
F49620-88-CK-0001 ..... N90-20053
F49620-89-C-022 ..... N90-20276
GRI-5069-242-1776 ..... N90-20483
JPL-956689 ..... N90-20515
JPL-958122 ..... N90-20550
MDA903-84-C-0031 ..... N90-20145
MDA903-86-K-0155 ..... N90-20644
MDA903-89-C-0003 ..... N90-20783
MDA972-88-J-1002 ..... N90-20873
MIPR-ARO-102-89 ..... N90-20210
MIPR-FY1455-89-N0655 ..... N90-20301
NAG1-270 ..... N90-20650
NAG1-613 ..... N90-20686
NAG1-703 ..... N90-20050
NAG1-901 ..... N90-20135
N90-20136
NAG2-426 ..... N90-20678
NAG3-519 ..... N90-20472
NAG3-536 ..... N90-20271
NAG3-740 ..... N90-20237
NAG3-816 ..... N90-20286
NAG3-828 ..... N90-20708
NAG3-964 ..... N90-20468
NAG5-528 ..... N90-20558
NAG5-557 ..... N90-20253
NAG5-1012 ..... N90-20582
NAG8-091 ..... N90-20194
NAG8-738 ..... N90-20918
NASA ORDER C-99066-G N90-20326
N90-20337
NASW-4430 ..... N90-20769
N90-20080
N90-20081
N90-20082
N90-20083
N90-20084
NAS1-16097 ..... N90-20088
NAS1-17499 ..... N90-20439
NAS1-17964 ..... N90-20694
NAS1-18107 ..... N90-20050
N90-20764
NAS1-18225 ..... N90-20112
NAS1-18444 ..... N90-20421
NAS1-18584 ..... N90-20284
NAS1-18599 ..... N90-20422
NAS1-18605 ..... N90-20049
N90-20050
N90-20650
N90-20768
NAS3-24564 ..... N90-20120
NAS3-24635 ..... N90-20469
NAS3-24680 ..... N90-20270
NAS3-25199 ..... N90-20471
NAS3-25355 ..... N90-20479
NAS5-28067 ..... N90-20554
N90-20561
N90-20713
NAS5-29452 ..... N90-20281
NAS7-918 ..... N90-20127
NAS8-30490 ..... N90-20113
NAS8-37745 ..... N90-20114
N90-20115
N90-20116
N90-20117
N90-20118
NAS9-15014 ..... N90-20662
NAS9-17900 ..... N90-20670
NAS9-17991 ..... N90-20461
NCA2-301 ..... N90-20686
NCC1-14 ..... N90-20430
NCC2-543 ..... N90-20052
NCC8-15 ..... N90-20324
NGR-36-008-161 ..... N90-20513
NGT-50063 ..... N90-20678
NIST PROJ. 4202464 ..... N90-20227
NRC-1886-8082-8B N90-20355
NSC78-0410-E014-02 ..... N90-20547
NSF ATM-86-08391 ..... N90-20276
NSF ATM-87-19781 ..... N90-20276
NSF ATM-88-11771 ..... N90-20913
NSF ATM-88-13454 ..... N90-20276
NSF CCR-89-07654 ..... N90-20770
NSF CHE-88-16581 ..... N90-20267
NSF DCR-85-1191 ..... N90-20728
NSF DCR-85-552543 ..... N90-20724
NSF DCR-86-05962 ..... N90-20693
N90-20728
N90-20754
NSF DMC-85-16114 ..... N90-20678
NSF DMR-85-13731 ..... N90-20858
NSF DMR-88-21571 ..... N90-20218
NSF DMS-87-01212 ..... N90-20776
NSF DMS-88-10150 ..... N90-20050
N90-20768
NSF DMS-88-11863 ..... N90-20650
NSF DMS-89-13089 ..... N90-20755
NSF DPP-87-001 ..... N90-20097
NSF DPP-87-19147 ..... N90-20526
NSF ECS-87-15811 ..... N90-20744
NSF IRI-86-16644 ..... N90-20725
NSF IST-86-12984 ..... N90-20678
NSF MCS-82-19196 ..... N90-20678
NSF PHY-88-20540 ..... N90-20267
NSF RII-86-10669 ..... N90-20916
NSG-5395 ..... N90-20914
N00014-81-K-0503 ..... N90-20399
N00014-83-K-0183 ..... N90-20327
N90-20329
N00014-83-K-0576 ..... N90-20836
N00014-84-C-0149 ..... N90-20292
N00014-84-C-0193 ..... N90-20796
N00014-84-K-0447 ..... N90-20216
N00014-84-K-0472 ..... N90-20255
N00014-84-K-0477 ..... N90-20230
N00014-84-K-0519 ..... N90-20274
N00014-85-C-2143 ..... N90-20367
N90-20368
N00014-85-K-0124 ..... N90-20724
N90-20751
N90-20752
N00014-86-C-0827 ..... N90-20497
N00014-86-C-2197 ..... N90-20347
N00014-86-C-2365 ..... N90-20584
N00014-86-C-2553 ..... N90-20893
N00014-86-K-0202 ..... N90-20278
N00014-86-K-0558 ..... N90-20366
N00014-86-K-0565 ..... N90-20328
N00014-86-K-0666 ..... N90-20895
N00014-86-K-0685 ..... N90-20752
N00014-86-K-0691 ..... N90-20650
N00014-86-K-0694 ..... N90-20267
N00014-86-K-0754 ..... N90-20768
N00014-86-K-0756 ..... N90-20213
N00014-86-K-0772 ..... N90-20158
N90-20215
N00014-86-K-0825 ..... N90-20387
N00014-87-C-0001 ..... N90-20449
N90-20700
N00014-87-G-0217 ..... N90-20143
N00014-87-K-0467 ..... N90-20693
N90-20728
N90-20754
N00014-87-K-0517 ..... N90-20211
N00014-87-K-0751 ..... N90-20275
N00014-87-K-0825 ..... N90-20287
N90-20687
N90-20729
N90-20742
N90-20756
N00014-88-C-0390 ..... N90-20498
N00014-88-C-0391 ..... N90-20464
N00014-88-C-0481 ..... N90-20277
N00014-88-C-0714 ..... N90-20233
N00014-88-K-0299 ..... N90-20267
N00014-88-K-0487 ..... N90-20725
N00014-88-K-0545 ..... N90-20643
N00014-88-K-0564 ..... N90-20866
N00014-88-K-0738 ..... N90-20287
N00014-88-K-2016 ..... N90-20912
N00014-89-C-0140 ..... N90-20214

N00014-89-J-1178 ..... N90-20826
N90-20827
N90-20864
N90-20865
N00014-89-J-1364 ..... N90-20567
N00014-89-J-1659 ..... N90-20755
N00014-89-J-1857 ..... N90-20919
N00014-89-J-3036 ..... N90-20734
N00014-89-J-3100 ..... N90-20732
N00014-90-J-1025 ..... N90-20770
N00014-90-J-1320 ..... N90-20229
N61533-88-C-0002 ..... N90-20212
N62271-86-M-0213 ..... N90-20837
N62271-87-M-0205 ..... N90-20837
N62271-6059-7873 ..... N90-20837
N62271-7183-4768 ..... N90-20837
RR01107 ..... N90-20836
R0148 ..... N90-20449
SRC-88-SJ-055 ..... N90-20267
SRI PROJ. 2915 ..... N90-20814
W-31-109-ENG-38 ..... N90-20201
N90-20258
N90-20394
N90-20400
N90-20401
N90-20460
N90-20480
N90-20703
N90-20709
N90-20888
W-7405-ENG-36 ..... N90-20168
N90-20283
N90-20365
N90-20369
N90-20374
N90-20379
N90-20436
N90-20485
N90-20702
N90-20785
N90-20786
N90-20809
N90-20834
N90-20841
N90-20847
N90-20849
N90-20863
N90-20887
N90-20916
W-7405-ENG-48 ..... N90-20169
N90-20171
N90-20203
N90-20204
N90-20205
N90-20257
N90-20260
N90-20261
N90-20269
N90-20299
N90-20300
N90-20304
N90-20305
N90-20336
N90-20359
N90-20360
N90-20371
N90-20372
N90-20373
N90-20376
N90-20378
N90-20382
N90-20437
N90-20440
N90-20573
N90-20588
N90-20589
N90-20620
N90-20691
N90-20704
N90-20705
N90-20711
N90-20735
N90-20762
N90-20808
N90-20822
N90-20823
N90-20833
N90-20853
N90-20880
N90-20883
N90-20884
N90-20885
N90-20904
307-07-00 ..... N90-20086
323-51-20-06 ..... N90-20281
474-12-10 ..... N90-20120
474-46-20 ..... N90-20181
505-60-01 ..... N90-20333
N90-20358
505-61-51 ..... N90-20325
505-62-3B N90-20392
505-62-4D N90-20051
505-62-21 ..... N90-20090
N90-20326
N90-20337
N90-20769
505-62-71 ..... N90-20338
505-63-1A N90-20130
505-63-1B N90-20138
N90-20391
N90-20431
N90-20432
505-63-01-05 ..... N90-20080
N90-20081
N90-20082
N90-20083
N90-20084
N90-20427
505-63-01-10 ..... N90-20421
N90-20422
505-63-01-11 ..... N90-20068
505-63-11 ..... N90-20139
505-63-21-04 ..... N90-20047
N90-20071
N90-20093
505-63-31 ..... N90-20438
505-63-51-01 ..... N90-20439
505-63-51-09 ..... N90-20430
505-66-21-03 ..... N90-20694
505-80-31-01 ..... N90-20088
505-90-21-01 ..... N90-20049
N90-20050
N90-20650
N90-20764
N90-20768
506-41-3F N90-20301
506-41-21 ..... N90-20454
506-41-41 ..... N90-20085
506-42-00 ..... N90-20110
506-43-11 ..... N90-20353
506-43-21-05 ..... N90-20137
506-43-31-05 ..... N90-20426
506-43-41-02 ..... N90-20121
506-44-2C N90-20286
506-44-20 ..... N90-20302
N90-20886
506-44-21 ..... N90-20393
506-46-21-01 ..... N90-20122
510-01-0A N90-20151
N90-20428
533-06-01 ..... N90-20087
535-03-01 ..... N90-20794
535-03-01-02 ..... N90-20046
535-05-01 ..... N90-20708
560-63-00 ..... N90-20645
643-10-01 ..... N90-20264
646-75-01-01 ..... N90-20112
647-27-05 ..... N90-20194
650-20-26 ..... N90-20270
672-22-20-70 ..... N90-20583
674-26-05 ..... N90-20237
676-00-00 ..... N90-20566
694-03-03 ..... N90-20253
N90-20352
763-01-41-27 ..... N90-20795

Typical Report Number Index Listing

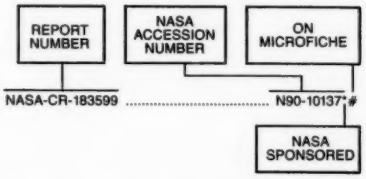

Listings in this index are arranged alphanumerically by report number. The NASA accession number denotes the number by which the citation is identified. An asterisk (*) indicates that the item is a NASA report. A pound sign (#) indicates that the item is available on microfiche.

A-88017 ..... N90-20333* #
A-89239 ..... N90-20087* #
A-90048 ..... N90-20325* #

AAMRL-TR-89-034 ..... N90-20799 #
AAMRL-TR-89-035 ..... N90-20800 #
AAMRL-TR-89-042 ..... N90-20640 #
AAMRL-TR-89-043 ..... N90-20639 #
AAMRL-TR-89-045 ..... N90-20749 #
AAMRL-TR-89-049 ..... N90-20641 #

ACT-110 ..... N90-20701 #

AD-A215107 ..... N90-20754 #
AD-A215110 ..... N90-20693 #
AD-A215111 ..... N90-20728 #
AD-A215191 ..... N90-20755 #
AD-A216685 ..... N90-20482 #
AD-A217114 ..... N90-20697 #
AD-A217117 ..... N90-20287 #
AD-A217119 ..... N90-20742 #
AD-A217120 ..... N90-20687 #
AD-A217121 ..... N90-20756 #
AD-A217123 ..... N90-20729 #
AD-A217126 ..... N90-20730 #
AD-A217161 ..... N90-20156 #
AD-A217165 ..... N90-20211 #
AD-A217166 ..... N90-20048 #
AD-A217167 ..... N90-20688 #
AD-A217168 ..... N90-20157 #
AD-A217175 ..... N90-20731 #
AD-A217178 ..... N90-20265 #
AD-A217180 ..... N90-20212 #
AD-A217181 ..... N90-20288 #
AD-A217182 ..... N90-20584 #
AD-A217184 ..... N90-20826 #
AD-A217185 ..... N90-20827 #
AD-A217186 ..... N90-20864 #
AD-A217187 ..... N90-20865 #
AD-A217188 ..... N90-20912 #
AD-A217189 ..... N90-20140 #
AD-A217200 ..... N90-20567 #
AD-A217202 ..... N90-20255 #
AD-A217203 ..... N90-20618 #
AD-A217204 ..... N90-20619 #
AD-A217207 ..... N90-20638 #
AD-A217216 ..... N90-20732 #
AD-A217218 ..... N90-20698 #
AD-A217219 ..... N90-20757 #
AD-A217231 ..... N90-20646 #
AD-A217233 ..... N90-20141 #
AD-A217234 ..... N90-20142 #
AD-A217261 ..... N90-20289 #
AD-A217262 ..... N90-20196 #
AD-A217264 ..... N90-20609 #
AD-A217300 ..... N90-20733 #
AD-A217302 ..... N90-20699 #
AD-A217308 ..... N90-20327 #
AD-A217310 ..... N90-20092 #
AD-A217318 ..... N90-20266 #
AD-A217330 ..... N90-20758 #
AD-A217331 ..... N90-20759 #
AD-A217332 ..... N90-20290 #
AD-A217333 ..... N90-20828 #
AD-A217334 ..... N90-20585 #
AD-A217336 ..... N90-20829 #
AD-A217337 ..... N90-20105 #
AD-A217343 ..... N90-20291 #
AD-A217348 ..... N90-20780 #
AD-A217366 ..... N90-20073 #
AD-A217375 ..... N90-20866 #
AD-A217378 ..... N90-20586 #
AD-A217380 ..... N90-20143 #
AD-A217383 ..... N90-20328 #
AD-A217384 ..... N90-20433 #
AD-A217393 ..... N90-20743 #
AD-A217396 ..... N90-20089 #
AD-A217398 ..... N90-20568 #
AD-A217401 ..... N90-20256 #
AD-A217412 ..... N90-20500 #
AD-A217413 ..... N90-20830 #
AD-A217418 ..... N90-20213 #
AD-A217421 ..... N90-20734 #
AD-A217426 ..... N90-20760 #
AD-A217431 ..... N90-20144 #
AD-A217432 ..... N90-20831 #
AD-A217448 ..... N90-20587 #
AD-A217452 ..... N90-20214 #
AD-A217455 ..... N90-20434 #
AD-A217459 ..... N90-20292 #
AD-A217460 ..... N90-20267 #
AD-A217479 ..... N90-20293 #
AD-A217492 ..... N90-20329 #
AD-A217496 ..... N90-20867 #
AD-A217498 ..... N90-20781 #
AD-A217510 ..... N90-20366 #
AD-A217518 ..... N90-20294 #
AD-A217527 ..... N90-20782 #
AD-A217572 ..... N90-20569 #
AD-A217573 ..... N90-20158 #
AD-A217574 ..... N90-20215 #
AD-A217578 ..... N90-20159 #
AD-A217581 ..... N90-20761 #
AD-A217585 ..... N90-20216 #
AD-A217598 ..... N90-20367 #
AD-A217599 ..... N90-20368 #
AD-A217610 ..... N90-20783 #
AD-A217611 ..... N90-20145 #
AD-A217617 ..... N90-20784 #
AD-A217620 ..... N90-20295 #
AD-A217621 ..... N90-20146 #
AD-A217622 ..... N90-20868 #
AD-A217630 ..... N90-20330 #
AD-A217638 ..... N90-20097 #
AD-A217640 ..... N90-20796 #
AD-A217642 ..... N90-20700 #
AD-A217652 ..... N90-20449 #
AD-A217667 ..... N90-20217 #
AD-A217672 ..... N90-20331 #
AD-A217674 ..... N90-20639 #
AD-A217675 ..... N90-20640 #
AD-A217678 ..... N90-20805 #
AD-A217679 ..... N90-20160 #
AD-A217681 ..... N90-20832 #
AD-A217682 ..... N90-20689 #
AD-A217684 ..... N90-20744 #
AD-A217685 ..... N90-20701 #
AD-A217692 ..... N90-20778 #
AD-A217694 ..... N90-20714 #
AD-A217696 ..... N90-20812 #
AD-A217697 ..... N90-20889 #
AD-A217699 ..... N90-20647 #
AD-A217708 ..... N90-20590 #
AD-A217709 ..... N90-20272 #
AD-A217711 ..... N90-20613 #
AD-A217712 ..... N90-20614 #
AD-A217713 ..... N90-20174 #
AD-A217723 ..... N90-20890 #
AD-A217724 ..... N90-20152 #
AD-A217729 ..... N90-20341 #
AD-A217730 ..... N90-20094 #
AD-A217731 ..... N90-20835 #
AD-A217732 ..... N90-20342 #
AD-A217735 ..... N90-20856 #
AD-A217736 ..... N90-20101 #
AD-A217737 ..... N90-20790 #
AD-A217738 ..... N90-20343 #
AD-A217739 ..... N90-20641 #
AD-A217740 ..... N90-20622 #
AD-A217742 ..... N90-20175 #
AD-A217743 ..... N90-20813 #
AD-A217744 ..... N90-20415 #
AD-A217745 ..... N90-20307 #
AD-A217746 ..... N90-20919 #
AD-A217748 ..... N90-20226 #
AD-A217752 ..... N90-20227 #
AD-A217765 ..... N90-20715 #
AD-A217768 ..... N90-20814 #
AD-A217769 ..... N90-20344 #
AD-A217770 ..... N90-20452 #
AD-A217771 ..... N90-20383 #
AD-A217772 ..... N90-20345 #
AD-A217775 ..... N90-20416 #
AD-A217776 ..... N90-20361 #
AD-A217778 ..... N90-20815 #
AD-A217779 ..... N90-20273 #
AD-A217782 ..... N90-20308 #
AD-A217784 ..... N90-20384 #
AD-A217786 ..... N90-20309 #
AD-A217789 ..... N90-20235 #
AD-A217792 ..... N90-20891 #
AD-A217796 ..... N90-20176 #
AD-A217799 ..... N90-20091 #
AD-A217808 ..... N90-20747 #
AD-A217810 ..... N90-20692 #
AD-A217822 ..... N90-20497 #
AD-A217824 ..... N90-20274 #
AD-A217825 ..... N90-20836 #
AD-A217840 ..... N90-20498 #
AD-A217841 ..... N90-20275 #
AD-A217843 ..... N90-20132 #
AD-A217854 ..... N90-20899 #
AD-A217855 ..... N90-20310 #
AD-A217862 ..... N90-20648 #
AD-A217877 ..... N90-20123 #
AD-A217878 ..... N90-20441 #
AD-A217880 ..... N90-20716 #
AD-A217882 ..... N90-20053 #
AD-A217887 ..... N90-20623 #
AD-A217889 ..... N90-20346 #
AD-A217894 ..... N90-20574 #
AD-A217896 ..... N90-20624 #
AD-A217897 ..... N90-20625 #
AD-A217899 ..... N90-20626 #
AD-A217907 ..... N90-20627 #
AD-A217908 ..... N90-20276 #
AD-A217910 ..... N90-20385 #
AD-A217920 ..... N90-20837 #
AD-A217924 ..... N90-20717 #
AD-A217925 ..... N90-20074 #
AD-A217936 ..... N90-20718 #
AD-A217939 ..... N90-20797 #
AD-A217940 ..... N90-20791 #
AD-A217947 ..... N90-20719 #
AD-A217950 ..... N90-20591 #
AD-A217952 ..... N90-20592 #
AD-A217953 ..... N90-20892 #
AD-A217957 ..... N90-20177 #
AD-A217961 ..... N90-20311 #
AD-A217962 ..... N90-20628 #
AD-A217964 ..... N90-20312 #
AD-A217965 ..... N90-20770 #
AD-A217969 ..... N90-20629 #
AD-A217972 ..... N90-20313 #
AD-A217976 ..... N90-20314 #
AD-A217978 ..... N90-20575 #
AD-A217980 ..... N90-20720 #
AD-A217981 ..... N90-20095 #
AD-A217986 ..... N90-20893 #
AD-A217987 ..... N90-20894 #
AD-A217989 ..... N90-20792 #
AD-A217993 ..... N90-20347 #
AD-A217997 ..... N90-20315 #
AD-A218003 ..... N90-20816 #
AD-A218013 ..... N90-20228 #
AD-A218015 ..... N90-20386 #
AD-A218017 ..... N90-20593 #

AD-A218018 ..... N90-20798 #
AD-A218019 ..... N90-20576 #
AD-A218020 ..... N90-20348 #
AD-A218024 ..... N90-20630 #
AD-A218025 ..... N90-20913 #
AD-A218027 ..... N90-20721 #
AD-A218035 ..... N90-20069 #
AD-A218041 ..... N90-20799 #
AD-A218048 ..... N90-20800 #
AD-A218052 ..... N90-20098 #
AD-A218057 ..... N90-20577 #
AD-A218064 ..... N90-20722 #
AD-A218066 ..... N90-20771 #
AD-A218069 ..... N90-20642 #
AD-A218070 ..... N90-20277 #
AD-A218075 ..... N90-20405 #
AD-A218077 ..... N90-20362 #
AD-A218079 ..... N90-20124 #
AD-A218080 ..... N90-20453 #
AD-A218088 ..... N90-20838 #
AD-A218089 ..... N90-20153 #
AD-A218093 ..... N90-20229 #
AD-A218096 ..... N90-20316 #
AD-A218097 ..... N90-20772 #
AD-A218098 ..... N90-20631 #
AD-A218103 ..... N90-20594 #
AD-A218105 ..... N90-20099 #
AD-A218106 ..... N90-20178 #
AD-A218107 ..... N90-20748 #
AD-A218115 ..... N90-20903 #
AD-A218116 ..... N90-20917 #
AD-A218119 ..... N90-20649 #
AD-A218120 ..... N90-20595 #
AD-A218121 ..... N90-20578 #
AD-A218124 ..... N90-20908 #
AD-A218141 ..... N90-20317 #
AD-A218143 ..... N90-20749 #
AD-A218145 ..... N90-20817 #
AD-A218146 ..... N90-20773 #
AD-A218148 ..... N90-20774 #
AD-A218149 ..... N90-20208 #
AD-A218157 ..... N90-20103 #
AD-A218162 ..... N90-20909 #
AD-A218163 ..... N90-20818 #
AD-A218165 ..... N90-20596 #
AD-A218168 ..... N90-20750 #
AD-A218170 ..... N90-20751 #
AD-A218174 ..... N90-20597 #
AD-A218175 ..... N90-20598 #
AD-A218180 ..... N90-20599 #
AD-A218183 ..... N90-20632 #
AD-A218184 ..... N90-20607 #
AD-A218192 ..... N90-20615 #
AD-A218195 ..... N90-20633 #
AD-A218202 ..... N90-20579 #
AD-A218203 ..... N90-20318 #
AD-A218207 ..... N90-20839 #
AD-A218208 ..... N90-20723 #
AD-A218211 ..... N90-20895 #
AD-A218212 ..... N90-20276 #
AD-A218214 ..... N90-20634 #
AD-A218215 ..... N90-20387 #
AD-A218218 ..... N90-20752 #
AD-A218219 ..... N90-20724 #
AD-A218220 ..... N90-20725 #
AD-A218224 ..... N90-20635 #
AD-A218233 ..... N90-20643 #
AD-A218234 ..... N90-20230 #
AD-A218236 ..... N90-20279 #
AD-A218244 ..... N90-20075 #
AD-A218249 ..... N90-20179 #
AD-A218253 ..... N90-20076 #
AD-A218262 ..... N90-20636 #
AD-A218268 ..... N90-20644 #
AD-A218271 ..... N90-20104 #
AD-A218272 ..... N90-20775 #
AD-A218273 ..... N90-20600 #
AD-A218276 ..... N90-20726 #
AD-A218277 ..... N90-20601 #
AD-A218280 ..... N90-20727 #
AD-A218282 ..... N90-20077 #
AD-A218284 ..... N90-20602 #
AD-A218285 ..... N90-20580 #
AD-A218286 ..... N90-20581 #
AD-A218287 ..... N90-20262 #
AD-A218298 ..... N90-20349 #
AD-A218312 ..... N90-20603 #
AD-A218316 ..... N90-20637 #
AD-A218321 ..... N90-20741 #
AD-A218325 ..... N90-20604 #
AD-A218330 ..... N90-20231 #
AD-A218331 ..... N90-20232 #
AD-A218336 ..... N90-20787 #
AD-A218337 ..... N90-20776 #
AD-A218338 ..... N90-20779 #
AD-A218339 ..... N90-20777 #
AD-A218340 ..... N90-20417 #
AD-A218344 ..... N90-20605 #
AD-A218345 ..... N90-20125 #
AD-A218347 ..... N90-20233 #
AD-A218349 ..... N90-20100 #
AD-A218353 ..... N90-20319 #
AD-A218366 ..... N90-20406 #
AD-A218367 ..... N90-20407 #

AD-D014317 ..... N90-20685

AD-E501189 ..... N90-20783 #
AD-E501190 ..... N90-20145 #
AD-E501190 ..... N90-20295 #
AD-E501190 ..... N90-20784 #
AD-E501191 ..... N90-20075 #
AD-E501191 ..... N90-20230 #
AD-E501191 ..... N90-20279 #
AD-E501191 ..... N90-20643 #

AEDC-TSR-89-V25 ..... N90-20331 #

AERE-M-3759 ..... N90-20185 #

AERE-R-12898 ..... N90-20424 #
AERE-R-13005 ..... N90-20423 #
AERE-R-13012 ..... N90-20425 #
AERE-R-13286 ..... N90-20209 #
AERE-R-13330 ..... N90-20134 #
AERE-R-13334 ..... N90-20410 #
AERE-R-13348 ..... N90-20190 #
AERE-R-13350 ..... N90-20411 #
AERE-R-13361 ..... N90-20193 #
AERE-R-13440 ..... N90-20192 #
AERE-R-13464 ..... N90-20189 #
AERE-R-13518 ..... N90-20187 #
AERE-R-13524 ..... N90-20191 #
AERE-R-13544 ..... N90-20862 #
AERE-R-13548 ..... N90-20182 #
AERE-R-13557 ..... N90-20861 #
AERE-R-13559 ..... N90-20188 #
AERE-R-13591 ..... N90-20184 #
AERE-R-13599 ..... N90-20183 #
AERE-R-13651 ..... N90-20186 #
AERE-R-13661 ..... N90-20860 #
AERE-R-13662 ..... N90-20801 #

AFGL-TR-89-0044 ..... N90-20595 #
AFGL-TR-89-0070 ..... N90-20578 #
AFGL-TR-89-0290 ..... N90-20839 #

AFHRL-TP-89-5 ..... N90-20642 #

AFIT/CI/CIA-88-227 ..... N90-20433 #
AFIT/CI/CIA-89-018 ..... N90-20599 #
AFIT/CI/CIA-89-023 ..... N90-20179 #
AFIT/CI/CIA-89-024 ..... N90-20592 #
AFIT/CI/CIA-89-025 ..... N90-20177 #
AFIT/CI/CIA-89-026 ..... N90-20178 #
AFIT/CI/CIA-89-028 ..... N90-20717 #
AFIT/CI/CIA-89-031 ..... N90-20568 #
AFIT/CI/CIA-89-035 ..... N90-20586 #
AFIT/CI/CIA-89-036 ..... N90-20272 #
AFIT/CI/CIA-89-037 ..... N90-20590 #
AFIT/CI/CIA-89-039 ..... N90-20276 #
AFIT/CI/CIA-89-041 ..... N90-20741 #
AFIT/CI/CIA-89-049 ..... N90-20601 #
AFIT/CI/CIA-89-050 ..... N90-20349 #
AFIT/CI/CIA-89-052 ..... N90-20598 #
AFIT/CI/CIA-89-060 ..... N90-20597 #
AFIT/CI/CIA-89-063 ..... N90-20600 #
AFIT/CI/CIA-89-064 ..... N90-20580 #
AFIT/CI/CIA-89-066 ..... N90-20603 #
AFIT/CI/CIA-89-068 ..... N90-20605 #
AFIT/CI/CIA-89-070 ..... N90-20125 #
AFIT/CI/CIA-89-073 ..... N90-20581 #
AFIT/CI/CIA-89-075 ..... N90-20604 #
AFIT/CI/CIA-89-076 ..... N90-20727 #
AFIT/CI/CIA-89-077 ..... N90-20726 #
AFIT/CI/CIA-89-081 ..... N90-20750 #
AFIT/CI/CIA-89-083 ..... N90-20818 #
AFIT/CI/CIA-89-085 ..... N90-20602 #
AFIT/CI/CIA-89-087 ..... N90-20596 #
AFIT/CI/CIA-89-096 ..... N90-20104 #
AFIT/CI/CIA-89-099 ..... N90-20892 #
AFIT/CI/CIA-89-101 ..... N90-20899 #
AFIT/CI/CIA-89-102 ..... N90-20313 #
AFIT/CI/CIA-89-104 ..... N90-20099 #
AFIT/CI/CIA-89-105 ..... N90-20074 #
AFIT/CI/CIA-89-107 ..... N90-20089 #
AFIT/CI/CIA-89-108 ..... N90-20775 #
AFIT/CI/CIA-89-111 ..... N90-20434 #
AFIT/CI/CIA-89-122 ..... N90-20591 #
AFIT/CI/CIA-89-124 ..... N90-20721 #
AFIT/CI/CIA-89-128 ..... N90-20644 #
AFIT/CI/CIA-89-138D ..... N90-20310 #
AFIT/CI/CIA-89-144 ..... N90-20577 #
AFIT/CI/CIA-89-148 ..... N90-20075 #
AFIT/CI/CIA-89-149 ..... N90-20346 #
AFIT/CI/CIA-89-152 ..... N90-20816 #
AFIT/CI/CIA-89-154 ..... N90-20627 #
AFIT/CI/CIA-89-155 ..... N90-20913 #
AFIT/CI/CIA-89-157 ..... N90-20903 #
AFIT/CI/CIA-89-158 ..... N90-20630 #
AFIT/CI/CIA-89-166 ..... N90-20632 #
AFIT/CI/CIA-89-172 ..... N90-20594 #
AFIT/CI/CIA-89-178 ..... N90-20262 #
AFIT/CI/CIA-89-180 ..... N90-20909 #
AFIT/CI/CIA-89-186 ..... N90-20100 #

AFIT/GAE/ENY/89D-01 ..... N90-20073 #

AFIT/GIR/LSR/89D-5 ..... N90-20908 #

AFOSR-89-1689TR ..... N90-20760 #
AFOSR-90-0001TR ..... N90-20343 #
AFOSR-90-0002TR ..... N90-20415 #
AFOSR-90-0003TR ..... N90-20814 #
AFOSR-90-0004TR ..... N90-20174 #
AFOSR-90-0011TR ..... N90-20361 #
AFOSR-90-0012TR ..... N90-20309 #
AFOSR-90-0013TR ..... N90-20227 #
AFOSR-90-0035TR ..... N90-20123 #
AFOSR-90-0049TR ..... N90-20386 #
AFOSR-90-0050TR ..... N90-20053 #
AFOSR-90-0058TR ..... N90-20778 #
AFOSR-90-0065TR ..... N90-20656 #
AFOSR-90-0070TR ..... N90-20714 #
AFOSR-90-0072TR ..... N90-20791 #
AFOSR-90-0073TR ..... N90-20632 #
AFOSR-90-0074TR ..... N90-20345 #
AFOSR-90-0075TR ..... N90-20692 #
AFOSR-90-0076TR ..... N90-20747 #
AFOSR-90-0077TR ..... N90-20715 #
AFOSR-90-0078TR ..... N90-20341 #
AFOSR-90-0079TR ..... N90-20342 #
AFOSR-90-0081TR ..... N90-20815 #
AFOSR-90-0084TR ..... N90-20175 #
AFOSR-90-0087TR ..... N90-20176 #
AFOSR-90-0088TR ..... N90-20441 #
AFOSR-90-0106TR ..... N90-20101 #
AFOSR-90-0116TR ..... N90-20159 #
AFOSR-90-0117TR ..... N90-20761 #
AFOSR-90-0118TR ..... N90-20416 #
AFOSR-90-0119TR ..... N90-20716 #
AFOSR-90-0120TR ..... N90-20813 #
AFOSR-90-0121TR ..... N90-20805 #
AFOSR-90-0122TR ..... N90-20160 #
AFOSR-90-0124TR ..... N90-20452 #
AFOSR-90-0125TR ..... N90-20383 #
AFOSR-90-0126TR ..... N90-20132 #
AFOSR-90-0236TR ..... N90-20231 #
AFOSR-90-0240TR ..... N90-20232 #
AFOSR-90-0268TR ..... N90-20417 #
AFOSR-90-0276TR ..... N90-20779 #
AFOSR-90-0277TR ..... N90-20777 #
AFOSR-90-0280TR ..... N90-20776 #

AGARD-CP-472 ..... N90-20054 #

AI-M-1082 ..... N90-20725 #
AI-M-1156 ..... N90-20724 #
AI-M-1184 ..... N90-20751 #
AI-M-1186 ..... N90-20752 #

AIAA-90-0283 ..... N90-20794* #

AL-TR-89-051 ..... N90-20812 #

ALLISON-EDR-14074 ..... N90-20091 #

ANL-89/23 ..... N90-20258 #
ANL-89/43 ..... N90-20709 #

ANL/ESD/TM-2 ..... N90-20394 #

ANL/PPRNT-90-204 ..... N90-20888 #

ARFSD-TR-89021 ..... N90-20105 #

ARI-RR-750 ..... N90-20214 #

ARINC-4247-01-01-5032 ..... N90-20120* #

ARL-FLIGHT-MECH-TM-412 ..... N90-20098 #

ARL-PROP-TM-464 ..... N90-20406 #
ARL-PROP-TM-468 ..... N90-20407 #

ARO-21684.204-EL-AI ..... N90-20743 #
ARO-22678.3-MS ..... N90-20217 #
ARO-23359.1-MS ..... N90-20157 #

ARO-23791.2-MS-F ..... N90-20226 #
ARO-23909.4-GS ..... N90-20831 #
ARO-24001.6-PH ..... N90-20288 #
ARO-24025.12-EG ..... N90-20048 #
ARO-24369.39-MA-SDI ..... N90-20731 #
ARO-24370.41-MA ..... N90-20265 #
ARO-24804.26-MS ..... N90-20144 #
ARO-25045.32-EL ..... N90-20835 #
ARO-25047.1-MS ..... N90-20790 #
ARO-25173.23-EL ..... N90-20697 #
ARO-26051-EL ..... N90-20894 #
ARO-26304.1-EL-CF-VOL-1039 ..... N90-20291 #
ARO-26588.1-EG-CF ..... N90-20140 #
ARO-26792.1-MA-SDI ..... N90-20698 #
ARO-26792.2-MA-SDI ..... N90-20757 #
ARO-26911.1-EL-CF ..... N90-20867 #
ARO-237781.1-MA-F ..... N30-20688 #

ASQBG-A-89-010 ..... N90-20266 #

ASQBG-I-89-013 ..... N90-20889 #

ATR-89(4785)-1 ..... N90-20344 #

BNL-42102 ..... N90-20509 #
BNL-43006 ..... N90-20857 #
BNL-43358 ..... N90-20210 #
BNL-43772 ..... N90-20218 #
BNL-43791 ..... N90-20807 #
BNL-43851 ..... N90-20870 #
BNL-43876 ..... N90-20150 #

CD-TR-89-003 ..... N90-20812 #

CERAMATEC-90610/55001 ..... N90-20497 #

CESAR-89/41 ..... N90-20395 #

CIM-48 ..... N90-20449 #

CMU-RI-TR-88-7 ..... N90-20388 #

CONF-890142-6 ..... N90-20885 #
CONF-890201-2 ..... N90-20170 #
CONF-890718-34 ..... N90-20883 #
CONF-890718-35 ..... N90-20884 #
CONF-891053-18 ..... N90-20510 #
CONF-891087-14 ..... N90-20691 #
CONF-891093-26 ..... N90-20205 #
CONF-891103-67 ..... N90-20808 #
CONF-891119-37 ..... N90-20857 #
CONF-891119-91 ..... N90-20858 #
CONF-891119-102 ..... N90-20164 #
CONF-891119-103 ..... N90-20873 #
CONF-891119-104 ..... N90-20872 #
CONF-891119-107 ..... N90-20149 #
CONF-891119-112 ..... N90-20225 #
CONF-891119-113 ..... N90-20172 #
CONF-891182-3 ..... N90-20847 #
CONF-891205-4 ..... N90-20299 #
CONF-891240-6 ..... N90-20843 #
CONF-891261-8 ..... N90-20365 #
CONF-891276-5 ..... N90-20357* #
CONF-891276-6 ..... N90-20360 #
CONF-891278-1 ..... N90-20916 #
CONF-891281-1 ..... N90-20906 #
CONF-891282-1 ..... N90-20710 #
CONF-900136-8 ..... N90-20492 #
CONF-900140-12-REV-1 ..... N90-20376 #
CONF-900140-13 ..... N90-20374 #
CONF-900140-14 ..... N90-20305 #
CONF-900143-23 ..... N90-20283 #
CONF-900147-2 ..... N90-20819 #
CONF-900174-1-VUGRAPHS ..... N90-20848 #
CONF-900176-1 ..... N90-20765 #
CONF-900178-1 ..... N90-20379 #
CONF-900178-2 ..... N90-20849 #
CONF-900179-1 ..... N90-20823 #
CONF-900206-4 ..... N90-20203 #
CONF-900206-5 ..... N90-20303 #
CONF-900210-23 ..... N90-20162 #
CONF-900210-29 ..... N90-20511 #
CONF-900264-3 ..... N90-20855 #
CONF-900271-2 ..... N90-20206 #
CONF-900280-2 ..... N90-20300 #
CONF-900285-1 ..... N90-20833 #
CONF-900285-2 ..... N90-20171 #
CONF-900287-1 ..... N90-20887 #
CONF-900288-4 ..... N90-20846 #
CONF-900290-2 ..... N90-20746 #
CONF-900377-2 ..... N90-20485 #
CONF-900377-3 ..... N90-20494 #
CONF-900393-2 ..... N90-20224 #
CONF-900403-4 ..... N90-20210 #
CONF-900406-36 ..... N90-20570 #
CONF-900418-8 ..... N90-20711 #
CONF-900419-2 ..... N90-20204 #
CONF-900530-1 ..... N90-20369 #
CONF-900530-2 ..... N90-20370 #
CONF-900530-4 ..... N90-20371 #
CONF-900530-5 ..... N90-20372 #
CONF-900530-6 ..... N90-20373 #
CONF-900530-7 ..... N90-20807 #
CONF-900530-8 ..... N90-20378 #
CONF-900559-1 ..... N90-20399 #
CONF-900559-2 ..... N90-20435 #
CONF-900559-3 ..... N90-20398 #
CONF-900559-4 ..... N90-20354 #
CONF-900559-5 ..... N90-20395 #
CONF-900559-6 ..... N90-20745 #
CONF-900559-7 ..... N90-20396 #
CONF-900559-8 ..... N90-20397 #
CONF-900559-9 ..... N90-20402 #
CONF-900559-10 ..... N90-20403 #
CONF-900559-12 ..... N90-20404 #
CONF-900562-1 ..... N90-20878 #
CONF-900562-2 ..... N90-20167 #
CONF-900566-1 ..... N90-20413 #
CONF-900580-1 ..... N90-20414 #
CONF-900580-2 ..... N90-20907 #
CONF-900588-1 ..... N90-20401 #
CONF-900588-2 ..... N90-20400 #
CONF-900597-1 ..... N90-20703 #
CONF-900598-1 ..... N90-20879 #
CONF-900599-1 ..... N90-20296 #
CONF-900599-3 ..... N90-20111 #
CONF-8806460-1 ..... N90-20509 #
CONF-8902142 ..... N90-20508 #
CONF-8902158-1 ..... N90-20505 #
CONF-8903169-3 ..... N90-20762 #
CONF-8905179-3 ..... N90-20201 #
CONF-8906270-2 ..... N90-20763 #
CONF-8908158-3 ..... N90-20336 #
CONF-8909113-7 ..... N90-20234 #
CONF-8909210-9 ..... N90-20810 #
CONF-8909297-1 ..... N90-20915 #
CONF-8909307-1 ..... N90-20870 #
CONF-8909308-1 ..... N90-20589 #
CONF-8910107-10 ..... N90-20304 #
CONF-8910107-11 ..... N90-20306 #
CONF-8910120-7 ..... N90-20859 #
CONF-8910120-8 ..... N90-20875 #
CONF-8910197-3 ..... N90-20375 #
CONF-8910302-1 ..... N90-20148 #
CONF-8910338-2 ..... N90-20588 #
CONF-8910350-2 ..... N90-20863 #
CONF-8910365-1 ..... N90-20834 #
CONF-8910366-1 ..... N90-20704 #
CONF-8910372 ..... N90-20709 #
CONF-8911130-5 ..... N90-20841 #
CONF-8911164-2 ..... N90-20897 #
CONF-8911168-1 ..... N90-20218 #
CONF-8911171-1 ..... N90-20168 #
CONF-8911172-1 ..... N90-20809 #
CONF-9003106-1 ..... N90-20359 #
CONF-9003111-1 ..... N90-20207 #
CONF-9004136-4 ..... N90-20106 #
CONF-9004136-5 ..... N90-20107 #
CONF-9004136-6 ..... N90-20108 #
CONF-9004138-2 ..... N90-20736 #
CONF-9004139-1 ..... N90-20197 #
CONF-9004140-1 ..... N90-20355 #
CONF-9004144-1 ..... N90-20737 #
CONF-9004147-1 ..... N90-20259 #
CONF-9004148-1 ..... N90-20707 #
CONF-9005105-4 ..... N90-20735 #
CONF-9005107-1 ..... N90-20221 #
CONF-9005108-1 ..... N90-20334 #
CONF-9005116-1 ..... N90-20268 #
CONF-9005118-1 ..... N90-20436 #
CONF-9005122-1 ..... N90-20437 #
CONF-9005133-1 ..... N90-20150 #

CRAD-2/89 ..... N90-20319 #

CRDEC-CR-058 ..... N90-20330 #

CRDEC-TR-067 ..... N90-20315 #

CRM-89-292 ..... N90-20700 #

CRREL-89-21 ..... N90-20097 #

CS-TR-189-88 ..... N90-20693 #
CS-TR-223-89 ..... N90-20728 #
CS-TR-228-89 ..... N90-20754 #

CSDL-T-1010 ..... N90-20433 #

CSG-121 ..... N90-20686* #

CTD-90/022 ..... N90-20270* #
CTN-89-007 ..... N90-20904 #

DC-115 ..... N90-20744 #

DCIEM-89-RR-47 ..... N90-20623 #
DCIEM-89-RR-48 ..... N90-20619 #
DCIEM-89-RR-50 ..... N90-20618 #

DE89-009447 ..... N90-20571 #
DE89-009473 ..... N90-20486 #
DE89-009475 ..... N90-20487 #
DE89-009479 ..... N90-20491 #
DE89-009487 ..... N90-20488 #
DE89-009493 ..... N90-20608 #
DE89-009503 ..... N90-20489 #
DE89-009512 ..... N90-20492 #
DE90-000300 ..... N90-20220 #
DE90-000315 ..... N90-20493 #
DE90-000317 ..... N90-20111 #
DE90-000443 ..... N90-20484 #
DE90-001678 ..... N90-20354 #
DE90-001731 ..... N90-20395 #
DE90-001952 ..... N90-20396 #
DE90-001953 ..... N90-20397 #
DE90-002101 ..... N90-20745 #
DE90-002238 ..... N90-20398 #
DE90-002313 ..... N90-20435 #
DE90-002585 ..... N90-20399 #
DE90-003220 ..... N90-20841 #
DE90-003687 ..... N90-20413 #
DE90-003957 ..... N90-20857 #
DE90-004186 ..... N90-20210 #
DE90-004655 ..... N90-20414 #
DE90-004841 ..... N90-20369 #
DE90-004936 ..... N90-20167 #
DE90-004969 ..... N90-20845 #
DE90-005196 ..... N90-20370 #
DE90-005593 ..... N90-20878 #
DE90-005632 ..... N90-20400 #
DE90-005633 ..... N90-20703 #
DE90-005685 ..... N90-20401 #
DE90-006020 ..... N90-20879 #
DE90-006183 ..... N90-20296 #
DE90-006366 ..... N90-20285 #
DE90-006453 ..... N90-20915 #
DE90-006528 ..... N90-20218 #
DE90-006535 ..... N90-20221 #
DE90-006537 ..... N90-20334 #
DE90-006569 ..... N90-20858 #
DE90-006620 ..... N90-20843 #
DE90-006721 ..... N90-20450 #
DE90-006772 ..... N90-20268 #
DE90-006811 ..... N90-20859 #
DE90-006991 ..... N90-20833 #
DE90-006995 ..... N90-20371 #
DE90-007013 ..... N90-20303 #
DE90-007018 ..... N90-20170 #
DE90-007088 ..... N90-20844 #
DE90-007160 ..... N90-20339 #
DE90-007178 ..... N90-20802 #
DE90-007184 ..... N90-20501 #
DE90-007216 ..... N90-20402 #
DE90-007257 ..... N90-20735 #
DE90-007260 ..... N90-20372 #
DE90-007261 ..... N90-20373 #
DE90-007293 ..... N90-20502 #
DE90-007348 ..... N90-20789 #
DE90-007425 ..... N90-20332 #
DE90-007479 ..... N90-20846 #
DE90-007481 ..... N90-20819 #
DE90-007483 ..... N90-20746 #
DE90-007485 ..... N90-20736 #
DE90-007497 ..... N90-20436 #
DE90-007507 ..... N90-20847 #
DE90-007509 ..... N90-20485 #
DE90-007523 ..... N90-20869 #
DE90-007528 ..... N90-20887 #
DE90-007534 ..... N90-20168 #
DE90-007540 ..... N90-20834 #
DE90-007545 ..... N90-20365 #
DE90-007547 ..... N90-20809 #
DE90-007555 ..... N90-20806 #
DE90-007560 ..... N90-20610 #
DE90-007565 ..... N90-20503 #
DE90-007575 ..... N90-20848 #
DE90-007576 ..... N90-20355 #
DE90-007607 ..... N90-20161 #
DE90-007622 ..... N90-20374 #
DE90-007623 ..... N90-20849 #
DE90-007624 ..... N90-20916 #
DE90-007626 ..... N90-20379 #
DE90-007627 ..... N90-20870 #
DE90-007653 ..... N90-20106 #
DE90-007658 ..... N90-20375 #
DE90-007676 ..... N90-20807 #
DE90-007677 ..... N90-20107 #

DE90-007680 ..... N90-20494 #
DE90-007683 ..... N90-20234 #
DE90-007685 ..... N90-20162 #
DE90-007687 ..... N90-20403 #
DE90-007693 ..... N90-20163 #
DE90-007694 ..... N90-20697 #
DE90-007696 ..... N90-20702 #
DE90-007754 ..... N90-20671 #
DE90-007759 ..... N90-20570 #
DE90-007761 ..... N90-20872 #
DE90-007764 ..... N90-20197 #
DE90-007767 ..... N90-20873 #
DE90-007778 ..... N90-20147 #
DE90-007779 ..... N90-20164 #
DE90-007782 ..... N90-20874 #
DE90-007803 ..... N90-20201 #
DE90-007820 ..... N90-20108 #
DE90-007821 ..... N90-20875 #
DE90-007836 ..... N90-20283 #
DE90-007849 ..... N90-20376 #
DE90-007854 ..... N90-20704 #
DE90-007857 ..... N90-20762 #
DE90-007858 ..... N90-20705 #
DE90-007880 ..... N90-20196 #
DE90-007889 ..... N90-20863 #
DE90-007996 ..... N90-20297 #
DE90-007997 ..... N90-20495 #
DE90-008005 ..... N90-20335 #
DE90-008015 ..... N90-20440 #
DE90-008016 ..... N90-20785 #
DE90-008020 ..... N90-20850 #
DE90-008028 ..... N90-20786 #
DE90-008029 ..... N90-20506 #
DE90-008040 ..... N90-20490 #
DE90-008042 ..... N90-20269 #
DE90-008043 ..... N90-20880 #
DE90-008044 ..... N90-20412 #
DE90-008047 ..... N90-20148 #
DE90-008049 ..... N90-20620 #
DE90-008054 ..... N90-20165 #
DE90-008061 ..... N90-20611 #
DE90-008069 ..... N90-20202 #
DE90-008072 ..... N90-20706 #
DE90-008075 ..... N90-20508 #
DE90-008077 ..... N90-20851 #
DE90-008082 ..... N90-20765 #
DE90-008090 ..... N90-20298 #
DE90-008093 ..... N90-20258 #
DE90-008095 ..... N90-20394 #
DE90-008108 ..... N90-20504 #
DE90-008119 ..... N90-20904 #
DE90-008122 ..... N90-20257 #
DE90-008130 ..... N90-20199 #
DE90-008136 ..... N90-20166 #
DE90-008140 ..... N90-20505 #
DE90-008163 ..... N90-20738 #
DE90-008165 ..... N90-20739 #
DE90-008166 ..... N90-20740 #
DE90-008169 ..... N90-20131 #
DE90-008246 ..... N90-20906 #
DE90-008249 ..... N90-20881 #
DE90-008250 ..... N90-20882 #
DE90-008252 ..... N90-20852 #
DE90-008253 ..... N90-20222 #
DE90-008272 ..... N90-20820 #
DE90-008273 ..... N90-20377 #
DE90-008281 ..... N90-20109 #
DE90-008292 ..... N90-20690 #
DE90-008301 ..... N90-20336 #
DE90-008302 ..... N90-20299 #
DE90-008303 ..... N90-20300 #
DE90-008306 ..... N90-20203 #
DE90-008307 ..... N90-20204 #
DE90-008308 ..... N90-20437 #
DE90-008309 ..... N90-20359 #
DE90-008314 ..... N90-20621 #
DE90-008322 ..... N90-20205 #
DE90-008324 ..... N90-20691 #
DE90-008325 ..... N90-20589 #
DE90-008326 ..... N90-20821 #
DE90-008329 ..... N90-20223 #
DE90-008330 ..... N90-20129 #
DE90-008343 ..... N90-20709 #
DE90-008348 ..... N90-20822 #
DE90-008349 ..... N90-20169 #
DE90-008352 ..... N90-20808 #
DE90-008354 ..... N90-20883 #
DE90-008361 ..... N90-20884 #
DE90-008363 ..... N90-20378 #
DE90-008366 ..... N90-20885 #
DE90-008390 ..... N90-20206 #
DE90-008403 ..... N90-20763 #
DE90-008409 ..... N90-20149 #
DE90-008415 ..... N90-20586 #
DE90-008424 ..... N90-20219 #
DE90-008428 ..... N90-20876 #
DE90-008429 ..... N90-20766 #
DE90-008430 ..... N90-20877 #
DE90-008439 ..... N90-20606 #
DE90-008440 ..... N90-20905 #
DE90-008444 ..... N90-20356 #
DE90-008446 ..... N90-20507 #
DE90-008497 ..... N90-20737 #
DE90-008501 ..... N90-20707 #
DE90-008503 ..... N90-20259 #
DE90-008518 ..... N90-20509 #
DE90-008526 ..... N90-20853 #
DE90-008527 ..... N90-20304 #
DE90-008529 ..... N90-20710 #
DE90-008539 ..... N90-20305 #
DE90-008542 ..... N90-20823 #
DE90-008545 ..... N90-20171 #
DE90-008547 ..... N90-20360 #
DE90-008548 ..... N90-20907 #
DE90-008558 ..... N90-20810 #
DE90-008565 ..... N90-20207 #
DE90-008575 ..... N90-20150 #
DE90-008599 ..... N90-20225 #
DE90-008607 ..... N90-20510 #
DE90-008622 ..... N90-20511 #
DE90-008633 ..... N90-20172 #
DE90-008640 ..... N90-20512 #
DE90-008642 ..... N90-20380 #
DE90-008647 ..... N90-20381 #
DE90-008648 ..... N90-20612 #
DE90-008660 ..... N90-20824 #
DE90-008663 ..... N90-20854 #
DE90-008665 ..... N90-20306 #
DE90-008667 ..... N90-20496 #
DE90-008668 ..... N90-20811 #
DE90-008683 ..... N90-20382 #
DE90-008687 ..... N90-20260 #
DE90-008688 ..... N90-20261 #
DE90-008699 ..... N90-20173 #
DE90-008707 ..... N90-20888 #
DE90-008724 ..... N90-20711 #
DE90-008733 ..... N90-20340 #
DE90-008751 ..... N90-20357* #
DE90-008753 ..... N90-20404 #
DE90-008758 ..... N90-20224 #
DE90-008787 ..... N90-20573 #
DE90-008799 ..... N90-20712 #
DE90-008812 ..... N90-20855 #
DE90-606958 ..... N90-20788 #
DE90-615185 ..... N90-20767 #
DE90-615205 ..... N90-20898 #
DE90-753026 ..... N90-20451 #

DFVLR-IB-333-89/3 ..... N90-20238 #

DNA-TR-89-150 ..... N90-20569 #

DODA-AR-005-629 ..... N90-20098 #
DODA-AR-005-643 ..... N90-20406 #
DODA-AR-006-058 ..... N90-20407 #

DOE/BP-1327 ..... N90-20507 #

DOE/CH-10093/58 ..... N90-20486 #
DOE/CH-10093/60 ..... N90-20487 #
DOE/CH-10093/64-VOL-1 ..... N90-20491 #
DOE/CH-10093/72 ..... N90-20488 #

DOE/DP-40200/120 ..... N90-20854 #

DOE/ER-0441 ..... N90-20504 #
DOE/ER-0447P ..... N90-20131 #
DOE/ER-10569/T5 ..... N90-20821 #
DOE/ER-13227/6 ..... N90-20380 #
DOE/ER-13405/T3 ..... N90-20381 #
DOE/ER-13441/6 ..... N90-20806 #
DOE/ER-13486/T1 ..... N90-20612 #
DOE/ER-13570/4 ..... N90-20869 #
DOE/ER-13937/2 ..... N90-20377 #
DOE/ER-14018/1 ..... N90-20163 #
DOE/ER-25015/29 ..... N90-20766 #
DOE/ER-25029/2 ..... N90-20690 #
DOE/ER-25063/2 ..... N90-20905 #
DOE/ER-40226/5 ..... N90-20802 #
DOE/ER-40272/94 ..... N90-20897 #
DOE/ER-40368/3 ..... N90-20820 #
DOE/ER-45061/6 ..... N90-20877 #
DOE/ER-45125/T2 ..... N90-20129 #
DOE/ER-45167/T1 ..... N90-20223 #
DOE/ER-45249/T1 ..... N90-20198 #
DOE/ER-45269/T1 ..... N90-20173 #
DOE/ER-45303/2 ..... N90-20219 #
DOE/ER-45310/20 ..... N90-20876 #
DOE/ER-45362/2 ..... N90-20881 #
DOE/ER-45396/1 ..... N90-20222 #
DOE/ER-45405/1 ..... N90-20882 #
DOE/ER-52111/T6 ..... N90-20109 #
DOE/ER-52158/1 ..... N90-20852 #
DOE/ER-60312/3 ..... N90-20501 #
DOE/ER-60348/12 ..... N90-20606 #
DOE/ER-60470/1 ..... N90-20450 #
DOE/ER-60512/3 ..... N90-20512 #
DOE/ER-60649/T2 ..... N90-20621 #
DOE/ER-60858/T1 ..... N90-20356 #
DOE/ER-60883/1 ..... N90-20503 #

DOE/ET-15601/35 ..... N90-20845 #
DOE/ET-53088/415 ..... N90-20844 #

DOE/MC-24222/2790 ..... N90-20484 #

DOE/NE-37944/1 ..... N90-20712 #

DOE/PC-88951/3 ..... N90-20332 #

DOE/PETC-TR/90/3 ..... N90-20339 #

DOE/SF-16496/T1 ..... N90-20824 #

DOT/FAA-CT-89/36-1 ..... N90-20081* #
DOT/FAA-CT-89/36-2 ..... N90-20080* #
DOT/FAA-CT-89/36-3 ..... N90-20082* #
DOT/FAA-CT-89/36-4 ..... N90-20083* #
DOT/FAA-CT-89/36-5 ..... N90-20084* #

DOT/FAA/CT-TN87/54-VOL-3 ..... N90-20500 #
DOT/FAA/CT-TN88/14 ..... N90-20072 #

DREO-TN-89-20 ..... N90-20294 #

DTRC-PAS-90/2 ..... N90-20797 #

DTRC/SME-CR-08-89 ..... N90-20212 #

DTRC/SME-89-67 ..... N90-20141 #
DTRC/SME-89-73 ..... N90-20142 #

E-4708 ..... N90-20454* #
E-4736 ..... N90-20264* #
E-4768 ..... N90-20392* #
E-5142 ..... N90-20181* #
E-5143 ..... N90-20432* #
E-5182 ..... N90-20138* #
E-5183 ..... N90-20901* #
E-5202 ..... N90-20338* #
E-5210 ..... N90-20794* #
E-5220 ..... N90-20194* #
E-5242 ..... N90-20708* #
E-5272 ..... N90-20085* #
E-5276 ..... N90-20428* #
E-5282 ..... N90-20237* #
E-5285 ..... N90-20286* #
E-5300 ..... N90-20391* #
E-5304 ..... N90-20352* #
E-5311 ..... N90-20431* #
E-5317 ..... N90-20353* #
E-5322 ..... N90-20090* #
E-5323 ..... N90-20769* #
E-5331 ..... N90-20326* #
E-5333 ..... N90-20337* #
E-5339 ..... N90-20253* #
E-5349 ..... N90-20139* #
E-5356 ..... N90-20393* #
E-5361 ..... N90-20130* #
E-5372 ..... N90-20438* #
E-5378 ..... N90-20151* #
E-5395 ..... N90-20886* #
E-5408 ..... N90-20301* #
E-5412 ..... N90-20358* #
E-5417 ..... N90-20110* #
E-5421 ..... N90-20051* #
E-5434 ..... N90-20302* #

EGG-M-88425 ..... N90-20170 #
EGG-M-89453 ..... N90-20303 #

EGG-10617-1066 ..... N90-20906 #
EGG-10617-2051 ..... N90-20357* #

ERIM-179100-40-F ..... N90-20748 #

ERP-1022 ..... N90-20595 #
ERP-1023 ..... N90-20578 #
ERP-1034 ..... N90-20917 #

ESD-TR-89-164 ..... N90-20290 #
ESD-TR-89-185 ..... N90-20828 #
ESD-TR-89-186 ..... N90-20759 #
ESD-TR-89-203 ..... N90-20585 #
ESD-TR-89-236 ..... N90-20758 #

ETN-90-95319 ..... N90-20902 #
ETN-90-95320 ..... N90-20499 #

ETN-90-95322 ..... N90-20803 #
ETN-90-95323 ..... N90-20825 #
ETN-90-95325 ..... N90-20364 #
ETN-90-95330 ..... N90-20155 #
ETN-90-95331 ..... N90-20804 #
ETN-90-95380 ..... N90-20195 #
ETN-90-95381 ..... N90-20695 #
ETN-90-95382 ..... N90-20429 #
ETN-90-95407 ..... N90-20696 #
ETN-90-95471 ..... N90-20067 #
ETN-90-95850 ..... N90-20238 #

FCPRL-8903 ..... N90-20109 #

FCR-10824 ..... N90-20498 #

FJSRL-TR-89-0010 ..... N90-20156 #

FNAL/C-90/40 ..... N90-20855 #

GEPP-TIS-1168 ..... N90-20412 #

GIT-85-019 ..... N90-20805 #

GL-AFSG-453 ..... N90-20574 #

GL-TR-89-0110 ..... N90-20838 #
GL-TR-89-0178 ..... N90-20917 #
GL-TR-89-0223 ..... N90-20574 #
GL-TR-89-0242 ..... N90-20723 #
GL-TR-89-0259 ..... N90-20579 #

GRI-89/0133 ..... N90-20483 #

GSJ-8902-270 ..... N90-20451 #

H-1542 ..... N90-20086* #

HDL-SR-89-4 ..... N90-20317 #

HDL-TR-2169 ..... N90-20891 #

HEL-TM-17-89 ..... N90-20095 #
HEL-TM-21-89 ..... N90-20646 #
HEL-TM-22-89 ..... N90-20720 #

HEL-TN-15-89 ..... N90-20648 #

IC-89/206 ..... N90-20788 #

ICASE-90-24 ..... N90-20764* #
ICASE-90-25 ..... N90-20650* #
ICASE-90-27 ..... N90-20768* #
ICASE-90-28 ..... N90-20049* #
ICASE-90-29 ..... N90-20050* #

ICMA-90-145 ..... N90-20770 #

ICOMP-90-01 ..... N90-20769* #
ICOMP-90-06 ..... N90-20326* #
ICOMP-90-07 ..... N90-20337* #

IDA-D-696 ..... N90-20145 #

IDA-M-513 ..... N90-20783 #

IDA/HQ-88-33759 ..... N90-20783 #
IDA/HQ-89-34967 ..... N90-20145 #

IFSR-415 ..... N90-20844 #

INPE-4746-RPE/580 ..... N90-20444 #
INPE-4761-TDL/349 ..... N90-20445 #
INPE-4859-TDL/370 ..... N90-20390 #
INPE-4874-PRE/1485 ..... N90-20442 #
INPE-4893-PRE/1494 ..... N90-20565 #
INPE-4949-RPE/598 ..... N90-20443 #
INPE-4964-TDL/392 ..... N90-20448 #
INPE-4969-RPE/604 ..... N90-20446 #
INPE-4980-RPE/606 ..... N90-20128 #
INPE-4984-TDL/394 ..... N90-20447 #

IPPCZ-290 ..... N90-20842 #

ISBN-0-8194-0074-2 ..... N90-20291 #
ISBN-1-55752-062-3 ..... N90-20832 #
ISBN-92-835-0539-5 ..... N90-20054 #

ISSN-0389-4010 ..... N90-20350 #
ISSN-0436-1199 ..... N90-20155 #
ISSN-0436-1199 ..... N90-20804 #

IZF-1989-32 ..... N90-20626 #

JA-1264-6 ..... N90-20112* #

JINR-R-2-88-851 ..... N90-20898 #
JINR-R-11-88-784 ..... N90-20767 #

JPL-PUBL-89-1 ..... N90-20281* #

K/CSD/INF-88/23 ..... N90-20340 #

K/CSD/TM-90 ..... N90-20335 #

KAPL-4713 ..... N90-20199 #

L-16441 ..... N90-20046* #

LA-UR-89-3720 ..... N90-20841 #
LA-UR-89-4110 ..... N90-20369 #
LA-UR-90-16 ..... N90-20283 #
LA-UR-90-112 ..... N90-20863 #
LA-UR-90-370 ..... N90-20809 #
LA-UR-90-413 ..... N90-20374 #
LA-UR-90-419 ..... N90-20849 #
LA-UR-90-432 ..... N90-20916 #
LA-UR-90-445 ..... N90-20379 #
LA-UR-90-449 ..... N90-20887 #
LA-UR-90-485 ..... N90-20168 #
LA-UR-90-537 ..... N90-20834 #
LA-UR-90-599 ..... N90-20365 #
LA-UR-90-650 ..... N90-20436 #
LA-UR-90-692 ..... N90-20847 #
LA-UR-90-698 ..... N90-20485 #

LA-11772-MS ..... N90-20702 #
LA-11774-MS ..... N90-20786 #
LA-11782-MS ..... N90-20785 #

LAIR-409 ..... N90-20614 #
LAIR-410 ..... N90-20613 #
LAIR-414 ..... N90-20609 #

LBL-PUB-3078 ..... N90-20871 #

LBL-27460 ..... N90-20611 #
LBL-27461 ..... N90-20873 #
LBL-27473 ..... N90-20165 #
LBL-27522 ..... N90-20872 #
LBL-27872 ..... N90-20508 #
LBL-27905 ..... N90-20148 #
LBL-27948 ..... N90-20706 #
LBL-27964 ..... N90-20306 #
LBL-28042 ..... N90-20610 #
LBL-28083 ..... N90-20496 #
LBL-28104 ..... N90-20811 #
LBL-28170 ..... N90-20789 #
LBL-28206 ..... N90-20164 #
LBL-28263 ..... N90-20147 #
LBL-28294 ..... N90-20197 #
LBL-28333 ..... N90-20570 #
LBL-28405 ..... N90-20206 #

LC-88-63146 ..... N90-20291 #

LIDS-P-1928 ..... N90-20274 #

LINO-1989-6 ..... N90-20696 #

LLNL-M-243-VOL-1 ..... N90-20260 #
LLNL-M-243-VOL-2 ..... N90-20261 #

LMSC/F186312/SSV-2167 ..... N90-20713* #

M-285 ..... N90-20705 #

MPIS-14/1988 ..... N90-20155 #
MPIS-19/1988 ..... N90-20804 #

MSFC-SPEC-1764-VOL-2 ..... N90-20114* #

MT-15/87 ..... N90-20364 #

MTL-TR-89-97 ..... N90-20196 #
MTL-TR-89-99 ..... N90-20152 #
MTL-TR-89-108 ..... N90-20792 #
MTL-TR-90-3 ..... N90-20890 #

MW-89-P-5 ..... N90-20835 #

NAE-AN-61 ..... N90-20575 #

NAL-TR-1017 ..... N90-20350 #

NAMRL-MONOGRAPH-39 ..... N90-20772 #

NAMRL-TM-89-3 ..... N90-20631 #

NAS 1.15:4191 ..... N90-20252* #
NAS 1.15:100038 ..... N90-20333* #
NAS 1.15:100390 ..... N90-20200* #

NAS 1.15:100392 ..... N90-20251* #
NAS 1.15:100729 ..... N90-20566* #
NAS 1.15:100730 ..... N90-20572* #
NAS 1.15:100754 ..... N90-20911* #
NAS 1.15:101453 ..... N90-20264* #
NAS 1.15:101689 ..... N90-20071* #
NAS 1.15:101696 ..... N90-20086* #
NAS 1.15:102158 ..... N90-20645* #
NAS 1.15:102231 ..... N90-20087* #
NAS 1.15:102271 ..... N90-20325* #
NAS 1.15:102403 ..... N90-20181* #
NAS 1.15:102417 ..... N90-20901* #
NAS 1.15:102440 ..... N90-20794* #
NAS 1.15:102445 ..... N90-20194* #
NAS 1.15:102454 ..... N90-20706* #
NAS 1.15:102482 ..... N90-20085* #
NAS 1.15:102494 ..... N90-20286* #
NAS 1.15:102503 ..... N90-20352* #
NAS 1.15:102509 ..... N90-20431* #
NAS 1.15:102514 ..... N90-20353* #
NAS 1.15:102515 ..... N90-20138* #
NAS 1.15:102518 ..... N90-20090* #
NAS 1.15:102519 ..... N90-20769* #
NAS 1.15:102524 ..... N90-20326* #
NAS 1.15:102525 ..... N90-20337* #
NAS 1.15:102529 ..... N90-20391* #
NAS 1.15:102530 ..... N90-20253* #
NAS 1.15:102532 ..... N90-20428* #
NAS 1.15:102536 ..... N90-20139* #
NAS 1.15:102537 ..... N90-20392* #
NAS 1.15:102544 ..... N90-20393* #
NAS 1.15:102549 ..... N90-20130* #
NAS 1.15:102556 ..... N90-20438* #
NAS 1.15:102558 ..... N90-20151* #
NAS 1.15:102566 ..... N90-20338* #
NAS 1.15:102567 ..... N90-20432* #
NAS 1.15:102571 ..... N90-20886* #
NAS 1.15:102577 ..... N90-20301* #
NAS 1.15:102581 ..... N90-20358* #
NAS 1.15:102590 ..... N90-20427* #
NAS 1.15:102595 ..... N90-20068* #
NAS 1.15:102596 ..... N90-20583* #
NAS 1.15:102604 ..... N90-20121* #
NAS 1.15:102606 ..... N90-20122* #
NAS 1.15:102611 ..... N90-20426* #
NAS 1.15:102617 ..... N90-20047* #
NAS 1.15:102618 ..... N90-20093* #
NAS 1.15:102621 ..... N90-20795* #
NAS 1.15:102625 ..... N90-20137* #
NAS 1.15:102965 ..... N90-20617* #
NAS 1.15:103096 ..... N90-20110* #
NAS 1.15:103100 ..... N90-20051* #
NAS 1.15:103110 ..... N90-20302* #
NAS 1.15:103318 ..... N90-20357* #
NAS 1.19:274 ..... N90-20900* #
NAS 1.26:4279 ..... N90-20422* #
NAS 1.26:180475 ..... N90-20582* #
NAS 1.26:180781 ..... N90-20713* #
NAS 1.26:181909-VOL-1 ..... N90-20081* #
NAS 1.26:181909-VOL-2 ..... N90-20080* #
NAS 1.26:181909-VOL-3 ..... N90-20082* #
NAS 1.26:181909-VOL-4 ..... N90-20083* #
NAS 1.26:181909-VOL-5 ..... N90-20084* #
NAS 1.26:181945 ..... N90-20088* #
NAS 1.26:181951 ..... N90-20421* #
NAS 1.26:181957 ..... N90-20430* #
NAS 1.26:181971 ..... N90-20112* #
NAS 1.26:181972 ..... N90-20694* #
NAS 1.26:181975 ..... N90-20439* #
NAS 1.26:182015 ..... N90-20764* #
NAS 1.26:182016 ..... N90-20650* #
NAS 1.26:182028 ..... N90-20768* #
NAS 1.26:182029 ..... N90-20049* #
NAS 1.26:182030 ..... N90-20050* #
NAS 1.26:183840 ..... N90-20113* #
NAS 1.26:183841 ..... N90-20114* #
NAS 1.26:183842 ..... N90-20115* #
NAS 1.26:183843 ..... N90-20116* #
NAS 1.26:183844 ..... N90-20117* #
NAS 1.26:183845 ..... N90-20118* #
NAS 1.26:183860 ..... N90-20127* #
NAS 1.26:185149 ..... N90-20270* #
NAS 1.26:185181 ..... N90-20120* #
NAS 1.26:185208 ..... N90-20237* #
NAS 1.26:185721 ..... N90-20513* #
NAS 1.26:185954 ..... N90-20281* #
NAS 1.26:186221 ..... N90-20263* #
NAS 1.26:186374 ..... N90-20914* #
NAS 1.26:186403 ..... N90-20324* #
NAS 1.26:186435 ..... N90-20052* #
NAS 1.26:186452 ..... N90-20686* #
NAS 1.26:186453 ..... N90-20136* #
NAS 1.26:186454 ..... N90-20135* #
NAS 1.26:186471 ..... N90-20918* #
NAS 1.26:186476 ..... N90-20284* #
NAS 1.26:186508 ..... N90-20271* #

NAS 1.55:3045 ..... N90-20651* #
NAS 1.55:3056 ..... N90-20454* #
NAS 1.60:2990 ..... N90-20046* #
NAS 1.61:1233-VOL-1 ..... N90-20562* #
NAS 1.61:1233-VOL-2 ..... N90-20563* #
NAS 1.61:1233-VOL-4 ..... N90-20564* #

NASA-CASE-ARC-11425-4 ..... N90-20133*

NASA-CASE-GSC-12442-2 ..... N90-20282*

NASA-CASE-KSC-11387-1 ..... N90-20236*

NASA-CASE-LAR-13273-2 ..... N90-20320*
NASA-CASE-LAR-13542-2-SB N90-20154*
NASA-CASE-LAR-13606-1 ..... N90-20409*
NASA-CASE-LAR-13734-1-CU N90-20096*
NASA-CASE-LAR-13741-1-SB N90-20180*
NASA-CASE-LAR-13761-1 ..... N90-20323*
NASA-CASE-LAR-13777-1 ..... N90-20078*
NASA-CASE-LAR-14031-1 ..... N90-20079*

NASA-CASE-MFS-25786-2 ..... N90-20696*
NASA-CASE-MFS-28234-1 ..... N90-20616*

NASA-CASE-MSC-18808-1 ..... N90-20280*
NASA-CASE-MSC-21253-1 ..... N90-20254*
NASA-CASE-MSC-21365-1 ..... N90-20408*
NASA-CASE-MSC-21366-1 ..... N90-20126*

NASA-CASE-NPO-16878-1-CU N90-20351*

NASA-CP-3045 ..... N90-20651* #
NASA-CP-3056 ..... N90-20454* #

NASA-CR-4279 ..... N90-20422* #
NASA-CR-180475 ..... N90-20582* #
NASA-CR-180781 ..... N90-20713* #
NASA-CR-181909-VOL-1 ..... N90-20081* #
NASA-CR-181909-VOL-2 ..... N90-20080* #
NASA-CR-181909-VOL-3 ..... N90-20082* #
NASA-CR-181909-VOL-4 ..... N90-20083* #
NASA-CR-181909-VOL-5 ..... N90-20084* #
NASA-CR-181945 ..... N90-20088* #
NASA-CR-181951 ..... N90-20421* #
NASA-CR-181957 ..... N90-20430* #
NASA-CR-181971 ..... N90-20112* #
NASA-CR-181972 ..... N90-20694* #
NASA-CR-181975 ..... N90-20439* #
NASA-CR-182015 ..... N90-20764* #
NASA-CR-182016 ..... N90-20650* #
NASA-CR-182028 ..... N90-20768* #
NASA-CR-182029 ..... N90-20049* #
NASA-CR-182030 ..... N90-20050* #
NASA-CR-183840 ..... N90-20113* #
NASA-CR-183841 ..... N90-20114* #
NASA-CR-183842 ..... N90-20115* #
NASA-CR-183843 ..... N90-20116* #
NASA-CR-183844 ..... N90-20117* #
NASA-CR-183845 ..... N90-20118* #
NASA-CR-183860 ..... N90-20127* #
NASA-CR-185149 ..... N90-20270* #
NASA-CR-185181 ..... N90-20120* #
NASA-CR-185208 ..... N90-20237* #
NASA-CR-185721 ..... N90-20513* #
NASA-CR-185954 ..... N90-20261* #
NASA-CR-186221 ..... N90-20263* #
NASA-CR-186374 ..... N90-20914* #
NASA-CR-186403 ..... N90-20324* #
NASA-CR-186435 ..... N90-20052* #
NASA-CR-186452 ..... N90-20686* #
NASA-CR-186453 ..... N90-20136* #
NASA-CR-186454 ..... N90-20135* #
NASA-CR-186471 ..... N90-20918* #
NASA-CR-186476 ..... N90-20284* #
NASA-CR-186508 ..... N90-20271* #

NASA-EP-274 ..... N90-20900* #

NASA-RP-1233-VOL-1 ..... N90-20562* #
NASA-RP-1233-VOL-2 ..... N90-20563* #
NASA-RP-1233-VOL-4 ..... N90-20564* #

NASA-TM-4191 ..... N90-20252* #
NASA-TM-100038 ..... N90-20333* #
NASA-TM-100390 ..... N90-20200* #
NASA-TM-100392 ..... N90-20251* #
NASA-TM-100729 ..... N90-20566* #
NASA-TM-100730 ..... N90-20572* #
NASA-TM-100754 ..... N90-20911* #
NASA-TM-101453 ..... N90-20264* #
NASA-TM-101689 ..... N90-20071* #
NASA-TM-101696 ..... N90-20086* #
NASA-TM-102158 ..... N90-20645* #
NASA-TM-102231 ..... N90-20087* #
NASA-TM-102271 ..... N90-20325* #
NASA-TM-102403 ..... N90-20181* #
NASA-TM-102417 ..... N90-20901* #
NASA-TM-102440 ..... N90-20794* #
NASA-TM-102445 ..... N90-20194* #
NASA-TM-102454 ..... N90-20708* #
NASA-TM-102482 ..... N90-20085* #
NASA-TM-102494 ..... N90-20286* #
NASA-TM-102503 ..... N90-20352* #
NASA-TM-102509 ..... N90-20431* #
NASA-TM-102514 ..... N90-20353* #
NASA-TM-102515 ..... N90-20138* #
NASA-TM-102518 ..... N90-20090* #
NASA-TM-102519 ..... N90-20769* #
NASA-TM-102524 ..... N90-20326* #
NASA-TM-102525 ..... N90-20337* #
NASA-TM-102529 ..... N90-20391* #
NASA-TM-102530 ..... N90-20253* #
NASA-TM-102532 ..... N90-20428* #
NASA-TM-102536 ..... N90-20139* #
NASA-TM-102537 ..... N90-20392* #
NASA-TM-102544 ..... N90-20393* #
NASA-TM-102549 ..... N90-20130* #
NASA-TM-102556 ..... N90-20438* #
NASA-TM-102558 ..... N90-20151* #
NASA-TM-102566 ..... N90-20338* #
NASA-TM-102567 ..... N90-20432* #
NASA-TM-102571 ..... N90-20886* #
NASA-TM-102577 ..... N90-20301* #
NASA-TM-102581 ..... N90-20358* #
NASA-TM-102590 ..... N90-20427* #
NASA-TM-102595 ..... N90-20068* #
NASA-TM-102596 ..... N90-20583* #
NASA-TM-102604 ..... N90-20121* #
NASA-TM-102606 ..... N90-20122* #
NASA-TM-102611 ..... N90-20426* #
NASA-TM-102617 ..... N90-20047* #
NASA-TM-102618 ..... N90-20093* #
NASA-TM-102621 ..... N90-20795* #
NASA-TM-102625 ..... N90-20137* #
NASA-TM-102965 ..... N90-20617* #
NASA-TM-103096 ..... N90-20110* #
NASA-TM-103100 ..... N90-20051* #
NASA-TM-103110 ..... N90-20302* #
NASA-TM-103318 ..... N90-20357* #

NASA-TP-2990 ..... N90-20046* #

NAVAIR-50-1C-556 ..... N90-20587 #

NDP-019/R1 ..... N90-20506 #

NMSU-ECE-89-005 ..... N90-20697 #

NPRDC-TN-90-9 ..... N90-20638 #

NPS61-89-011CR ..... N90-20837 #

NRC-31023 ..... N90-20575 #

NRL-MR-6586 ..... N90-20722 #
NRL-MR-6601 ..... N90-20771 #
NRL-MR-6605 ..... N90-20774 #
NRL-MR-6606 ..... N90-20773 #
NRL-MR-6607 ..... N90-20316 #
NRL-MR-6610 ..... N90-20817 #

NRL-9120 ..... N90-20273 #

ORNL/ATD-26/V2 ..... N90-20850 #

ORNL/CDIAC-30 ..... N90-20506 #

ORNL/TM-11420 ..... N90-20851 #
ORNL/TM-11488 ..... N90-20765 #

OSU-TR-716111-8 ..... N90-20271* #

PARGUM-89-06 ..... N90-20796 #

PB90-129974 ..... N90-20483 #

PME-FM-90-1 ..... N90-20329 #
PME-FM-90-2 ..... N90-20327 #

PNL-SA-16909 ..... N90-20510 #
PNL-SA-17226 ..... N90-20172 #
PNL-SA-17271 ..... N90-20225 #
PNL-SA-17283 ..... N90-20511 #
PNL-SA-17905 ..... N90-20505 #

PNL-7203 ..... N90-20298 #

PW-FR-20760 ..... N90-20208 #

R/D-5899A-CH-01 ..... N90-20482 #
RADC-TR-89-230 ..... N90-20308 #
RADC-TR-89-239 ..... N90-20293 #
RADC-TR-89-251 ..... N90-20830 #
RADC-TR-89-265 ..... N90-20295 #
RADC-TR-89-290 ..... N90-20384 #

RCC/RSG-318-89 ..... N90-20092 #

RDA-TR-022618902-002 ..... N90-20569 #

REPT-16/89 ..... N90-20902 #
REPT-89-62543 ..... N90-20088* #
REPT-89B00106 ..... N90-20572* #
REPT-89B00107 ..... N90-20566* #
REPT-89B00239 ..... N90-20562* #
REPT-89B00240 ..... N90-20563* #
REPT-89B00241 ..... N90-20564* #
REPT-90-068 ..... N90-20911* #
REPT-397 ..... N90-20513* #
REPT-718048-11 ..... N90-20278 #

RFP-4406 ..... N90-20502 #

RSD-TR-14-88 ..... N90-20256 #

S-594 ..... N90-20651* #

SAIC 89/1732 ..... N90-20347 #

SAIC-89/1746 ..... N90-20584 #

SAND-88-3291 ..... N90-20738 #
SAND-89-0412C ..... N90-20259 #
SAND-89-0773 ..... N90-20874 #
SAND-89-1480C ..... N90-20859 #
SAND-89-1514C ..... N90-20875 #
SAND-89-1890 ..... N90-20285 #
SAND-89-1930C ..... N90-20878 #
SAND-89-2044C ..... N90-20402 #
SAND-89-2106 ..... N90-20166 #
SAND-89-2111C ..... N90-20106 #
SAND-89-2112C ..... N90-20108 #
SAND-89-2113C ..... N90-20107 #
SAND-89-2236C ..... N90-20162 #
SAND-89-2293C ..... N90-20296 #
SAND-89-2399 ..... N90-20161 #
SAND-89-2414C ..... N90-20399 #
SAND-89-2506C ..... N90-20403 #
SAND-89-2510C ..... N90-20745 #
SAND-89-2511C ..... N90-20398 #
SAND-89-2522C ..... N90-20435 #
SAND-89-2527C ..... N90-20354 #
SAND-89-2534 ..... N90-20740 #
SAND-89-2696C ..... N90-20879 #
SAND-89-2781 ..... N90-20739 #
SAND-89-2783C ..... N90-20710 #
SAND-89-3025C ..... N90-20370 #
SAND-89-3039 ..... N90-20297 #
SAND-89-3040C ..... N90-20334 #
SAND-89-7040 ..... N90-20495 #
SAND-89-7041 ..... N90-20490 #
SAND-89-7096 ..... N90-20202 #
SAND-90-0052C ..... N90-20707 #
SAND-90-0077C ..... N90-20221 #
SAND-90-0231C ..... N90-20268 #
SAND-90-0259C ..... N90-20234 #
SAND-90-0438C ..... N90-20494 #
SAND-90-0746C ..... N90-20907 #

SBRC-90-0045 ..... N90-20893 #

SCA-142 ..... N90-20235 #

SC5537.FR ..... N90-20791 #

SERI/STR-232-3569 ..... N90-20608 #

SERI/TP-257-3603 ..... N90-20492 #
SERI/TP-257-3663 ..... N90-20111 #

SERI/TR-211-3571 ..... N90-20489 #
SERI/TR-215-3513A-VOL-1 ..... N90-20571 #
SERI/TR-234-3610 ..... N90-20220 #
SERI/TR-253-3549 ..... N90-20493 #

SOL-89-15 ..... N90-20755 #

SRI-MP-90-001 ..... N90-20814 #

SU-CLASSIC-90-07 ..... N90-20328 #

SU-JIAA-TR-92 ..... N90-20052* #

SU-SLAC-PUB-5161 ..... N90-20915 #

TACOM-TR-13463 ..... N90-20748 #

TF-45 ..... N90-20343 #

TOXICOLOGY-SER-167 ..... N90-20614 #
TOXICOLOGY-SER-177 ..... N90-20609 #
TOXICOLOGY-SER-178 ..... N90-20613 #

TR-9 ..... N90-20211 #
TR-14 ..... N90-20255 #
TR-21 ..... N90-20213 #
TR-36 ..... N90-20158 #
TR-52 ..... N90-20216 #
TR-54 ..... N90-20230 #
TR-89-15 ..... N90-20053 #
TR-89-48 ..... N90-20698 #
TR-89-49 ..... N90-20757 #
TR-274 ..... N90-20777 #
TR-281 ..... N90-20776 #
TR-282 ..... N90-20779 #
TR-454 ..... N90-20643 #
TR-860 ..... N90-20290 #
TR-864 ..... N90-20585 #
TR-865 ..... N90-20828 #
TR-868 ..... N90-20759 #

TRW-SCS-89-T1-VOL-6 ..... N90-20118* #
TRW-SCS-89-T2-VOL-5 ..... N90-20117* #
TRW-SCS-89-T4-VOL-4 ..... N90-20116* #
TRW-SCS-89-T5-VOL-3 ..... N90-20115* #
TRW-SCS-89-T7-VOL-1 ..... N90-20113* #

TT-73 ..... N90-20758 #

TWR-50138 ..... N90-20127* #

UCB/ERL-89/1 ..... N90-20311 #

UCID-21679-REV-1 ..... N90-20904 #
UCID-21792 ..... N90-20269 #
UCID-21823-REV-1 ..... N90-20620 #
UCID-21864 ..... N90-20257 #
UCID-21873 ..... N90-20880 #

UCRL-21233 ..... N90-20822 #
UCRL-21264 ..... N90-20304 #
UCRL-21268 ..... N90-20169 #
UCRL-21274 ..... N90-20573 #
UCRL-21275 ..... N90-20382 #
UCRL-21298 ..... N90-20853 #
UCRL-53945 ..... N90-20440 #
UCRL-98747 ..... N90-20205 #
UCRL-99094 ..... N90-20885 #
UCRL-99707 ..... N90-20762 #
UCRL-99967-REV-1 ..... N90-20376 #
UCRL-100480 ..... N90-20884 #
UCRL-100992 ..... N90-20691 #
UCRL-101262 ..... N90-20808 #
UCRL-101287 ..... N90-20883 #
UCRL-101479 ..... N90-20299 #
UCRL-101560 ..... N90-20711 #
UCRL-101574 ..... N90-20833 #
UCRL-101575 ..... N90-20171 #
UCRL-102017 ..... N90-20204 #
UCRL-102046 ..... N90-20704 #
UCRL-102525 ..... N90-20378 #
UCRL-102536 ..... N90-20372 #
UCRL-102537 ..... N90-20373 #
UCRL-102538 ..... N90-20305 #
UCRL-102559 ..... N90-20360 #
UCRL-102620 ..... N90-20300 #
UCRL-102645 ..... N90-20371 #
UCRL-102663 ..... N90-20735 #
UCRL-102793 ..... N90-20589 #
UCRL-102806 ..... N90-20823 #
UCRL-102861 ..... N90-20588 #
UCRL-102966 ..... N90-20336 #
UCRL-102971 ..... N90-20203 #
UCRL-102995 ..... N90-20437 #
UCRL-102996 ..... N90-20359 #

UDR-TR-88-39 ..... N90-20069 #
UDR-TR-89-33 ..... N90-20289 #

UFIFT-HEP-90-3 ..... N90-20897 #

UILI-ENG-90-2201 ..... N90-20701 #

UILU-ENG-89-2236 ..... N90-20265 #
UILU-ENG-89-2243 ..... N90-20292 #
UILU-ENG-90-2202 ..... N90-20744 #
UILU-ENG-90-2207 ..... N90-20686* #

US-PATENT-APPL-SN-054985 ..... N90-20133*
US-PATENT-APPL-SN-082766 ..... N90-20096*
US-PATENT-APPL-SN-084062 ..... N90-20351*
US-PATENT-APPL-SN-087281 ..... N90-20616*
US-PATENT-APPL-SN-090874 ..... N90-20180*
US-PATENT-APPL-SN-125677 ..... N90-20280*
US-PATENT-APPL-SN-145719 ..... N90-20154*
US-PATENT-APPL-SN-210480 ..... N90-20078*
US-PATENT-APPL-SN-221388 ..... N90-20408*
US-PATENT-APPL-SN-232734 ..... N90-20236*
US-PATENT-APPL-SN-237036 ..... N90-20323*
US-PATENT-APPL-SN-251439 ..... N90-20254*
US-PATENT-APPL-SN-252081 ..... N90-20079*
US-PATENT-APPL-SN-267146 ..... N90-20409*
US-PATENT-APPL-SN-292123 ..... N90-20126*
US-PATENT-APPL-SN-441896 ..... N90-20896*
US-PATENT-APPL-SN-493864 ..... N90-20133*
US-PATENT-APPL-SN-522629 ..... N90-20133*
US-PATENT-APPL-SN-625436 ..... N90-20320*
US-PATENT-APPL-SN-641152 ..... N90-20133*
US-PATENT-APPL-SN-675471 ..... N90-20282*
US-PATENT-APPL-SN-811309 ..... N90-20896*
US-PATENT-APPL-SN-823719 ..... N90-20685
US-PATENT-APPL-SN-862942 ..... N90-20320*

US-PATENT-CLASS-55-46 ..... N90-20254*
US-PATENT-CLASS-55-105 ..... N90-20320*
US-PATENT-CLASS-55-139 ..... N90-20320*
US-PATENT-CLASS-55-159 ..... N90-20254*
US-PATENT-CLASS-55-160 ..... N90-20236*
US-PATENT-CLASS-55-182 ..... N90-20236*
US-PATENT-CLASS-55-205 ..... N90-20236*
US-PATENT-CLASS-73-178-T N90-20096*
US-PATENT-CLASS-73-831 ..... N90-20409*
US-PATENT-CLASS-73-860 ..... N90-20409*
US-PATENT-CLASS-137-154 ..... N90-20254*
US-PATENT-CLASS-141-45 ..... N90-20236*
US-PATENT-CLASS-141-93 ..... N90-20254*
US-PATENT-CLASS-156-616.4 ..... N90-20896*
US-PATENT-CLASS-156-616.41 ..... N90-20896*
US-PATENT-CLASS-165-41 ..... N90-20323*
US-PATENT-CLASS-165-104 ..... N90-20323*
US-PATENT-CLASS-165-133 ..... N90-20323*
US-PATENT-CLASS-165-180 ..... N90-20323*
US-PATENT-CLASS-165-905 ..... N90-20323*
US-PATENT-CLASS-166-343 ..... N90-20126*
US-PATENT-CLASS-204-157.51 ..... N90-20154*
US-PATENT-CLASS-219-121.28 ..... N90-20351*
US-PATENT-CLASS-239-543 ..... N90-20254*
US-PATENT-CLASS-244-54 ..... N90-20078*
US-PATENT-CLASS-244-55 ..... N90-20078*
US-PATENT-CLASS-244-130 ..... N90-20078*
US-PATENT-CLASS-244-130 ..... N90-20079*
US-PATENT-CLASS-244-137.4 ..... N90-20079*
US-PATENT-CLASS-244-159 ..... N90-20126*
US-PATENT-CLASS-244-161 ..... N90-20126*
US-PATENT-CLASS-250-310 ..... N90-20351*
US-PATENT-CLASS-250-396-ML N90-20351*
US-PATENT-CLASS-250-396-R N90-20351*
US-PATENT-CLASS-294-86.4 ..... N90-20408*
US-PATENT-CLASS-294-106 ..... N90-20408*
US-PATENT-CLASS-323-903 ..... N90-20320*
US-PATENT-CLASS-342-105 ..... N90-20280*
US-PATENT-CLASS-342-114 ..... N90-20280*
US-PATENT-CLASS-342-195 ..... N90-20280*
US-PATENT-CLASS-357-22 ..... N90-20282*
US-PATENT-CLASS-357-55 ..... N90-20282*
US-PATENT-CLASS-357-68 ..... N90-20282*
US-PATENT-CLASS-357-76 ..... N90-20282*
US-PATENT-CLASS-357-81 ..... N90-20282*
US-PATENT-CLASS-361-65 ..... N90-20320*
US-PATENT-CLASS-361-79 ..... N90-20320*
US-PATENT-CLASS-364-427 ..... N90-20096*
US-PATENT-CLASS-372-59 ..... N90-20154*
US-PATENT-CLASS-405-188 ..... N90-20126*
US-PATENT-CLASS-422-249 ..... N90-20896*
US-PATENT-CLASS-427-2 ..... N90-20616*
US-PATENT-CLASS-428-408 ..... N90-20616*
US-PATENT-CLASS-502-38 ..... N90-20154*
US-PATENT-CLASS-502-53 ..... N90-20154*
US-PATENT-CLASS-502-325 ..... N90-20180*
US-PATENT-CLASS-502-339 ..... N90-20154*
US-PATENT-CLASS-502-339 ..... N90-20180*
US-PATENT-CLASS-502-344 ..... N90-20180*
US-PATENT-CLASS-502-352 ..... N90-20154*
US-PATENT-CLASS-530-362 ..... N90-20616*
US-PATENT-CLASS-530-363 ..... N90-20616*
US-PATENT-CLASS-530-364 ..... N90-20616*
US-PATENT-CLASS-530-387 ..... N90-20616*
US-PATENT-CLASS-530-422 ..... N90-20616*
US-PATENT-CLASS-558-190 ..... N90-20133*
US-PATENT-CLASS-901-38 ..... N90-20408*
US-PATENT-CLASS-901-39 ..... N90-20408*

US-PATENT-4,605,424 ..... N90-20320*
US-PATENT-4,833,233 ..... N90-20616*
US-PATENT-4,838,346 ..... N90-20323*
US-PATENT-4,839,330 ..... N90-20154*
US-PATENT-4,843,440 ..... N90-20282*
US-PATENT-4,843,554 ..... N90-20096*
US-PATENT-4,846,854 ..... N90-20254*
US-PATENT-4,847,502 ..... N90-20351*
US-PATENT-4,848,987 ..... N90-20236*
US-PATENT-4,855,274 ..... N90-20180*
US-PATENT-4,858,857 ..... N90-20126*
US-PATENT-4,858,979 ..... N90-20408*
US-PATENT-4,860,014 ..... N90-20280*
US-PATENT-4,860,149 ..... N90-20320*
US-PATENT-4,862,406 ..... N90-20685
US-PATENT-4,863,118 ..... N90-20079*
US-PATENT-4,863,553 ..... N90-20896*
US-PATENT-4,864,050 ..... N90-20133*
US-PATENT-4,864,865 ..... N90-20409*
US-PATENT-4,867,394 ..... N90-20078*

USAAEFA-86-15 ..... N90-20076 #

USAARL-89-28 ..... N90-20634 #

USAFSAM-SR-89-6 ..... N90-20622 #

USARIEM-M5-90 ..... N90-20633 #
USARIEM-M7-90 ..... N90-20615 #
USARIEM-M8-90 ..... N90-20624 #
USARIEM-M13-90 ..... N90-20625 #

USARIEM-T7-90 ..... N90-20629 #
USARIEM-T8-90 ..... N90-20636 #

UVA-527387/CS90/102 ..... N90-20905 #

VLSI-MEMO-89-564 ..... N90-20287 #
VLSI-MEMO-89-565 ..... N90-20730 #
VLSI-MEMO-89-566 ..... N90-20729 #
VLSI-MEMO-89-569 ..... N90-20756 #
VLSI-MEMO-89-570 ..... N90-20687 #
VLSI-MEMO-89-571 ..... N90-20742 #

VPI-E-90-04 ..... N90-20136* #
VPI-E-90-05 ..... N90-20135* #

WL-TR-89-47 ..... N90-20829 #
WL-TR-89-80 ..... N90-20868 #

WRDC-TR-89-1118 ..... N90-20312 #
WRDC-TR-89-2023 ..... N90-20103 #
WRDC-TR-89-2056 ..... N90-20235 #
WRDC-TR-89-2065 ..... N90-20289 #
WRDC-TR-89-2079 ..... N90-20318 #
WRDC-TR-89-2118 ..... N90-20091 #
WRDC-TR-89-3075 ..... N90-20069 #
WRDC-TR-89-3114 ..... N90-20094 #
WRDC-TR-89-4035 ..... N90-20153 #
WRDC-TR-89-4095 ..... N90-20208 #
WRDC-TR-89-4107 ..... N90-20146 #
WRDC-TR-89-4112 ..... N90-20314 #
WRDC-TR-89-5046 ..... N90-20719 #
WRDC-TR-89-7006-VOL-1 ..... N90-20647 #
WRDC-TR-89-8037 ..... N90-20256 #

WSRC-RP-89-1100 ..... N90-20414 #

Appendix—About STAR

Scientific and Technical Aerospace Reports (STAR) is a major component of a comprehensive National Aeronautics and Space Administration information system covering aeronautics, space, and supporting disciplines. *STAR* is issued on the 8th and 23rd of each month and announces current publications of the following types:

- NASA, NASA contractor, and NASA grantee reports
- Reports issued by other U.S. Government agencies, domestic and foreign institutions, universities, and private firms
- Translations in report form
- NASA-owned patents and patent applications
- Other U.S. Government agency and foreign patents and patent applications
- Domestic and foreign dissertations and theses

Journal, book, and conference literature, cover-to-cover journal translations, and certain foreign dissertations are announced in a companion journal, *International Aerospace Abstracts (IAA),* available on subscription from the American Institute of Aeronautics and Astronautics, Technical Information Service, 555 West 57th Street, 12th Floor, New York, NY 10019.

SUBJECT SCOPE

The subject scope of *STAR* and *IAA* includes all aspects of aeronautics and space research and development, supporting basic and applied research, and applications. Aerospace aspects of earth resources, energy development, conservation, oceanography, environmental protection, urban transportation, and other topics of high national priority are also covered.

OTHER NASA PUBLICATIONS

Other NASA publications and information services are described in the publication, *The NASA Scientific and Technical Information System ... and How to Use It,* available without charge from the NASA Scientific and Technical Information Facility, P.O. Box 8757, BWI Airport, MD 21240.

HOW TO USE *STAR* SUBJECT CATEGORIES

STAR is categorized by 10 major subject divisions broken down further into 76 specific subject categories and one general division/category. The major subject divisions are listed on page ii in the Table of Contents, together with a note for each that defines its scope and provides any cross-references. For example:

AERONAUTICS

Includes aeronautics (general); aerodynamics; air transportation and safety; aircraft communications and navigation; aircraft design, testing and performance; aircraft instrumentation; aircraft propulsion and power; aircraft stability and control; and research and support facilities (air).

For related information see also *Astronautics.*

Each major division is further divided into as many as nine specific categories, which are identified by category numbers.

Abstracts in *STAR* are grouped by subject category, the categories appearing in sequential order. Category breaks in the abstract section are identified by the category number and title, and a scope note. Cross-references to other categories are provided as appropriate. For example:

02 AERODYNAMICS

Includes aerodynamics of bodies, combinations, wings, rotors, and control surfaces; and internal flow in ducts and turbomachinery.

For related information see also *34 Fluid Mechanics and Heat Transfer.*

CROSS-REFERENCES

Individual *STAR* abstracts are not ordinarily cross-referenced, except for certain conference reports or book translations that have had separate abstracts written for their component papers or chapters. Citations and abstracts of the components follow immediately after those of the parent document. When the subject content of a component differs sufficiently from the general content of the parent, a cross-reference citation also is printed at the end of the category to which it normally would have been assigned if it were independent.

DOCUMENTS ON MICROFICHE

Documents on microfiche[1] are designated by a pound sign (#) following the accession number. The pound sign is used without regard to the source or quality of the microfiche.

LIMITED REPRODUCIBILITY

A Note of Limited Reproducibility appears in the citation, if one or a combination of the following factors affect the reproducibility of more than 20% of the document. These factors include: faint or broken type, color photographs, black and white photographs, foldouts, dot matrix print, charts/graphs with script notation, non-Roman alphabet, or some other factor that limits the reproducibility of that document. This notation also appears on the microfiche header, with the specific causing factor checked off on a list visible in the second frame.

COLOR COPIES

An increasing number of NASA scientific and technical reports are being produced with color graphs, charts, illustrations, and photographs. A message indicating that a document has color pages follows the Sales and Pricing (SAP) information in the *STAR* citation.

Registered users of the NASA Scientific and Technical Information System will receive ordered documents with color at no *additional* cost, as long as stock copies of that document are available. Otherwise, an additional fee of $2.00 per color page, over and above the standard document price will be charged. The NASA STI Facility staff will work with registered users over the telephone to inform and meet each individual's ordering needs.

AVAILABILITIES

One or more sources from which a document announced in *STAR* is available to the public is given in each citation. The most commonly indicated sources and their acronyms or abbreviations are listed below. If the publication is available from a source other than those listed, the publisher and his address will be displayed on the availability line or in combination with the corporate source line.

Avail: NTIS. Sold by the National Technical Information Service. Prices for hard copy (HC) and microfiche (MF) are indicated by a price code following the letters HC or MF in the *STAR* citation. Current values for the price codes are given in the tables on page A-7.

(1) A microfiche is a transparent sheet of film, 105 by 148 mm in size, containing as many as 60 to 98 pages of information reduced to micro images (not to exceed 26:1 reduction).

Initially distributed microfiche under the NTIS SRIM (Selected Research in Microfiche) is available at greatly reduced unit prices. For this service and for information concerning subscription to NASA printed reports, consult the NTIS Subscription Section, Springfield, VA 22161.

NOTE ON ORDERING DOCUMENTS: When ordering NASA publications (those followed by the * symbol), use the N accession number. NASA patent applications (only the specifications are offered) should be ordered by the US-Patent-Appl-SN number. Non-NASA publications (no asterisk) should be ordered by the AD, PB, or other *report number* shown on the last line of the citation, not by the N accession number. It is also advisable to cite the title and other bibliographic identification.

Avail: SOD (or GPO). Sold by the Superintendent of Documents, U.S. Government Printing Office, in hard copy. The current price and order number are given following the availability line. (NTIS will fill microfiche requests, as indicated above, for those documents identified by a # symbol.)

Avail: BLL (formerly NLL): British Library Lending Division, Boston Spa, Wetherby, Yorkshire, England. Photocopies available from this organization at the price shown. (If none is given, address inquiry to the BLL.)

Avail: DOE Depository Libraries. Organizations in U.S. cities and abroad that maintain collections of Department of Energy reports, usually in microfiche form, are listed in *Energy Research Abstracts.* Services available from the DOE and its depositories are described in a booklet, *DOE Technical Information Center - Its Functions and Services* (TID-4660), which may be obtained without charge from the DOE Technical Information Center.

Avail: ESDU. Pricing information on specific data, computer programs, and details on Engineering Sciences Data Unit (ESDU) topic categories can be obtained from ESDU International Ltd. Requesters in North America should use the Virginia address while all other requesters should use the London address, both of which are on page A-6.

Avail: Fachinformationszentrum, Karlsruhe. Sold by the Fachinformationszentrum Energie, Physik, Mathematik GMBH, Eggenstein Leopoldshafen, Federal Republic of Germany, at the price shown in deutschmarks (DM).

Avail: HMSO. Publications of Her Majesty's Stationery Office are sold in the U.S. by Pendragon House, Inc. (PHI), Redwood City, CA. The U.S. price (including a service and mailing charge) is given, or a conversion table may be obtained from PHI.

Avail: NASA Public Document Rooms. Documents so indicated may be examined at or purchased from the National Aeronautics and Space Administration, Public Documents Room (Room 126), 600 Independence Ave., S.W., Washington, DC 20546, or public document rooms located at NASA installations, and the NASA Pasadena Office at the Jet Propulsion Laboratory.

Avail: Univ. Microfilms. Documents so indicated are dissertations selected from *Dissertation Abstracts* and are sold by University Microfilms as xerographic copy (HC) and microfilm. All requests should cite the author and the Order Number as they appear in the citation.

Avail: US Patent and Trademark Office. Sold by Commissioner of Patents and Trademarks, U.S. Patent and Trademark Office, at the standard price of

$1.50 each, postage free. (See discussion of NASA patents and patent applications below.)

Avail: (US Sales Only). These foreign documents are available to users within the United States from the National Technical Information Service (NTIS). They are available to users outside the United States through the International Nuclear Information Service (INIS) representative in their country, or by applying directly to the issuing organization.

Avail: USGS. Originals of many reports from the U.S. Geological Survey, which may contain color illustrations, or otherwise may not have the quality of illustrations preserved in the microfiche or facsimile reproduction, may be examined by the public at the libraries of the USGS field offices whose addresses are listed in this Introduction. The libraries may be queried concerning the availability of specific documents and the possible utilization of local copying services, such as color reproduction.

Avail: Issuing Activity, or Corporate Author, or no indication of availability. Inquiries as to the availability of these documents should be addressed to the organization shown in the citation as the corporate author of the document.

NASA PATENTS AND PATENT APPLICATIONS

Patents and patent applications owned by NASA are announced in *STAR* under appropriate subject categories and are referenced in the *STAR* indexes. In the Report/Accession Number Index, patents are indexed by the NASA Case Number (which appears in lieu of the report number in other indexes), the U.S. Patent Number, the U.S. Patent Application Serial Number, and the U.S. Patent Class. Patent applications for which patents have not yet been issued are indexed by the NASA Case Number and the U.S. Patent Application Serial Number.

NASA *patent application specifications* are sold in paper copy and microfiche by the National Technical Information Service (NTIS). The US-Patent-Appl-SN- number should be used in ordering either paper copy or microfiche from NTIS. Printed copies of *patents* (which are not microfiched) are available for purchase from:

Commissioner of Patents and Trademarks
U.S. Patent and Trademark Office
Washington, DC 20231

When ordering patents, the U.S. Patent Number should be used, and payment must be remitted in advance, by money order or check payable to the Commissioner of Patents and Trademarks. Prepaid purchase coupons for ordering are also available from the Patent and Trademark Office. The patents and patent applications announced in *STAR* are owned by NASA and are available for royalty-free licensing. Requests for licensing terms and further information should be addressed to:

Associate General Counsel for Intellectual Property/Code GP
National Aeronautics and Space Administration
Washington, DC 20546

ELIGIBILITY AND REGISTRATION FOR NASA INFORMATION PRODUCTS AND SERVICES

A variety of services is available to organizations of the following types that have registered with NASA to receive specific services or products:

1. NASA offices and installations, contractors, subcontractors, grantees, and consultants;
2. Other U.S. Government agencies and their contractors;
3. Libraries in the United States that have arrangements with NASA to maintain collections of NASA documents for public reference;
4. Other organizations in the United States having a need for NASA documents in work related to aeronautics and space research;
5. Organizations abroad that have established reciprocal document exchange arrangements with NASA.

Only the central service points or central points of document acquisition and control within qualified organizations are eligible to register for NASA products and services. Domestic organizations that may be eligible to receive various classes of NASA publications and services should address their requests for registration or for further information to:

NASA Scientific and Technical Information Facility
ATTN: Registration Services
P.O. Box 8757
BWI Airport, MD 21240
301-621-0153

Organizations abroad should direct requests to Manager, International STI Activities, NTT, NASA Headquarters, Washington, DC 20546.

AVAILABILITY OF *STAR* ABSTRACTS ON MICROFICHE

Microfiche of the abstract sections of this issue and other issues of *STAR* are available on annual subscription from NTIS as PB90-911300, Attn: Subscriptions, 5285 Port Royal Road, Springfield, VA 22161. Annual subscription rates are $75.50 North America; $151.00 foreign. Abstract sections for previous years retroactive to 1964 are available at the current rates. Microfiche for individual *STAR* issue abstract sections are not available.

PUBLIC COLLECTIONS OF NASA DOCUMENTS

DOMESTIC: NASA and NASA-sponsored documents and a large number of aerospace publications are available to the public for reference purposes at the library maintained by the American Institute of Aeronautics and Astronautics, Technical Information Service, 555 West 57th Street, 12th Floor, New York, NY 10019

EUROPEAN: An extensive collection of NASA and NASA-sponsored publications is maintained by the British Library Lending Division, Boston Spa, Wetherby, Yorkshire, England, for public access. The British Library Lending Division also has available many of the non-NASA publications cited in *STAR*. European requesters may purchase facsimile copy or microfiche of NASA and NASA-sponsored documents, those identified by both the symbols # and * from ESA - Information Retrieval Service, European Space Agency, 8-10 rue Mario-Nikis, 75738 Paris CEDEX 15, France.

FEDERAL DEPOSITORY LIBRARY PROGRAM

In order to provide the general public with greater access to U.S. Government publications, Congress established the Federal Depository Library Program under the Government Printing Office (GPO), with 51 regional depositories responsible for permanent retention of material, inter-library loan, and reference services. At least one copy of nearly every NASA and NASA-sponsored publication, either in printed or microfiche format, is received and retained by the 51 regional depositories. A list of the regional GPO libraries, arranged alphabetically by state, appears on the inside back cover. These libraries are *not* sales outlets. A local library can contact a Regional Depository to help locate specific reports, or direct contact may be made by an individual.

ADDRESSES OF ORGANIZATIONS

American Institute of Aeronautics and Astronautics
Technical Information Service
555 West 57th Street, 12th Floor
New York, New York 10019

British Library Lending Division,
Boston Spa, Wetherby, Yorkshire,
England

Commissioner of Patents and Trademarks
U.S. Patent and Trademark Office
Washington, DC 20231

Department of Energy
Technical Information Center
P.O. Box 62
Oak Ridge, Tennessee 37830

European Space Agency-Information Retrieval Service
ESRIN
Via Galileo Galilei
00044 Frascati (Rome) Italy

Engineering Sciences Data Unit International
P.O. Box 1633
Manassas, Virginia 22110

Engineering Sciences Data Unit International, Ltd.
251-259 Regent Street
London, W1R 7AD, England

Fachinformationszentrum Energie, Physik, Mathematik
GMBH
7514 Eggenstein Leopoldshafen
Federal Republic of Germany

Her Majesty's Stationery Office
P.O. Box 569, S.E. 1
London, England

NASA Scientific and Technical Information Facility
P.O. Box 8757
BWI Airport, Maryland 21240

National Aeronautics and Space Administration
Scientific and Technical Information Division (NTT)
Washington, DC 20546

National Technical Information Service
5285 Port Royal Road
Springfield, Virginia 22161

Pendragon House, Inc.
899 Broadway Avenue
Redwood City, California 94063

Superintendent of Documents
U.S. Government Printing Office
Washington, DC 20402

University Microfilms
A Xerox Company
300 North Zeeb Road
Ann Arbor, Michigan 48106

University Microfilms, Ltd.
Tylers Green
London, England

U.S. Geological Survey Library National Center
MS 950
12201 Sunrise Valley Drive
Reston, Virginia 22092

U.S. Geological Survey Library
2255 North Gemini Drive
Flagstaff, Arizona 86001

U.S. Geological Survey
345 Middlefield Road
Menlo Park, California 94025

U.S. Geological Survey Library
Box 25046
Denver Federal Center, MS914
Denver, Colorado 80225

NTIS PRICE SCHEDULES

(Effective January 1, 1990)

Schedule A
STANDARD PRICE DOCUMENTS AND MICROFICHE

PRICE CODE	NORTH AMERICAN PRICE	FOREIGN PRICE
A01	$ 8.00	$ 16.00
A02	11.00	22.00
A03	15.00	30.00
A04-A05	17.00	34.00
A06-A09	23.00	46.00
A10-A13	31.00	62.00
A14-A17	39.00	78.00
A18-A21	45.00	90.00
A22-A25	53.00	106.00
A99	*	*
N01	60.00	120.00
N02	59.00	118.00
N03	20.00	40.00

Schedule E
EXCEPTION PRICE DOCUMENTS AND MICROFICHE

PRICE CODE	NORTH AMERICAN PRICE	FOREIGN PRICE
E01	$10.00	$ 20.00
E02	12.00	24.00
E03	14.00	28.00
E04	16.50	33.00
E05	18.50	37.00
E06	21.50	43.00
E07	24.00	48.00
E08	27.00	54.00
E09	29.50	59.00
E10	32.50	65.00
E11	35.00	70.00
E12	38.50	77.00
E13	41.00	82.00
E14	45.00	90.00
E15	48.50	97.00
E16	53.00	106.00
E17	57.50	115.00
E18	62.00	124.00
E19	69.00	138.00
E20	80.00	160.00
E99	*	*

* Contact NTIS for price quote.

IMPORTANT NOTICE

NTIS Shipping and Handling Charges

U.S., Canada, Mexico — ADD $3.00 per TOTAL ORDER

All Other Countries — ADD $4.00 per TOTAL ORDER

Exceptions — Does NOT apply to:

ORDERS REQUESTING NTIS RUSH HANDLING
ORDERS FOR SUBSCRIPTION OR STANDING ORDER PRODUCTS *ONLY*

NOTE: Each additional delivery address on an order requires a separate shipping and handling charge.

FEDERAL REGIONAL DEPOSITORY LIBRARIES

ALABAMA

AUBURN UNIV. AT MONTGOMERY LIBRARY
Documents Department
Montgomery, AL 36193
(205) 279-9110 ext.253

UNIV. OF ALABAMA LIBRARY
Reference Department/Documents
Box S
Tuscaloosa, AL 35486
(205) 348-6046

ARIZONA

DEPT. OF LIBRARY, ARCHIVES, AND PUBLIC RECORDS
Third Floor State Capitol
1700 West Washington
Phoenix, AZ 85007
(602) 255-4121

ARKANSAS

ARKANSAS STATE LIBRARY
Documents Service Section
One Capitol Mall
Little Rock, AR 72201
(501) 371-2090

CALIFORNIA

CALIFORNIA STATE LIBRARY
Govt. Publications Section
914 Capitol Mall
Sacramento, CA 95814
(916) 322-4572

COLORADO

UNIV. OF COLORADO
Norlin Library
Government Publications Division
Campus Box 184
Boulder, CO 80309
(303) 492-8834

DENVER PUBLIC LIBRARY
Govt. Pub. Department
1357 Broadway
Denver, CO 80203
(303) 571-2346

CONNECTICUT

CONNECTICUT STATE LIBRARY
231 Capitol Avenue
Hartford, CT 06106
(203) 566-4971

FLORIDA

UNIV. OF FLORIDA LIBRARIES
Documents Department
Library West
Gainesville, FL 32611
(904) 392-0367

GEORGIA

UNIV. OF GEORGIA LIBRARIES
Government Documents Dept.
Athens, GA 30602
(404) 542-8949

HAWAII

UNIV. OF HAWAII
Hamilton Library
Government Documents Collection
2550 The Mall
Honolulu, HI 96822
(808) 948-8230

IDAHO

UNIV. OF IDAHO LIBRARY
Documents Section
Moscow, ID 83843
(208) 885-6344

ILLINOIS

ILLINOIS STATE LIBRARY
Federal Documents
Centennial Building
Springfield, IL 62756
(217) 782-5012

INDIANA

INDIANA STATE LIBRARY
Serials Section
140 North Senate Avenue
Indianapolis, IN 46204
(317) 232-3686

IOWA

UNIV. OF IOWA LIBRARIES
Government Publications Dept.
Iowa City, IA 52242
(319) 335-5926

KANSAS

UNIVERSITY OF KANSAS
Spencer Research Library
Government Documents
Lawrence, KS 66045
(913) 864-4662

KENTUCKY

UNIV. OF KENTUCKY LIBRARIES
Government Publications/Maps Dept.
Lexington, KY 40506
(606) 257-8400

LOUISIANA

LOUISIANA STATE UNIVERSITY
Middleton Library
Government Documents Dept.
Baton Rouge, LA 70803
(504) 388-2570

LOUISIANA TECHNICAL UNIV.
Prescott Memorial Library
Government Documents Dept.
Ruston, LA 71272
(318) 257-4962

MAINE

UNIVERSITY OF MAINE
Raymond H. Fogler Library
Govt. Documents & Microforms Dept.
Orono, ME 04469
(207) 581-1680

MARYLAND

UNIVERSITY OF MARYLAND
McKeldin Library
Documents/Maps Room
College Park, MD 20742
(301) 454-3034

MASSACHUSETTS

BOSTON PUBLIC LIBRARY
Government Documents Dept.
666 Boylston Street
Boston, MA 02117
(617) 536-5400 ext.226

MICHIGAN

DETROIT PUBLIC LIBRARY
5201 Woodward Avenue
Detroit, MI 48202
(313) 833-1409

LIBRARY OF MICHIGAN
Government Documents
P.O. Box 30007
735 E. Michigan Avenue
Lansing, MI 48909
(517) 373-1593

MINNESOTA

UNIVERSITY OF MINNESOTA
Wilson Library
Government Publications
309 Nineteenth Avenue South
Minneapolis, MN 55455
(612) 373-7813

MISSISSIPPI

UNIV. OF MISSISSIPPI LIB.
Government Documents Dept.
106 Old Gym Bldg.
University, MS 38677
(601) 232-5857

MISSOURI

University of Missouri at Columbia Library
Government Documents
Columbia, MO 65201
(314) 882-6733

MONTANA

UNIV. OF MONTANA
Mansfield Library
Documents Division
Missoula, MT 59812
(406) 243-6700

NEBRASKA

UNIVERSITY OF NEBRASKA - LINCOLN
Love Memorial Library
Documents Department
Lincoln, NE 68588
(402) 472-2562

NEVADA

UNIV. OF NEVADA-RENO LIB.
Govt. Pub. Department
Reno, NV 89557
(702) 784-6579

NEW JERSEY

NEWARK PUBLIC LIBRARY
U.S. Documents Division
5 Washington Street
P.O. Box 630
Newark, NJ 07101
(201) 733-7812

NEW MEXICO

UNIVERSITY OF NEW MEXICO
General Library
Government Publications/Maps Dept.
Albuquerque, NM 87131
(505) 277-5441

NEW MEXICO STATE LIBRARY
325 Don Gaspar Avenue
Santa Fe, NM 87501
(505) 827-3826

NEW YORK

NEW YORK STATE LIBRARY
Documents Sect. Cultural Educ. Ctr.
Empire State Plaza
Albany, NY 12230
(518) 474-5563

NORTH CAROLINA

UNIVERSITY OF NORTH CAROLINA AT CHAPEL HILL
Davis Library 080A
BA/SS Department Documents
Chapel Hill, NC 27514
(919) 962-1151

NORTH DAKOTA

NORTH DAKOTA STATE UNIVERSITY LIBRARY
Government Documents Dept.
Fargo, ND 58105
(701) 237-8352
In cooperation with Univ. of North Dakota, Chester Fritz Library
Grand Forks

OHIO

STATE LIBRARY OF OHIO
Documents Section
65 South Front Street
Columbus, OH 43266
(614) 644-7051

OKLAHOMA

OKLAHOMA DEPT. OF LIBRARIES
Government Documents
200 NE 18th Street
Oklahoma City, OK 73105
(405) 521-2502, ext. 252

OKLAHOMA STATE UNIV. LIB.
Documents Department
Stillwater, OK 74078
(405) 624-0489

OREGON

PORTLAND STATE UNIV.
Millar Library
934 SW Harrison - P.O. Box 1151
Portland, OR 97207
(503) 229-3673

PENNSYLVANIA

STATE LIBRARY OF PENN.
Government Publications Section
Box 1601
Walnut St. & Commonwealth Ave.
Harrisburg, PA 17105
(717) 787-3752

SOUTH CAROLINA

CLEMSON UNIV. COOPER LIB.
Documents Department
Clemson, SC 29634
(803) 656-5174
In cooperation with Univ. of South Carolina, Thomas Cooper Library, Columbia

TEXAS

TEXAS STATE LIBRARY
Public Services Department
P.O. Box 12927 - 1201 Brazos
Austin, TX 78711
(512) 463-5455

TEXAS TECH. UNIV. LIBRARY
Documents Department
Lubbock, TX 79409
(806) 742-2268

UTAH

UTAH STATE UNIVERSITY
Merrill Library & Learning Resources Center, UMC-30
Documents Department
Logan, UT 84322
(801) 750-2682

VIRGINIA

UNIVERSITY OF VIRGINIA
Alderman Library
Government Documents
Charlottesville, VA 22903
(804) 924-3133

WASHINGTON

WASHINGTON STATE LIBRARY
Document Section
Olympia, WA 98504
(206) 753-4027

WEST VIRGINIA

WEST VIRGINIA UNIV. LIB.
Government Documents Section
P.O. Box 6069
Morgantown, WV 26506
(304) 293-3640

WISCONSIN

ST. HIST SOC. OF WISCONSIN LIB.
Government Pub. Section
816 State Street
Madison, WI 53706
(608) 262-2781
In cooperation with Univ. of Wisconsin-Madison, Memorial Library

MILWAUKEE PUBLIC LIBRARY
Documents Division
814 West Wisconsin Avenue
Milwaukee, WI 53233
(414) 278-3065

WYOMING

WYOMING STATE LIBRARY
Supreme Court & Library Bldg.
Cheyenne, WY 82002
(307) 777-5919

National Aeronautics and
Space Administration
Code NTT
Washington, D.C.
20546

Official Business

Penalty for Private Use, $300

SPECIAL FOURTH-CLASS RATE
POSTAGE & FEES PAID
NASA
PERMIT No. G27

NASA

POSTMASTER: If Undeliverable (Section 158 Postal Manual) Do Not Return